Title: Dark Matter Halos in 6D

Date: Sep 22, 2011 11:20 AM

URL: http://pirsa.org/11090109

Abstract: I will describe various efforts to understand the phase space structure of dark matter halos. Implications for dark matter detection experiments will also be discussed.

Dark Matter Halos in 6D

Unravelling Dark Matter
Perimeter Institute
September 2011

Larry Widrow
Queen's University
in collaboration with
David Stiff, Pascal Elahi, and Robert Thacker

figure from Fantin et al 2008

Formation of dark matter halos within
the context of the standard CDM paradigm
is a relatively "clean" physics problem

The System:
collisionless particles
Newtonian gravity

Initial Conditions:
negligible velocity dispersion
linear, random perturbations
power spectrum given by "fundamental physics" (inflation)

Formation of dark matter halos within
the context of the standard CDM paradigm
is a relatively "clean" physics problem

The System:
collisionless particles
Newtonian gravity

Initial Conditions:
negligible velocity dispersion
linear, random perturbations
power spectrum given by "fundamental physics" (inflation)

Formation of dark matter halos within
the context of the standard CDM paradigm
is a relatively "clean" physics problem

The System:
collisionless particles
Newtonian gravity

Initial Conditions:
negligible velocity dispersion
linear, random perturbations
power spectrum given by "fundamental physics" (inflation)

dark halo phenomenology from simulations

spherically-averaged density profile (from Navarro, 2010)

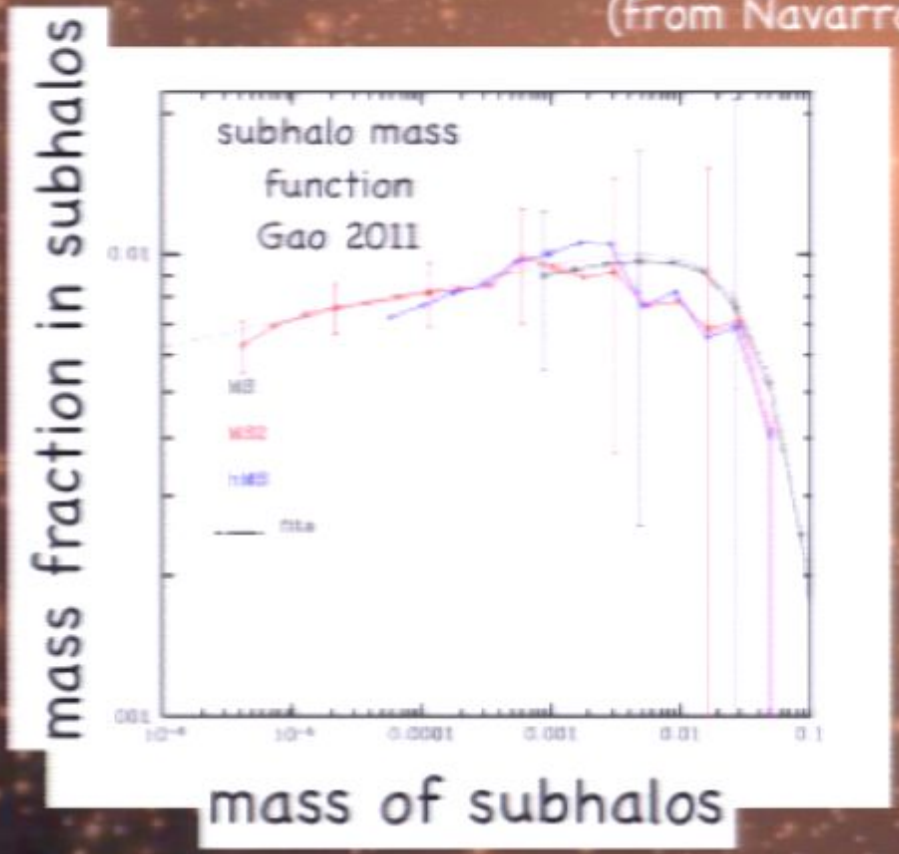

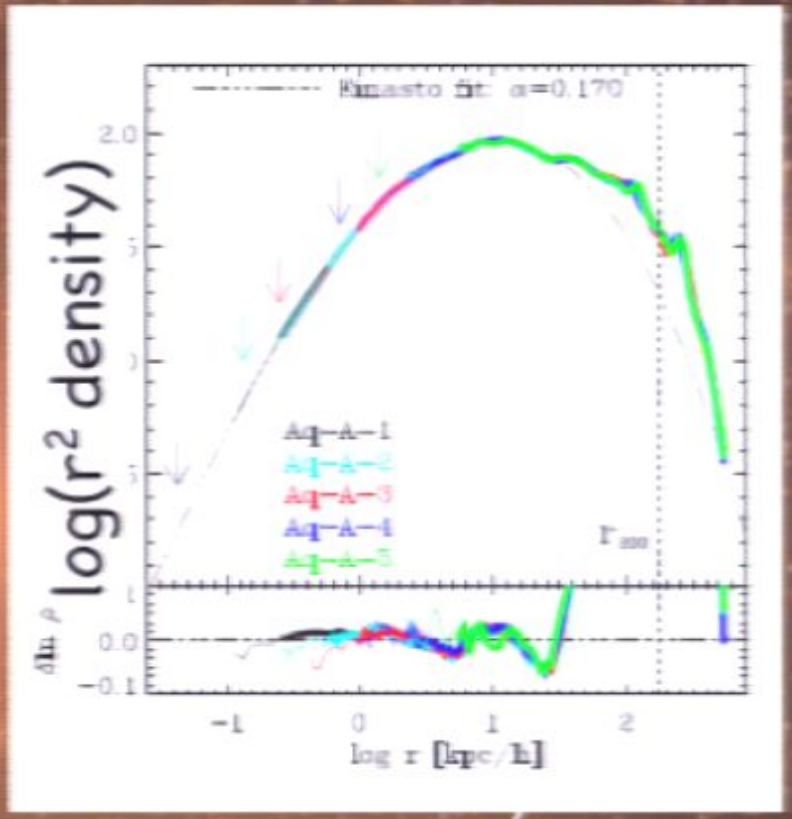

velocity anisotropy profile
pseudo-phase space profile
rotation
streams

figure from Diemand et al. 2006

dark halo phenomenology from simulations

spherically-averaged density profile (from Navarro, 2010)

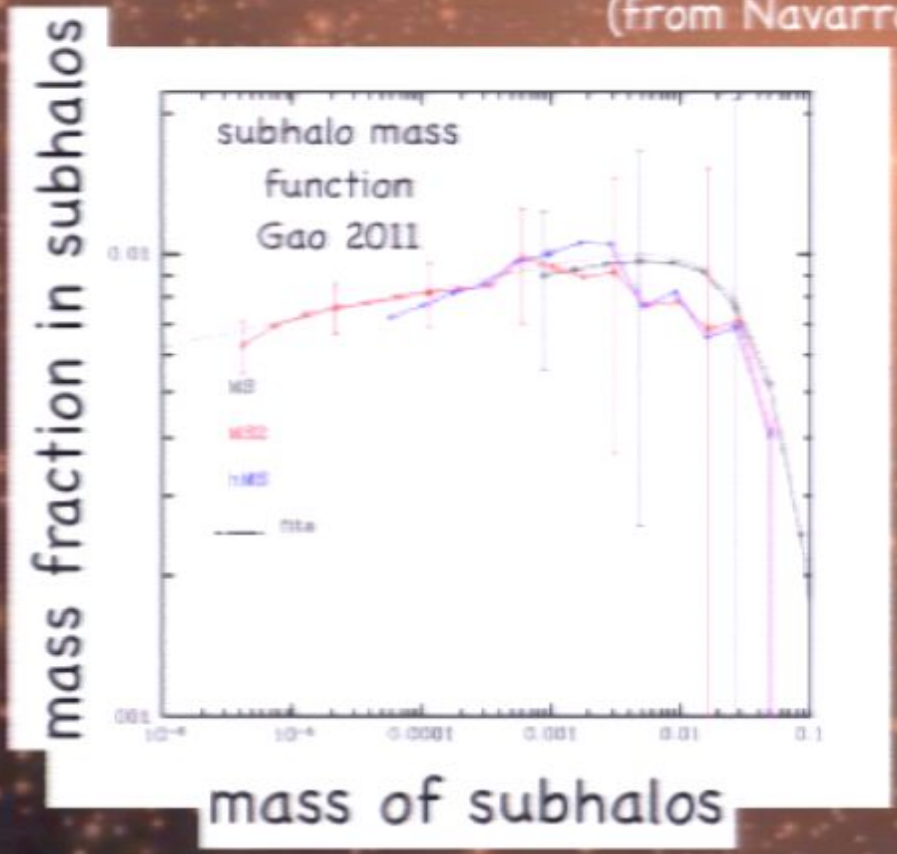

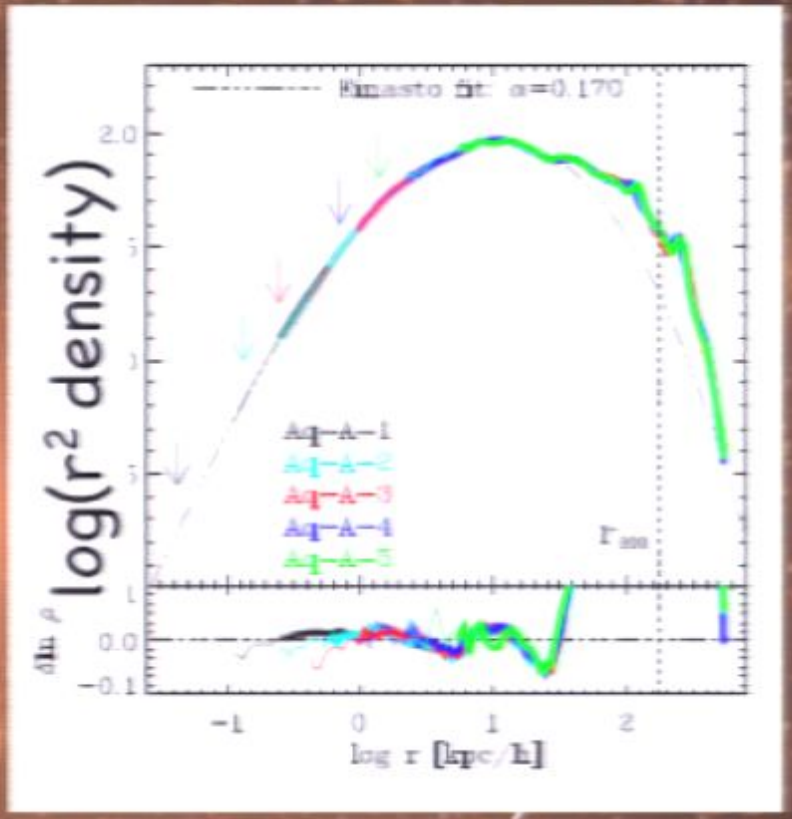

velocity anisotropy profile
pseudo-phase space profile
rotation
streams

figure from Diemand et al. 2006

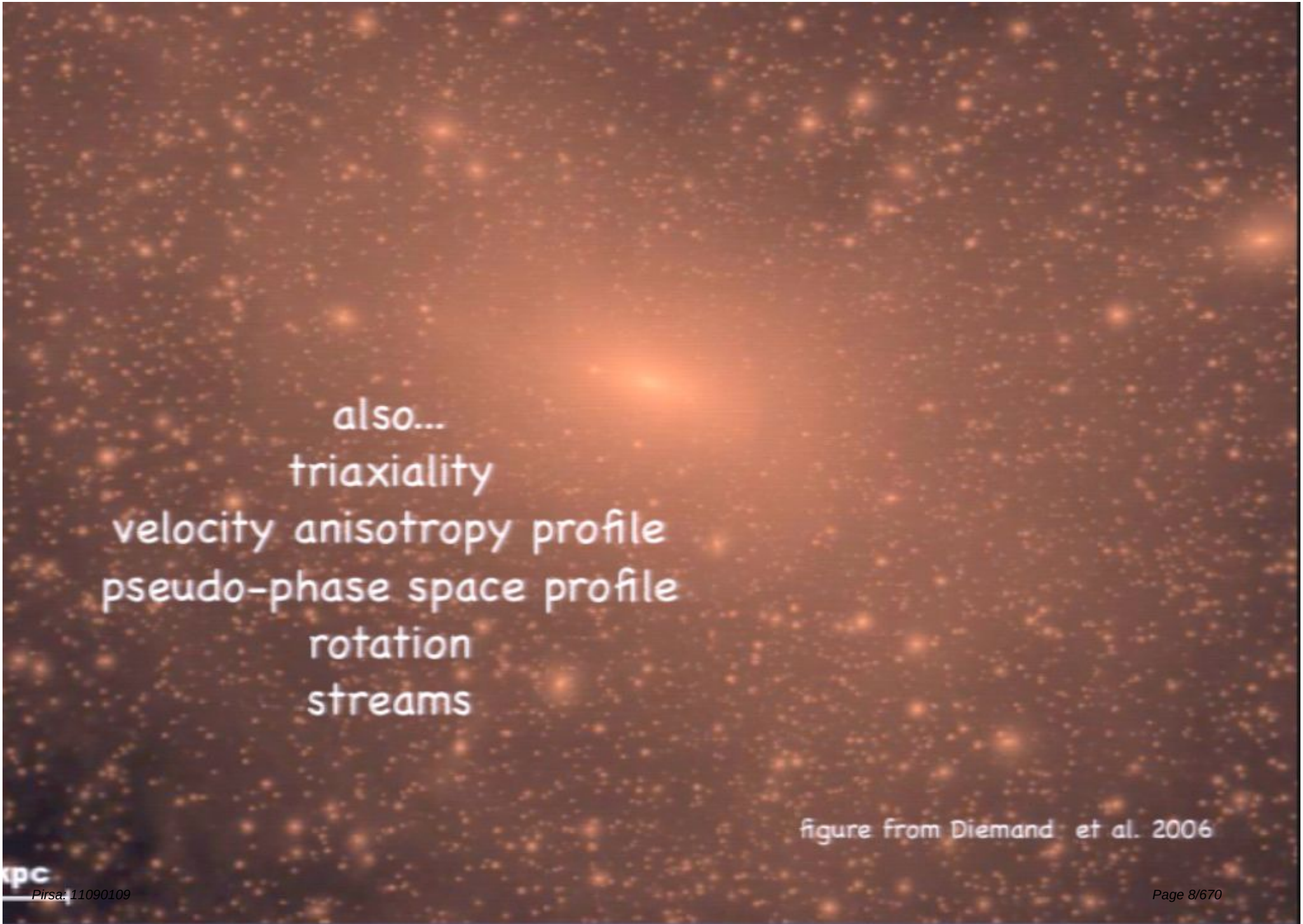
also...
triaxiality
velocity anisotropy profile
pseudo-phase space profile
rotation
streams
figure from Diemand et al. 2006
kpc

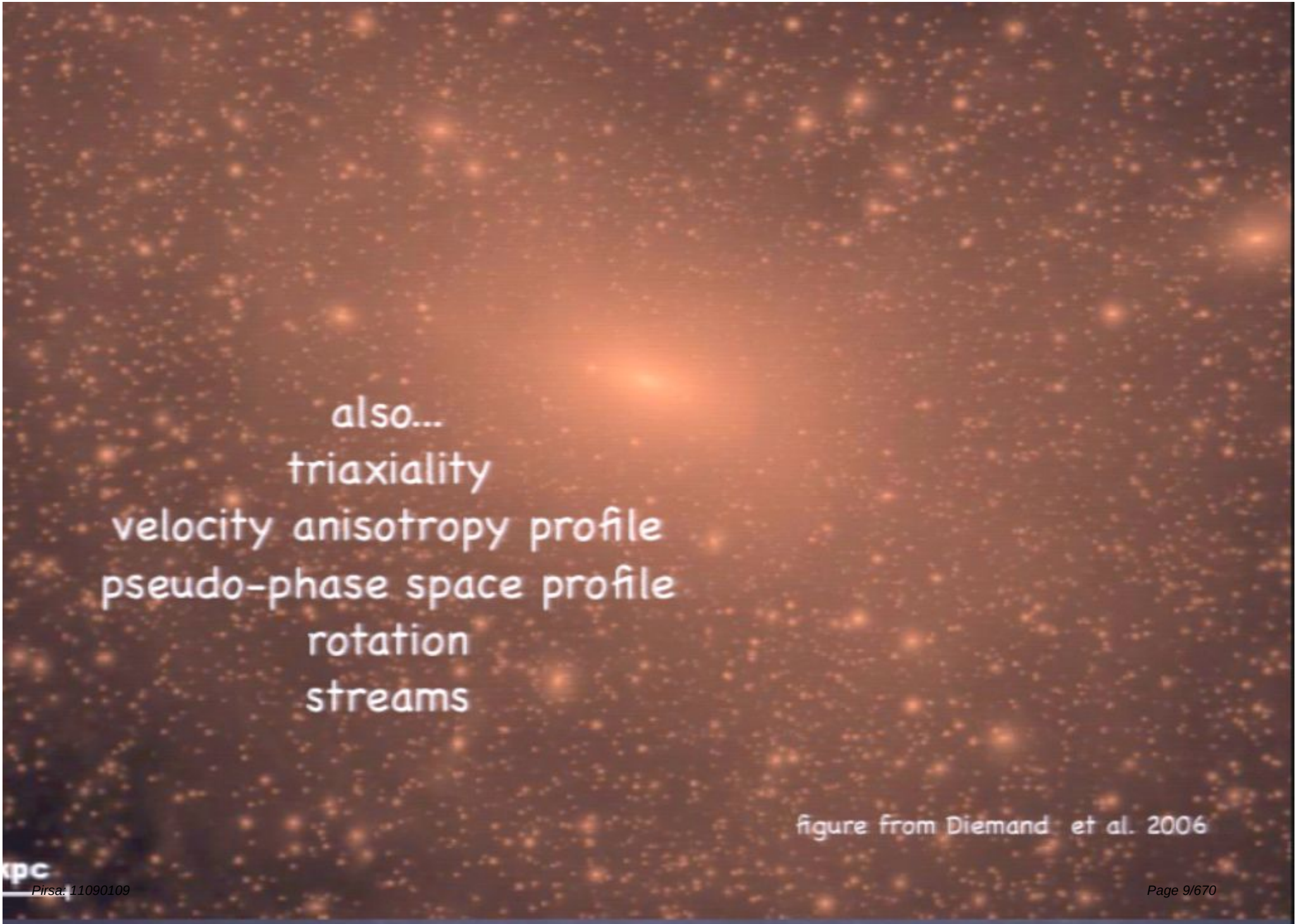
also...
triaxiality
velocity anisotropy profile
pseudo-phase space profile
rotation
streams
figure from Diemand et al. 2006
kpc


also...
triaxiality
velocity anisotropy profile
pseudo-phase space profile
rotation
streams
figure from Diemand et al. 2006
kpc

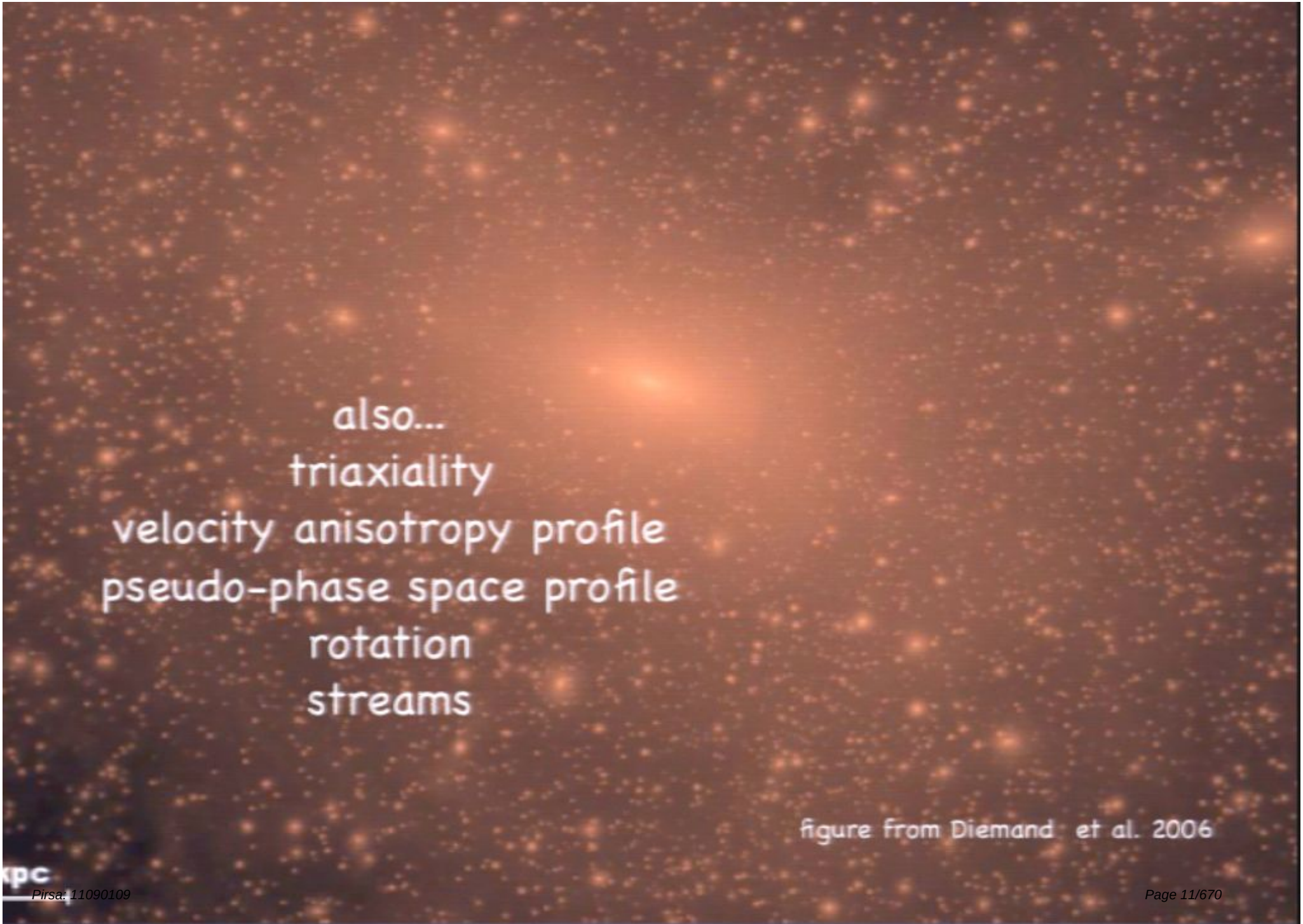
also...
triaxiality
velocity anisotropy profile
pseudo-phase space profile
rotation
streams
figure from Diemand et al. 2006
kpc

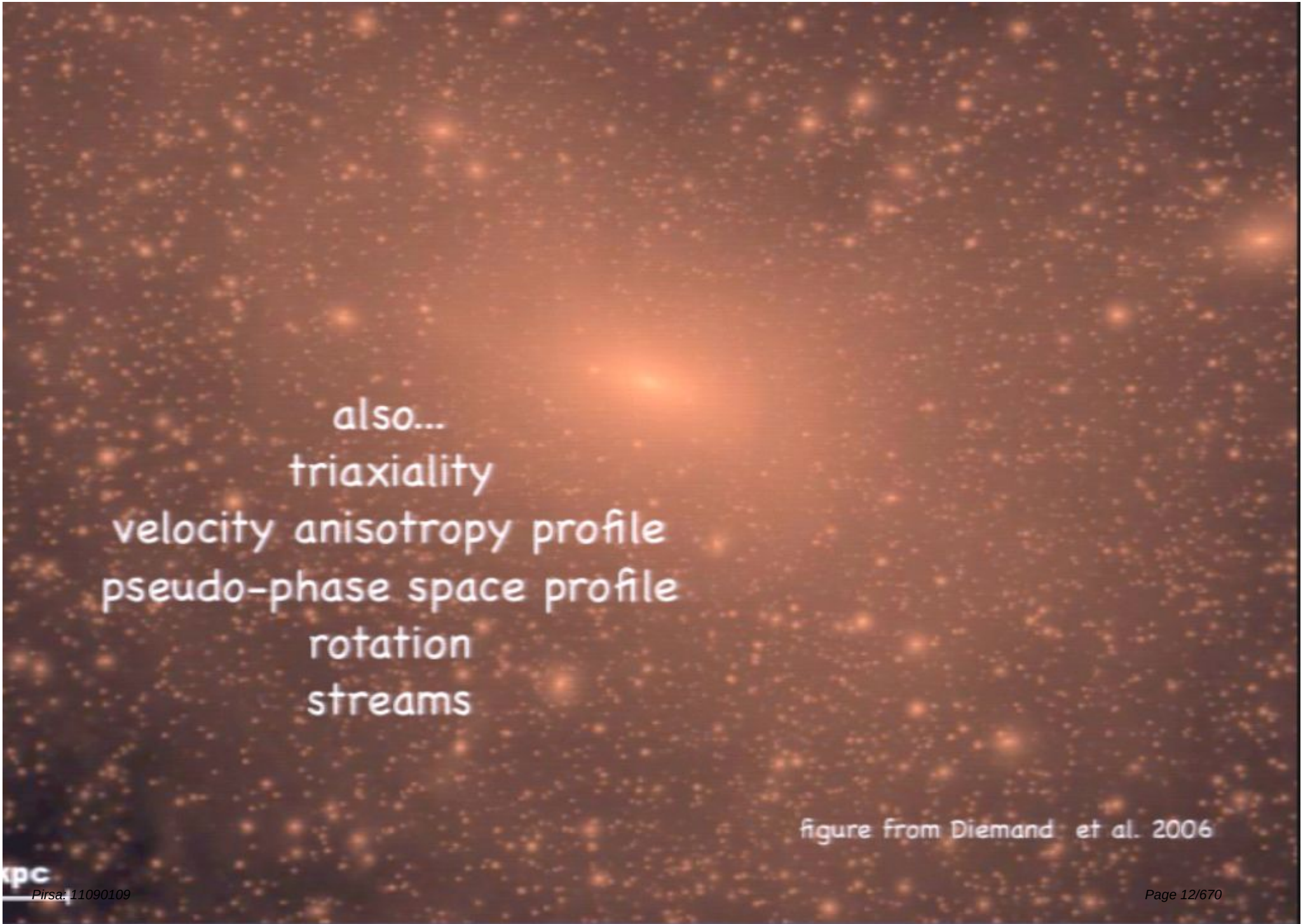
also...
triaxiality
velocity anisotropy profile
pseudo-phase space profile
rotation
streams
figure from Diemand et al. 2006
kpc

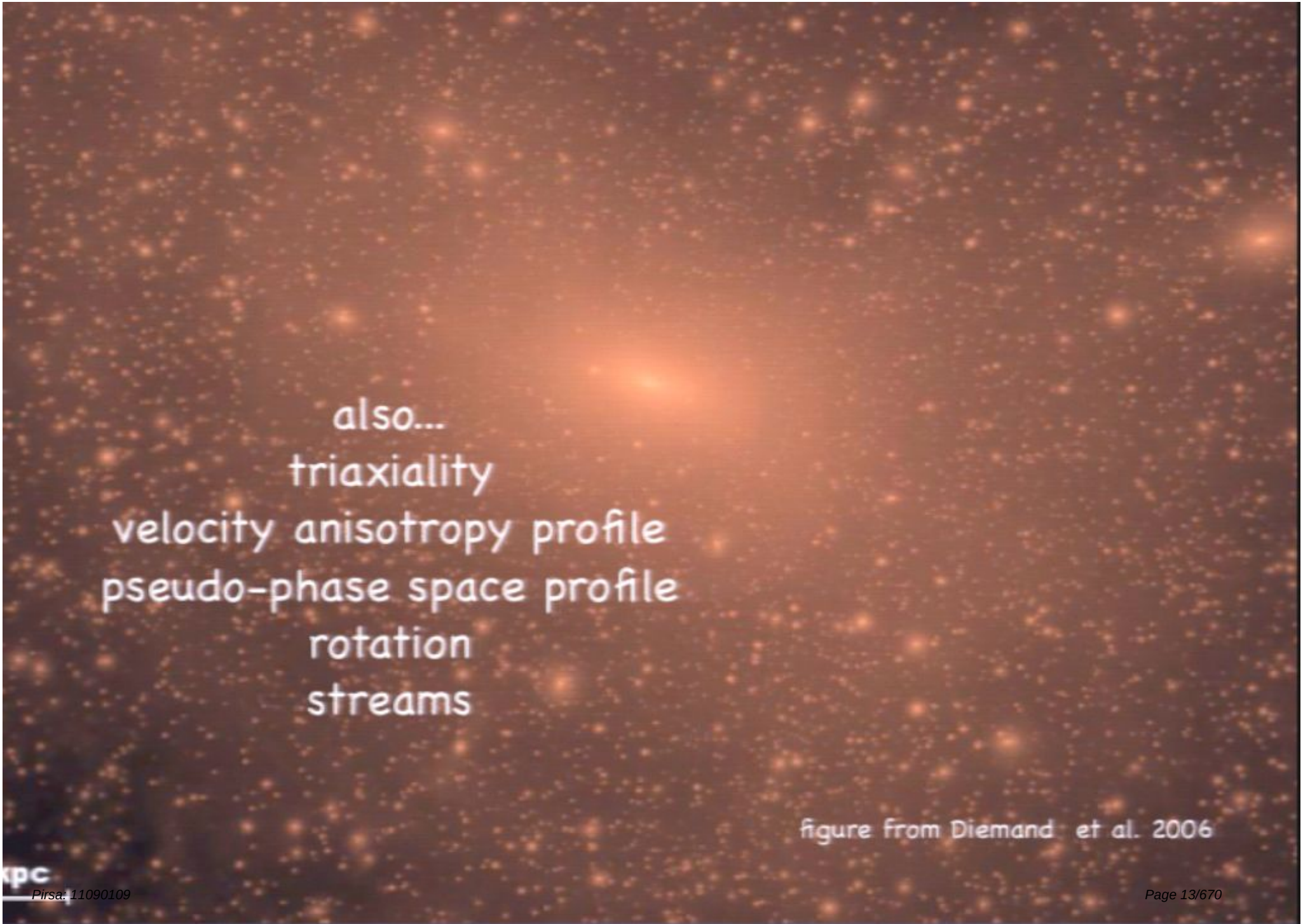
also...
triaxiality
velocity anisotropy profile
pseudo-phase space profile
rotation
streams
figure from Diemand et al. 2006
kpc

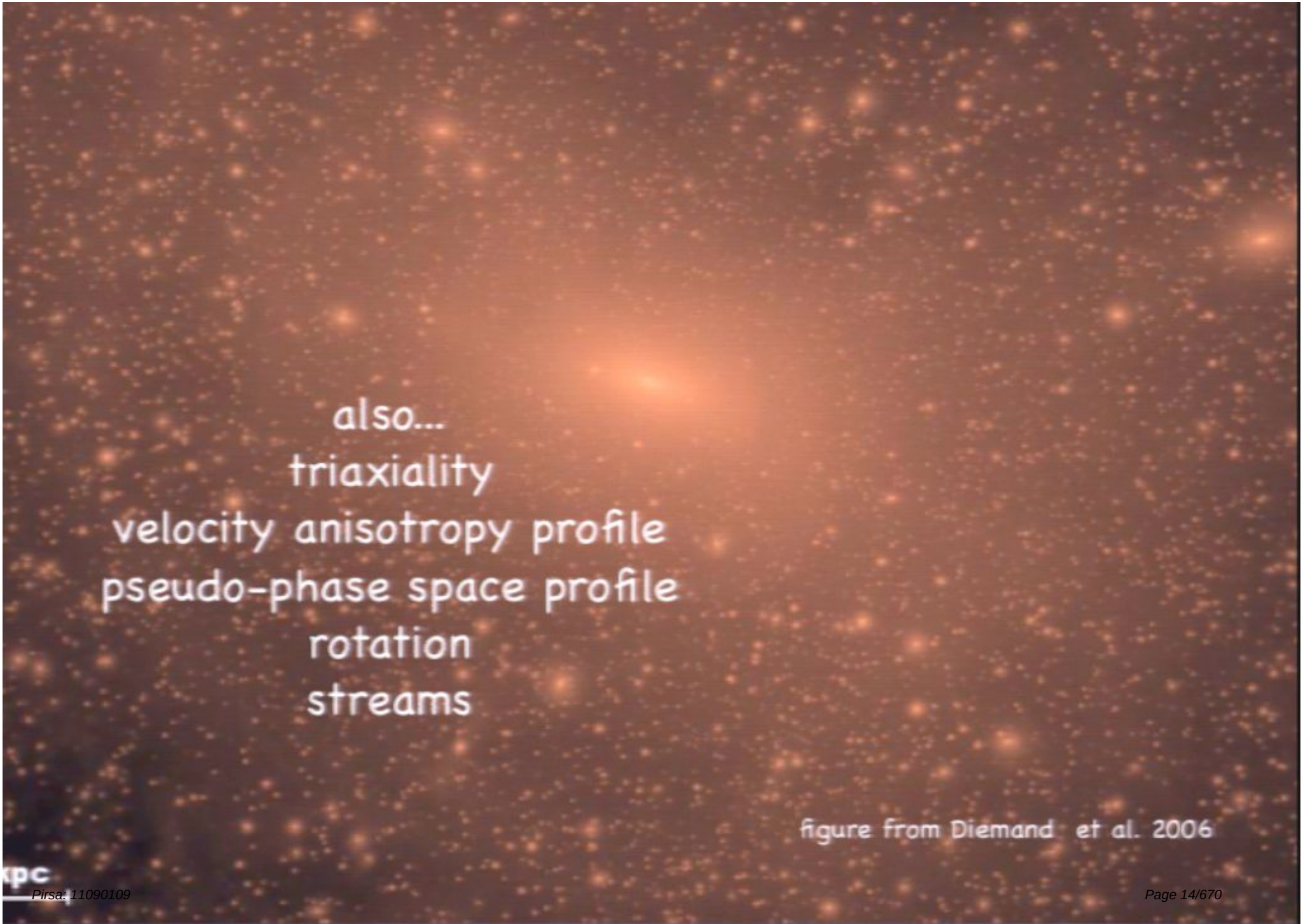
also...
triaxiality
velocity anisotropy profile
pseudo-phase space profile
rotation
streams
figure from Diemand et al. 2006
kpc

In addition, there are hints of self-similarity between halos of a different size

cluster halo

galaxy halo

Moore et al. 1999

In addition, there are hints of self-similarity between halos of a different size

cluster halo

galaxy halo

Moore et al. 1999

Ultimate goal as dark matter theorists:
to develop a generative, theoretical
(or at least phenomenological)
model for dark matter halos

build synthetic halos
indistinguishable from the halos
found in simulations

Generative model ⟶

push beyond resolution limits
of present-day simulations

see also work by other conference participants Taylor, Afshordi, Vogelsberger, Kuhlen,

Ultimate goal as dark matter theorists:
to develop a generative, theoretical
(or at least phenomenological)
model for dark matter halos

build synthetic halos
indistinguishable from the halos
found in simulations

Generative model ⟶

push beyond resolution limits
of present-day simulations

see also work by other conference participants Taylor, Afshordi, Vogelsberger, Kuhlen,

In short, we aim to model the phase space distribution function of dark matter particles

$$\mathrm{f}(\mathbf{x}, \mathbf{v}, \mathrm{t})$$

All dark matter detection experiments probe the DF, i.e., detector response involves some integral over the DF

$$\mathcal{R}(E, ...) \sim \int f(\mathbf{x}, \mathbf{v})\, I(E, ...; \mathbf{x}, \mathbf{v})\, d^3x\, d^3v$$

In short, we aim to model the phase space distribution function of dark matter particles

$$\mathrm{f}(\mathbf{x}, \mathbf{v}, \mathrm{t})$$

All dark matter detection experiments probe the DF, i.e., detector response involves some integral over the DF

$$\mathcal{R}(E, ...) \sim \int f(\mathbf{x}, \mathbf{v})\, I(E, ...; \mathbf{x}, \mathbf{v})\, d^3x\, d^3v$$

In short, we aim to model the phase space distribution function of dark matter particles

$$\mathrm{f}(\mathbf{x}, \mathbf{v}, \mathrm{t})$$

All dark matter detection experiments probe the DF, i.e., detector response involves some integral over the DF

$$\mathcal{R}(E, ...) \sim \int f(\mathbf{x}, \mathbf{v})\, I(E, ...; \mathbf{x}, \mathbf{v})\, d^3x\, d^3v$$

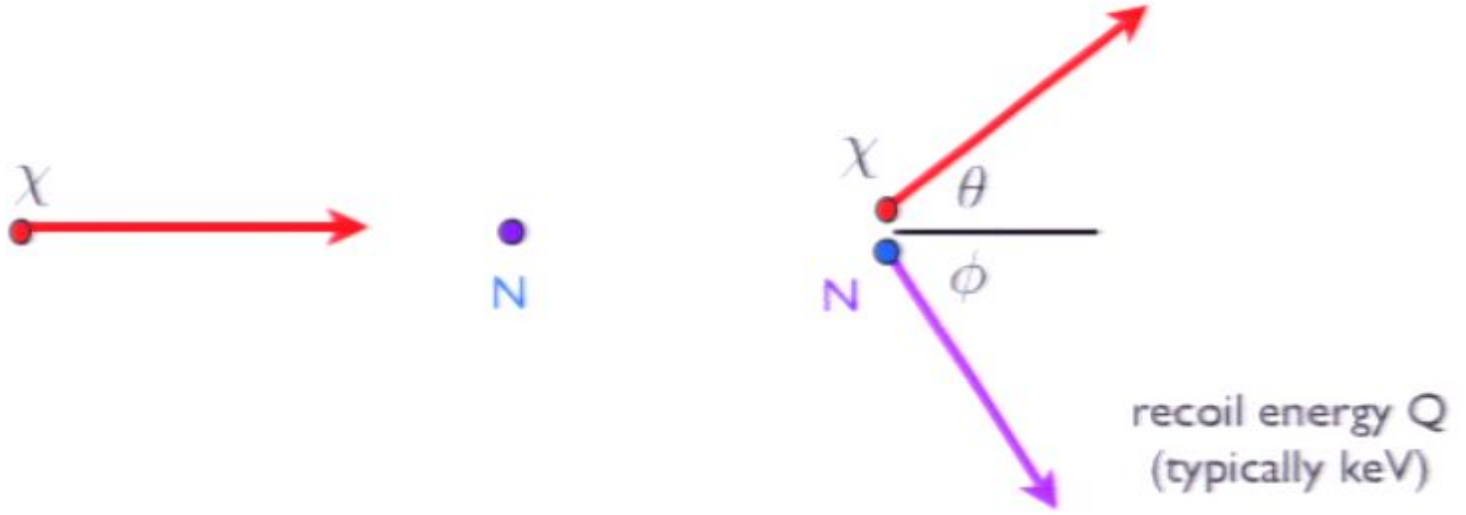

$$\frac{dR}{dQ} = \frac{\rho_L \sigma_0}{2 m_r^2 m_\chi} G^2(Q) \int_{v_{\min}}^{\infty} F(v) \frac{dv}{v}$$

if all WIMPs had the same speed....

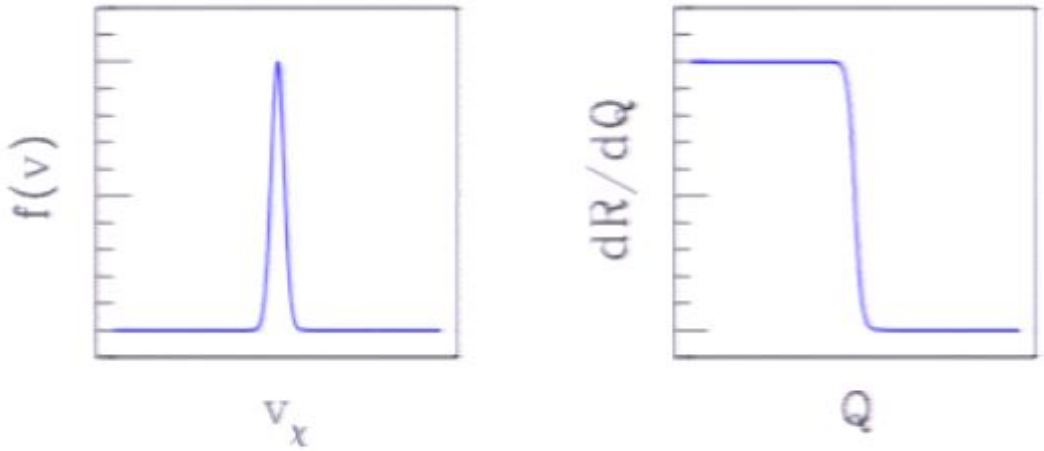

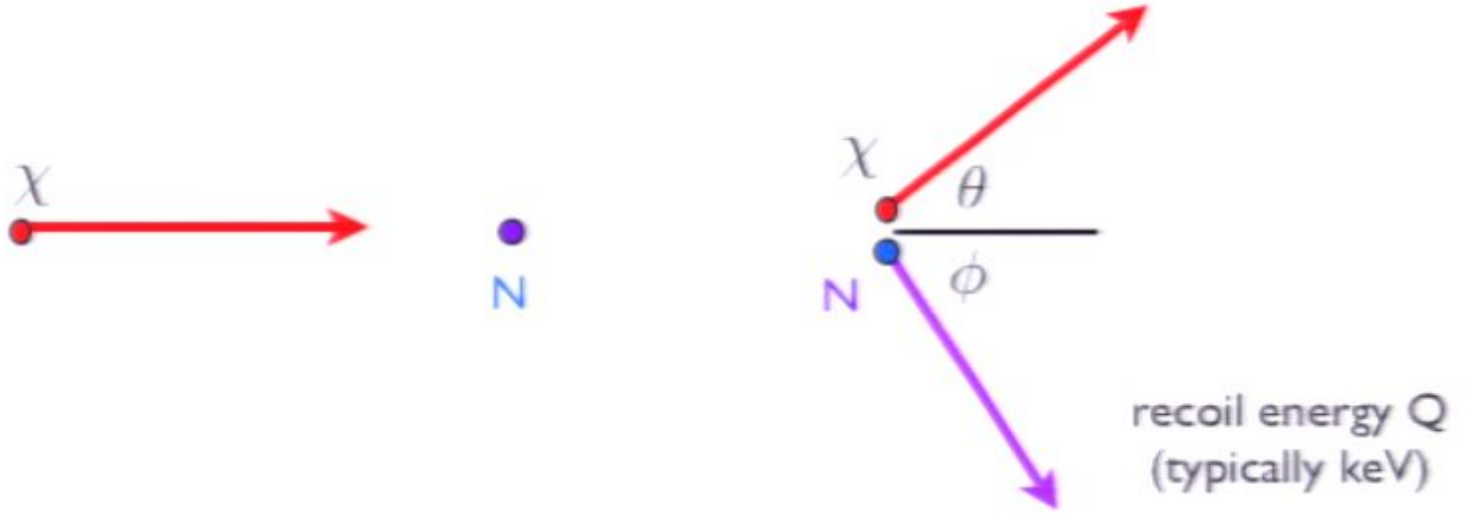

$$\frac{dR}{dQ} = \frac{\rho_L \sigma_0}{2 m_r^2 m_\chi} G^2(Q) \int_{v_{\min}}^{\infty} F(v) \frac{dv}{v}$$

if all WIMPs had the same speed....

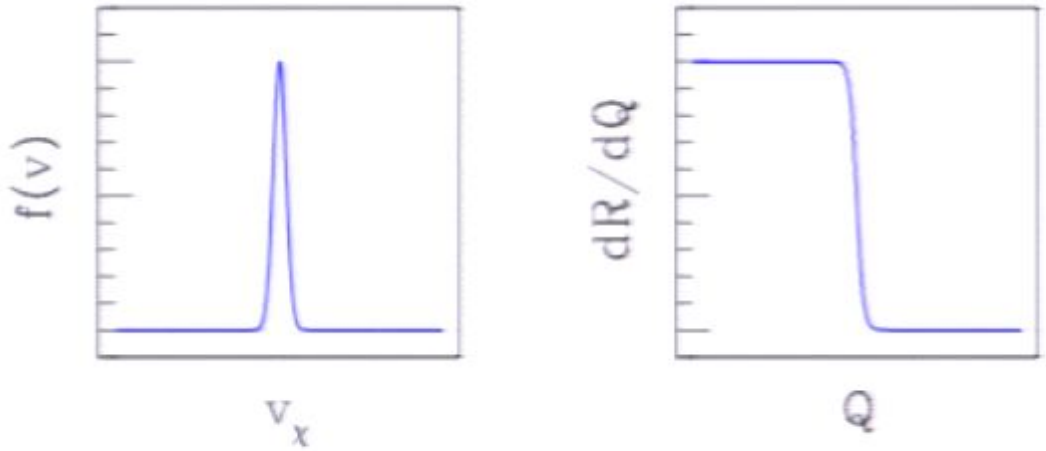

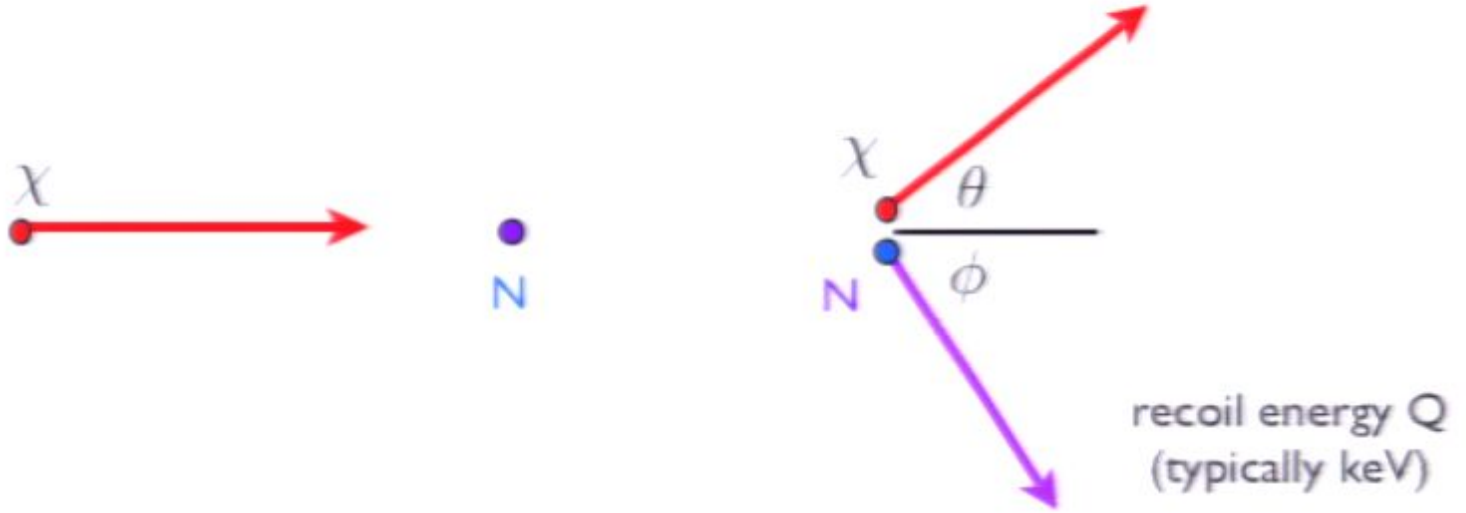

$$\frac{dR}{dQ} = \frac{\rho_L \sigma_0}{2 m_r^2 m_\chi} G^2(Q) \int_{v_{\min}}^{\infty} F(v) \frac{dv}{v}$$

if all WIMPs had the same speed....

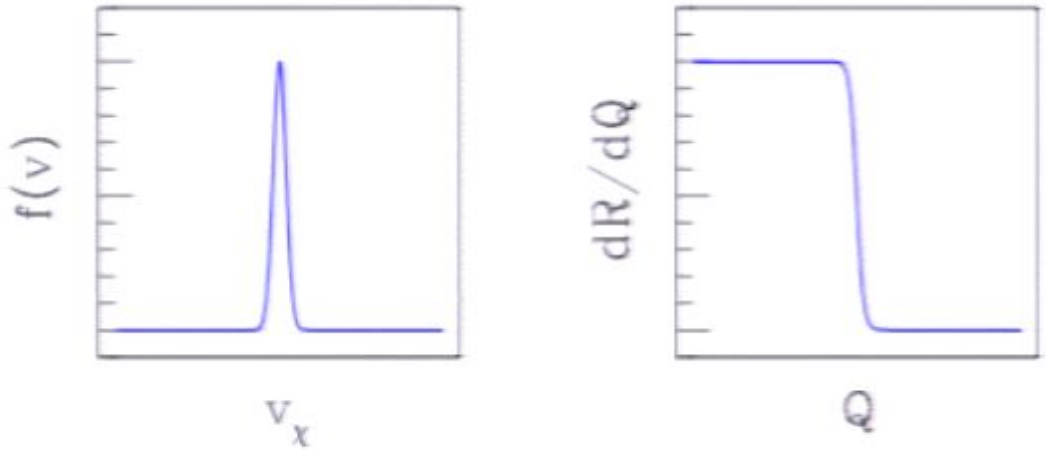

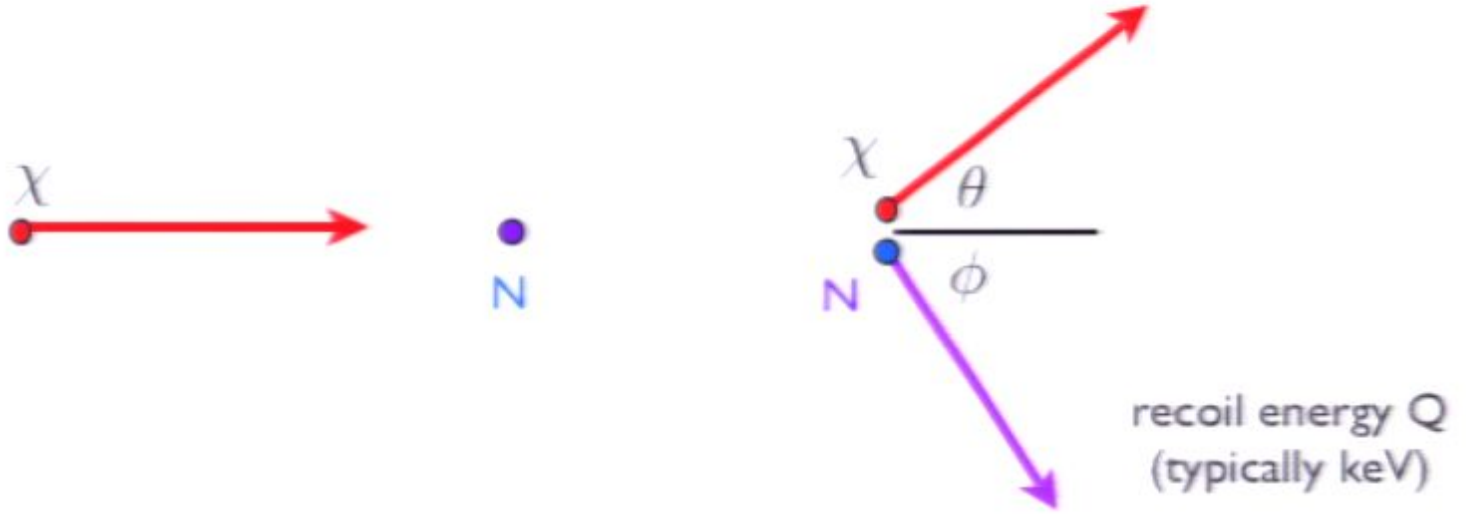

$$\frac{dR}{dQ} = \frac{\rho_L \sigma_0}{2 m_r^2 m_\chi} G^2(Q) \int_{v_{\min}}^{\infty} F(v) \frac{dv}{v}$$

if all WIMPs had the same speed....

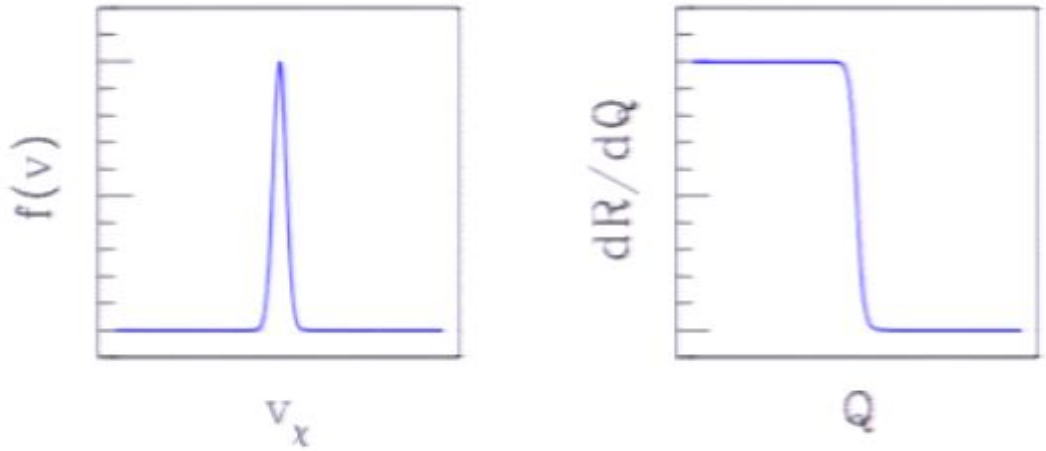

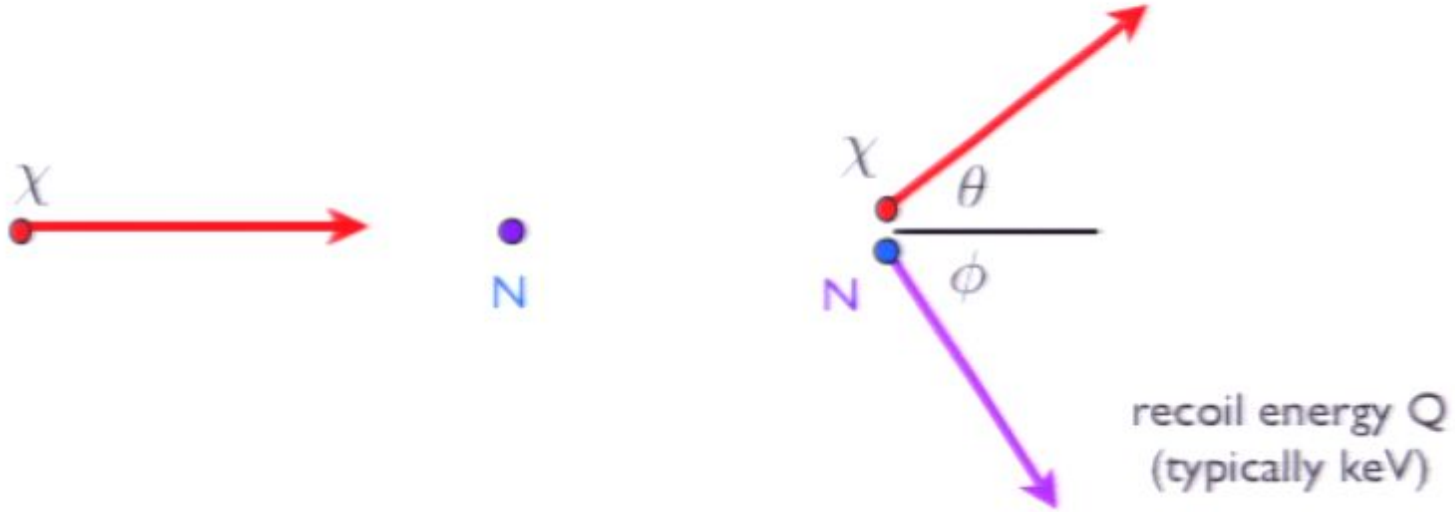

$$\frac{dR}{dQ} = \frac{\rho_L \sigma_0}{2 m_r^2 m_\chi} G^2(Q) \int_{v_{\min}}^{\infty} F(v) \frac{dv}{v}$$

if all WIMPs had the same speed....

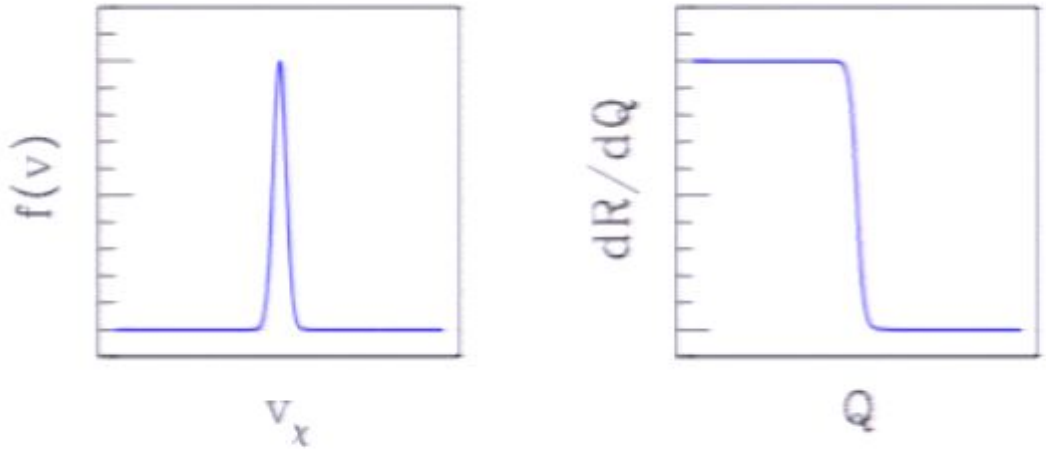

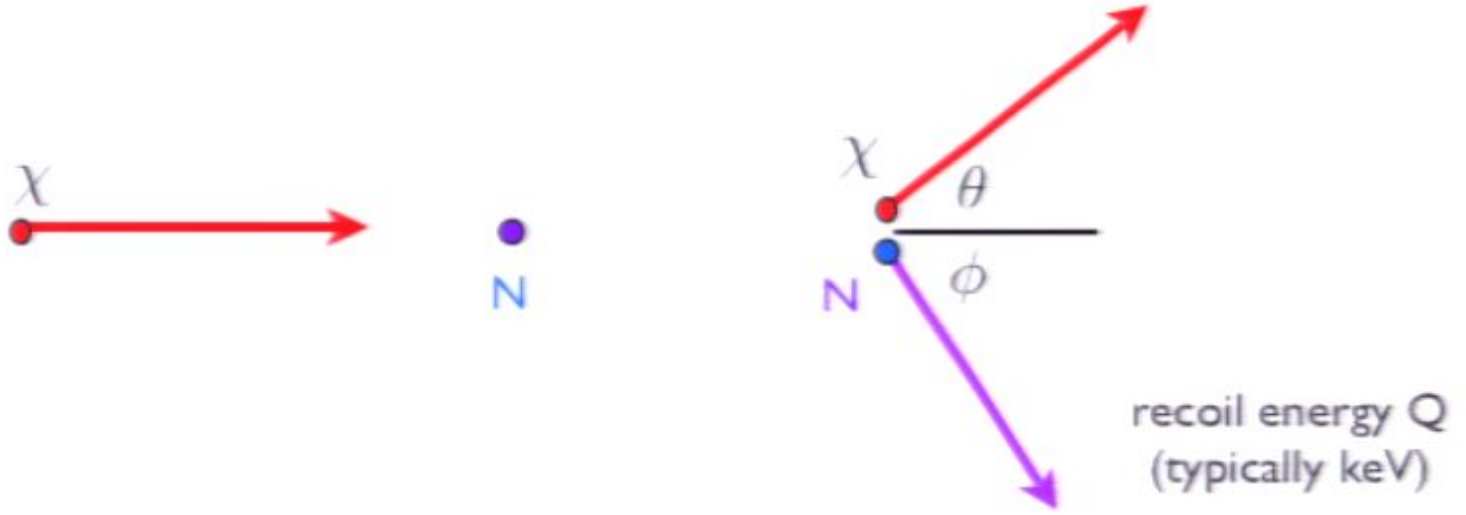

$$\frac{dR}{dQ} = \frac{\rho_L \sigma_0}{2 m_r^2 m_\chi} G^2(Q) \int_{v_{\min}}^{\infty} F(v) \frac{dv}{v}$$

if all WIMPs had the same speed....

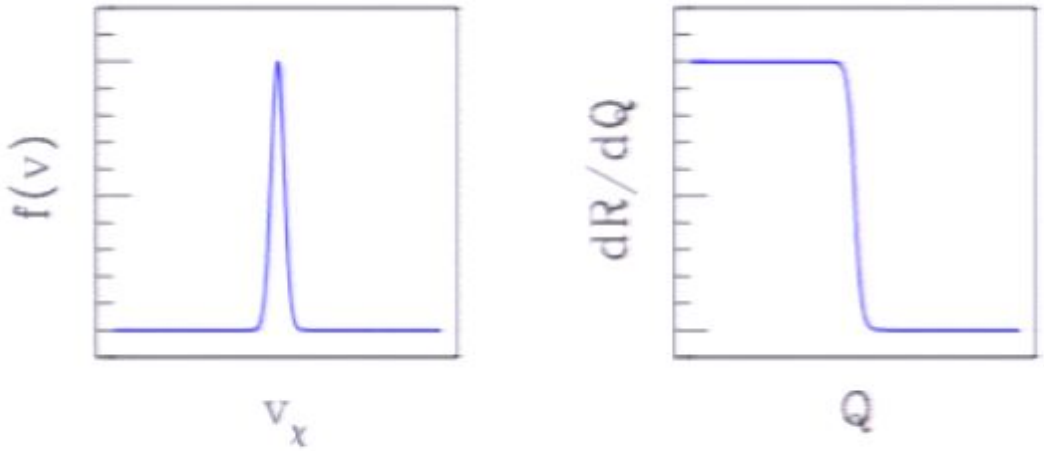

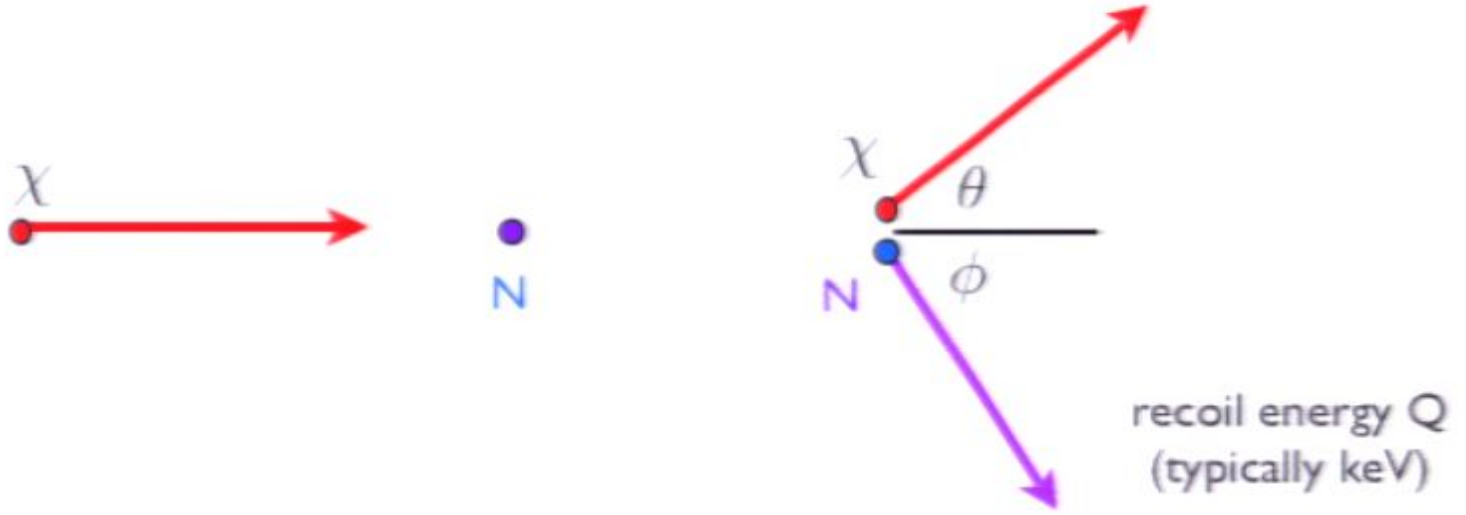

$$\frac{dR}{dQ} = \frac{\rho_L \sigma_0}{2 m_r^2 m_\chi} G^2(Q) \int_{v_{\min}}^{\infty} F(v) \frac{dv}{v}$$

if all WIMPs had the same speed....

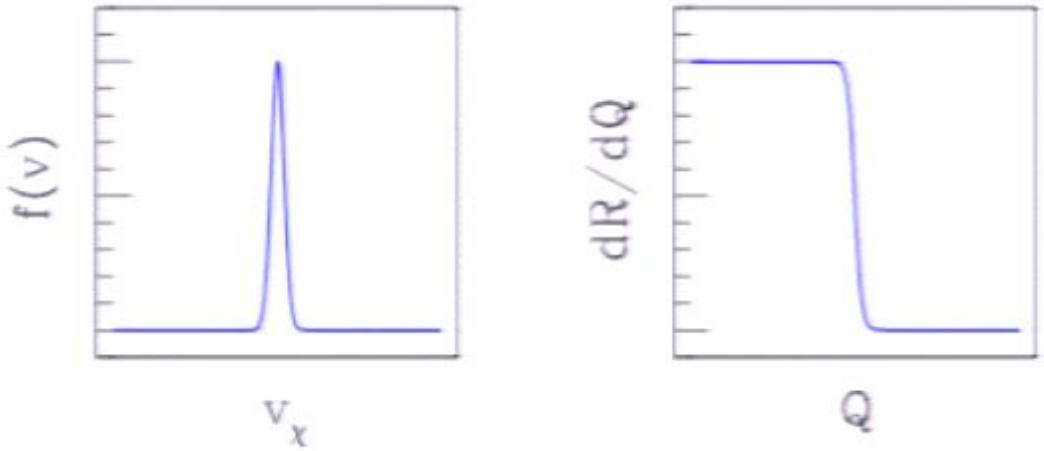

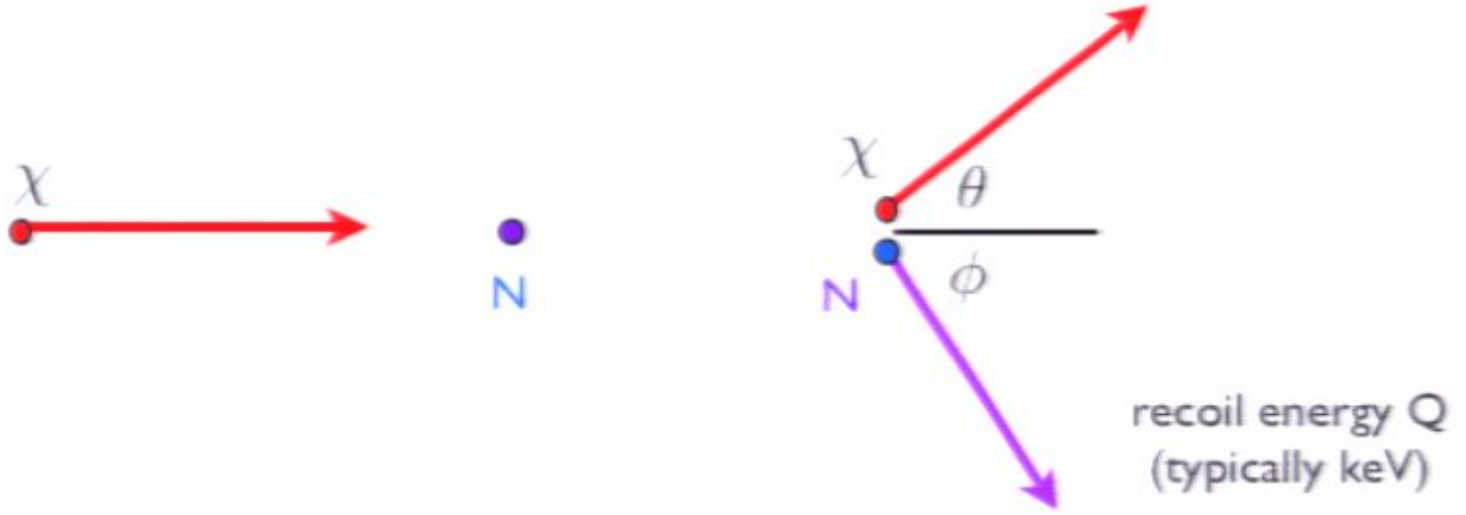

$$\frac{dR}{dQ} = \frac{\rho_L \sigma_0}{2 m_r^2 m_\chi} G^2(Q) \int_{v_{\min}}^{\infty} F(v) \frac{dv}{v}$$

if all WIMPs had the same speed....

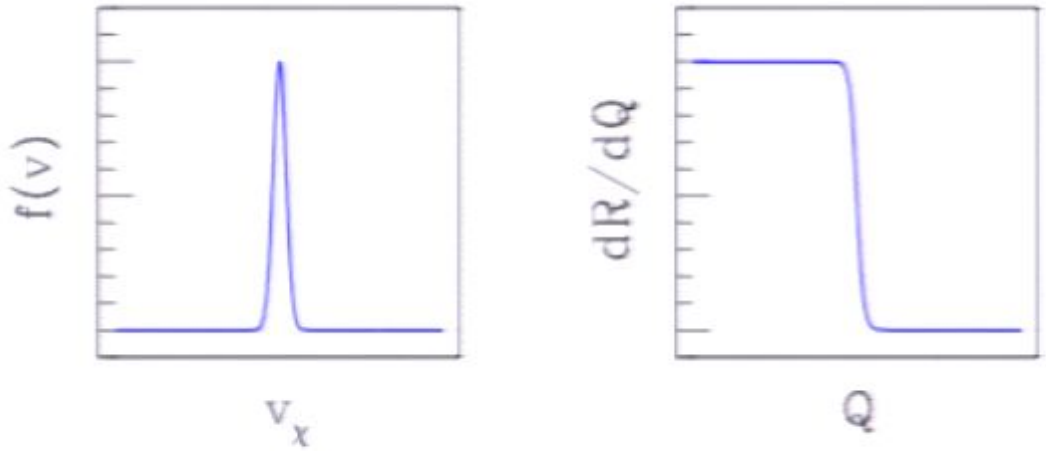

standard model used in DM detection experiments assumes a Maxwellian velocities in the Galactic rest frame

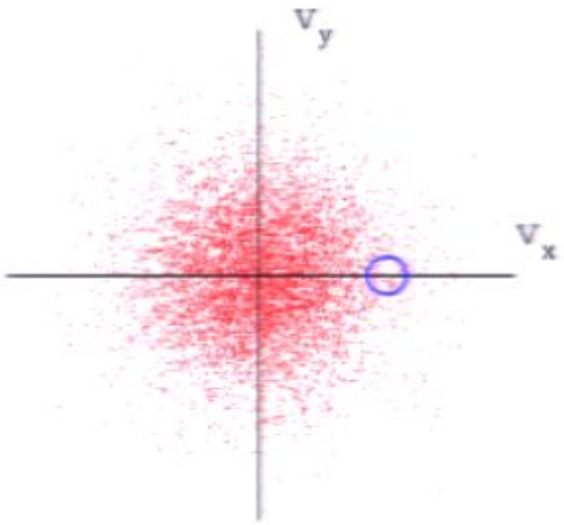

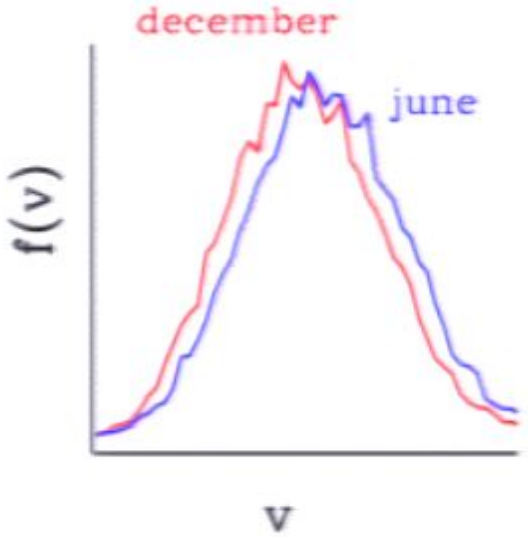

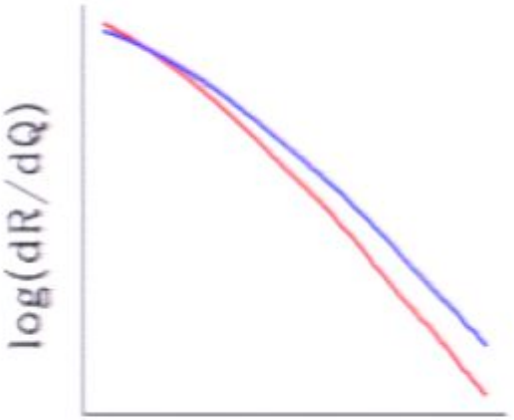

CDMS collaboration, 2011

standard model used in DM detection experiments assumes a Maxwellian velocities in the Galactic rest frame

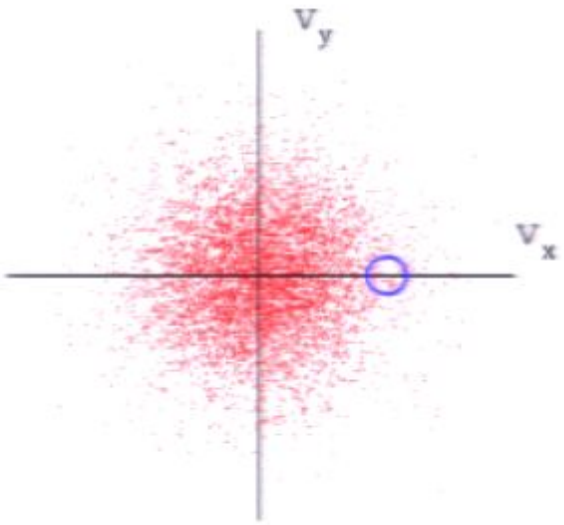

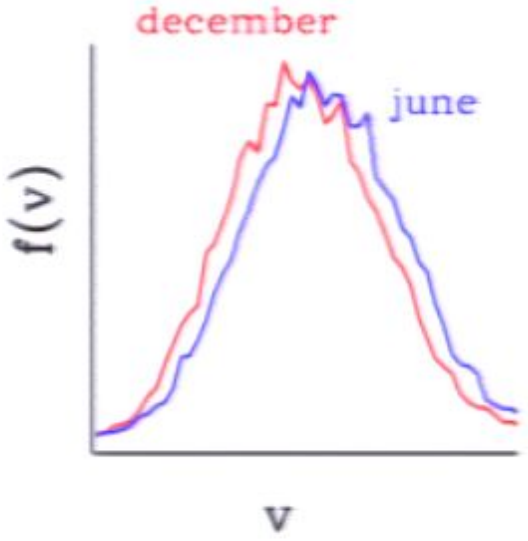

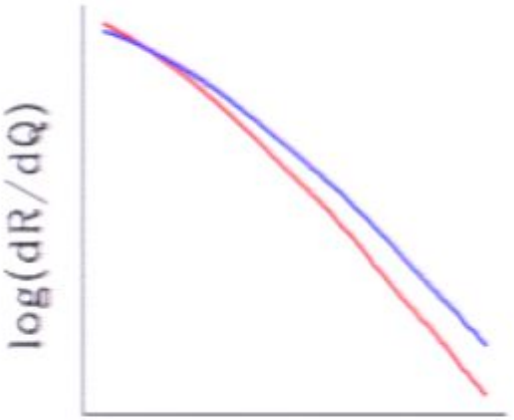

CDMS collaboration, 2011

standard model used in DM detection experiments assumes a Maxwellian velocities in the Galactic rest frame

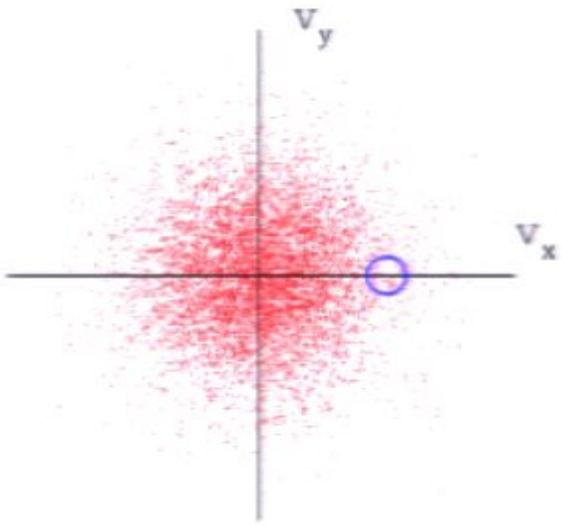

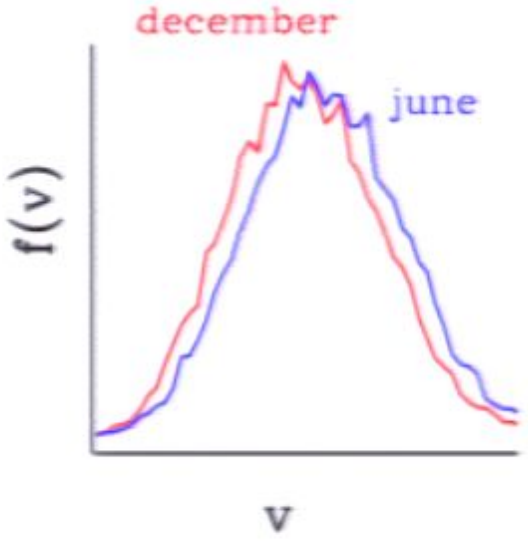

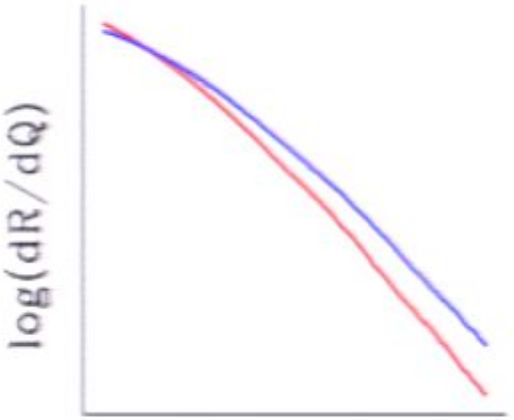

CDMS collaboration, 2011

standard model used in DM detection experiments assumes a Maxwellian velocities in the Galactic rest frame

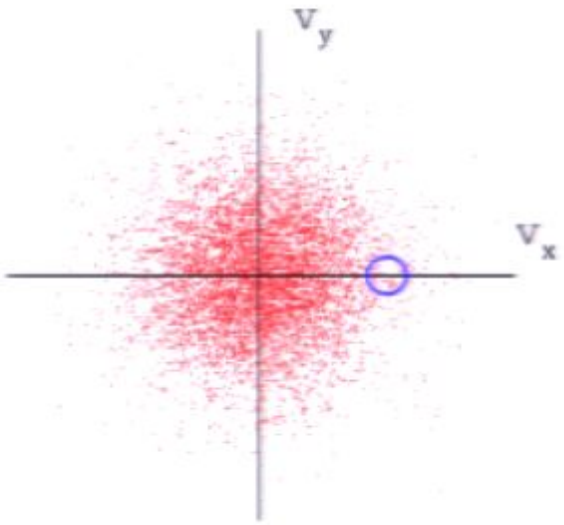

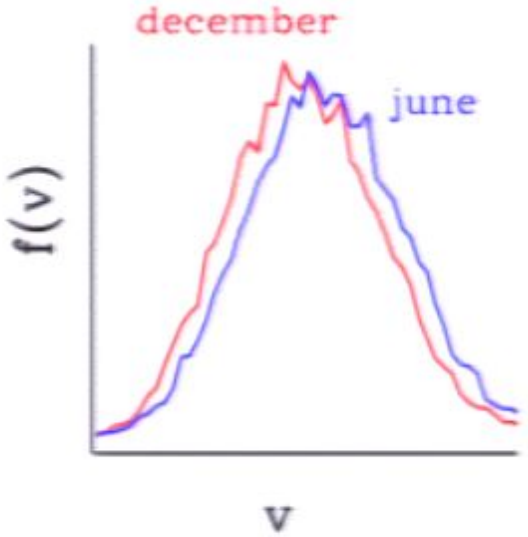

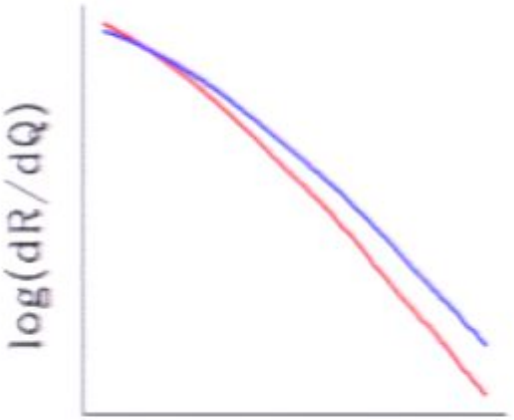

CDMS collaboration, 2011

standard model used in DM detection experiments assumes a Maxwellian velocities in the Galactic rest frame

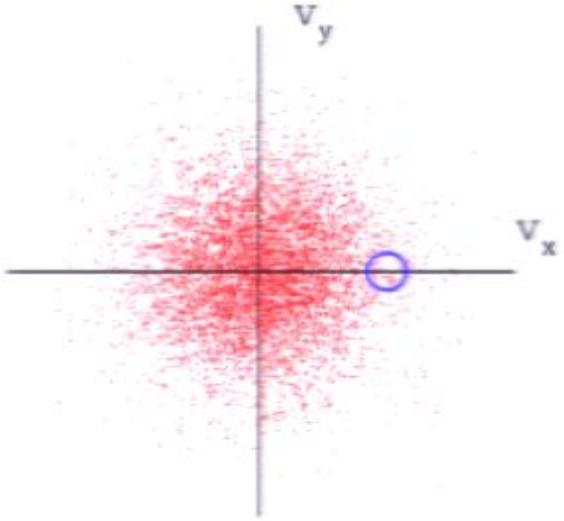

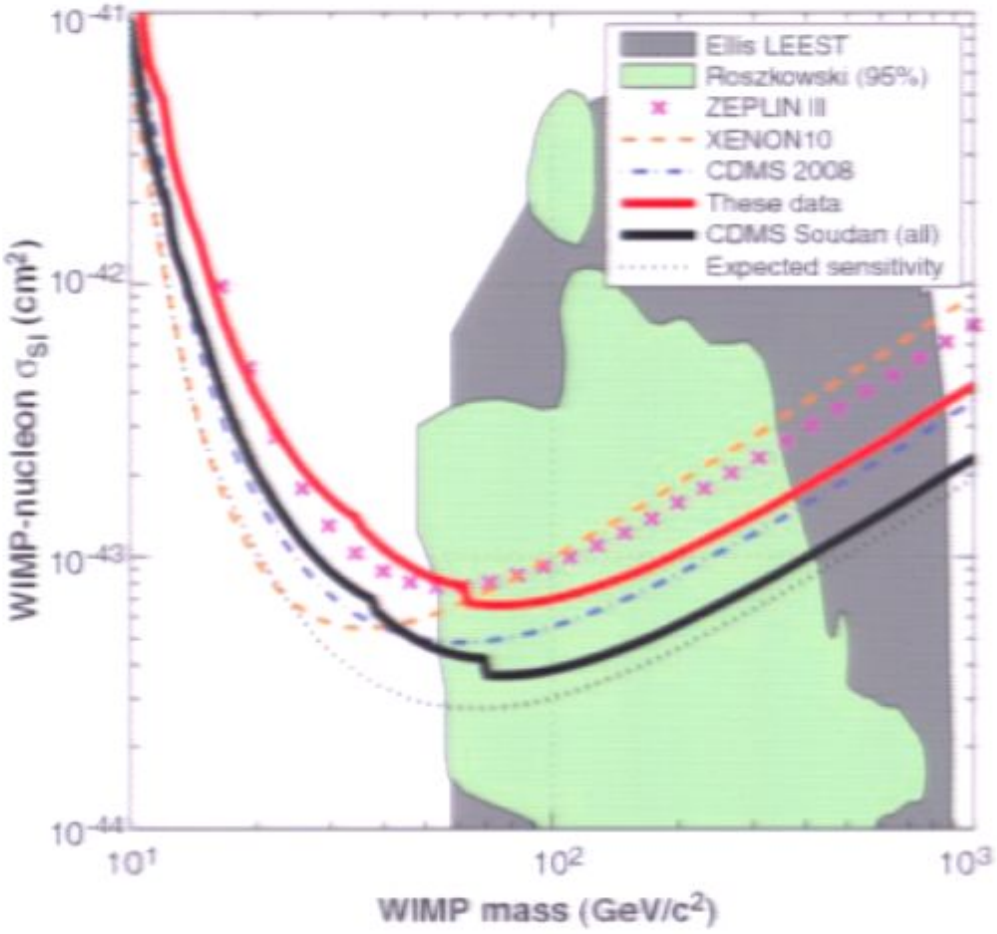

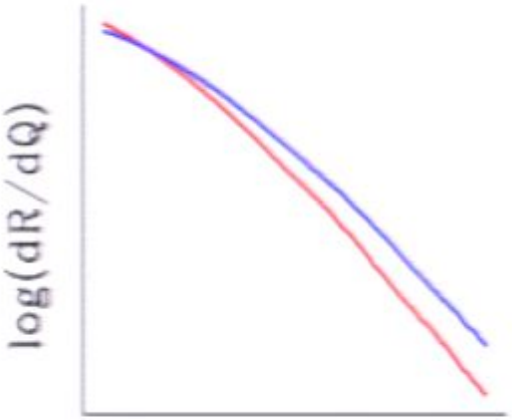

CDMS collaboration, 2011

Baby steps toward a generative model:

Given $\rho(r)$ and the assumptions of spherical symmetry and isotropic velocities, find $f(E)$ via the Eddington inversion formula

For "flattened" and rotating halos, consider $f(E, L_z)$

For velocity anisotropy, consider $f(E, L)$

... three integral DFs

Baby steps toward a generative model:

Given $\rho(r)$ and the assumptions of spherical symmetry and isotropic velocities, find $f(E)$ via the Eddington inversion formula

For "flattened" and rotating halos, consider $f(E, L_z)$

For velocity anisotropy, consider $f(E, L)$

... three integral DFs

Baby steps toward a generative model:

Given $\rho(r)$ and the assumptions of spherical symmetry and isotropic velocities, find $f(E)$ via the Eddington inversion formula

For "flattened" and rotating halos, consider $f(E, L_z)$

For velocity anisotropy, consider $f(E, L)$

... three integral DFs

Baby steps toward a generative model:

Given $\rho(r)$ and the assumptions of spherical symmetry and isotropic velocities, find $f(E)$ via the Eddington inversion formula

For "flattened" and rotating halos, consider $f(E, L_z)$

For velocity anisotropy, consider $f(E, L)$

... three integral DFs

Baby steps toward a generative model:

Given $\rho(r)$ and the assumptions of spherical symmetry and isotropic velocities, find $f(E)$ via the Eddington inversion formula

For "flattened" and rotating halos, consider $f(E, L_z)$

For velocity anisotropy, consider $f(E, L)$

... three integral DFs

Baby steps toward a generative model:

Given $\rho(r)$ and the assumptions of spherical symmetry and isotropic velocities, find $f(E)$ via the Eddington inversion formula

For "flattened" and rotating halos, consider $f(E, L_z)$

For velocity anisotropy, consider $f(E, L)$

... three integral DFs

Challenges, I
Limited resolution

The best present-day simulations for MW-sized halos are performed with of order 1 billion particles or a mass resolution

$$\sim 10^3 M_\odot$$

In typical WIMP models, the first objects to form in the Earth. Thus, we are 9 or more orders of magnitude short of doing fully realistic simulations of a MW-sized halo

Challenges, I
Limited resolution

The best present-day simulations for MW-sized halos are performed with of order 1 billion particles or a mass resolution

$$\sim 10^3 M_\odot$$

In typical WIMP models, the first objects to form in the Earth. Thus, we are 9 or more orders of magnitude short of doing fully realistic simulations of a MW-sized halo

Challenges, I
Limited resolution

The best present-day simulations for MW-sized halos are performed with of order 1 billion particles or a mass resolution

$$\sim 10^3 M_\odot$$

In typical WIMP models, the first objects to form in the Earth. Thus, we are 9 or more orders of magnitude short of doing fully realistic simulations of a MW-sized halo

Challenges, I
Limited resolution

The best present-day simulations for MW-sized halos are performed with of order 1 billion particles or a mass resolution

$$\sim 10^3 M_\odot$$

In typical WIMP models, the first objects to form in the Earth. Thus, we are 9 or more orders of magnitude short of doing fully realistic simulations of a MW-sized halo

12 orders of magnitude to the bottom of the CDM hierarchy

$$\frac{dN}{d\ln f} = Af^{-\alpha}$$

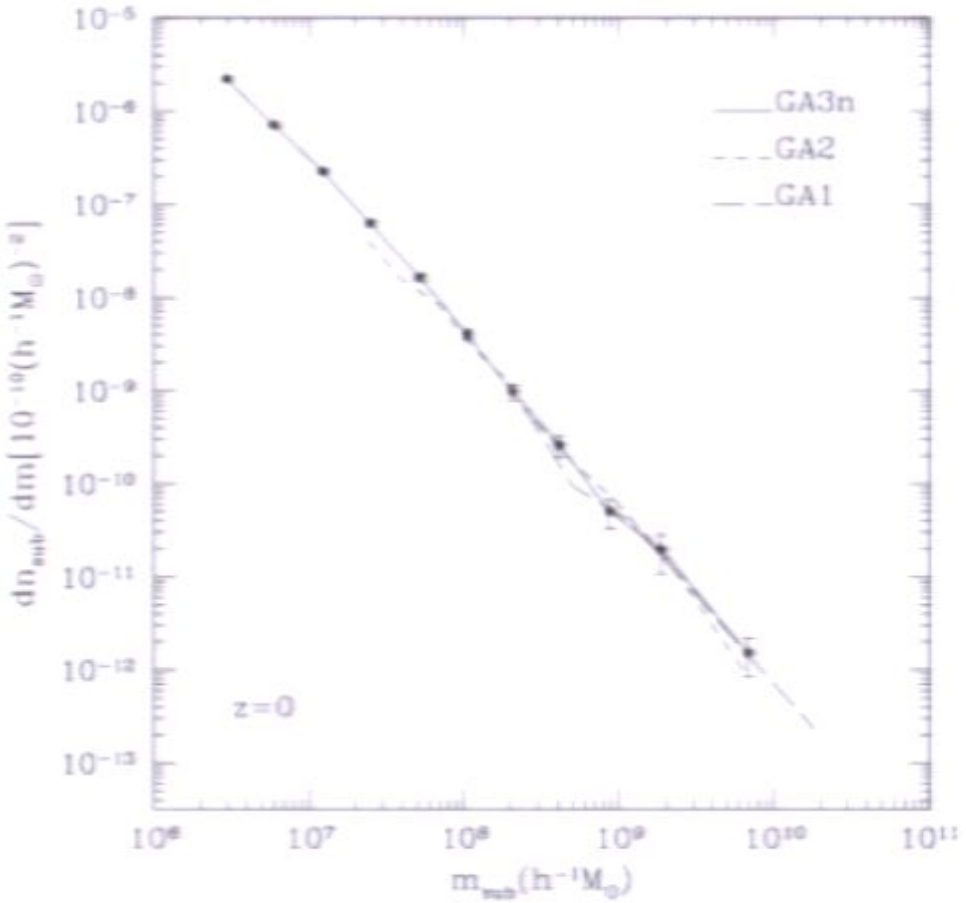

subhalo mass function from Gao et al. 2004

12 orders of magnitude to the bottom of the CDM hierarchy

$$\frac{dN}{d\ln f} = Af^{-\alpha}$$

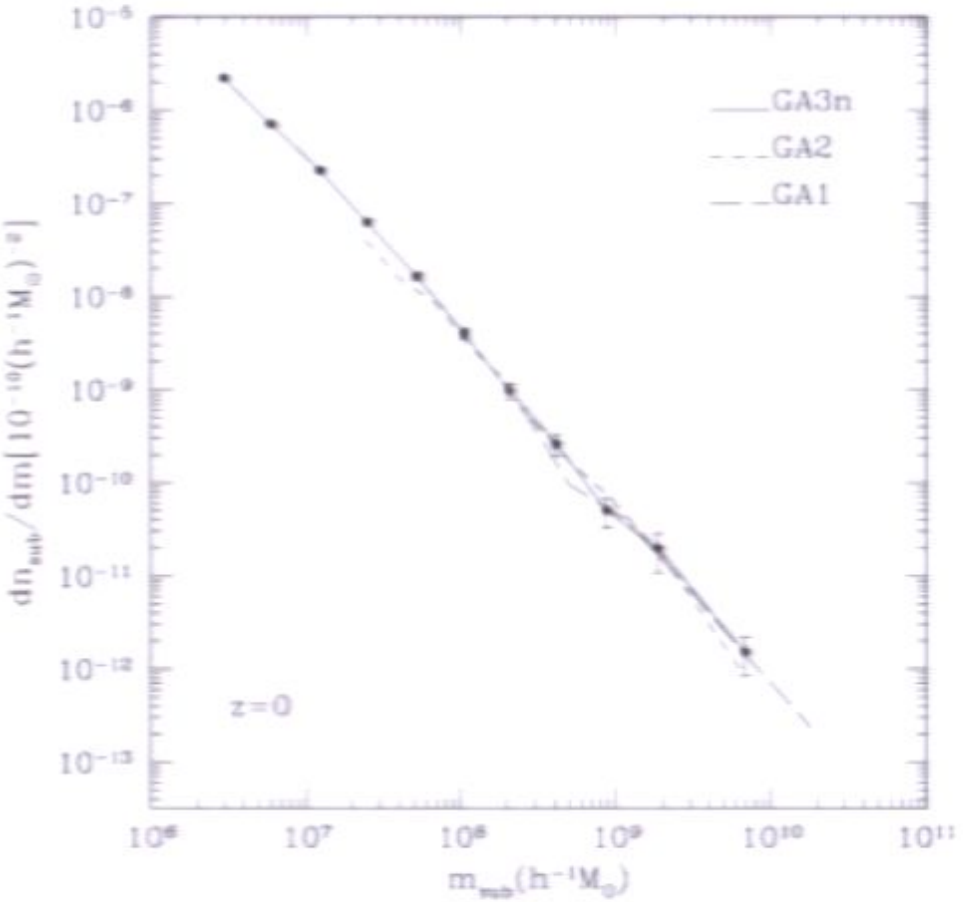

subhalo mass function from Gao et al. 2004

12 orders of magnitude to the bottom of the CDM hierarchy

$$\frac{dN}{d\ln f} = Af^{-\alpha}$$

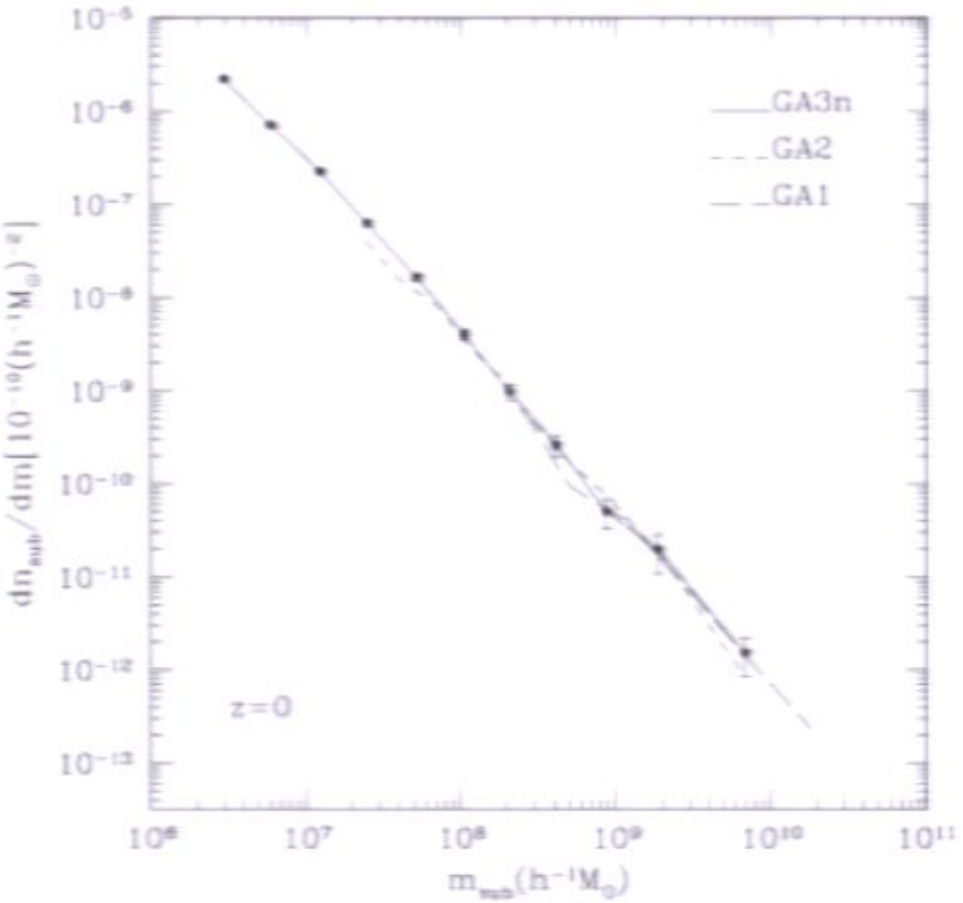

subhalo mass function from Gao et al. 2004

12 orders of magnitude to the bottom of the CDM hierarchy

$$\frac{dN}{d\ln f} = Af^{-\alpha}$$

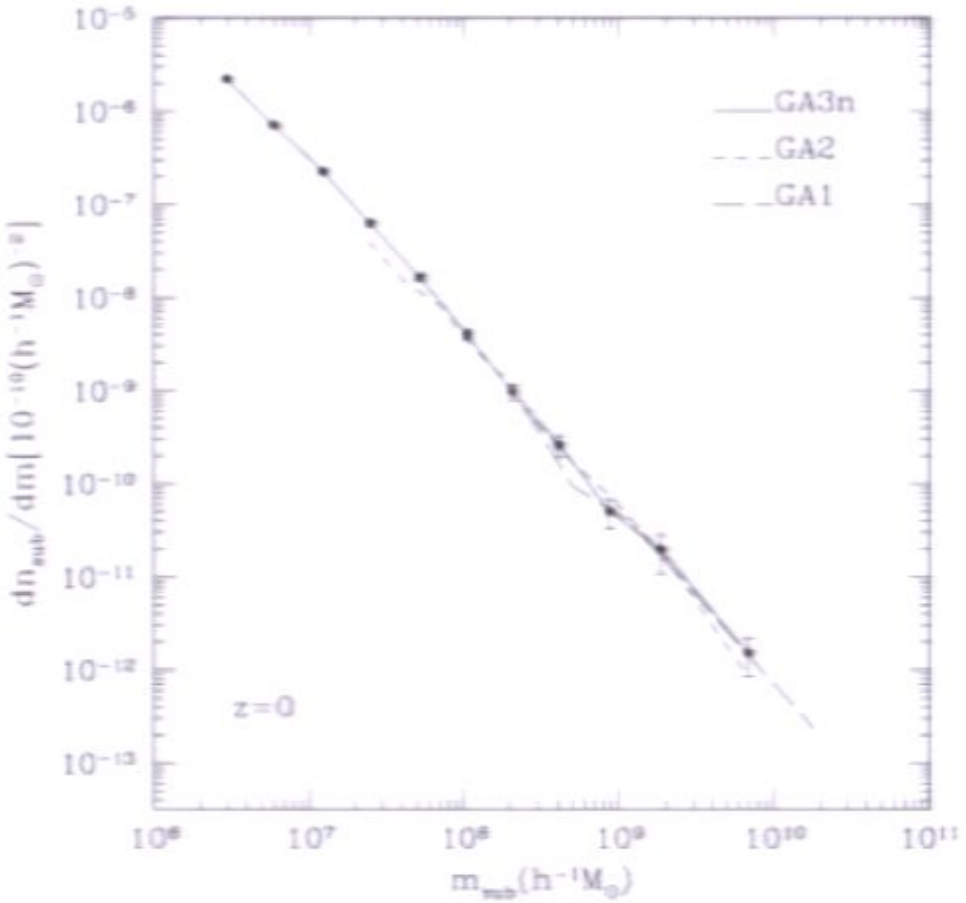

subhalo mass function from Gao et al. 2004

12 orders of magnitude to the bottom of the CDM hierarchy

$$\frac{dN}{d\ln f} = Af^{-\alpha}$$

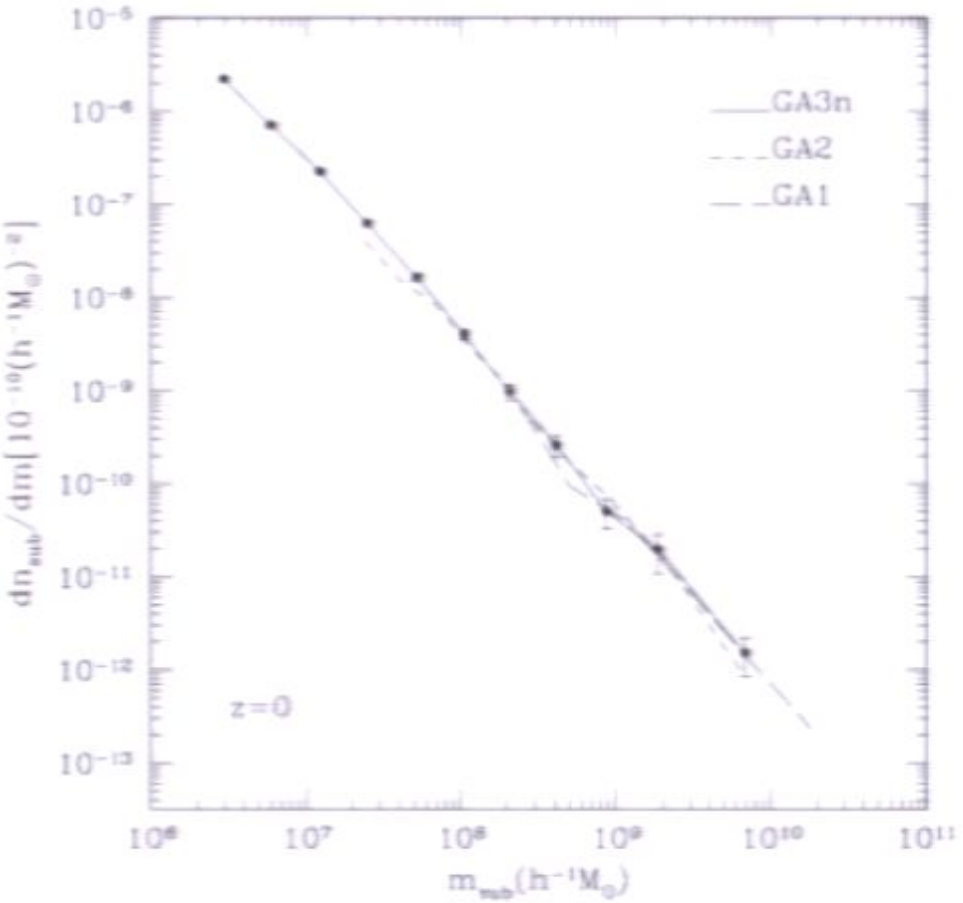

subhalo mass function from Gao et al. 2004

12 orders of magnitude to the bottom of the CDM hierarchy

$$\frac{dN}{d\ln f} = Af^{-\alpha}$$

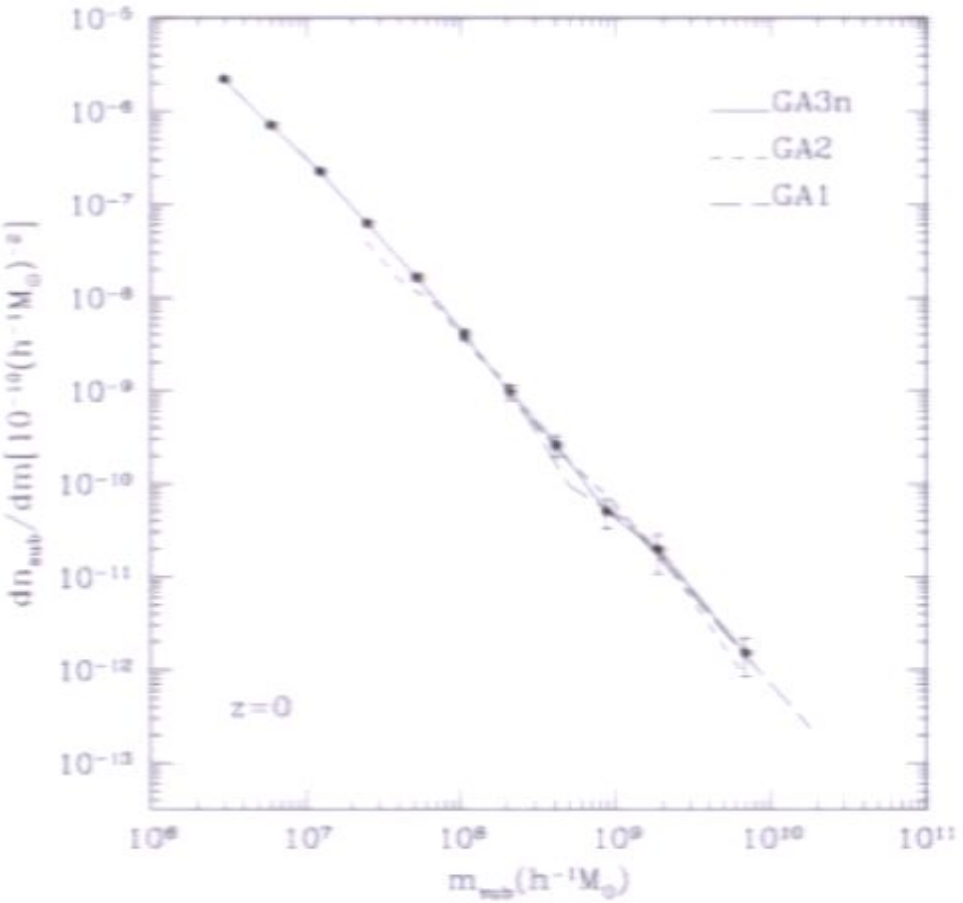

subhalo mass function from Gao et al. 2004

12 orders of magnitude to the bottom of the CDM hierarchy

$$\frac{dN}{d\ln f} = Af^{-\alpha}$$

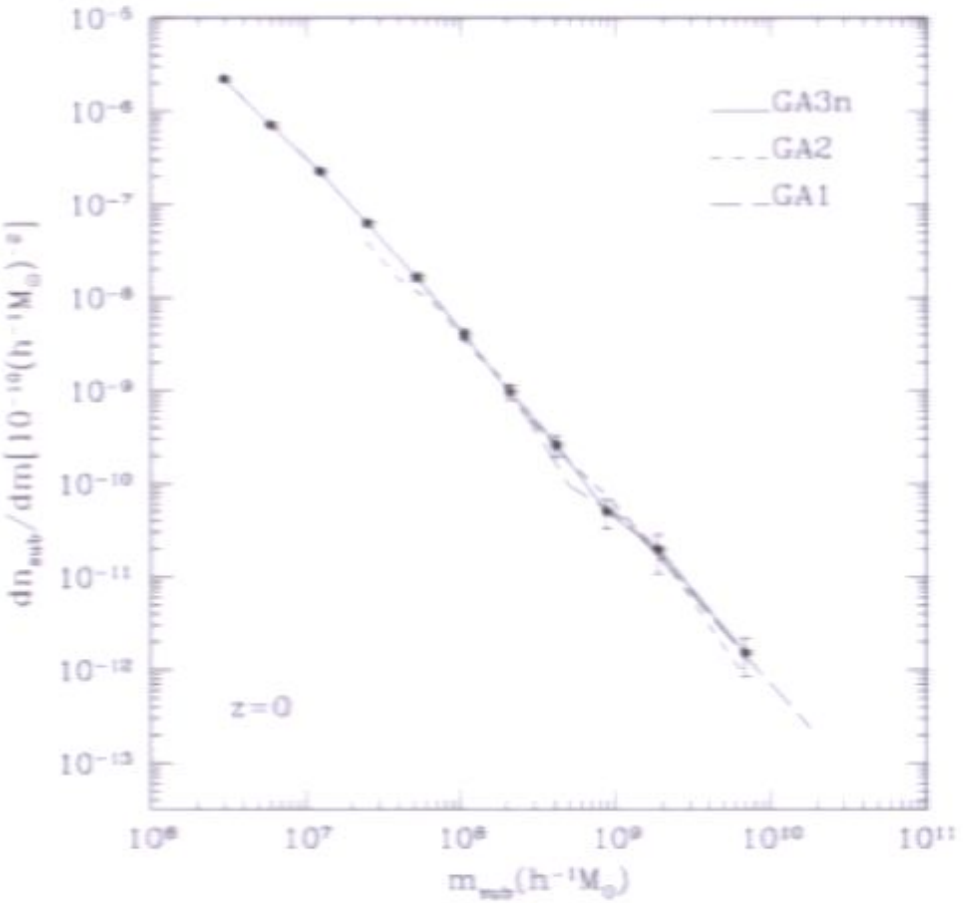

subhalo mass function from Gao et al. 2004

12 orders of magnitude to the bottom of the CDM hierarchy

$$\frac{dN}{d\ln f} = Af^{-\alpha}$$

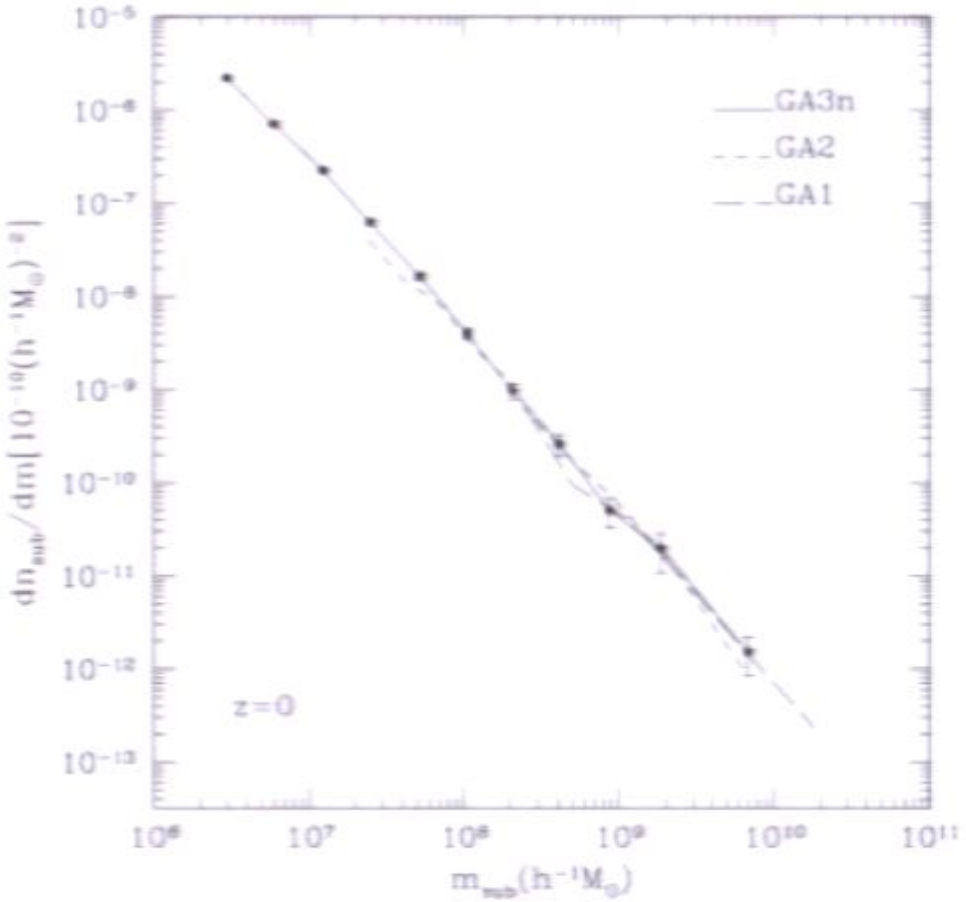

subhalo mass function from Gao et al. 2004

12 orders of magnitude to the bottom of the CDM hierarchy

$$\frac{dN}{d\ln f} = Af^{-\alpha}$$

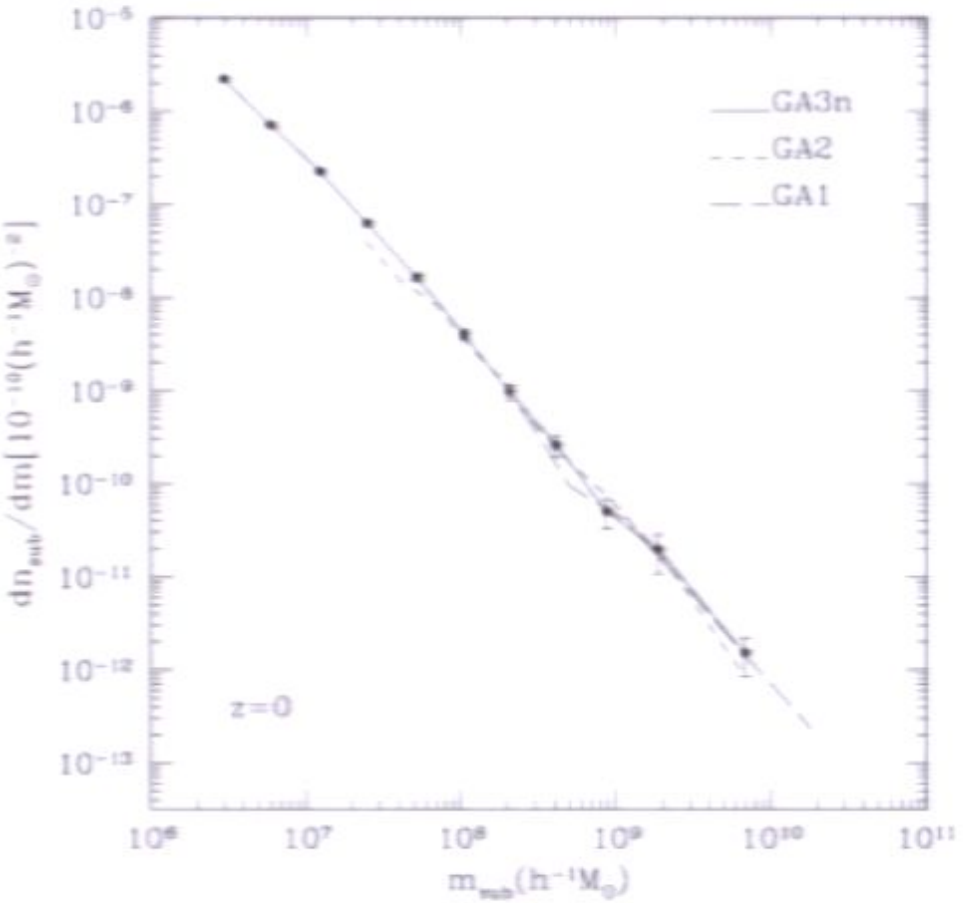

subhalo mass function from Gao et al. 2004

12 orders of magnitude to the bottom of the CDM hierarchy

$$\frac{dN}{d\ln f} = Af^{-\alpha}$$

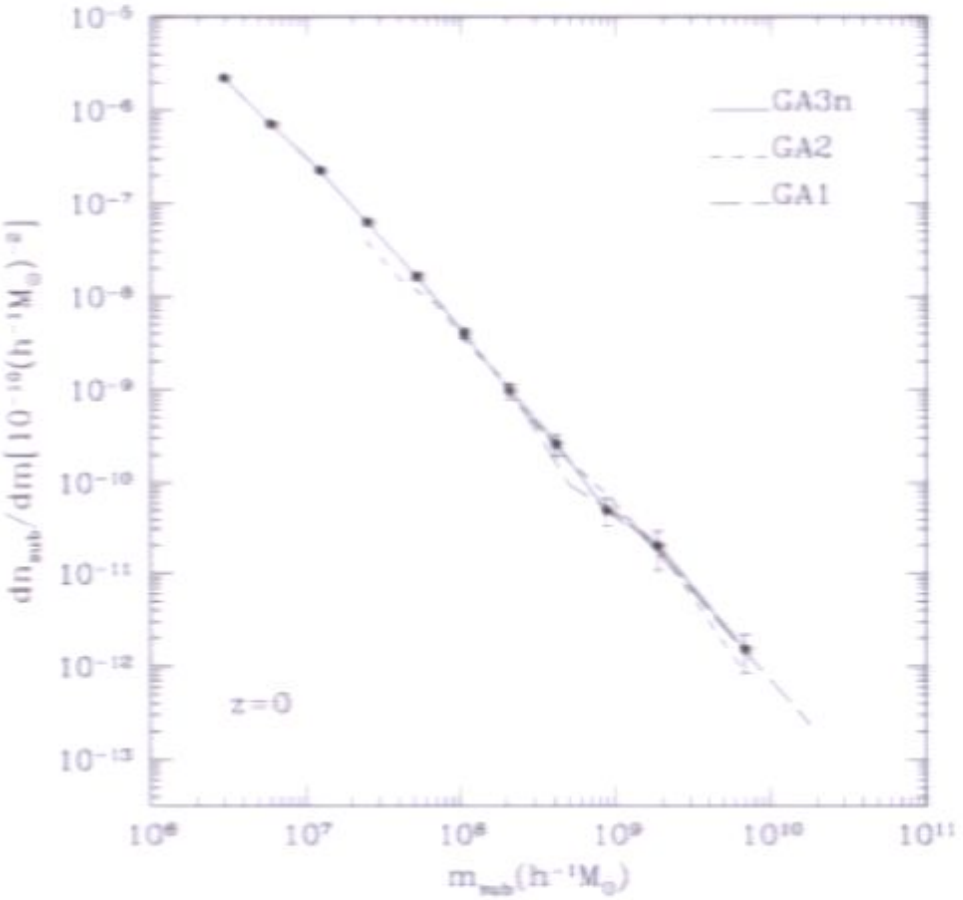

subhalo mass function from Gao et al. 2004

12 orders of magnitude to the bottom of the CDM hierarchy

$$\frac{dN}{d\ln f} = Af^{-\alpha}$$

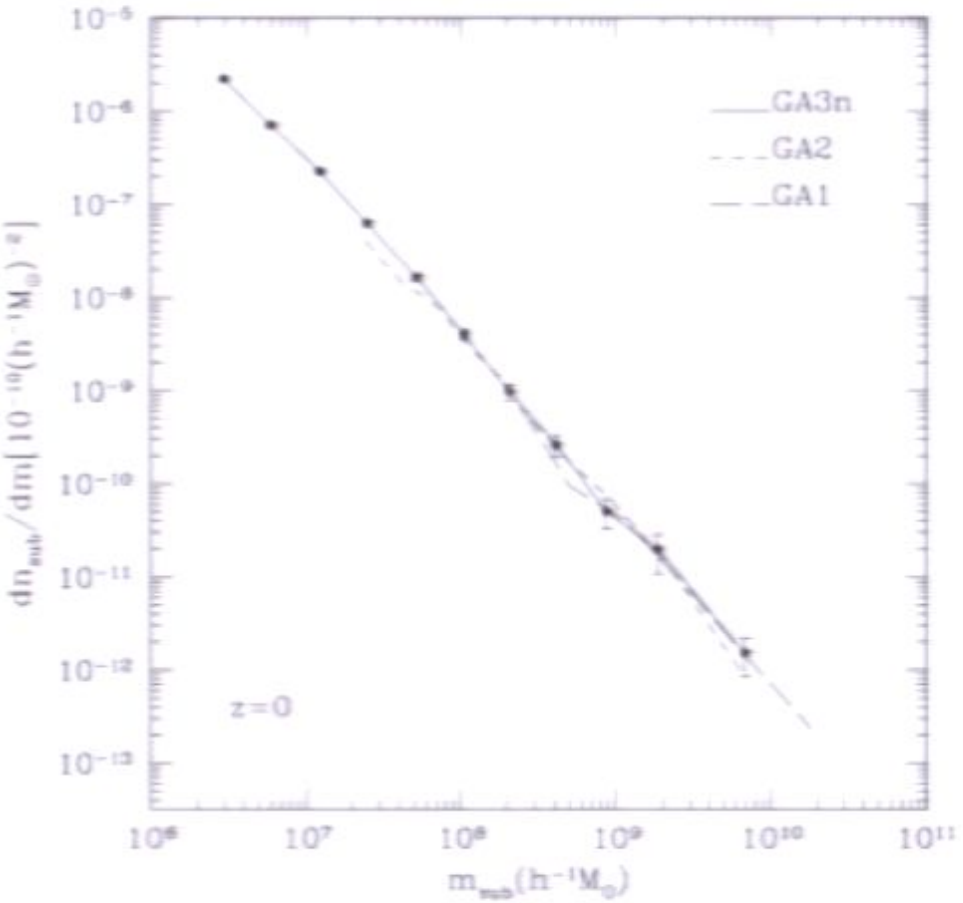

subhalo mass function from Gao et al. 2004

12 orders of magnitude to the bottom of the CDM hierarchy

$$\frac{dN}{d\ln f} = Af^{-\alpha}$$

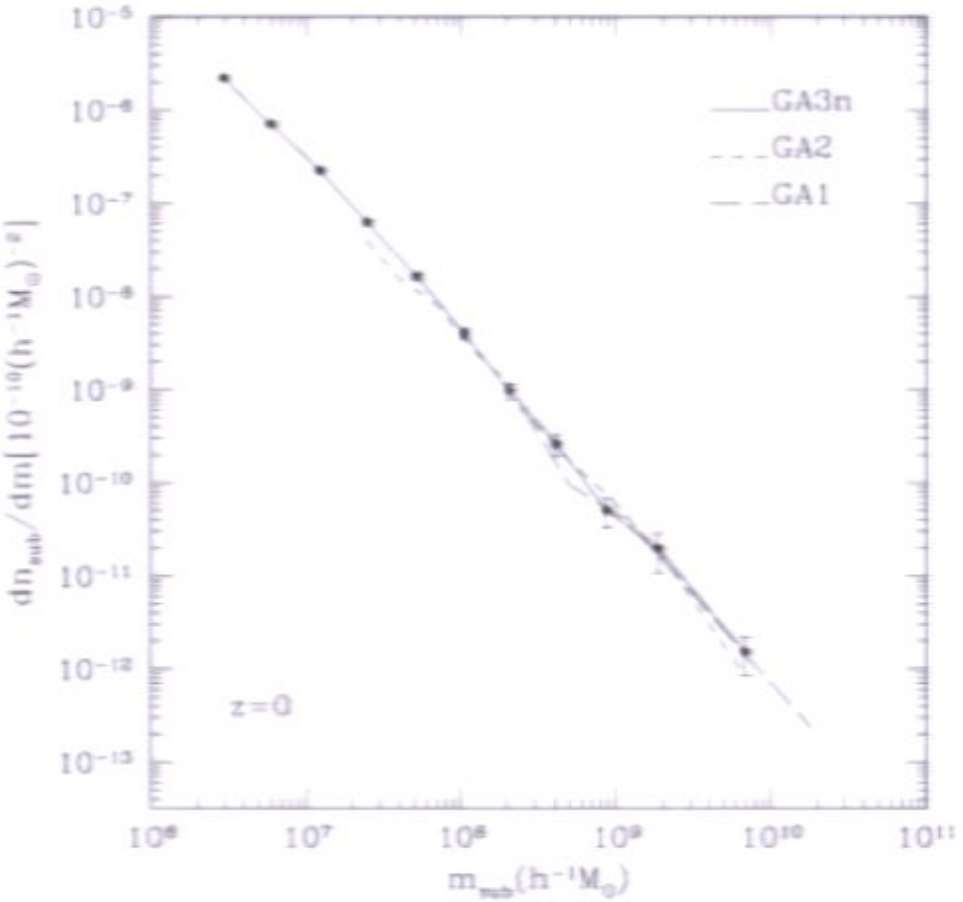

subhalo mass function from Gao et al. 2004

Challenges, II

Pathological behavior of the CDM power spectrum at very small scales

For the first objects in the CDM hierarchy structures form over a wide range of scales nearly simultaneously.

Clustering no longer hierarchical and a significant dynamic range in simulations is difficult to achieve.

Other schemes to understand structure formation (e.g., perturbation theory) also have problems

Challenges, II

Pathological behavior of the CDM power spectrum at very small scales

For the first objects in the CDM hierarchy structures form over a wide range of scales nearly simultaneously.

Clustering no longer hierarchical and a significant dynamic range in simulations is difficult to achieve.

Other schemes to understand structure formation (e.g., perturbation theory) also have problems

Challenges, II

Pathological behavior of the CDM power spectrum at very small scales

For the first objects in the CDM hierarchy structures form over a wide range of scales nearly simultaneously.

Clustering no longer hierarchical and a significant dynamic range in simulations is difficult to achieve.

Other schemes to understand structure formation (e.g., perturbation theory) also have problems

Challenges, II

Pathological behavior of the CDM power spectrum at very small scales

For the first objects in the CDM hierarchy structures form over a wide range of scales nearly simultaneously.

Clustering no longer hierarchical and a significant dynamic range in simulations is difficult to achieve.

Other schemes to understand structure formation (e.g., perturbation theory) also have problems

Challenges, II

Pathological behavior of the CDM power spectrum at very small scales

For the first objects in the CDM hierarchy structures form over a wide range of scales nearly simultaneously.

Clustering no longer hierarchical and a significant dynamic range in simulations is difficult to achieve.

Other schemes to understand structure formation (e.g., perturbation theory) also have problems

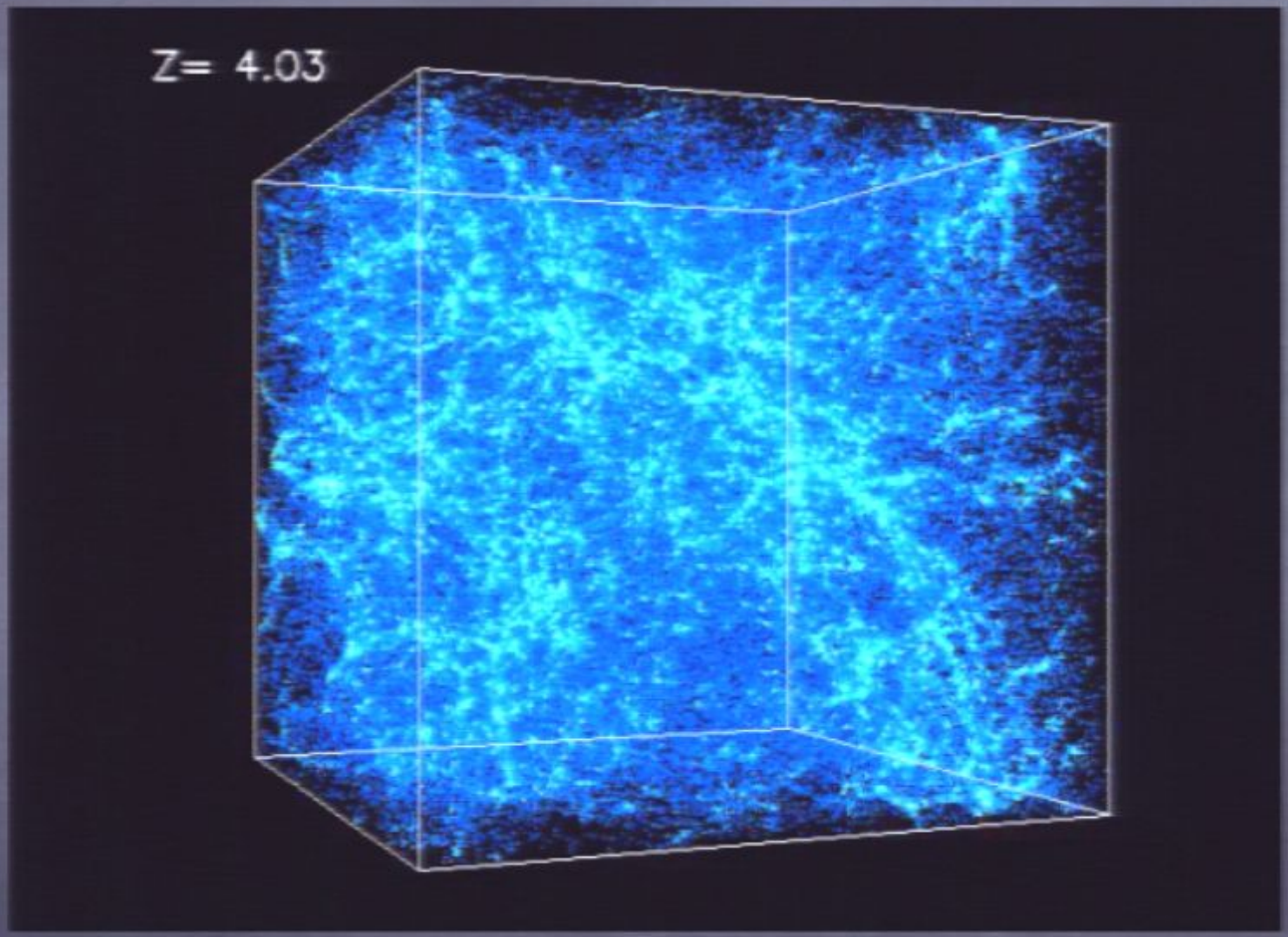

from University of Chicago
Center for Cosmological Physics website

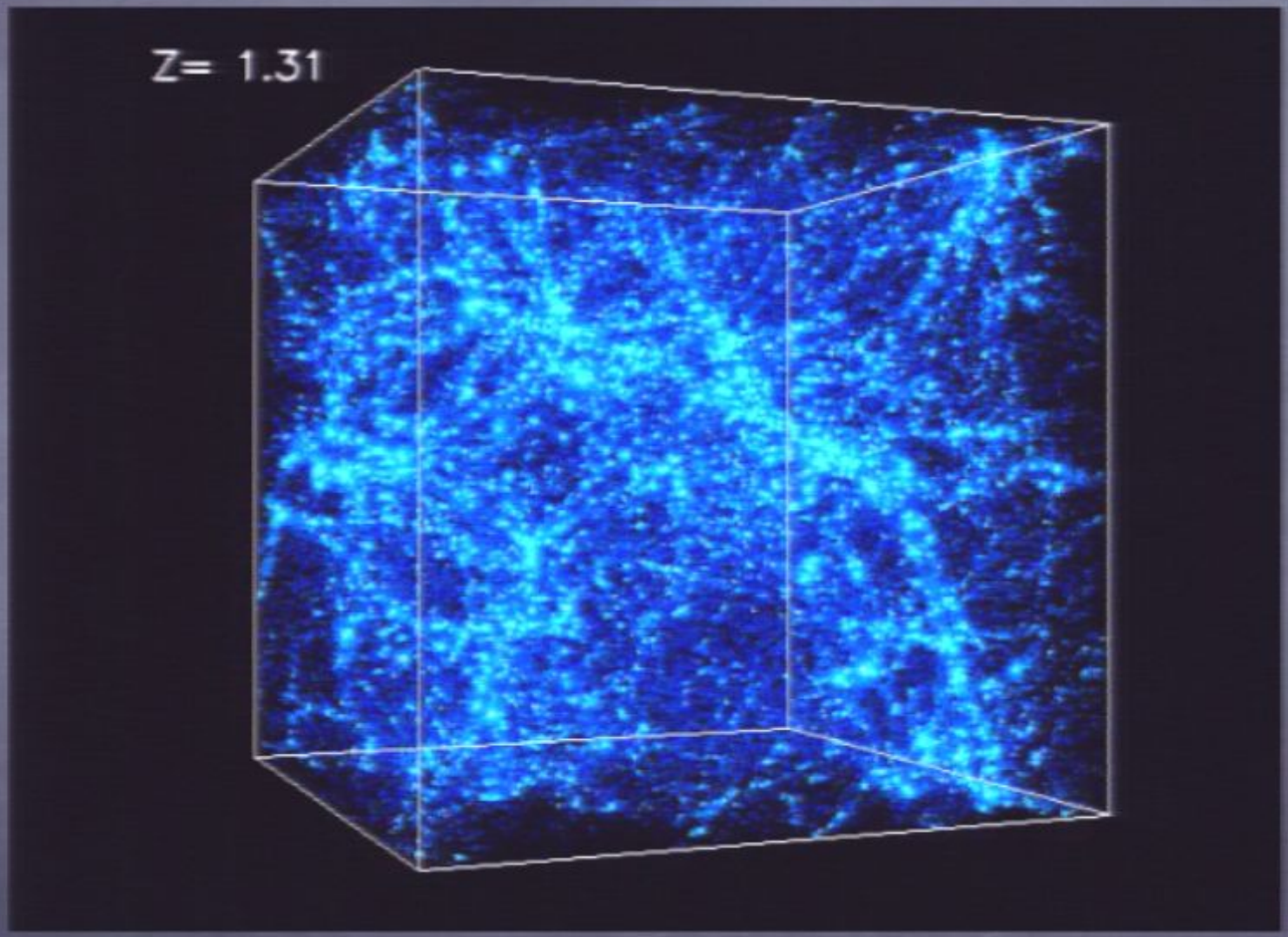

from University of Chicago
Center for Cosmological Physics website

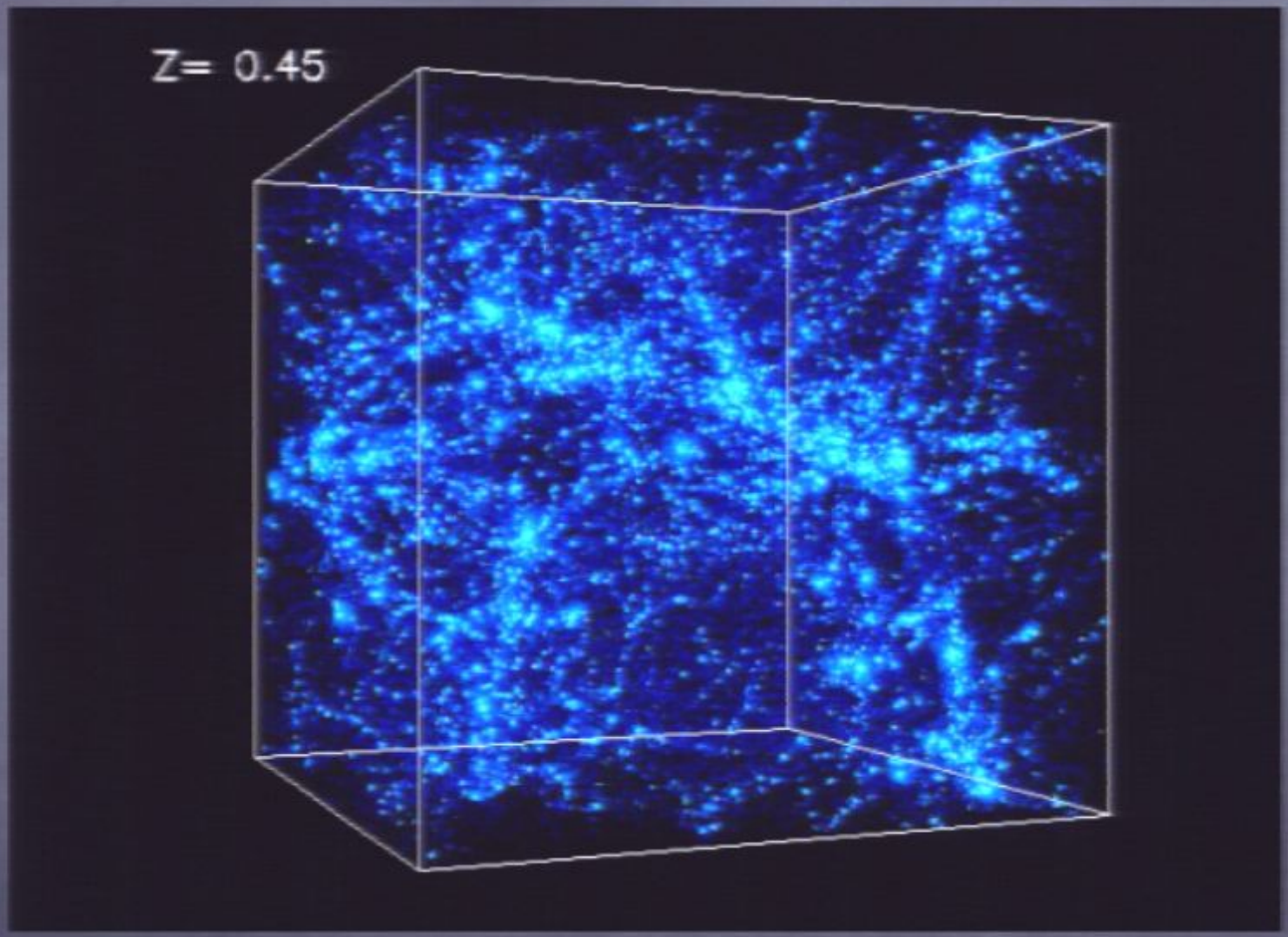

from University of Chicago
Center for Cosmological Physics website

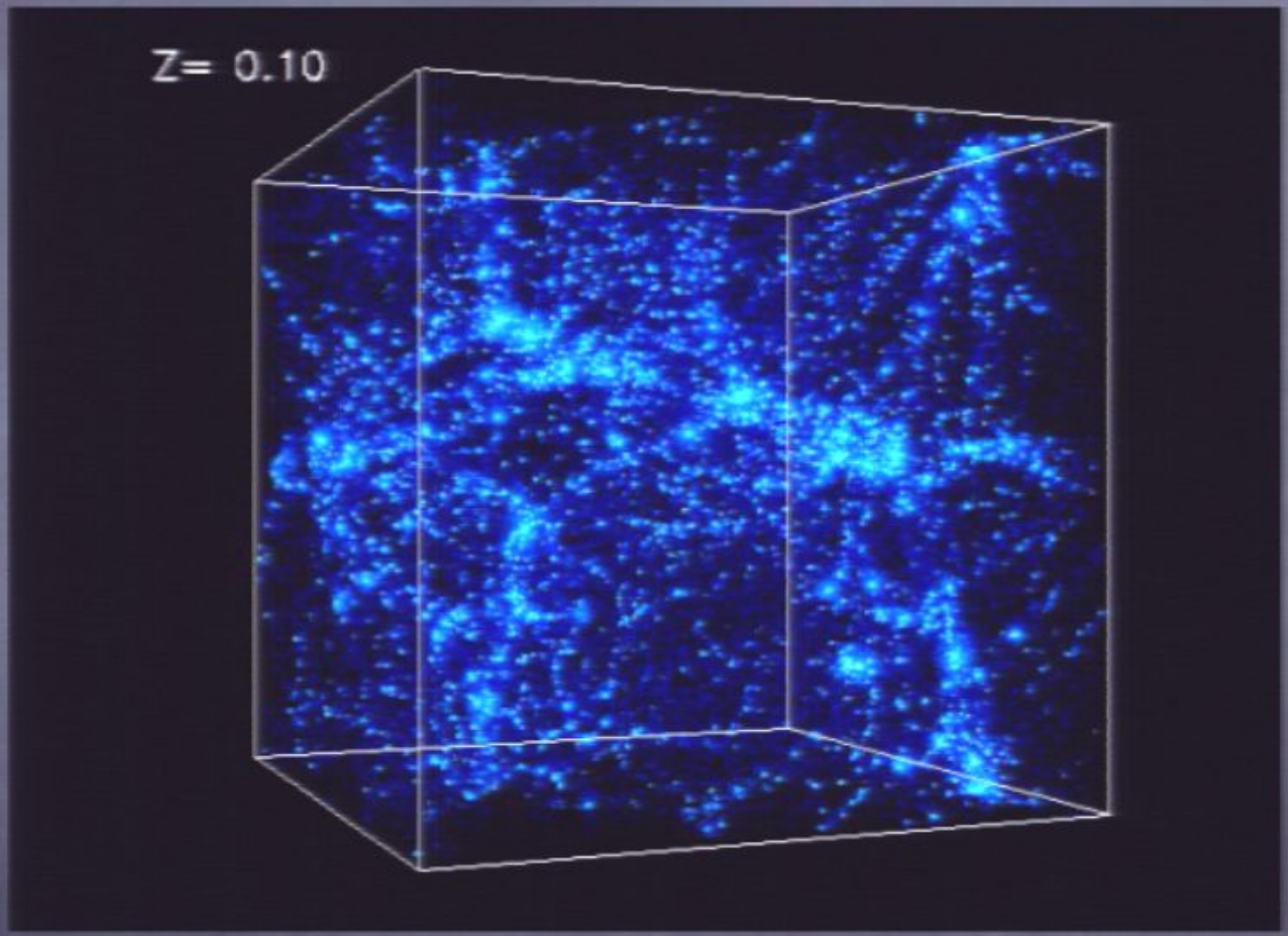

from University of Chicago
Center for Cosmological Physics website

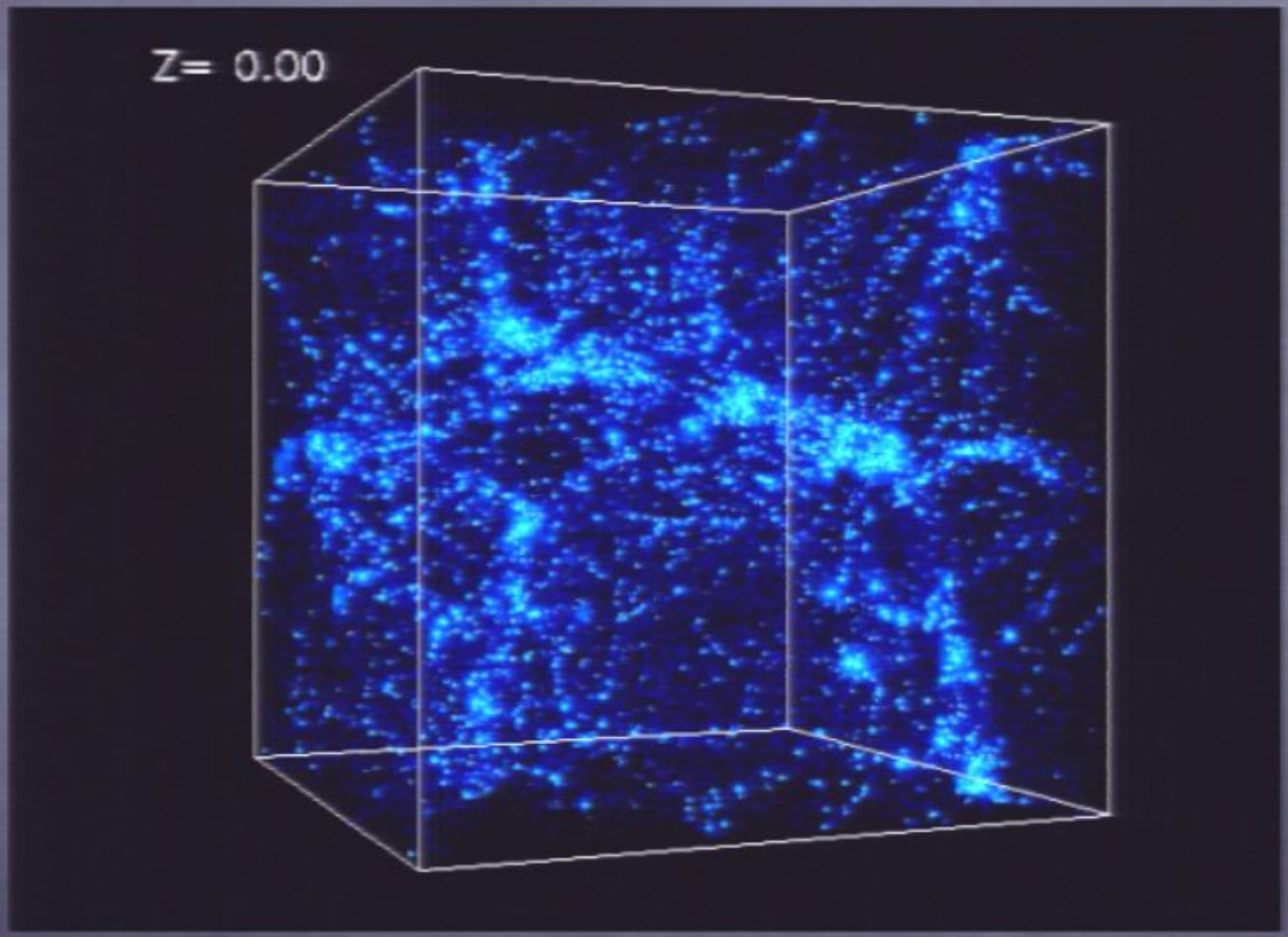

from University of Chicago
Center for Cosmological Physics website

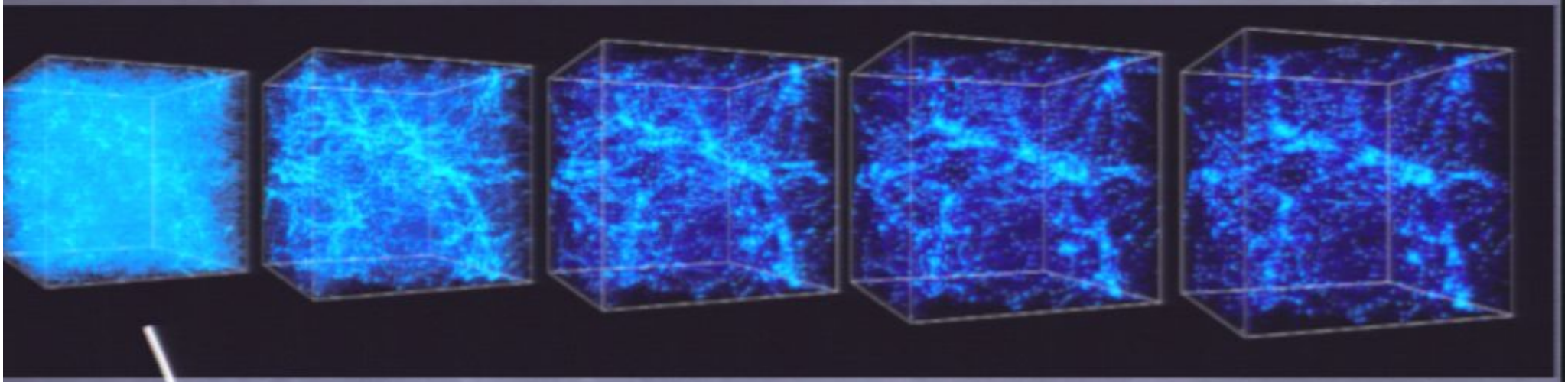

ICs:
mass fluctuation
associated with scale

$$\lambda \sim \frac{2\pi}{k}$$

power per logarithmic bin in k

$$k^3 \left(\frac{\delta\rho_k}{\rho}\right)^2 \equiv k^3 P(k)$$

$$\equiv \Delta^2(k)$$

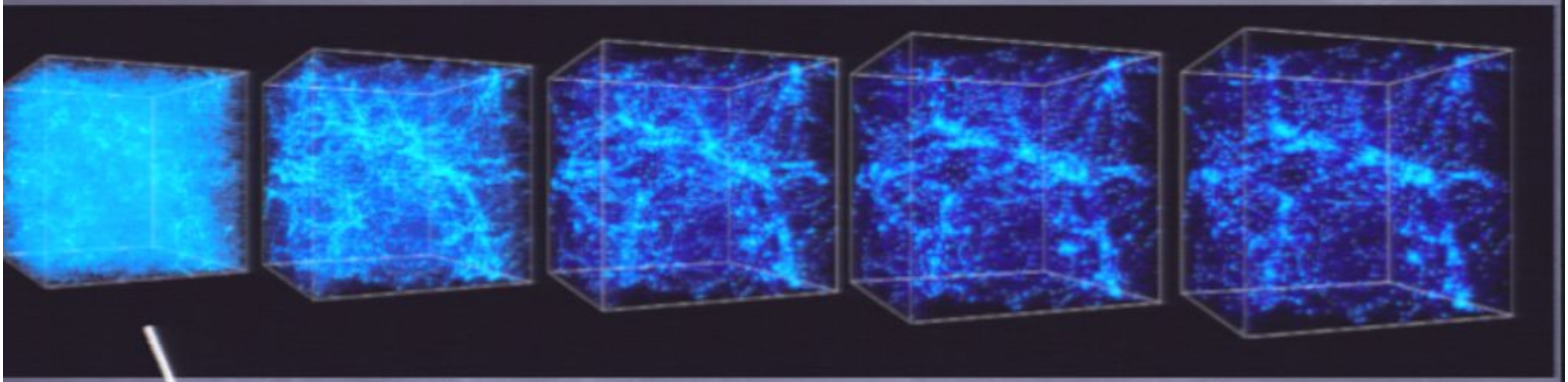

ICs:
mass fluctuation
associated with scale

$$\lambda \sim \frac{2\pi}{k}$$

power per logarithmic bin in k

$$k^3 \left(\frac{\delta \rho_k}{\rho} \right)^2 \equiv k^3 P(k)$$

$$\equiv \Delta^2(k)$$

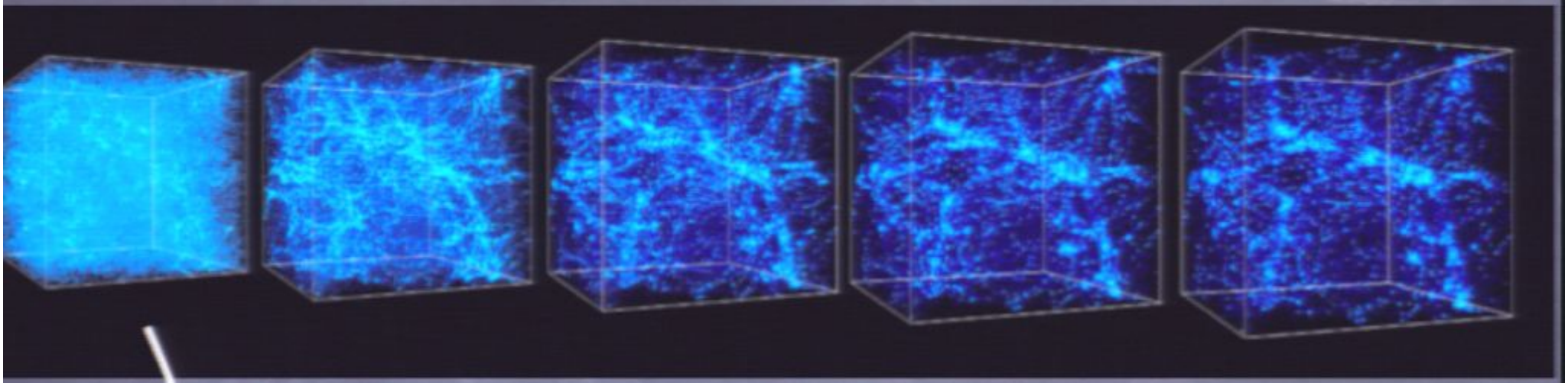

ICs:
mass fluctuation
associated with scale

$$\lambda \sim \frac{2\pi}{k}$$

power per logarithmic bin in k

$$k^3 \left(\frac{\delta\rho_k}{\rho}\right)^2 \equiv k^3 P(k)$$

$$\equiv \Delta^2(k)$$

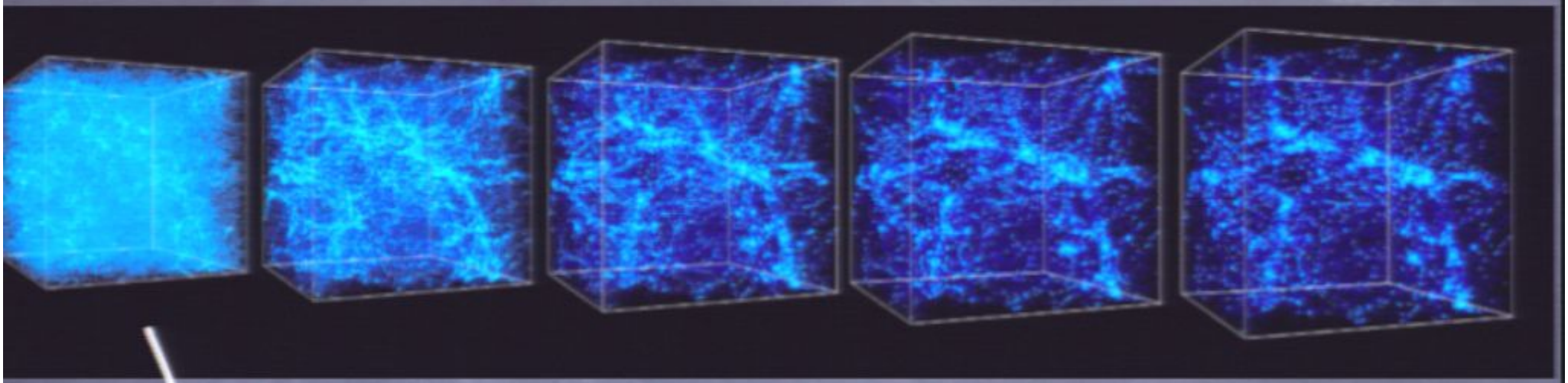

ICs:
mass fluctuation
associated with scale

$$\lambda \sim \frac{2\pi}{k}$$

power per logarithmic bin in k

$$k^3 \left(\frac{\delta \rho_k}{\rho} \right)^2 \equiv k^3 P(k)$$

$$\equiv \Delta^2(k)$$

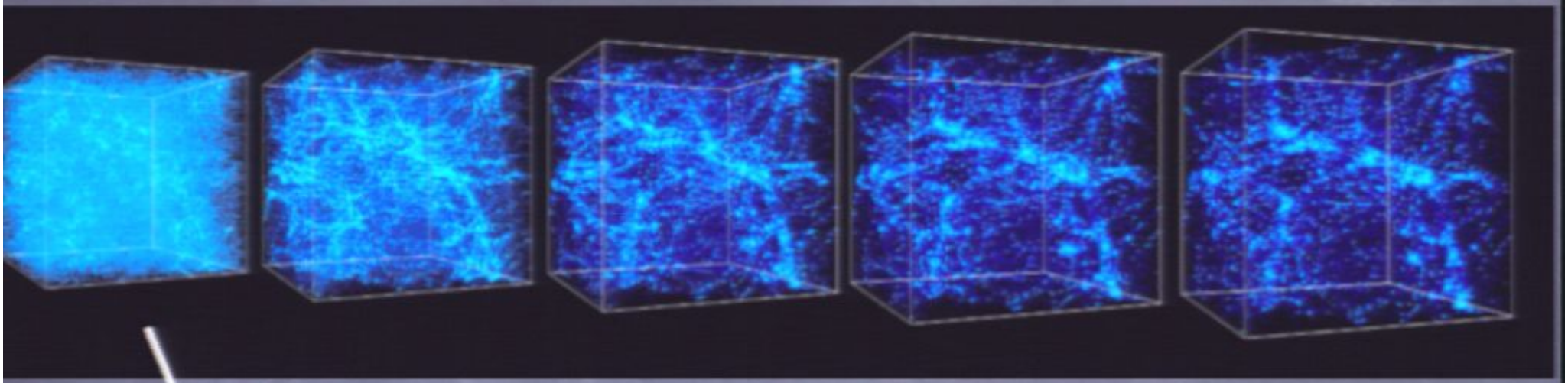

ICs:
mass fluctuation
associated with scale

$$\lambda \sim \frac{2\pi}{k}$$

power per logarithmic bin in k

$$k^3 \left(\frac{\delta \rho_k}{\rho} \right)^2 \equiv k^3 P(k)$$

$$\equiv \Delta^2(k)$$

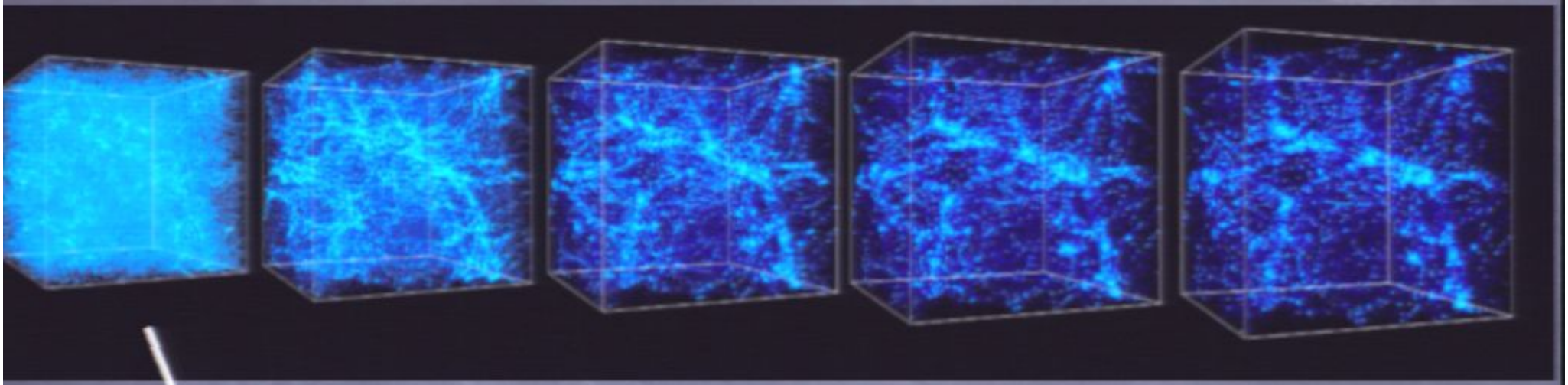

ICs:
mass fluctuation
associated with scale

$$\lambda \sim \frac{2\pi}{k}$$

power per logarithmic bin in k

$$k^3 \left(\frac{\delta\rho_k}{\rho}\right)^2 \equiv k^3 P(k)$$

$$\equiv \Delta^2(k)$$

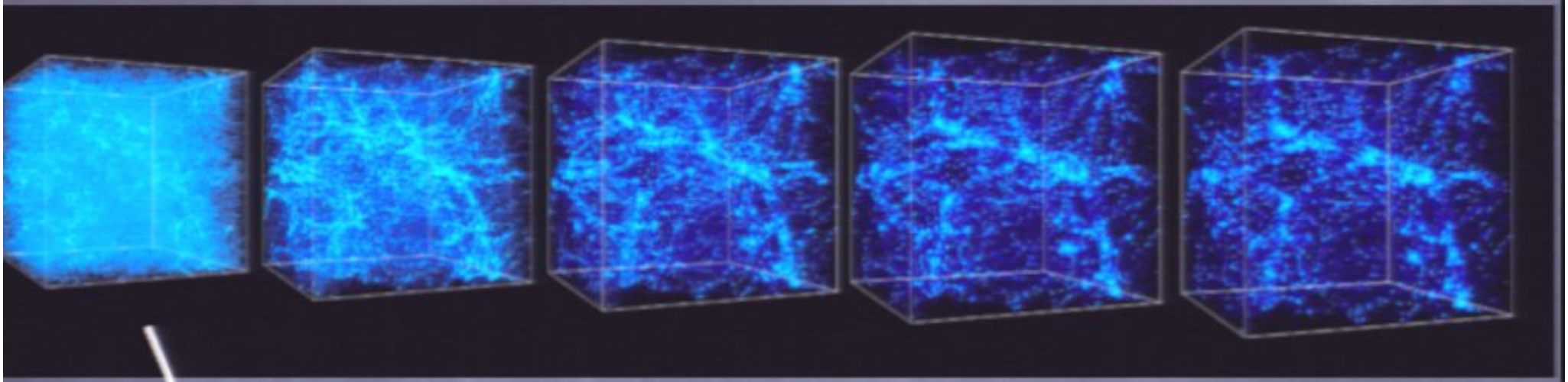

ICs:
mass fluctuation
associated with scale

$$\lambda \sim \frac{2\pi}{k}$$

power per logarithmic bin in k

$$k^3 \left(\frac{\delta \rho_k}{\rho} \right)^2 \equiv k^3 P(k)$$

$$\equiv \Delta^2(k)$$

$$\begin{aligned}
\Delta^2(k) &= k^3 P(k) \\
&= k^3 P_{\rm primordial}(k) T^2(k) \\
&\sim k^{n_{\rm eff}+3} \qquad \text{(over small range in k)} \\
&\sim \text{const.} \quad (i.e., n_{\rm eff} \simeq -3) \quad \text{for } k \to \infty
\end{aligned}$$

$$\begin{aligned}
\Delta^2(k) &= k^3 P(k) \\
&= k^3 P_{\rm primordial}(k) T^2(k) \\
&\sim k^{n_{\rm eff}+3} \qquad \text{(over small range in k)} \\
&\sim \text{const.} \quad (i.e., n_{\rm eff} \simeq -3) \quad \text{for } k \to \infty
\end{aligned}$$

$$\begin{aligned}
\Delta^2(k) &= k^3 P(k) \\
&= k^3 P_{\rm primordial}(k) T^2(k) \\
&\sim k^{n_{\rm eff}+3} \qquad \text{(over small range in k)} \\
&\sim \text{const.} \quad (i.e., n_{\rm eff} \simeq -3) \quad \text{for } k \to \infty
\end{aligned}$$

$$\begin{aligned}
\Delta^2(k) &= k^3 P(k) \\
&= k^3 P_{\rm primordial}(k) T^2(k) \\
&\sim k^{n_{\rm eff}+3} \qquad \text{(over small range in k)} \\
&\sim \text{const.} \quad (i.e., n_{\rm eff} \simeq -3) \quad \text{for } k \to \infty
\end{aligned}$$

Moore et al. 1999

cluster
n = -1.8

galaxy
n = -2.2

simulations with scale-free power-spectra $P(k) \propto k^n$

$n = -1$

$n = -2.5$

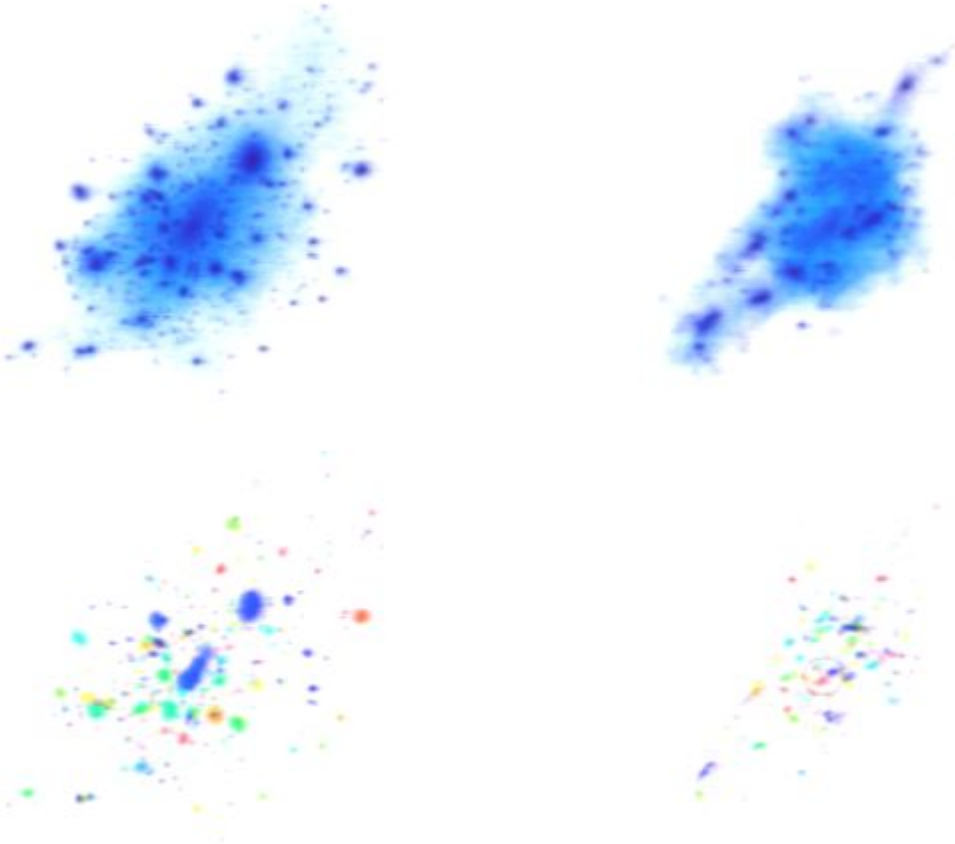

from Elahi, LMW, & Thacker, 2009

Moore et al. 1999

cluster
n = -1.8

galaxy
n = -2.2

simulations with scale-free power-spectra $P(k) \propto k^n$

$n = -1$

$n = -2.5$

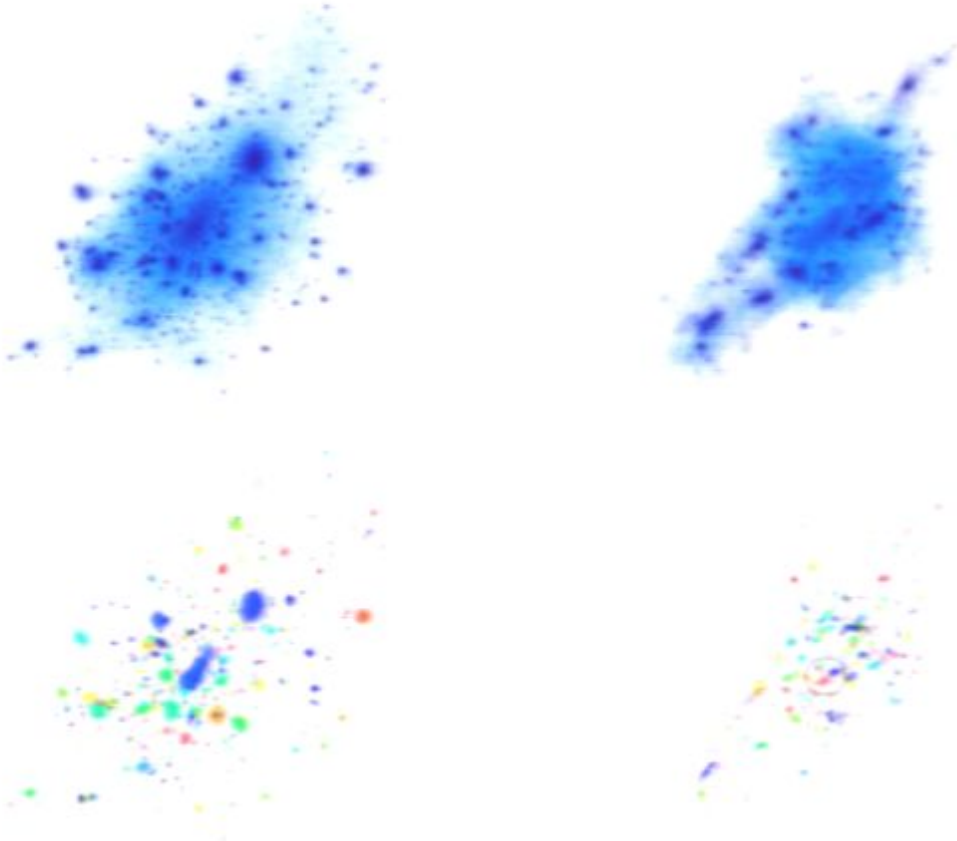

from Elahi, LMW, & Thacker, 2009

Moore et al. 1999

cluster
n = -1.8

galaxy
n = -2.2

simulations with scale-free power-spectra $P(k) \propto k^n$

$n = -1$

$n = -2.5$

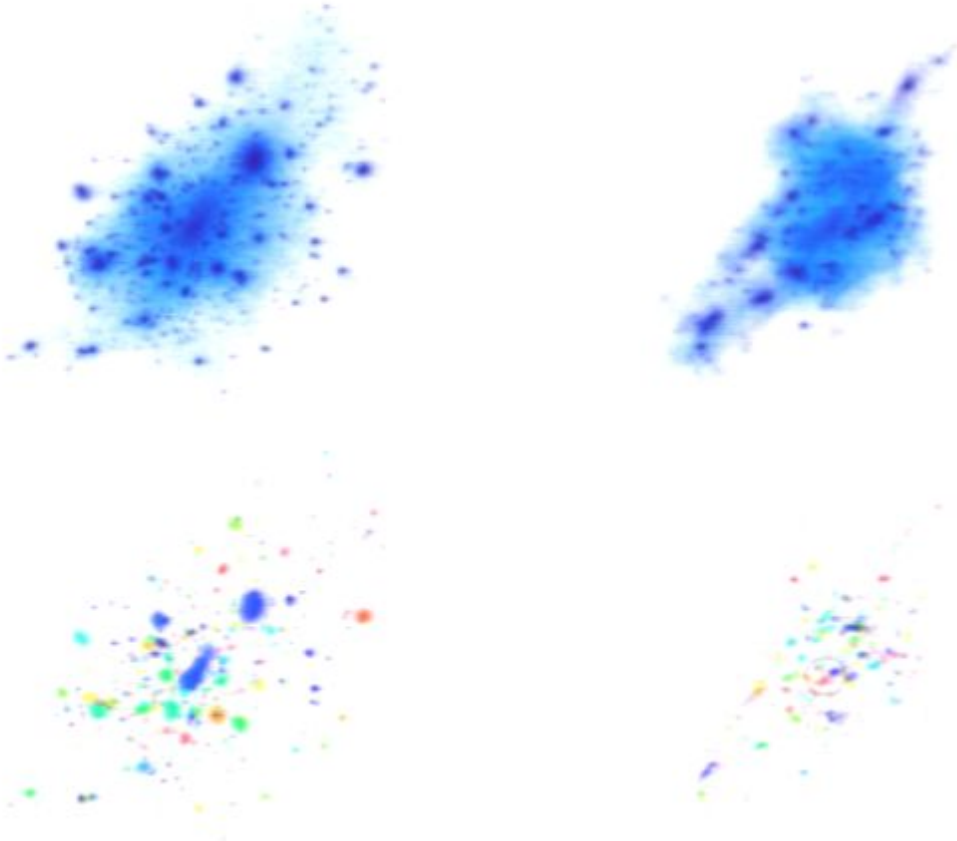

from Elahi, LMW, & Thacker, 2009

Moore et al. 1999

cluster
n = -1.8

galaxy
n = -2.2

simulations with scale-free power-spectra $P(k) \propto k^n$

$n = -1$

$n = -2.5$

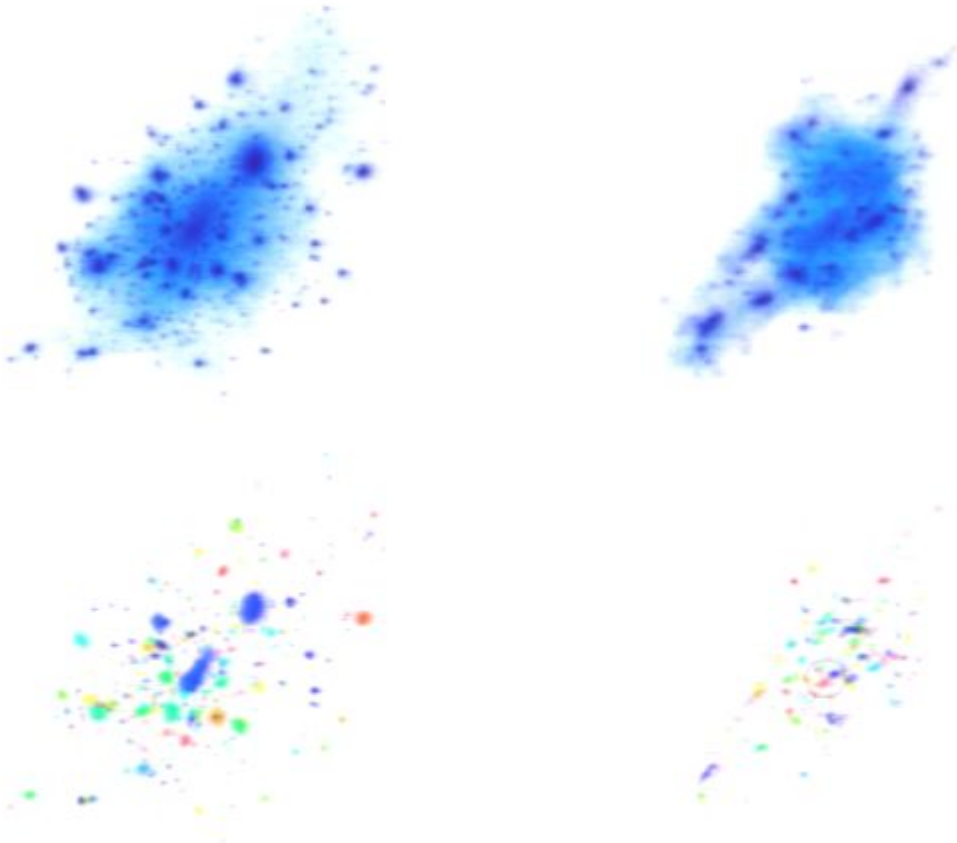

from Elahi, LMW, & Thacker, 2009

Moore et al. 1999

cluster
n = -1.8

galaxy
n = -2.2

simulations with scale-free power-spectra $P(k) \propto k^n$

$n = -1$

$n = -2.5$

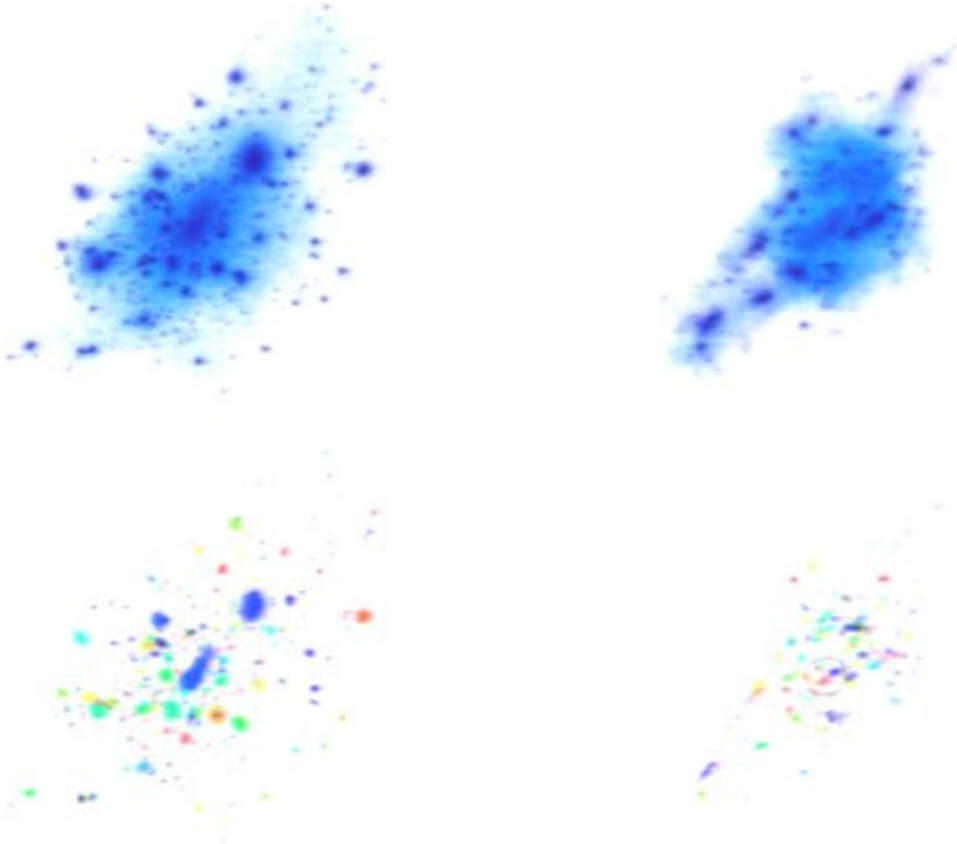

from Elahi, LMW, & Thacker, 2009

Moore et al. 1999

cluster
n = -1.8

galaxy
n = -2.2

simulations with scale-free power-spectra $P(k) \propto k^n$

$n = -1$

$n = -2.5$

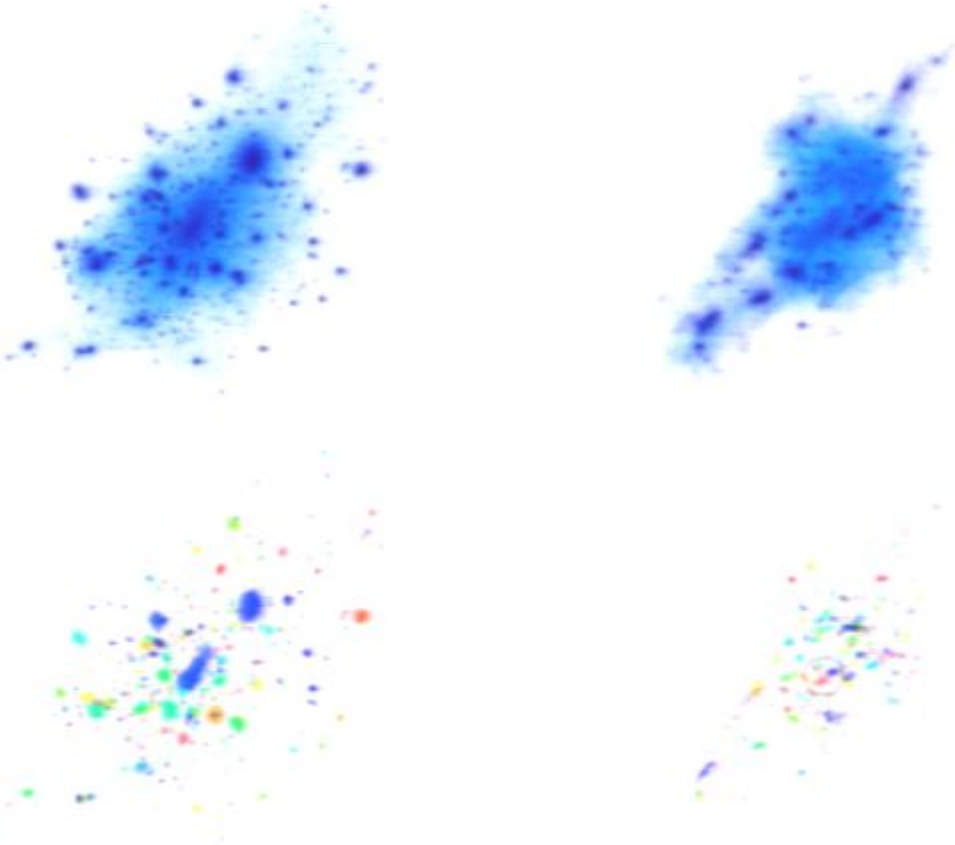

from Elahi, LMW, & Thacker, 2009

Moore et al. 1999

cluster
n = -1.8

galaxy
n = -2.2

simulations with scale-free power-spectra $P(k) \propto k^n$

$n = -1$

$n = -2.5$

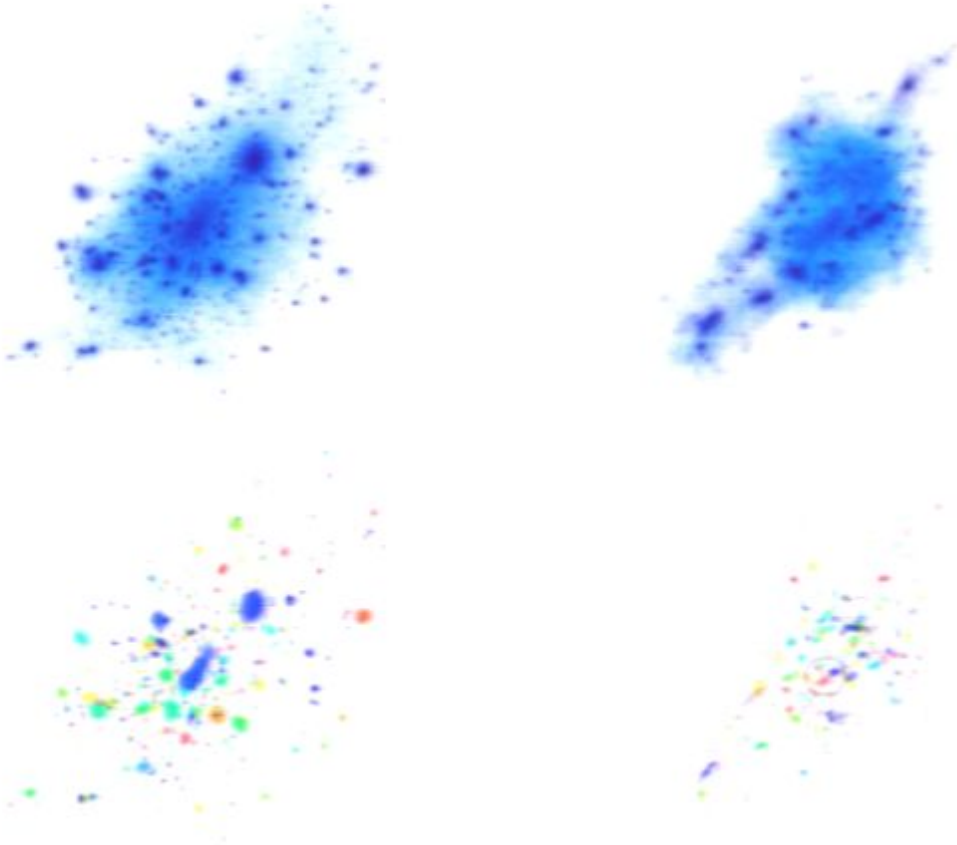

from Elahi, LMW, & Thacker, 2009

Moore et al. 1999

cluster
n = -1.8

galaxy
n = -2.2

simulations with scale-free power-spectra $P(k) \propto k^n$

$n = -1$

$n = -2.5$

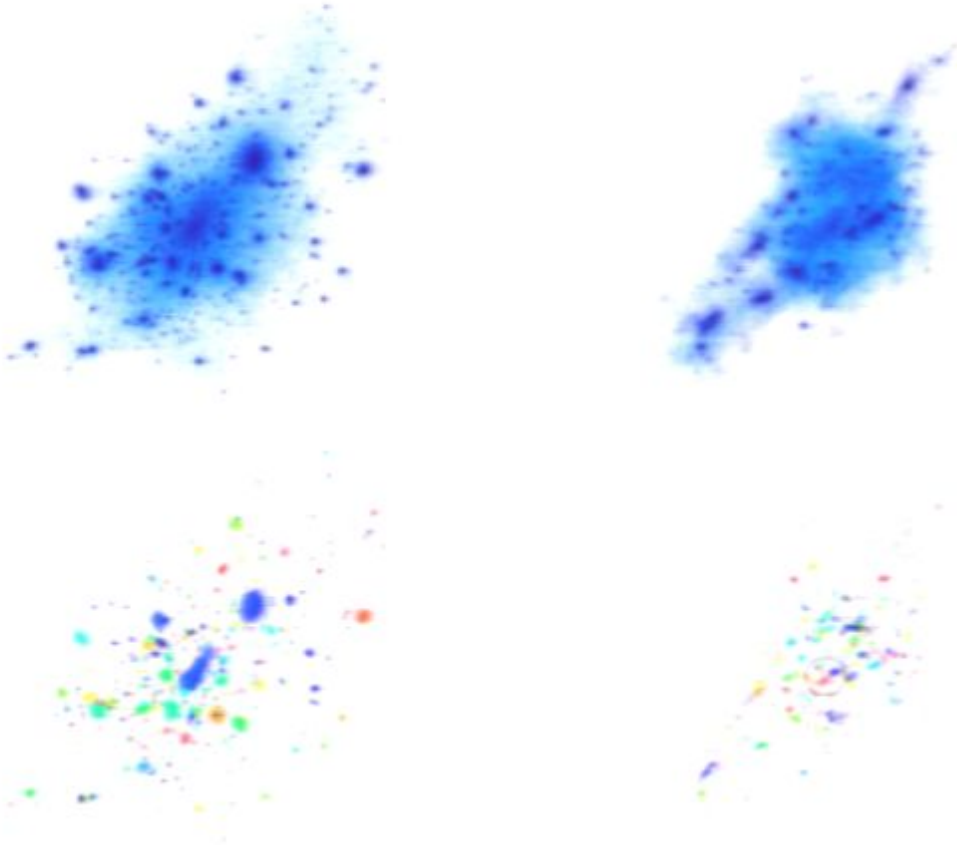

from Elahi, LMW, & Thacker, 2009

Moore et al. 1999

cluster
n = -1.8

galaxy
n = -2.2

simulations with scale-free power-spectra $P(k) \propto k^n$

$n = -1$

$n = -2.5$

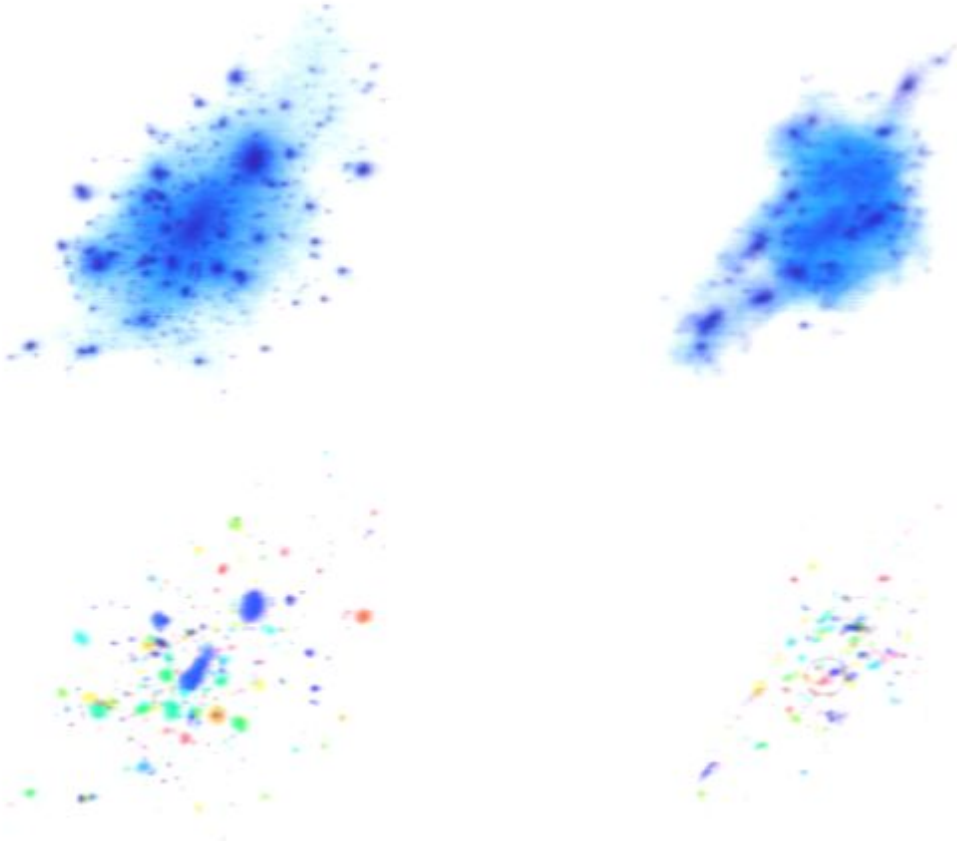

from Elahi, LMW, & Thacker, 2009

Moore et al. 1999

cluster
n = -1.8

galaxy
n = -2.2

simulations with scale-free power-spectra $P(k) \propto k^n$

$n = -1$

$n = -2.5$

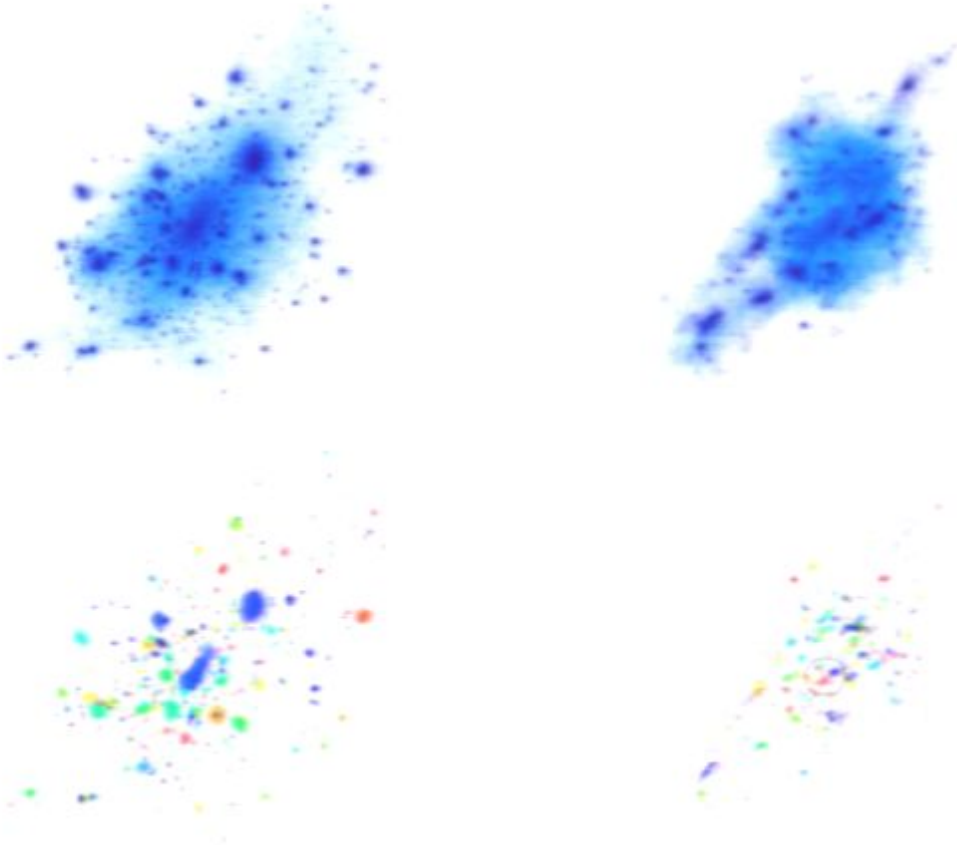

from Elahi, LMW, & Thacker, 2009

Moore et al. 1999

cluster
n = -1.8

galaxy
n = -2.2

simulations with scale-free power-spectra $P(k) \propto k^n$

$n = -1$

$n = -2.5$

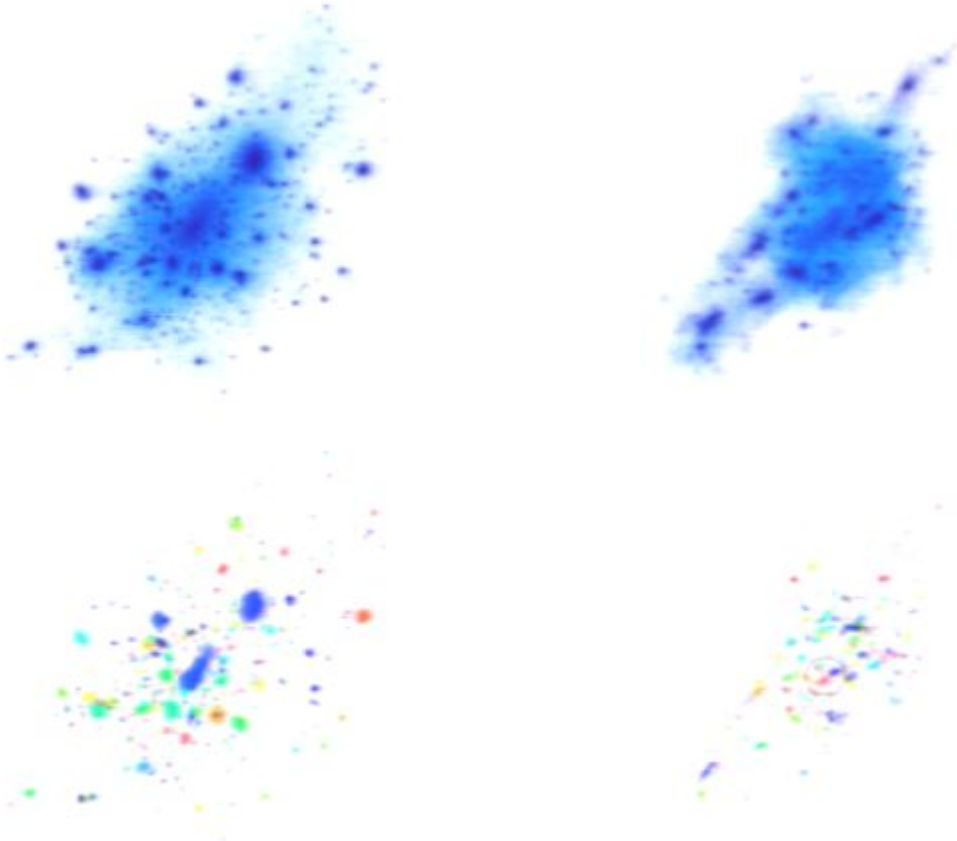

from Elahi, LMW, & Thacker, 2009

Moore et al. 1999

cluster
n = -1.8

galaxy
n = -2.2

simulations with scale-free power-spectra $P(k) \propto k^n$

$n = -1$

$n = -2.5$

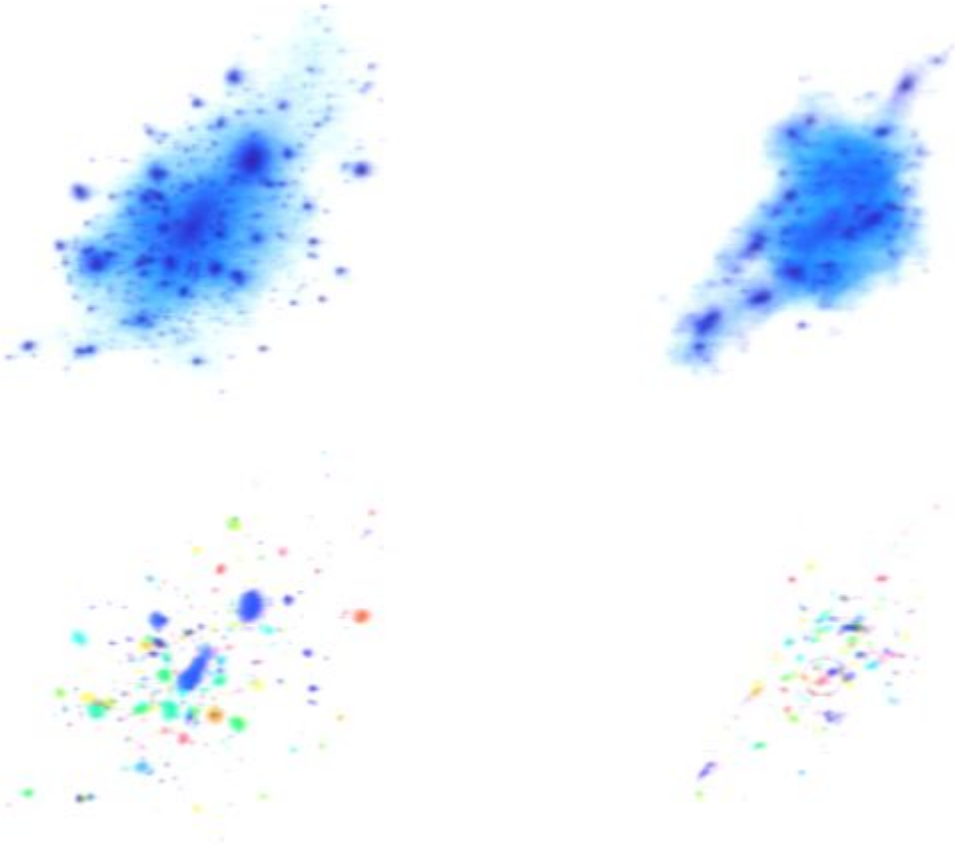

from Elahi, LMW, & Thacker, 2009

Moore et al. 1999

cluster
n = -1.8

galaxy
n = -2.2

simulations with scale-free power-spectra $P(k) \propto k^n$

$n = -1$

$n = -2.5$

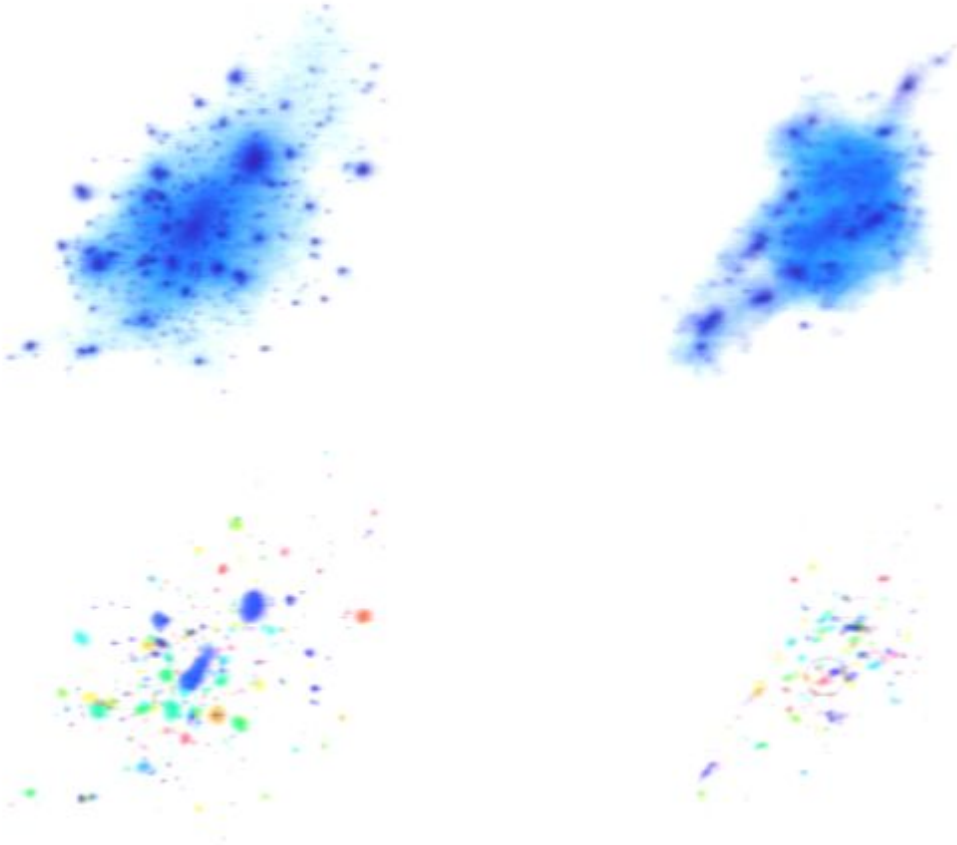

from Elahi, LMW, & Thacker, 2009

Moore et al. 1999

cluster
n = -1.8

galaxy
n = -2.2

simulations with scale-free power-spectra $P(k) \propto k^n$

$n = -1$

$n = -2.5$

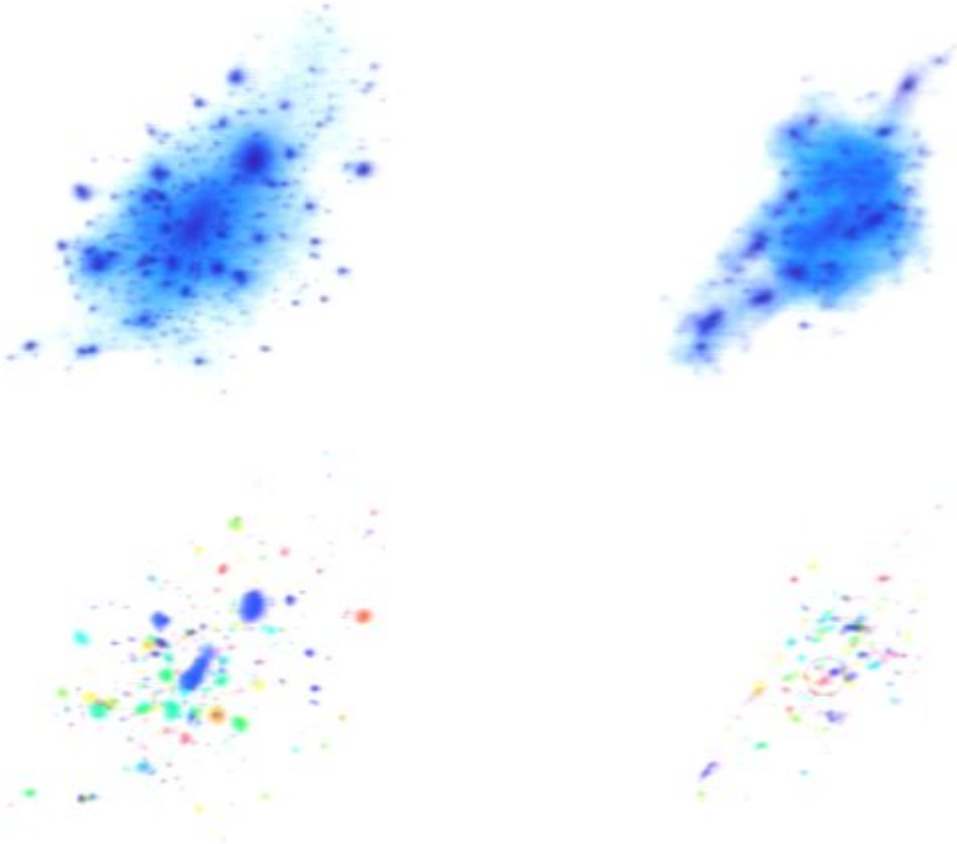

from Elahi, LMW, & Thacker, 2009

Moore et al. 1999

cluster
n = -1.8

galaxy
n = -2.2

simulations with scale-free power-spectra $P(k) \propto k^n$

$n = -1$

$n = -2.5$

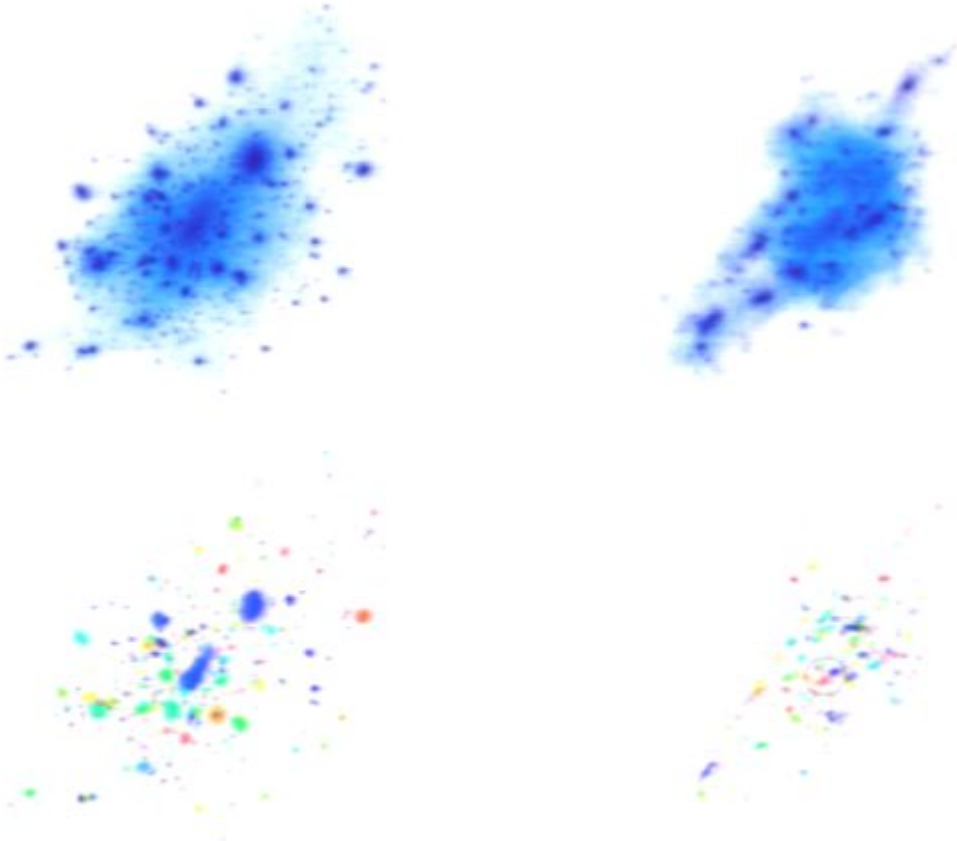

from Elahi, LMW, & Thacker, 2009

Moore et al. 1999

cluster
n = -1.8

galaxy
n = -2.2

simulations with scale-free power-spectra $P(k) \propto k^n$

$n = -1$

$n = -2.5$

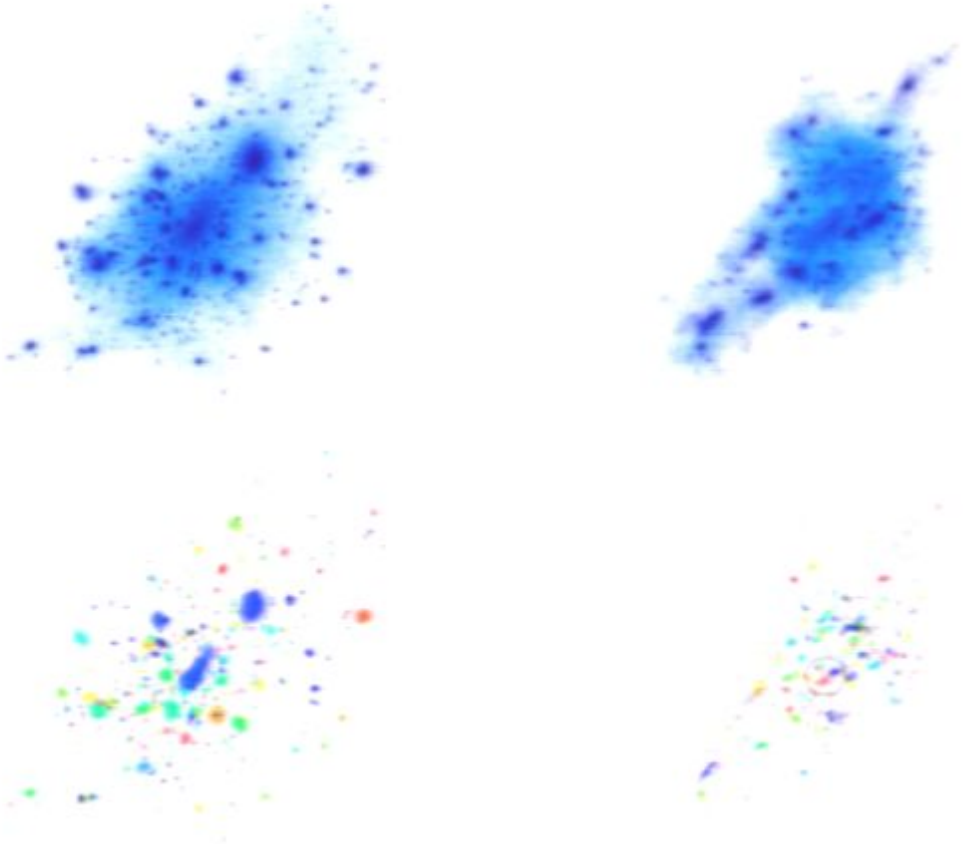

from Elahi, LMW, & Thacker, 2009

Moore et al. 1999

cluster
n = -1.8

galaxy
n = -2.2

simulations with scale-free power-spectra $P(k) \propto k^n$

$n = -1$

$n = -2.5$

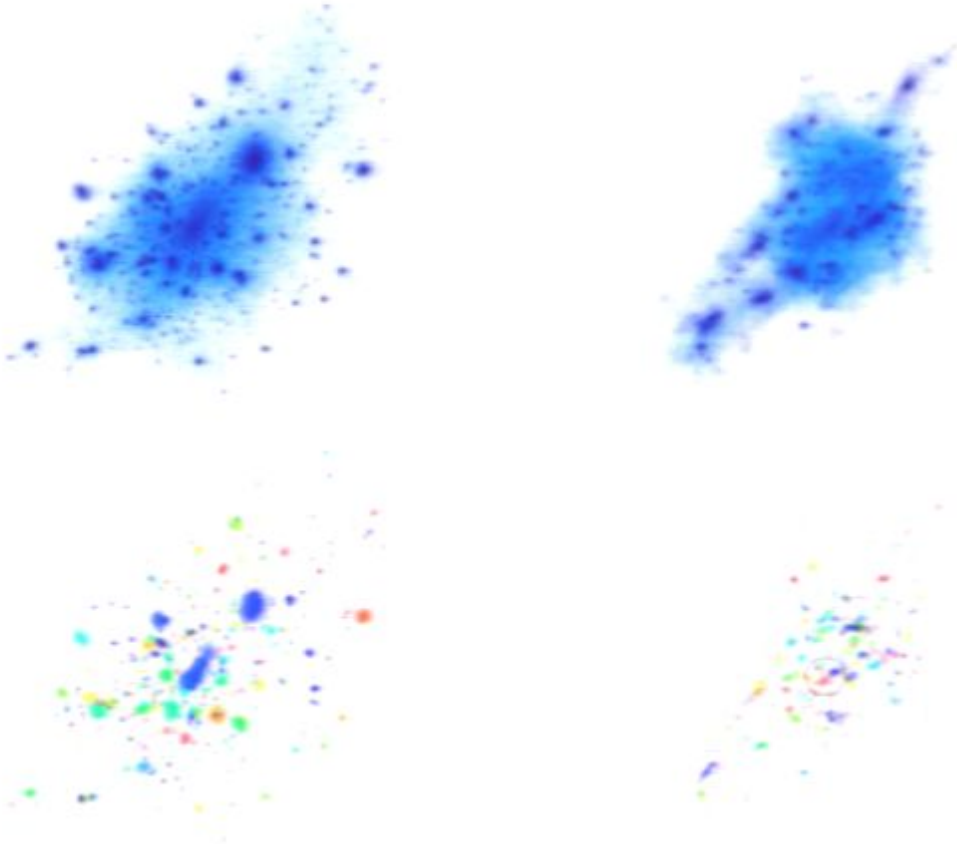

from Elahi, LMW, & Thacker, 2009

Moore et al. 1999

cluster
n = -1.8

galaxy
n = -2.2

simulations with scale-free power-spectra $P(k) \propto k^n$

$n = -1$

$n = -2.5$

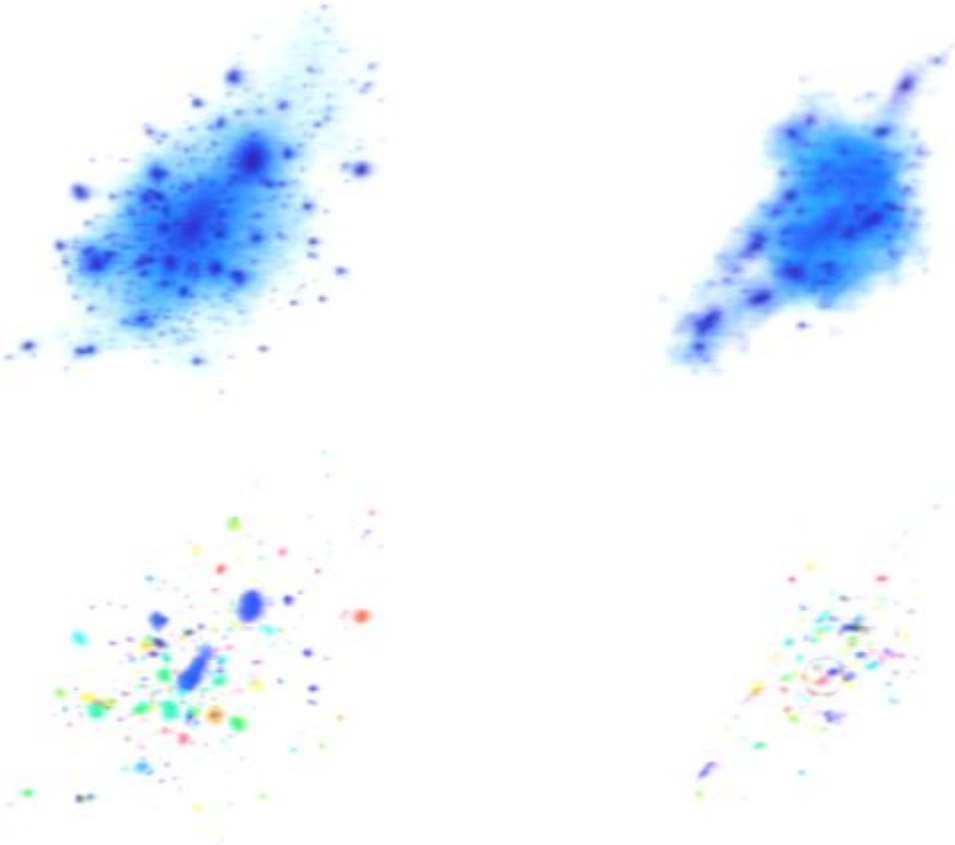

from Elahi, LMW, & Thacker, 2009

EARLY SUPERSYMMETRIC COLD DARK MATTER SUBSTRUCTURE

JÜRG DIEMAND, MICHAEL KUHLEN, AND PIERO MADAU
Department of Astronomy and Astrophysics, 477 Clark Kerr Hall, University of California, Santa Cruz, CA 95064; diemand@ucolick.org
Received 2006 February 26; accepted 2006 May 31

ABSTRACT

Earth-mass "microhalos" may be the first objects to virialize in the early universe. Their ability to survive the hierarchical clustering process as substructure in the larger halos that form subsequently has implications for dark matter detection experiments. We present a large N-body simulation of early substructure in a supersymmetric cold dark matter (SUSY-CDM) scenario characterized by an exponential cutoff in the power spectrum at $M_c = 10^{-6}\ M_\odot$. The simulation resolves a $0.014\ M_\odot$ parent SUSY halo at $z = 75$ with 14 million particles. On these scales, the effective index of the power spectrum approaches -3, and a range of mass scales collapses almost simultaneously.

galactic scale

microhalo scale

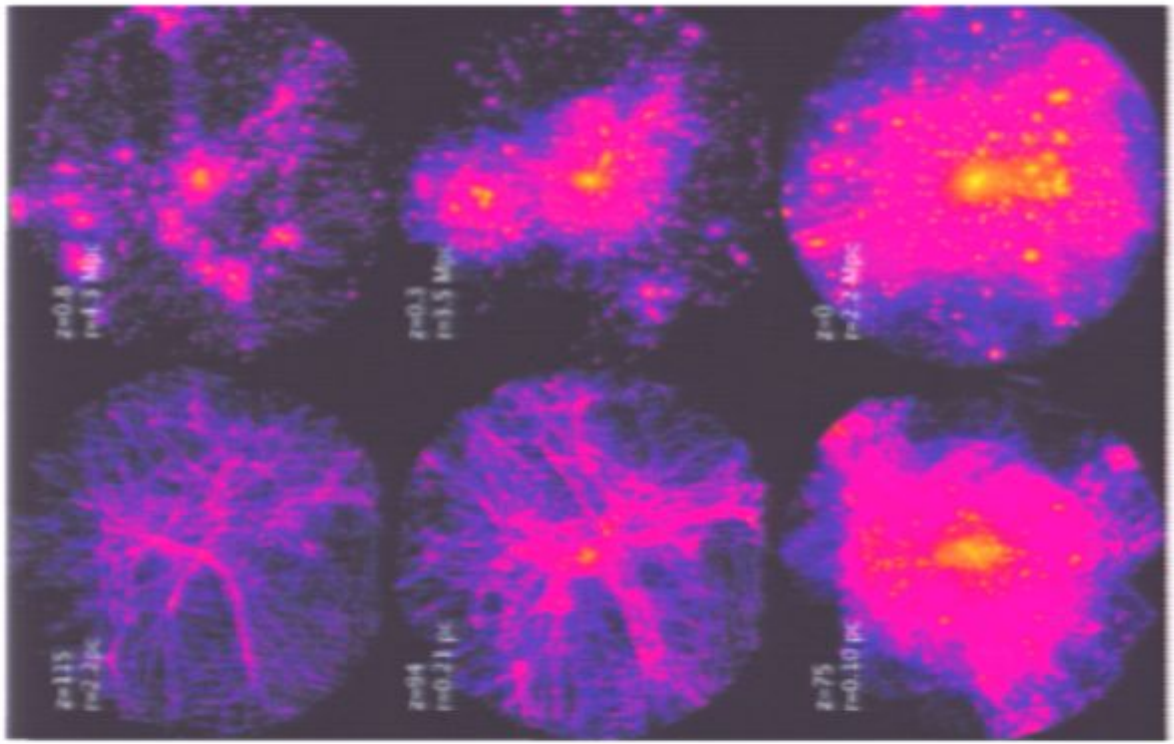

time ⟶

EARLY SUPERSYMMETRIC COLD DARK MATTER SUBSTRUCTURE

JÜRG DIEMAND, MICHAEL KUHLEN, AND PIERO MADAU
Department of Astronomy and Astrophysics, 477 Clark Kerr Hall, University of California, Santa Cruz, CA 95064; diemand@ucolick.org
Received 2006 February 26; accepted 2006 May 31

ABSTRACT

Earth-mass "microhalos" may be the first objects to virialize in the early universe. Their ability to survive the hierarchical clustering process as substructure in the larger halos that form subsequently has implications for dark matter detection experiments. We present a large N-body simulation of early substructure in a supersymmetric cold dark matter (SUSY-CDM) scenario characterized by an exponential cutoff in the power spectrum at $M_c = 10^{-6}\ M_\odot$. The simulation resolves a $0.014\ M_\odot$ parent SUSY halo at $z = 75$ with 14 million particles. On these scales, the effective index of the power spectrum approaches -3, and a range of mass scales collapses almost simultaneously.

galactic scale

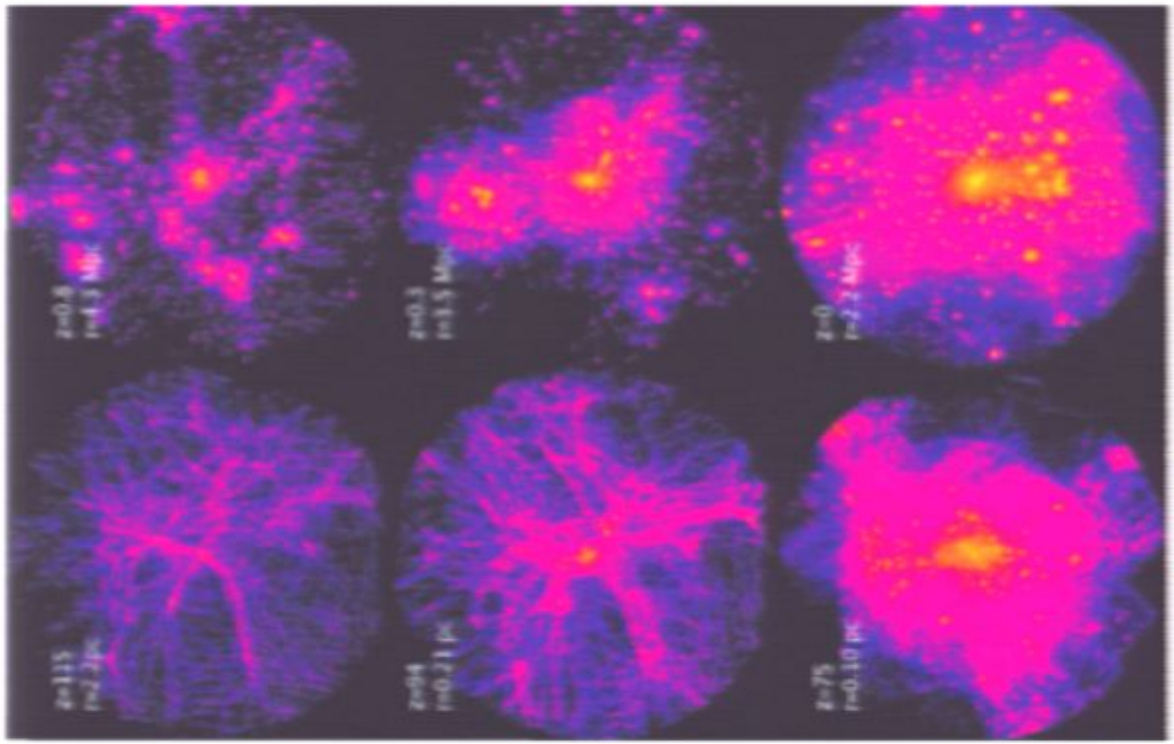

microhalo scale

time ⟶

EARLY SUPERSYMMETRIC COLD DARK MATTER SUBSTRUCTURE

JÜRG DIEMAND, MICHAEL KUHLEN, AND PIERO MADAU
Department of Astronomy and Astrophysics, 477 Clark Kerr Hall, University of California, Santa Cruz, CA 95064; diemandj@ucolick.org
Received 2006 February 26; accepted 2006 May 31

ABSTRACT

Earth-mass "microhalos" may be the first objects to virialize in the early universe. Their ability to survive the hierarchical clustering process as substructure in the larger halos that form subsequently has implications for dark matter detection experiments. We present a large N-body simulation of early substructure in a supersymmetric cold dark matter (SUSY-CDM) scenario characterized by an exponential cutoff in the power spectrum at $M_c = 10^{-6}\ M_\odot$. The simulation resolves a $0.014\ M_\odot$ parent SUSY halo at $z = 75$ with 14 million particles. On these scales, the effective index of the power spectrum approaches -3, and a range of mass scales collapses almost simultaneously.

galactic scale

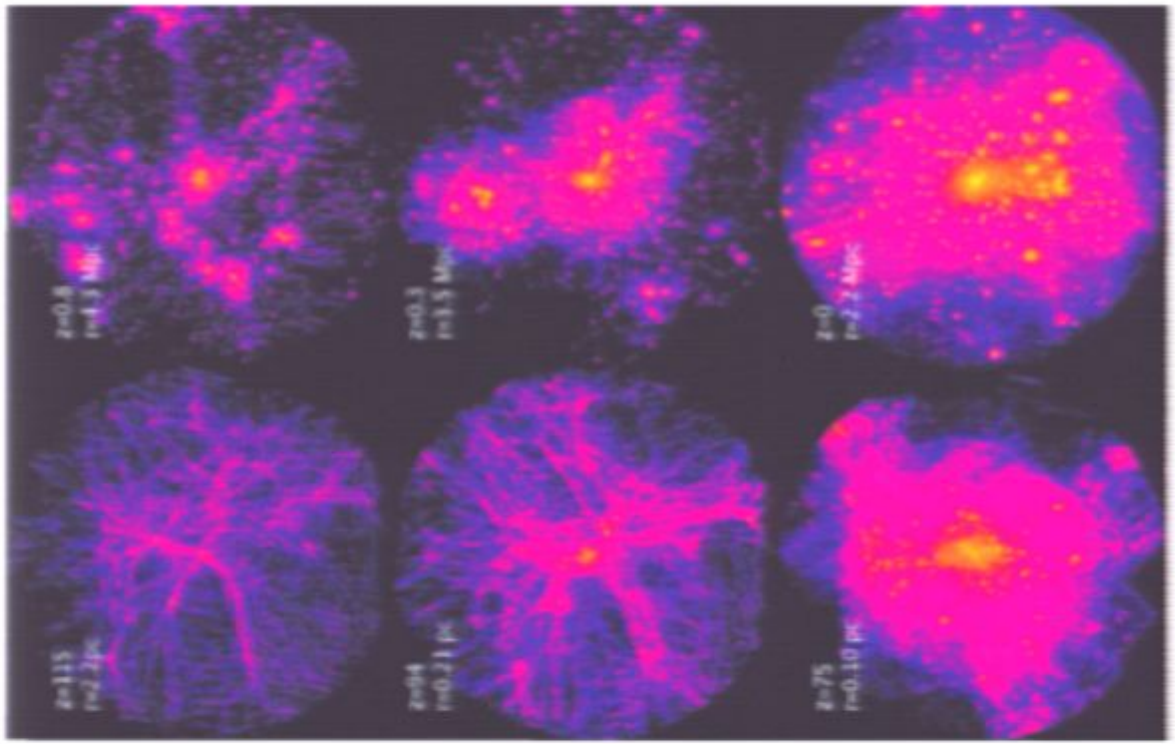

microhalo scale

time ⟶

EARLY SUPERSYMMETRIC COLD DARK MATTER SUBSTRUCTURE

JÜRG DIEMAND, MICHAEL KUHLEN, AND PIERO MADAU
Department of Astronomy and Astrophysics, 477 Clark Kerr Hall, University of California, Santa Cruz, CA 95064; diemand@ucolick.org
Received 2006 February 26; accepted 2006 May 31

ABSTRACT

Earth-mass "microhalos" may be the first objects to virialize in the early universe. Their ability to survive the hierarchical clustering process as substructure in the larger halos that form subsequently has implications for dark matter detection experiments. We present a large N-body simulation of early substructure in a supersymmetric cold dark matter (SUSY-CDM) scenario characterized by an exponential cutoff in the power spectrum at $M_c = 10^{-6}\ M_\odot$. The simulation resolves a $0.014\ M_\odot$ parent SUSY halo at $z = 75$ with 14 million particles. On these scales, the effective index of the power spectrum approaches -3, and a range of mass scales collapses almost simultaneously.

galactic scale

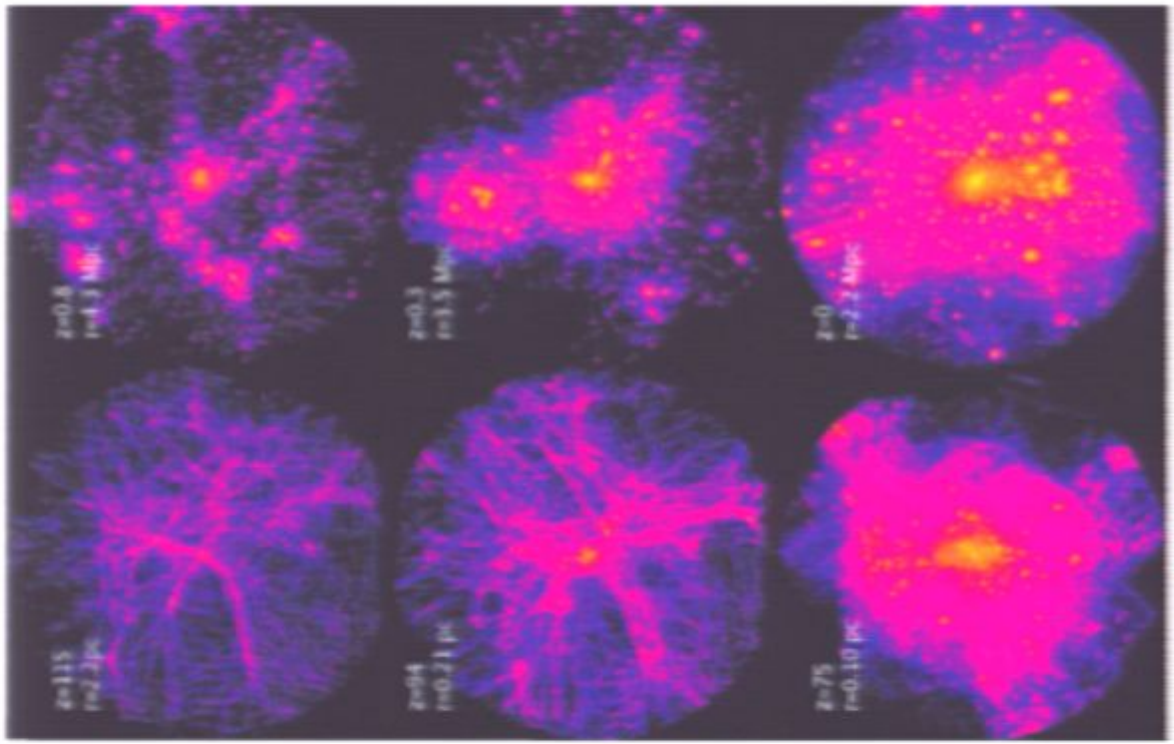

microhalo scale

time ⟶

EARLY SUPERSYMMETRIC COLD DARK MATTER SUBSTRUCTURE

JÜRG DIEMAND, MICHAEL KUHLEN, AND PIERO MADAU
Department of Astronomy and Astrophysics, 477 Clark Kerr Hall, University of California, Santa Cruz, CA 95064; diemand@ucolick.org
Received 2006 February 26; accepted 2006 May 31

ABSTRACT

Earth-mass "microhalos" may be the first objects to virialize in the early universe. Their ability to survive the hierarchical clustering process as substructure in the larger halos that form subsequently has implications for dark matter detection experiments. We present a large N-body simulation of early substructure in a supersymmetric cold dark matter (SUSY-CDM) scenario characterized by an exponential cutoff in the power spectrum at $M_c = 10^{-6}\ M_\odot$. The simulation resolves a $0.014\ M_\odot$ parent SUSY halo at $z = 75$ with 14 million particles. On these scales, the effective index of the power spectrum approaches -3, and a range of mass scales collapses almost simultaneously.

galactic scale

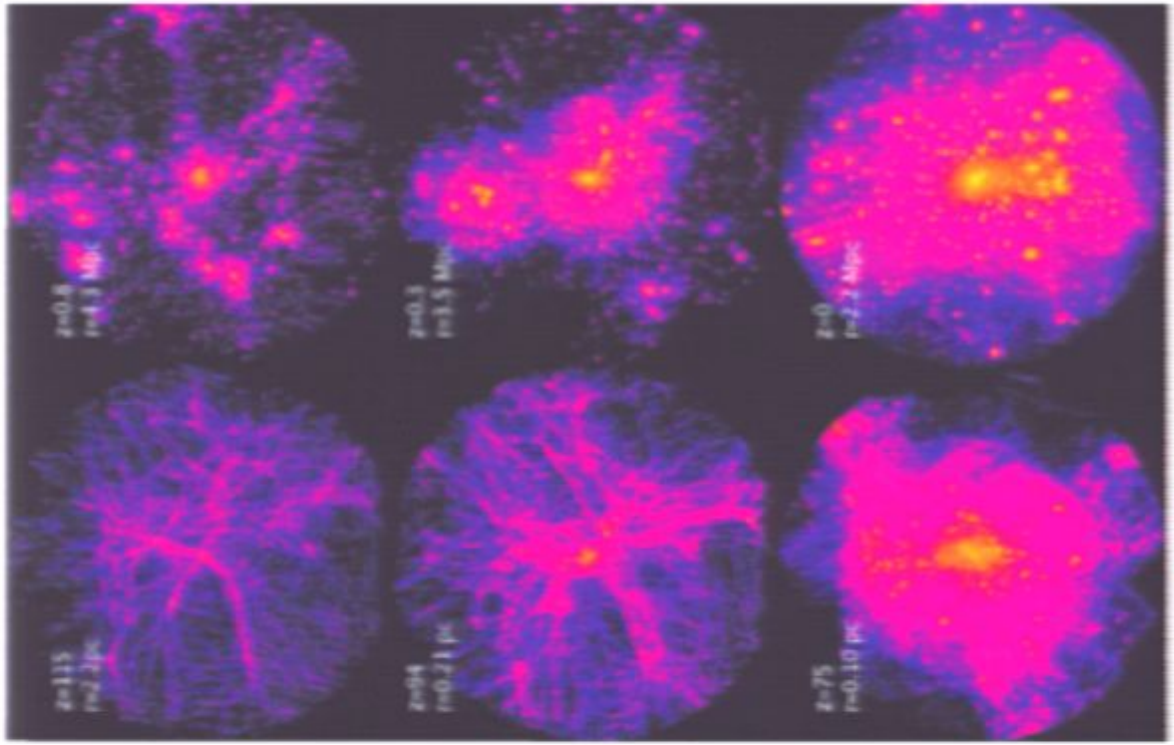

microhalo scale

time ⟶

EARLY SUPERSYMMETRIC COLD DARK MATTER SUBSTRUCTURE

JÜRG DIEMAND, MICHAEL KUHLEN, AND PIERO MADAU
Department of Astronomy and Astrophysics, 477 Clark Kerr Hall, University of California, Santa Cruz, CA 95064; diemand@ucolick.org
Received 2006 February 26; accepted 2006 May 31

ABSTRACT

Earth-mass "microhalos" may be the first objects to virialize in the early universe. Their ability to survive the hierarchical clustering process as substructure in the larger halos that form subsequently has implications for dark matter detection experiments. We present a large N-body simulation of early substructure in a supersymmetric cold dark matter (SUSY-CDM) scenario characterized by an exponential cutoff in the power spectrum at $M_c = 10^{-6}\ M_\odot$. The simulation resolves a $0.014\ M_\odot$ parent SUSY halo at $z = 75$ with 14 million particles. On these scales, the effective index of the power spectrum approaches -3, and a range of mass scales collapses almost simultaneously.

galactic scale

microhalo scale

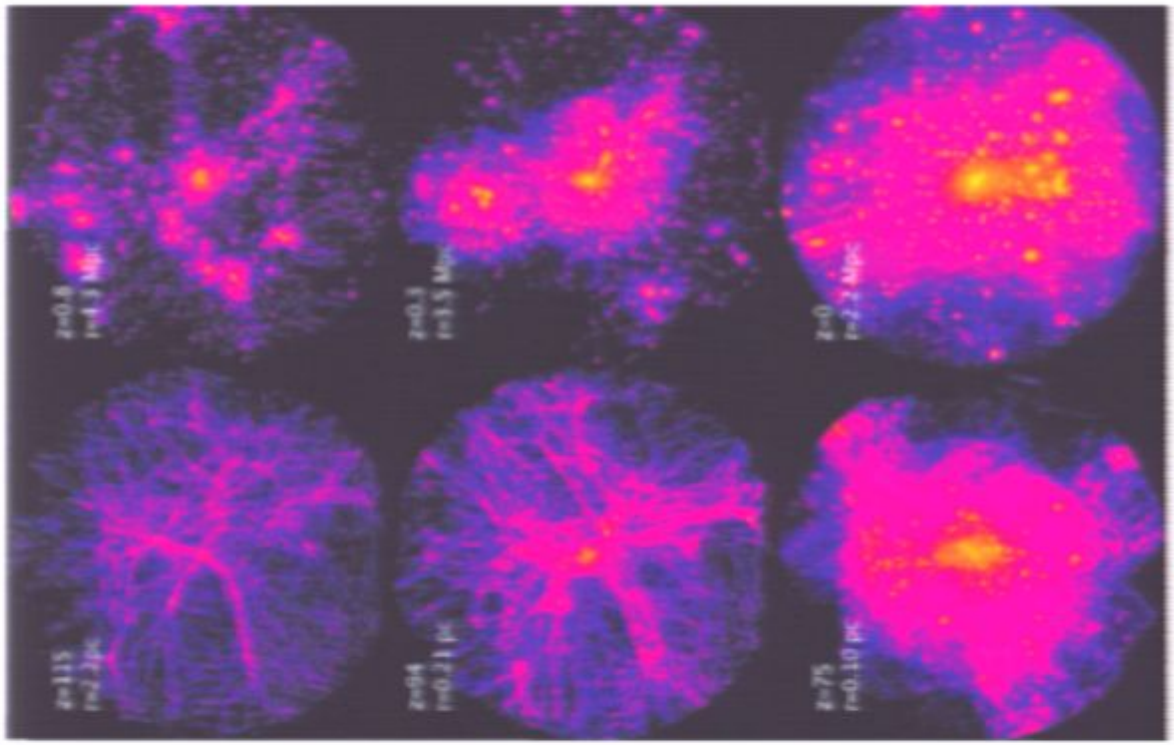

time ⟶

EARLY SUPERSYMMETRIC COLD DARK MATTER SUBSTRUCTURE

JÜRG DIEMAND, MICHAEL KUHLEN, AND PIERO MADAU
Department of Astronomy and Astrophysics, 477 Clark Kerr Hall, University of California, Santa Cruz, CA 95064; diemand@ucolick.org
Received 2006 February 26; accepted 2006 May 31

ABSTRACT

Earth-mass "microhalos" may be the first objects to virialize in the early universe. Their ability to survive the hierarchical clustering process as substructure in the larger halos that form subsequently has implications for dark matter detection experiments. We present a large N-body simulation of early substructure in a supersymmetric cold dark matter (SUSY-CDM) scenario characterized by an exponential cutoff in the power spectrum at $M_c = 10^{-6}\ M_\odot$. The simulation resolves a $0.014\ M_\odot$ parent SUSY halo at $z = 75$ with 14 million particles. On these scales, the effective index of the power spectrum approaches -3, and a range of mass scales collapses almost simultaneously.

galactic scale

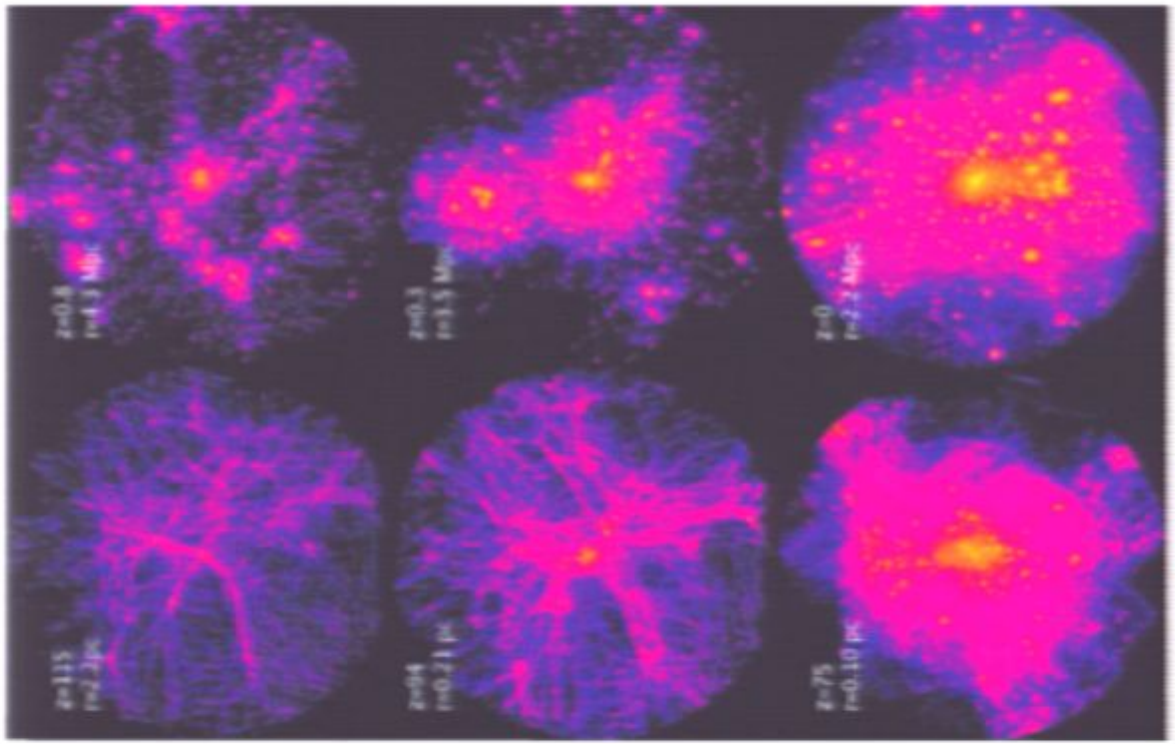

microhalo scale

time ⟶

EARLY SUPERSYMMETRIC COLD DARK MATTER SUBSTRUCTURE

JÜRG DIEMAND, MICHAEL KUHLEN, AND PIERO MADAU
Department of Astronomy and Astrophysics, 477 Clark Kerr Hall, University of California, Santa Cruz, CA 95064; diemand@ucolick.org
Received 2006 February 26; accepted 2006 May 31

ABSTRACT

Earth-mass "microhalos" may be the first objects to virialize in the early universe. Their ability to survive the hierarchical clustering process as substructure in the larger halos that form subsequently has implications for dark matter detection experiments. We present a large N-body simulation of early substructure in a supersymmetric cold dark matter (SUSY-CDM) scenario characterized by an exponential cutoff in the power spectrum at $M_c = 10^{-6}\ M_\odot$. The simulation resolves a $0.014\ M_\odot$ parent SUSY halo at $z = 75$ with 14 million particles. On these scales, the effective index of the power spectrum approaches -3, and a range of mass scales collapses almost simultaneously.

galactic scale

microhalo scale

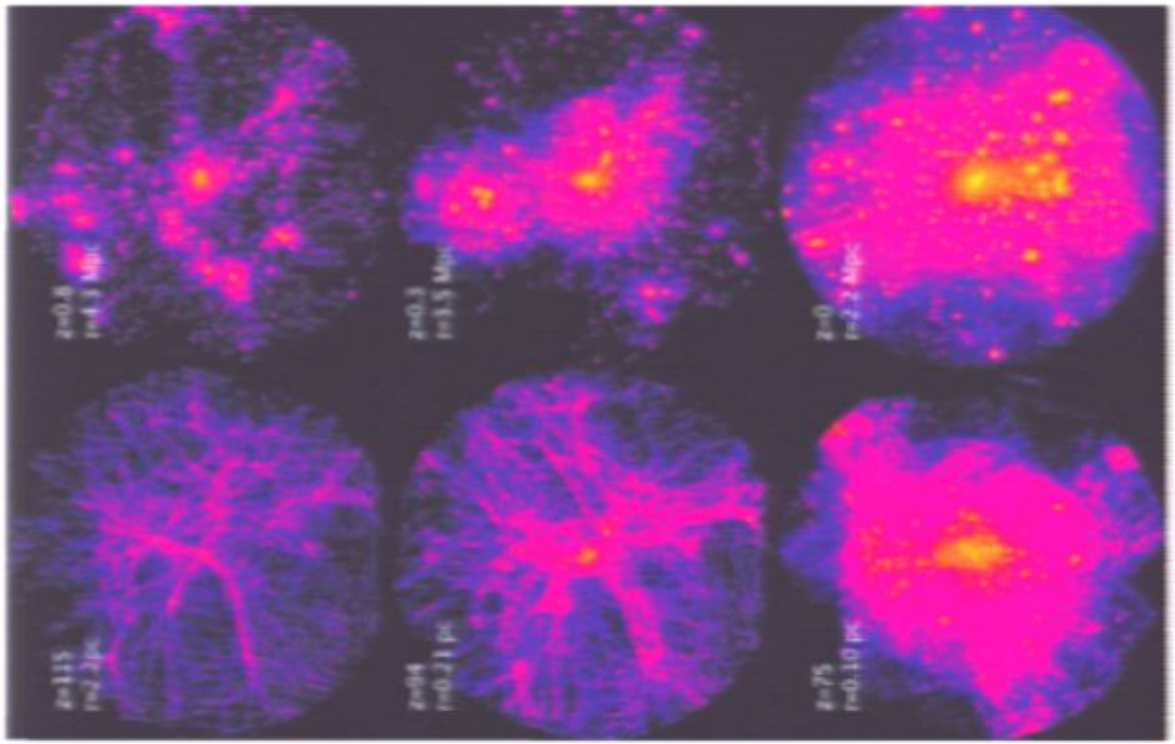

time ⟶

computing requirements for performing simulations at the "bottom of the CDM hierarchy become prohibitive

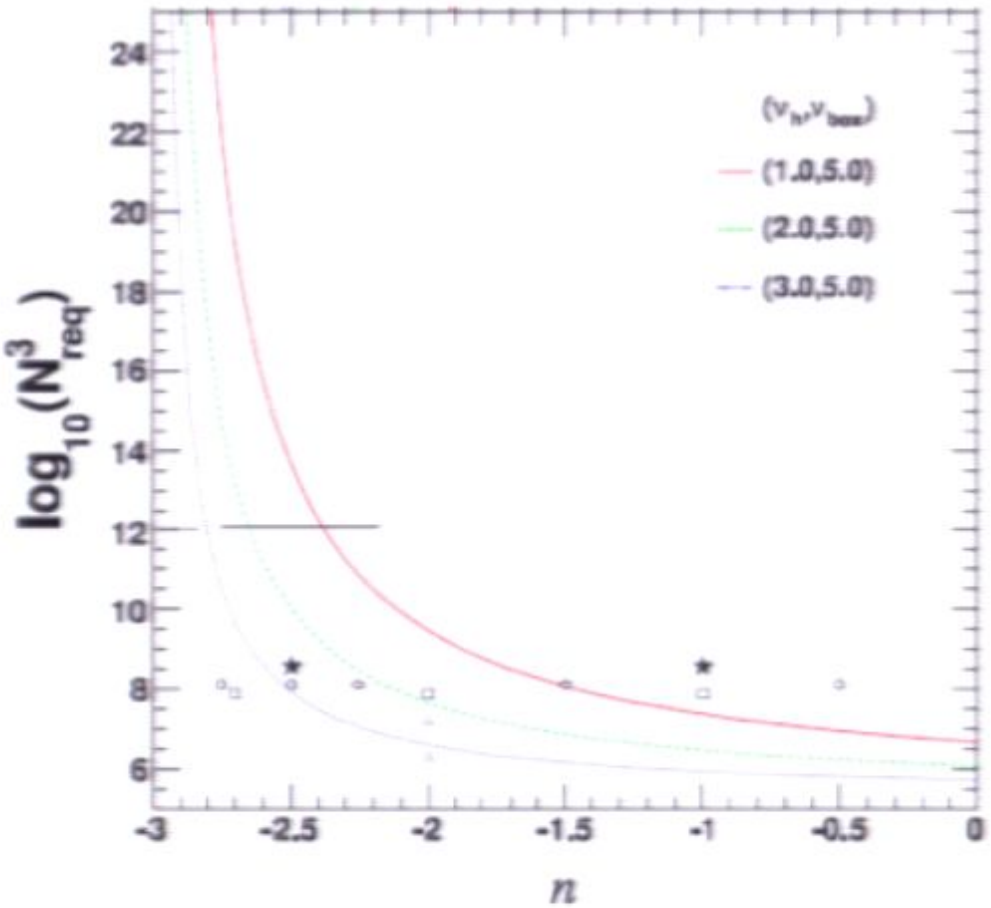

see Elahi, et al. 2009
and Smith et al. 2003

computing requirements for performing simulations at the "bottom of the CDM hierarchy become prohibitive

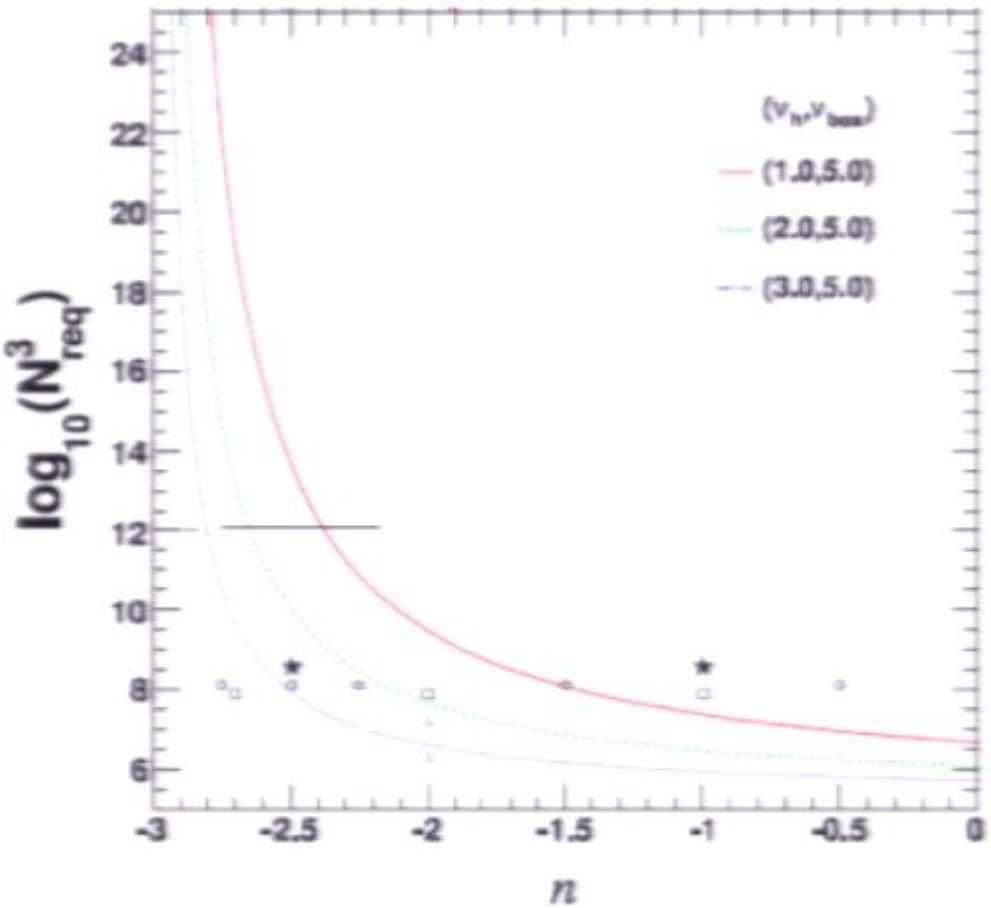

see Elahi, et al. 2009
and Smith et al. 2003

computing requirements for performing simulations at the "bottom of the CDM hierarchy become prohibitive

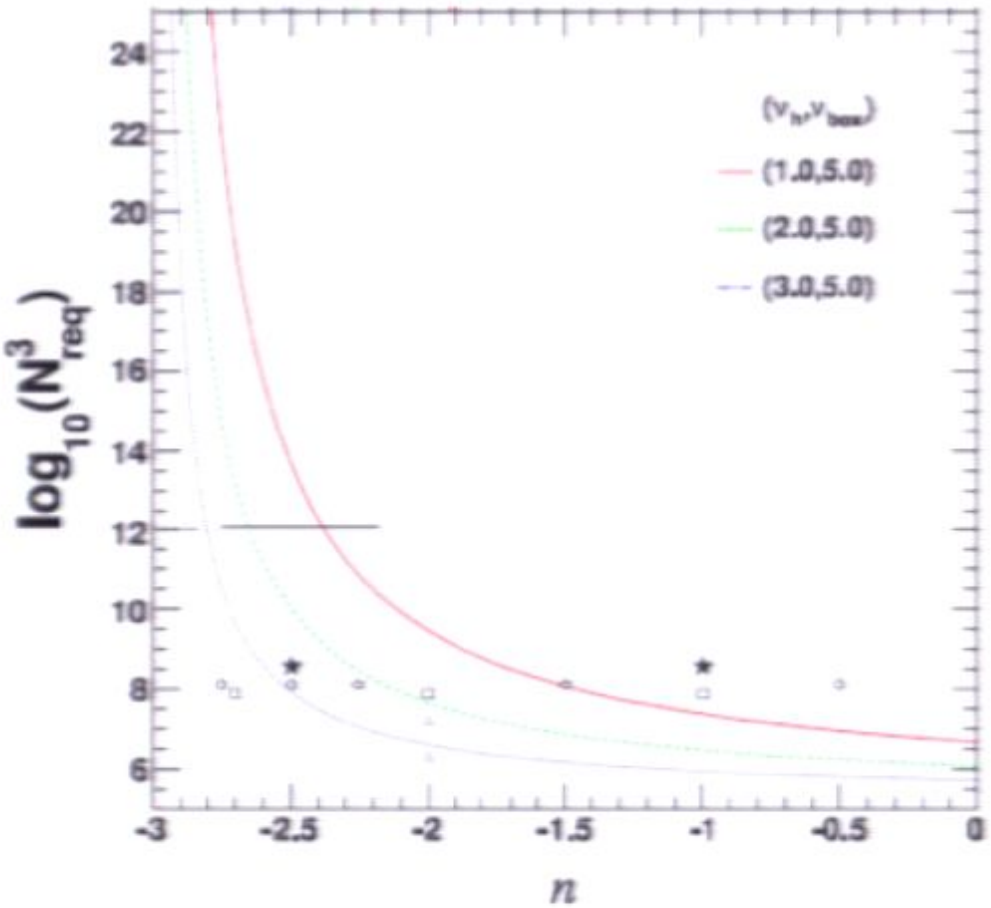

see Elahi, et al. 2009 and Smith et al. 2003

computing requirements for performing simulations at the "bottom of the CDM hierarchy become prohibitive

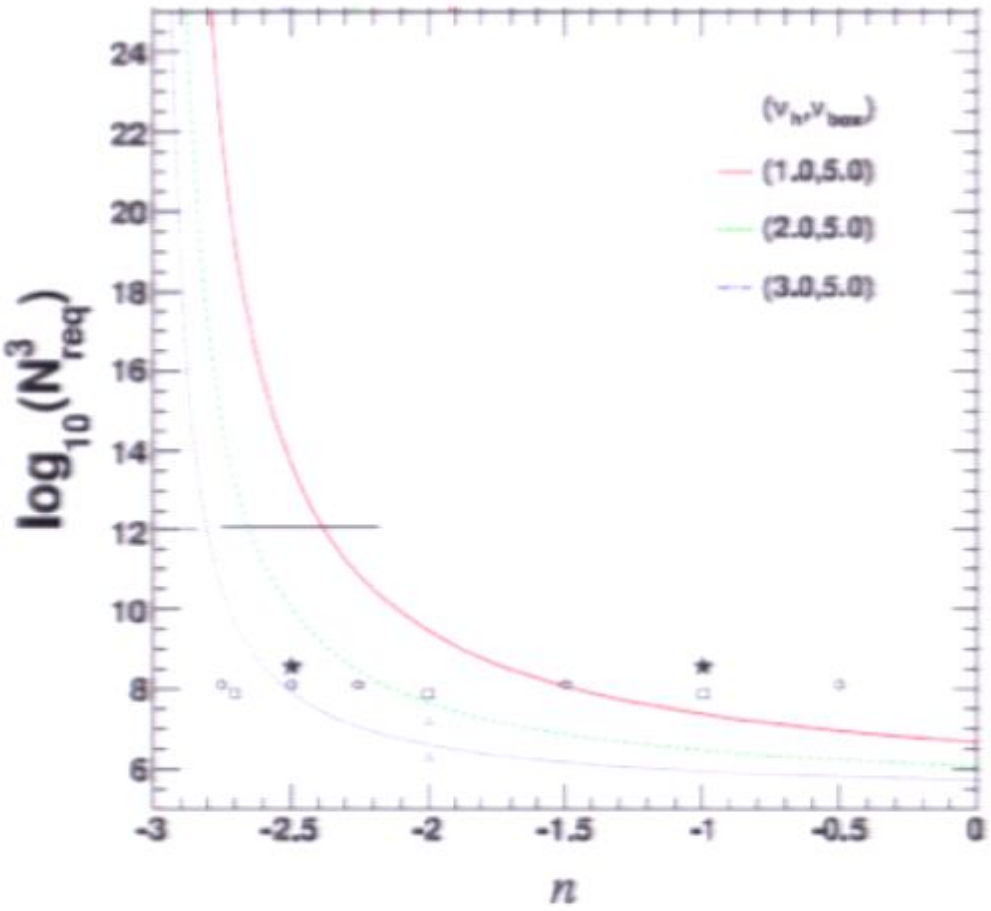

see Elahi, et al. 2009
and Smith et al. 2003

computing requirements for performing simulations at the "bottom of the CDM hierarchy become prohibitive

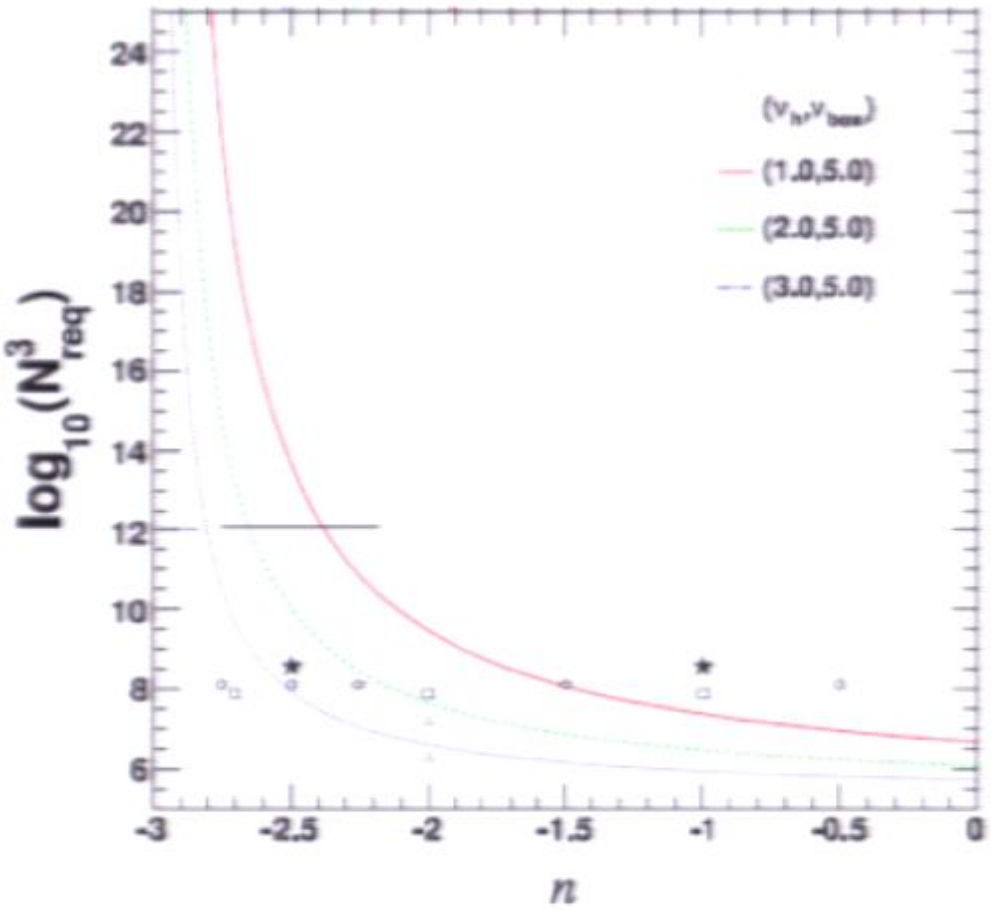

see Elahi, et al. 2009 and Smith et al. 2003

computing requirements for performing simulations at the "bottom of the CDM hierarchy become prohibitive

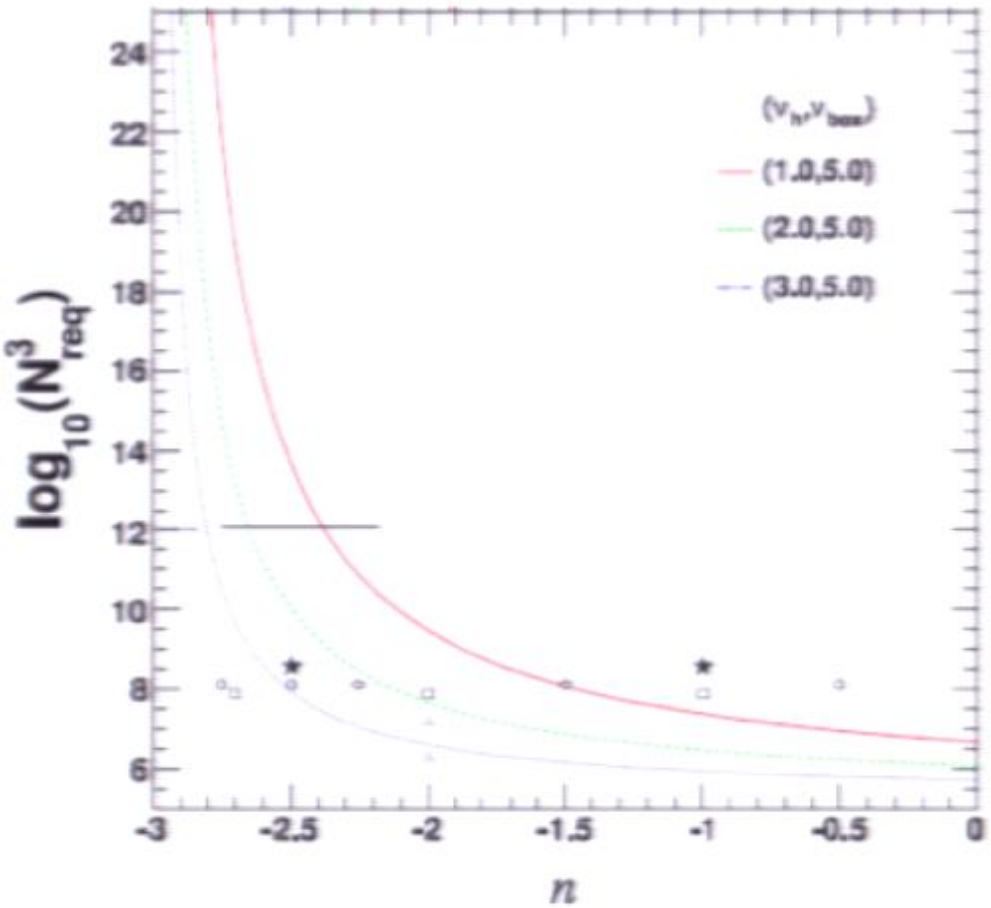

see Elahi, et al. 2009
and Smith et al. 2003

computing requirements for performing simulations at the "bottom of the CDM hierarchy become prohibitive

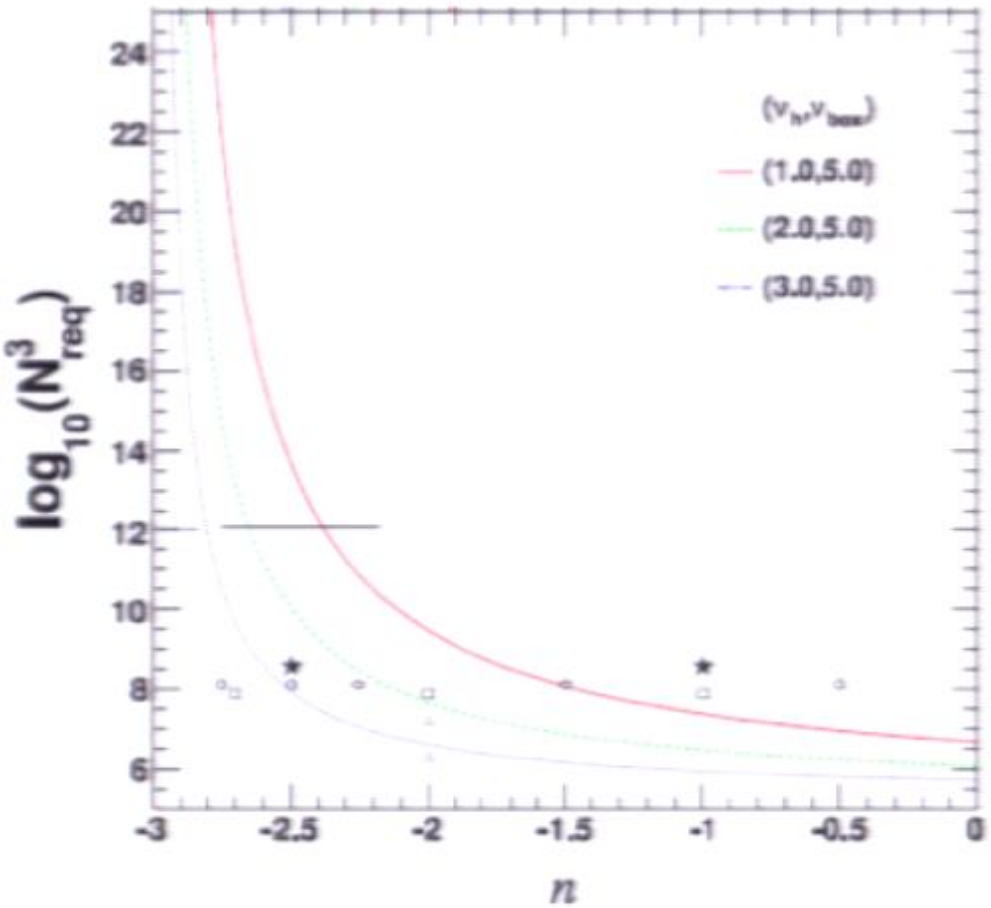

see Elahi, et al. 2009
and Smith et al. 2003

computing requirements for performing simulations at the "bottom of the CDM hierarchy become prohibitive

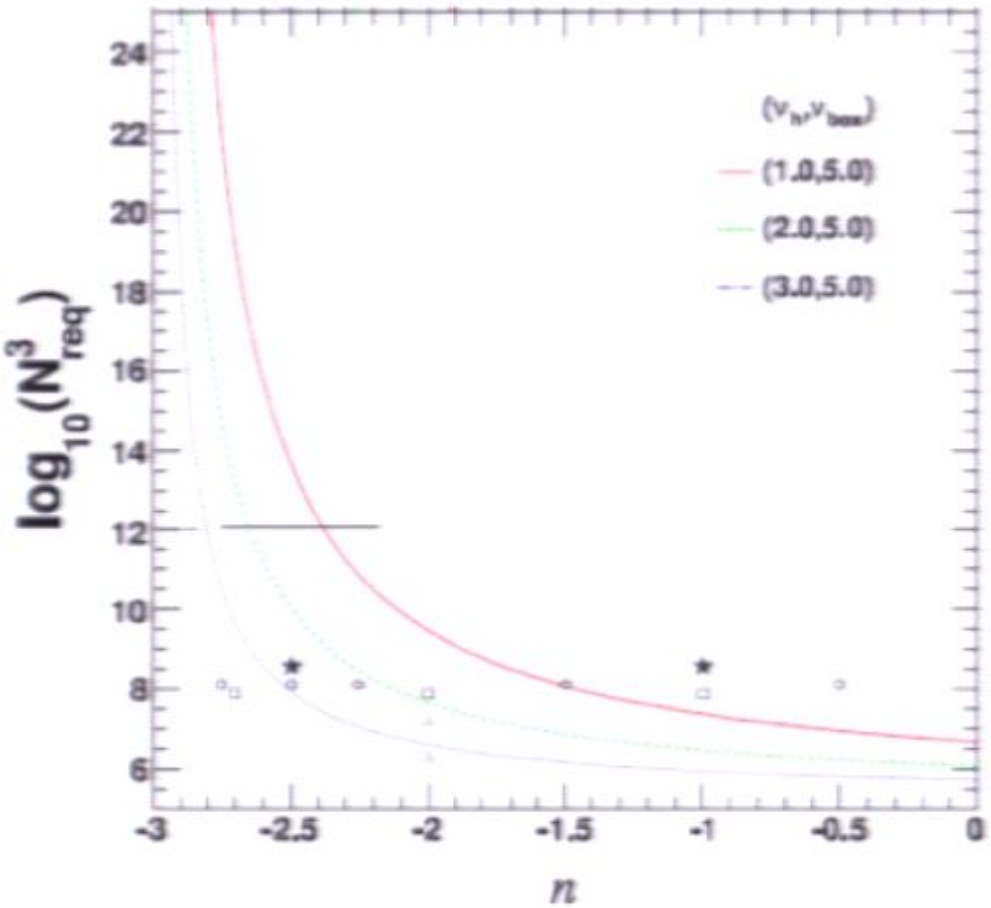

see Elahi, et al. 2009
and Smith et al. 2003

computing requirements for performing simulations at the "bottom of the CDM hierarchy become prohibitive

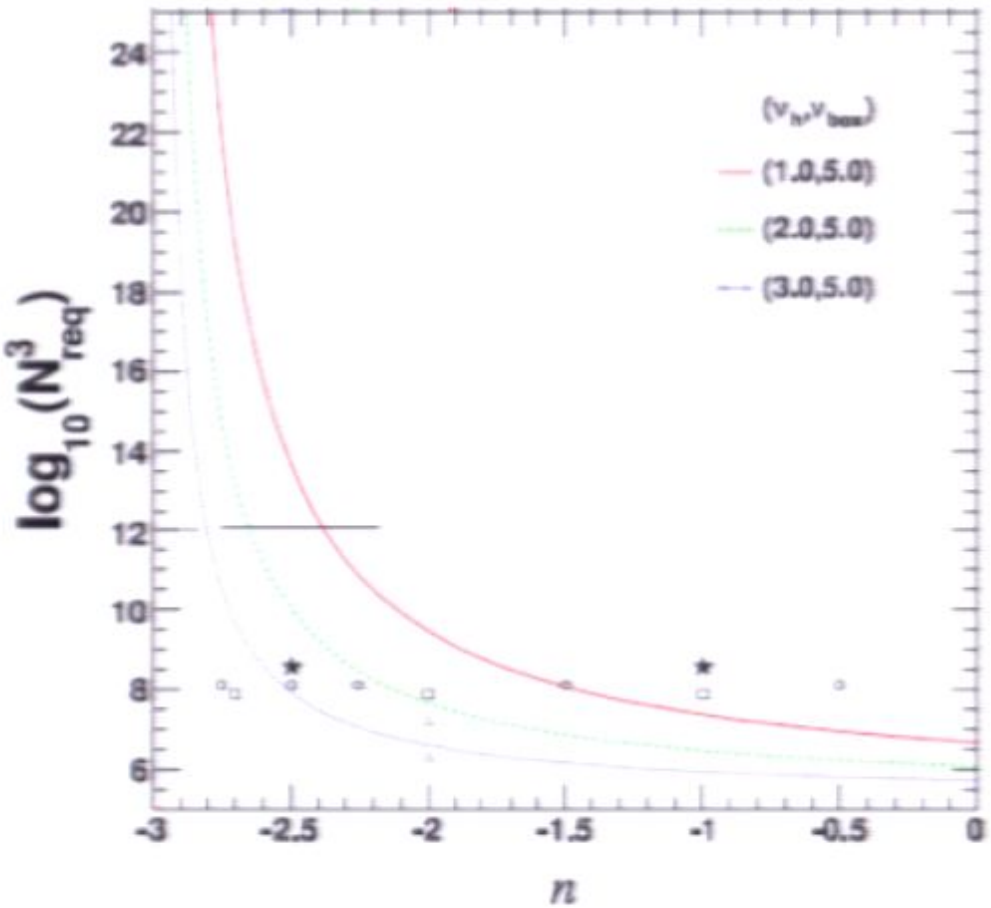

see Elahi, et al. 2009
and Smith et al. 2003

computing requirements for performing simulations at the "bottom of the CDM hierarchy become prohibitive

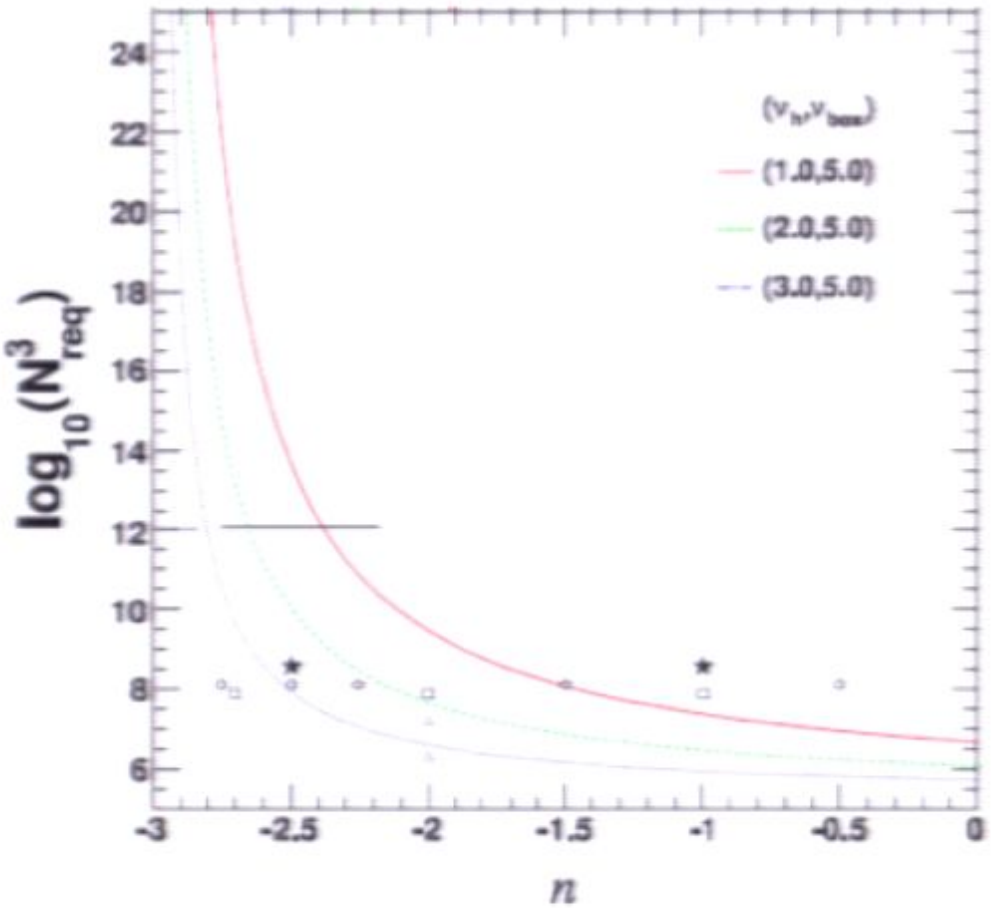

see Elahi, et al. 2009 and Smith et al. 2003

computing requirements for performing simulations at the "bottom of the CDM hierarchy become prohibitive

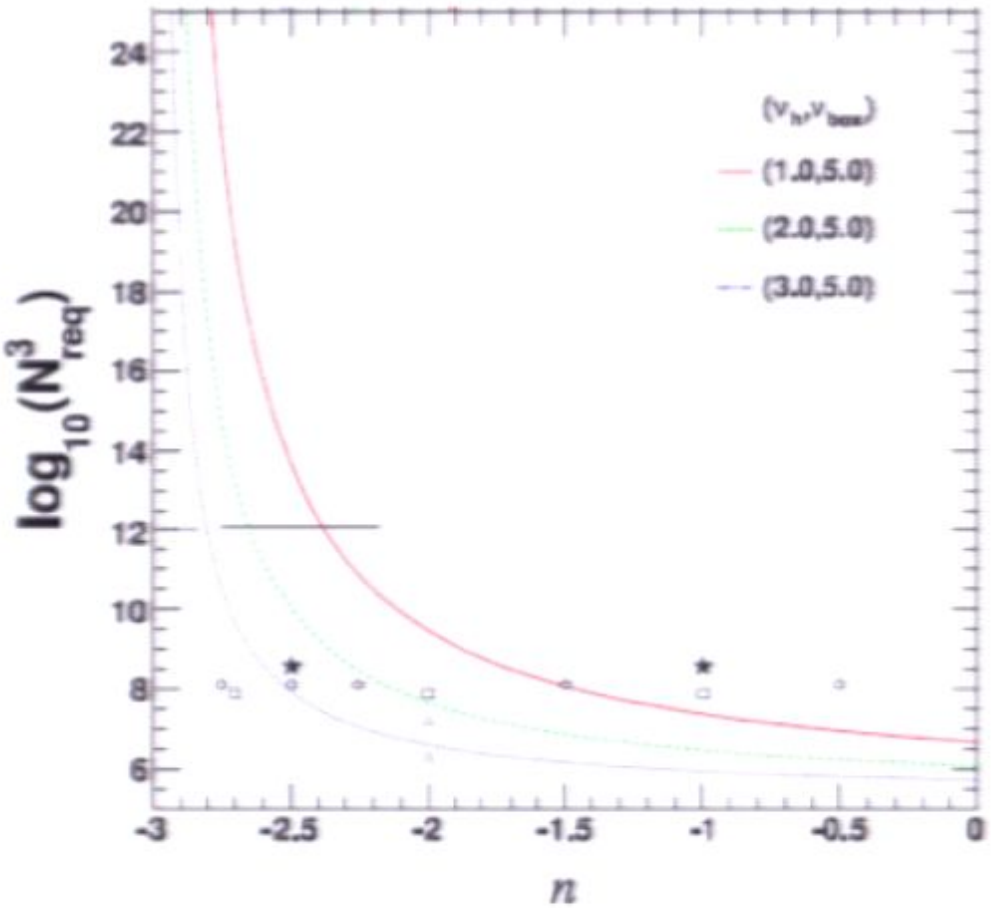

see Elahi, et al. 2009
and Smith et al. 2003

computing requirements for performing simulations at the "bottom of the CDM hierarchy become prohibitive

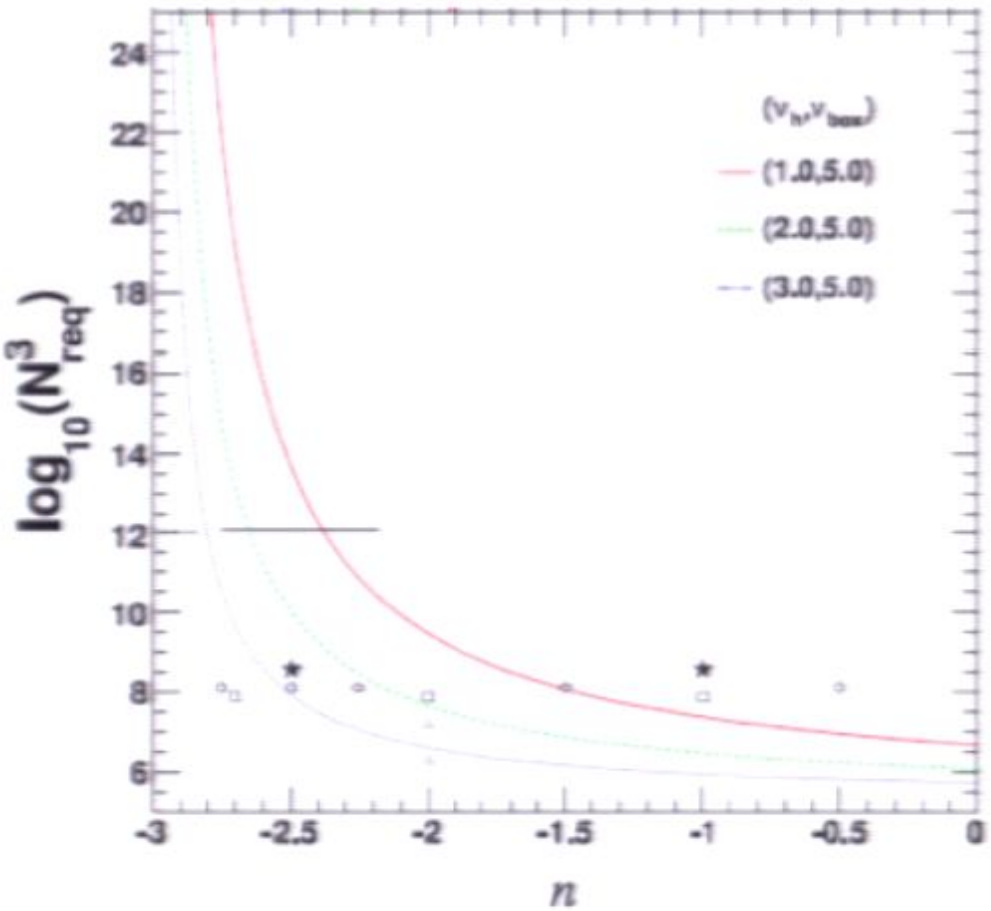

see Elahi, et al. 2009
and Smith et al. 2003

computing requirements for performing simulations at the "bottom of the CDM hierarchy become prohibitive

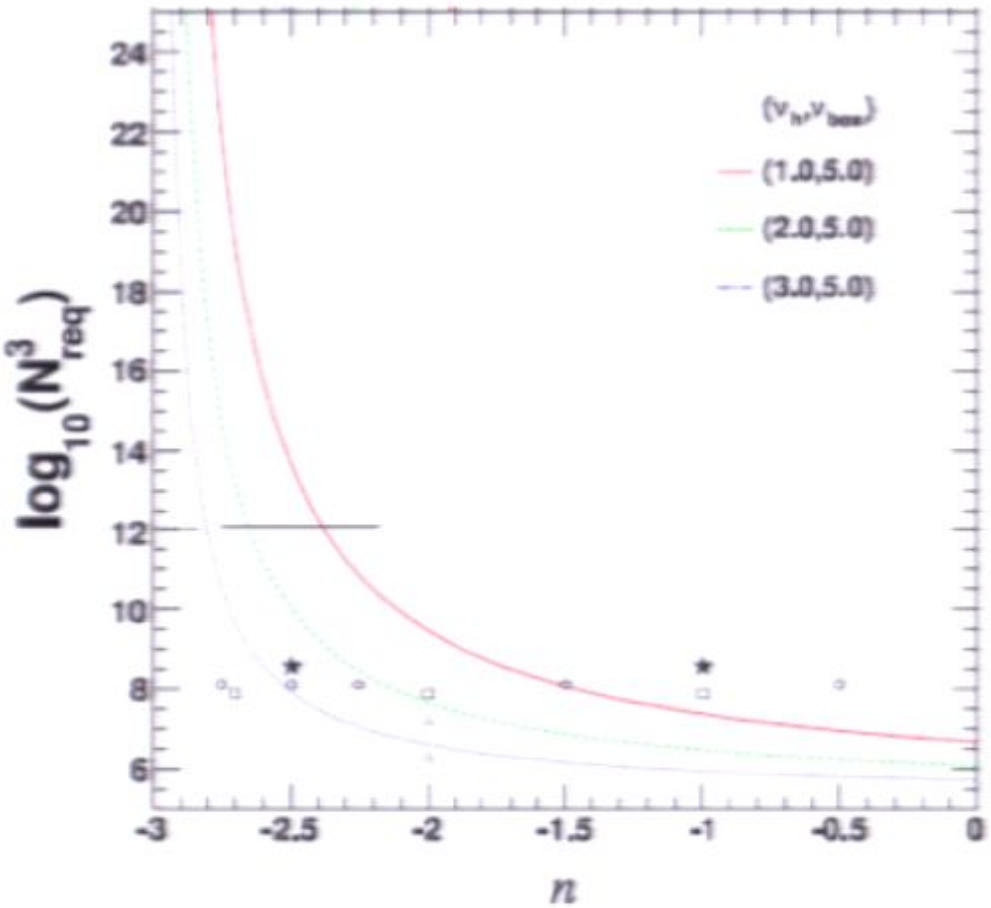

see Elahi, et al. 2009
and Smith et al. 2003

computing requirements for performing simulations at the "bottom of the CDM hierarchy become prohibitive

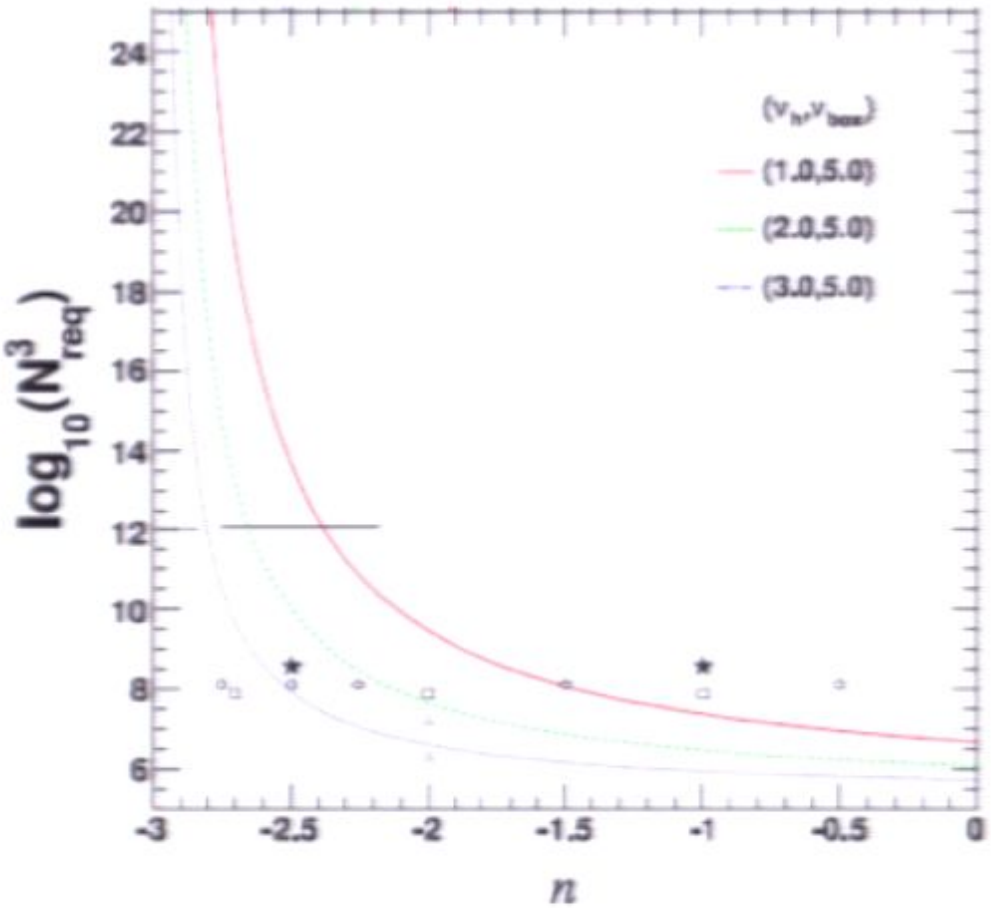

see Elahi, et al. 2009
and Smith et al. 2003

computing requirements for performing simulations at the "bottom of the CDM hierarchy become prohibitive

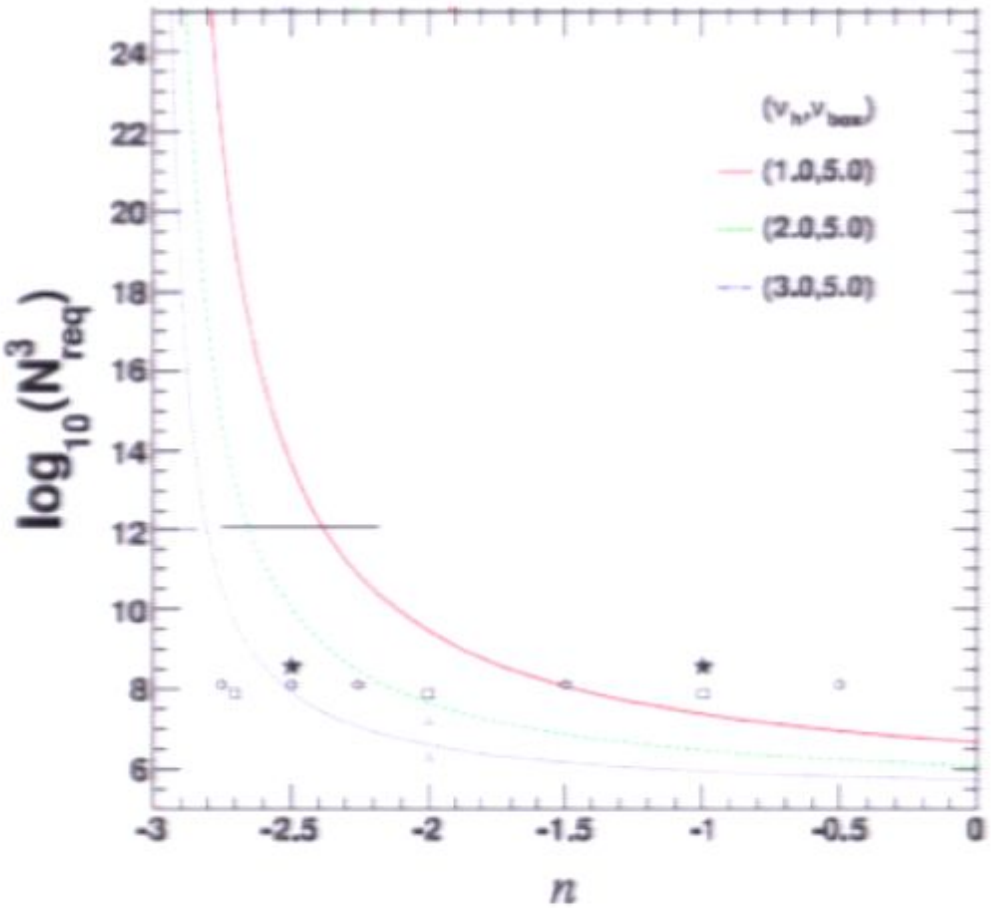

see Elahi, et al. 2009
and Smith et al. 2003

computing requirements for performing simulations at the "bottom of the CDM hierarchy become prohibitive

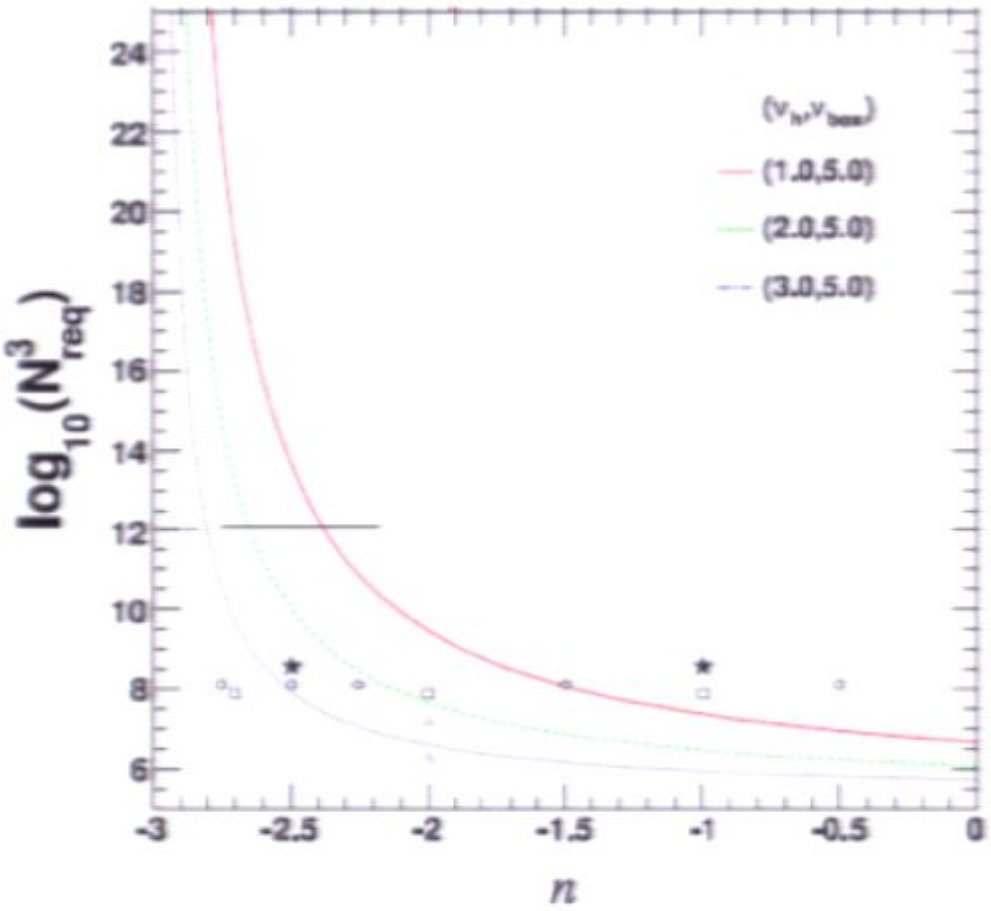

see Elahi, et al. 2009
and Smith et al. 2003

substructure can enhance the signal from
indirect detection experiments, which probe annihilation by-products
and are therefore sensitive to the line-of-sight integral of ρ^2

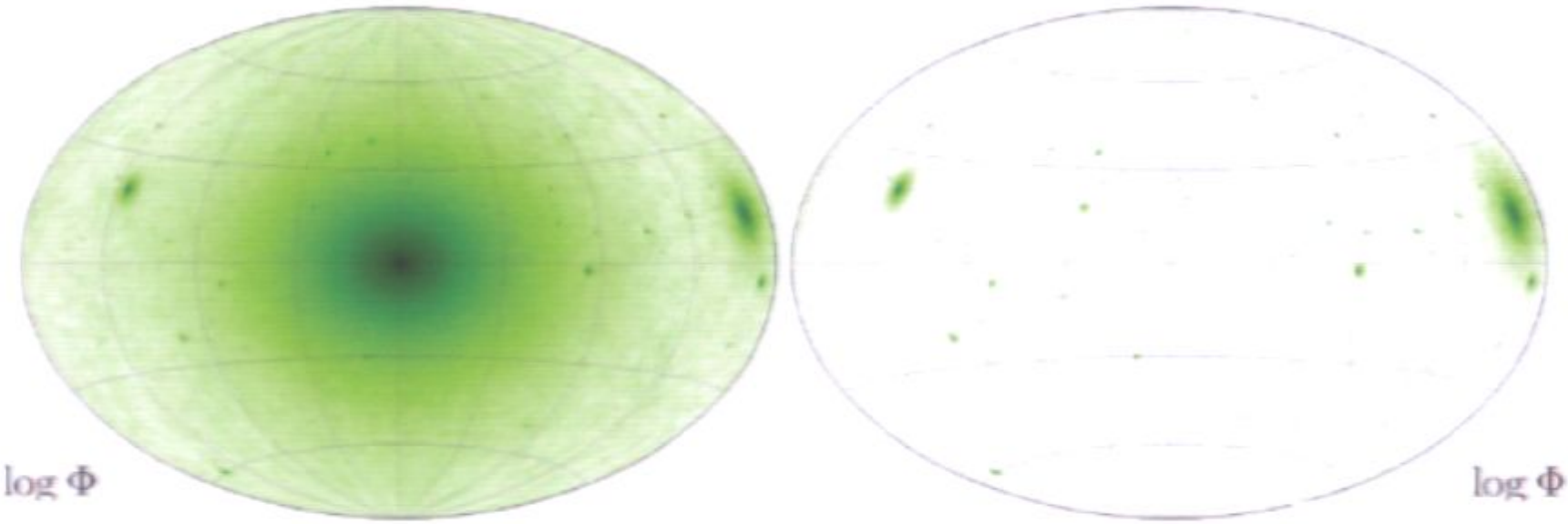

integrated los density-squared from simulations
from Kuhlen et al, 2008

substructure can enhance the signal from
indirect detection experiments, which probe annihilation by-products
and are therefore sensitive to the line-of-sight integral of ρ^2

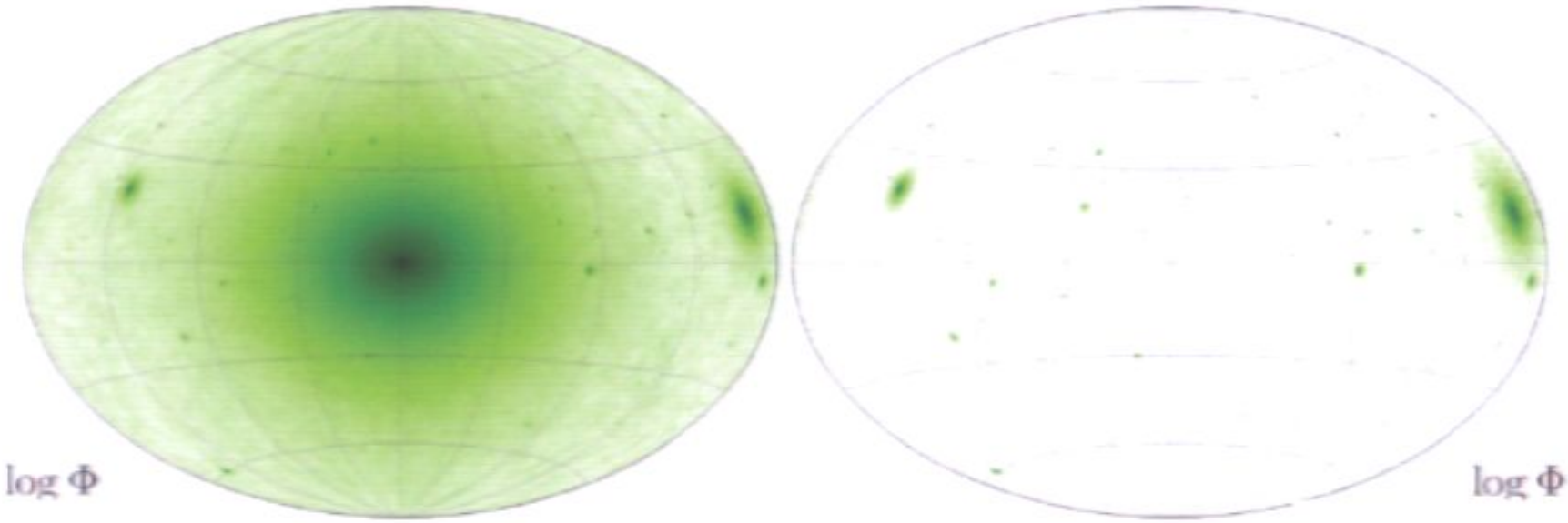

integrated los density-squared from simulations
from Kuhlen et al, 2008

substructure can enhance the signal from
indirect detection experiments, which probe annihilation by-products
and are therefore sensitive to the line-of-sight integral of ρ^2

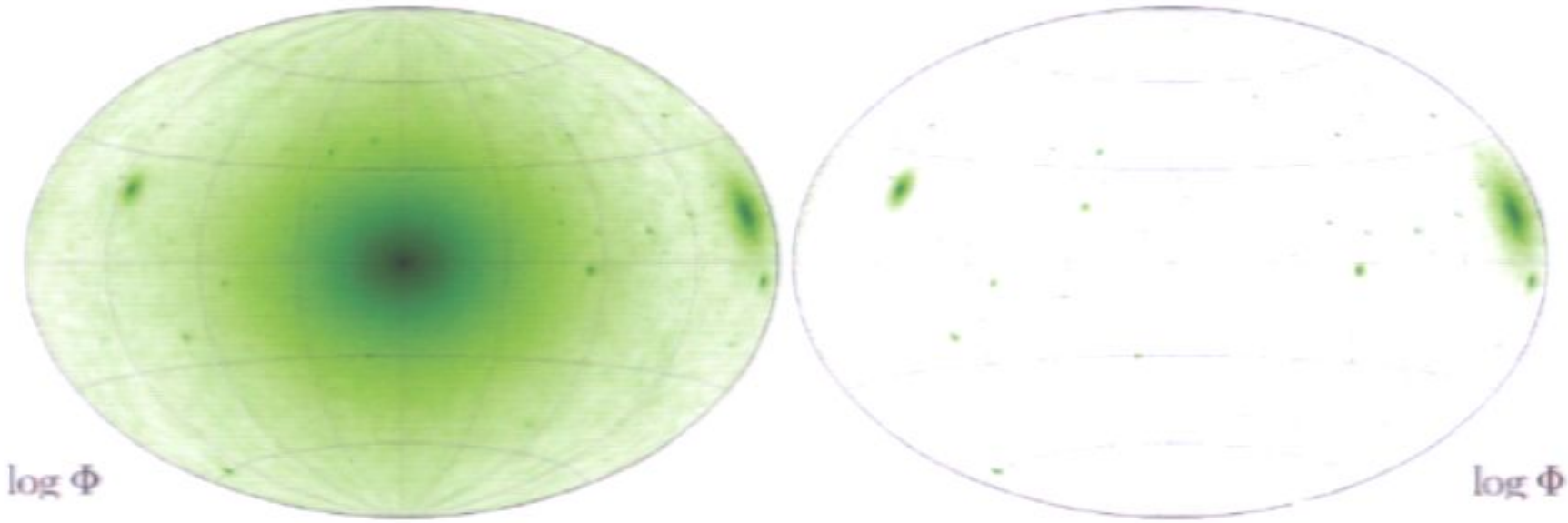

integrated los density-squared from simulations
from Kuhlen et al, 2008

substructure can enhance the signal from
indirect detection experiments, which probe annihilation by-products
and are therefore sensitive to the line-of-sight integral of ρ^2

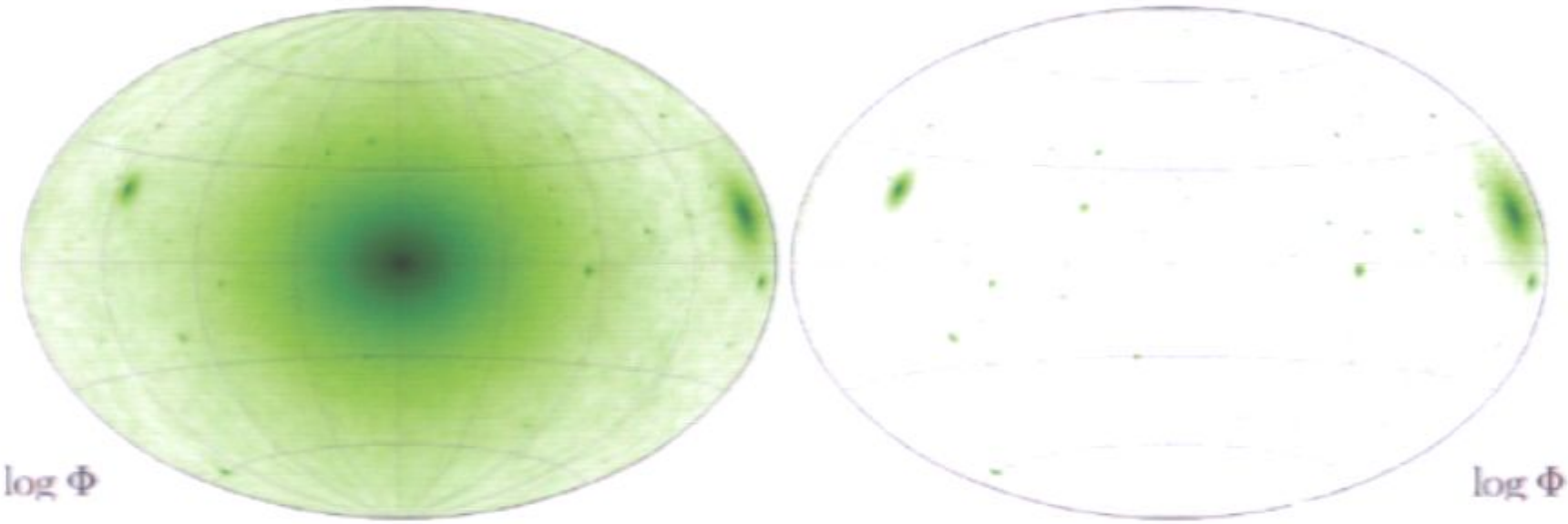

integrated los density-squared from simulations
from Kuhlen et al, 2008

substructure can enhance the signal from
indirect detection experiments, which probe annihilation by-products
and are therefore sensitive to the line-of-sight integral of ρ^2

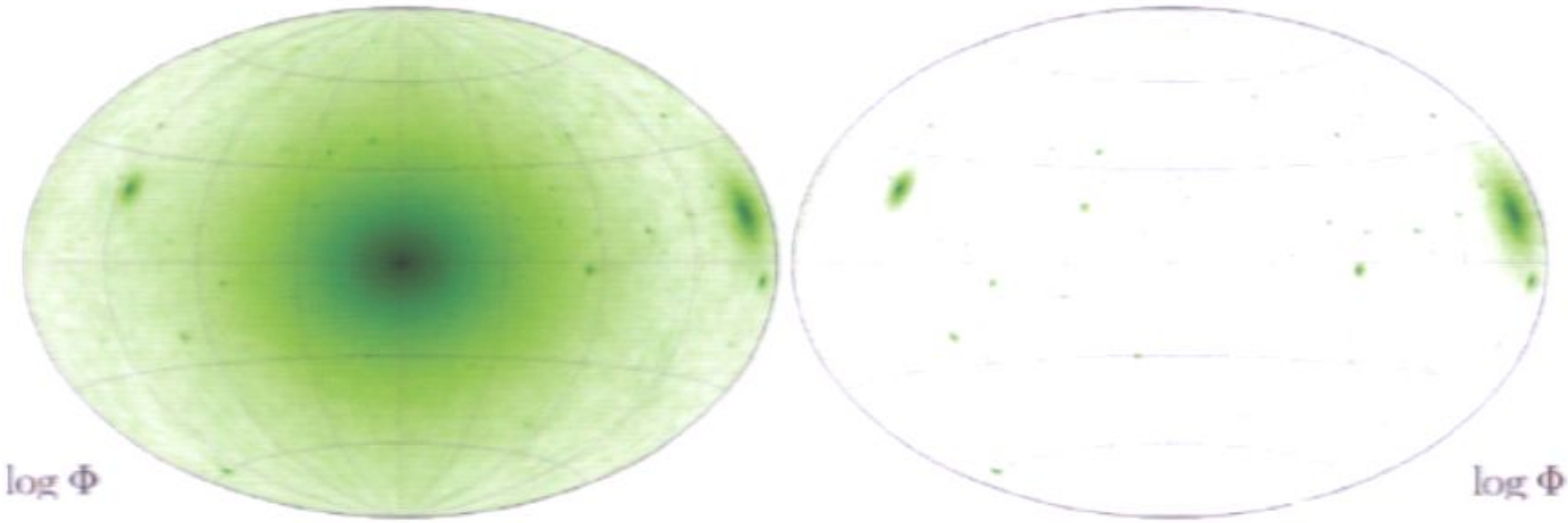

integrated los density-squared from simulations
from Kuhlen et al, 2008

substructure can enhance the signal from
indirect detection experiments, which probe annihilation by-products
and are therefore sensitive to the line-of-sight integral of ρ^2

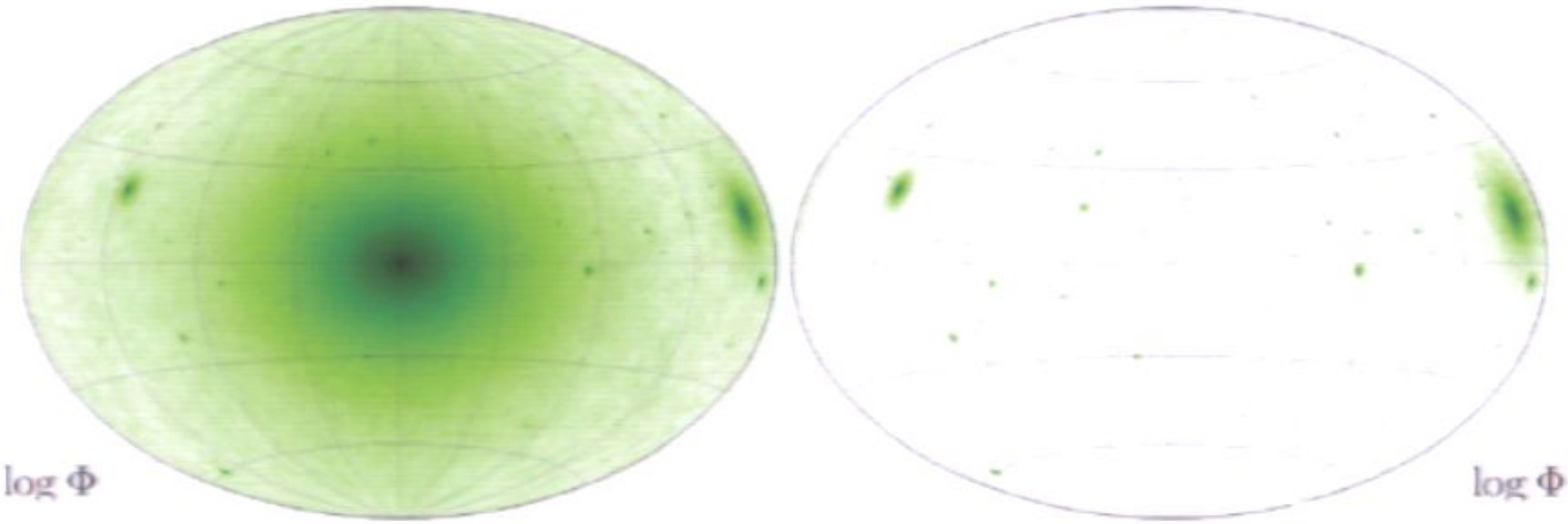

integrated los density-squared from simulations
from Kuhlen et al, 2008

substructure can enhance the signal from
indirect detection experiments, which probe annihilation by-products
and are therefore sensitive to the line-of-sight integral of ρ^2

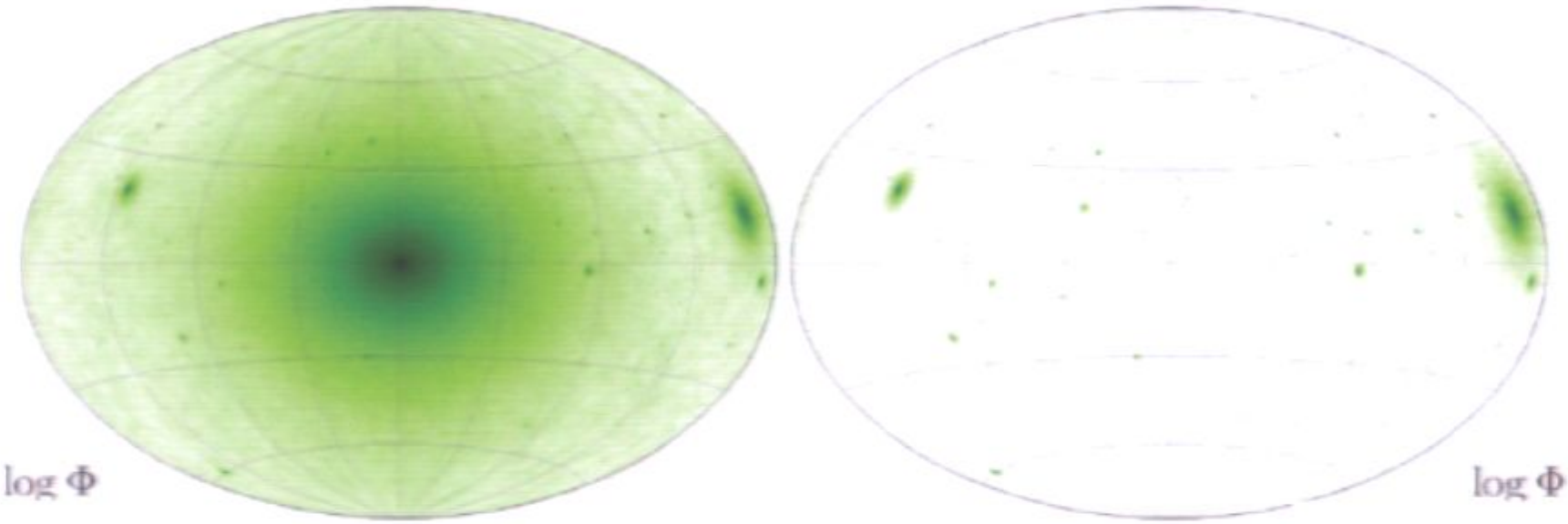

integrated los density-squared from simulations
from Kuhlen et al, 2008

substructure can enhance the signal from
indirect detection experiments, which probe annihilation by-products
and are therefore sensitive to the line-of-sight integral of ρ^2

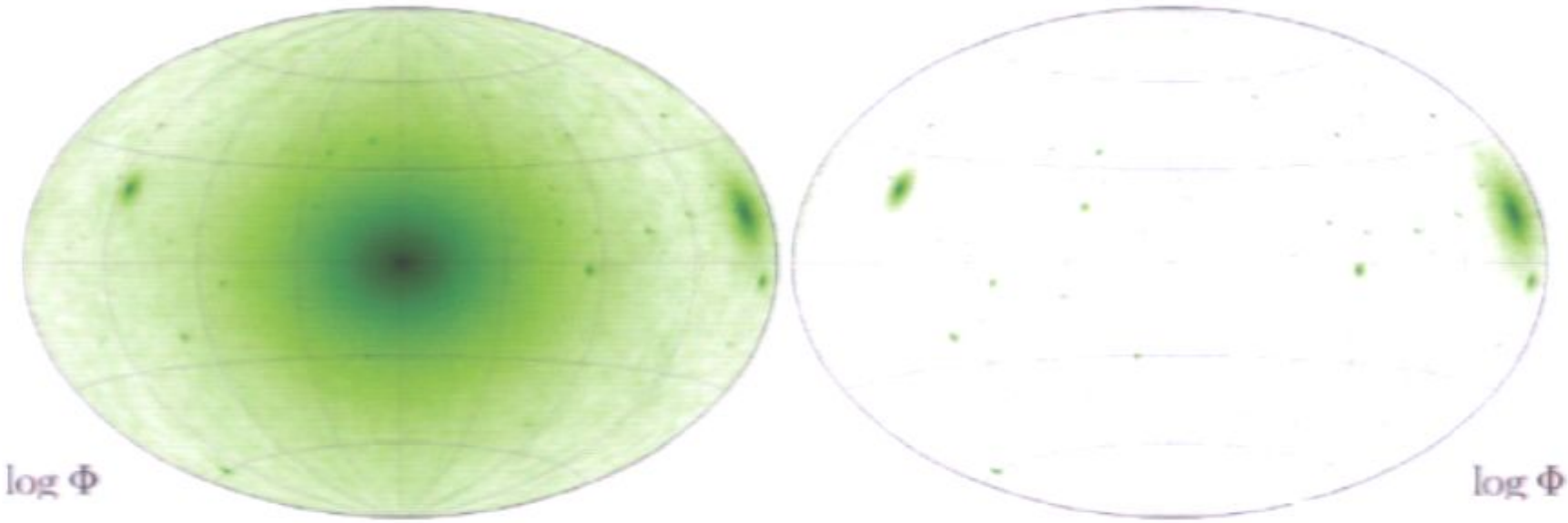

integrated los density-squared from simulations
from Kuhlen et al, 2008

substructure can enhance the signal from
indirect detection experiments, which probe annihilation by-products
and are therefore sensitive to the line-of-sight integral of ρ^2

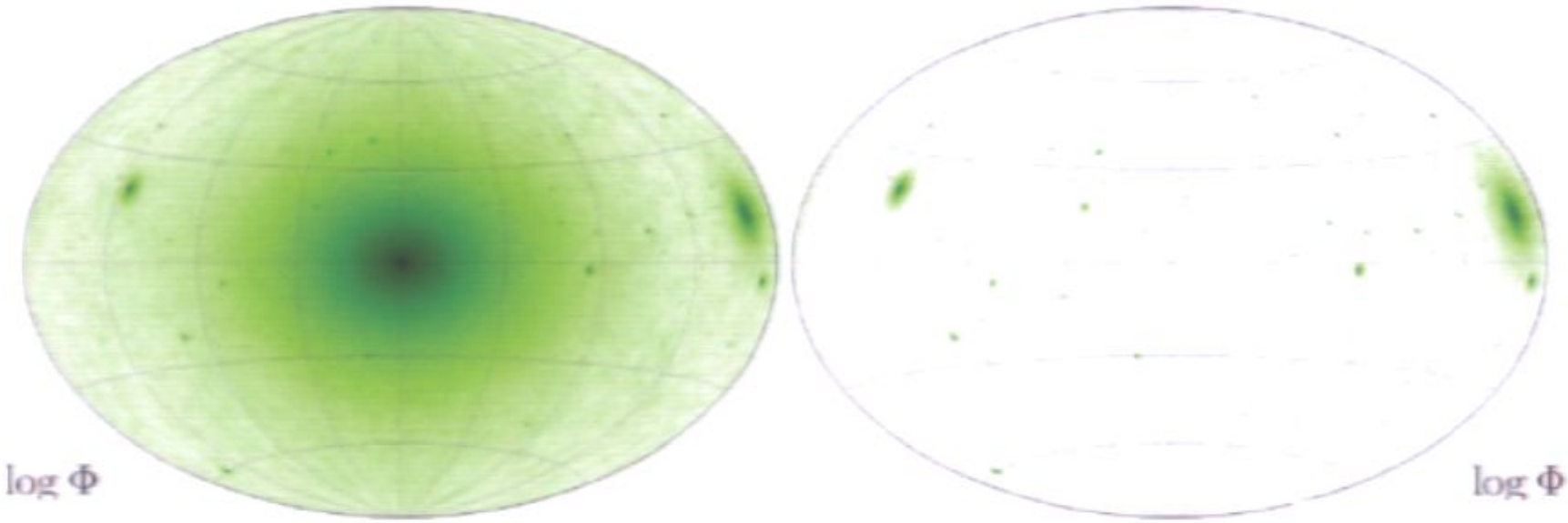

integrated los density-squared from simulations
from Kuhlen et al, 2008

meta-analysis of subhalo mass function derived from 21 different simulation studies (see Elahi et al 2009)

slope

$$\frac{dN}{d\ln f} = Af^{-\alpha}$$

normalization

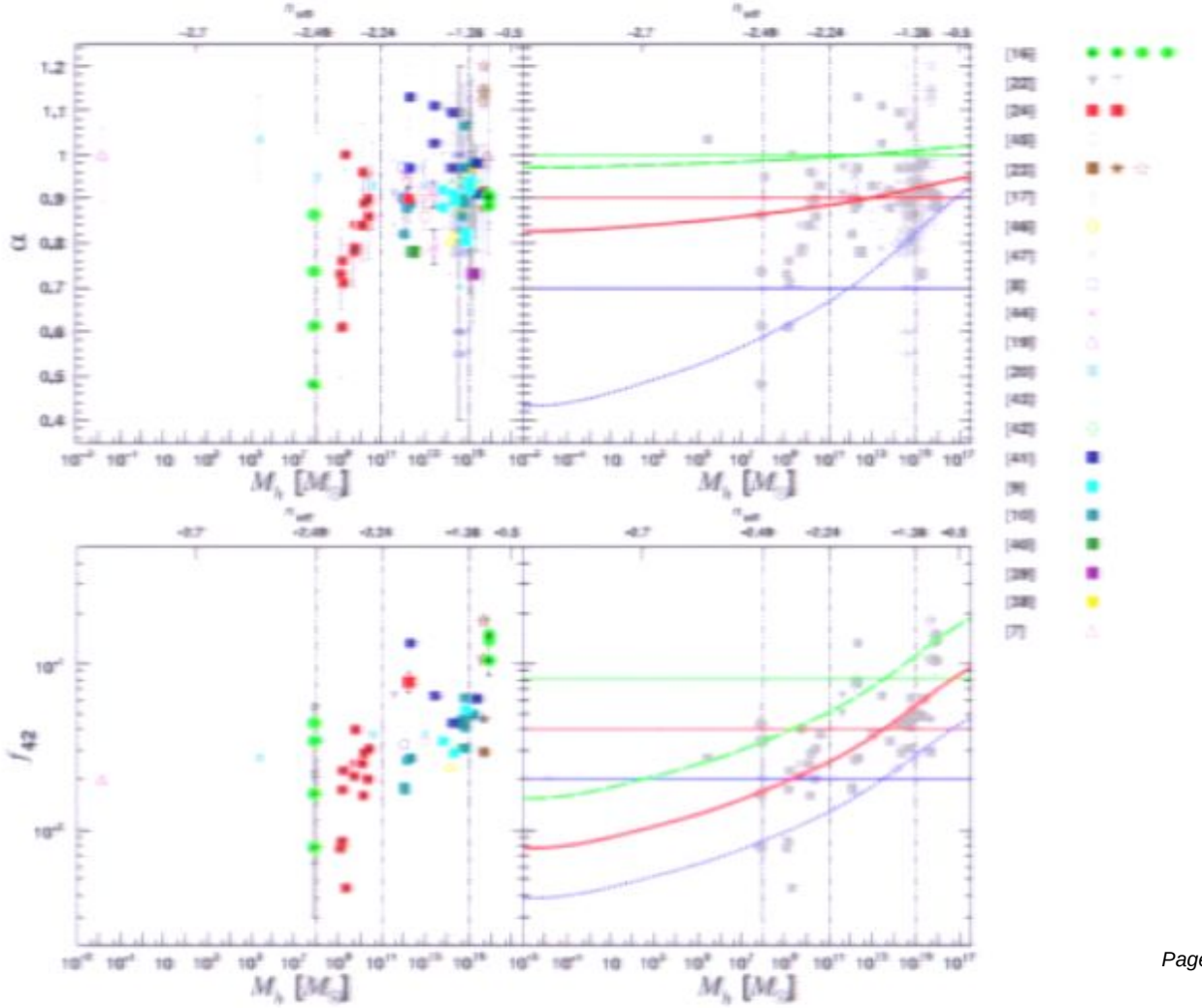

meta-analysis of subhalo mass function derived from 21 different simulation studies (see Elahi et al 2009)

slope

$$\frac{dN}{d\ln f} = Af^{-\alpha}$$

normalization

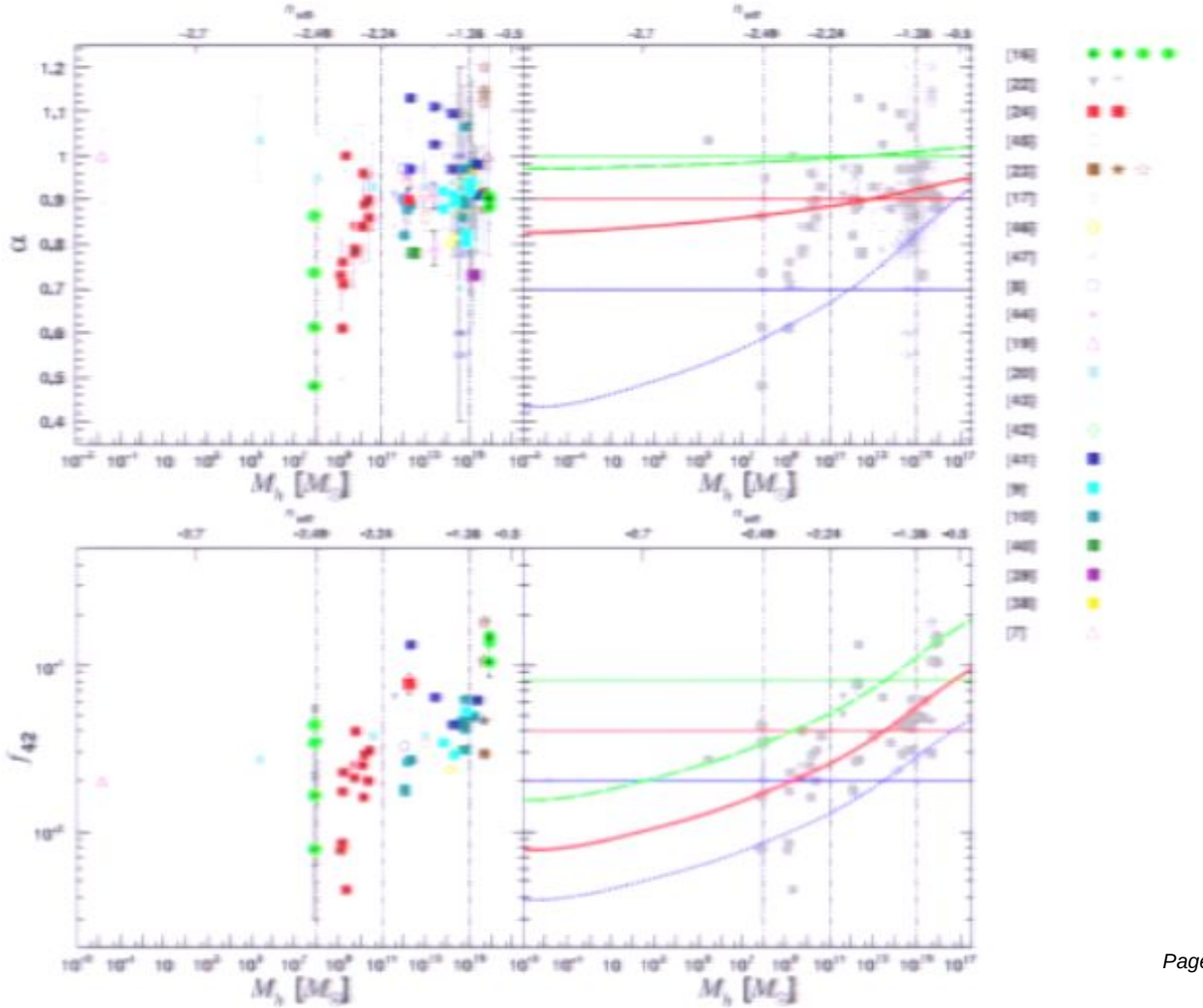

meta-analysis of subhalo mass function derived from 21 different simulation studies (see Elahi et al 2009)

slope

normalization

$$\frac{dN}{d\ln f} = Af^{-\alpha}$$

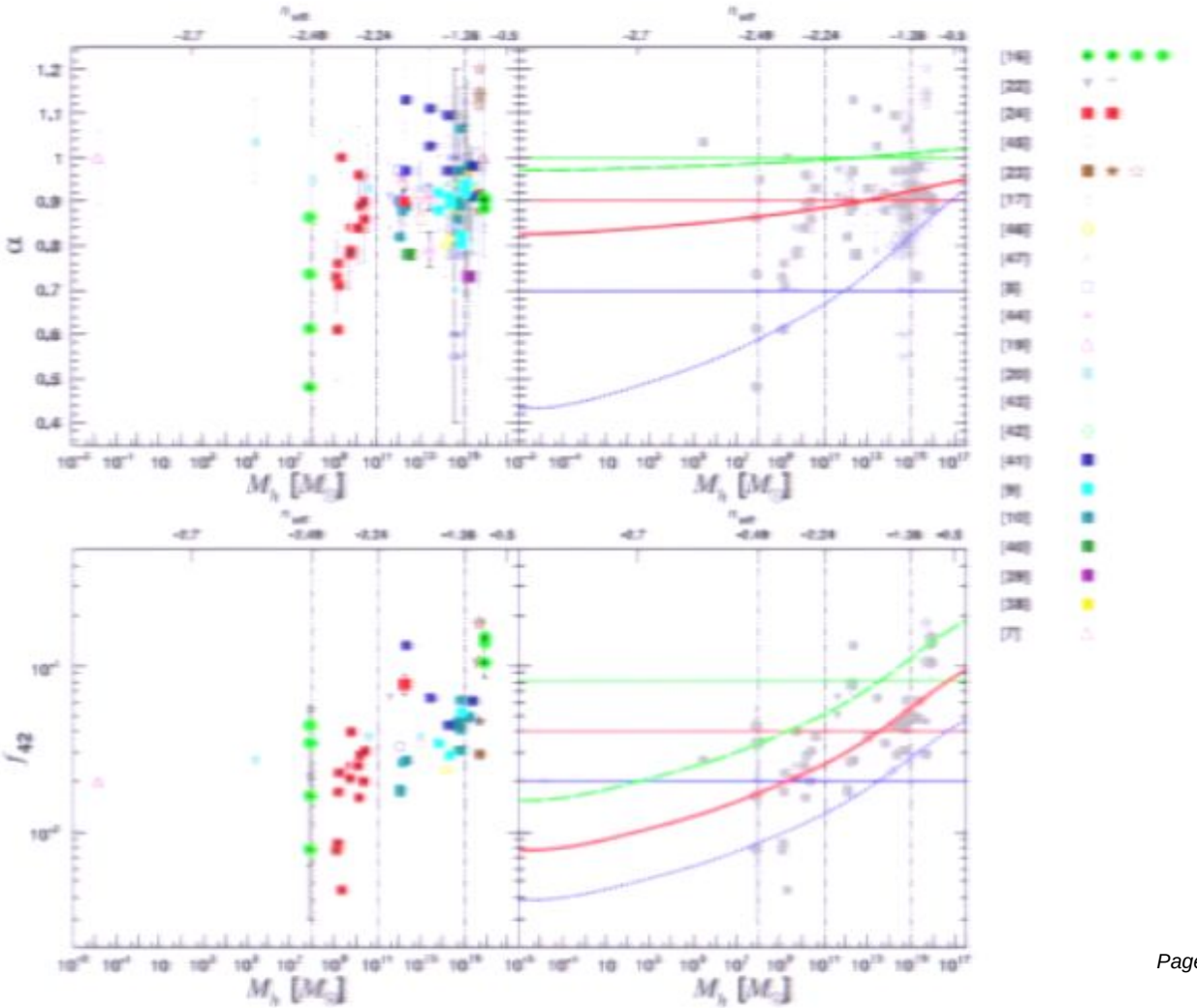

meta-analysis of subhalo mass function derived from 21 different simulation studies (see Elahi et al 2009)

slope

normalization

$$\frac{dN}{d\ln f} = Af^{-\alpha}$$

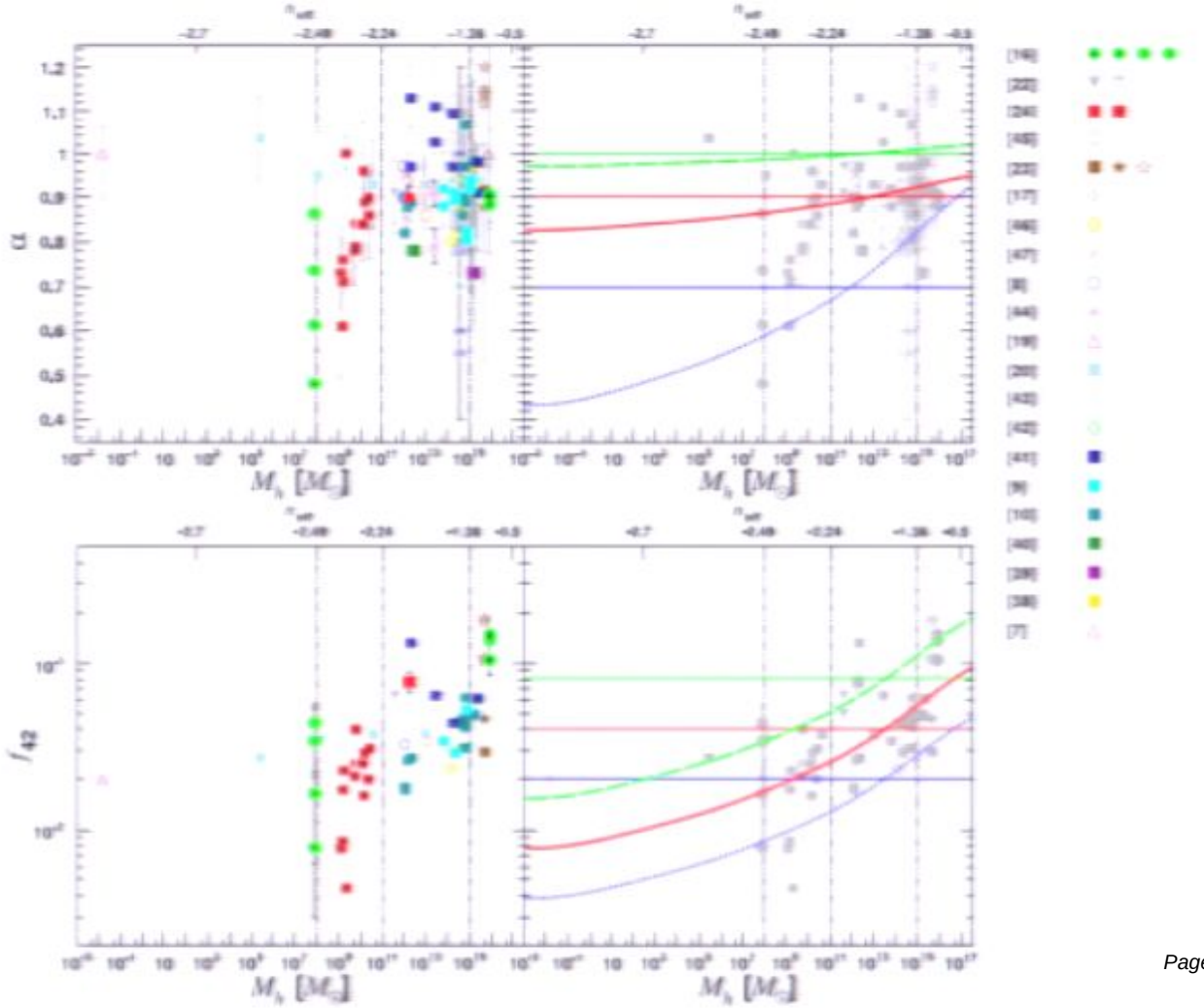

meta-analysis of subhalo mass function derived from 21 different simulation studies (see Elahi et al 2009)

slope

normalization

$$\frac{dN}{d\ln f} = Af^{-\alpha}$$

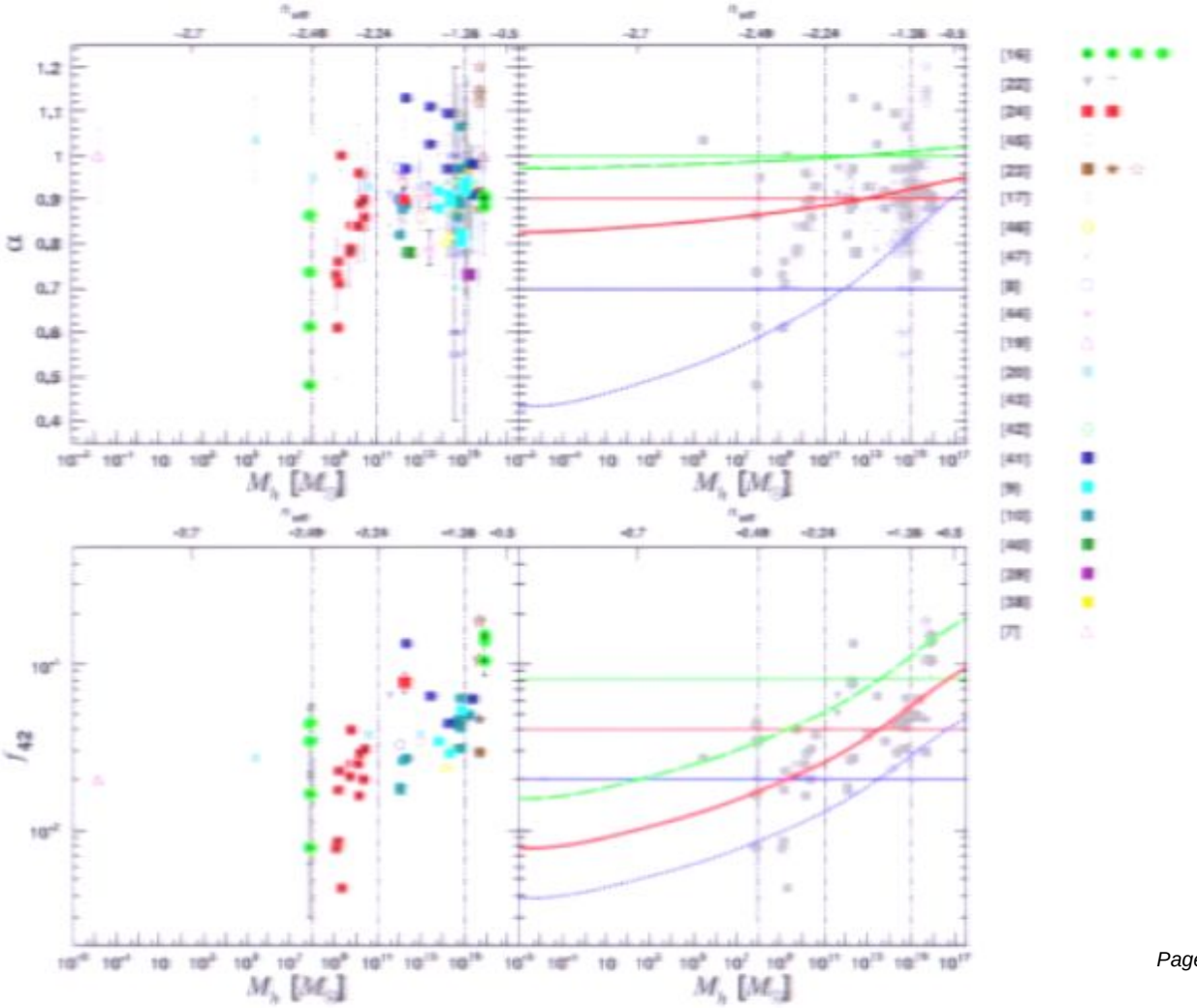

meta-analysis of subhalo mass function derived from 21 different simulation studies (see Elahi et al 2009)

slope

normalization

$$\frac{dN}{d\ln f} = Af^{-\alpha}$$

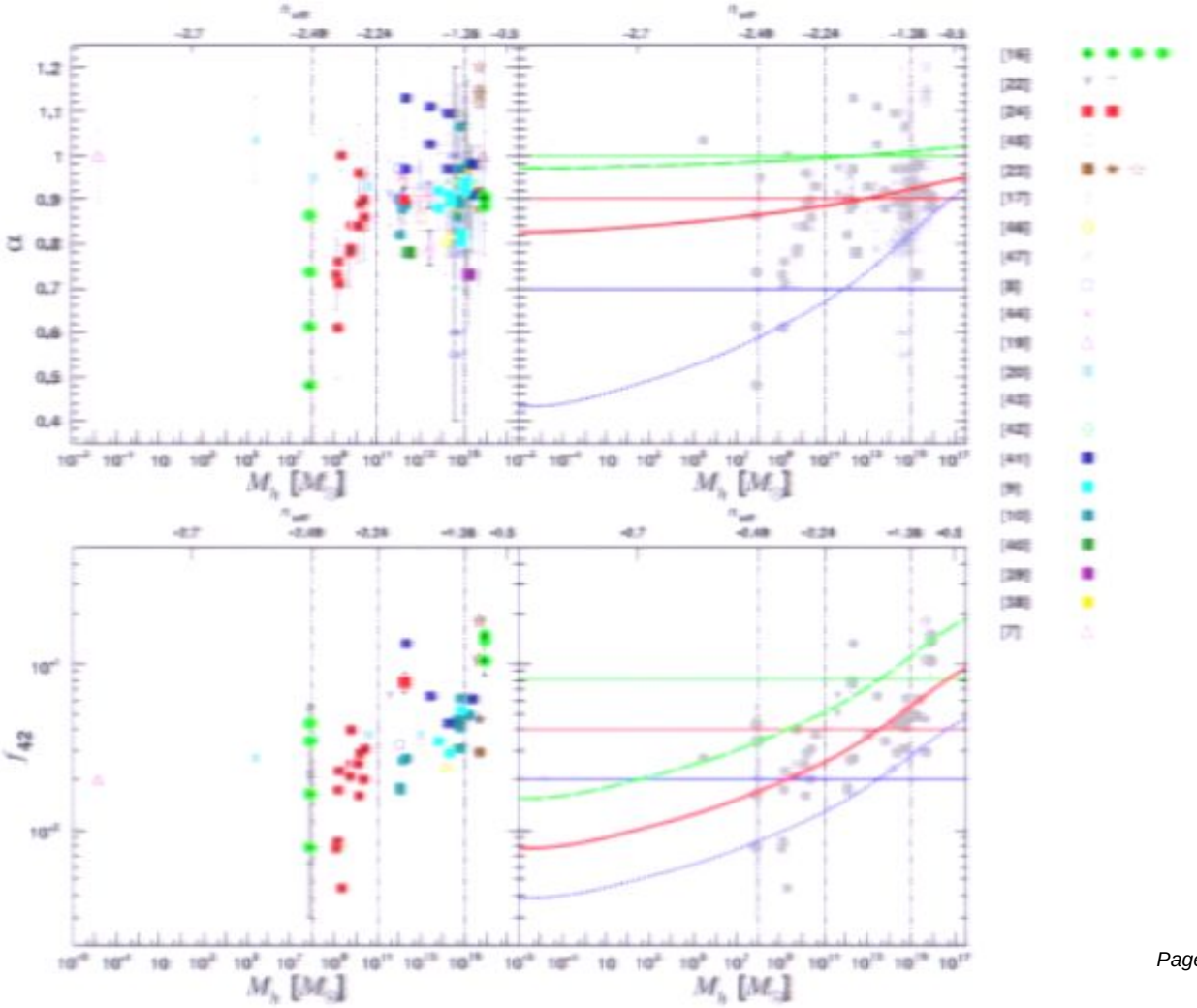

meta-analysis of subhalo mass function derived from 21 different simulation studies (see Elahi et al 2009)

slope

$$\frac{dN}{d\ln f} = Af^{-\alpha}$$

normalization

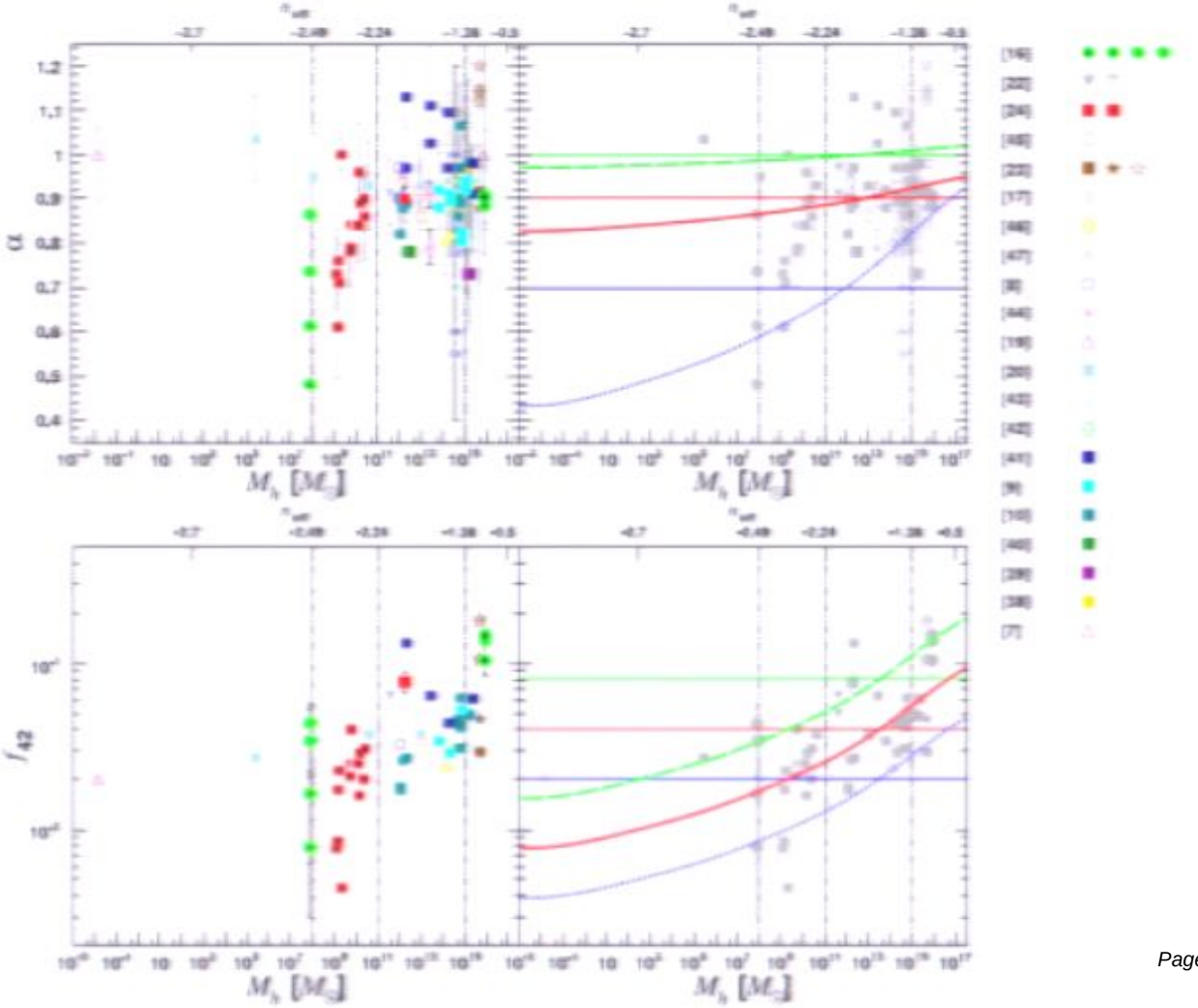

meta-analysis of subhalo mass function derived from 21 different simulation studies (see Elahi et al 2009)

slope

normalization

$$\frac{dN}{d\ln f} = Af^{-\alpha}$$

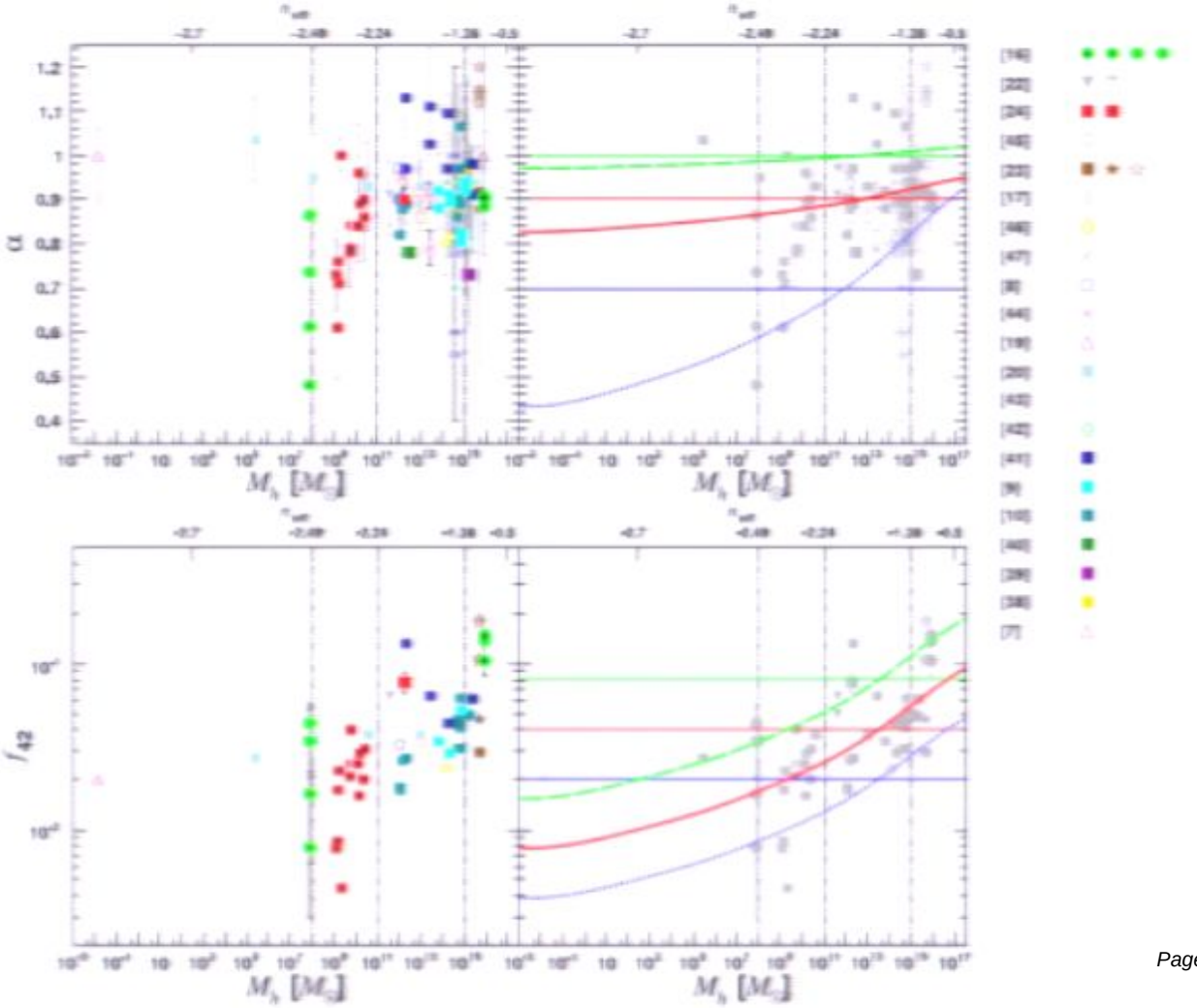

meta-analysis of subhalo mass function derived from 21 different simulation studies (see Elahi et al 2009)

slope

normalization

$$\frac{dN}{d\ln f} = Af^{-\alpha}$$

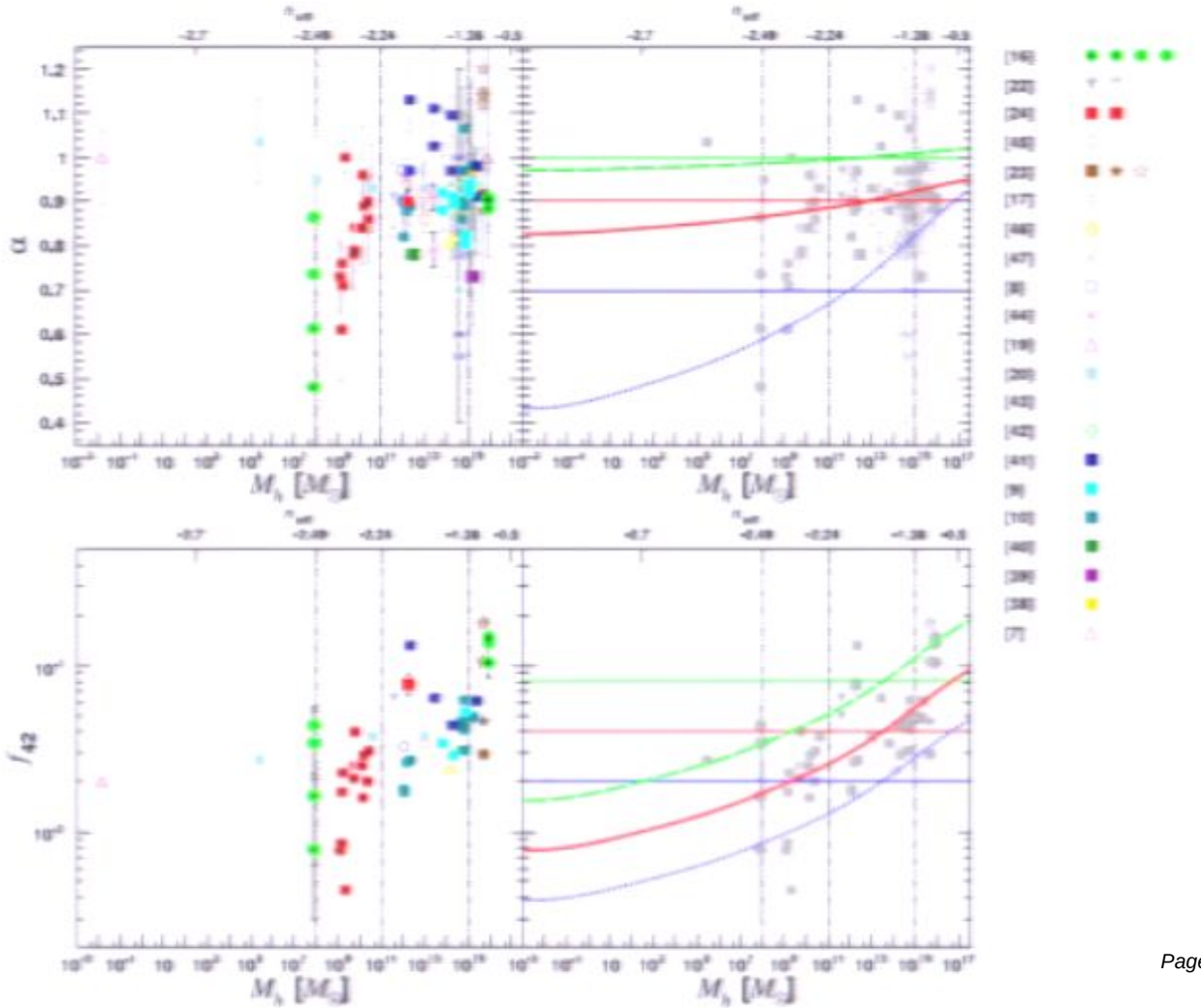

meta-analysis of subhalo mass function derived from 21 different simulation studies (see Elahi et al 2009)

slope

normalization

$$\frac{dN}{d\ln f} = Af^{-\alpha}$$

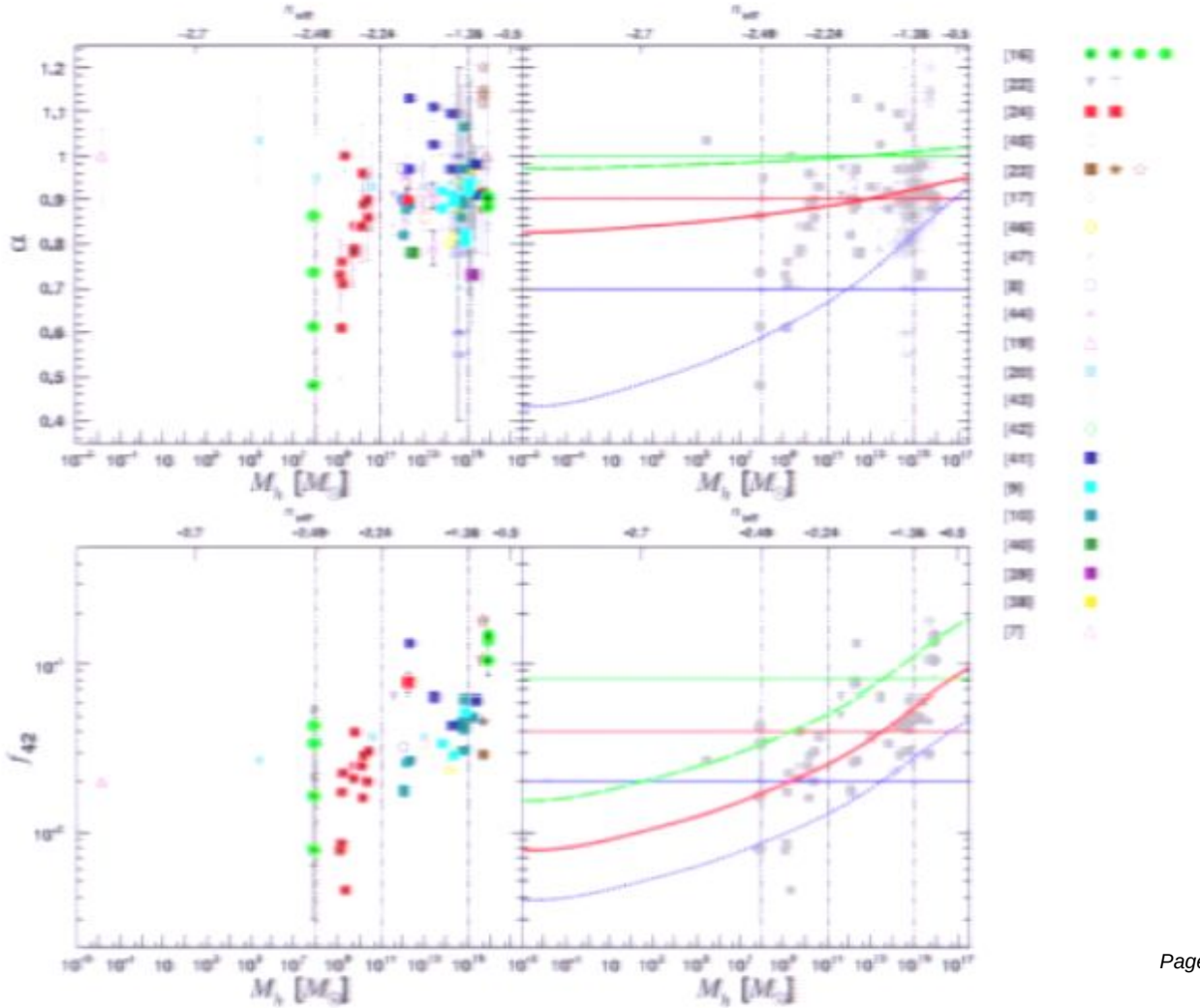

meta-analysis of subhalo mass function derived from 21 different simulation studies (see Elahi et al 2009)

slope

normalization

$$\frac{dN}{d\ln f} = Af^{-\alpha}$$

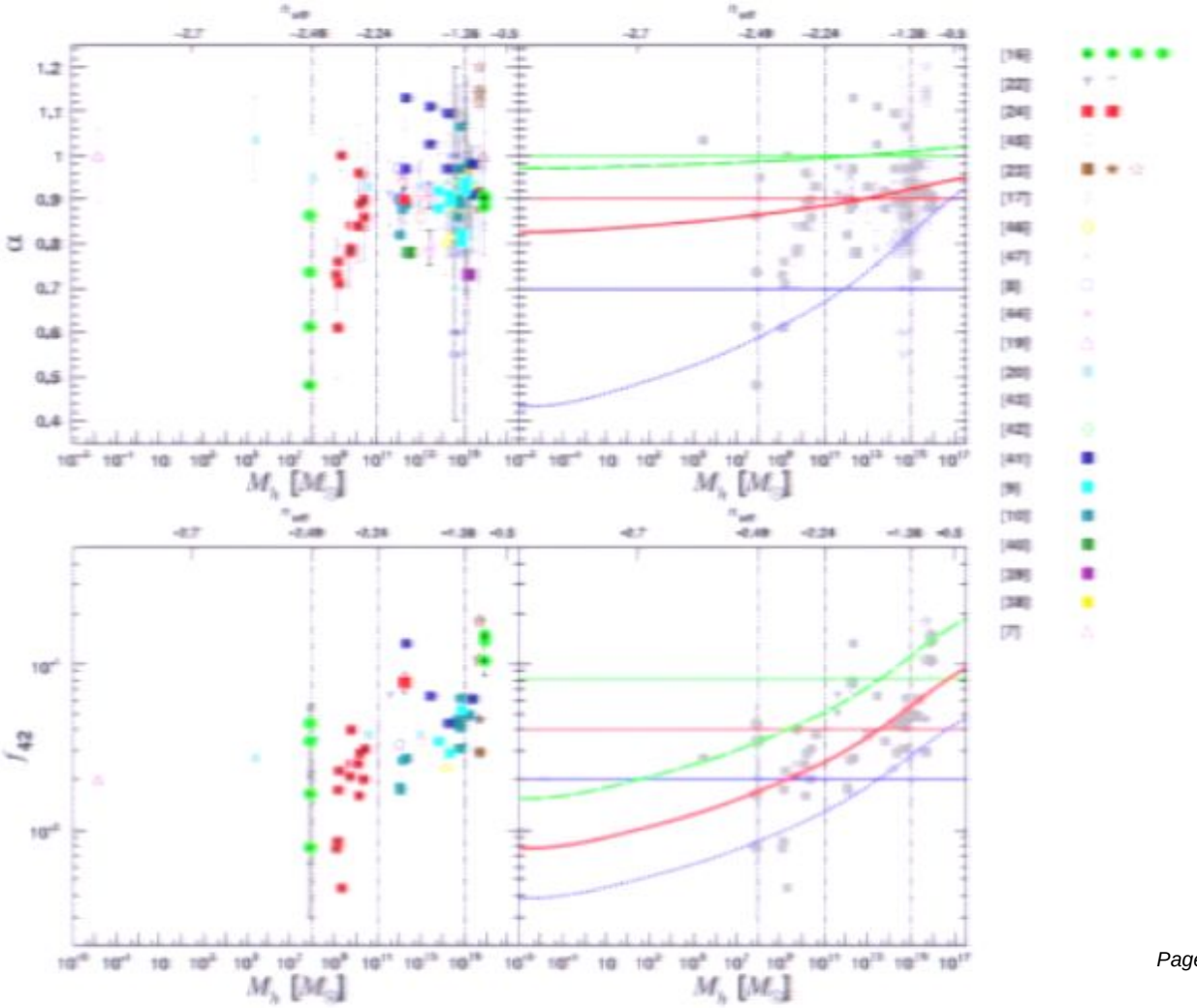

meta-analysis of subhalo mass function derived from 21 different simulation studies (see Elahi et al 2009)

slope

$$\frac{dN}{d\ln f} = Af^{-\alpha}$$

normalization

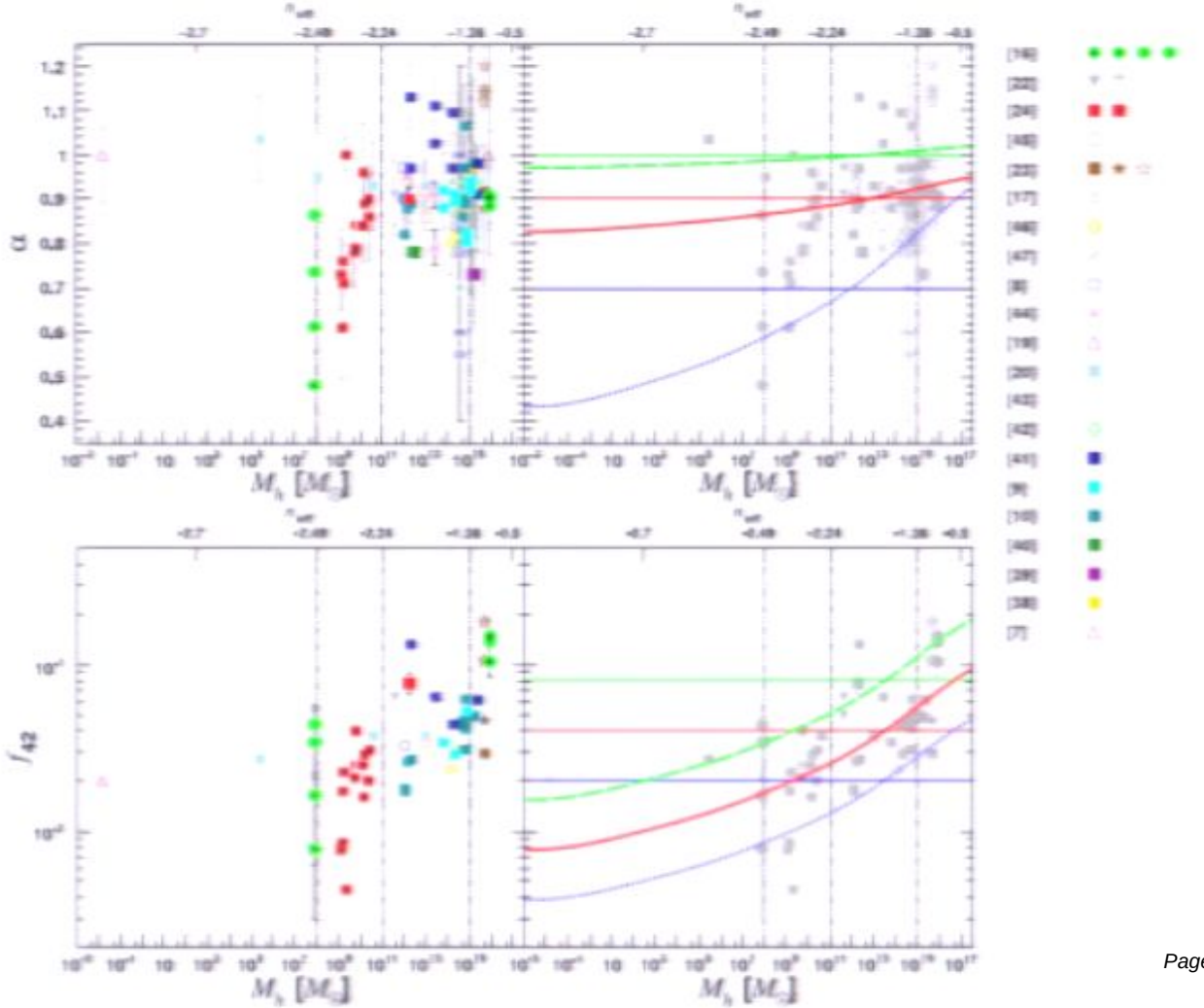

meta-analysis of subhalo mass function derived from 21 different simulation studies (see Elahi et al 2009)

slope

$$\frac{dN}{d\ln f} = Af^{-\alpha}$$

normalization

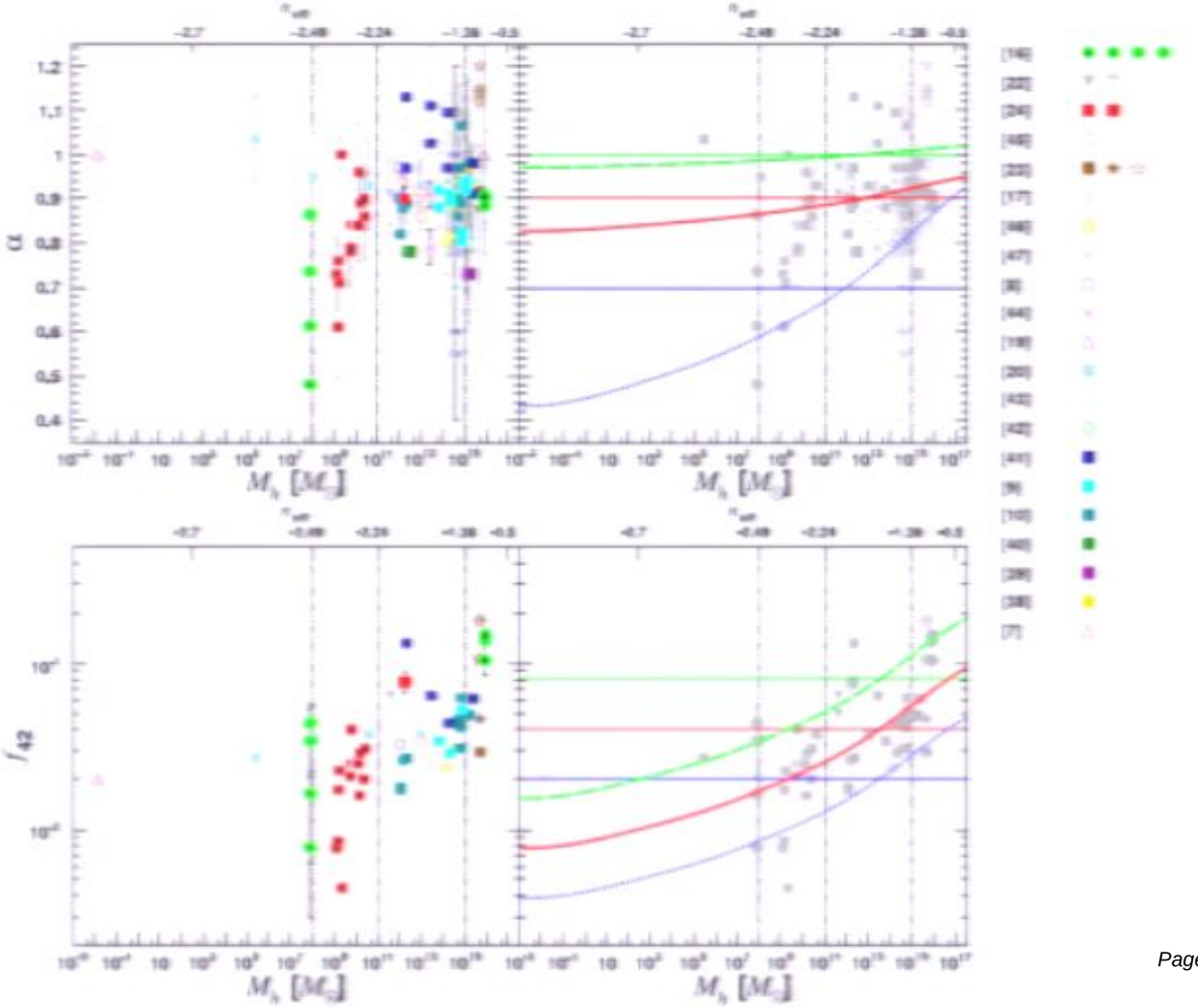

meta-analysis of subhalo mass function derived from 21 different simulation studies (see Elahi et al 2009)

slope

$$\frac{dN}{d\ln f} = Af^{-\alpha}$$

normalization

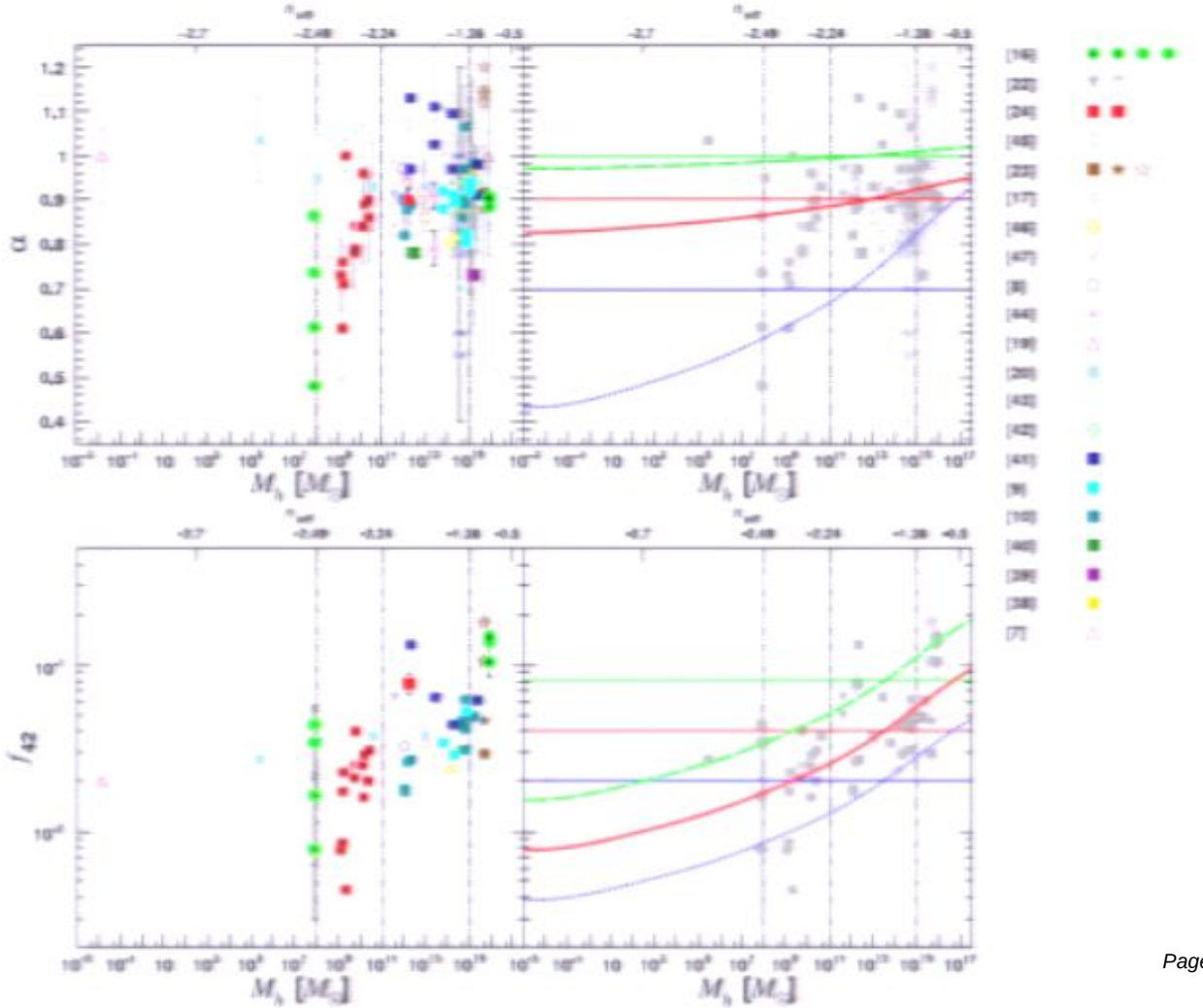

meta-analysis of subhalo mass function derived from 21 different simulation studies (see Elahi et al 2009)

slope

normalization

$$\frac{dN}{d\ln f} = Af^{-\alpha}$$

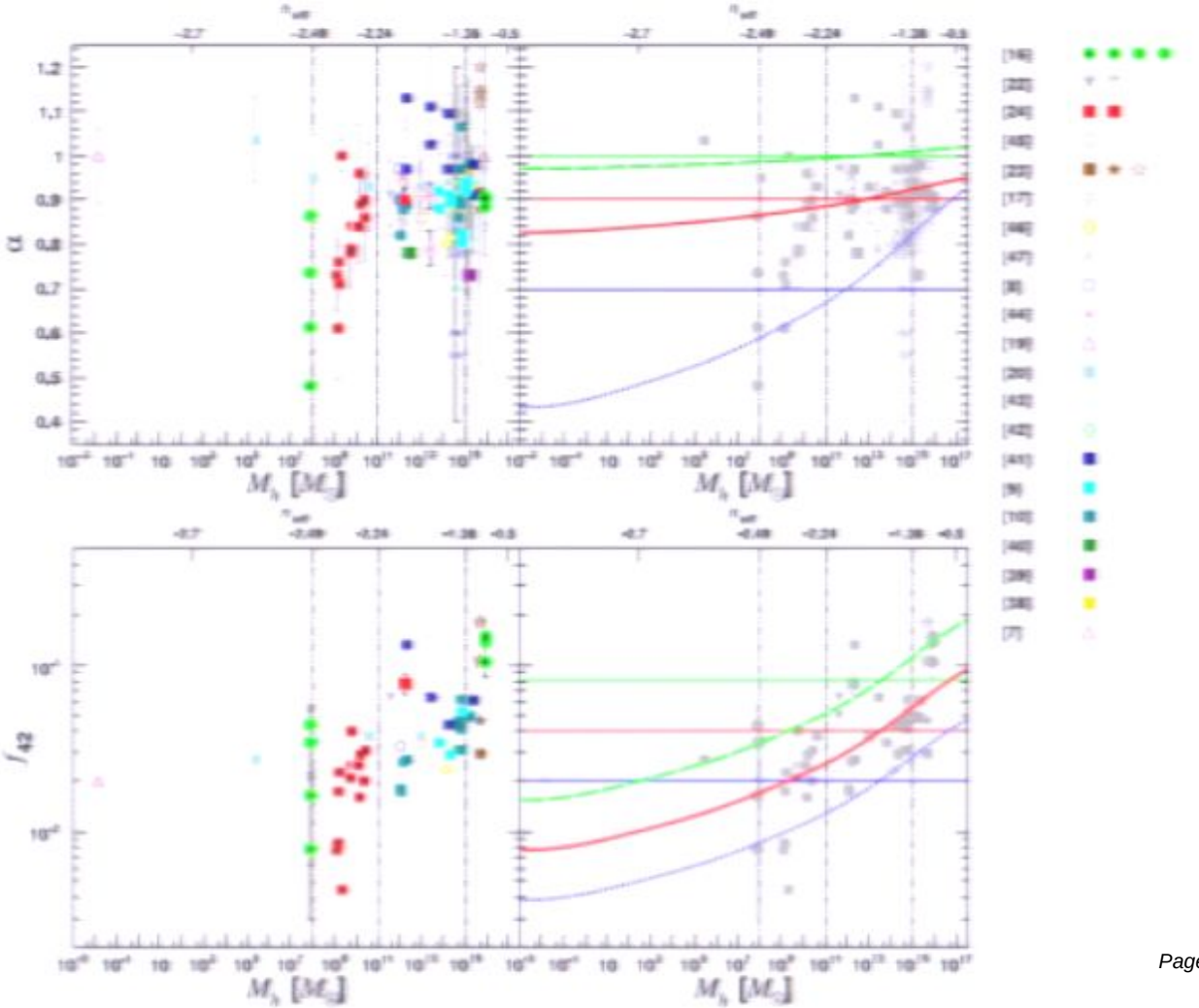

meta-analysis of subhalo mass function derived from 21 different simulation studies (see Elahi et al 2009)

slope

normalization

$$\frac{dN}{d\ln f} = Af^{-\alpha}$$

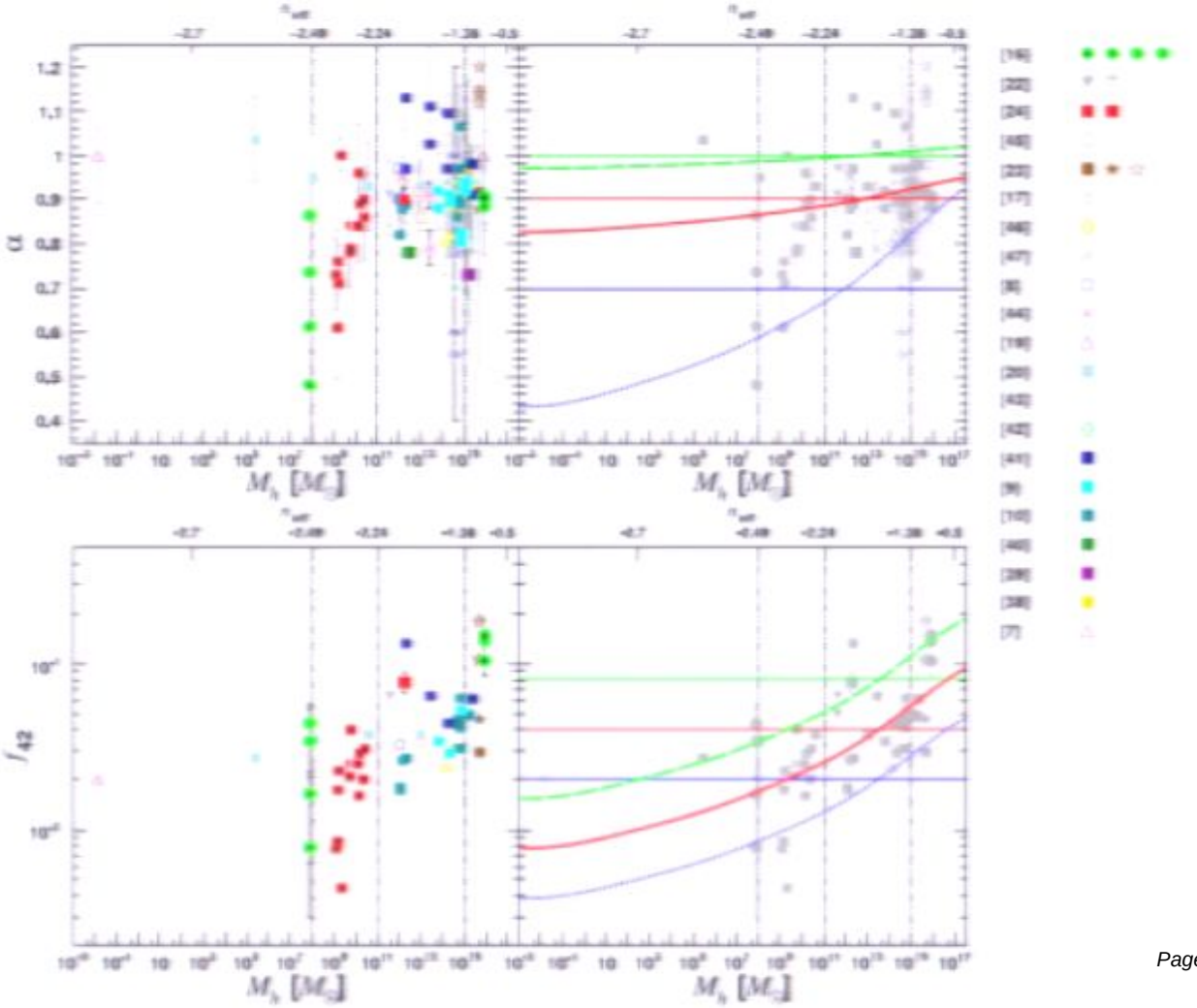

meta-analysis of subhalo mass function derived from 21 different simulation studies (see Elahi et al 2009)

slope

$$\frac{dN}{d\ln f} = Af^{-\alpha}$$

normalization

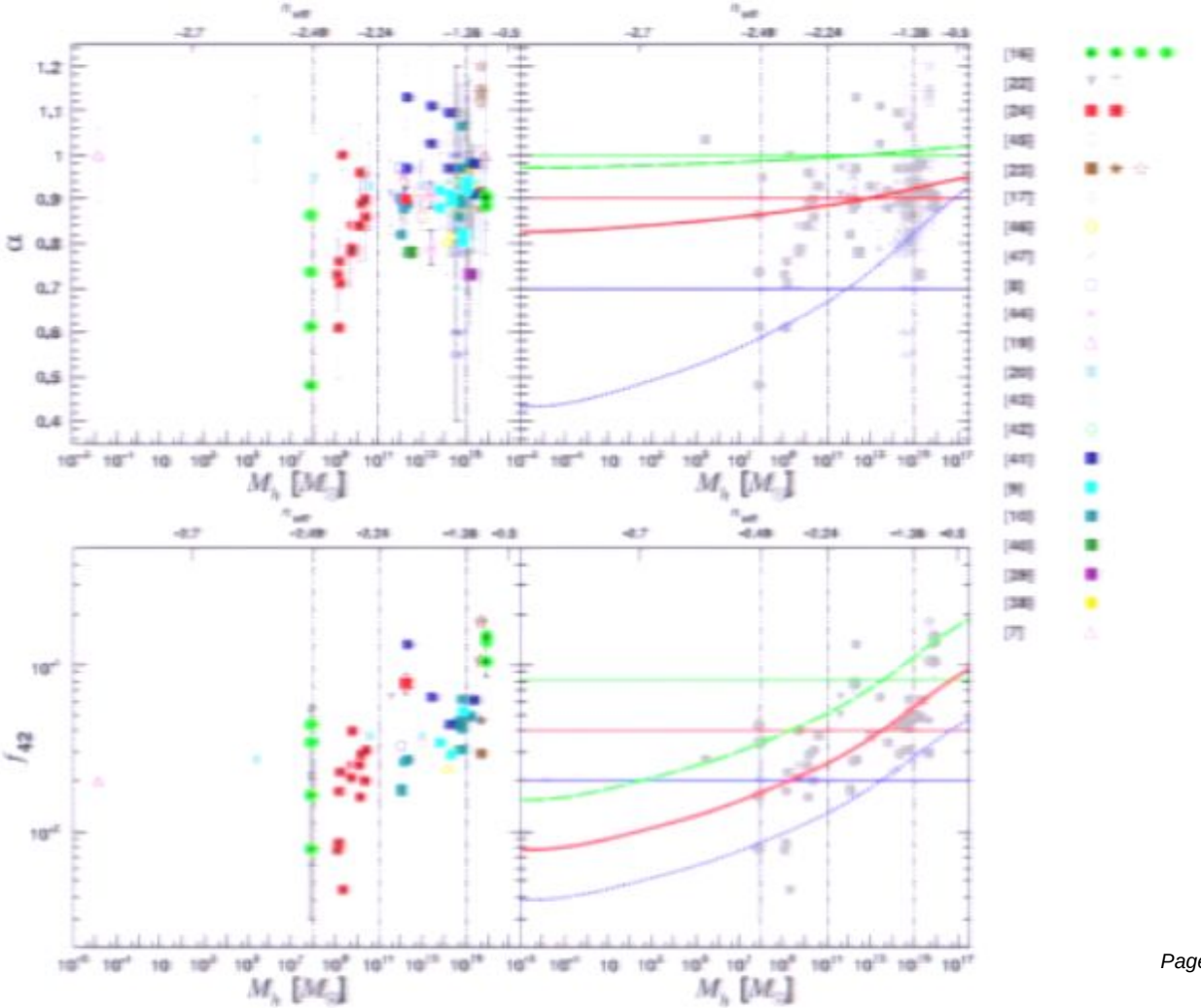

meta-analysis of subhalo mass function derived from 21 different simulation studies (see Elahi et al 2009)

$$\frac{dN}{d\ln f} = Af^{-\alpha}$$

slope

normalization

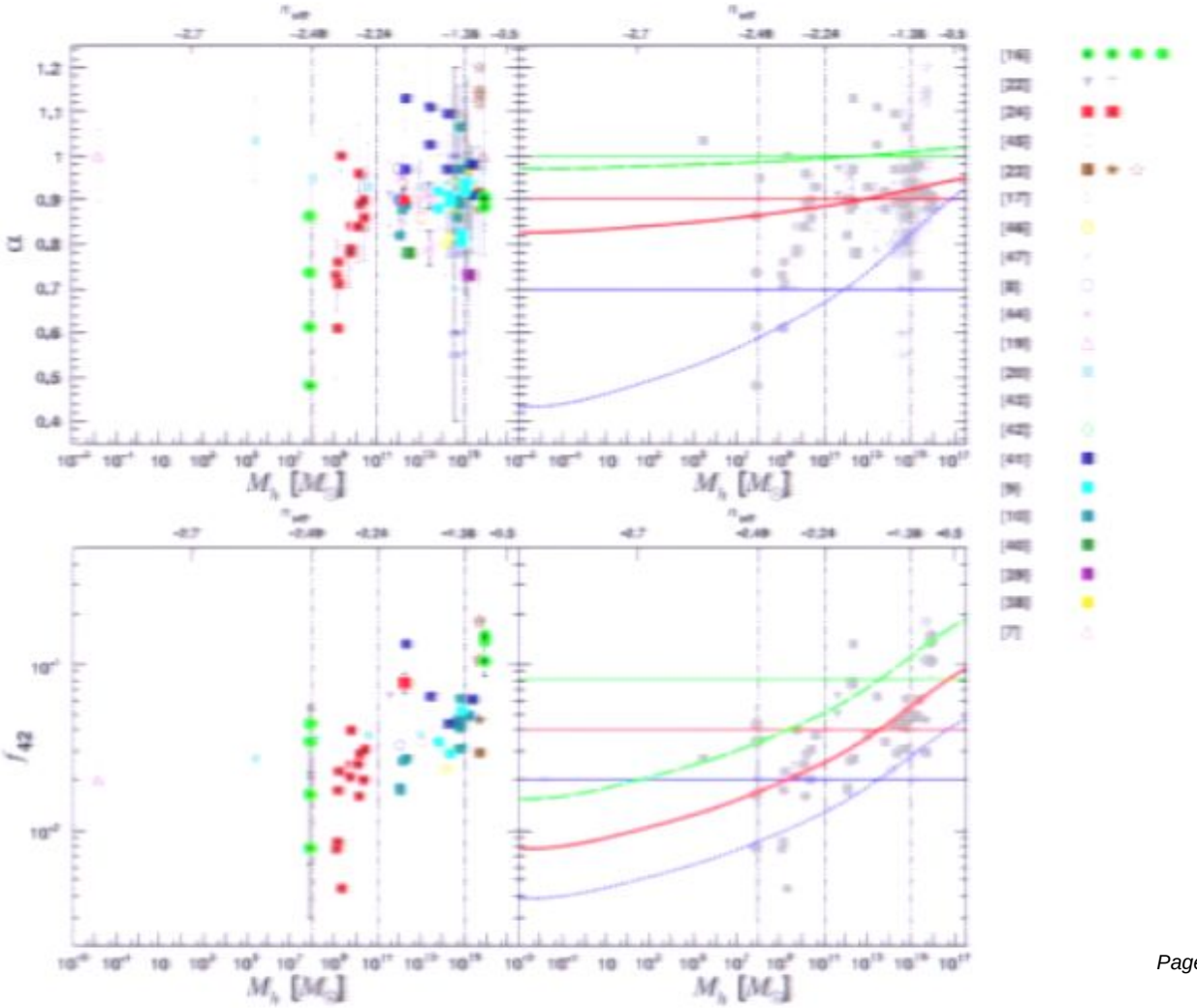

meta-analysis of subhalo mass function derived from 21 different simulation studies (see Elahi et al 2009)

slope

normalization

$$\frac{dN}{d\ln f} = Af^{-\alpha}$$

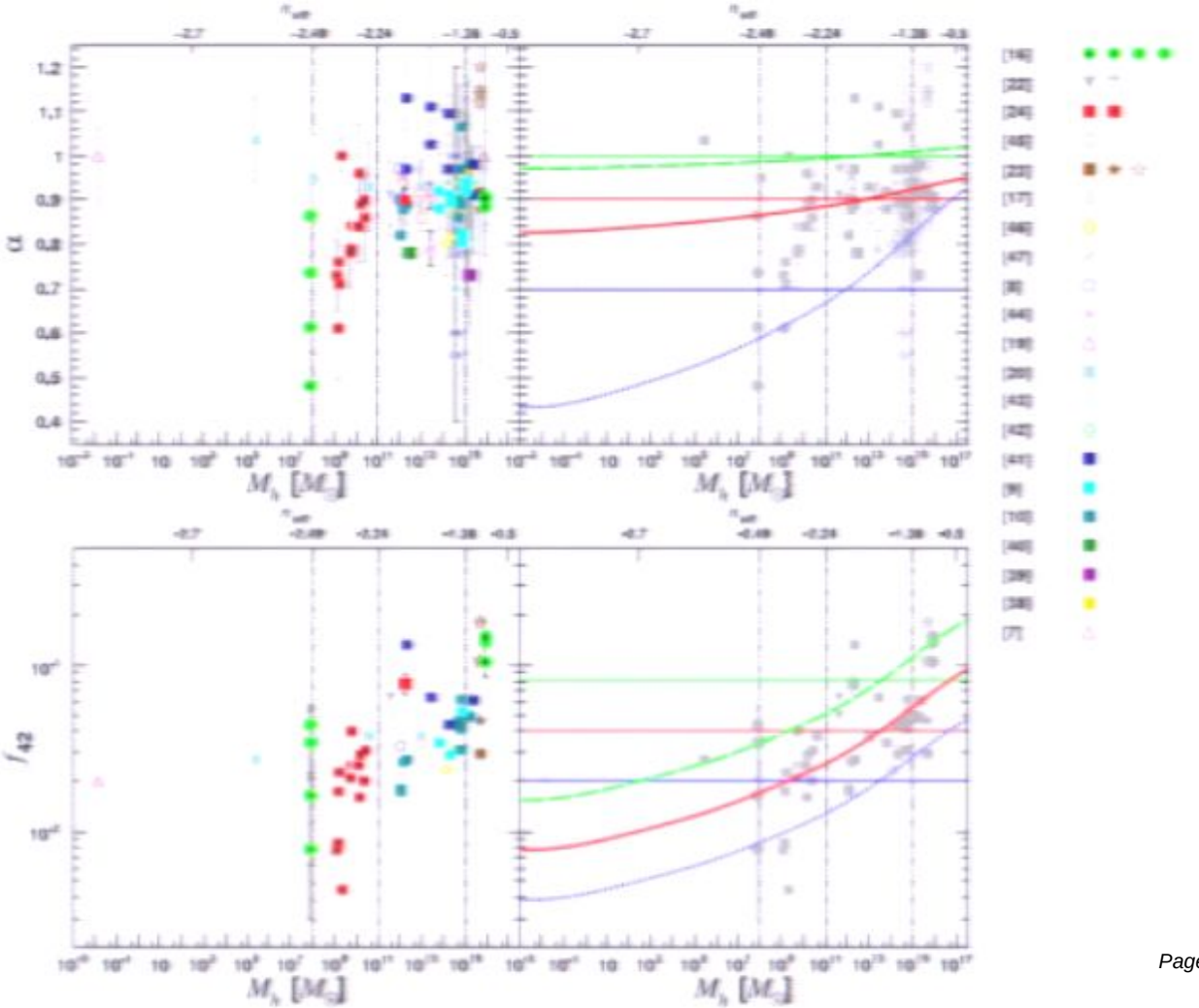

meta-analysis of subhalo mass function derived from 21 different simulation studies (see Elahi et al 2009)

slope

normalization

$$\frac{dN}{d\ln f} = Af^{-\alpha}$$

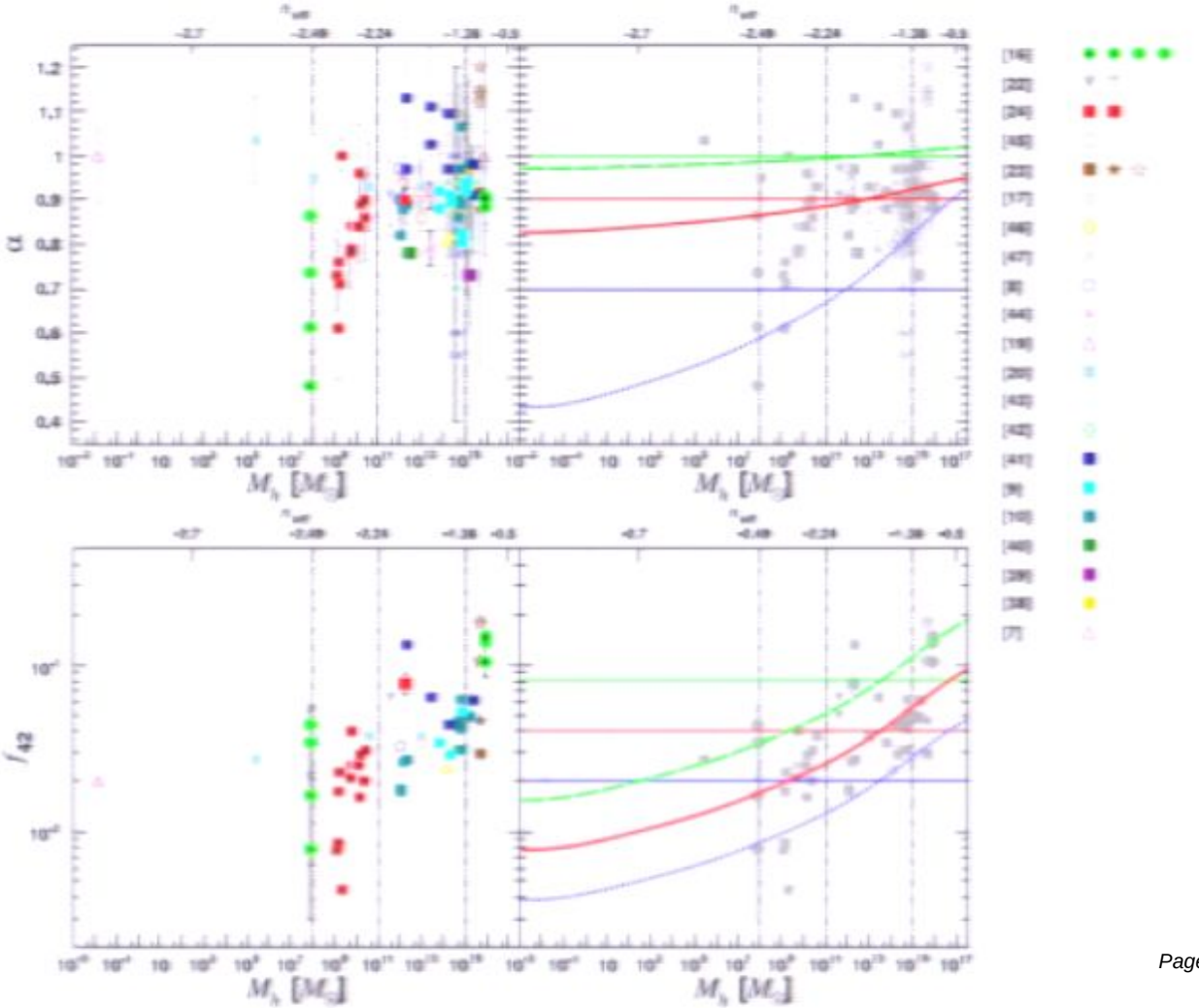

meta-analysis of subhalo mass function derived from 21 different simulation studies (see Elahi et al 2009)

slope

$$\frac{dN}{d\ln f} = Af^{-\alpha}$$

normalization

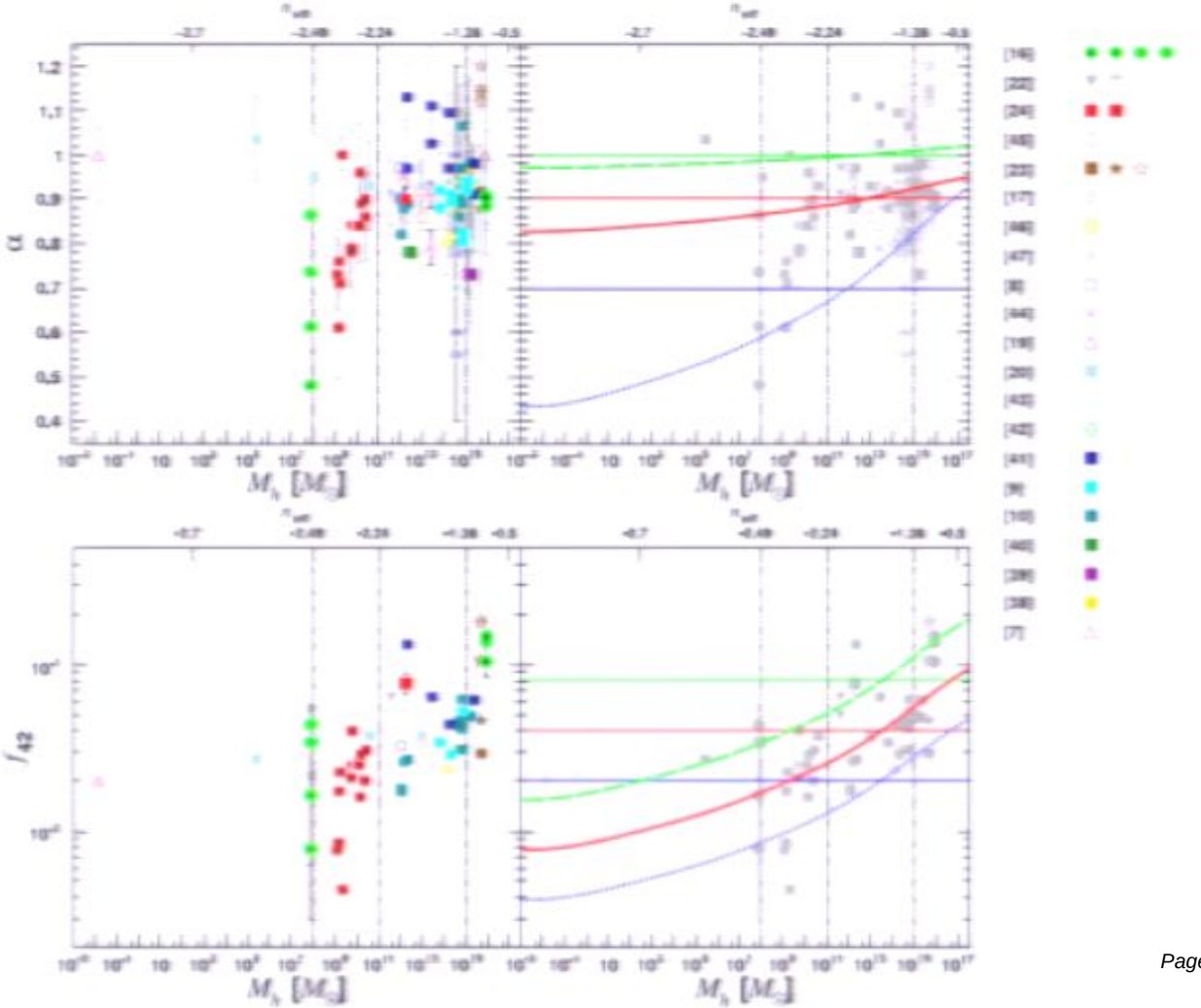

meta-analysis of subhalo mass function derived from 21 different simulation studies (see Elahi et al 2009)

slope

normalization

$$\frac{dN}{d\ln f} = Af^{-\alpha}$$

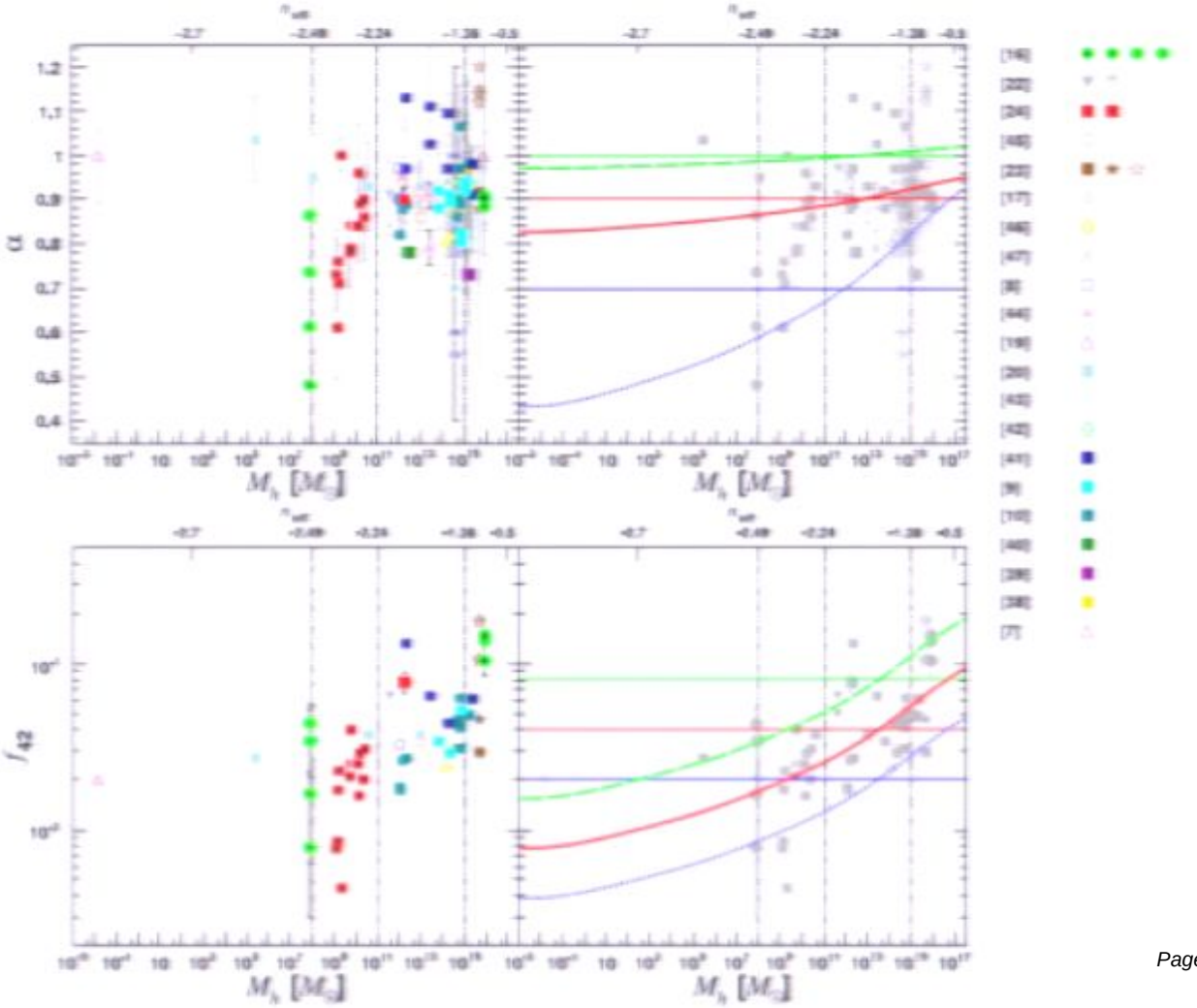

meta-analysis of subhalo mass function derived from 21 different simulation studies (see Elahi et al 2009)

slope

normalization

$$\frac{dN}{d\ln f} = Af^{-\alpha}$$

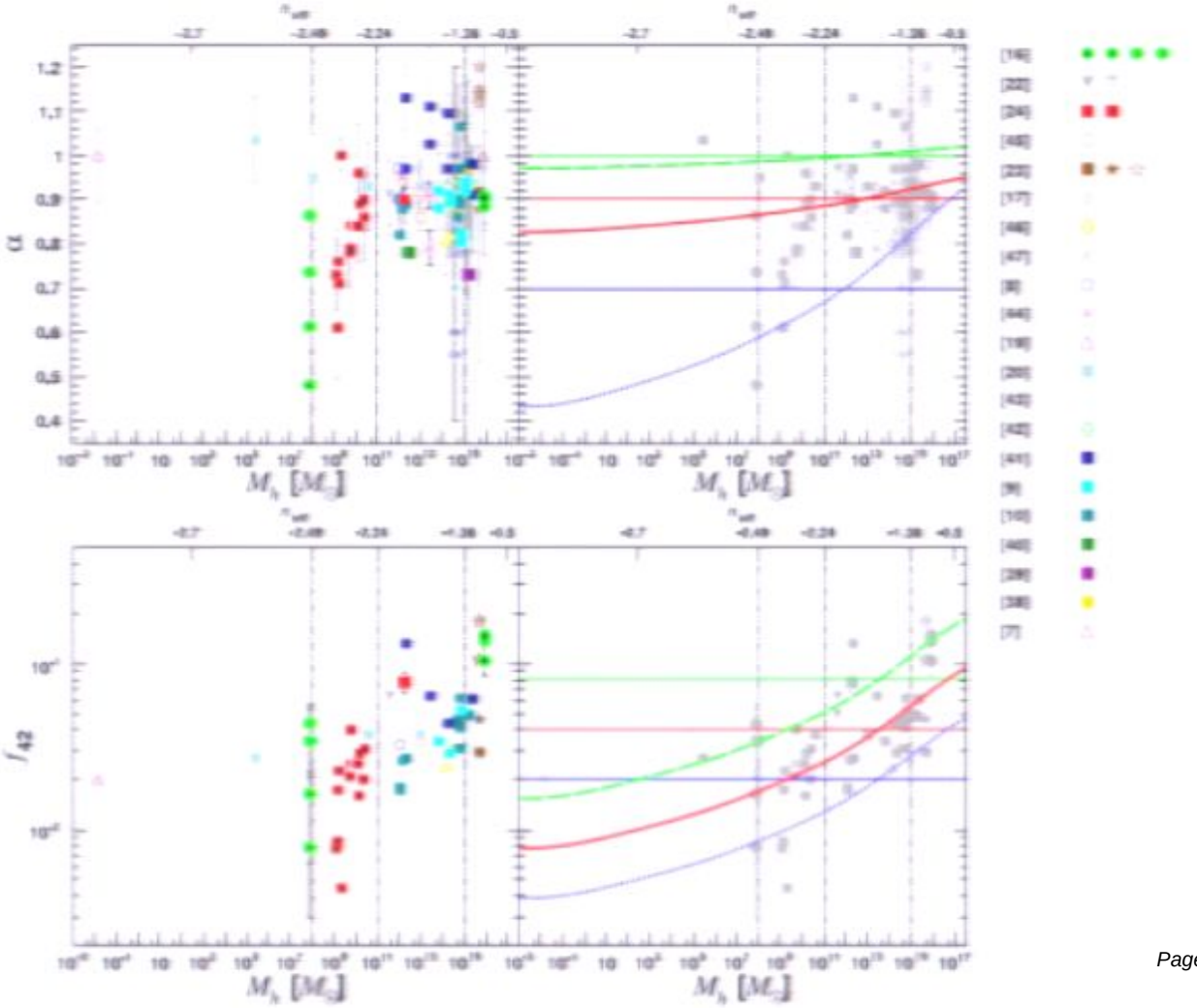

calculation of the boost factor requires a bold extrapolation of the subhalo mass function to small scales. Our analysis found relatively modest boost factors for "realistic" extrapolations

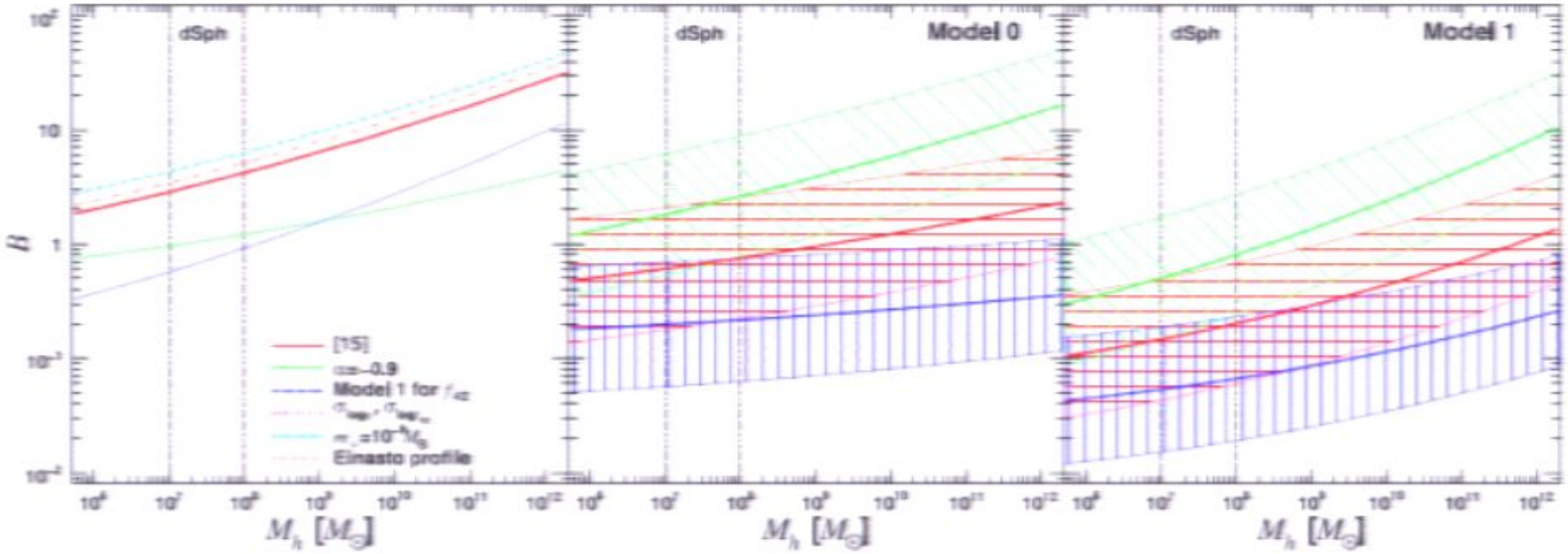

Elahi et al 2009

calculation of the boost factor requires a bold extrapolation of the subhalo mass function to small scales. Our analysis found relatively modest boost factors for "realistic" extrapolations

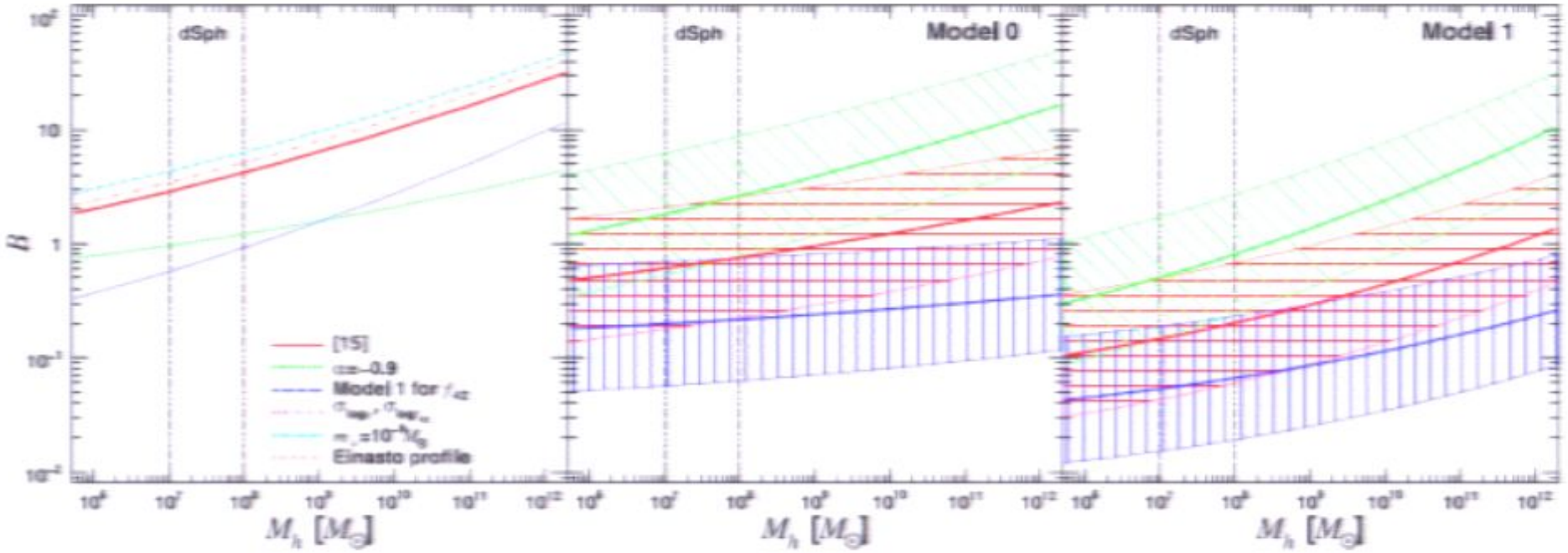

Elahi et al 2009

calculation of the boost factor requires a bold extrapolation of the subhalo mass function to small scales. Our analysis found relatively modest boost factors for "realistic" extrapolations

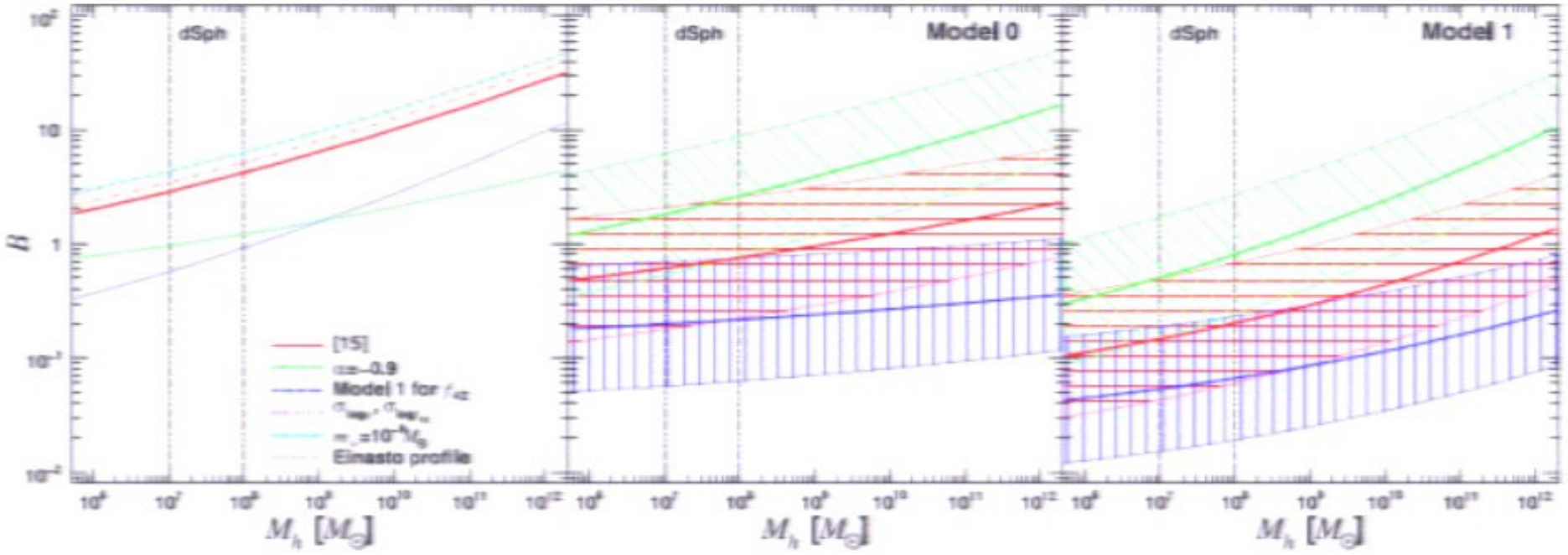

Elahi et al 2009

calculation of the boost factor requires a bold extrapolation of the subhalo mass function to small scales. Our analysis found relatively modest boost factors for "realistic" extrapolations

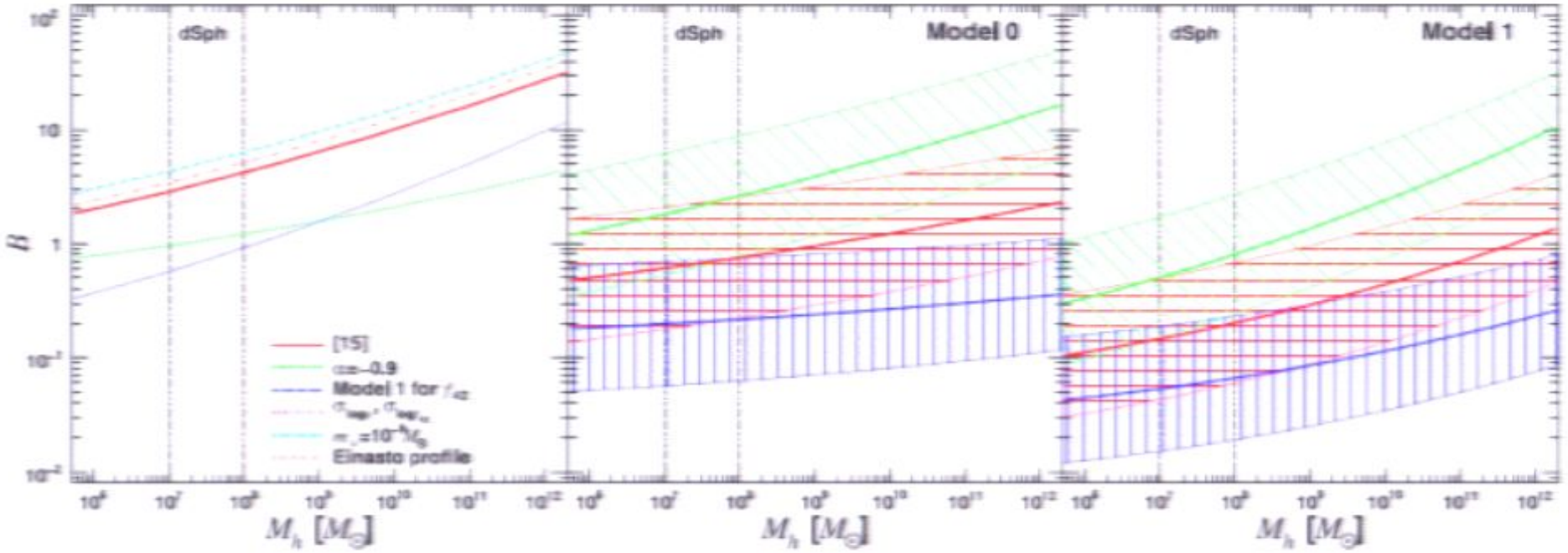

Elahi et al 2009

calculation of the boost factor requires a bold extrapolation of the subhalo mass function to small scales. Our analysis found relatively modest boost factors for "realistic" extrapolations

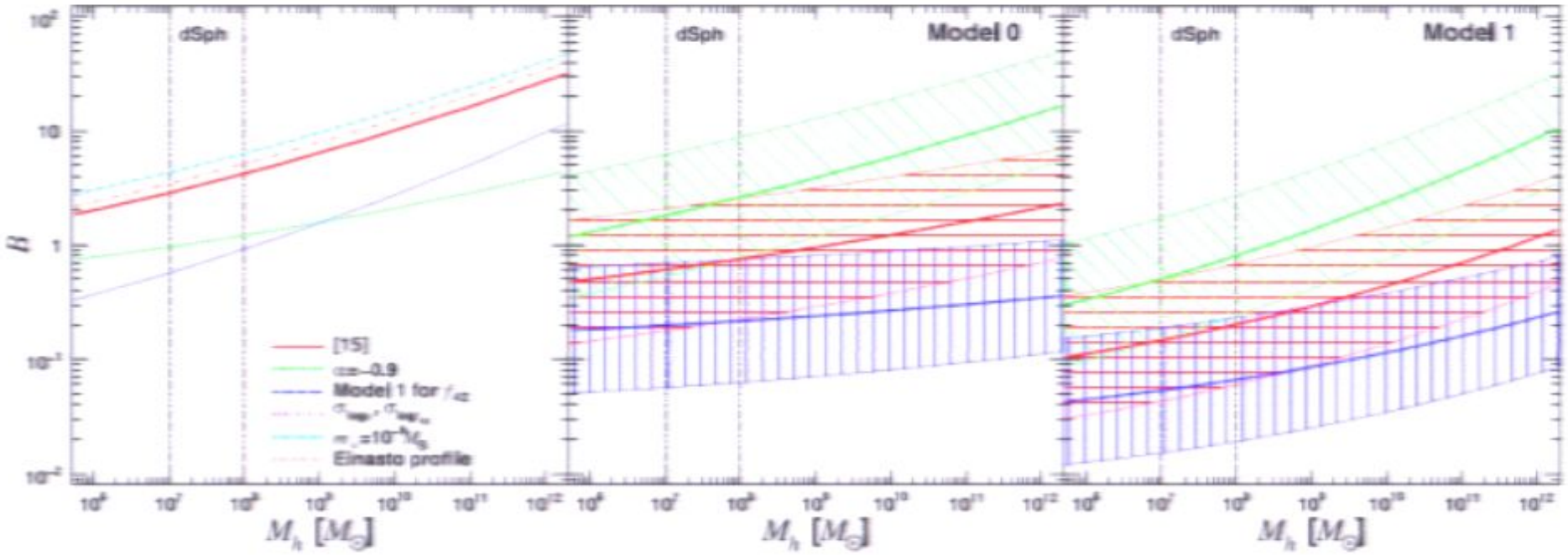

Elahi et al 2009

calculation of the boost factor requires a bold extrapolation of the subhalo mass function to small scales. Our analysis found relatively modest boost factors for "realistic" extrapolations

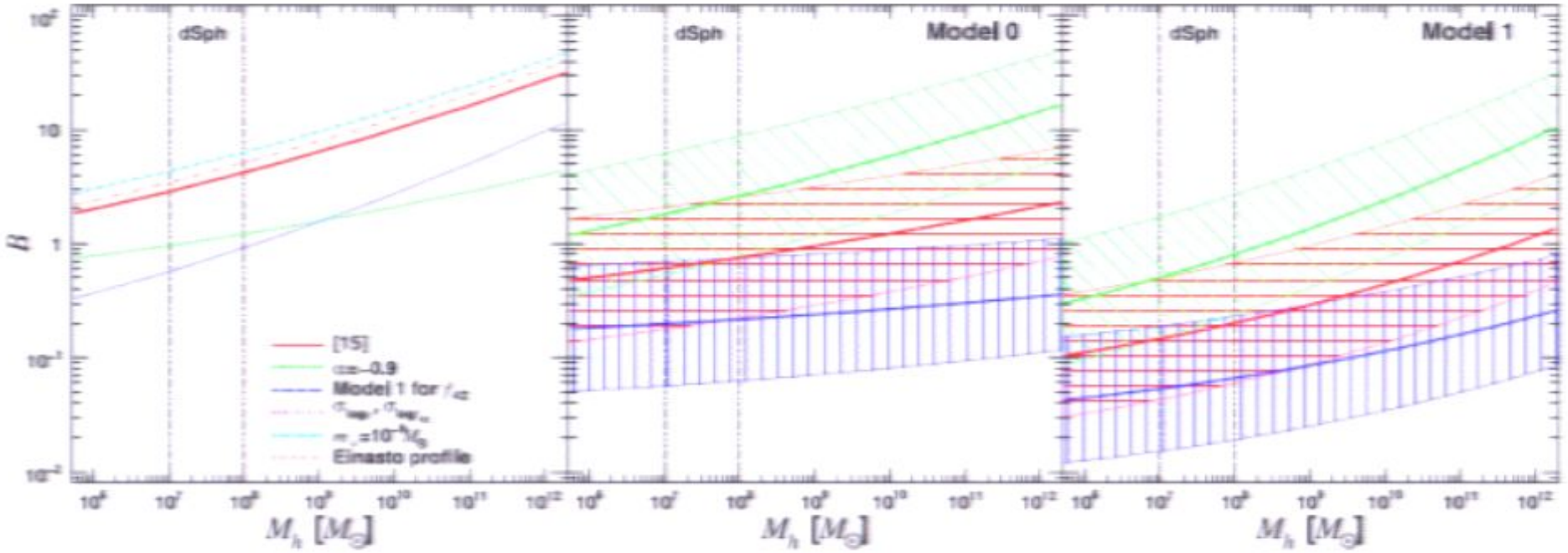

Elahi et al 2009

Challenges, III
Liouville's theorem and the phase-space sheet

for collisionless system's, the phase space density along a particle's orbit is constant

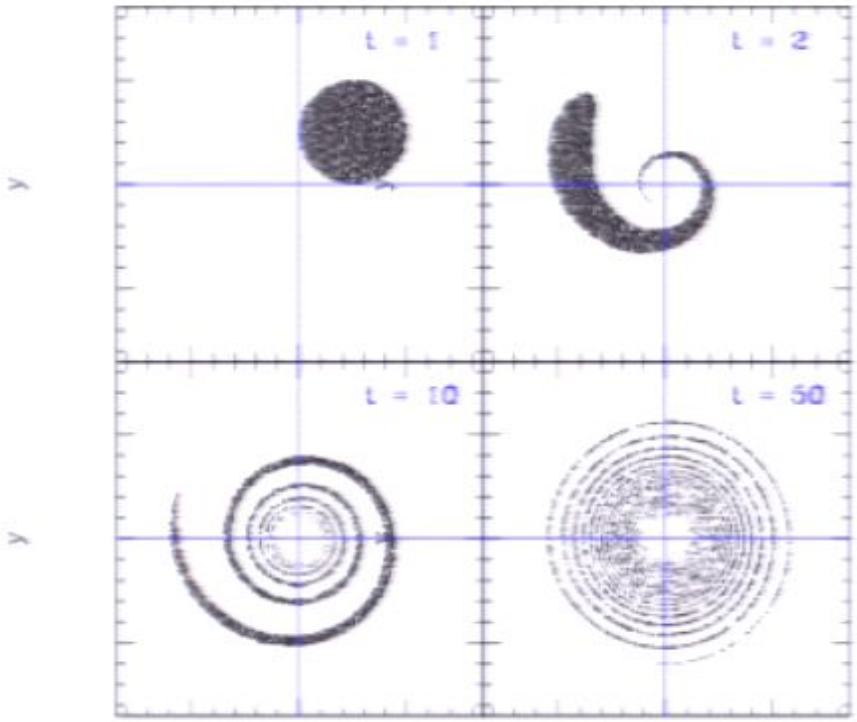

phase mixing in a simple toy model
NB: evolution is reversible!

adapted from Tremaine, 1999

Challenges, III
Liouville's theorem and the phase-space sheet

for collisionless system's, the phase space density along a particle's orbit is constant

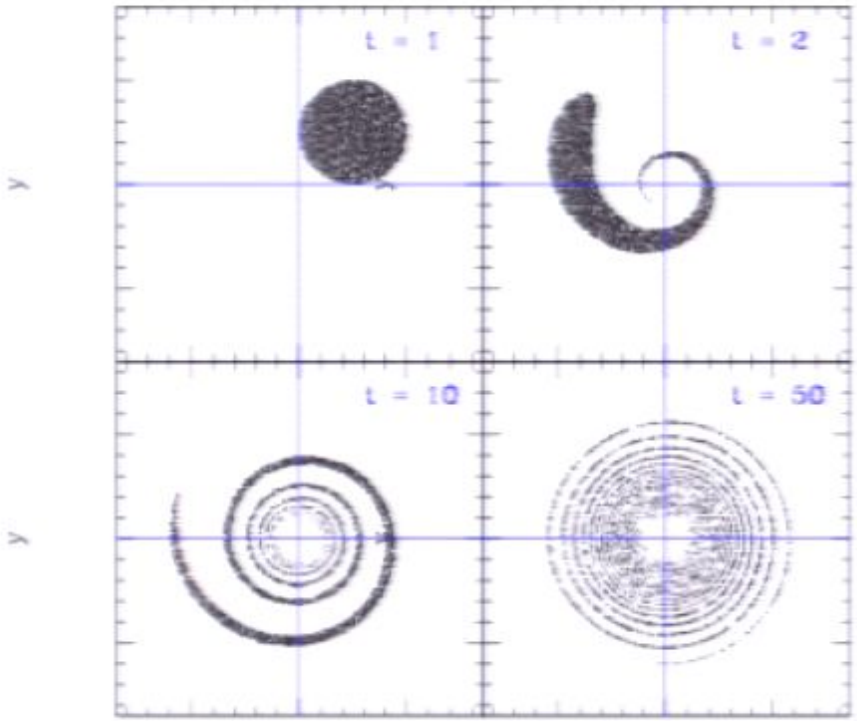

phase mixing in a simple toy model
NB: evolution is reversible!

adapted from Tremaine, 1999

Challenges, III
Liouville's theorem and the phase-space sheet

for collisionless system's, the phase space density along a particle's orbit is constant

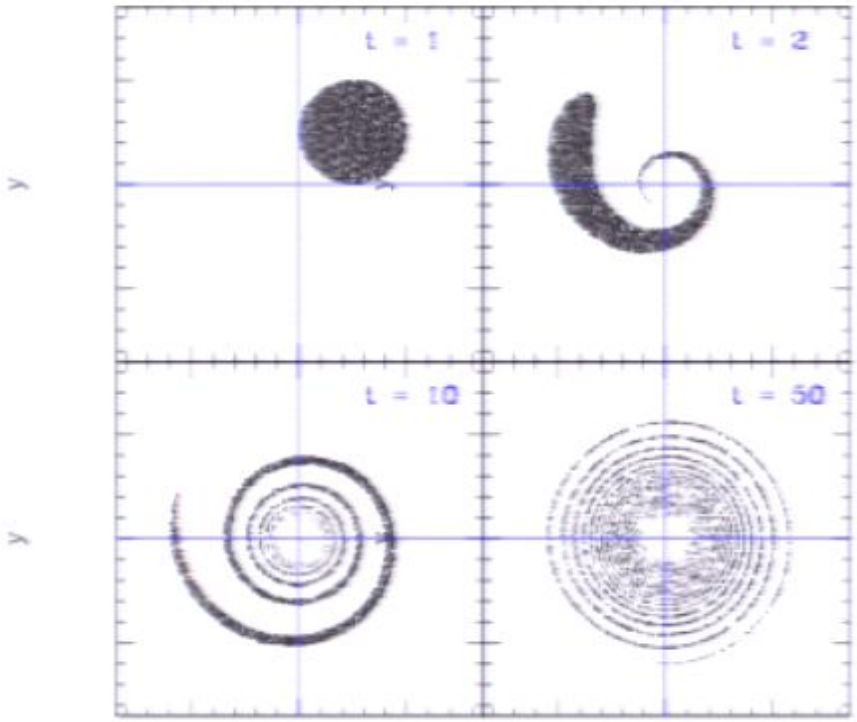

phase mixing in a simple toy model
NB: evolution is reversible!

adapted from Tremaine, 1999

Challenges, III
Liouville's theorem and the phase-space sheet

for collisionless system's, the phase space density along a particle's orbit is constant

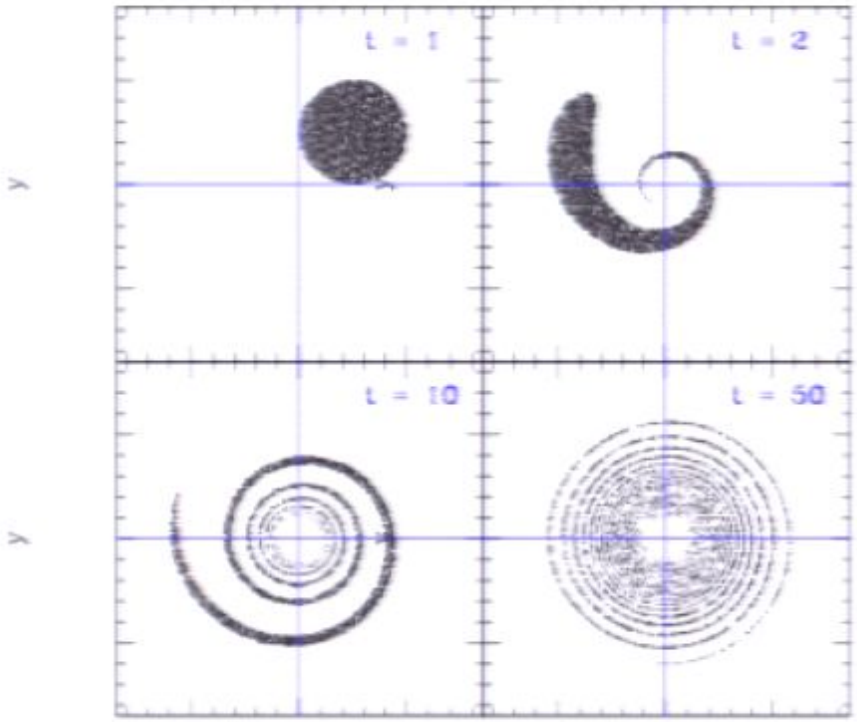

phase mixing in a simple toy model
NB: evolution is reversible!

adapted from Tremaine, 1999

Challenges, III
Liouville's theorem and the phase-space sheet

for collisionless system's, the phase space density along a particle's orbit is constant

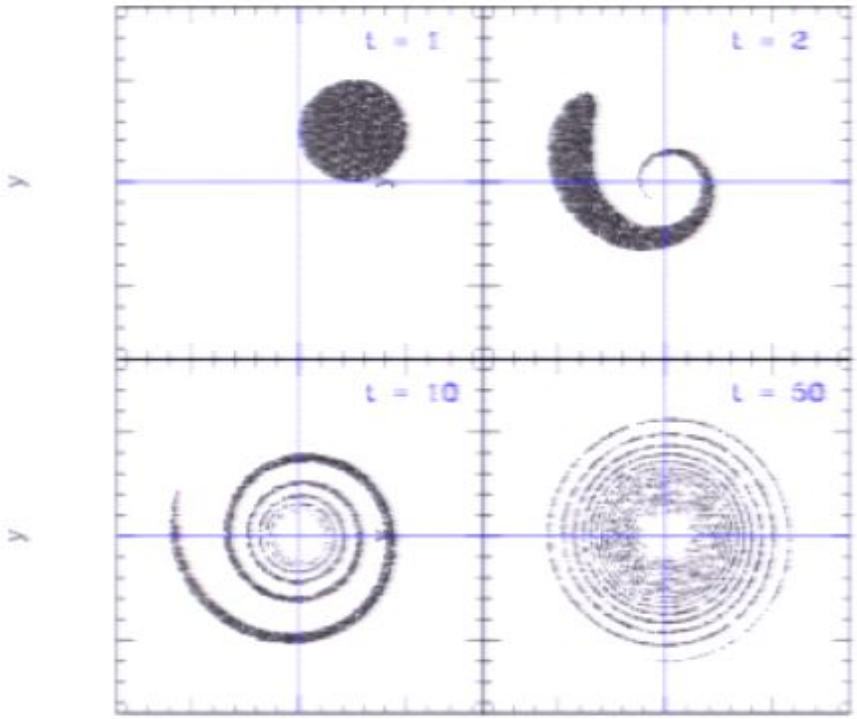

phase mixing in a simple toy model
NB: evolution is reversible!

adapted from Tremaine, 1999

Challenges, III
Liouville's theorem and the phase-space sheet

for collisionless system's, the phase space density along a particle's orbit is constant

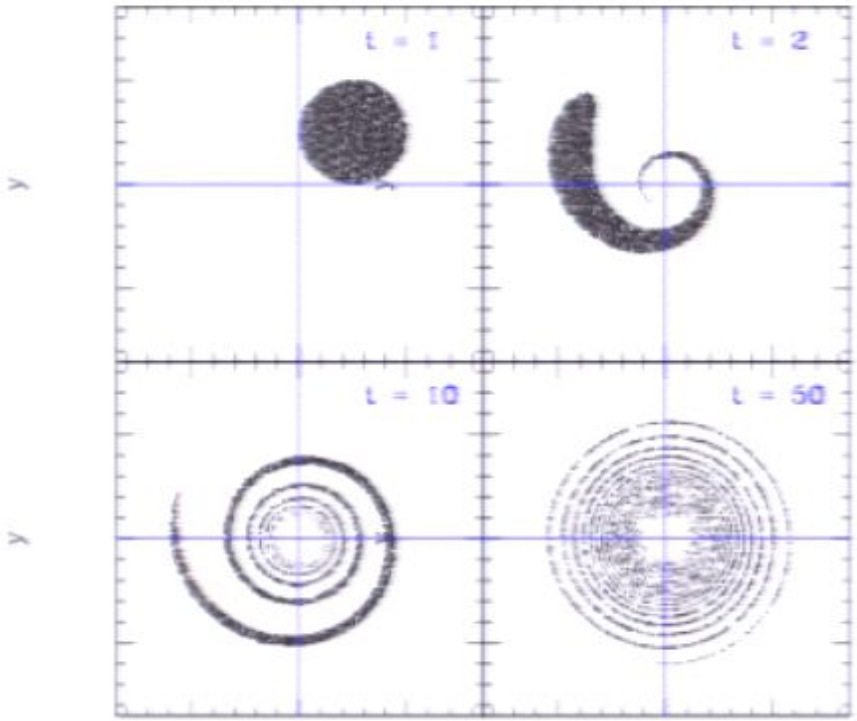

phase mixing in a simple toy model
NB: evolution is reversible!

adapted from Tremaine, 1999

Challenges, III
Liouville's theorem and the phase-space sheet

for collisionless system's, the phase space density along a particle's orbit is constant

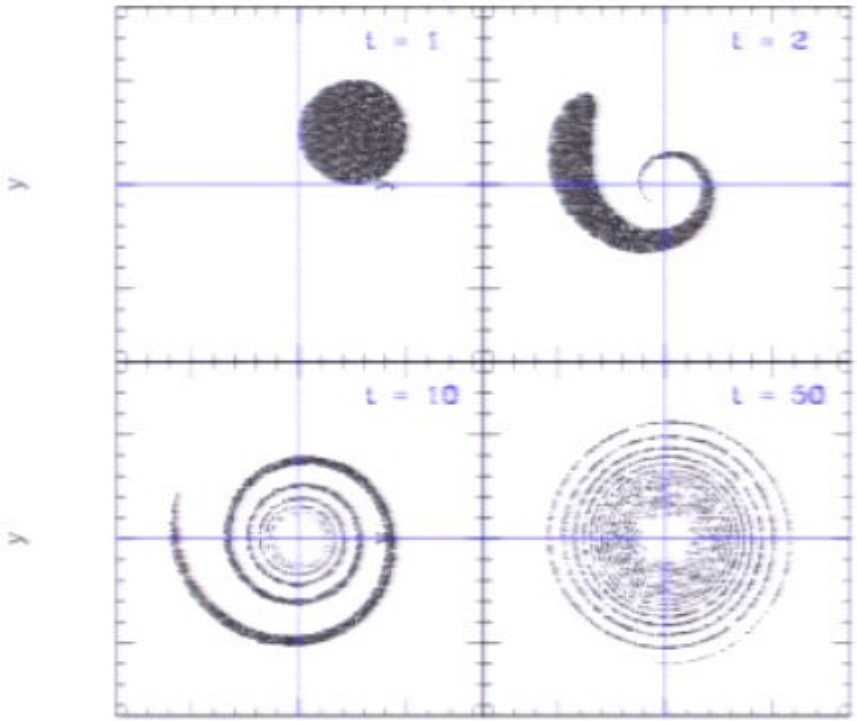

phase mixing in a simple toy model
NB: evolution is reversible!

adapted from Tremaine, 1999

Challenges, III
Liouville's theorem and the phase-space sheet

for collisionless system's, the phase space density along a particle's orbit is constant

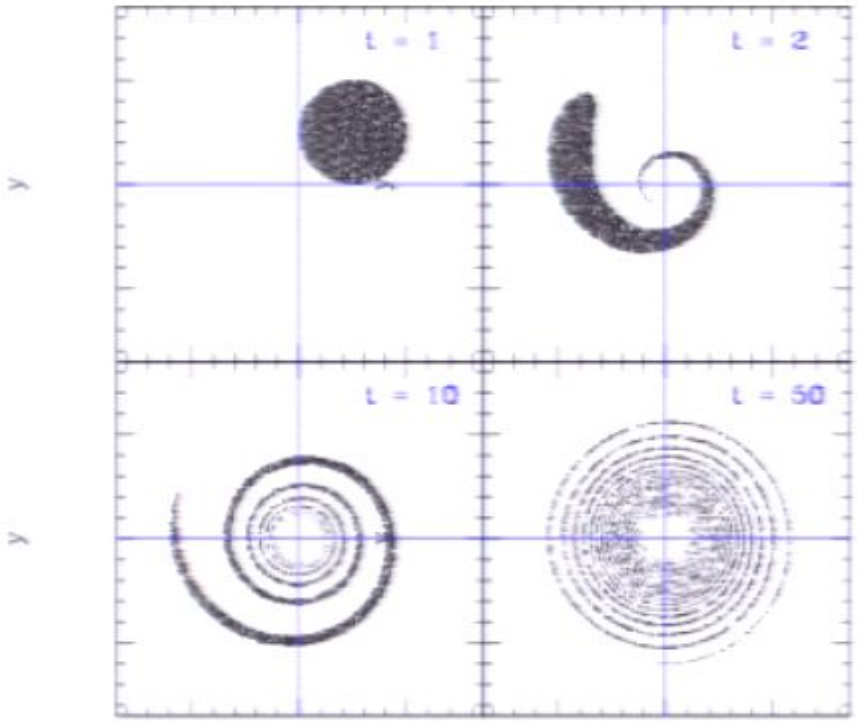

phase mixing in a simple toy model
NB: evolution is reversible!

adapted from Tremaine, 1999

Challenges, III
Liouville's theorem and the phase-space sheet

for collisionless system's, the phase space density along a particle's orbit is constant

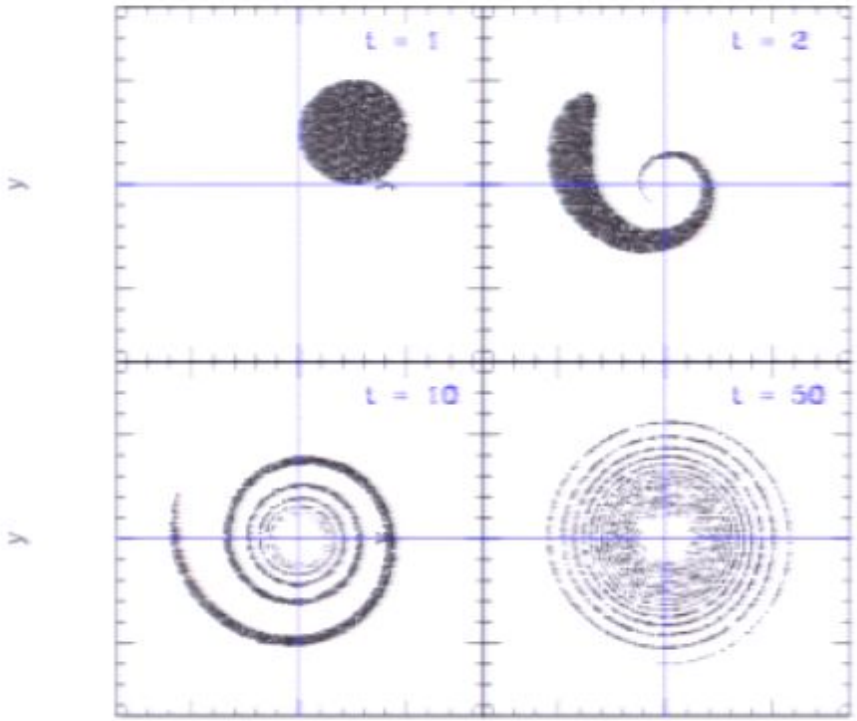

phase mixing in a simple toy model
NB: evolution is reversible!

adapted from Tremaine, 1999

Challenges, III
Liouville's theorem and the phase-space sheet

for collisionless system's, the phase space density along a particle's orbit is constant

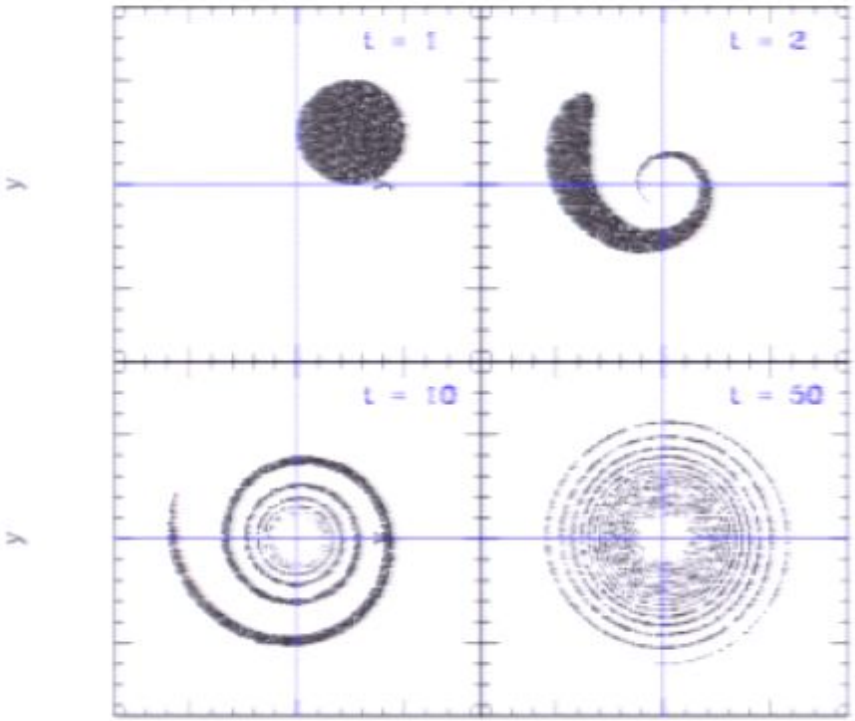

phase mixing in a simple toy model
NB: evolution is reversible!

adapted from Tremaine, 1999

Challenges, III
Liouville's theorem and the phase-space sheet

for collisionless system's, the phase space density along a particle's orbit is constant

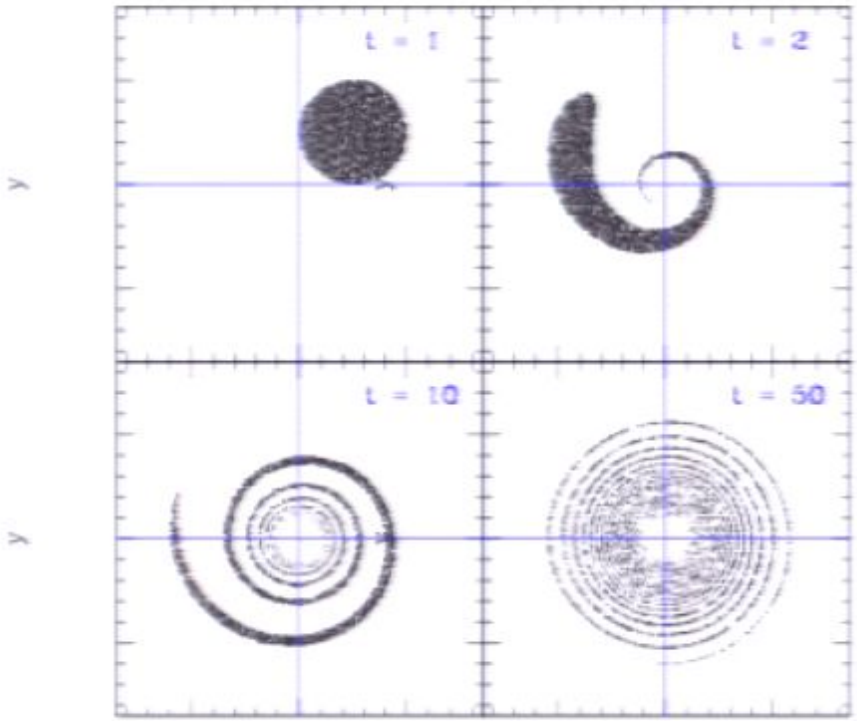

phase mixing in a simple toy model
NB: evolution is reversible!

adapted from Tremaine, 1999

Challenges, III
Liouville's theorem and the phase-space sheet

for collisionless system's, the phase space density along a particle's orbit is constant

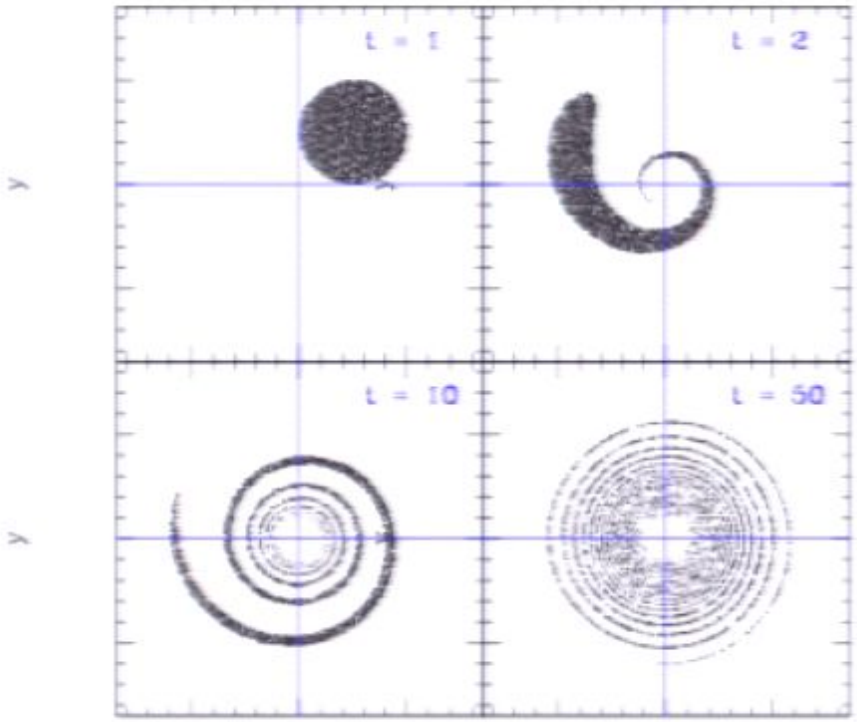

phase mixing in a simple toy model
NB: evolution is reversible!

adapted from Tremaine, 1999

Challenges, III
Liouville's theorem and the phase-space sheet

for collisionless system's, the phase space density along a particle's orbit is constant

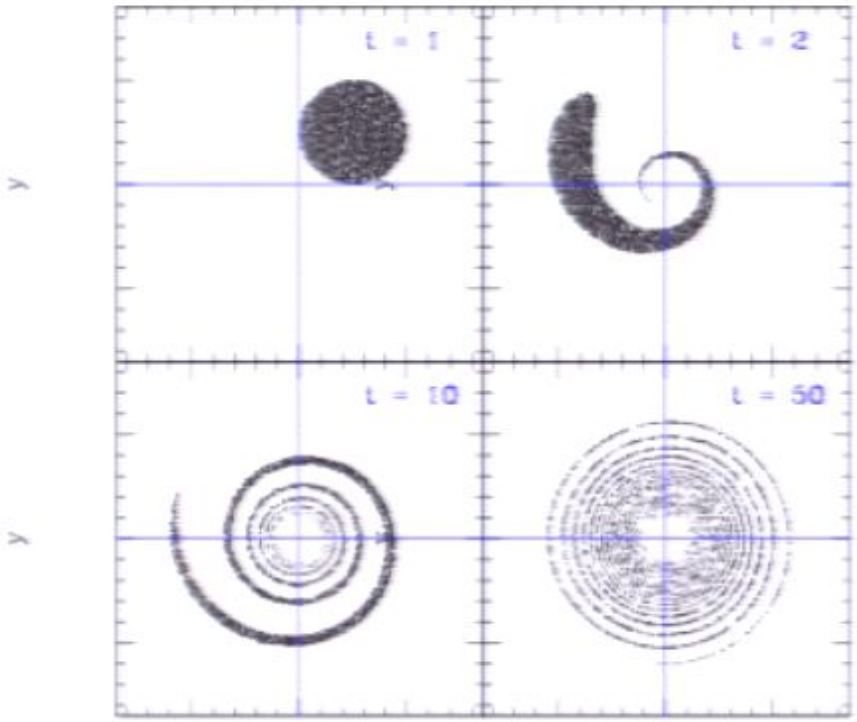

phase mixing in a simple toy model
NB: evolution is reversible!

adapted from Tremaine, 1999

Challenges, III
Liouville's theorem and the phase-space sheet

for collisionless system's, the phase space density along a particle's orbit is constant

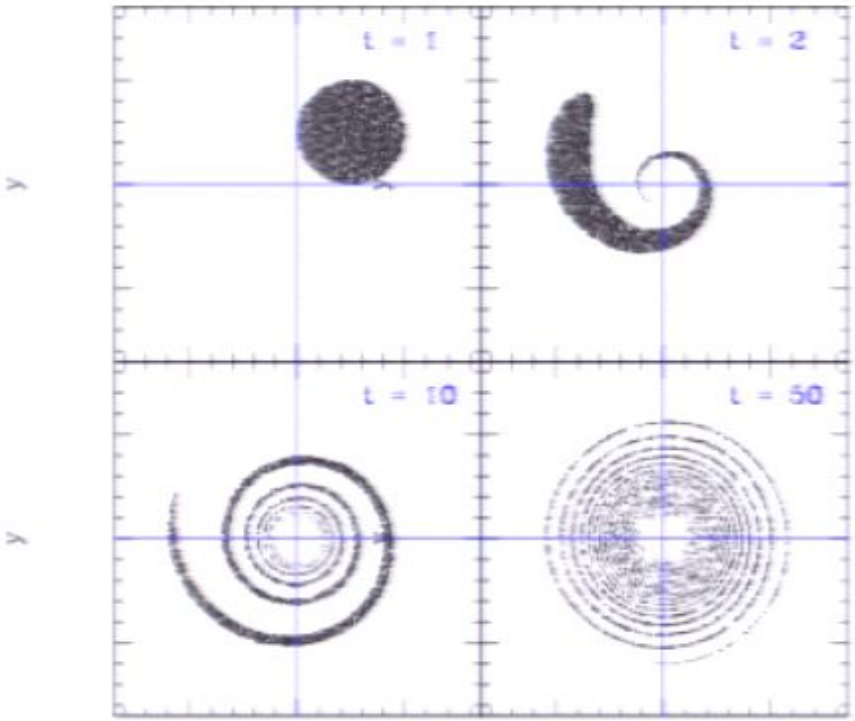

phase mixing in a simple toy model
NB: evolution is reversible!

adapted from Tremaine, 1999

Challenges, III
Liouville's theorem and the phase-space sheet

for collisionless system's, the phase space density along a particle's orbit is constant

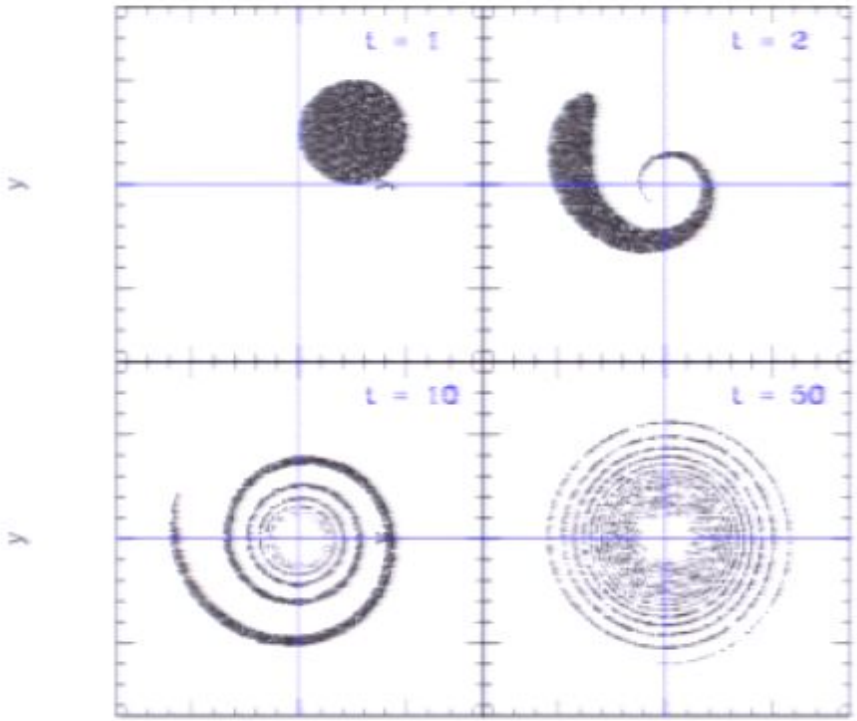

phase mixing in a simple toy model
NB: evolution is reversible!

adapted from Tremaine, 1999

Challenges, III
Liouville's theorem and the phase-space sheet

for collisionless system's, the phase space density along a particle's orbit is constant

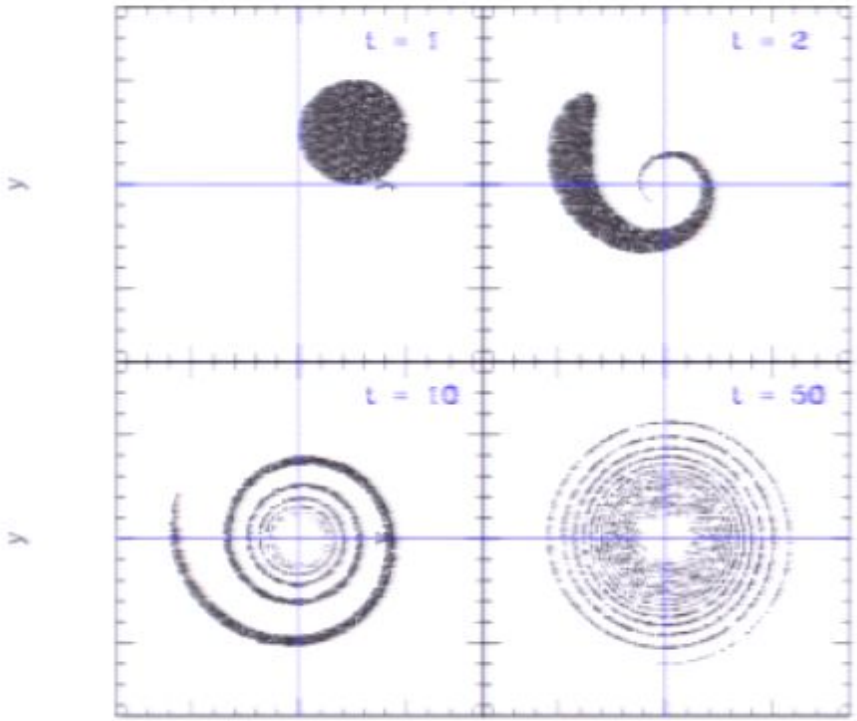

phase mixing in a simple toy model
NB: evolution is reversible!

adapted from Tremaine, 1999

Challenges, III
Liouville's theorem and the phase-space sheet

for collisionless system's, the phase space density along a particle's orbit is constant

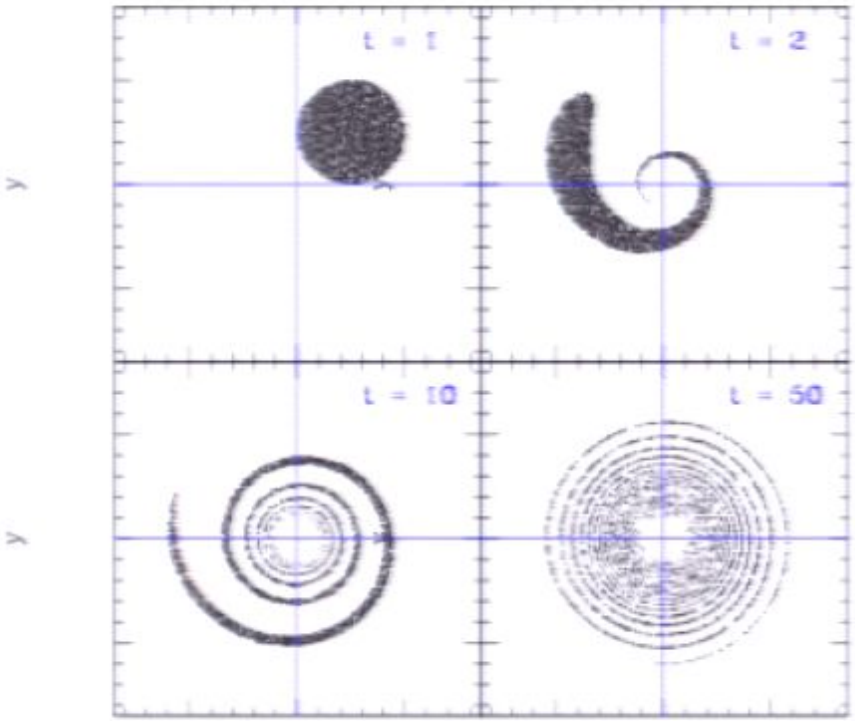

phase mixing in a simple toy model
NB: evolution is reversible!

adapted from Tremaine, 1999

Challenges, III
Liouville's theorem and the phase-space sheet

for collisionless system's, the phase space density along a particle's orbit is constant

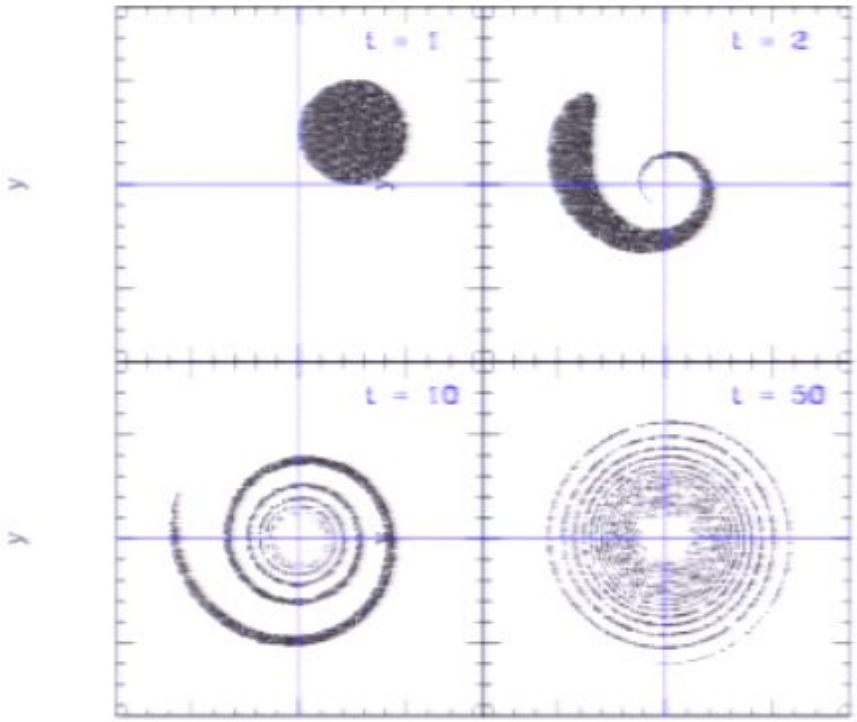

phase mixing in a simple toy model
NB: evolution is reversible!

adapted from Tremaine, 1999

Challenges, III
Liouville's theorem and the phase-space sheet

for collisionless system's, the phase space density along a particle's orbit is constant

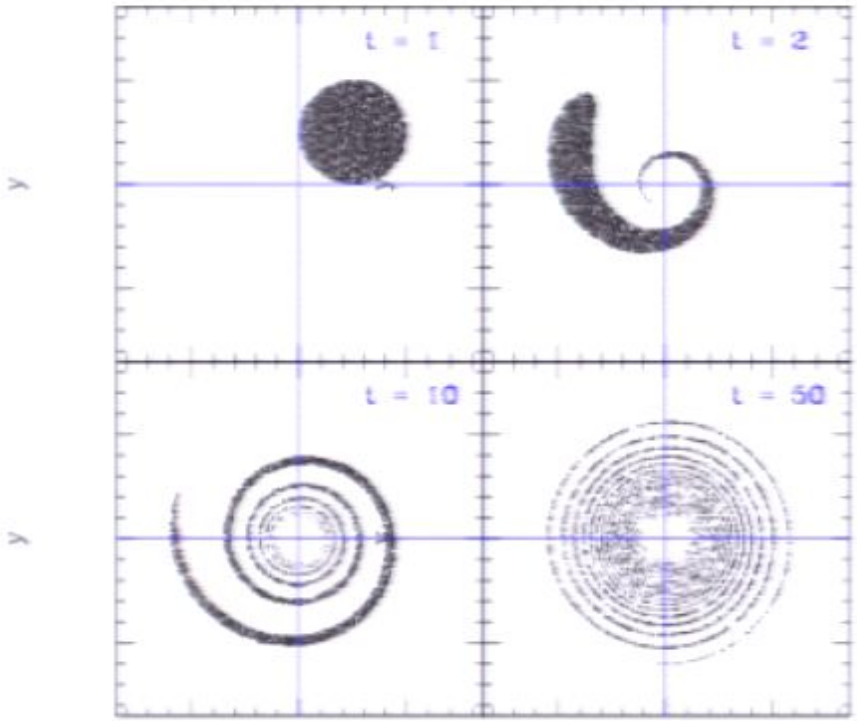

phase mixing in a simple toy model
NB: evolution is reversible!

adapted from Tremaine, 1999

Challenges, III
Liouville's theorem and the phase-space sheet

for collisionless system's, the phase space density along a particle's orbit is constant

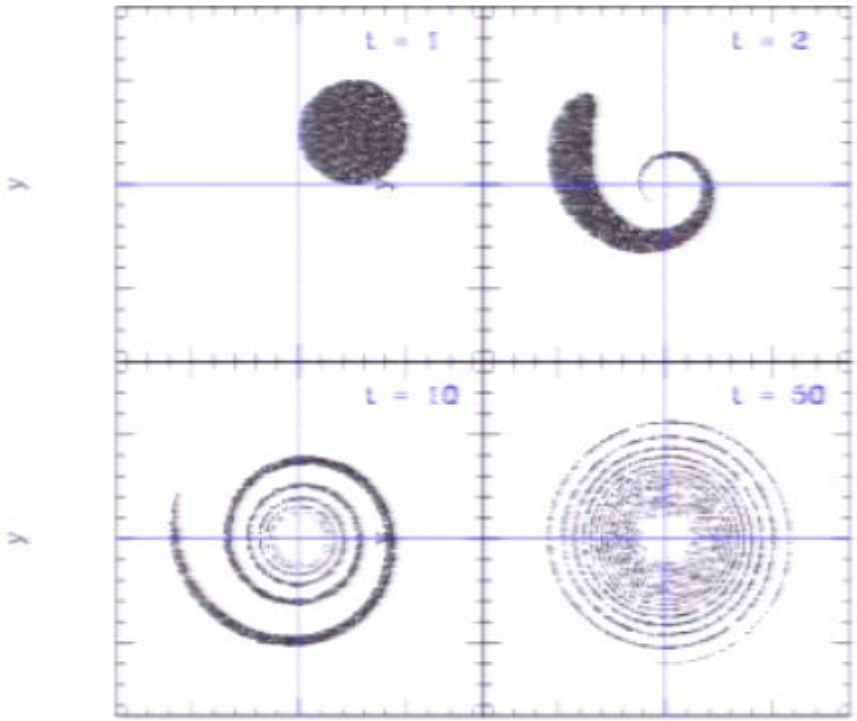

phase mixing in a simple toy model
NB: evolution is reversible!

adapted from Tremaine, 1999

Challenges, III
Liouville's theorem and the phase-space sheet

for collisionless system's, the phase space density along a particle's orbit is constant

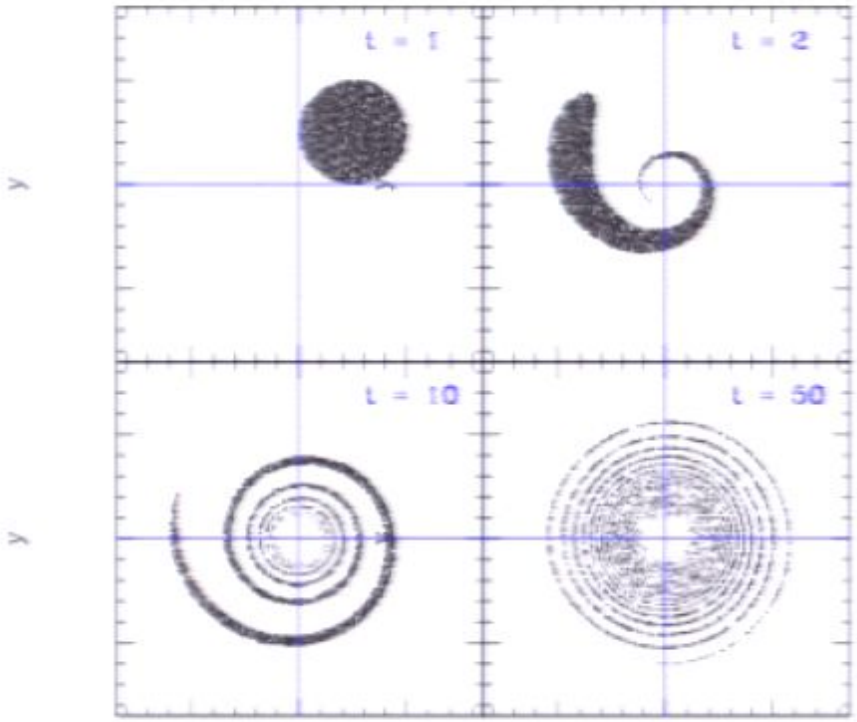

phase mixing in a simple toy model
NB: evolution is reversible!

adapted from Tremaine, 1999

Challenges, III
Liouville's theorem and the phase-space sheet

for collisionless system's, the phase space density along a particle's orbit is constant

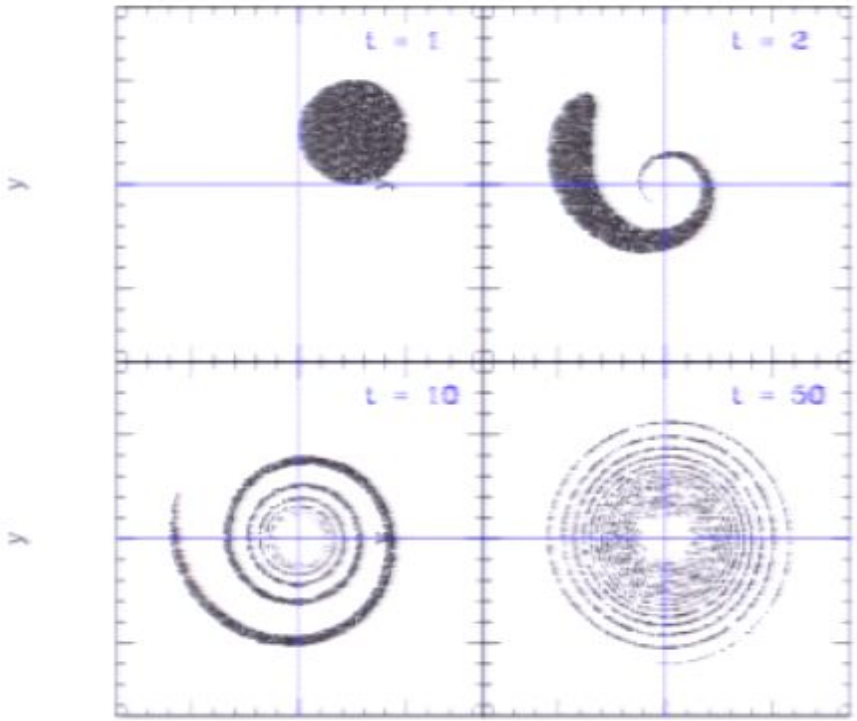

phase mixing in a simple toy model
NB: evolution is reversible!

adapted from Tremaine, 1999

Challenges, III
Liouville's theorem and the phase-space sheet

for collisionless system's, the phase space density along a particle's orbit is constant

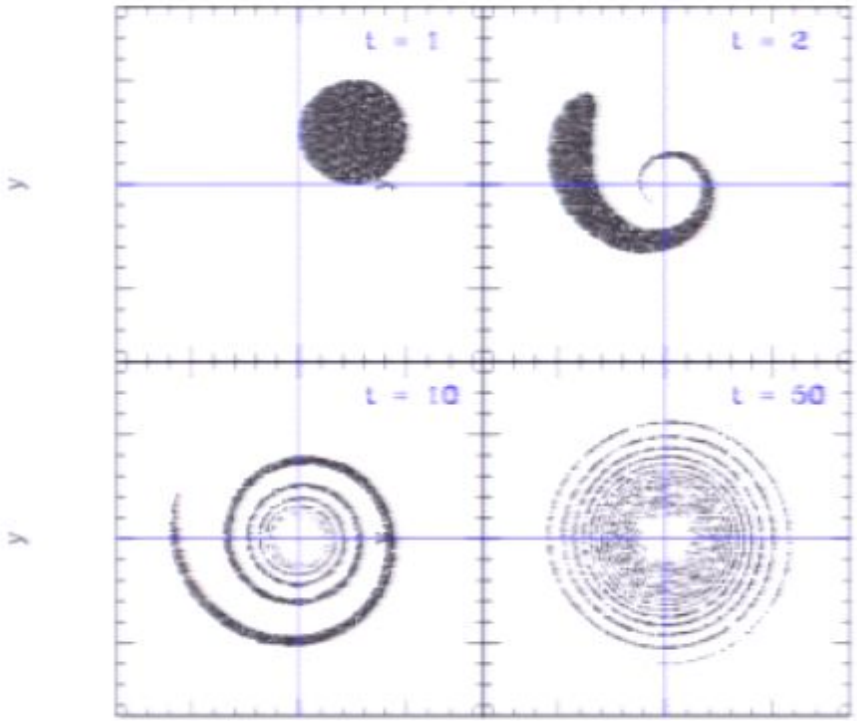

phase mixing in a simple toy model
NB: evolution is reversible!

adapted from Tremaine, 1999

Phase-space structure of cold dark matter halos

P. Sikivie [a,b] and James R. Ipser [b]

[a] *Institute for Theoretical Physics, University of California, Santa Barbara, CA 93106-4030, USA*

[b] *Physics Department, University of Florida, Gainesville, FL 32611, USA*

Received 3 July 1992

We discuss the extent to which the phase-space distribution of cold dark matter particles is thermalized in a galactic halo and find that there are large deviations from a thermal distribution in that the highest energy particles have discrete values of velocity. The central values and intensities of the corresponding peaks provide detailed information on the history of the Galaxy. This information becomes immediately available if a signal is found in a cavity detector of galactic halo axions.

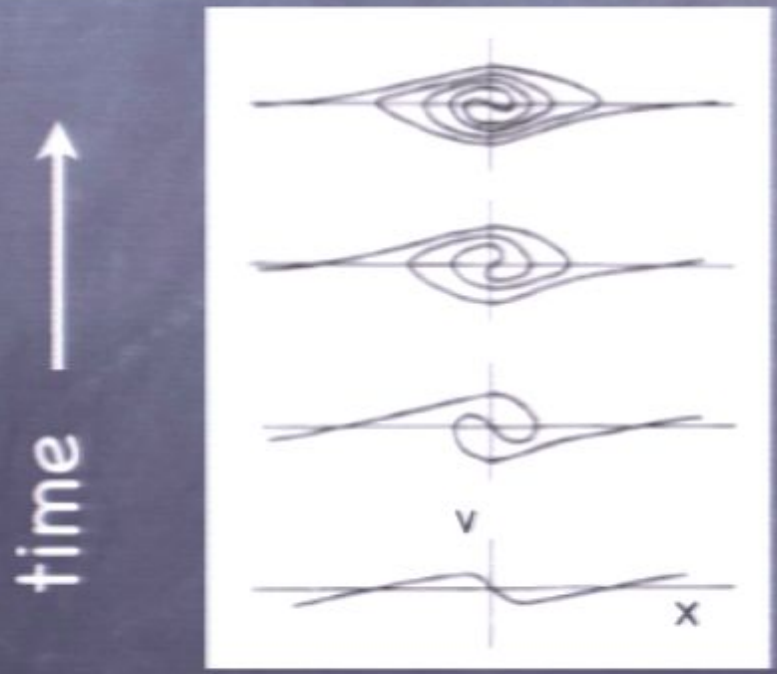

Phase-space structure of cold dark matter halos

P. Sikivie [a,b] and James R. Ipser [b]

[a] *Institute for Theoretical Physics, University of California, Santa Barbara, CA 93106-4030, USA*

[b] *Physics Department, University of Florida, Gainesville, FL 32611, USA*

Received 3 July 1992

We discuss the extent to which the phase-space distribution of cold dark matter particles is thermalized in a galactic halo and find that there are large deviations from a thermal distribution in that the highest energy particles have discrete values of velocity. The central values and intensities of the corresponding peaks provide detailed information on the history of the Galaxy. This information becomes immediately available if a signal is found in a cavity detector of galactic halo axions.

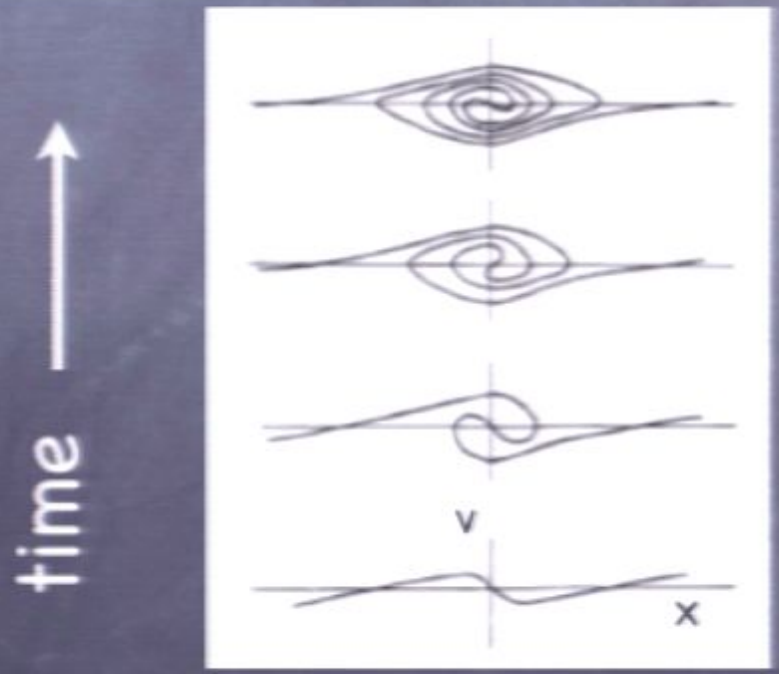

Phase-space structure of cold dark matter halos

P. Sikivie [a,b] and James R. Ipser [b]

[a] *Institute for Theoretical Physics, University of California, Santa Barbara, CA 93106-4030, USA*

[b] *Physics Department, University of Florida, Gainesville, FL 32611, USA*

Received 3 July 1992

We discuss the extent to which the phase-space distribution of cold dark matter particles is thermalized in a galactic halo and find that there are large deviations from a thermal distribution in that the highest energy particles have discrete values of velocity. The central values and intensities of the corresponding peaks provide detailed information on the history of the Galaxy. This information becomes immediately available if a signal is found in a cavity detector of galactic halo axions.

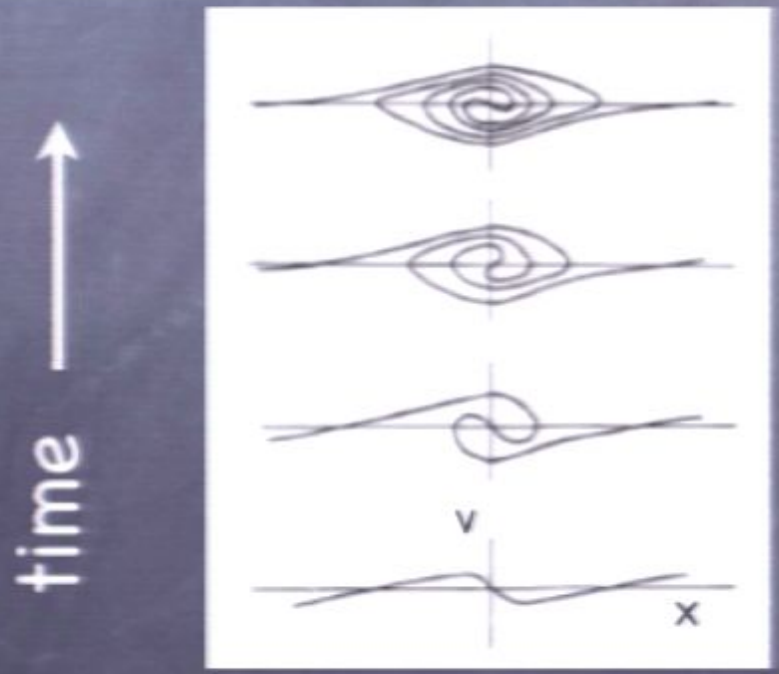

Phase-space structure of cold dark matter halos

P. Sikivie [a,b] and James R. Ipser [b]

[a] *Institute for Theoretical Physics, University of California, Santa Barbara, CA 93106-4030, USA*

[b] *Physics Department, University of Florida, Gainesville, FL 32611, USA*

Received 3 July 1992

We discuss the extent to which the phase-space distribution of cold dark matter particles is thermalized in a galactic halo and find that there are large deviations from a thermal distribution in that the highest energy particles have discrete values of velocity. The central values and intensities of the corresponding peaks provide detailed information on the history of the Galaxy. This information becomes immediately available if a signal is found in a cavity detector of galactic halo axions.

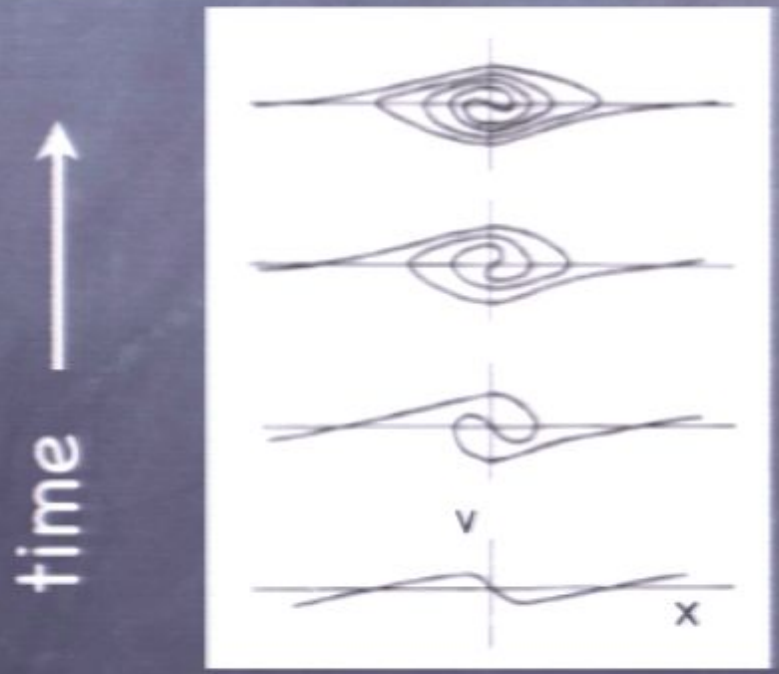

Phase-space structure of cold dark matter halos

P. Sikivie [a,b] and James R. Ipser [b]

[a] *Institute for Theoretical Physics, University of California, Santa Barbara, CA 93106-4030, USA*

[b] *Physics Department, University of Florida, Gainesville, FL 32611, USA*

Received 3 July 1992

We discuss the extent to which the phase-space distribution of cold dark matter particles is thermalized in a galactic halo and find that there are large deviations from a thermal distribution in that the highest energy particles have discrete values of velocity. The central values and intensities of the corresponding peaks provide detailed information on the history of the Galaxy. This information becomes immediately available if a signal is found in a cavity detector of galactic halo axions.

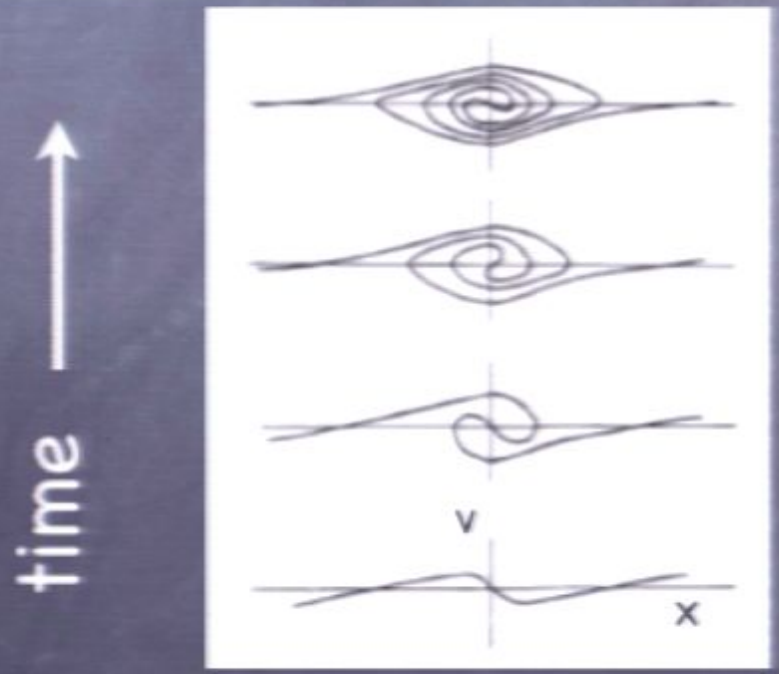

Phase-space structure of cold dark matter halos

P. Sikivie [a,b] and James R. Ipser [b]

[a] *Institute for Theoretical Physics, University of California, Santa Barbara, CA 93106-4030, USA*

[b] *Physics Department, University of Florida, Gainesville, FL 32611, USA*

Received 3 July 1992

We discuss the extent to which the phase-space distribution of cold dark matter particles is thermalized in a galactic halo and find that there are large deviations from a thermal distribution in that the highest energy particles have discrete values of velocity. The central values and intensities of the corresponding peaks provide detailed information on the history of the Galaxy. This information becomes immediately available if a signal is found in a cavity detector of galactic halo axions.

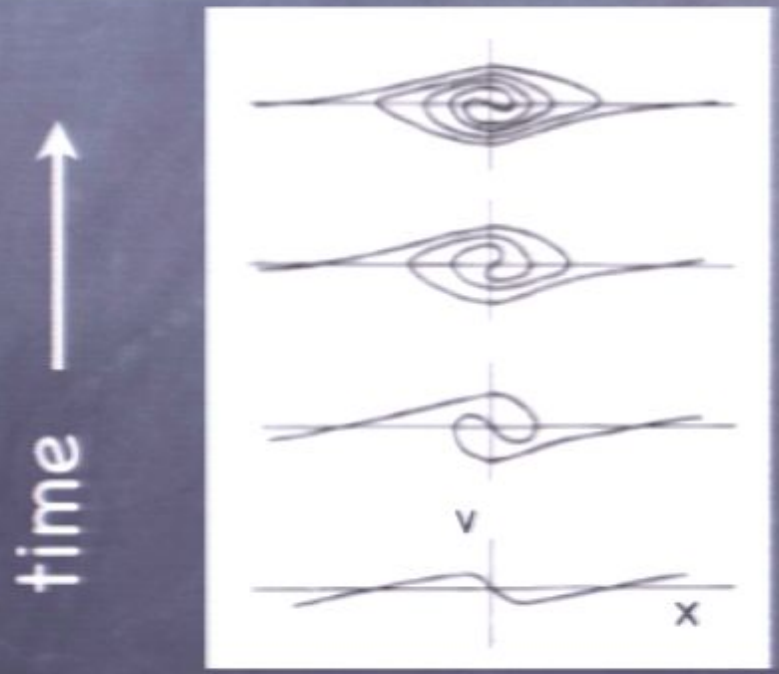

Phase-space structure of cold dark matter halos

P. Sikivie [a,b] and James R. Ipser [b]

[a] *Institute for Theoretical Physics, University of California, Santa Barbara, CA 93106-4030, USA*

[b] *Physics Department, University of Florida, Gainesville, FL 32611, USA*

Received 3 July 1992

We discuss the extent to which the phase-space distribution of cold dark matter particles is thermalized in a galactic halo and find that there are large deviations from a thermal distribution in that the highest energy particles have discrete values of velocity. The central values and intensities of the corresponding peaks provide detailed information on the history of the Galaxy. This information becomes immediately available if a signal is found in a cavity detector of galactic halo axions.

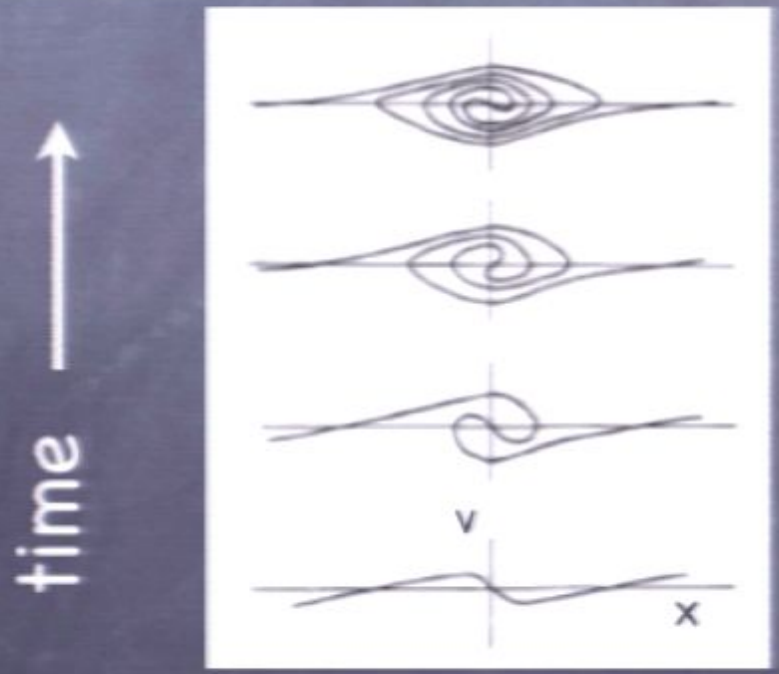

Phase-space structure of cold dark matter halos

P. Sikivie [a,b] and James R. Ipser [b]

[a] *Institute for Theoretical Physics, University of California, Santa Barbara, CA 93106-4030, USA*

[b] *Physics Department, University of Florida, Gainesville, FL 32611, USA*

Received 3 July 1992

We discuss the extent to which the phase-space distribution of cold dark matter particles is thermalized in a galactic halo and find that there are large deviations from a thermal distribution in that the highest energy particles have discrete values of velocity. The central values and intensities of the corresponding peaks provide detailed information on the history of the Galaxy. This information becomes immediately available if a signal is found in a cavity detector of galactic halo axions.

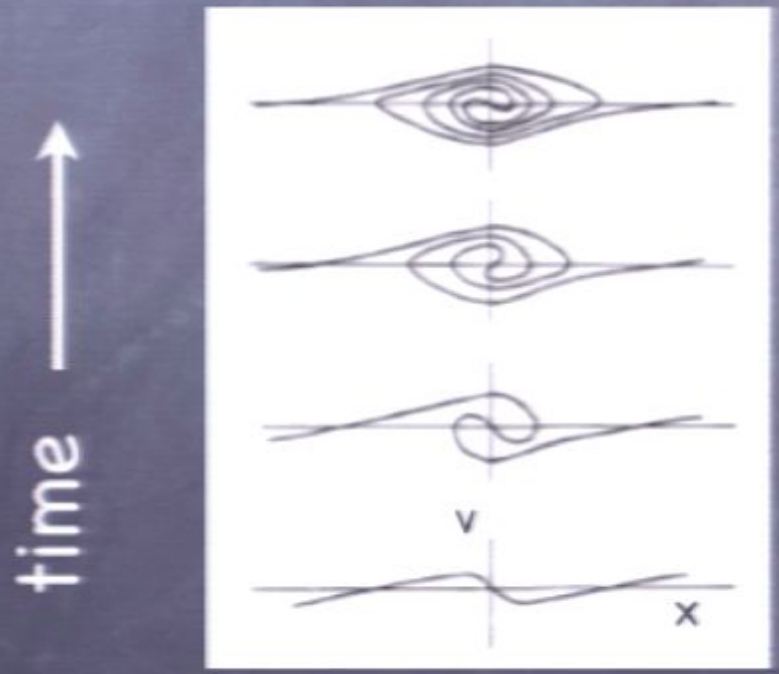

Another baby step toward a theoretical model for a dark matter halo: spherical collapse of a scale-free perturbation in an expanding Universe

each point on curve represents spherical shell with radial velocity dr/dt and radius r(t)

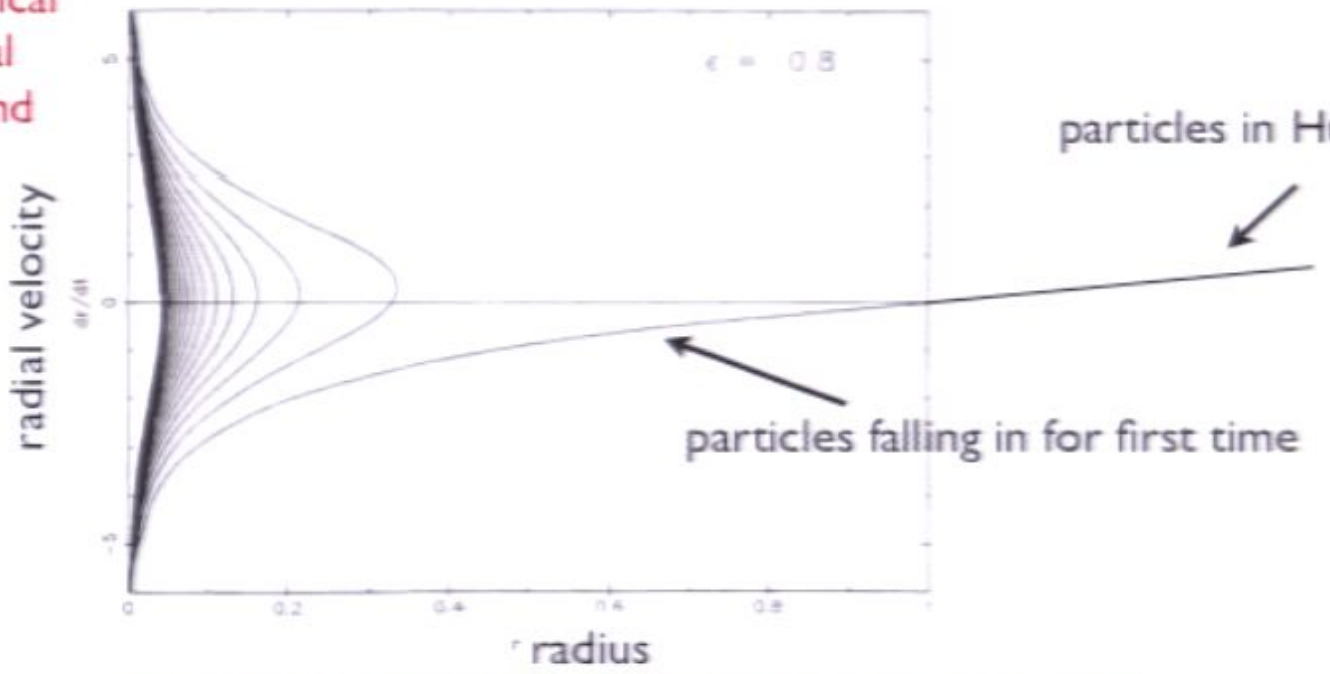

Fillmore & Goldreich, 1984 and Bertschinger, 1985

Note that this solution

(a) satisfies Liouville's theorem (i.e., phase space DF remains a cold, 3D sheet in 6D phase space)

(b) solution is time-reversible

Another baby step toward a theoretical model for a dark matter halo: spherical collapse of a scale-free perturbation in an expanding Universe

each point on curve represents spherical shell with radial velocity dr/dt and radius r(t)

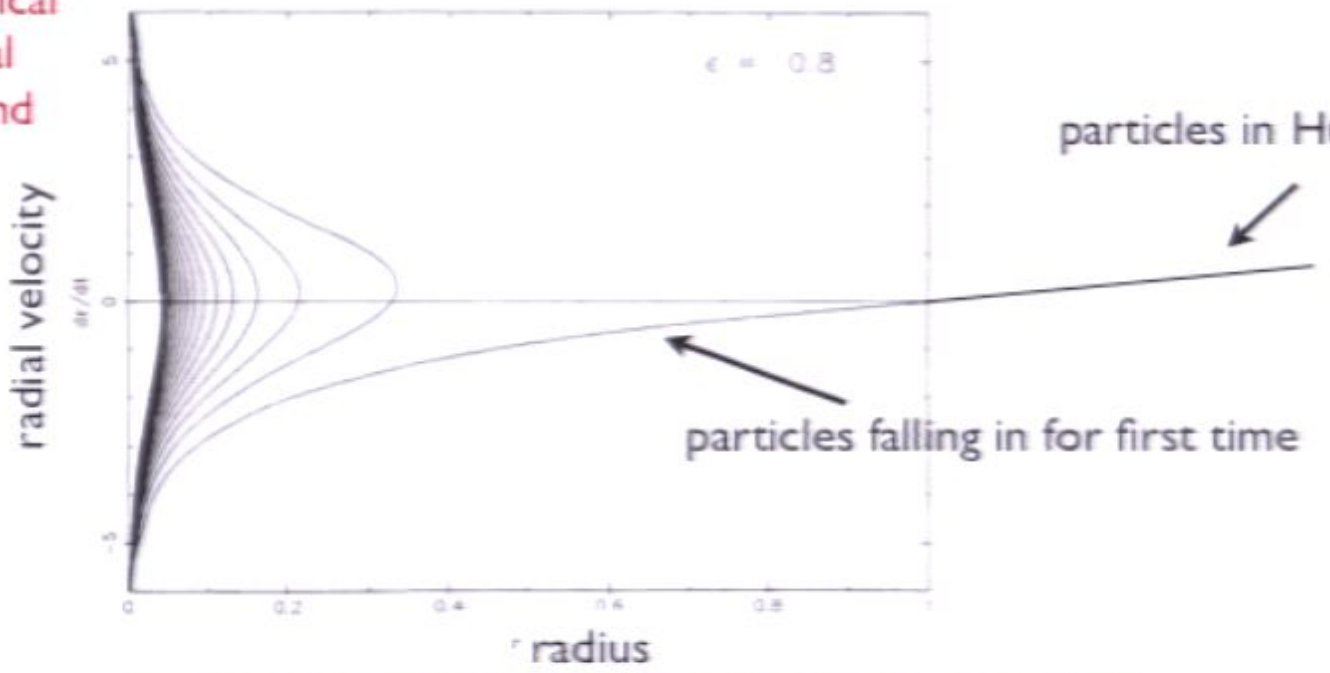

Fillmore & Goldreich, 1984 and Bertschinger, 1985

Note that this solution

(a) satisfies Liouville's theorem (i.e., phase space DF remains a cold, 3D sheet in 6D phase space)

(b) solution is time-reversible

Another baby step toward a theoretical model for a dark matter halo: spherical collapse of a scale-free perturbation in an expanding Universe

each point on curve represents spherical shell with radial velocity dr/dt and radius r(t)

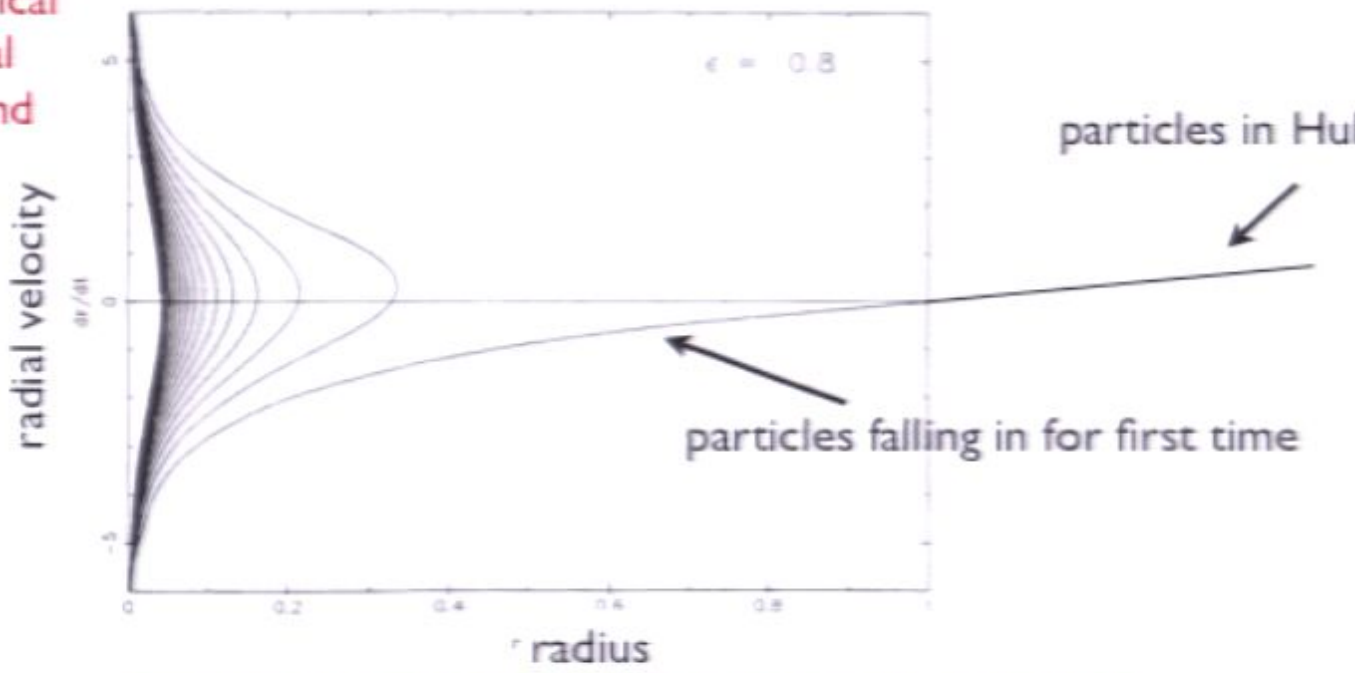

Fillmore & Goldreich, 1984 and Bertschinger, 1985

Note that this solution

(a) satisfies Liouville's theorem (i.e., phase space DF remains a cold, 3D sheet in 6D phase space)

(b) solution is time-reversible

Another baby step toward a theoretical model for a dark matter halo: spherical collapse of a scale-free perturbation in an expanding Universe

each point on curve represents spherical shell with radial velocity dr/dt and radius r(t)

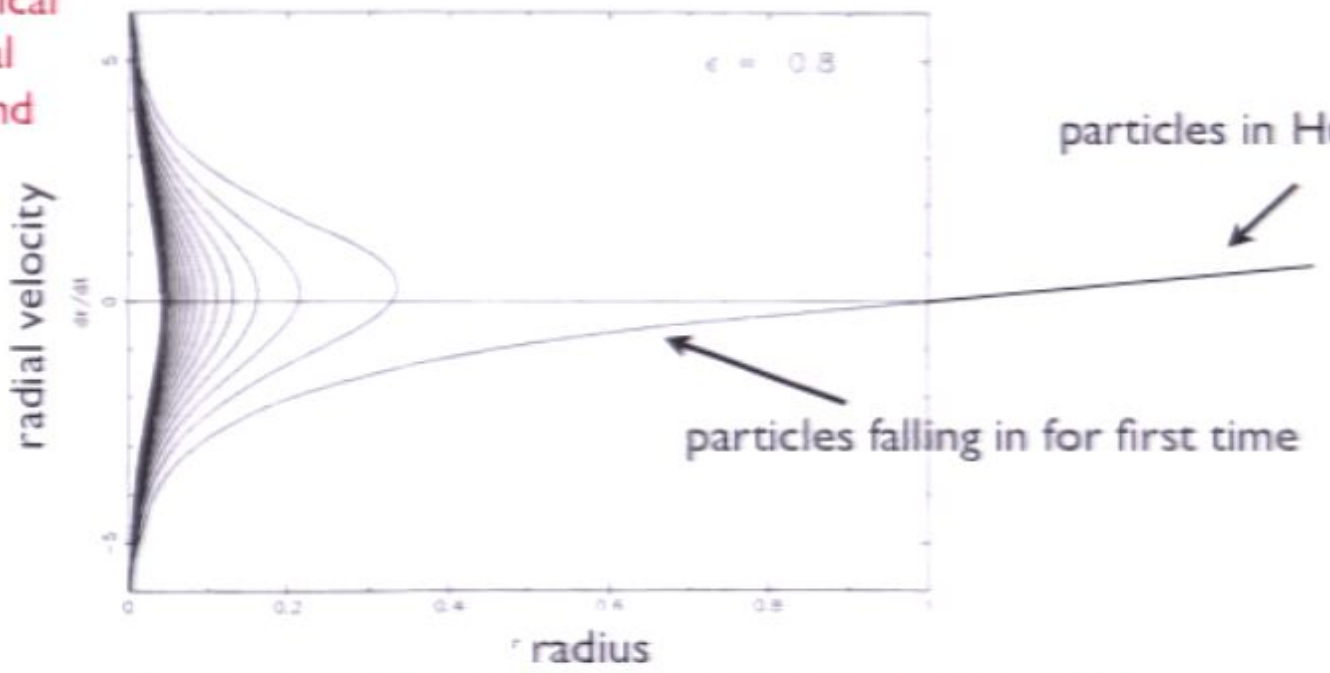

Fillmore & Goldreich, 1984 and Bertschinger, 1985

Note that this solution

(a) satisfies Liouville's theorem (i.e., phase space DF remains a cold, 3D sheet in 6D phase space)

(b) solution is time-reversible

Another baby step toward a theoretical model for a dark matter halo: spherical collapse of a scale-free perturbation in an expanding Universe

each point on curve represents spherical shell with radial velocity dr/dt and radius r(t)

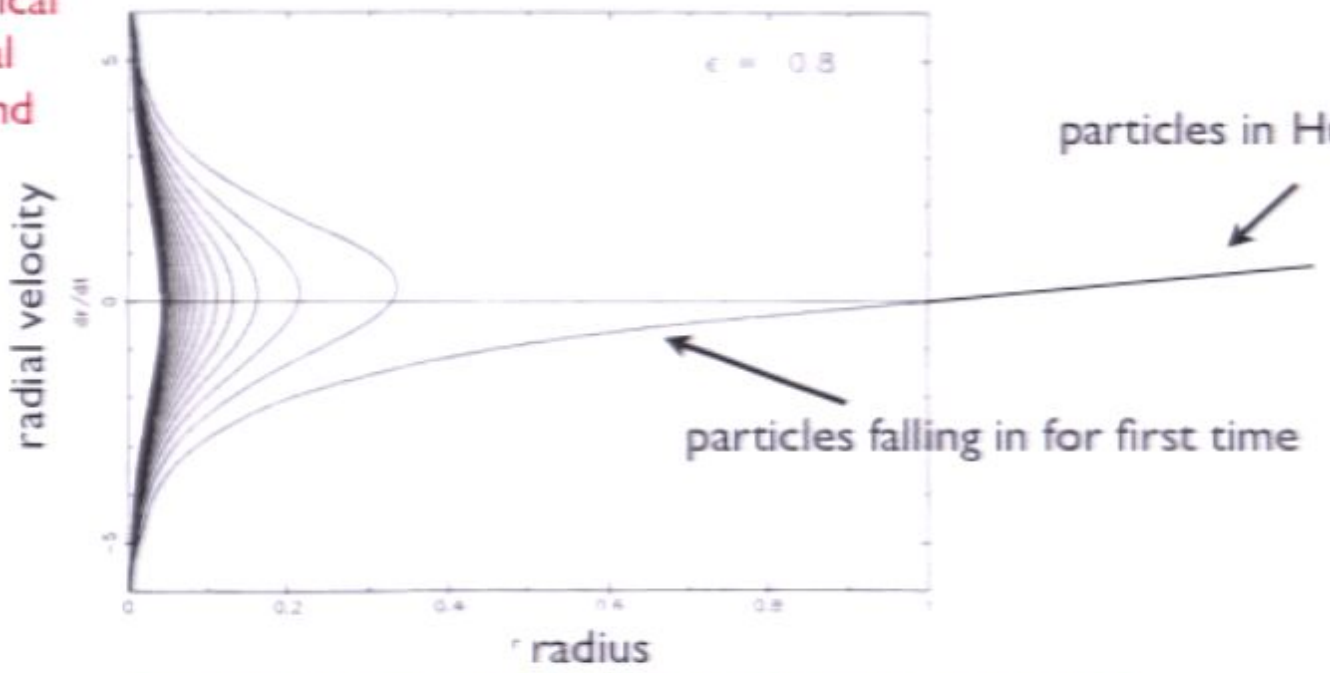

Fillmore & Goldreich, 1984 and Bertschinger, 1985

Note that this solution

(a) satisfies Liouville's theorem (i.e., phase space DF remains a cold, 3D sheet in 6D phase space)

(b) solution is time-reversible

Another baby step toward a theoretical model for a dark matter halo: spherical collapse of a scale-free perturbation in an expanding Universe

each point on curve represents spherical shell with radial velocity dr/dt and radius r(t)

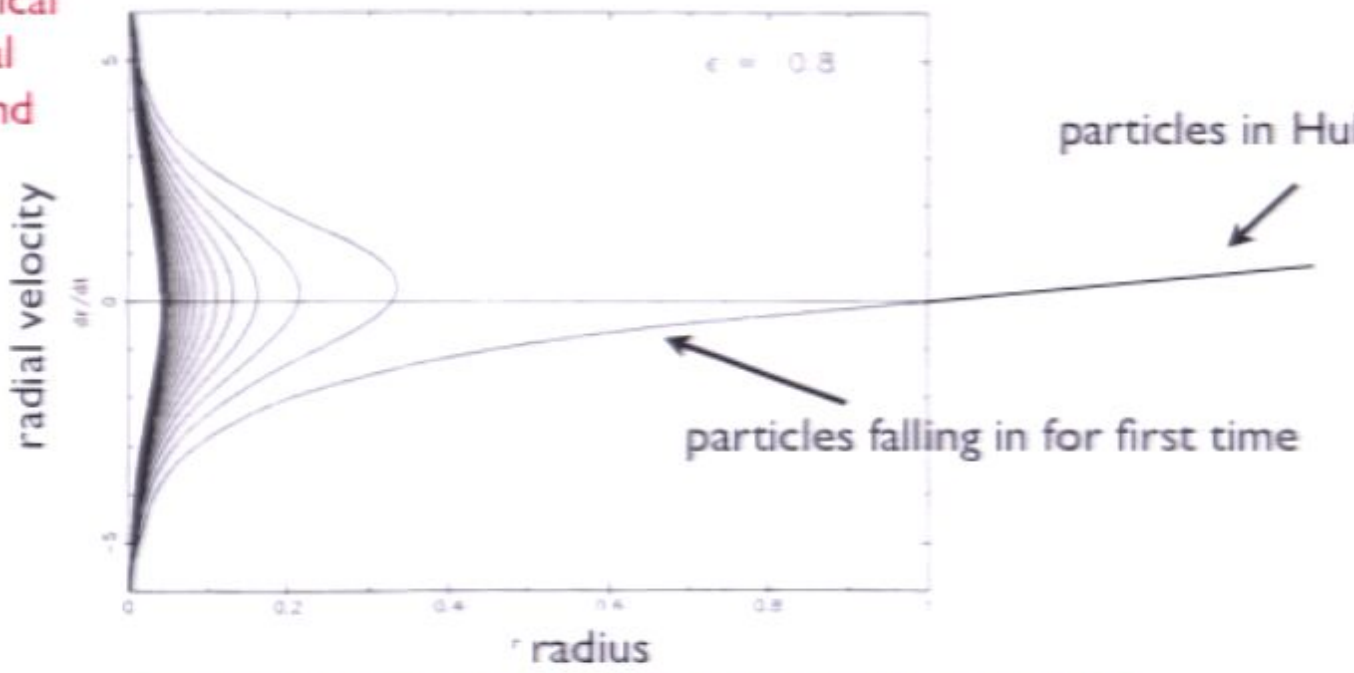

Fillmore & Goldreich, 1984 and Bertschinger, 1985

Note that this solution

(a) satisfies Liouville's theorem (i.e., phase space DF remains a cold, 3D sheet in 6D phase space)

(b) solution is time-reversible

Another baby step toward a theoretical model for a dark matter halo: spherical collapse of a scale-free perturbation in an expanding Universe

each point on curve represents spherical shell with radial velocity dr/dt and radius r(t)

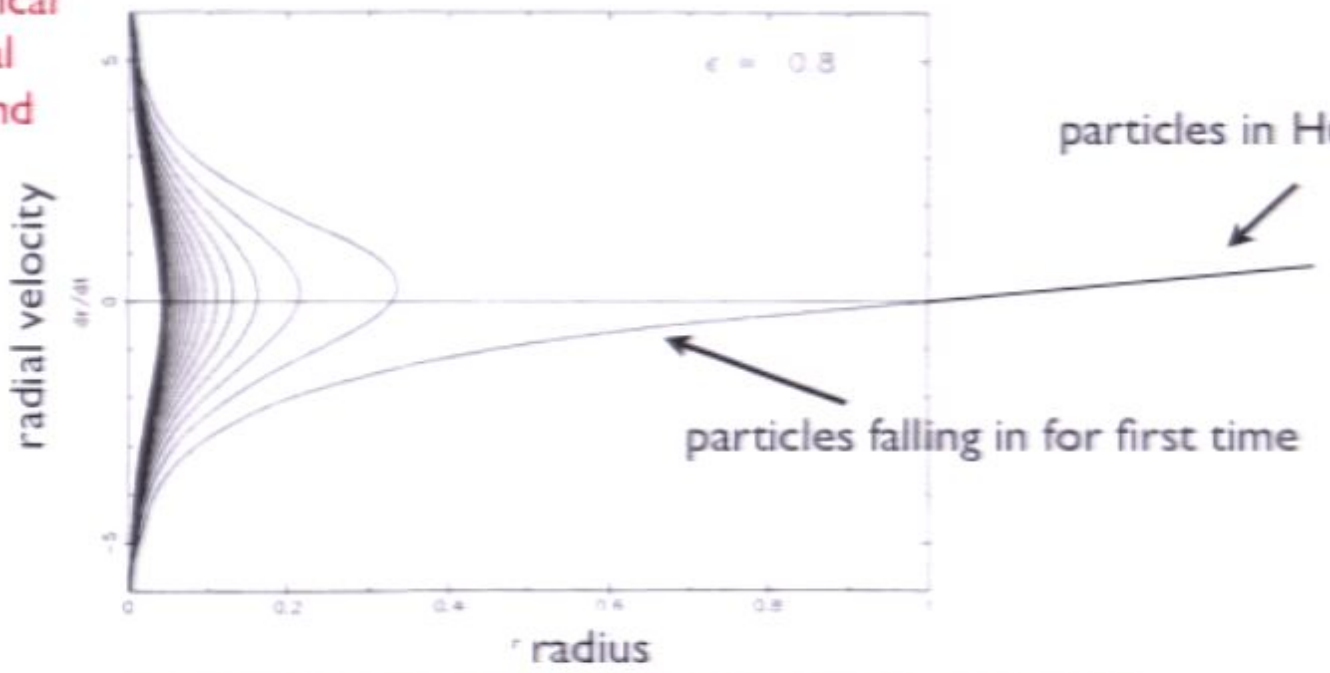

Fillmore & Goldreich, 1984 and Bertschinger, 1985

Note that this solution

(a) satisfies Liouville's theorem (i.e., phase space DF remains a cold, 3D sheet in 6D phase space)

(b) solution is time-reversible

Another baby step toward a theoretical model for a dark matter halo: spherical collapse of a scale-free perturbation in an expanding Universe

each point on curve represents spherical shell with radial velocity dr/dt and radius r(t)

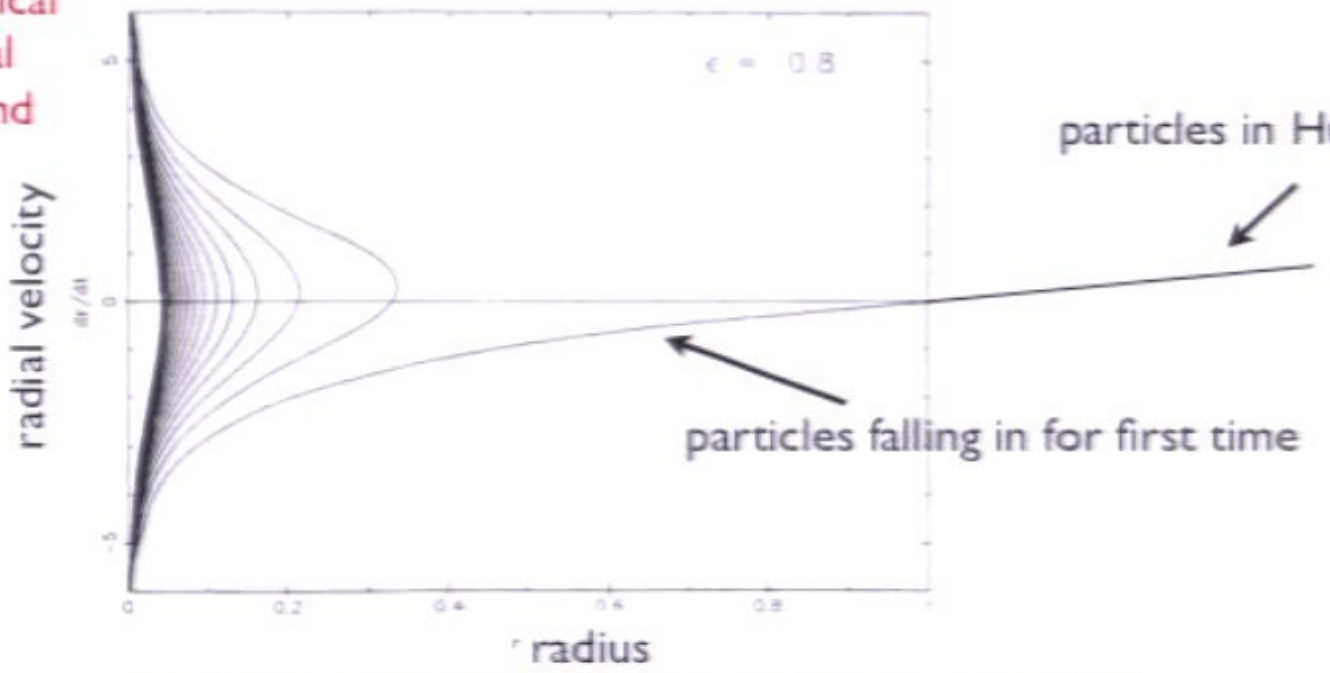

Fillmore & Goldreich, 1984 and Bertschinger, 1985

Note that this solution

(a) satisfies Liouville's theorem (i.e., phase space DF remains a cold, 3D sheet in 6D phase space)

(b) solution is time-reversible

Another baby step toward a theoretical model for a dark matter halo: spherical collapse of a scale-free perturbation in an expanding Universe

each point on curve represents spherical shell with radial velocity dr/dt and radius r(t)

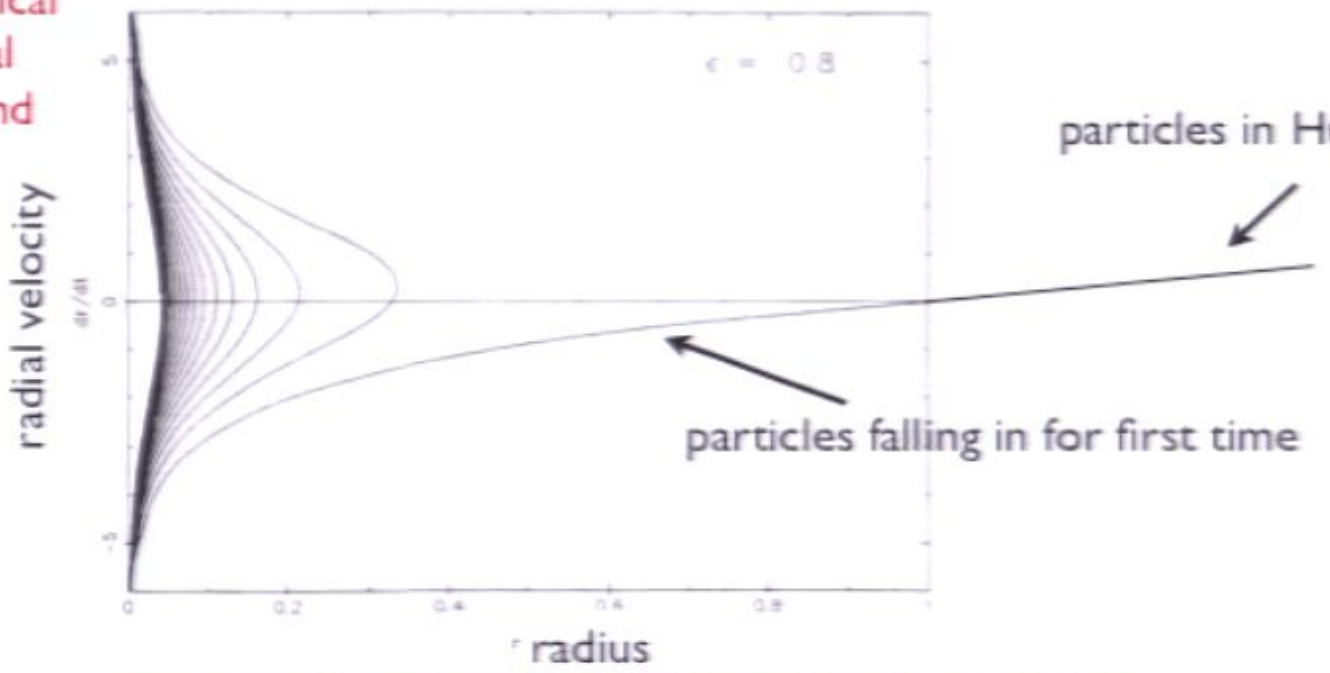

Fillmore & Goldreich, 1984 and Bertschinger, 1985

Note that this solution

(a) satisfies Liouville's theorem (i.e., phase space DF remains a cold, 3D sheet in 6D phase space)

(b) solution is time-reversible

Another baby step toward a theoretical model for a dark matter halo: spherical collapse of a scale-free perturbation in an expanding Universe

each point on curve represents spherical shell with radial velocity dr/dt and radius r(t)

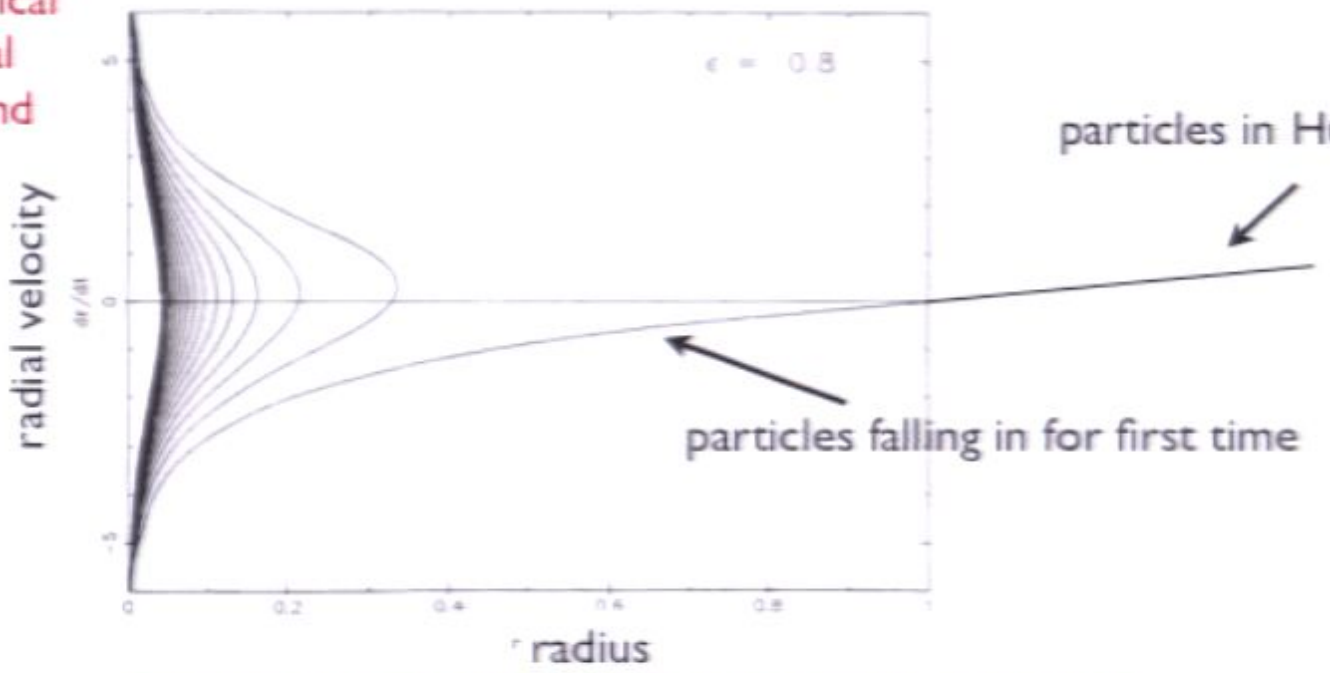

Fillmore & Goldreich, 1984 and Bertschinger, 1985

Note that this solution

(a) satisfies Liouville's theorem (i.e., phase space DF remains a cold, 3D sheet in 6D phase space)

(b) solution is time-reversible

Another baby step toward a theoretical model for a dark matter halo: spherical collapse of a scale-free perturbation in an expanding Universe

each point on curve represents spherical shell with radial velocity dr/dt and radius r(t)

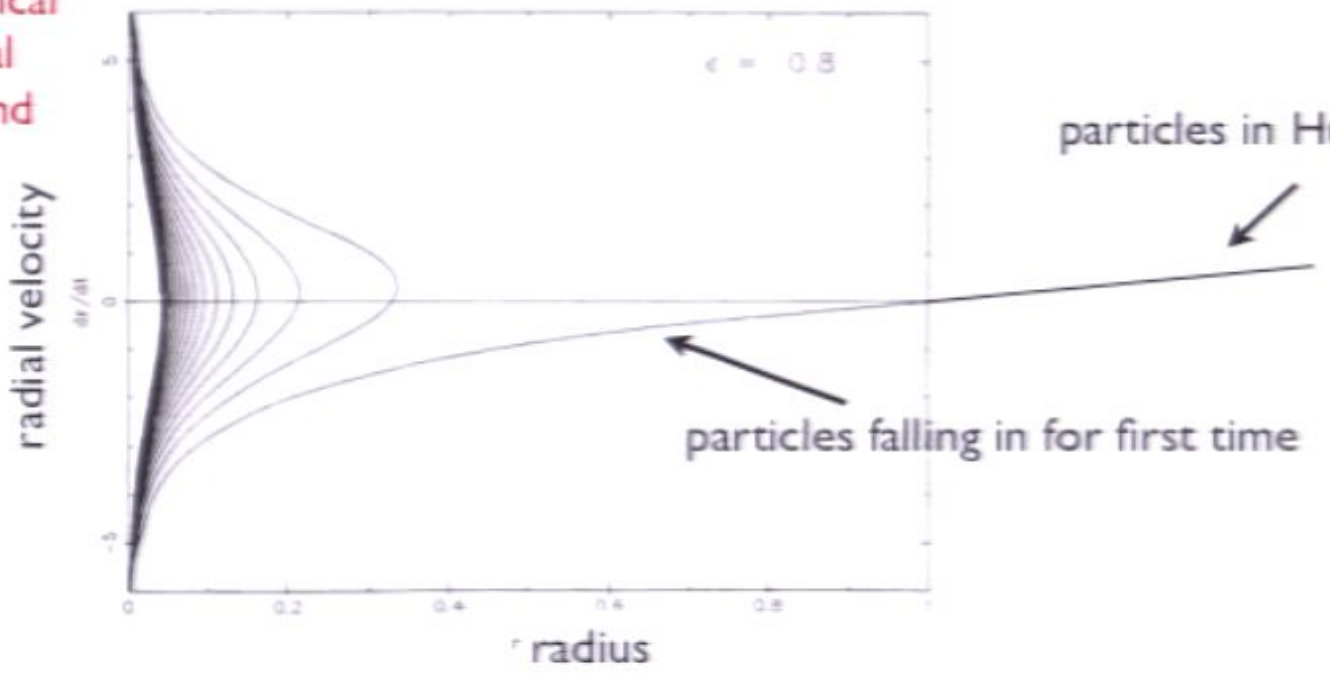

Fillmore & Goldreich, 1984 and Bertschinger, 1985

Note that this solution

(a) satisfies Liouville's theorem (i.e., phase space DF remains a cold, 3D sheet in 6D phase space)

(b) solution is time-reversible

Another baby step toward a theoretical model for a dark matter halo: spherical collapse of a scale-free perturbation in an expanding Universe

each point on curve represents spherical shell with radial velocity dr/dt and radius r(t)

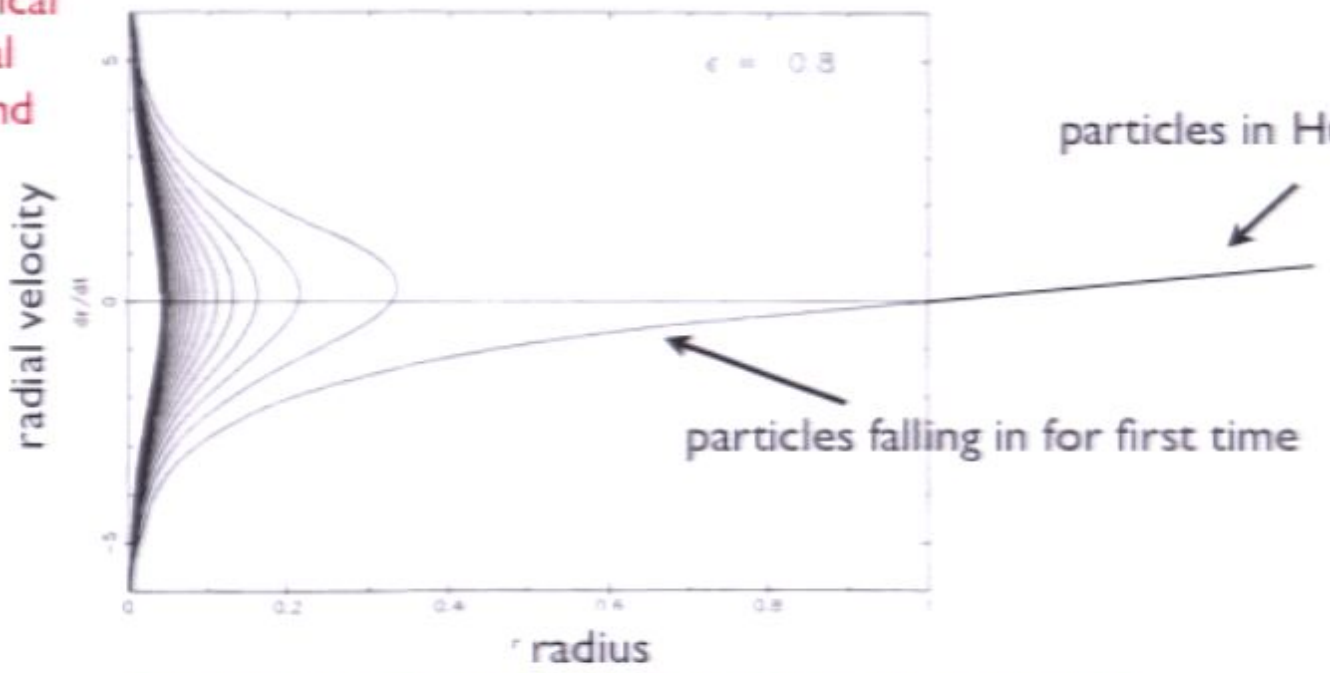

Fillmore & Goldreich, 1984 and Bertschinger, 1985

Note that this solution

(a) satisfies Liouville's theorem (i.e., phase space DF remains a cold, 3D sheet in 6D phase space)

(b) solution is time-reversible

Another baby step toward a theoretical model for a dark matter halo: spherical collapse of a scale-free perturbation in an expanding Universe

each point on curve represents spherical shell with radial velocity dr/dt and radius r(t)

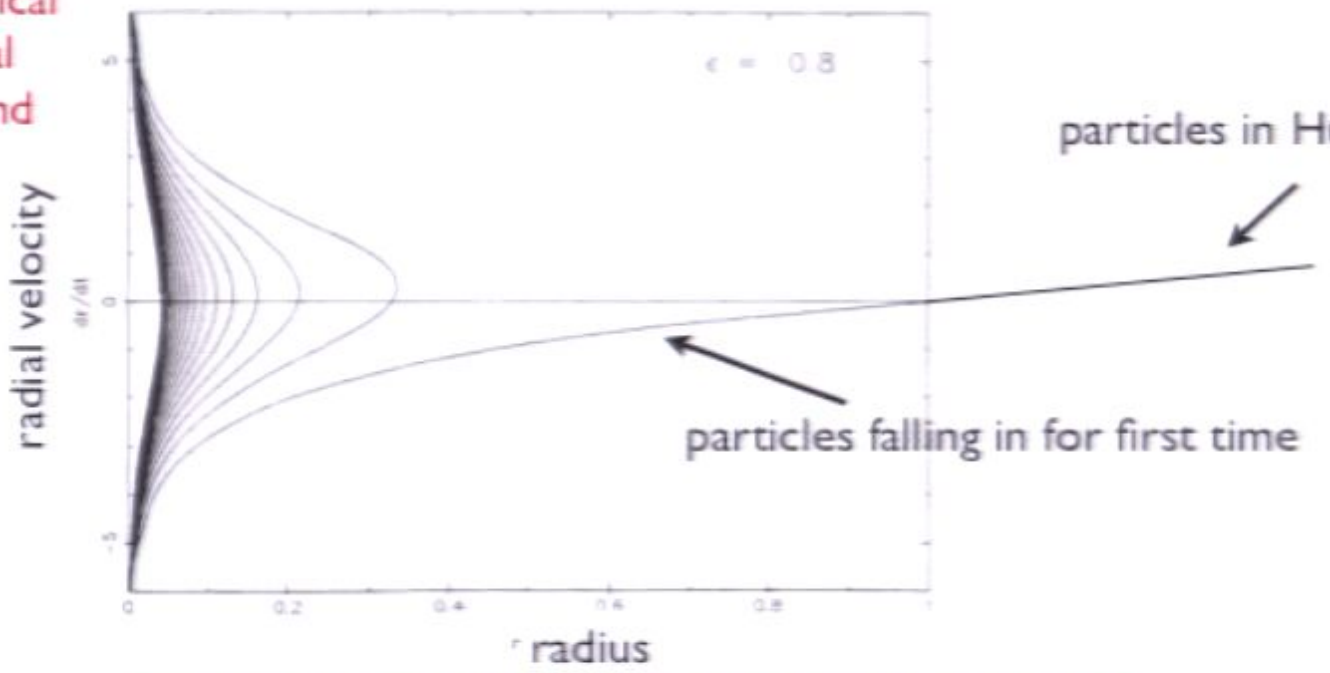

Fillmore & Goldreich, 1984 and Bertschinger, 1985

Note that this solution

(a) satisfies Liouville's theorem (i.e., phase space DF remains a cold, 3D sheet in 6D phase space)

(b) solution is time-reversible

Another baby step toward a theoretical model for a dark matter halo: spherical collapse of a scale-free perturbation in an expanding Universe

each point on curve represents spherical shell with radial velocity dr/dt and radius r(t)

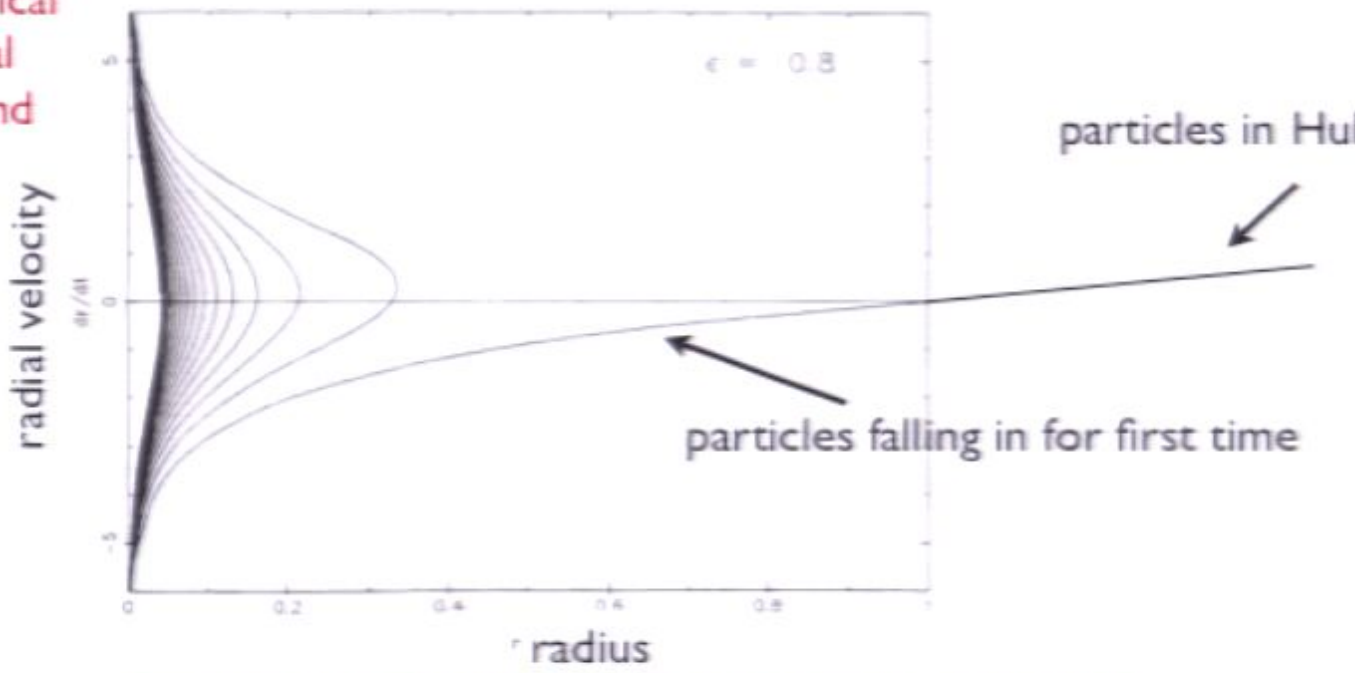

Fillmore & Goldreich, 1984 and Bertschinger, 1985

Note that this solution

(a) satisfies Liouville's theorem (i.e., phase space DF remains a cold, 3D sheet in 6D phase space)

(b) solution is time-reversible

Another baby step toward a theoretical model for a dark matter halo: spherical collapse of a scale-free perturbation in an expanding Universe

each point on curve represents spherical shell with radial velocity dr/dt and radius r(t)

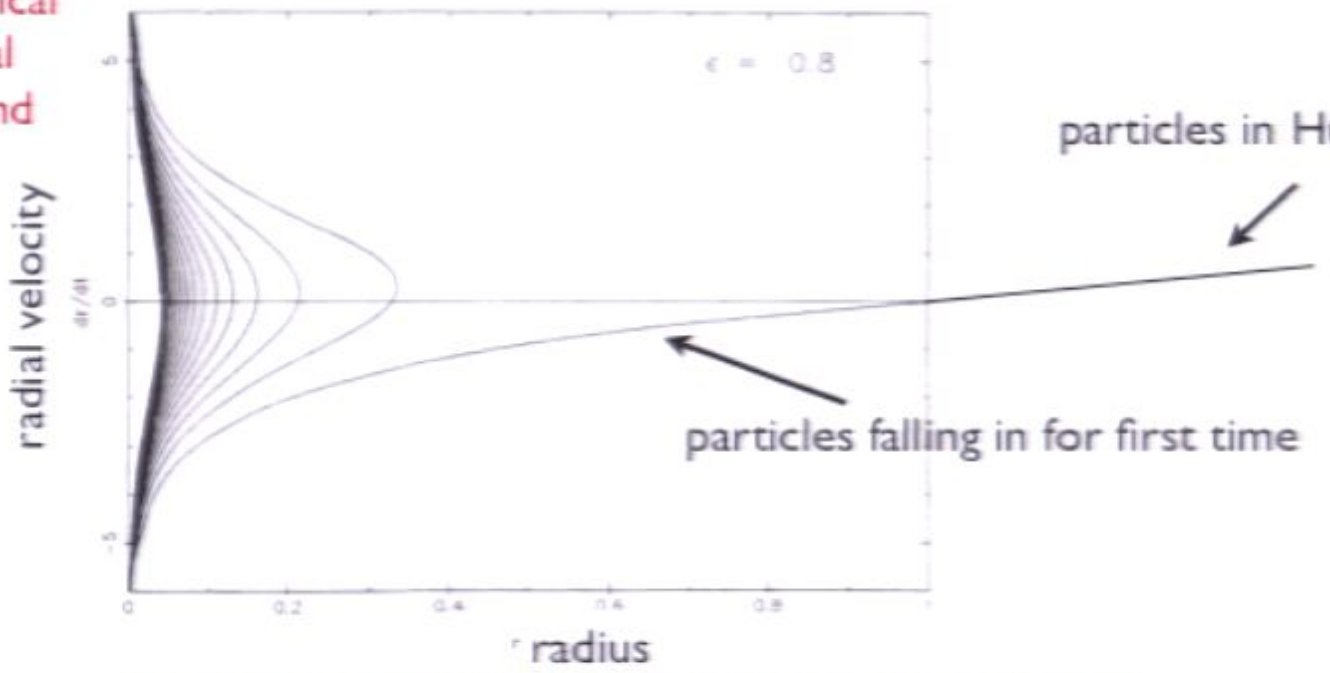

Fillmore & Goldreich, 1984 and Bertschinger, 1985

Note that this solution

(a) satisfies Liouville's theorem (i.e., phase space DF remains a cold, 3D sheet in 6D phase space)

(b) solution is time-reversible

Another baby step toward a theoretical model for a dark matter halo: spherical collapse of a scale-free perturbation in an expanding Universe

each point on curve represents spherical shell with radial velocity dr/dt and radius r(t)

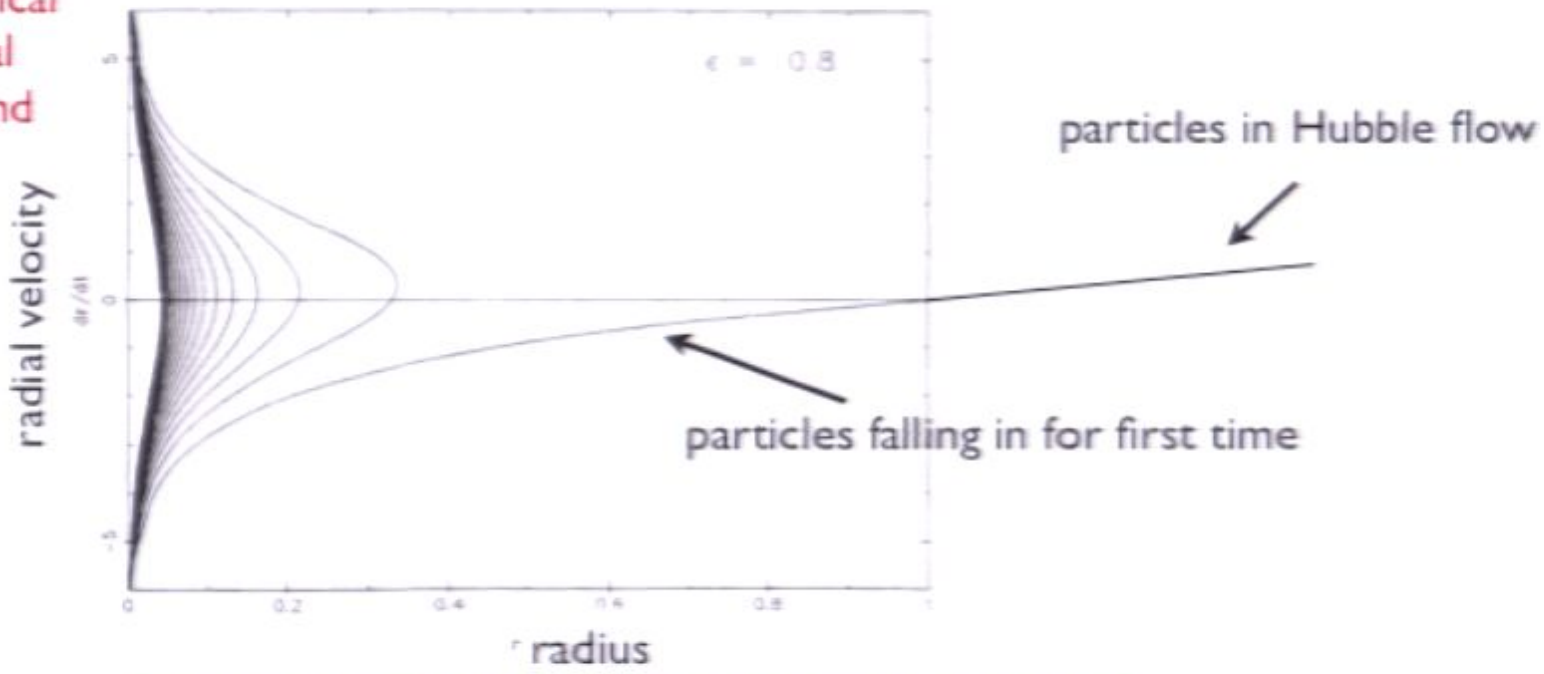

Fillmore & Goldreich, 1984 and Bertschinger, 1985

Note that this solution

(a) satisfies Liouville's theorem (i.e., phase space DF remains a cold, 3D sheet in 6D phase space)

(b) solution is time-reversible

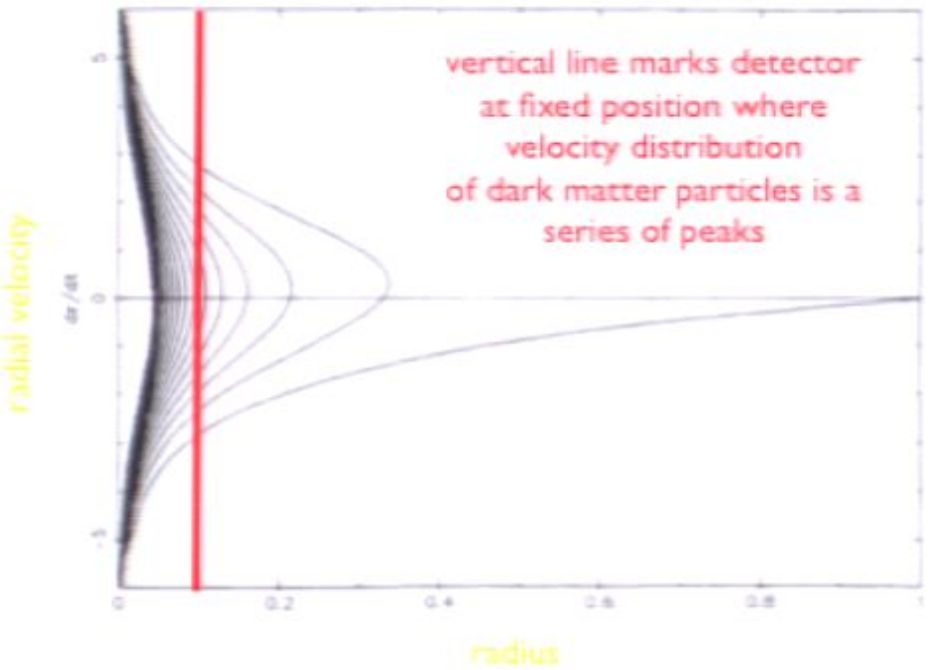

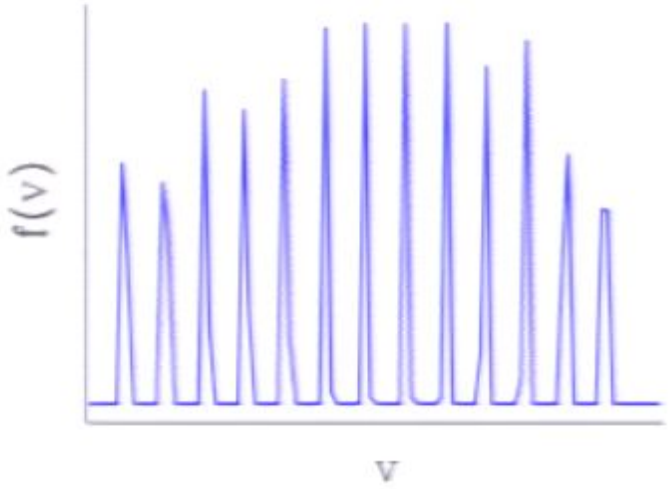

see papers on axion detection
by Sikivie and collaborators

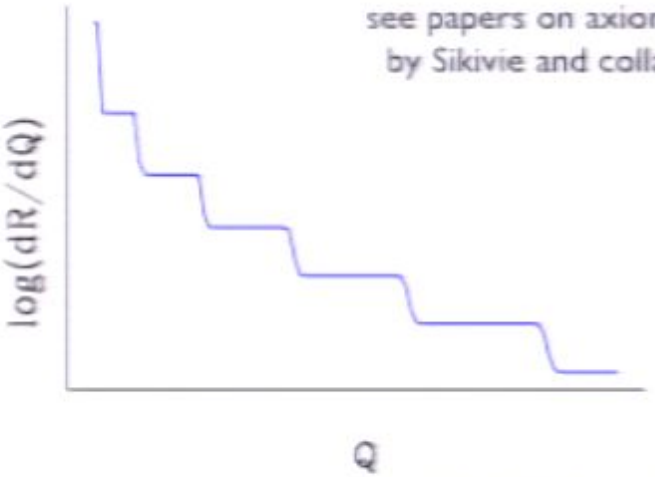

for WIMPs we have a series
of steps in recoil energy, Q
(see Stiff, LMW, Frieman 2001)

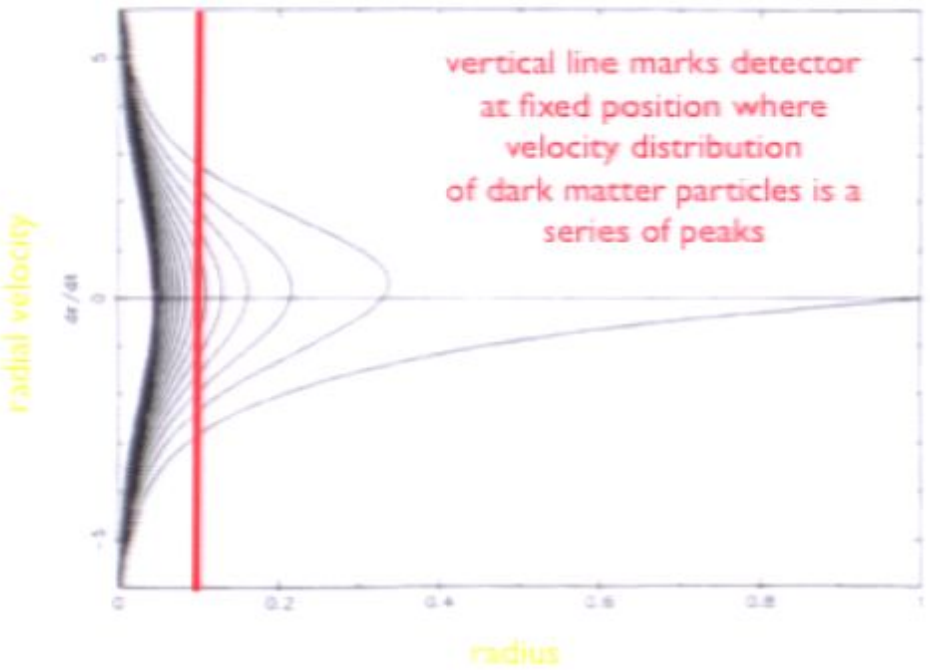

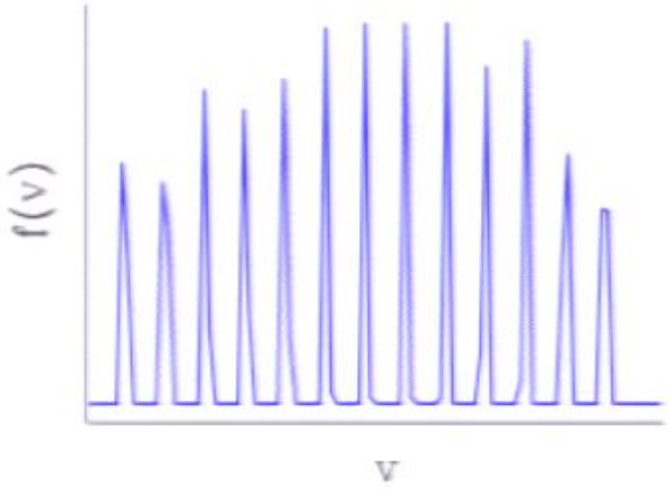

see papers on axion detection
by Sikivie and collaborators

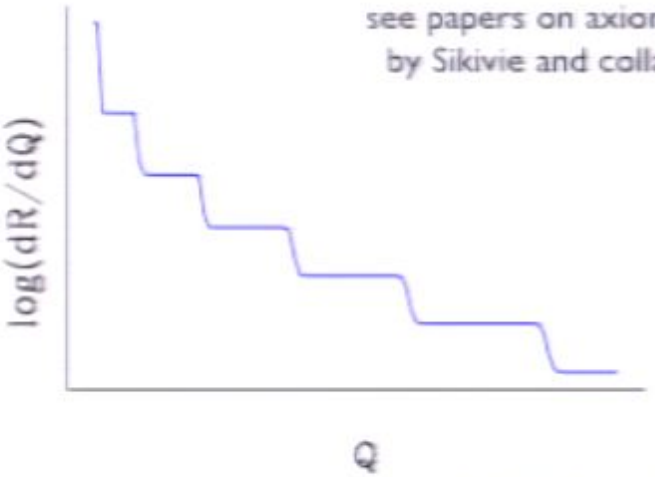

for WIMPs we have a series
of steps in recoil energy, Q
(see Stiff, LMW, Frieman 2001)

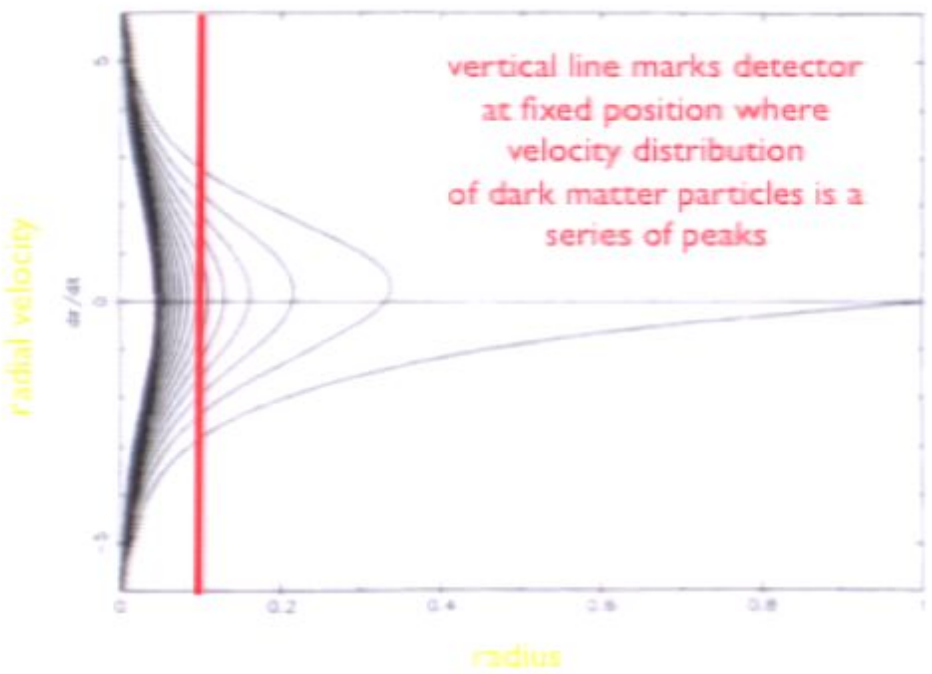

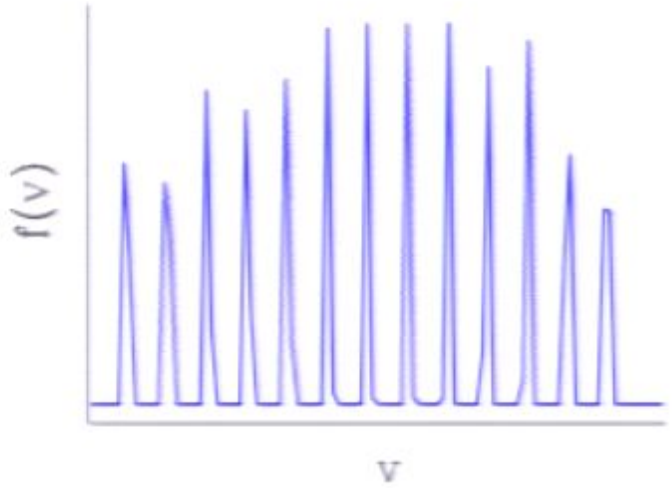

see papers on axion detection
by Sikivie and collaborators

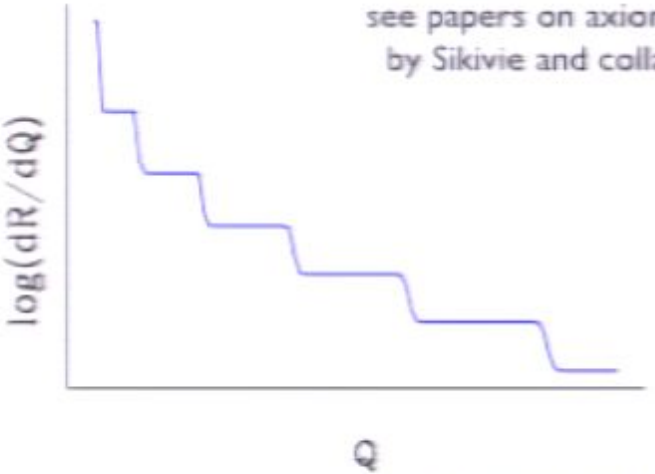

for WIMPs we have a series
of steps in recoil energy, Q
(see Stiff, LMW, Frieman 2001)

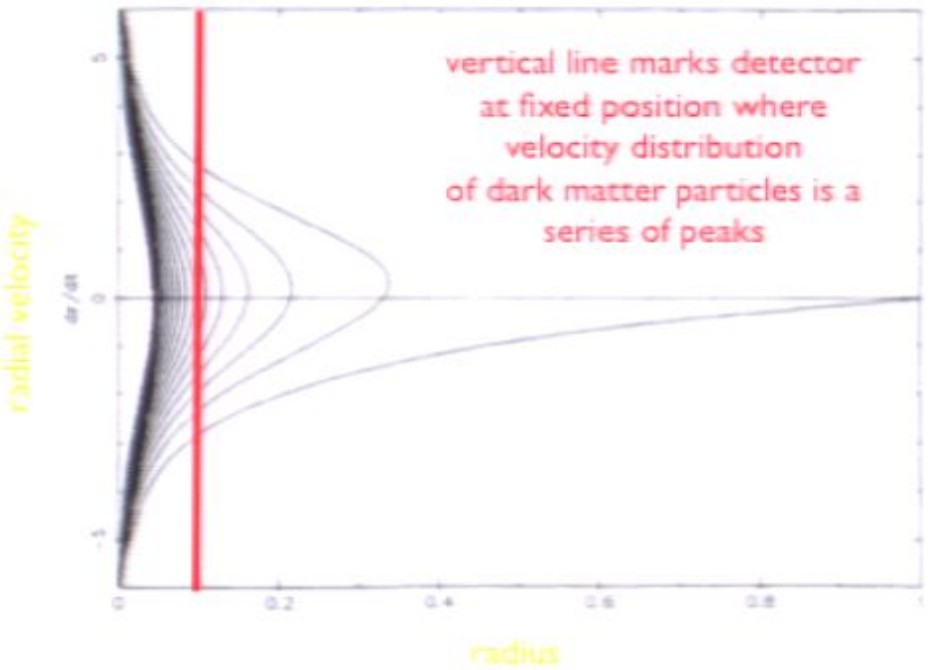

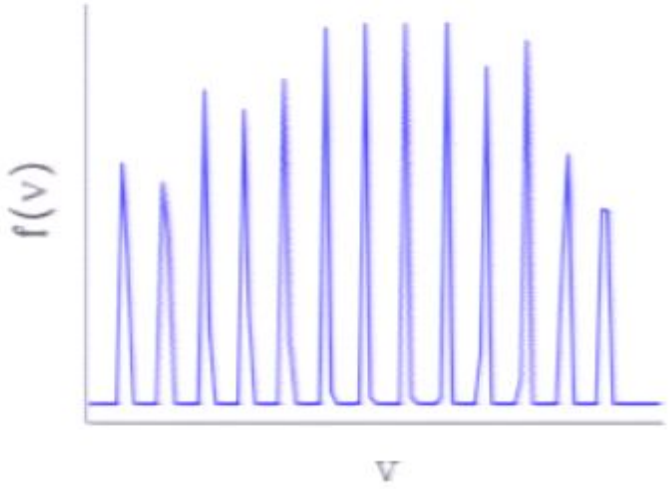

see papers on axion detection
by Sikivie and collaborators

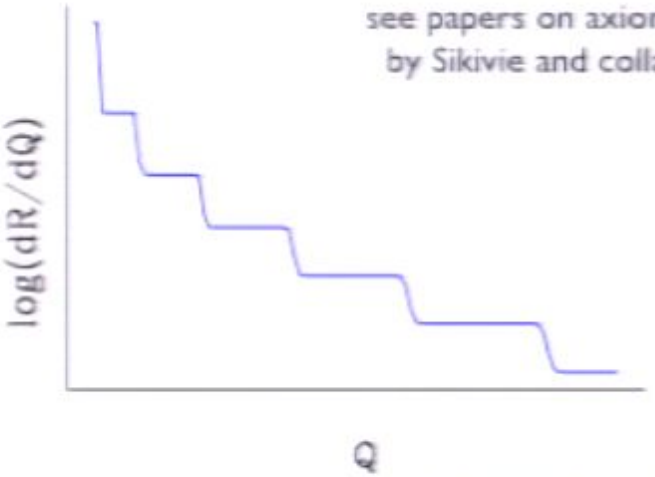

for WIMPs we have a series
of steps in recoil energy, Q
(see Stiff, LMW, Frieman 2001)

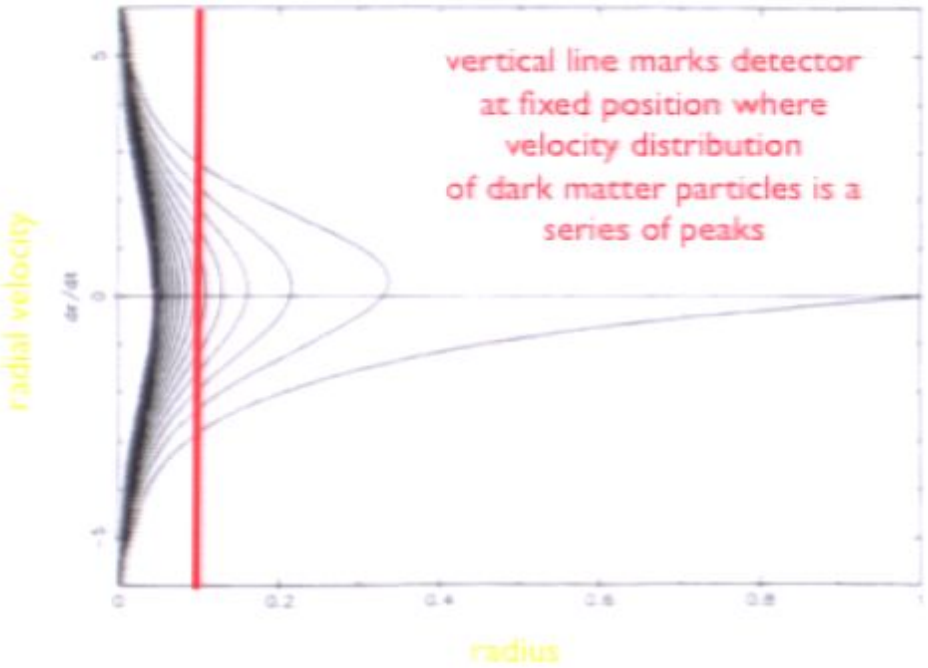

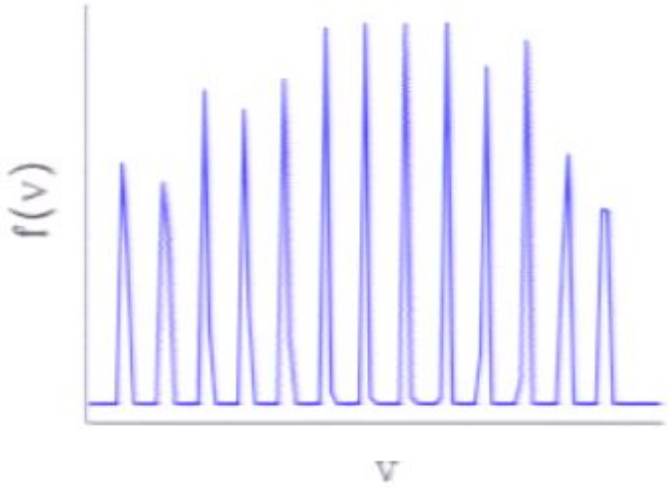

see papers on axion detection
by Sikivie and collaborators

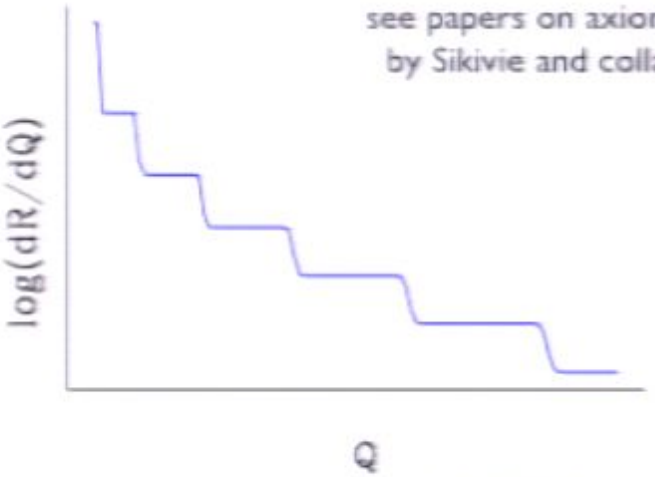

for WIMPs we have a series
of steps in recoil energy, Q
(see Stiff, LMW, Frieman 2001)

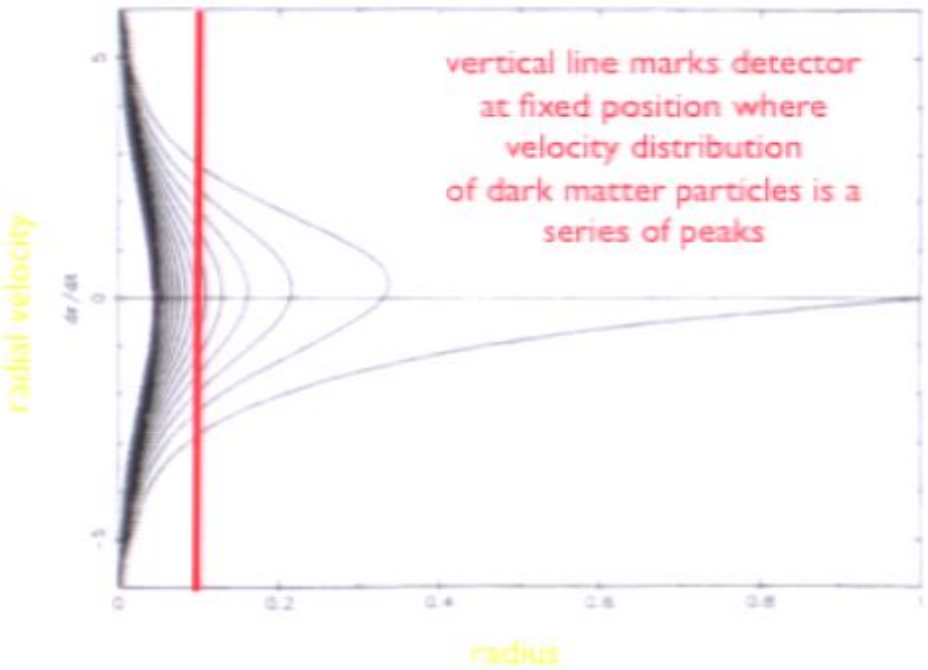

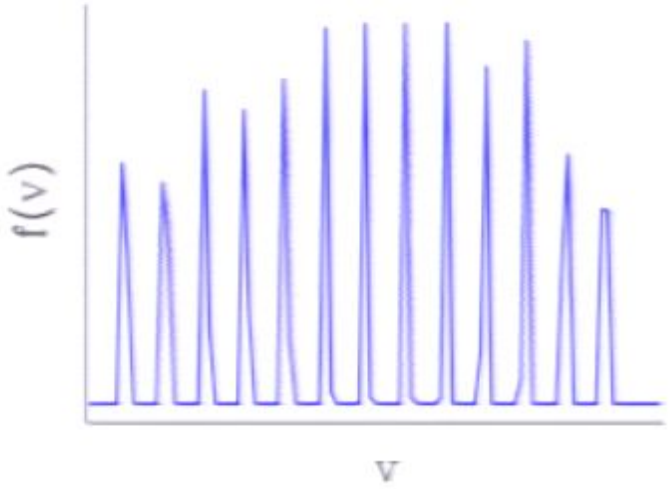

see papers on axion detection
by Sikivie and collaborators

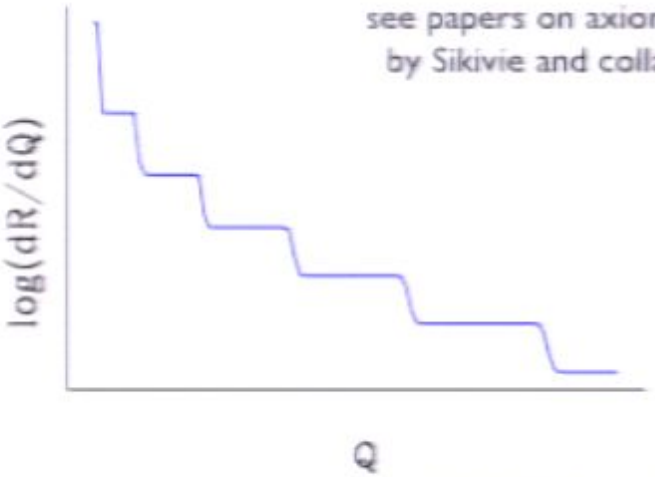

for WIMPs we have a series
of steps in recoil energy, Q
(see Stiff, LMW, Frieman 2001)

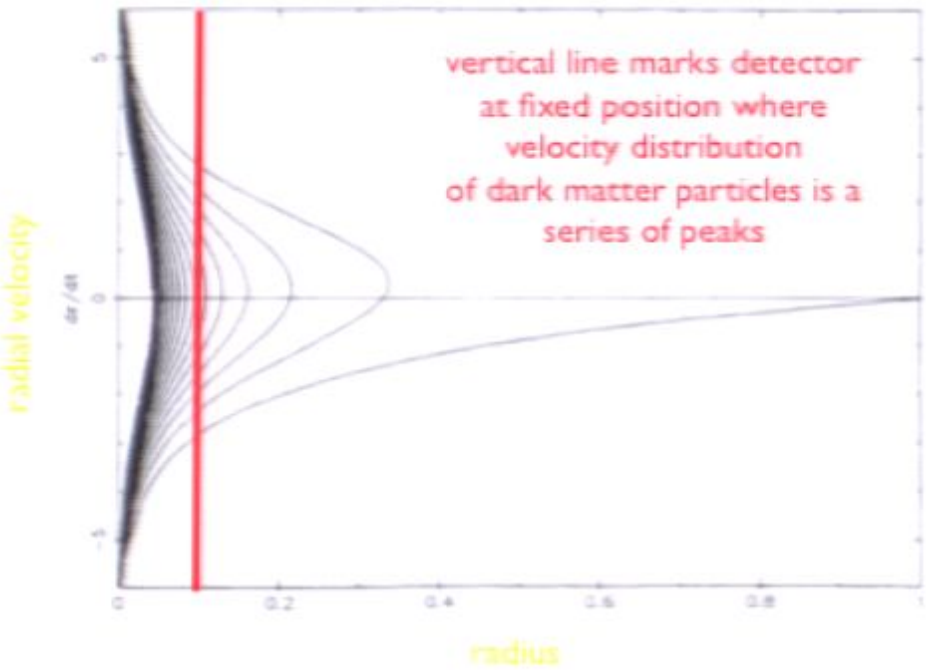

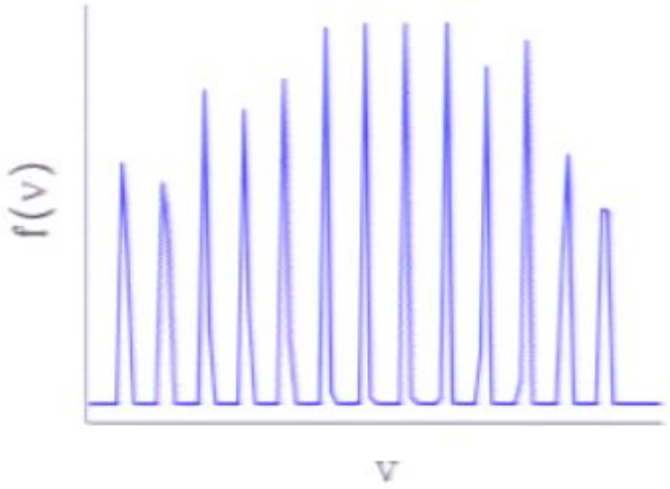

see papers on axion detection
by Sikivie and collaborators

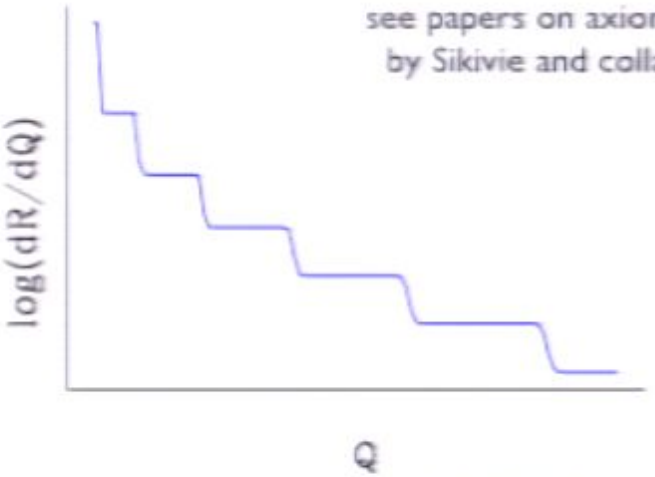

for WIMPs we have a series
of steps in recoil energy, Q
(see Stiff, LMW, Frieman 2001)

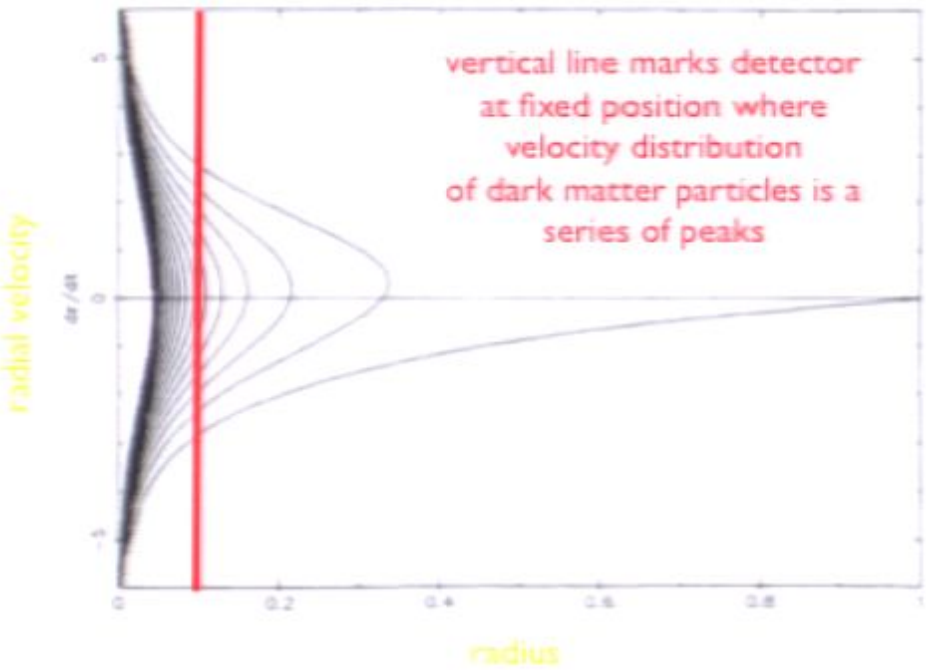

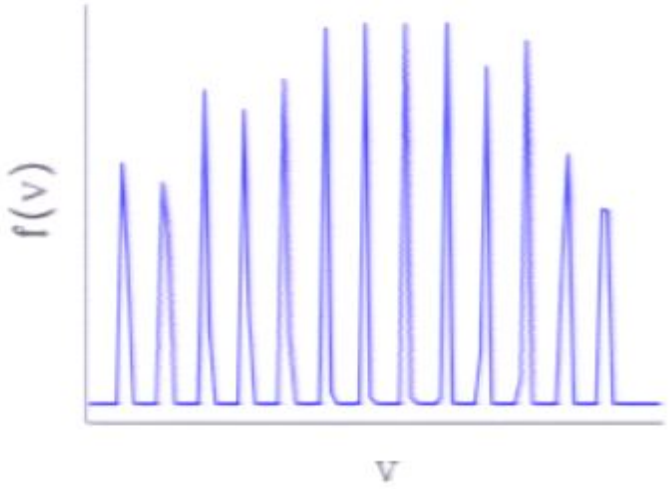

see papers on axion detection
by Sikivie and collaborators

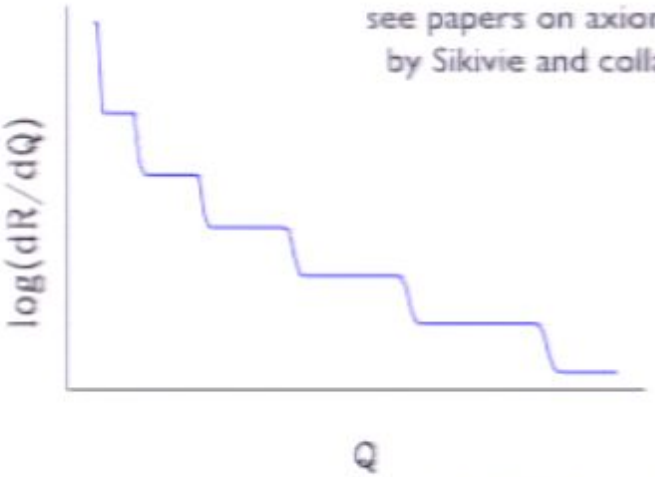

for WIMPs we have a series
of steps in recoil energy, Q
(see Stiff, LMW, Frieman 2001)

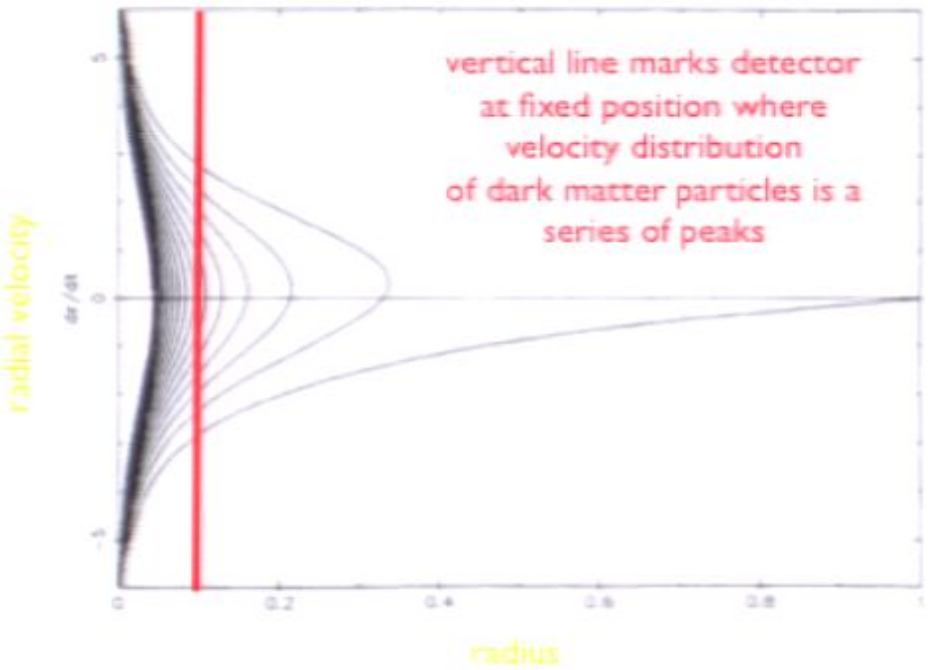

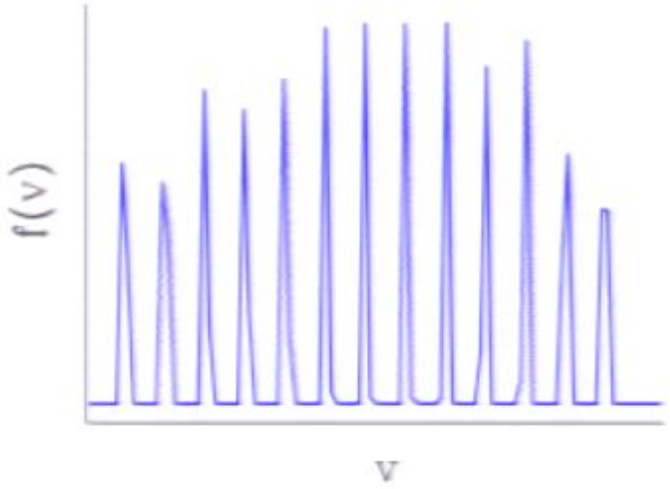

see papers on axion detection
by Sikivie and collaborators

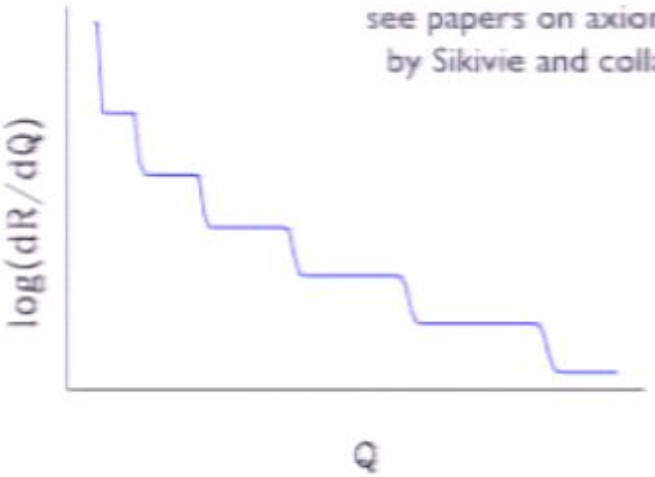

for WIMPs we have a series
of steps in recoil energy, Q
(see Stiff, LMW, Frieman 2001)

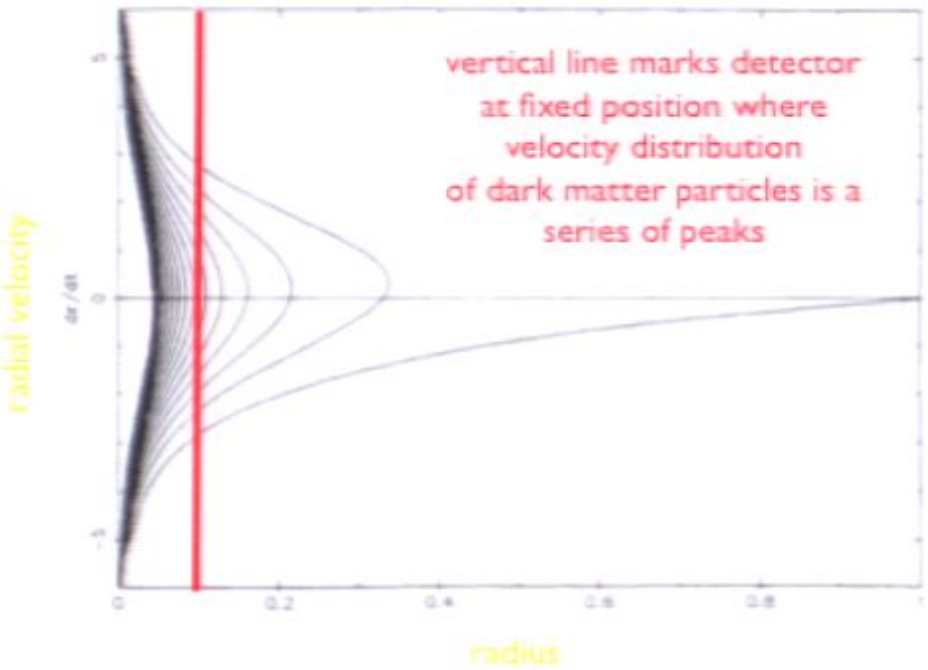

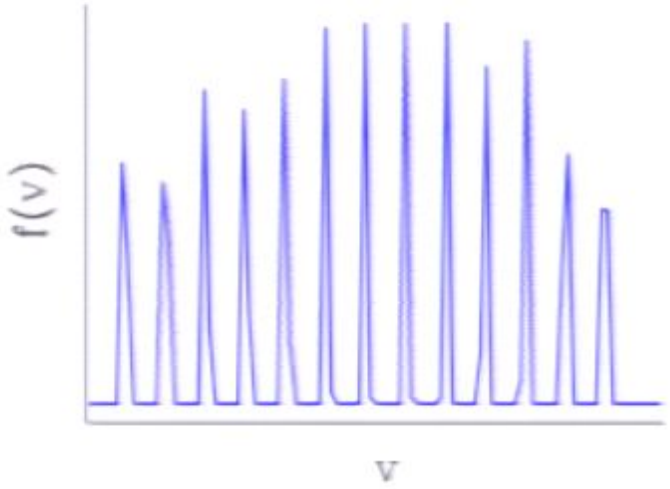

see papers on axion detection
by Sikivie and collaborators

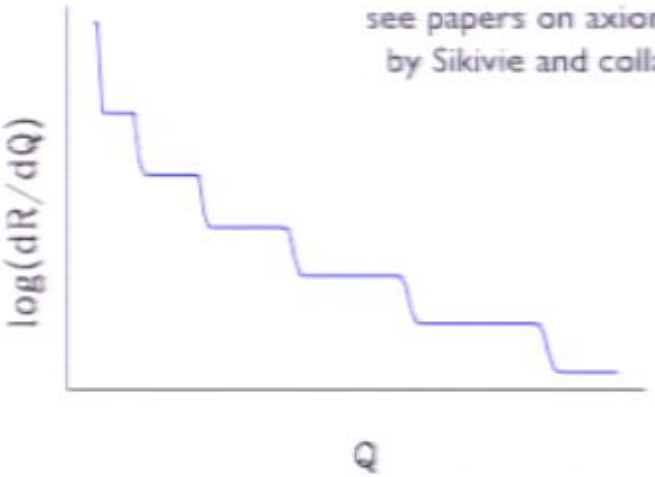

for WIMPs we have a series
of steps in recoil energy, Q
(see Stiff, LMW, Frieman 2001)

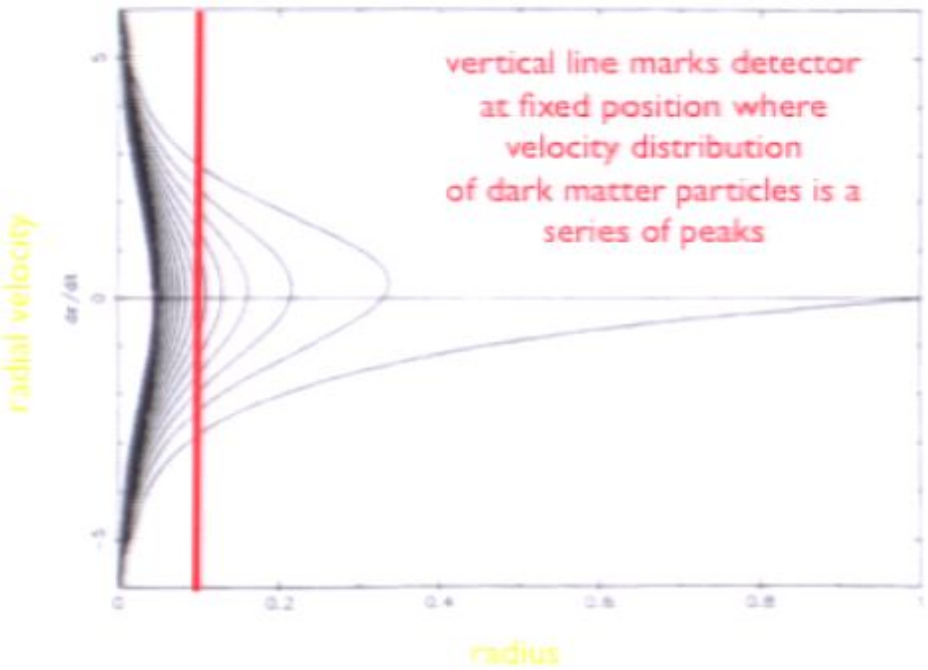

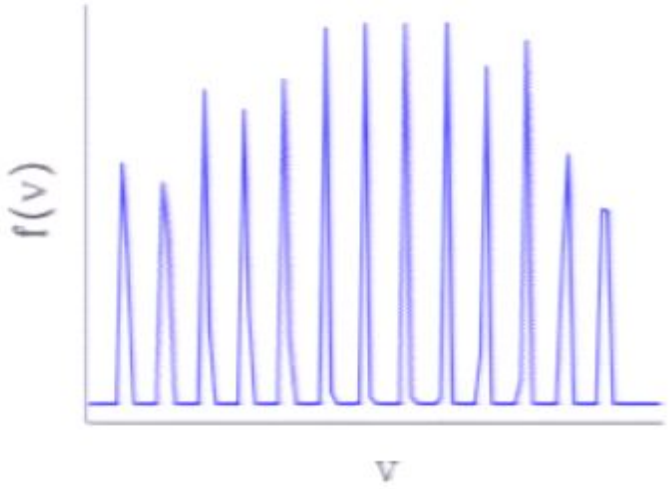

see papers on axion detection
by Sikivie and collaborators

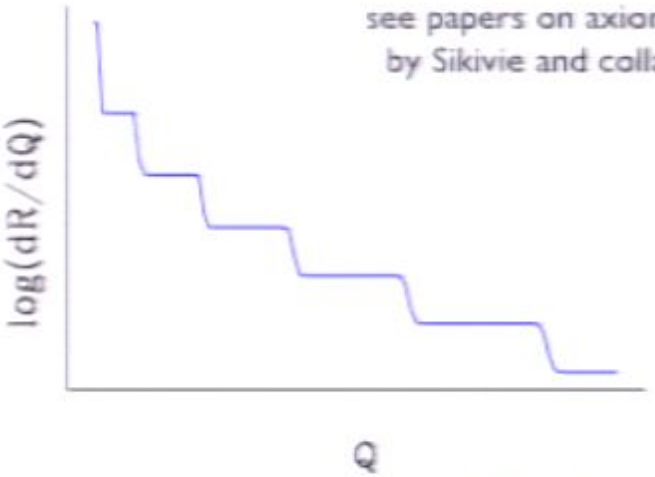

for WIMPs we have a series
of steps in recoil energy, Q
(see Stiff, LMW, Frieman 2001)

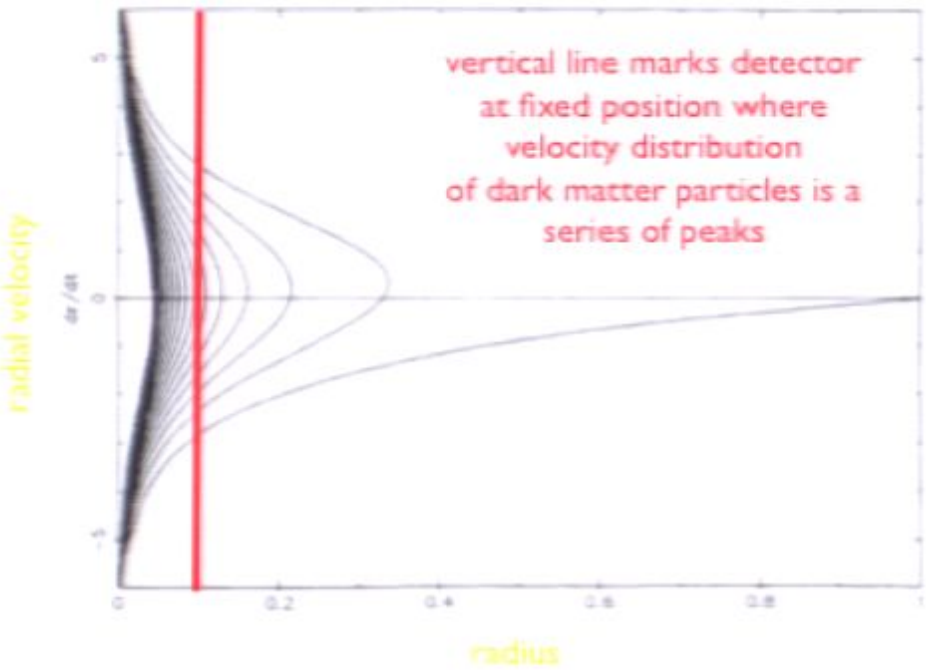

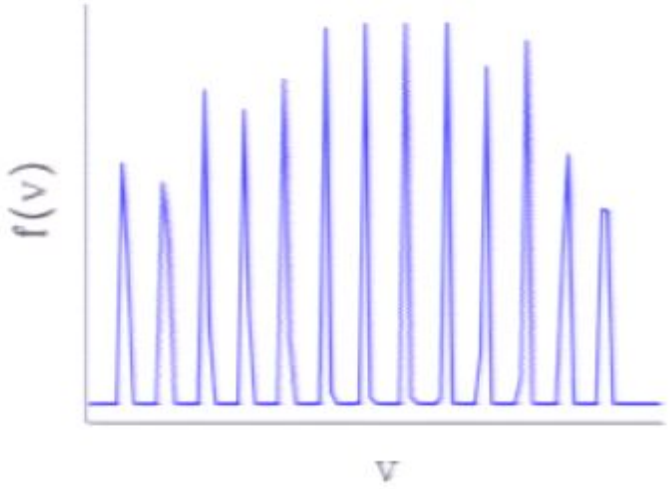

see papers on axion detection
by Sikivie and collaborators

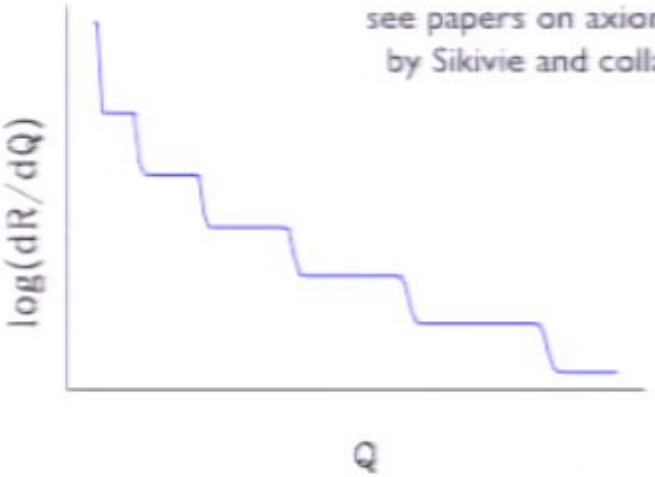

for WIMPs we have a series
of steps in recoil energy, Q
(see Stiff, LMW, Frieman 2001)

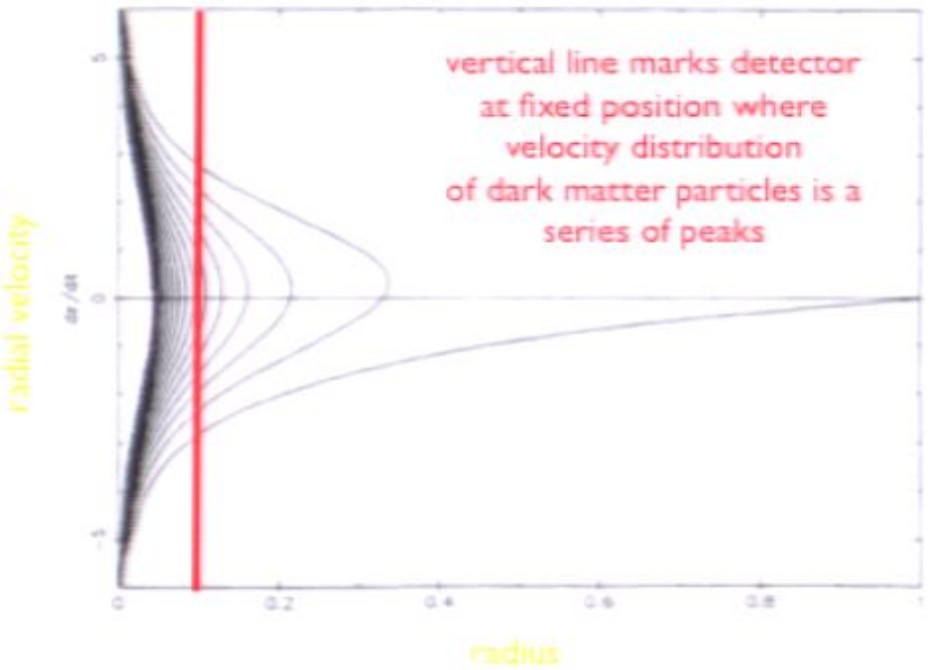

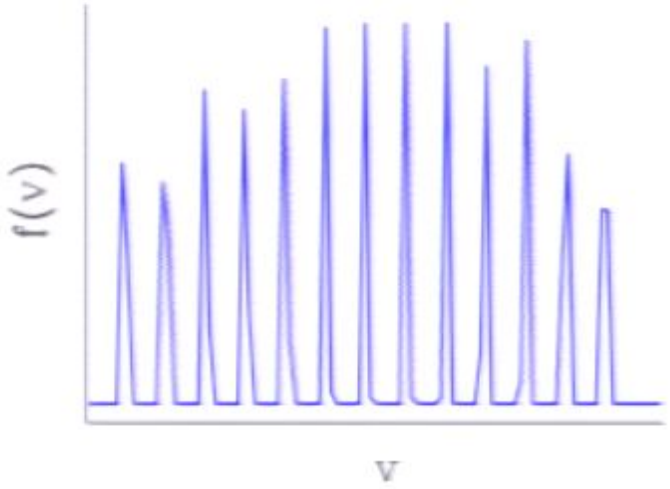

see papers on axion detection
by Sikivie and collaborators

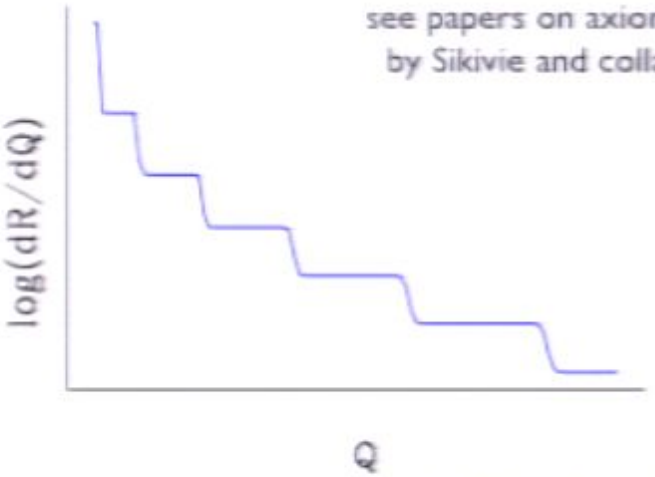

for WIMPs we have a series
of steps in recoil energy, Q
(see Stiff, LMW, Frieman 2001)

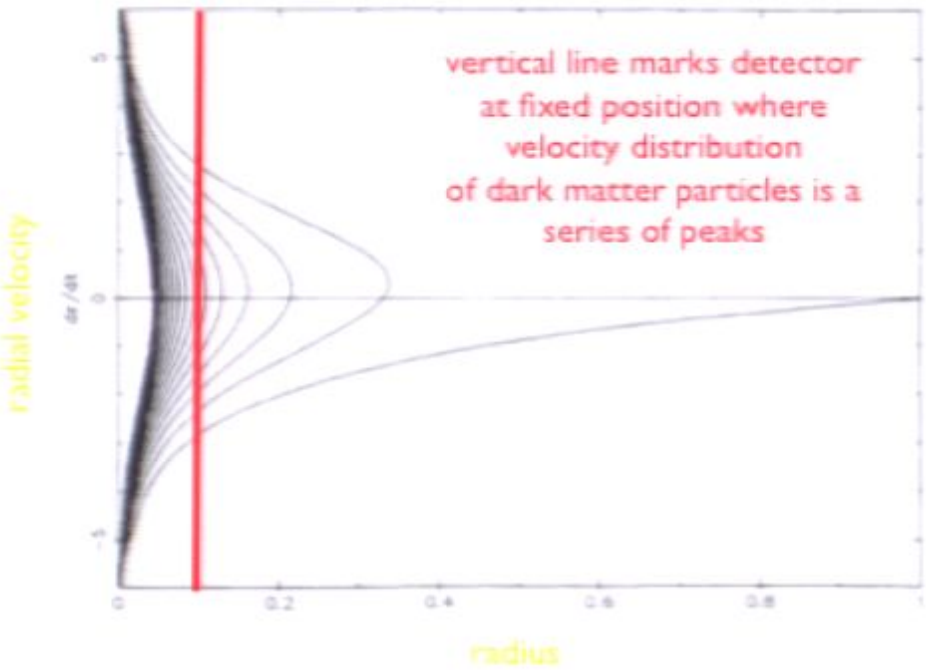

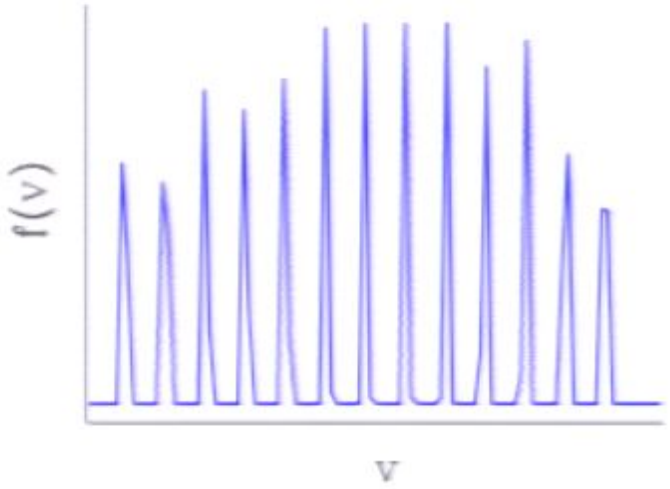

see papers on axion detection
by Sikivie and collaborators

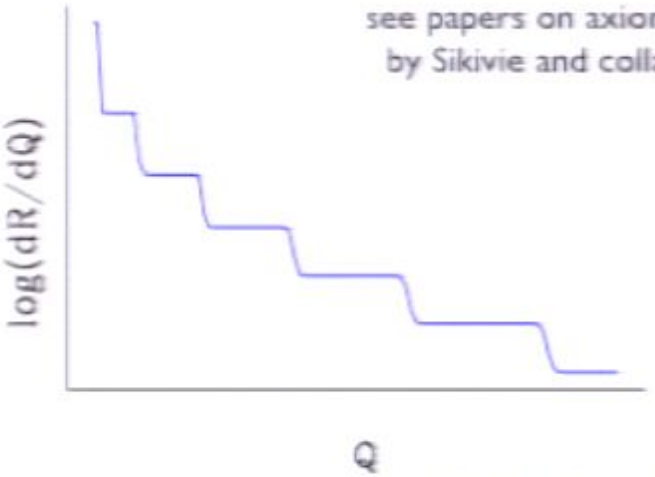

for WIMPs we have a series
of steps in recoil energy, Q
(see Stiff, LMW, Frieman 2001)

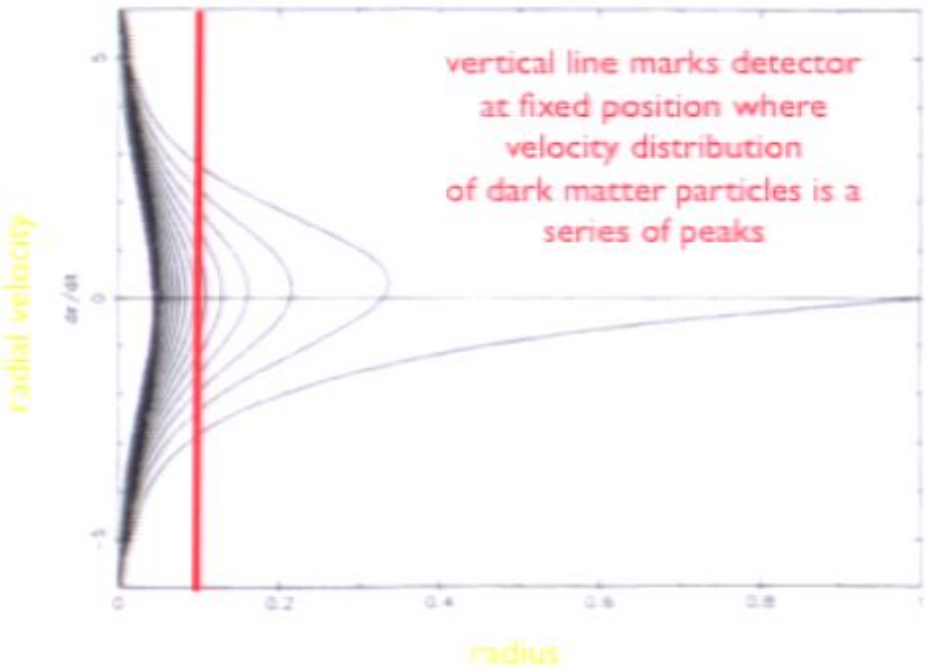

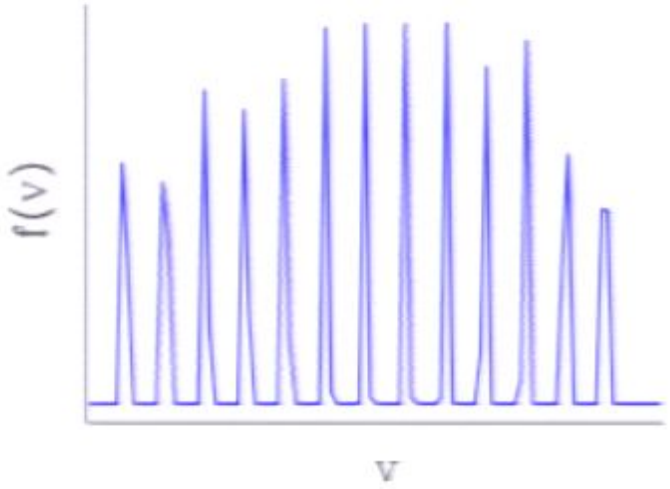

see papers on axion detection
by Sikivie and collaborators

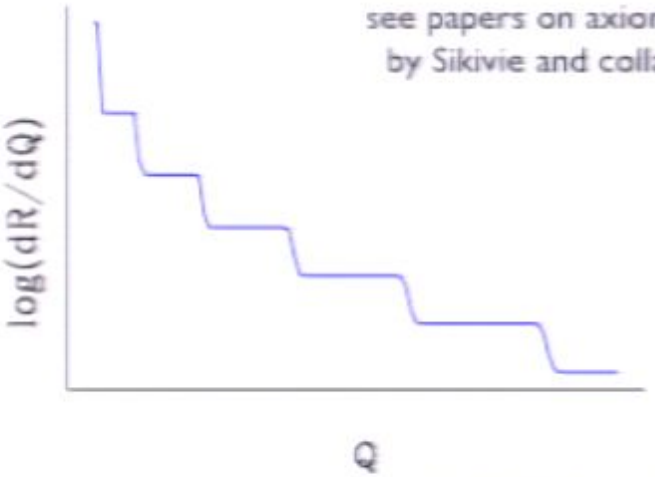

for WIMPs we have a series
of steps in recoil energy, Q
(see Stiff, LMW, Frieman 2001)

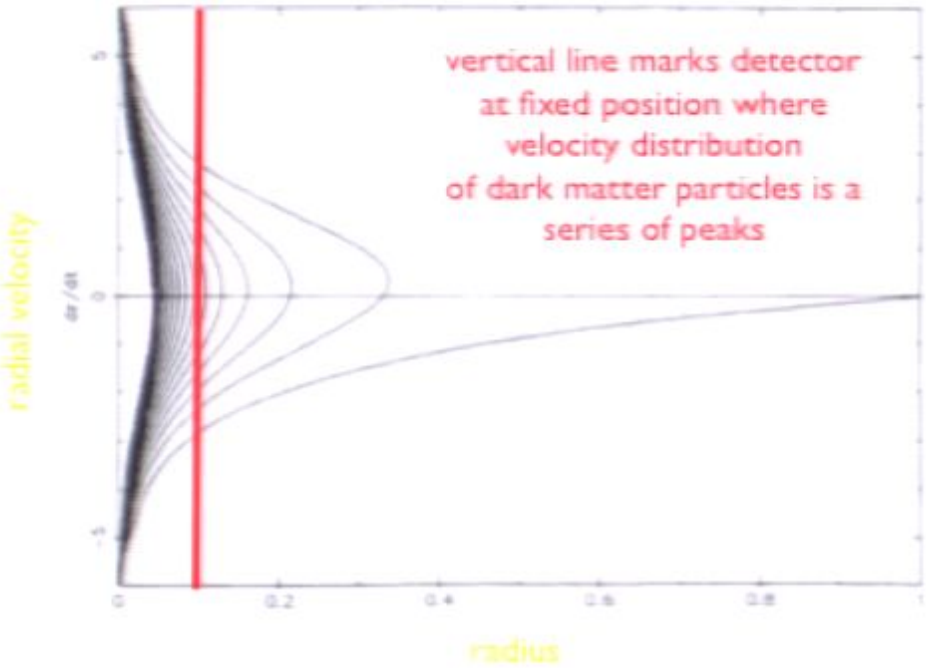

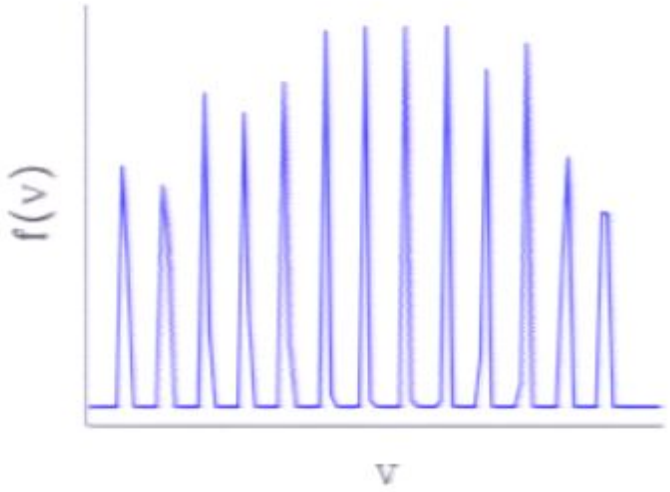

see papers on axion detection
by Sikivie and collaborators

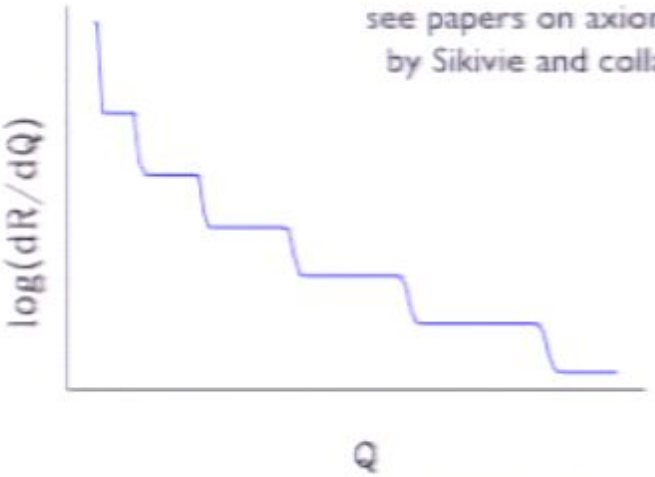

for WIMPs we have a series
of steps in recoil energy, Q
(see Stiff, LMW, Frieman 2001)

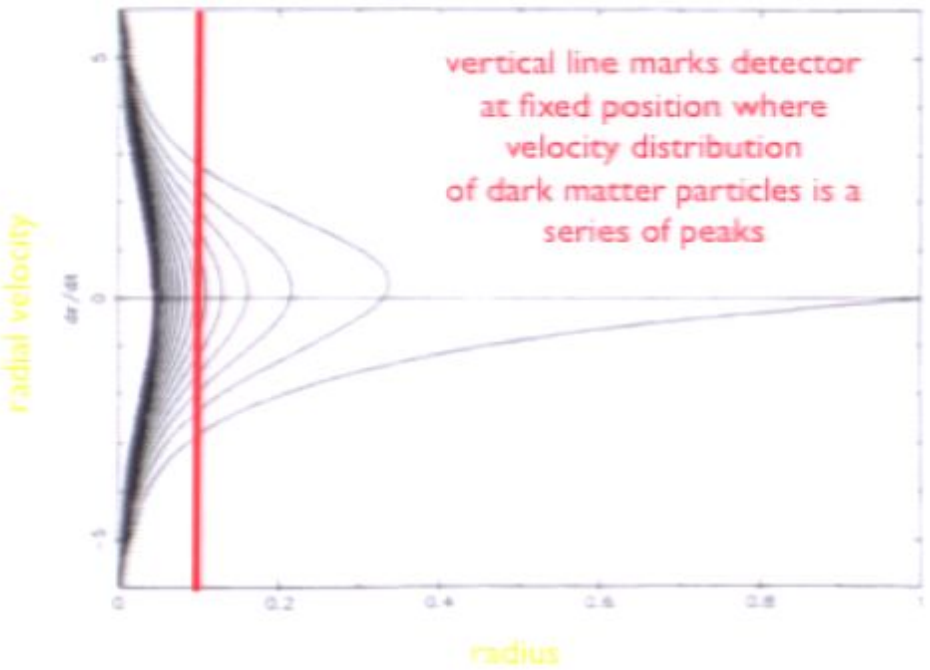

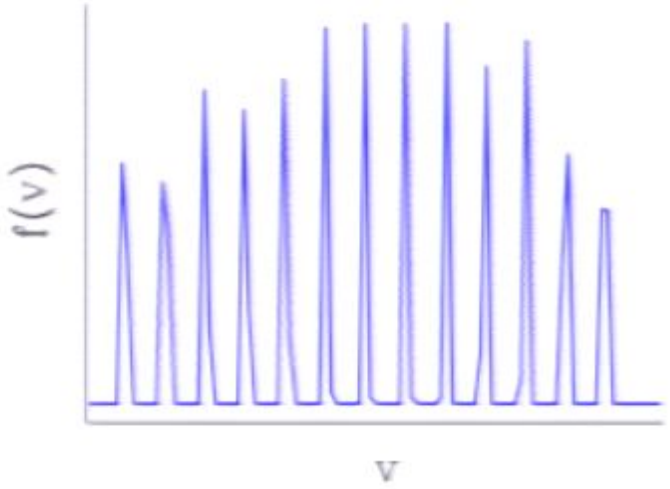

see papers on axion detection
by Sikivie and collaborators

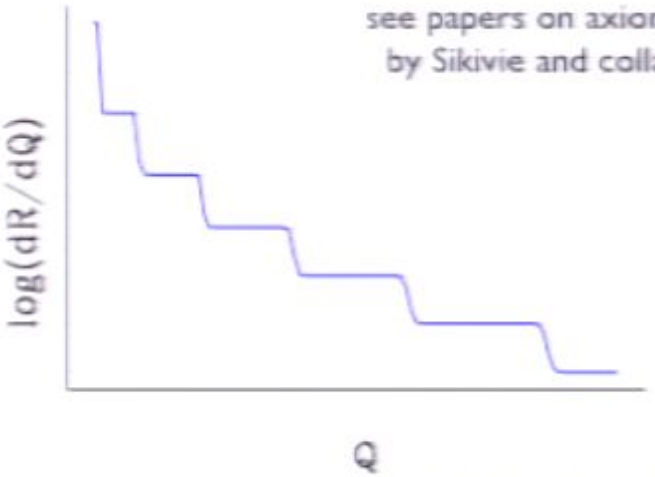

for WIMPs we have a series
of steps in recoil energy, Q
(see Stiff, LMW, Frieman 2001)

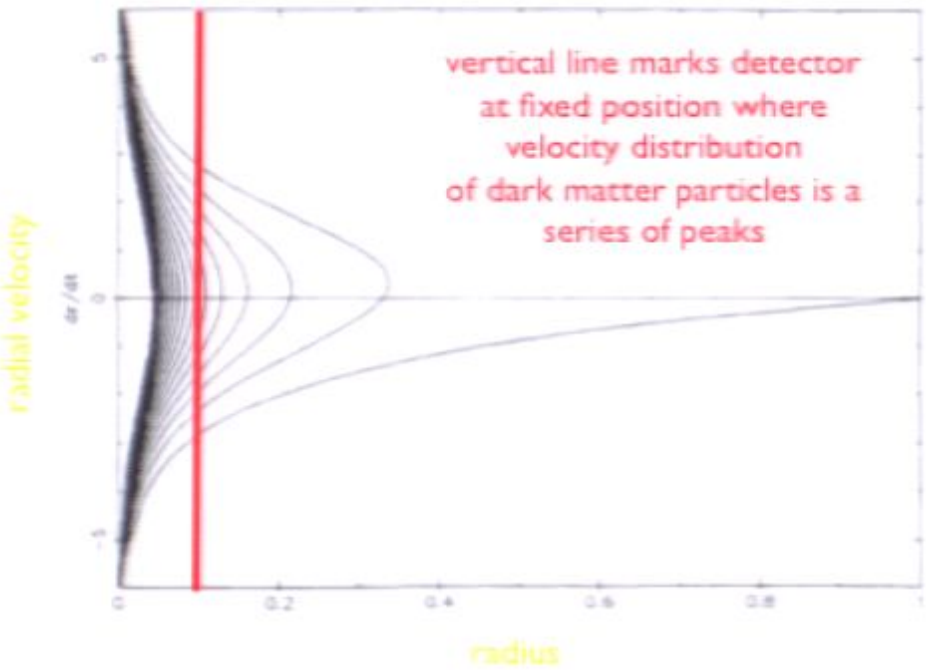

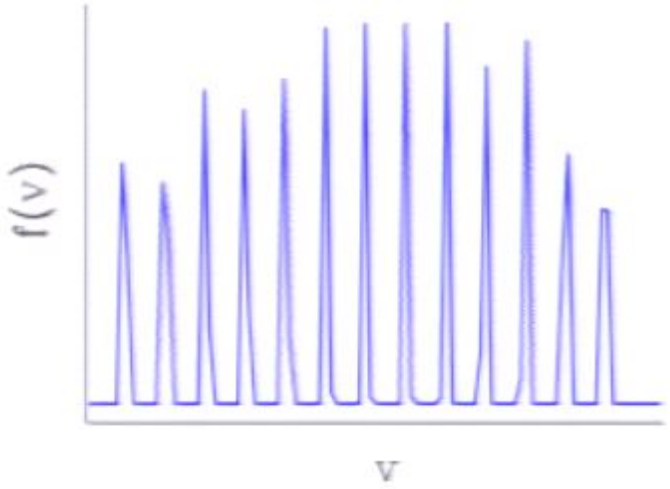

see papers on axion detection
by Sikivie and collaborators

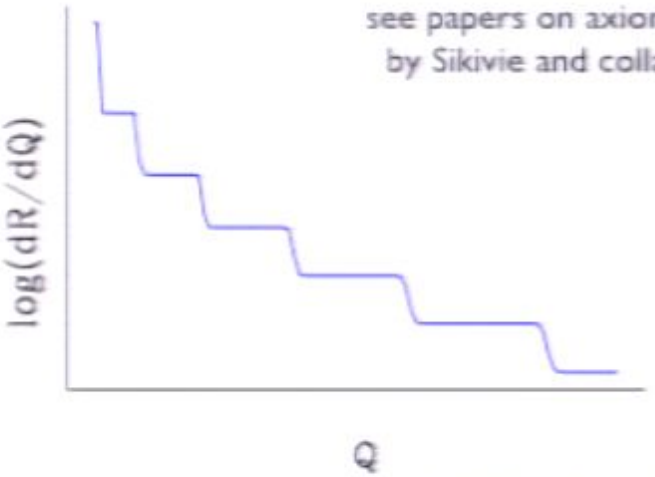

for WIMPs we have a series
of steps in recoil energy, Q
(see Stiff, LMW, Frieman 2001)

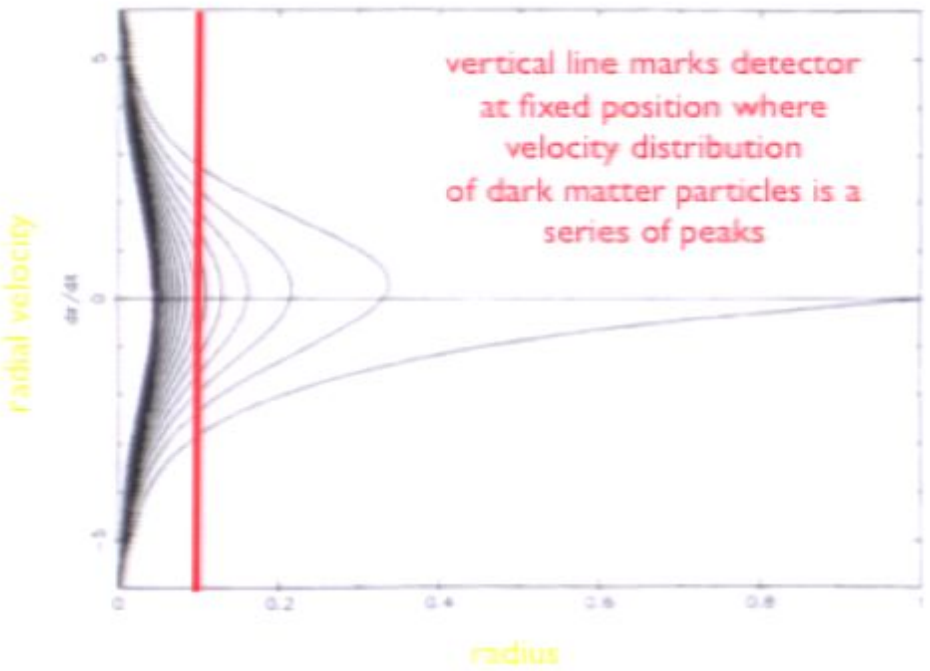

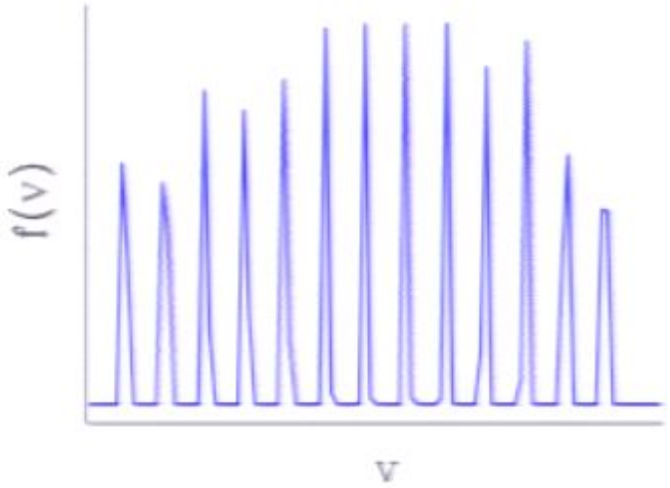

see papers on axion detection
by Sikivie and collaborators

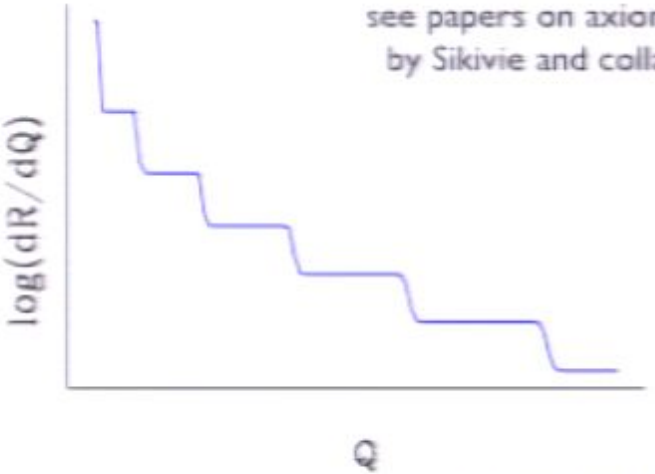

for WIMPs we have a series
of steps in recoil energy, Q
(see Stiff, LMW, Frieman 2001)

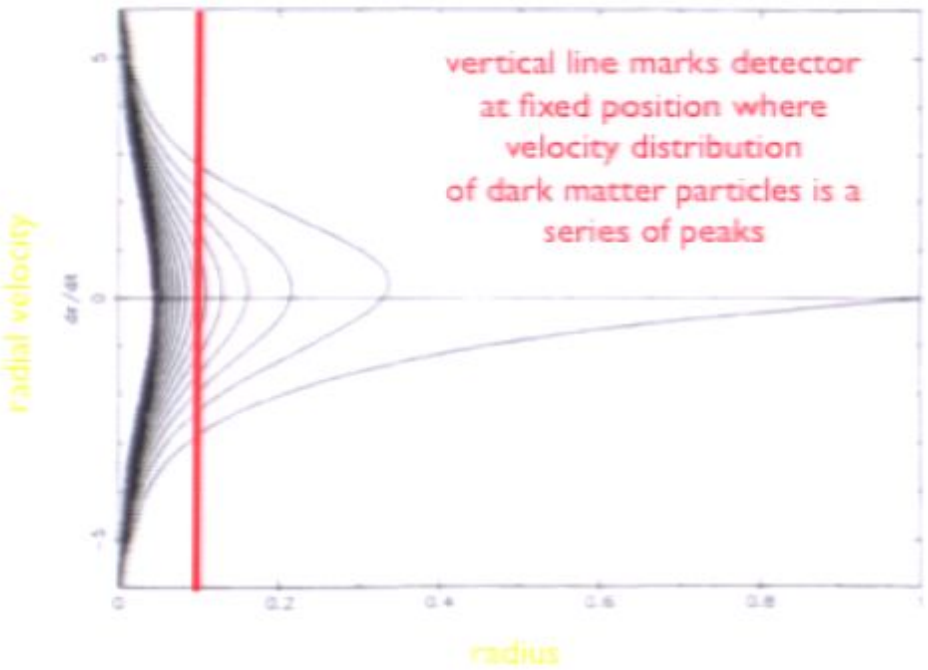

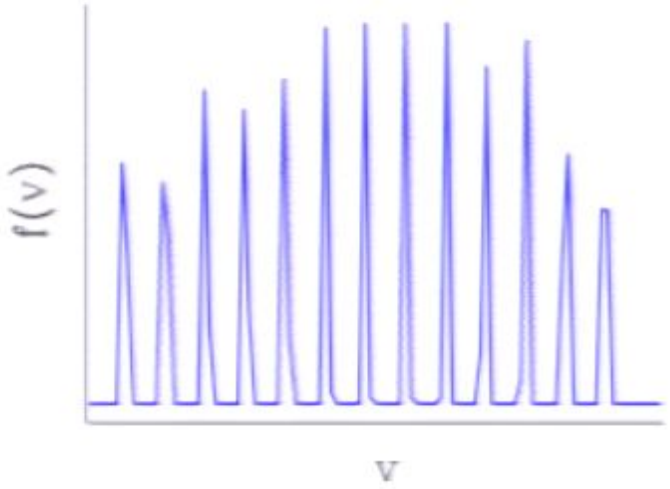

see papers on axion detection
by Sikivie and collaborators

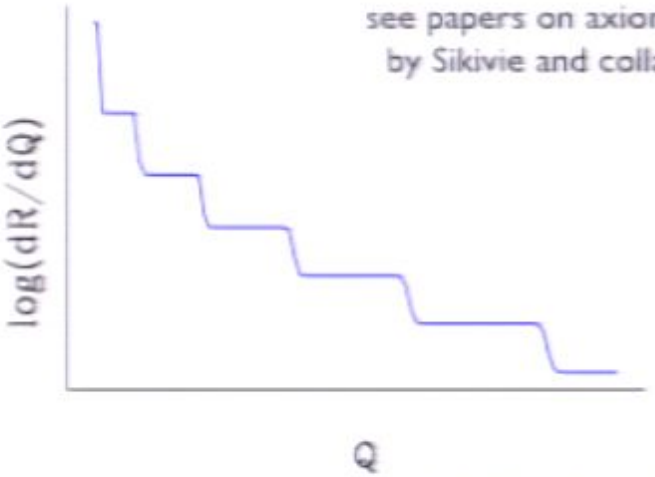

for WIMPs we have a series
of steps in recoil energy, Q
(see Stiff, LMW, Frieman 2001)

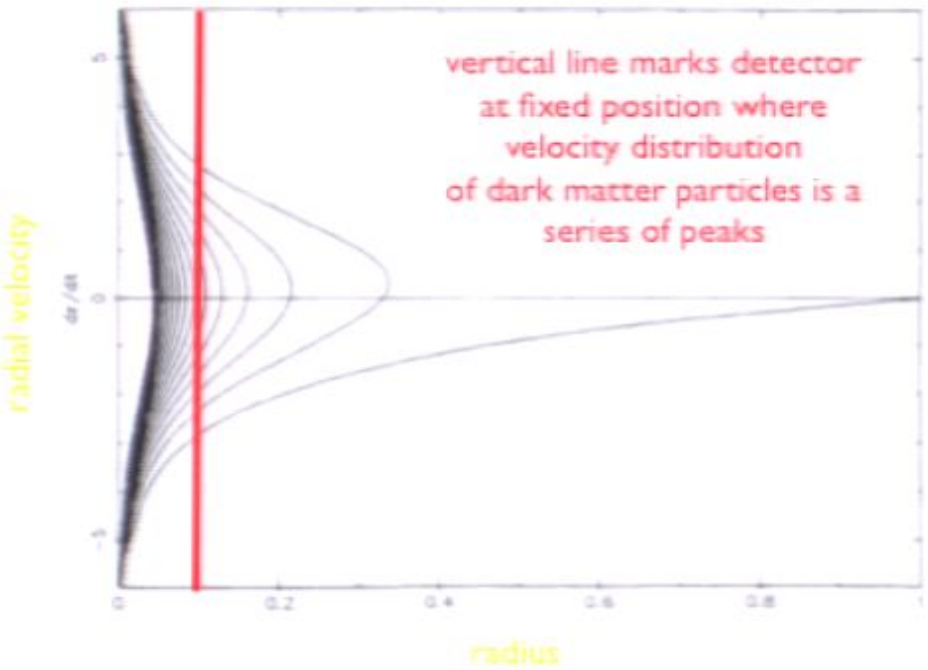

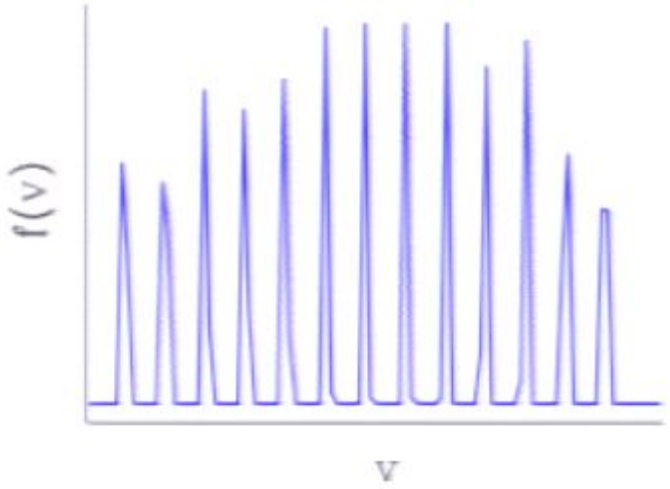

see papers on axion detection
by Sikivie and collaborators

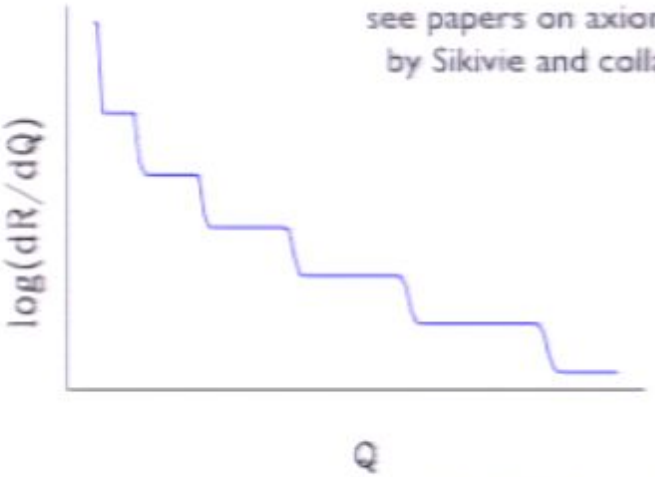

for WIMPs we have a series
of steps in recoil energy, Q
(see Stiff, LMW, Frieman 2001)

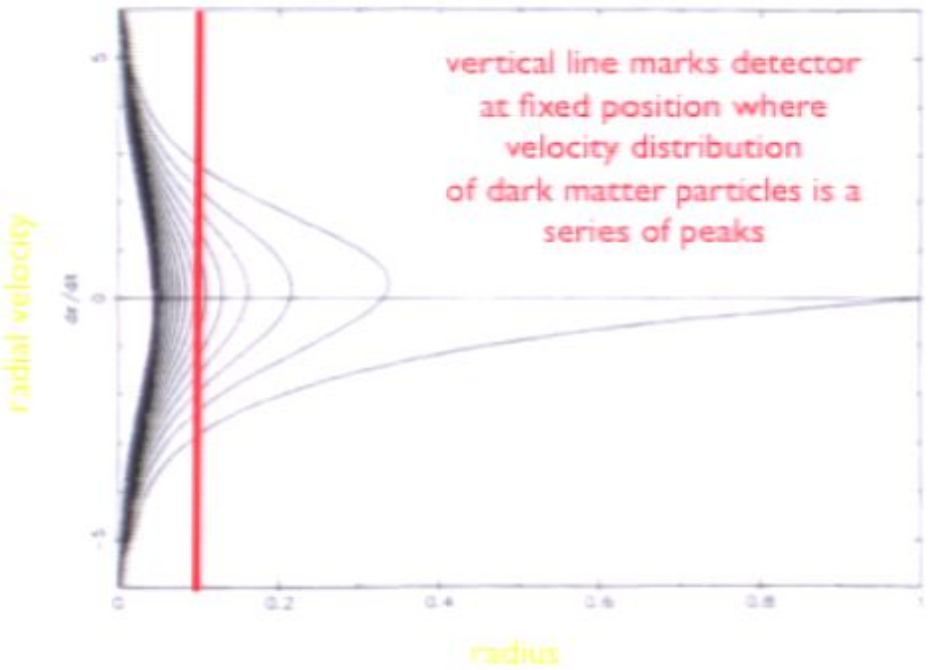

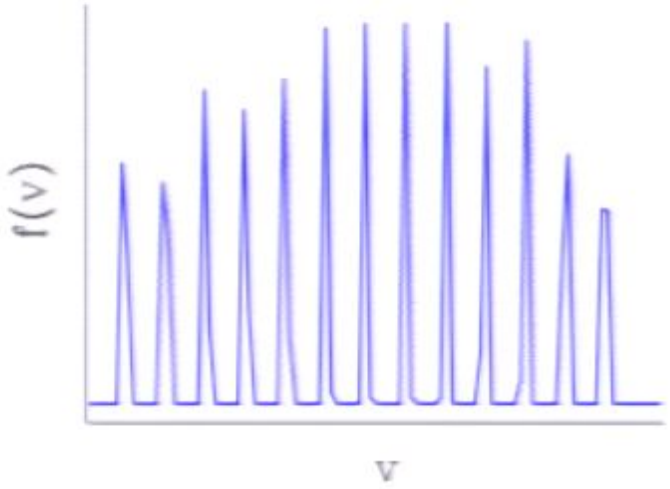

see papers on axion detection
by Sikivie and collaborators

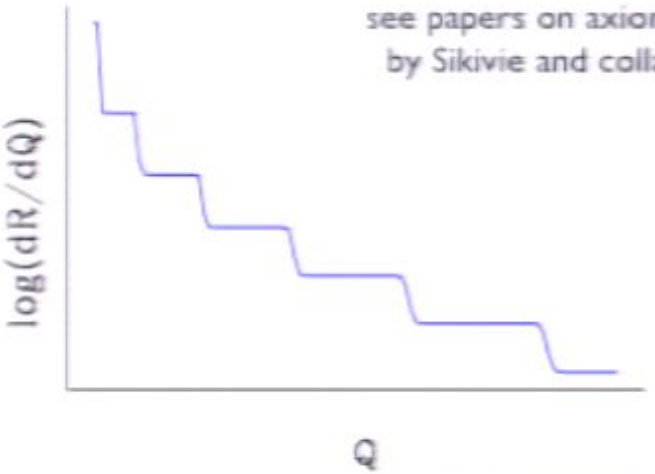

for WIMPs we have a series
of steps in recoil energy, Q
(see Stiff, LMW, Frieman 2001)

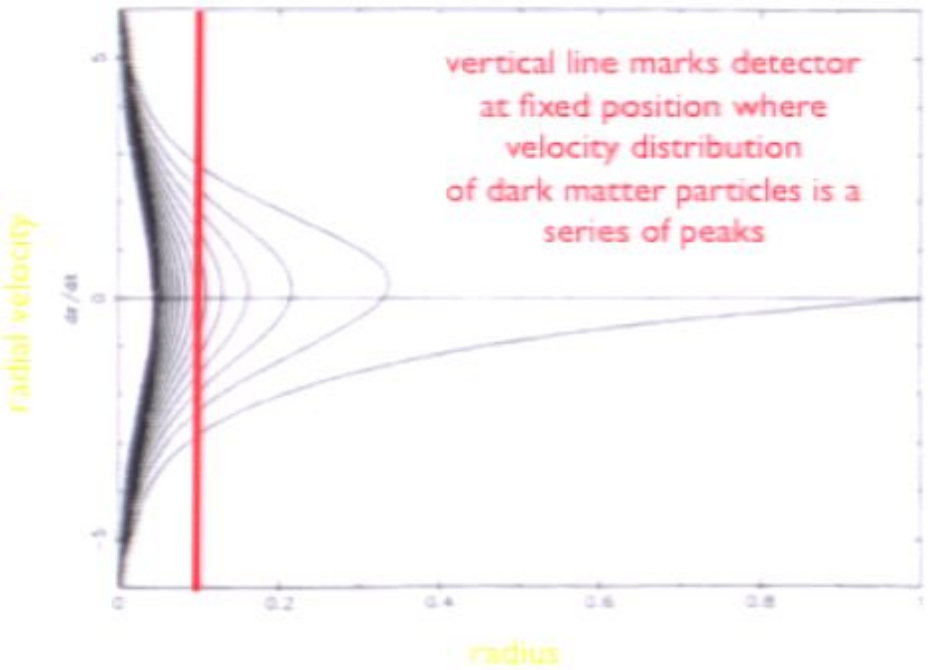

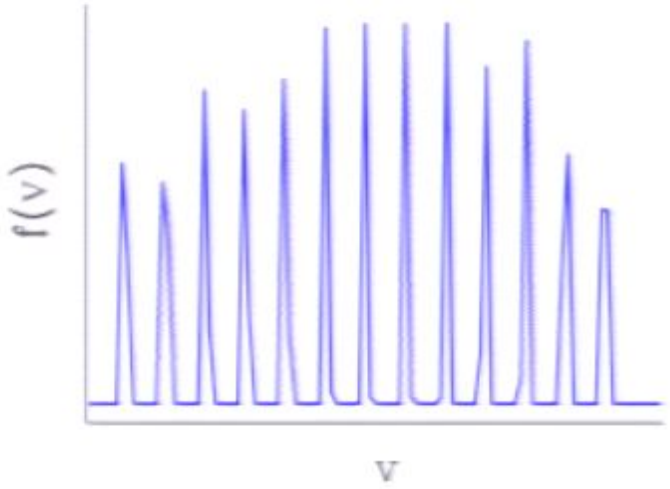

see papers on axion detection
by Sikivie and collaborators

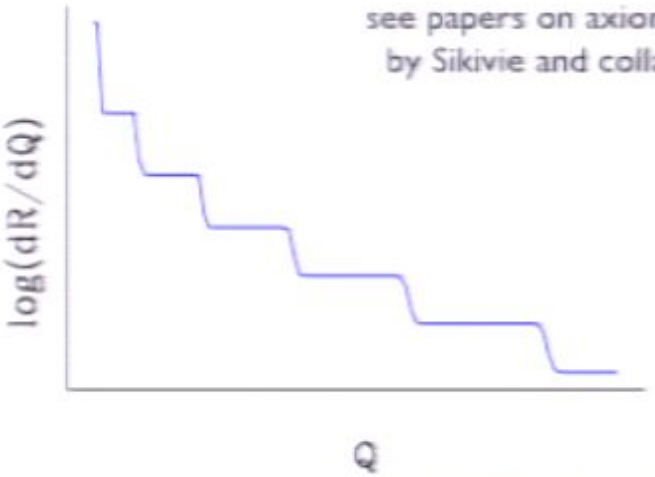

for WIMPs we have a series
of steps in recoil energy, Q
(see Stiff, LMW, Frieman 2001)

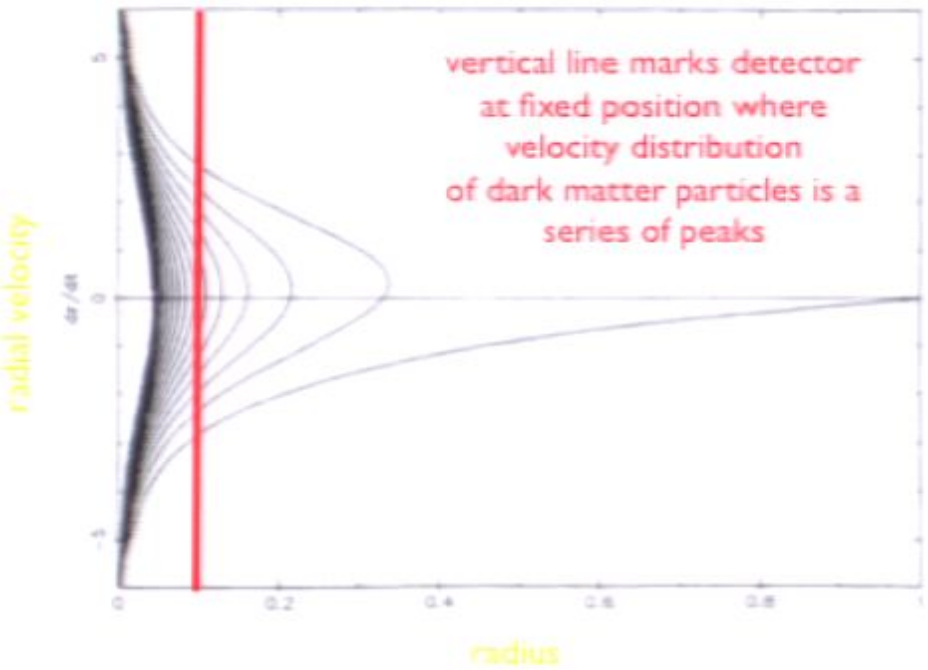

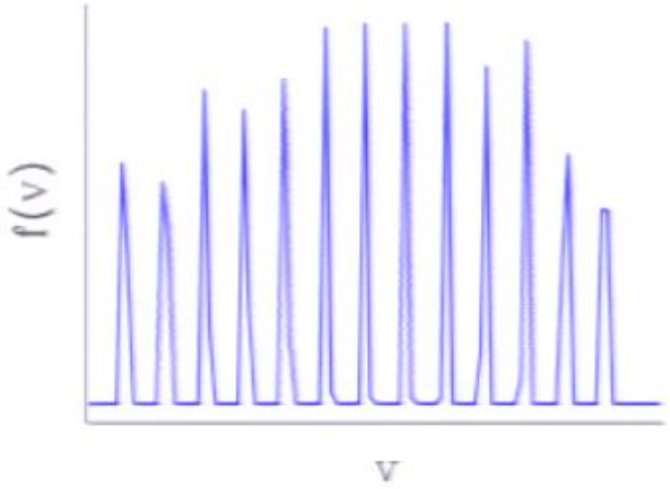

see papers on axion detection
by Sikivie and collaborators

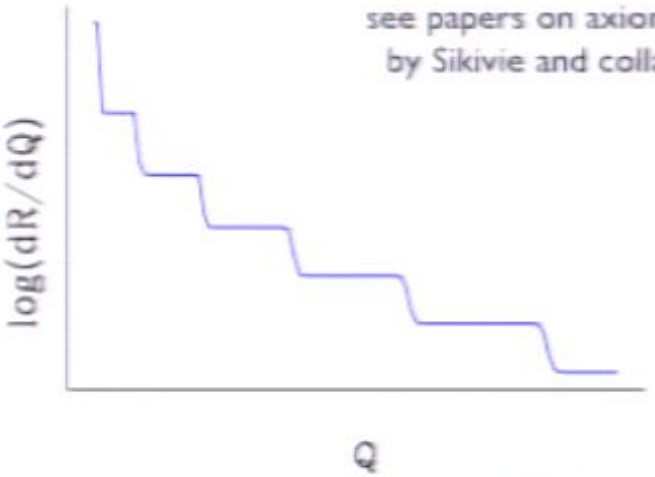

for WIMPs we have a series
of steps in recoil energy, Q
(see Stiff, LMW, Frieman 2001)

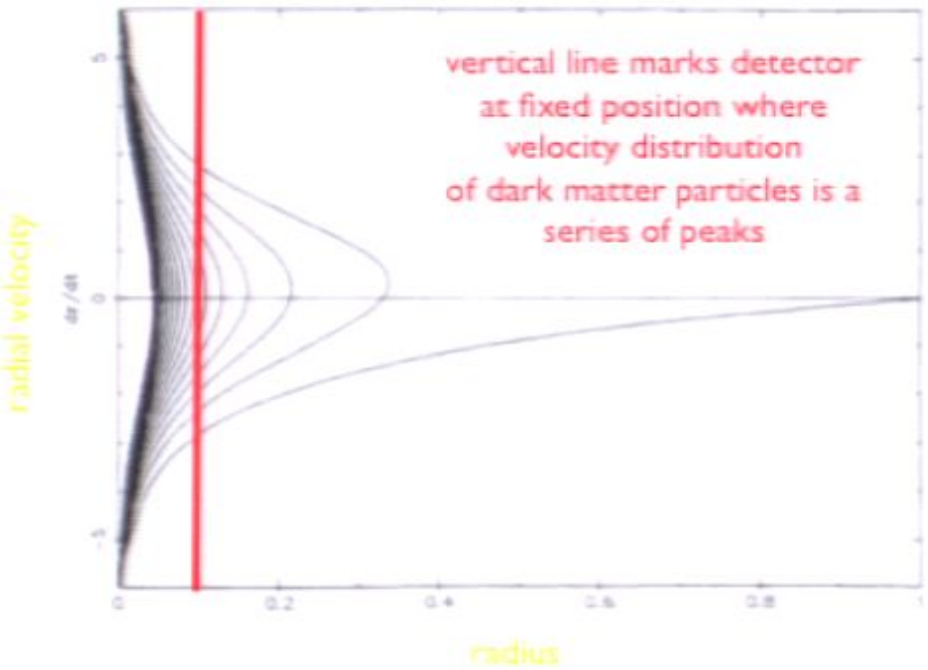

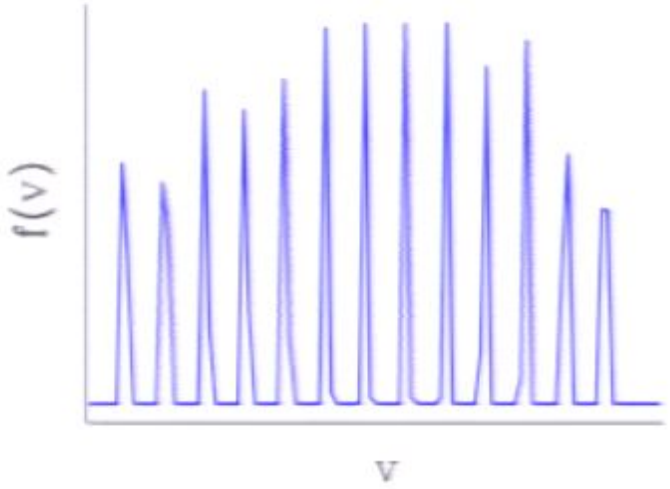

see papers on axion detection
by Sikivie and collaborators

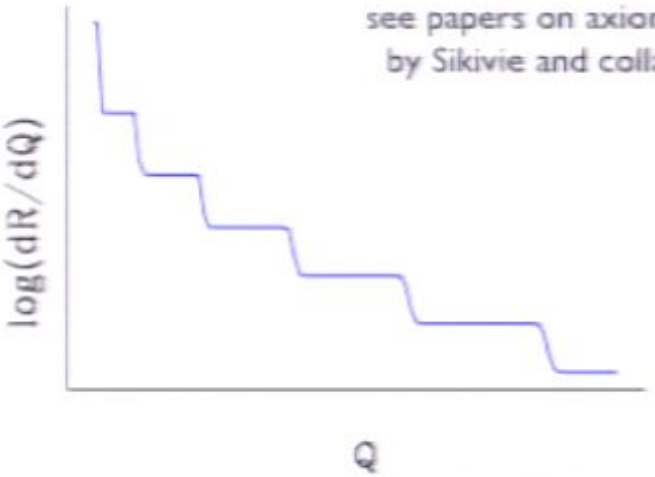

for WIMPs we have a series
of steps in recoil energy, Q
(see Stiff, LMW, Frieman 2001)

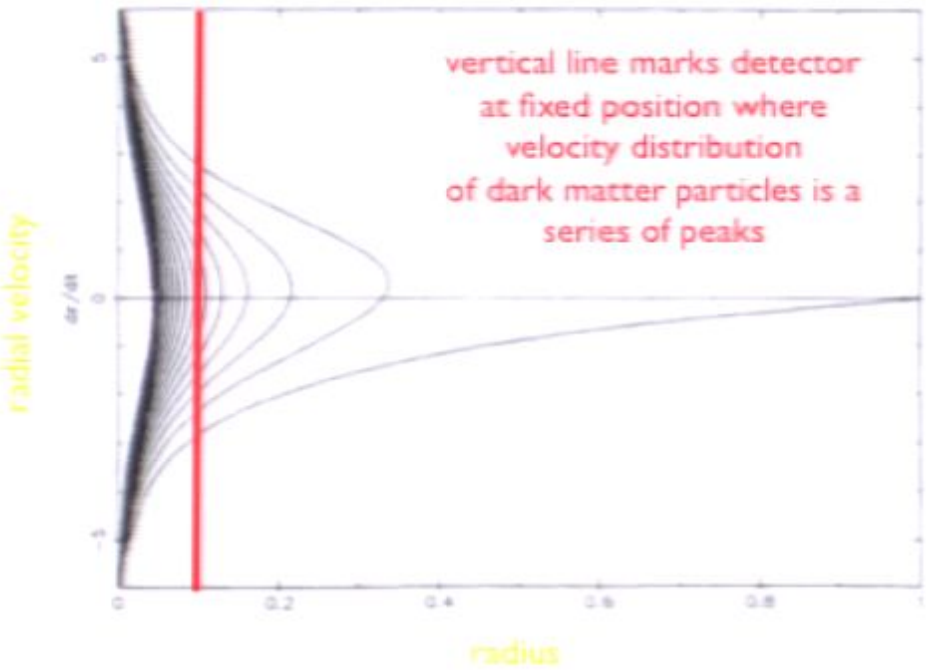

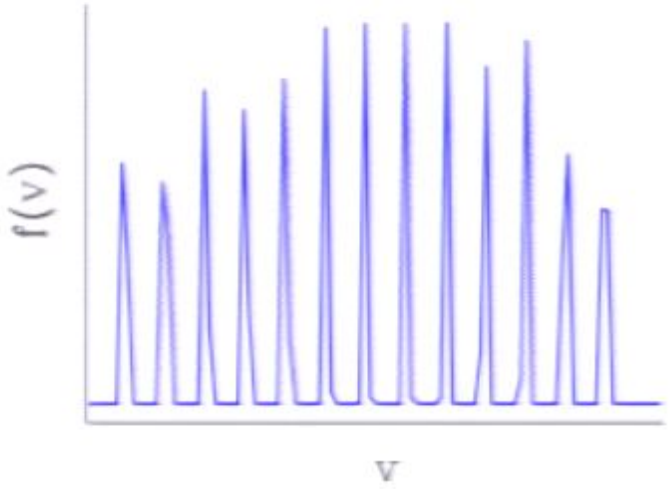

see papers on axion detection
by Sikivie and collaborators

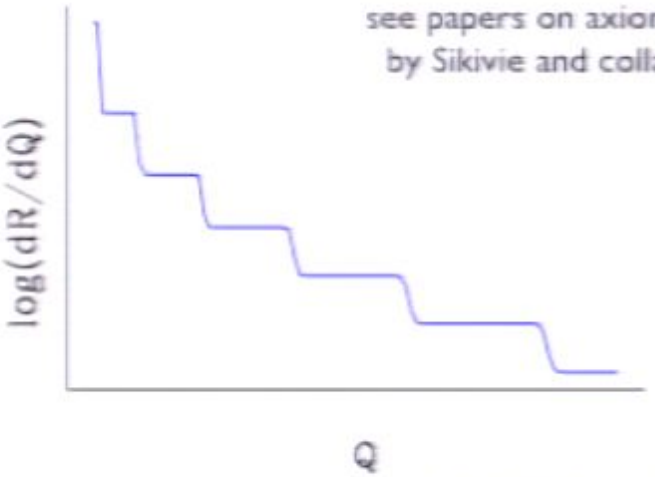

for WIMPs we have a series
of steps in recoil energy, Q
(see Stiff, LMW, Frieman 2001)

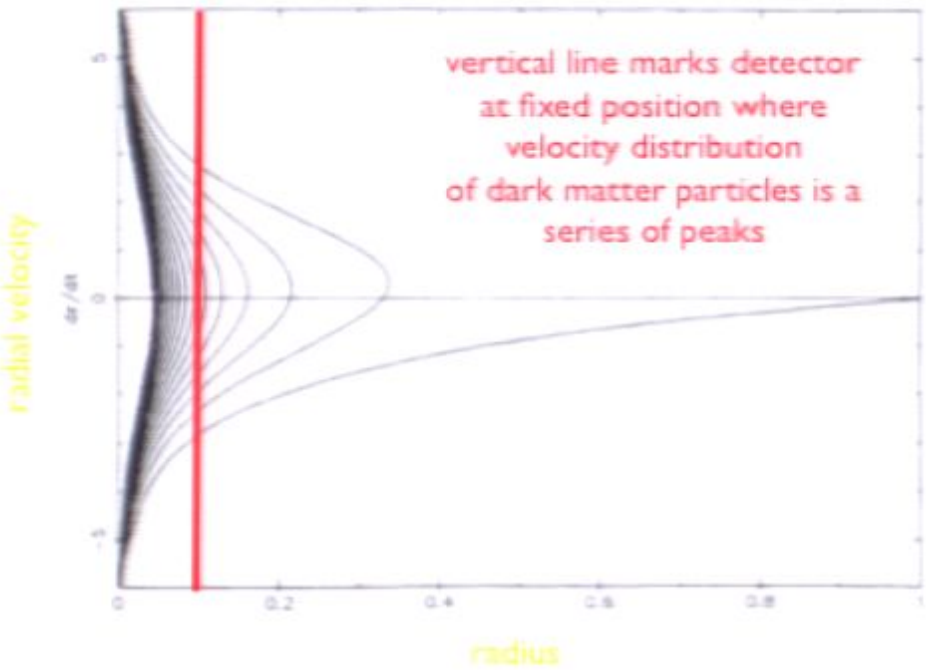

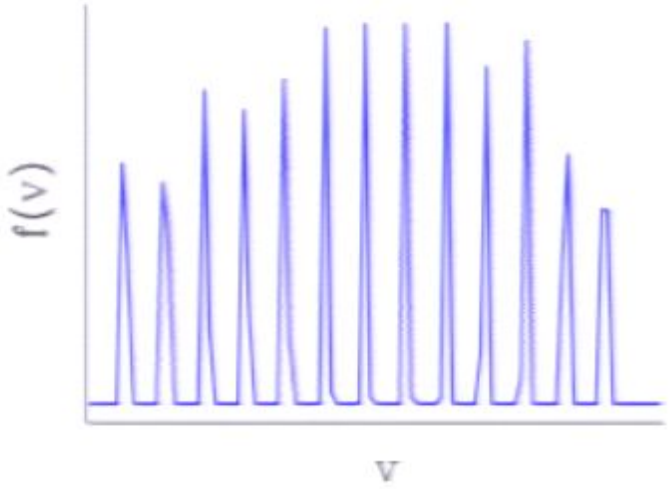

see papers on axion detection
by Sikivie and collaborators

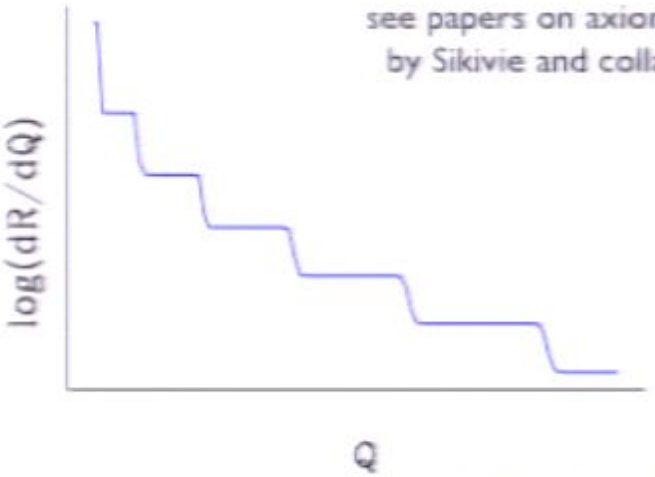

for WIMPs we have a series
of steps in recoil energy, Q
(see Stiff, LMW, Frieman 2001)

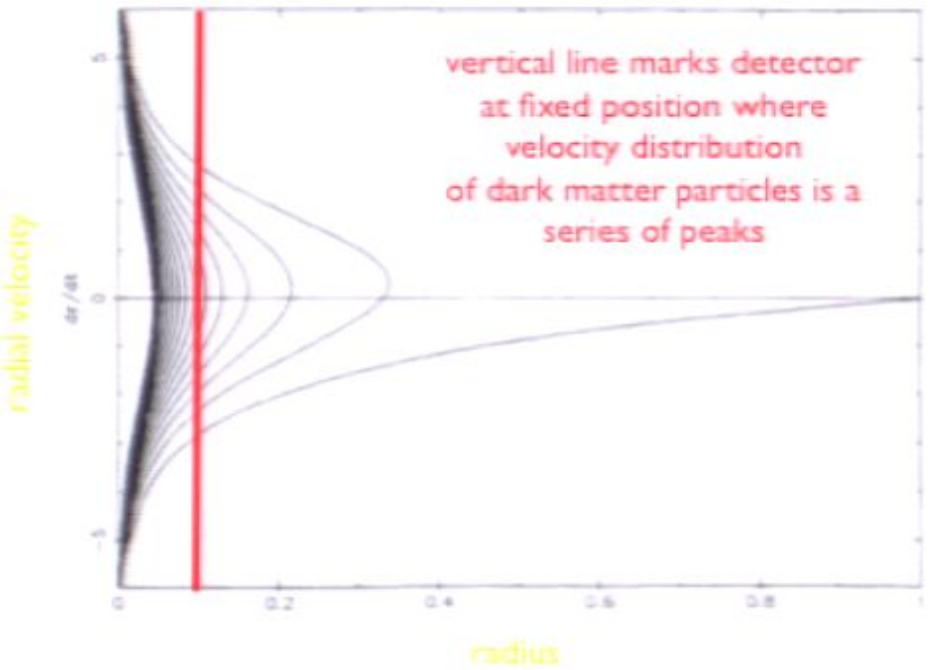

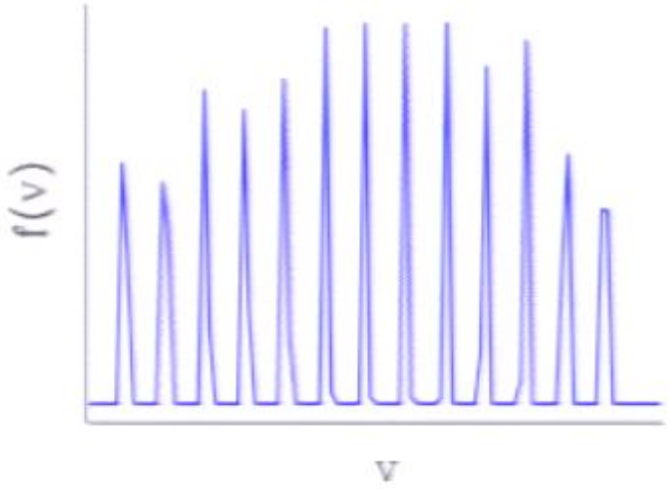

see papers on axion detection
by Sikivie and collaborators

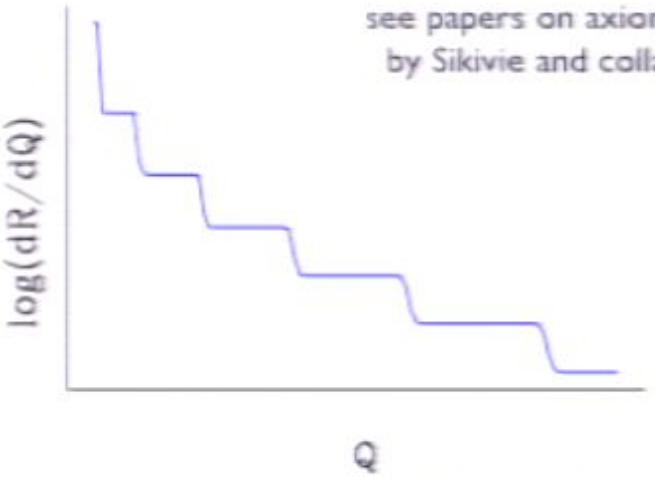

for WIMPs we have a series
of steps in recoil energy, Q
(see Stiff, LMW, Frieman 2001)

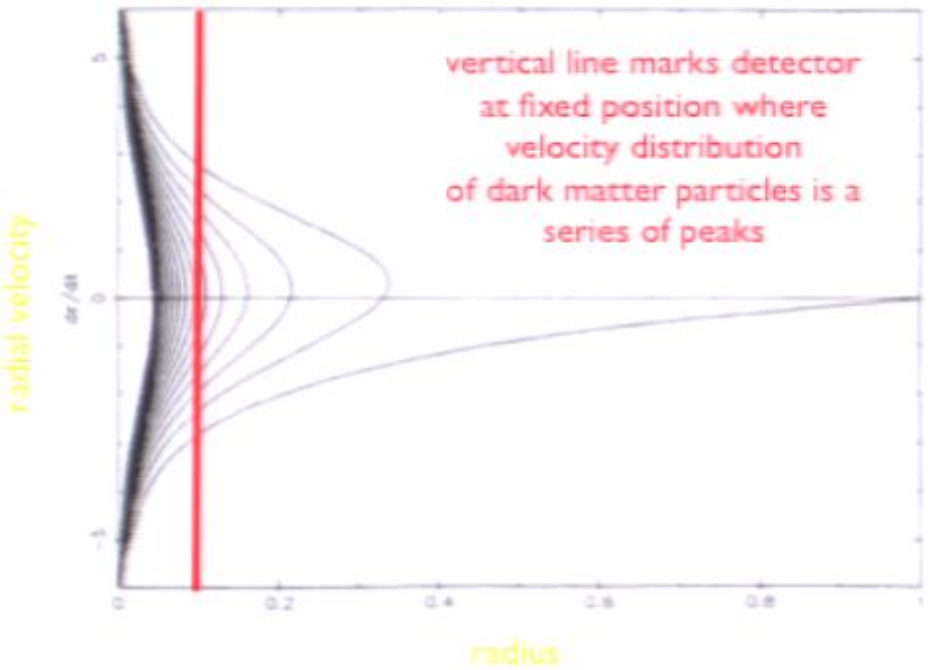

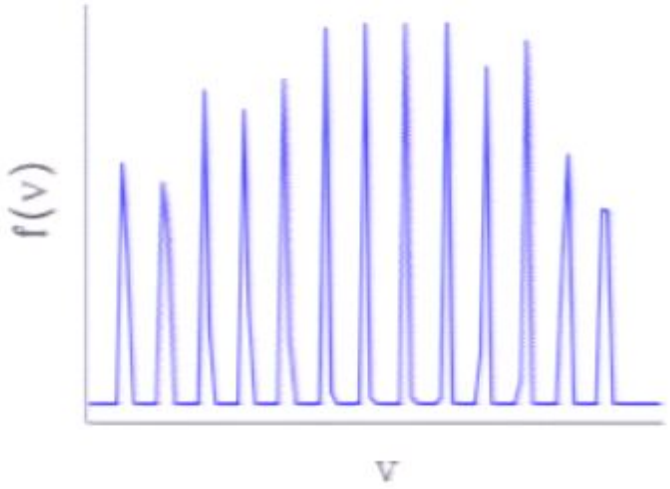

see papers on axion detection
by Sikivie and collaborators

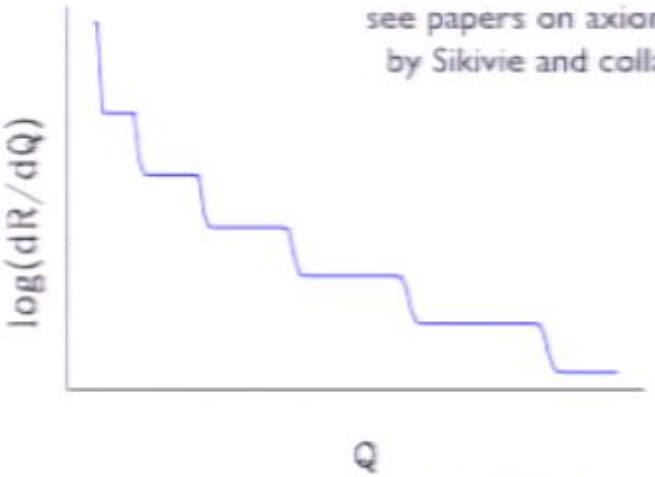

for WIMPs we have a series
of steps in recoil energy, Q
(see Stiff, LMW, Frieman 2001)

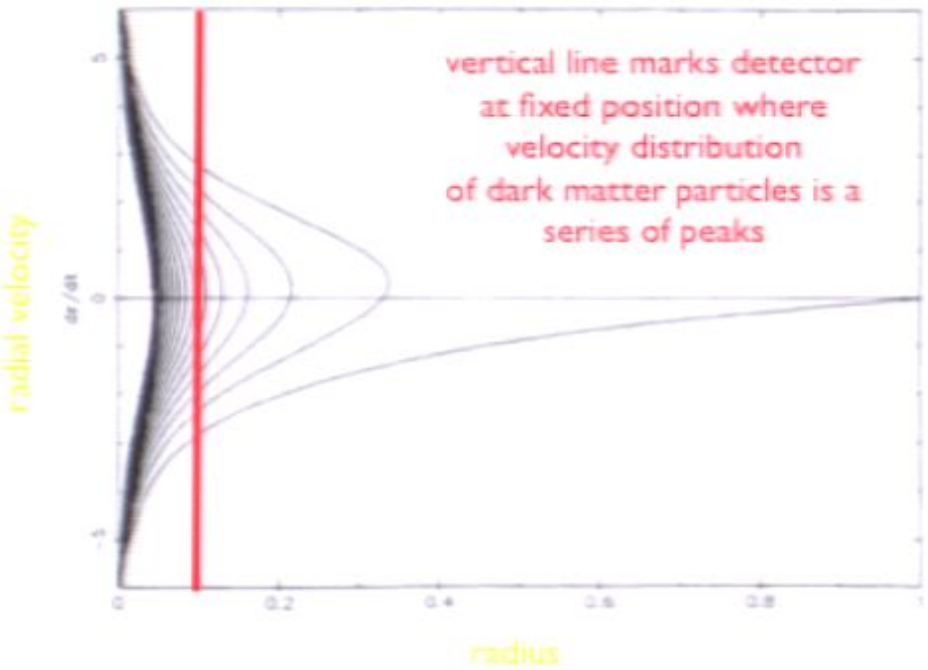

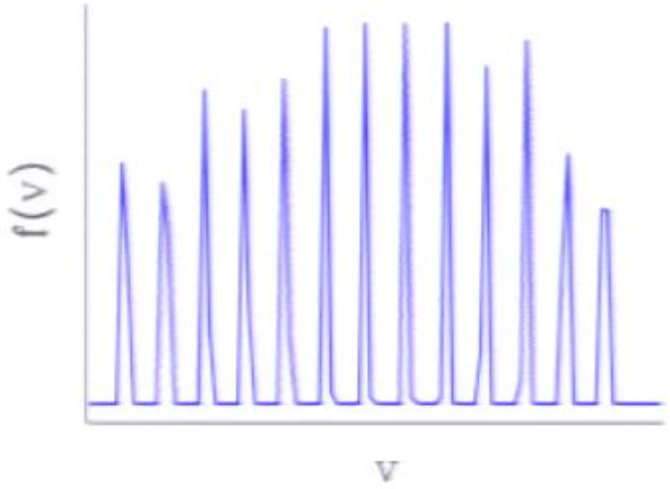

see papers on axion detection
by Sikivie and collaborators

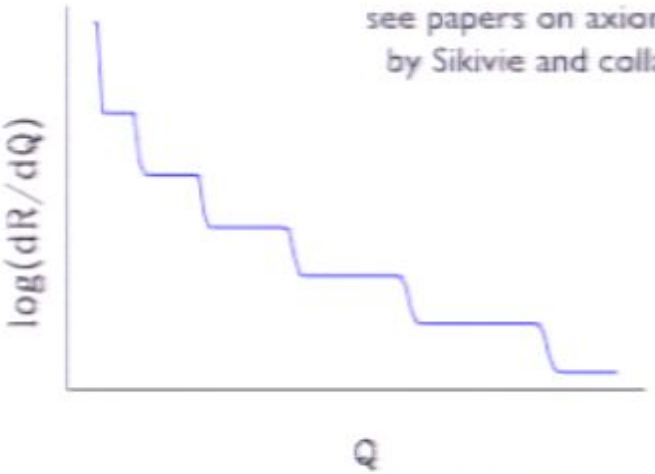

for WIMPs we have a series
of steps in recoil energy, Q
(see Stiff, LMW, Frieman 2001)

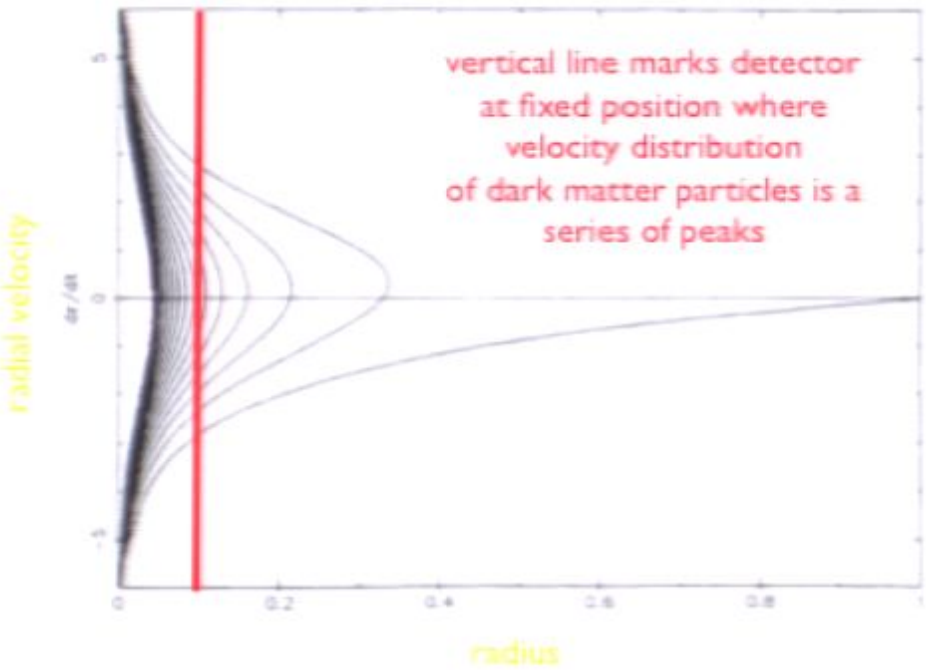

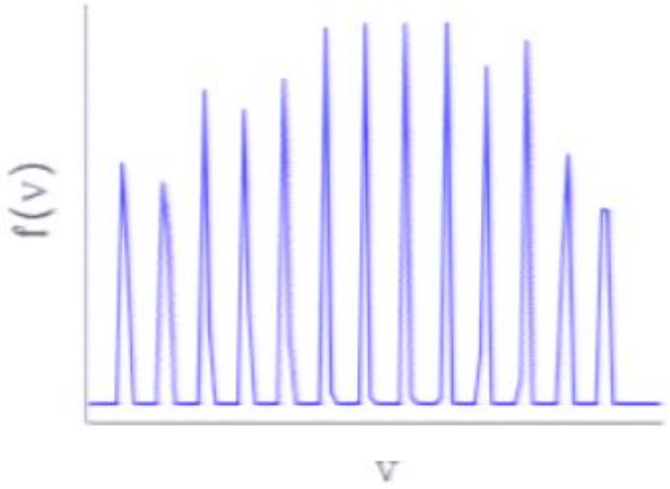

see papers on axion detection
by Sikivie and collaborators

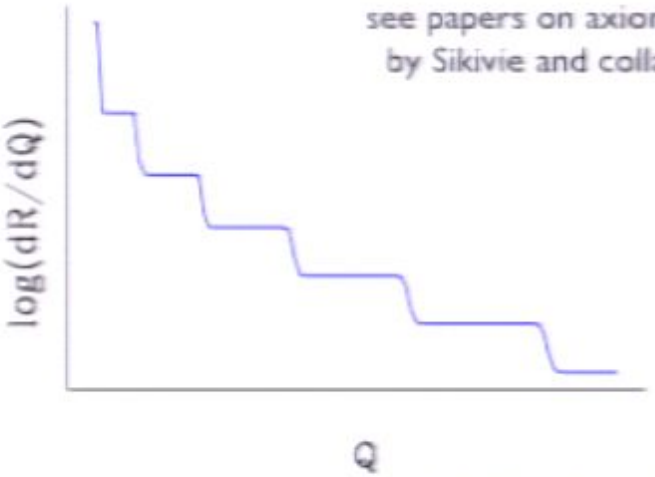

for WIMPs we have a series
of steps in recoil energy, Q
(see Stiff, LMW, Frieman 2001)

The Fillmore-Goldreich-Bertschinger solutions assume smooth, spherical infall. Initial perturbation is monotonic in r.

In the standard model for structure formation on all scales and structure formation proceeds perturbations exist hierarchically

single mode -- planar collapse

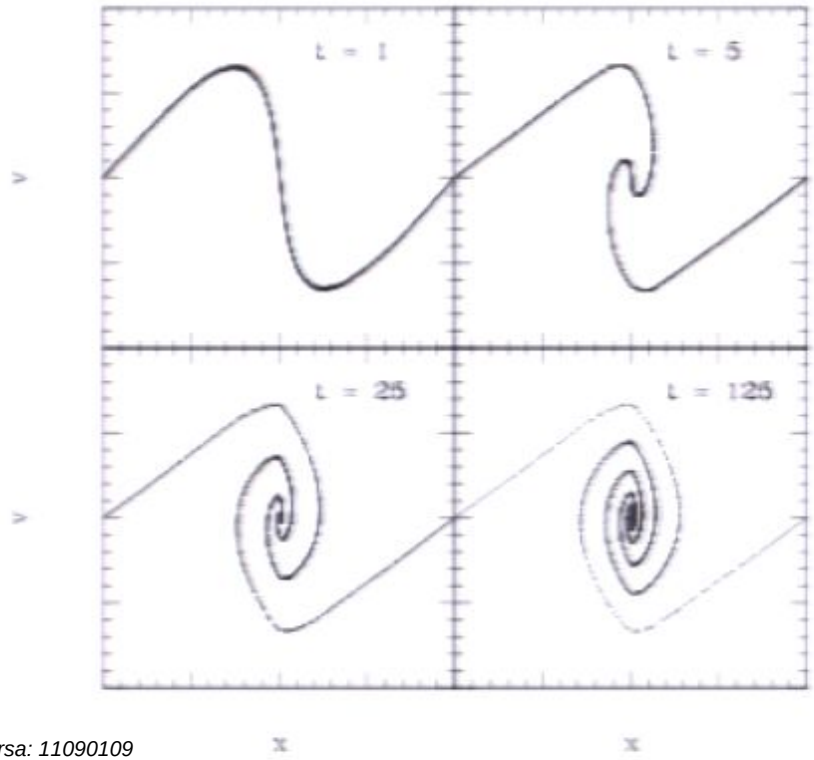

1D spectrum of modes

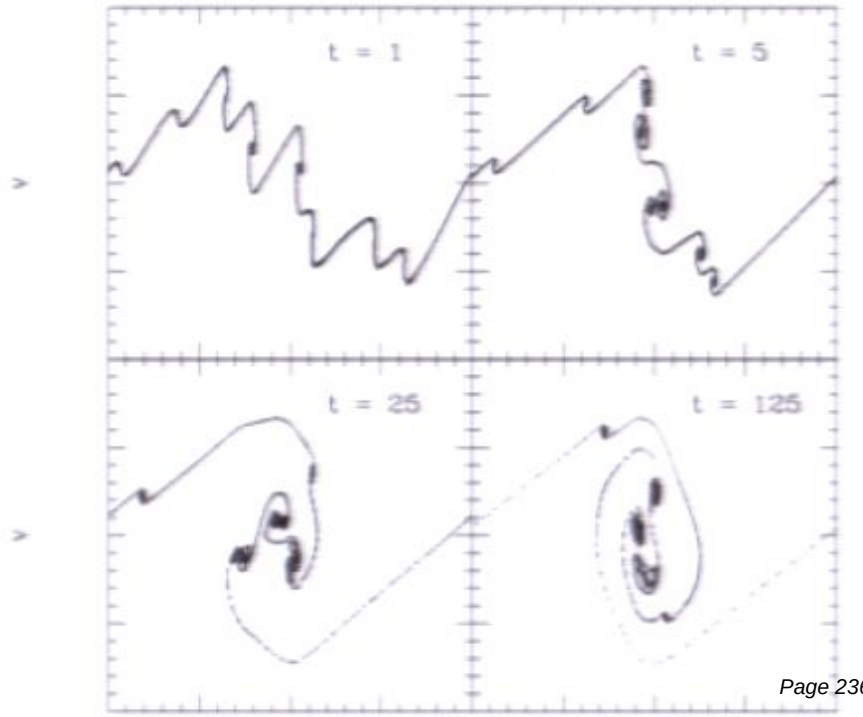

The Fillmore-Goldreich-Bertschinger solutions assume smooth, spherical infall. Initial perturbation is monotonic in r.

In the standard model for structure formation on all scales and structure formation proceeds perturbations exist hierarchically

single mode -- planar collapse

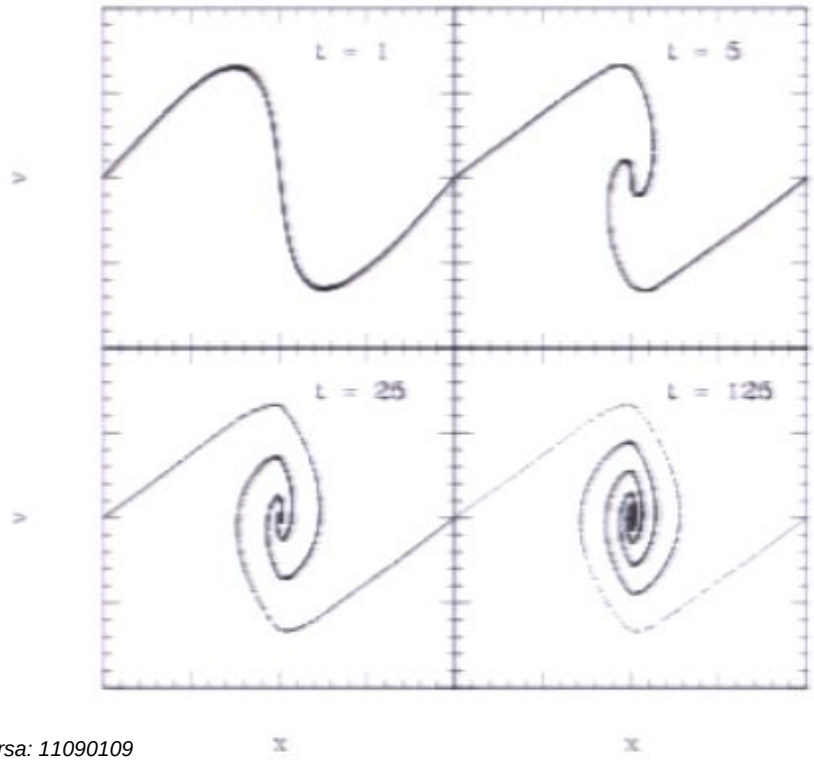

1D spectrum of modes

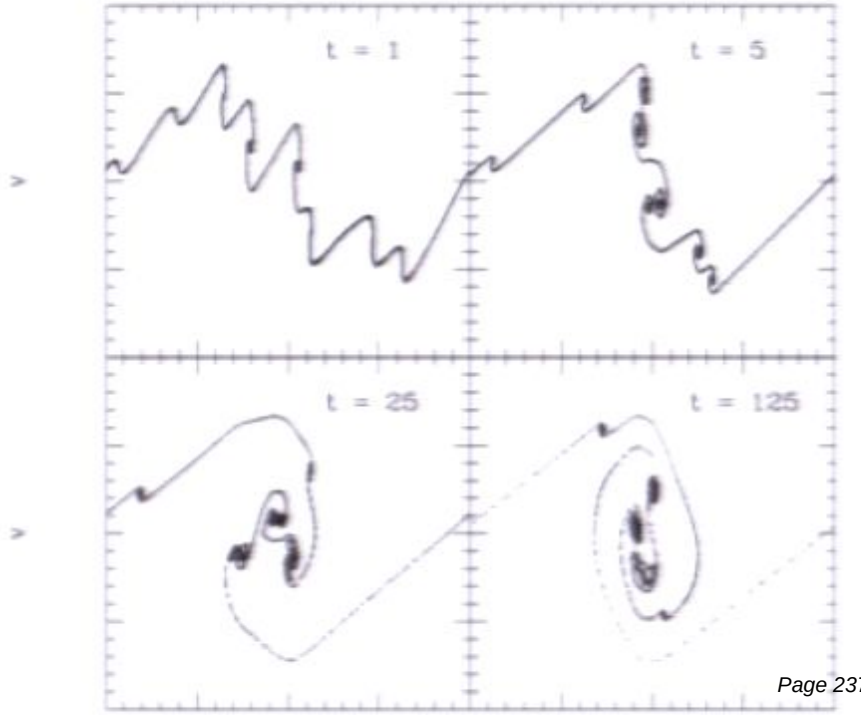

The Fillmore-Goldreich-Bertschinger solutions assume smooth, spherical infall. Initial perturbation is monotonic in r.

In the standard model for structure formation on all scales and structure formation proceeds perturbations exist hierarchically

single mode -- planar collapse

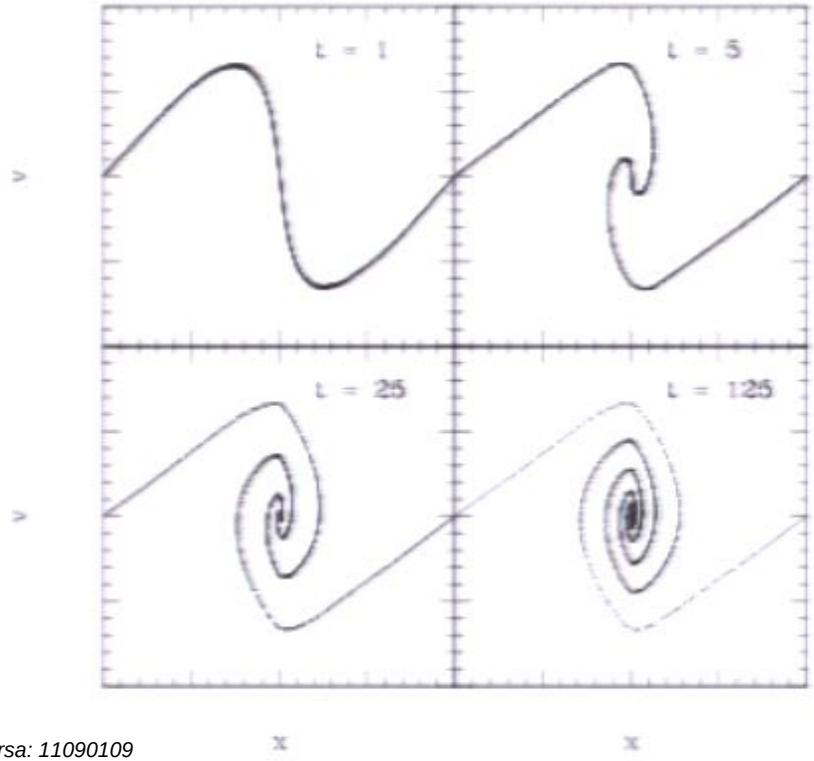

1D spectrum of modes

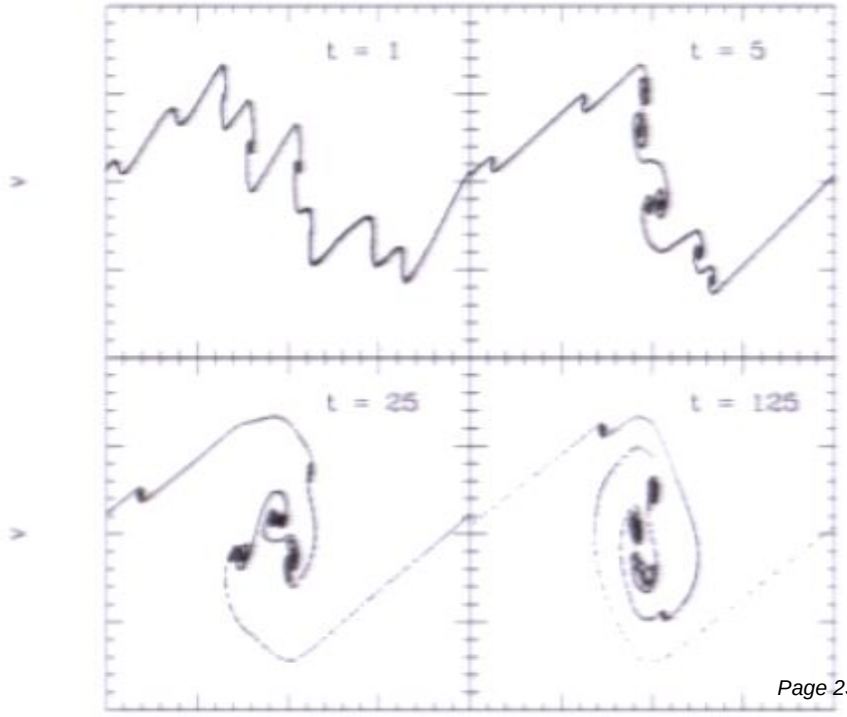

The Fillmore-Goldreich-Bertschinger solutions assume smooth, spherical infall. Initial perturbation is monotonic in r.

In the standard model for structure formation on all scales and structure formation proceeds perturbations exist hierarchically

single mode -- planar collapse

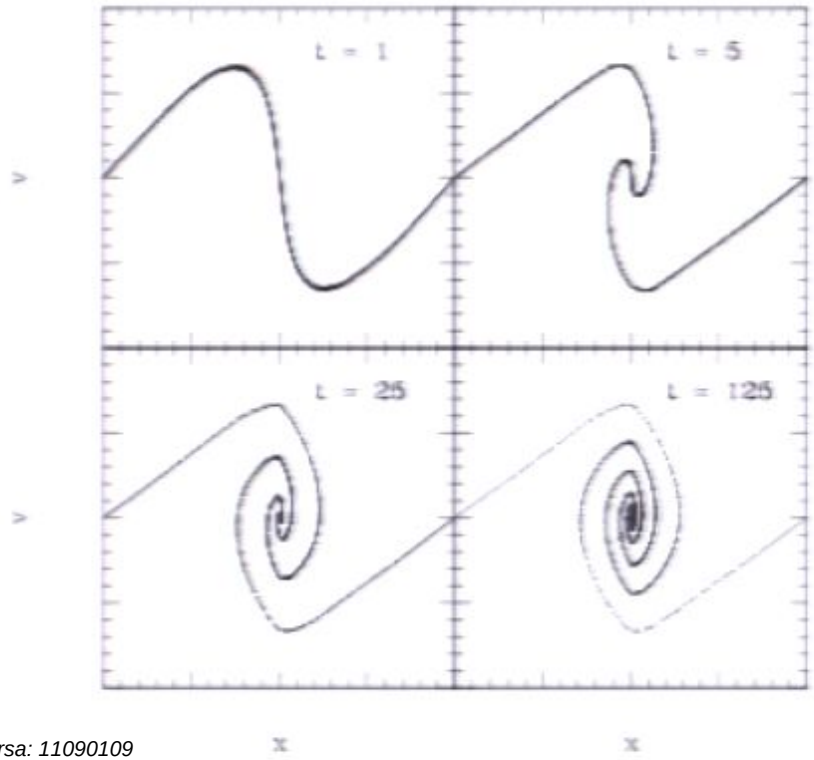

1D spectrum of modes

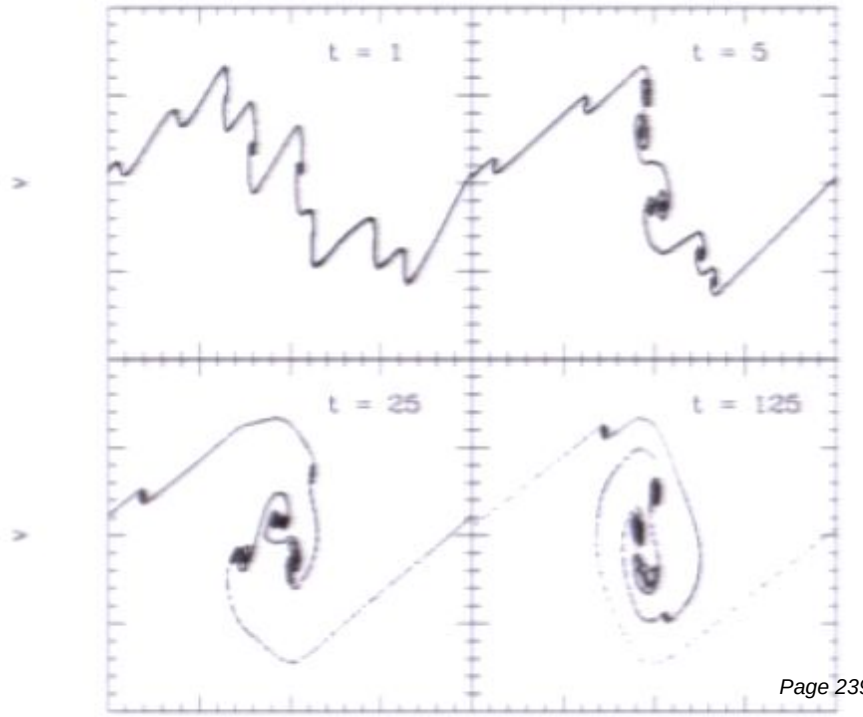

The Fillmore-Goldreich-Bertschinger solutions assume smooth, spherical infall. Initial perturbation is monotonic in r.

In the standard model for structure formation on all scales and structure formation proceeds perturbations exist hierarchically

single mode -- planar collapse

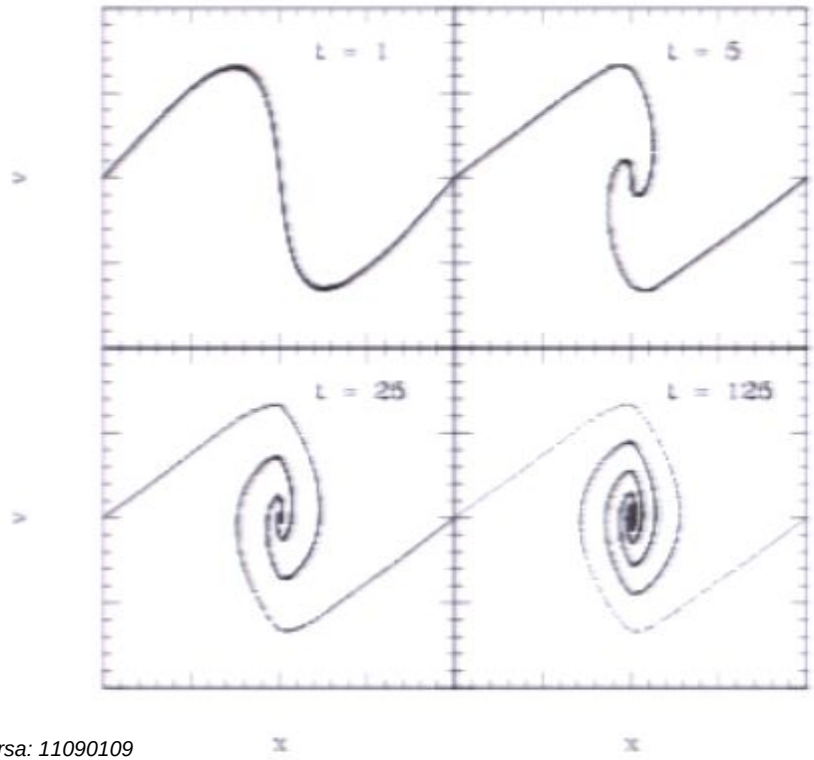

1D spectrum of modes

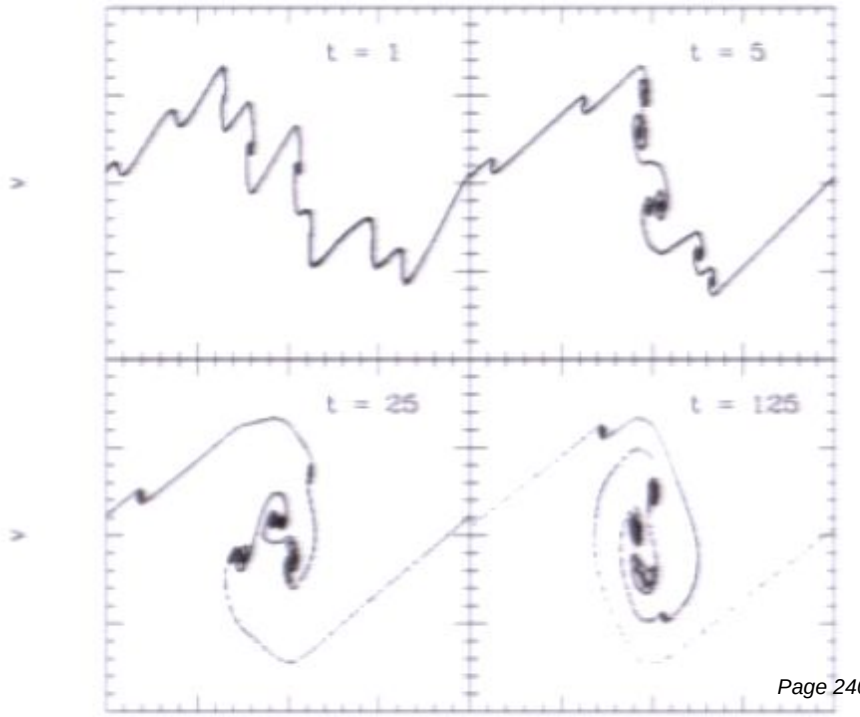

The Fillmore-Goldreich-Bertschinger solutions assume smooth, spherical infall. Initial perturbation is monotonic in r.

In the standard model for structure formation on all scales and structure formation proceeds perturbations exist hierarchically

single mode -- planar collapse

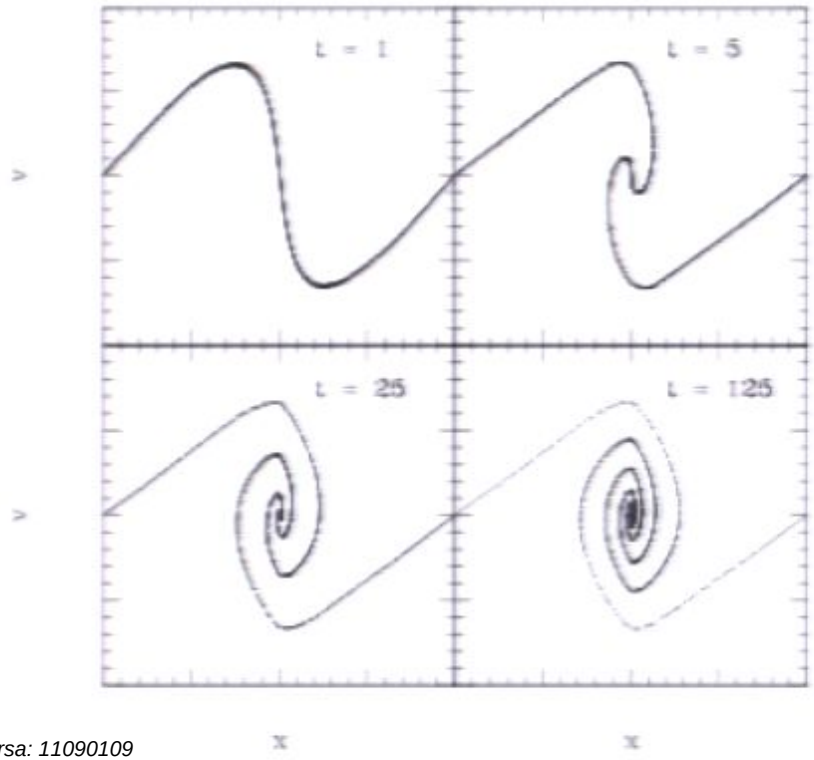

1D spectrum of modes

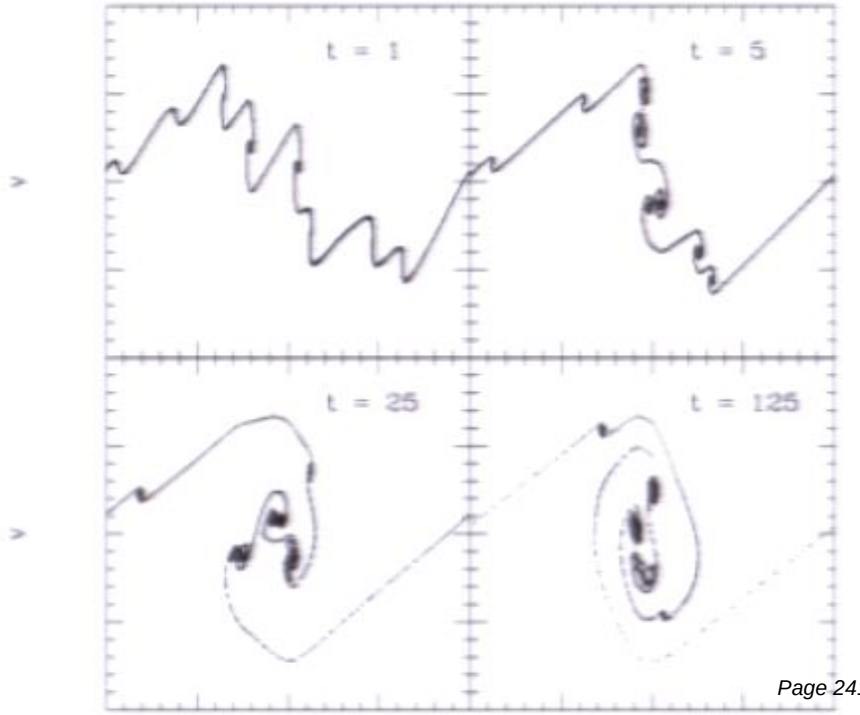

The Fillmore-Goldreich-Bertschinger solutions assume smooth, spherical infall. Initial perturbation is monotonic in r.

In the standard model for structure formation on all scales and structure formation proceeds perturbations exist hierarchically

single mode -- planar collapse

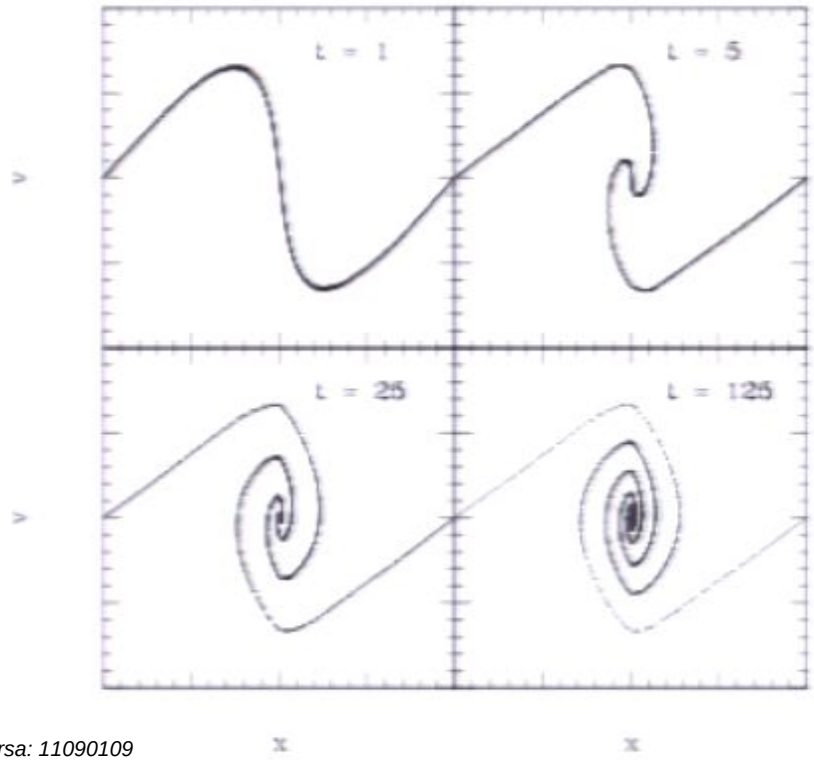

1D spectrum of modes

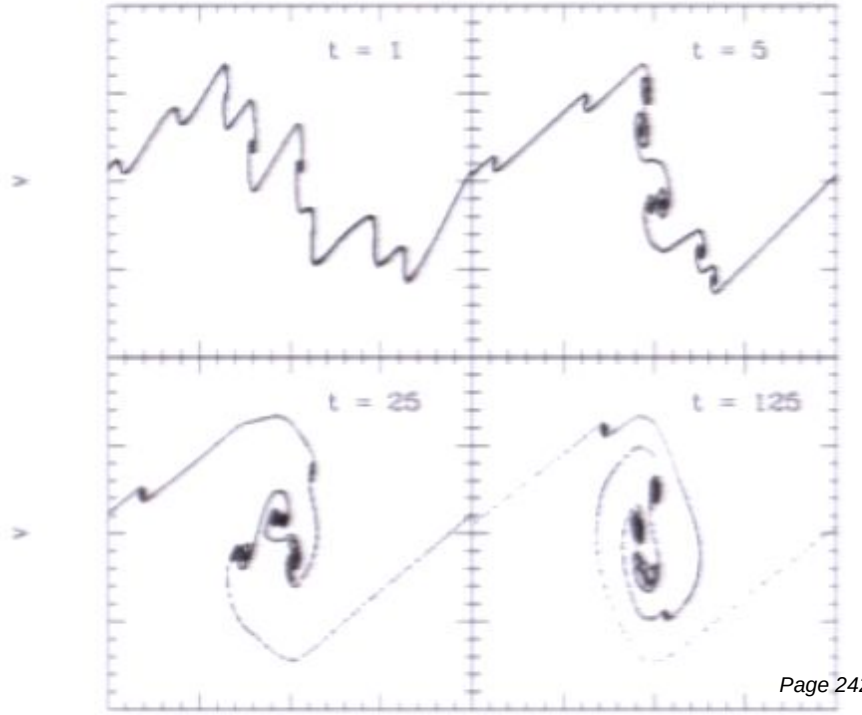

The Fillmore-Goldreich-Bertschinger solutions assume smooth, spherical infall. Initial perturbation is monotonic in r.

In the standard model for structure formation on all scales and structure formation proceeds perturbations exist hierarchically

single mode -- planar collapse

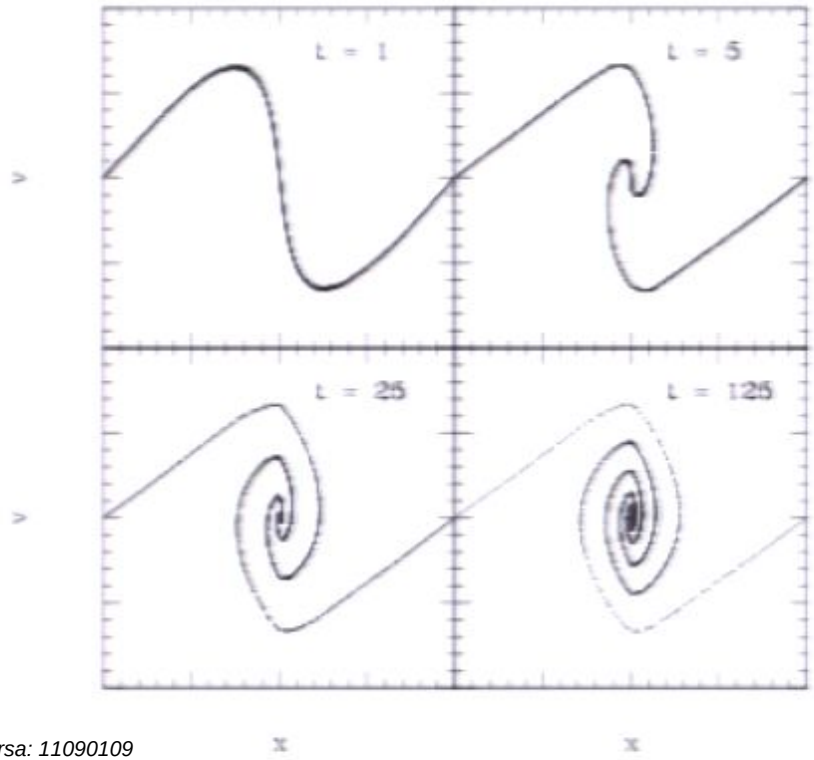

1D spectrum of modes

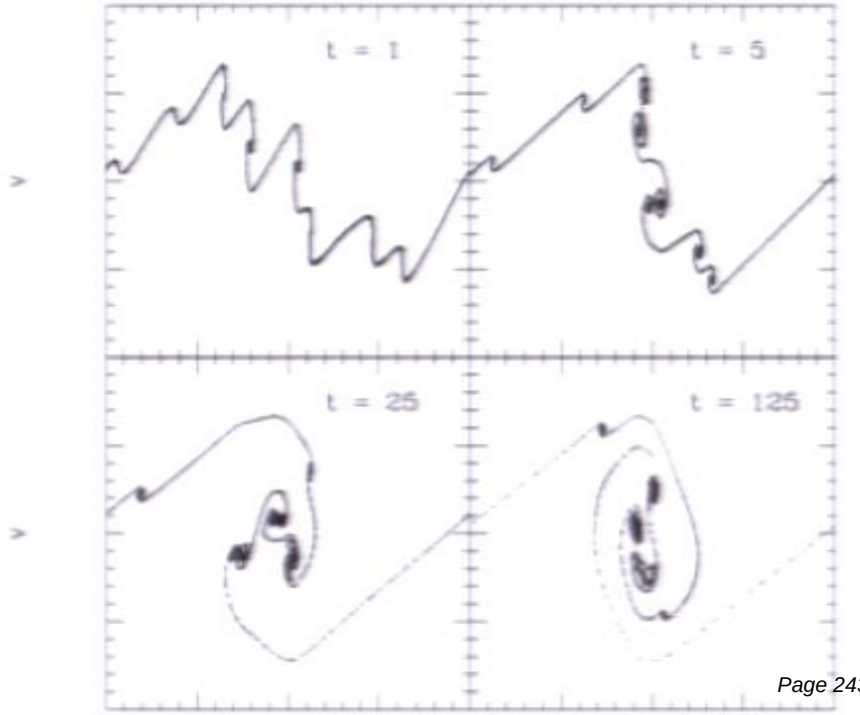

The Fillmore-Goldreich-Bertschinger solutions assume smooth, spherical infall. Initial perturbation is monotonic in r.

In the standard model for structure formation on all scales and structure formation proceeds perturbations exist hierarchically

single mode -- planar collapse

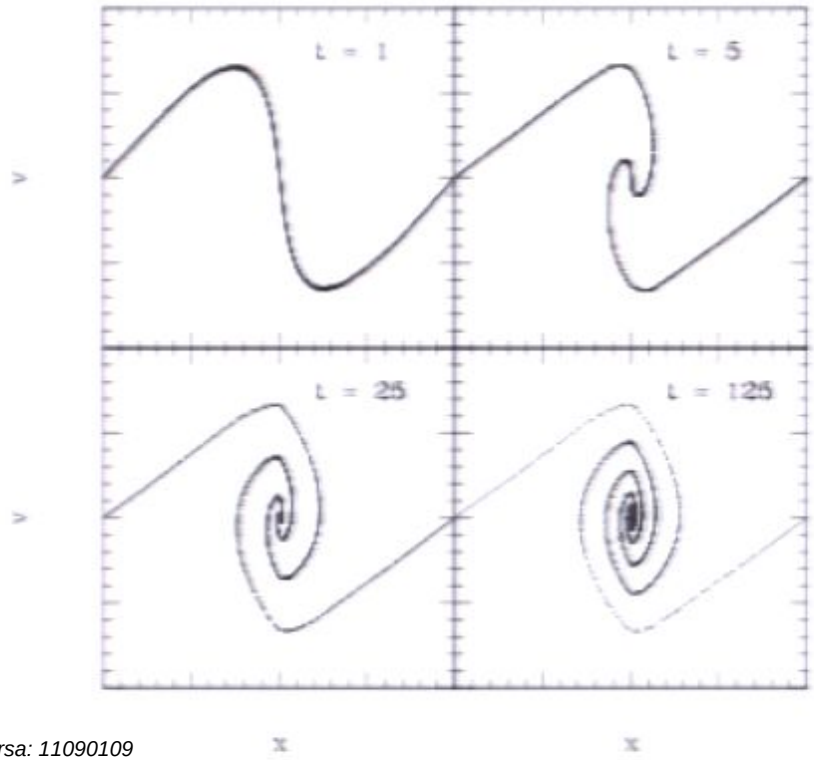

1D spectrum of modes

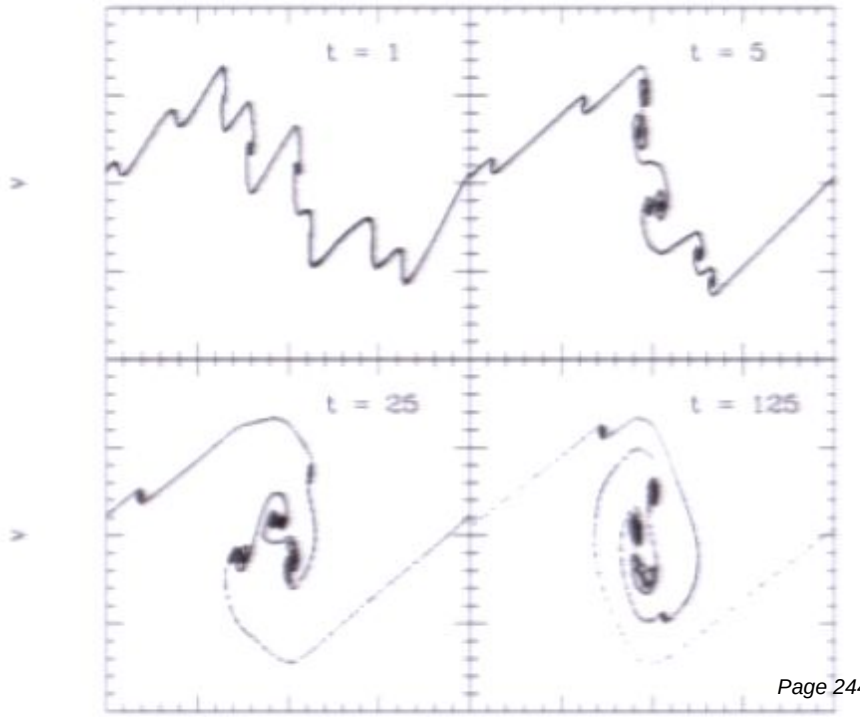

The Fillmore-Goldreich-Bertschinger solutions assume smooth, spherical infall. Initial perturbation is monotonic in r.

In the standard model for structure formation on all scales and structure formation proceeds perturbations exist hierarchically

single mode -- planar collapse

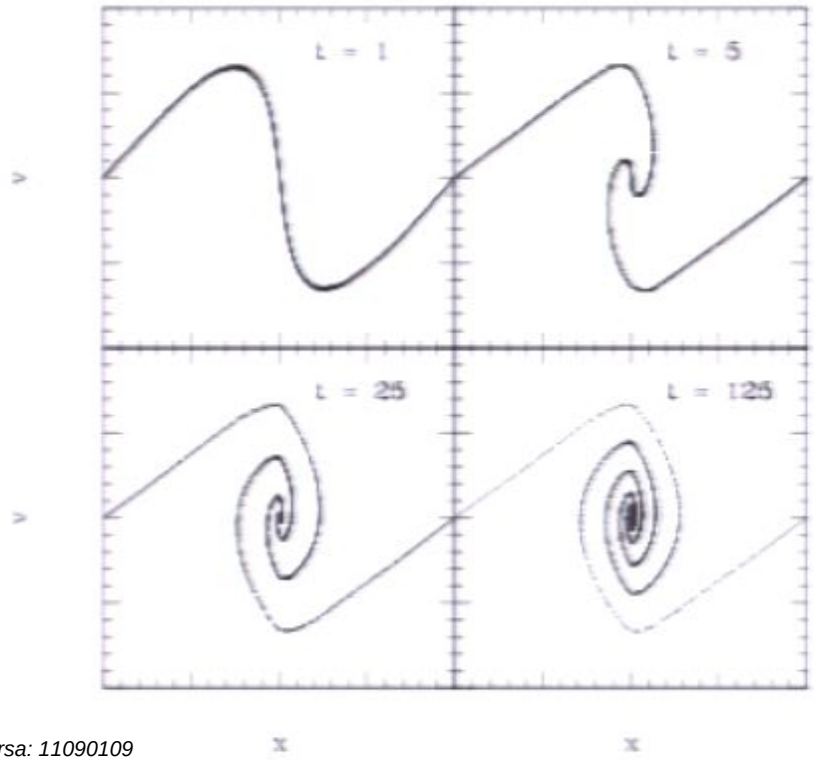

1D spectrum of modes

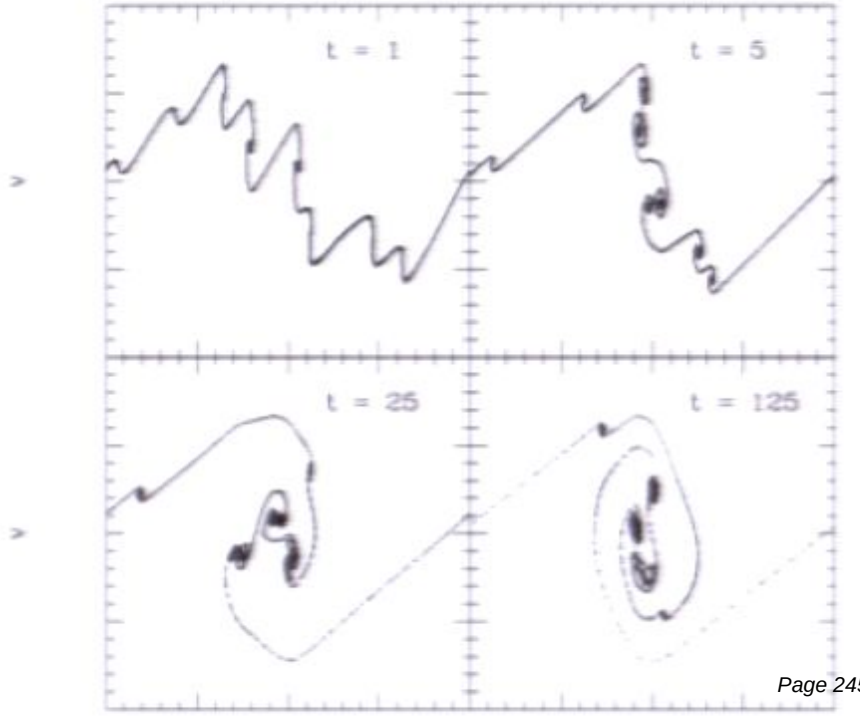

The Fillmore-Goldreich-Bertschinger solutions assume smooth, spherical infall. Initial perturbation is monotonic in r.

In the standard model for structure formation on all scales and structure formation proceeds perturbations exist hierarchically

single mode -- planar collapse

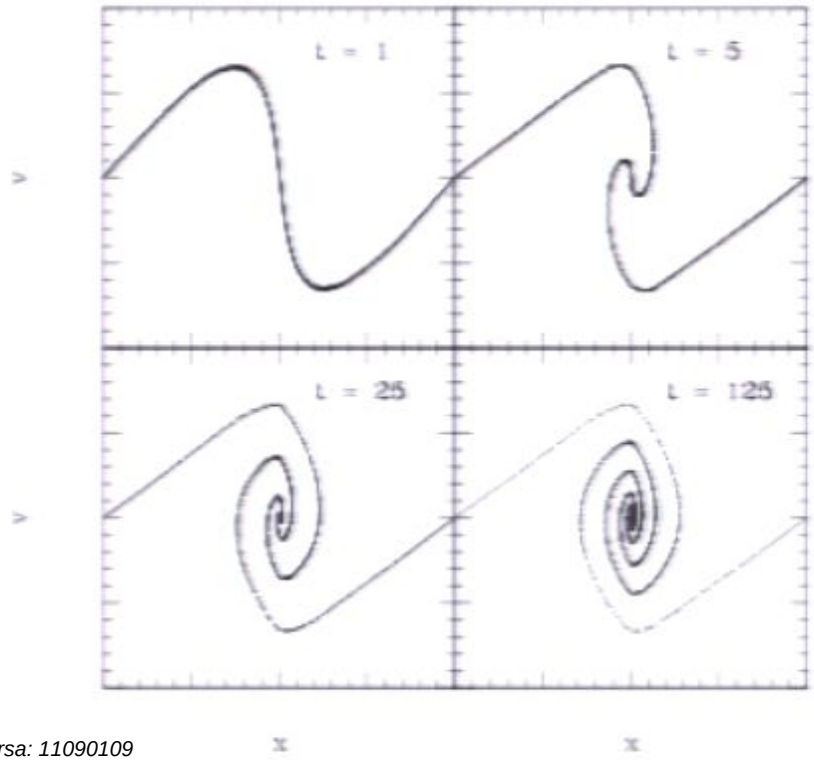

1D spectrum of modes

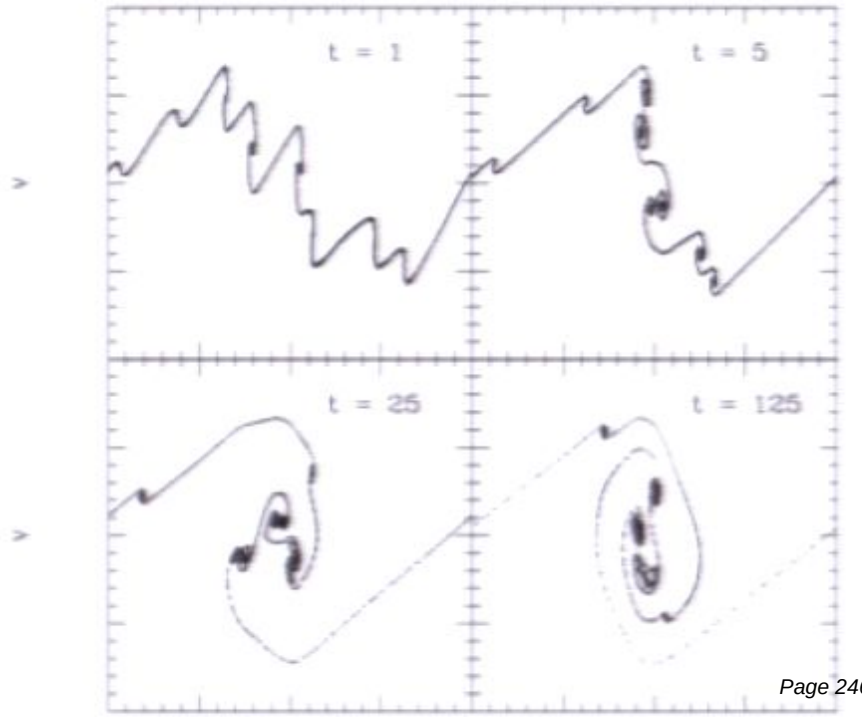

The Fillmore-Goldreich-Bertschinger solutions assume smooth, spherical infall. Initial perturbation is monotonic in r.

In the standard model for structure formation on all scales and structure formation proceeds perturbations exist hierarchically

single mode -- planar collapse

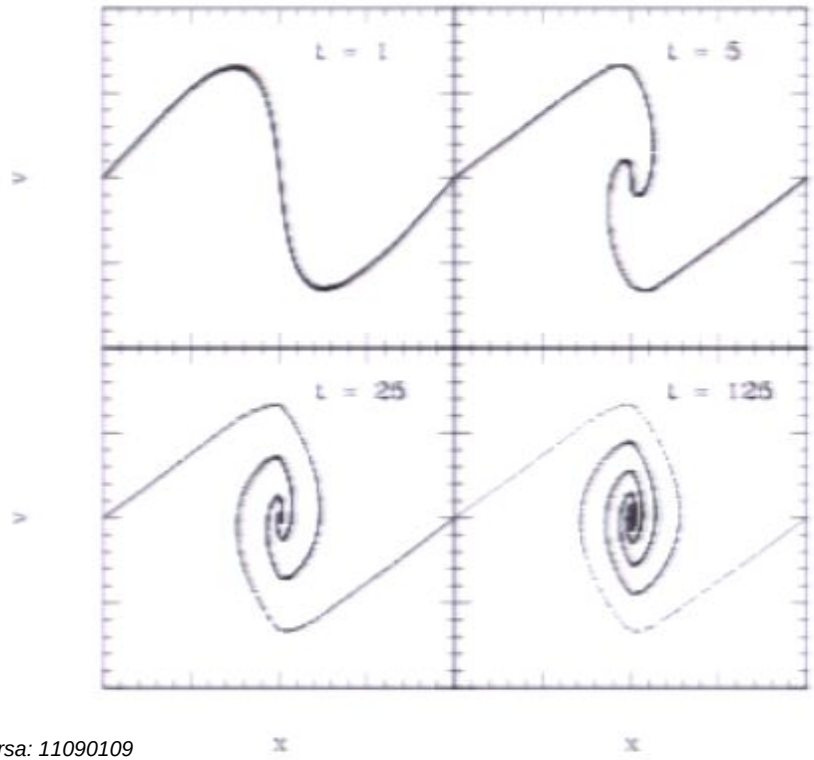

1D spectrum of modes

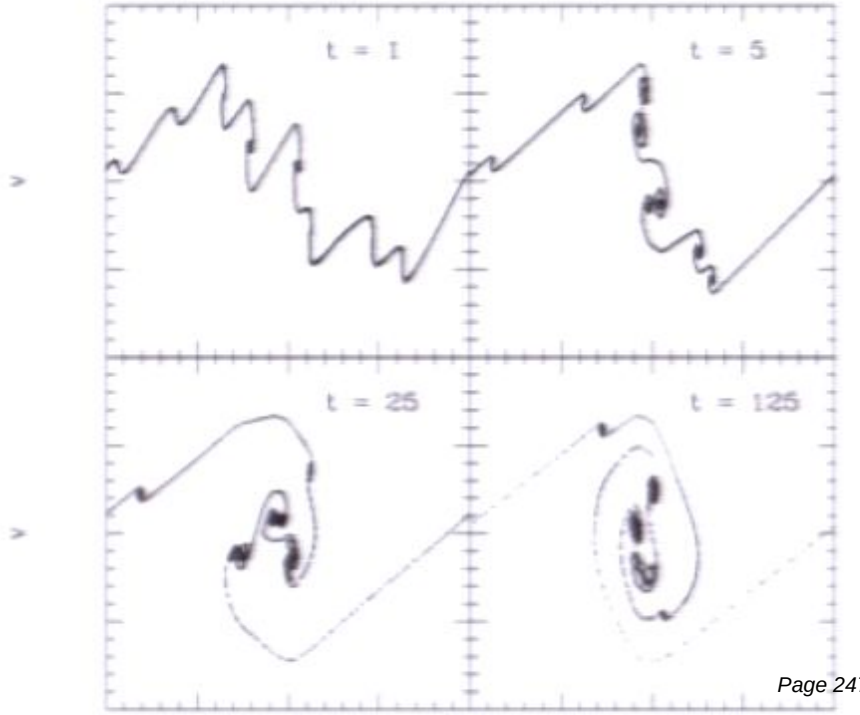

The Fillmore-Goldreich-Bertschinger solutions assume smooth, spherical infall. Initial perturbation is monotonic in r.

In the standard model for structure formation on all scales and structure formation proceeds perturbations exist hierarchically

single mode -- planar collapse

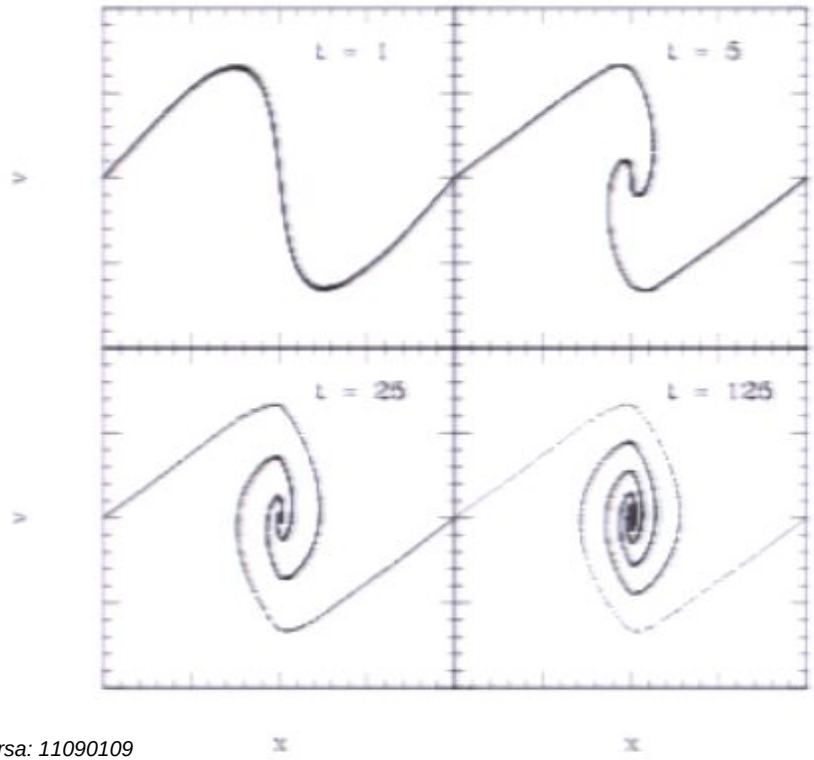

1D spectrum of modes

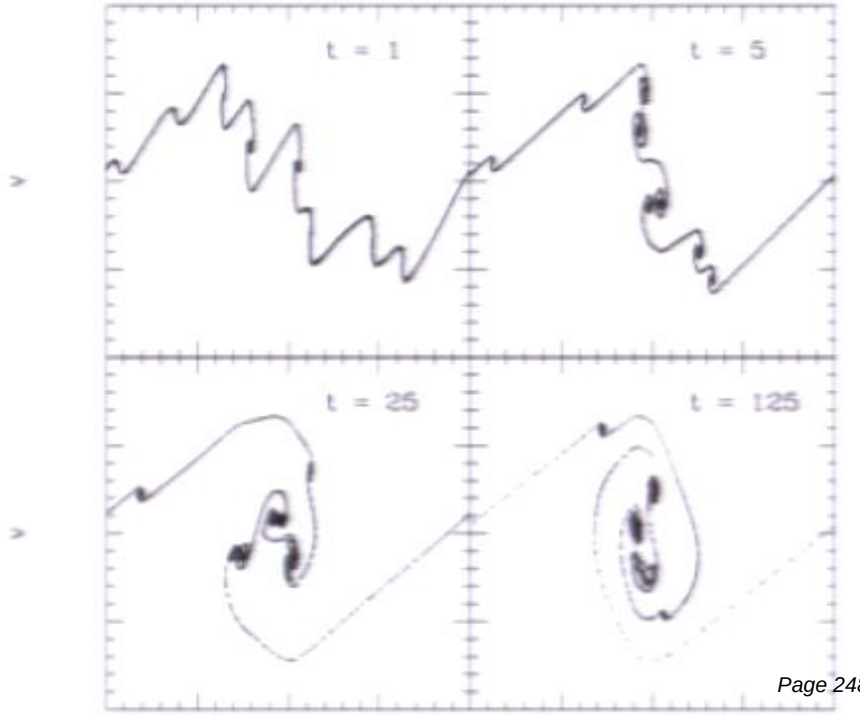

The Fillmore-Goldreich-Bertschinger solutions assume smooth, spherical infall. Initial perturbation is monotonic in r.

In the standard model for structure formation on all scales and structure formation proceeds perturbations exist hierarchically

single mode -- planar collapse

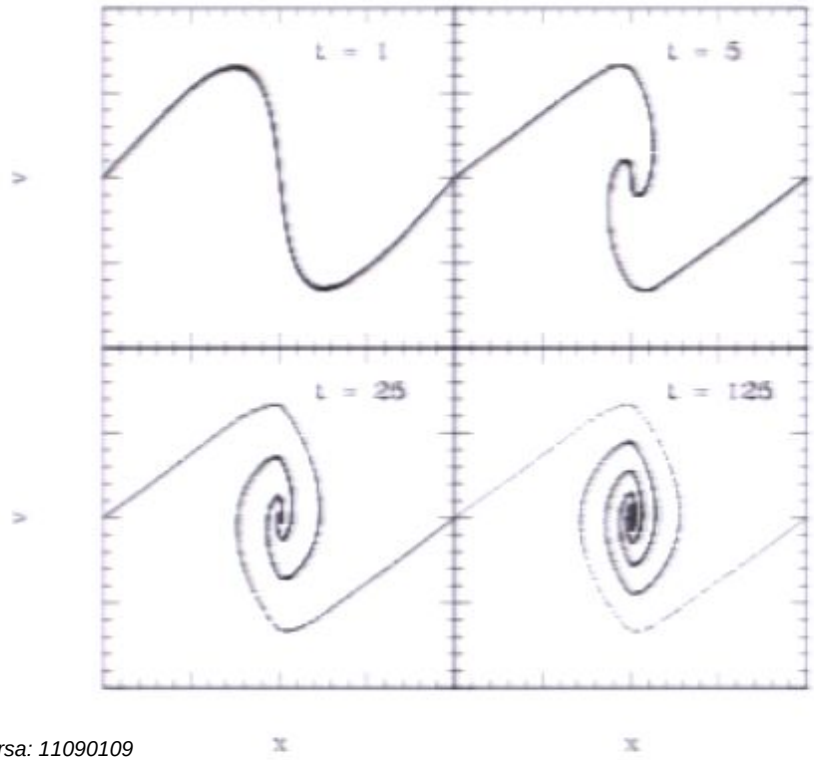

1D spectrum of modes

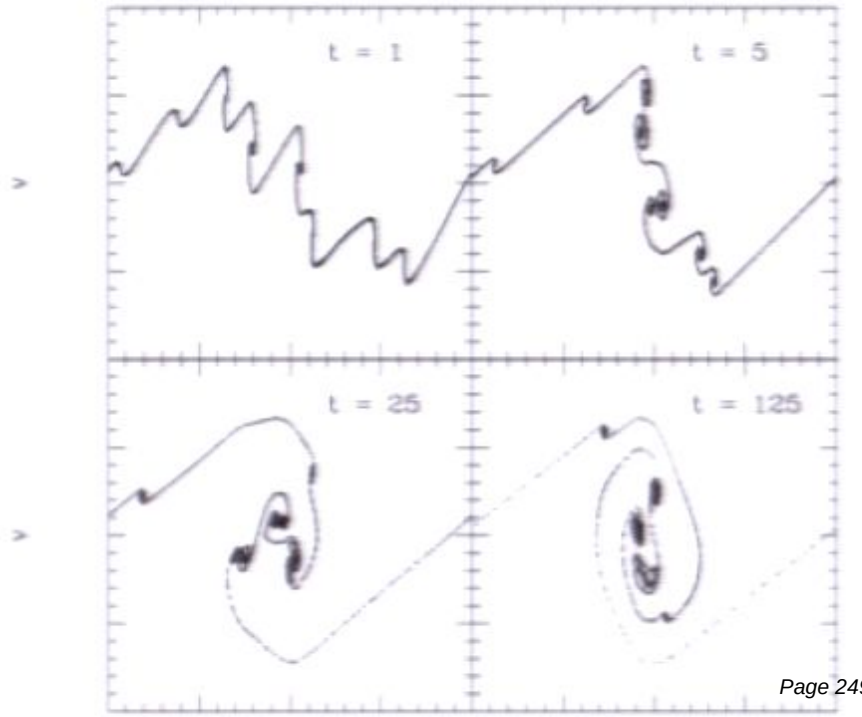

The Fillmore-Goldreich-Bertschinger solutions assume smooth, spherical infall. Initial perturbation is monotonic in r.

In the standard model for structure formation on all scales and structure formation proceeds perturbations exist hierarchically

single mode -- planar collapse

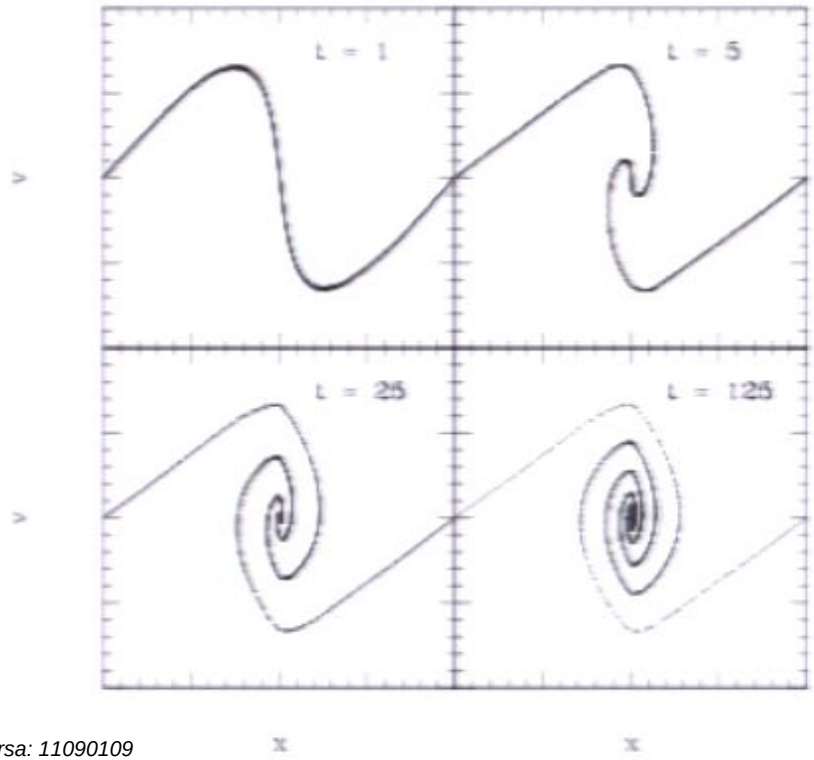

1D spectrum of modes

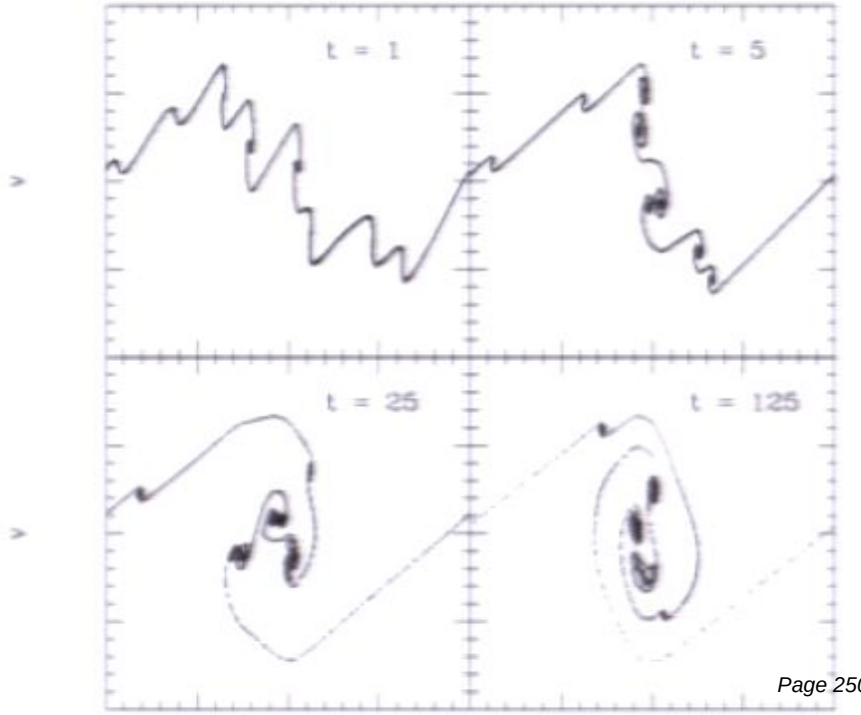

The Fillmore-Goldreich-Bertschinger solutions assume smooth, spherical infall. Initial perturbation is monotonic in r.

In the standard model for structure formation on all scales and structure formation proceeds perturbations exist hierarchically

single mode -- planar collapse

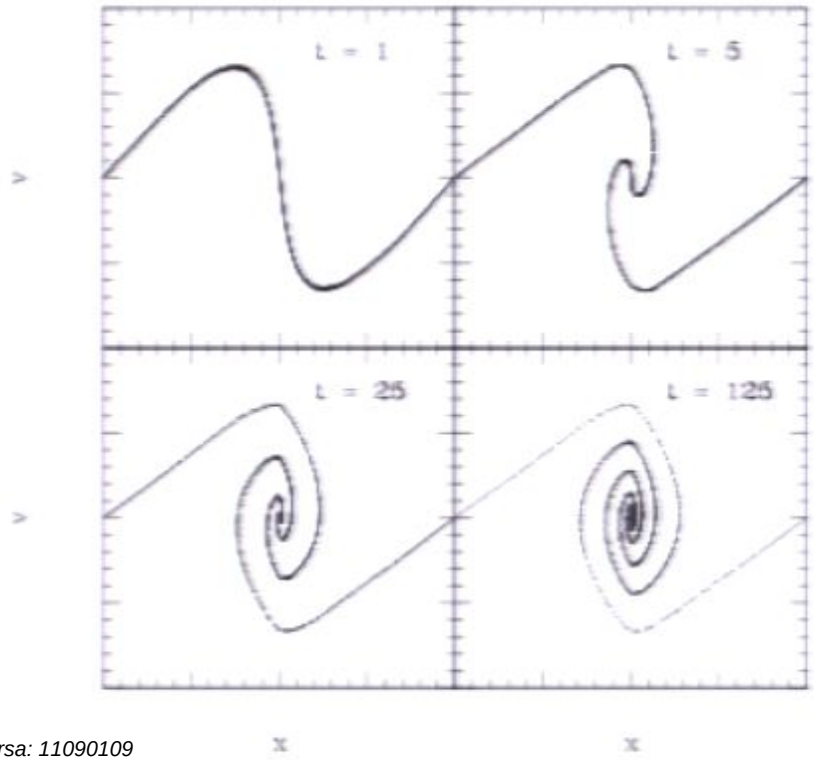

1D spectrum of modes

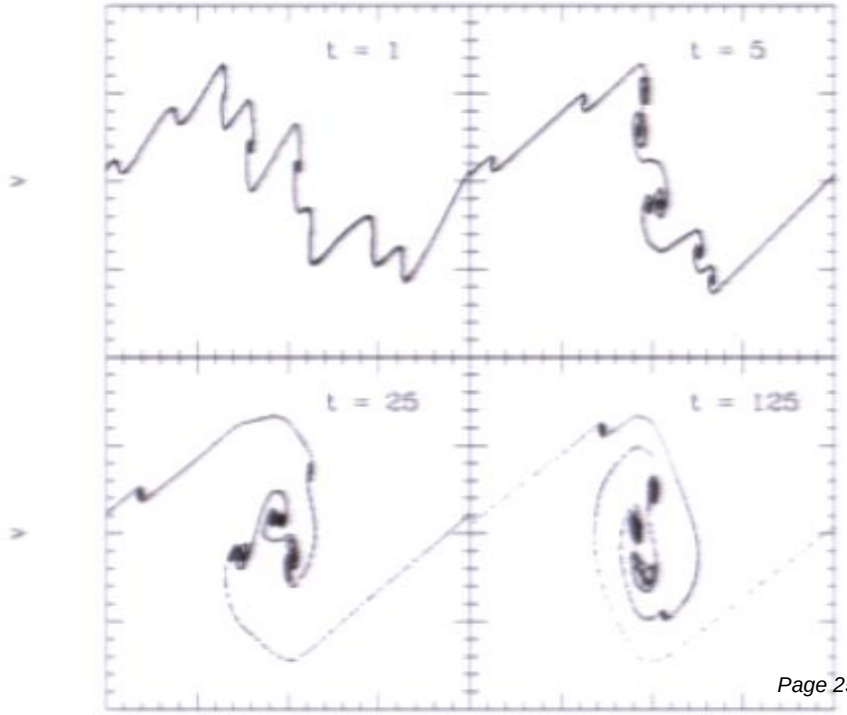

The Fillmore-Goldreich-Bertschinger solutions assume smooth, spherical infall. Initial perturbation is monotonic in r.

In the standard model for structure formation on all scales and structure formation proceeds perturbations exist hierarchically

single mode -- planar collapse

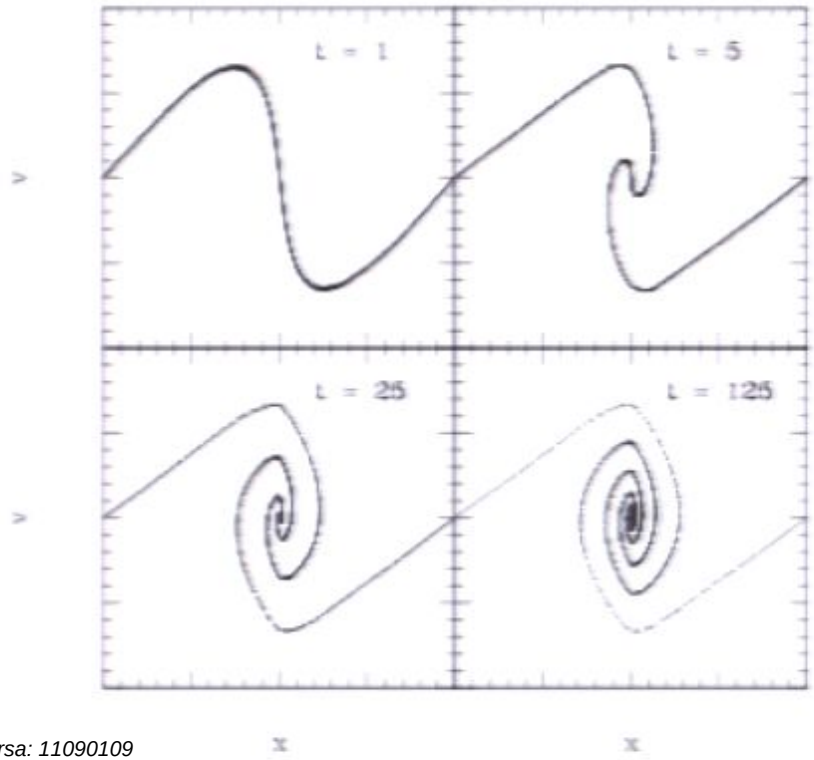

1D spectrum of modes

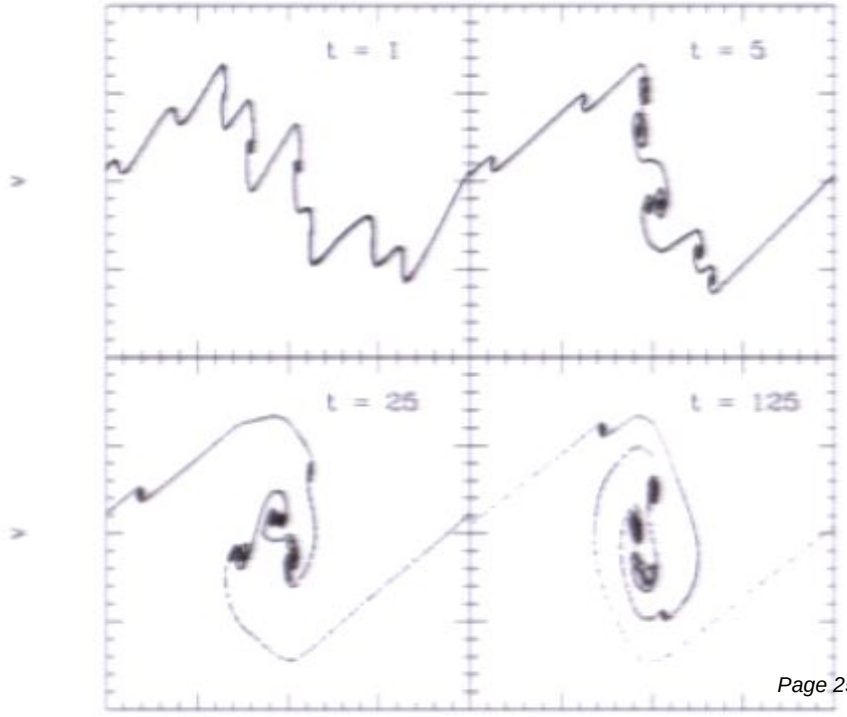

The Fillmore-Goldreich-Bertschinger solutions assume smooth, spherical infall. Initial perturbation is monotonic in r.

In the standard model for structure formation on all scales and structure formation proceeds perturbations exist hierarchically

single mode -- planar collapse

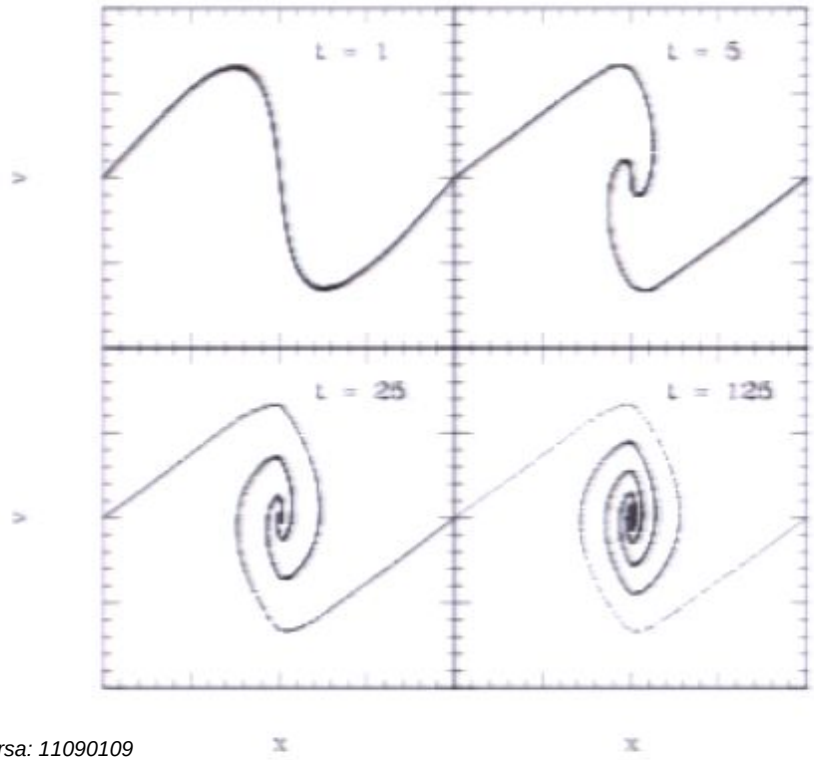

1D spectrum of modes

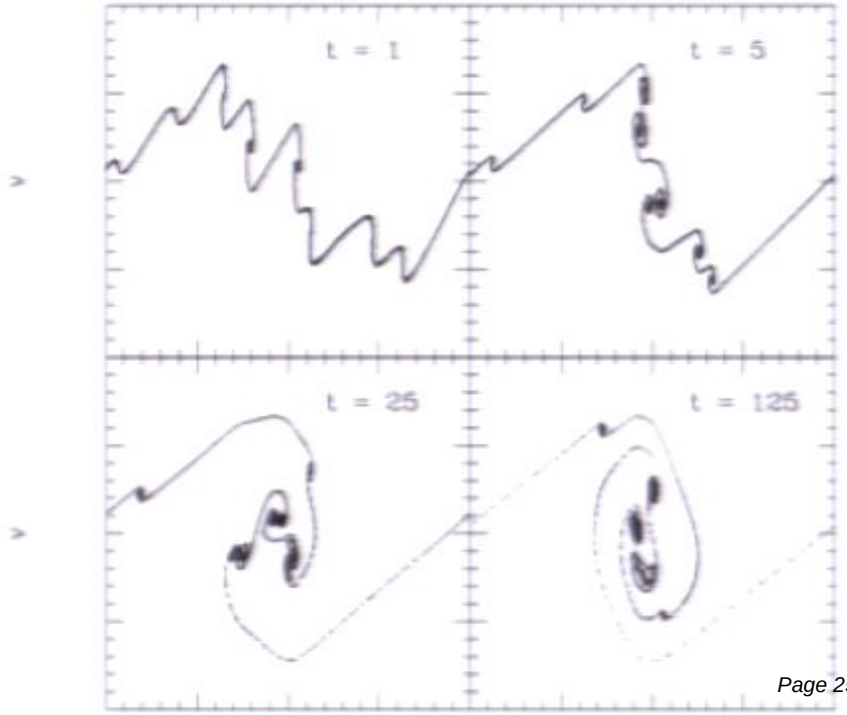

The Fillmore-Goldreich-Bertschinger solutions assume smooth, spherical infall. Initial perturbation is monotonic in r.

In the standard model for structure formation on all scales and structure formation proceeds perturbations exist hierarchically

single mode -- planar collapse

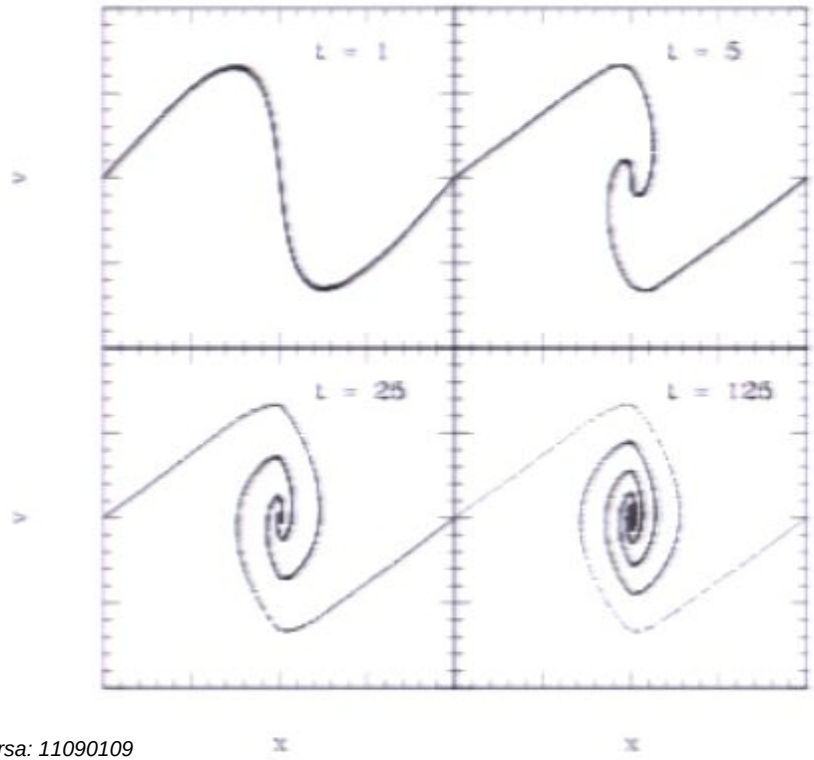

1D spectrum of modes

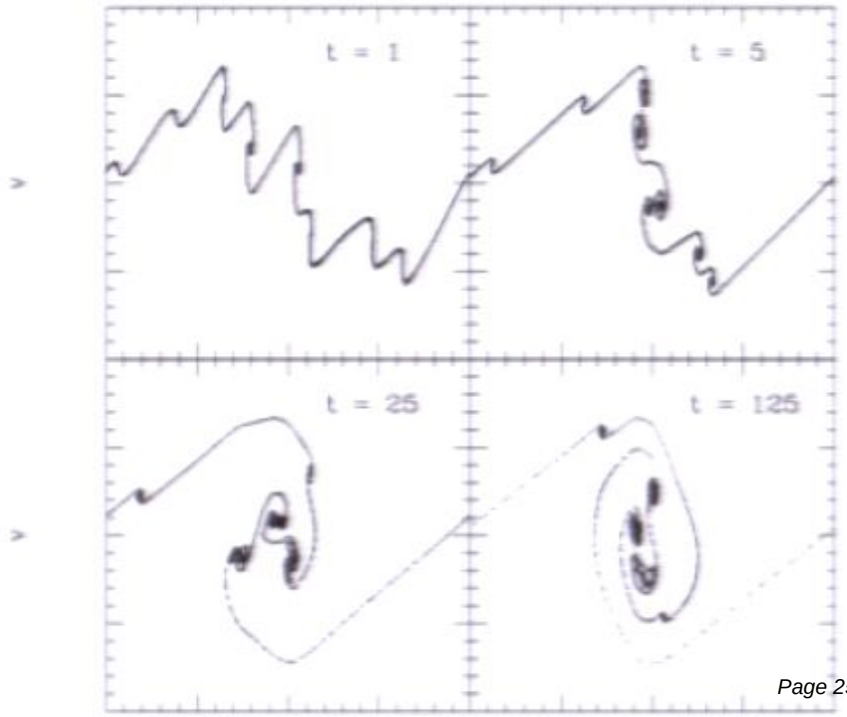

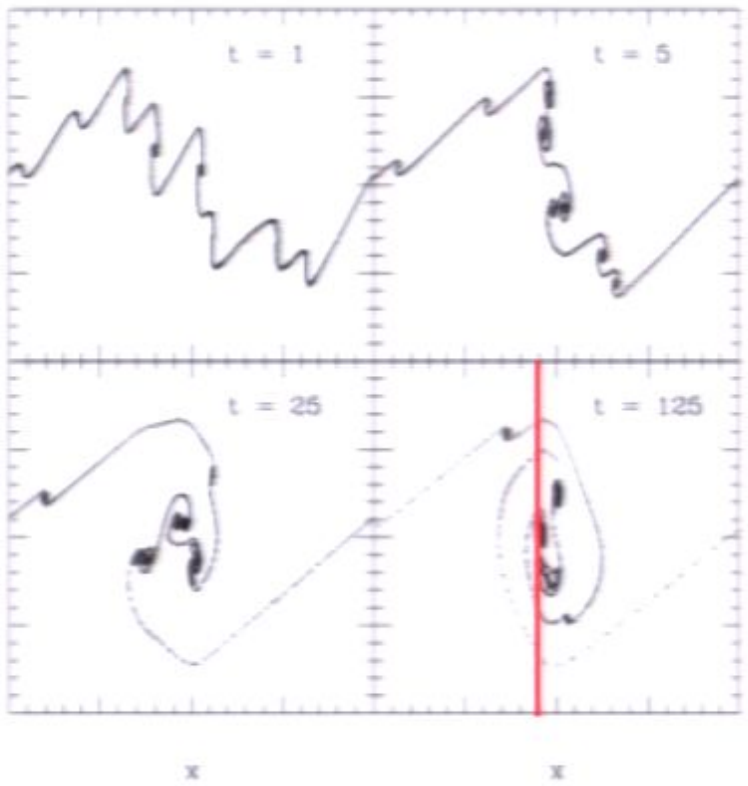

dark matter detector at
position of red line
"sees" particles with
complicated velocity
distribution (peaks and subpeaks)

ideal terrestrial detector occupies a 3D plane
(fixed position, all of velocity-space accessible)
If DF is a 3D surface (albeit curled up on all scales),
$f(\mathbf{v})$ will be a collection of peaks and subpeaks

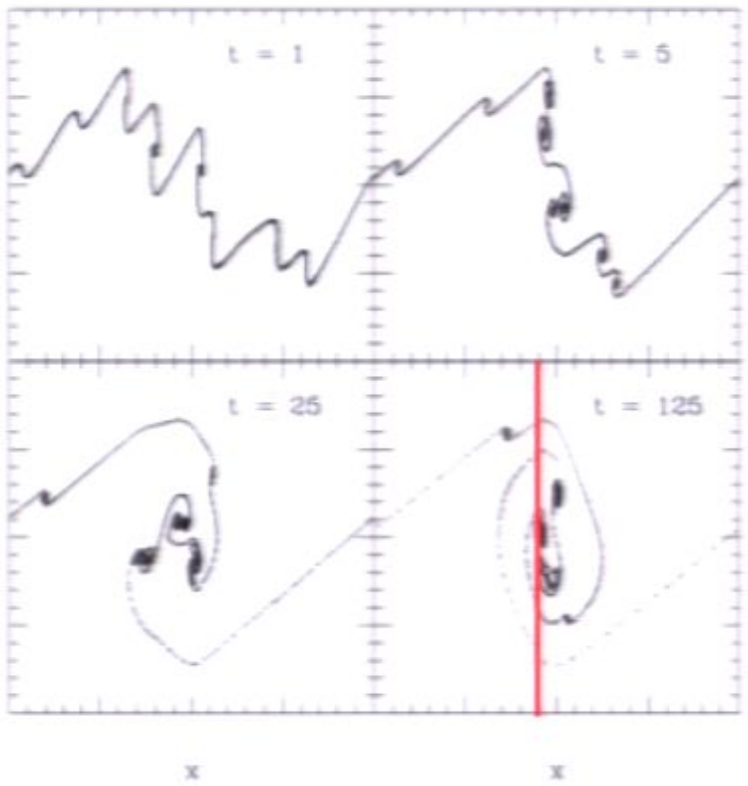

dark matter detector at
position of red line
"sees" particles with
complicated velocity
distribution (peaks and subpeaks)

ideal terrestrial detector occupies a 3D plane
(fixed position, all of velocity-space accessible)
If DF is a 3D surface (albeit curled up on all scales),
$f(\mathbf{v})$ will be a collection of peaks and subpeaks

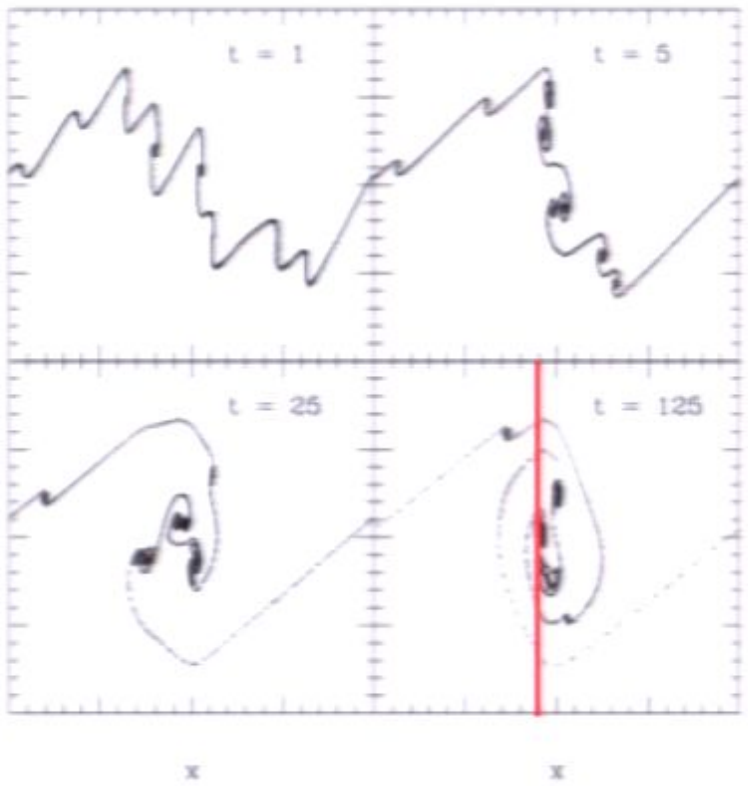

dark matter detector at
position of red line
"sees" particles with
complicated velocity
distribution (peaks and subpeaks)

ideal terrestrial detector occupies a 3D plane
(fixed position, all of velocity-space accessible)
If DF is a 3D surface (albeit curled up on all scales),
$f(\mathbf{v})$ will be a collection of peaks and subpeaks

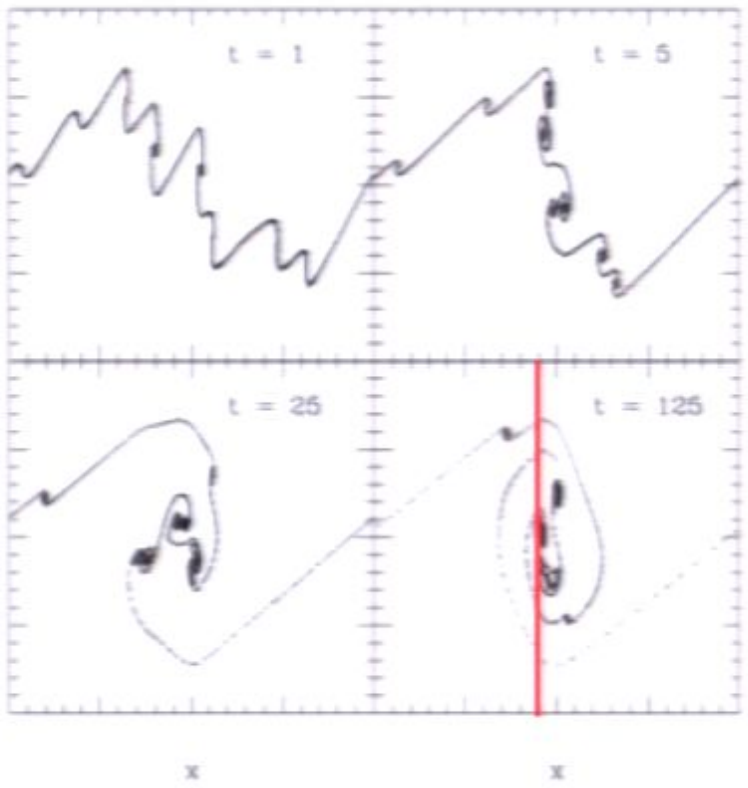

dark matter detector at
position of red line
"sees" particles with
complicated velocity
distribution (peaks and subpeaks)

ideal terrestrial detector occupies a 3D plane
(fixed position, all of velocity-space accessible)
If DF is a 3D surface (albeit curled up on all scales),
$f(\mathbf{v})$ will be a collection of peaks and subpeaks

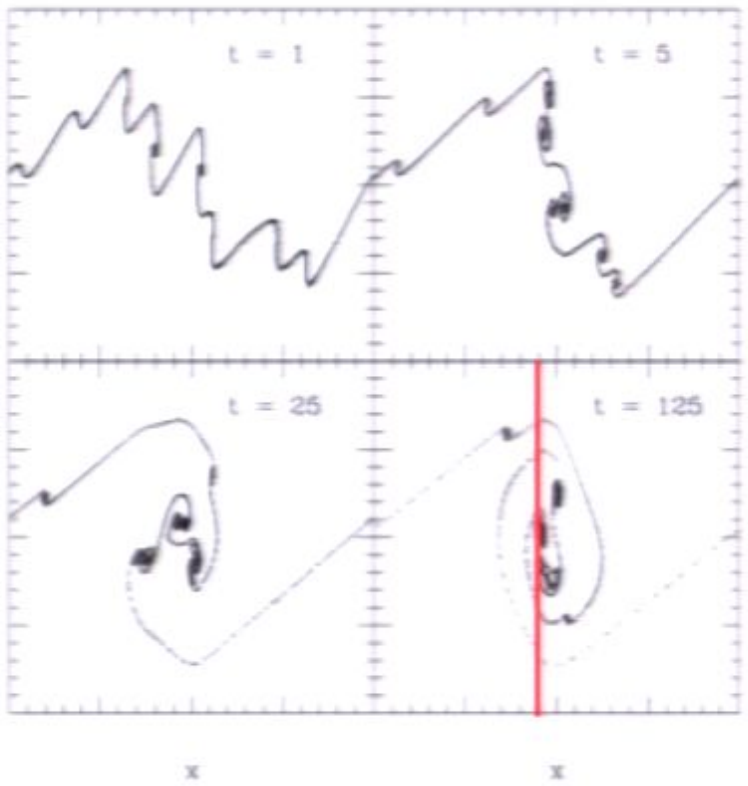

dark matter detector at
position of red line
"sees" particles with
complicated velocity
distribution (peaks and subpeaks)

ideal terrestrial detector occupies a 3D plane
(fixed position, all of velocity-space accessible)
If DF is a 3D surface (albeit curled up on all scales),
$f(\mathbf{v})$ will be a collection of peaks and subpeaks

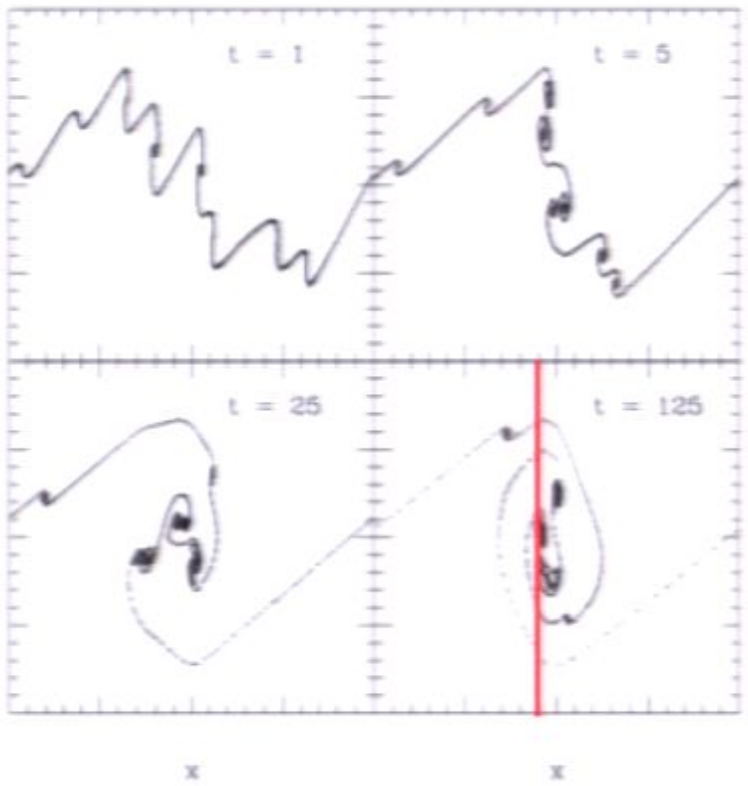

dark matter detector at
position of red line
"sees" particles with
complicated velocity
distribution (peaks and subpeaks)

ideal terrestrial detector occupies a 3D plane
(fixed position, all of velocity-space accessible)
If DF is a 3D surface (albeit curled up on all scales),
$f(\mathbf{v})$ will be a collection of peaks and subpeaks

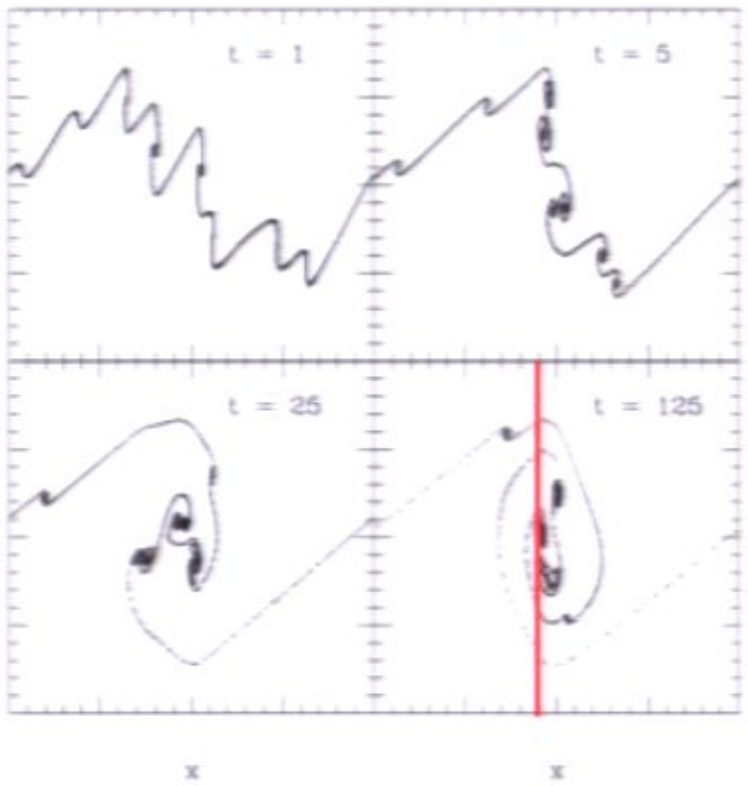

dark matter detector at
position of red line
"sees" particles with
complicated velocity
distribution (peaks and subpeaks)

ideal terrestrial detector occupies a 3D plane
(fixed position, all of velocity-space accessible)
If DF is a 3D surface (albeit curled up on all scales),
$f(\mathbf{v})$ will be a collection of peaks and subpeaks

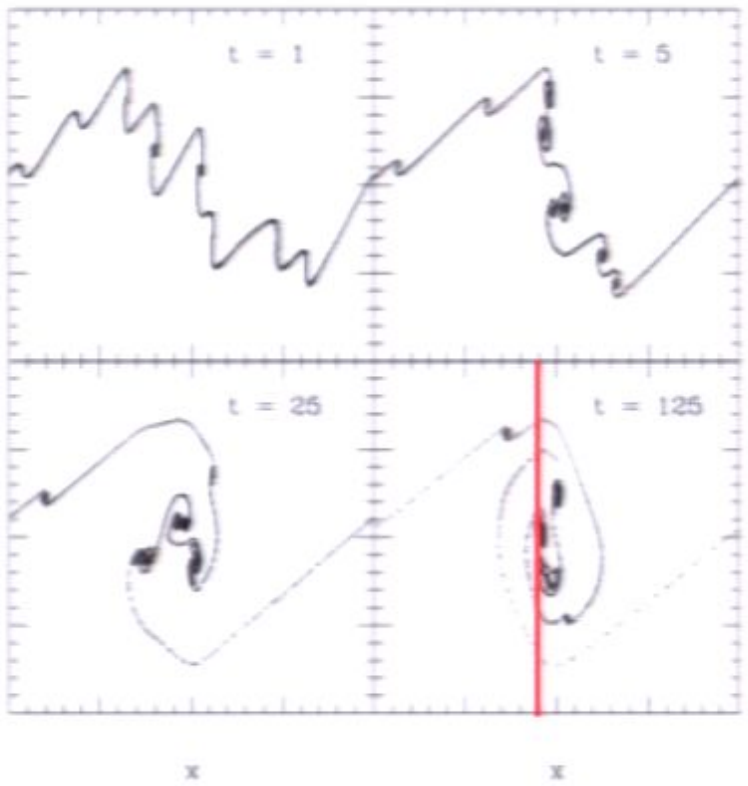

dark matter detector at
position of red line
"sees" particles with
complicated velocity
distribution (peaks and subpeaks)

ideal terrestrial detector occupies a 3D plane
(fixed position, all of velocity-space accessible)
If DF is a 3D surface (albeit curled up on all scales),
$f(\mathbf{v})$ will be a collection of peaks and subpeaks

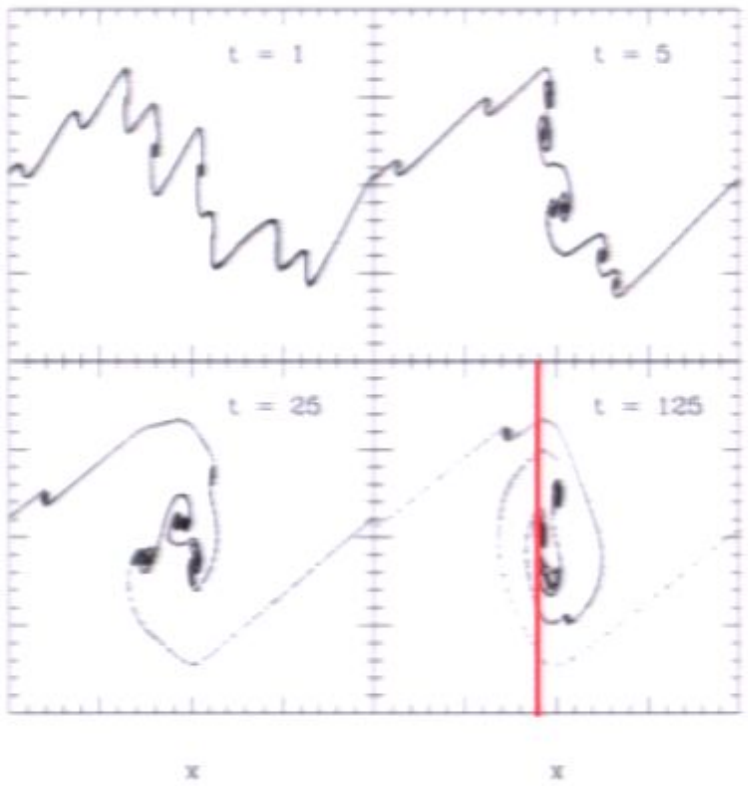

dark matter detector at
position of red line
"sees" particles with
complicated velocity
distribution (peaks and subpeaks)

ideal terrestrial detector occupies a 3D plane
(fixed position, all of velocity-space accessible)
If DF is a 3D surface (albeit curled up on all scales),
$f(\mathbf{v})$ will be a collection of peaks and subpeaks

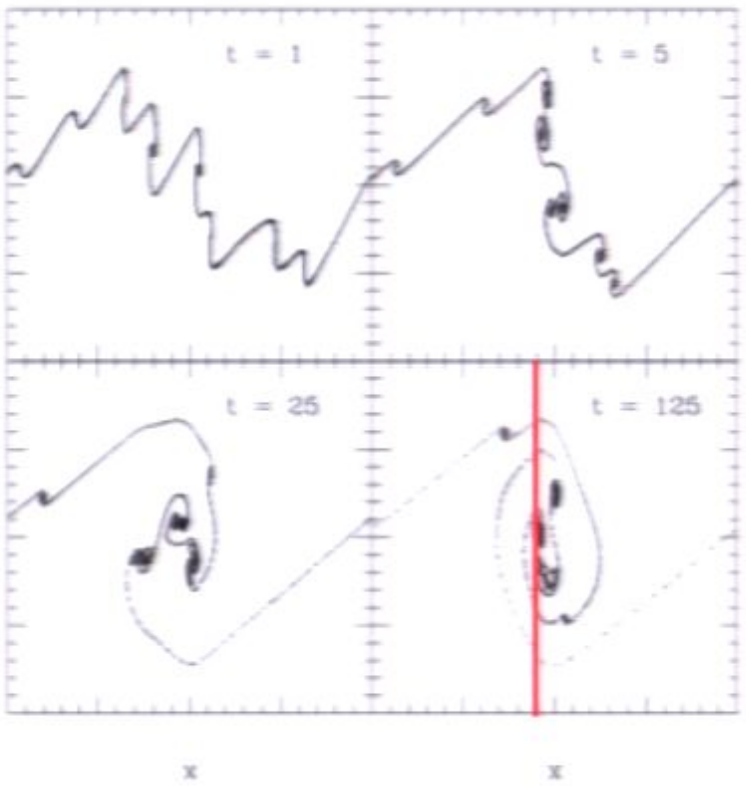

dark matter detector at
position of red line
"sees" particles with
complicated velocity
distribution (peaks and subpeaks)

ideal terrestrial detector occupies a 3D plane
(fixed position, all of velocity-space accessible)
If DF is a 3D surface (albeit curled up on all scales),
$f(\mathbf{v})$ will be a collection of peaks and subpeaks

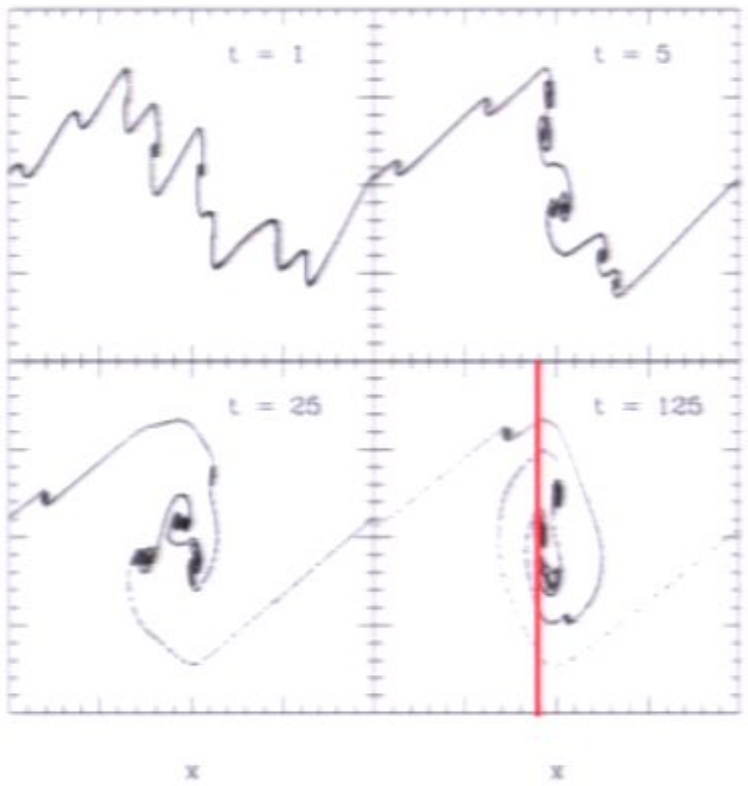

dark matter detector at
position of red line
"sees" particles with
complicated velocity
distribution (peaks and subpeaks)

ideal terrestrial detector occupies a 3D plane
(fixed position, all of velocity-space accessible)
If DF is a 3D surface (albeit curled up on all scales),
$f(\mathbf{v})$ will be a collection of peaks and subpeaks

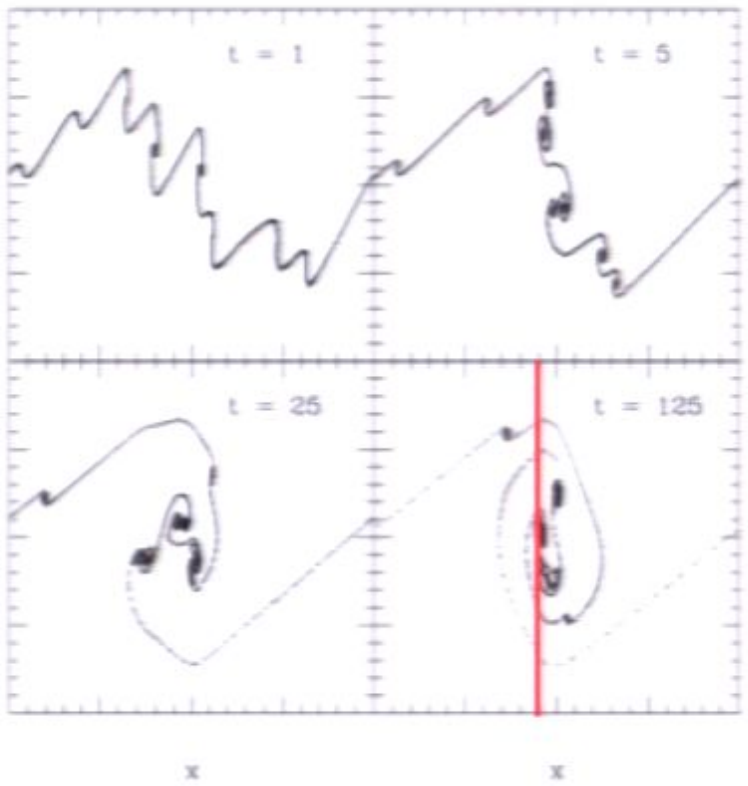

dark matter detector at
position of red line
"sees" particles with
complicated velocity
distribution (peaks and subpeaks)

ideal terrestrial detector occupies a 3D plane
(fixed position, all of velocity-space accessible)
If DF is a 3D surface (albeit curled up on all scales),
$f(\mathbf{v})$ will be a collection of peaks and subpeaks

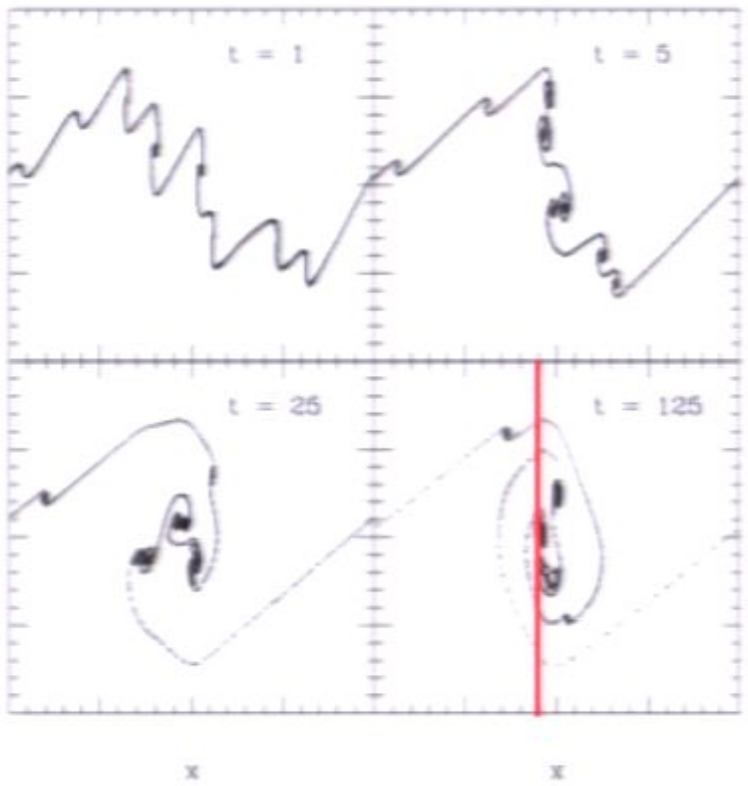

dark matter detector at
position of red line
"sees" particles with
complicated velocity
distribution (peaks and subpeaks)

ideal terrestrial detector occupies a 3D plane
(fixed position, all of velocity-space accessible)
If DF is a 3D surface (albeit curled up on all scales),
$f(\mathbf{v})$ will be a collection of peaks and subpeaks

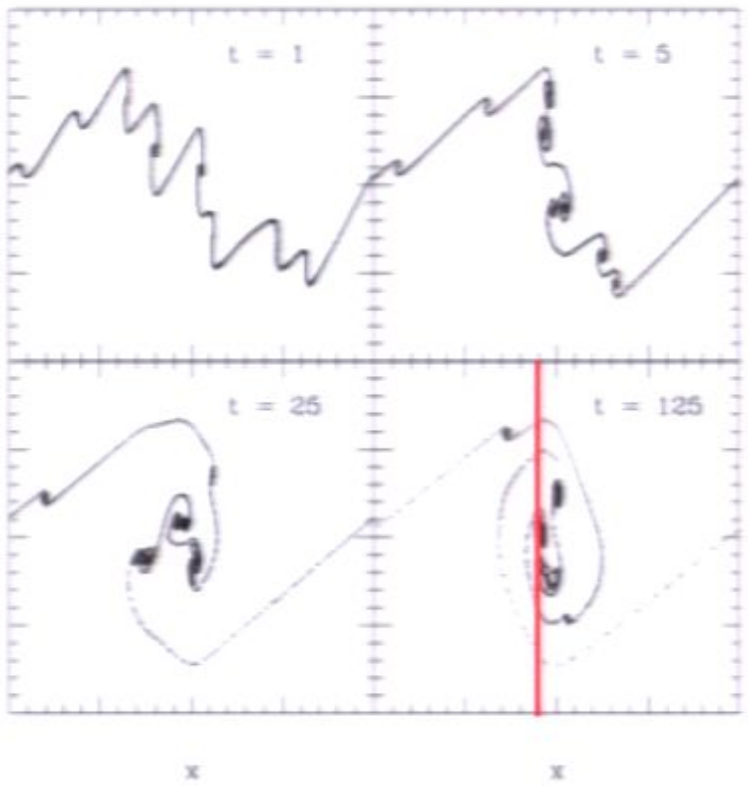

dark matter detector at
position of red line
"sees" particles with
complicated velocity
distribution (peaks and subpeaks)

ideal terrestrial detector occupies a 3D plane
(fixed position, all of velocity-space accessible)
If DF is a 3D surface (albeit curled up on all scales),
$f(\mathbf{v})$ will be a collection of peaks and subpeaks

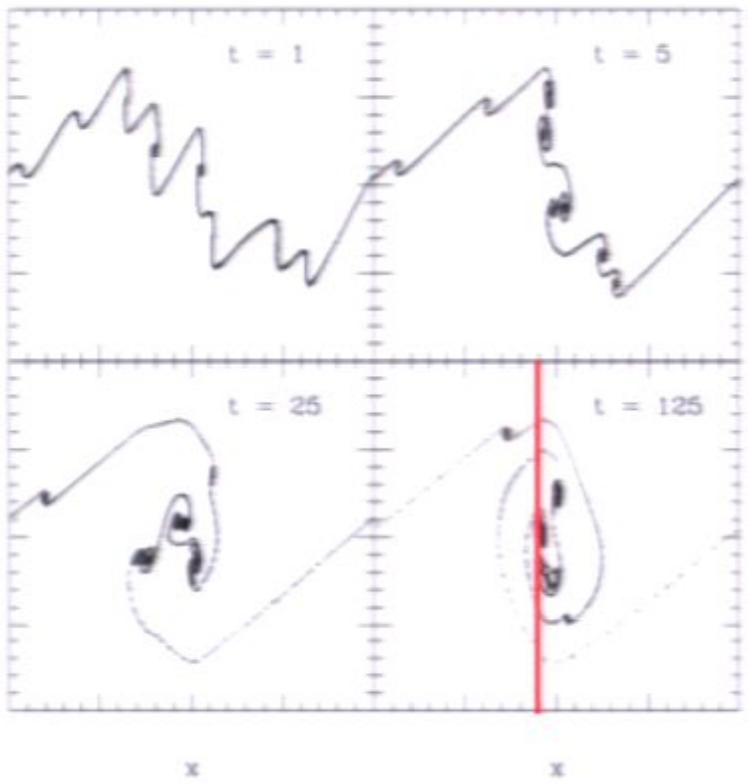

dark matter detector at
position of red line
"sees" particles with
complicated velocity
distribution (peaks and subpeaks)

ideal terrestrial detector occupies a 3D plane
(fixed position, all of velocity-space accessible)
If DF is a 3D surface (albeit curled up on all scales),
$f(\mathbf{v})$ will be a collection of peaks and subpeaks

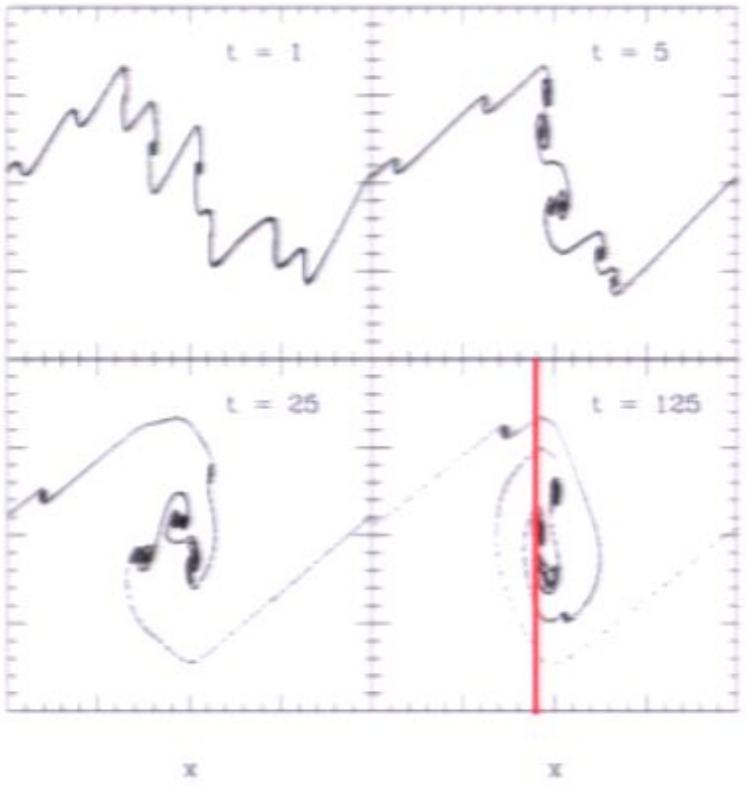

dark matter detector at
position of red line
"sees" particles with
complicated velocity
distribution (peaks and subpeaks)

ideal terrestrial detector occupies a 3D plane
(fixed position, all of velocity-space accessible)
If DF is a 3D surface (albeit curled up on all scales),
$f(\mathbf{v})$ will be a collection of peaks and subpeaks

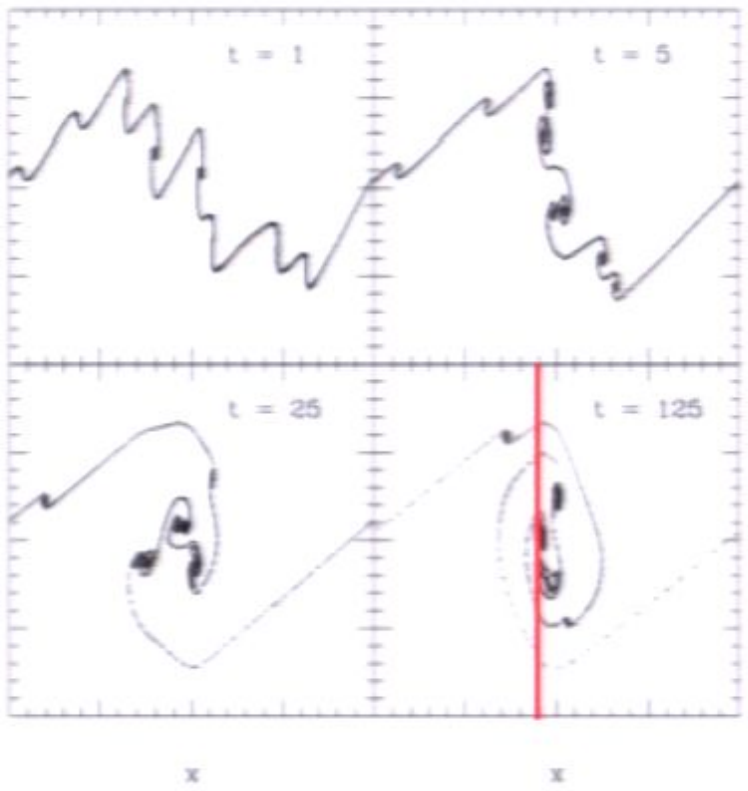

dark matter detector at
position of red line
"sees" particles with
complicated velocity
distribution (peaks and subpeaks)

ideal terrestrial detector occupies a 3D plane
(fixed position, all of velocity-space accessible)
If DF is a 3D surface (albeit curled up on all scales),
$f(\mathbf{v})$ will be a collection of peaks and subpeaks

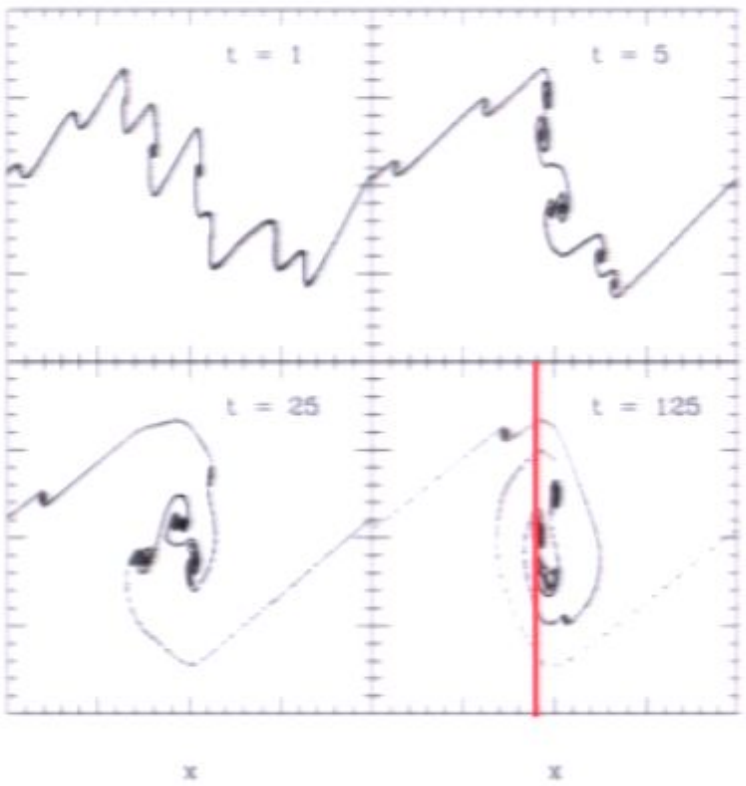

dark matter detector at
position of red line
"sees" particles with
complicated velocity
distribution (peaks and subpeaks)

ideal terrestrial detector occupies a 3D plane
(fixed position, all of velocity-space accessible)
If DF is a 3D surface (albeit curled up on all scales),
$f(\mathbf{v})$ will be a collection of peaks and subpeaks

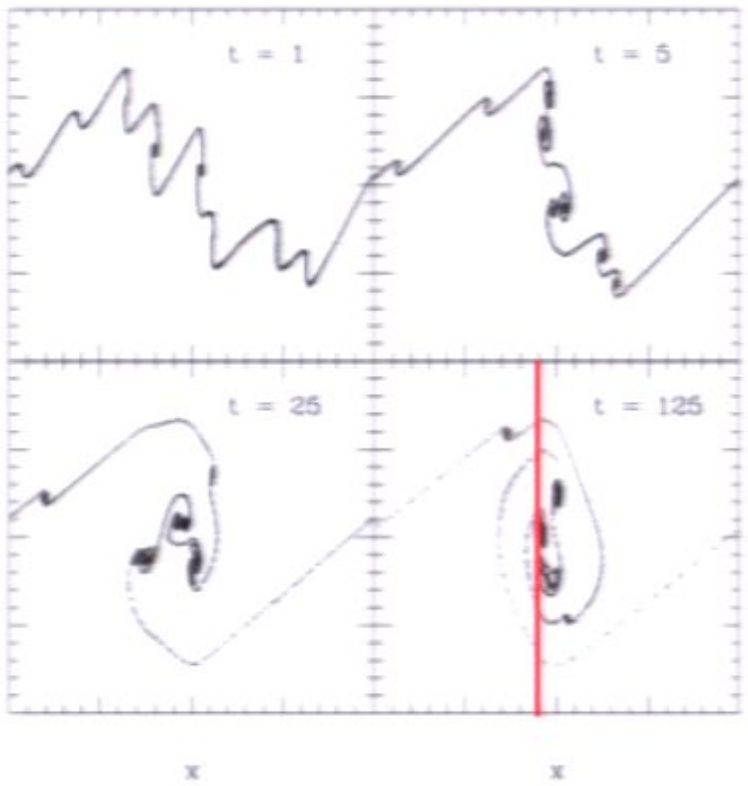

dark matter detector at
position of red line
"sees" particles with
complicated velocity
distribution (peaks and subpeaks)

ideal terrestrial detector occupies a 3D plane
(fixed position, all of velocity-space accessible)
If DF is a 3D surface (albeit curled up on all scales),
$f(\mathbf{v})$ will be a collection of peaks and subpeaks

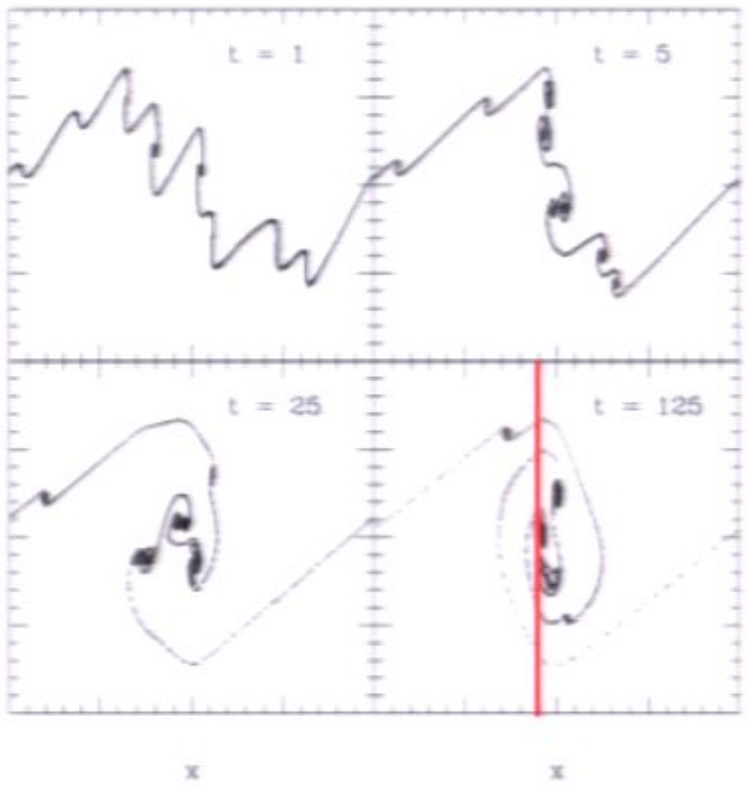

dark matter detector at
position of red line
"sees" particles with
complicated velocity
distribution (peaks and subpeaks)

ideal terrestrial detector occupies a 3D plane
(fixed position, all of velocity-space accessible)
If DF is a 3D surface (albeit curled up on all scales),
$f(\mathbf{v})$ will be a collection of peaks and subpeaks

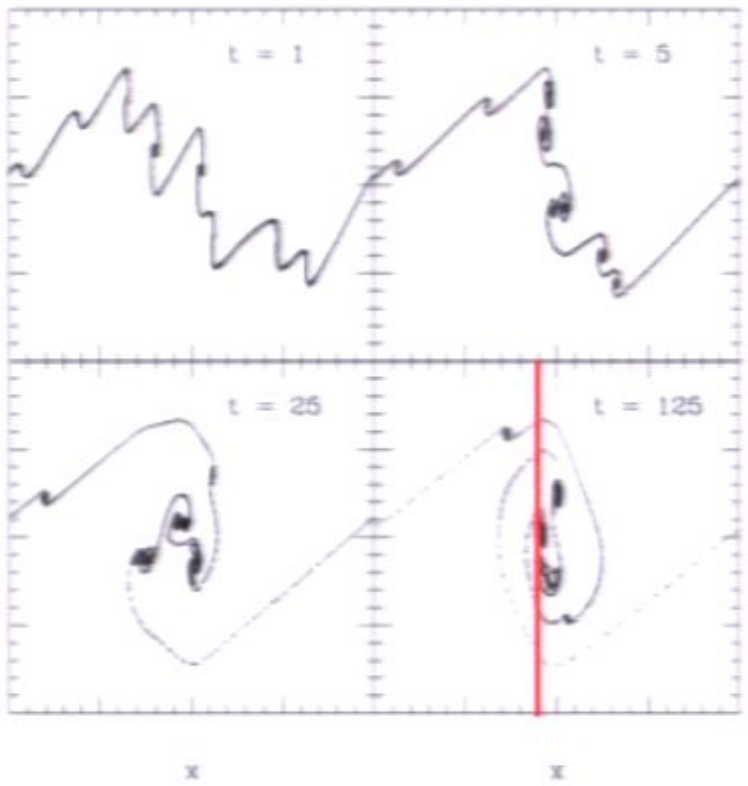

dark matter detector at
position of red line
"sees" particles with
complicated velocity
distribution (peaks and subpeaks)

ideal terrestrial detector occupies a 3D plane
(fixed position, all of velocity-space accessible)
If DF is a 3D surface (albeit curled up on all scales),
$f(\mathbf{v})$ will be a collection of peaks and subpeaks

Two Questions:

Do N-body simulations correctly
evolve the phase space sheet?

If they did, can we properly visualize/study it?

Two Questions:

Do N-body simulations correctly
evolve the phase space sheet?

If they did, can we properly visualize/study it?

Two Questions:

Do N-body simulations correctly
evolve the phase space sheet?

If they did, can we properly visualize/study it?

Two Questions:

Do N-body simulations correctly
evolve the phase space sheet?

If they did, can we properly visualize/study it?

Two Questions:

Do N-body simulations correctly evolve the phase space sheet?

If they did, can we properly visualize/study it?

Two Questions:

Do N-body simulations correctly
evolve the phase space sheet?

If they did, can we properly visualize/study it?

Two Questions:

Do N-body simulations correctly evolve the phase space sheet?

If they did, can we properly visualize/study it?

Two Questions:

Do N-body simulations correctly evolve the phase space sheet?

If they did, can we properly visualize/study it?

Two Questions:

Do N-body simulations correctly evolve the phase space sheet?

If they did, can we properly visualize/study it?

Use simulation to characterize

$$f(\mathbf{v}, \mathbf{x}_d)$$

see LMW & Dubinski 1998; Moore et al. 2001 and many others

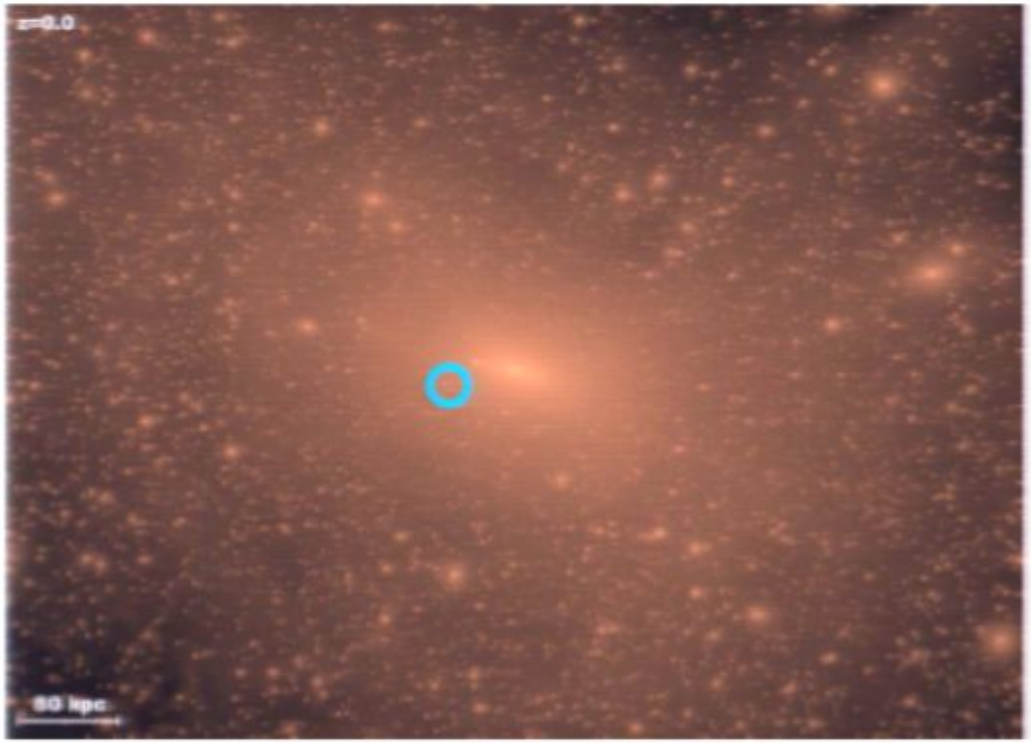

Pick a region of the simulated halo representative of the Earth. Select particles in this region and compute f(v).
From f(v), compute dR/dQ

"Uncertainty principle" for phase space:
Larger volumes give better velocity-space resolution but worse spatial resolution, and vice versa

Use simulation to characterize

$$f(\mathbf{v}, \mathbf{x}_d)$$

see LMW & Dubinski 1998; Moore et al. 2001 and many others

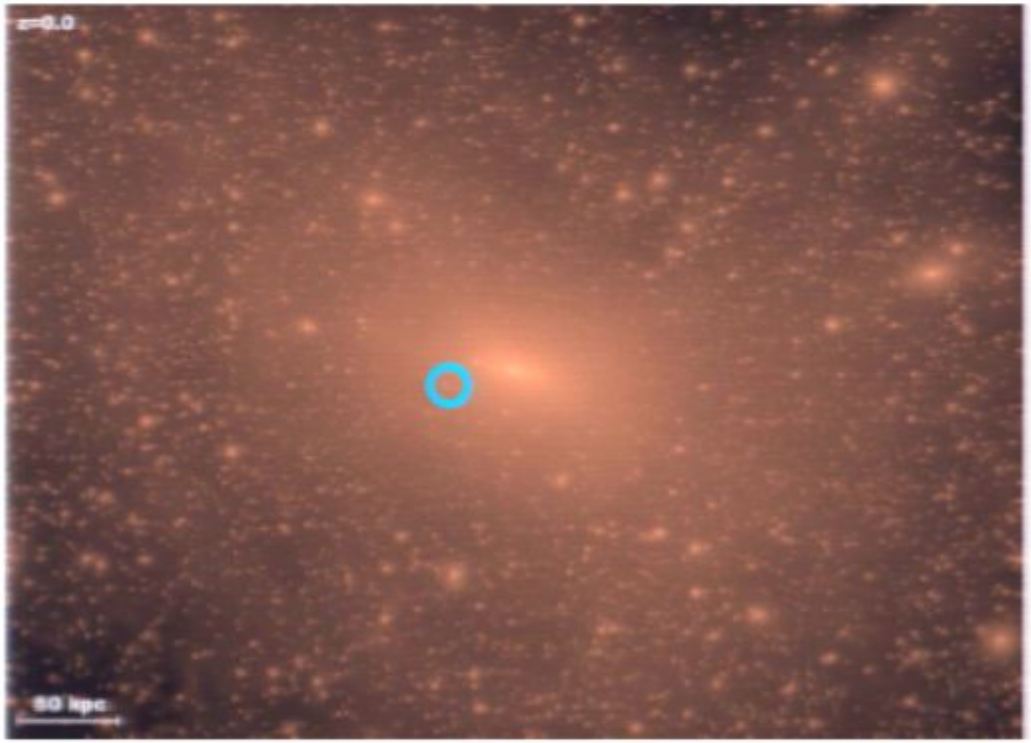

Pick a region of the simulated halo representative of the Earth. Select particles in this region and compute f(v).
From f(v), compute dR/dQ

"Uncertainty principle" for phase space:
Larger volumes give better velocity-space resolution but worse spatial resolution, and vice versa

Use simulation to characterize

$$f(\mathbf{v}, \mathbf{x}_d)$$

see LMW & Dubinski 1998; Moore et al. 2001 and many others

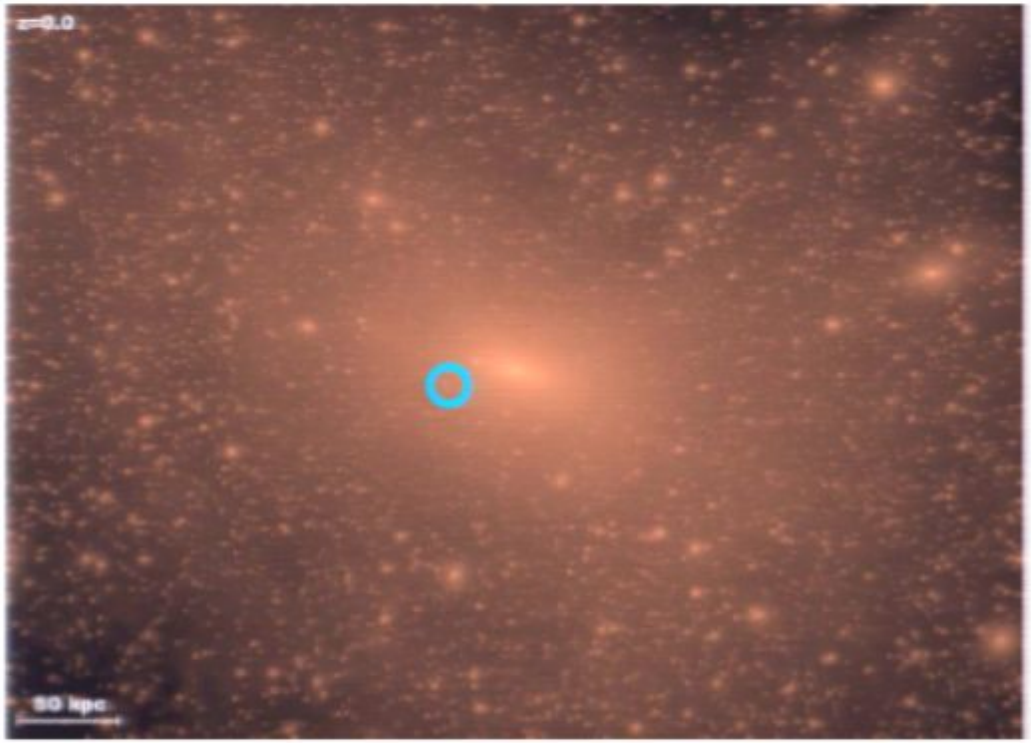

Pick a region of the simulated halo representative of the Earth. Select particles in this region and compute f(v).
From f(v), compute dR/dQ

"Uncertainty principle" for phase space:
Larger volumes give better velocity-space resolution but worse spatial resolution, and vice versa

Use simulation to characterize

$$f(\mathbf{v}, \mathbf{x}_d)$$

see LMW & Dubinski 1998; Moore et al. 2001 and many others

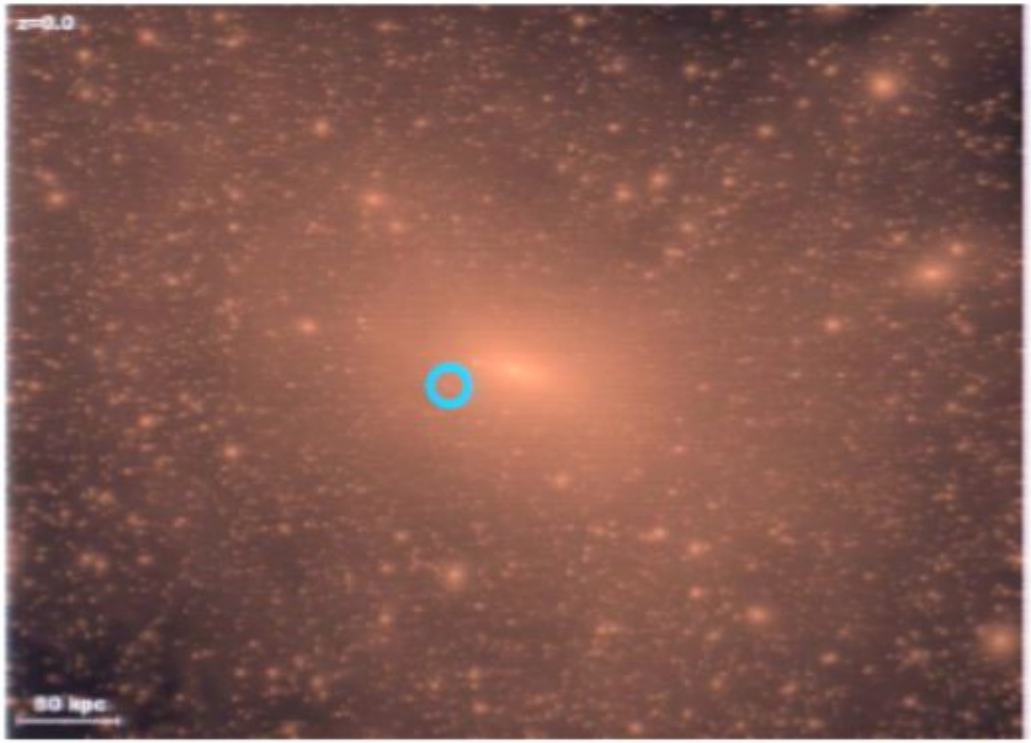

Pick a region of the simulated halo representative of the Earth. Select particles in this region and compute f(v).
From f(v), compute dR/dQ

"Uncertainty principle" for phase space:
Larger volumes give better velocity-space resolution but worse spatial resolution, and vice versa

Use simulation to characterize

$$f(\mathbf{v}, \mathbf{x}_d)$$

see LMW & Dubinski 1998; Moore et al. 2001 and many others

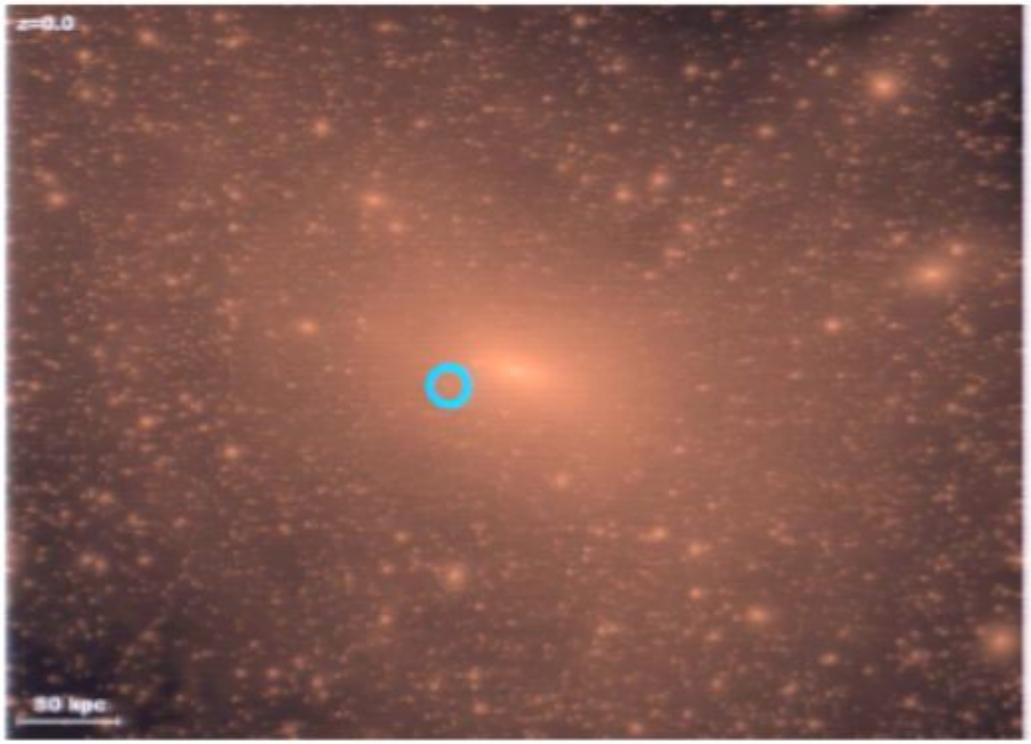

Pick a region of the simulated halo representative of the Earth. Select particles in this region and compute f(v).
From f(v), compute dR/dQ

"Uncertainty principle" for phase space:
Larger volumes give better velocity-space resolution but worse spatial resolution, and vice versa

Use simulation to characterize

$$f(\mathbf{v}, \mathbf{x}_d)$$

see LMW & Dubinski 1998; Moore et al. 2001 and many others

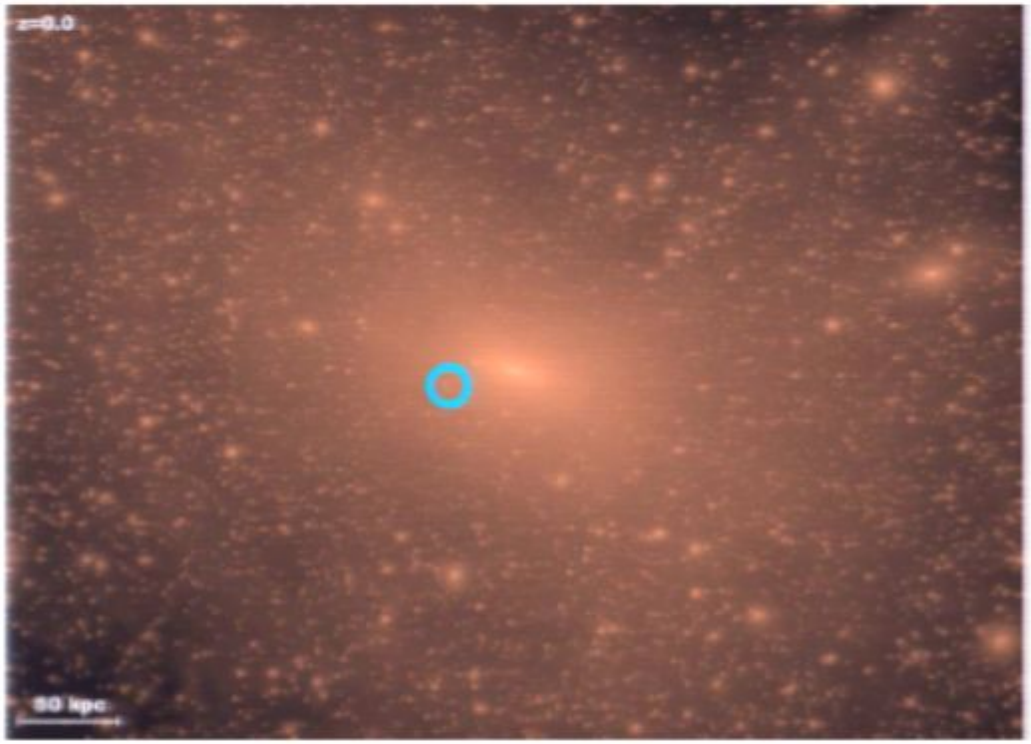

Pick a region of the simulated halo representative of the Earth. Select particles in this region and compute f(v).
From f(v), compute dR/dQ

"Uncertainty principle" for phase space:
Larger volumes give better velocity-space resolution but worse spatial resolution, and vice versa

Use simulation to characterize

$$f(\mathbf{v}, \mathbf{x}_d)$$

see LMW & Dubinski 1998; Moore et al. 2001 and many others

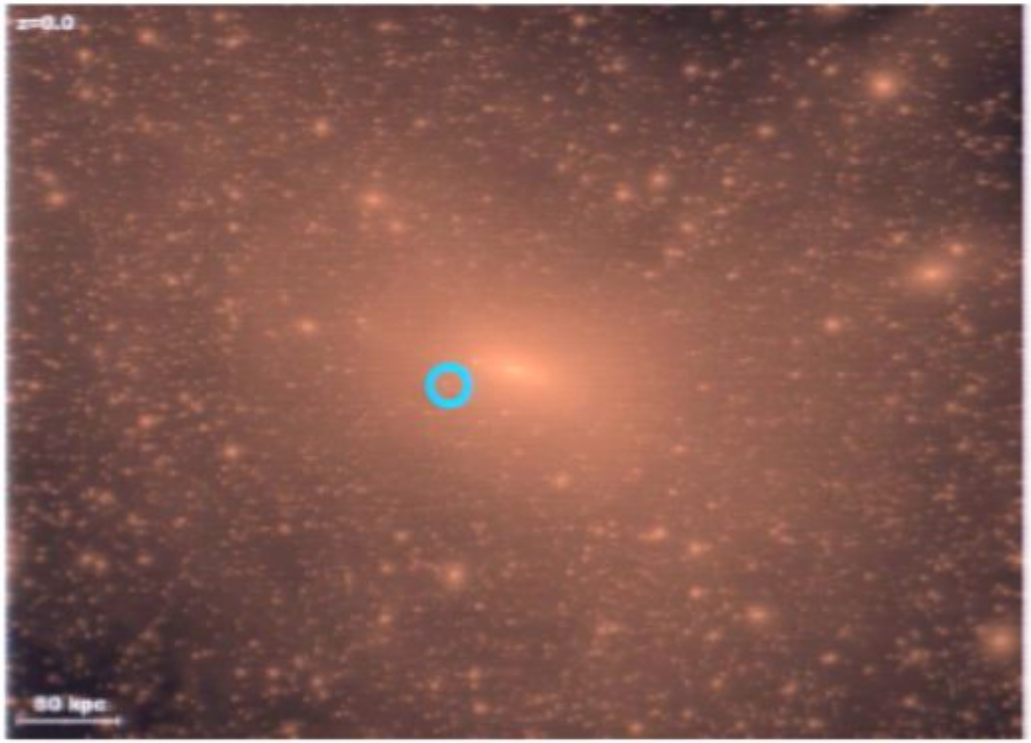

Pick a region of the simulated halo representative of the Earth. Select particles in this region and compute f(v).
From f(v), compute dR/dQ

"Uncertainty principle" for phase space:
Larger volumes give better velocity-space resolution but worse spatial resolution, and vice versa

Use simulation to characterize

$$f(\mathbf{v}, \mathbf{x}_d)$$

see LMW & Dubinski 1998; Moore et al. 2001 and many others

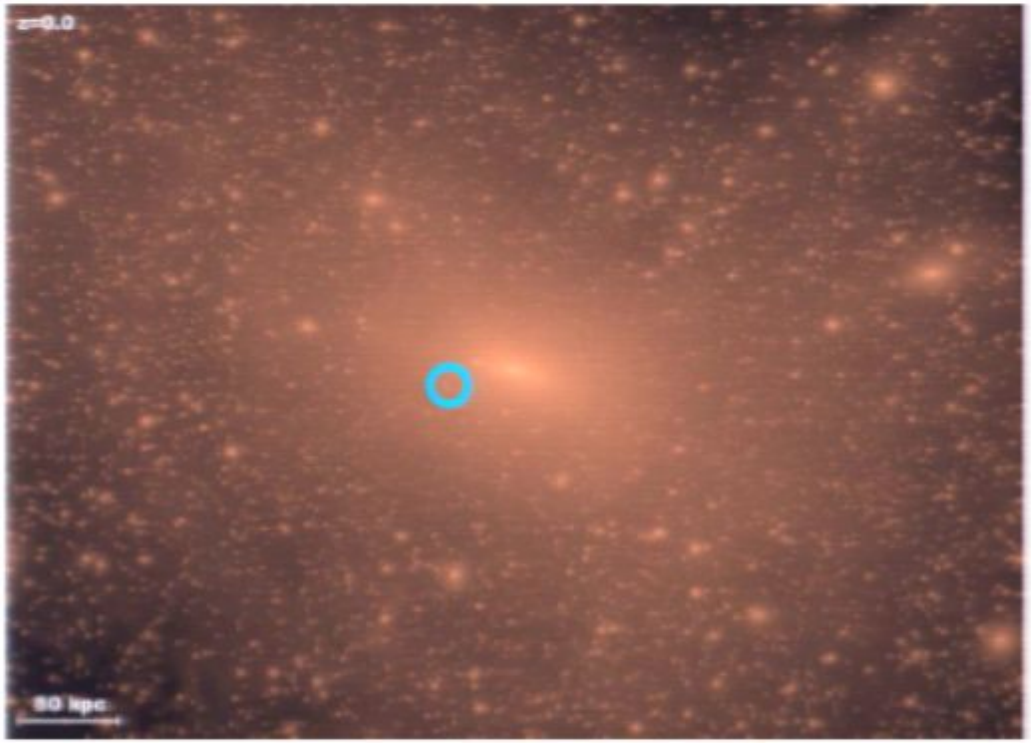

Pick a region of the simulated halo representative of the Earth. Select particles in this region and compute f(v).
From f(v), compute dR/dQ

"Uncertainty principle" for phase space:
Larger volumes give better velocity-space resolution but worse spatial resolution, and vice versa

Use simulation to characterize

$$f(\mathbf{v}, \mathbf{x}_d)$$

see LMW & Dubinski 1998; Moore et al. 2001 and many others

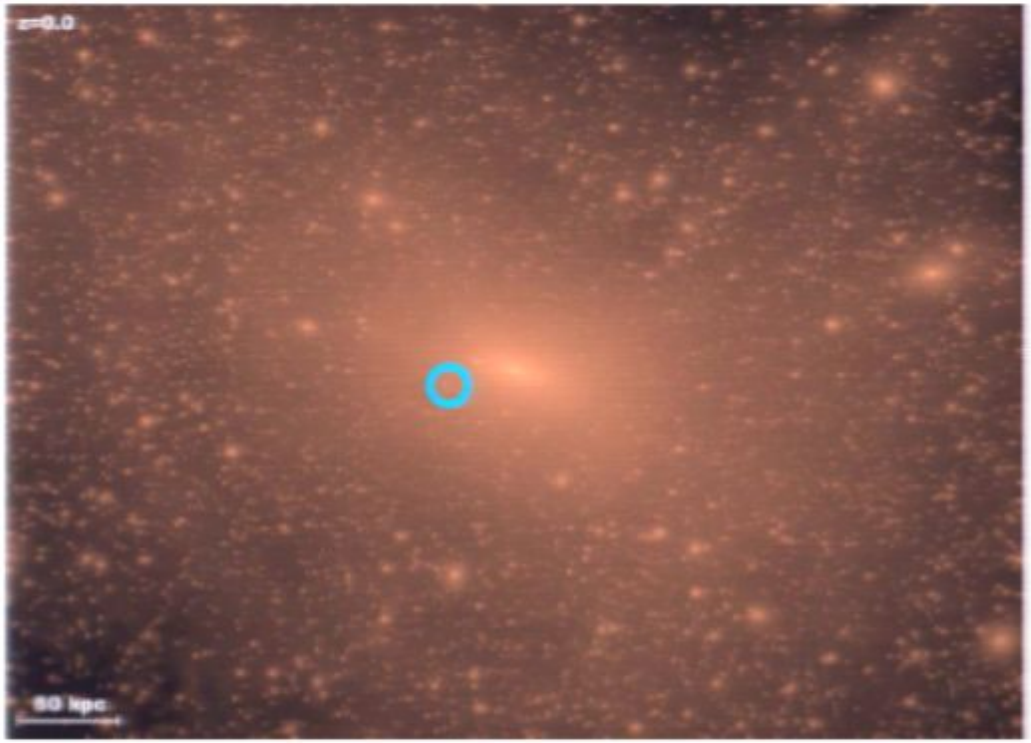

Pick a region of the simulated halo representative of the Earth. Select particles in this region and compute f(v).
From f(v), compute dR/dQ

"Uncertainty principle" for phase space:
Larger volumes give better velocity-space resolution but worse spatial resolution, and vice versa

Use simulation to characterize

$$f(\mathbf{v}, \mathbf{x}_d)$$

see LMW & Dubinski 1998; Moore et al. 2001 and many others

Pick a region of the simulated halo representative of the Earth. Select particles in this region and compute f(v).
From f(v), compute dR/dQ

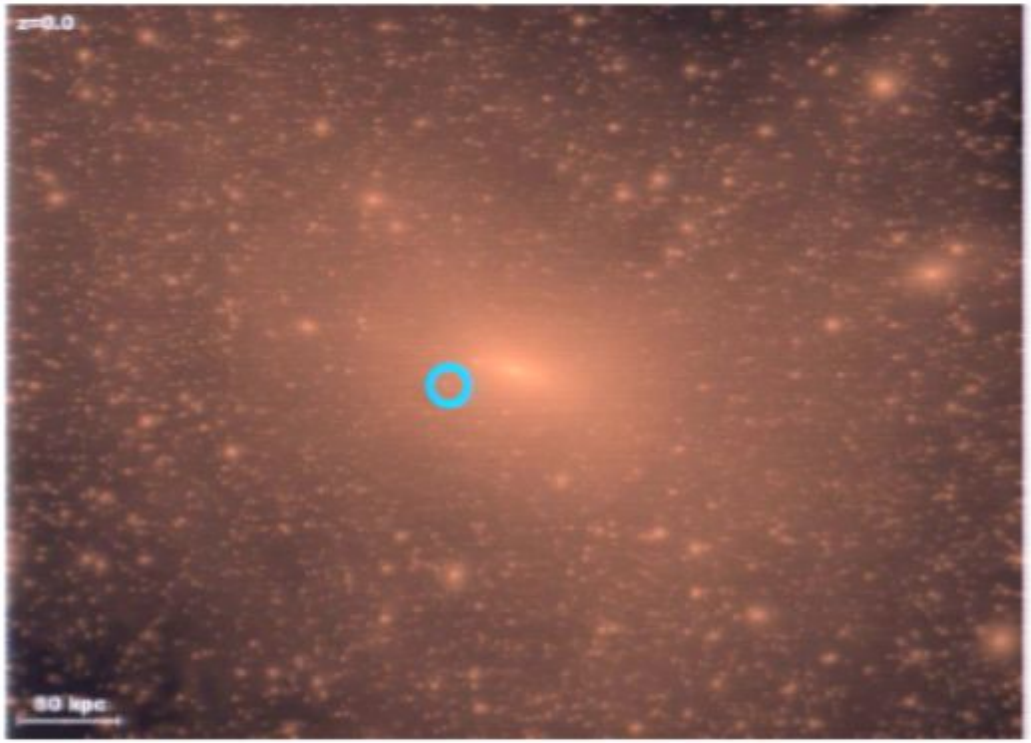

"Uncertainty principle" for phase space:
Larger volumes give better velocity-space resolution but worse spatial resolution, and vice versa

Use simulation to characterize

$$f(\mathbf{v}, \mathbf{x}_d)$$

see LMW & Dubinski 1998; Moore et al. 2001 and many others

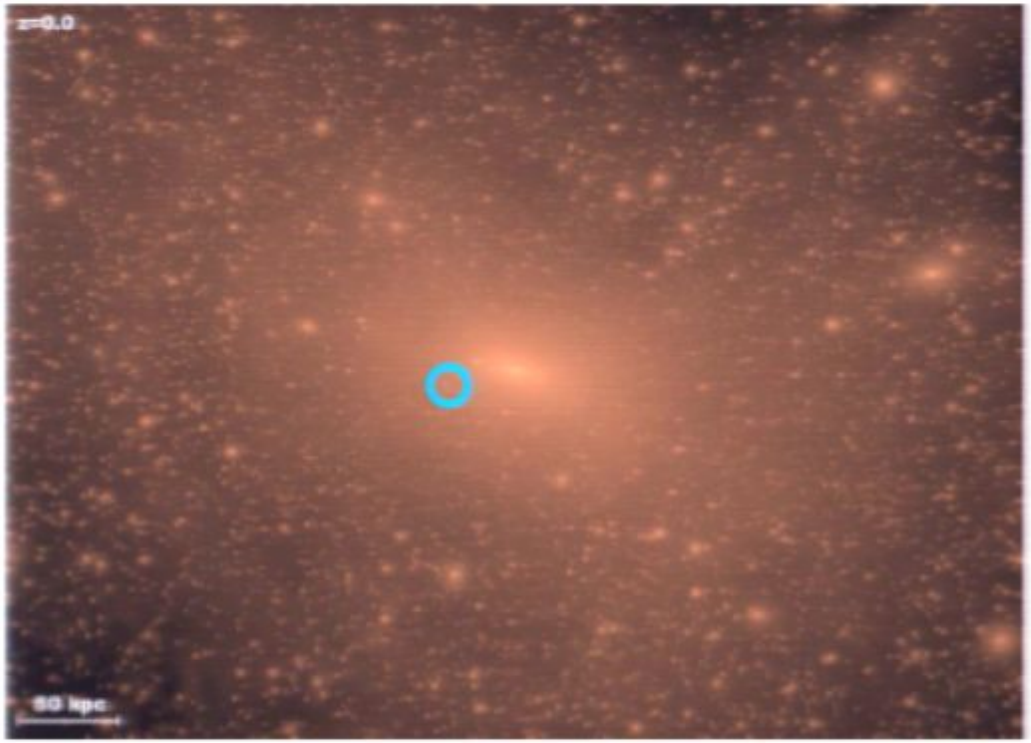

Pick a region of the simulated halo representative of the Earth. Select particles in this region and compute f(v).
From f(v), compute dR/dQ

"Uncertainty principle" for phase space:
Larger volumes give better velocity-space resolution but worse spatial resolution, and vice versa

Use simulation to characterize

$$f(\mathbf{v}, \mathbf{x}_d)$$

see LMW & Dubinski 1998; Moore et al. 2001 and many others

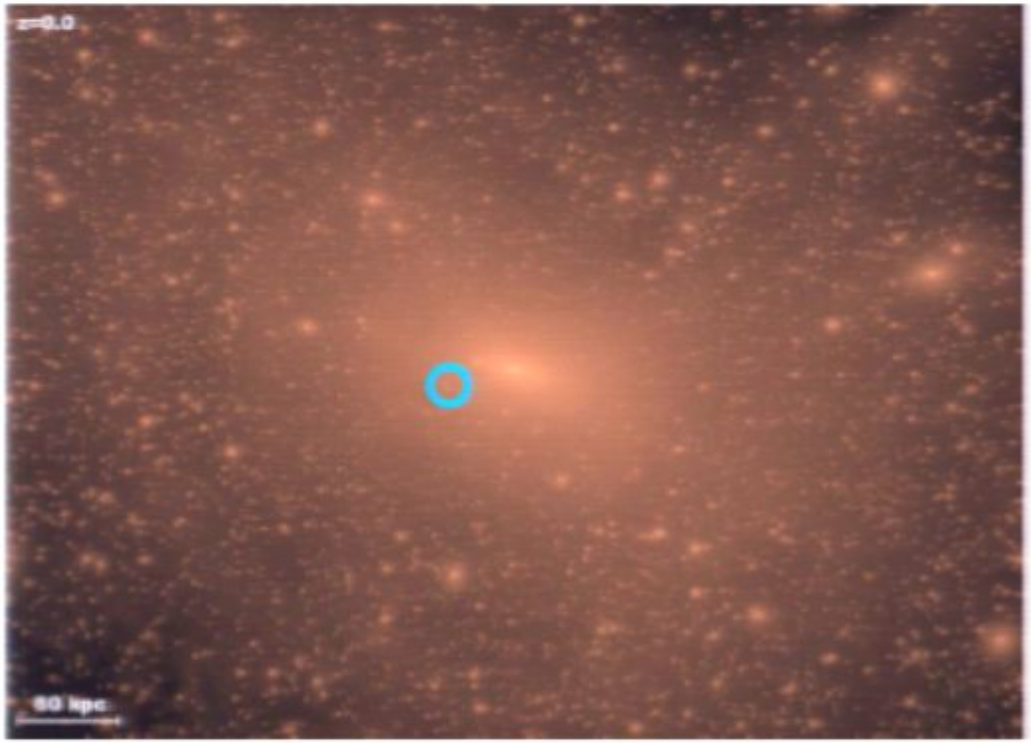

Pick a region of the simulated halo representative of the Earth. Select particles in this region and compute f(v).
From f(v), compute dR/dQ

"Uncertainty principle" for phase space:
Larger volumes give better velocity-space resolution but worse spatial resolution, and vice versa

Use simulation to characterize

$$f(\mathbf{v}, \mathbf{x}_d)$$

see LMW & Dubinski 1998; Moore et al. 2001 and many others

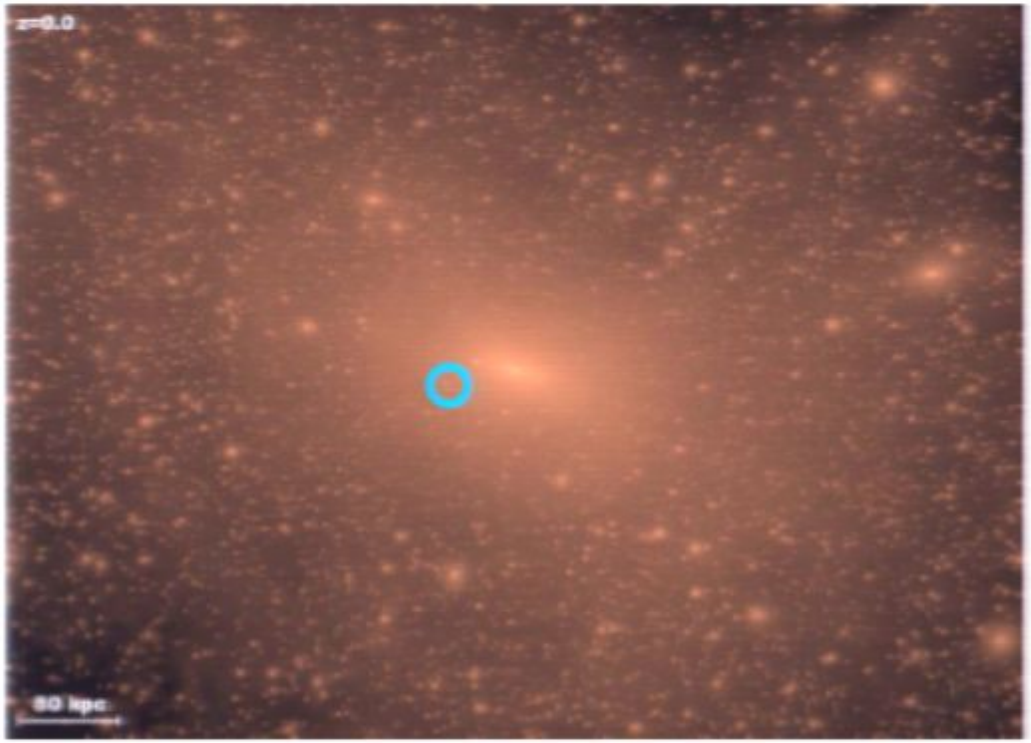

Pick a region of the simulated halo representative of the Earth. Select particles in this region and compute f(v).
From f(v), compute dR/dQ

"Uncertainty principle" for phase space:
Larger volumes give better velocity-space resolution but worse spatial resolution, and vice versa

Use simulation to characterize

$$f(\mathbf{v}, \mathbf{x}_d)$$

see LMW & Dubinski 1998; Moore et al. 2001 and many others

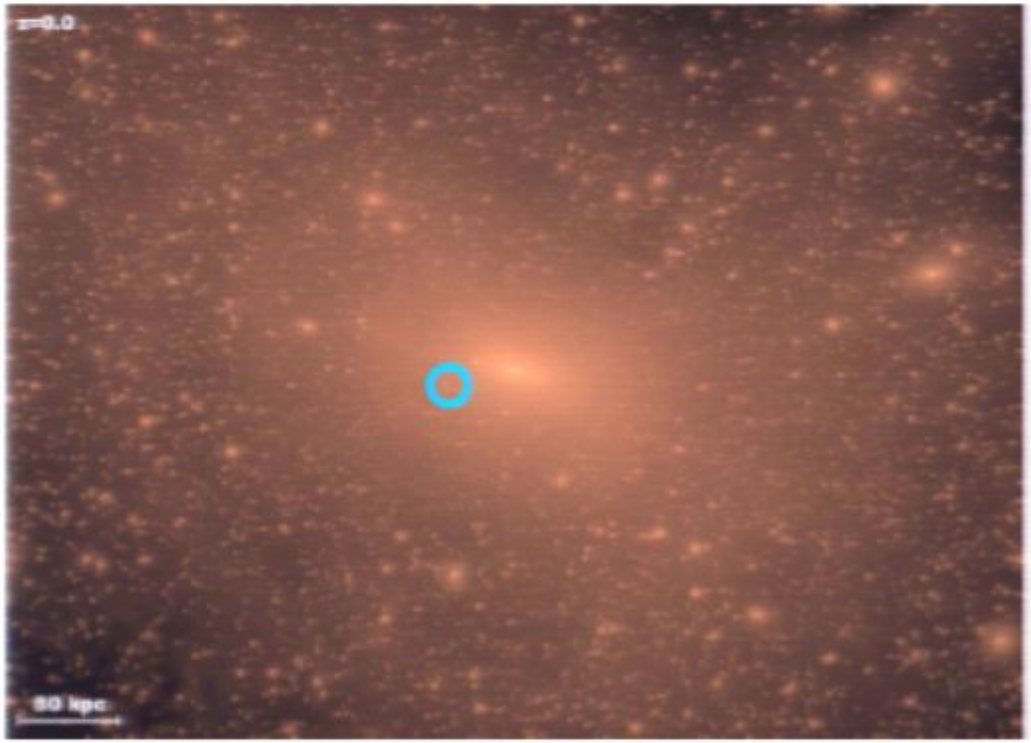

Pick a region of the simulated halo representative of the Earth. Select particles in this region and compute f(v).
From f(v), compute dR/dQ

"Uncertainty principle" for phase space:
Larger volumes give better velocity-space resolution but worse spatial resolution, and vice versa

Use simulation to characterize

$$f(\mathbf{v}, \mathbf{x}_d)$$

see LMW & Dubinski 1998; Moore et al. 2001 and many others

Pick a region of the simulated halo representative of the Earth. Select particles in this region and compute f(v).
From f(v), compute dR/dQ

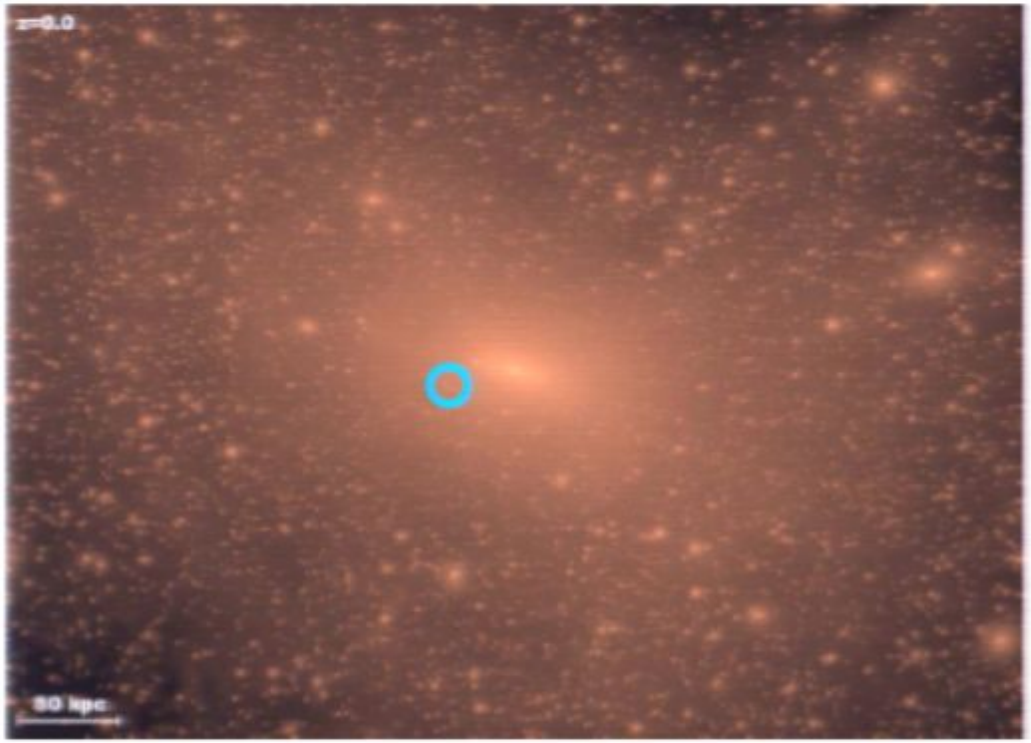

"Uncertainty principle" for phase space:
Larger volumes give better velocity-space resolution but worse spatial resolution, and vice versa

Use simulation to characterize

$$f(\mathbf{v}, \mathbf{x}_d)$$

see LMW & Dubinski 1998; Moore et al. 2001 and many others

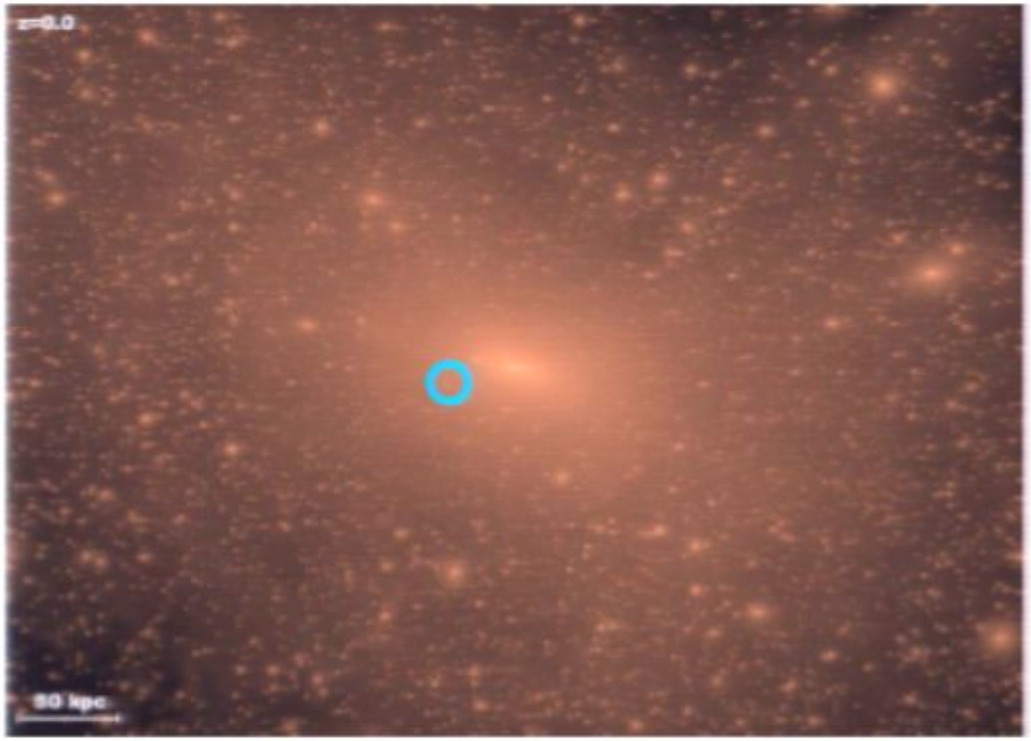

Pick a region of the simulated halo representative of the Earth. Select particles in this region and compute f(v).
From f(v), compute dR/dQ

"Uncertainty principle" for phase space:
Larger volumes give better velocity-space resolution but worse spatial resolution, and vice versa

Stiff & LMW (PRL, 2003)

Follow the formation of a halo using a simulation.

At the final frame, select a position representative of the dark matter detector.

At that position, lay down test particles that cover the full velocity space.

Evolve the full system, including the test particles,
backward in time to the initial epoch.

Test particles at the initial epoch with zero velocity map out region of velocity space in the final frame where the dark matter DF is non-zero.

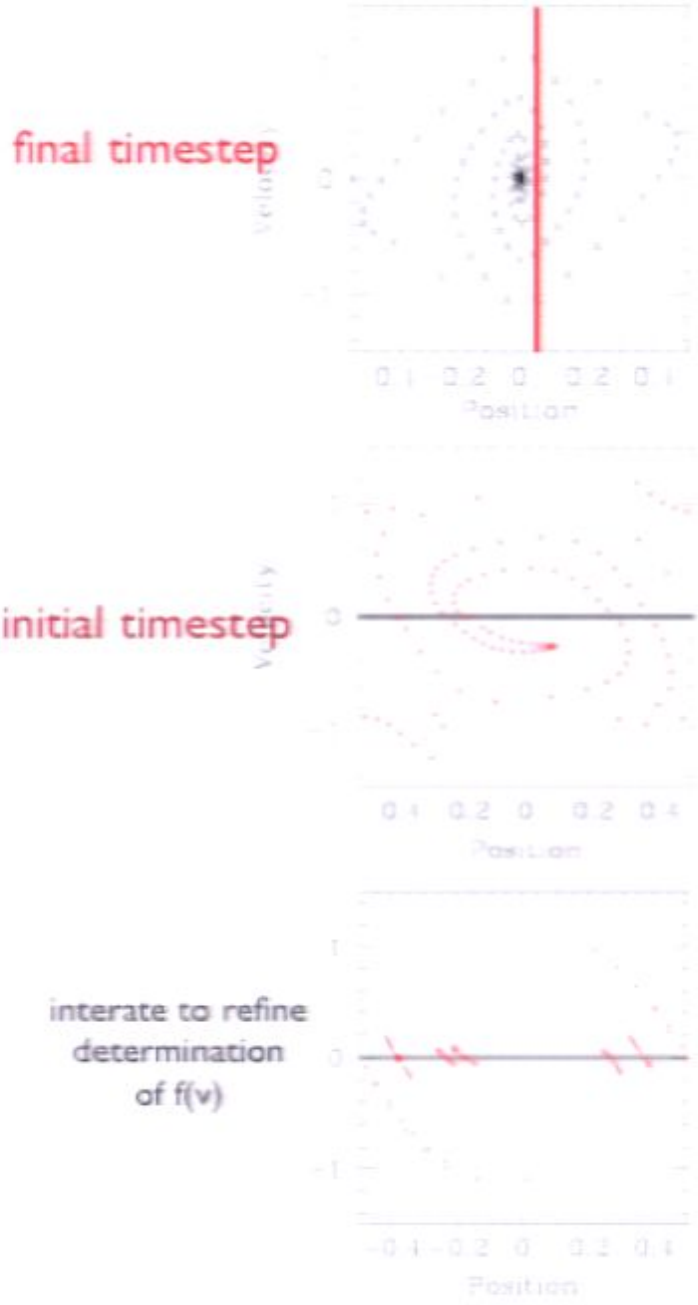

Stiff & LMW (PRL, 2003)

Follow the formation of a halo using a simulation.

At the final frame, select a position representative of the dark matter detector.

At that position, lay down test particles that cover the full velocity space.

Evolve the full system, including the test particles,
backward in time to the initial epoch.

Test particles at the initial epoch with zero velocity map out region of velocity space in the final frame where the dark matter DF is non-zero.

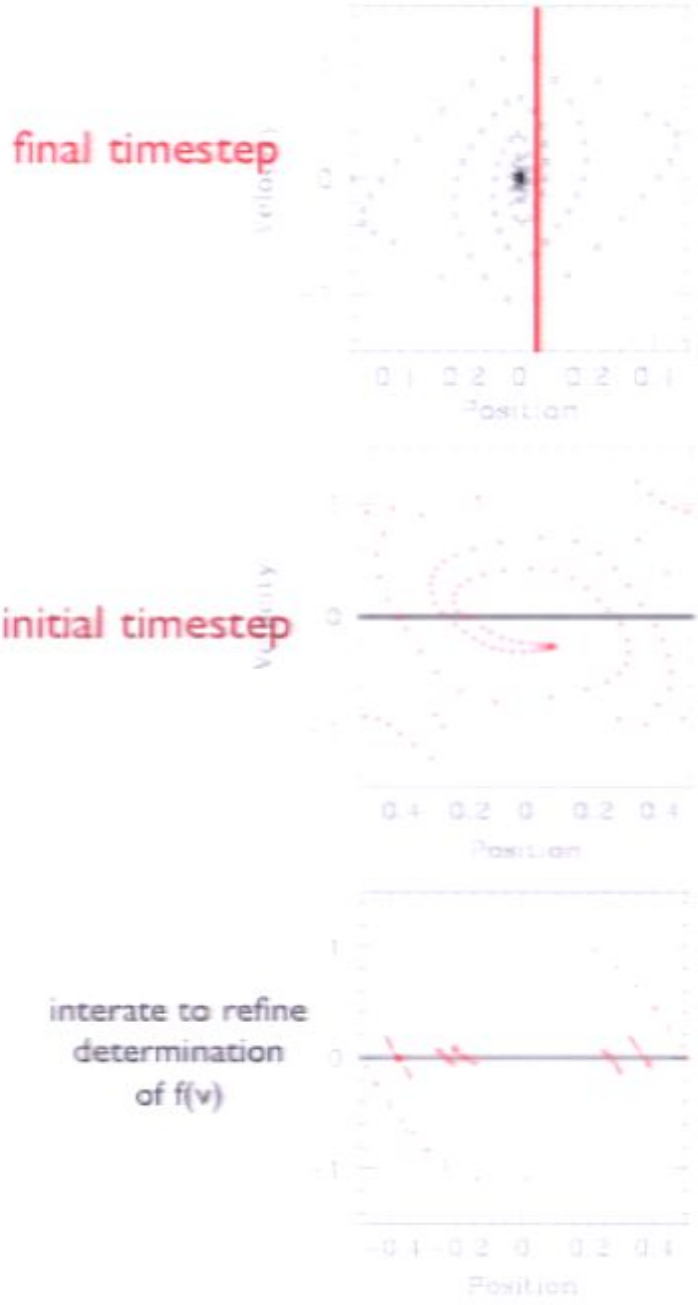

Stiff & LMW (PRL, 2003)

Follow the formation of a halo using a simulation.

At the final frame, select a position representative of the dark matter detector.

At that position, lay down test particles that cover the full velocity space.

Evolve the full system, including the test particles,
backward in time to the initial epoch.

Test particles at the initial epoch with zero velocity map out region of velocity space in the final frame where the dark matter DF is non-zero.

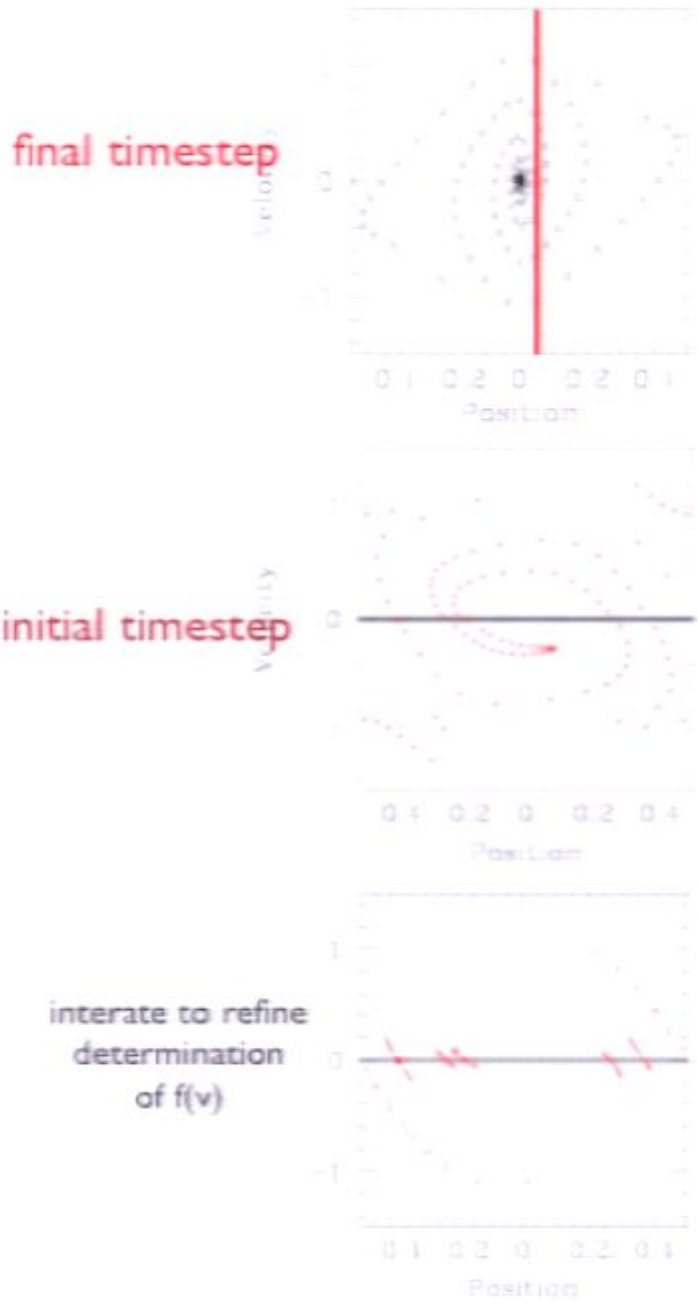

Stiff & LMW (PRL, 2003)

Follow the formation of a halo using a simulation.

At the final frame, select a position representative of the dark matter detector.

At that position, lay down test particles that cover the full velocity space.

Evolve the full system, including the test particles,
backward in time to the initial epoch.

Test particles at the initial epoch with zero velocity map out region of velocity space in the final frame where the dark matter DF is non-zero.

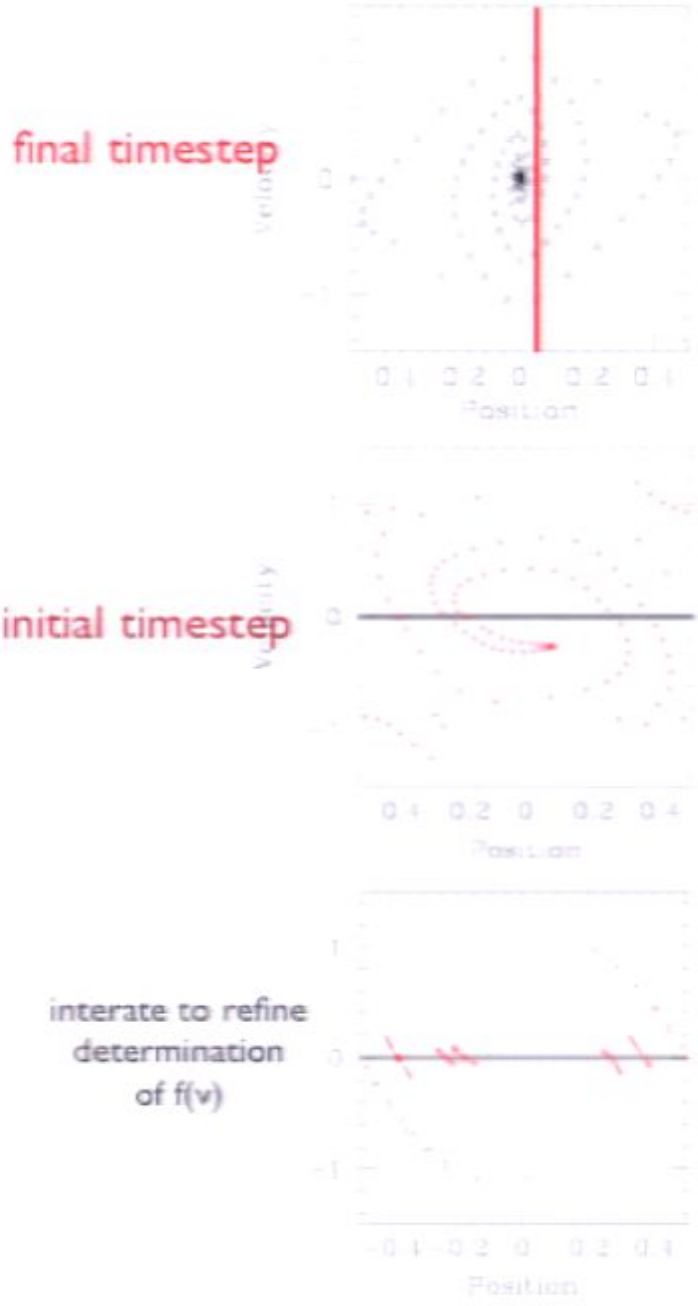

Stiff & LMW (PRL, 2003)

Follow the formation of a halo using a simulation.

At the final frame, select a position representative of the dark matter detector.

At that position, lay down test particles that cover the full velocity space.

Evolve the full system, including the test particles,
backward in time to the initial epoch.

Test particles at the initial epoch with zero velocity map out region of velocity space in the final frame where the dark matter DF is non-zero.

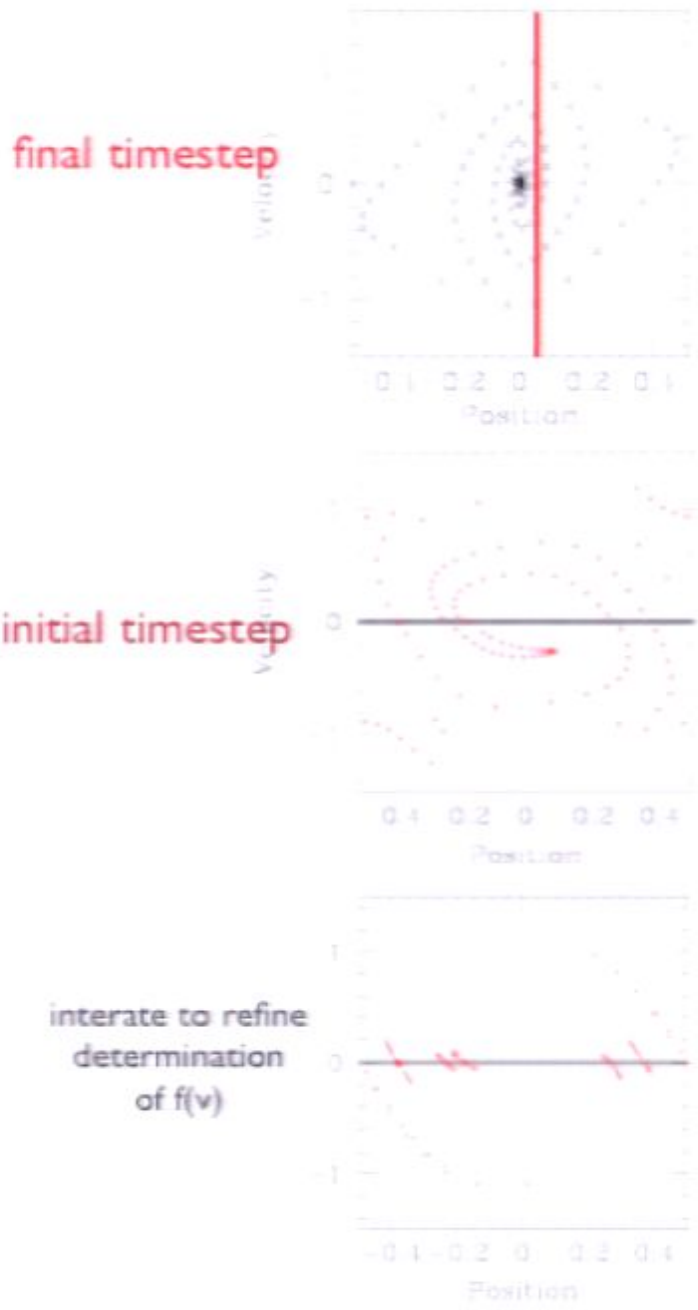

Stiff & LMW (PRL, 2003)

Follow the formation of a halo using a simulation.

At the final frame, select a position representative of the dark matter detector.

At that position, lay down test particles that cover the full velocity space.

Evolve the full system, including the test particles,
backward in time to the initial epoch.

Test particles at the initial epoch with zero velocity map out region of velocity space in the final frame where the dark matter DF is non-zero.

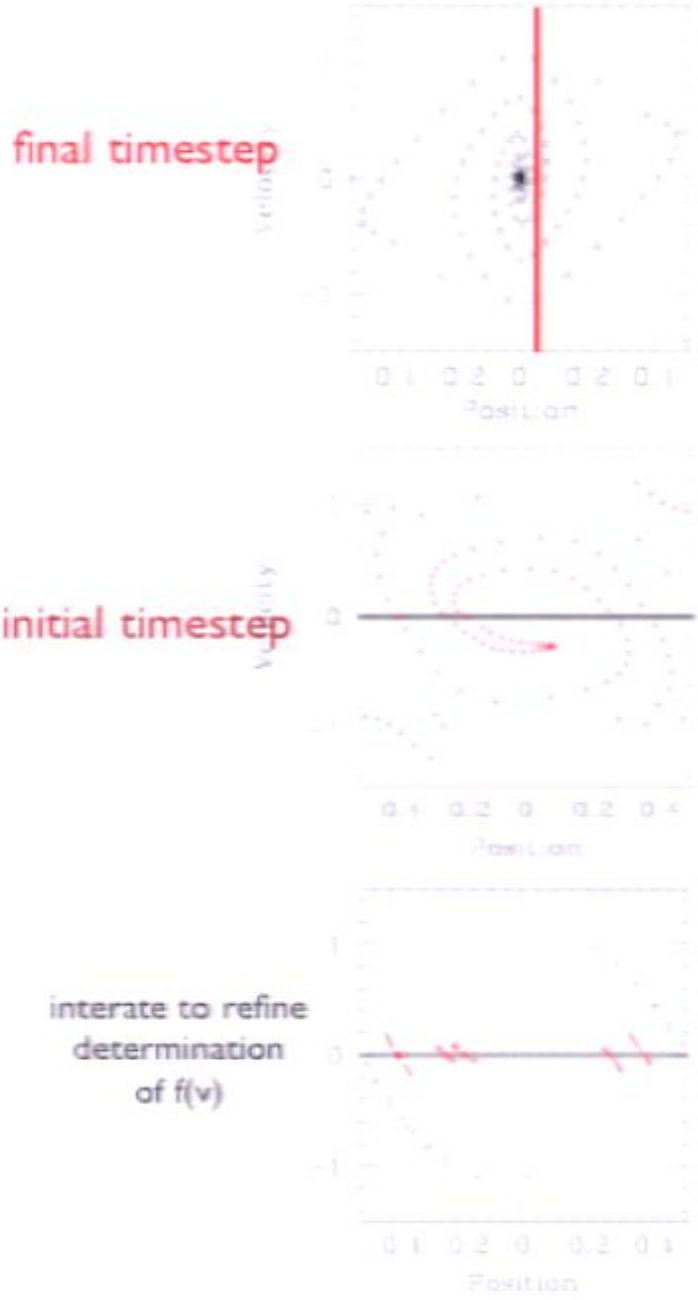

Stiff & LMW (PRL, 2003)

Follow the formation of a halo using a simulation.

At the final frame, select a position representative of the dark matter detector.

At that position, lay down test particles that cover the full velocity space.

Evolve the full system, including the test particles,
backward in time to the initial epoch.

Test particles at the initial epoch with zero velocity map out region of velocity space in the final frame where the dark matter DF is non-zero.

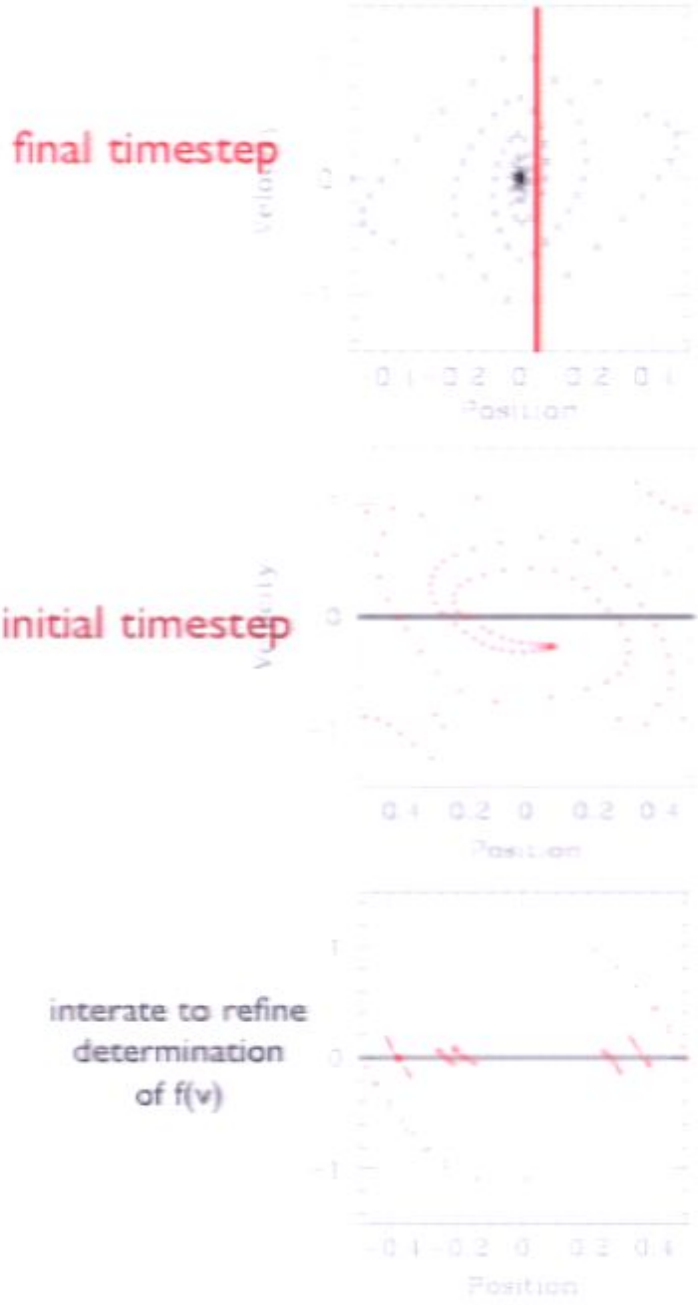

Stiff & LMW (PRL, 2003)

Follow the formation of a halo using a simulation.

At the final frame, select a position representative of the dark matter detector.

At that position, lay down test particles that cover the full velocity space.

Evolve the full system, including the test particles,
backward in time to the initial epoch.

Test particles at the initial epoch with zero velocity map out region of velocity space in the final frame where the dark matter DF is non-zero.

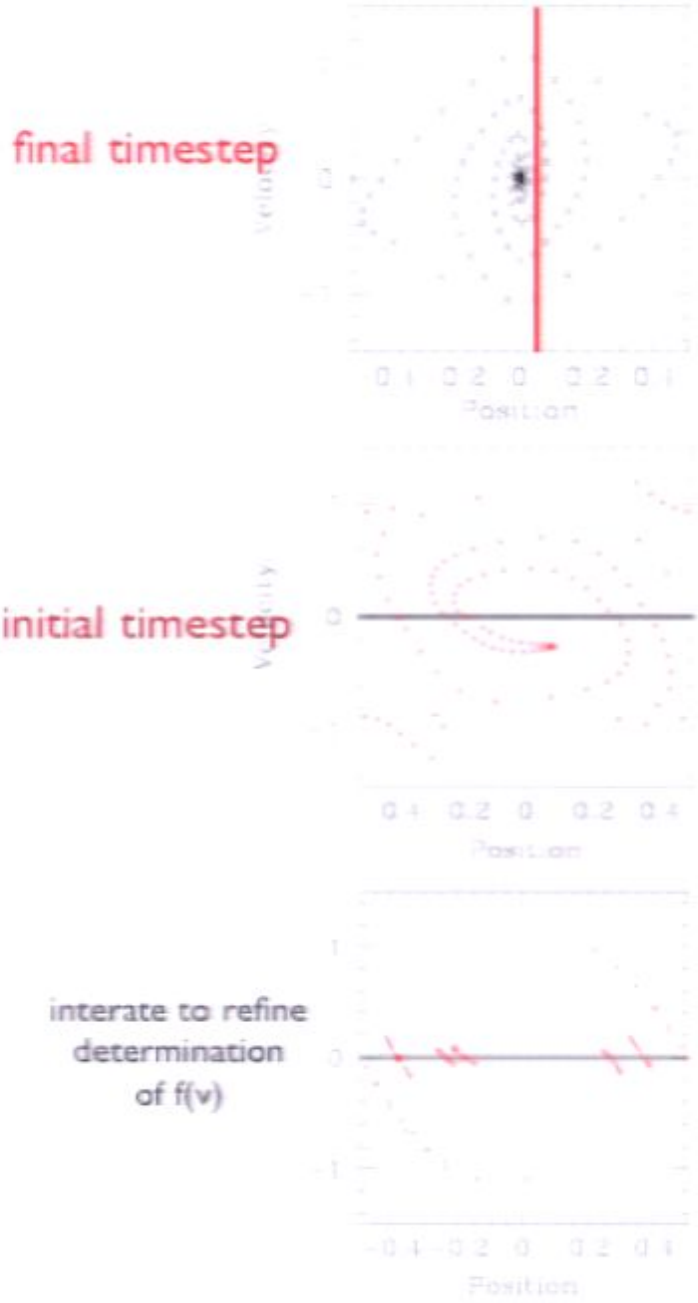

Stiff & LMW (PRL, 2003)

Follow the formation of a halo using a simulation.

At the final frame, select a position representative of the dark matter detector.

At that position, lay down test particles that cover the full velocity space.

Evolve the full system, including the test particles,
backward in time to the initial epoch.

Test particles at the initial epoch with zero velocity map out region of velocity space in the final frame where the dark matter DF is non-zero.

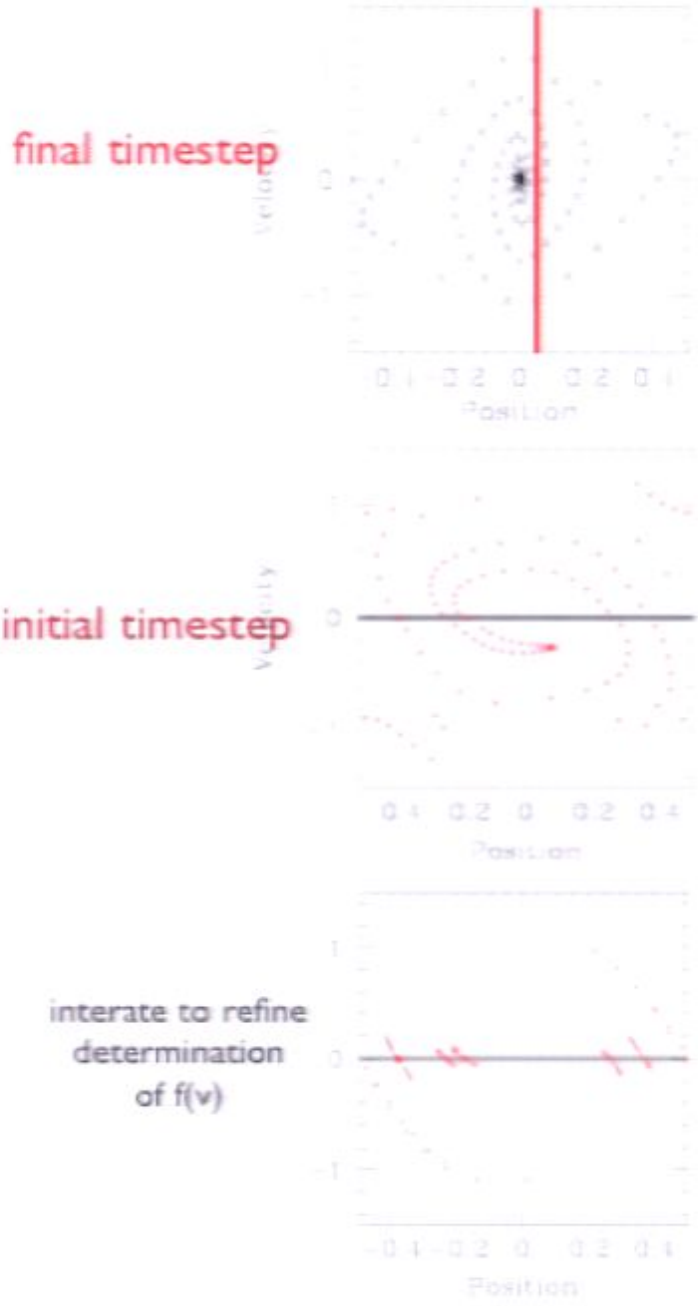

Stiff & LMW (PRL, 2003)

Follow the formation of a halo using a simulation.

At the final frame, select a position representative of the dark matter detector.

At that position, lay down test particles that cover the full velocity space.

Evolve the full system, including the test particles,
backward in time to the initial epoch.

Test particles at the initial epoch with zero velocity map out region of velocity space in the final frame where the dark matter DF is non-zero.

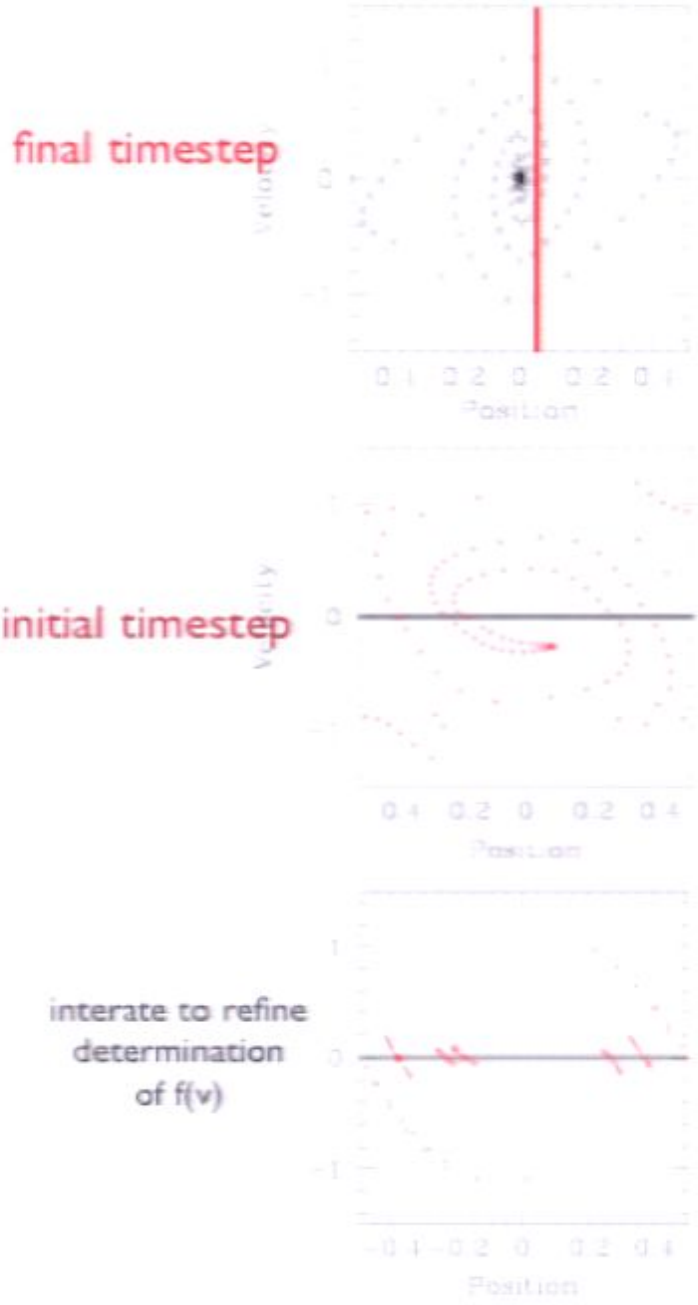

Stiff & LMW (PRL, 2003)

Follow the formation of a halo using a simulation.

At the final frame, select a position representative of the dark matter detector.

At that position, lay down test particles that cover the full velocity space.

Evolve the full system, including the test particles,
backward in time to the initial epoch.

Test particles at the initial epoch with zero velocity map out region of velocity space in the final frame where the dark matter DF is non-zero.

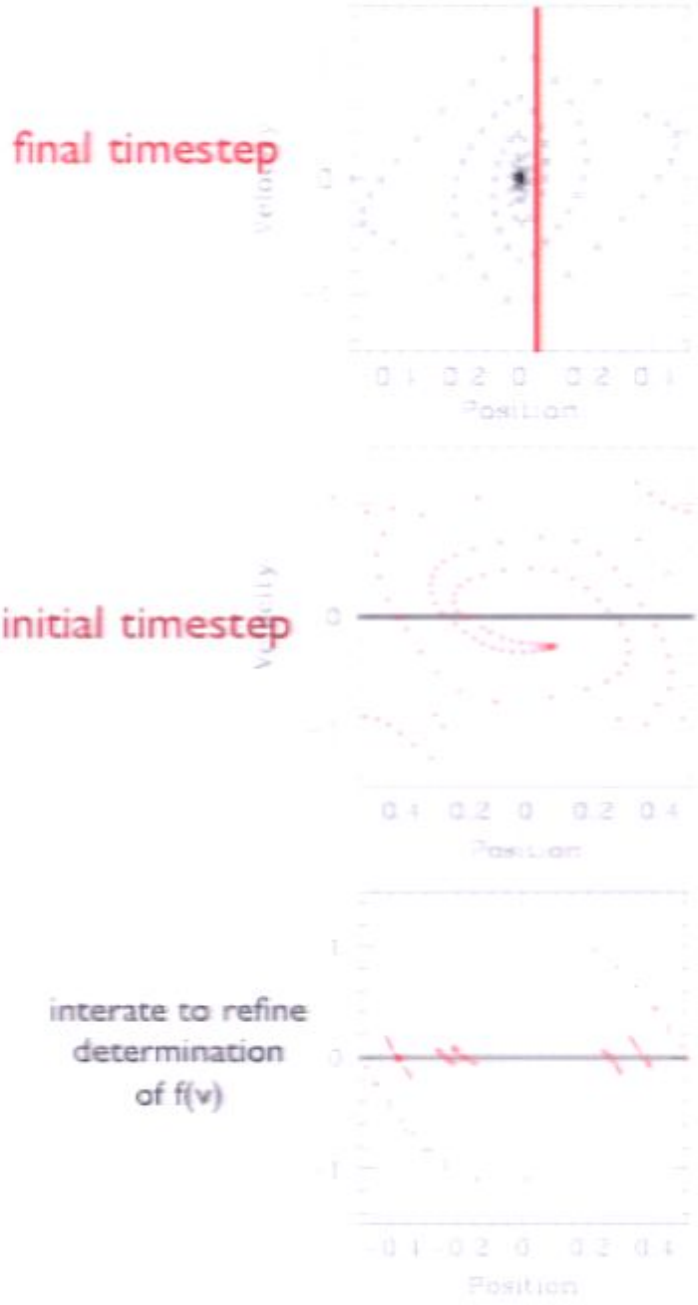

Stiff & LMW (PRL, 2003)

Follow the formation of a halo using a simulation.

At the final frame, select a position representative of the dark matter detector.

At that position, lay down test particles that cover the full velocity space.

Evolve the full system, including the test particles,
backward in time to the initial epoch.

Test particles at the initial epoch with zero velocity map out region of velocity space in the final frame where the dark matter DF is non-zero.

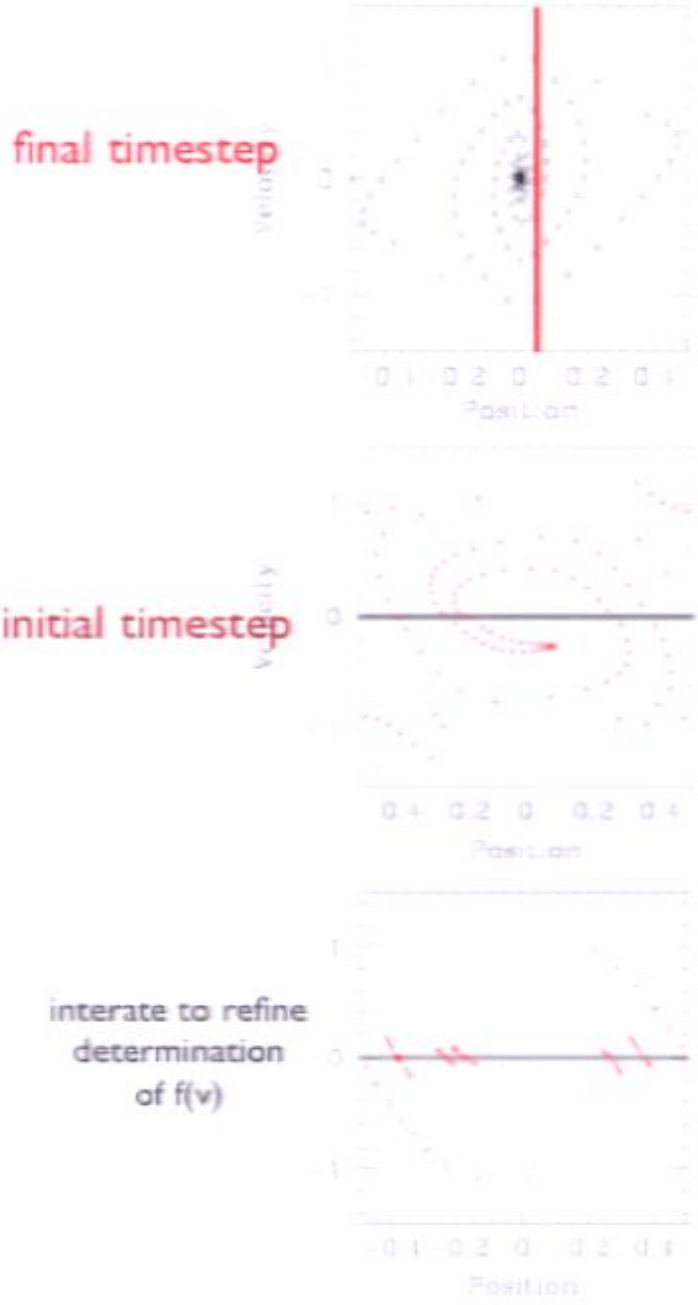

Stiff & LMW (PRL, 2003)

Follow the formation of a halo using a simulation.

At the final frame, select a position representative of the dark matter detector.

At that position, lay down test particles that cover the full velocity space.

Evolve the full system, including the test particles,
backward in time to the initial epoch.

Test particles at the initial epoch with zero velocity map out region of velocity space in the final frame where the dark matter DF is non-zero.

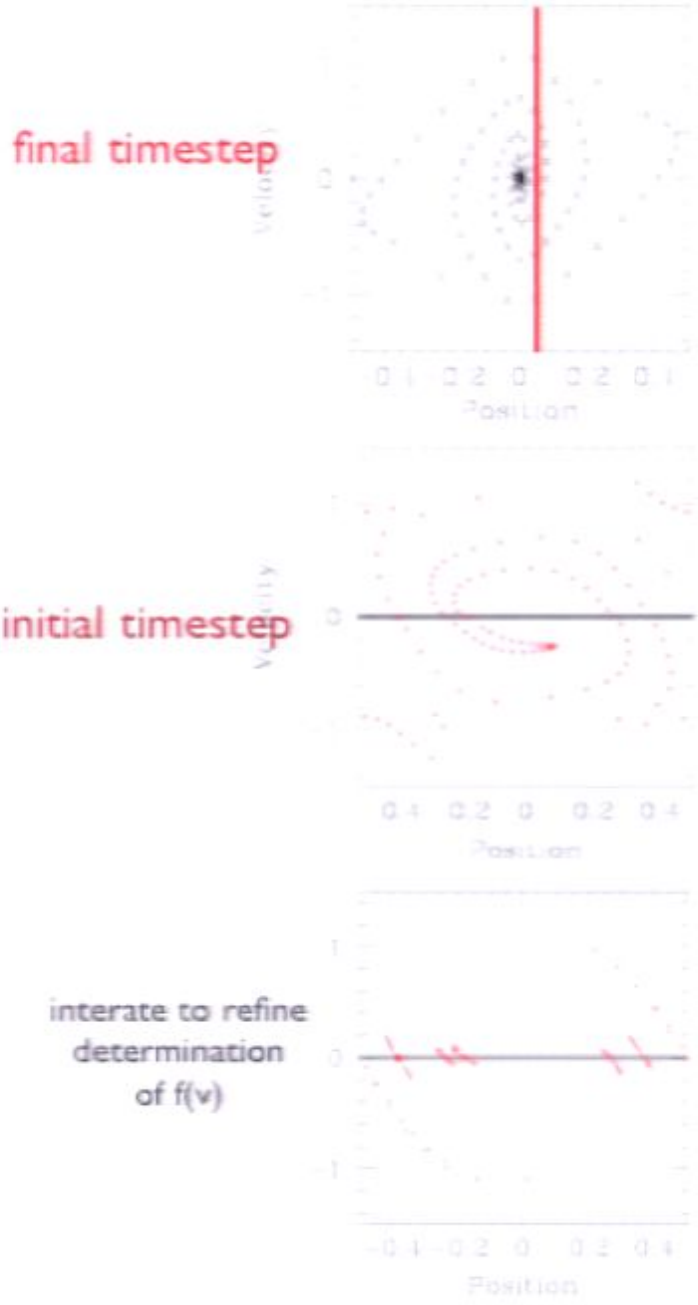

Stiff & LMW (PRL, 2003)

Follow the formation of a halo using a simulation.

At the final frame, select a position representative of the dark matter detector.

At that position, lay down test particles that cover the full velocity space.

Evolve the full system, including the test particles,
backward in time to the initial epoch.

Test particles at the initial epoch with zero velocity map out region of velocity space in the final frame where the dark matter DF is non-zero.

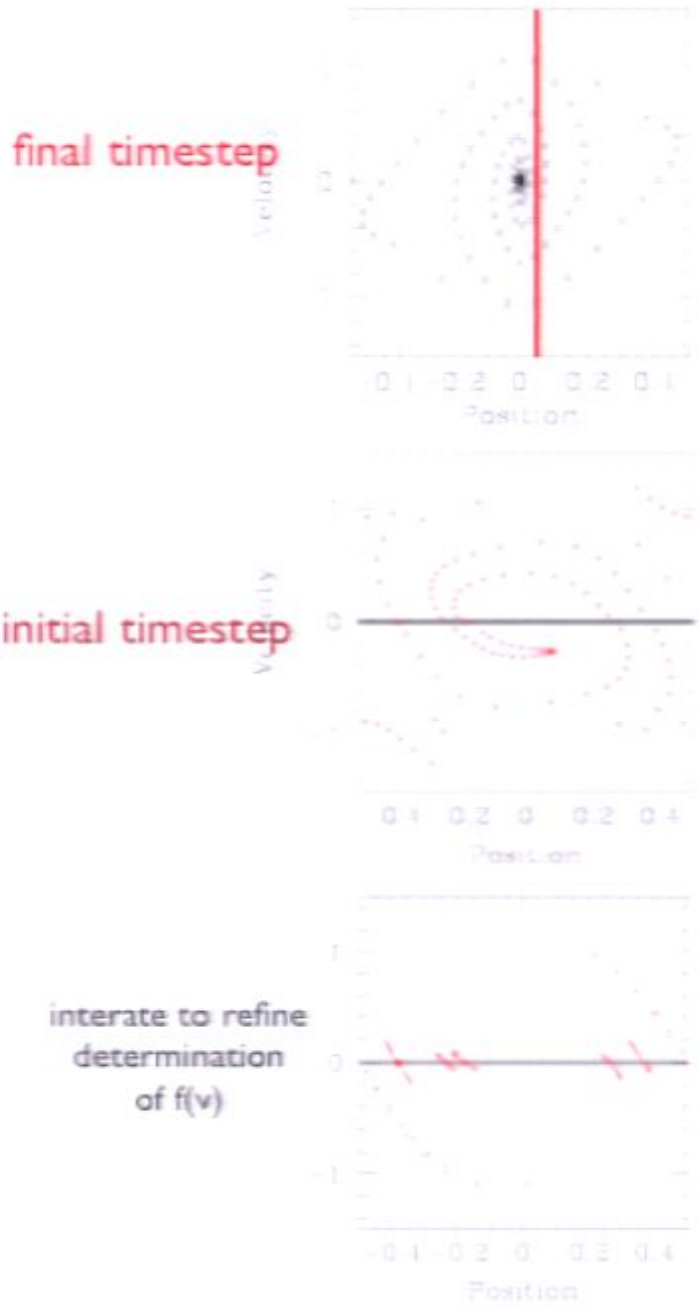

Stiff & LMW (PRL, 2003)

Follow the formation of a halo using a simulation.

At the final frame, select a position representative of the dark matter detector.

At that position, lay down test particles that cover the full velocity space.

Evolve the full system, including the test particles,
backward in time to the initial epoch.

Test particles at the initial epoch with zero velocity map out region of velocity space in the final frame where the dark matter DF is non-zero.

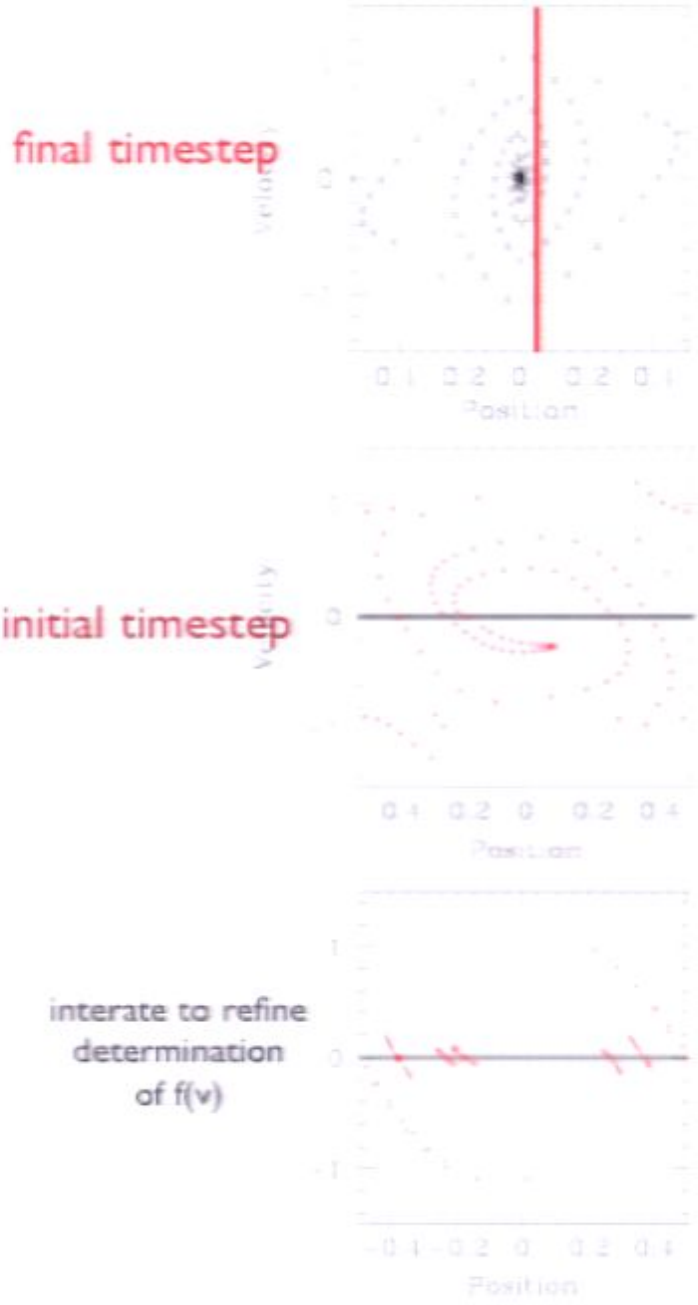

Stiff & LMW (PRL, 2003)

Follow the formation of a halo using a simulation.

At the final frame, select a position representative of the dark matter detector.

At that position, lay down test particles that cover the full velocity space.

Evolve the full system, including the test particles,
backward in time to the initial epoch.

Test particles at the initial epoch with zero velocity map out region of velocity space in the final frame where the dark matter DF is non-zero.

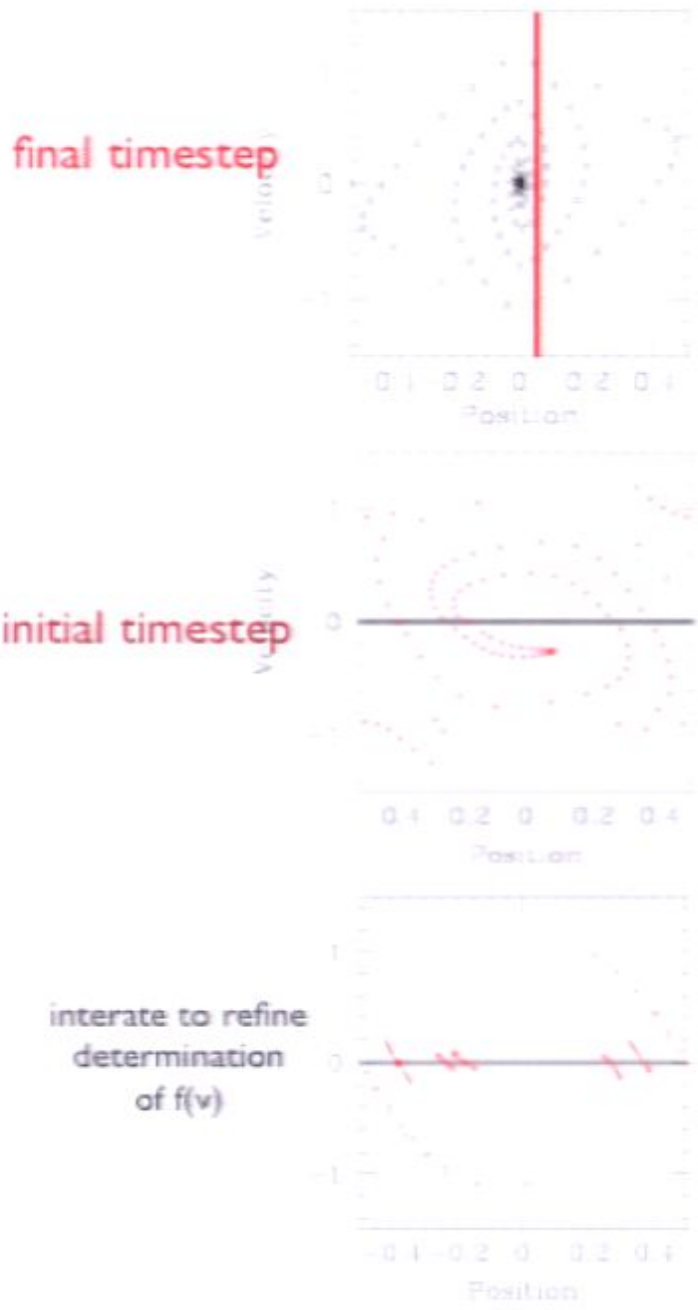

Stiff & LMW (PRL, 2003)

Follow the formation of a halo using a simulation.

At the final frame, select a position representative of the dark matter detector.

At that position, lay down test particles that cover the full velocity space.

Evolve the full system, including the test particles,
backward in time to the initial epoch.

Test particles at the initial epoch with zero velocity map out region of velocity space in the final frame where the dark matter DF is non-zero.

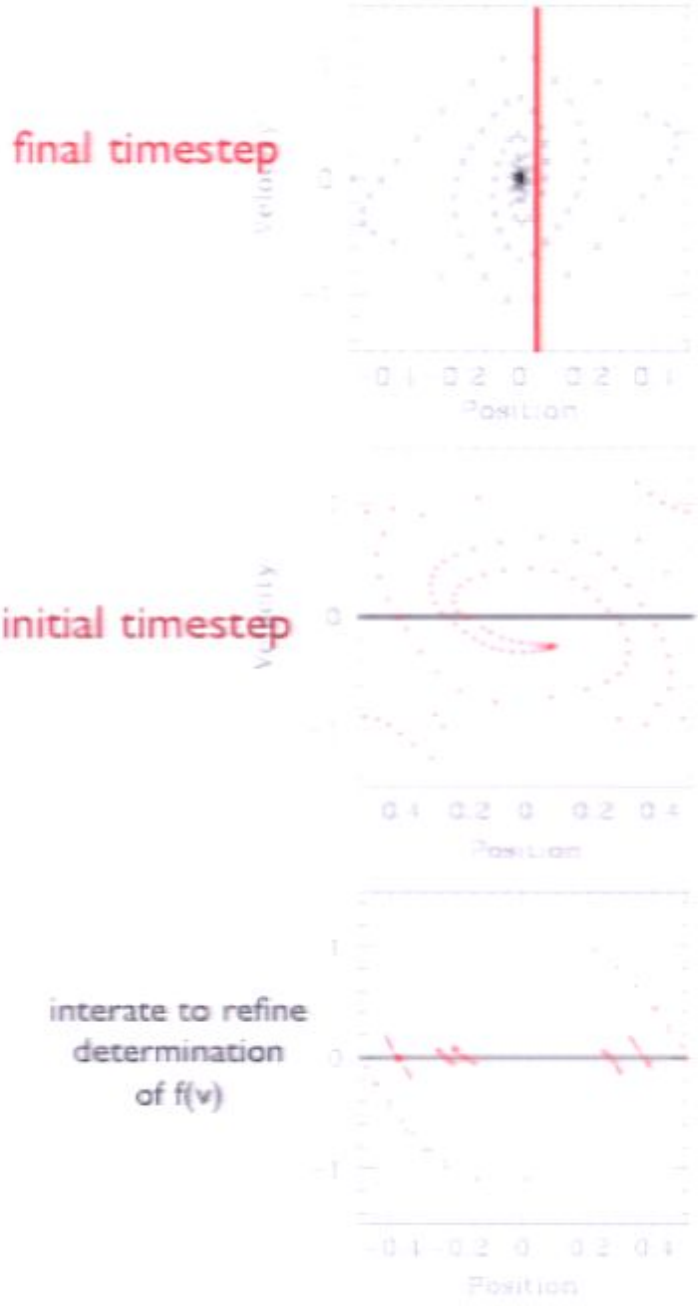

Stiff & LMW (PRL, 2003)

Follow the formation of a halo using a simulation.

At the final frame, select a position representative of the dark matter detector.

At that position, lay down test particles that cover the full velocity space.

Evolve the full system, including the test particles,
backward in time to the initial epoch.

Test particles at the initial epoch with zero velocity map out region of velocity space in the final frame where the dark matter DF is non-zero.

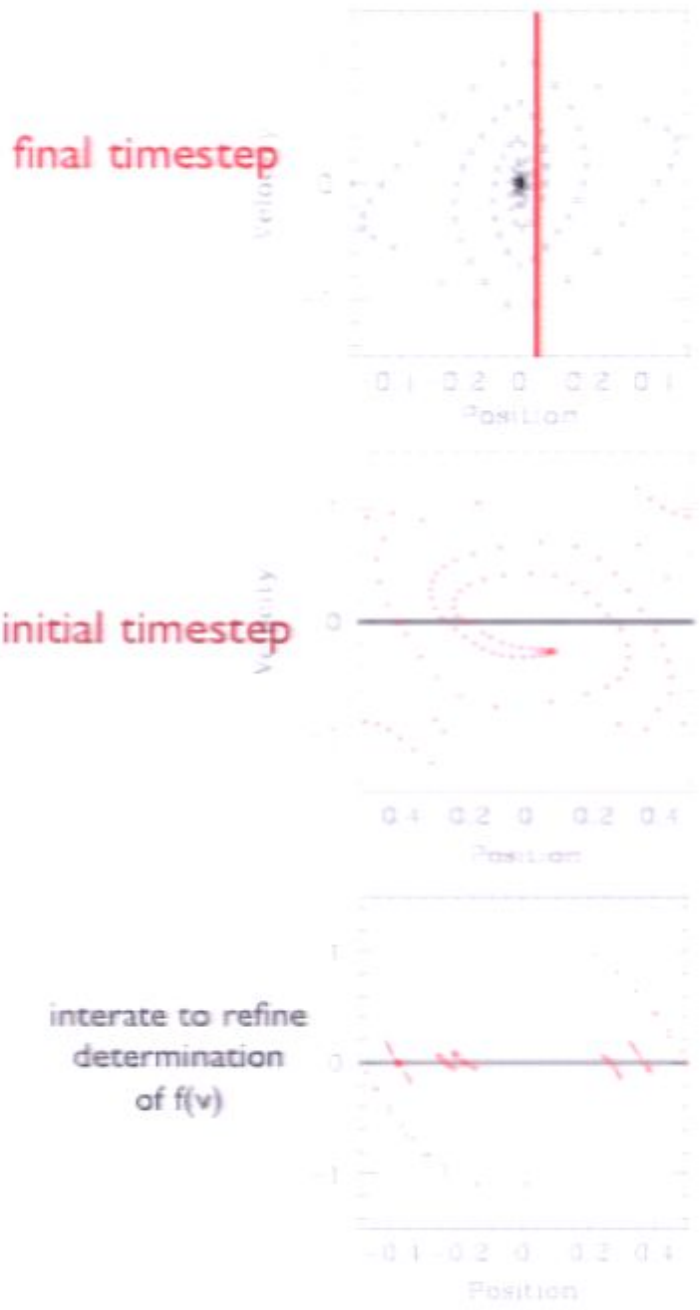

Stiff & LMW (PRL, 2003)

Follow the formation of a halo using a simulation.

At the final frame, select a position representative of the dark matter detector.

At that position, lay down test particles that cover the full velocity space.

Evolve the full system, including the test particles,
backward in time to the initial epoch.

Test particles at the initial epoch with zero velocity map out region of velocity space in the final frame where the dark matter DF is non-zero.

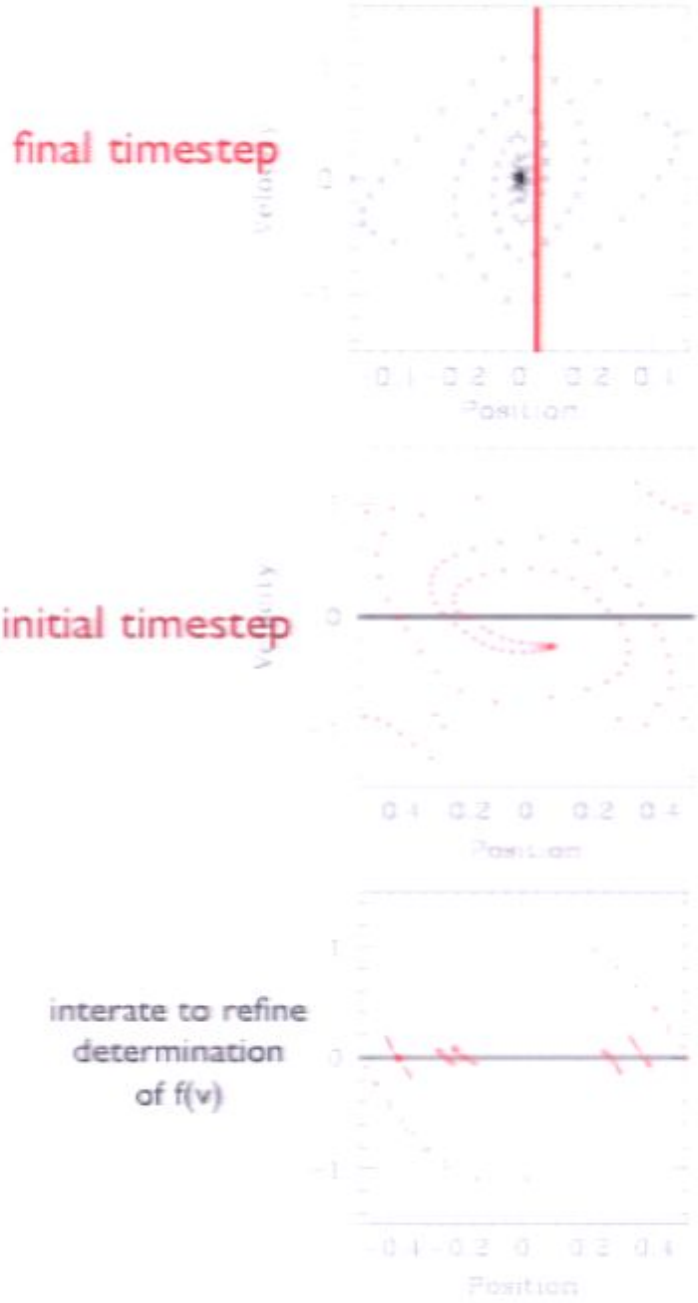

Stiff & LMW (PRL, 2003)

Follow the formation of a halo using a simulation.

At the final frame, select a position representative of the dark matter detector.

At that position, lay down test particles that cover the full velocity space.

Evolve the full system, including the test particles,
backward in time to the initial epoch.

Test particles at the initial epoch with zero velocity map out region of velocity space in the final frame where the dark matter DF is non-zero.

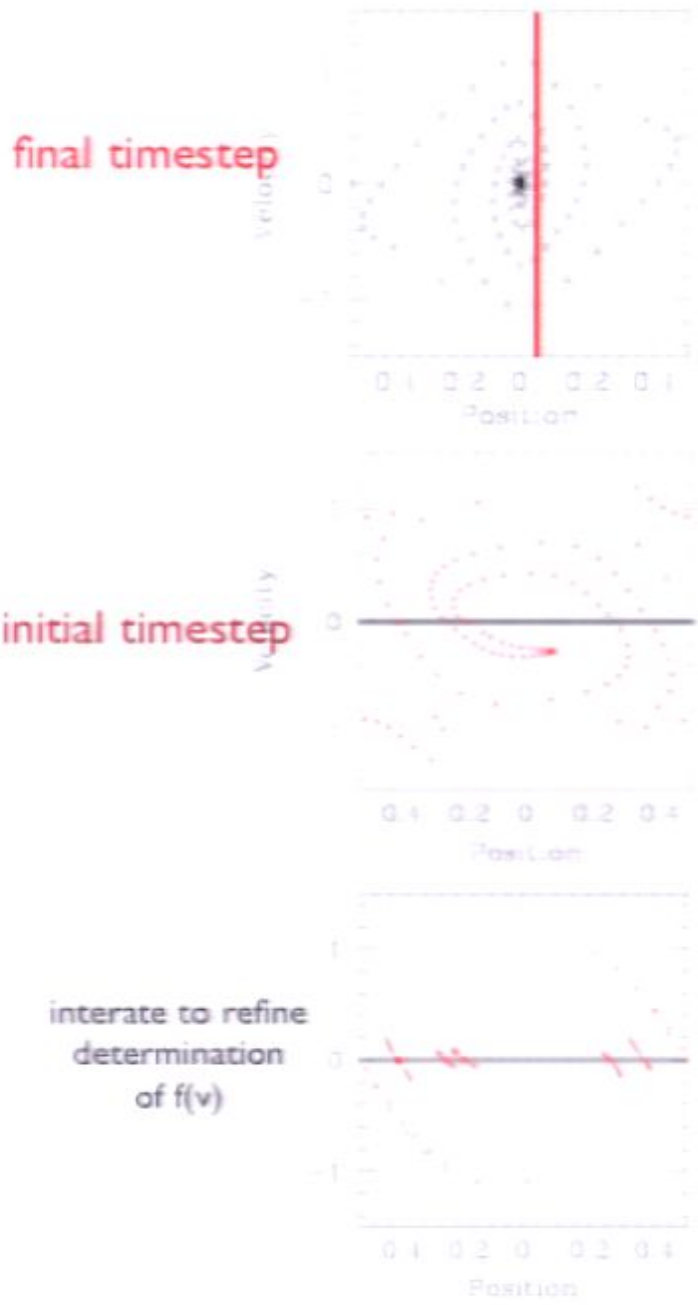

Stiff & LMW (PRL, 2003)

Follow the formation of a halo using a simulation.

At the final frame, select a position representative of the dark matter detector.

At that position, lay down test particles that cover the full velocity space.

Evolve the full system, including the test particles,
backward in time to the initial epoch.

Test particles at the initial epoch with zero velocity map out region of velocity space in the final frame where the dark matter DF is non-zero.

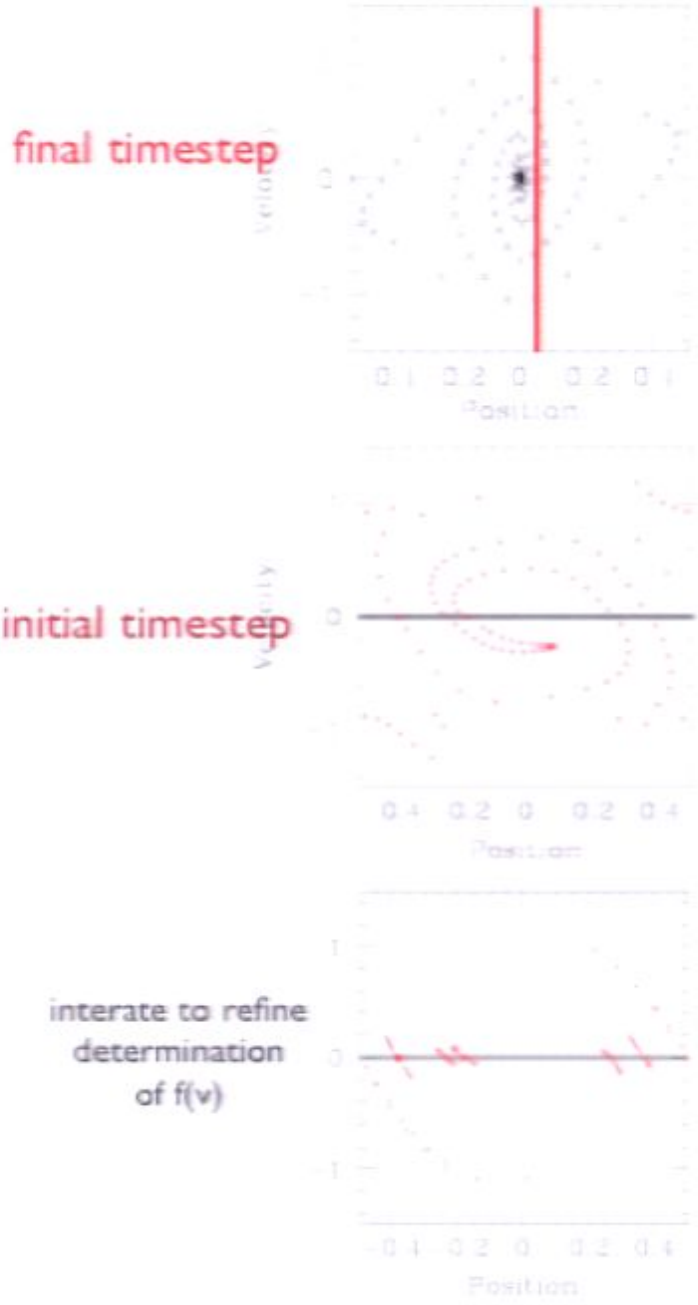

Stiff & LMW (PRL, 2003)

Follow the formation of a halo using a simulation.

At the final frame, select a position representative of the dark matter detector.

At that position, lay down test particles that cover the full velocity space.

Evolve the full system, including the test particles,
backward in time to the initial epoch.

Test particles at the initial epoch with zero velocity map out region of velocity space in the final frame where the dark matter DF is non-zero.

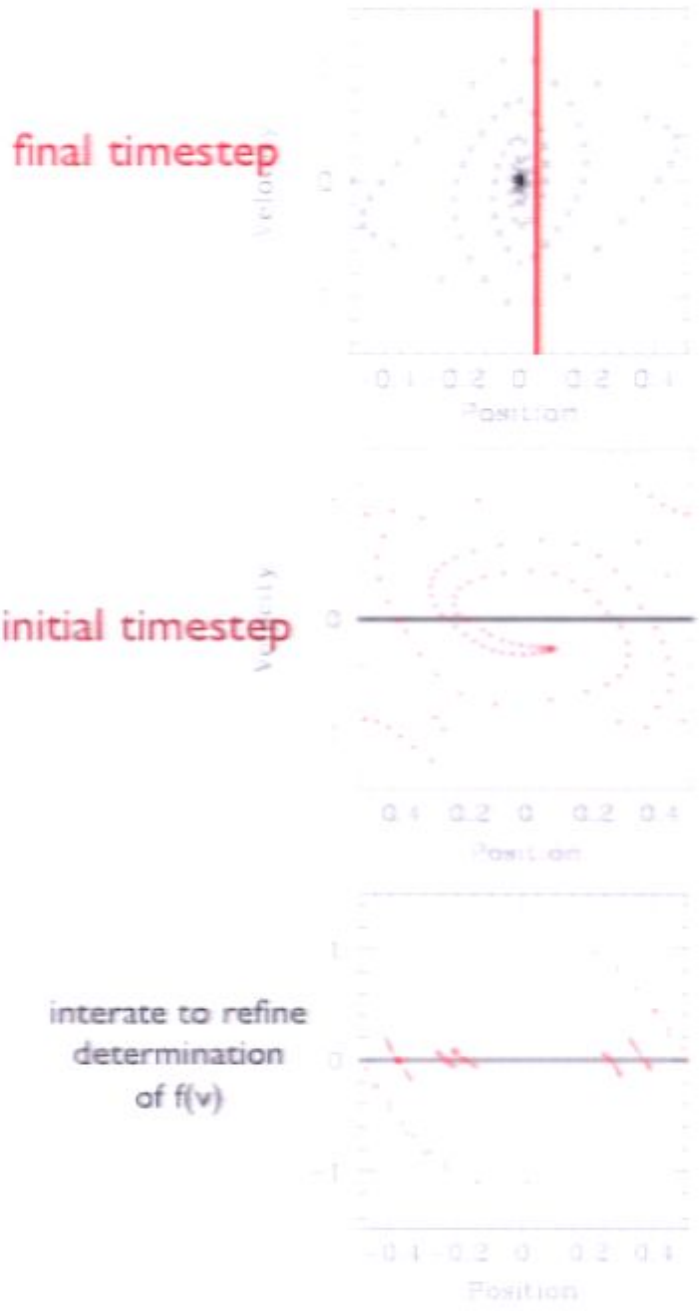

Stiff & LMW (PRL, 2003)

Follow the formation of a halo using a simulation.

At the final frame, select a position representative of the dark matter detector.

At that position, lay down test particles that cover the full velocity space.

Evolve the full system, including the test particles,
backward in time to the initial epoch.

Test particles at the initial epoch with zero velocity map out region of velocity space in the final frame where the dark matter DF is non-zero.

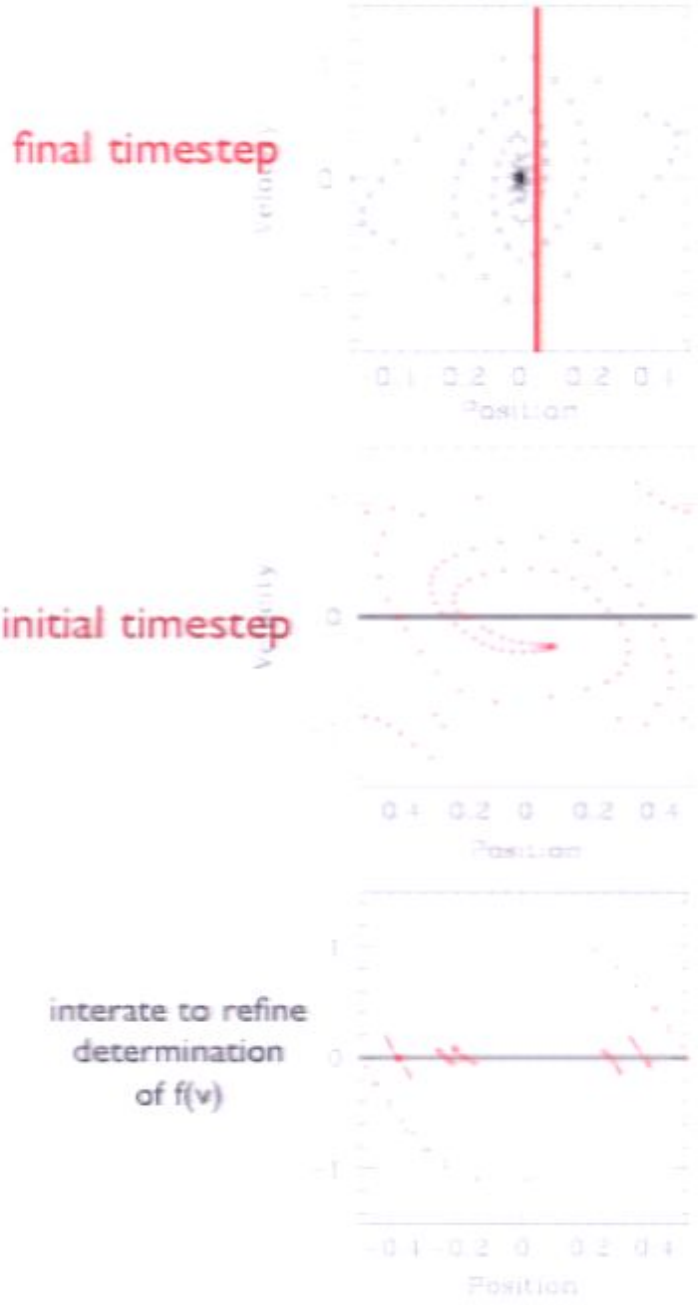

Stiff & LMW (PRL, 2003)

Follow the formation of a halo using a simulation.

At the final frame, select a position representative of the dark matter detector.

At that position, lay down test particles that cover the full velocity space.

Evolve the full system, including the test particles,
backward in time to the initial epoch.

Test particles at the initial epoch with zero velocity map out region of velocity space in the final frame where the dark matter DF is non-zero.

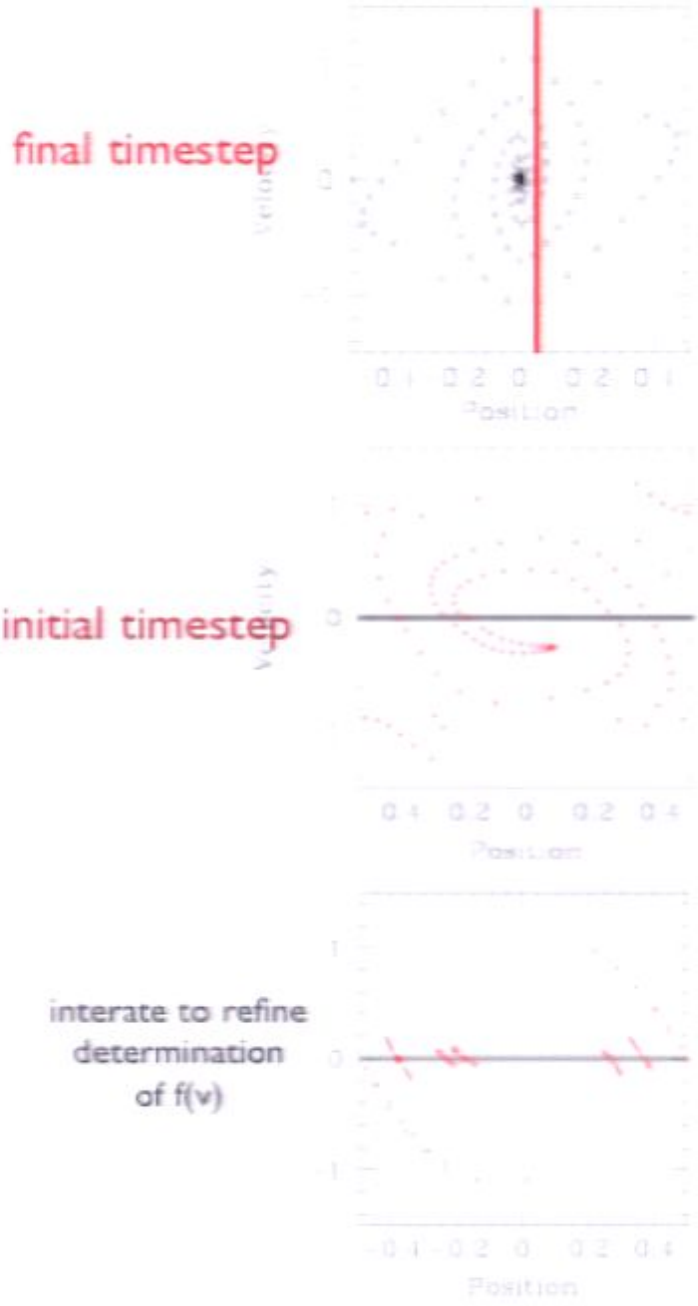

Stiff & LMW (PRL, 2003)

Follow the formation of a halo using a simulation.

At the final frame, select a position representative of the dark matter detector.

At that position, lay down test particles that cover the full velocity space.

Evolve the full system, including the test particles,
backward in time to the initial epoch.

Test particles at the initial epoch with zero velocity map out region of velocity space in the final frame where the dark matter DF is non-zero.

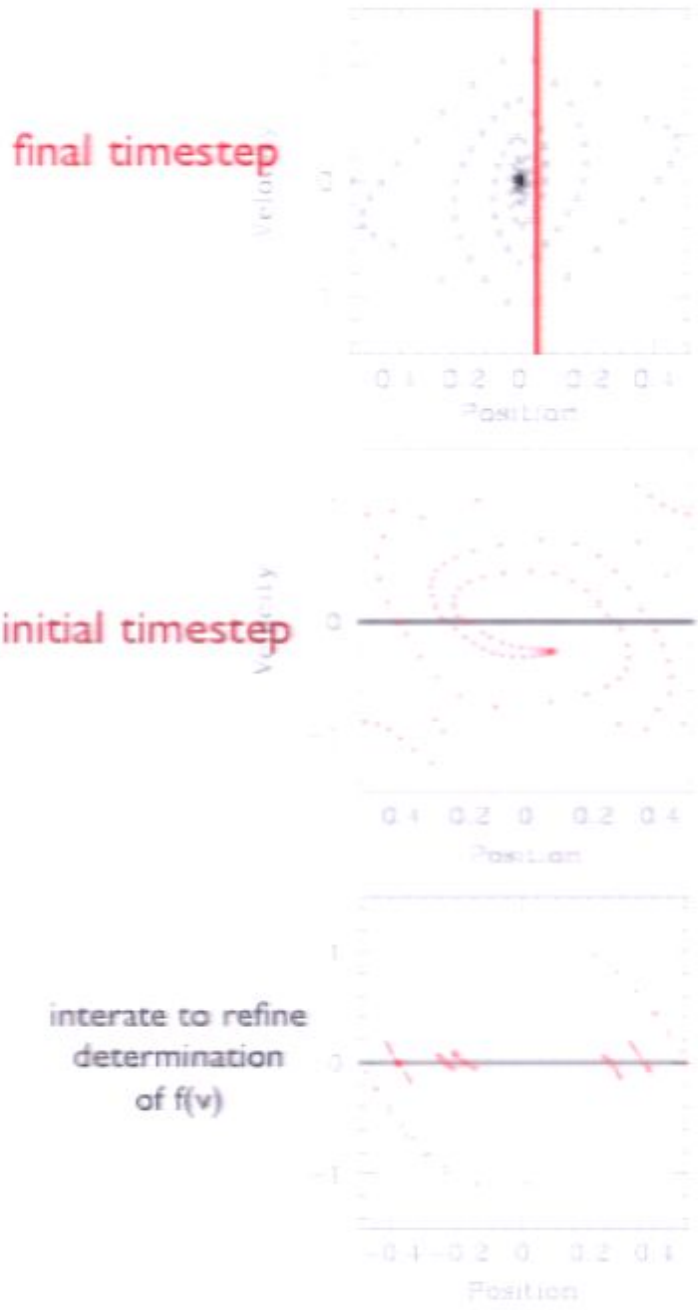

Stiff & LMW (PRL, 2003)

Follow the formation of a halo using a simulation.

At the final frame, select a position representative of the dark matter detector.

At that position, lay down test particles that cover the full velocity space.

Evolve the full system, including the test particles,
backward in time to the initial epoch.

Test particles at the initial epoch with zero velocity map out region of velocity space in the final frame where the dark matter DF is non-zero.

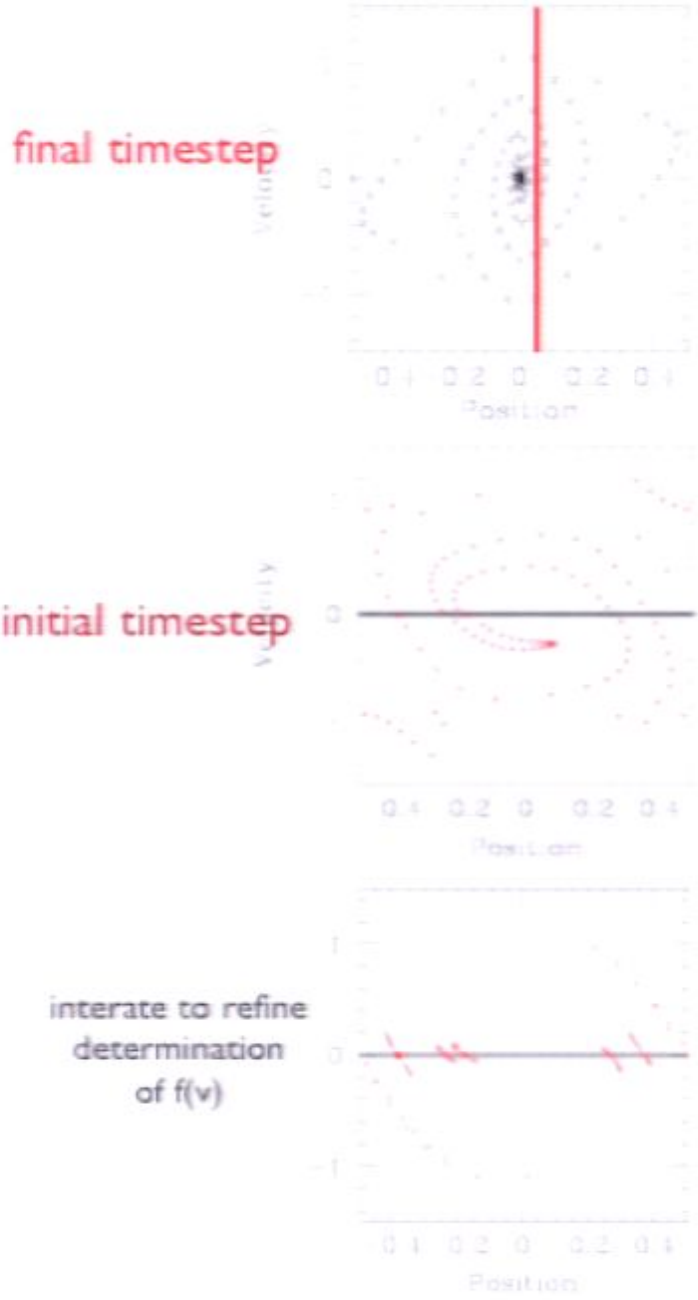

Stiff & LMW (PRL, 2003)

Follow the formation of a halo using a simulation.

At the final frame, select a position representative of the dark matter detector.

At that position, lay down test particles that cover the full velocity space.

Evolve the full system, including the test particles,
backward in time to the initial epoch.

Test particles at the initial epoch with zero velocity map out region of velocity space in the final frame where the dark matter DF is non-zero.

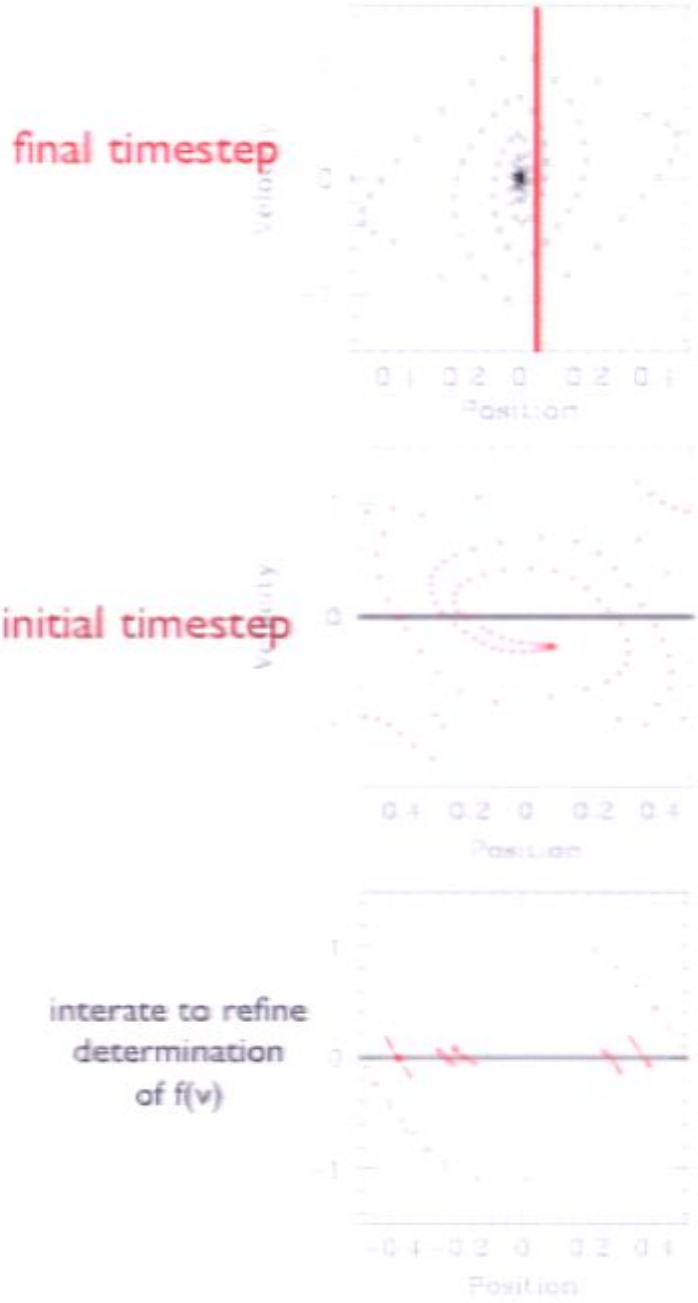

Stiff & LMW (PRL, 2003)

Follow the formation of a halo using a simulation.

At the final frame, select a position representative of the dark matter detector.

At that position, lay down test particles that cover the full velocity space.

Evolve the full system, including the test particles,
backward in time to the initial epoch.

Test particles at the initial epoch with zero velocity map out region of velocity space in the final frame where the dark matter DF is non-zero.

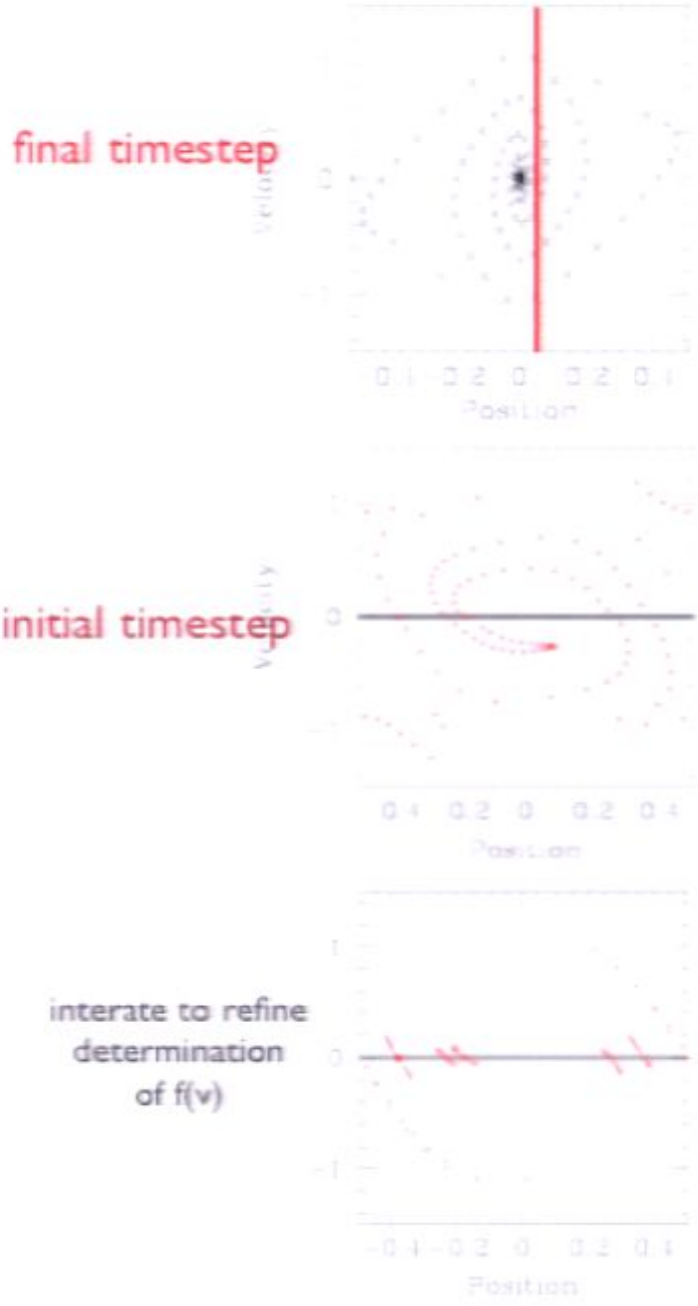

Stiff & LMW (PRL, 2003)

Follow the formation of a halo using a simulation.

At the final frame, select a position representative of the dark matter detector.

At that position, lay down test particles that cover the full velocity space.

Evolve the full system, including the test particles,
backward in time to the initial epoch.

Test particles at the initial epoch with zero velocity map out region of velocity space in the final frame where the dark matter DF is non-zero.

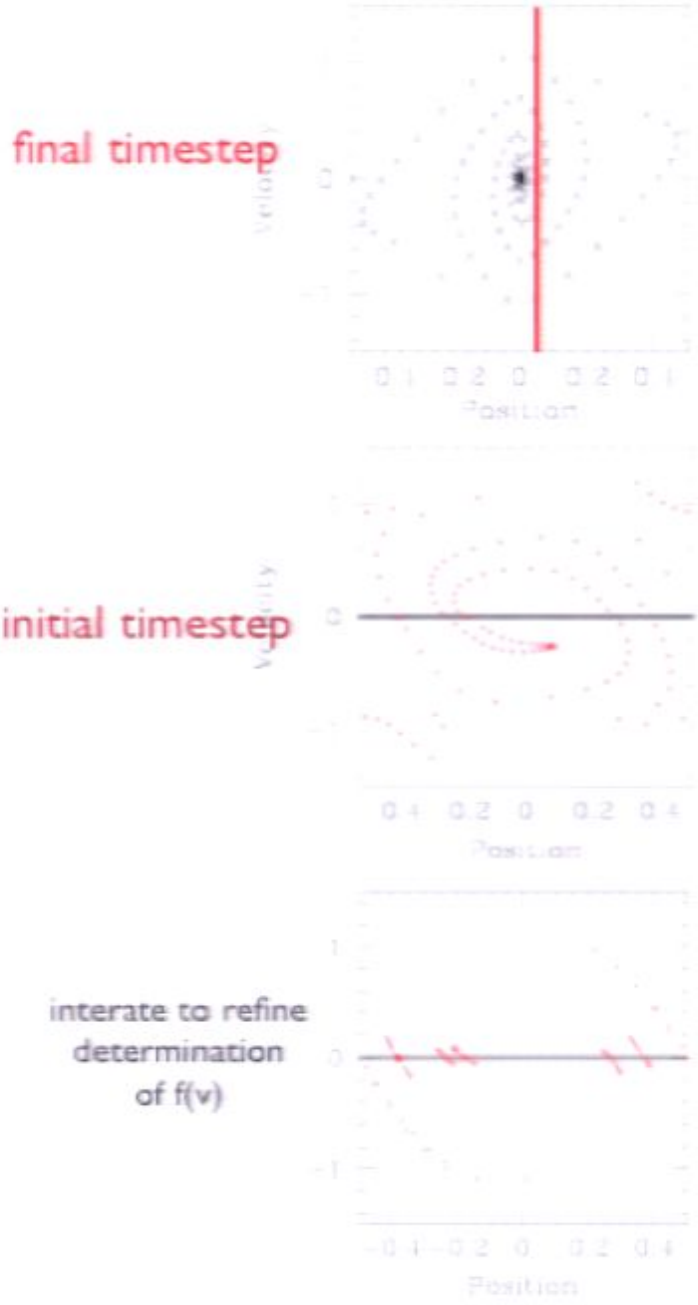

Stiff & LMW (PRL, 2003)

Follow the formation of a halo using a simulation.

At the final frame, select a position representative of the dark matter detector.

At that position, lay down test particles that cover the full velocity space.

Evolve the full system, including the test particles,
backward in time to the initial epoch.

Test particles at the initial epoch with zero velocity map out region of velocity space in the final frame where the dark matter DF is non-zero.

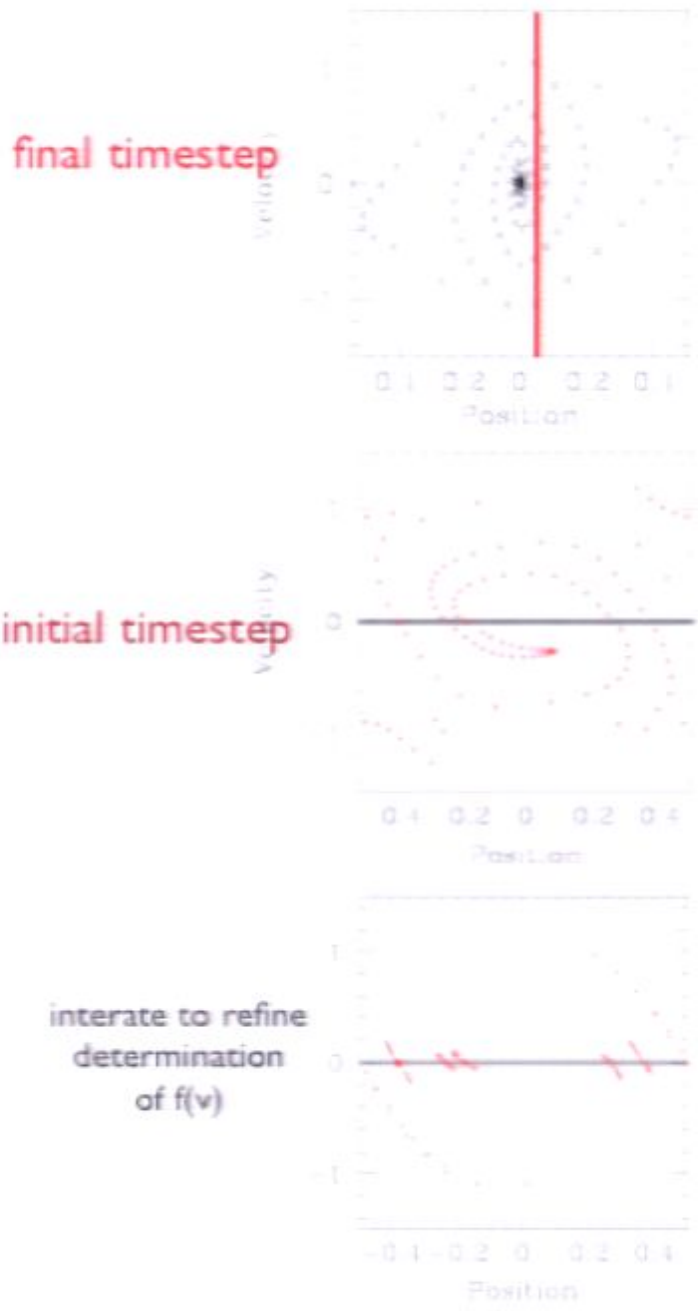

Stiff & LMW (PRL, 2003)

Follow the formation of a halo using a simulation.

At the final frame, select a position representative of the dark matter detector.

At that position, lay down test particles that cover the full velocity space.

Evolve the full system, including the test particles,
backward in time to the initial epoch.

Test particles at the initial epoch with zero velocity map out region of velocity space in the final frame where the dark matter DF is non-zero.

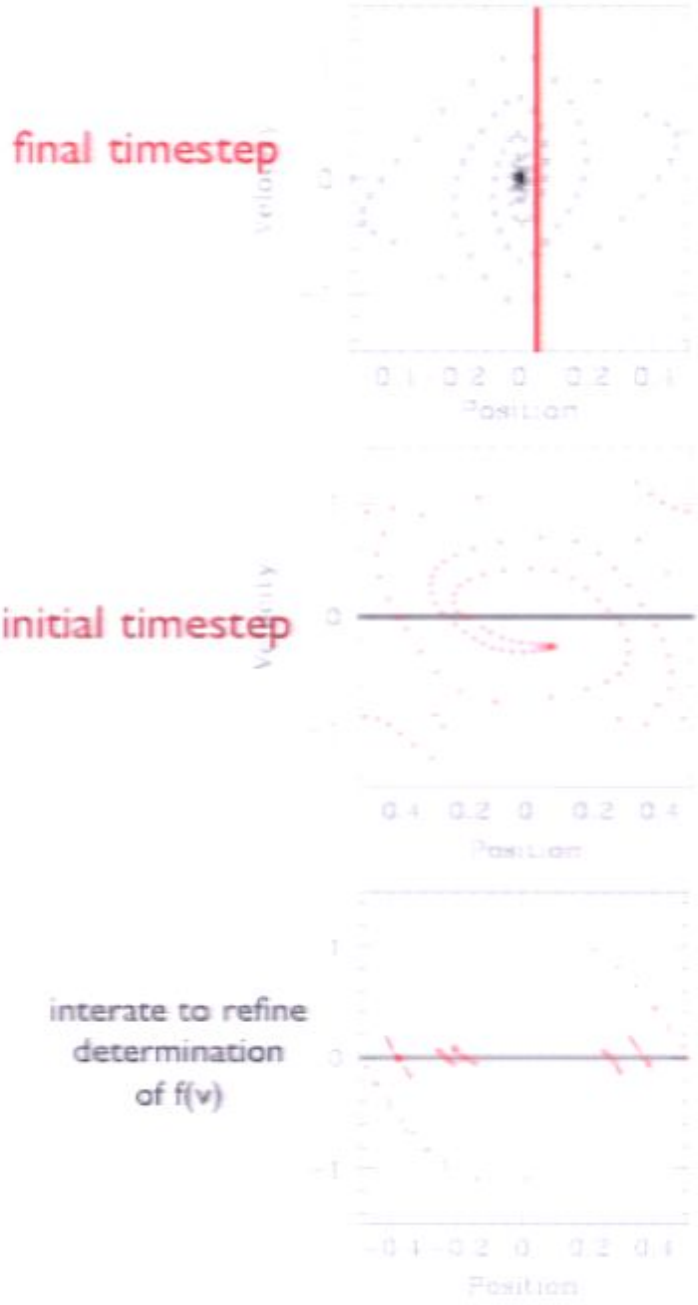

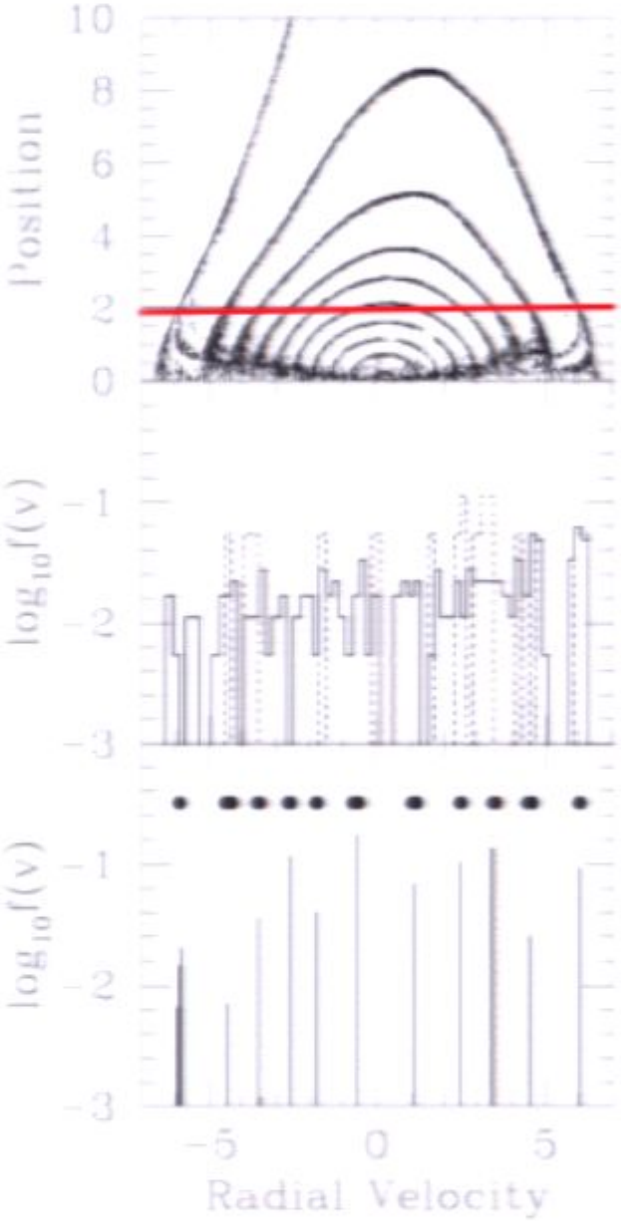

final frame for spherical collapse
from high-res shell-model calculation

red line marks position of detector

velocity distribution measured
using standard method with low-res simulation
too few particles to map out true
peak structure in velocity space

reverse-run method picks
out peaks in velocity space
even with low-res simulation

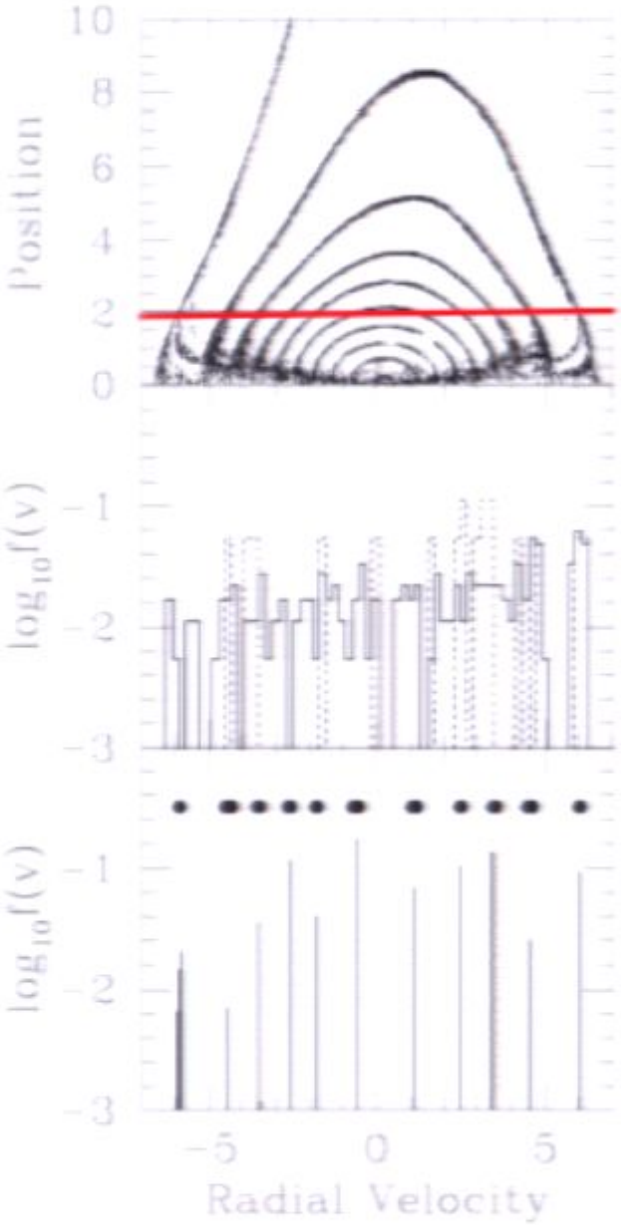

final frame for spherical collapse
from high-res shell-model calculation

red line marks position of detector

velocity distribution measured
using standard method with low-res simulation
too few particles to map out true
peak structure in velocity space

reverse-run method picks
out peaks in velocity space
even with low-res simulation

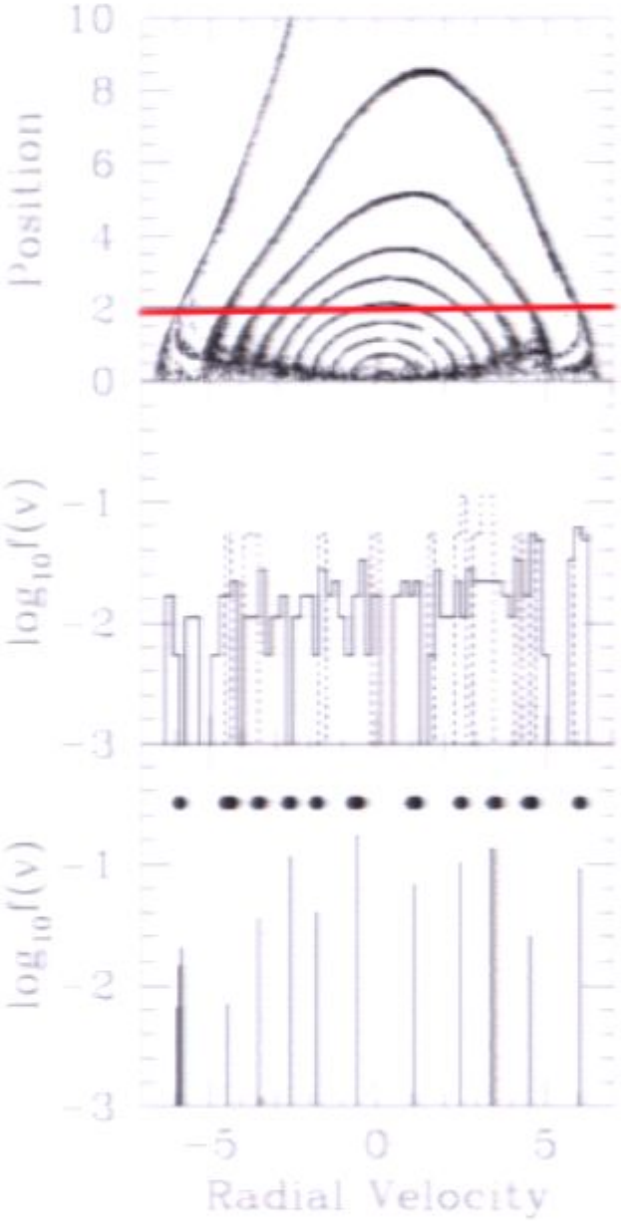

final frame for spherical collapse
from high-res shell-model calculation

red line marks position of detector

velocity distribution measured
using standard method with low-res simulation
too few particles to map out true
peak structure in velocity space

reverse-run method picks
out peaks in velocity space
even with low-res simulation

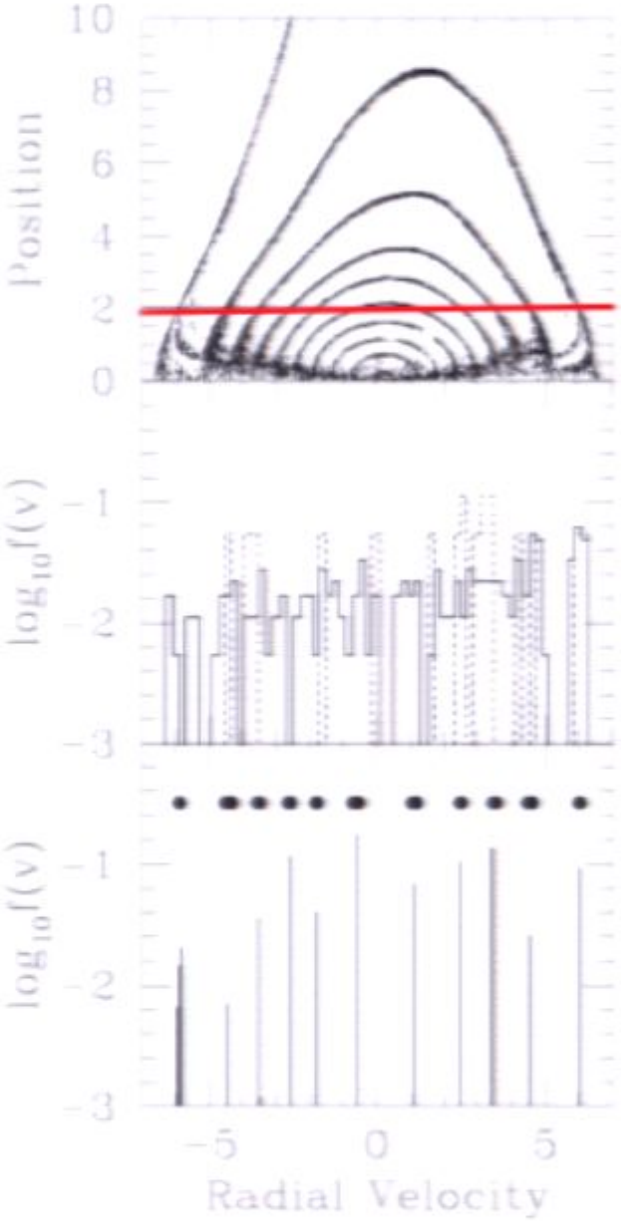

final frame for spherical collapse
from high-res shell-model calculation

red line marks position of detector

velocity distribution measured
using standard method with low-res simulation
too few particles to map out true
peak structure in velocity space

reverse-run method picks
out peaks in velocity space
even with low-res simulation

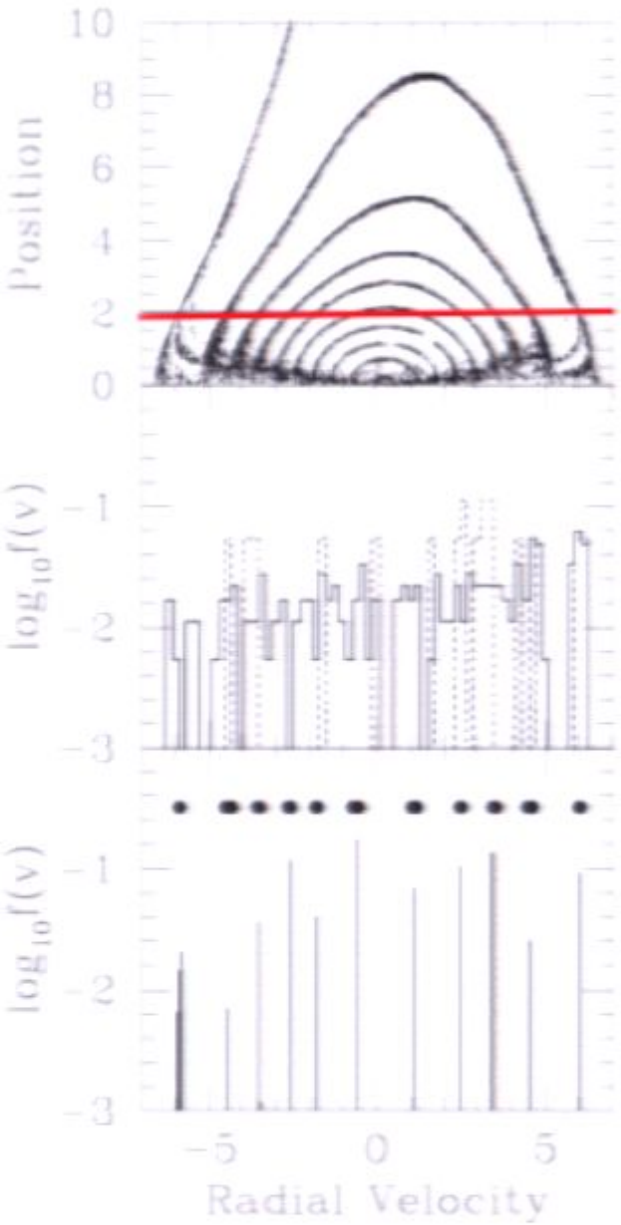

final frame for spherical collapse
from high-res shell-model calculation

red line marks position of detector

velocity distribution measured
using standard method with low-res simulation
too few particles to map out true
peak structure in velocity space

reverse-run method picks
out peaks in velocity space
even with low-res simulation

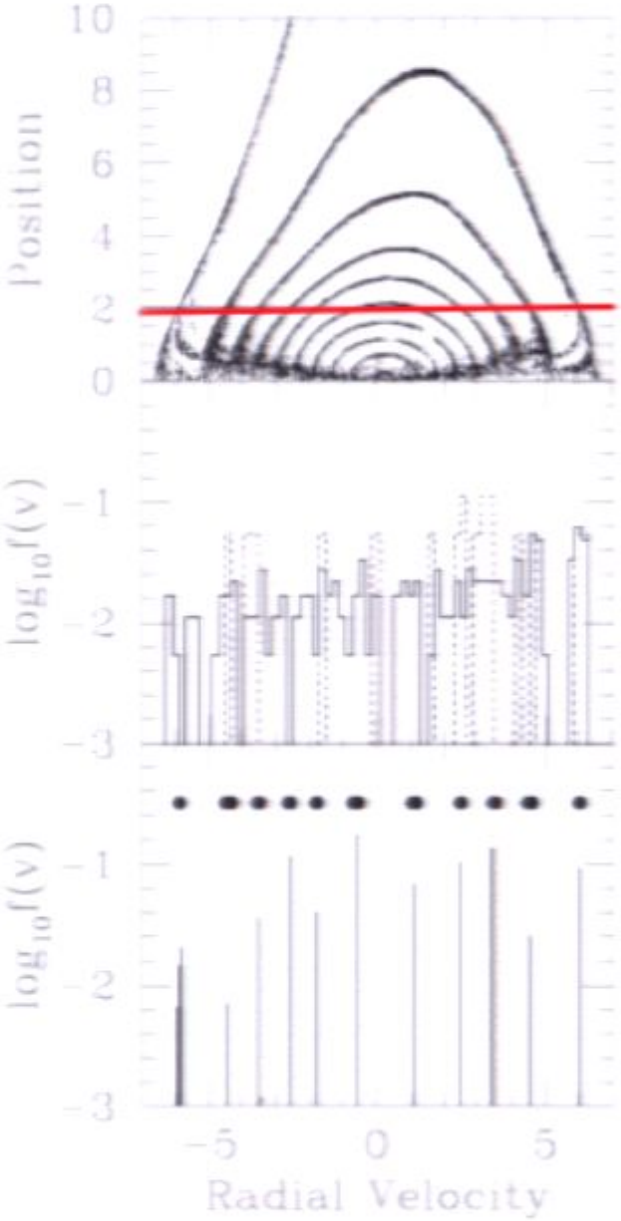

final frame for spherical collapse
from high-res shell-model calculation

red line marks position of detector

velocity distribution measured
using standard method with low-res simulation
too few particles to map out true
peak structure in velocity space

reverse-run method picks
out peaks in velocity space
even with low-res simulation

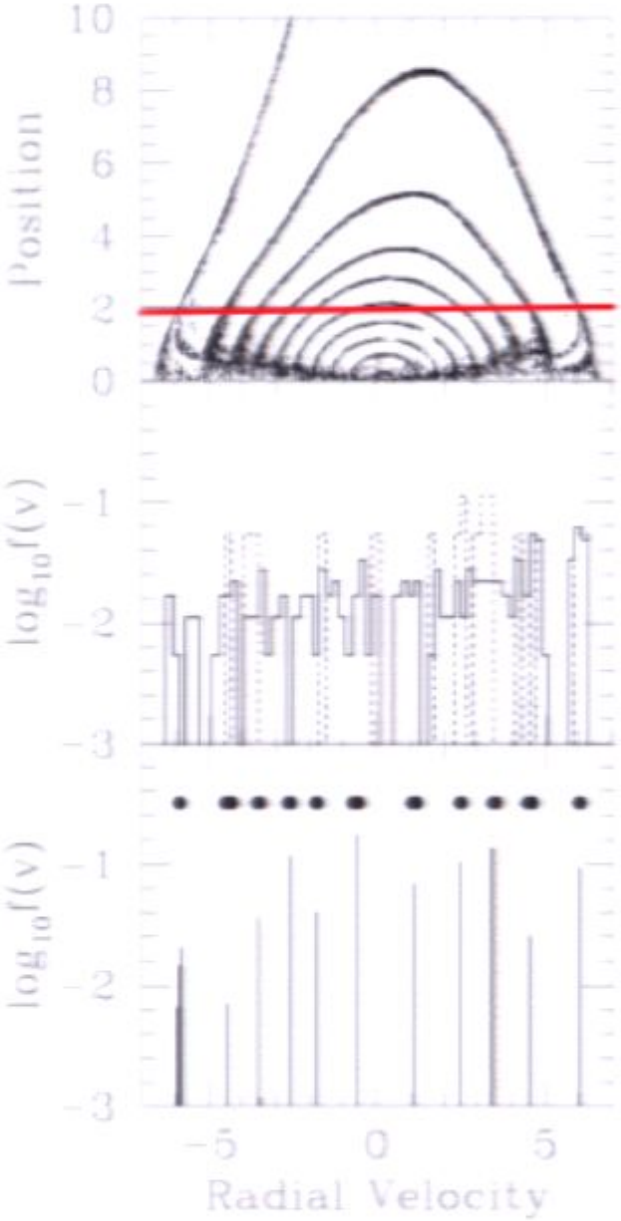

final frame for spherical collapse
from high-res shell-model calculation

red line marks position of detector

velocity distribution measured
using standard method with low-res simulation
too few particles to map out true
peak structure in velocity space

reverse-run method picks
out peaks in velocity space
even with low-res simulation

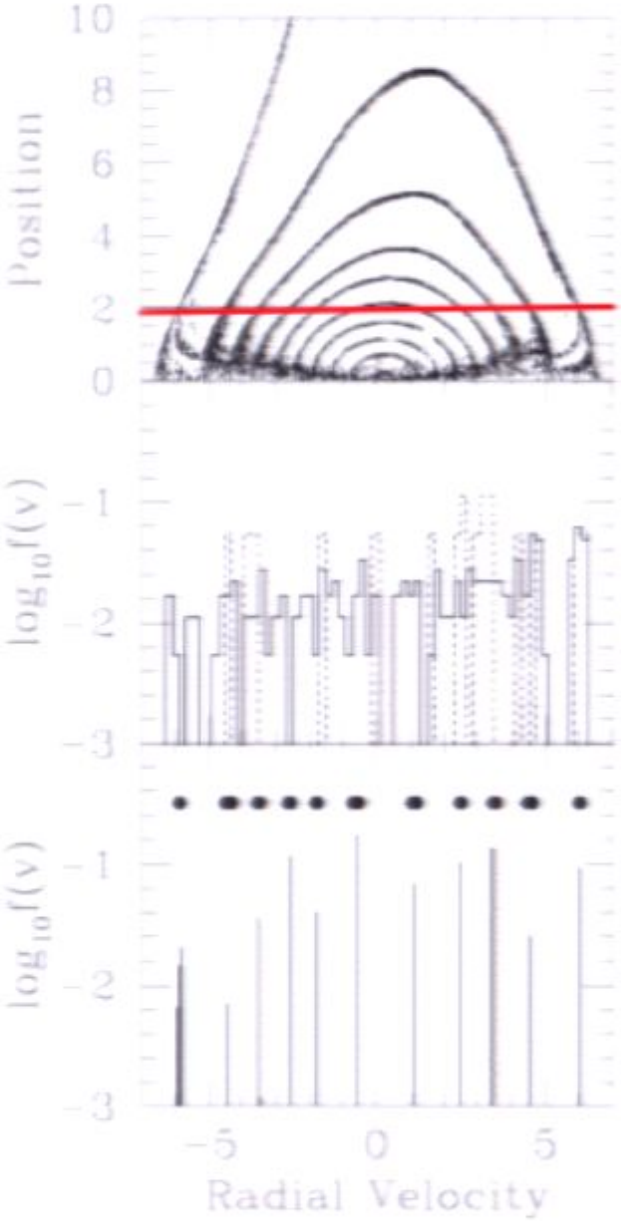

final frame for spherical collapse
from high-res shell-model calculation

red line marks position of detector

velocity distribution measured
using standard method with low-res simulation
too few particles to map out true
peak structure in velocity space

reverse-run method picks
out peaks in velocity space
even with low-res simulation

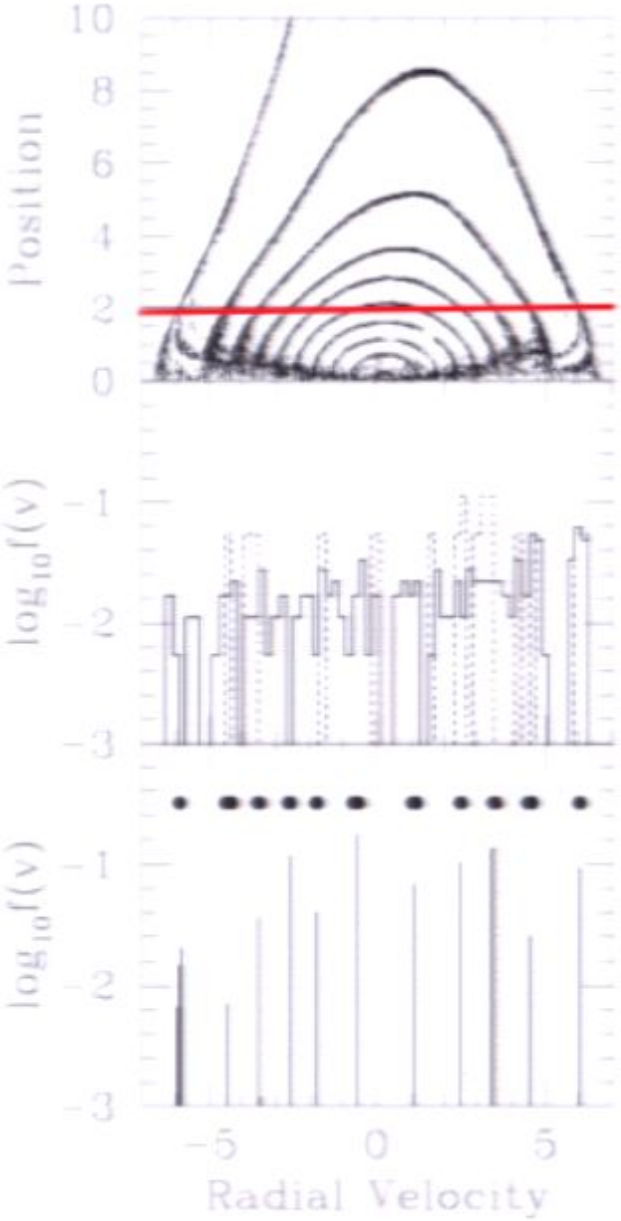

final frame for spherical collapse
from high-res shell-model calculation

red line marks position of detector

velocity distribution measured
using standard method with low-res simulation
too few particles to map out true
peak structure in velocity space

reverse-run method picks
out peaks in velocity space
even with low-res simulation

Reversibility ... there's the rub

Our method requires that the simulation be reversible
Liouville's theorem must be satisfied.

Of course, cosmological N-body simulations
are never reversible

Our fix: use an extra large softening length

Reversibility ... there's the rub

Our method requires that the simulation be reversible
Liouville's theorem must be satisfied.

Of course, cosmological N-body simulations
are never reversible

Our fix: use an extra large softening length

Reversibility ... there's the rub

Our method requires that the simulation be reversible
Liouville's theorem must be satisfied.

Of course, cosmological N-body simulations
are never reversible

Our fix: use an extra large softening length

Reversibility ... there's the rub

Our method requires that the simulation be reversible
Liouville's theorem must be satisfied.

Of course, cosmological N-body simulations
are never reversible

Our fix: use an extra large softening length

Reversibility ... there's the rub

Our method requires that the simulation be reversible
Liouville's theorem must be satisfied.

Of course, cosmological N-body simulations
are never reversible

Our fix: use an extra large softening length

Reversibility ... there's the rub

Our method requires that the simulation be reversible
Liouville's theorem must be satisfied.

Of course, cosmological N-body simulations
are never reversible

Our fix: use an extra large softening length

Reversibility ... there's the rub

Our method requires that the simulation be reversible
Liouville's theorem must be satisfied.

Of course, cosmological N-body simulations
are never reversible

Our fix: use an extra large softening length

Reversibility ... there's the rub

Our method requires that the simulation be reversible
Liouville's theorem must be satisfied.

Of course, cosmological N-body simulations
are never reversible

Our fix: use an extra large softening length

Reversibility ... there's the rub

Our method requires that the simulation be reversible
Liouville's theorem must be satisfied.

Of course, cosmological N-body simulations
are never reversible

Our fix: use an extra large softening length

Reversibility ... there's the rub

Our method requires that the simulation be reversible
Liouville's theorem must be satisfied.

Of course, cosmological N-body simulations
are never reversible

Our fix: use an extra large softening length

An aside on softening in N-body simulations:

Generally, the inverse-square force-law of gravity is "softened" to damp down unphysical two-body interactions.

Softening lengths used in N-body simulations are large enough to suppress the most significant two-body interactions. But particles still "jump" from one phase-space sheet to another, thereby spoiling Liouville's theorem and reversibility.

An aside on softening in N-body simulations:

Generally, the inverse-square force-law of gravity is "softened" to damp down unphysical two-body interactions.

Softening lengths used in N-body simulations are large enough to suppress the most significant two-body interactions. But particles still "jump" from one phase-space sheet to another, thereby spoiling Liouville's theorem and reversibility.

here, the Fillmore-Goldreich-Bertschinger solution goes unstable ---
once particles jump from one phase space sheet
to another, reversibility is lost

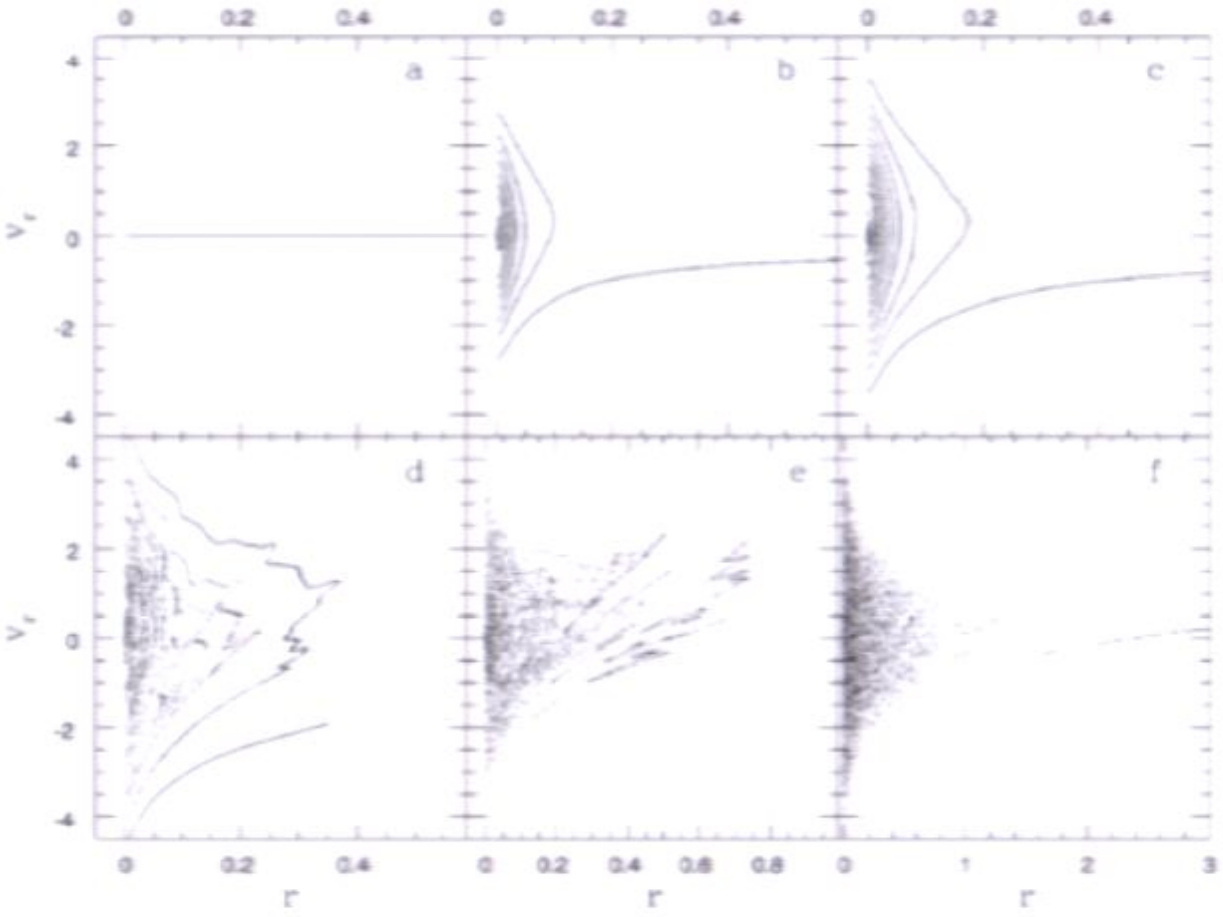

Henriksen & Widrow, 1997

here, the Fillmore-Goldreich-Bertschinger solution goes unstable ---
once particles jump from one phase space sheet
to another, reversibility is lost

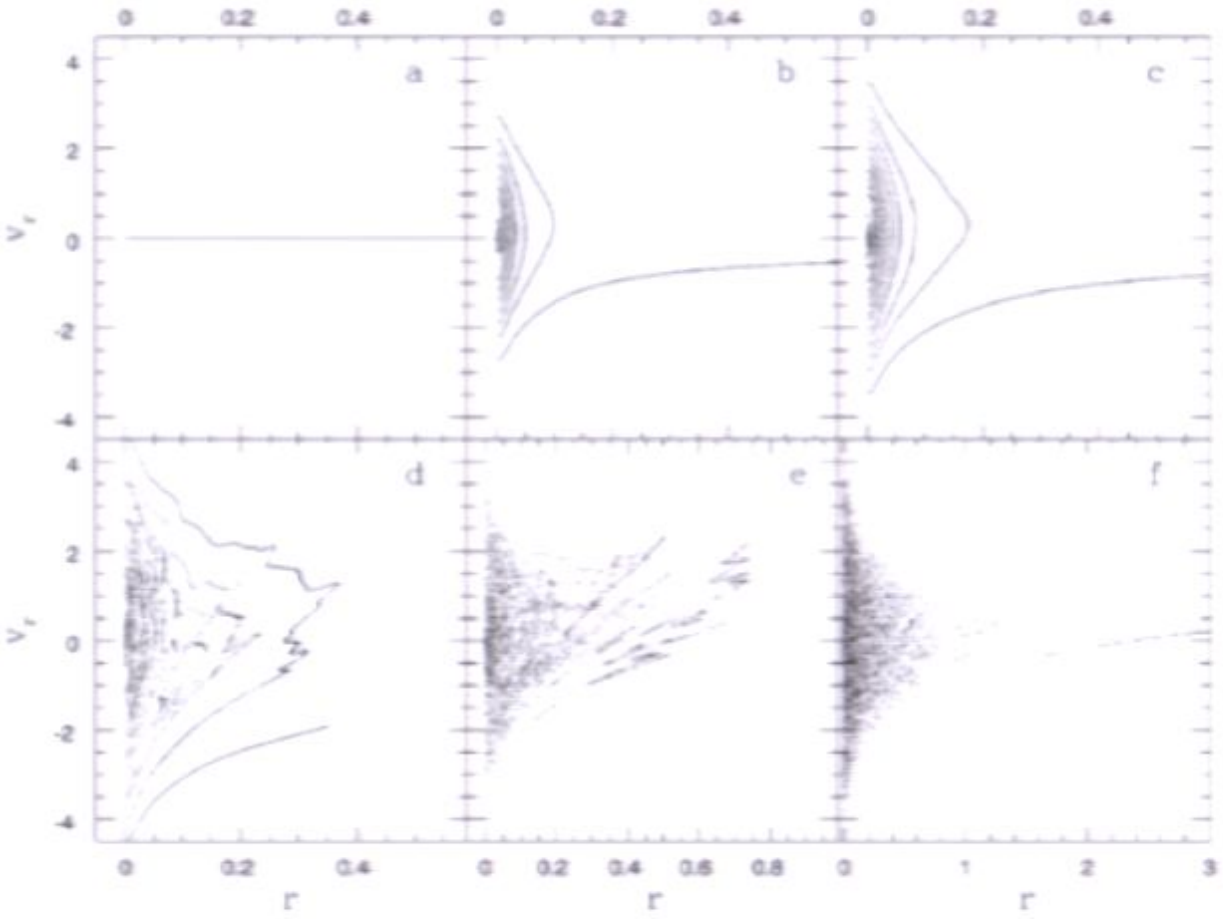

Henriksen & Widrow, 1997

Fantin, Merrifield, & Green, 2007 and 2011

use backward integration method on a simpler problem:
tidal disruption of a satellite in a fixed isochrone potential
which admits analytic angle-action variables

$$\Phi(r) = \frac{GM}{b + \sqrt{b^2 + r^2}}$$

FMG pick position of detector at final epoch and consider test-particles at this postion with different velocities.

These particles are evolved backward in time to initial epoch
("trivial" one-step calculation)

phase space coordinates of test particles at initial epoch
are compared to DF for initial satellite

$$f_{\rm sat}\left(\mathbf{x},\,\mathbf{v},\,t_i\right) \;\propto\; e^{-\left((\mathbf{x}-\mathbf{x}_i)^2/2\Delta_x^2\right)}\, e^{-\left((\mathbf{v}-\mathbf{v}_i)^2/2\Delta_v^2\right)}$$

Fantin, Merrifield, & Green, 2007 and 2011

use backward integration method on a simpler problem:
tidal disruption of a satellite in a fixed isochrone potential
which admits analytic angle-action variables

$$\Phi(r) = \frac{GM}{b + \sqrt{b^2 + r^2}}$$

FMG pick position of detector at final epoch and consider test-particles at this postion with different velocities.

These particles are evolved backward in time to initial epoch
("trivial" one-step calculation)

phase space coordinates of test particles at initial epoch
are compared to DF for initial satellite

$$f_{\rm sat}\left(\mathbf{x},\,\mathbf{v},\,t_i\right) \;\propto\; e^{-\left((\mathbf{x}-\mathbf{x}_i)^2/2\Delta_x^2\right)}\, e^{-\left((\mathbf{v}-\mathbf{v}_i)^2/2\Delta_v^2\right)}$$

Fantin, Merrifield, & Green, 2007 and 2011

use backward integration method on a simpler problem:
tidal disruption of a satellite in a fixed isochrone potential
which admits analytic angle-action variables

$$\Phi(r) = \frac{GM}{b + \sqrt{b^2 + r^2}}$$

FMG pick position of detector at final epoch and consider test-particles at this postion with different velocities.

These particles are evolved backward in time to initial epoch
("trivial" one-step calculation)

phase space coordinates of test particles at initial epoch
are compared to DF for initial satellite

$$f_{\rm sat}\left(\mathbf{x},\,\mathbf{v},\,t_i\right) \;\propto\; e^{-\left((\mathbf{x}-\mathbf{x}_i)^2/2\Delta_x^2\right)}\, e^{-\left((\mathbf{v}-\mathbf{v}_i)^2/2\Delta_v^2\right)}$$

Fantin, Merrifield, & Green, 2007 and 2011

use backward integration method on a simpler problem:
tidal disruption of a satellite in a fixed isochrone potential
which admits analytic angle-action variables

$$\Phi(r) = \frac{GM}{b + \sqrt{b^2 + r^2}}$$

FMG pick position of detector at final epoch and consider test-particles at this postion with different velocities.

These particles are evolved backward in time to initial epoch
("trivial" one-step calculation)

phase space coordinates of test particles at initial epoch
are compared to DF for initial satellite

$$f_{\rm sat}\left(\mathbf{x},\,\mathbf{v},\,t_i\right) \;\propto\; e^{-\left((\mathbf{x}-\mathbf{x}_i)^2/2\Delta_x^2\right)}\, e^{-\left((\mathbf{v}-\mathbf{v}_i)^2/2\Delta_v^2\right)}$$

Fantin, Merrifield, & Green, 2007 and 2011

use backward integration method on a simpler problem:
tidal disruption of a satellite in a fixed isochrone potential
which admits analytic angle-action variables

$$\Phi(r) = \frac{GM}{b + \sqrt{b^2 + r^2}}$$

FMG pick position of detector at final epoch and consider test-particles at this postion with different velocities.

These particles are evolved backward in time to initial epoch
("trivial" one-step calculation)

phase space coordinates of test particles at initial epoch
are compared to DF for initial satellite

$$f_{\rm sat}\left(\mathbf{x},\,\mathbf{v},\,t_i\right) \;\propto\; e^{-\left((\mathbf{x}-\mathbf{x}_i)^2/2\Delta_x^2\right)}\, e^{-\left((\mathbf{v}-\mathbf{v}_i)^2/2\Delta_v^2\right)}$$

Fantin, Merrifield, & Green, 2007 and 2011

use backward integration method on a simpler problem:
tidal disruption of a satellite in a fixed isochrone potential
which admits analytic angle-action variables

$$\Phi(r) = \frac{GM}{b + \sqrt{b^2 + r^2}}$$

FMG pick position of detector at final epoch and consider test-particles at this postion with different velocities.

These particles are evolved backward in time to initial epoch
("trivial" one-step calculation)

phase space coordinates of test particles at initial epoch
are compared to DF for initial satellite

$$f_{\rm sat}\left(\mathbf{x},\,\mathbf{v},\,t_i\right) \;\propto\; e^{-\left((\mathbf{x}-\mathbf{x}_i)^2/2\Delta_x^2\right)}\, e^{-\left((\mathbf{v}-\mathbf{v}_i)^2/2\Delta_v^2\right)}$$

Fantin, Merrifield, & Green, 2007 and 2011

use backward integration method on a simpler problem:
tidal disruption of a satellite in a fixed isochrone potential
which admits analytic angle-action variables

$$\Phi(r) = \frac{GM}{b + \sqrt{b^2 + r^2}}$$

FMG pick position of detector at final epoch and consider test-particles at this postion with different velocities.

These particles are evolved backward in time to initial epoch
("trivial" one-step calculation)

phase space coordinates of test particles at initial epoch
are compared to DF for initial satellite

$$f_{\rm sat}\left(\mathbf{x},\,\mathbf{v},\,t_i\right) \;\propto\; e^{-\left((\mathbf{x}-\mathbf{x}_i)^2/2\Delta_x^2\right)}\, e^{-\left((\mathbf{v}-\mathbf{v}_i)^2/2\Delta_v^2\right)}$$

Fantin, Merrifield, & Green, 2007 and 2011

use backward integration method on a simpler problem:
tidal disruption of a satellite in a fixed isochrone potential
which admits analytic angle-action variables

$$\Phi(r) = \frac{GM}{b + \sqrt{b^2 + r^2}}$$

FMG pick position of detector at final epoch and consider test-particles at this postion with different velocities.

These particles are evolved backward in time to initial epoch
("trivial" one-step calculation)

phase space coordinates of test particles at initial epoch
are compared to DF for initial satellite

$$f_{\rm sat}\left(\mathbf{x},\,\mathbf{v},\,t_i\right) \;\propto\; e^{-\left((\mathbf{x}-\mathbf{x}_i)^2/2\Delta_x^2\right)}\, e^{-\left((\mathbf{v}-\mathbf{v}_i)^2/2\Delta_v^2\right)}$$

Fantin, Merrifield, & Green, 2007 and 2011

use backward integration method on a simpler problem:
tidal disruption of a satellite in a fixed isochrone potential
which admits analytic angle-action variables

$$\Phi(r) = \frac{GM}{b + \sqrt{b^2 + r^2}}$$

FMG pick position of detector at final epoch and consider test-particles at this postion with different velocities.

These particles are evolved backward in time to initial epoch
("trivial" one-step calculation)

phase space coordinates of test particles at initial epoch
are compared to DF for initial satellite

$$f_{\rm sat}\left(\mathbf{x},\,\mathbf{v},\,t_i\right) \;\propto\; e^{-\left((\mathbf{x}-\mathbf{x}_i)^2/2\Delta_x^2\right)}\, e^{-\left((\mathbf{v}-\mathbf{v}_i)^2/2\Delta_v^2\right)}$$

Fantin, Merrifield, & Green, 2007 and 2011

use backward integration method on a simpler problem:
tidal disruption of a satellite in a fixed isochrone potential
which admits analytic angle-action variables

$$\Phi(r) = \frac{GM}{b + \sqrt{b^2 + r^2}}$$

FMG pick position of detector at final epoch and consider test-particles at this postion with different velocities.

These particles are evolved backward in time to initial epoch
("trivial" one-step calculation)

phase space coordinates of test particles at initial epoch
are compared to DF for initial satellite

$$f_{\rm sat}\left(\mathbf{x},\,\mathbf{v},\,t_i\right) \;\propto\; e^{-\left((\mathbf{x}-\mathbf{x}_i)^2/2\Delta_x^2\right)}\, e^{-\left((\mathbf{v}-\mathbf{v}_i)^2/2\Delta_v^2\right)}$$

Fantin, Merrifield, & Green, 2007 and 2011

use backward integration method on a simpler problem:
tidal disruption of a satellite in a fixed isochrone potential
which admits analytic angle-action variables

$$\Phi(r) = \frac{GM}{b + \sqrt{b^2 + r^2}}$$

FMG pick position of detector at final epoch and consider test-particles at this postion with different velocities.

These particles are evolved backward in time to initial epoch
("trivial" one-step calculation)

phase space coordinates of test particles at initial epoch
are compared to DF for initial satellite

$$f_{\rm sat}\left(\mathbf{x},\,\mathbf{v},\,t_i\right) \;\propto\; e^{-\left((\mathbf{x}-\mathbf{x}_i)^2/2\Delta_x^2\right)}\, e^{-\left((\mathbf{v}-\mathbf{v}_i)^2/2\Delta_v^2\right)}$$

Fantin, Merrifield, & Green, 2007 and 2011

use backward integration method on a simpler problem:
tidal disruption of a satellite in a fixed isochrone potential
which admits analytic angle-action variables

$$\Phi(r) = \frac{GM}{b + \sqrt{b^2 + r^2}}$$

FMG pick position of detector at final epoch and consider test-particles at this postion with different velocities.

These particles are evolved backward in time to initial epoch
("trivial" one-step calculation)

phase space coordinates of test particles at initial epoch
are compared to DF for initial satellite

$$f_{\rm sat}\left(\mathbf{x},\,\mathbf{v},\,t_i\right) \;\propto\; e^{-\left((\mathbf{x}-\mathbf{x}_i)^2/2\Delta_x^2\right)}\, e^{-\left((\mathbf{v}-\mathbf{v}_i)^2/2\Delta_v^2\right)}$$

Fantin, Merrifield, & Green, 2007 and 2011

use backward integration method on a simpler problem:
tidal disruption of a satellite in a fixed isochrone potential
which admits analytic angle-action variables

$$\Phi(r) = \frac{GM}{b + \sqrt{b^2 + r^2}}$$

FMG pick position of detector at final epoch and consider test-particles at this postion with different velocities.

These particles are evolved backward in time to initial epoch
("trivial" one-step calculation)

phase space coordinates of test particles at initial epoch
are compared to DF for initial satellite

$$f_{\rm sat}\left(\mathbf{x},\,\mathbf{v},\,t_i\right) \;\propto\; e^{-\left((\mathbf{x}-\mathbf{x}_i)^2/2\Delta_x^2\right)}\, e^{-\left((\mathbf{v}-\mathbf{v}_i)^2/2\Delta_v^2\right)}$$

Fantin, Merrifield, & Green, 2007 and 2011

use backward integration method on a simpler problem:
tidal disruption of a satellite in a fixed isochrone potential
which admits analytic angle-action variables

$$\Phi(r) = \frac{GM}{b + \sqrt{b^2 + r^2}}$$

FMG pick position of detector at final epoch and consider test-particles at this postion with different velocities.

These particles are evolved backward in time to initial epoch
("trivial" one-step calculation)

phase space coordinates of test particles at initial epoch
are compared to DF for initial satellite

$$f_{\rm sat}\left(\mathbf{x},\,\mathbf{v},\,t_i\right) \;\propto\; e^{-\left((\mathbf{x}-\mathbf{x}_i)^2/2\Delta_x^2\right)}\, e^{-\left((\mathbf{v}-\mathbf{v}_i)^2/2\Delta_v^2\right)}$$

Fantin, Merrifield, & Green, 2007 and 2011

use backward integration method on a simpler problem:
tidal disruption of a satellite in a fixed isochrone potential
which admits analytic angle-action variables

$$\Phi(r) = \frac{GM}{b + \sqrt{b^2 + r^2}}$$

FMG pick position of detector at final epoch and consider test-particles at this postion with different velocities.

These particles are evolved backward in time to initial epoch
("trivial" one-step calculation)

phase space coordinates of test particles at initial epoch
are compared to DF for initial satellite

$$f_{\rm sat}\left(\mathbf{x},\,\mathbf{v},\,t_i\right) \;\propto\; e^{-\left((\mathbf{x}-\mathbf{x}_i)^2/2\Delta_x^2\right)}\, e^{-\left((\mathbf{v}-\mathbf{v}_i)^2/2\Delta_v^2\right)}$$

Fantin, Merrifield, & Green, 2007 and 2011

use backward integration method on a simpler problem:
tidal disruption of a satellite in a fixed isochrone potential
which admits analytic angle-action variables

$$\Phi(r) = \frac{GM}{b + \sqrt{b^2 + r^2}}$$

FMG pick position of detector at final epoch and consider test-particles at this postion with different velocities.

These particles are evolved backward in time to initial epoch
("trivial" one-step calculation)

phase space coordinates of test particles at initial epoch
are compared to DF for initial satellite

$$f_{\rm sat}\left(\mathbf{x},\,\mathbf{v},\,t_i\right) \;\propto\; e^{-\left((\mathbf{x}-\mathbf{x}_i)^2/2\Delta_x^2\right)}\, e^{-\left((\mathbf{v}-\mathbf{v}_i)^2/2\Delta_v^2\right)}$$

Fantin et al. explore different orbits and effect of initial internal dispersion of the satellite

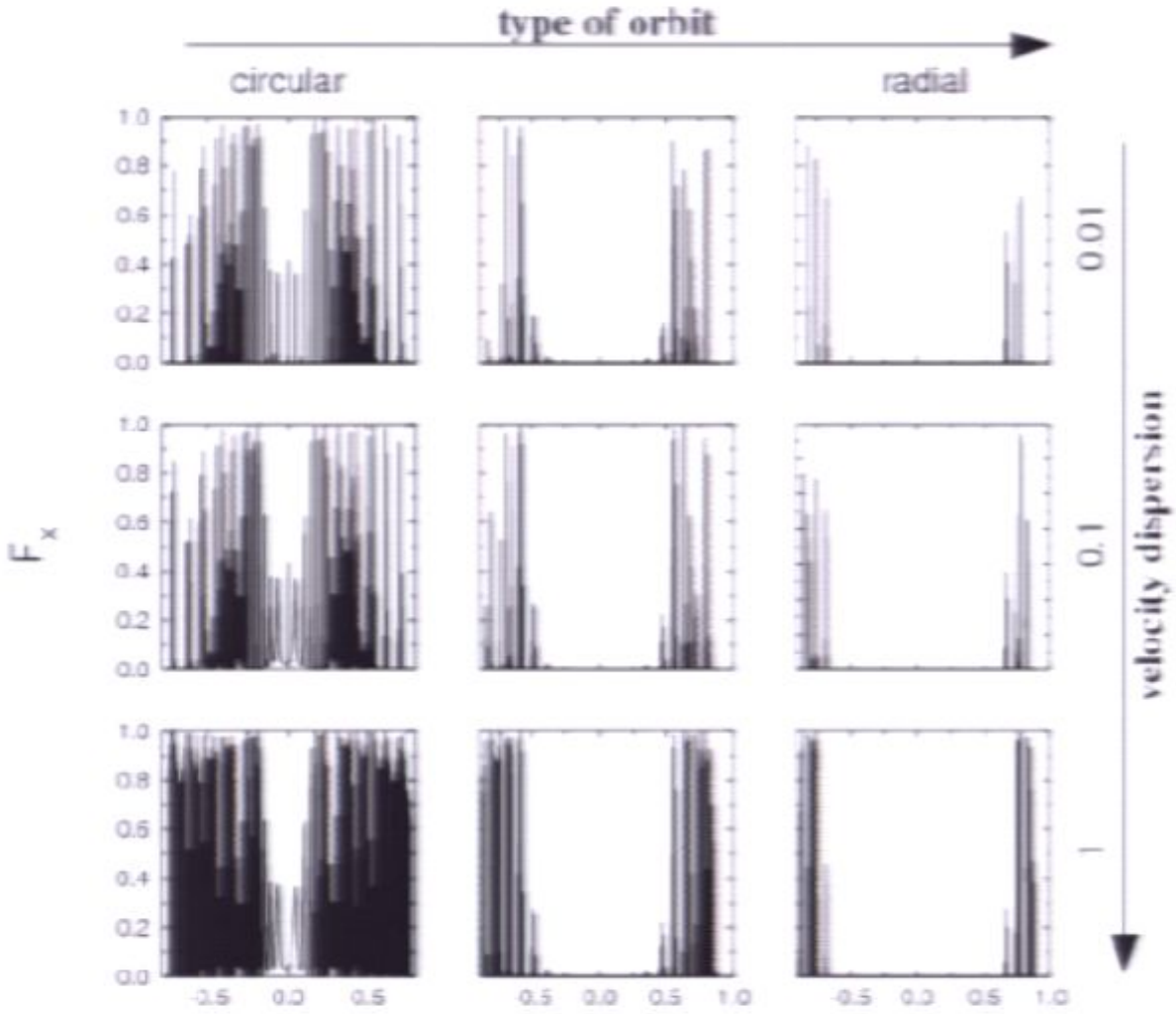

Fantin et al. explore different orbits and effect of initial internal dispersion of the satellite

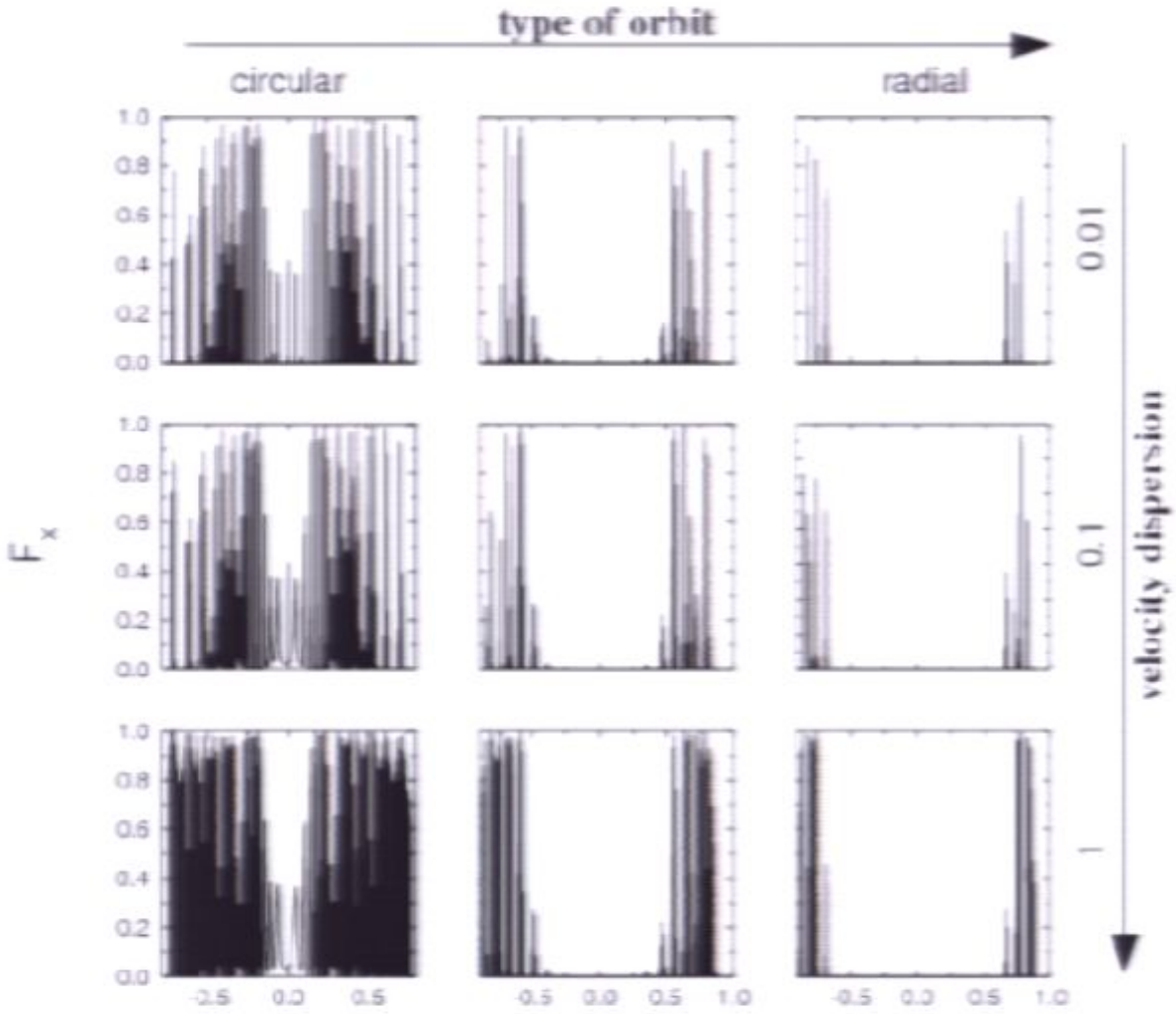

Fantin et al. explore different orbits and effect of initial internal dispersion of the satellite

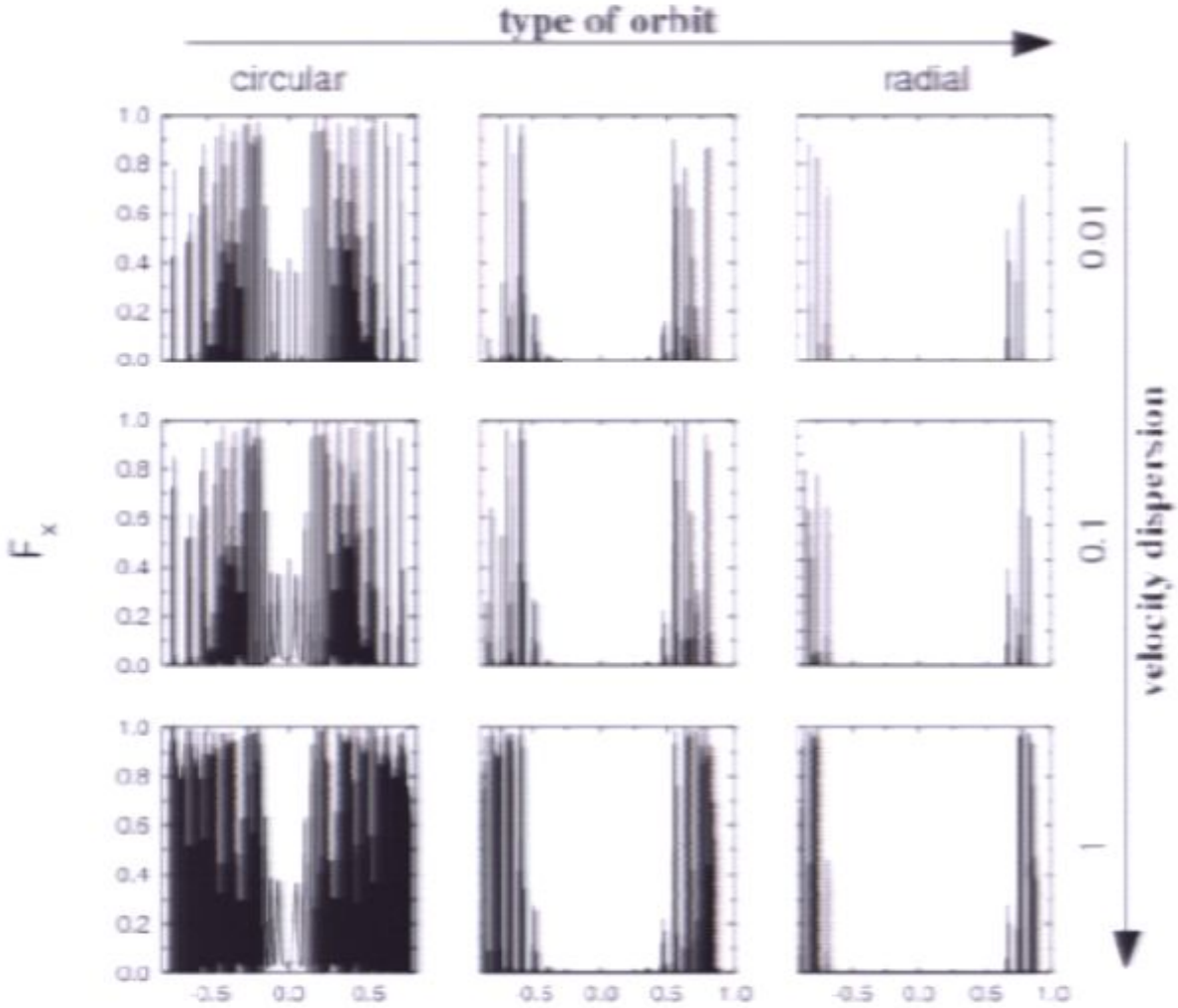

velocity-space distribution in a terrestrial detector due to three subhalos (Fantin et al. 2007)

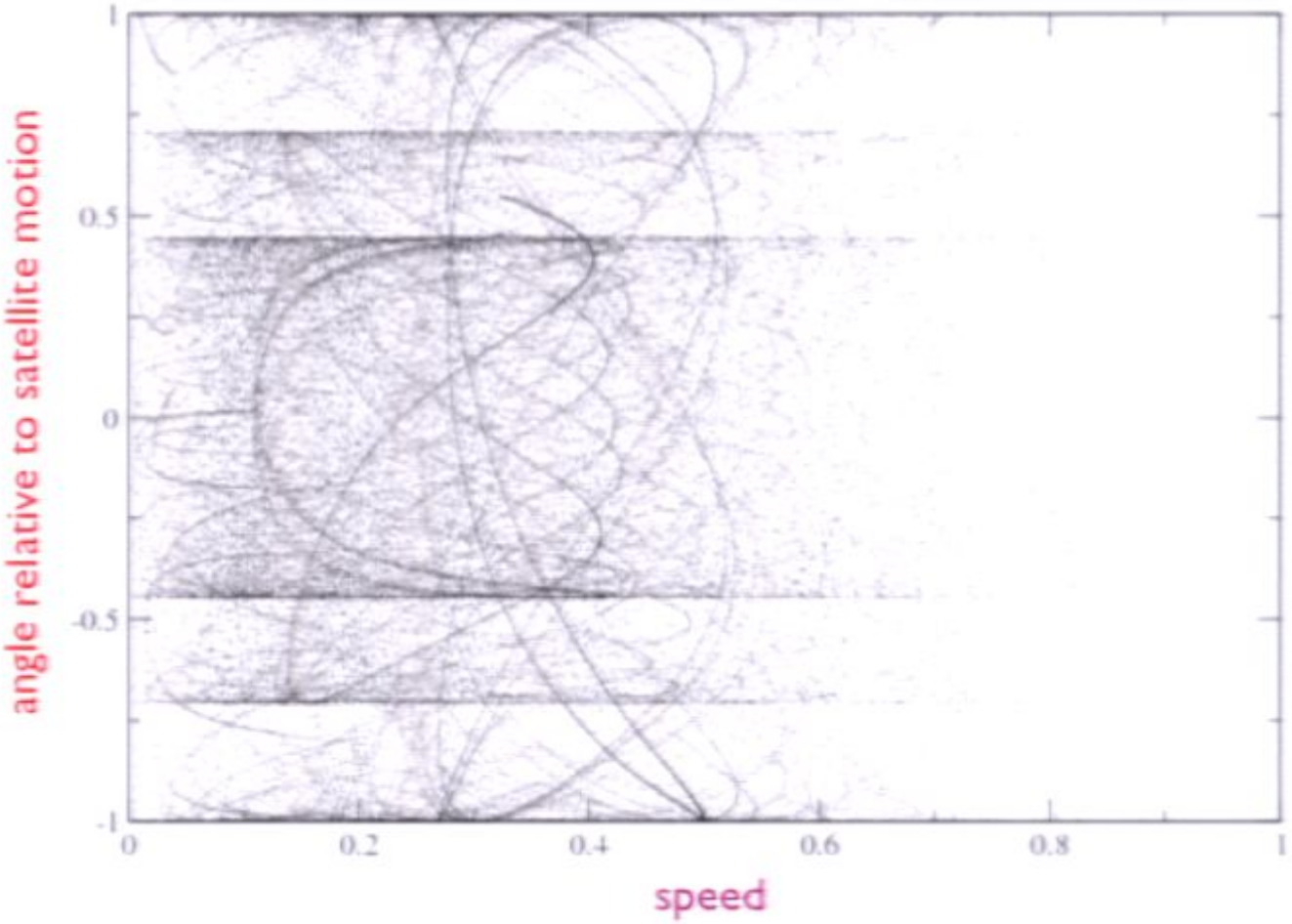

For a different approach based on "geodesic deviation" for nearby orbits, see Vogelsberger et al. 2008

velocity-space distribution in a terrestrial detector due to three subhalos (Fantin et al. 2007)

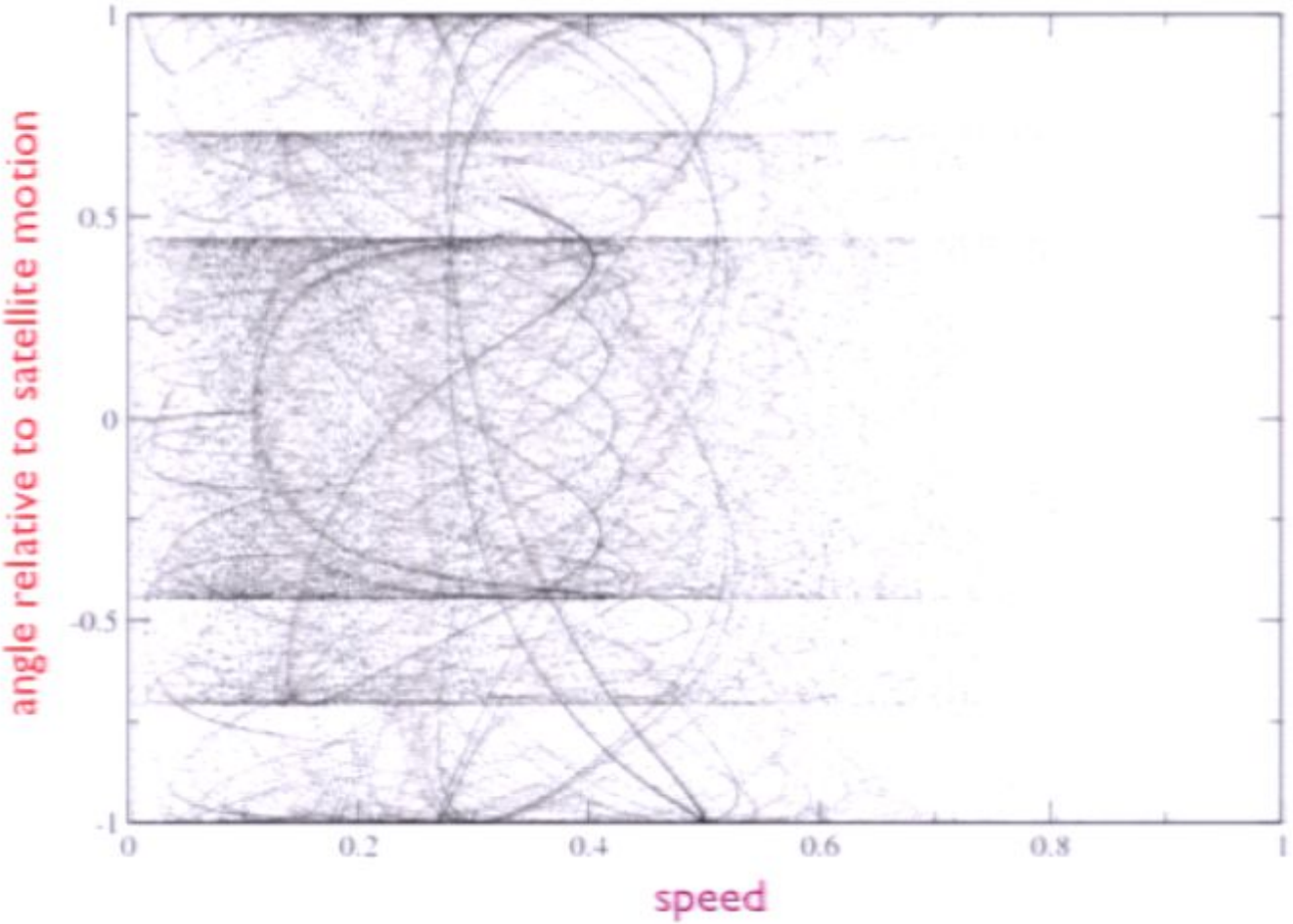

For a different approach based on "geodesic deviation" for nearby orbits, see Vogelsberger et al. 2008

velocity-space distribution in a terrestrial detector due to three subhalos (Fantin et al. 2007)

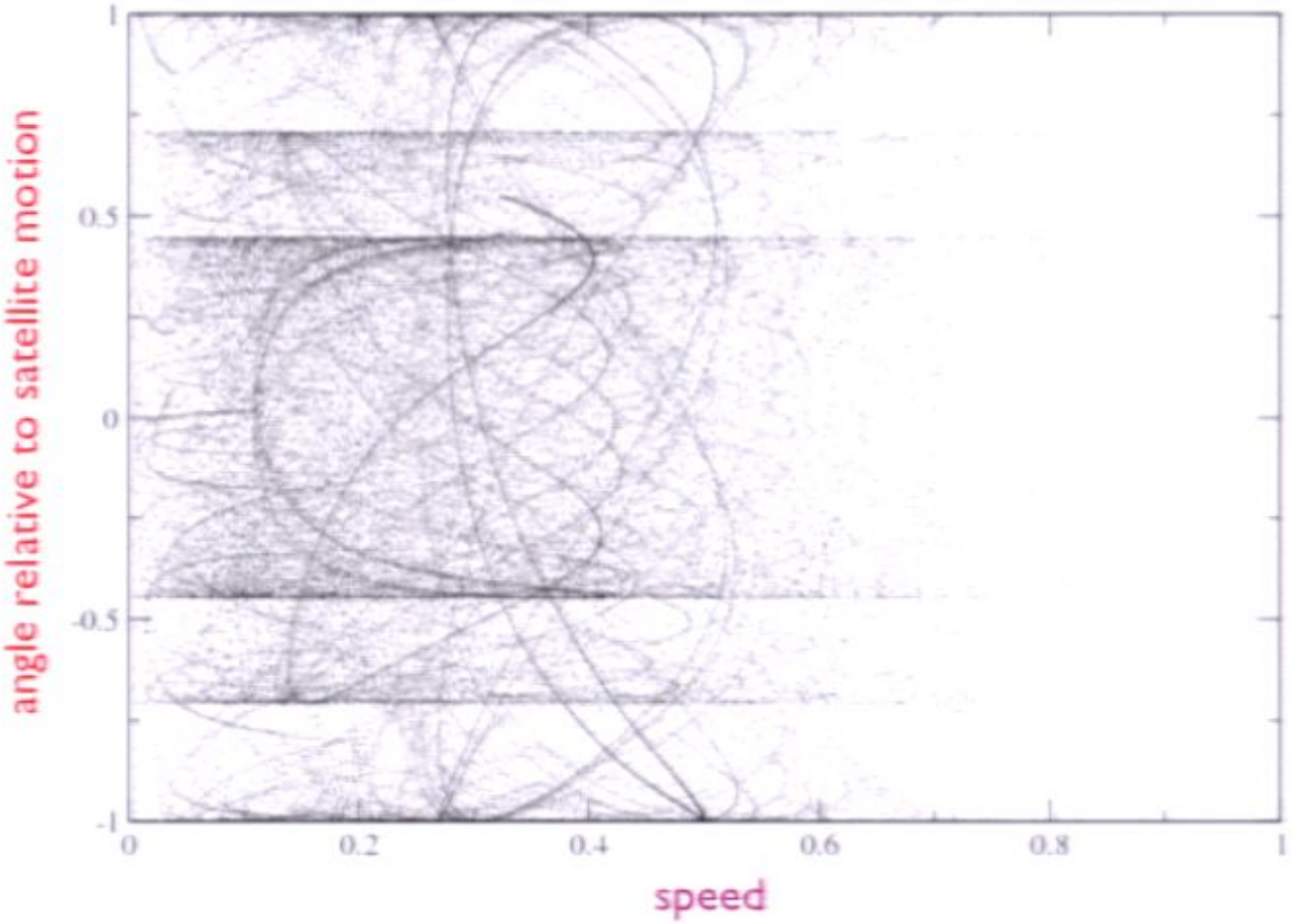

For a different approach based on "geodesic deviation" for nearby orbits, see Vogelsberger et al. 2008

velocity-space distribution in a terrestrial detector due to three subhalos (Fantin et al. 2007)

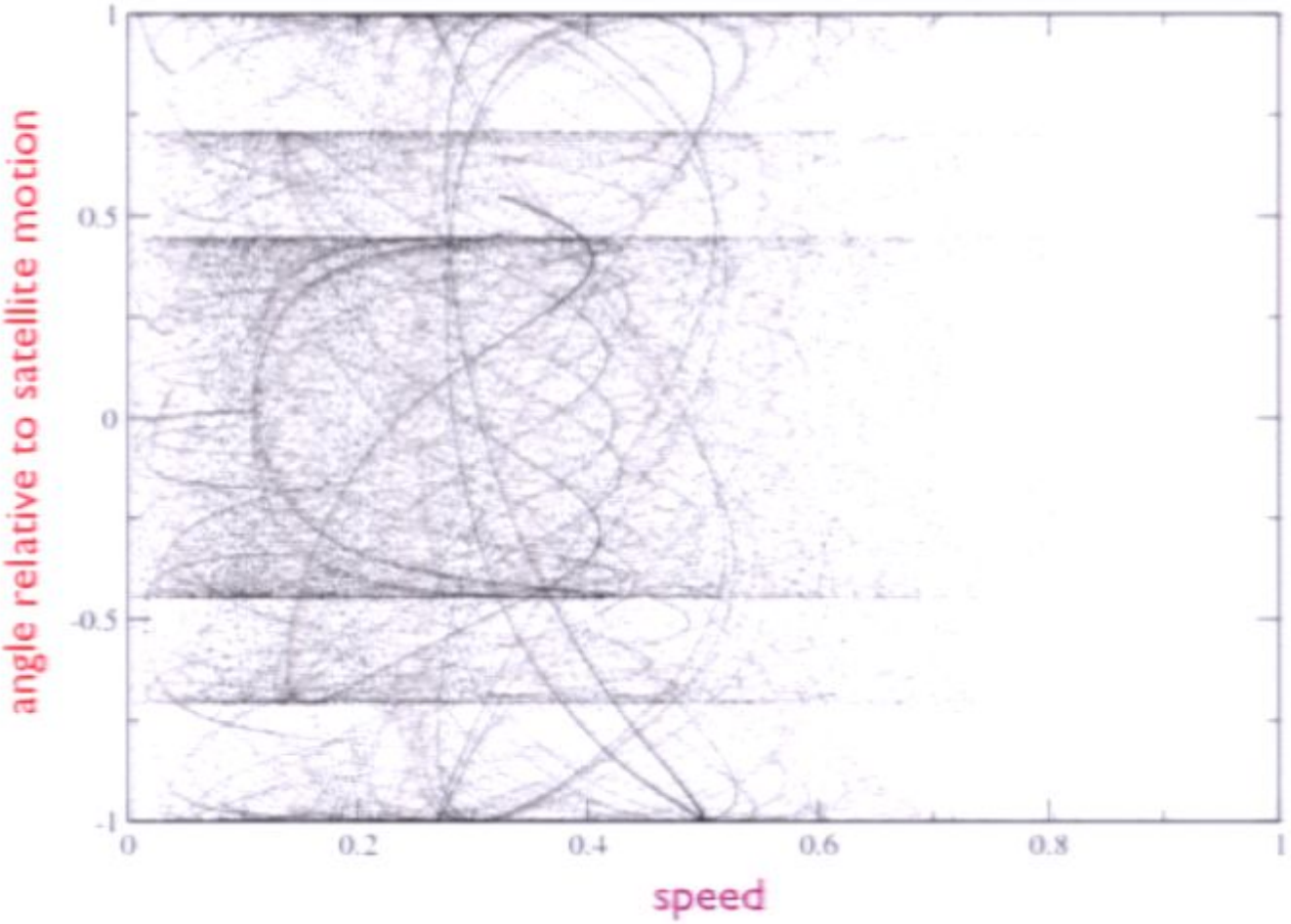

For a different approach based on "geodesic deviation" for nearby orbits, see Vogelsberger et al. 2008

velocity-space distribution in a terrestrial detector due to three subhalos (Fantin et al. 2007)

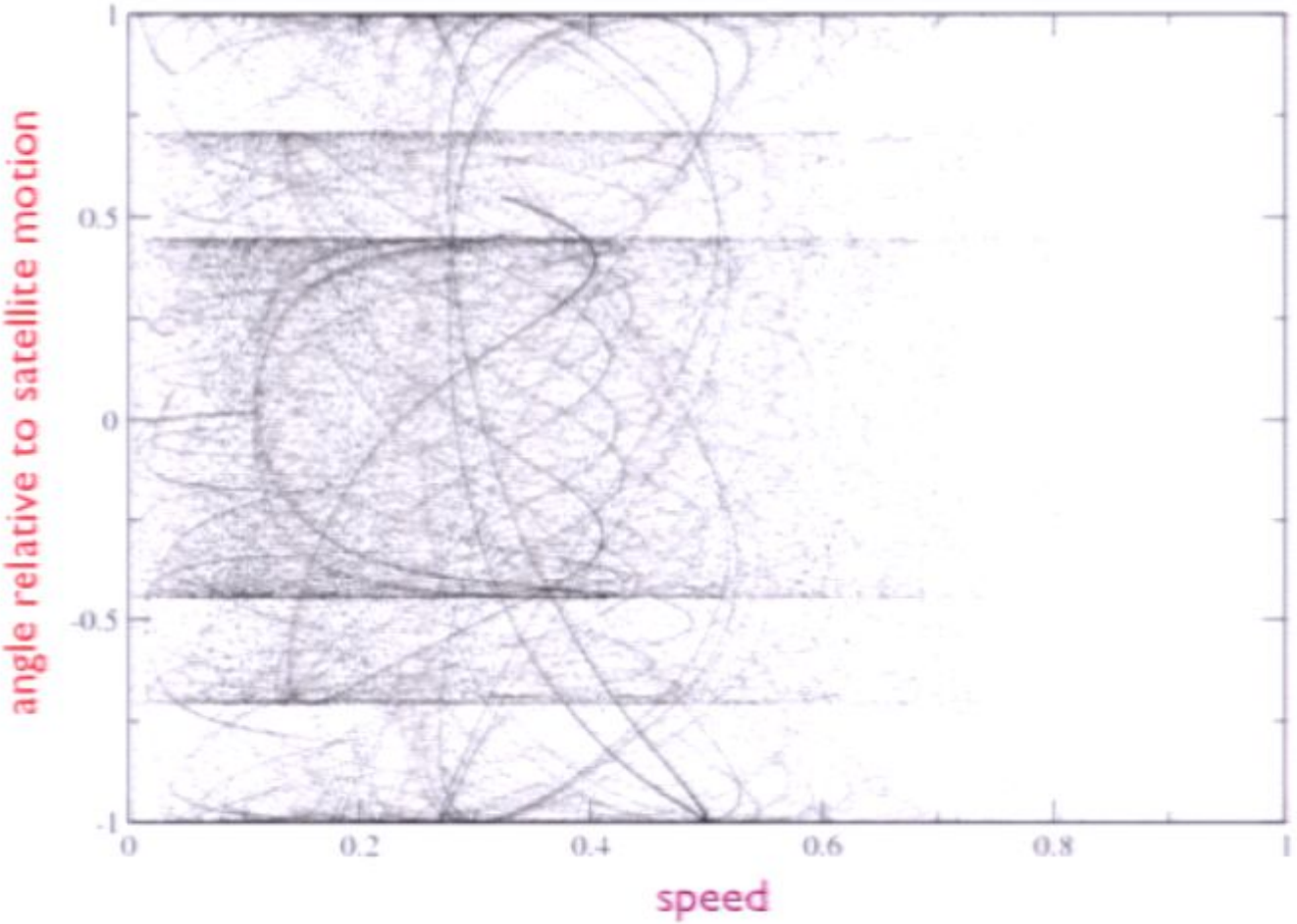

For a different approach based on "geodesic deviation" for nearby orbits, see Vogelsberger et al. 2008

velocity-space distribution in a terrestrial detector due to three subhalos (Fantin et al. 2007)

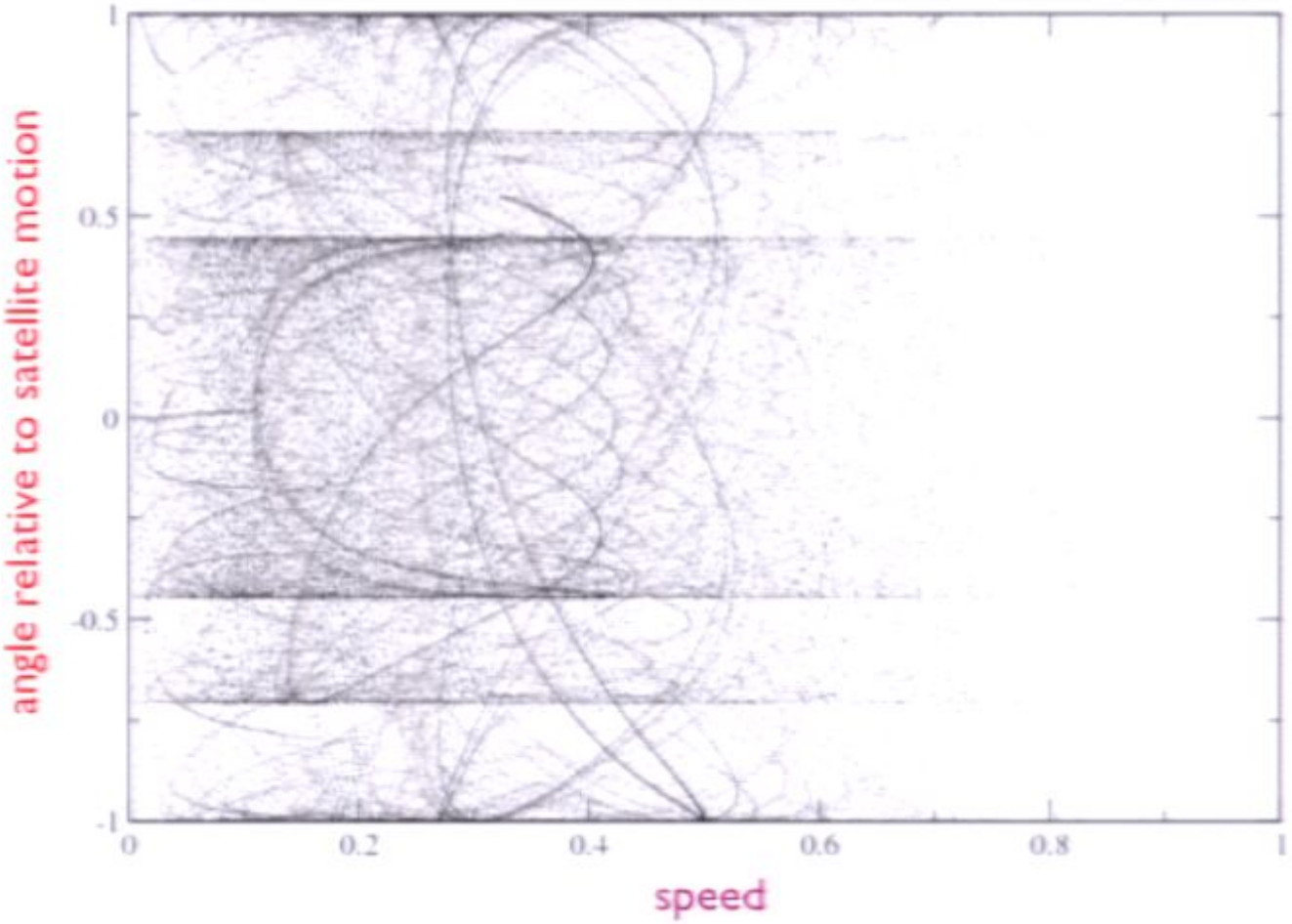

For a different approach based on "geodesic deviation" for nearby orbits, see Vogelsberger et al. 2008

velocity-space distribution in a terrestrial detector due to three subhalos (Fantin et al. 2007)

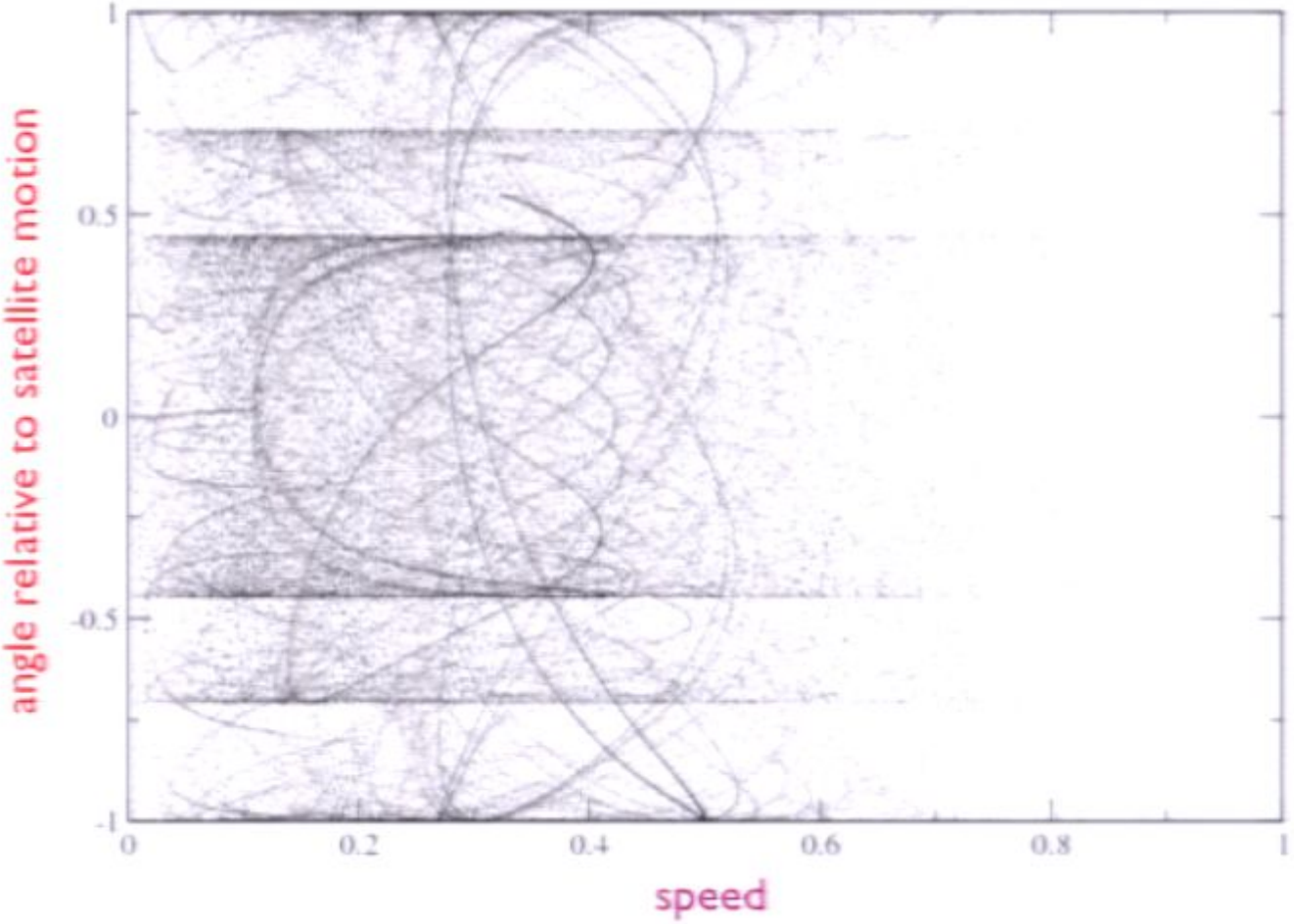

For a different approach based on "geodesic deviation" for nearby orbits, see Vogelsberger et al. 2008

velocity-space distribution in a terrestrial detector due to three subhalos (Fantin et al. 2007)

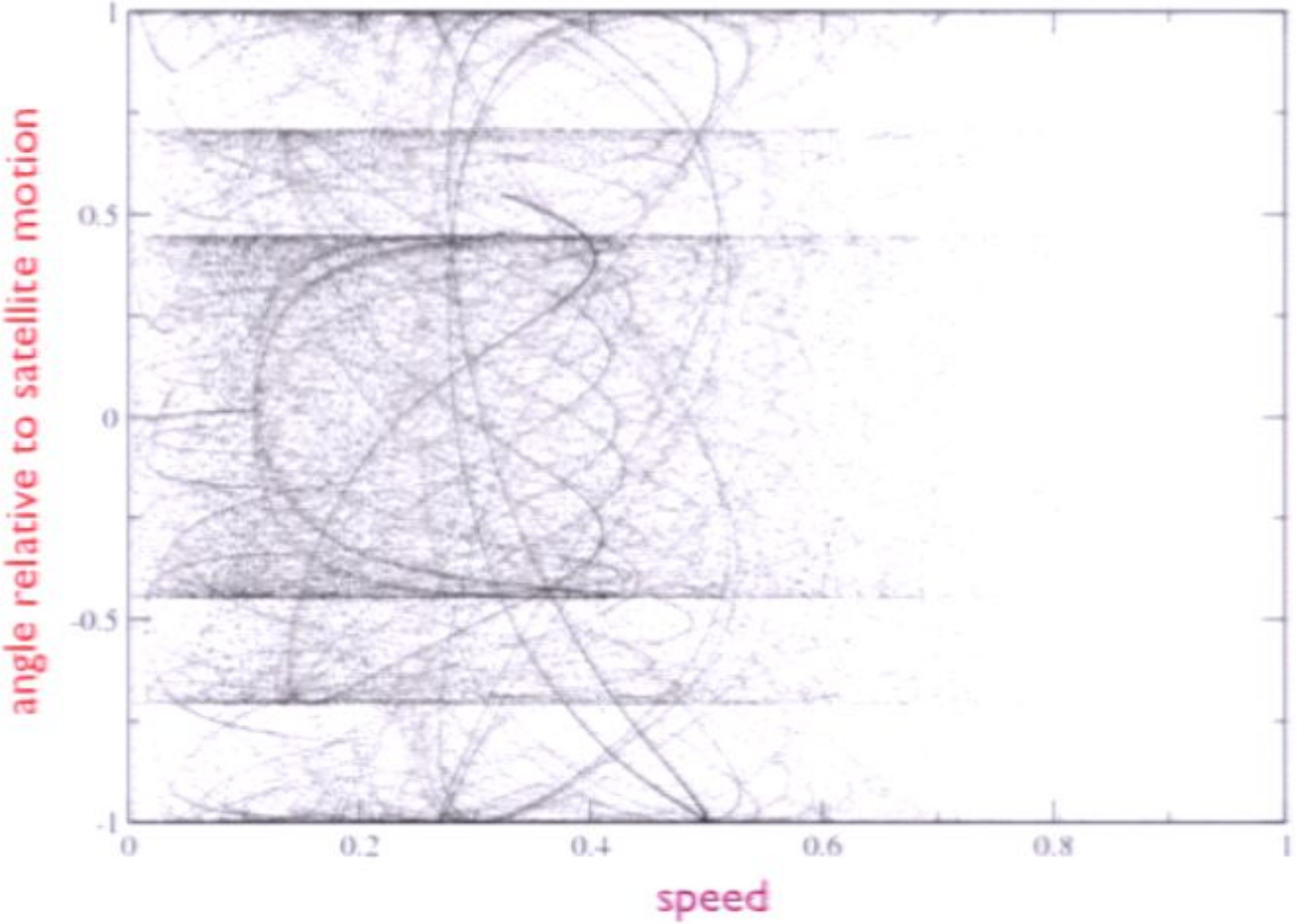

For a different approach based on "geodesic deviation" for nearby orbits, see Vogelsberger et al. 2008

velocity-space distribution in a terrestrial detector due to three subhalos (Fantin et al. 2007)

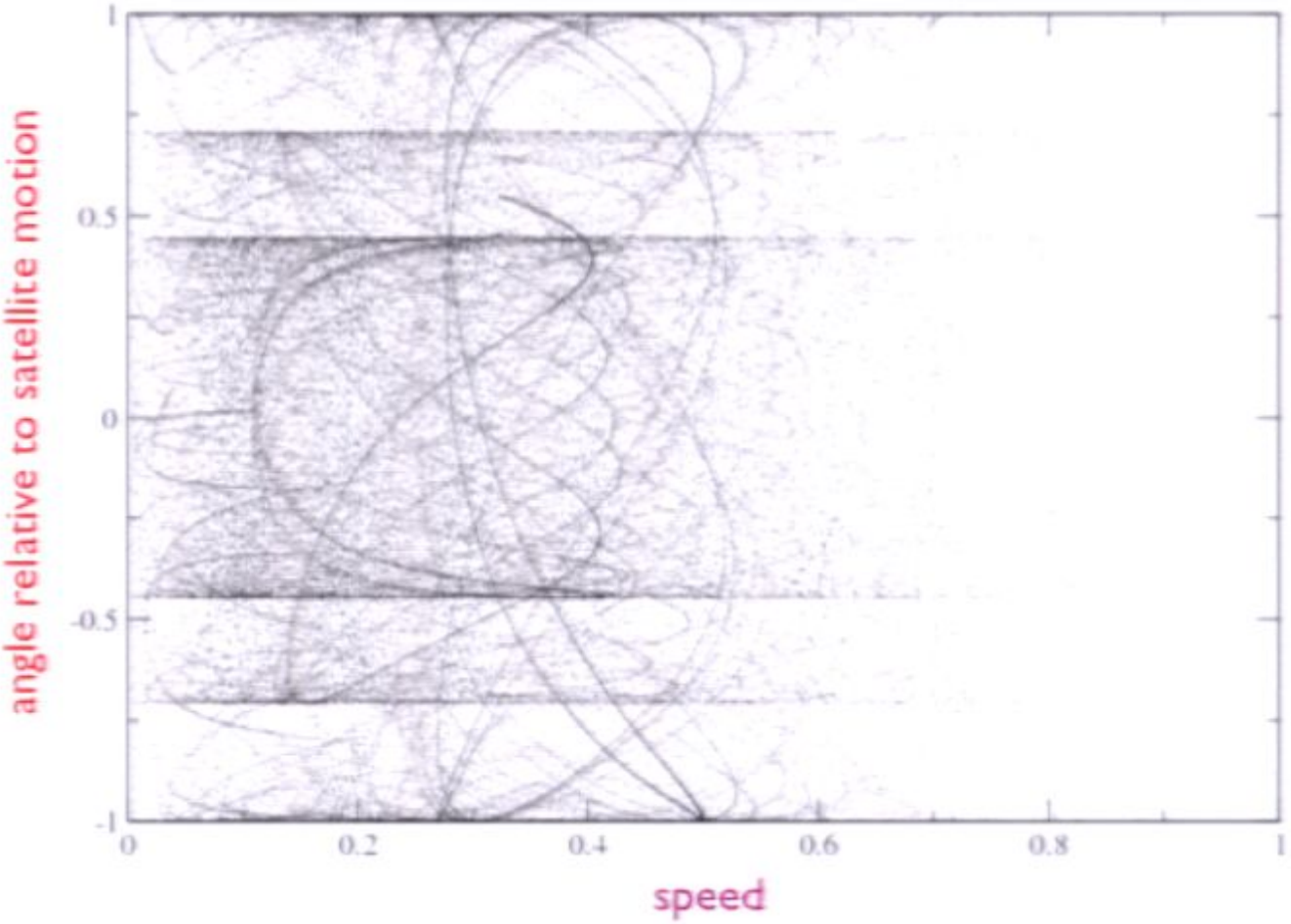

For a different approach based on "geodesic deviation" for nearby orbits, see Vogelsberger et al. 2008

velocity-space distribution in a terrestrial detector due to three subhalos (Fantin et al. 2007)

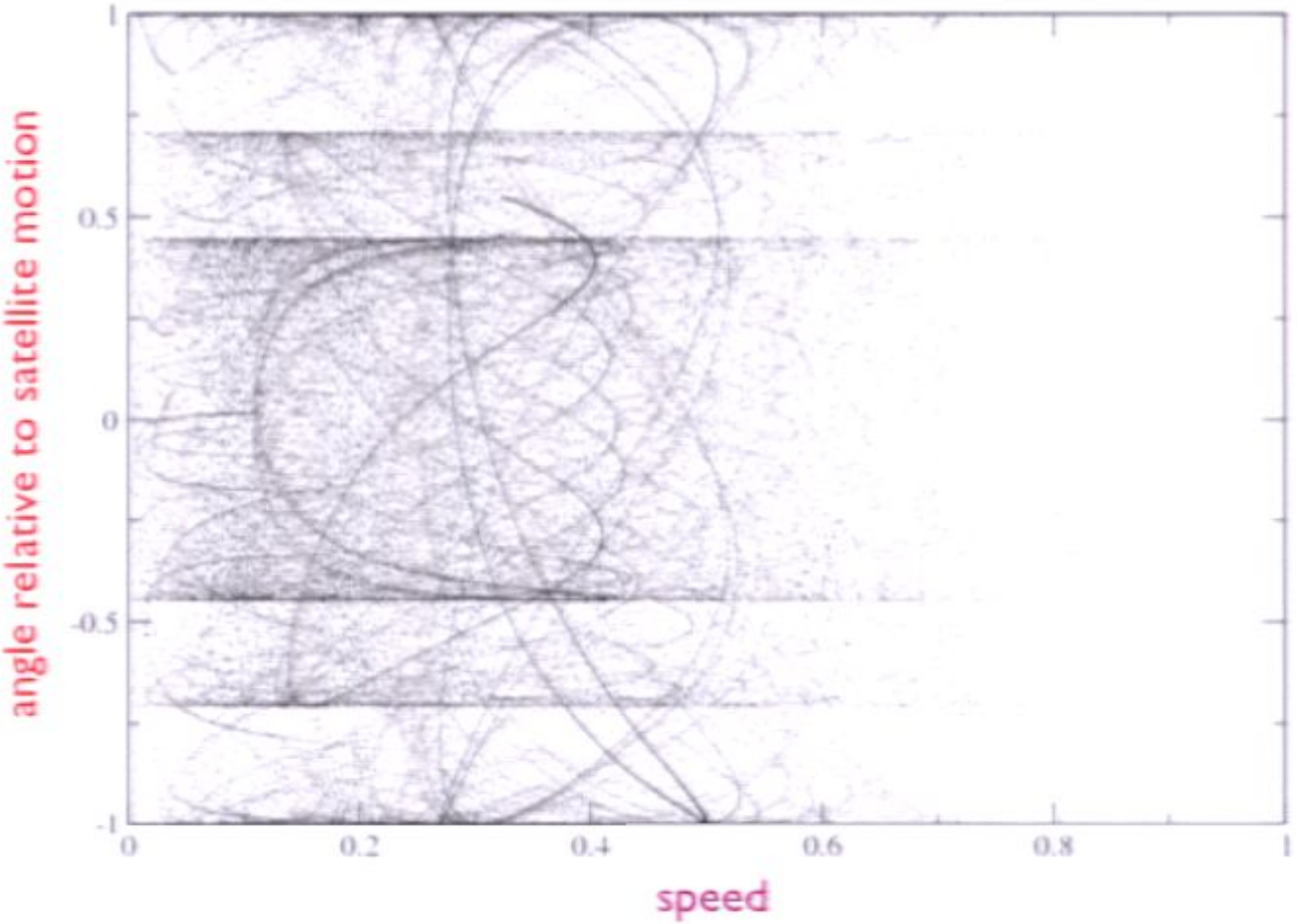

For a different approach based on "geodesic deviation" for nearby orbits, see Vogelsberger et al. 2008

velocity-space distribution in a terrestrial detector due to three subhalos (Fantin et al. 2007)

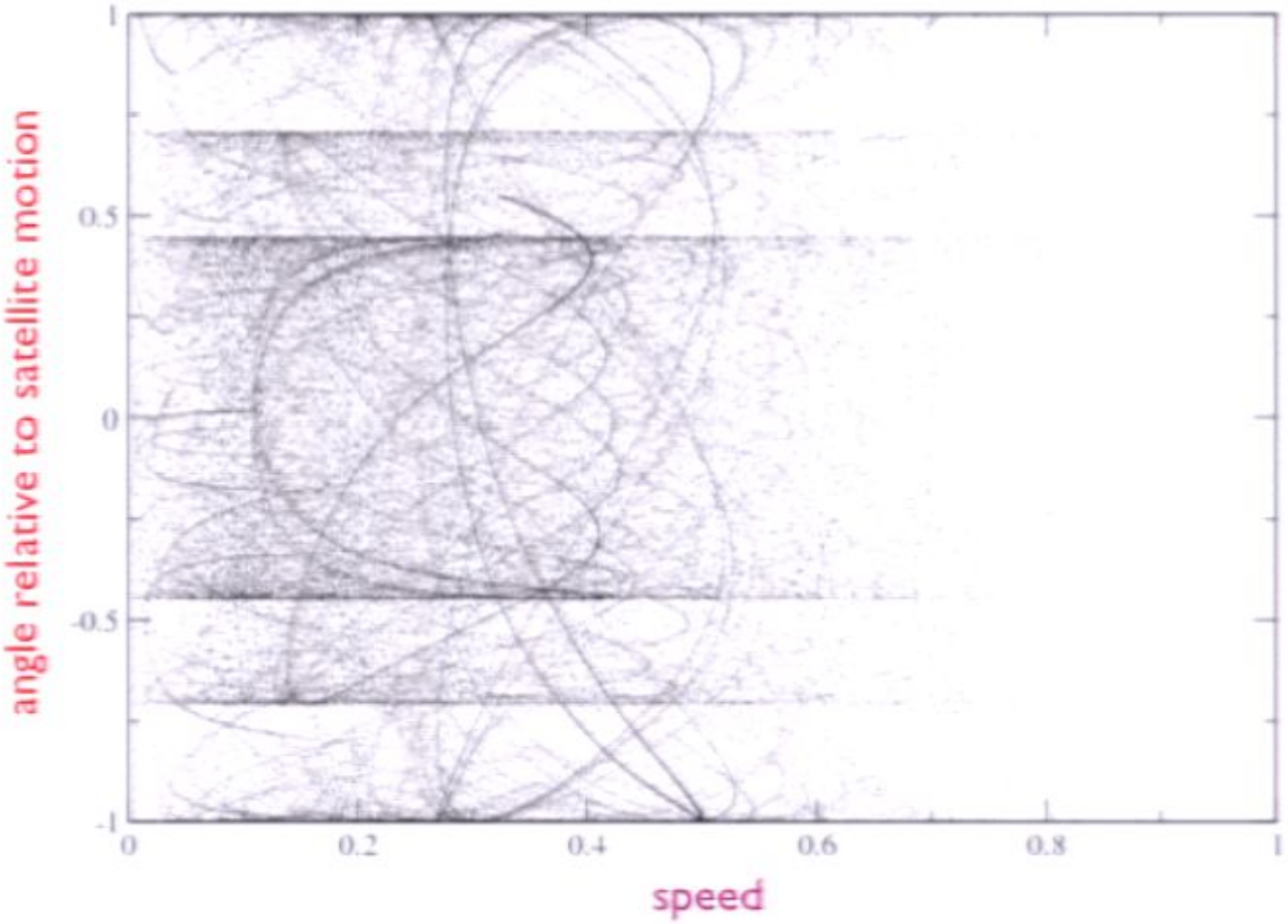

For a different approach based on "geodesic deviation" for nearby orbits, see Vogelsberger et al. 2008

velocity-space distribution in a terrestrial detector due to three subhalos (Fantin et al. 2007)

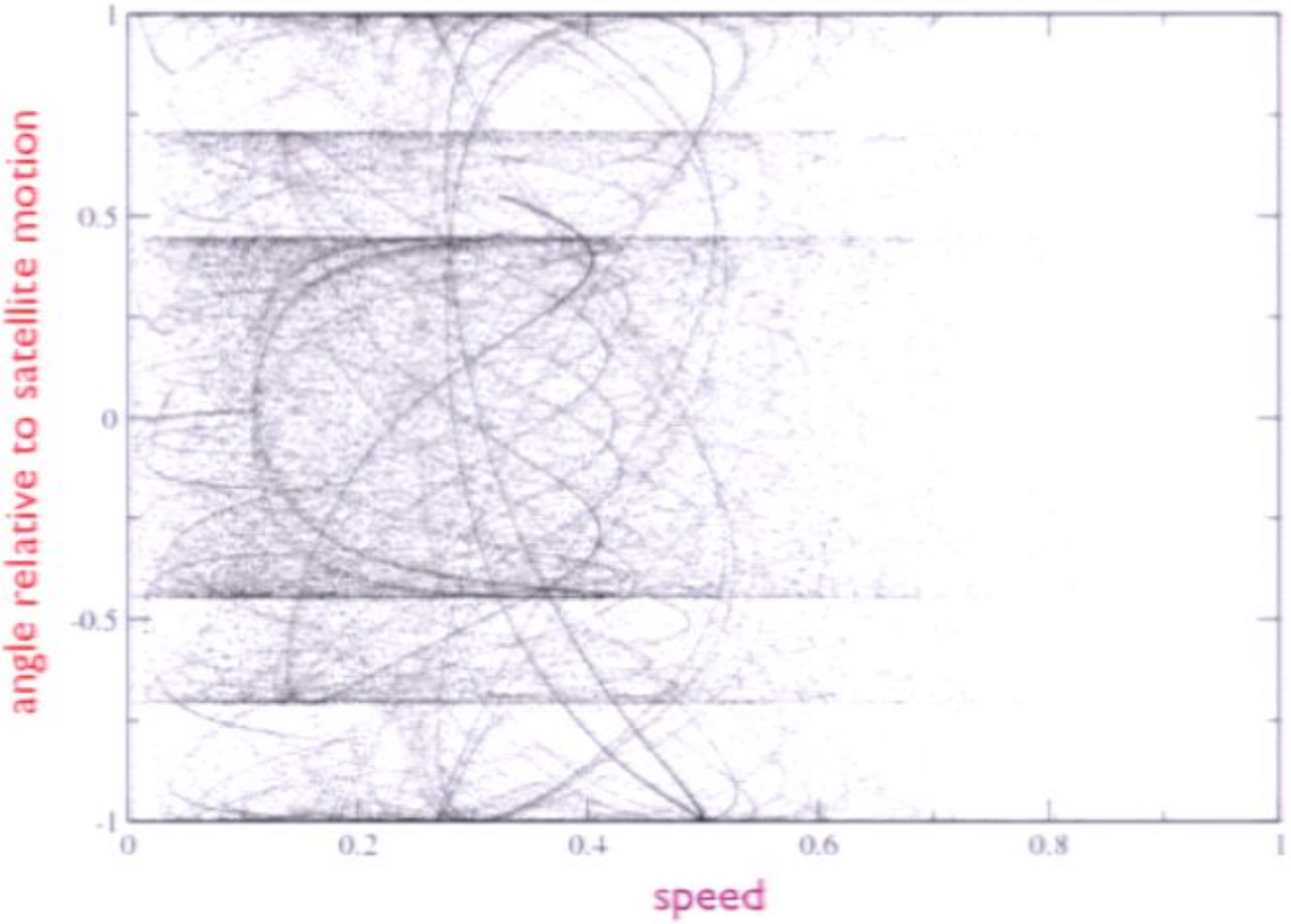

For a different approach based on "geodesic deviation" for nearby orbits, see Vogelsberger et al. 2008

velocity-space distribution in a terrestrial detector due to three subhalos (Fantin et al. 2007)

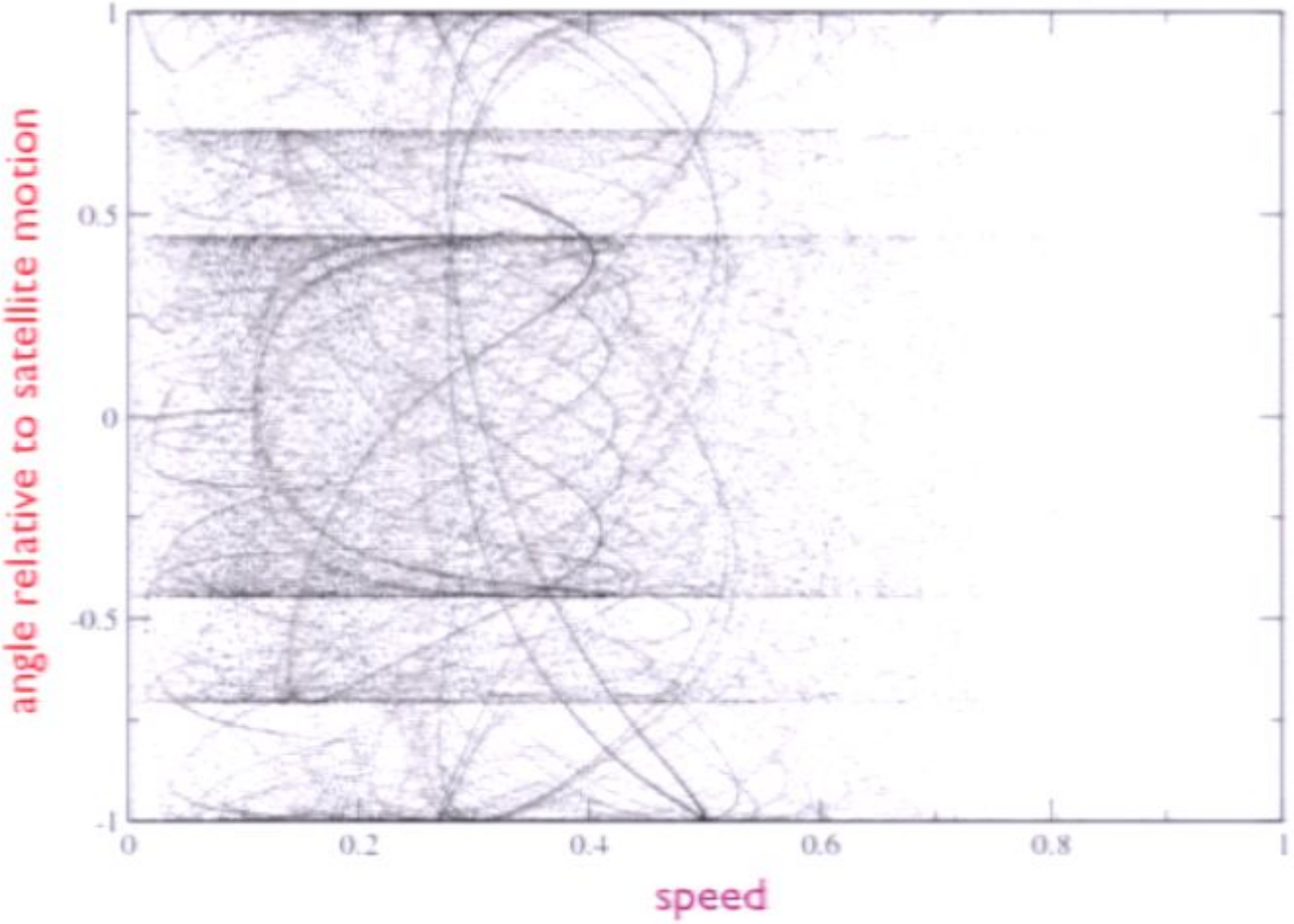

For a different approach based on "geodesic deviation" for nearby orbits, see Vogelsberger et al. 2008

velocity-space distribution in a terrestrial detector due to three subhalos (Fantin et al. 2007)

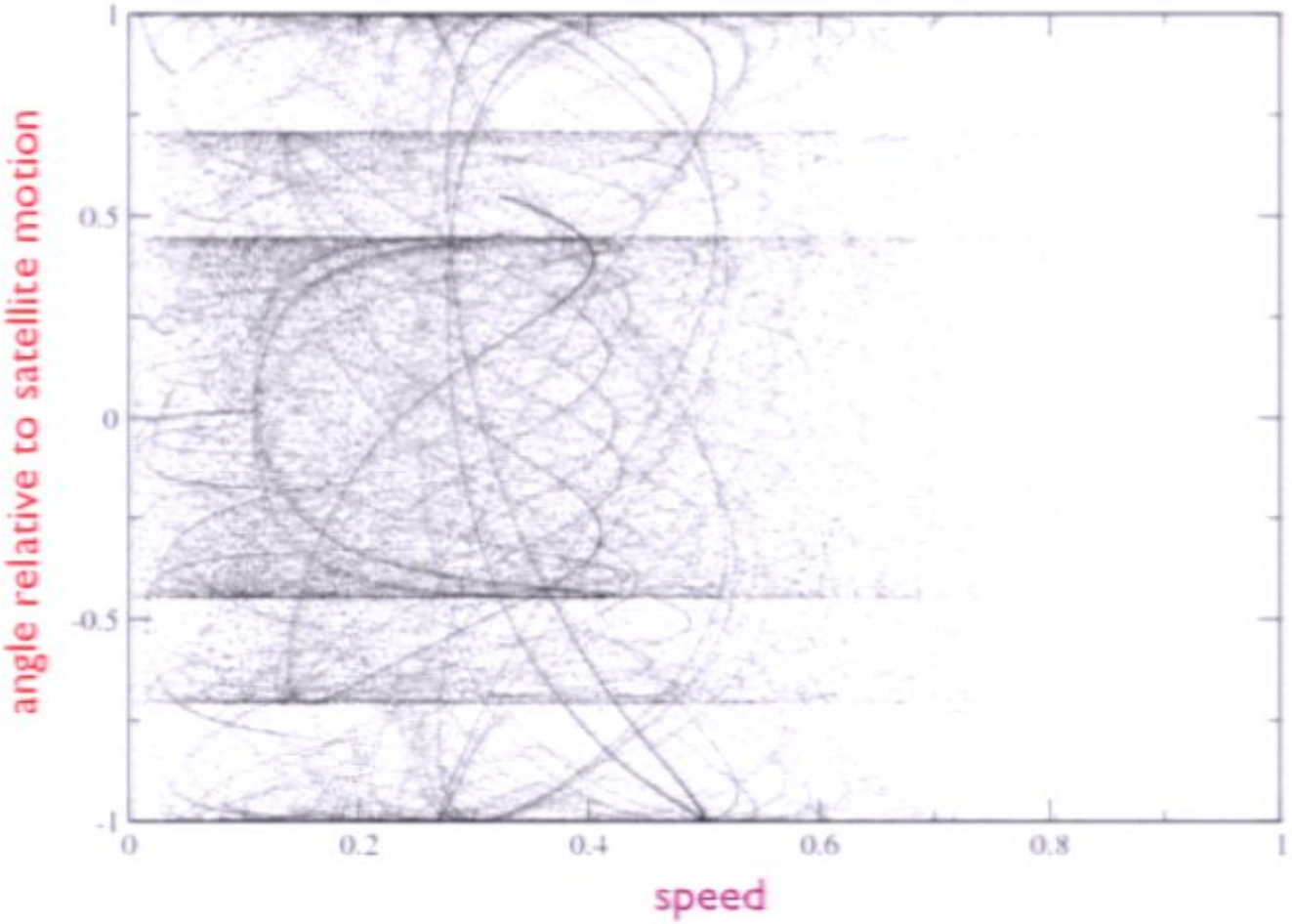

For a different approach based on "geodesic deviation" for nearby orbits, see Vogelsberger et al. 2008

velocity-space distribution in a terrestrial detector due to three subhalos (Fantin et al. 2007)

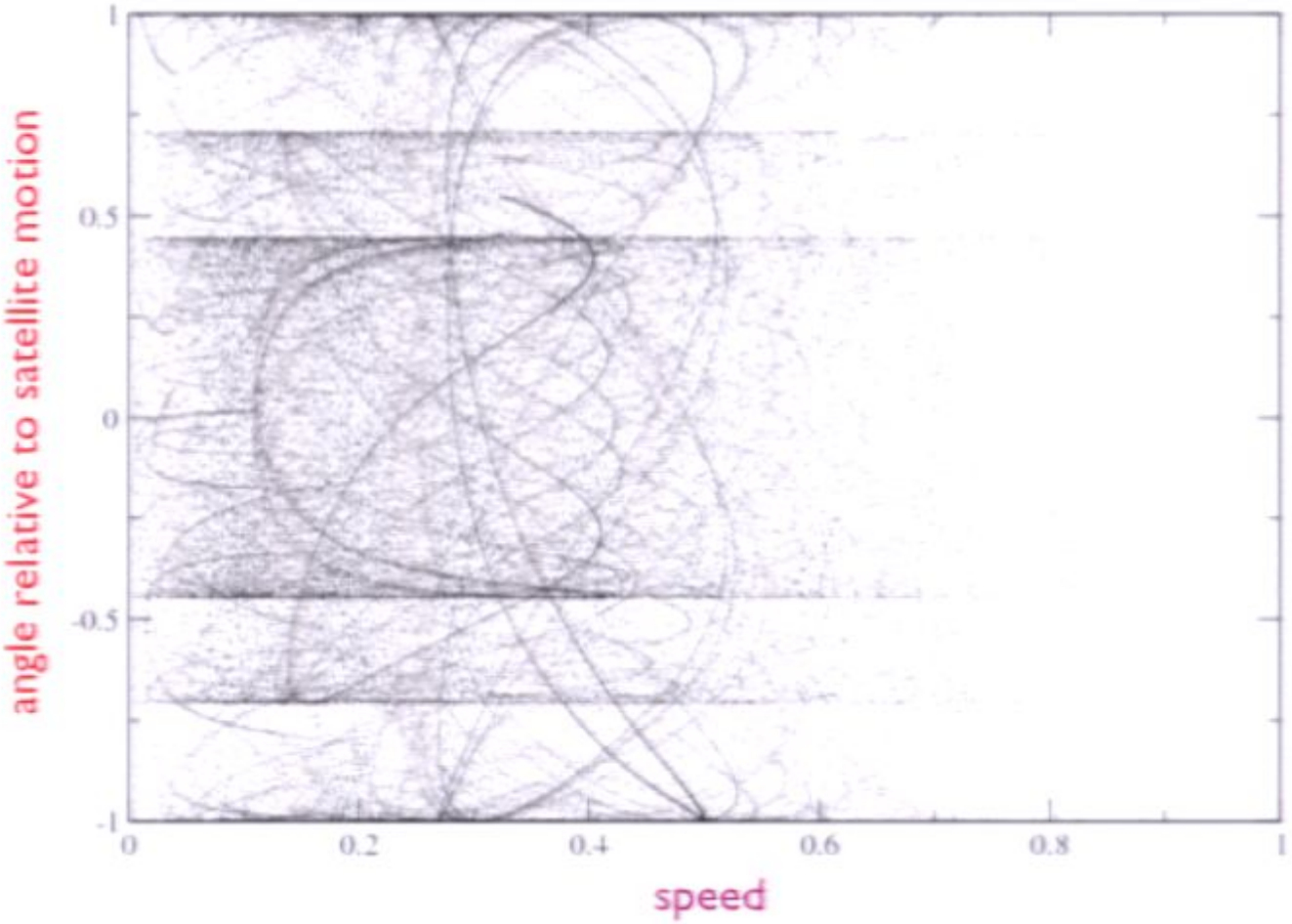

For a different approach based on "geodesic deviation" for nearby orbits, see Vogelsberger et al. 2008

velocity-space distribution in a terrestrial detector due to three subhalos (Fantin et al. 2007)

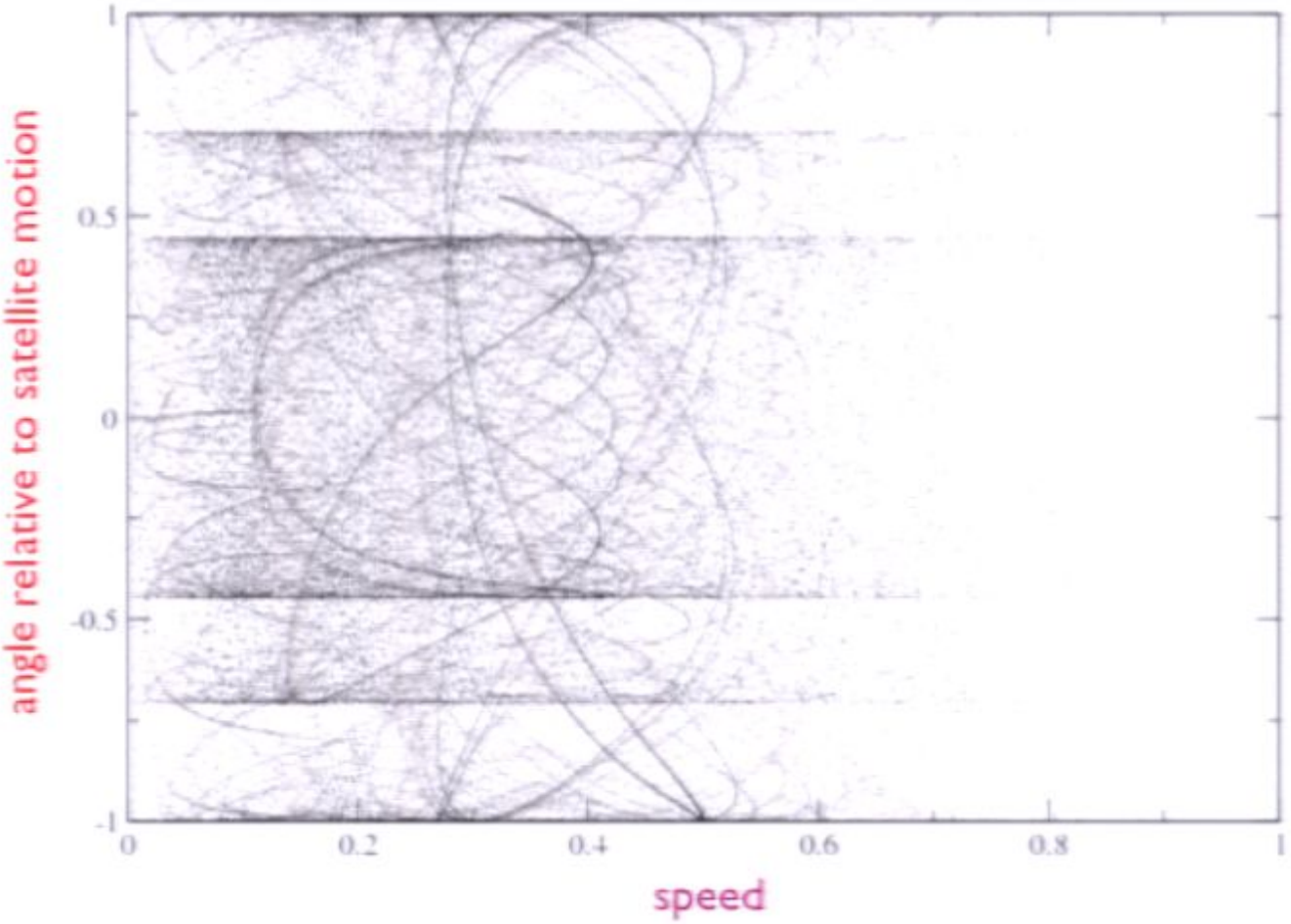

For a different approach based on "geodesic deviation" for nearby orbits, see Vogelsberger et al. 2008

Fantin et al. explore different orbits and effect of initial internal dispersion of the satellite

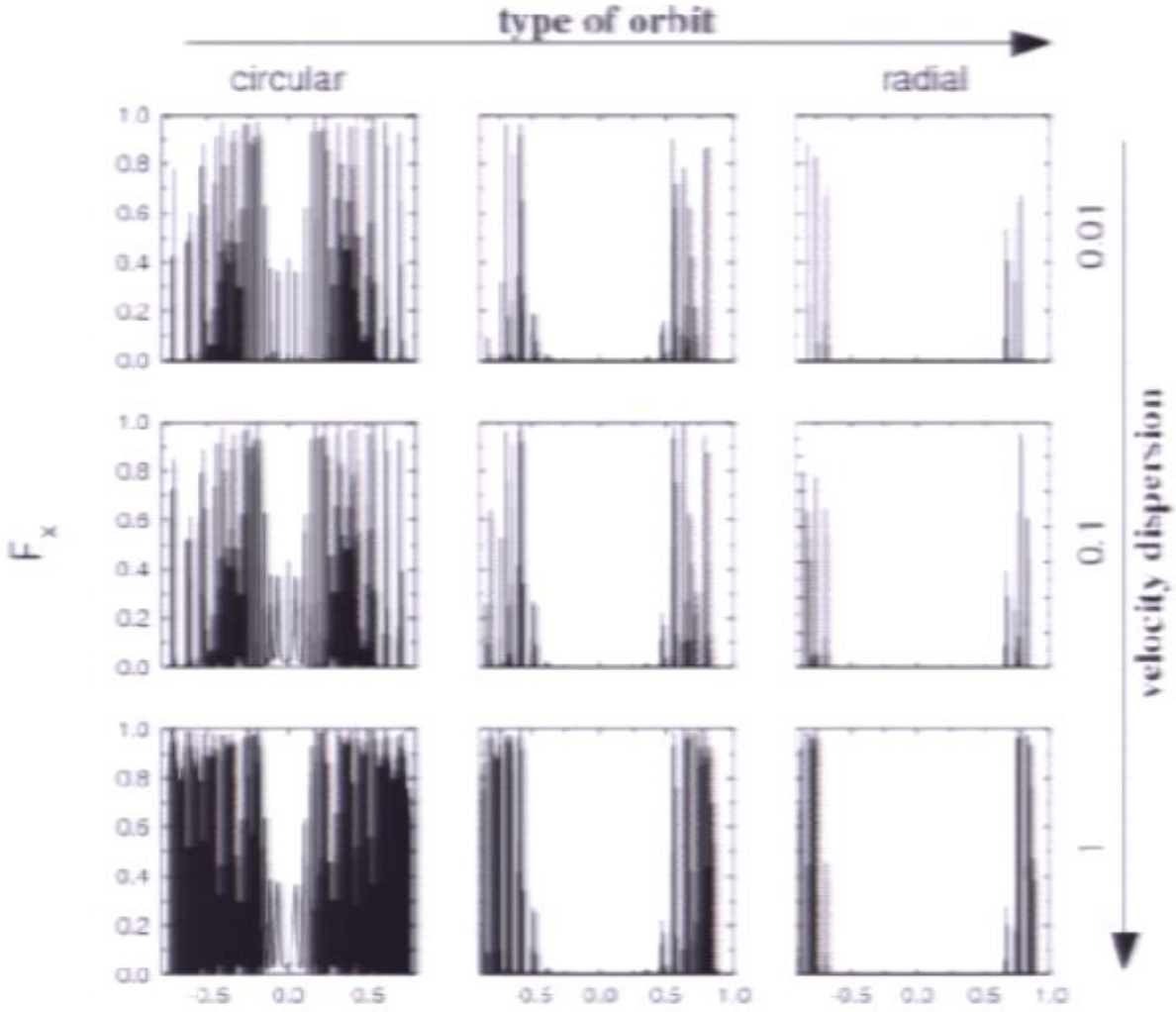

Fantin et al. explore different orbits and effect of initial internal dispersion of the satellite

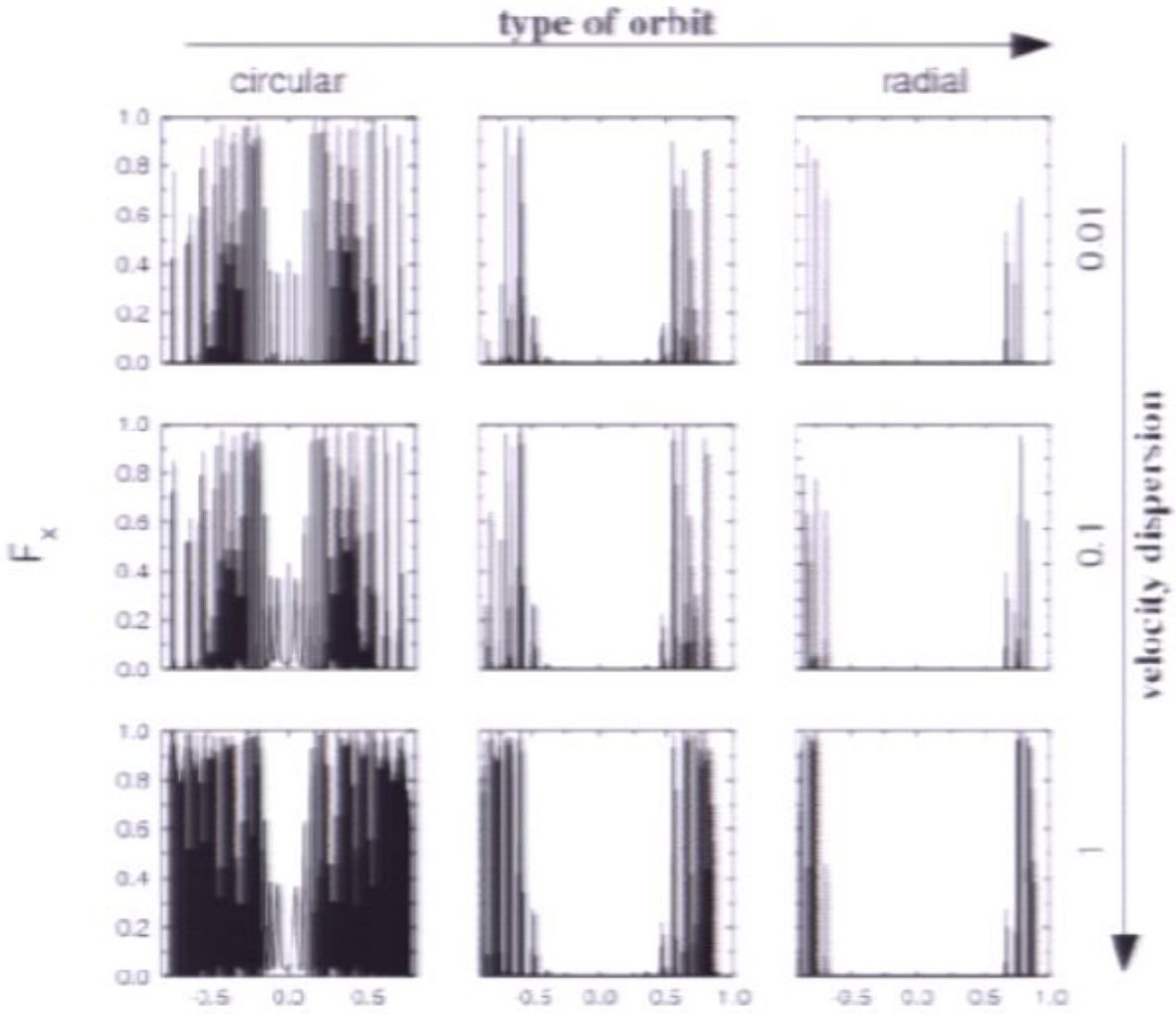

Fantin et al. explore different orbits and effect of initial internal dispersion of the satellite

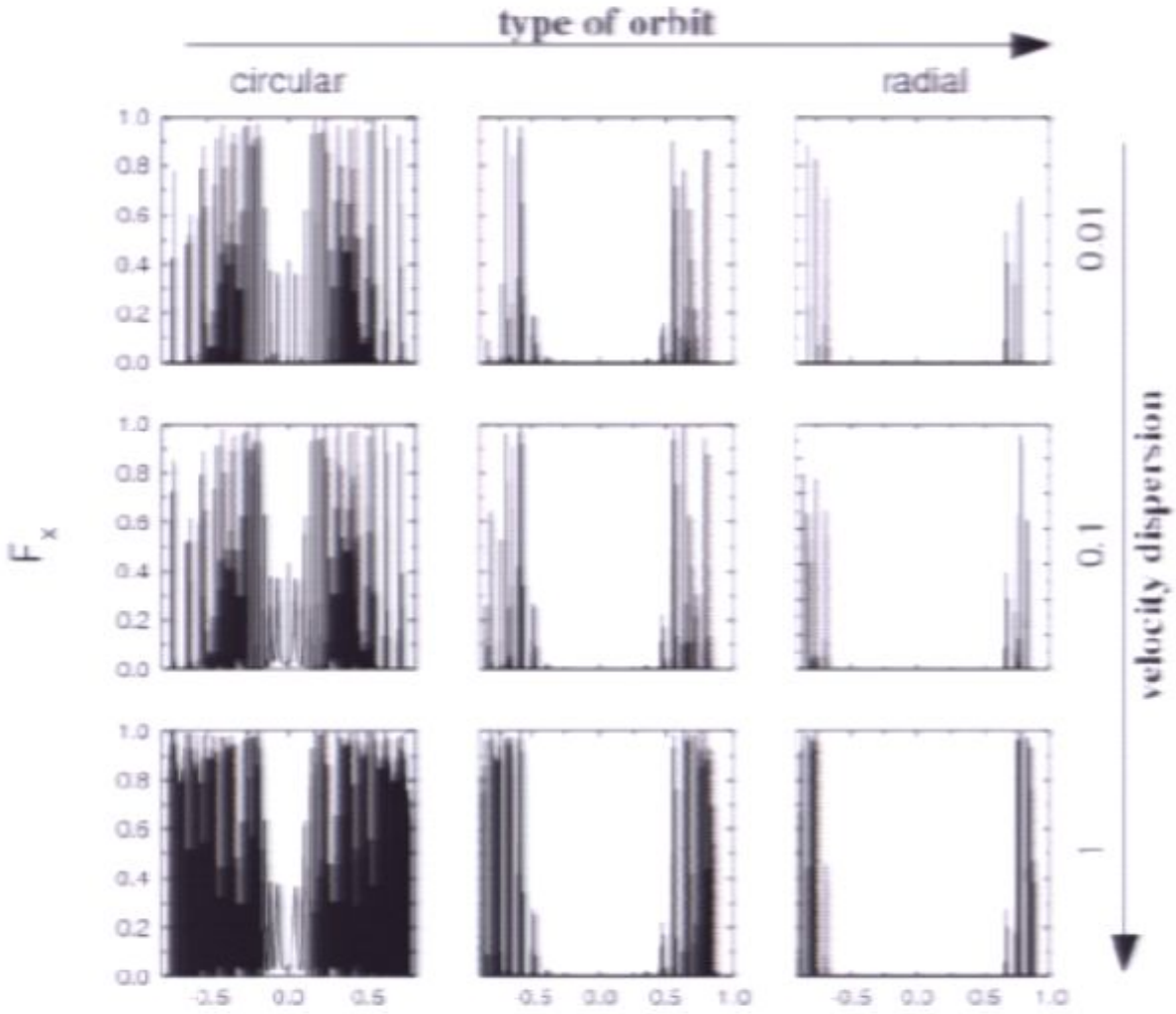

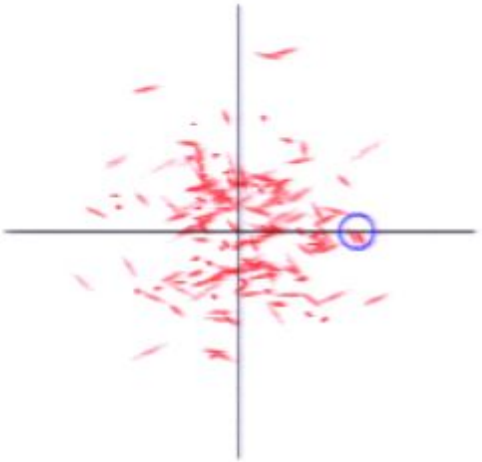

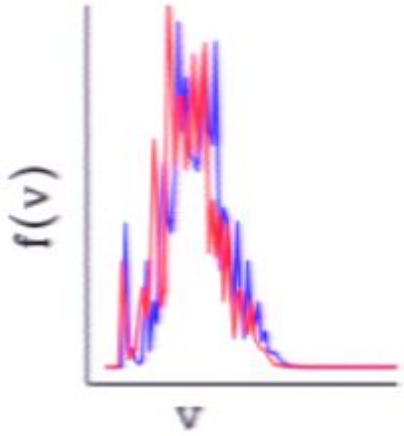

Possible phenomenological model for local f(v)

$$f(\mathbf{v}) = \sum_{\text{streams}} f_s\left(\bar{\mathbf{v}}_i, \sigma_{ij,s}\right)$$

key question: how many streams and what is their distribution (see Helmi & White 1999 Vogelsberger et al. 2008)

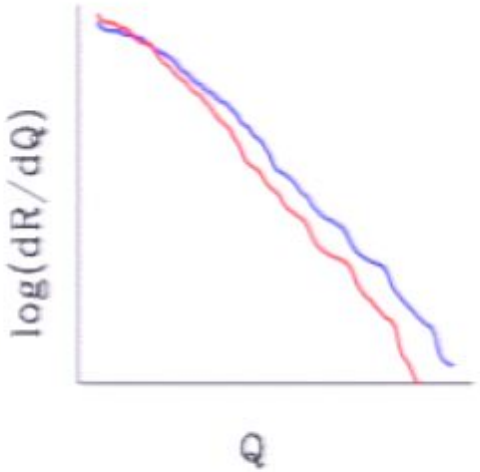

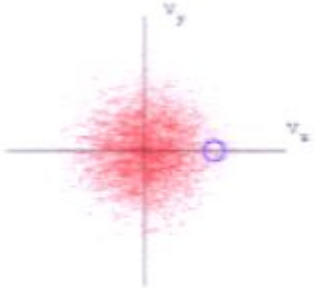

standard Maxwellian

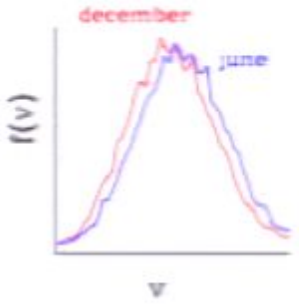

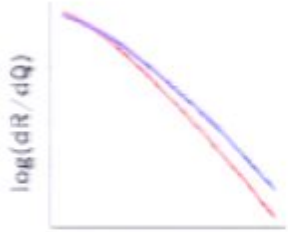

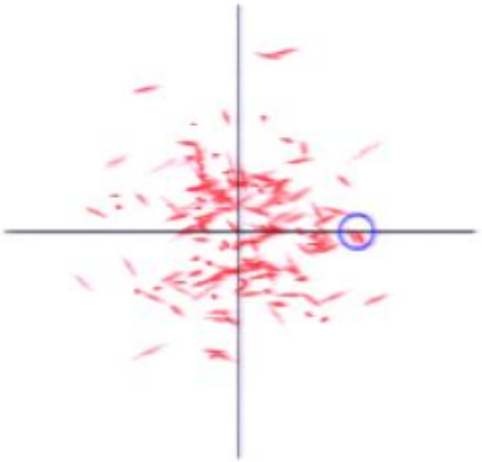

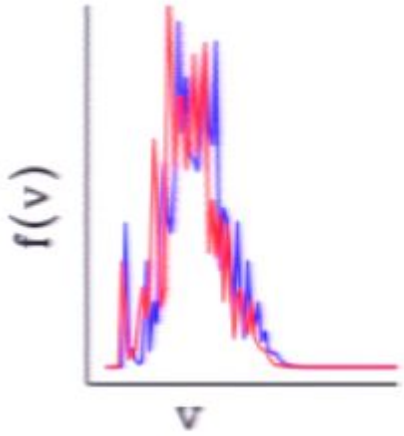

Possible phenomenological model for local f(v)

$$f(\mathbf{v}) = \sum_{\text{streams}} f_s\left(\bar{\mathbf{v}}_i, \sigma_{ij,s}\right)$$

key question: how many streams and what is their distribution (see Helmi & White 1999 Vogelsberger et al. 2008)

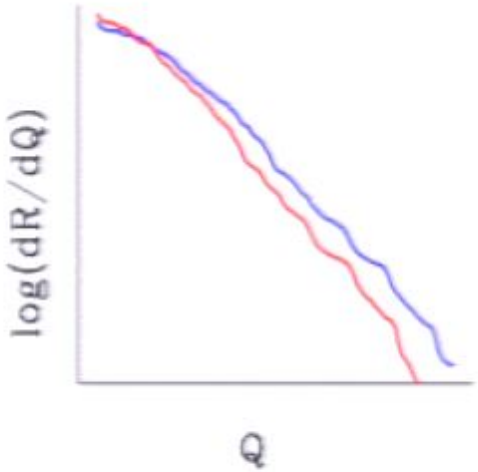

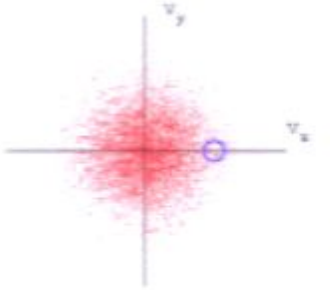

standard Maxwellian

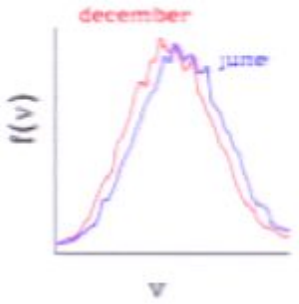

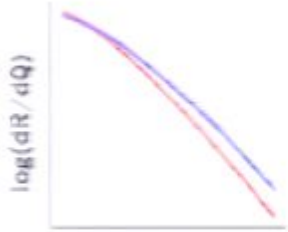

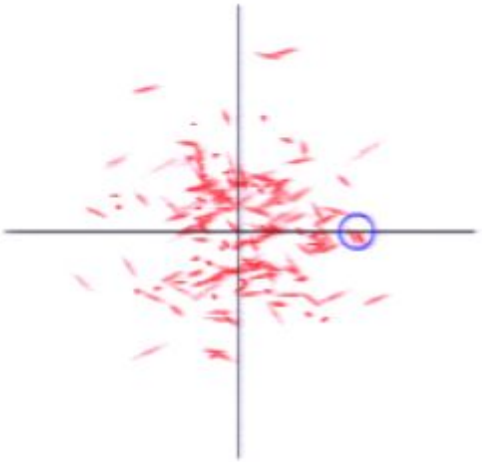

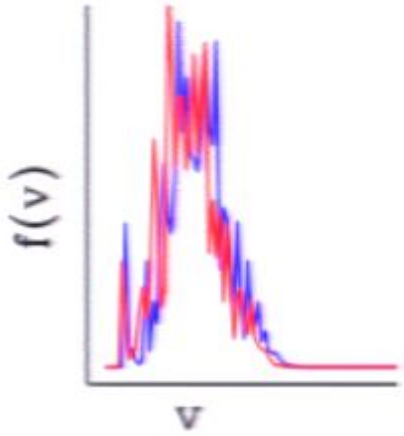

Possible phenomenological model for local f(v)

$$f(\mathbf{v}) = \sum_{\text{streams}} f_s\left(\bar{\mathbf{v}}_i, \sigma_{ij,s}\right)$$

key question: how many streams and what is their distribution (see Helmi & White 1999 Vogelsberger et al. 2008)

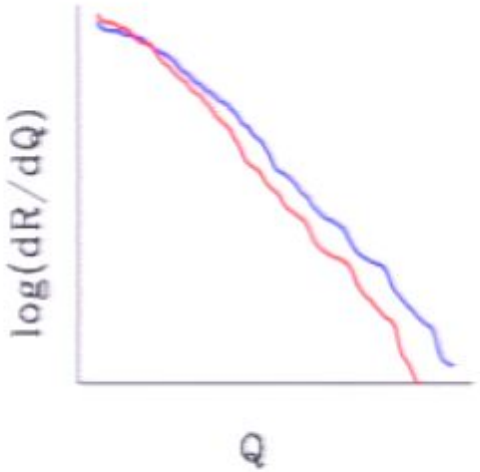

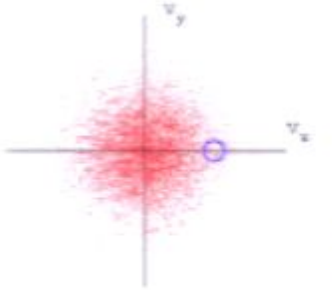

standard Maxwellian

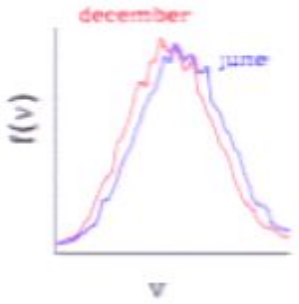

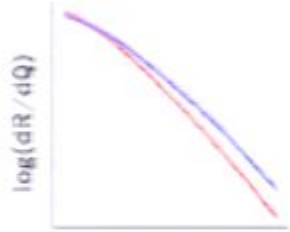

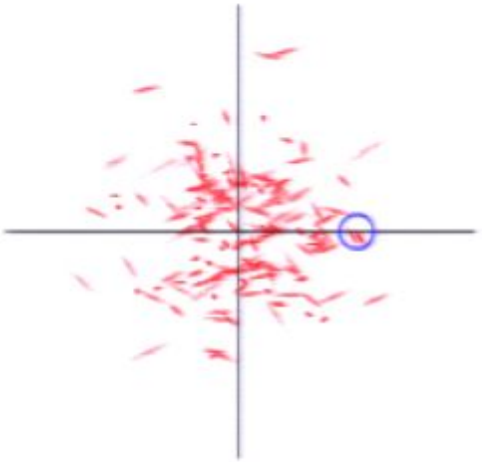

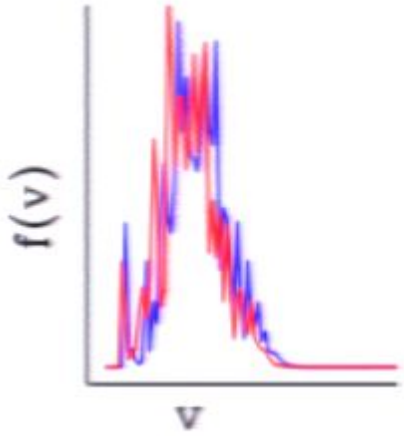

Possible phenomenological model for local f(v)

$$f(\mathbf{v}) = \sum_{\text{streams}} f_s\left(\bar{\mathbf{v}}_i,\, \sigma_{ij,s}\right)$$

key question: how many streams and what is their distribution (see Helmi & White 1999 Vogelsberger et al. 2008)

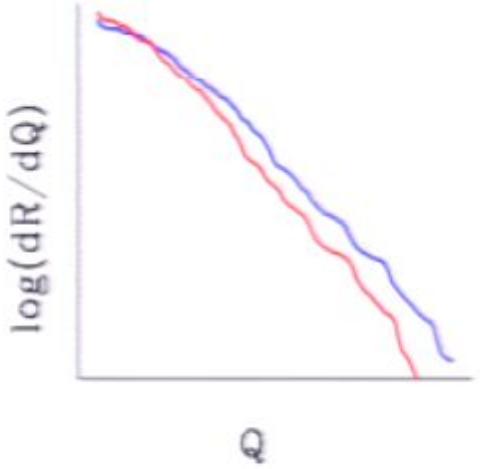

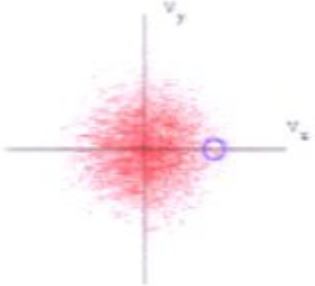

standard Maxwellian

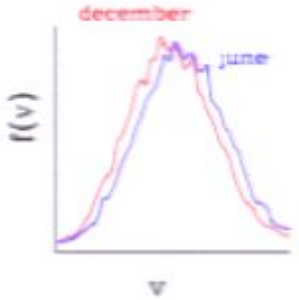

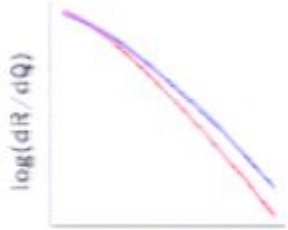

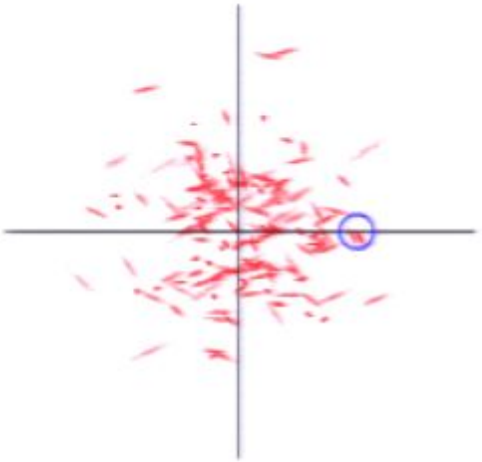

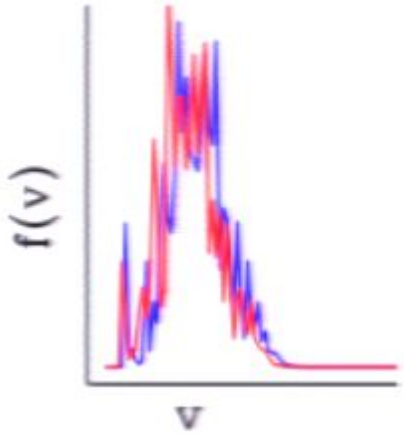

Possible phenomenological model for local f(v)

$$f(\mathbf{v}) = \sum_{\text{streams}} f_s\left(\bar{\mathbf{v}}_i, \sigma_{ij,s}\right)$$

key question: how many streams and what is their distribution (see Helmi & White 1999 Vogelsberger et al. 2008)

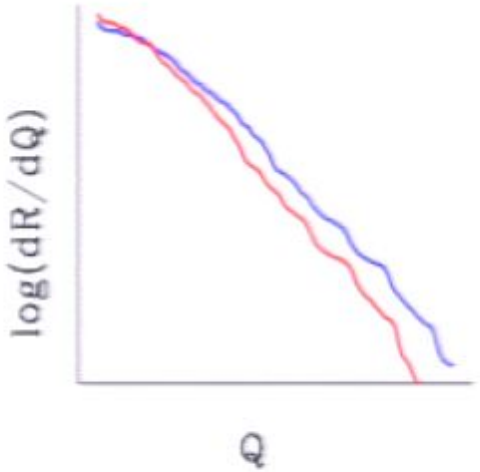

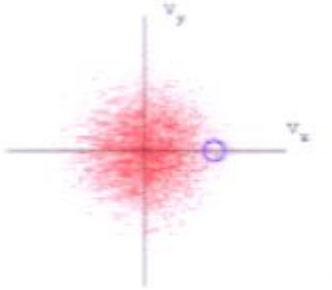

standard Maxwellian

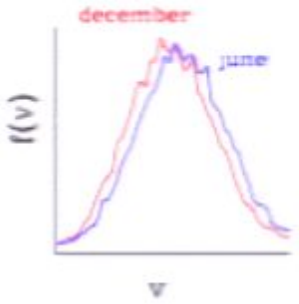

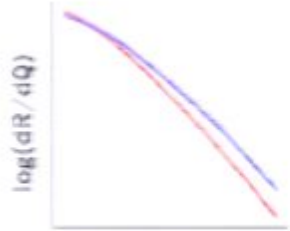

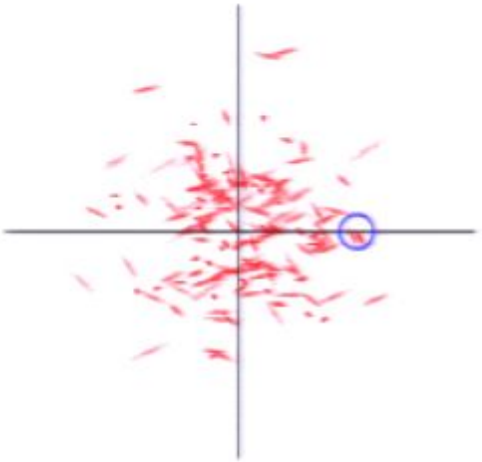

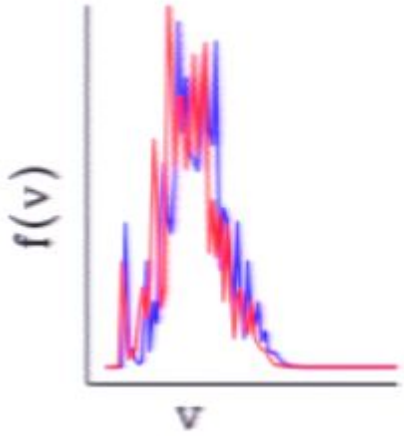

Possible phenomenological model for local f(v)

$$f(\mathbf{v}) = \sum_{\text{streams}} f_s\left(\bar{\mathbf{v}}_i,\, \sigma_{ij,s}\right)$$

key question: how many streams and what is their distribution (see Helmi & White 1999 Vogelsberger et al. 2008)

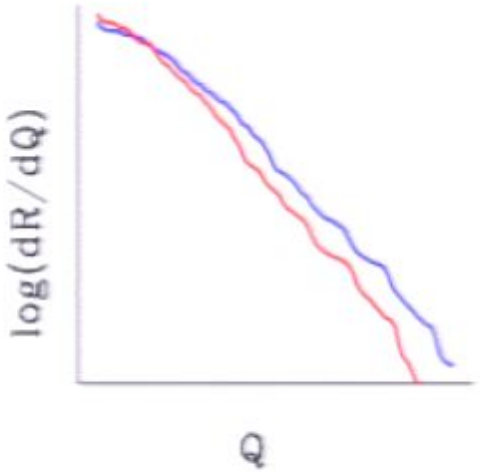

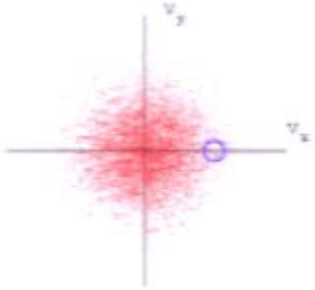

standard Maxwellian

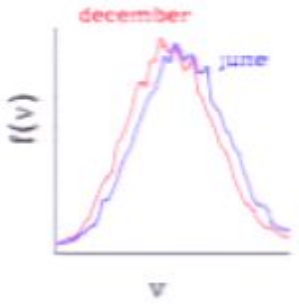

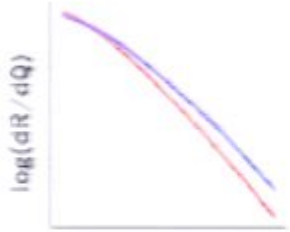

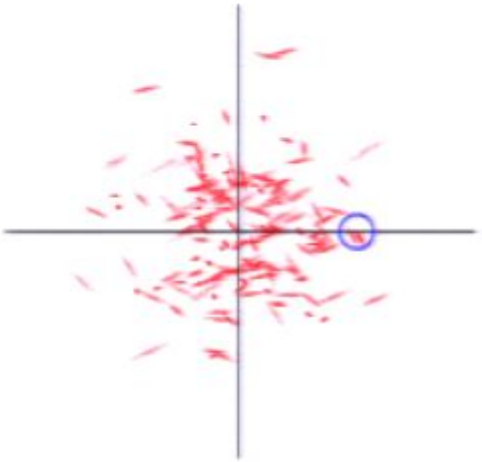

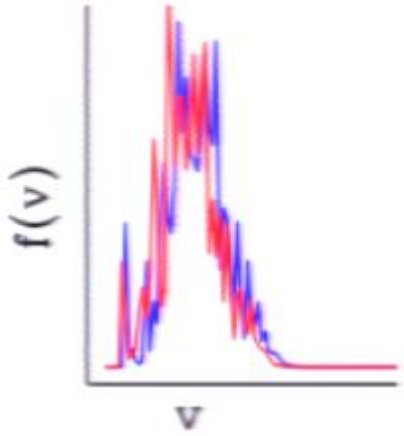

Possible phenomenological model for local f(v)

$$f(\mathbf{v}) = \sum_{\text{streams}} f_s\left(\bar{\mathbf{v}}_i,\, \sigma_{ij,s}\right)$$

key question: how many streams and what is their distribution (see Helmi & White 1999 Vogelsberger et al. 2008)

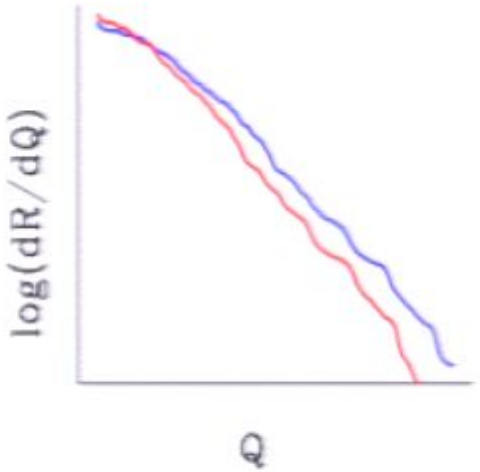

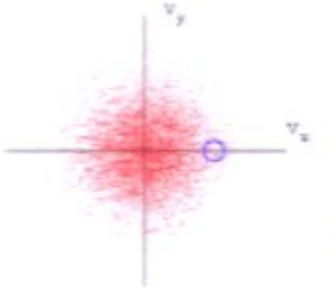

standard Maxwellian

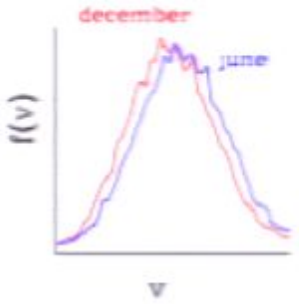

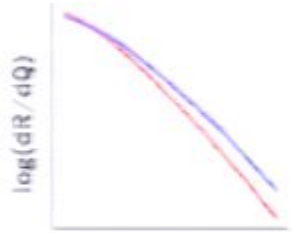

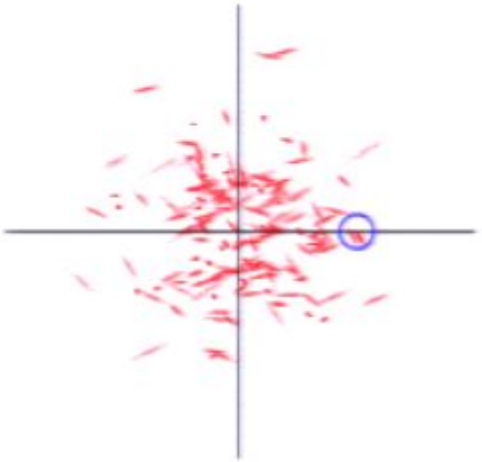

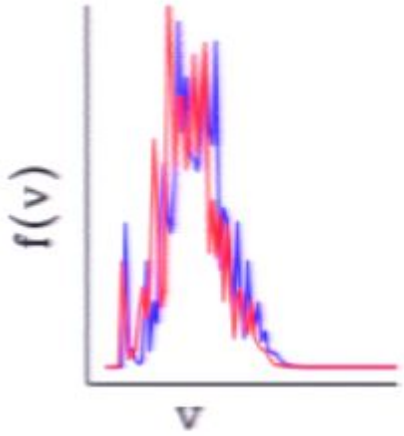

Possible phenomenological model for local f(v)

$$f(\mathbf{v}) = \sum_{\text{streams}} f_s\left(\bar{\mathbf{v}}_i, \sigma_{ij,s}\right)$$

key question: how many streams and what is their distribution (see Helmi & White 1999 Vogelsberger et al. 2008)

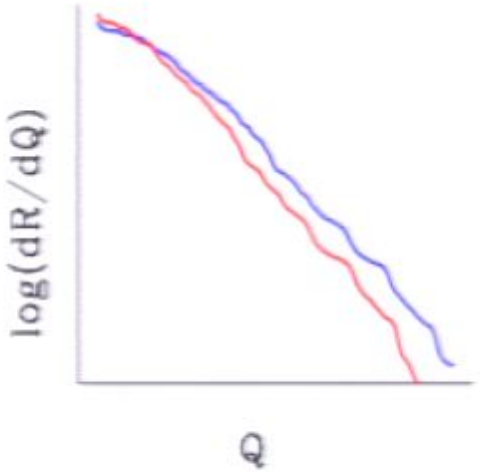

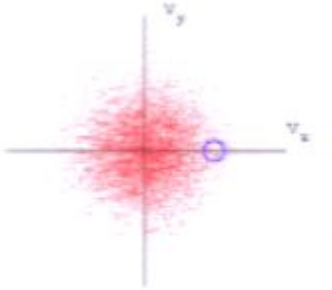

standard Maxwellian

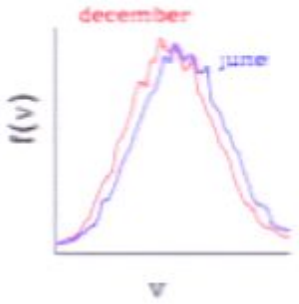

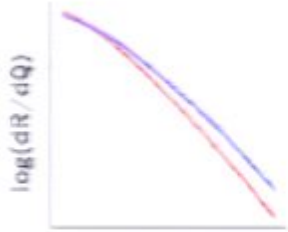

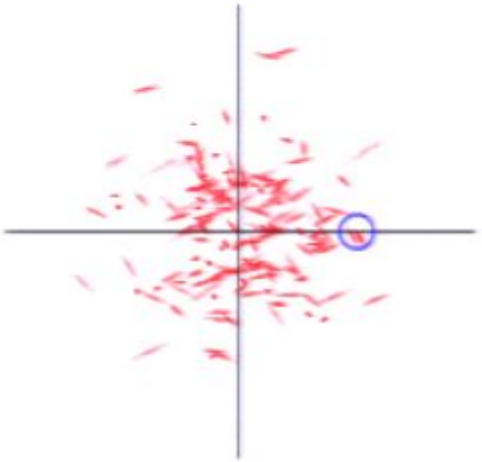

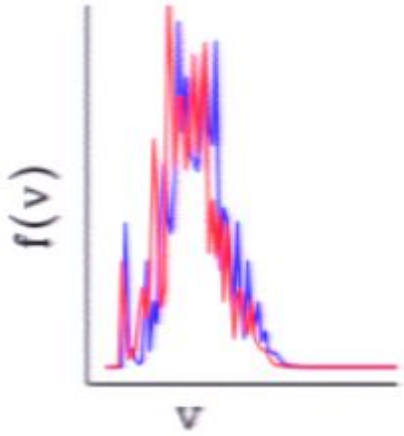

Possible phenomenological model for local f(v)

$$f(\mathbf{v}) = \sum_{\text{streams}} f_s\left(\bar{\mathbf{v}}_i, \sigma_{ij,s}\right)$$

key question: how many streams and what is their distribution (see Helmi & White 1999 Vogelsberger et al. 2008)

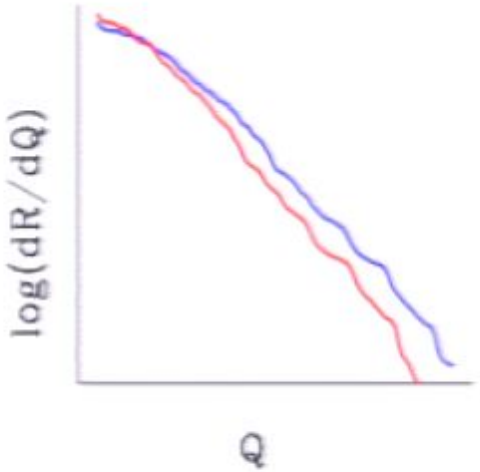

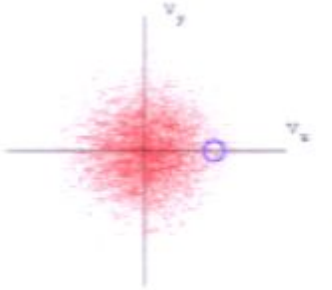

standard Maxwellian

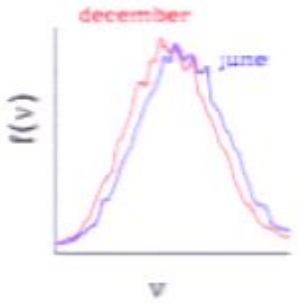

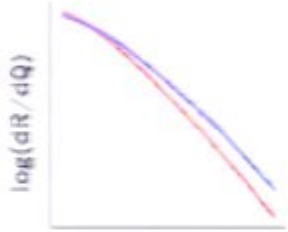

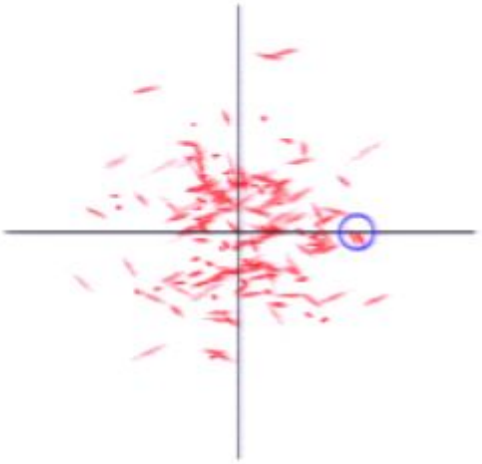

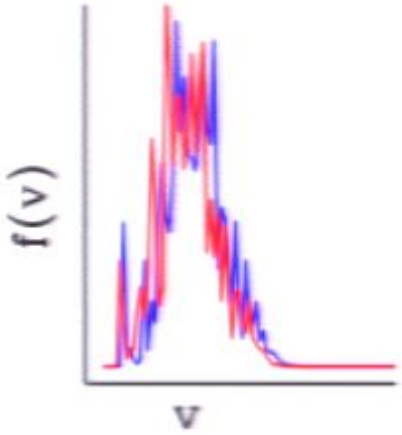

Possible phenomenological model for local f(v)

$$f(\mathbf{v}) = \sum_{\text{streams}} f_s\left(\bar{\mathbf{v}}_i,\, \sigma_{ij,s}\right)$$

key question: how many streams and what is their distribution (see Helmi & White 1999 Vogelsberger et al. 2008)

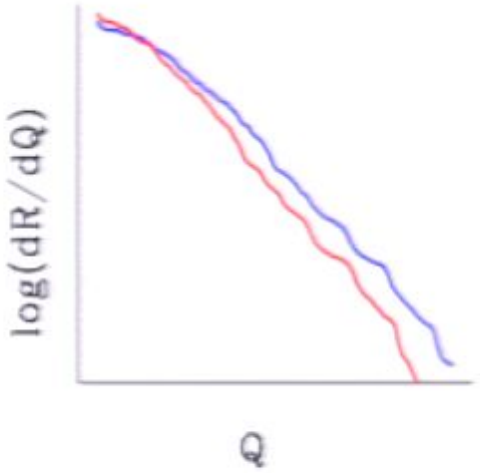

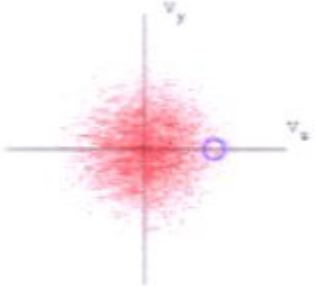

standard Maxwellian

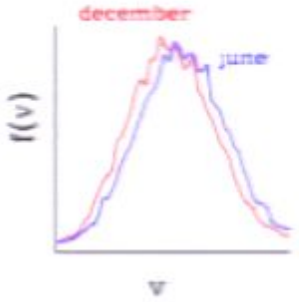

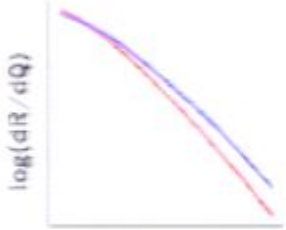

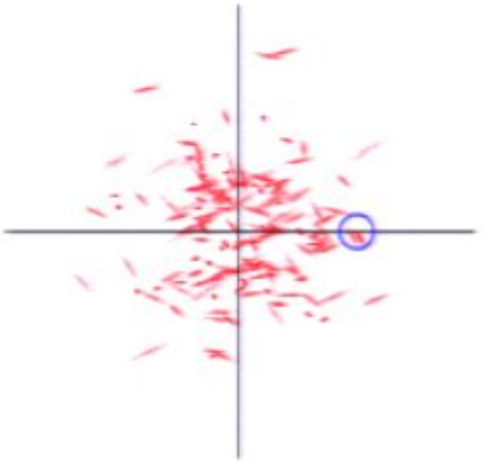

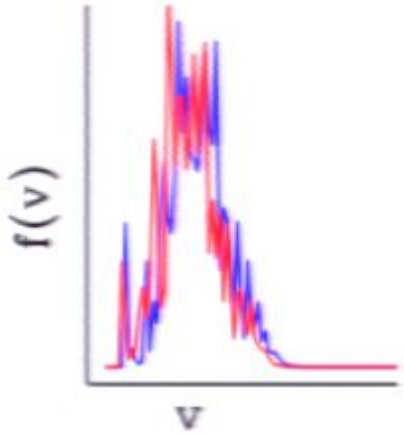

Possible phenomenological model for local f(v)

$$f(\mathbf{v}) = \sum_{\text{streams}} f_s\left(\bar{\mathbf{v}}_i, \sigma_{ij,s}\right)$$

key question: how many streams and what is their distribution (see Helmi & White 1999 Vogelsberger et al. 2008)

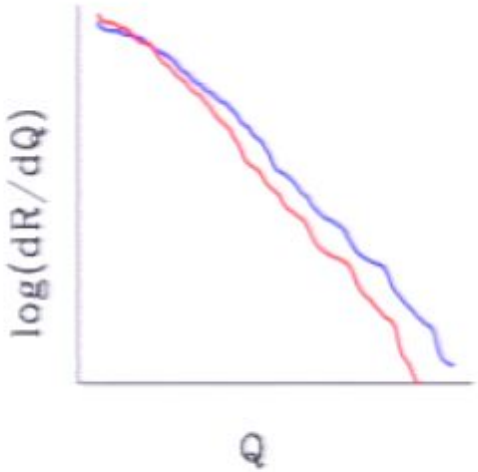

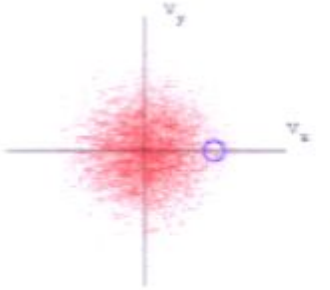

standard Maxwellian

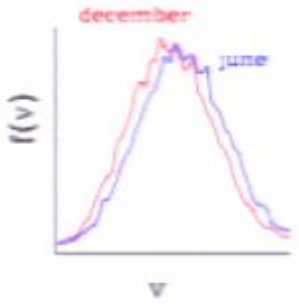

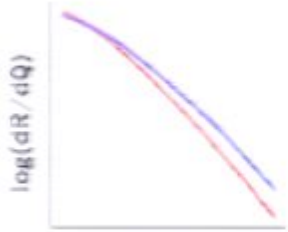

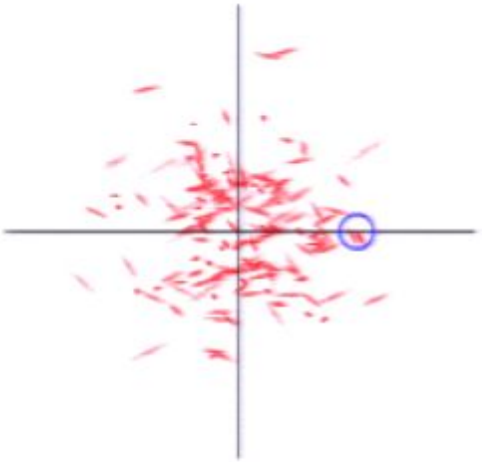

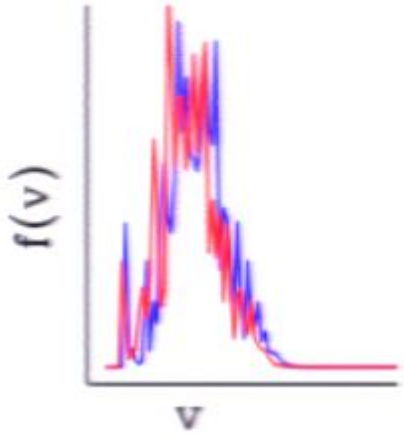

Possible phenomenological model for local f(v)

$$f(\mathbf{v}) = \sum_{\text{streams}} f_s\left(\bar{\mathbf{v}}_i, \sigma_{ij,s}\right)$$

key question: how many streams and what is their distribution (see Helmi & White 1999 Vogelsberger et al. 2008)

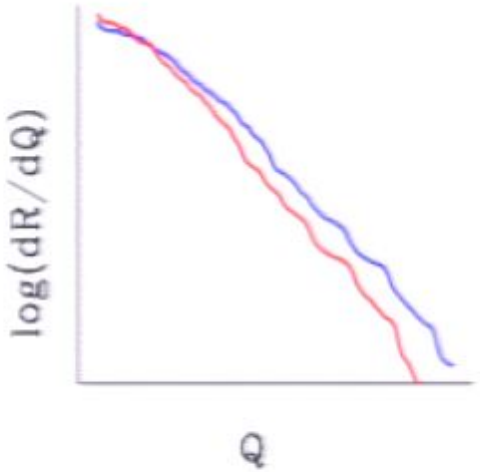

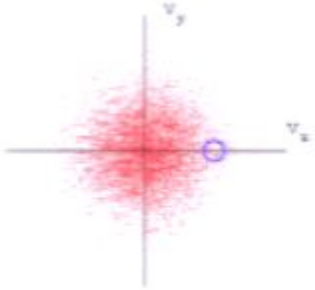

standard Maxwellian

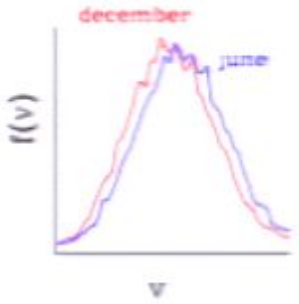

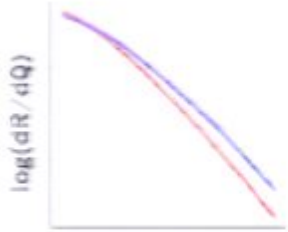

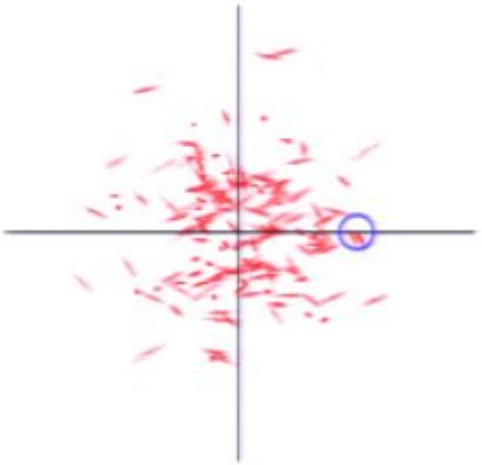

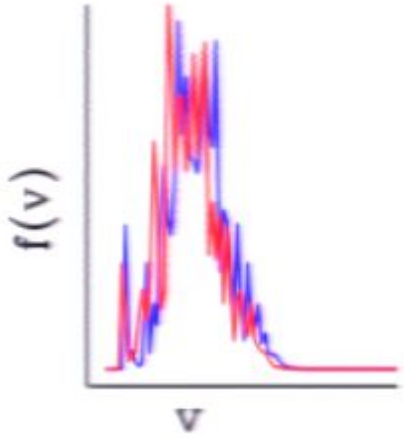

Possible phenomenological model for local f(v)

$$f(\mathbf{v}) = \sum_{\text{streams}} f_s\left(\bar{\mathbf{v}}_i, \sigma_{ij,s}\right)$$

key question: how many streams and what is their distribution (see Helmi & White 1999 Vogelsberger et al. 2008)

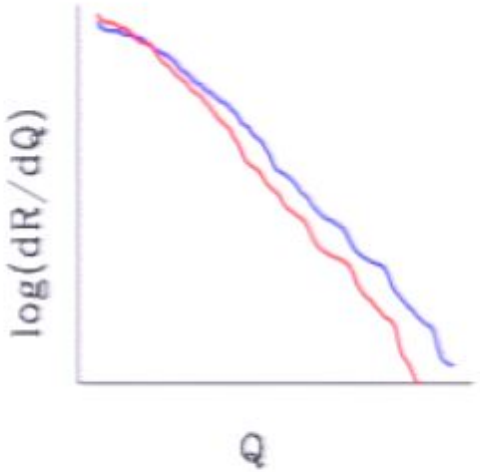

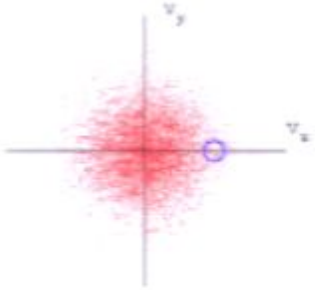

standard Maxwellian

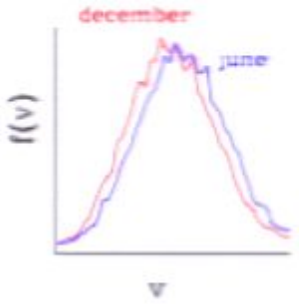

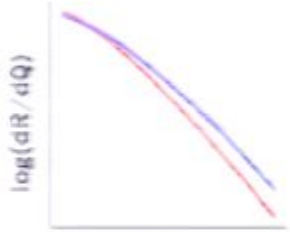

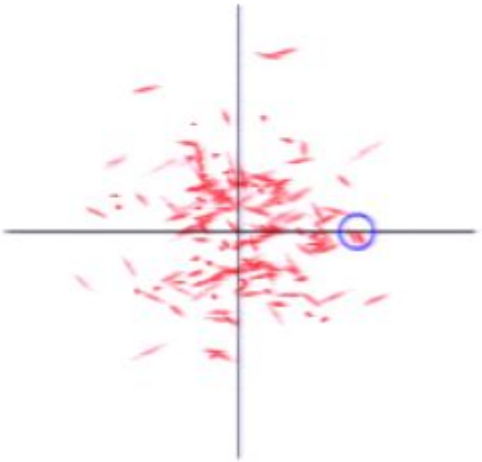

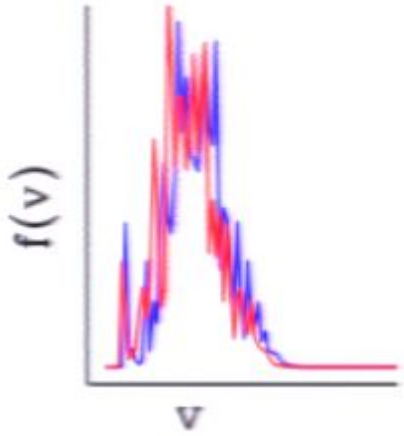

Possible phenomenological model for local f(v)

$$f(\mathbf{v}) = \sum_{\text{streams}} f_s\left(\bar{\mathbf{v}}_i, \sigma_{ij,s}\right)$$

key question: how many streams and what is their distribution (see Helmi & White 1999 Vogelsberger et al. 2008)

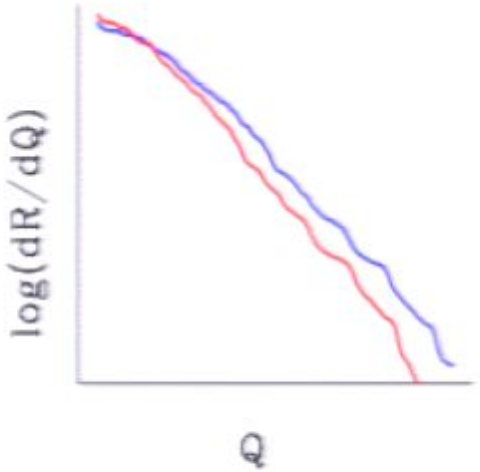

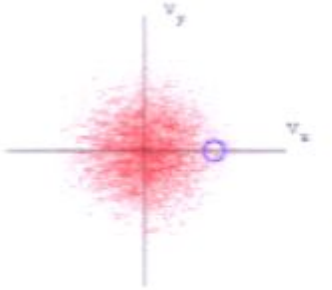

standard Maxwellian

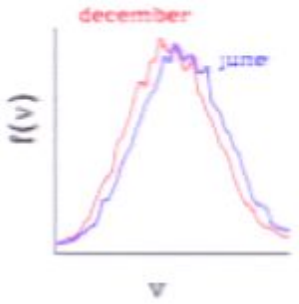

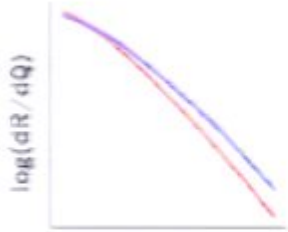

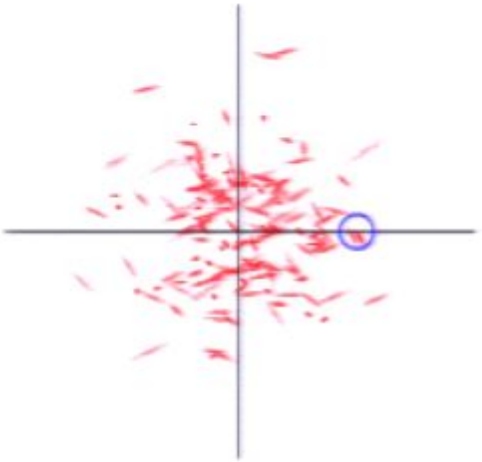

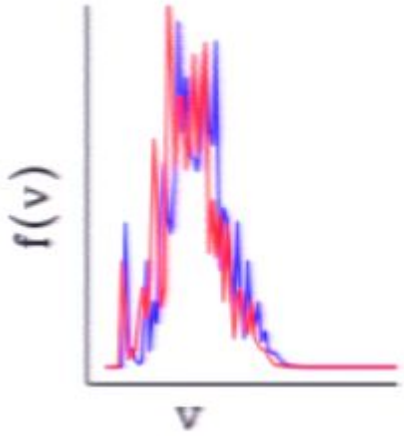

Possible phenomenological model for local f(v)

$$f(\mathbf{v}) = \sum_{\text{streams}} f_s\left(\bar{\mathbf{v}}_i, \sigma_{ij,s}\right)$$

key question: how many streams and what is their distribution (see Helmi & White 1999 Vogelsberger et al. 2008)

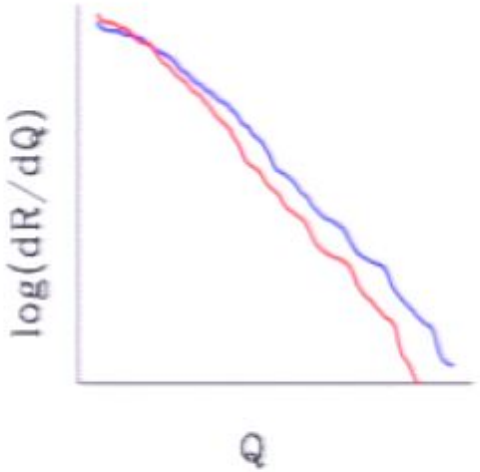

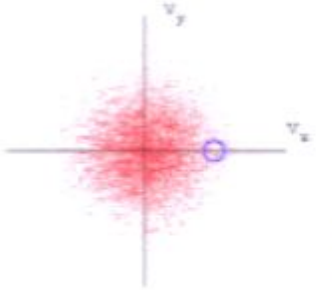

standard Maxwellian

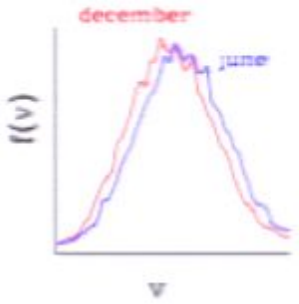

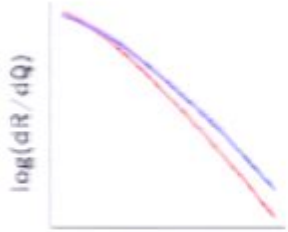

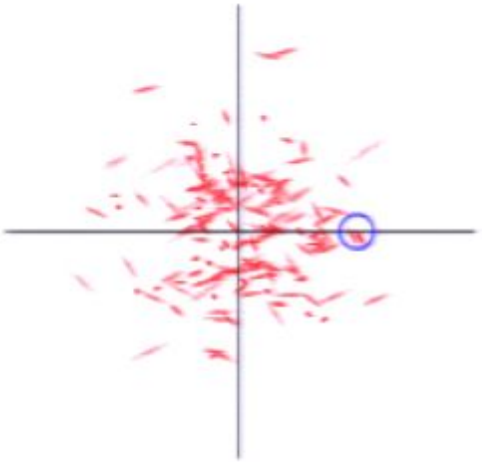

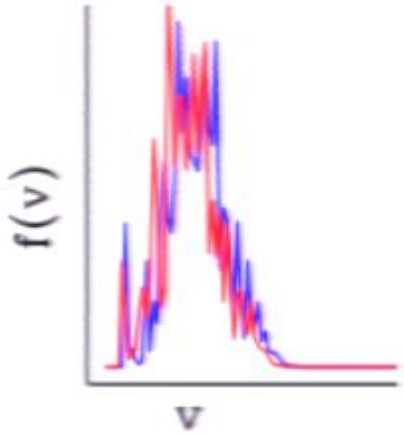

Possible phenomenological model for local f(v)

$$f(\mathbf{v}) = \sum_{\text{streams}} f_s\left(\bar{\mathbf{v}}_i, \sigma_{ij,s}\right)$$

key question: how many streams and what is their distribution (see Helmi & White 1999 Vogelsberger et al. 2008)

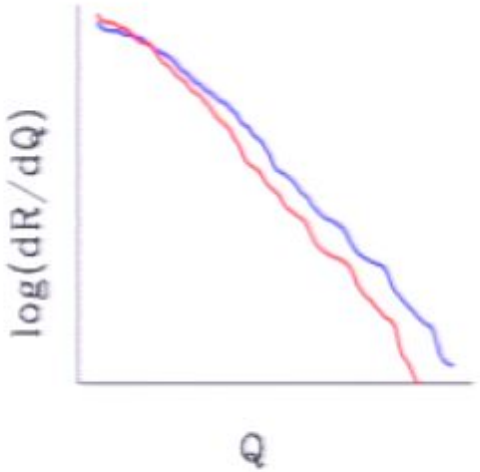

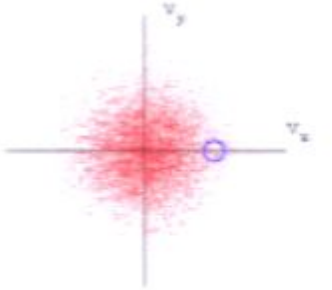

standard Maxwellian

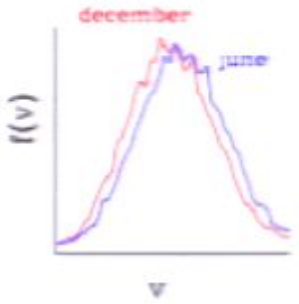

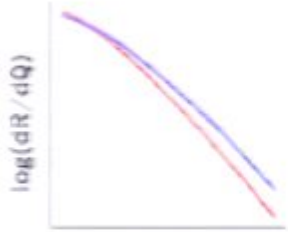

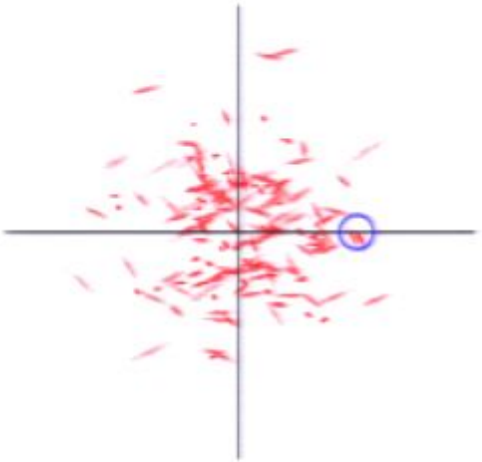

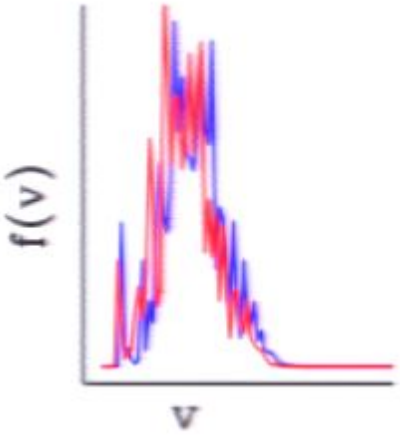

Possible phenomenological model for local f(v)

$$f(\mathbf{v}) = \sum_{\text{streams}} f_s\left(\bar{\mathbf{v}}_i, \sigma_{ij,s}\right)$$

key question: how many streams and what is their distribution (see Helmi & White 1999 Vogelsberger et al. 2008)

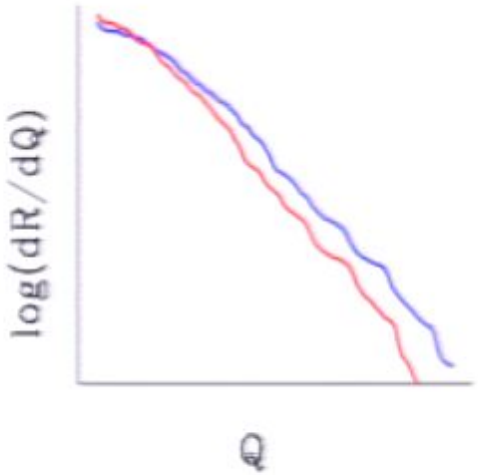

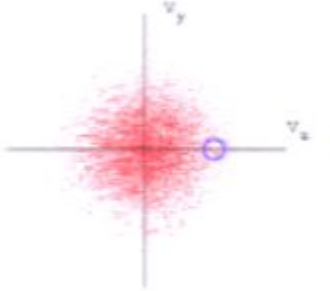

standard Maxwellian

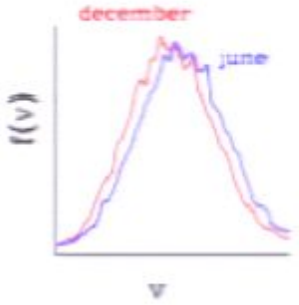

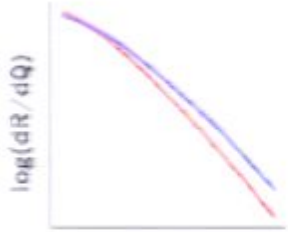

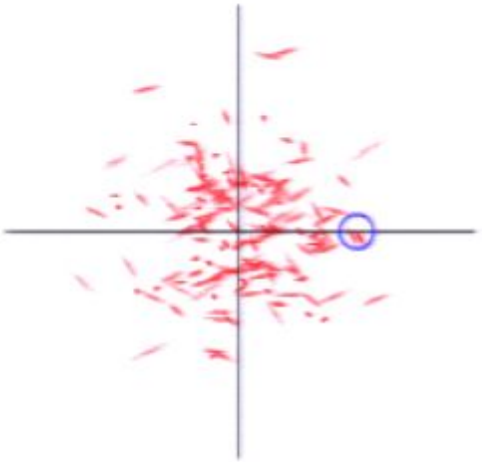

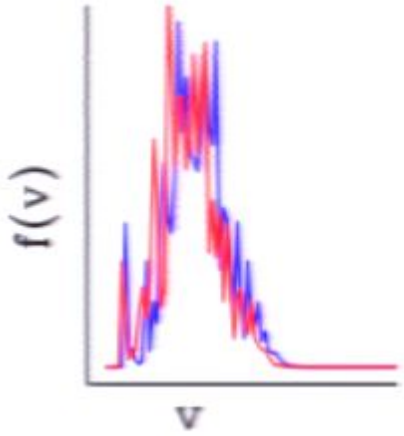

Possible phenomenological model for local f(v)

$$f(\mathbf{v}) = \sum_{\text{streams}} f_s\left(\bar{\mathbf{v}}_i, \sigma_{ij,s}\right)$$

key question: how many streams and what is their distribution (see Helmi & White 1999 Vogelsberger et al. 2008)

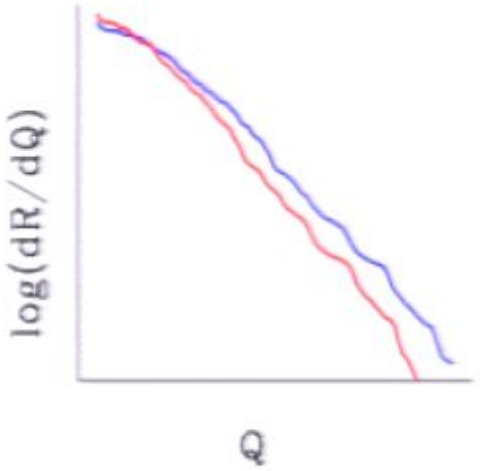

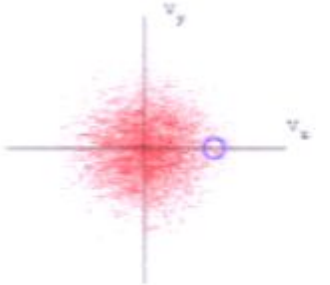

standard Maxwellian

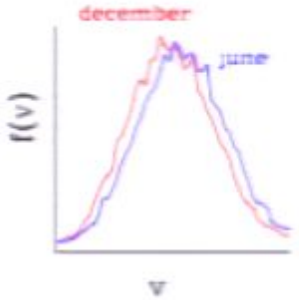

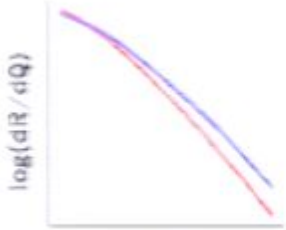

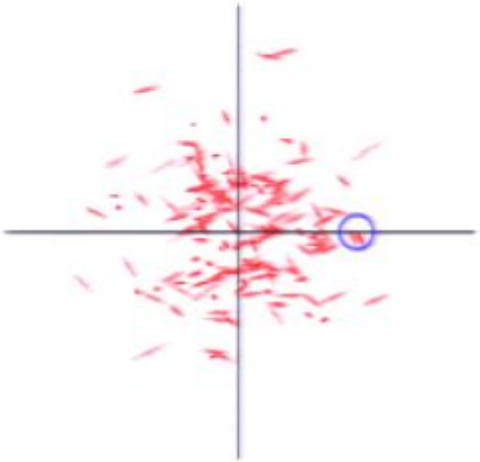

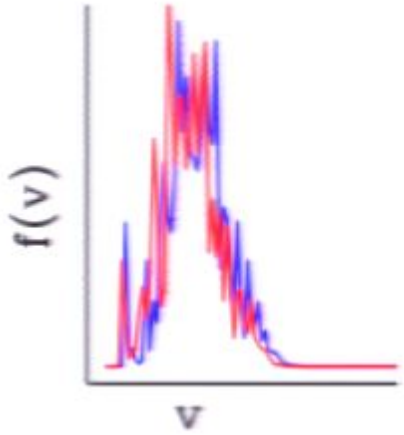

Possible phenomenological model for local f(v)

$$f(\mathbf{v}) = \sum_{\text{streams}} f_s\left(\bar{\mathbf{v}}_i, \sigma_{ij,s}\right)$$

key question: how many streams and what is their distribution (see Helmi & White 1999 Vogelsberger et al. 2008)

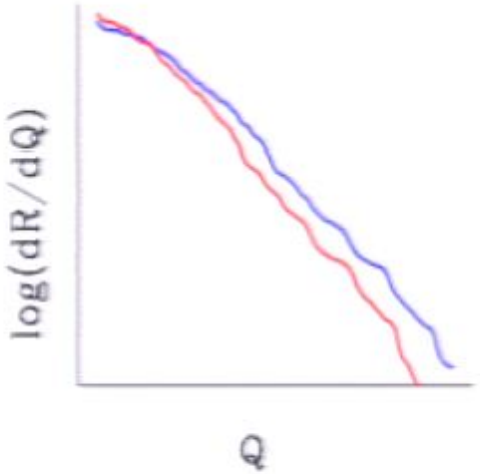

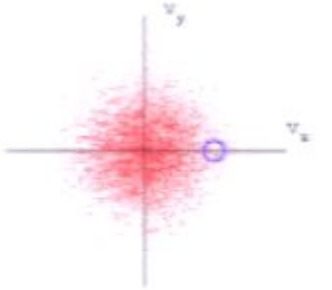

standard Maxwellian

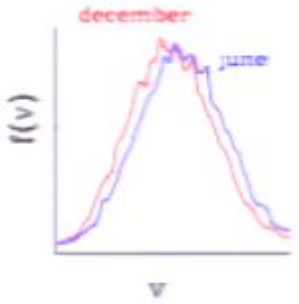

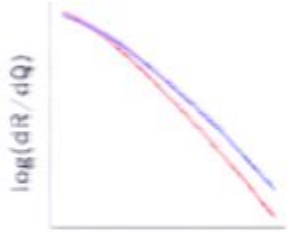

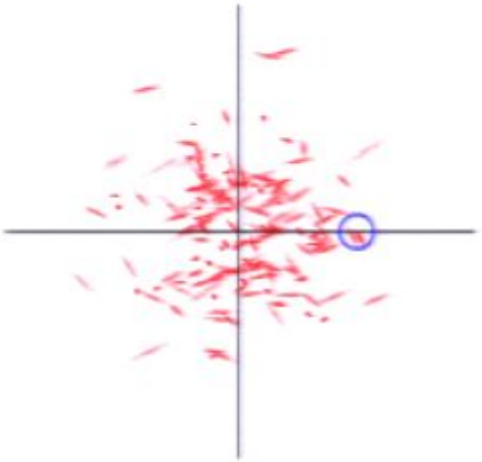

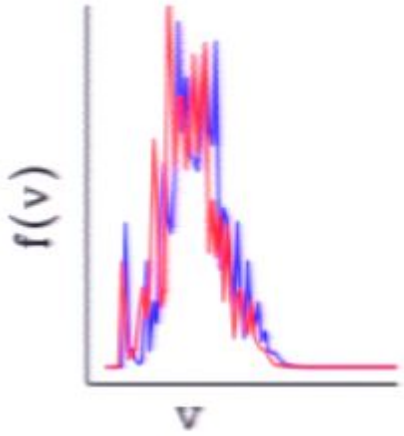

Possible phenomenological model for local f(v)

$$f(\mathbf{v}) = \sum_{\text{streams}} f_s\left(\bar{\mathbf{v}}_i, \sigma_{ij,s}\right)$$

key question: how many streams and what is their distribution (see Helmi & White 1999 Vogelsberger et al. 2008)

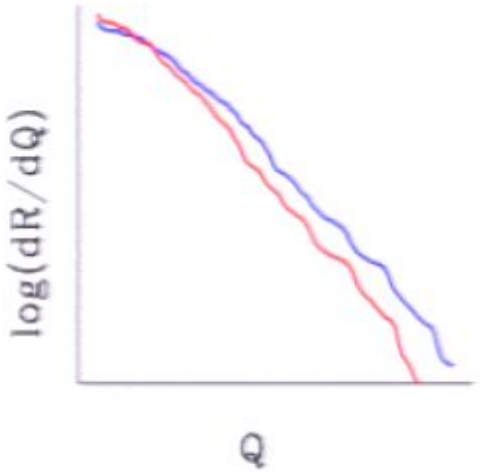

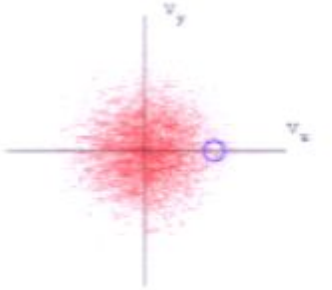

standard Maxwellian

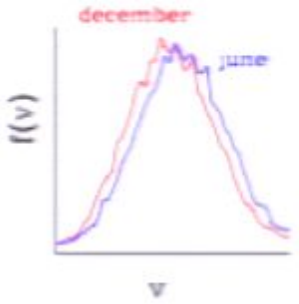

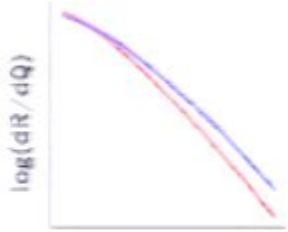

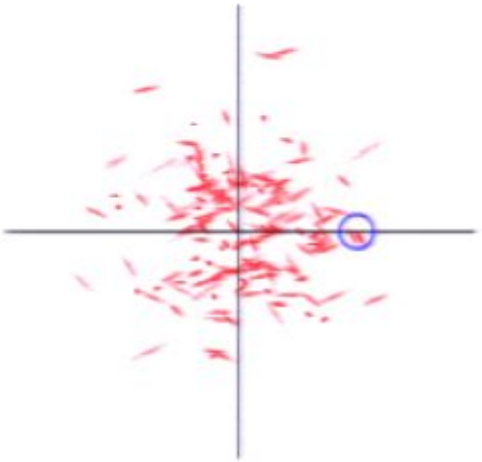

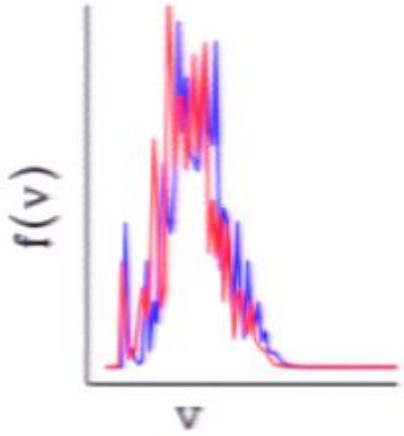

Possible phenomenological model for local f(v)

$$f(\mathbf{v}) = \sum_{\text{streams}} f_s\left(\bar{\mathbf{v}}_i,\, \sigma_{ij,s}\right)$$

key question: how many streams and what is their distribution (see Helmi & White 1999 Vogelsberger et al. 2008)

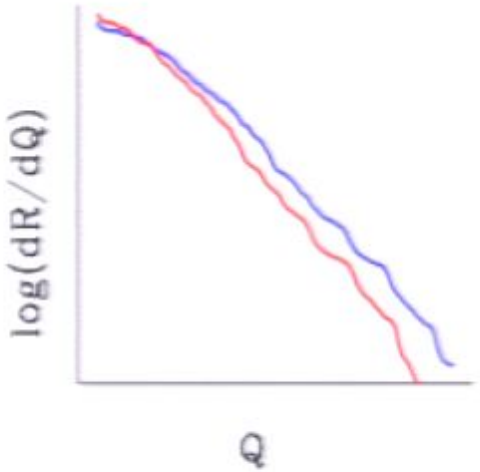

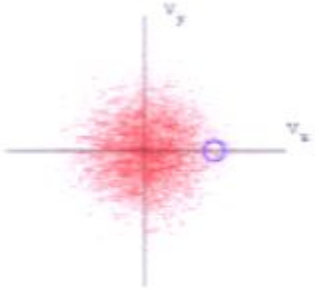

standard Maxwellian

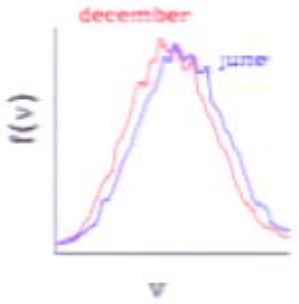

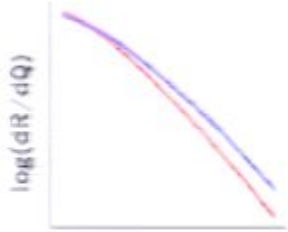

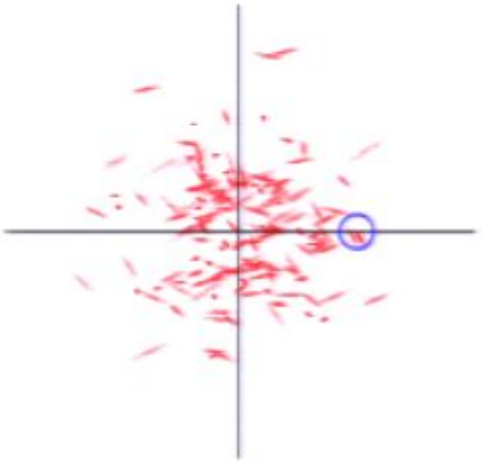

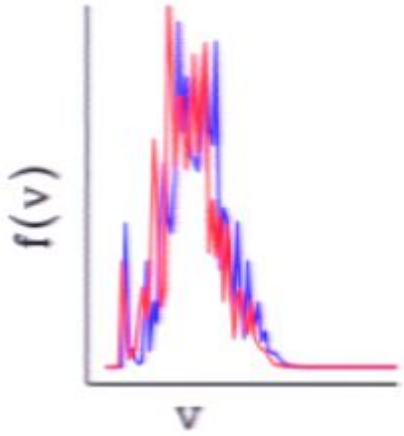

Possible phenomenological model for local f(v)

$$f(\mathbf{v}) = \sum_{\text{streams}} f_s\left(\bar{\mathbf{v}}_i,\, \sigma_{ij,s}\right)$$

key question: how many streams and what is their distribution (see Helmi & White 1999 Vogelsberger et al. 2008)

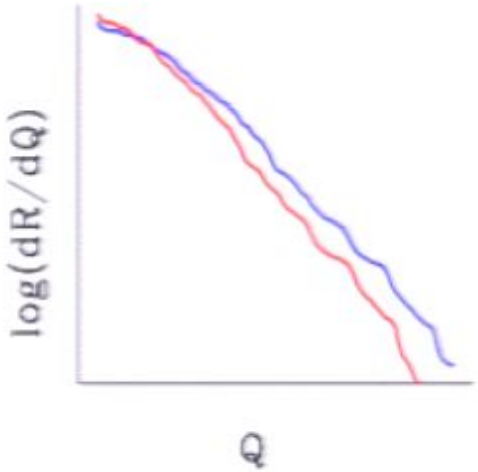

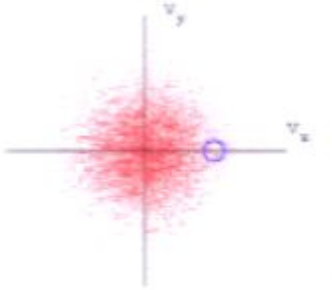

standard Maxwellian

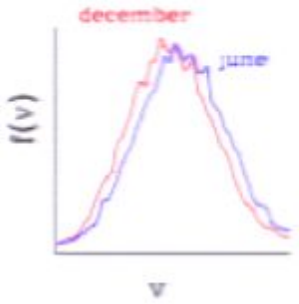

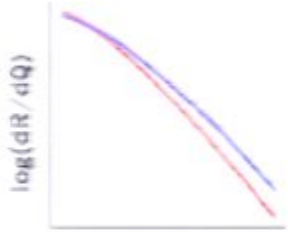

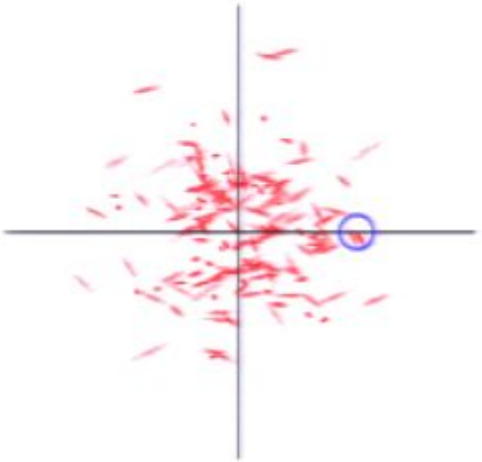

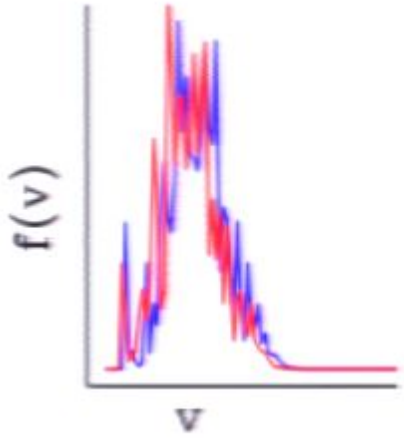

Possible phenomenological model for local f(v)

$$f(\mathbf{v}) = \sum_{\text{streams}} f_s\left(\bar{\mathbf{v}}_i, \sigma_{ij,s}\right)$$

key question: how many streams and what is their distribution (see Helmi & White 1999 Vogelsberger et al. 2008)

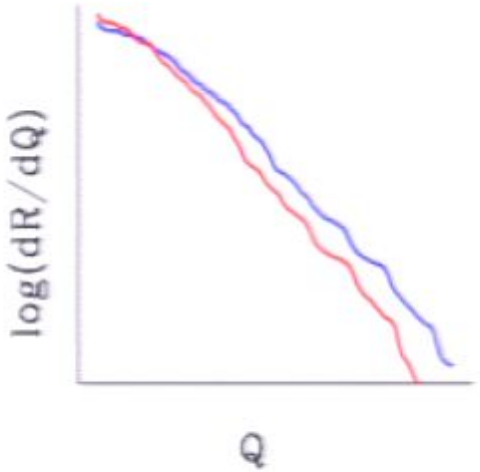

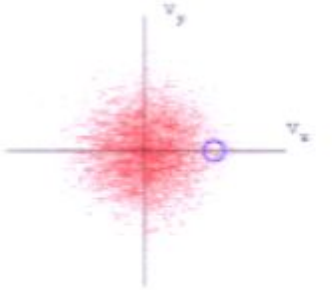

standard Maxwellian

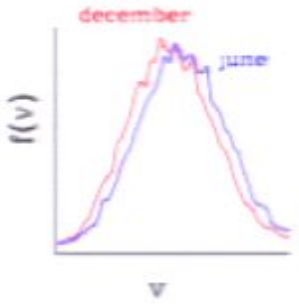

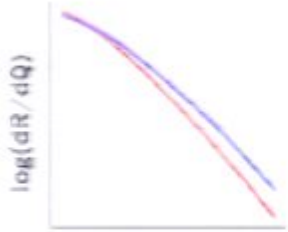

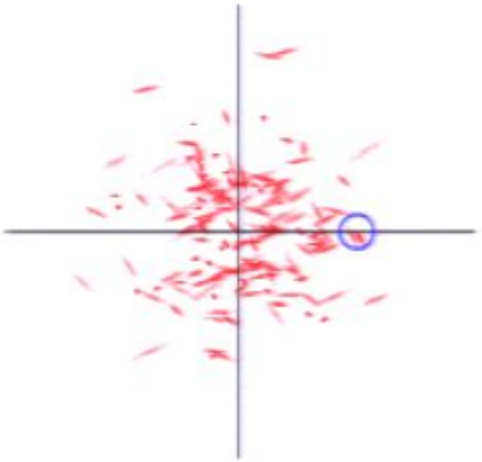

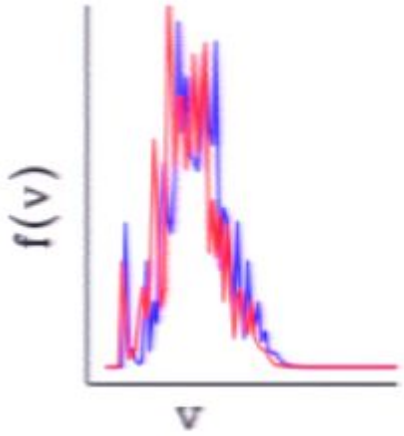

Possible phenomenological model for local f(v)

$$f(\mathbf{v}) = \sum_{\text{streams}} f_s\left(\bar{\mathbf{v}}_i, \sigma_{ij,s}\right)$$

key question: how many streams and what is their distribution (see Helmi & White 1999 Vogelsberger et al. 2008)

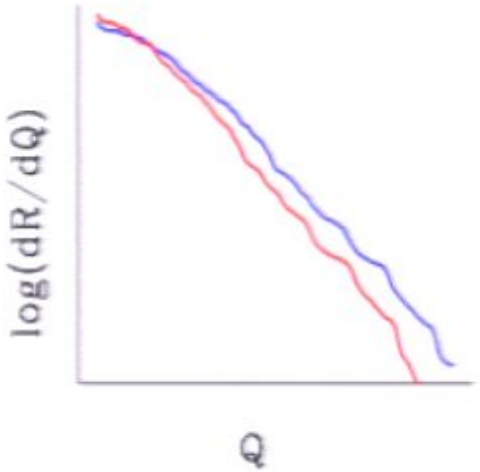

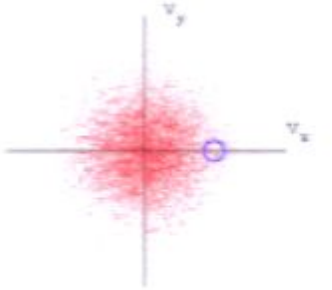

standard Maxwellian

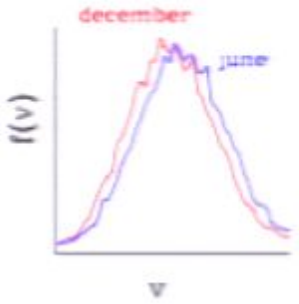

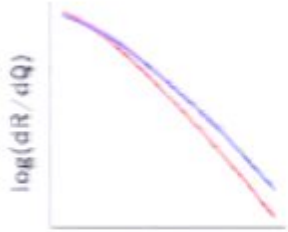

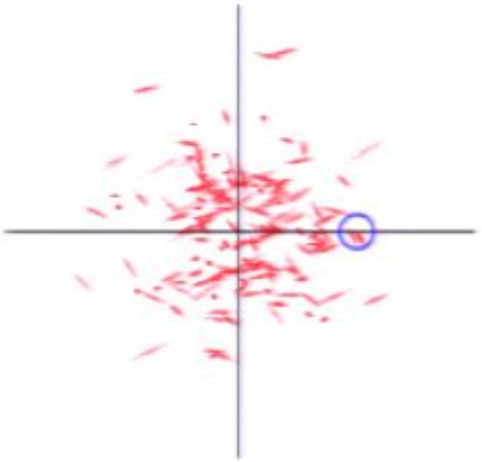

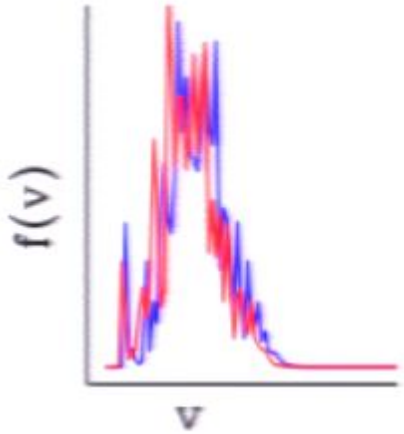

Possible phenomenological model for local f(v)

$$f(\mathbf{v}) = \sum_{\text{streams}} f_s\left(\bar{\mathbf{v}}_i, \sigma_{ij,s}\right)$$

key question: how many streams and what is their distribution (see Helmi & White 1999 Vogelsberger et al. 2008)

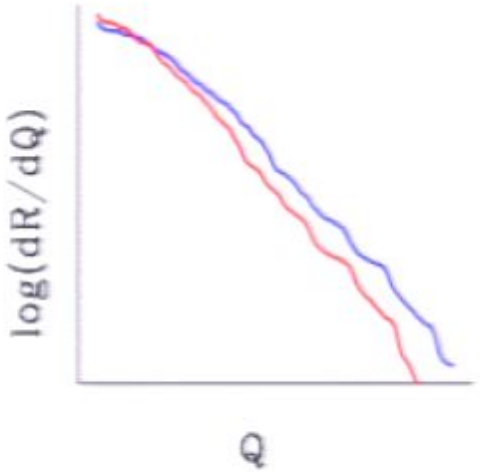

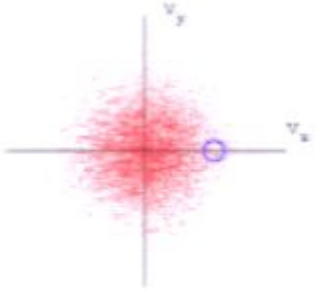

standard Maxwellian

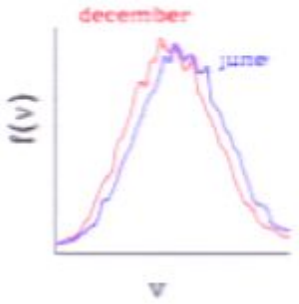

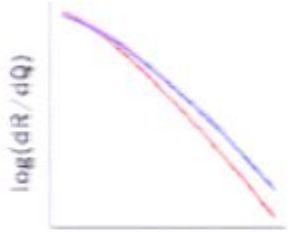

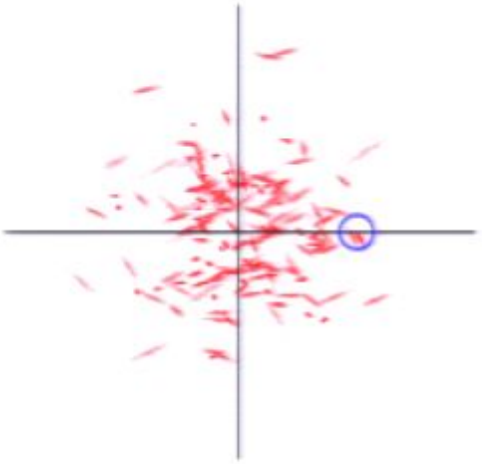

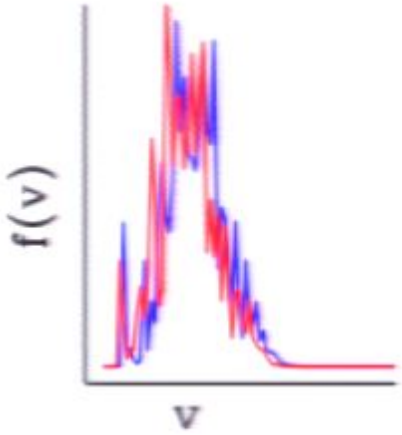

Possible phenomenological model for local f(v)

$$f(\mathbf{v}) = \sum_{\text{streams}} f_s\left(\bar{\mathbf{v}}_i, \sigma_{ij,s}\right)$$

key question: how many streams and what is their distribution (see Helmi & White 1999 Vogelsberger et al. 2008)

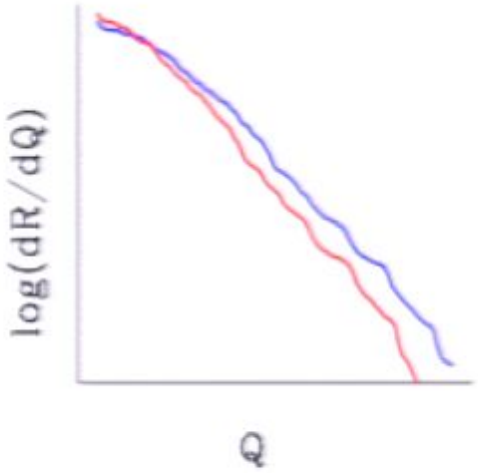

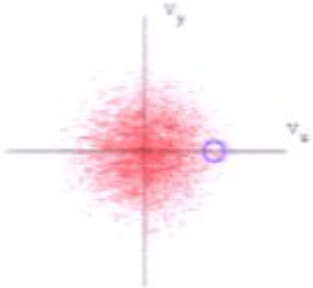

standard Maxwellian

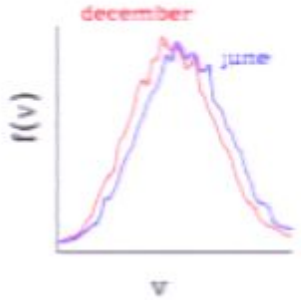

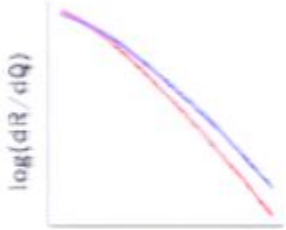

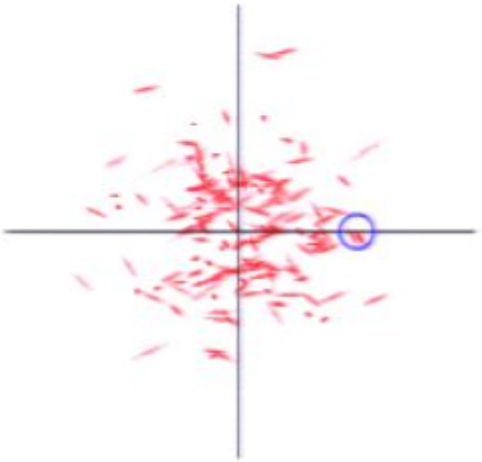

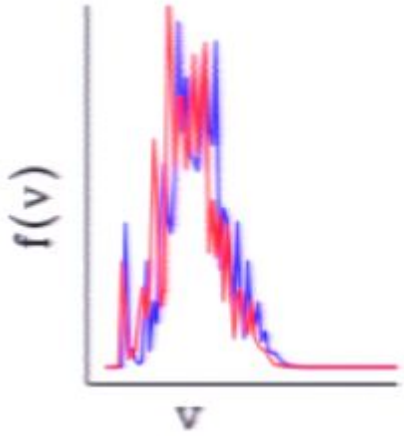

Possible phenomenological model for local f(v)

$$f(\mathbf{v}) = \sum_{\text{streams}} f_s\left(\bar{\mathbf{v}}_i, \sigma_{ij,s}\right)$$

key question: how many streams and what is their distribution (see Helmi & White 1999 Vogelsberger et al. 2008)

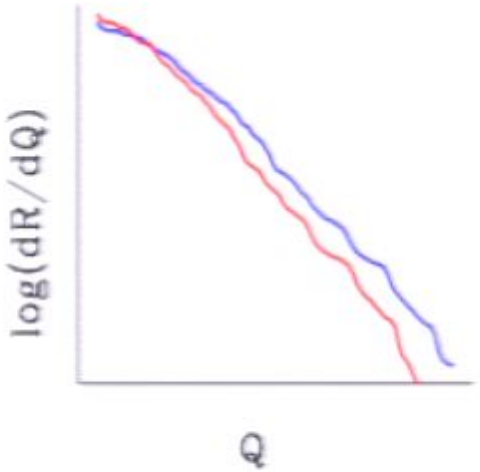

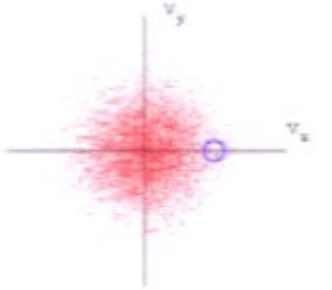

standard Maxwellian

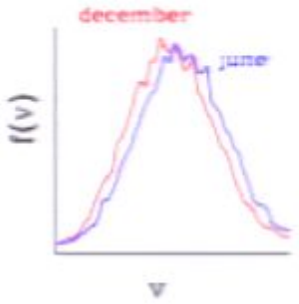

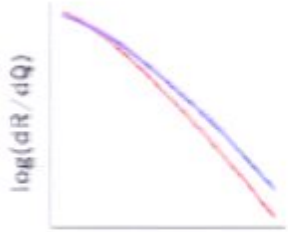

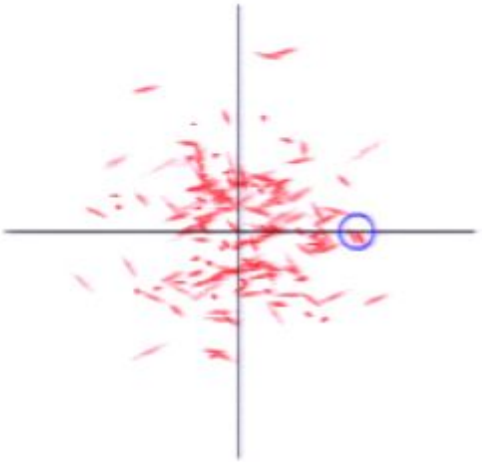

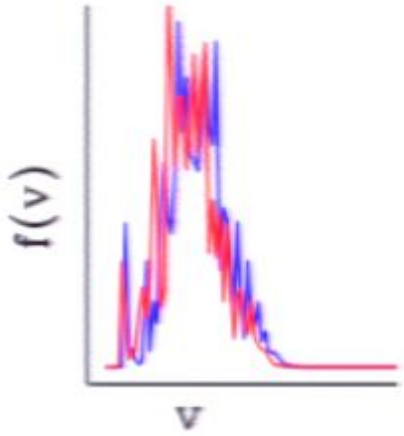

Possible phenomenological model for local f(v)

$$f(\mathbf{v}) = \sum_{\text{streams}} f_s\left(\bar{\mathbf{v}}_i, \sigma_{ij,s}\right)$$

key question: how many streams and what is their distribution (see Helmi & White 1999 Vogelsberger et al. 2008)

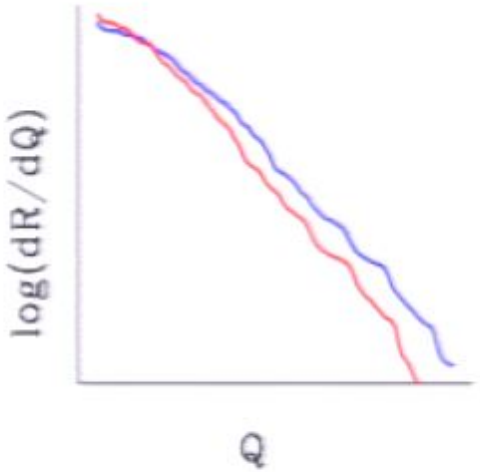

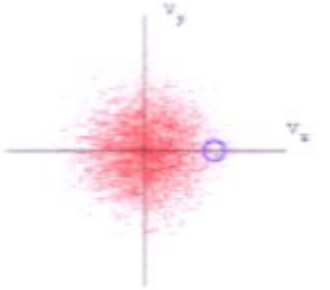

standard Maxwellian

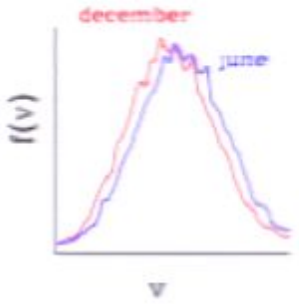

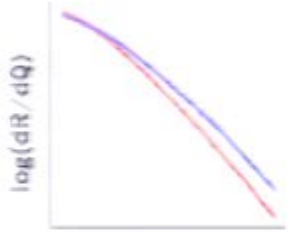

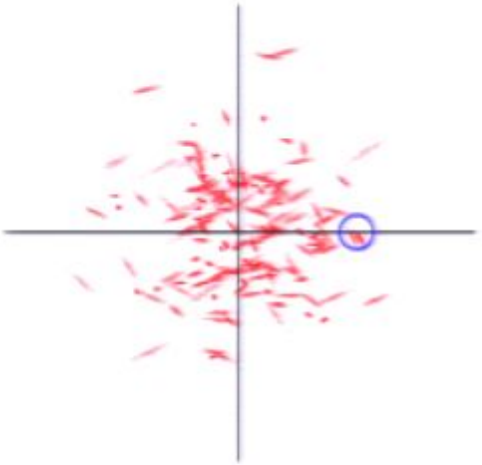

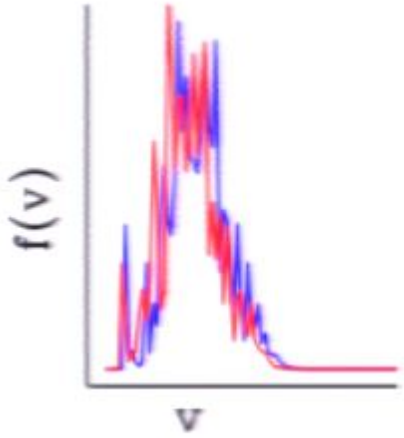

Possible phenomenological model for local f(v)

$$f(\mathbf{v}) = \sum_{\text{streams}} f_s\left(\bar{\mathbf{v}}_i, \sigma_{ij,s}\right)$$

key question: how many streams and what is their distribution (see Helmi & White 1999 Vogelsberger et al. 2008)

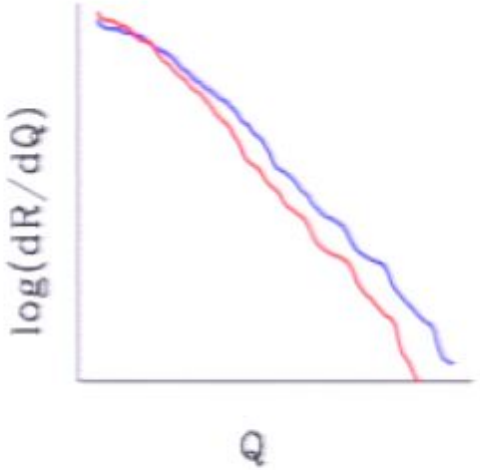

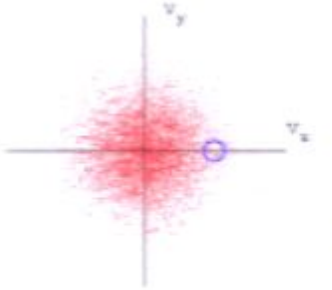

standard Maxwellian

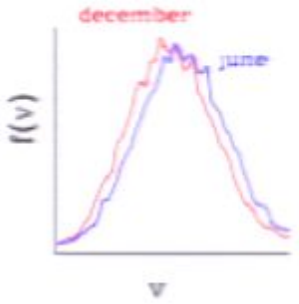

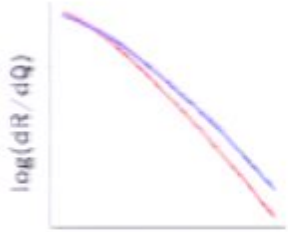

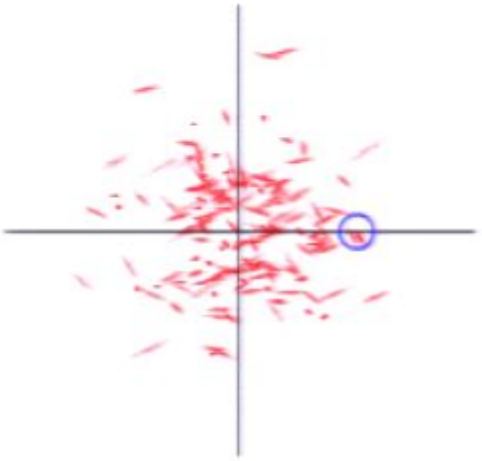

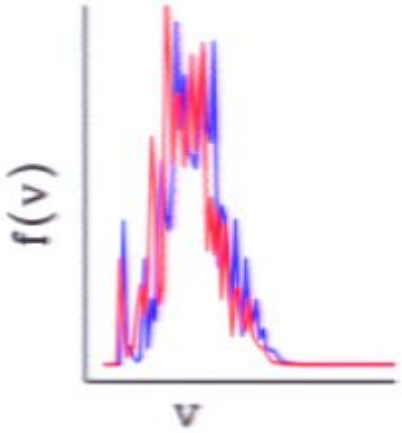

Possible phenomenological model for local f(v)

$$f(\mathbf{v}) = \sum_{\text{streams}} f_s\left(\bar{\mathbf{v}}_i, \sigma_{ij,s}\right)$$

key question: how many streams and what is their distribution (see Helmi & White 1999 Vogelsberger et al. 2008)

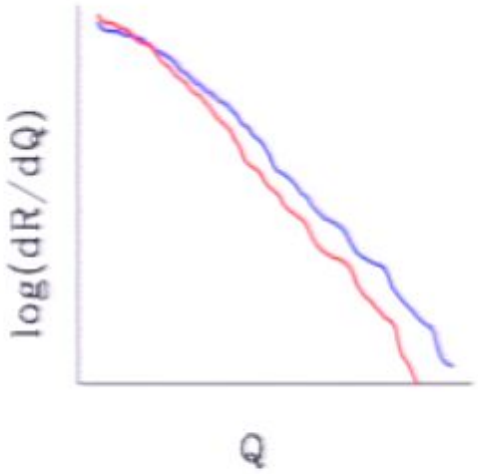

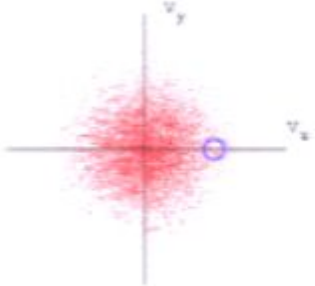

standard Maxwellian

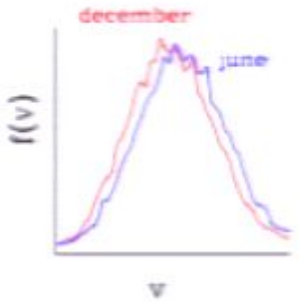

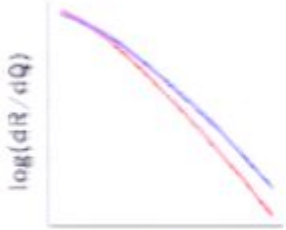

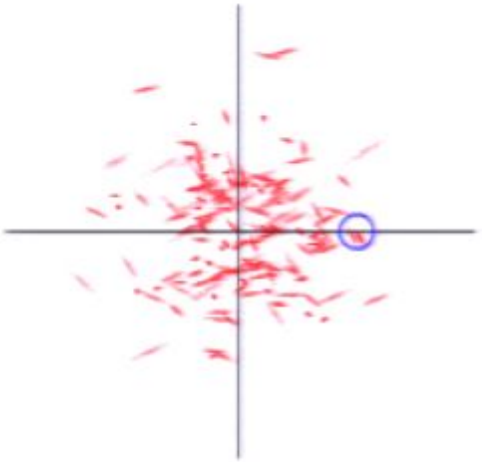

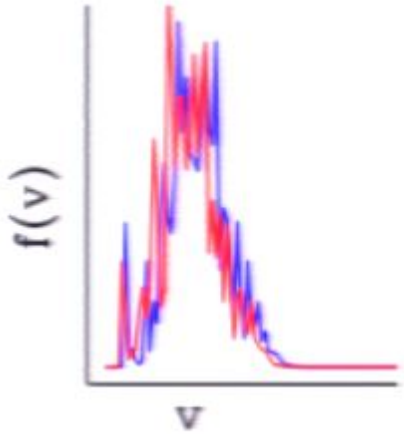

Possible phenomenological model for local f(v)

$$f(\mathbf{v}) = \sum_{\text{streams}} f_s\left(\bar{\mathbf{v}}_i, \sigma_{ij,s}\right)$$

key question: how many streams and what is their distribution (see Helmi & White 1999 Vogelsberger et al. 2008)

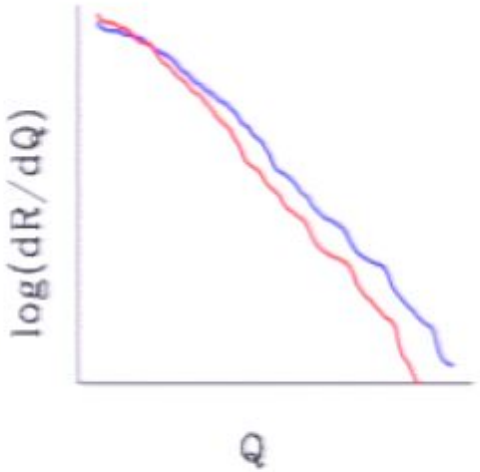

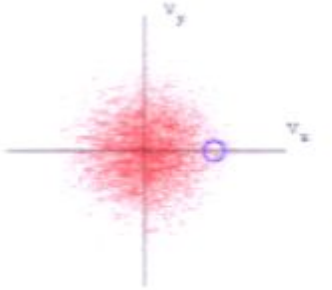

standard Maxwellian

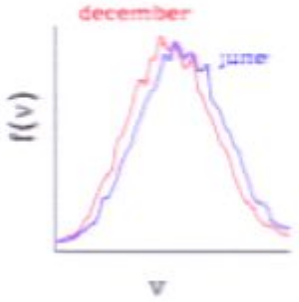

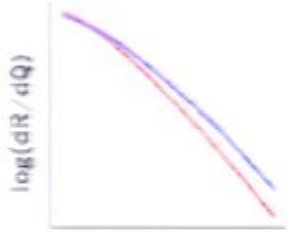

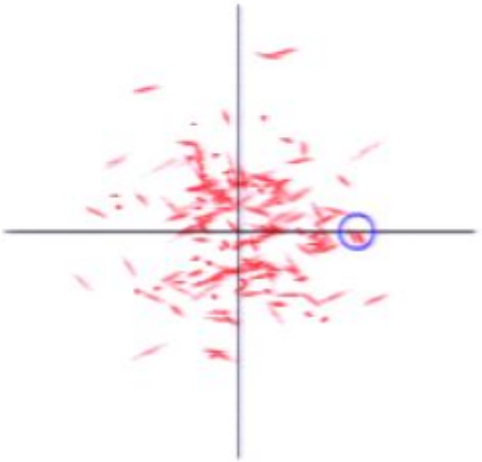

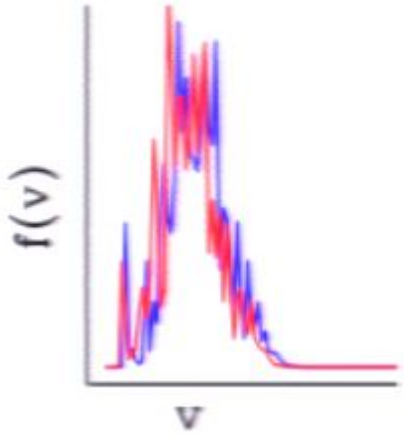

Possible phenomenological model for local f(v)

$$f(\mathbf{v}) = \sum_{\text{streams}} f_s\left(\bar{\mathbf{v}}_i, \sigma_{ij,s}\right)$$

key question: how many streams and what is their distribution (see Helmi & White 1999 Vogelsberger et al. 2008)

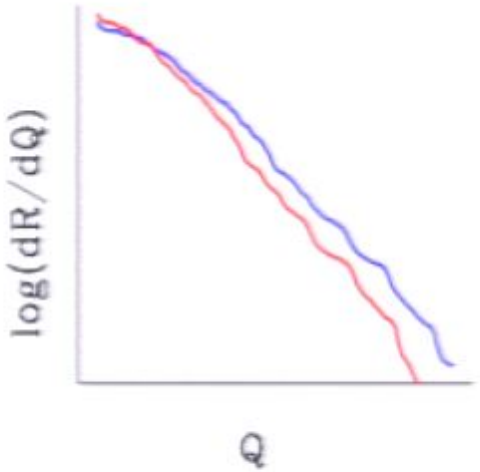

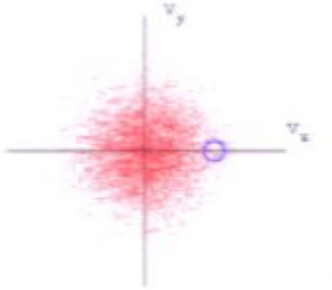

standard Maxwellian

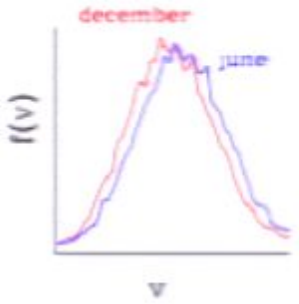

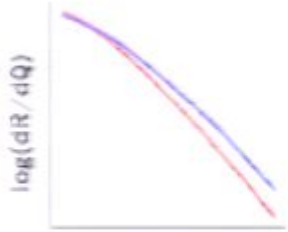

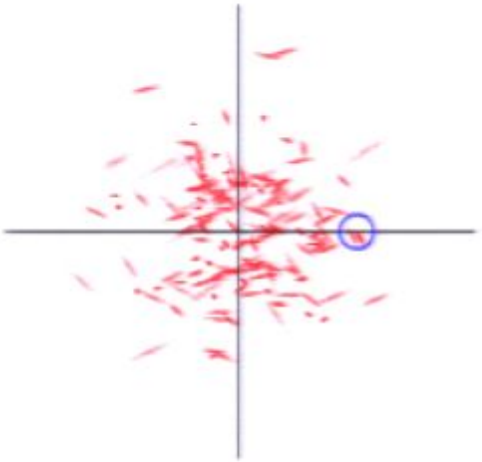

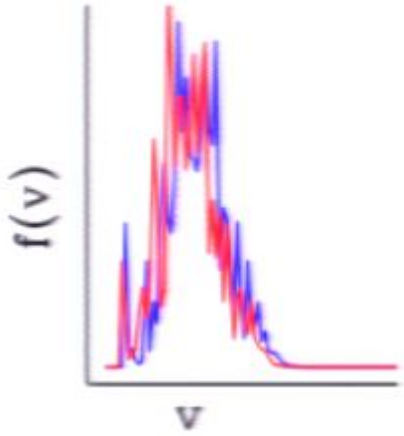

Possible phenomenological model for local f(v)

$$f(\mathbf{v}) = \sum_{\text{streams}} f_s\left(\bar{\mathbf{v}}_i,\, \sigma_{ij,s}\right)$$

key question: how many streams and what is their distribution (see Helmi & White 1999 Vogelsberger et al. 2008)

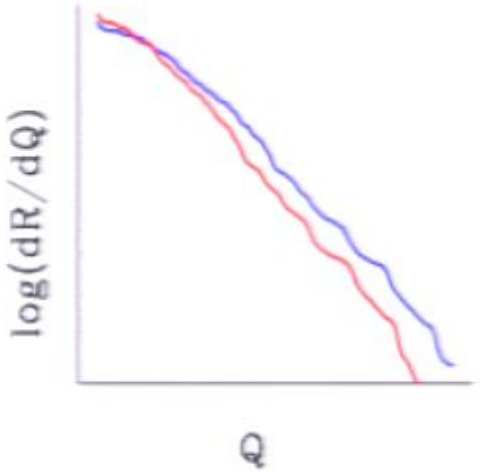

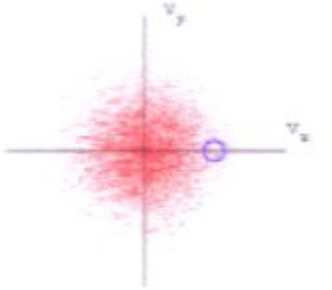

standard Maxwellian

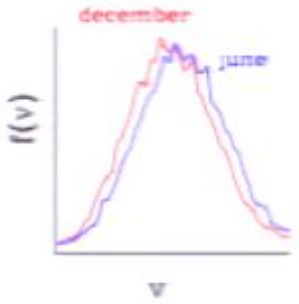

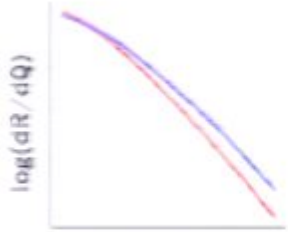

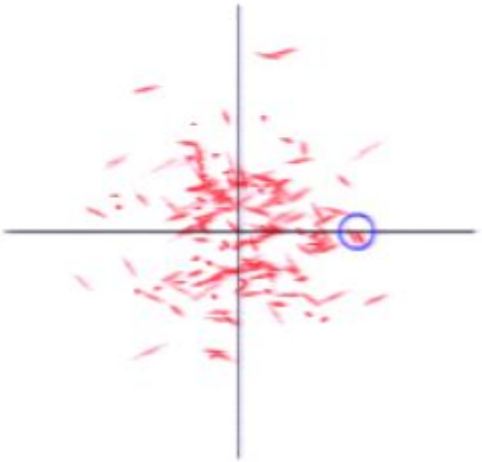

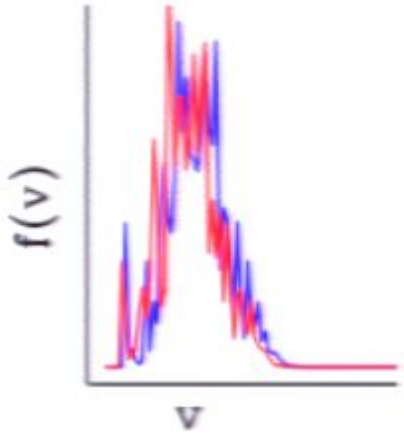

Possible phenomenological model for local f(v)

$$f(\mathbf{v}) = \sum_{\text{streams}} f_s\left(\bar{\mathbf{v}}_i, \sigma_{ij,s}\right)$$

key question: how many streams and what is their distribution (see Helmi & White 1999 Vogelsberger et al. 2008)

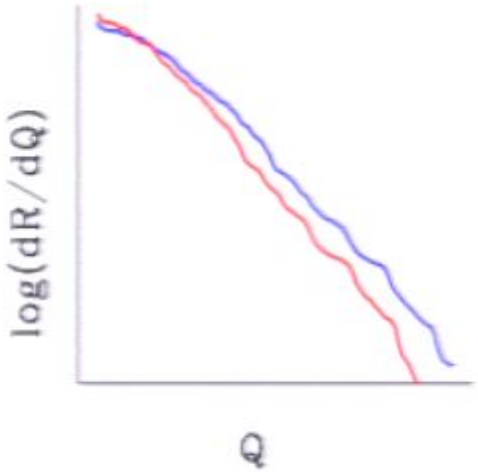

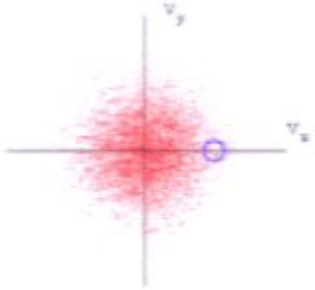

standard Maxwellian

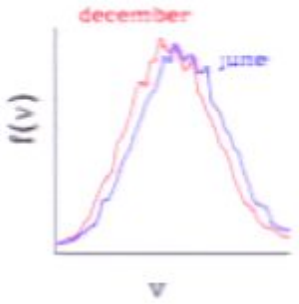

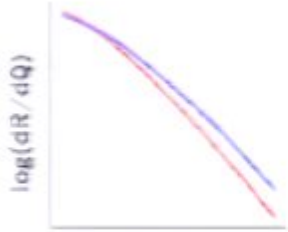

Challenges, IV
Identification of substructure

Identification of halos, subhalos, and tidal streams is a time-honored endeavor in numerical cosmology

Methods include:

FOF (Davis et al 1985)

DENMAX (Bertschinger & Gelb 1991)

SKID (Stadel 2001)

SUBFIND (Springel et al 2001)

6DFOF (Diemand et al 2006)

ENLINK (Sharma & Johnston 2009)

HSF (Maciejewski et al 2009)

.....

Challenges, IV
Identification of substructure

Identification of halos, subhalos, and tidal streams is a time-honored endeavor in numerical cosmology

Methods include:

FOF (Davis et al 1985)

DENMAX (Bertschinger & Gelb 1991)

SKID (Stadel 2001)

SUBFIND (Springel et al 2001)

6DFOF (Diemand et al 2006)

ENLINK (Sharma & Johnston 2009)

HSF (Maciejewski et al 2009)

.....

Challenges, IV
Identification of substructure

Identification of halos, subhalos, and tidal streams is a time-honored endeavor in numerical cosmology

Methods include:

FOF (Davis et al 1985)

DENMAX (Bertschinger & Gelb 1991)

SKID (Stadel 2001)

SUBFIND (Springel et al 2001)

6DFOF (Diemand et al 2006)

ENLINK (Sharma & Johnston 2009)

HSF (Maciejewski et al 2009)

.....

Challenges, IV
Identification of substructure

Identification of halos, subhalos, and tidal streams is a time-honored endeavor in numerical cosmology

Methods include:

FOF (Davis et al 1985)

DENMAX (Bertschinger & Gelb 1991)

SKID (Stadel 2001)

SUBFIND (Springel et al 2001)

6DFOF (Diemand et al 2006)

ENLINK (Sharma & Johnston 2009)

HSF (Maciejewski et al 2009)

.....

Challenges, IV
Identification of substructure

Identification of halos, subhalos, and tidal streams is a time-honored endeavor in numerical cosmology

Methods include:

FOF (Davis et al 1985)

DENMAX (Bertschinger & Gelb 1991)

SKID (Stadel 2001)

SUBFIND (Springel et al 2001)

6DFOF (Diemand et al 2006)

ENLINK (Sharma & Johnston 2009)

HSF (Maciejewski et al 2009)

.....

Challenges, IV
Identification of substructure

Identification of halos, subhalos, and tidal streams is a time-honored endeavor in numerical cosmology

Methods include:

FOF (Davis et al 1985)

DENMAX (Bertschinger & Gelb 1991)

SKID (Stadel 2001)

SUBFIND (Springel et al 2001)

6DFOF (Diemand et al 2006)

ENLINK (Sharma & Johnston 2009)

HSF (Maciejewski et al 2009)

.....

Challenges, IV
Identification of substructure

Identification of halos, subhalos, and tidal streams is a time-honored endeavor in numerical cosmology

Methods include:

FOF (Davis et al 1985)

DENMAX (Bertschinger & Gelb 1991)

SKID (Stadel 2001)

SUBFIND (Springel et al 2001)

6DFOF (Diemand et al 2006)

ENLINK (Sharma & Johnston 2009)

HSF (Maciejewski et al 2009)

.....

STructure Finder

hunting for peaks above the Maxwellian Sea

(Elahi, LMW, Thacker 2011)

Model the distribution of dark matter as a smooth background (the parent halo DF) and contributions from substructure (streams and subhalos)

$$f(\mathbf{x}, \mathbf{v}) = f_h(\mathbf{x}, \mathbf{v}) + \sum_s f_s(\mathbf{x}, \mathbf{v})$$

In a small region of the parent halo, DF is the product of density and an anisotropic Maxwellian-like velocity distribution

$$f_h(\mathbf{x}, \mathbf{v}) = \rho_h(\mathbf{x})\, e^{-v_i \sigma^{ij} v_j / 2\sigma_h^2}$$

STructure Finder

hunting for peaks above the Maxwellian Sea

(Elahi, LMW, Thacker 2011)

Model the distribution of dark matter as a smooth background (the parent halo DF) and contributions from substructure (streams and subhalos)

$$f(\mathbf{x}, \mathbf{v}) = f_h(\mathbf{x}, \mathbf{v}) + \sum_s f_s(\mathbf{x}, \mathbf{v})$$

In a small region of the parent halo, DF is the product of density and an anisotropic Maxwellian-like velocity distribution

$$f_h(\mathbf{x}, \mathbf{v}) = \rho_h(\mathbf{x})\, e^{-v_i \sigma^{ij} v_j / 2\sigma_h^2}$$

STructure Finder

hunting for peaks above the Maxwellian Sea

(Elahi, LMW, Thacker 2011)

Model the distribution of dark matter as a smooth background (the parent halo DF) and contributions from substructure (streams and subhalos)

$$f(\mathbf{x}, \mathbf{v}) = f_h(\mathbf{x}, \mathbf{v}) + \sum_s f_s(\mathbf{x}, \mathbf{v})$$

In a small region of the parent halo, DF is the product of density and an anisotropic Maxwellian-like velocity distribution

$$f_h(\mathbf{x}, \mathbf{v}) = \rho_h(\mathbf{x})\, e^{-v_i \sigma^{ij} v_j / 2\sigma_h^2}$$

STructure Finder

hunting for peaks above the Maxwellian Sea

(Elahi, LMW, Thacker 2011)

Model the distribution of dark matter as a smooth background (the parent halo DF) and contributions from substructure (streams and subhalos)

$$f(\mathbf{x}, \mathbf{v}) = f_h(\mathbf{x}, \mathbf{v}) + \sum_s f_s(\mathbf{x}, \mathbf{v})$$

In a small region of the parent halo, DF is the product of density and an anisotropic Maxwellian-like velocity distribution

$$f_h(\mathbf{x}, \mathbf{v}) = \rho_h(\mathbf{x})\, e^{-v_i \sigma^{ij} v_j / 2\sigma_h^2}$$

STructure Finder

hunting for peaks above the Maxwellian Sea

(Elahi, LMW, Thacker 2011)

Model the distribution of dark matter as a smooth background (the parent halo DF) and contributions from substructure (streams and subhalos)

$$f(\mathbf{x}, \mathbf{v}) = f_h(\mathbf{x}, \mathbf{v}) + \sum_s f_s(\mathbf{x}, \mathbf{v})$$

In a small region of the parent halo, DF is the product of density and an anisotropic Maxwellian-like velocity distribution

$$f_h(\mathbf{x}, \mathbf{v}) = \rho_h(\mathbf{x})\, e^{-v_i \sigma^{ij} v_j / 2\sigma_h^2}$$

STructure Finder

hunting for peaks above the Maxwellian Sea

(Elahi, LMW, Thacker 2011)

Model the distribution of dark matter as a smooth background (the parent halo DF) and contributions from substructure (streams and subhalos)

$$f(\mathbf{x}, \mathbf{v}) = f_h(\mathbf{x}, \mathbf{v}) + \sum_s f_s(\mathbf{x}, \mathbf{v})$$

In a small region of the parent halo, DF is the product of density and an anisotropic Maxwellian-like velocity distribution

$$f_h(\mathbf{x}, \mathbf{v}) = \rho_h(\mathbf{x})\, e^{-v_i \sigma^{ij} v_j / 2\sigma_h^2}$$

STructure Finder

hunting for peaks above the Maxwellian Sea

(Elahi, LMW, Thacker 2011)

Model the distribution of dark matter as a smooth background (the parent halo DF) and contributions from substructure (streams and subhalos)

$$f(\mathbf{x}, \mathbf{v}) = f_h(\mathbf{x}, \mathbf{v}) + \sum_s f_s(\mathbf{x}, \mathbf{v})$$

In a small region of the parent halo, DF is the product of density and an anisotropic Maxwellian-like velocity distribution

$$f_h(\mathbf{x}, \mathbf{v}) = \rho_h(\mathbf{x})\, e^{-v_i \sigma^{ij} v_j / 2\sigma_h^2}$$

STructure Finder

hunting for peaks above the Maxwellian Sea

(Elahi, LMW, Thacker 2011)

Model the distribution of dark matter as a smooth background (the parent halo DF) and contributions from substructure (streams and subhalos)

$$f(\mathbf{x}, \mathbf{v}) = f_h(\mathbf{x}, \mathbf{v}) + \sum_s f_s(\mathbf{x}, \mathbf{v})$$

In a small region of the parent halo, DF is the product of density and an anisotropic Maxwellian-like velocity distribution

$$f_h(\mathbf{x}, \mathbf{v}) = \rho_h(\mathbf{x})\, e^{-v_i \sigma^{ij} v_j / 2\sigma_h^2}$$

STructure Finder

hunting for peaks above the Maxwellian Sea

(Elahi, LMW, Thacker 2011)

Model the distribution of dark matter as a smooth background (the parent halo DF) and contributions from substructure (streams and subhalos)

$$f(\mathbf{x}, \mathbf{v}) = f_h(\mathbf{x}, \mathbf{v}) + \sum_s f_s(\mathbf{x}, \mathbf{v})$$

In a small region of the parent halo, DF is the product of density and an anisotropic Maxwellian-like velocity distribution

$$f_h(\mathbf{x}, \mathbf{v}) = \rho_h(\mathbf{x})\, e^{-v_i \sigma^{ij} v_j / 2\sigma_h^2}$$

STructure Finder

hunting for peaks above the Maxwellian Sea

(Elahi, LMW, Thacker 2011)

Model the distribution of dark matter as a smooth background (the parent halo DF) and contributions from substructure (streams and subhalos)

$$f(\mathbf{x}, \mathbf{v}) = f_h(\mathbf{x}, \mathbf{v}) + \sum_s f_s(\mathbf{x}, \mathbf{v})$$

In a small region of the parent halo, DF is the product of density and an anisotropic Maxwellian-like velocity distribution

$$f_h(\mathbf{x}, \mathbf{v}) = \rho_h(\mathbf{x})\, e^{-v_i \sigma^{ij} v_j / 2\sigma_h^2}$$

STructure Finder

hunting for peaks above the Maxwellian Sea

(Elahi, LMW, Thacker 2011)

Model the distribution of dark matter as a smooth background (the parent halo DF) and contributions from substructure (streams and subhalos)

$$f(\mathbf{x}, \mathbf{v}) = f_h(\mathbf{x}, \mathbf{v}) + \sum_s f_s(\mathbf{x}, \mathbf{v})$$

In a small region of the parent halo, DF is the product of density and an anisotropic Maxwellian-like velocity distribution

$$f_h(\mathbf{x}, \mathbf{v}) = \rho_h(\mathbf{x})\, e^{-v_i \sigma^{ij} v_j / 2\sigma_h^2}$$

Likewise, we write the DF for the substructure as

$$f_s(\mathbf{x}, \mathbf{v}) = \rho_s(\mathbf{x} - \mathbf{x}_0)\, g(\mathbf{v} - \mathbf{v}_0; \sigma_s)$$

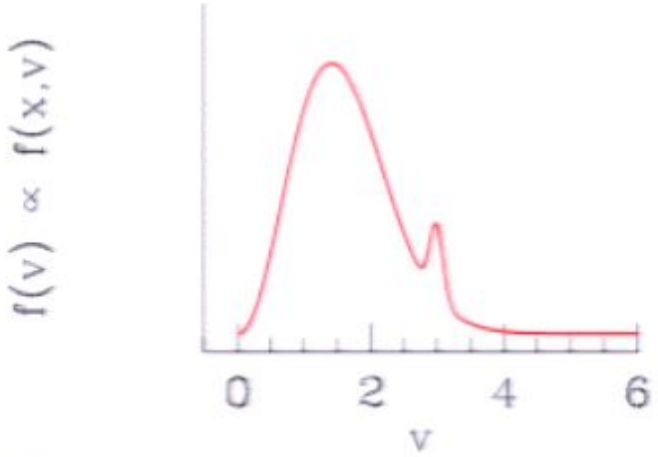

to pick out substructure (streams or subhalos) divide out by the local Maxwellian

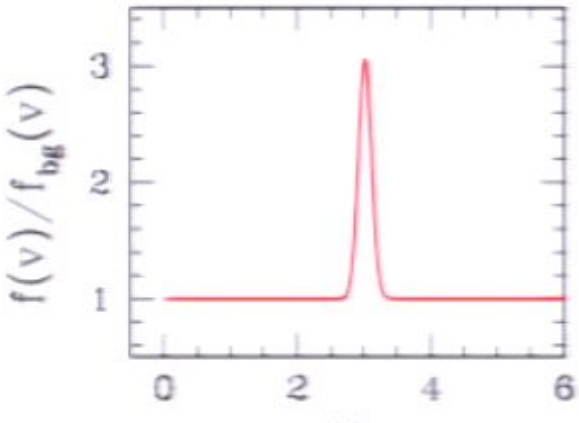

Likewise, we write the DF for the substructure as

$$f_s(\mathbf{x}, \mathbf{v}) = \rho_s(\mathbf{x} - \mathbf{x}_0)\, g(\mathbf{v} - \mathbf{v}_0; \sigma_s)$$

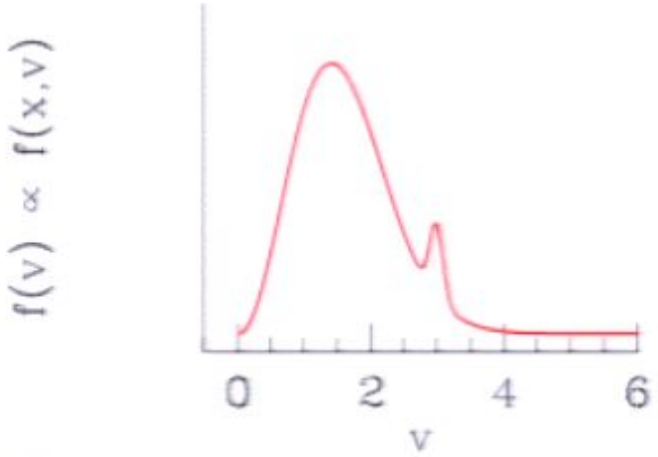

to pick out substructure (streams or subhalos) divide out by the local Maxwellian

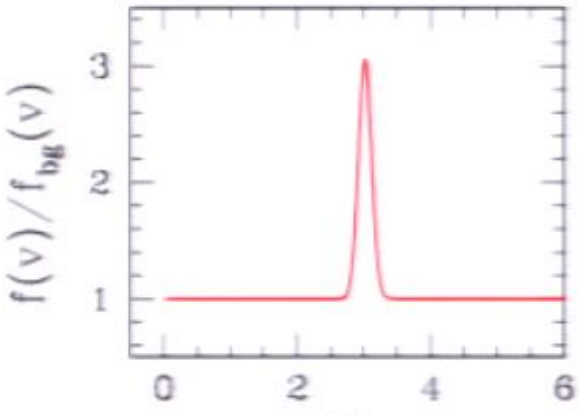

Likewise, we write the DF for the substructure as

$$f_s(\mathbf{x}, \mathbf{v}) = \rho_s(\mathbf{x} - \mathbf{x}_0)\, g(\mathbf{v} - \mathbf{v}_0; \sigma_s)$$

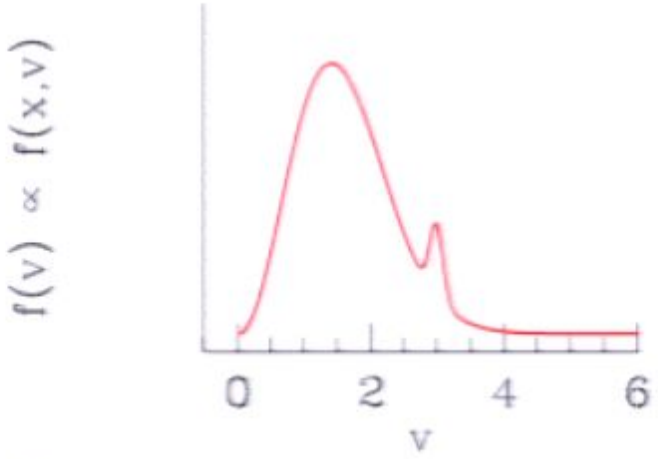

to pick out substructure (streams or subhalos) divide out by the local Maxwellian

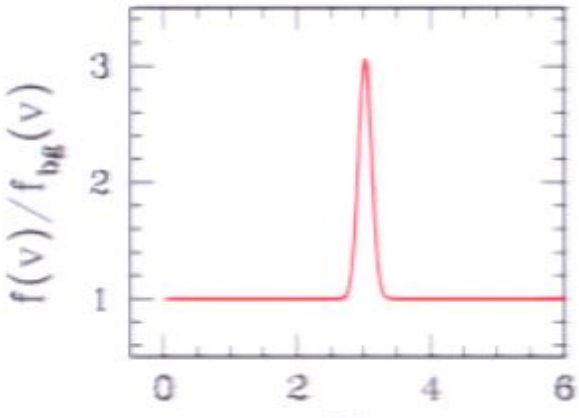

Likewise, we write the DF for the substructure as

$$f_s(\mathbf{x}, \mathbf{v}) = \rho_s(\mathbf{x} - \mathbf{x}_0)\, g(\mathbf{v} - \mathbf{v}_0; \sigma_s)$$

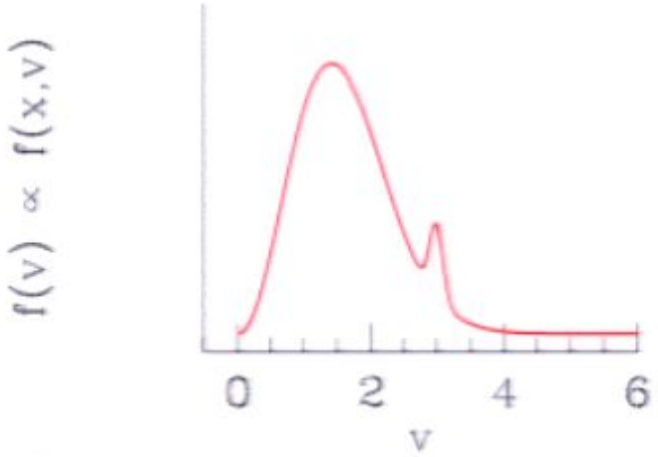

to pick out substructure (streams or subhalos) divide out by the local Maxwellian

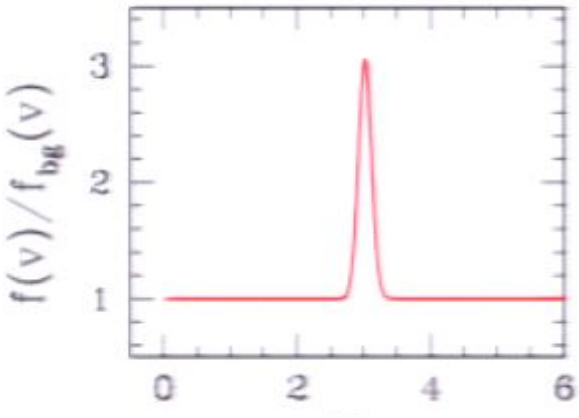

Likewise, we write the DF for the substructure as

$$f_s(\mathbf{x}, \mathbf{v}) = \rho_s(\mathbf{x} - \mathbf{x}_0)\, g(\mathbf{v} - \mathbf{v}_0; \sigma_s)$$

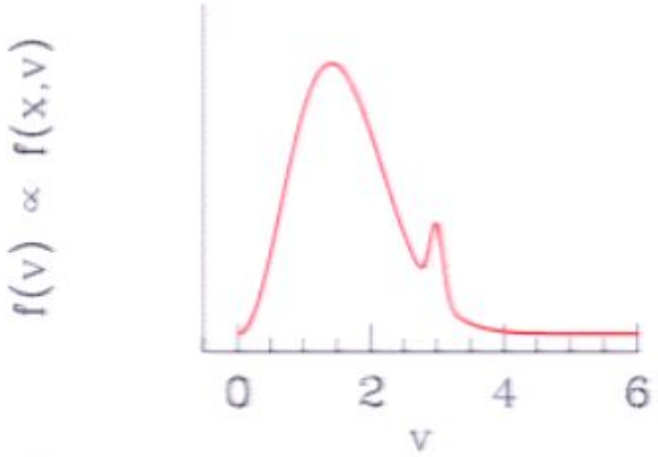

to pick out substructure (streams or subhalos) divide out by the local Maxwellian

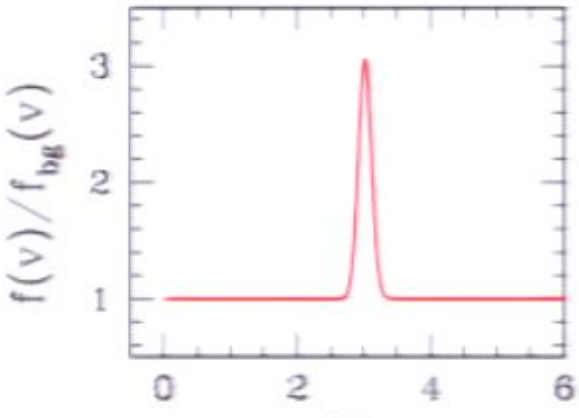

Likewise, we write the DF for the substructure as

$$f_s(\mathbf{x}, \mathbf{v}) = \rho_s(\mathbf{x} - \mathbf{x}_0)\, g(\mathbf{v} - \mathbf{v}_0; \sigma_s)$$

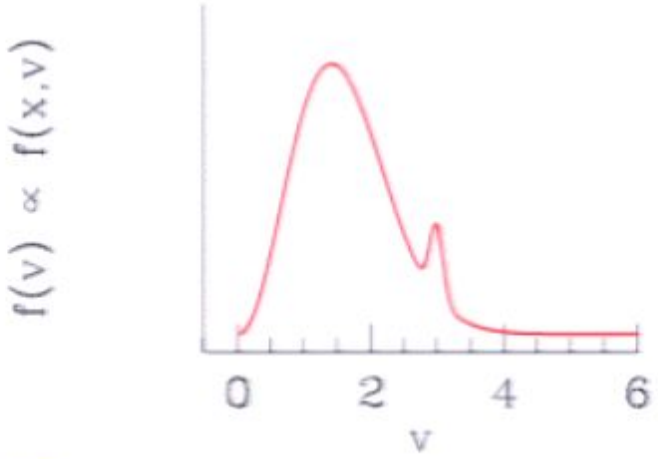

to pick out substructure (streams or subhalos) divide out by the local Maxwellian

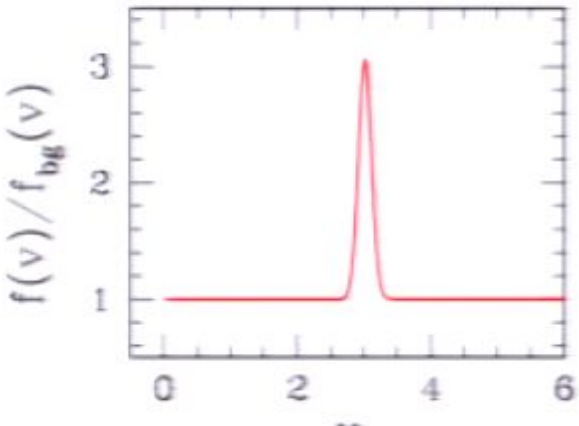

Likewise, we write the DF for the substructure as

$$f_s(\mathbf{x}, \mathbf{v}) = \rho_s(\mathbf{x} - \mathbf{x}_0)\, g(\mathbf{v} - \mathbf{v}_0; \sigma_s)$$

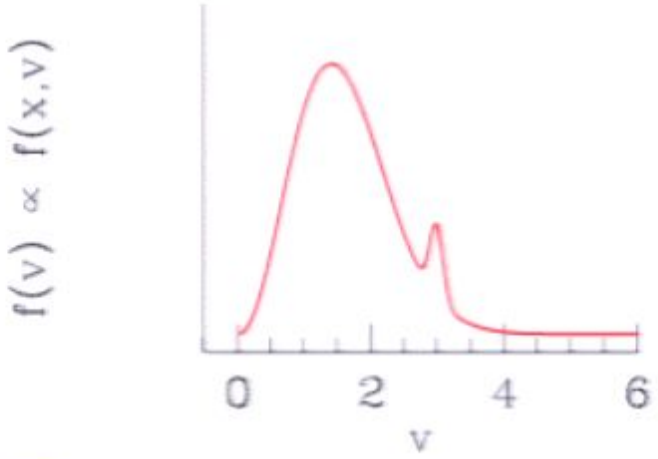

to pick out substructure (streams or subhalos) divide out by the local Maxwellian

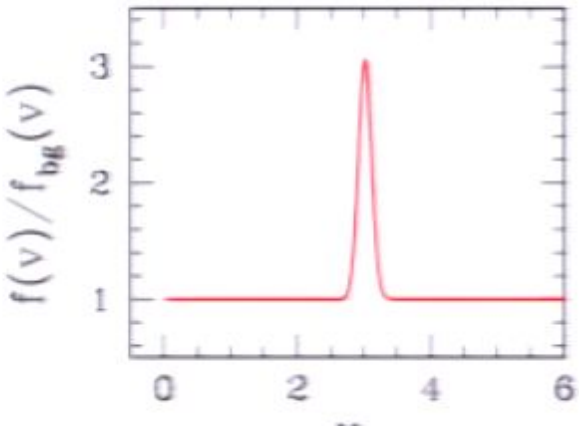

Likewise, we write the DF for the substructure as

$$f_s(\mathbf{x}, \mathbf{v}) = \rho_s(\mathbf{x} - \mathbf{x}_0)\, g(\mathbf{v} - \mathbf{v}_0; \sigma_s)$$

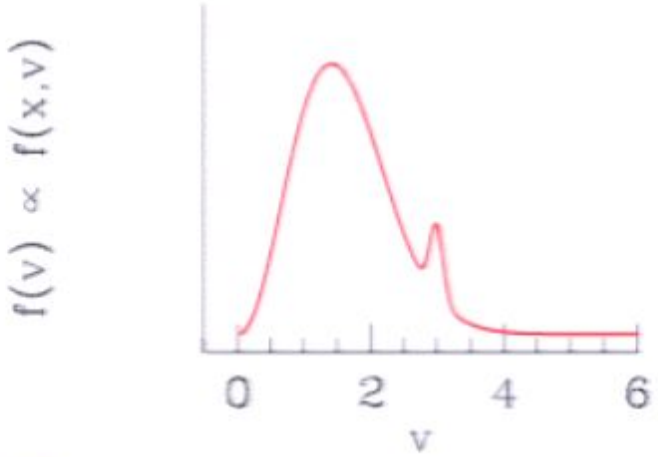

to pick out substructure (streams or subhalos) divide out by the local Maxwellian

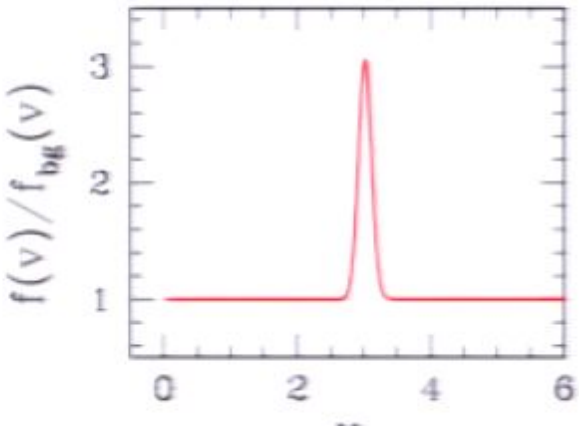

Likewise, we write the DF for the substructure as

$$f_s(\mathbf{x}, \mathbf{v}) = \rho_s(\mathbf{x} - \mathbf{x}_0)\, g(\mathbf{v} - \mathbf{v}_0; \sigma_s)$$

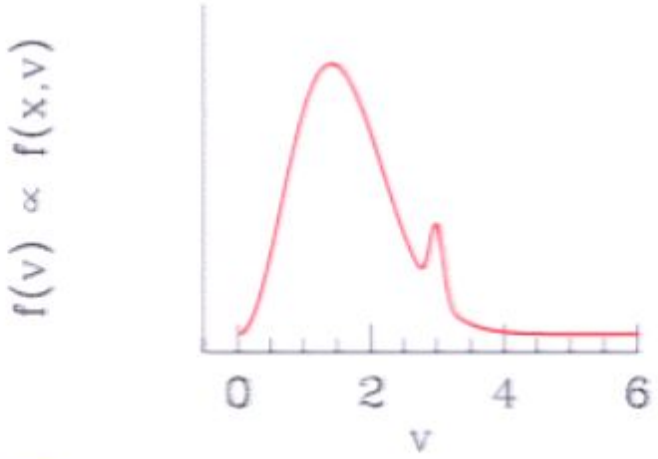

to pick out substructure (streams or subhalos) divide out by the local Maxwellian

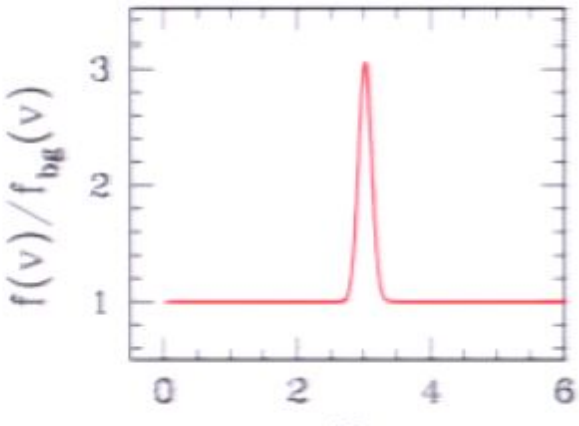

Likewise, we write the DF for the substructure as

$$f_s(\mathbf{x}, \mathbf{v}) = \rho_s(\mathbf{x} - \mathbf{x}_0)\, g(\mathbf{v} - \mathbf{v}_0; \sigma_s)$$

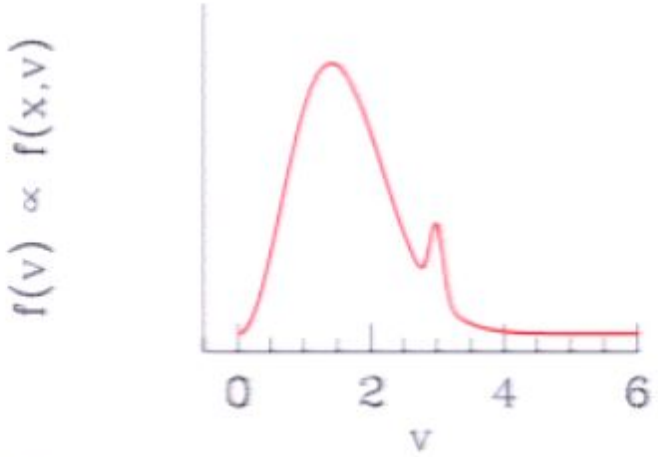

to pick out substructure (streams or subhalos) divide out by the local Maxwellian

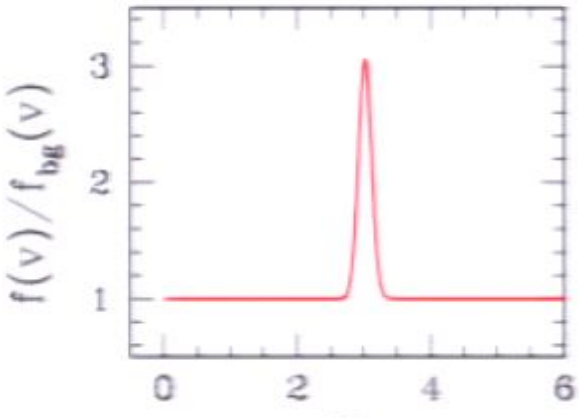

Likewise, we write the DF for the substructure as

$$f_s(\mathbf{x}, \mathbf{v}) = \rho_s(\mathbf{x} - \mathbf{x}_0)\, g(\mathbf{v} - \mathbf{v}_0; \sigma_s)$$

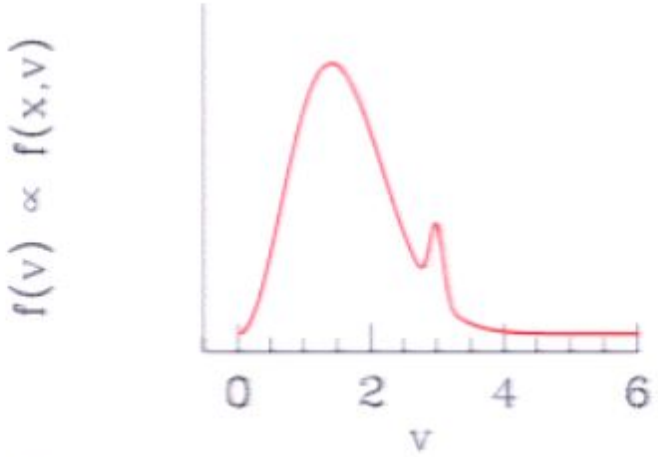

to pick out substructure (streams or subhalos) divide out by the local Maxwellian

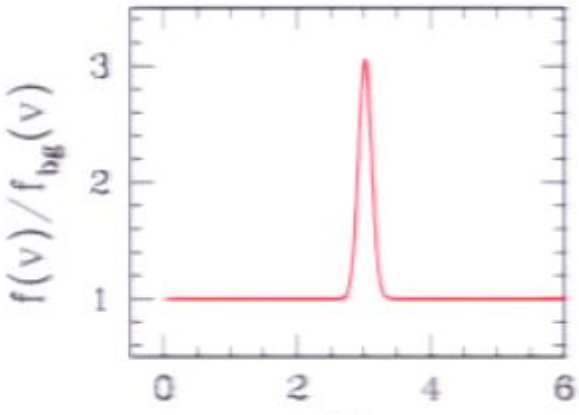

Likewise, we write the DF for the substructure as

$$f_s(\mathbf{x}, \mathbf{v}) = \rho_s(\mathbf{x} - \mathbf{x}_0)\, g(\mathbf{v} - \mathbf{v}_0; \sigma_s)$$

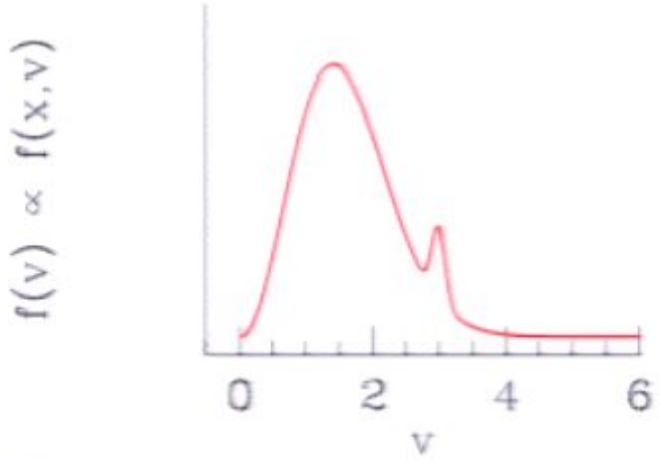

to pick out substructure (streams or subhalos) divide out by the local Maxwellian

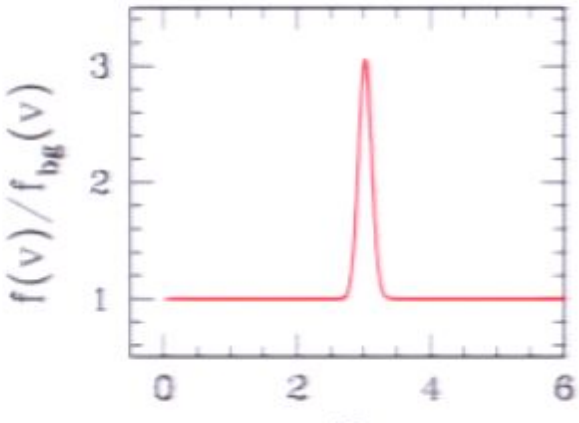

Likewise, we write the DF for the substructure as

$$f_s(\mathbf{x}, \mathbf{v}) = \rho_s(\mathbf{x} - \mathbf{x}_0)\, g(\mathbf{v} - \mathbf{v}_0; \sigma_s)$$

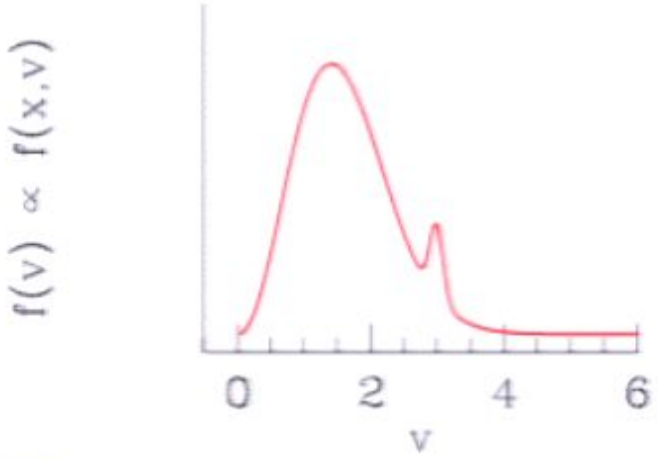

to pick out substructure (streams or subhalos) divide out by the local Maxwellian

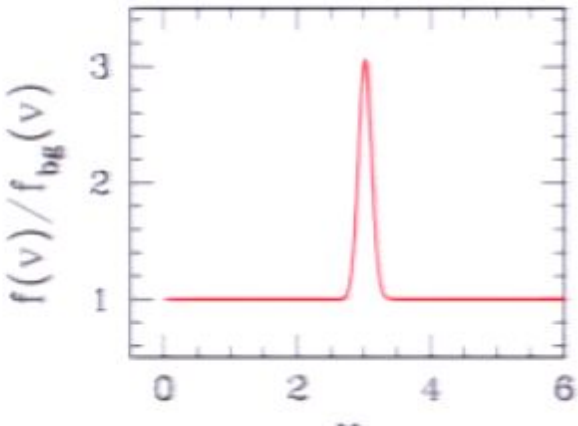

Likewise, we write the DF for the substructure as

$$f_s(\mathbf{x}, \mathbf{v}) = \rho_s(\mathbf{x} - \mathbf{x}_0)\, g(\mathbf{v} - \mathbf{v}_0; \sigma_s)$$

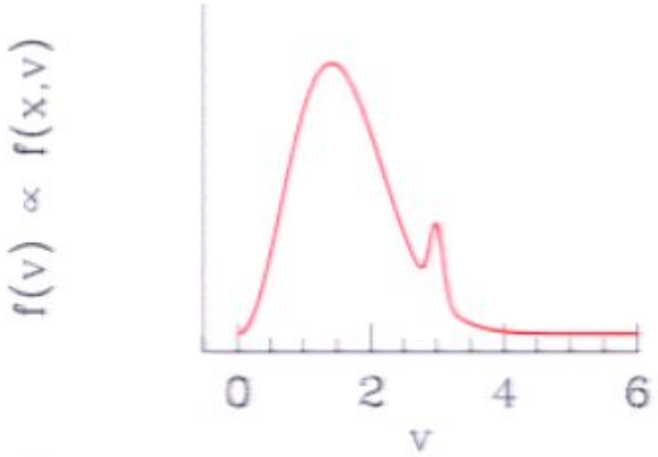

to pick out substructure (streams or subhalos) divide out by the local Maxwellian

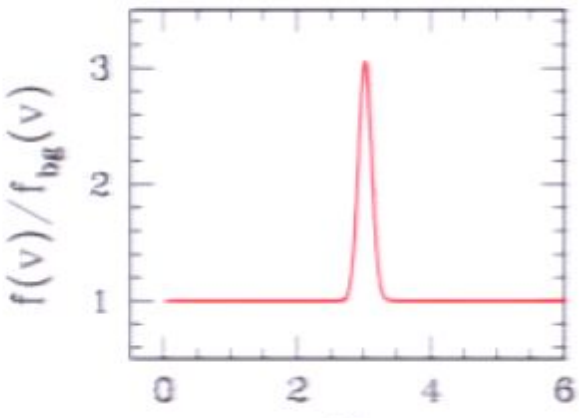

Likewise, we write the DF for the substructure as

$$f_s(\mathbf{x}, \mathbf{v}) = \rho_s(\mathbf{x} - \mathbf{x}_0)\, g(\mathbf{v} - \mathbf{v}_0; \sigma_s)$$

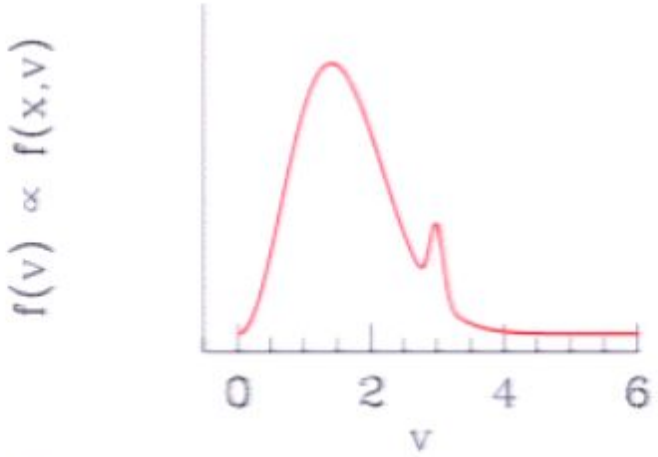

to pick out substructure (streams or subhalos) divide out by the local Maxwellian

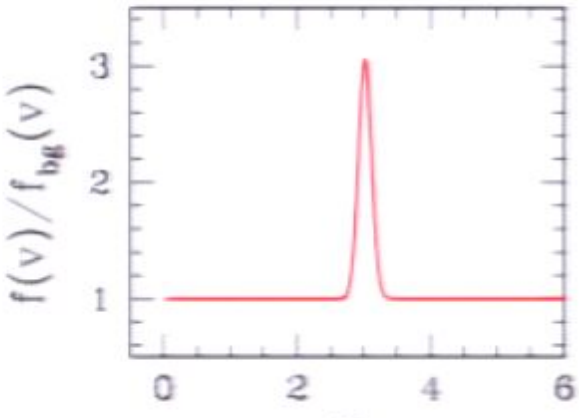

Likewise, we write the DF for the substructure as

$$f_s(\mathbf{x}, \mathbf{v}) = \rho_s(\mathbf{x} - \mathbf{x}_0)\, g(\mathbf{v} - \mathbf{v}_0; \sigma_s)$$

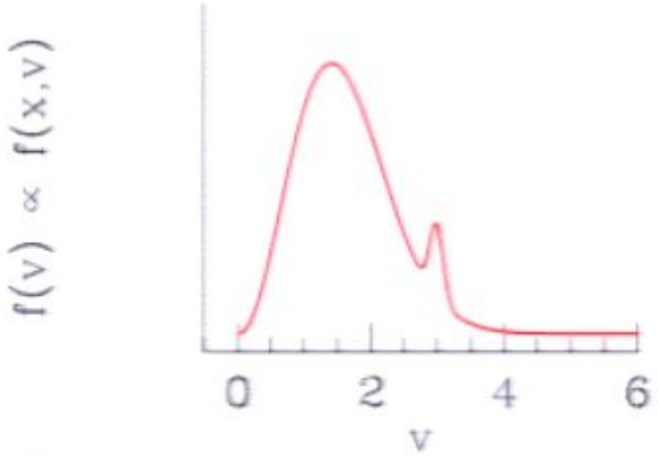

to pick out substructure (streams or subhalos) divide out by the local Maxwellian

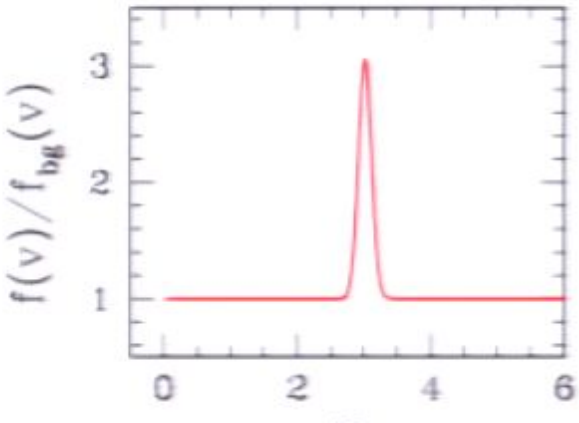

Likewise, we write the DF for the substructure as

$$f_s(\mathbf{x}, \mathbf{v}) = \rho_s(\mathbf{x} - \mathbf{x}_0)\, g(\mathbf{v} - \mathbf{v}_0; \sigma_s)$$

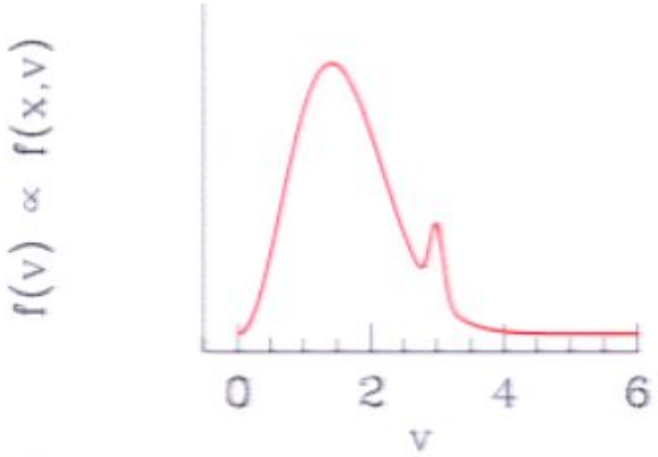

to pick out substructure (streams or subhalos) divide out by the local Maxwellian

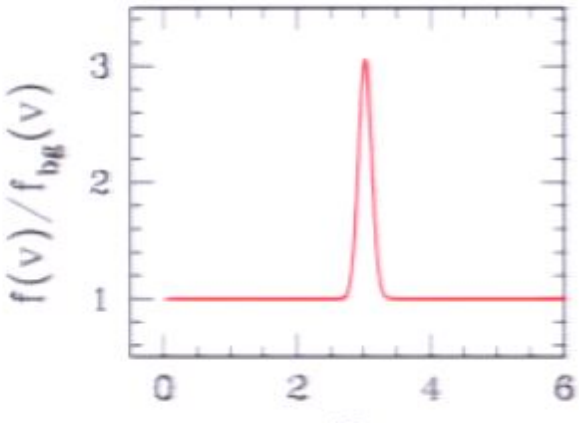

Likewise, we write the DF for the substructure as

$$f_s(\mathbf{x}, \mathbf{v}) = \rho_s(\mathbf{x} - \mathbf{x}_0)\, g(\mathbf{v} - \mathbf{v}_0; \sigma_s)$$

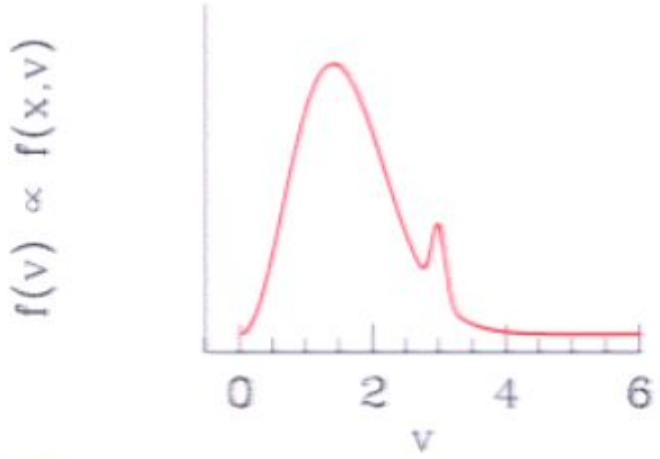

to pick out substructure (streams or subhalos) divide out by the local Maxwellian

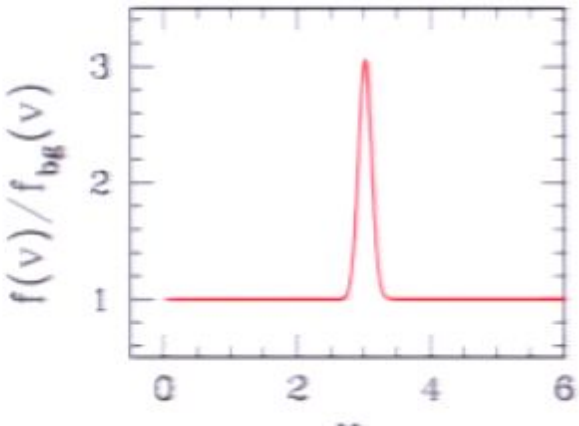

Likewise, we write the DF for the substructure as

$$f_s(\mathbf{x}, \mathbf{v}) = \rho_s(\mathbf{x} - \mathbf{x}_0)\, g(\mathbf{v} - \mathbf{v}_0; \sigma_s)$$

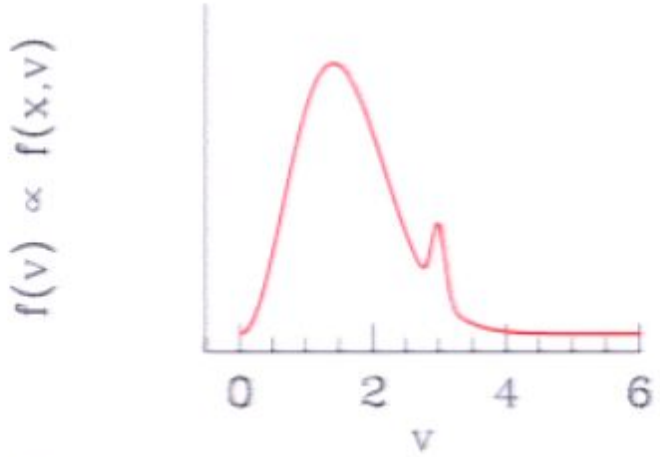

to pick out substructure (streams or subhalos) divide out by the local Maxwellian

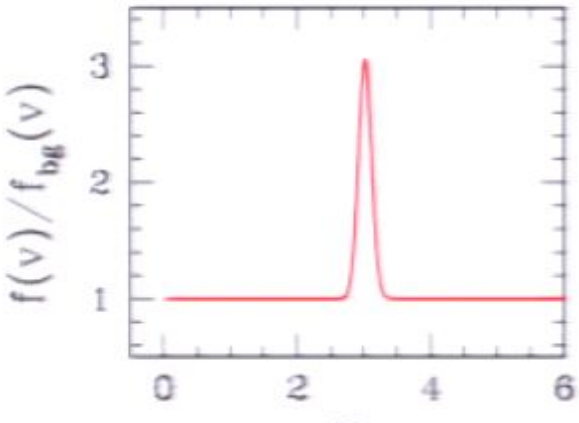

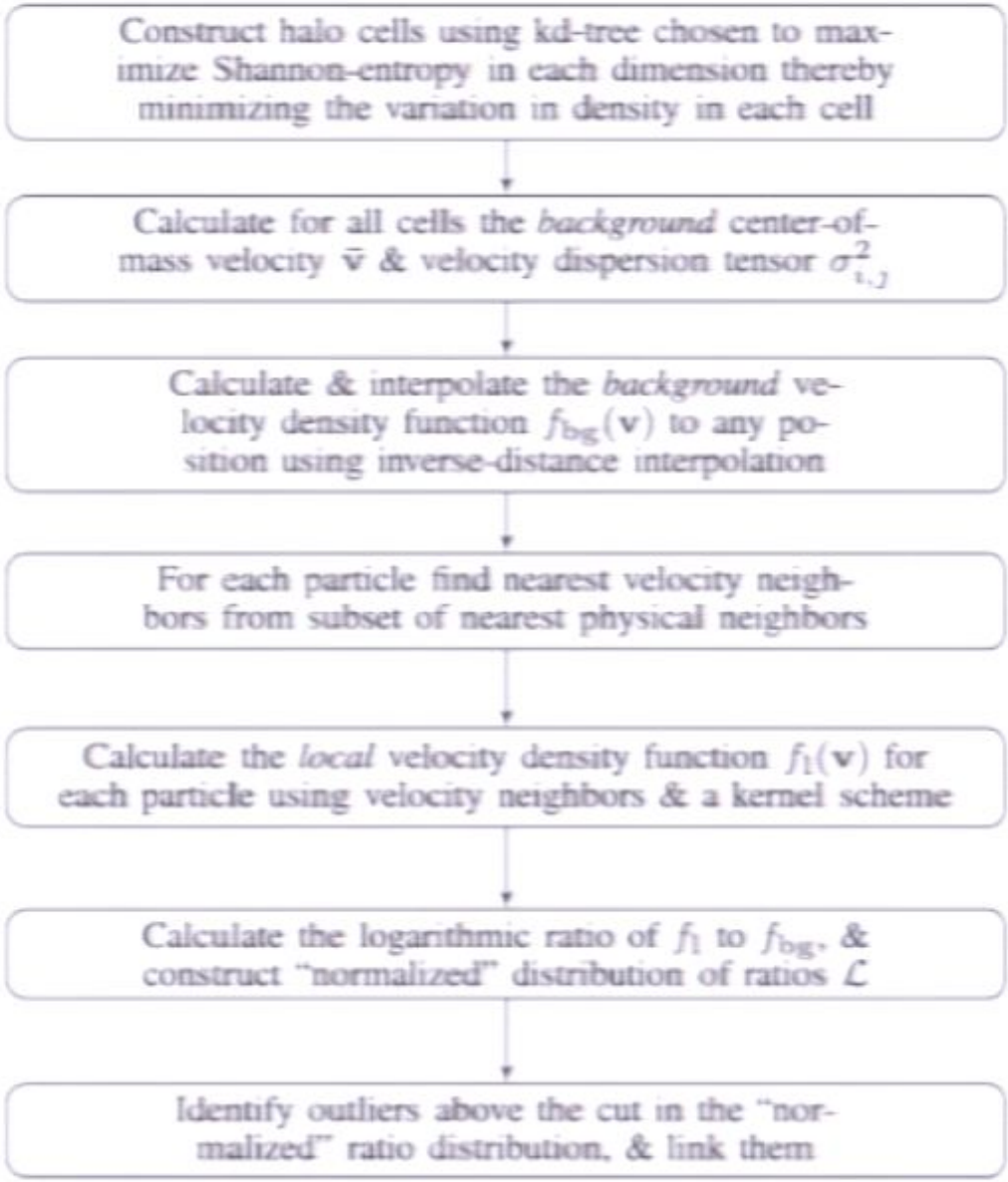

Figure 1. Flow chart of STF algorithm.

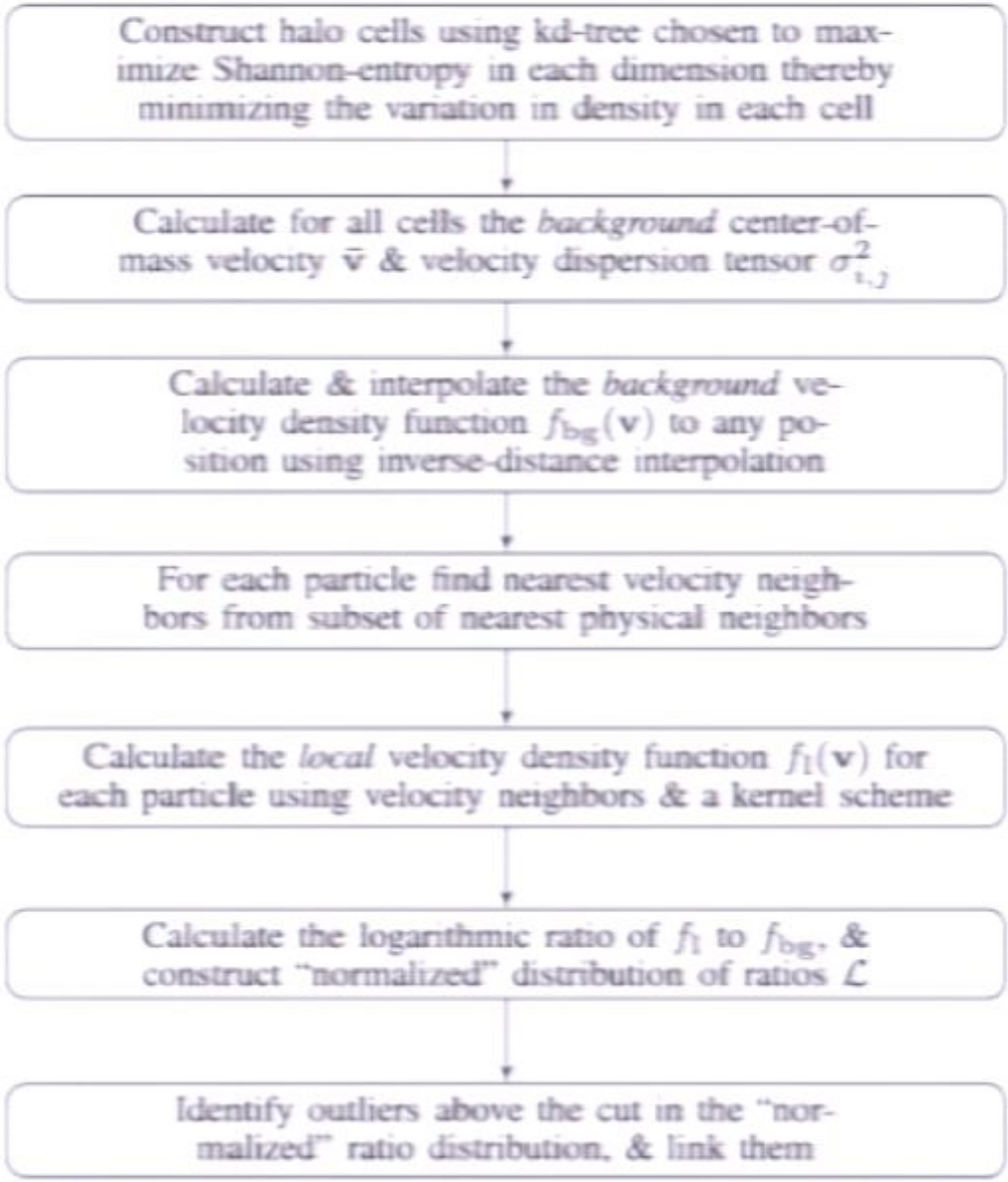

Figure 1. Flow chart of STF algorithm.

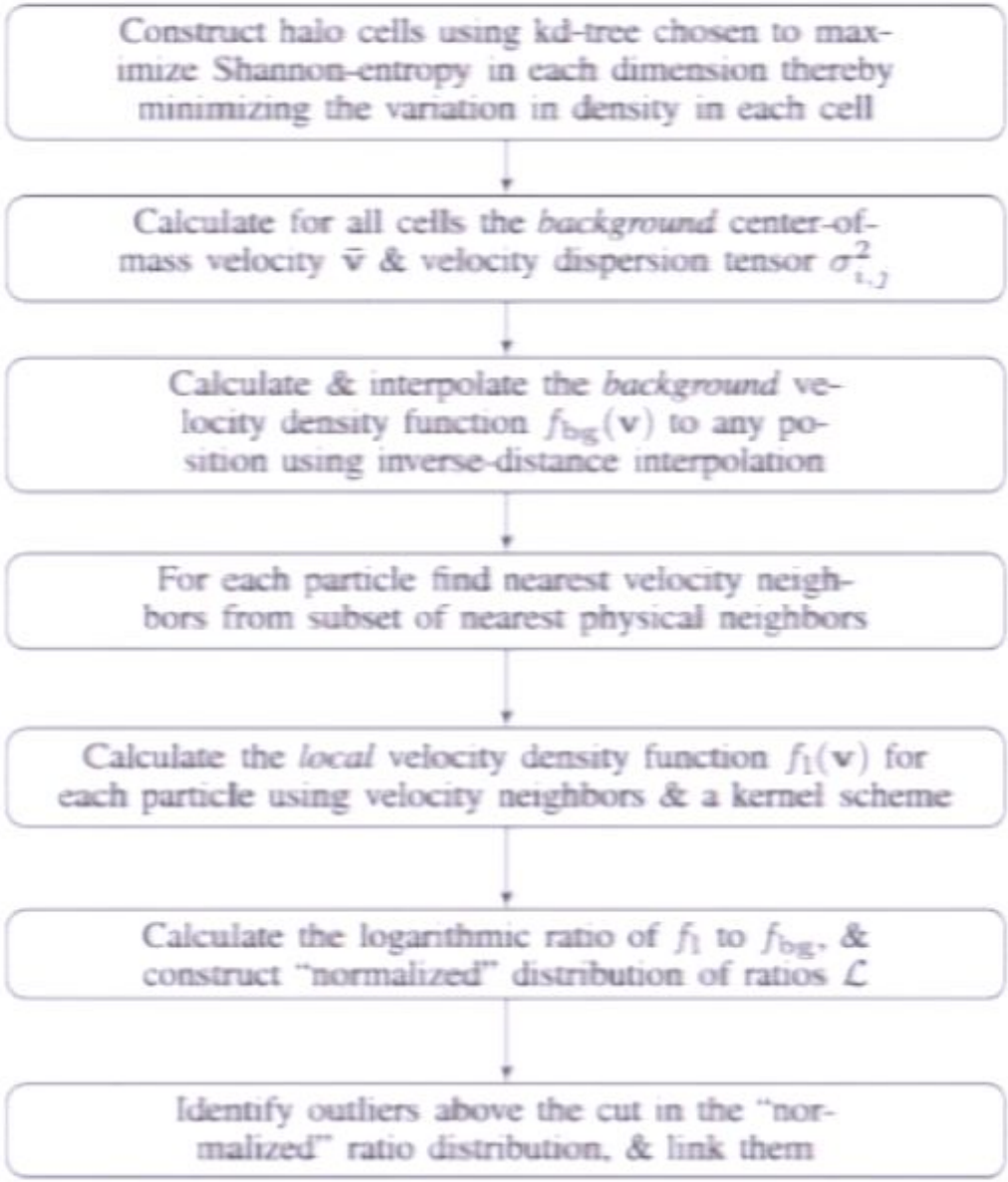

Figure 1. Flow chart of STF algorithm.

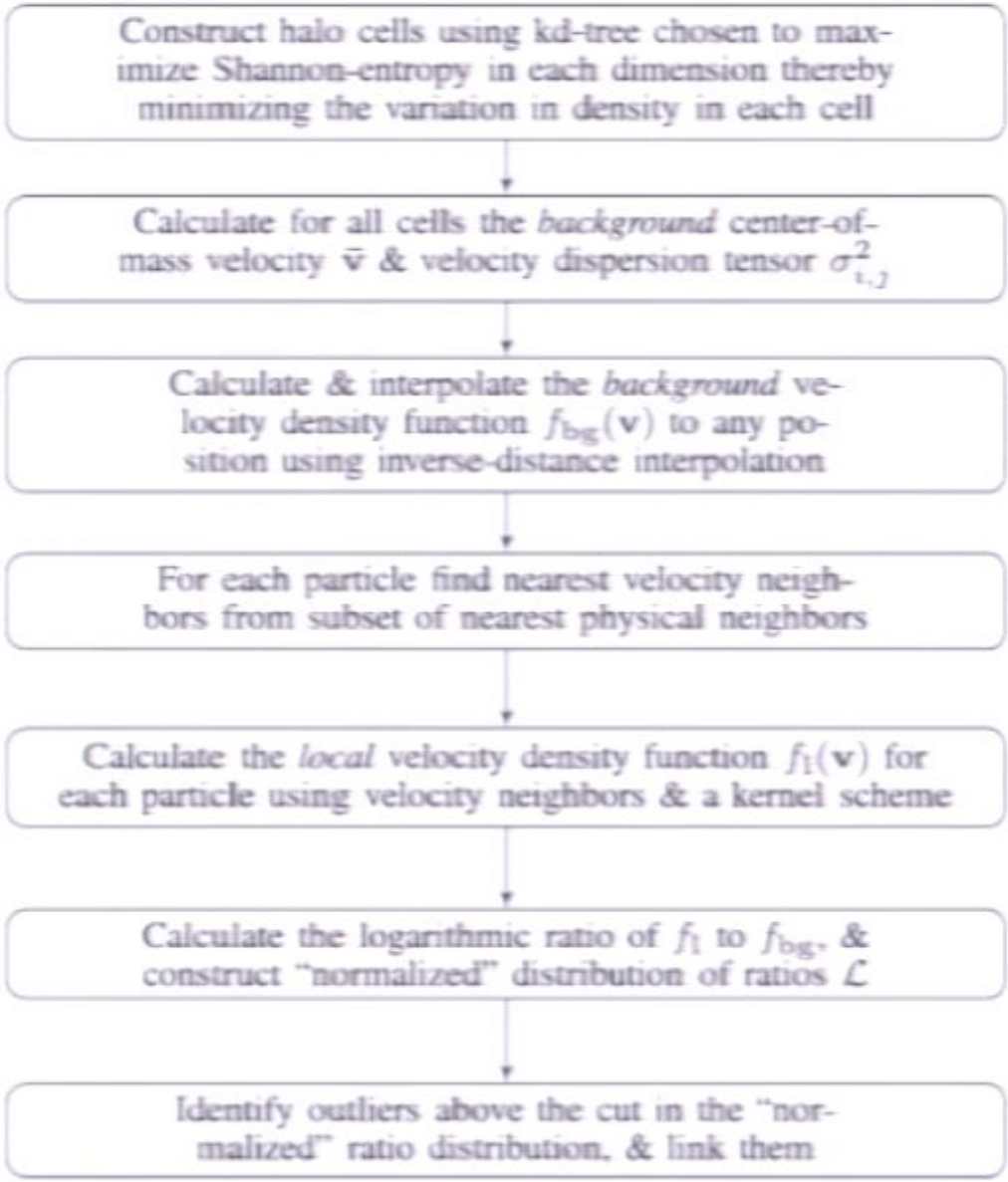

Figure 1. Flow chart of STF algorithm.

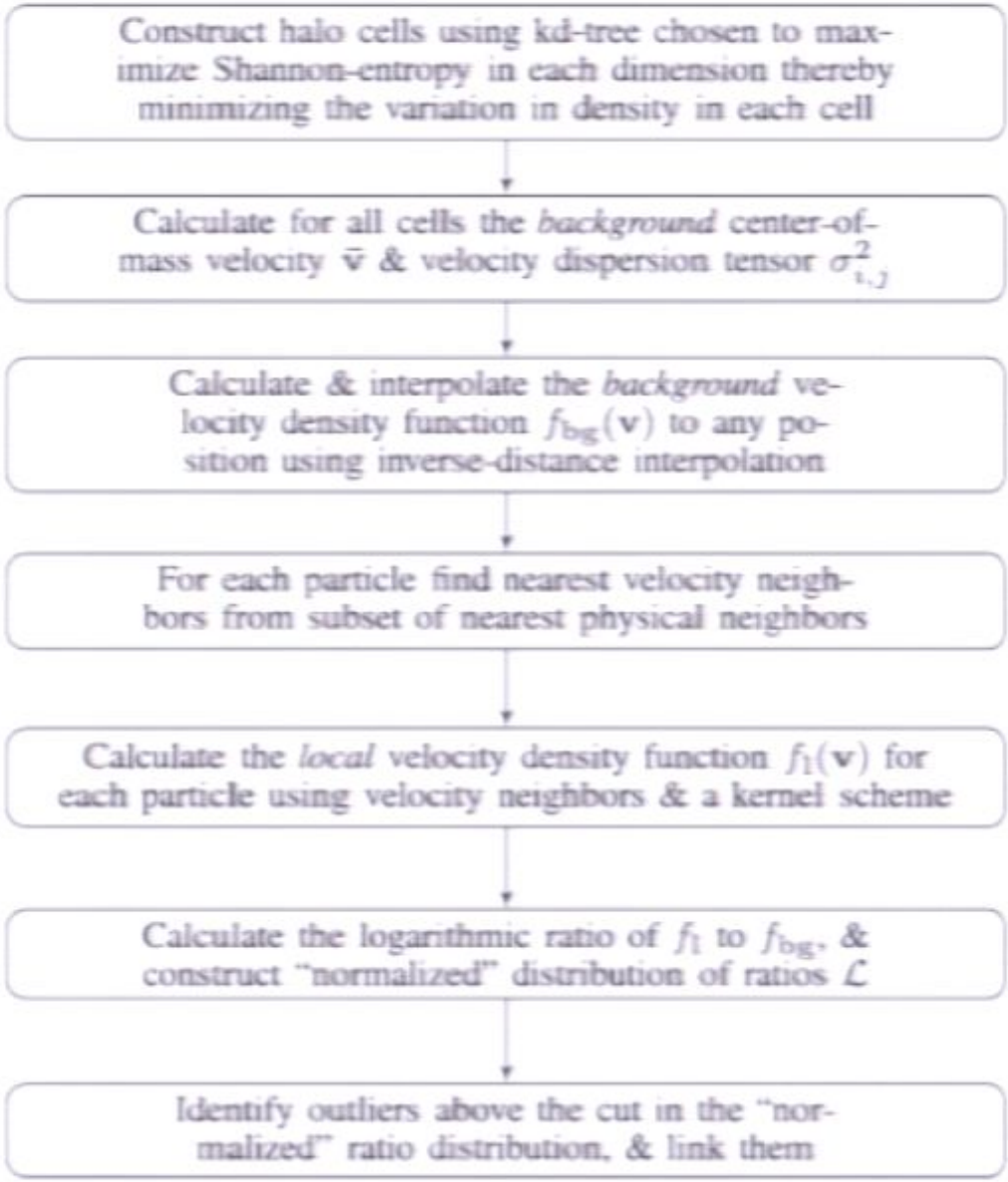

Figure 1. Flow chart of STF algorithm.

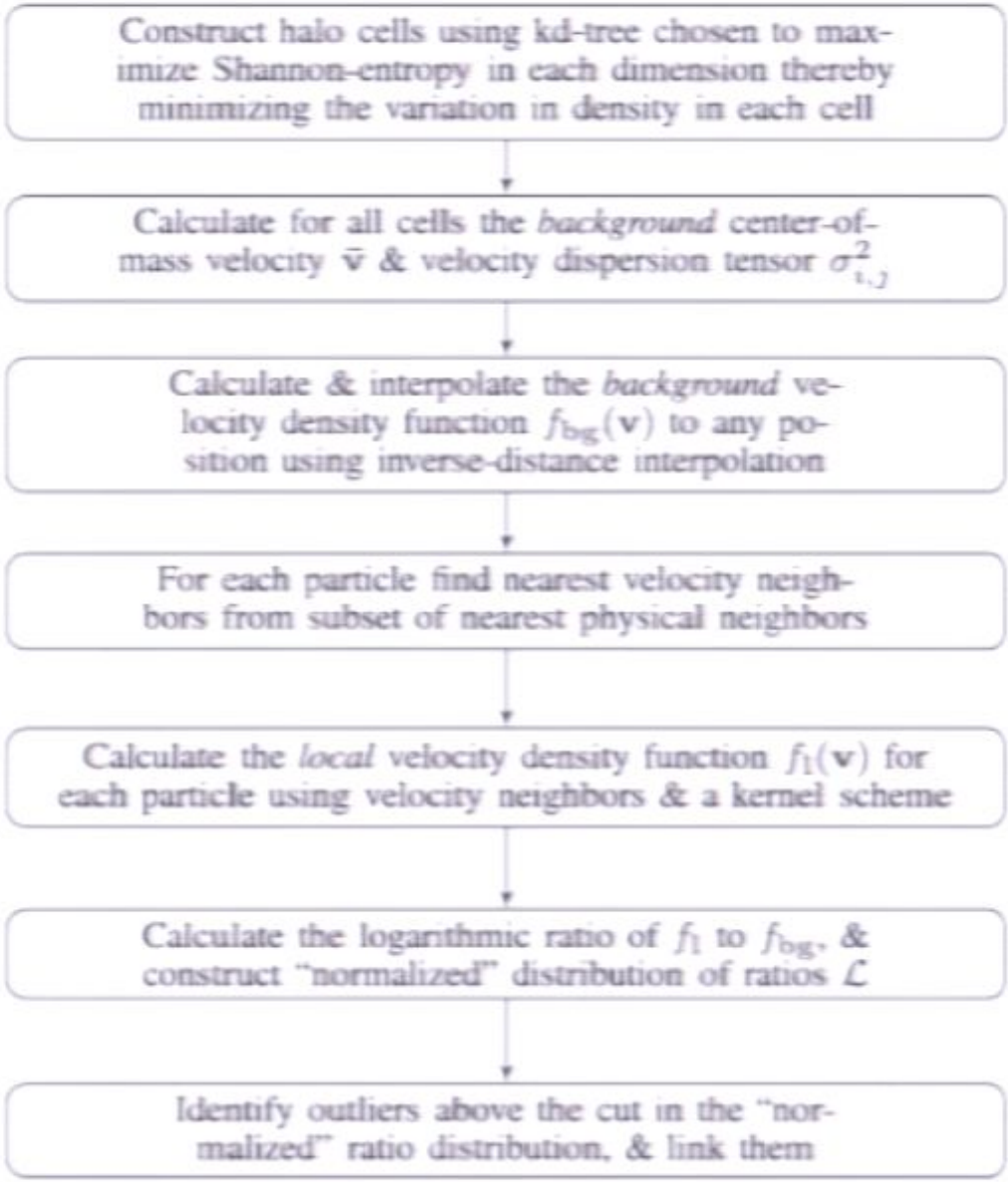

Figure 1. Flow chart of STF algorithm.

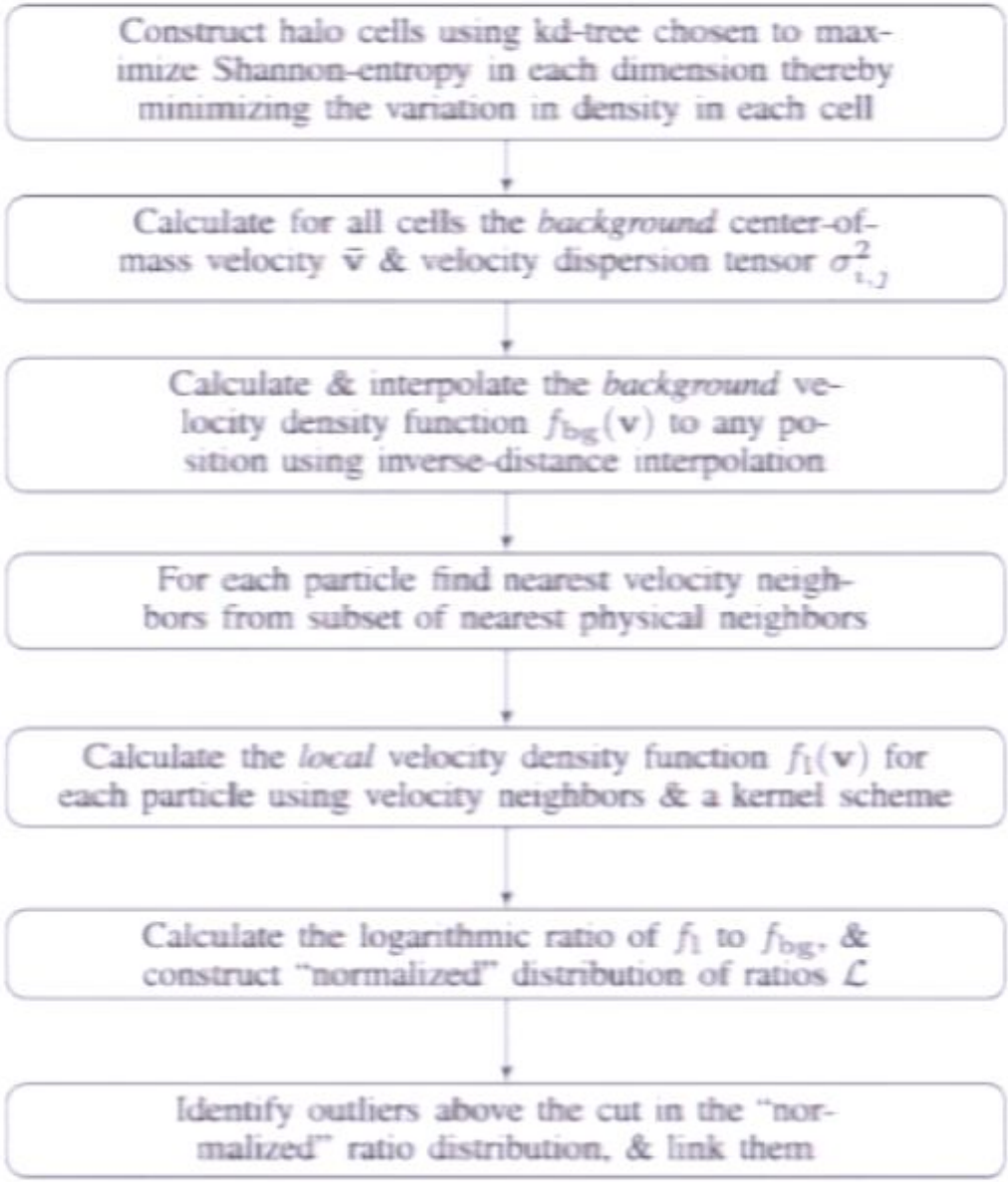

Figure 1. Flow chart of STF algorithm.

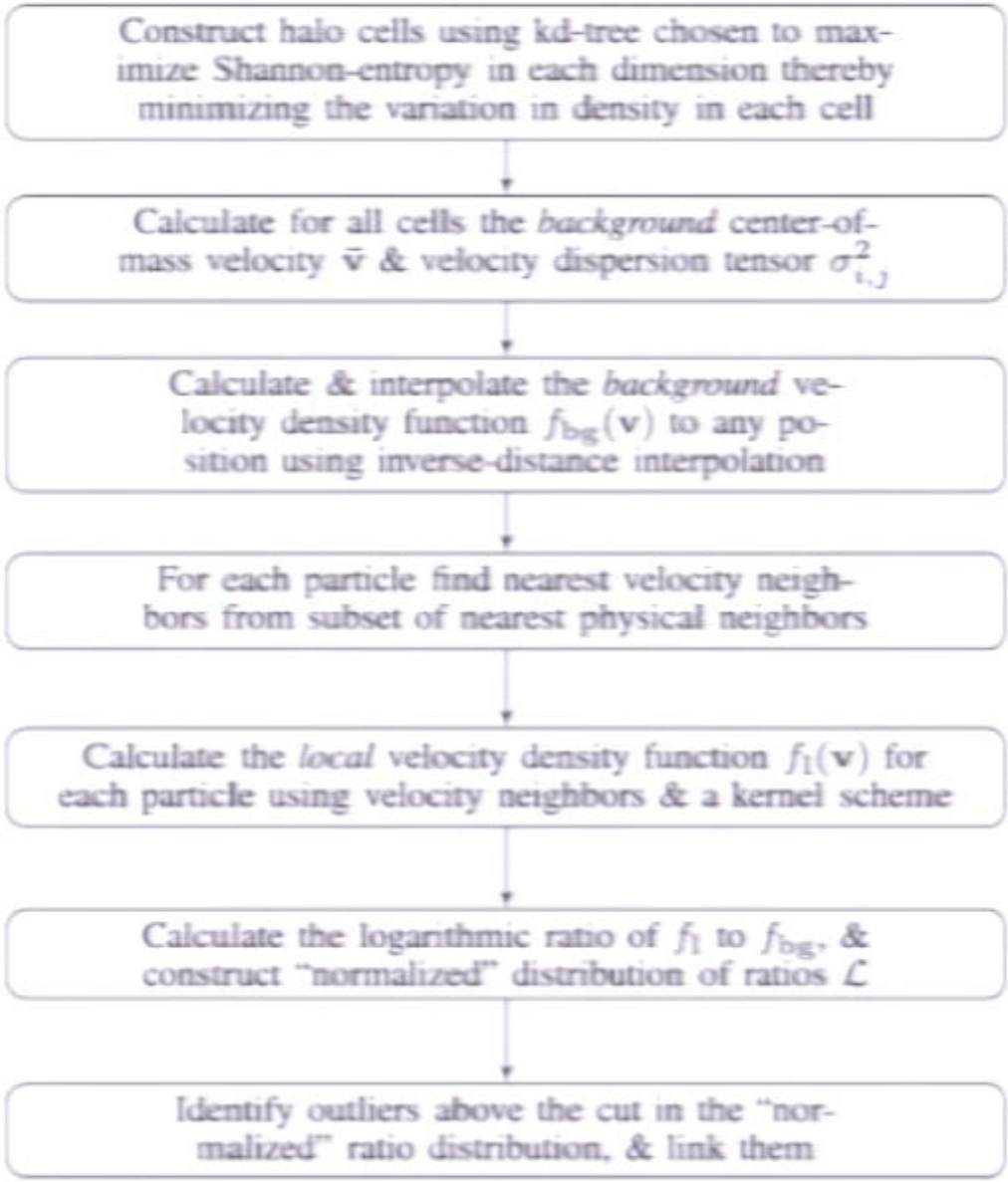

Figure 1. Flow chart of STF algorithm.

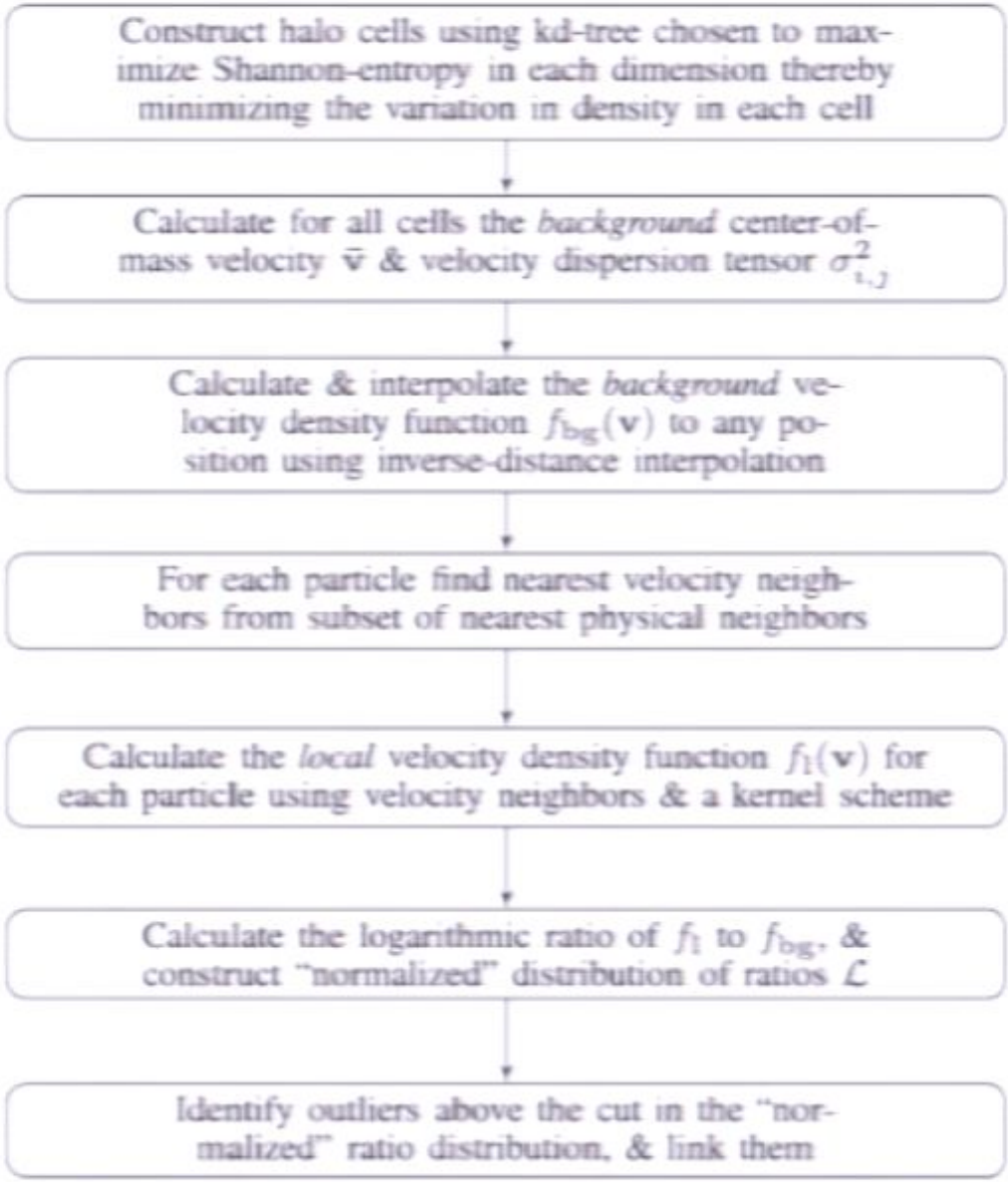

Figure 1. Flow chart of STF algorithm.

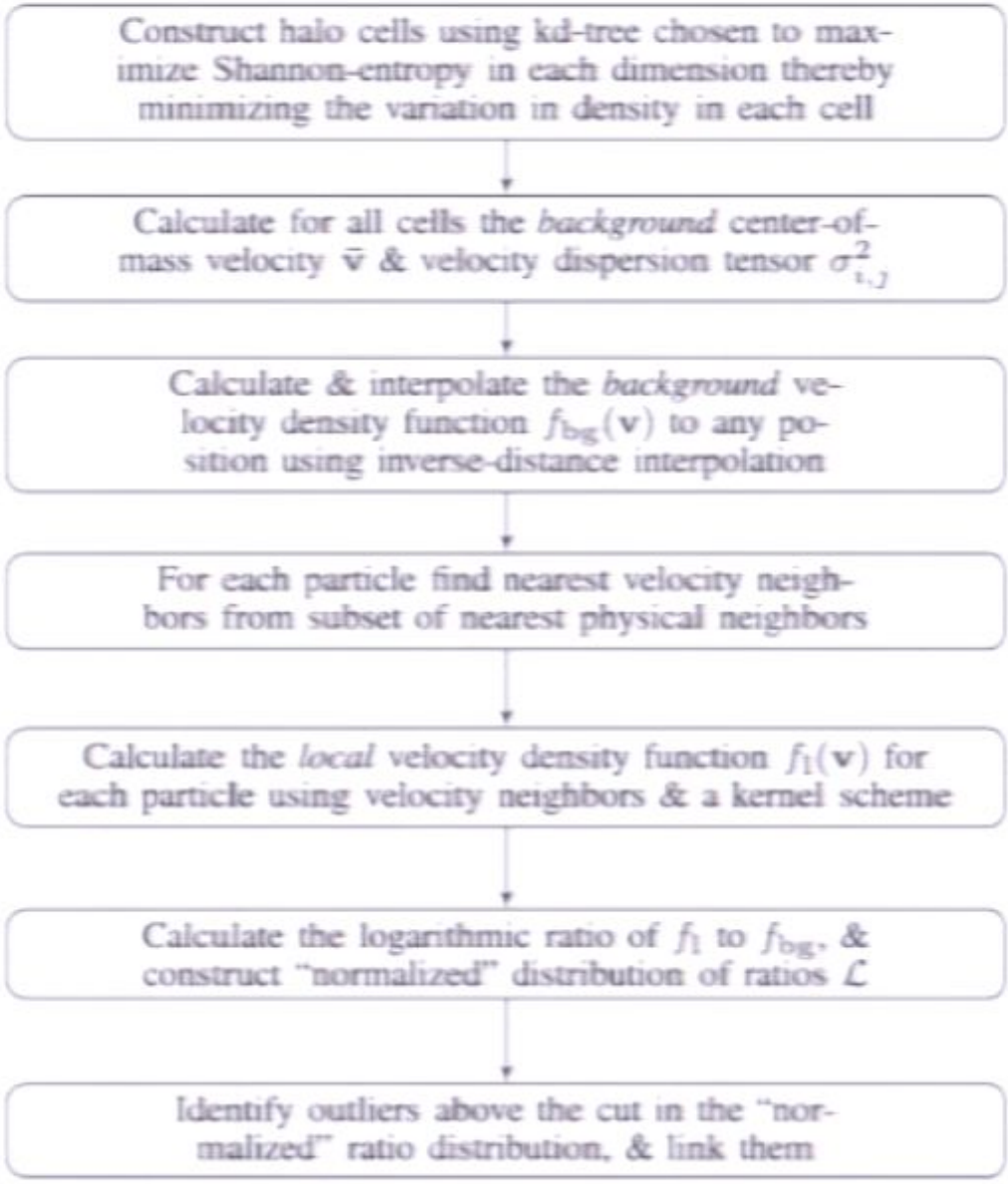

Figure 1. Flow chart of STF algorithm.

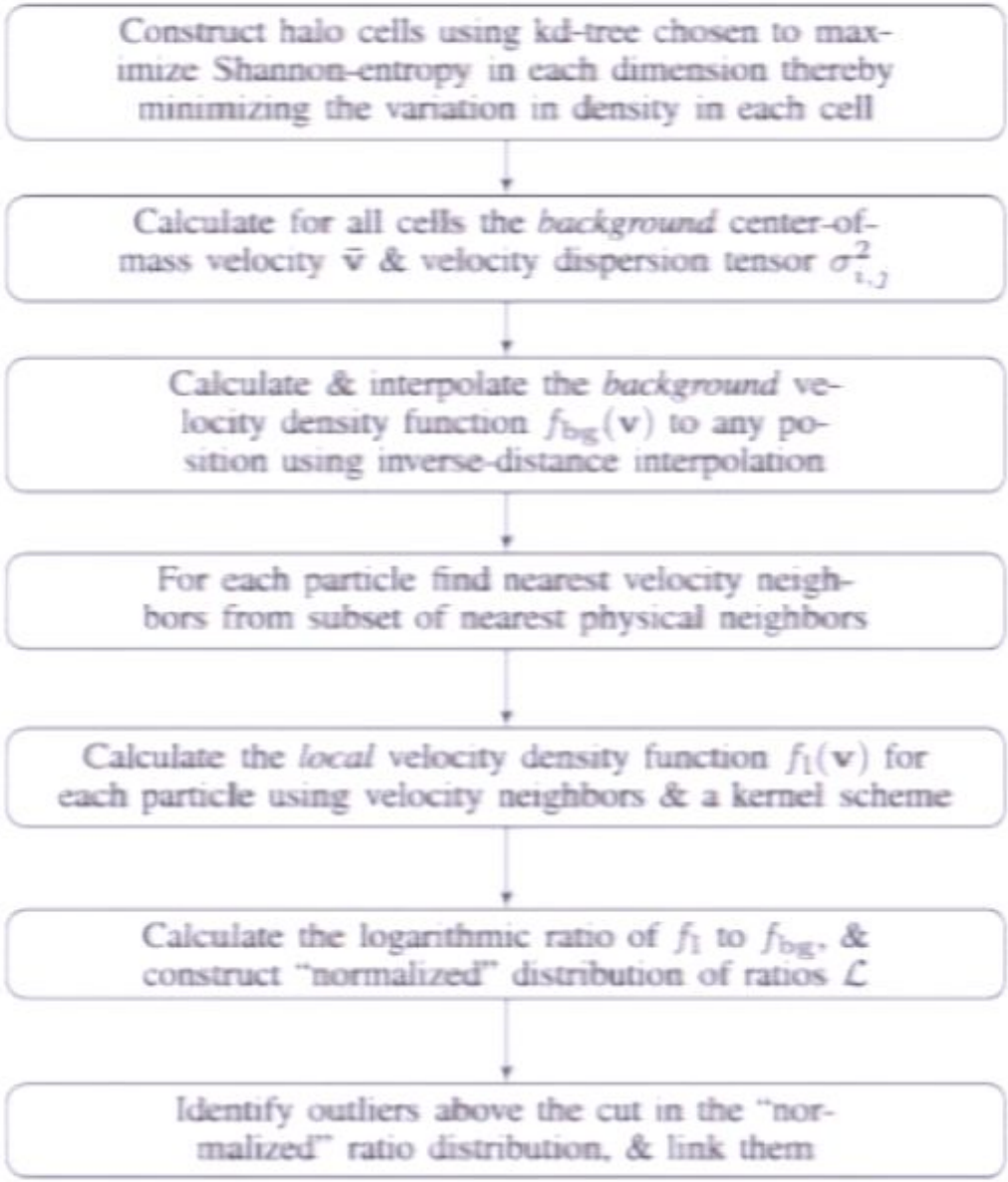

Figure 1. Flow chart of STF algorithm.

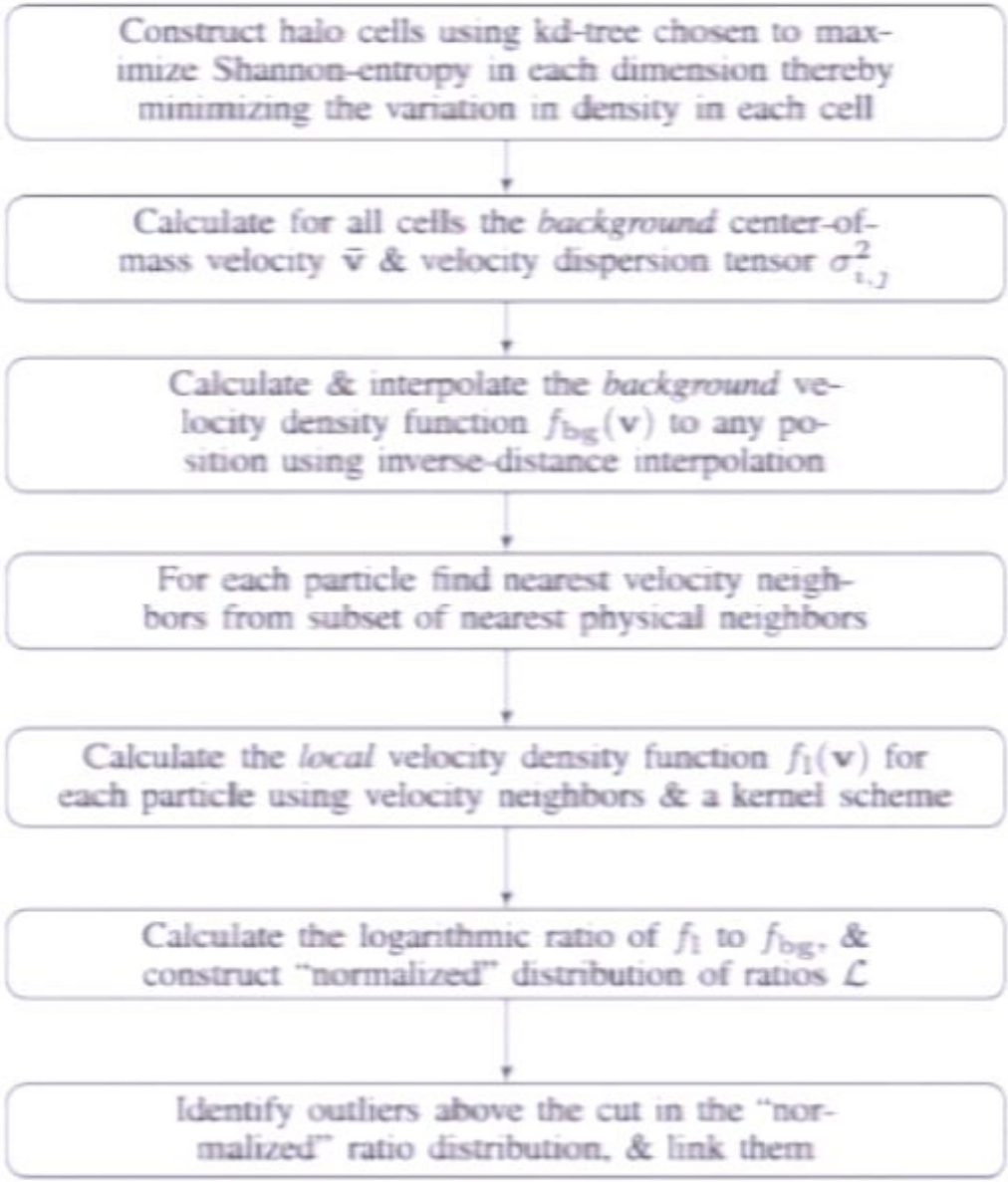

Figure 1. Flow chart of STF algorithm.

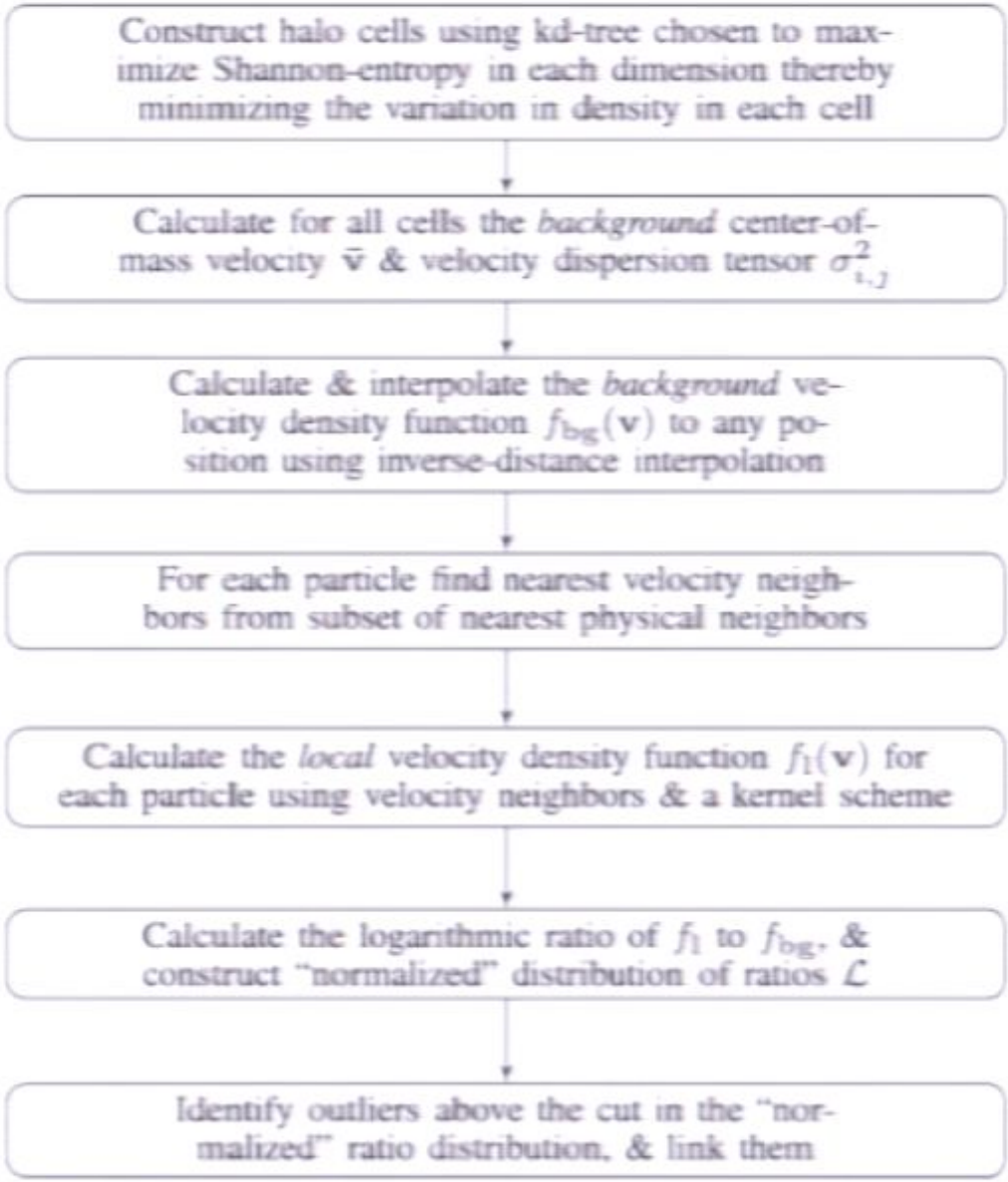

Figure 1. Flow chart of STF algorithm.

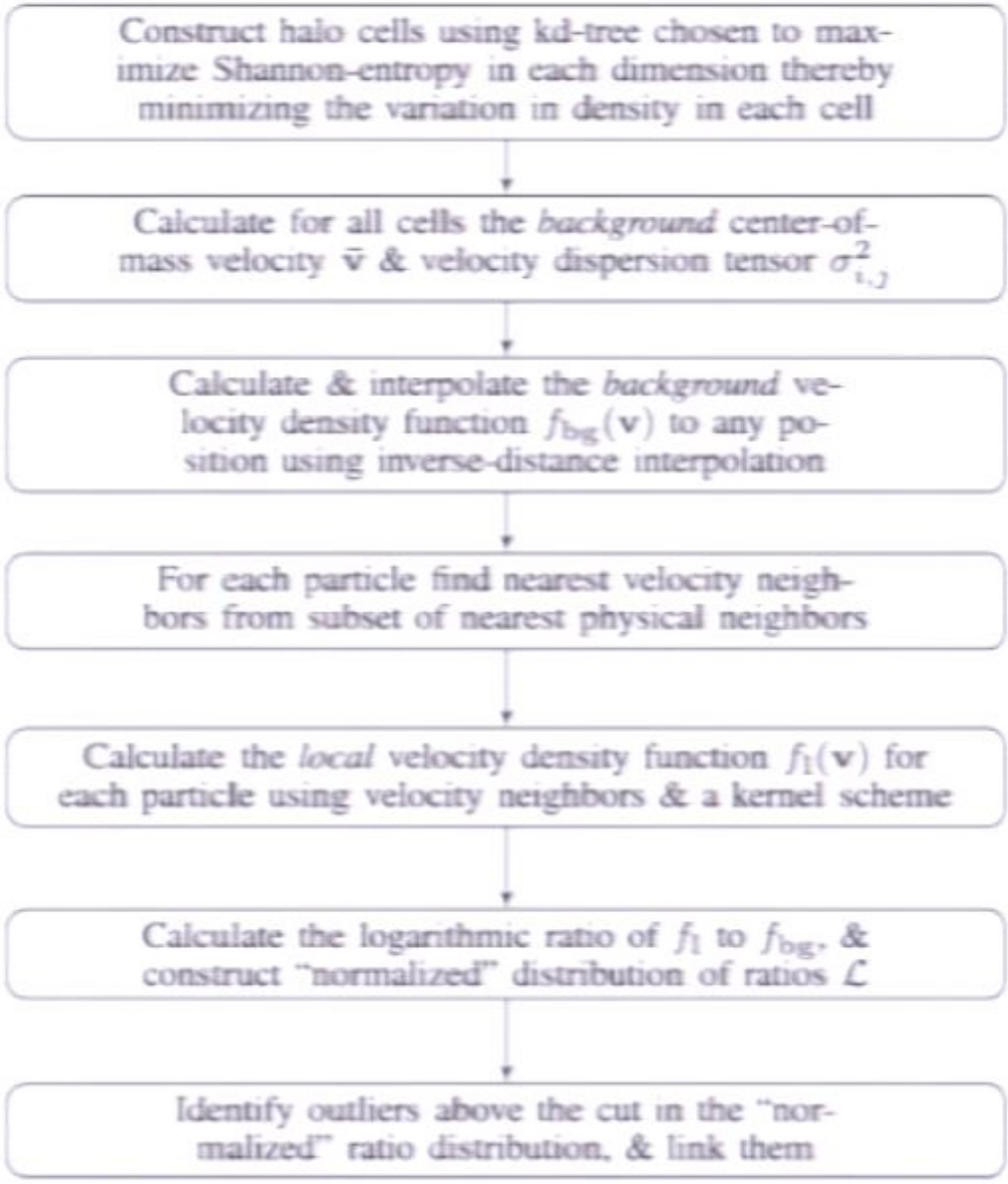

Figure 1. Flow chart of STF algorithm.

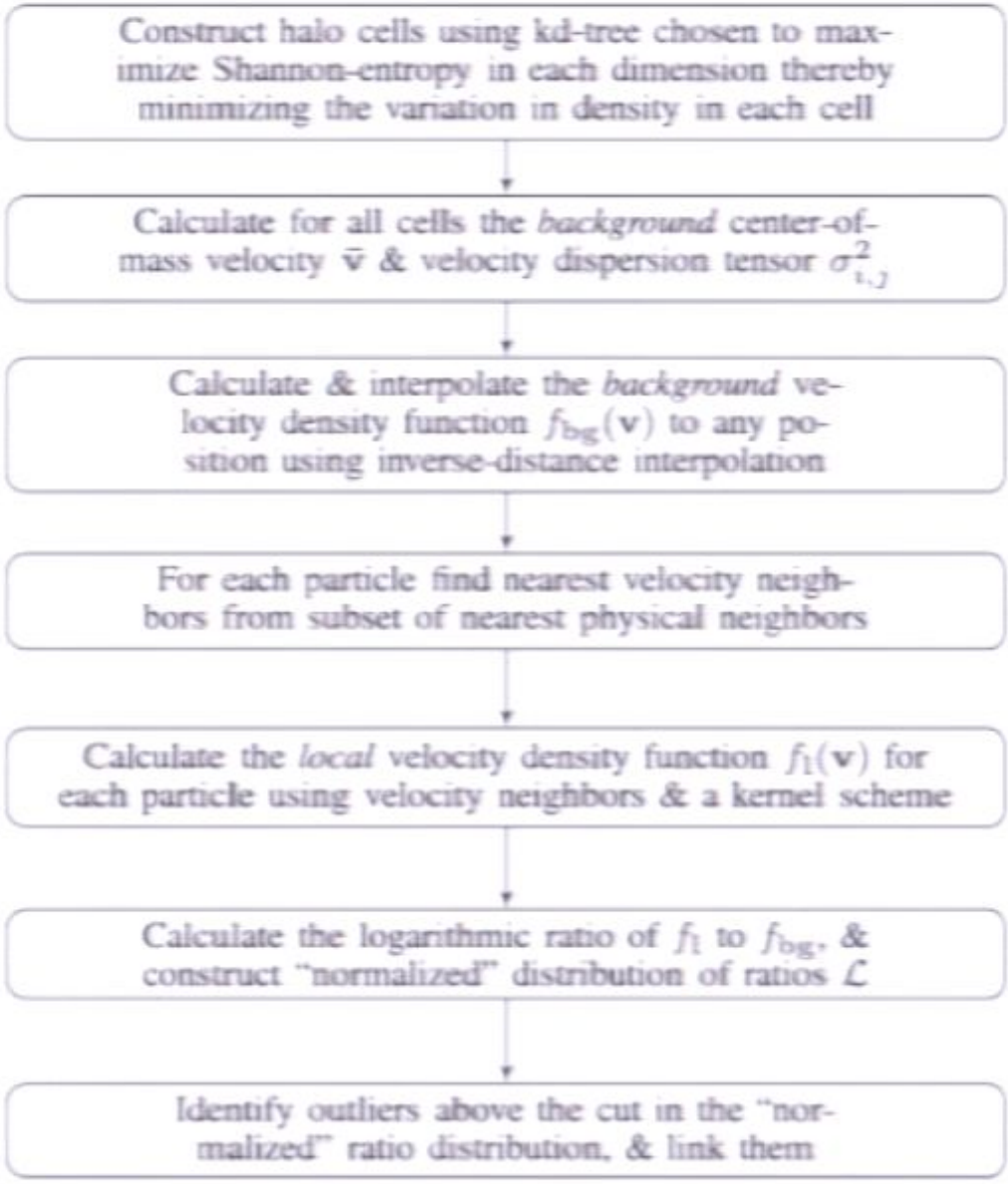

Figure 1. Flow chart of STF algorithm.

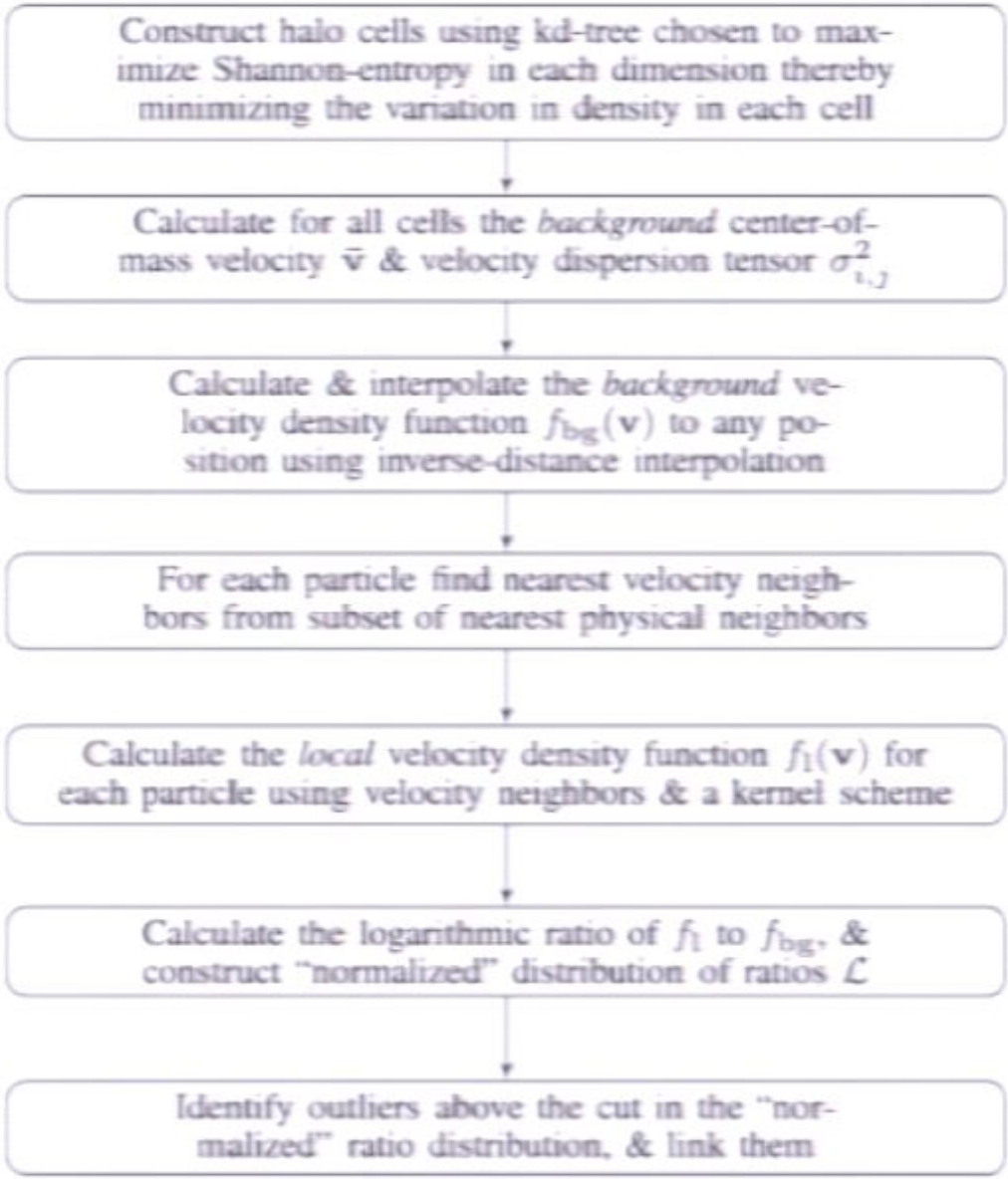

Figure 1. Flow chart of STF algorithm.

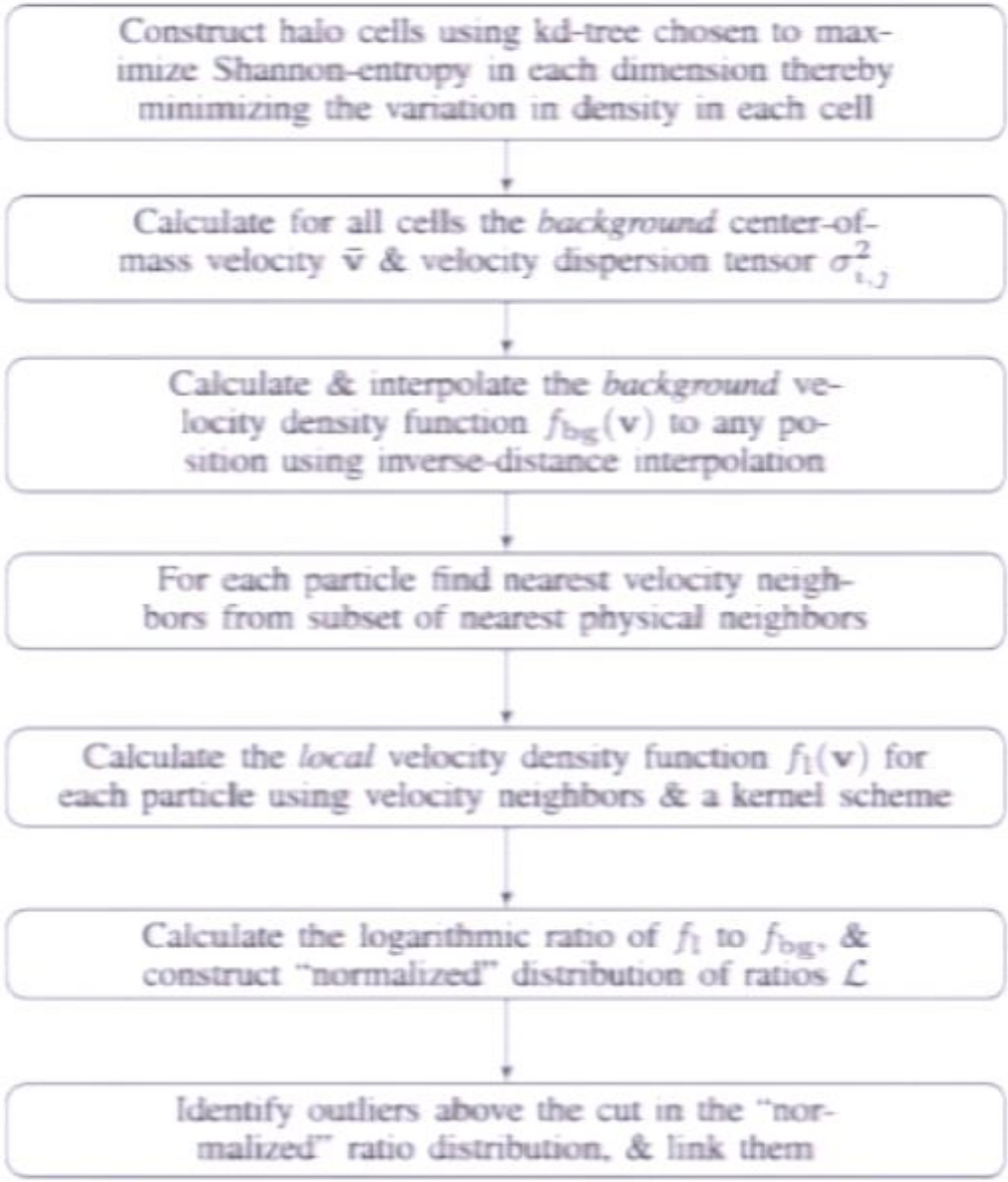

Figure 1. Flow chart of STF algorithm.

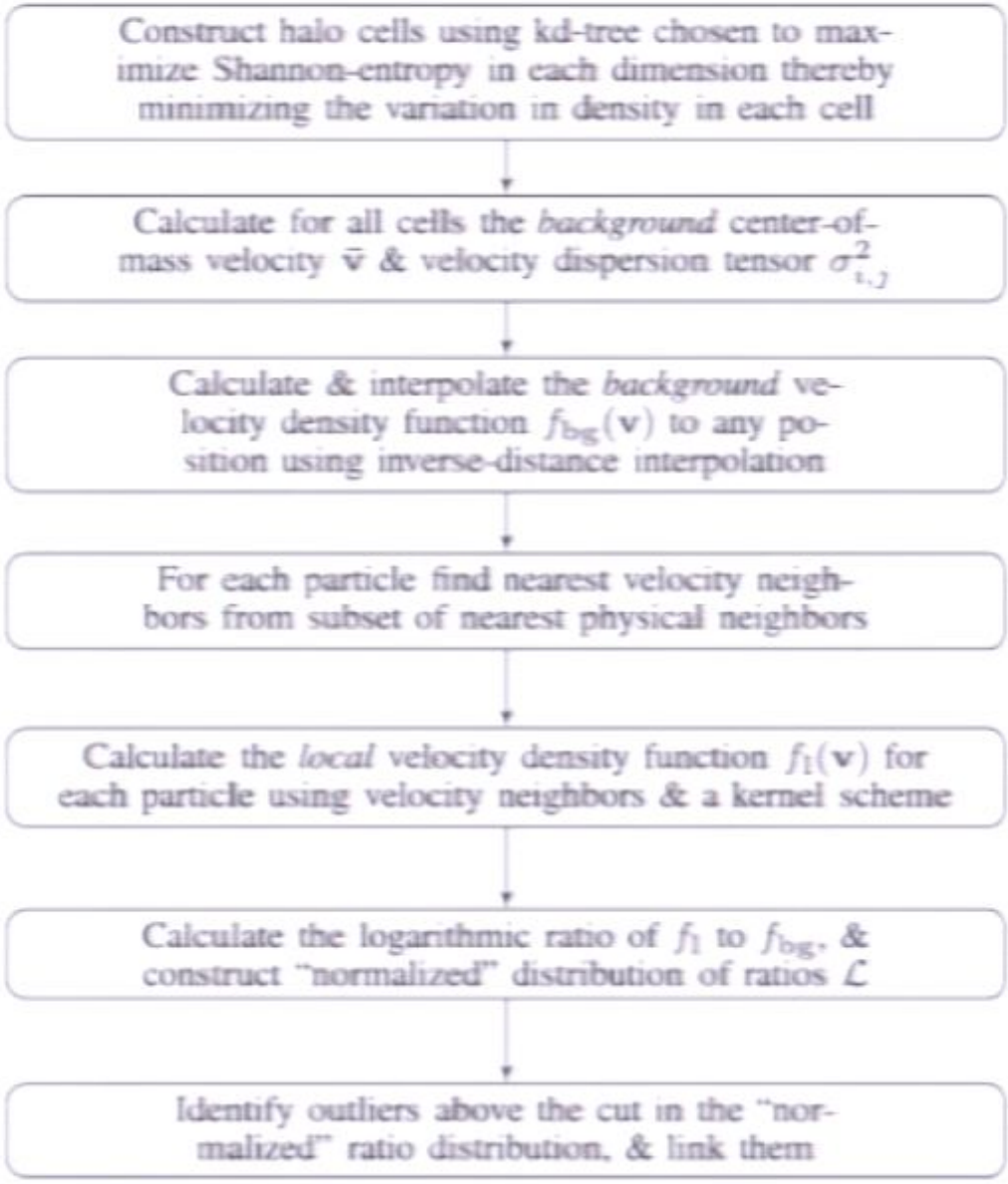

Figure 1. Flow chart of STF algorithm.

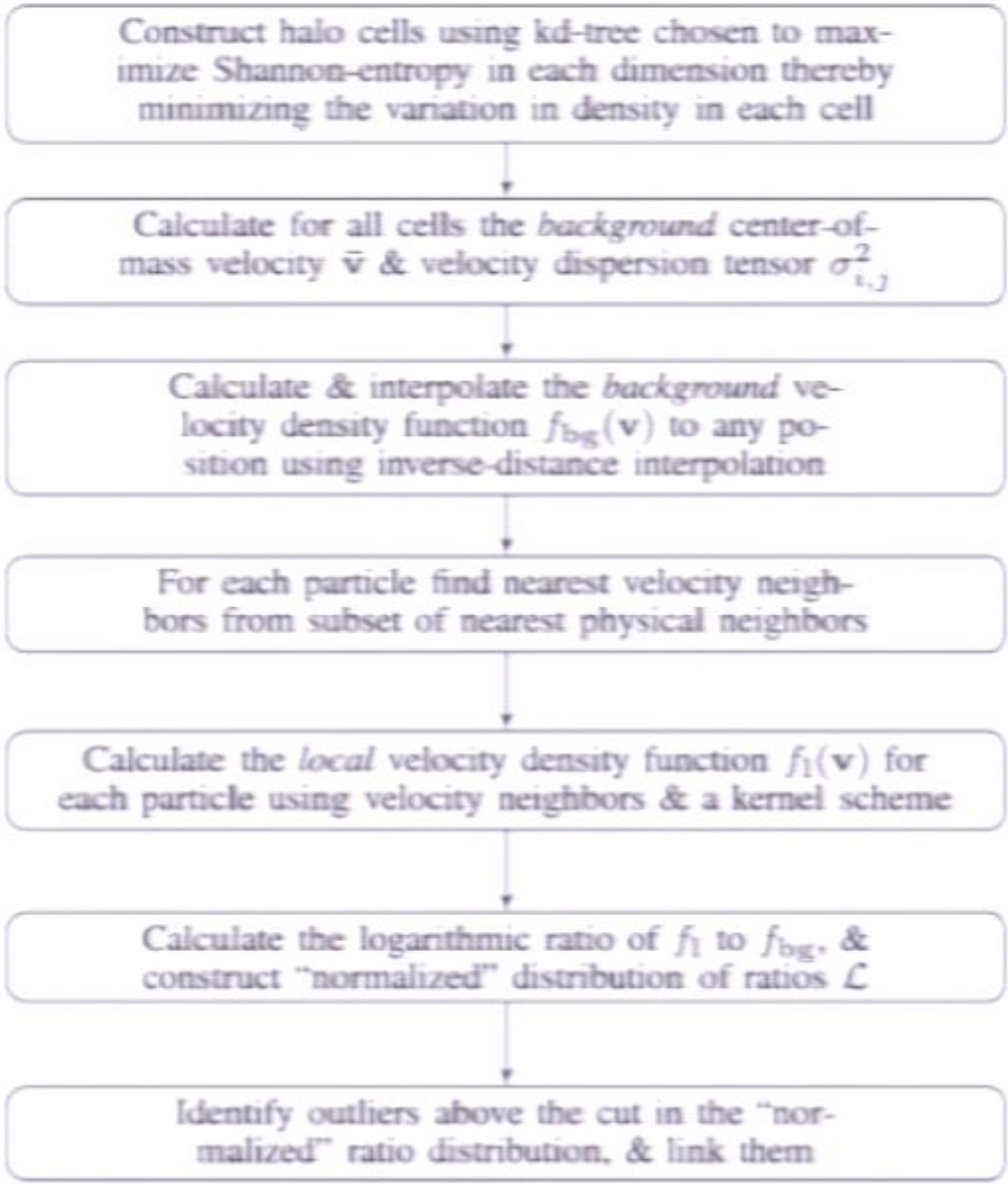

Figure 1. Flow chart of STF algorithm.

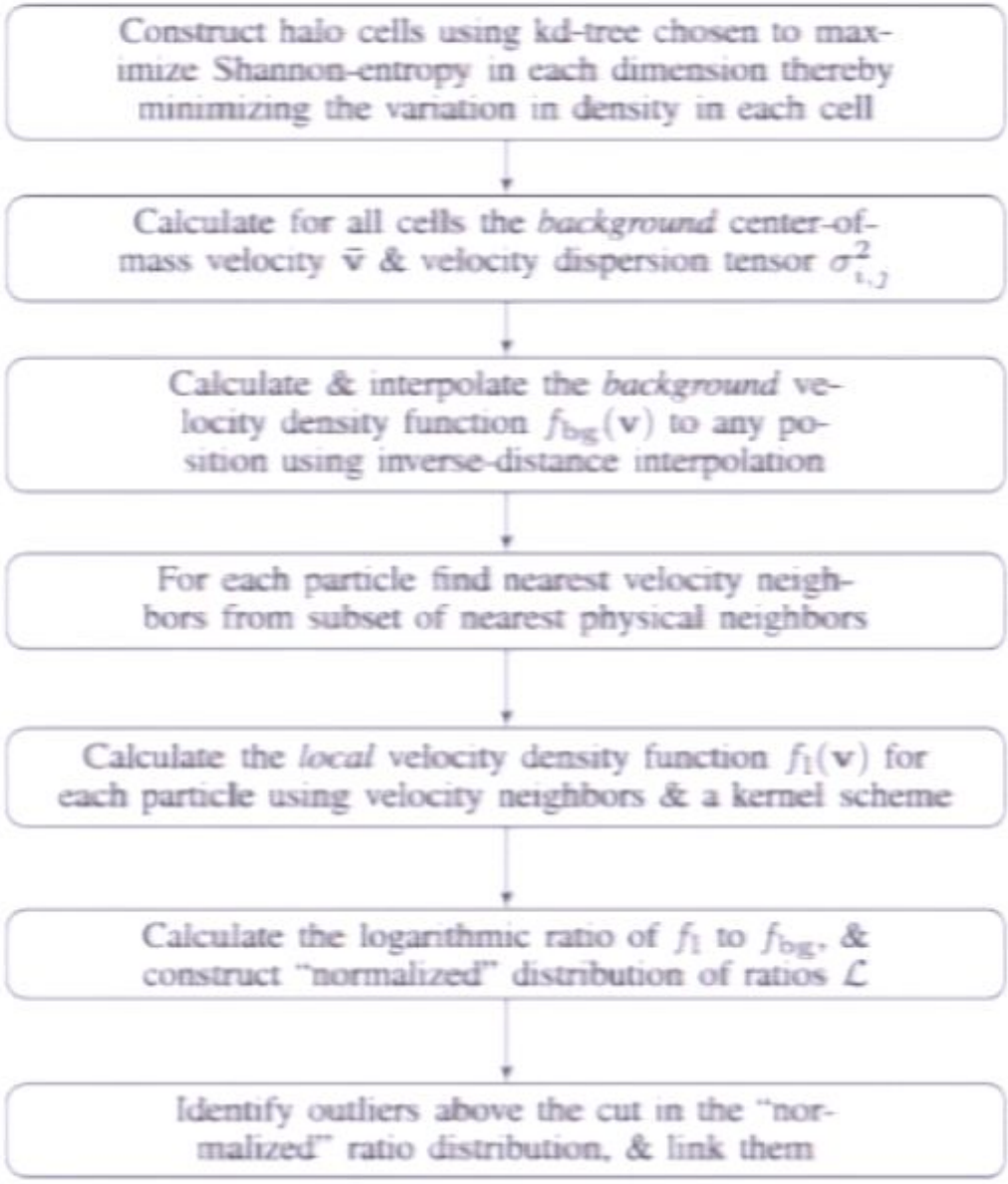

Figure 1. Flow chart of STF algorithm.

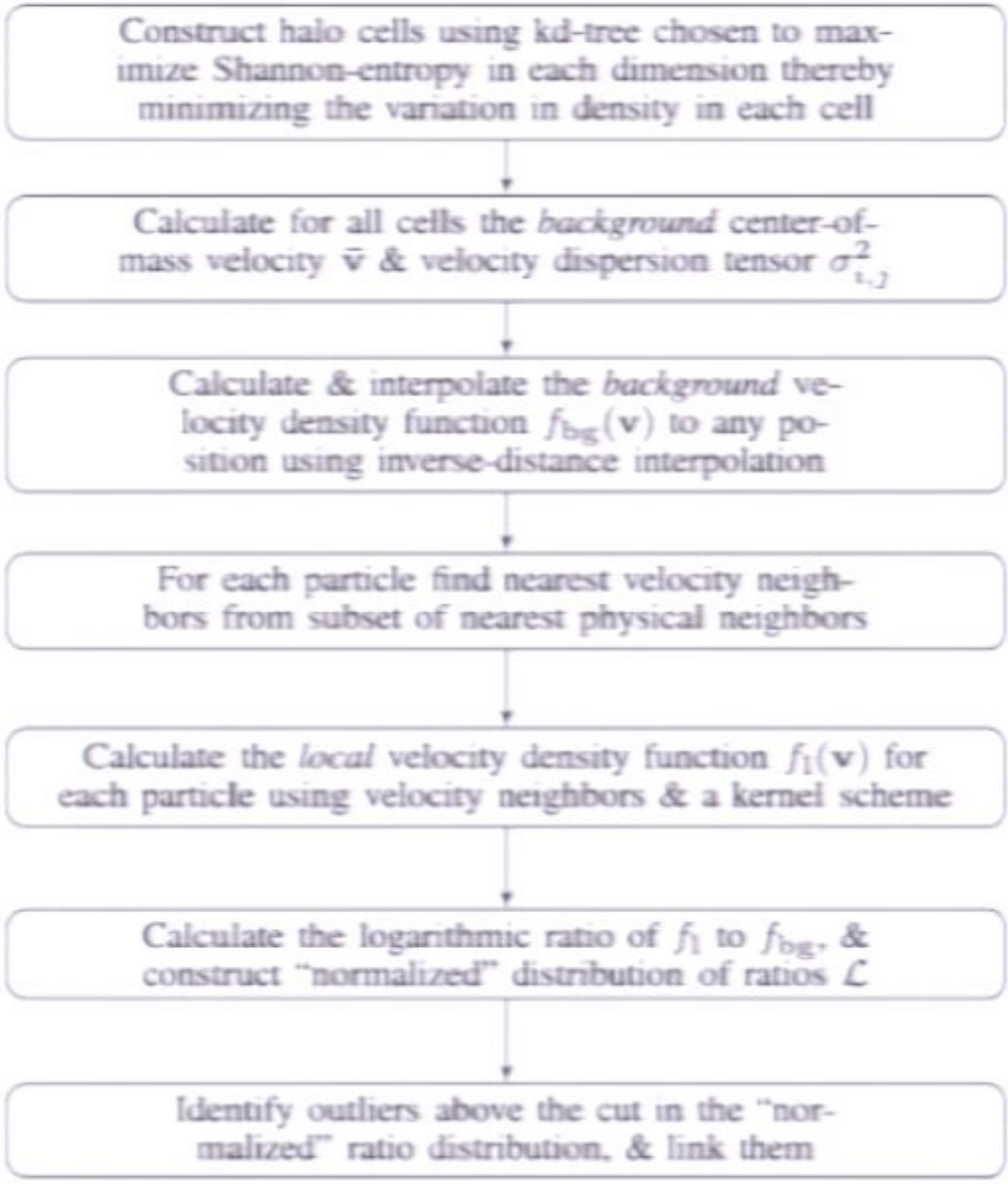

Figure 1. Flow chart of STF algorithm.

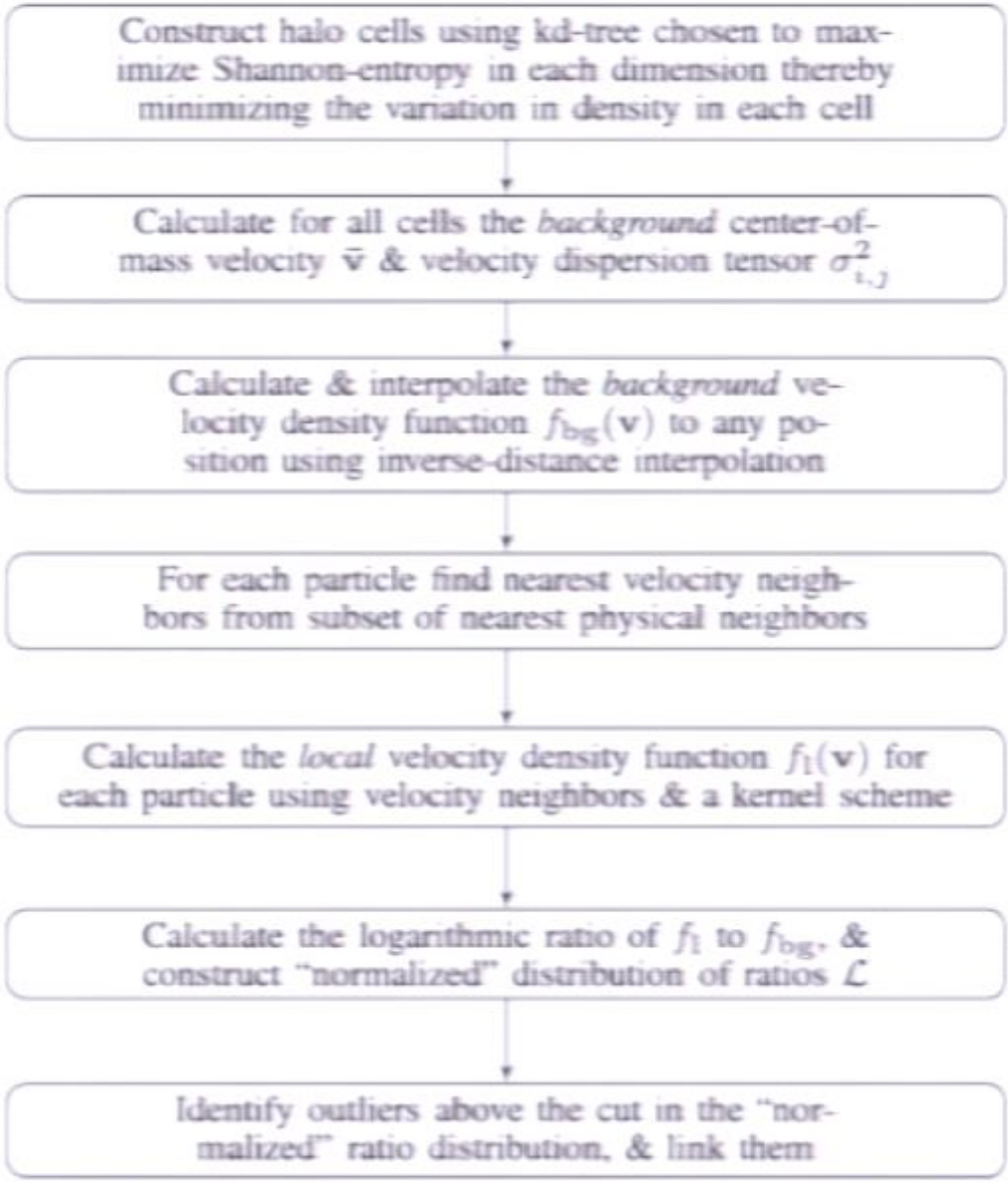

Figure 1. Flow chart of STF algorithm.

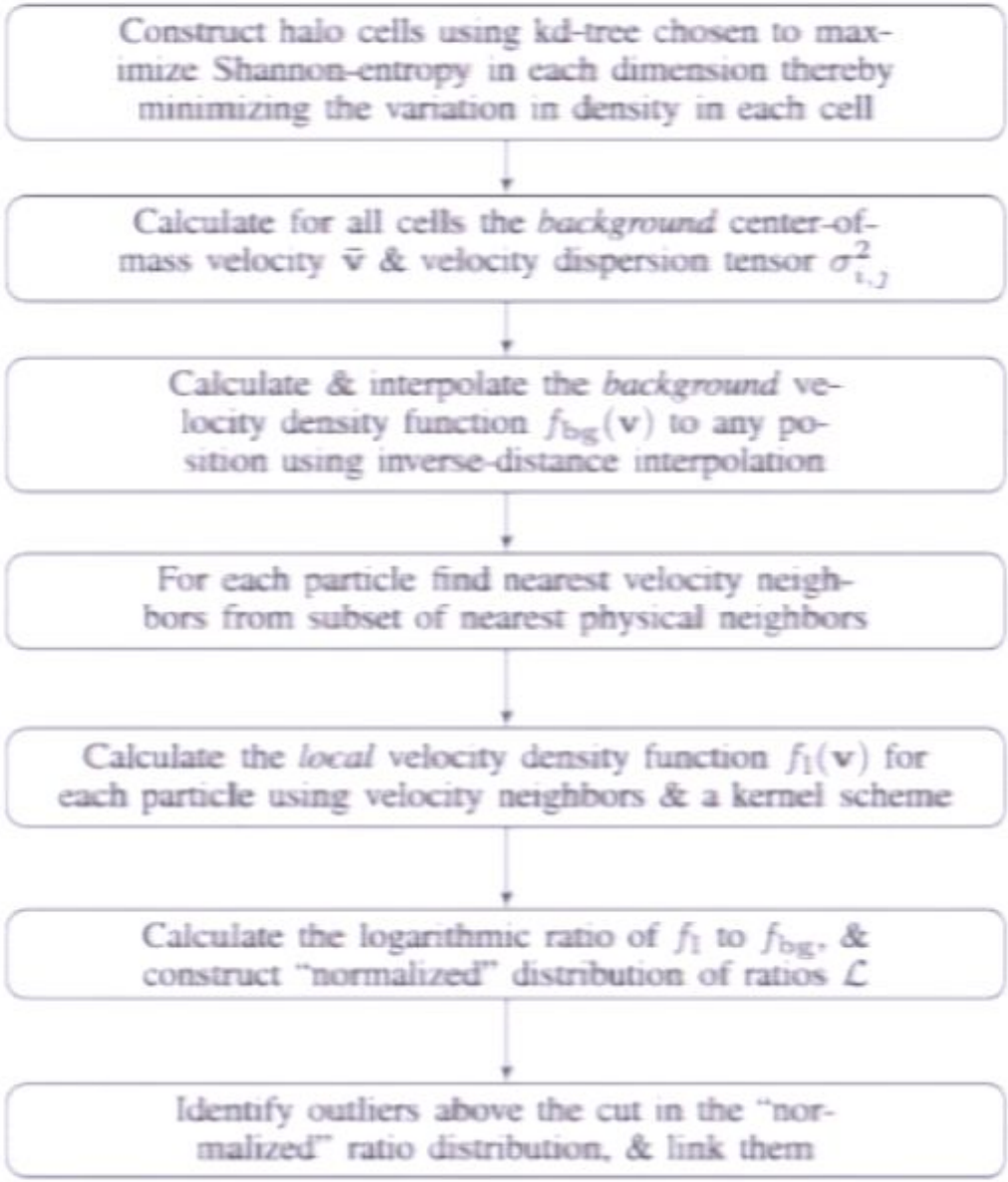

Figure 1. Flow chart of STF algorithm.

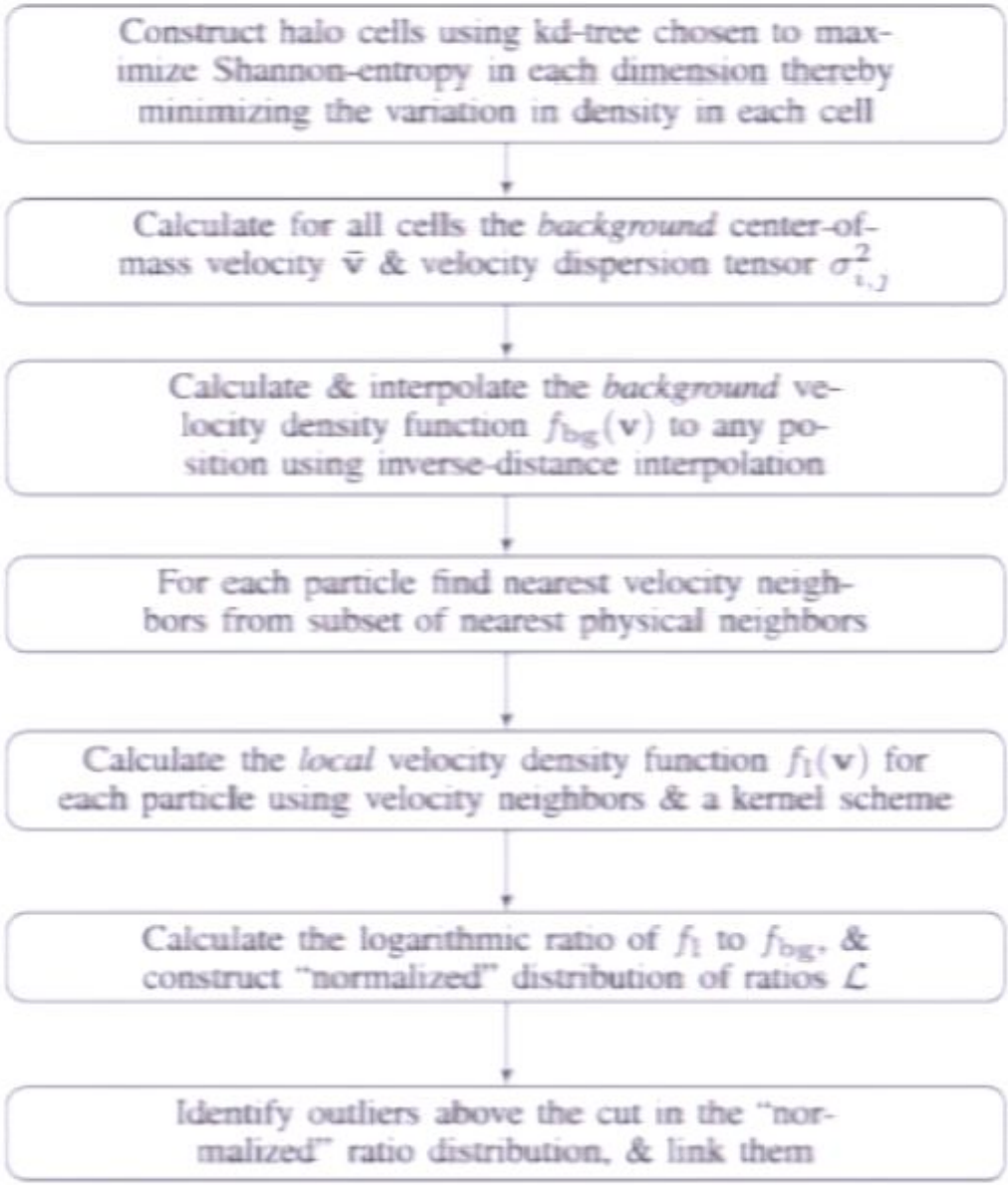

Figure 1. Flow chart of STF algorithm.

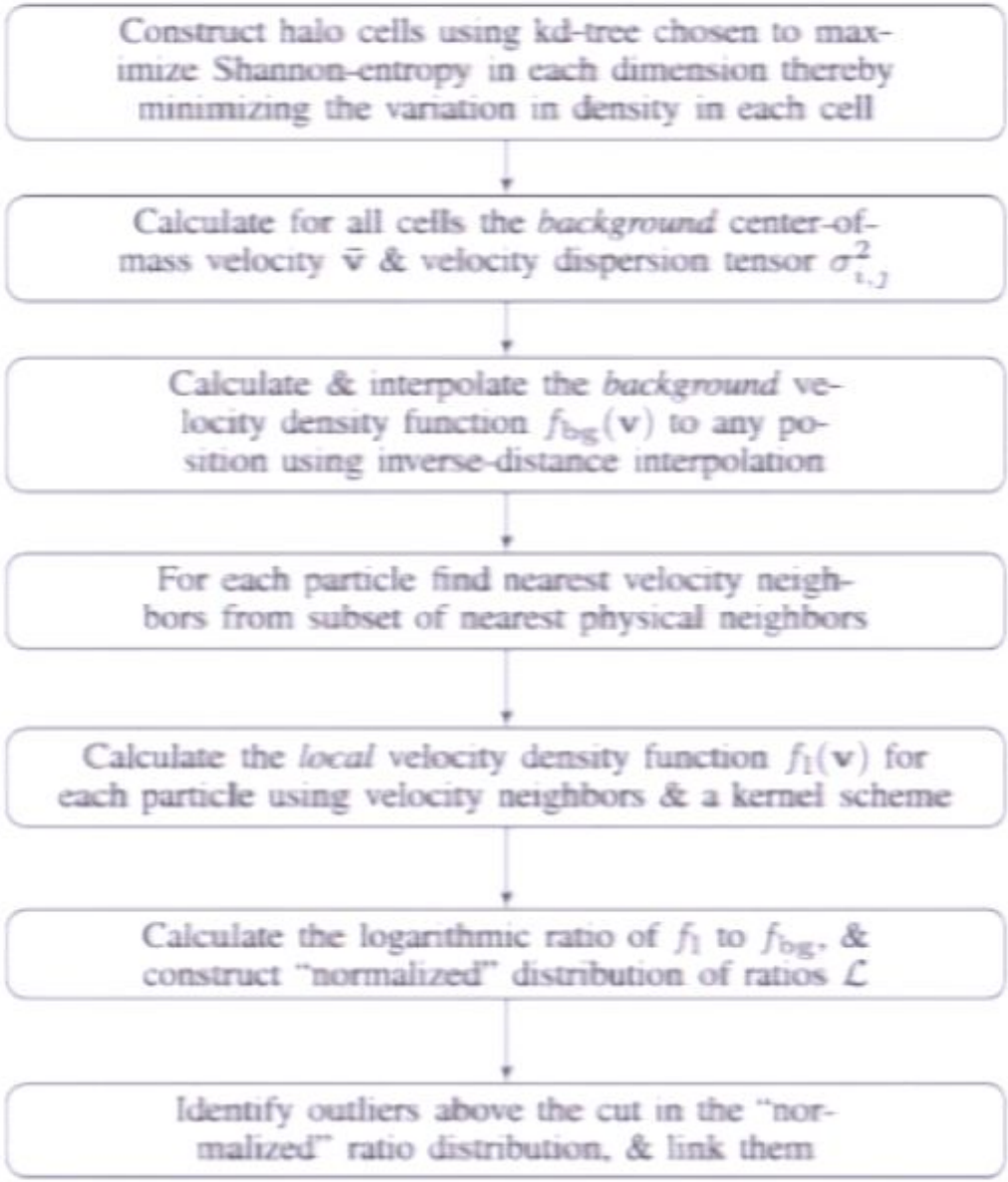

Figure 1. Flow chart of STF algorithm.

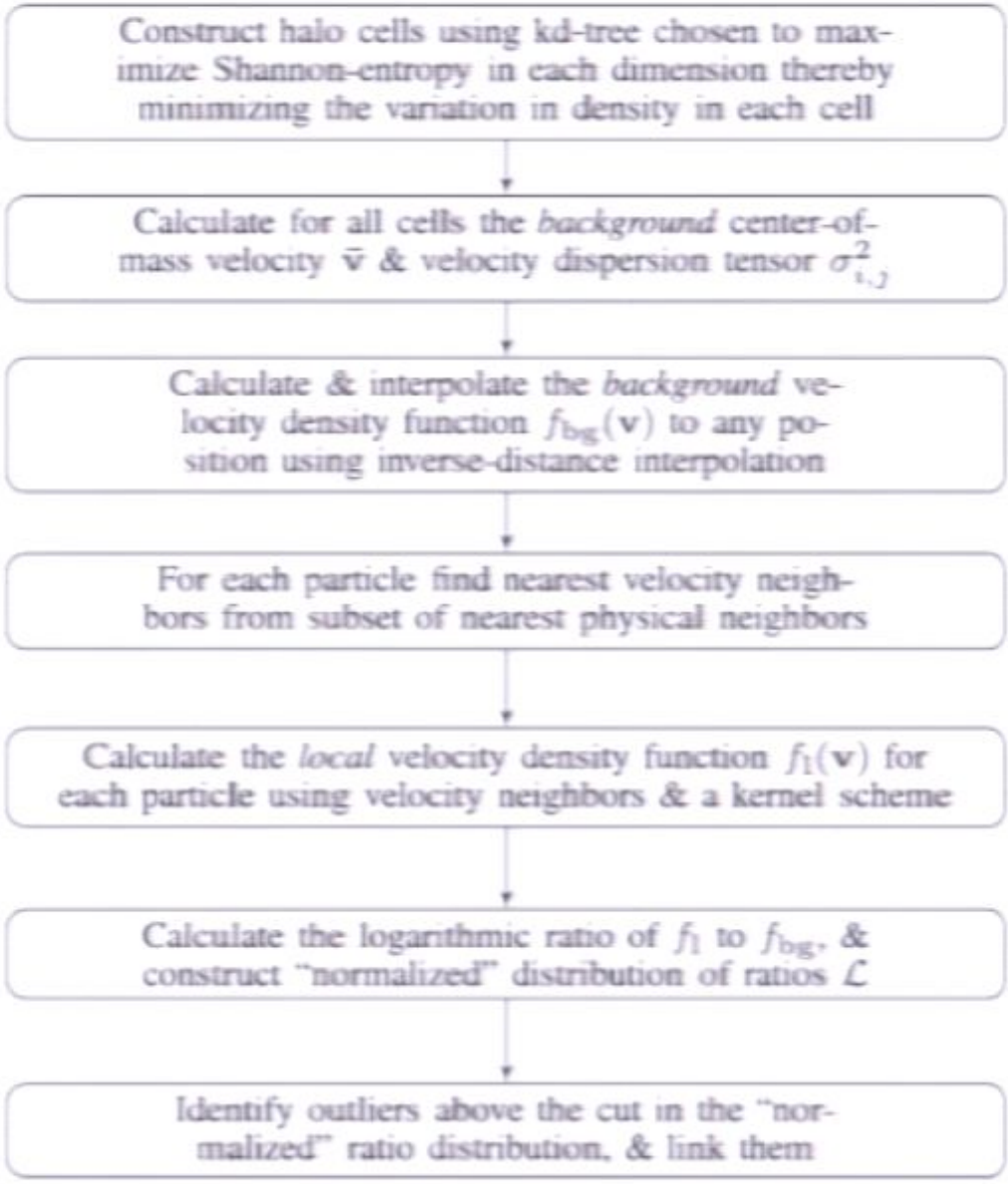

Figure 1. Flow chart of STF algorithm.

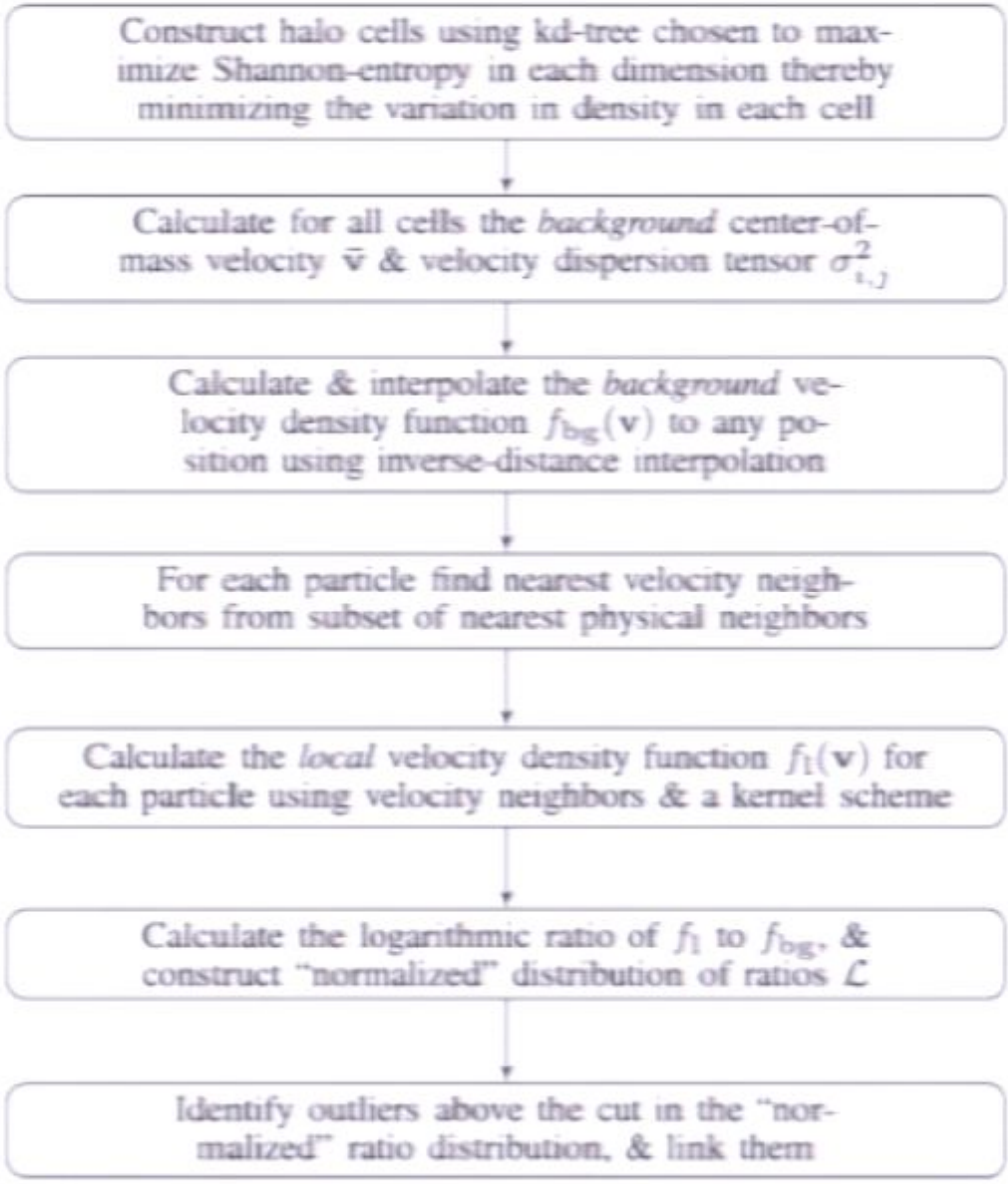

Figure 1. Flow chart of STF algorithm.

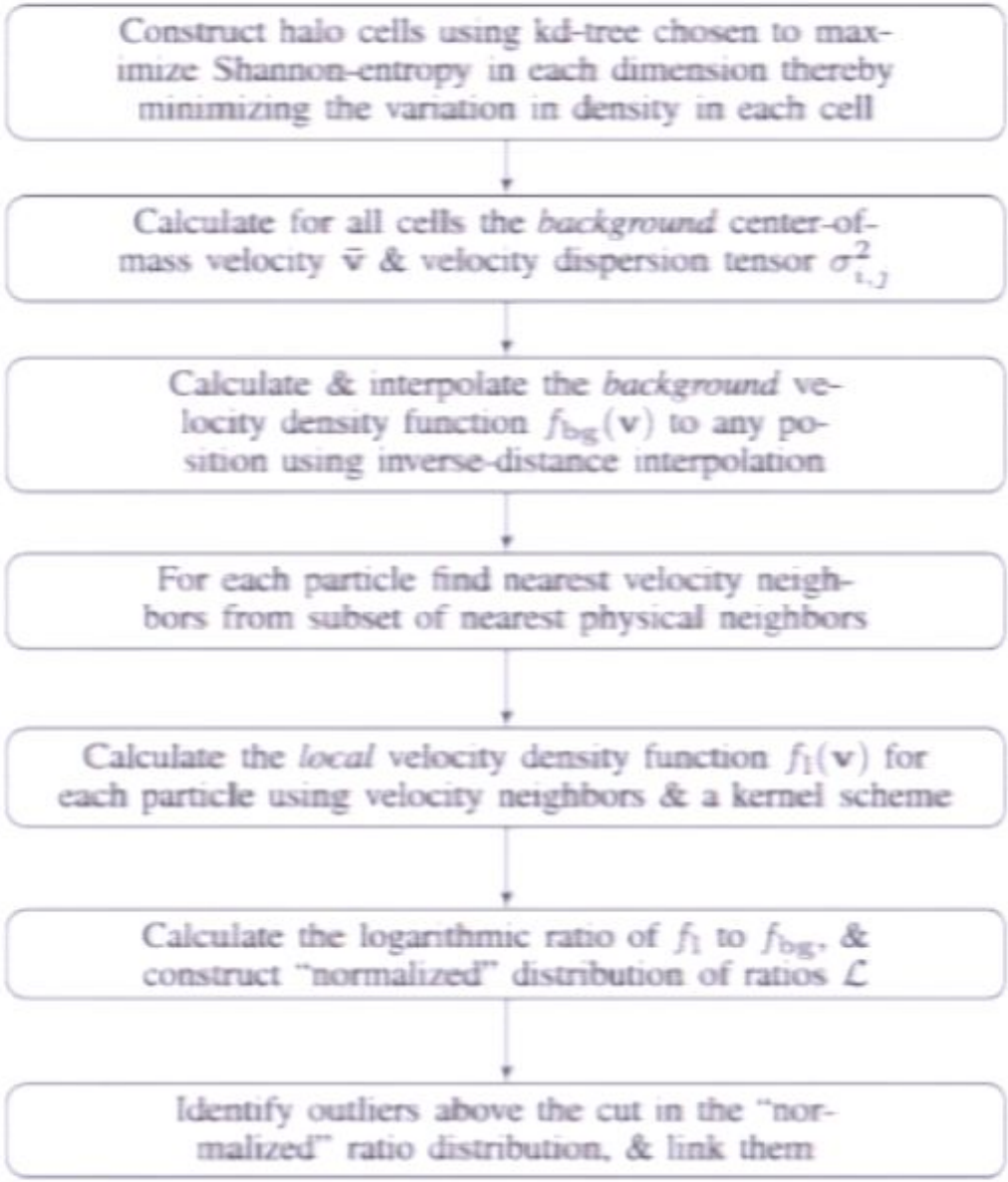

Figure 1. Flow chart of STF algorithm.

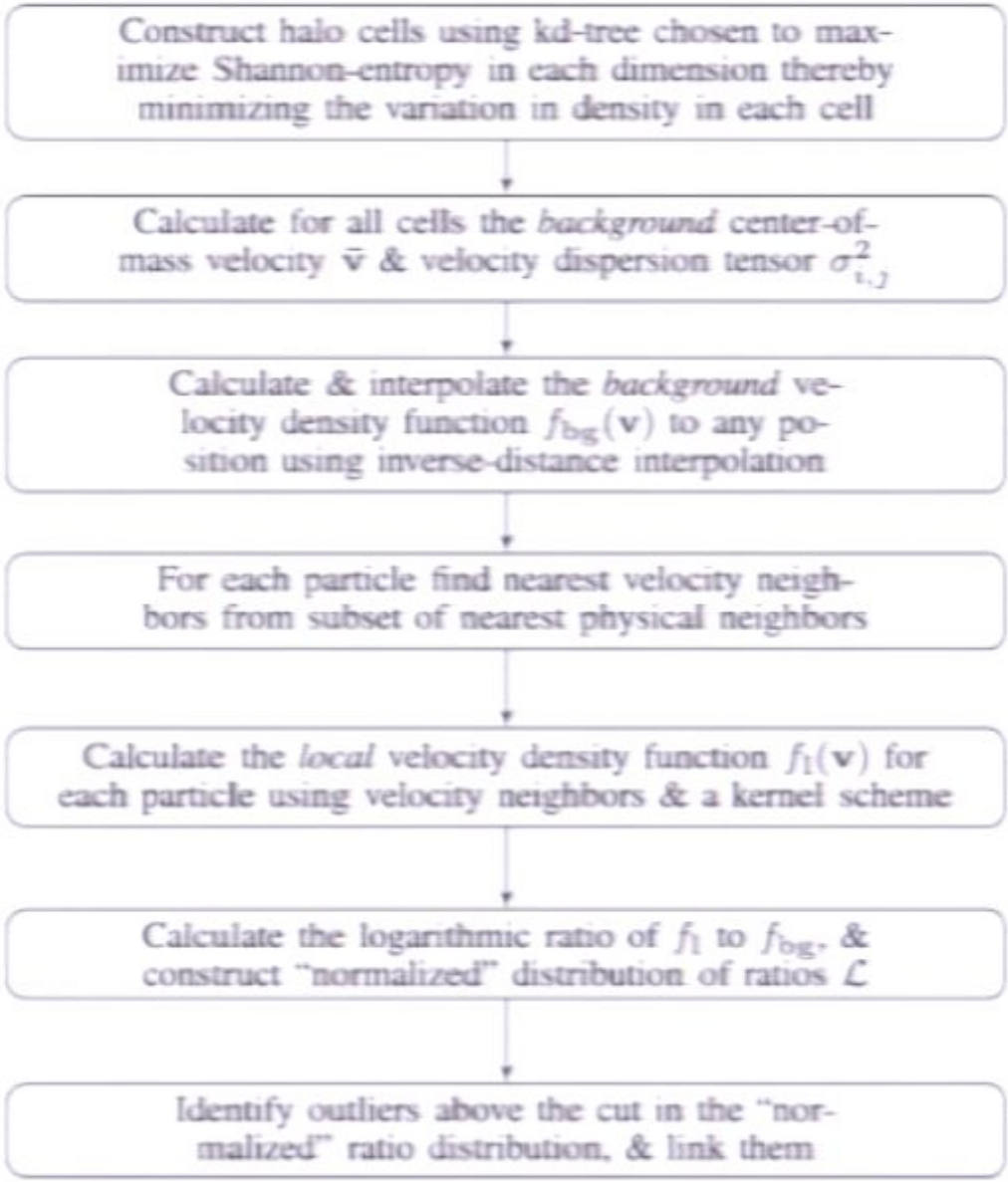

Figure 1. Flow chart of STF algorithm.

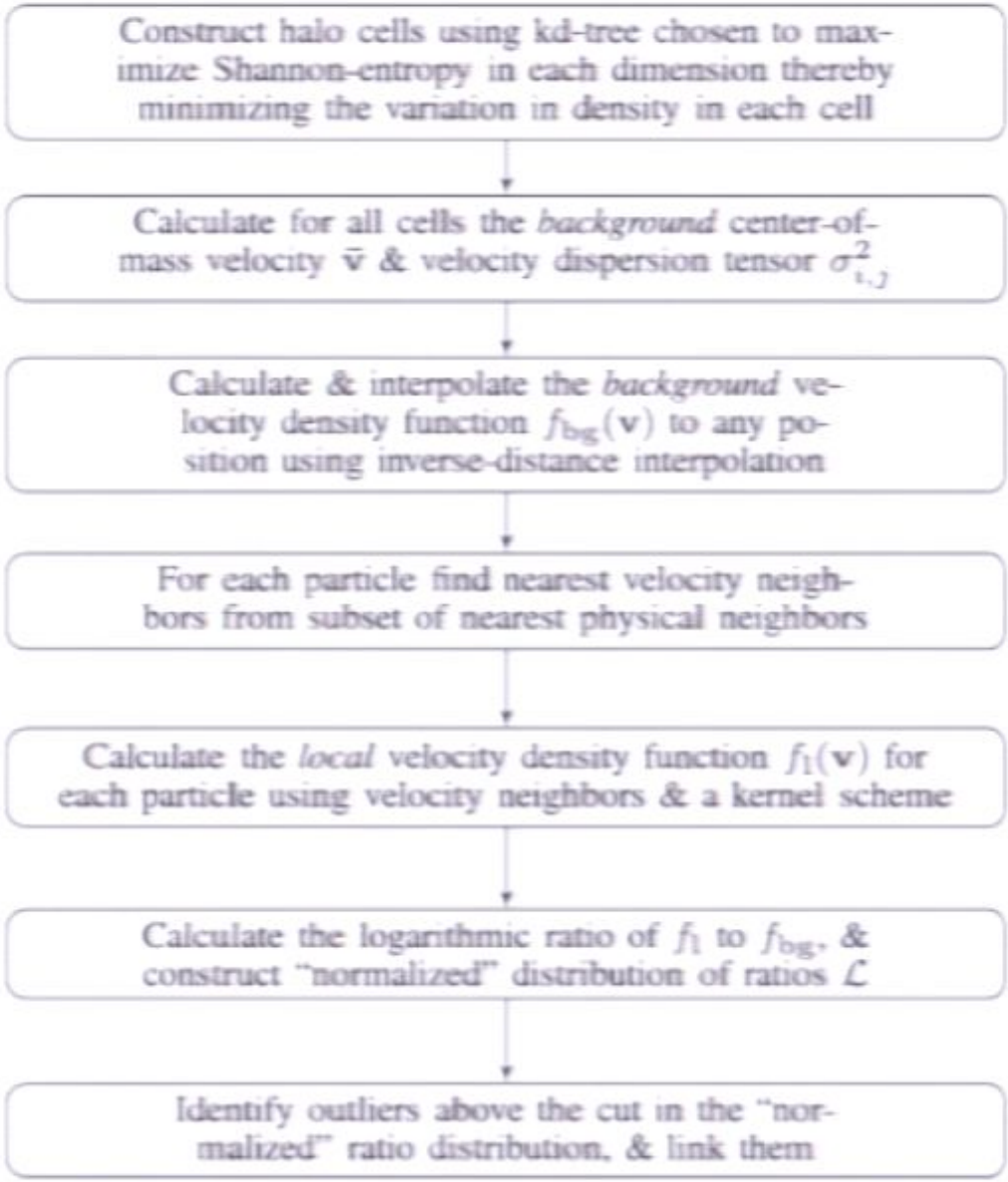

Figure 1. Flow chart of STF algorithm.

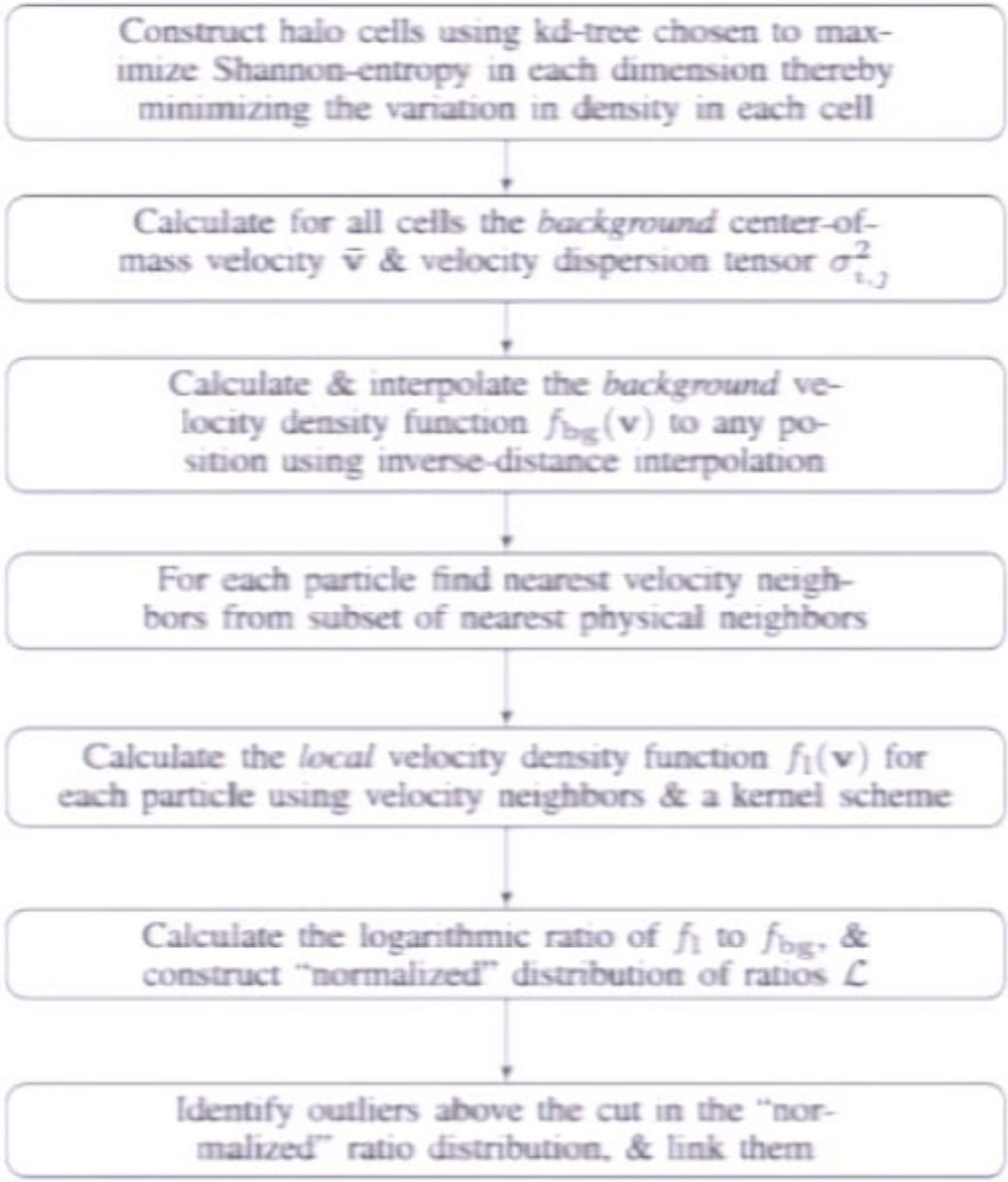

Figure 1. Flow chart of STF algorithm.

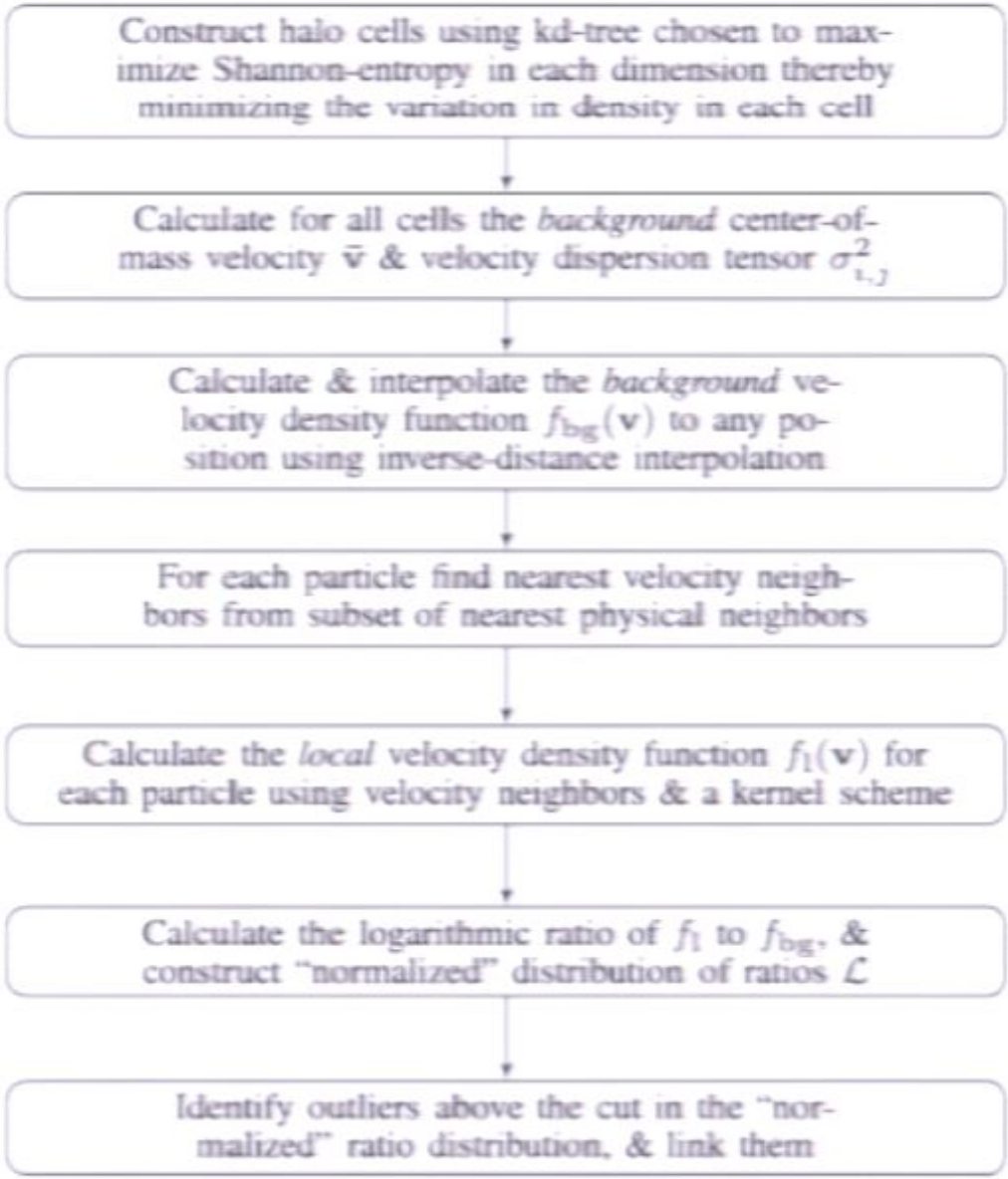

Figure 1. Flow chart of STF algorithm.

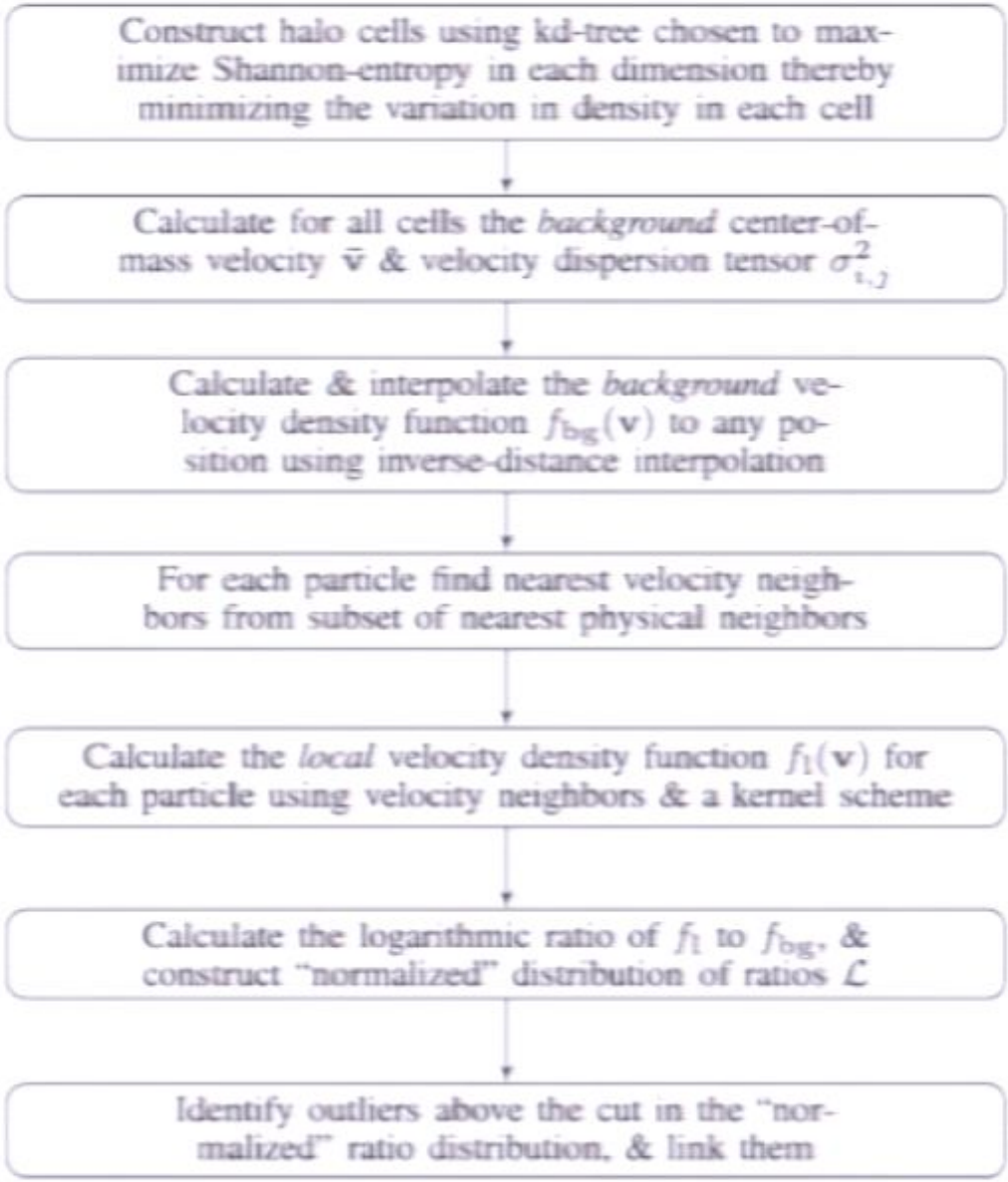

Figure 1. Flow chart of STF algorithm.

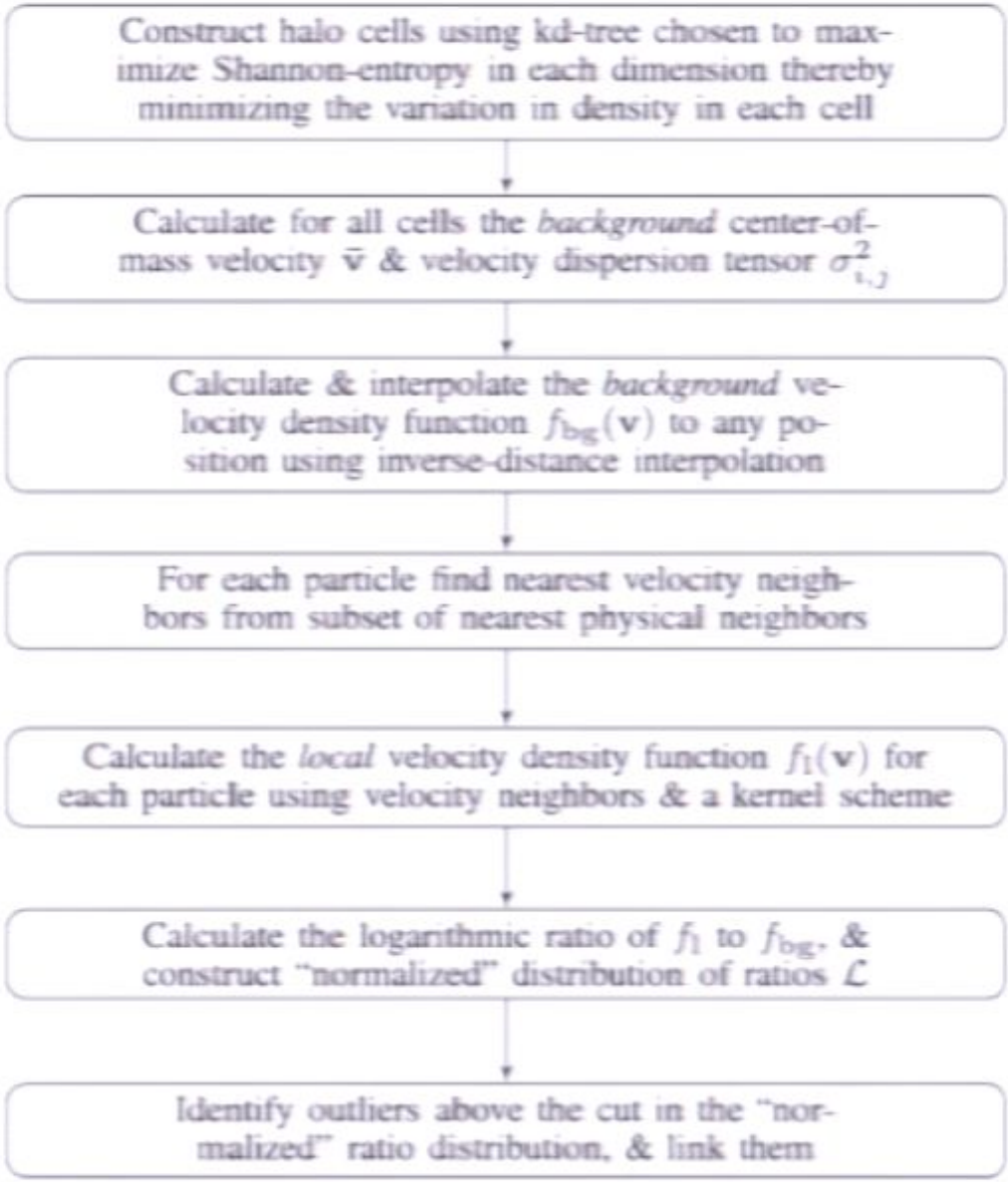

Figure 1. Flow chart of STF algorithm.

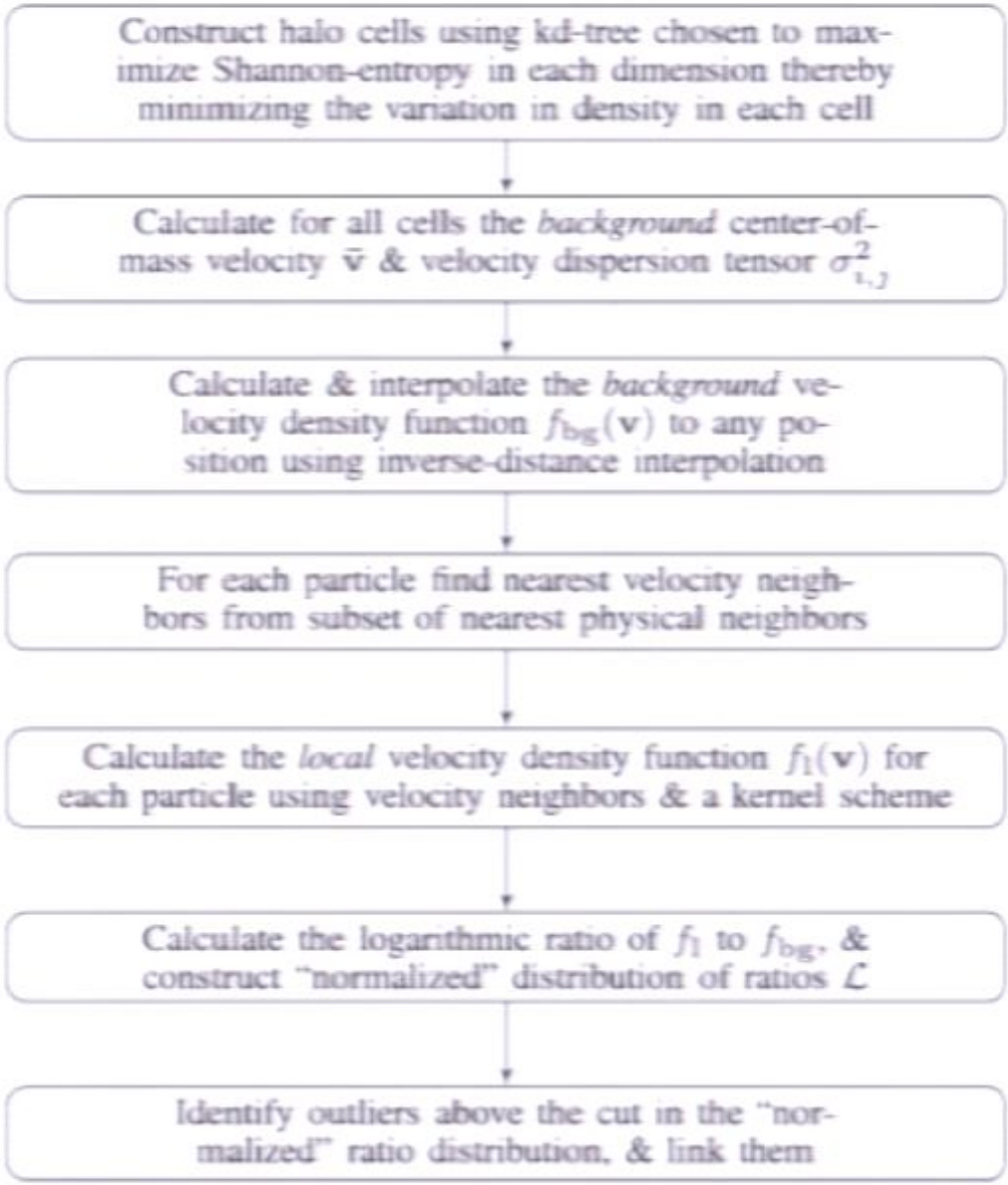

Figure 1. Flow chart of STF algorithm.

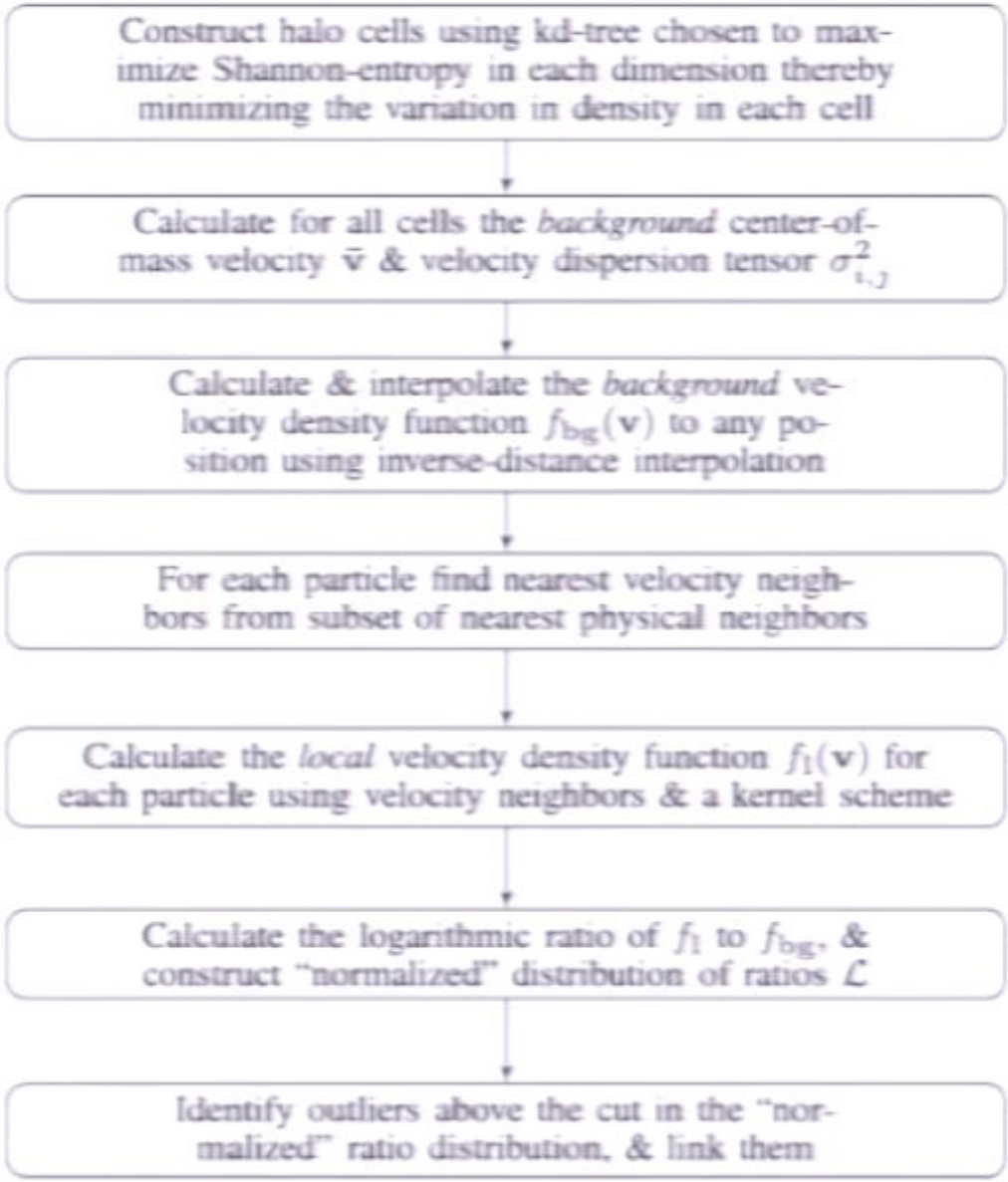

Figure 1. Flow chart of STF algorithm.

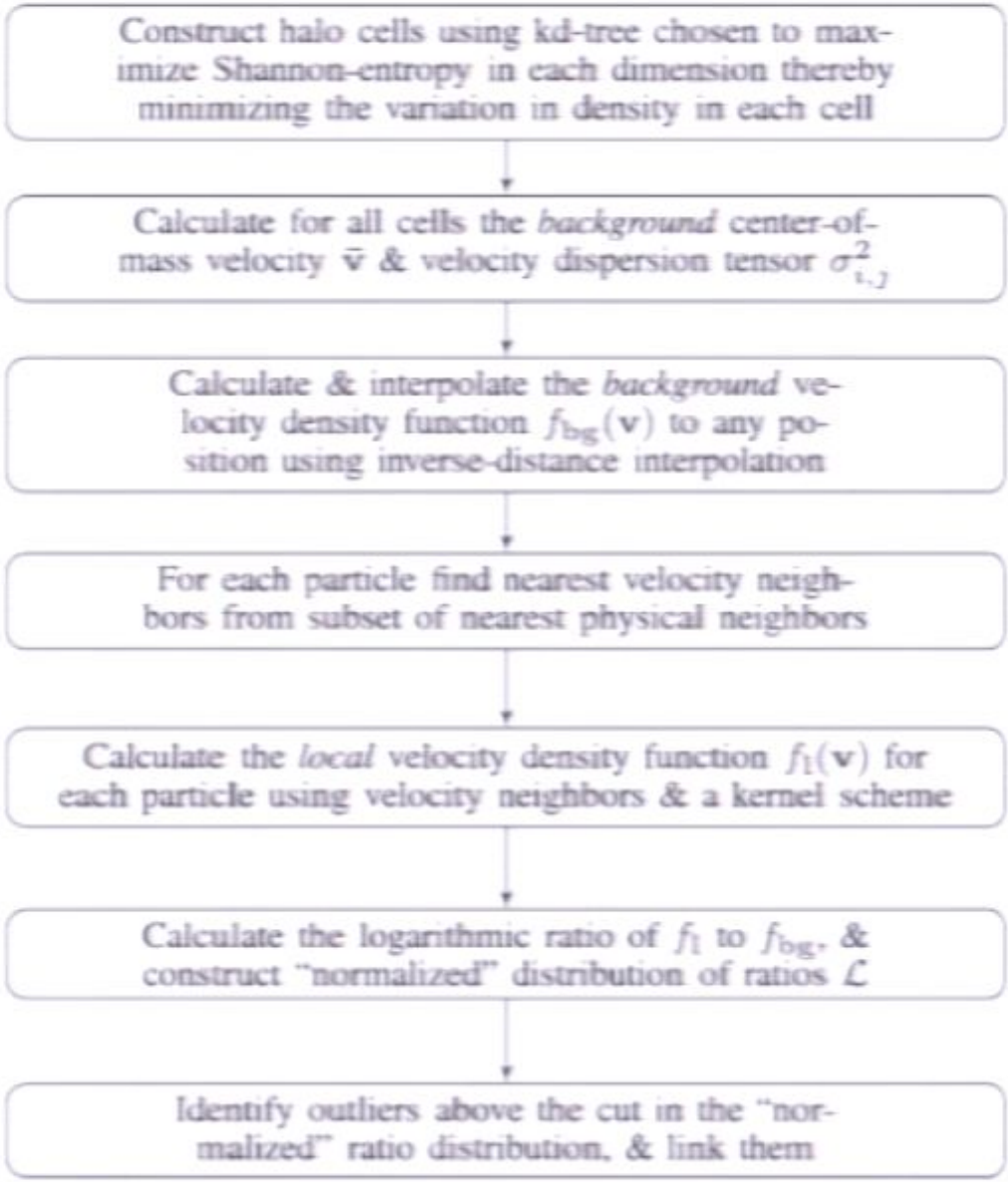

Figure 1. Flow chart of STF algorithm.

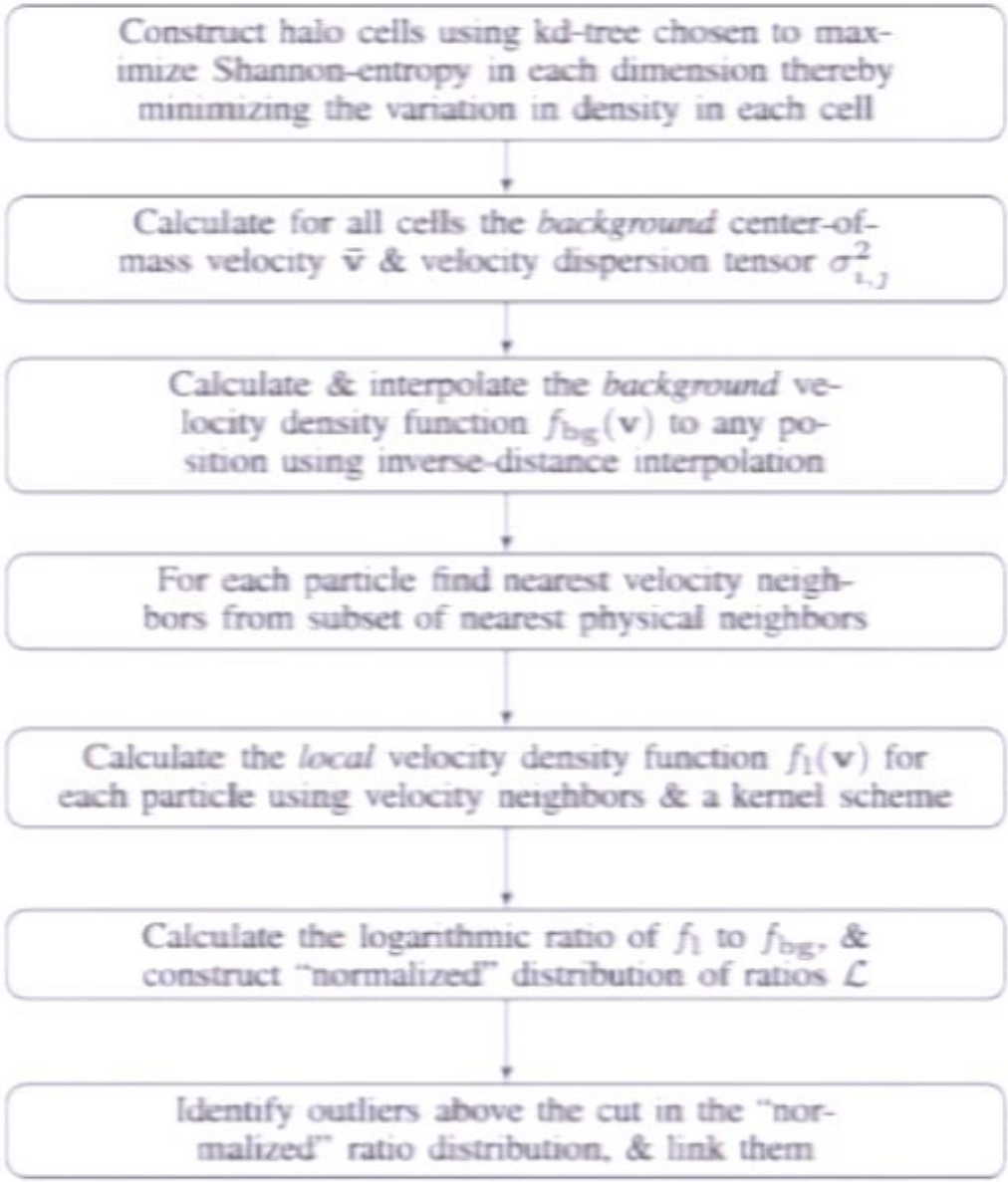

Figure 1. Flow chart of STF algorithm.

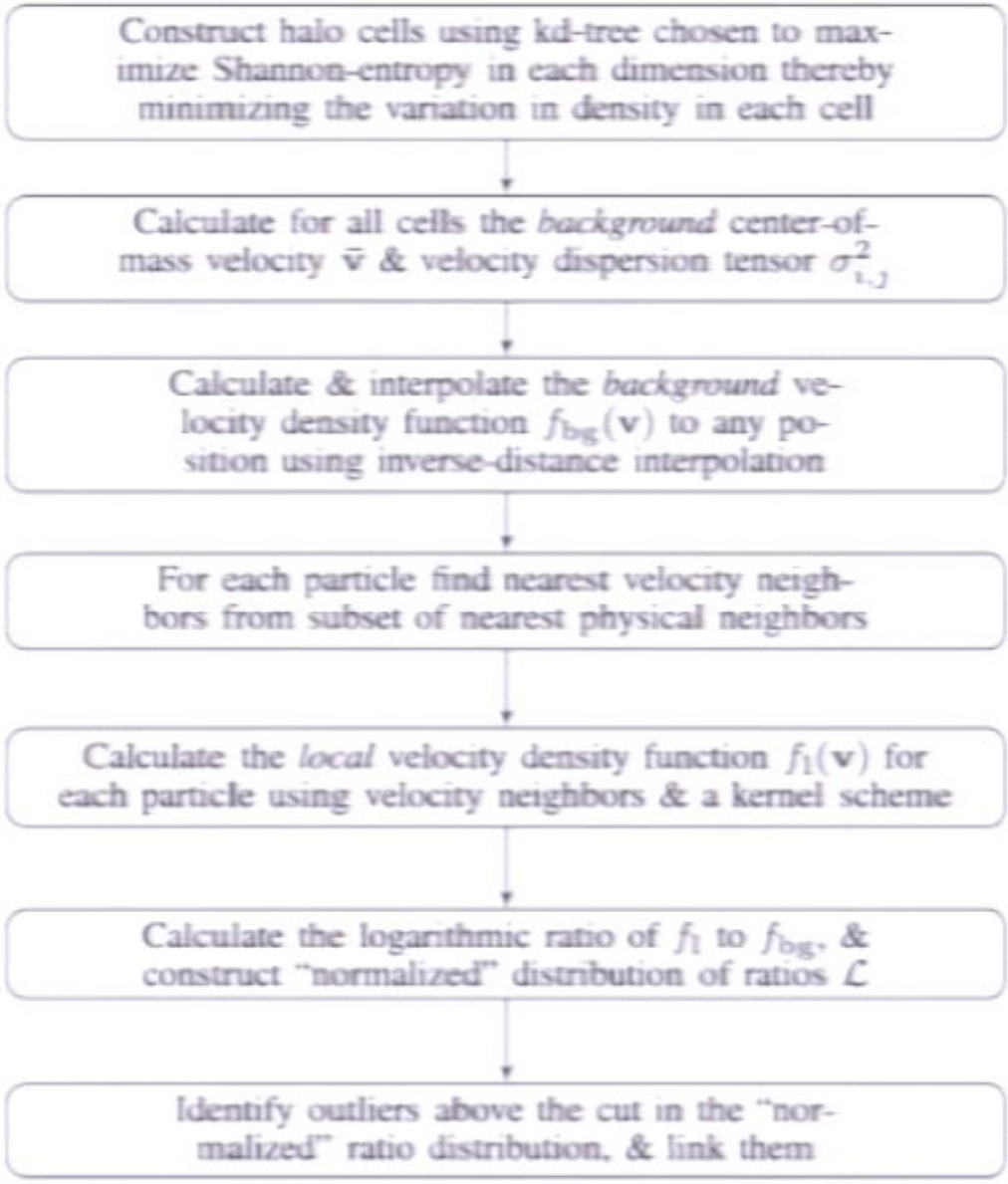

Figure 1. Flow chart of STF algorithm.

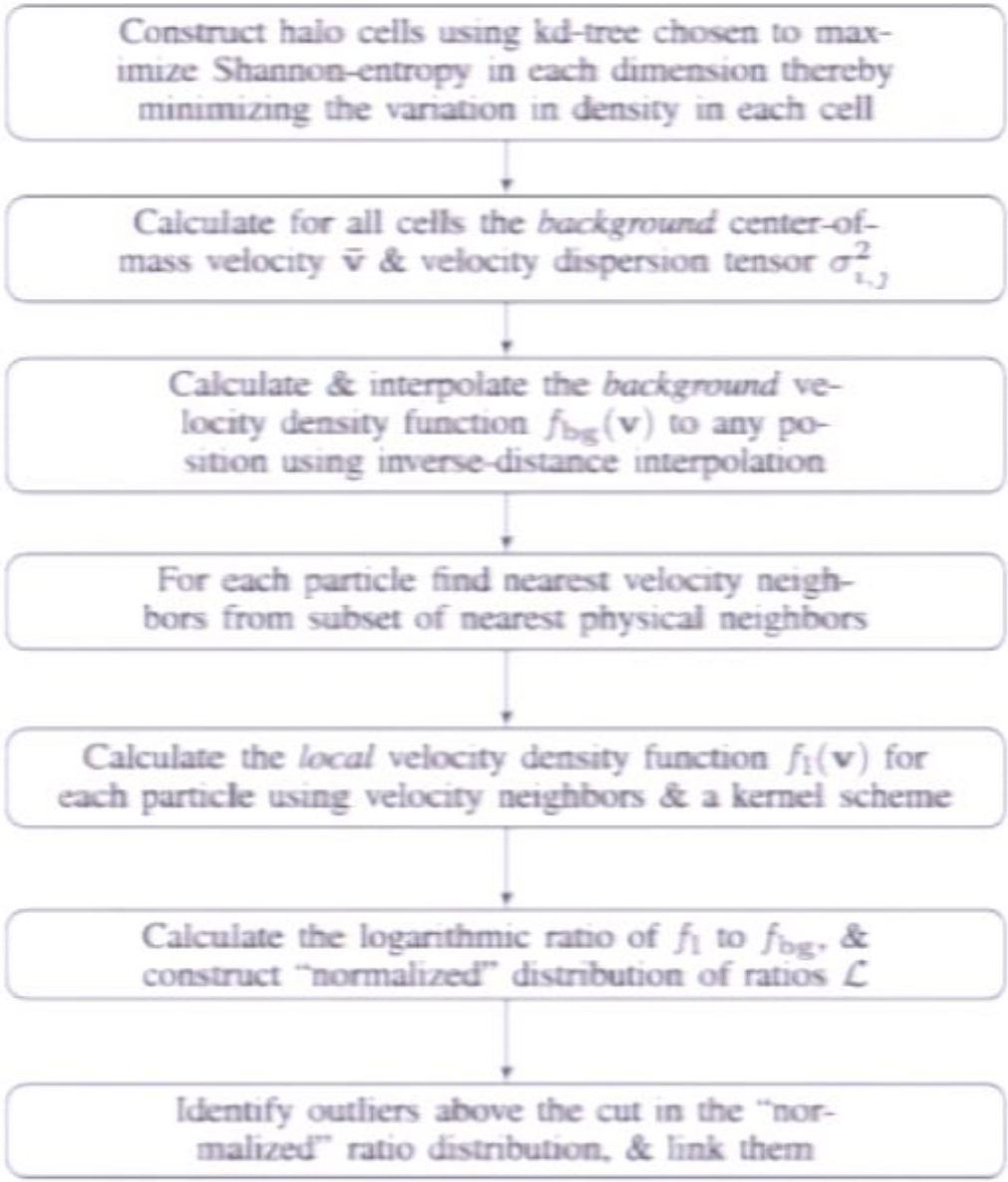

Figure 1. Flow chart of STF algorithm.

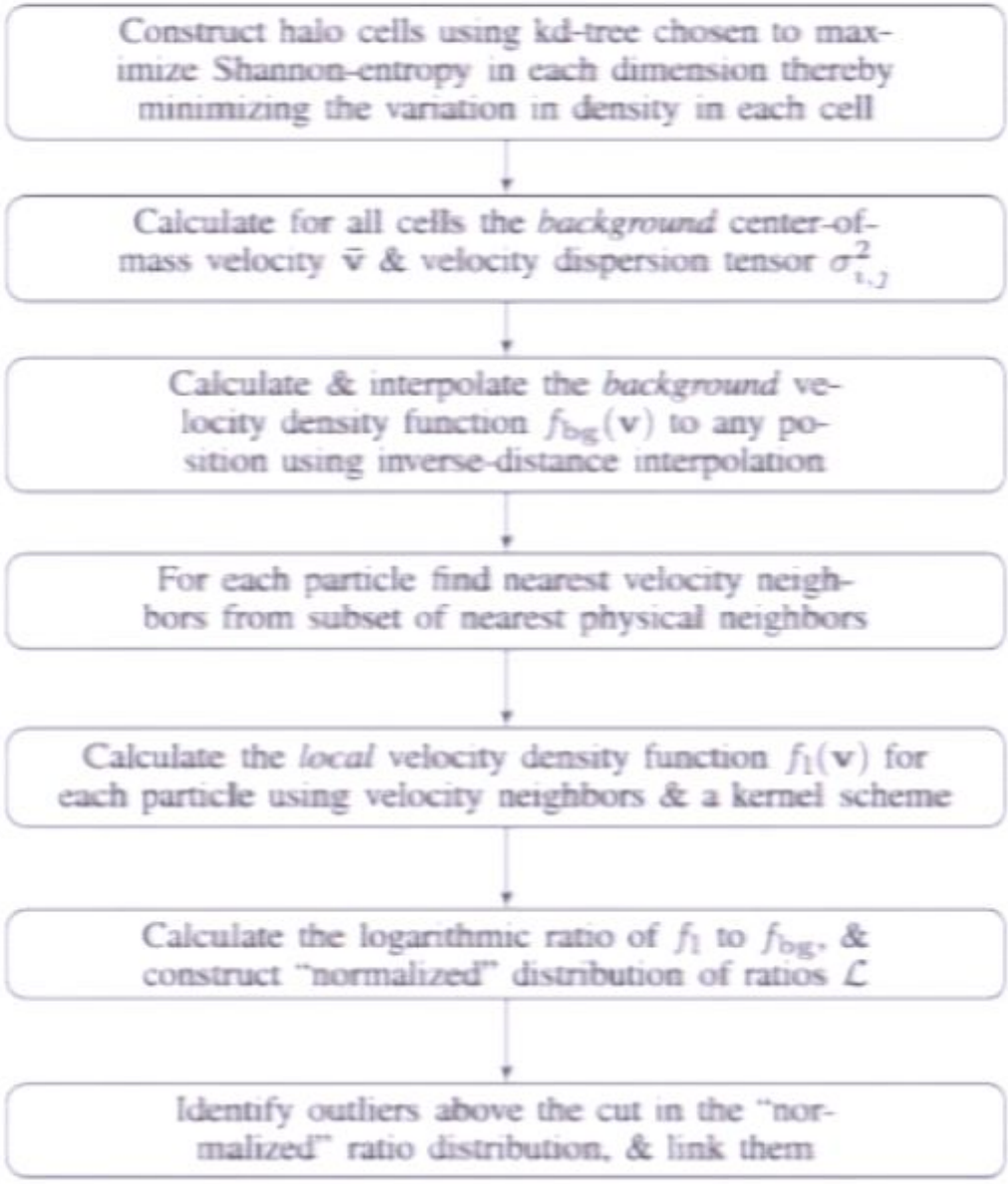

Figure 1. Flow chart of STF algorithm.

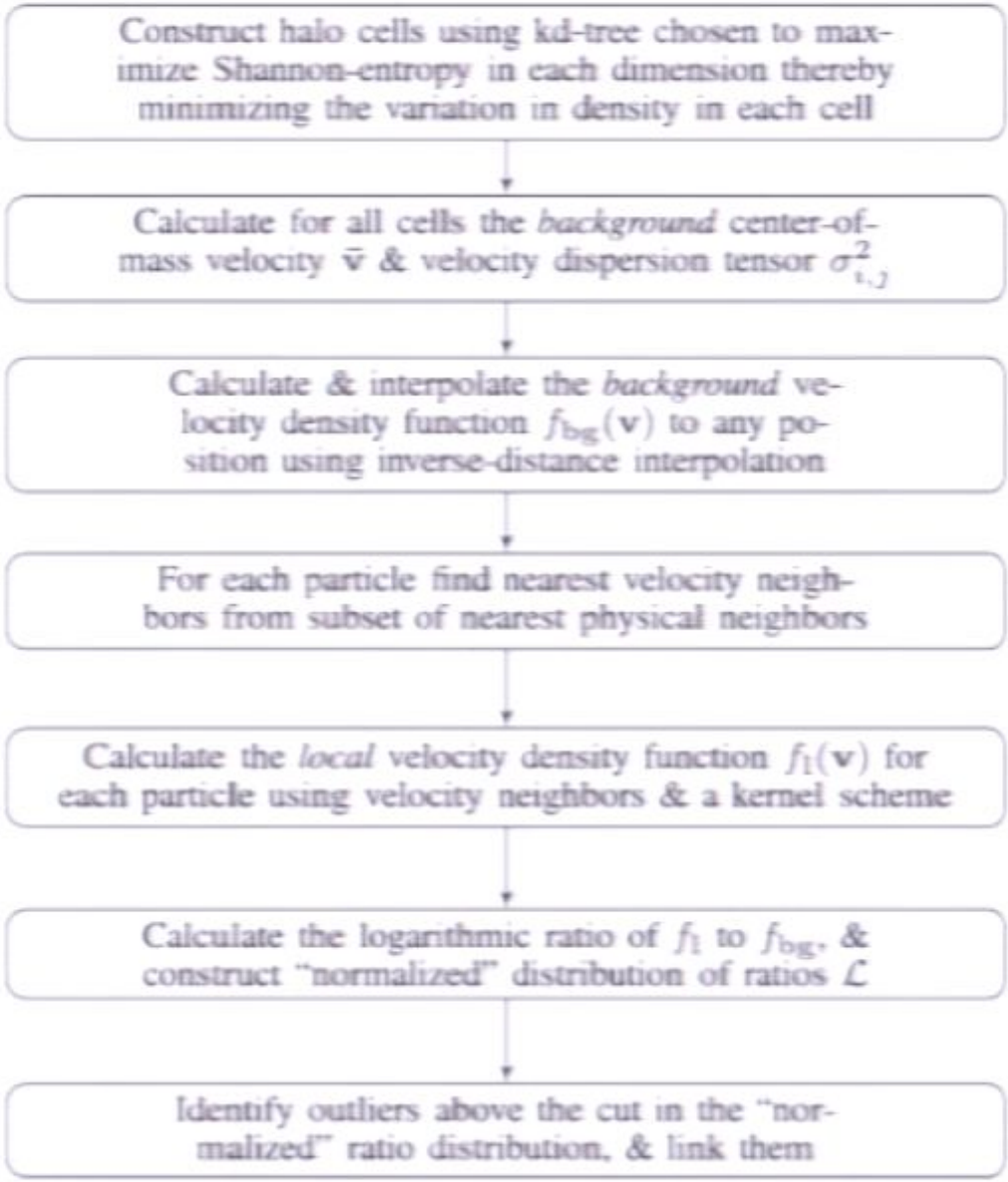

Figure 1. Flow chart of STF algorithm.

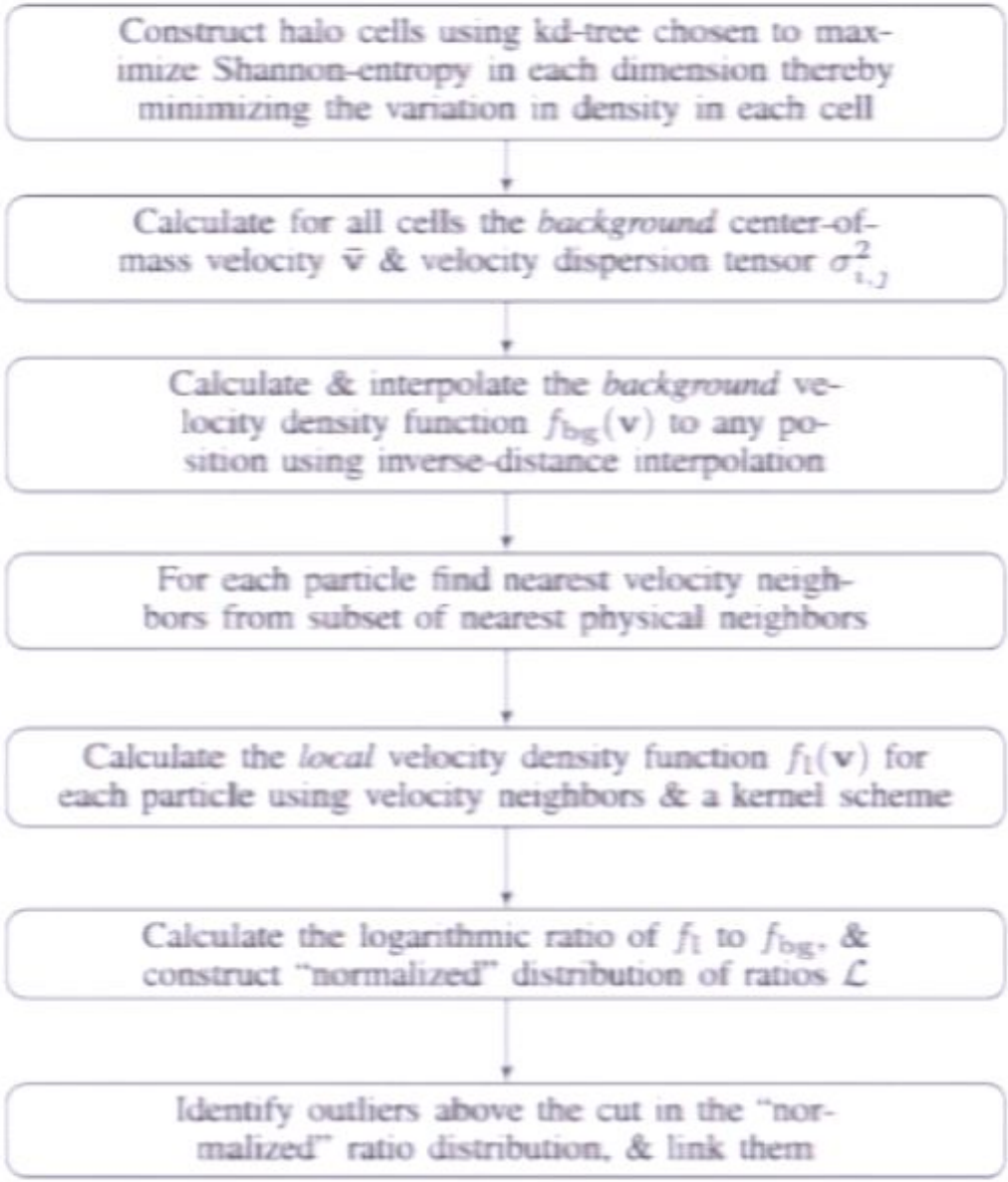

Figure 1. Flow chart of STF algorithm.

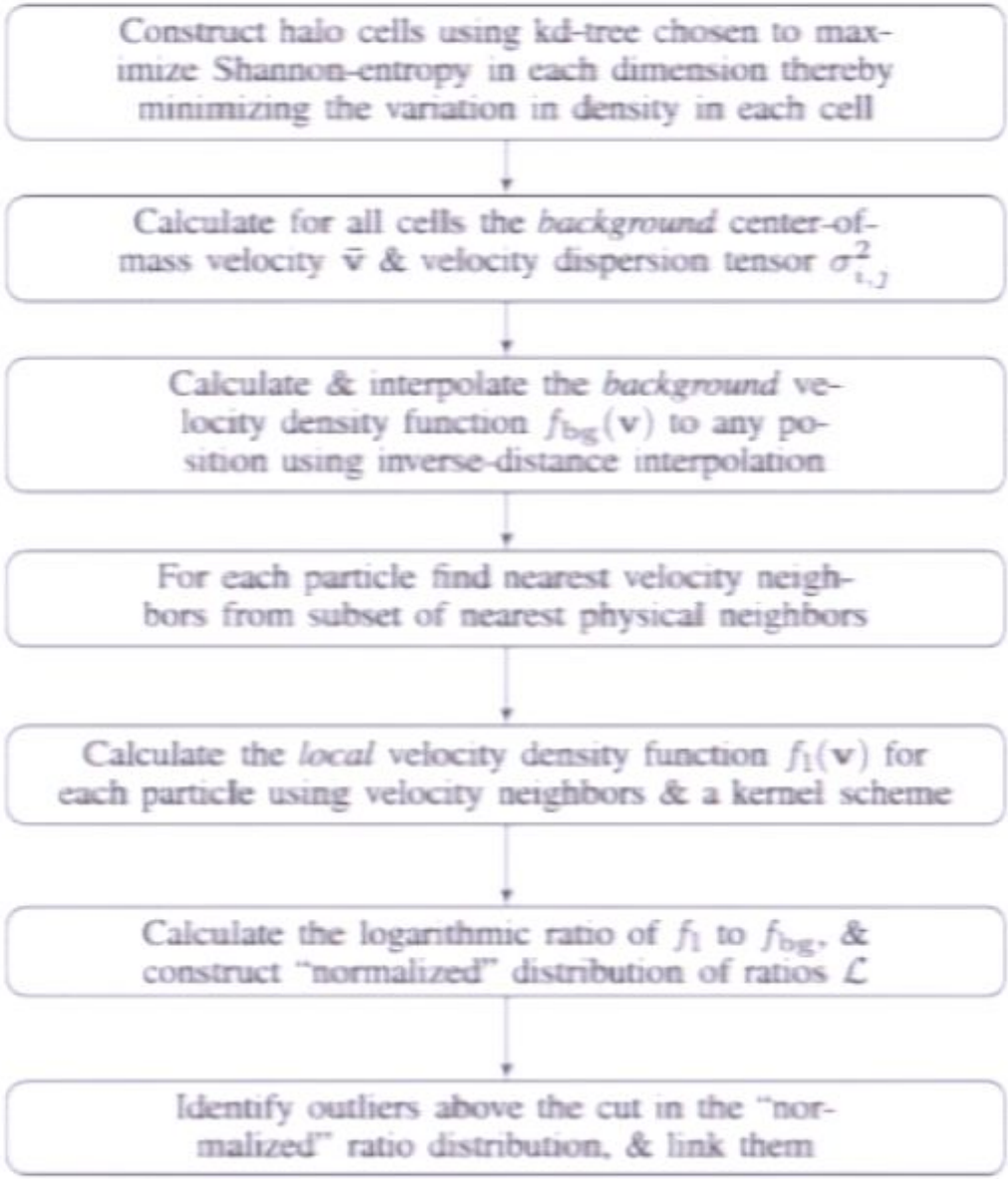

Figure 1. Flow chart of STF algorithm.

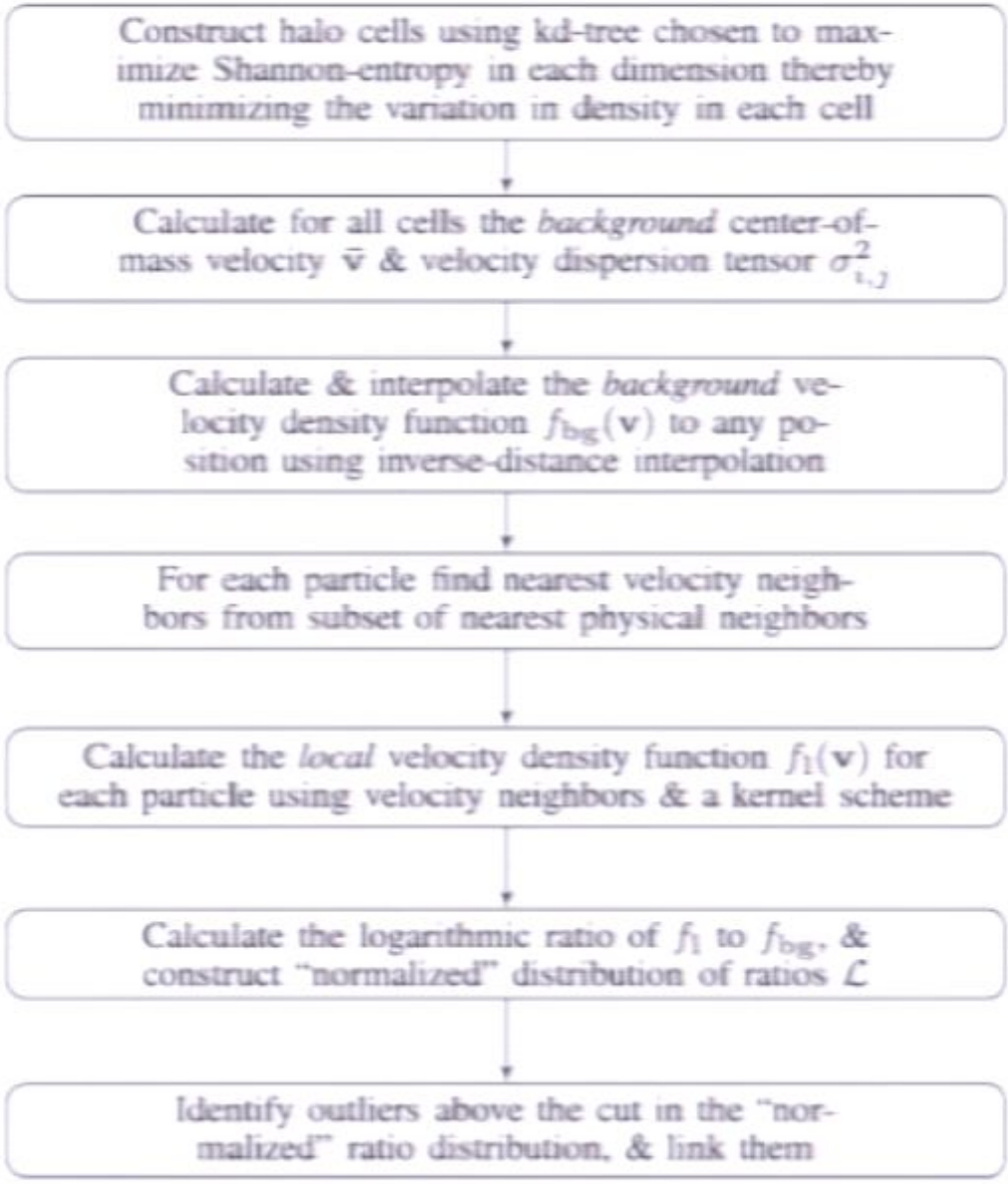

Figure 1. Flow chart of STF algorithm.

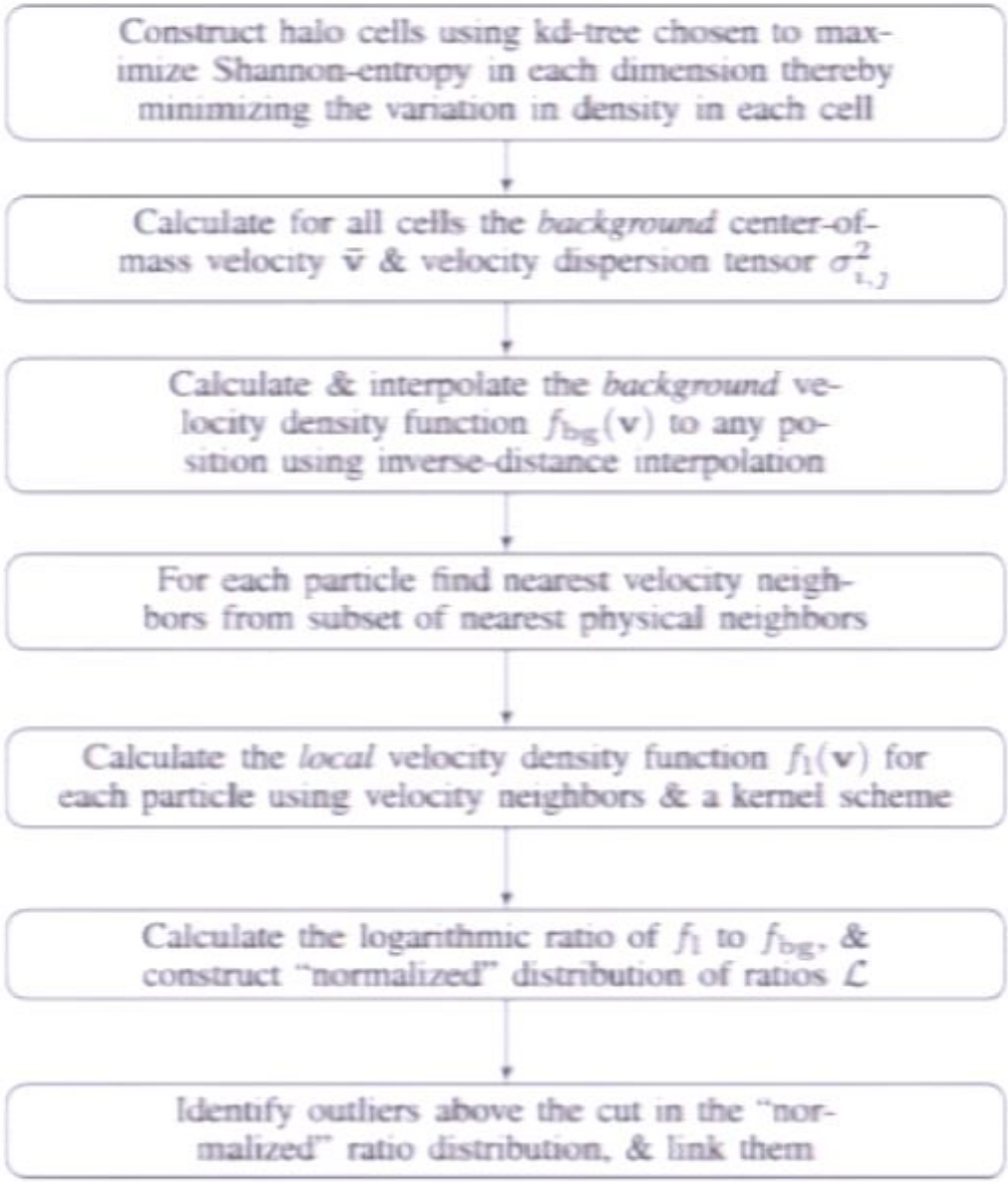

Figure 1. Flow chart of STF algorithm.

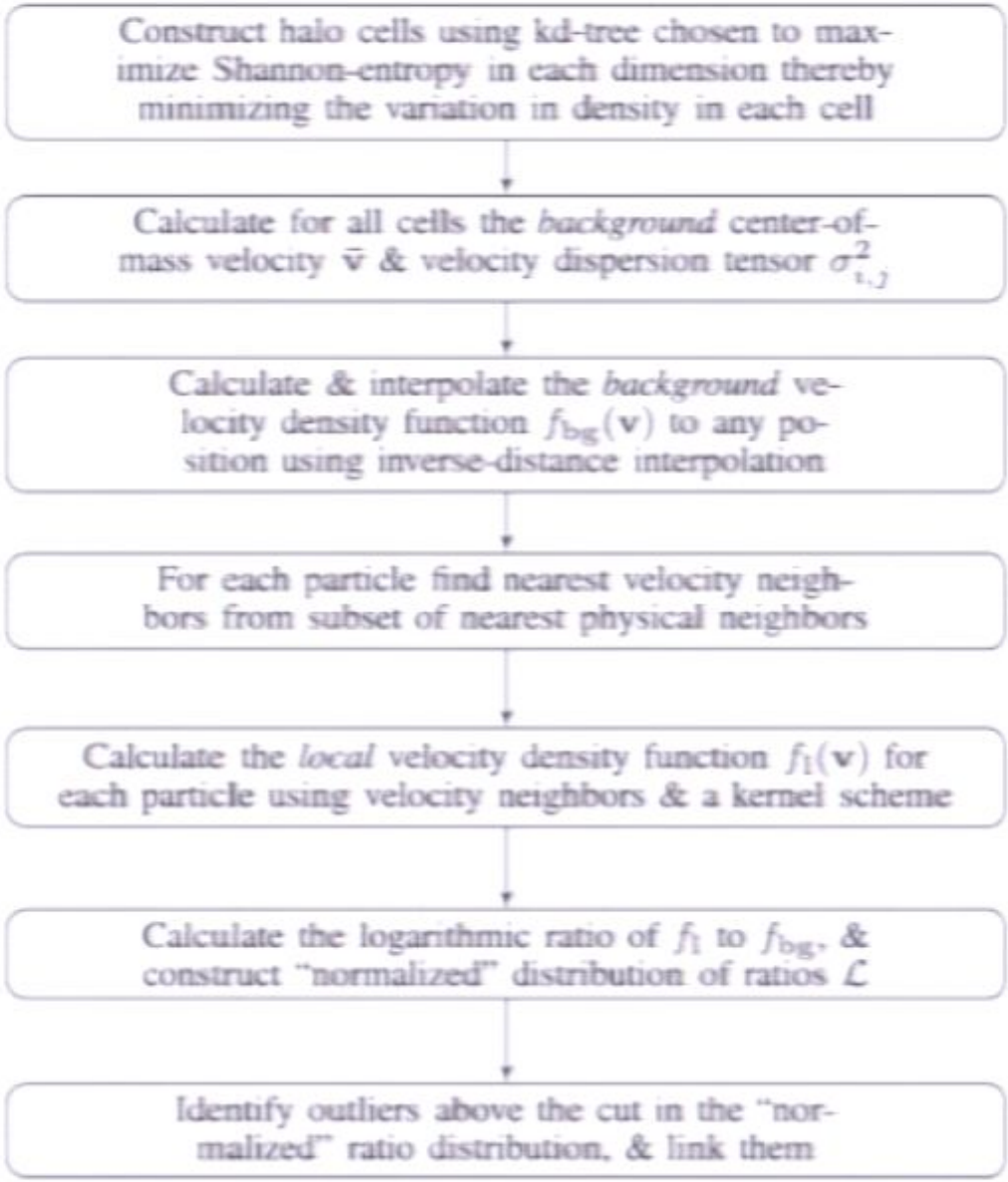

Figure 1. Flow chart of STF algorithm.

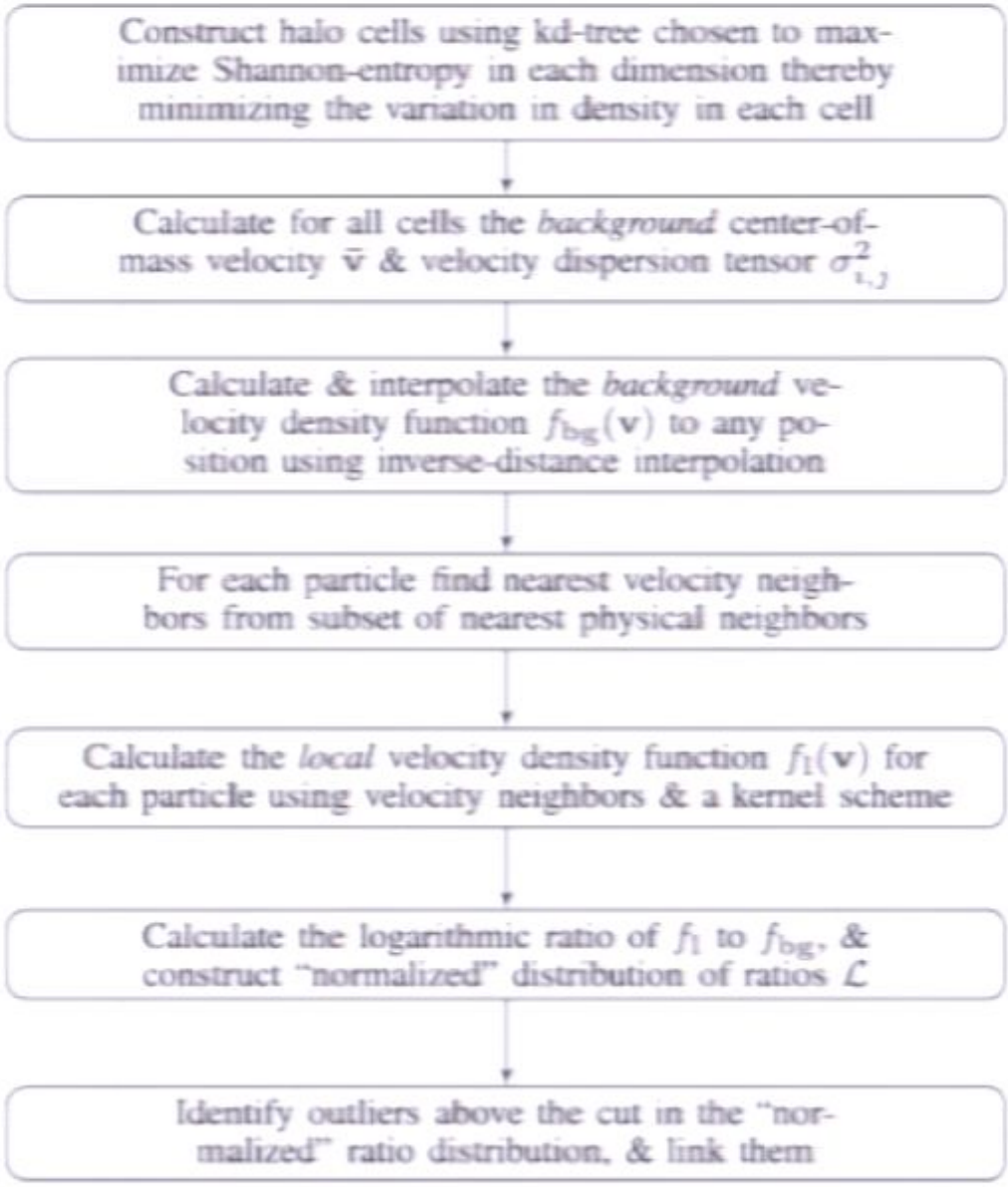

Figure 1. Flow chart of STF algorithm.

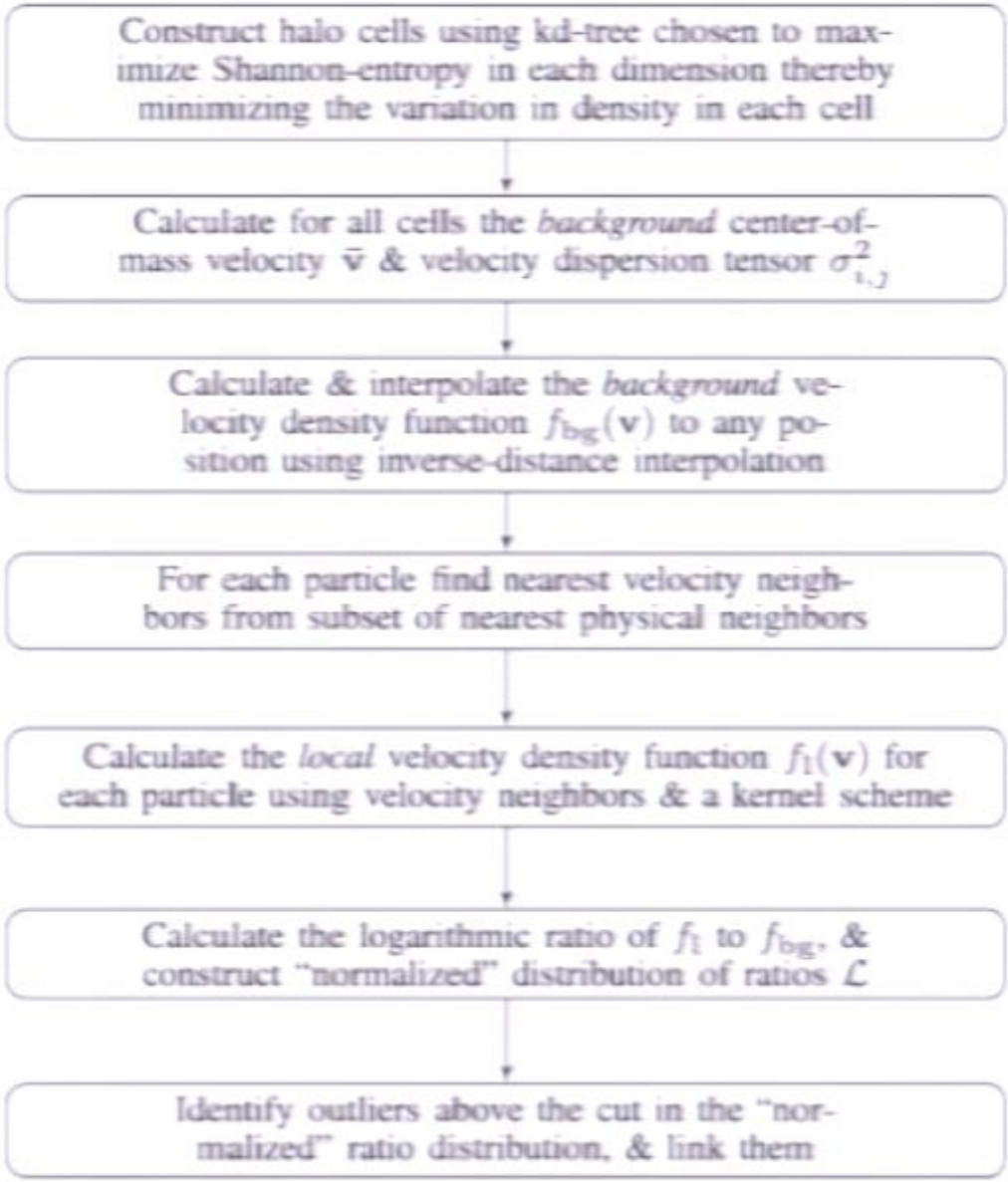

Figure 1. Flow chart of STF algorithm.

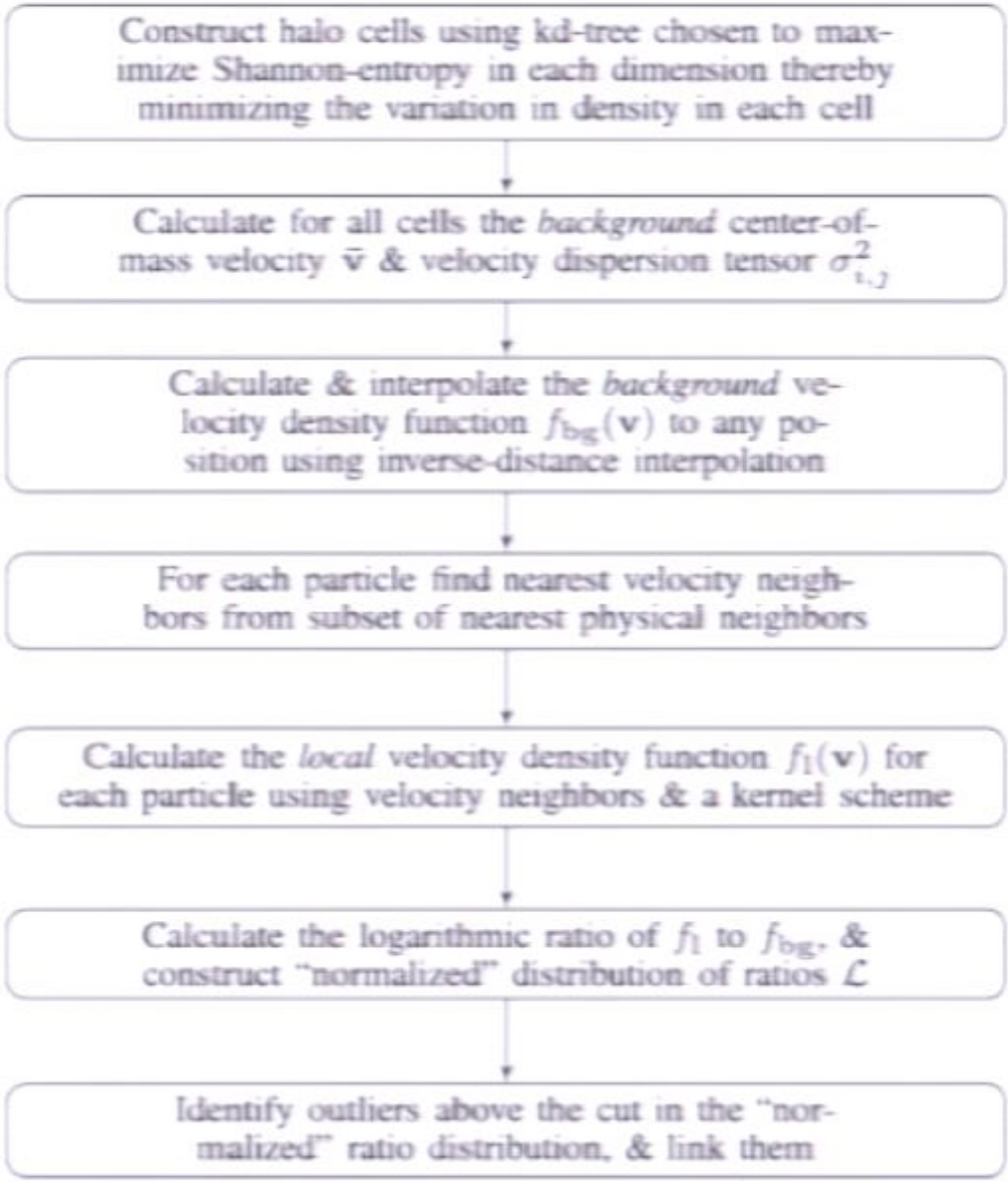

Figure 1. Flow chart of STF algorithm.

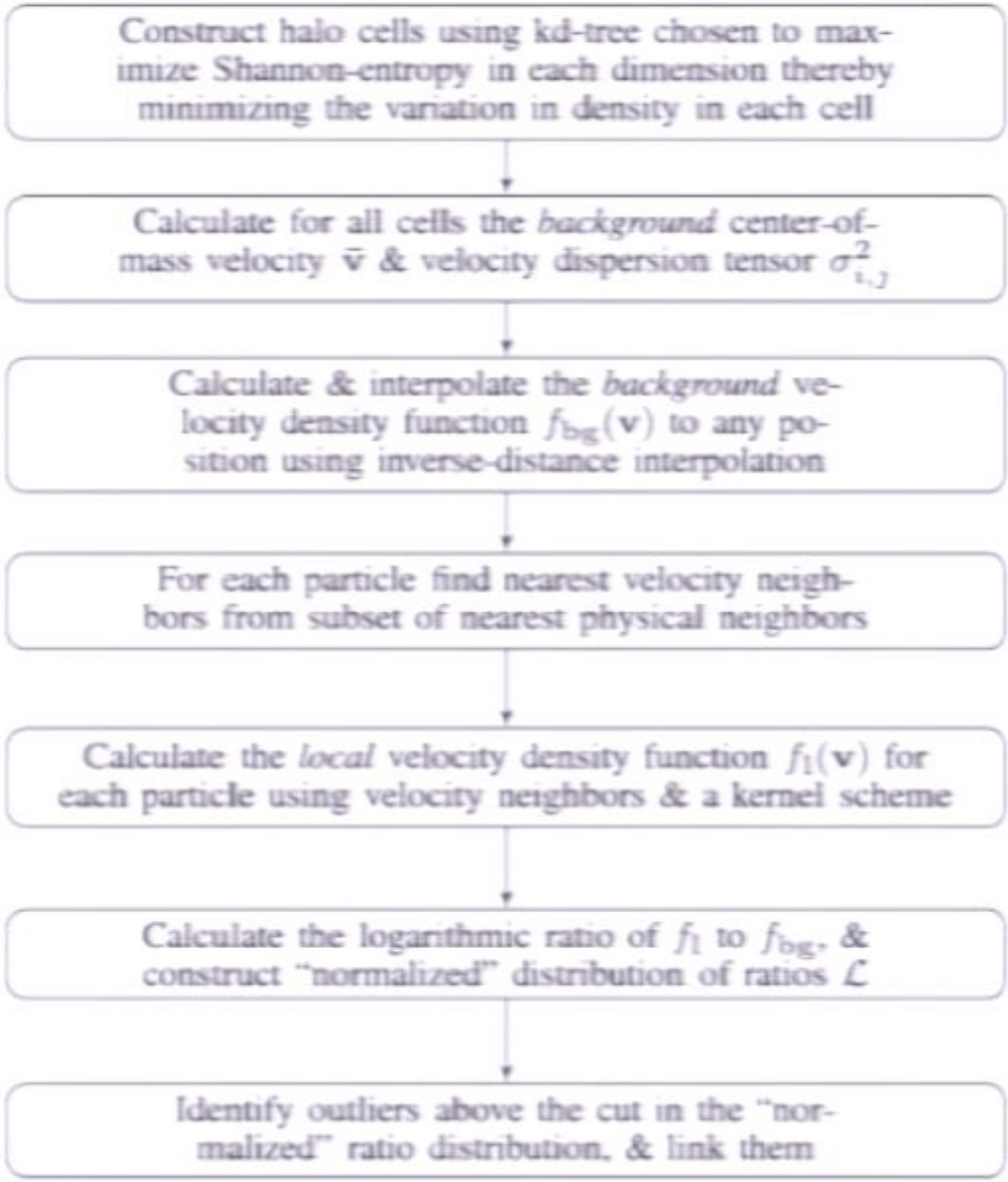

Figure 1. Flow chart of STF algorithm.

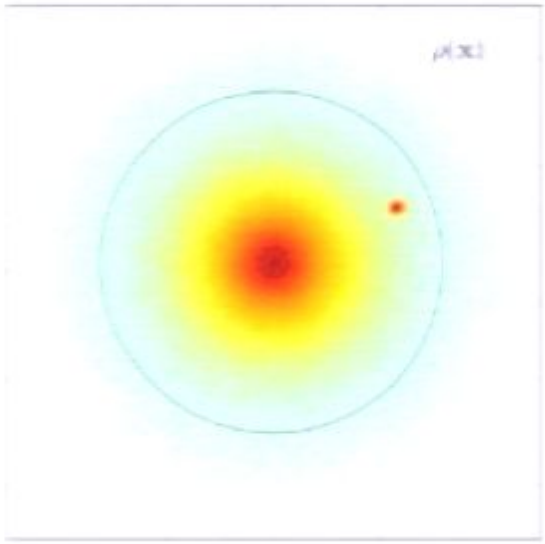
$\rho(\mathbf{x})$

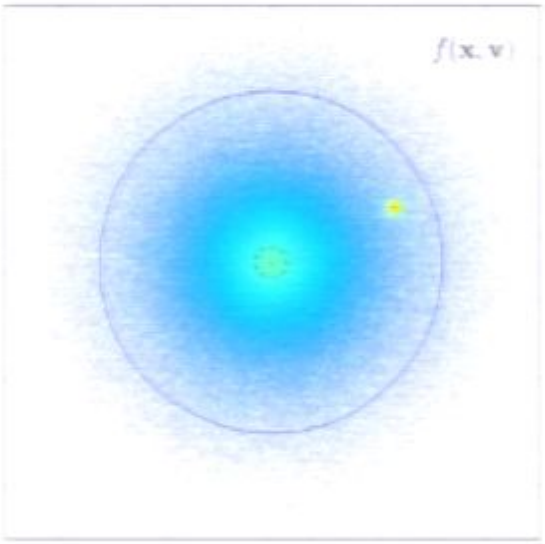
$f(\mathbf{x}, \mathbf{v})$

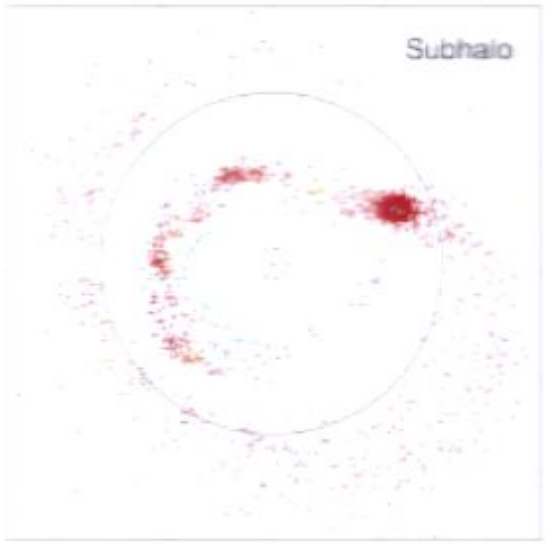
Subhalo

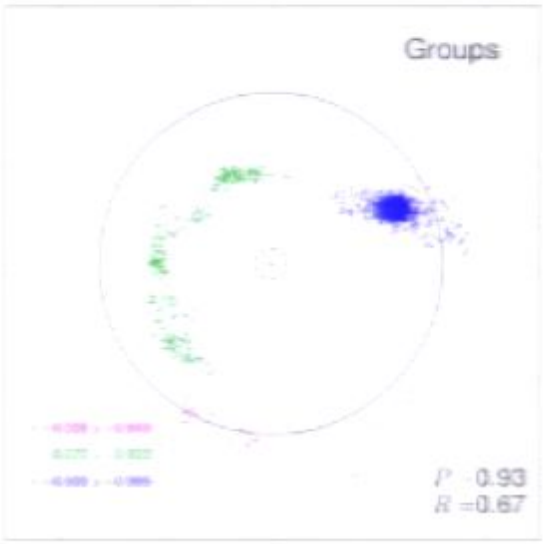
Groups
P 0.93
R =0.67

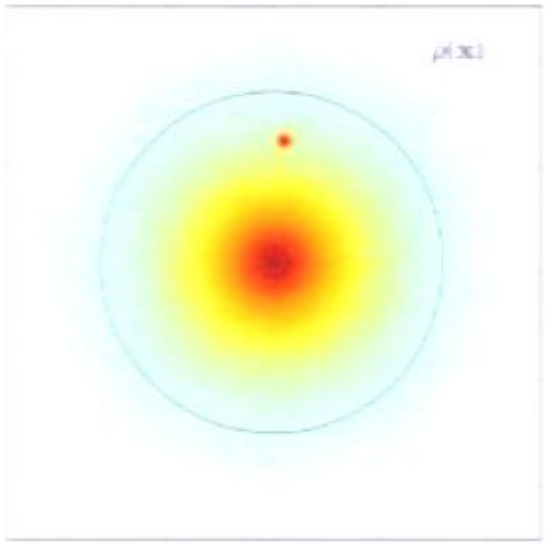
$\rho(\mathbf{x})$

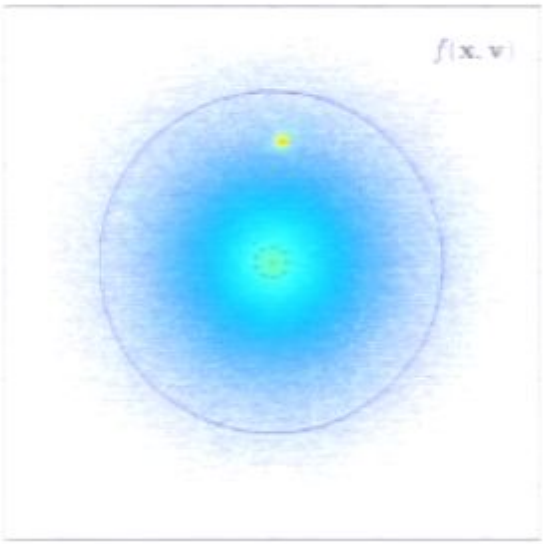
$f(\mathbf{x}, \mathbf{v})$

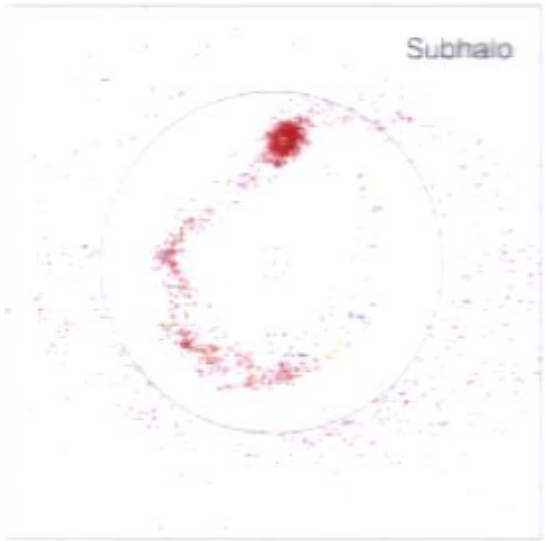
Subhalo

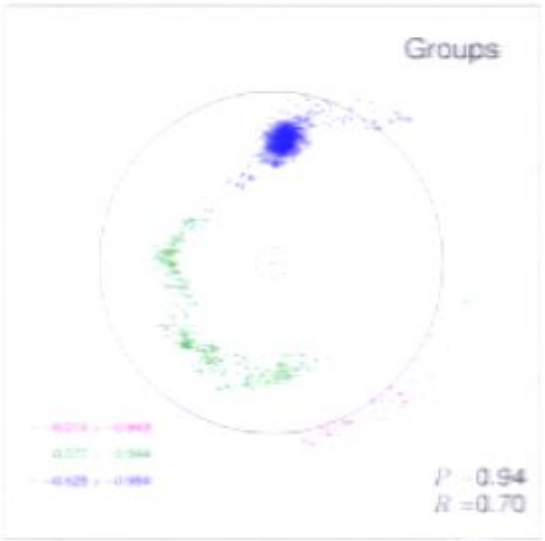
Groups
P 0.94
R =0.70

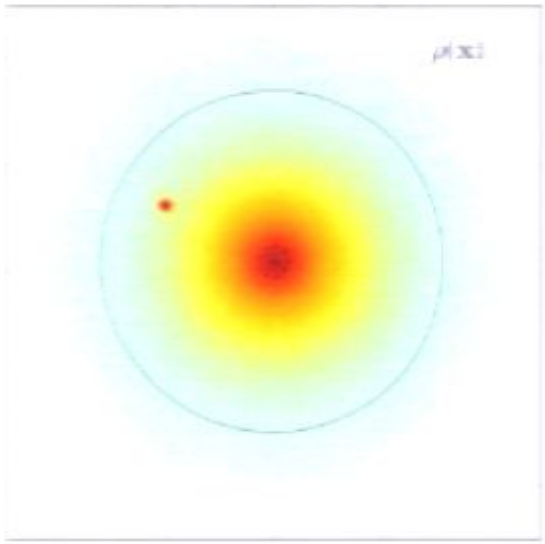
$\rho(\mathbf{x})$

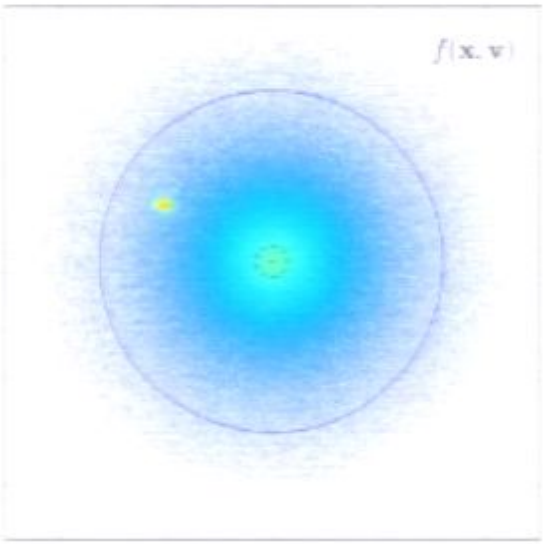
$f(\mathbf{x}, \mathbf{v})$

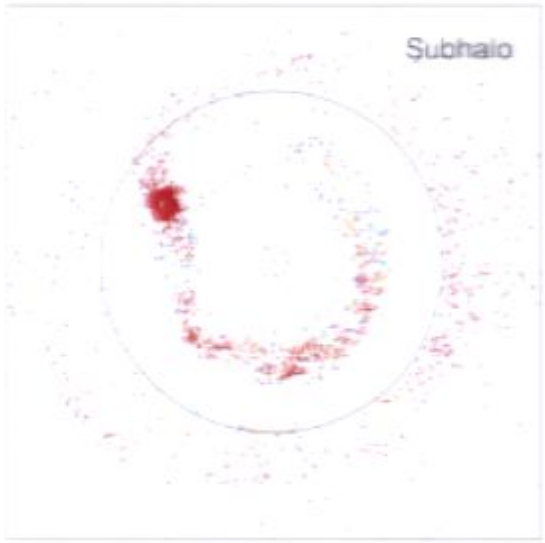
Subhalo

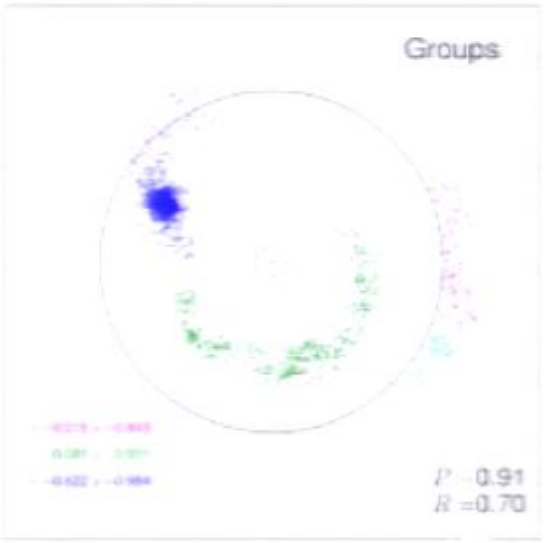
Groups
P 0.91
R =0.70

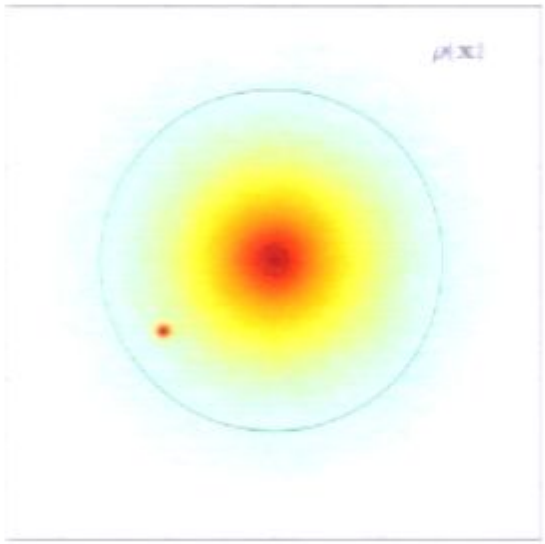
$\rho(\mathbf{x})$

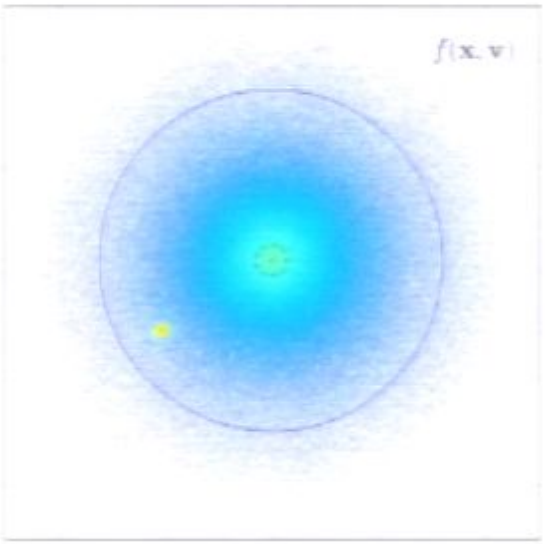
$f(\mathbf{x}, \mathbf{v})$

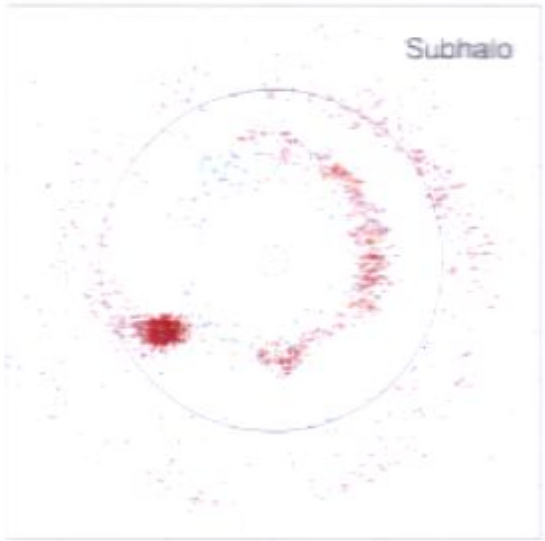
Subhalo

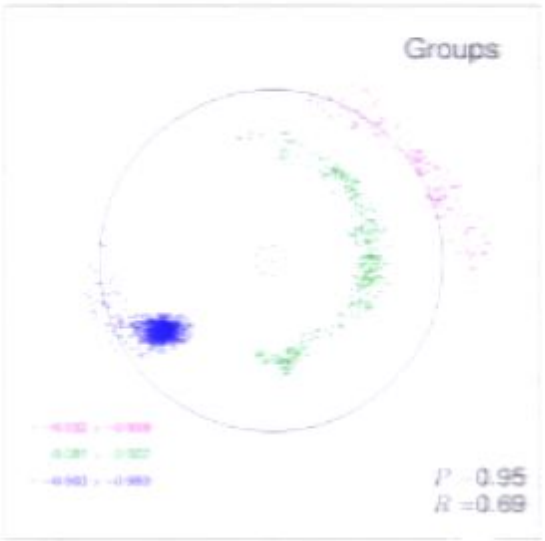
Groups
P 0.95
R =0.69

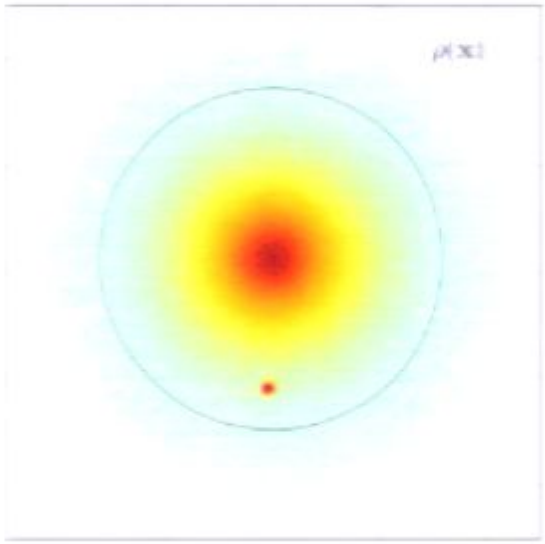
$\rho(\mathbf{x})$

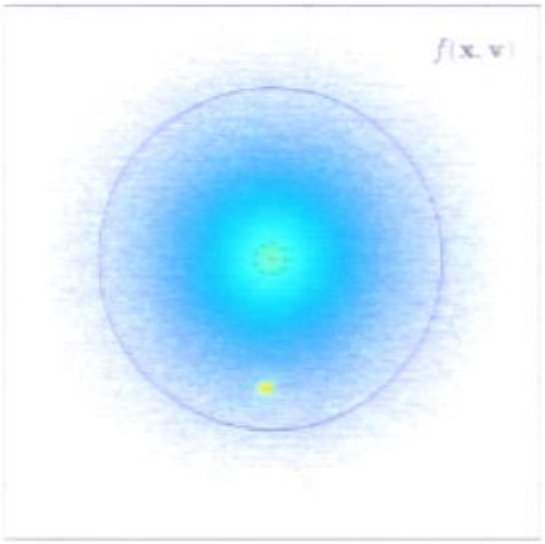
$f(\mathbf{x}, \mathbf{v})$

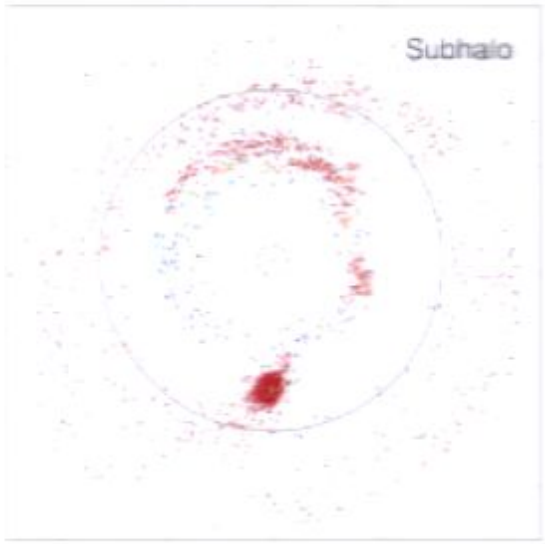
Subhalo

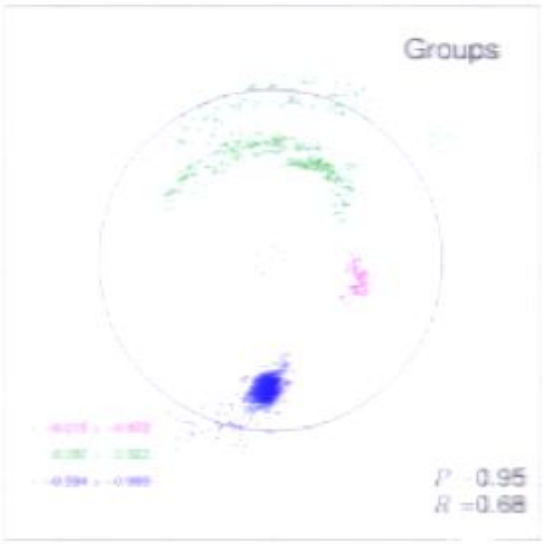
Groups
P 0.95
R =0.68

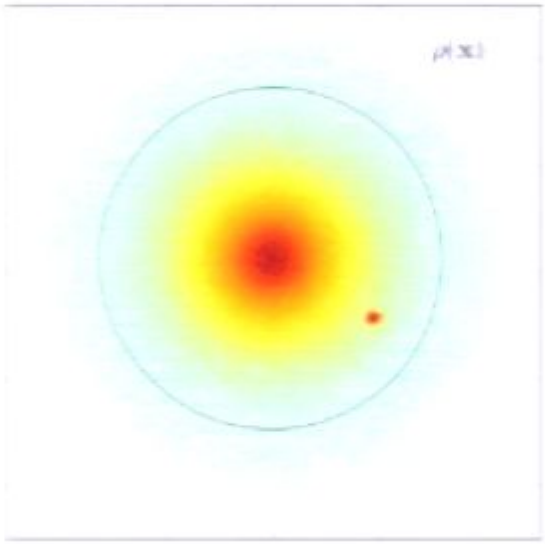
$\rho(\mathbf{x})$

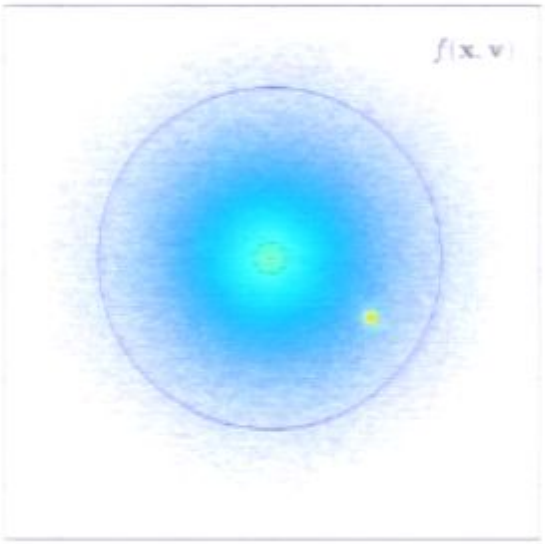
$f(\mathbf{x}, \mathbf{v})$

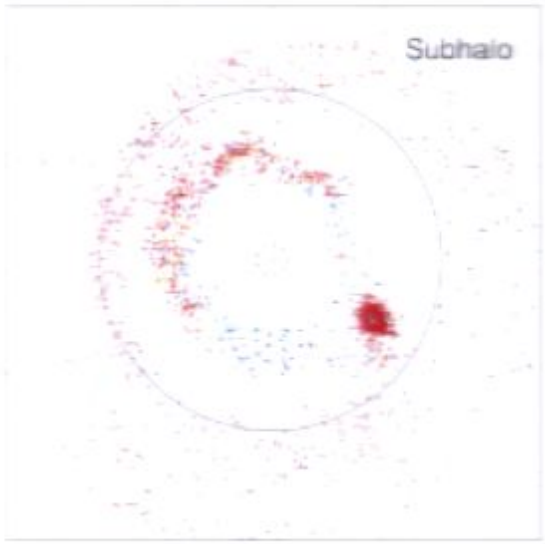
Subhalo

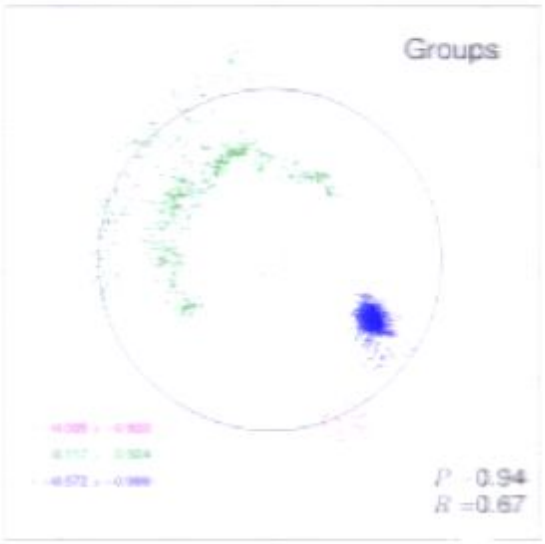
Groups
P 0.94
R =0.67

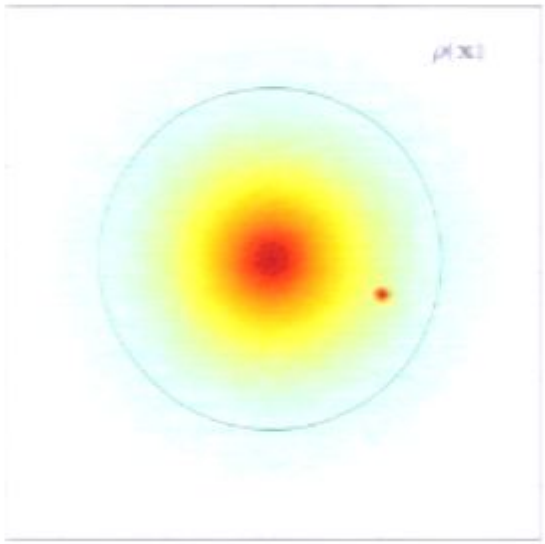
$\rho(\mathbf{x})$

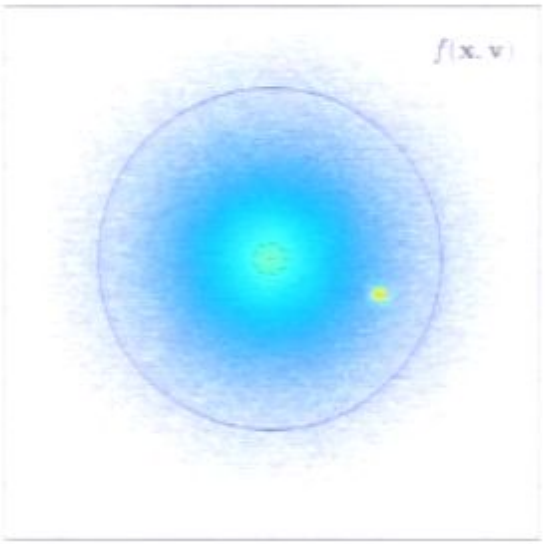
$f(\mathbf{x}, \mathbf{v})$

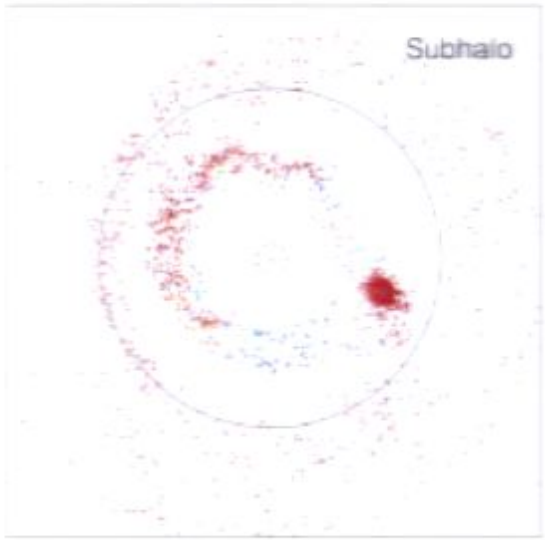
Subhalo

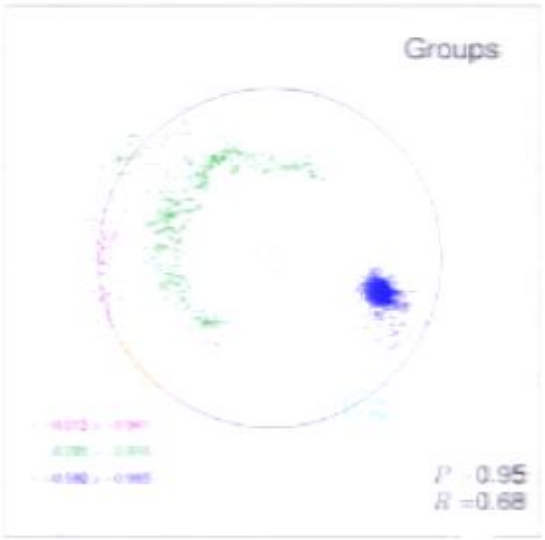
Groups
P 0.95
R =0.68

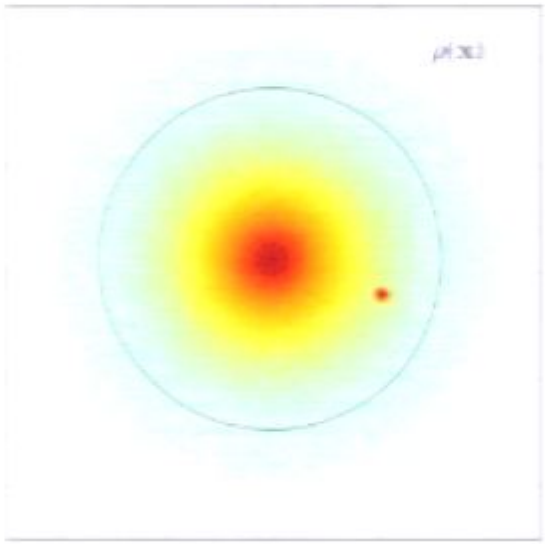
$\rho(\mathbf{x})$

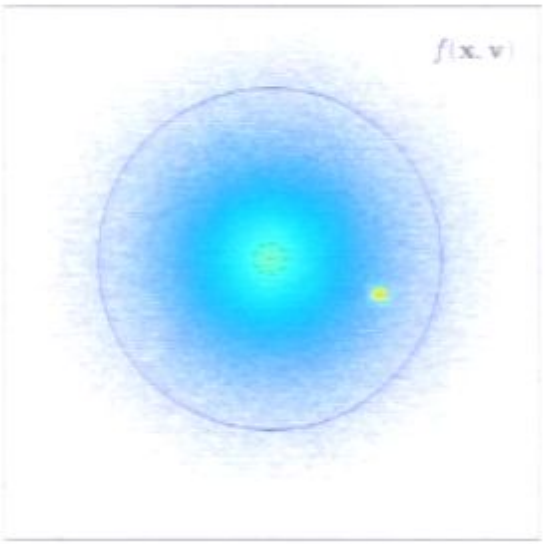
$f(\mathbf{x}, \mathbf{v})$

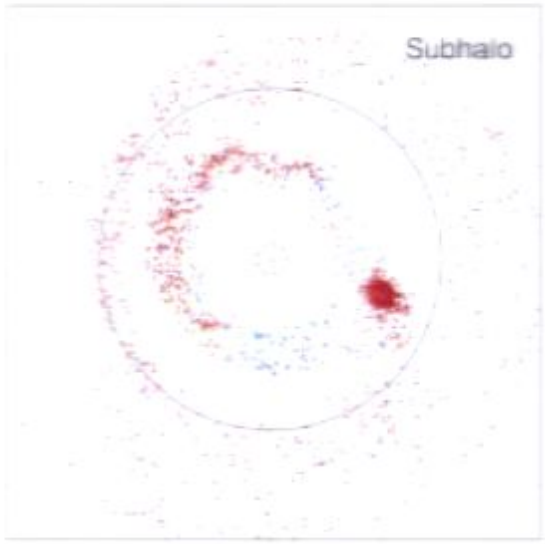
Subhalo

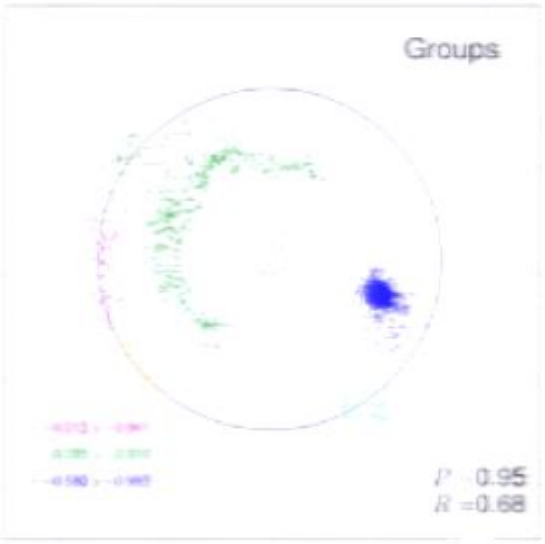
Groups
P 0.95
R =0.68

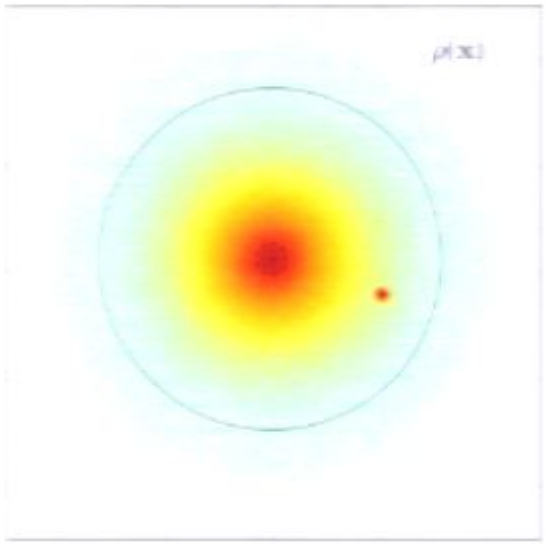
$\rho(\mathbf{x})$

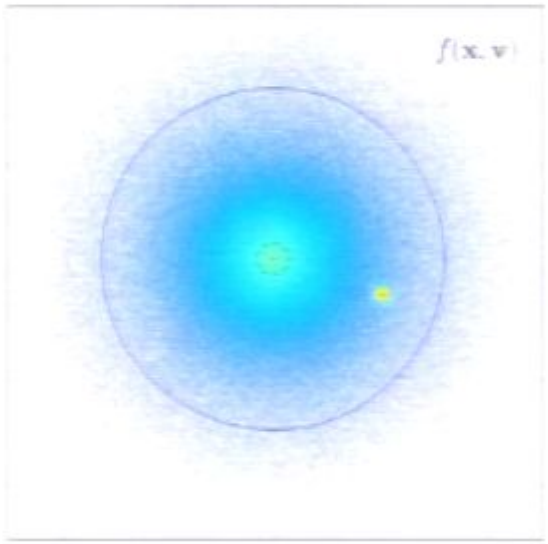
$f(\mathbf{x}, \mathbf{v})$

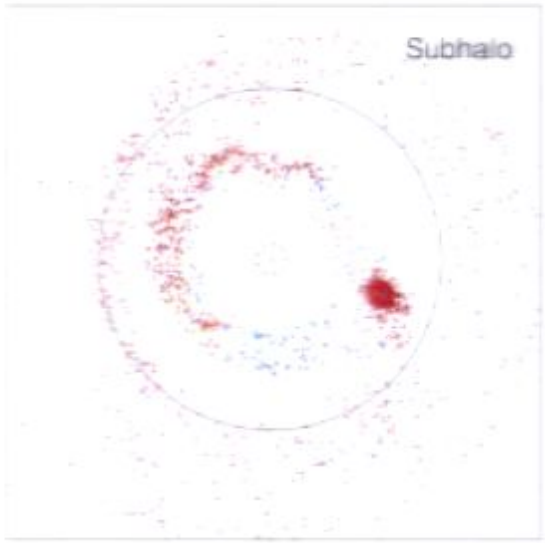
Subhalo

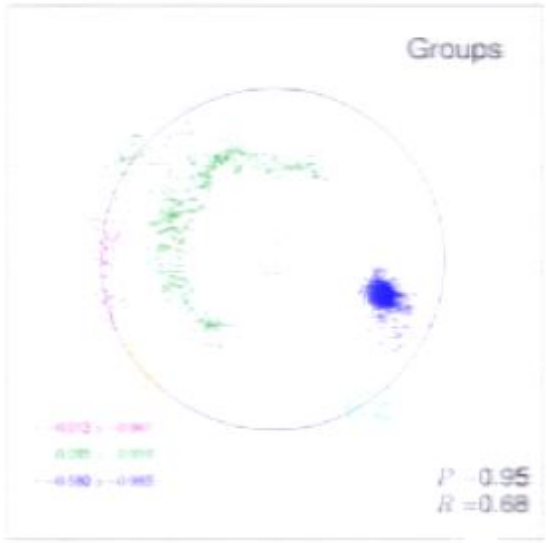
Groups
P 0.95
R =0.68

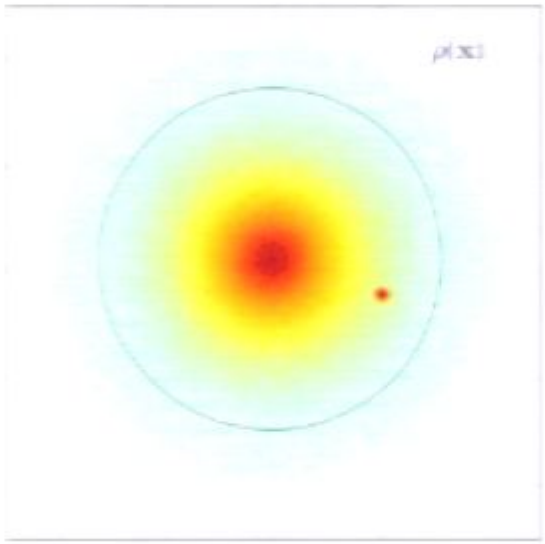
$\rho(\mathbf{x})$

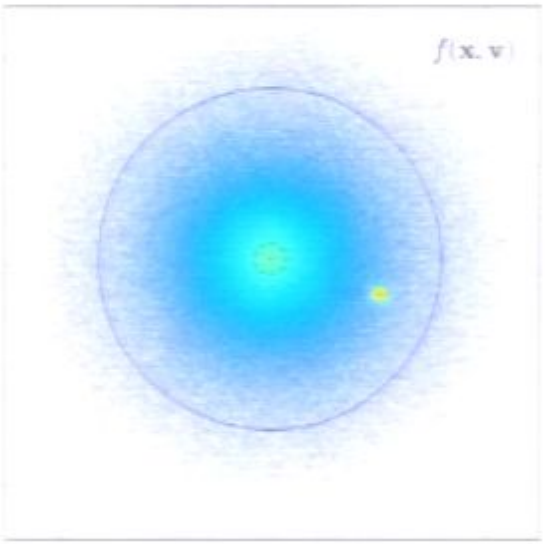
$f(\mathbf{x}, \mathbf{v})$

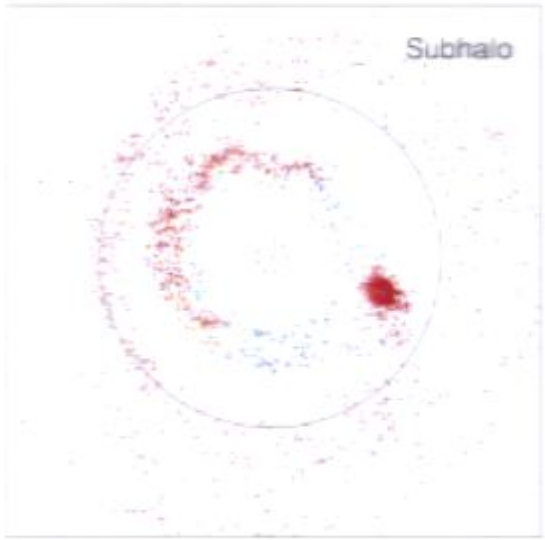
Subhalo

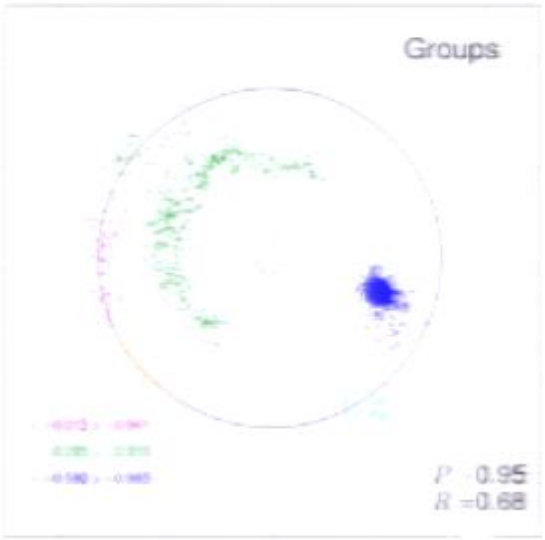
Groups
P 0.95
R =0.68

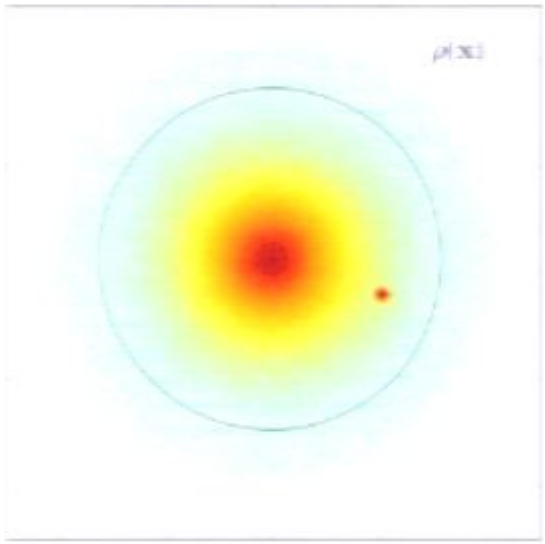
$\rho(\mathbf{x})$

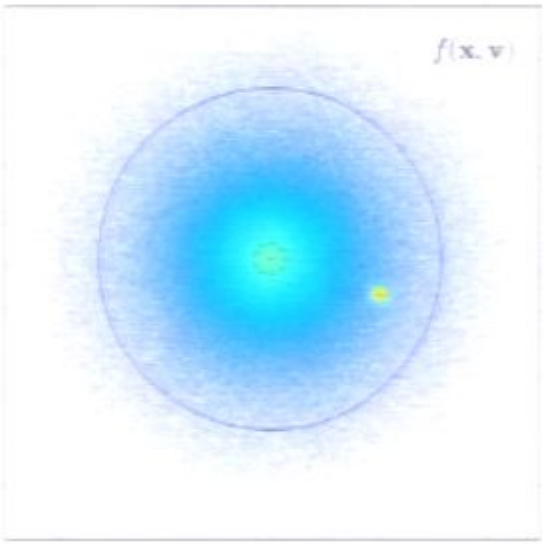
$f(\mathbf{x}, \mathbf{v})$

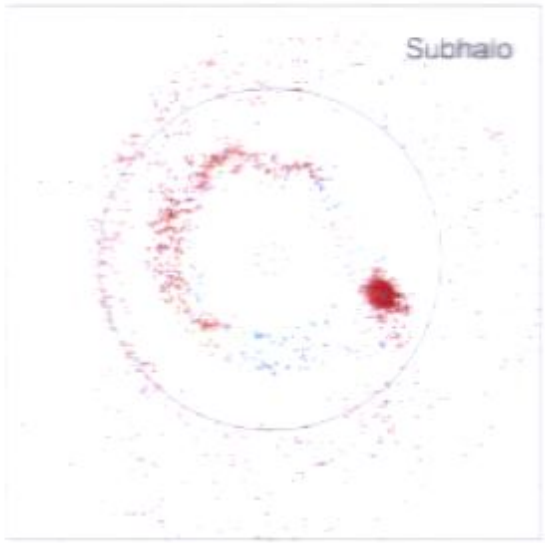
Subhalo

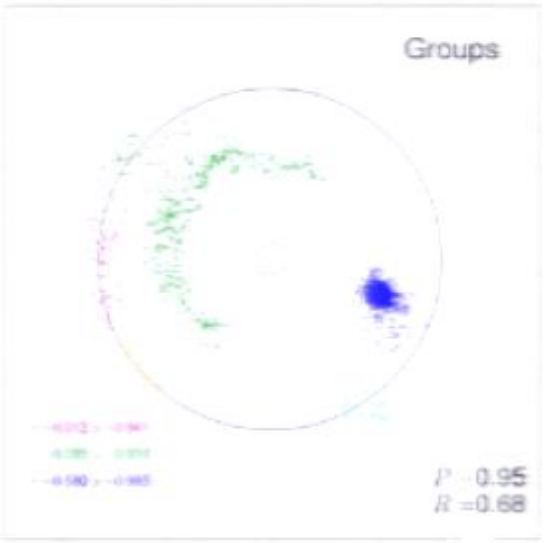
Groups
P 0.95
R =0.68

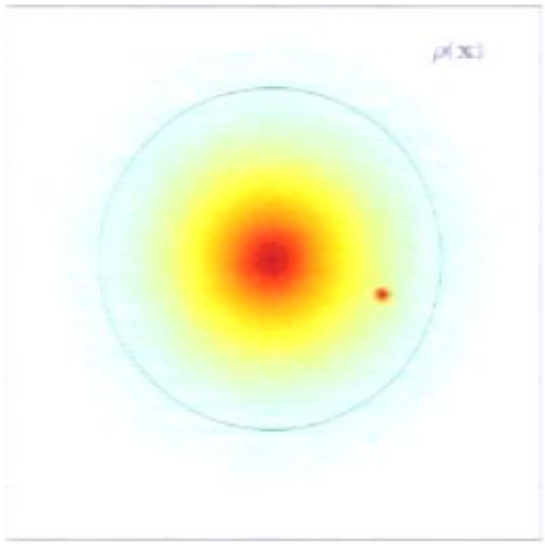
$\rho(\mathbf{x})$

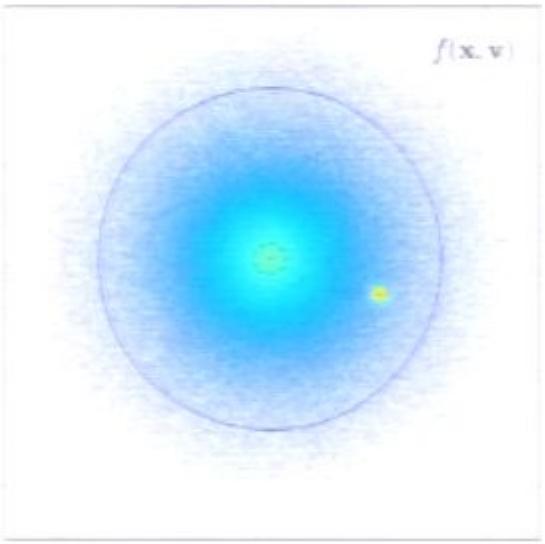
$f(\mathbf{x}, \mathbf{v})$

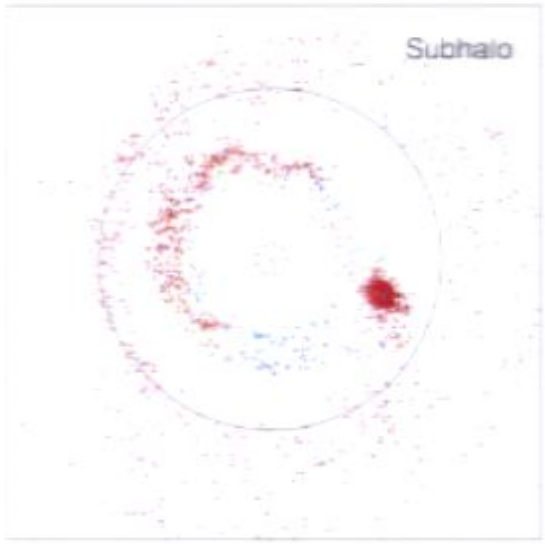
Subhalo

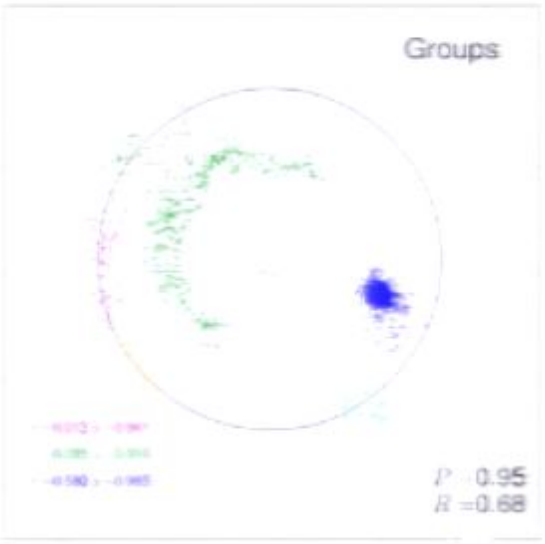
Groups
P 0.95
R =0.68

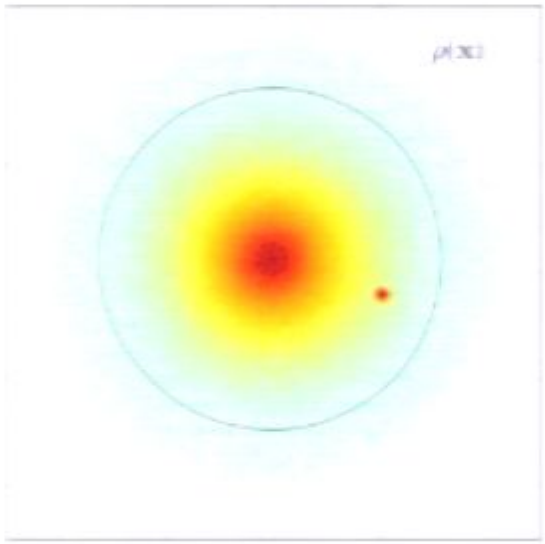
$\rho(\mathbf{x})$

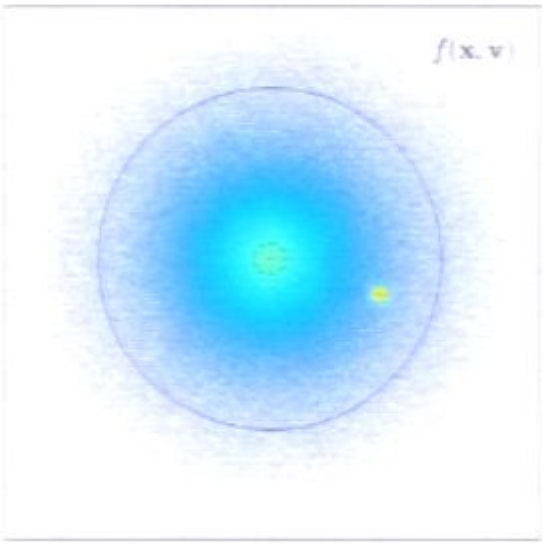
$f(\mathbf{x}, \mathbf{v})$

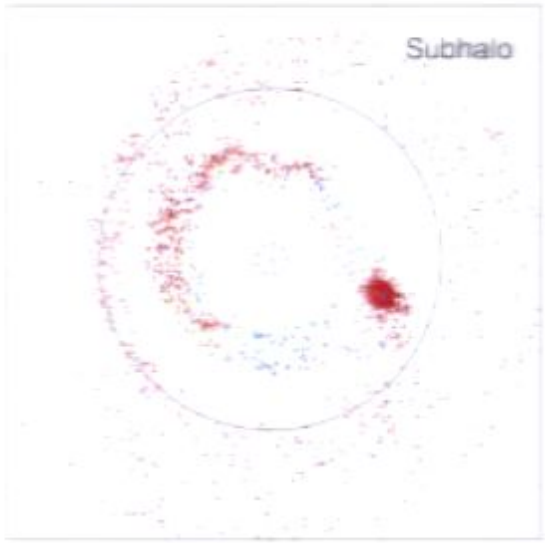
Subhalo

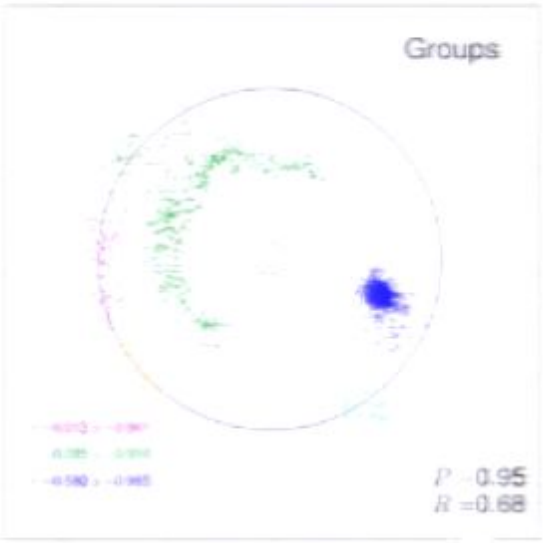
Groups
P =0.95
R =0.68

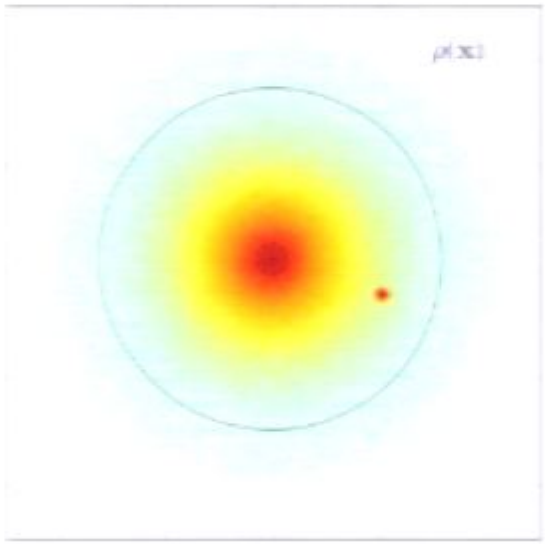
$\rho(\mathbf{x})$

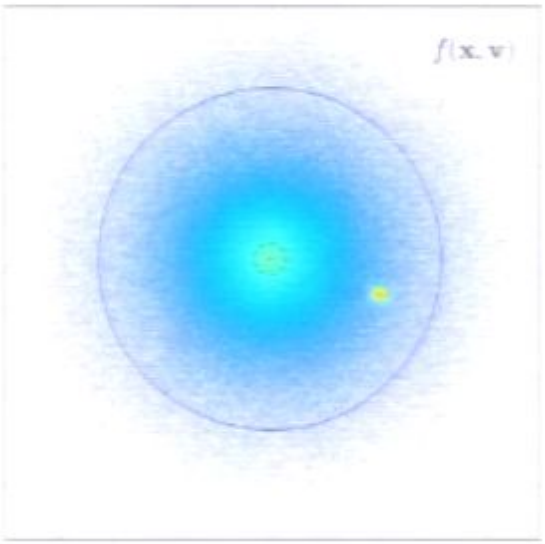
$f(\mathbf{x}, \mathbf{v})$

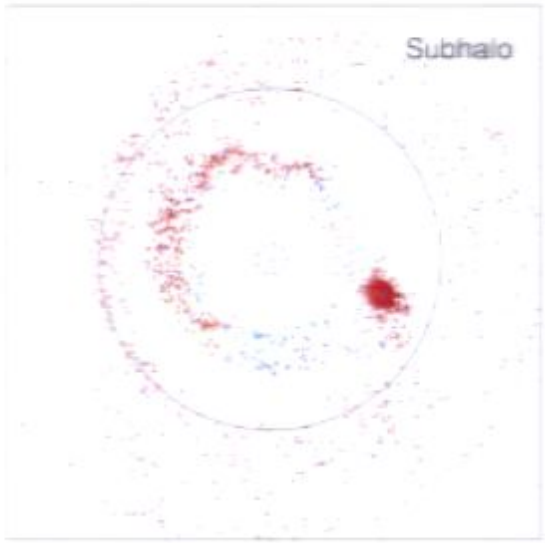
Subhalo

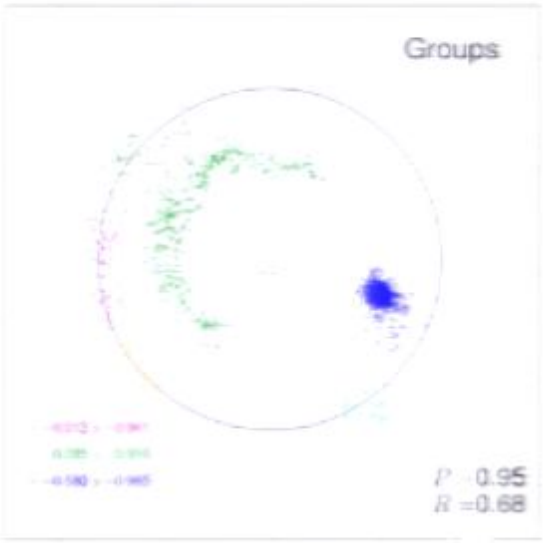
Groups
P 0.95
R =0.68

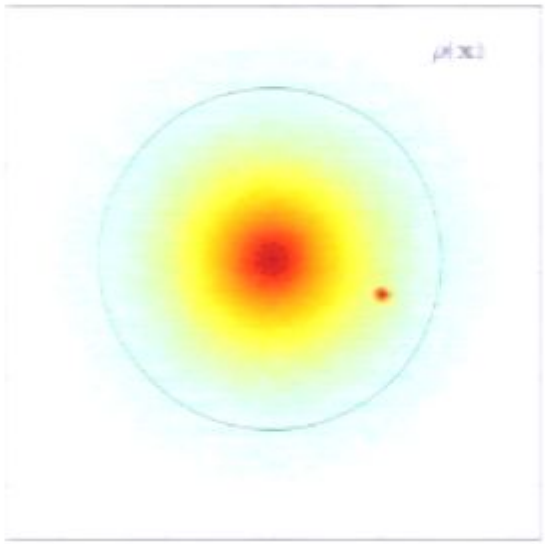
$\rho(\mathbf{x})$

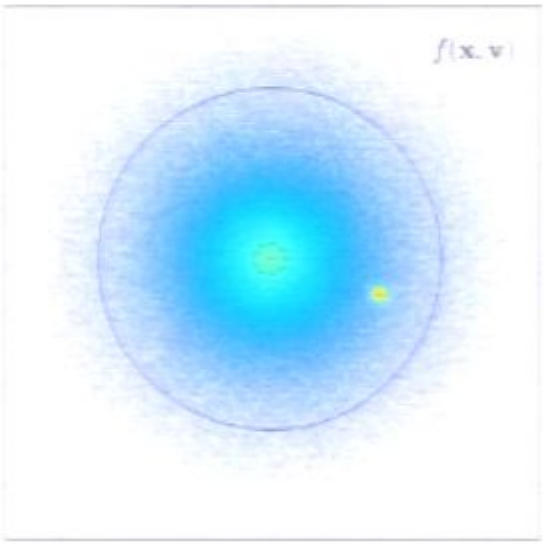
$f(\mathbf{x}, \mathbf{v})$

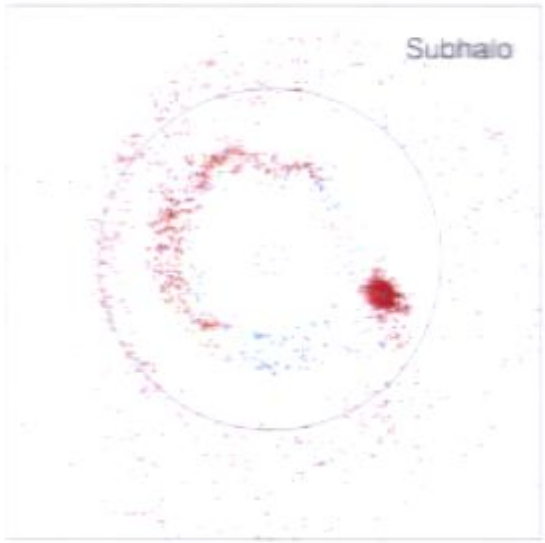
Subhalo

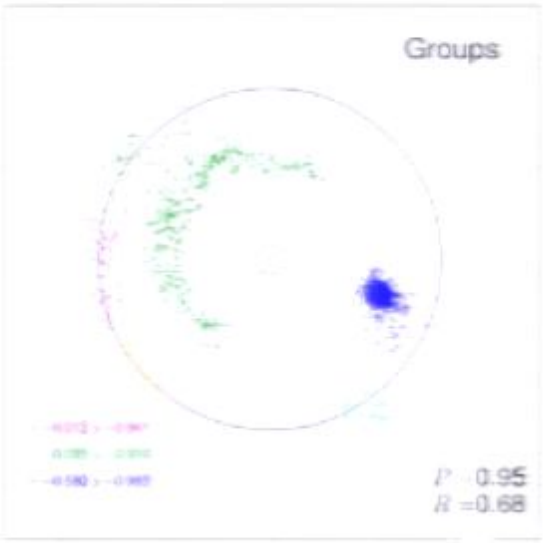
Groups
P 0.95
R =0.68

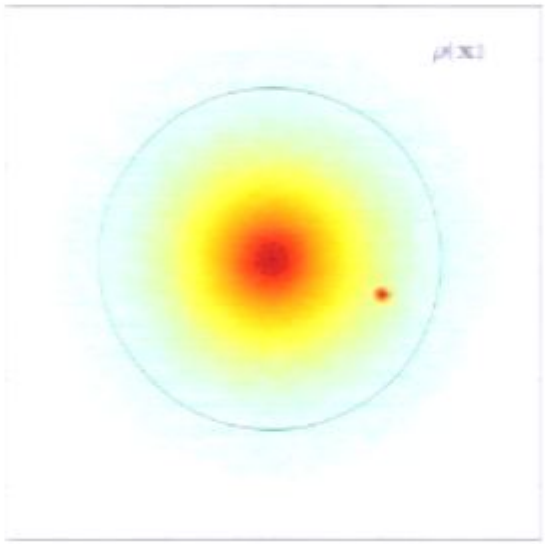
$\rho(\mathbf{x})$

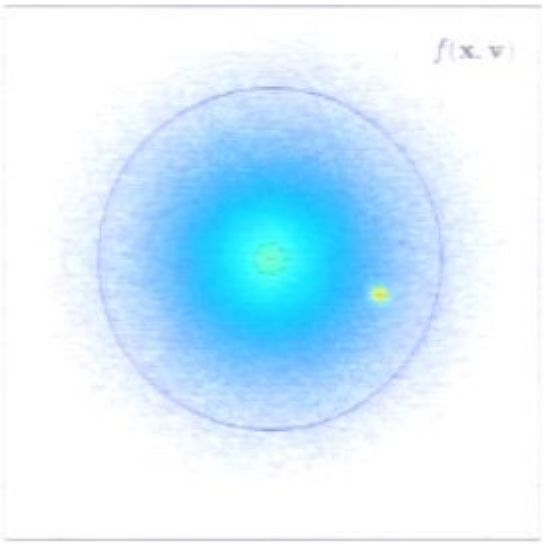
$f(\mathbf{x}, \mathbf{v})$

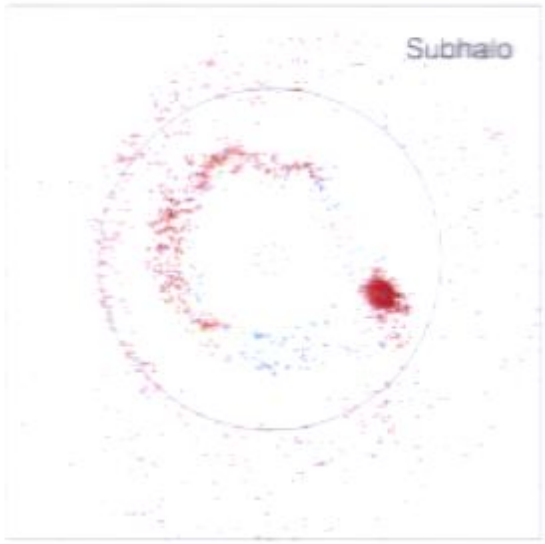
Subhalo

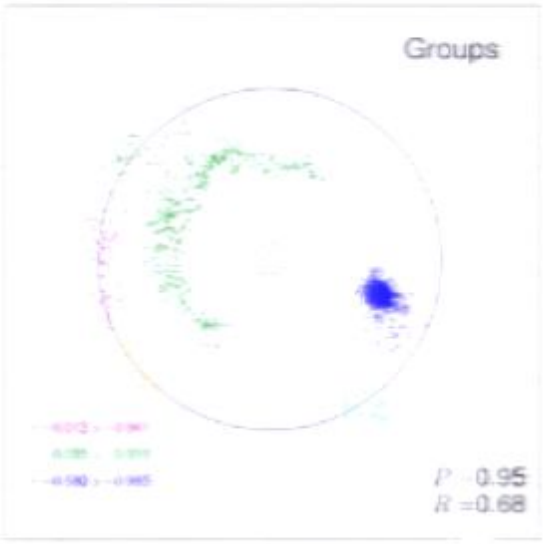
Groups
P 0.95
R =0.68

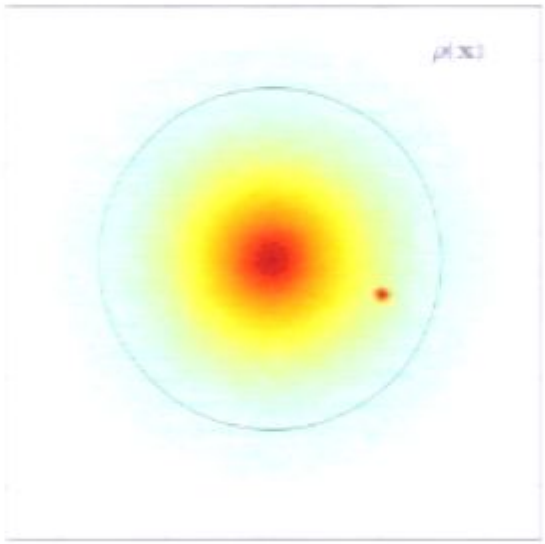
$\rho(\mathbf{x})$

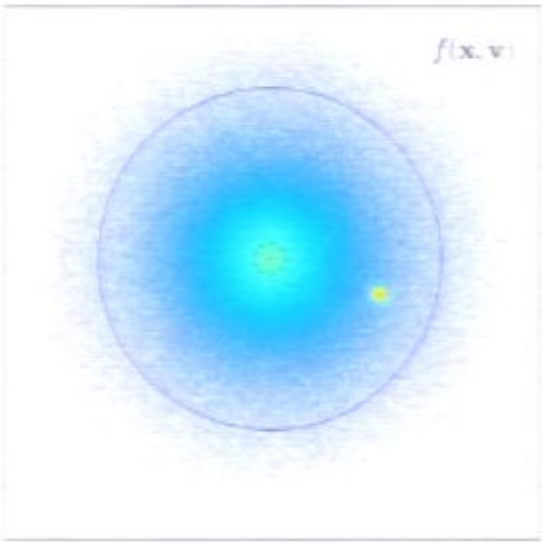
$f(\mathbf{x}, \mathbf{v})$

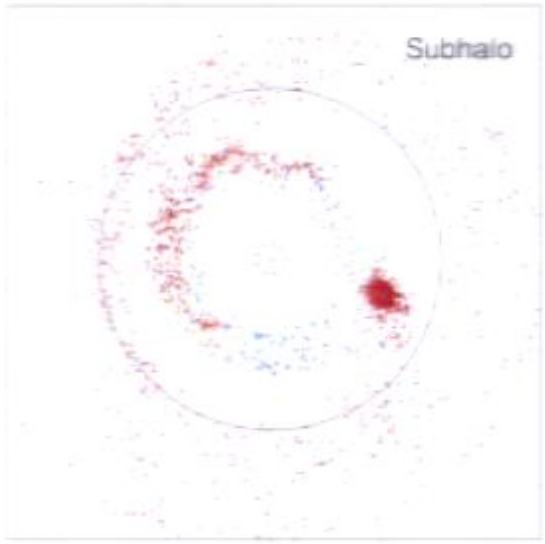
Subhalo

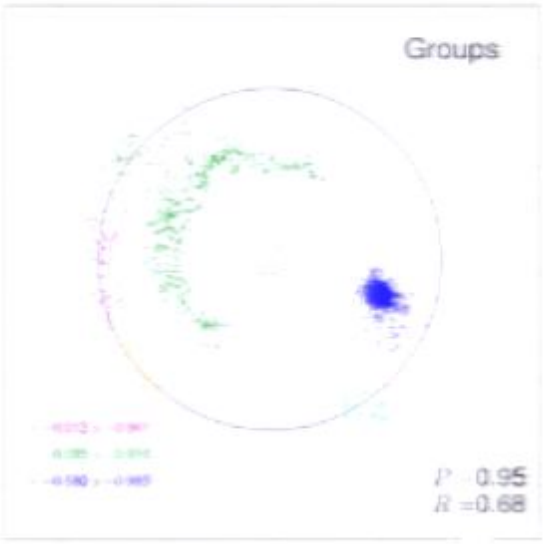
Groups
P 0.95
R =0.68

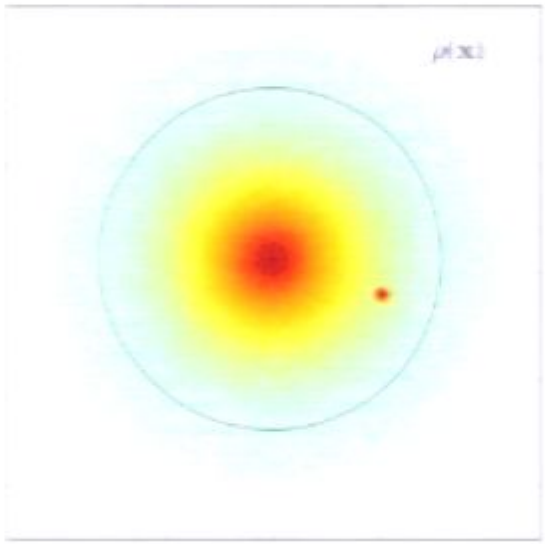
$\rho(\mathbf{x})$

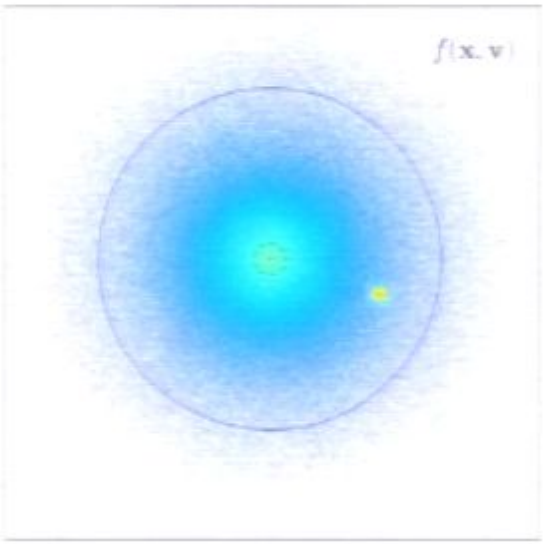
$f(\mathbf{x}, \mathbf{v})$

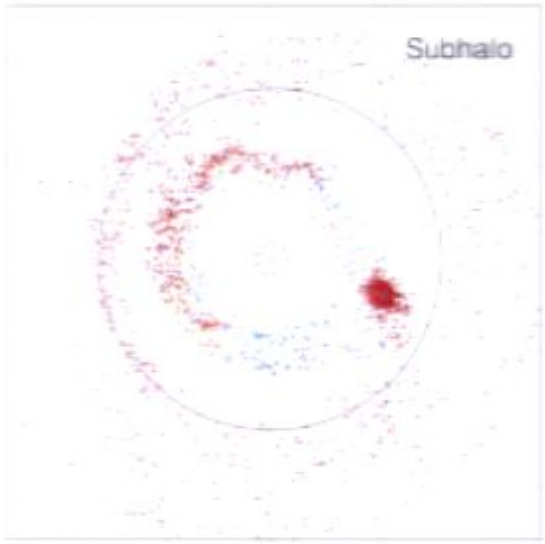
Subhalo

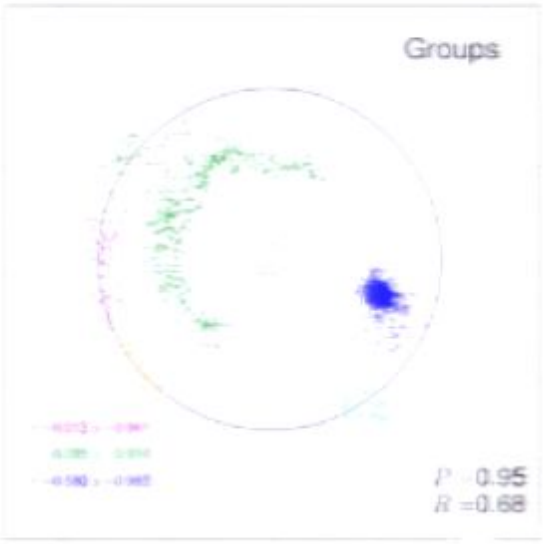
Groups
P 0.95
R =0.68

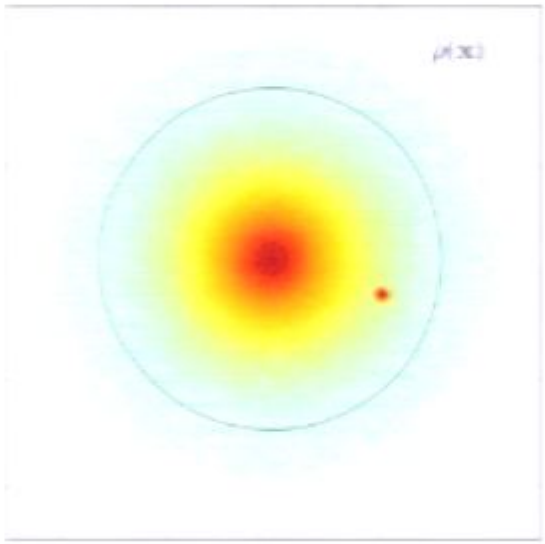
$\rho(\mathbf{x})$

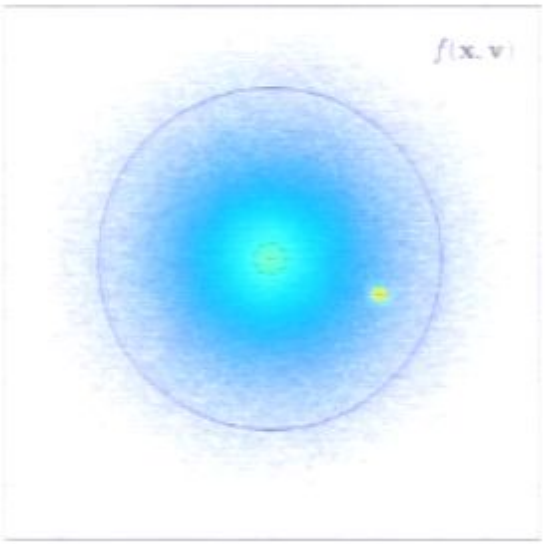
$f(\mathbf{x}, \mathbf{v})$

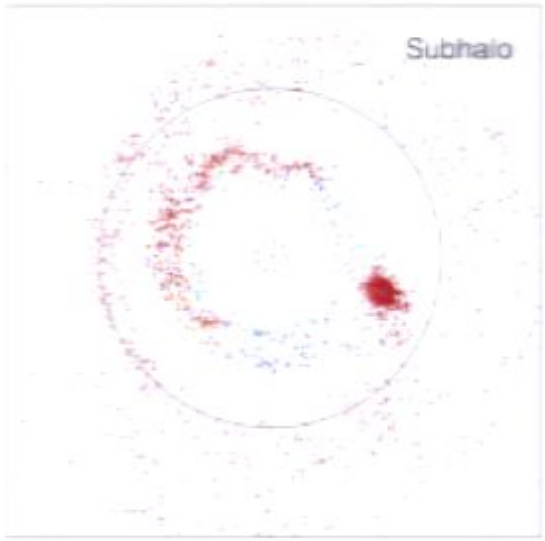
Subhalo

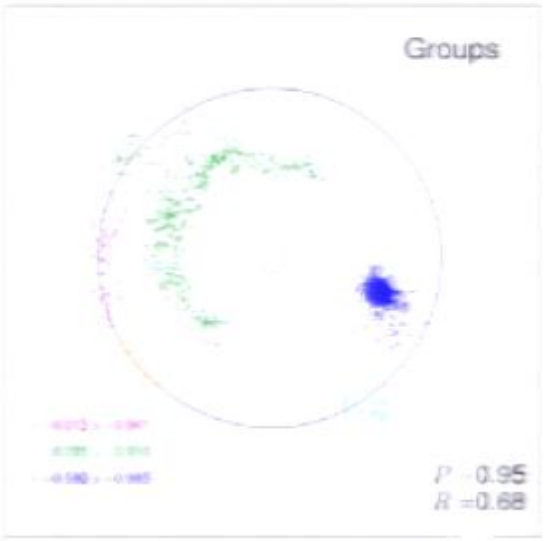
Groups
P 0.95
R =0.68

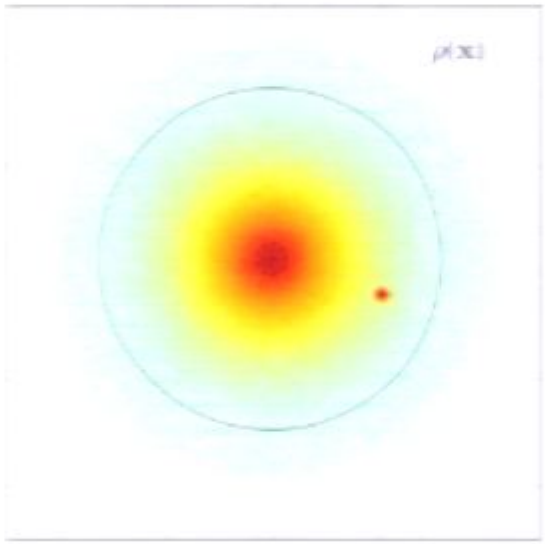
$\rho(\mathbf{x})$

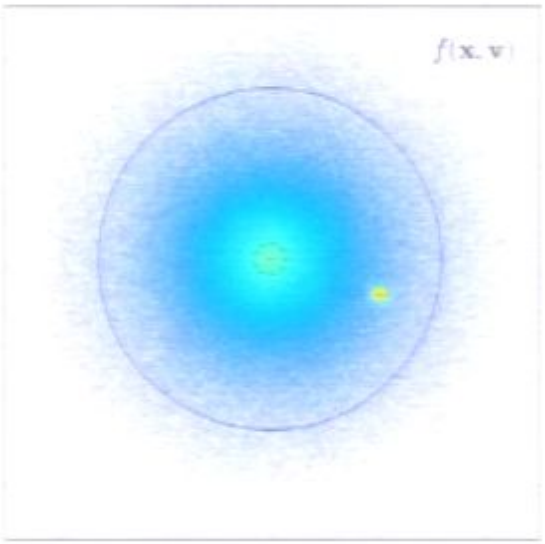
$f(\mathbf{x}, \mathbf{v})$

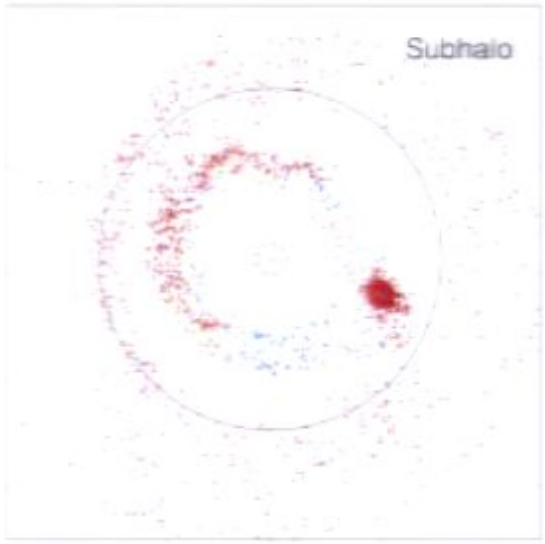
Subhalo

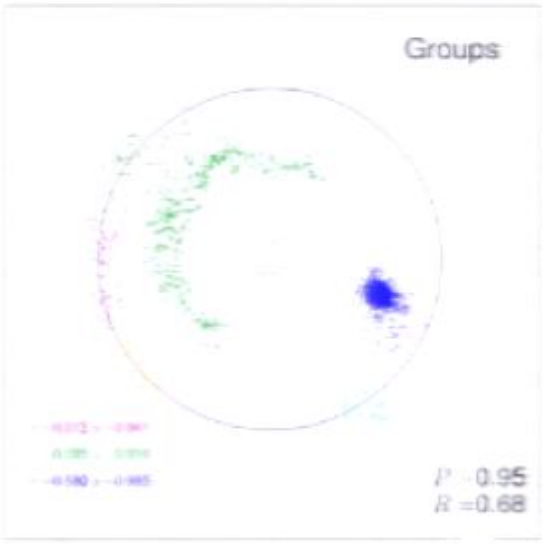
Groups
P 0.95
R =0.68

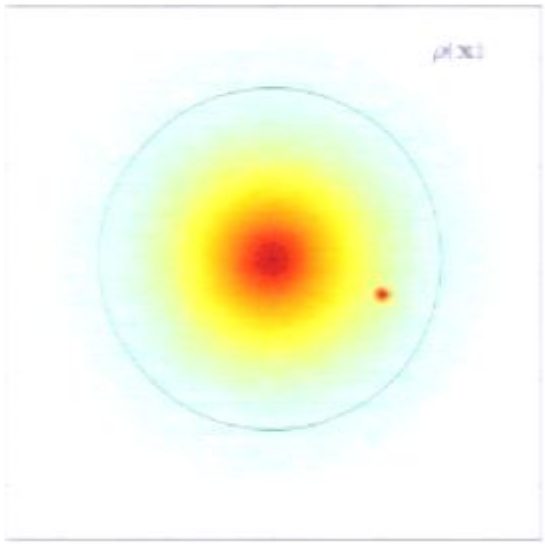
$\rho(\mathbf{x})$

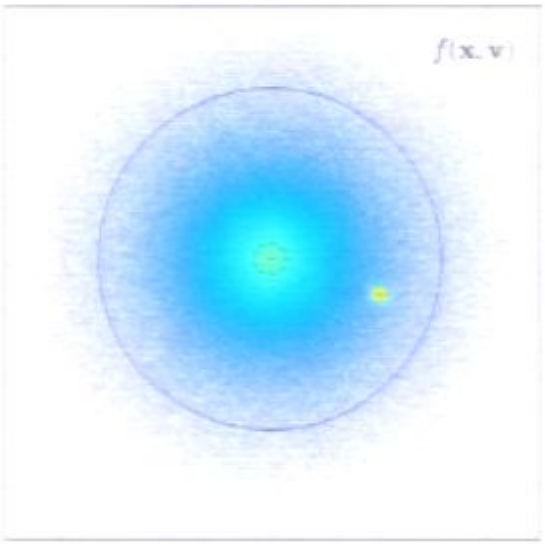
$f(\mathbf{x}, \mathbf{v})$

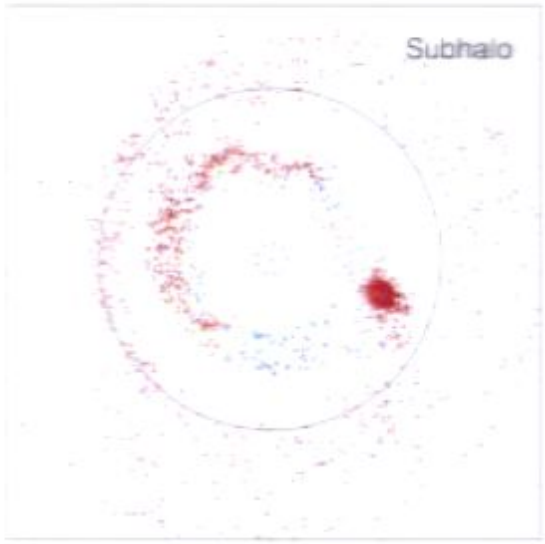
Subhalo

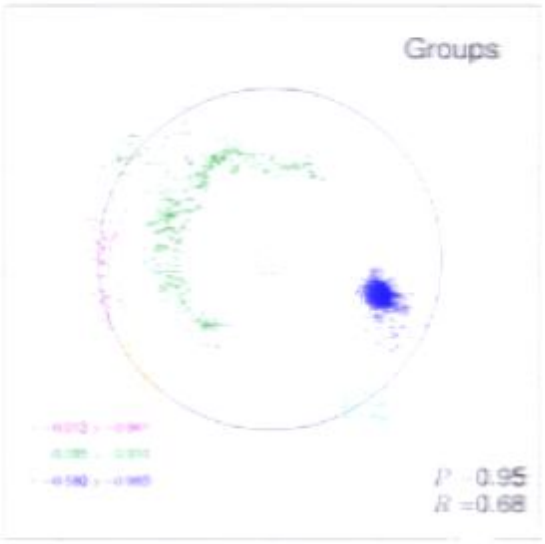
Groups
P 0.95
R =0.68

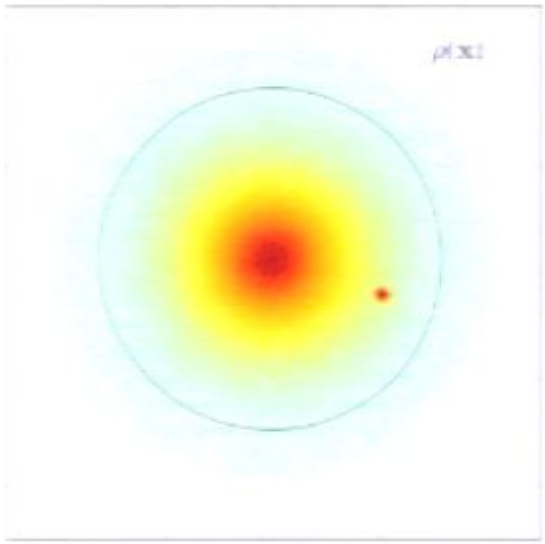
$\rho(\mathbf{x})$

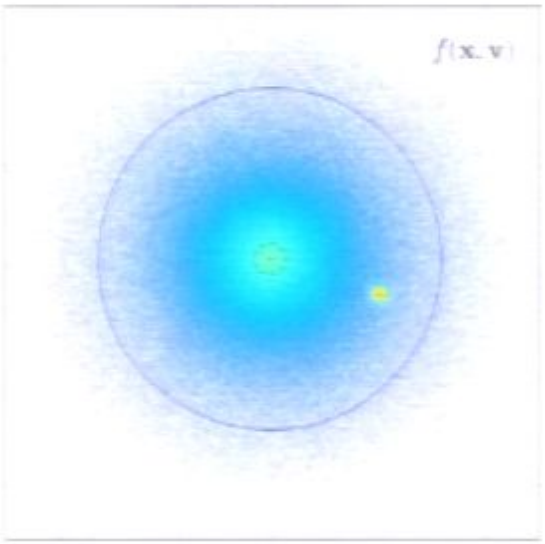
$f(\mathbf{x}, \mathbf{v})$

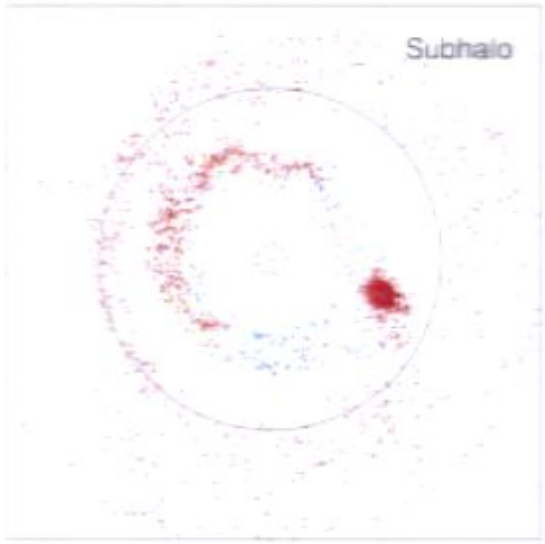
Subhalo

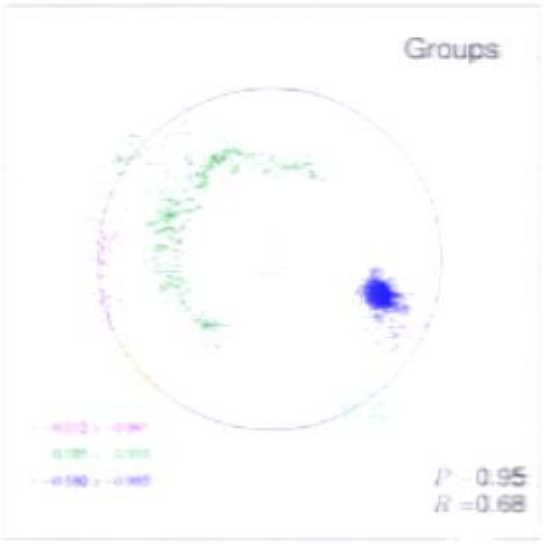
Groups
P 0.95
R =0.68

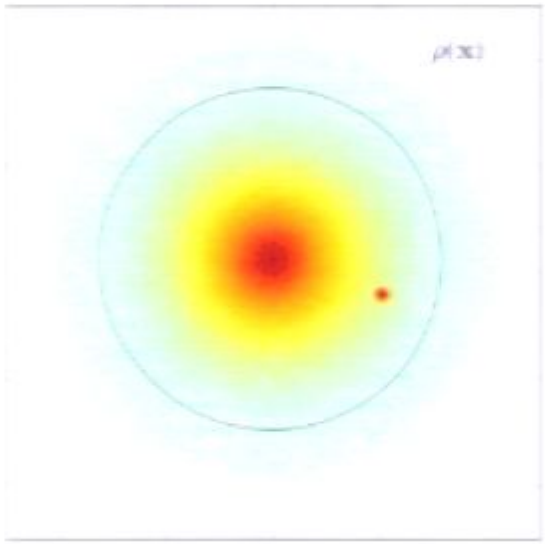
$\rho(\mathbf{x})$

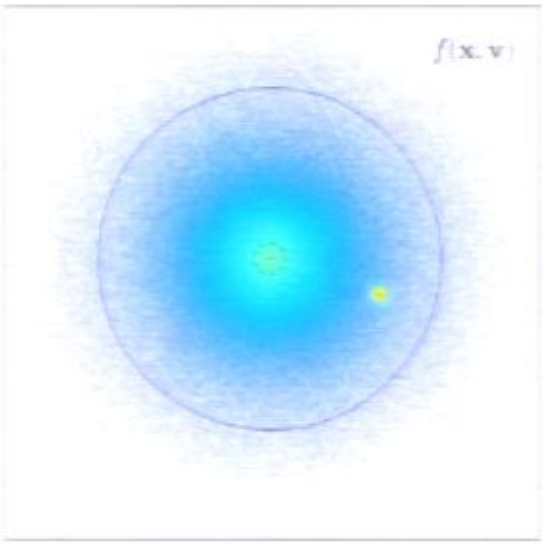
$f(\mathbf{x}, \mathbf{v})$

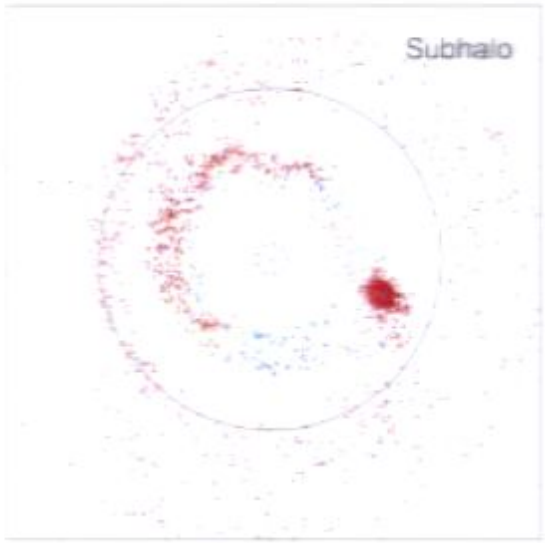
Subhalo

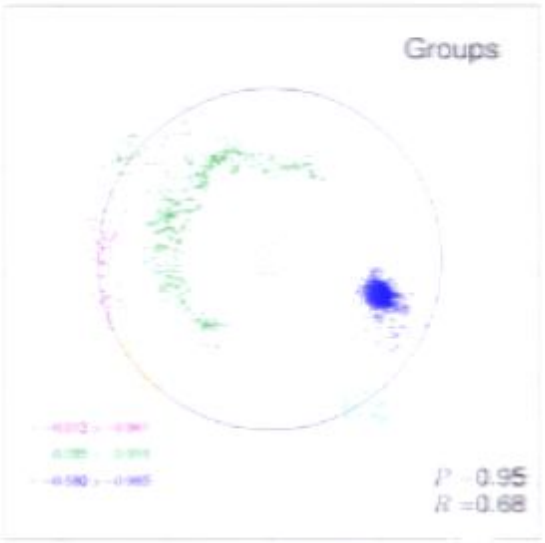
Groups
P =0.95
R =0.68

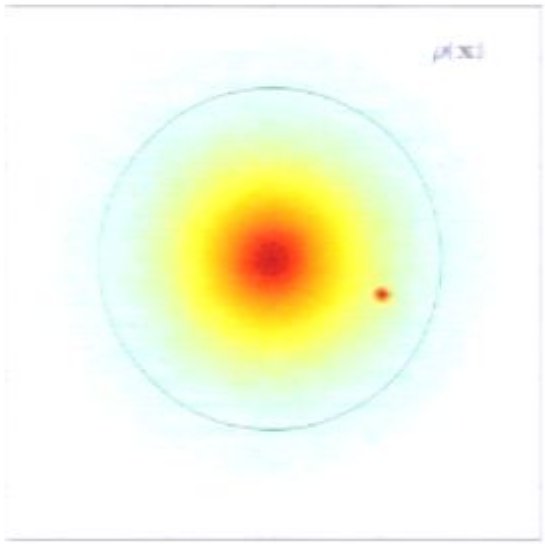
$\rho(\mathbf{x})$

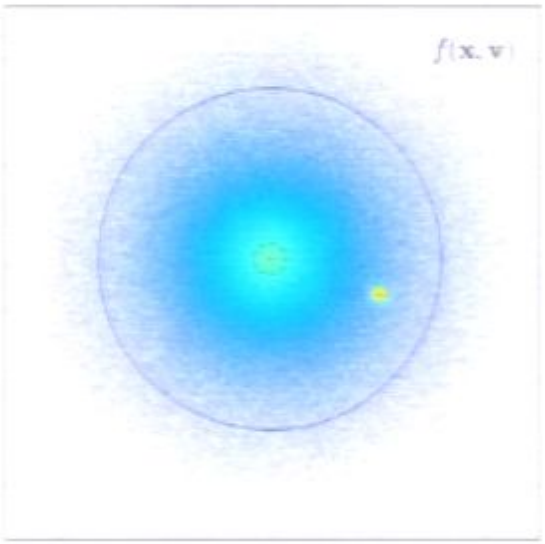
$f(\mathbf{x}, \mathbf{v})$

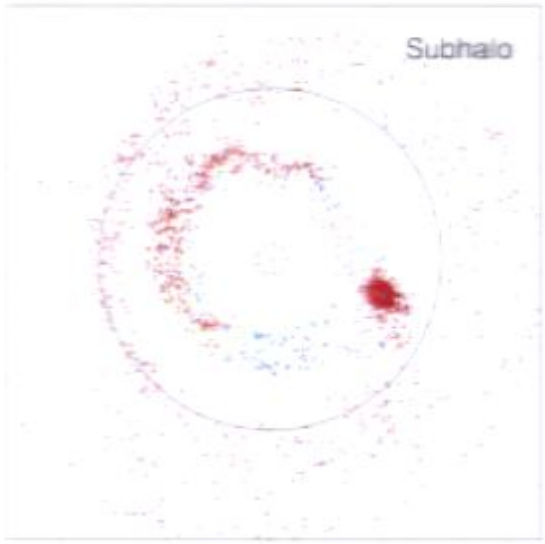
Subhalo

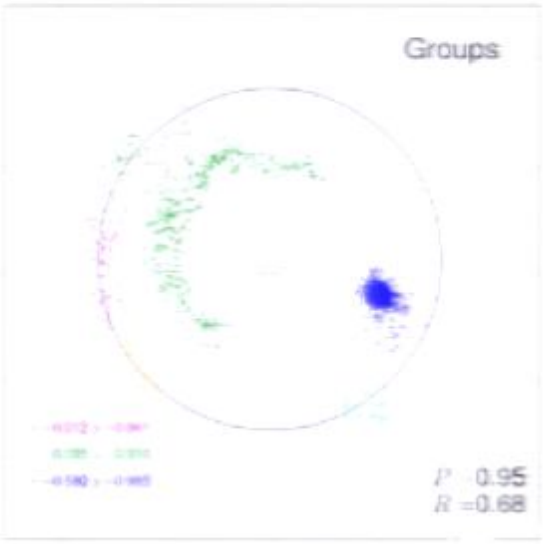
Groups
P 0.95
R =0.68

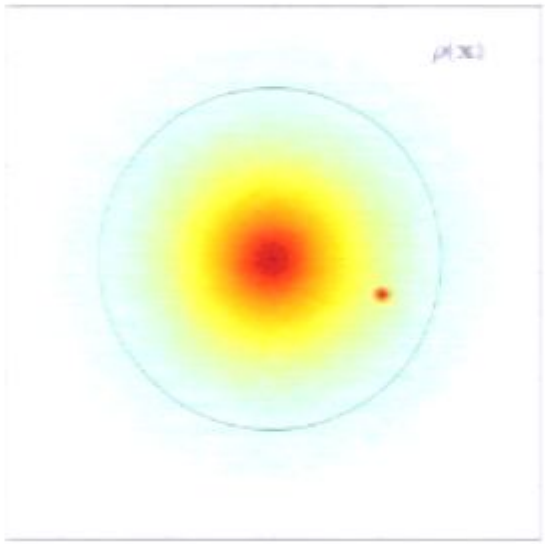
$\rho(\mathbf{x})$

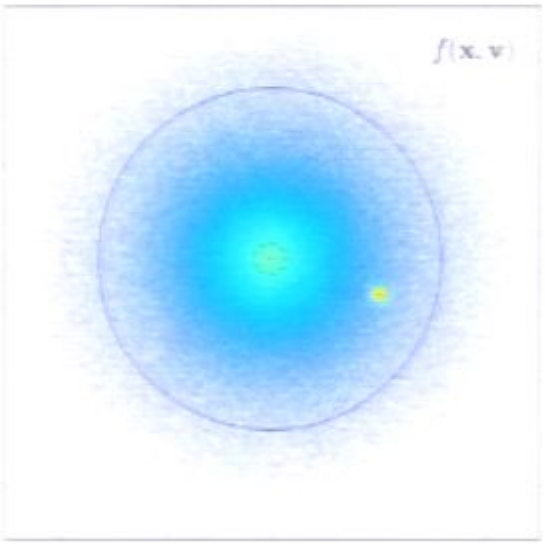
$f(\mathbf{x}, \mathbf{v})$

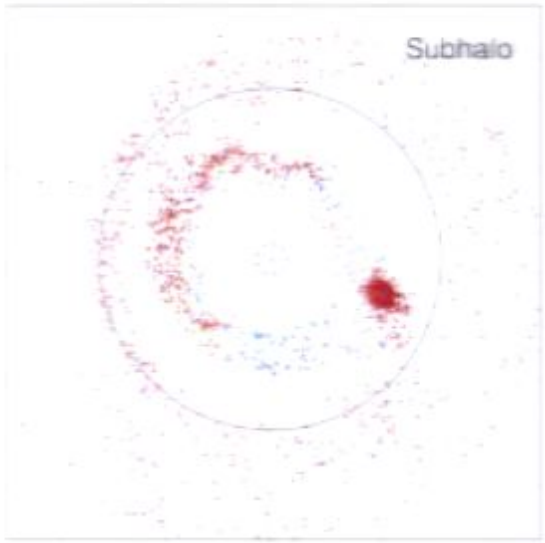
Subhalo

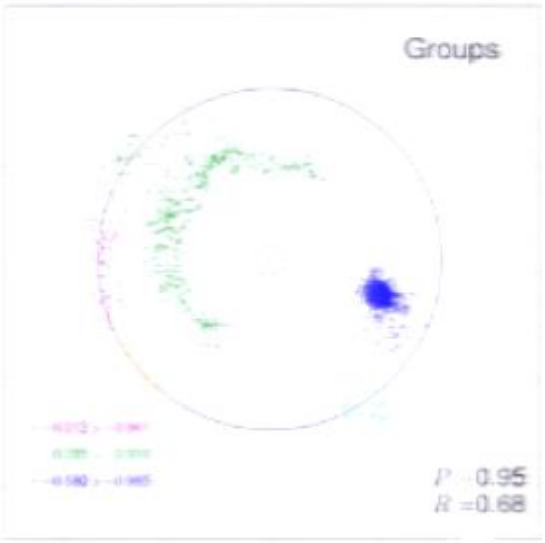
Groups
P 0.95
R =0.68

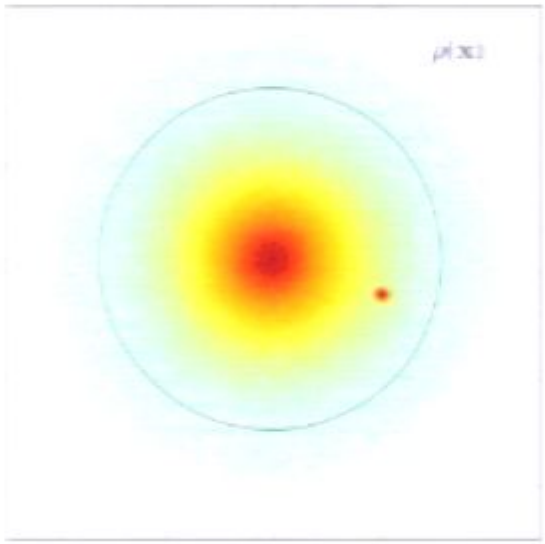
$\rho(\mathbf{x})$

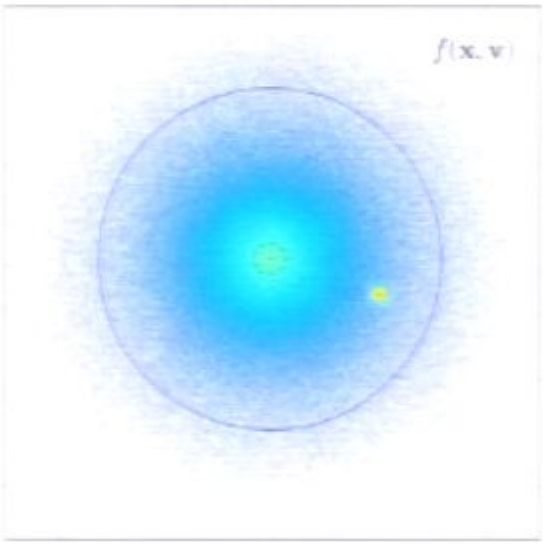
$f(\mathbf{x}, \mathbf{v})$

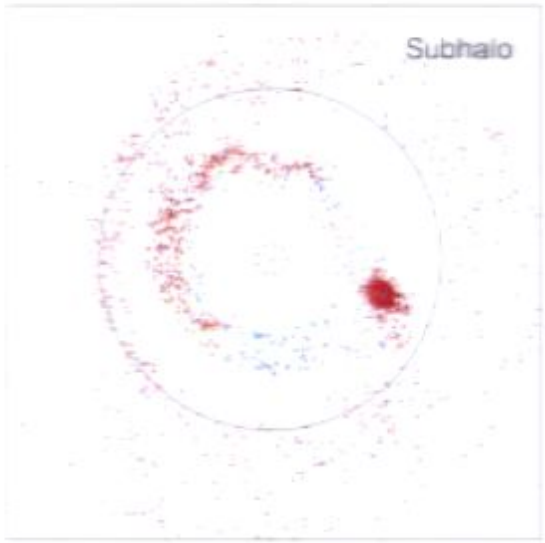
Subhalo

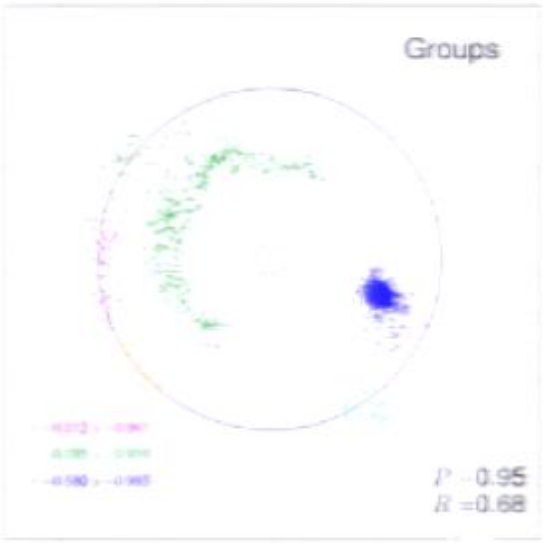
Groups
P =0.95
R =0.68

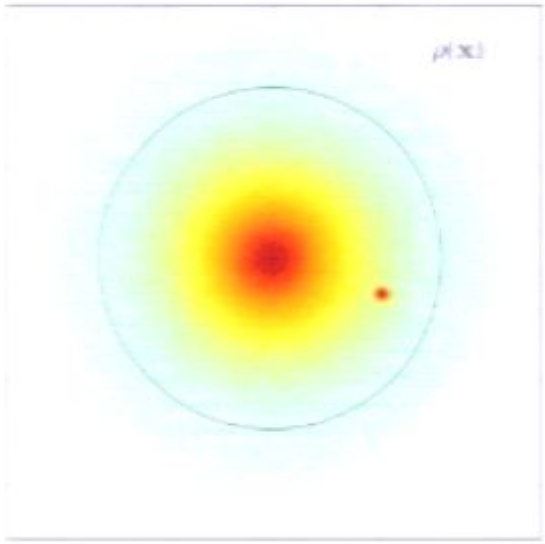
$\rho(\mathbf{x})$

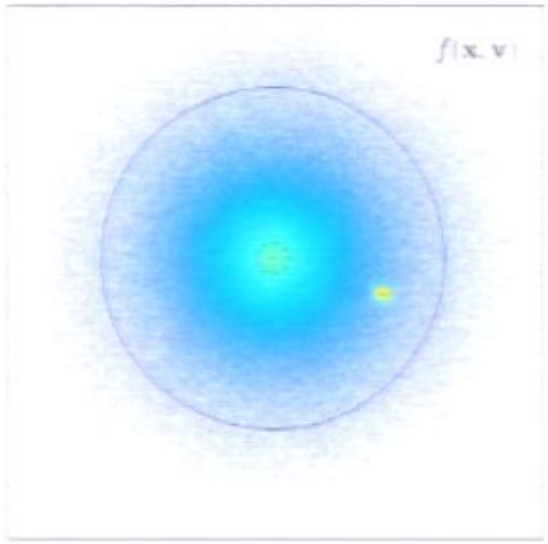
$f(\mathbf{x}, \mathbf{v})$

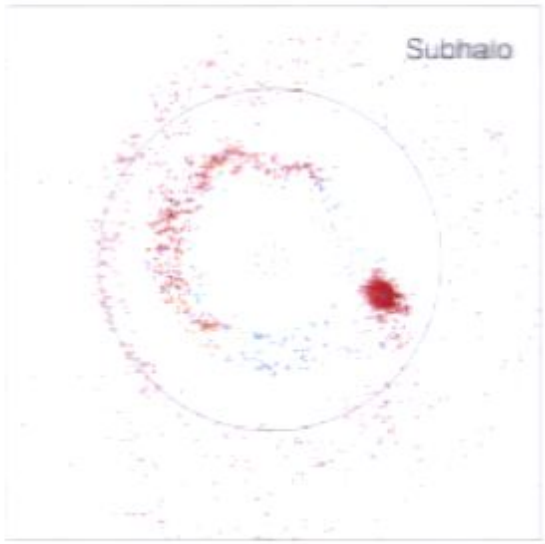
Subhalo

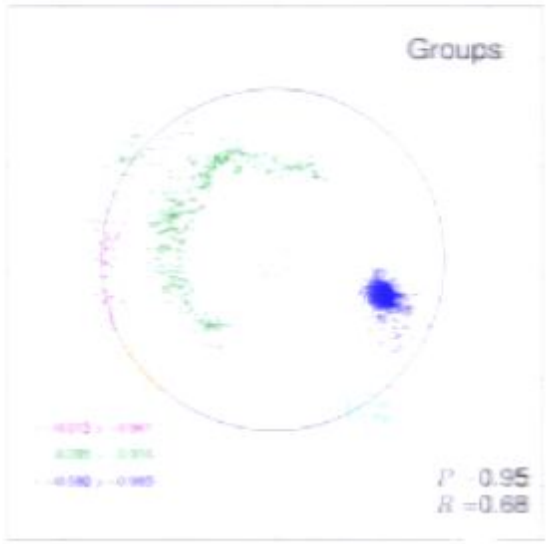
Groups
P 0.95
R =0.68

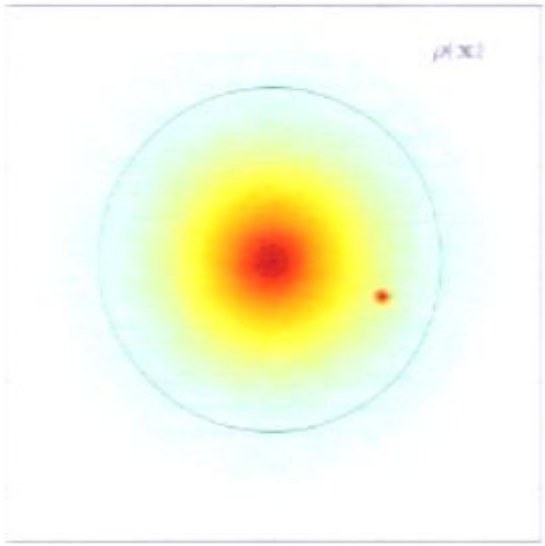
ρ(x)

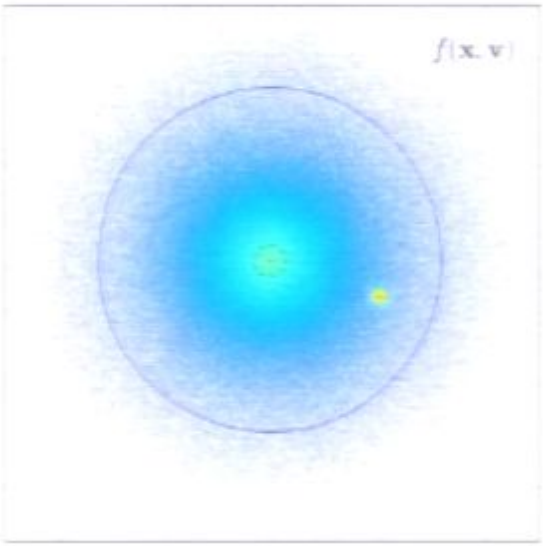
f(x, v)

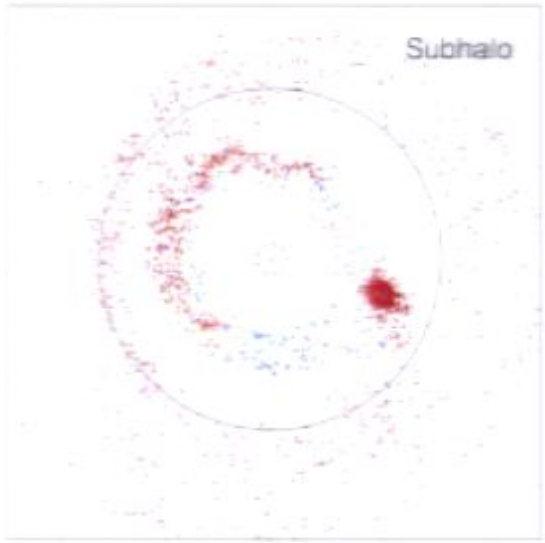
Subhalo

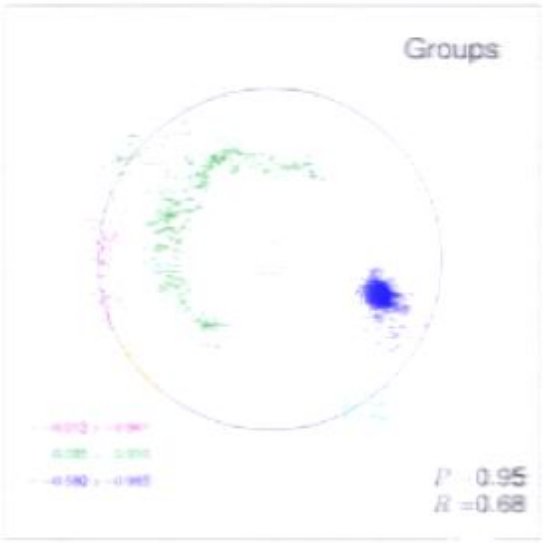
Groups
P 0.95
R =0.68

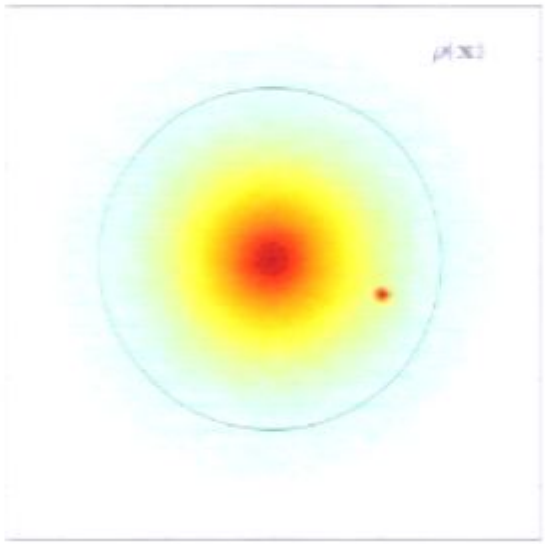
$\rho(\mathbf{x})$

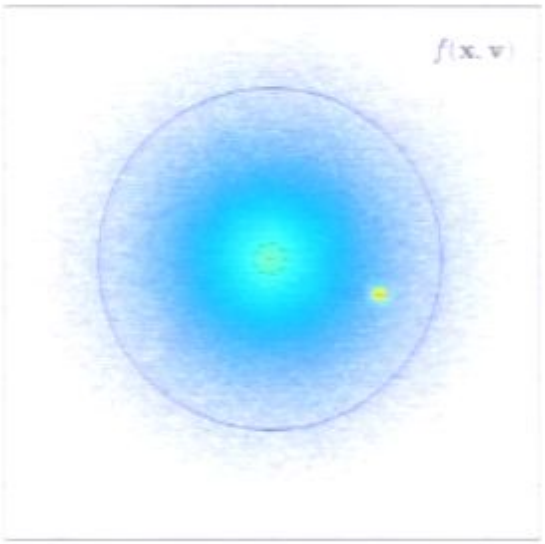
$f(\mathbf{x}, \mathbf{v})$

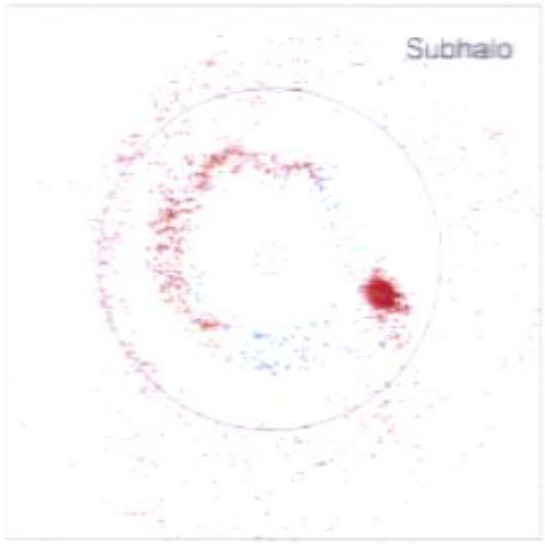
Subhalo

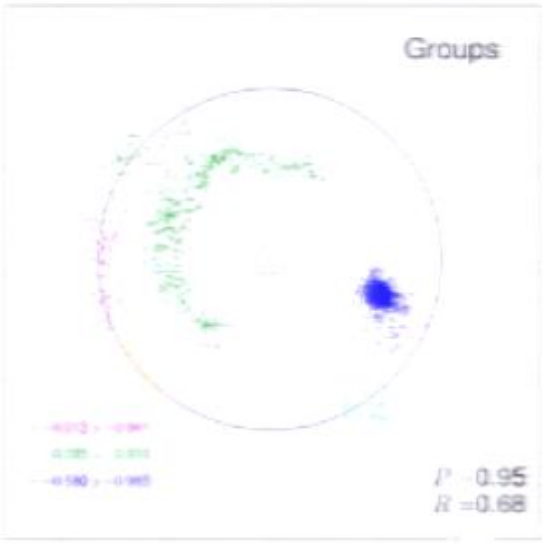
Groups
P 0.95
R =0.68

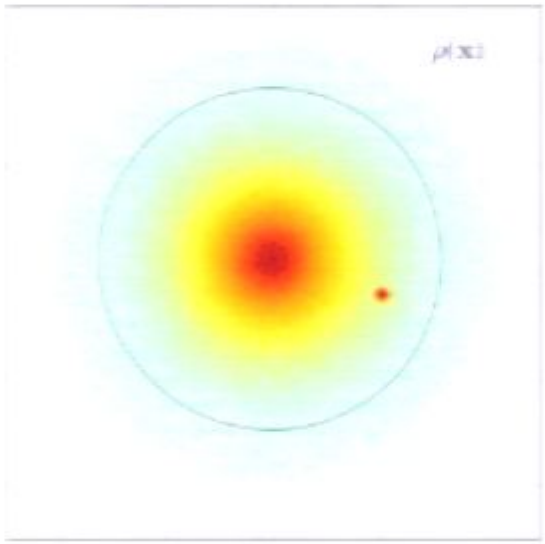
$\rho(\mathbf{x})$

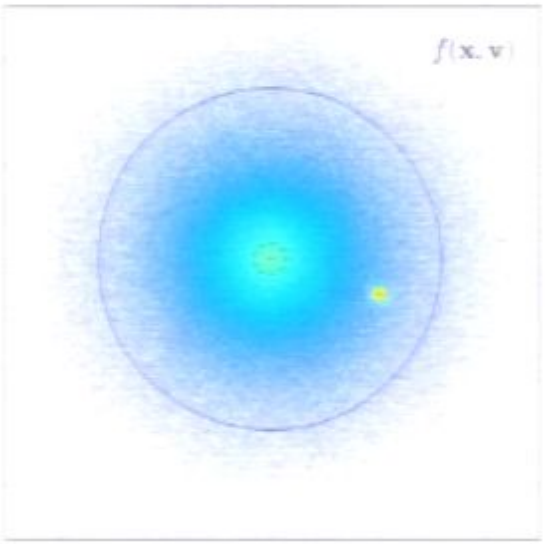
$f(\mathbf{x}, \mathbf{v})$

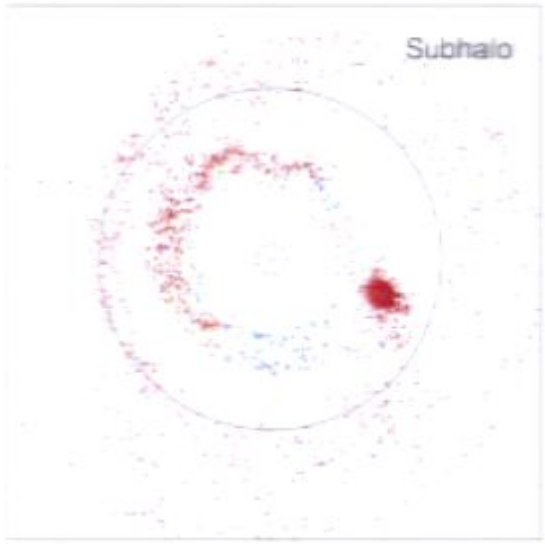
Subhalo

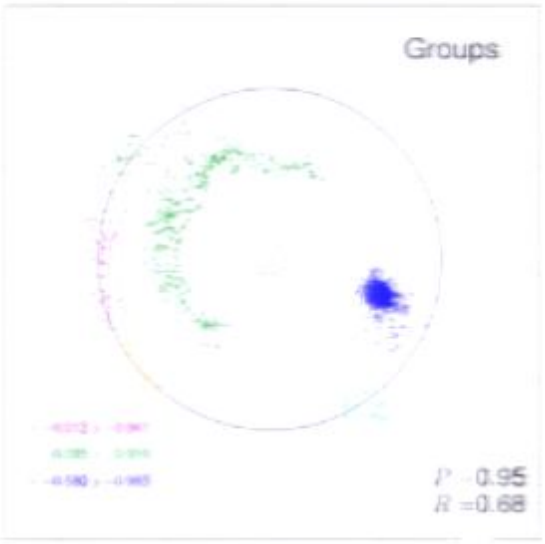
Groups
P =0.95
R =0.68

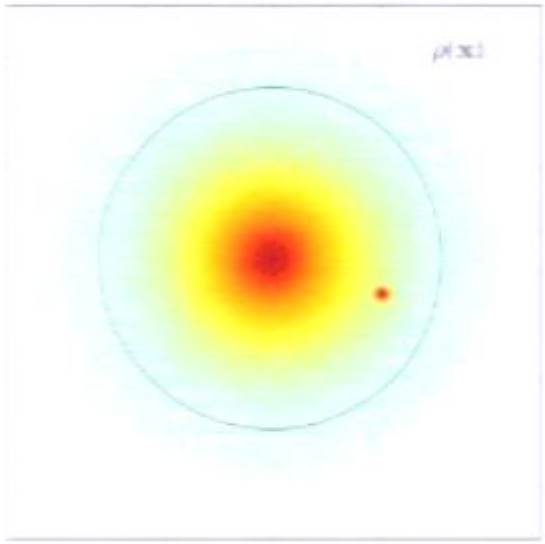
$\rho(\mathbf{x})$

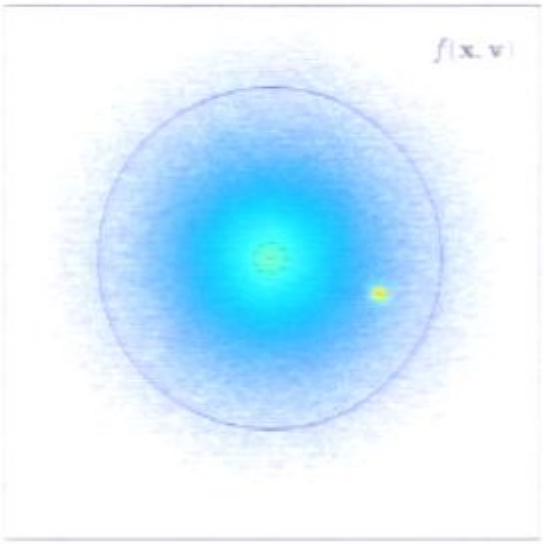
$f(\mathbf{x}, \mathbf{v})$

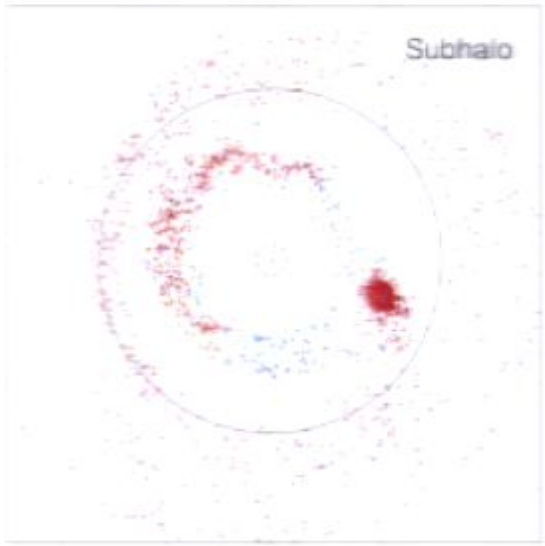
Subhalo

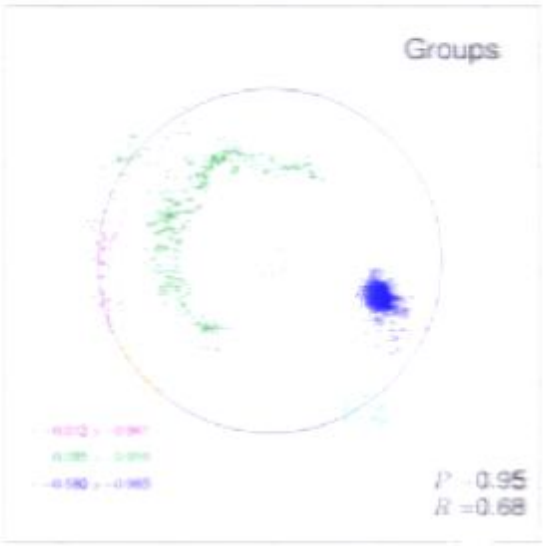
Groups
P 0.95
R =0.68

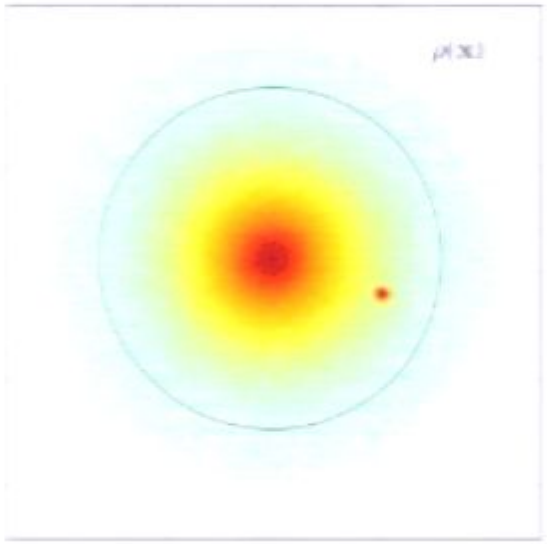
$\rho(\mathbf{x})$

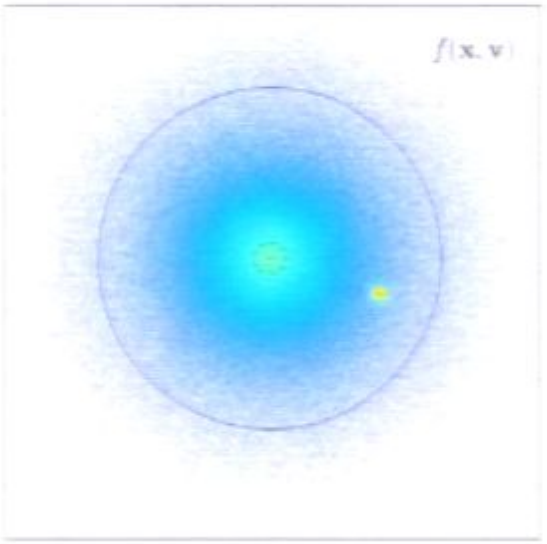
$f(\mathbf{x}, \mathbf{v})$

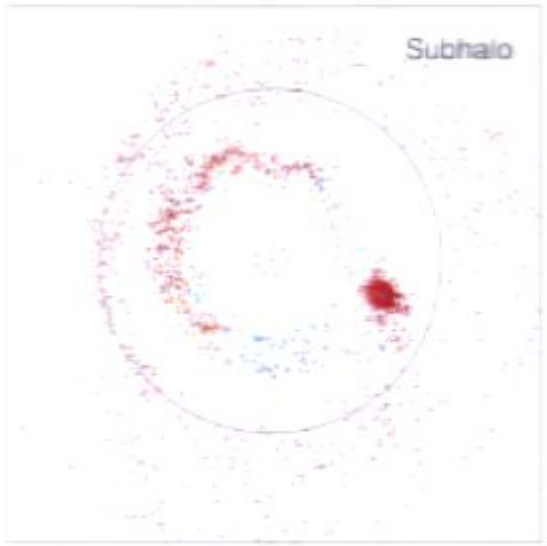
Subhalo

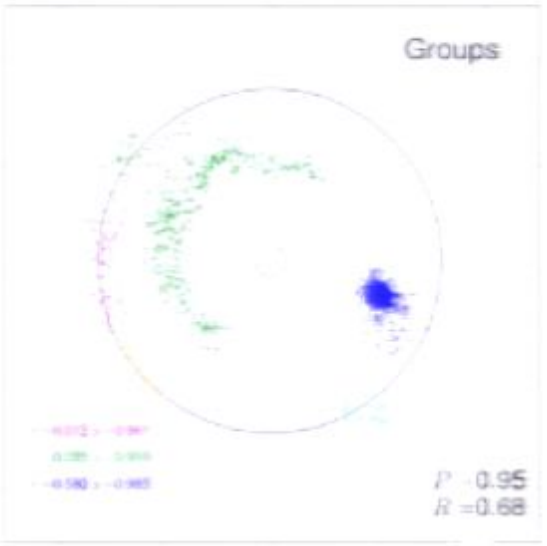
Groups
P 0.95
R =0.68

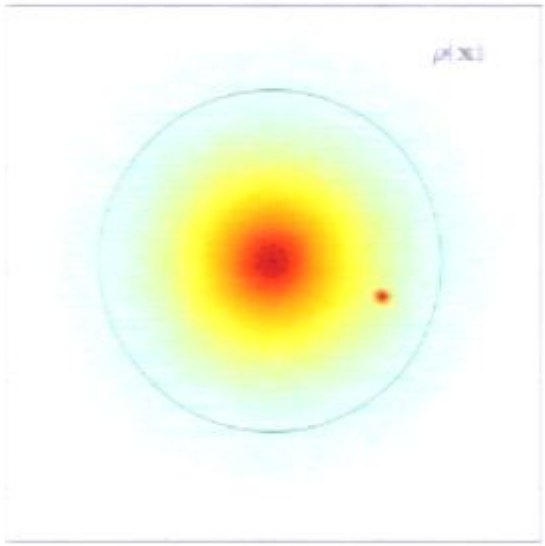
$\rho(\mathbf{x})$

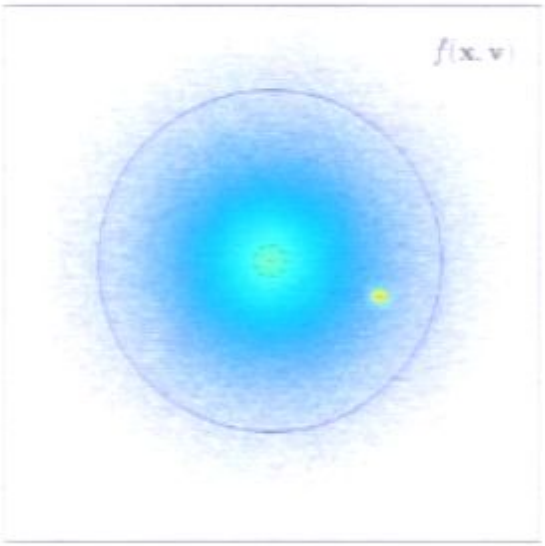
$f(\mathbf{x}, \mathbf{v})$

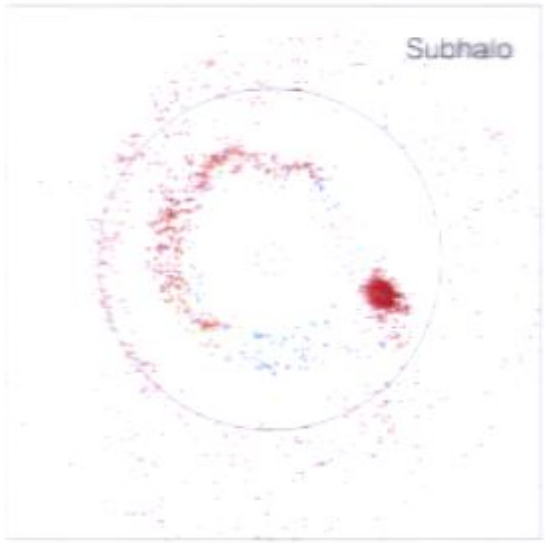
Subhalo

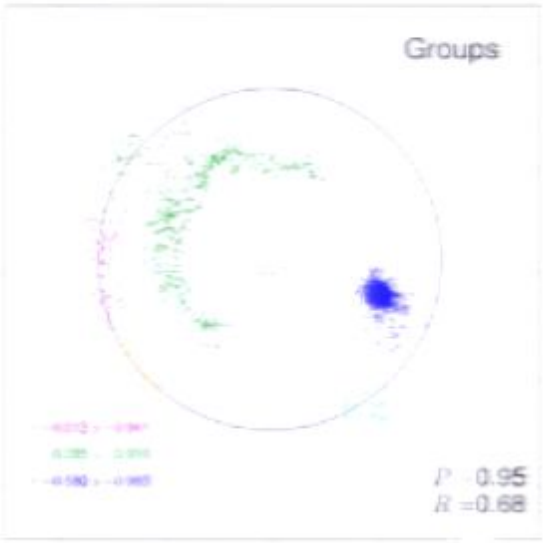
Groups
P 0.95
R =0.68

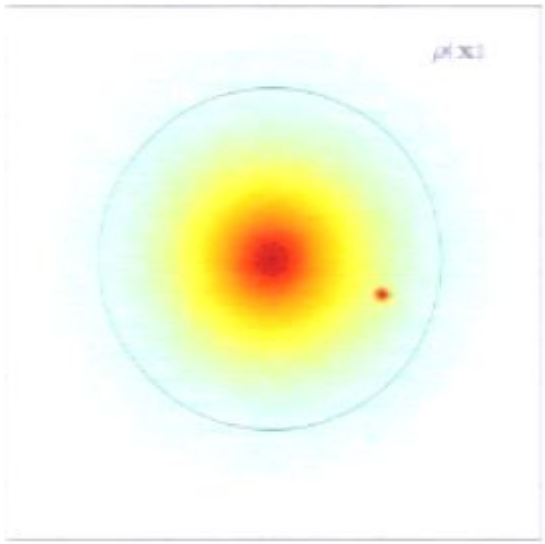
$\rho(\mathbf{x})$

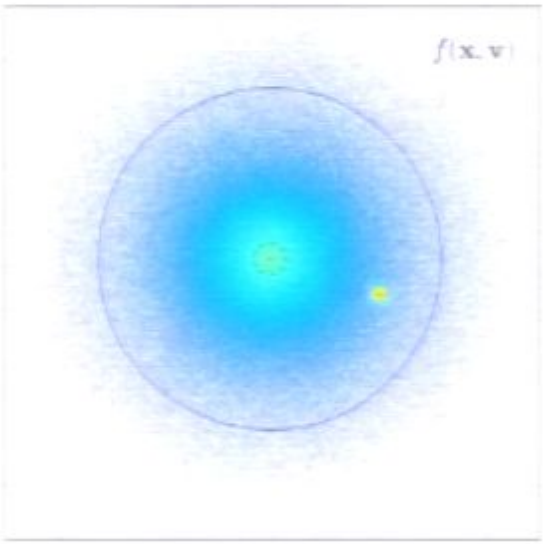
$f(\mathbf{x}, \mathbf{v})$

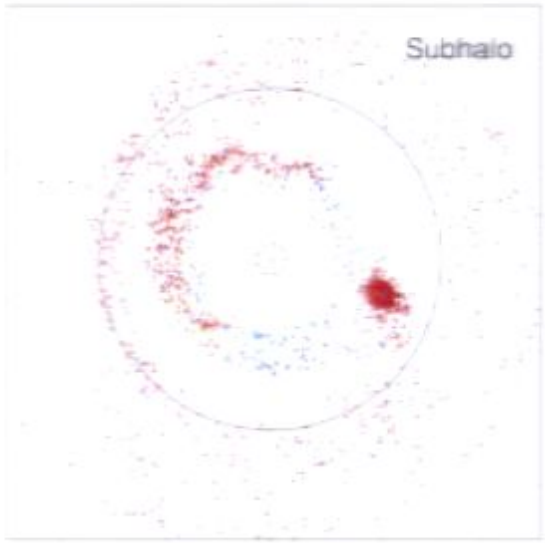
Subhalo

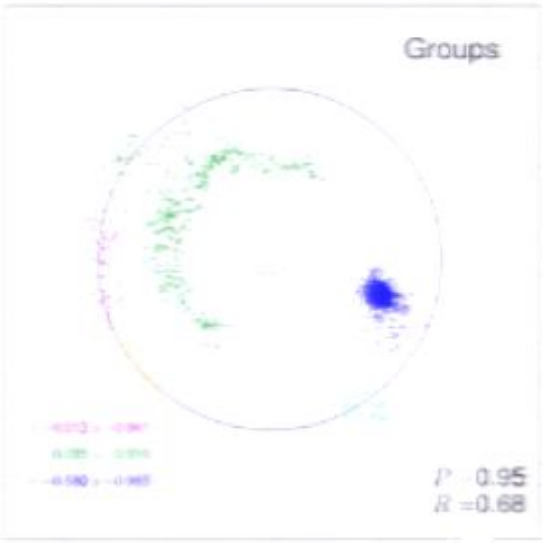
Groups
P 0.95
R =0.68

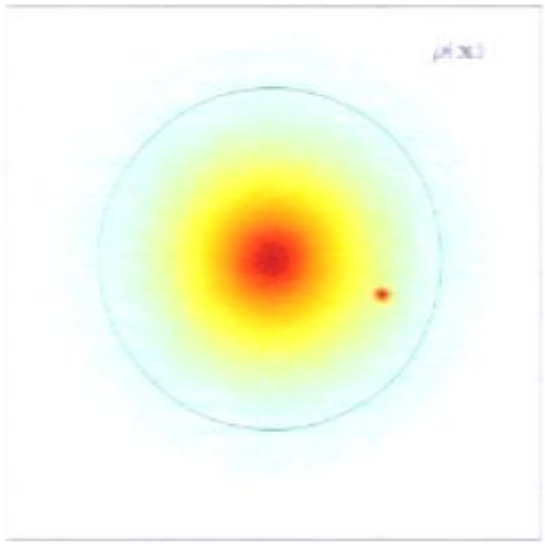
$\rho(\mathbf{x})$

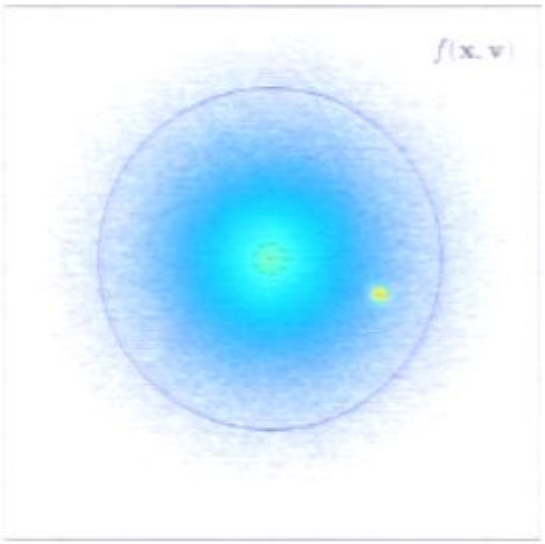
$f(\mathbf{x}, \mathbf{v})$

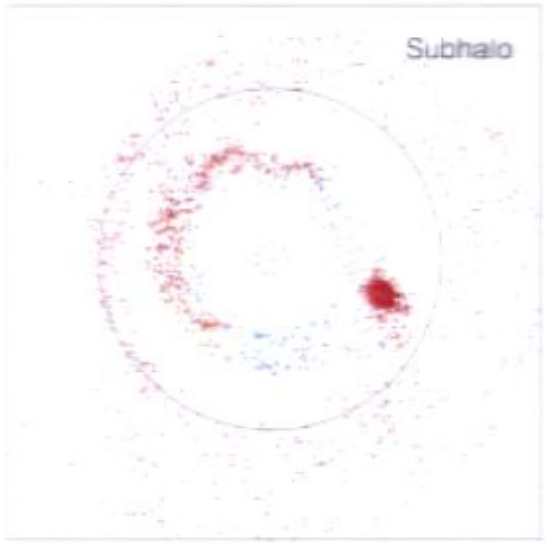
Subhalo

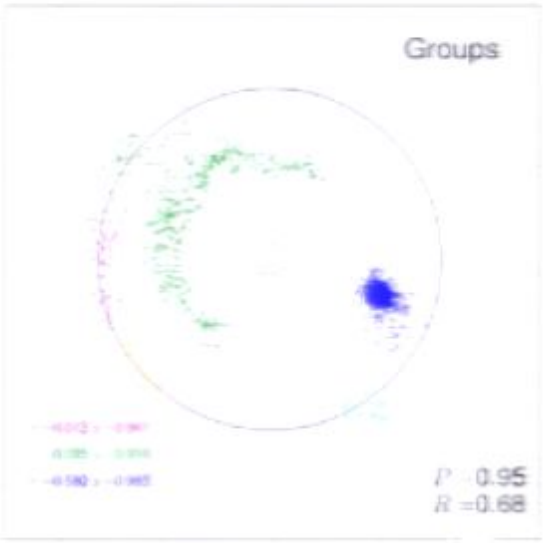
Groups
P 0.95
R =0.68

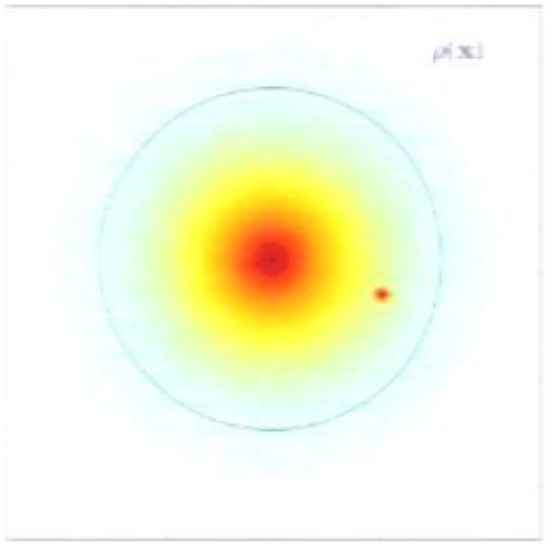
$\rho(\mathbf{x})$

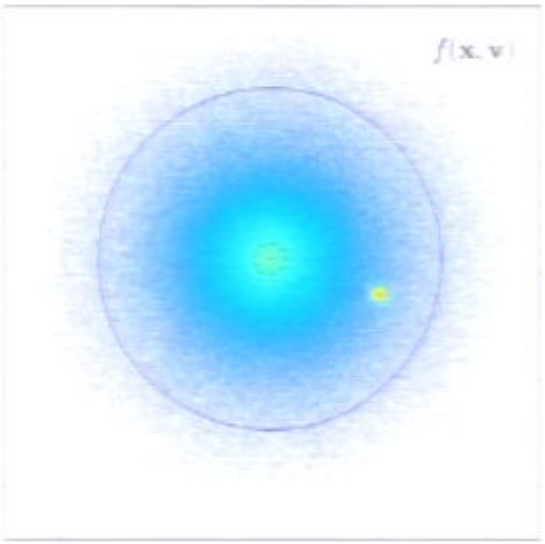
$f(\mathbf{x}, \mathbf{v})$

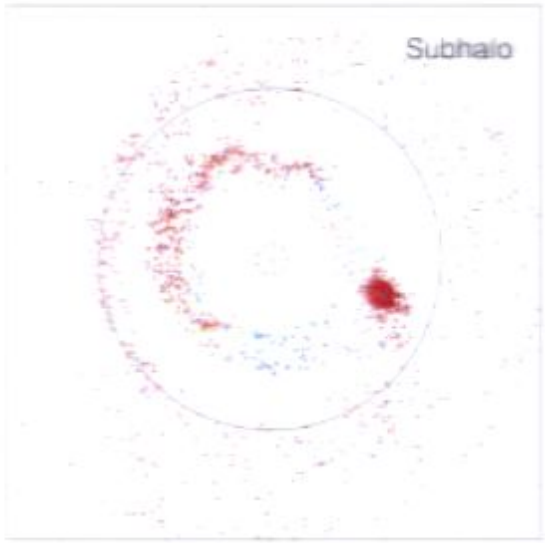
Subhalo

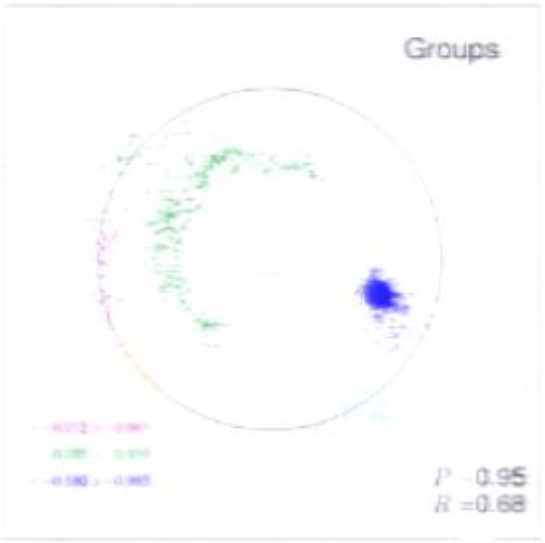
Groups
P 0.95
R =0.68

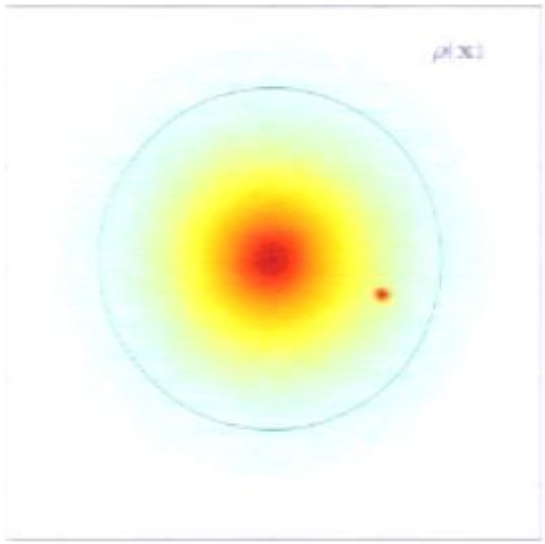
$\rho(\mathbf{x})$

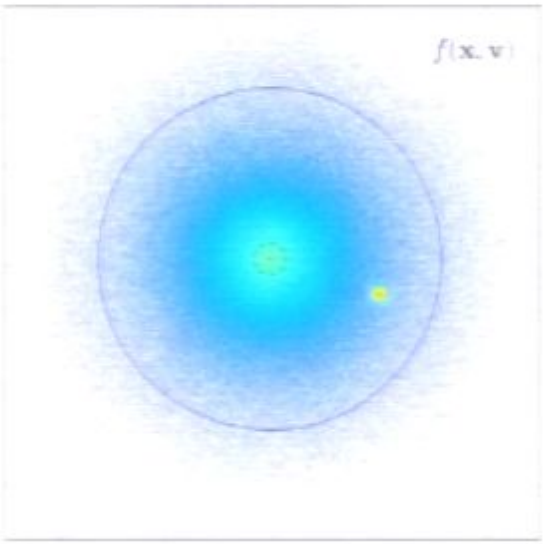
$f(\mathbf{x}, \mathbf{v})$

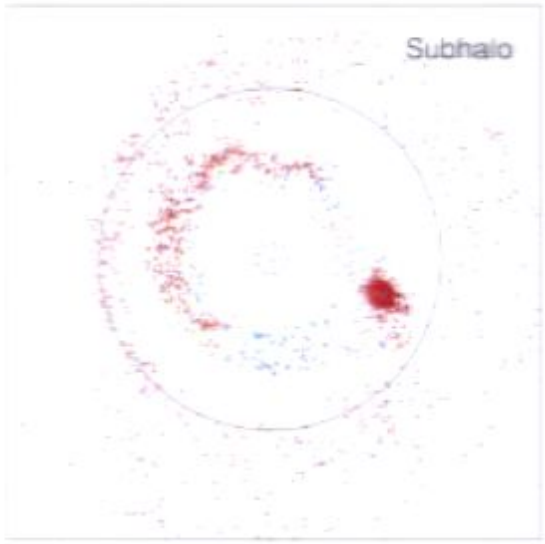
Subhalo

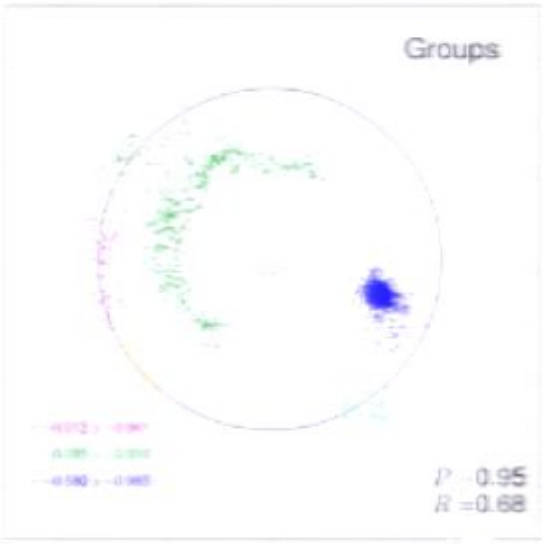
Groups
P 0.95
R =0.68

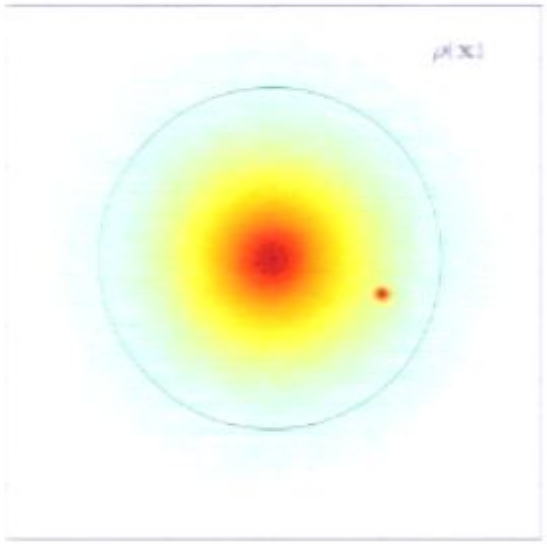
ρ(x)

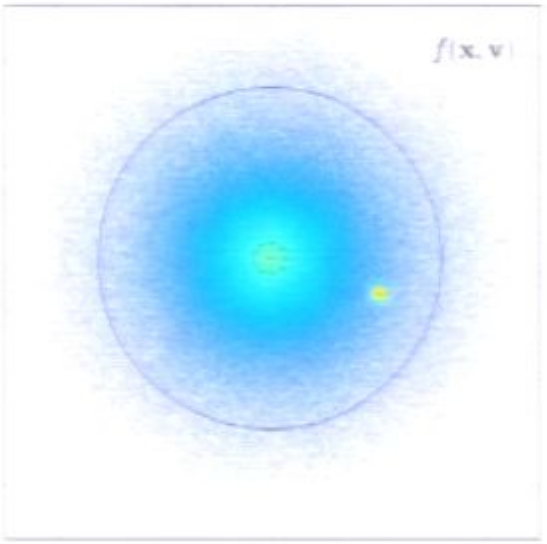
f(x, v)

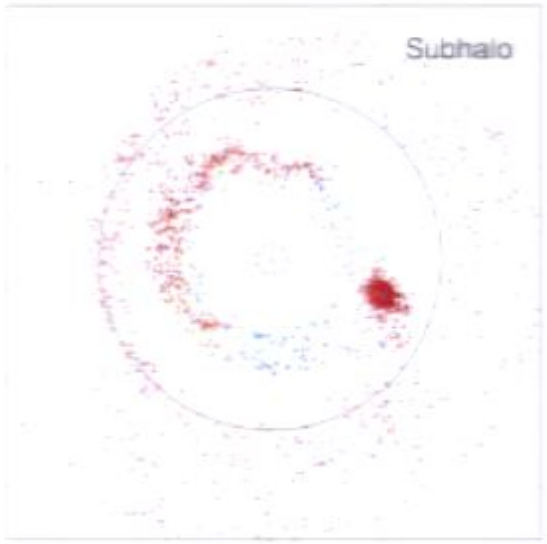
Subhalo

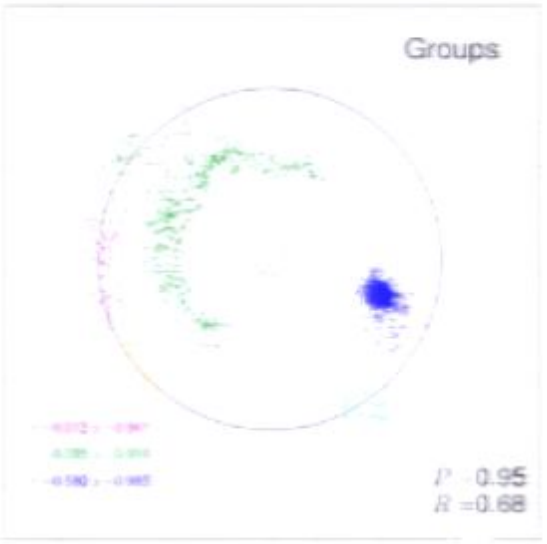
Groups
P 0.95
R =0.68

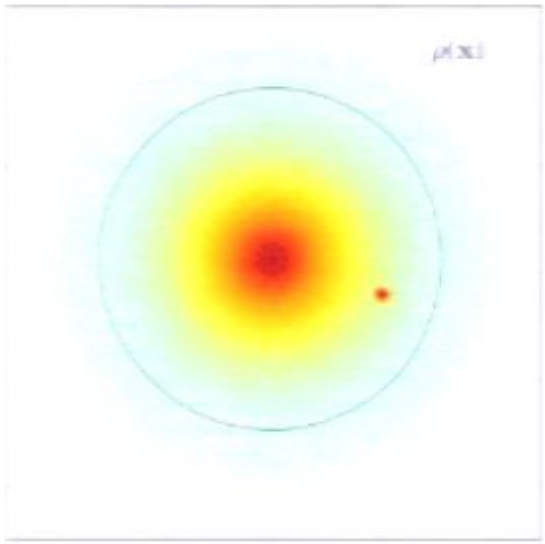
$\rho(\mathbf{x})$

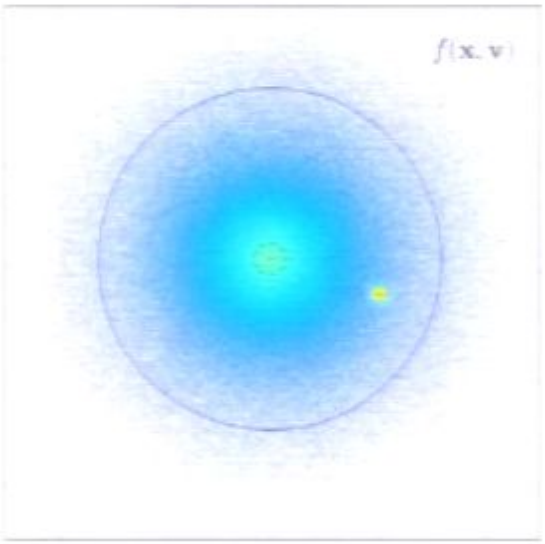
$f(\mathbf{x}, \mathbf{v})$

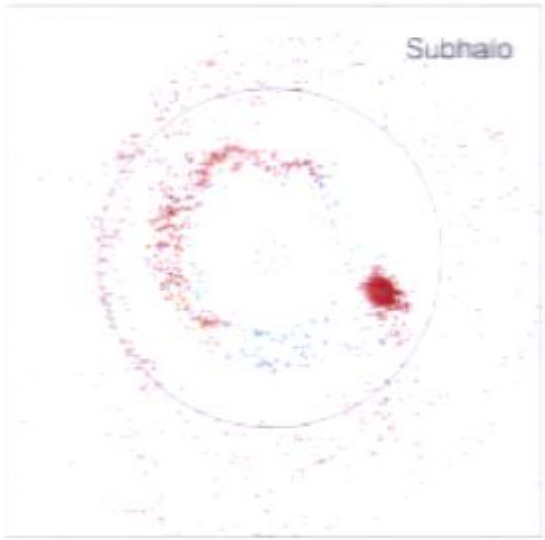
Subhalo

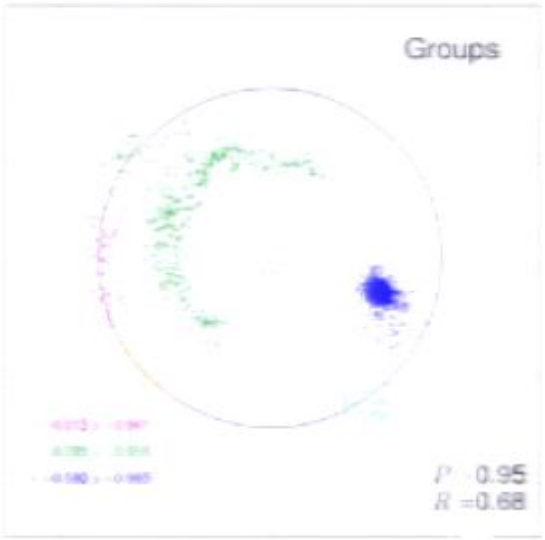
Groups
P 0.95
R =0.68

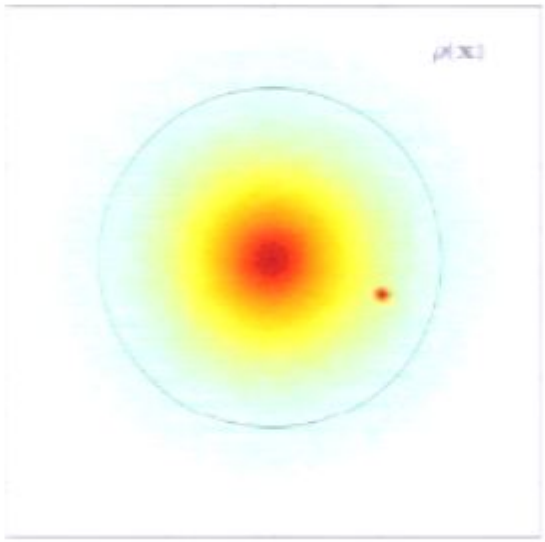
$\rho(\mathbf{x})$

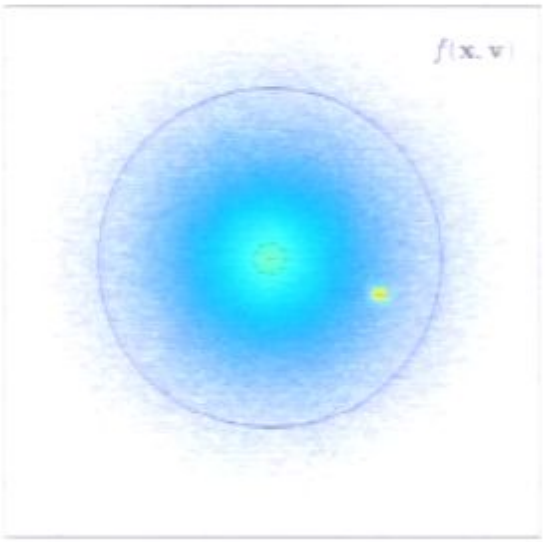
$f(\mathbf{x}, \mathbf{v})$

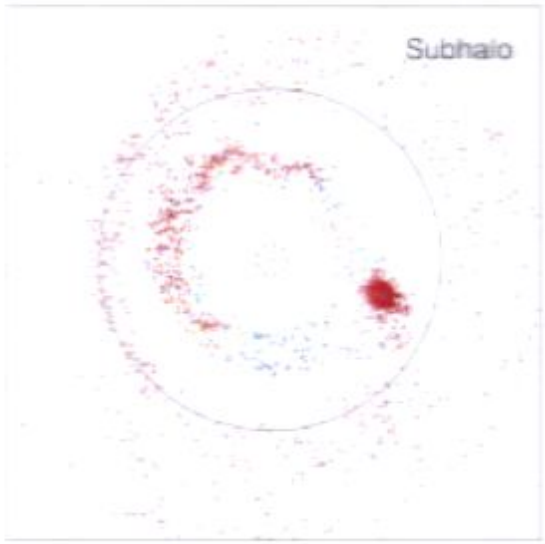
Subhalo

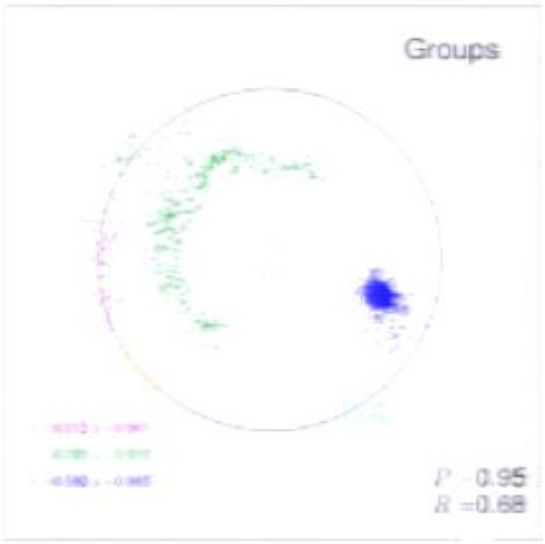
Groups
P 0.95
R =0.68

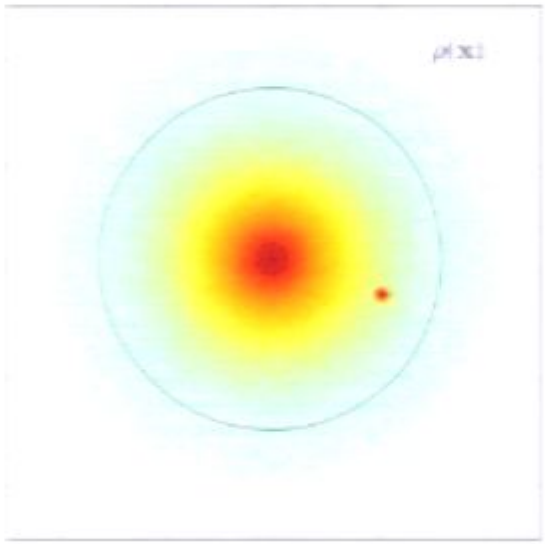
$\rho(\mathbf{x})$

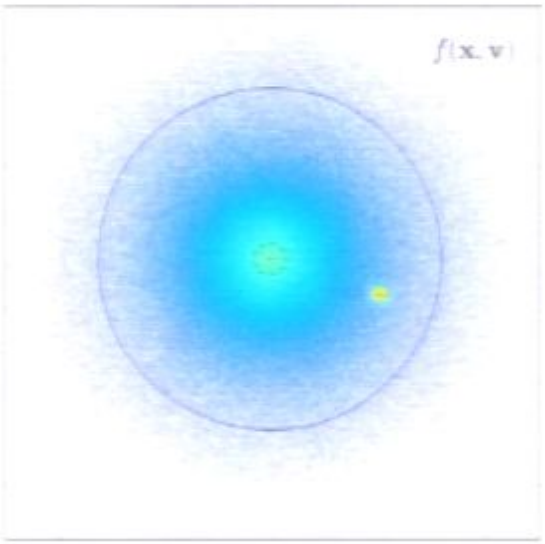
$f(\mathbf{x}, \mathbf{v})$

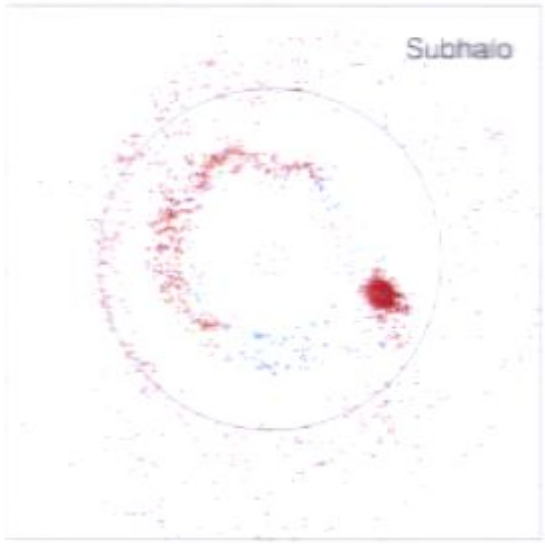
Subhalo

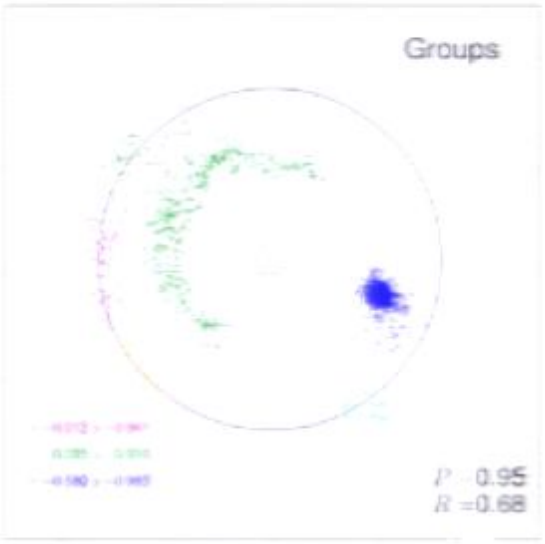
Groups
P 0.95
R =0.68

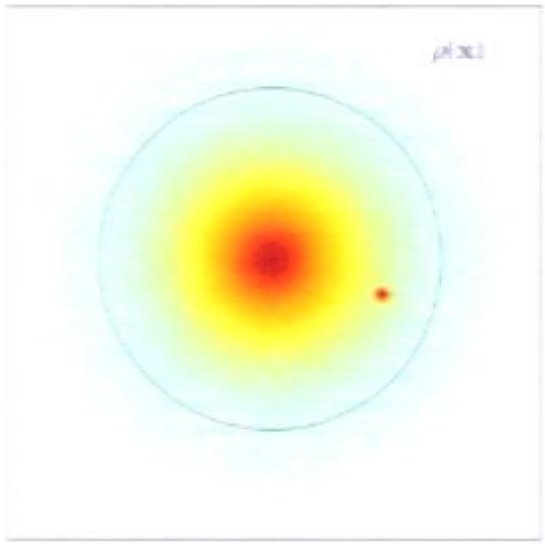
$\rho(\mathbf{x})$

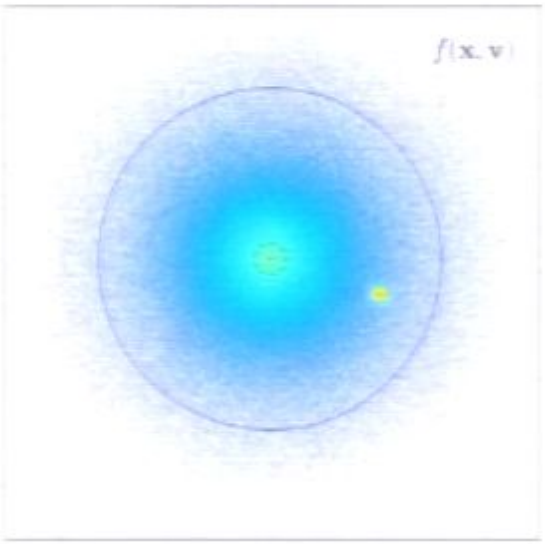
$f(\mathbf{x}, \mathbf{v})$

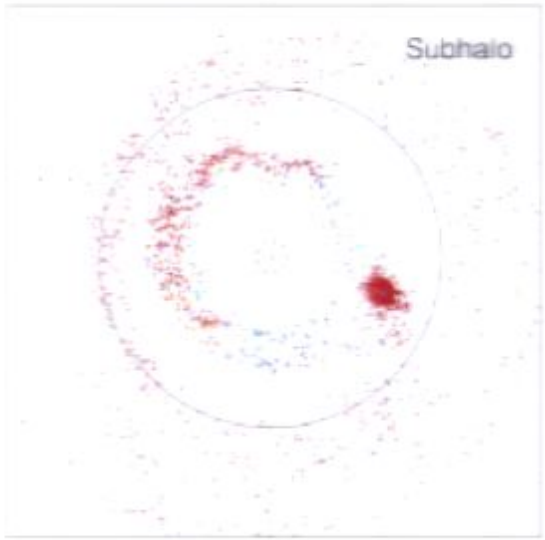
Subhalo

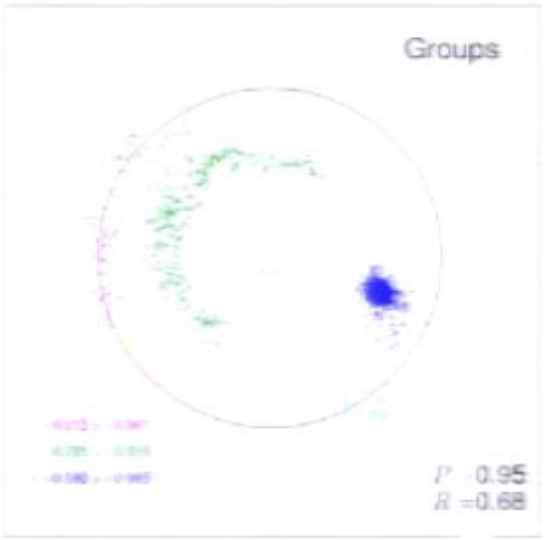
Groups
P 0.95
R =0.68

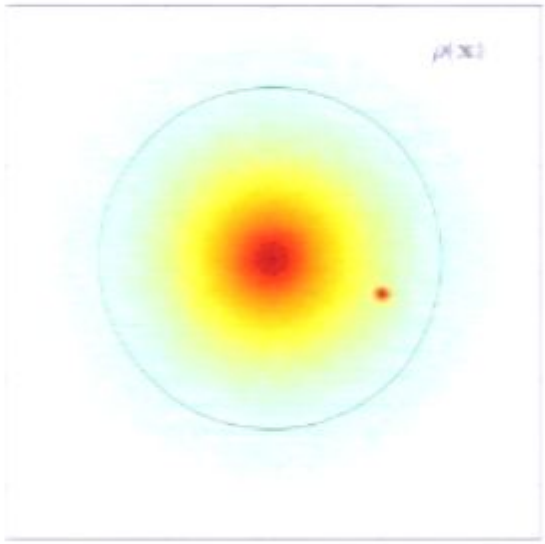
$\rho(\mathbf{x})$

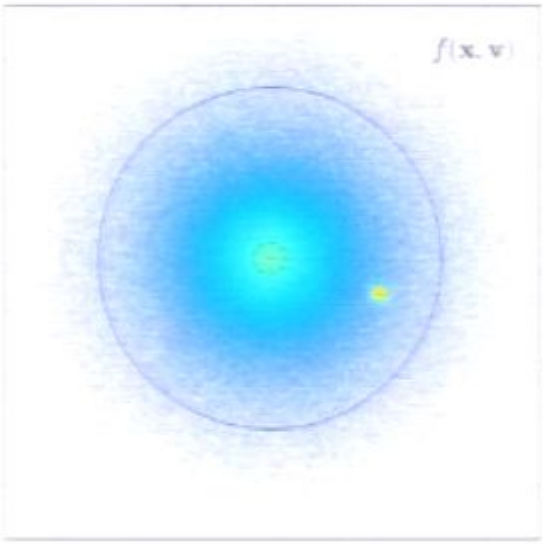
$f(\mathbf{x}, \mathbf{v})$

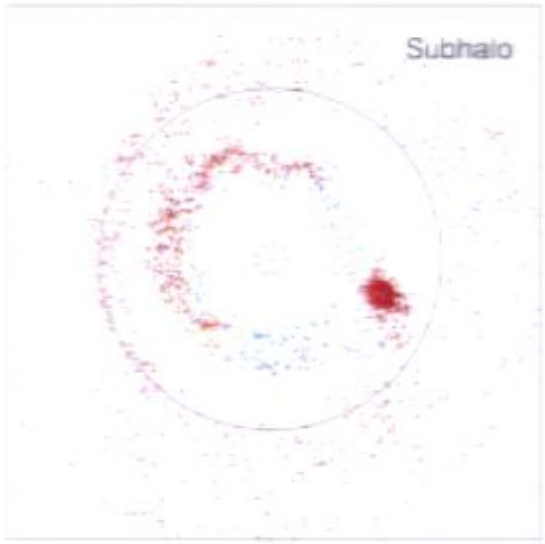
Subhalo

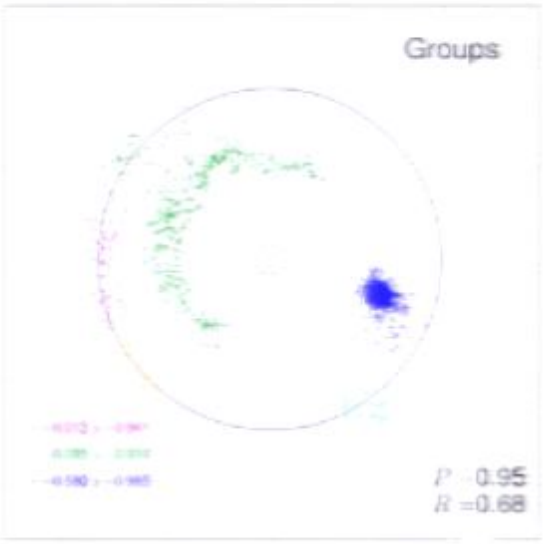
Groups
P 0.95
R =0.68

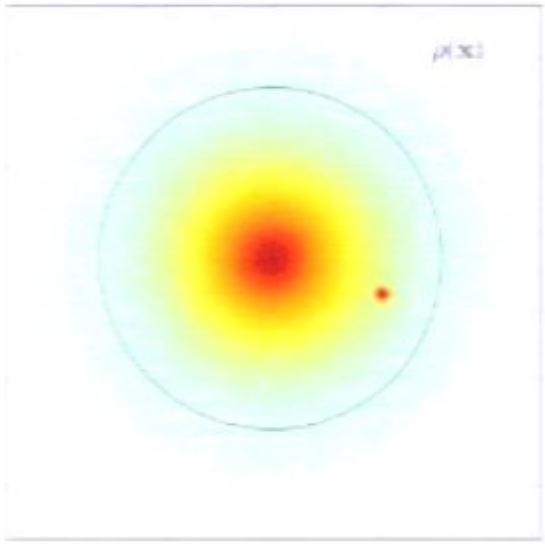
$\rho(\mathbf{x})$

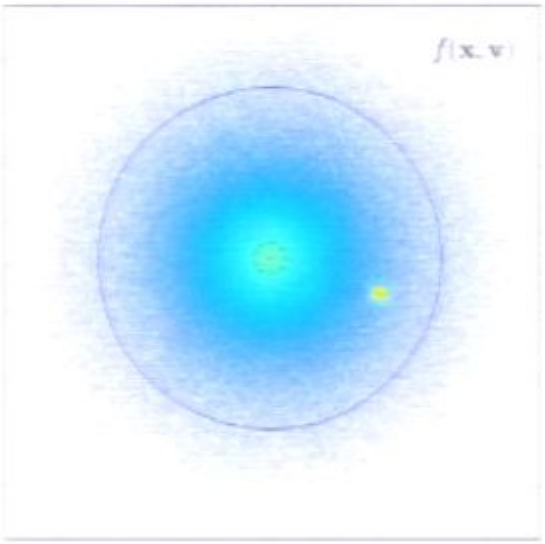
$f(\mathbf{x}, \mathbf{v})$

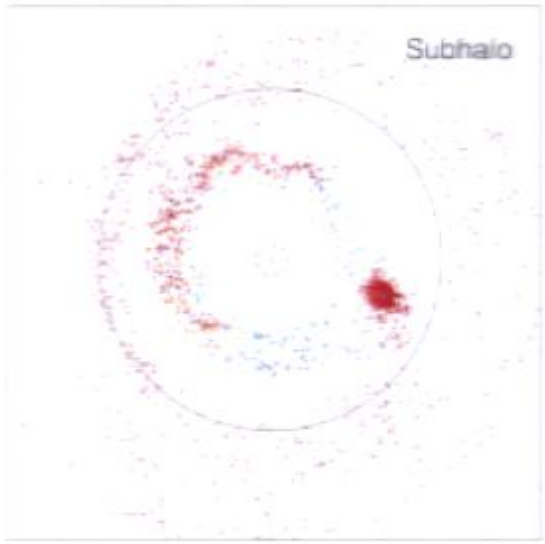
Subhalo

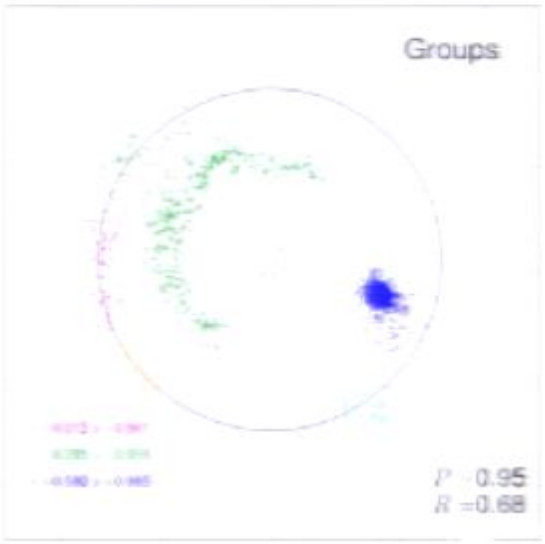
Groups
P 0.95
R =0.68

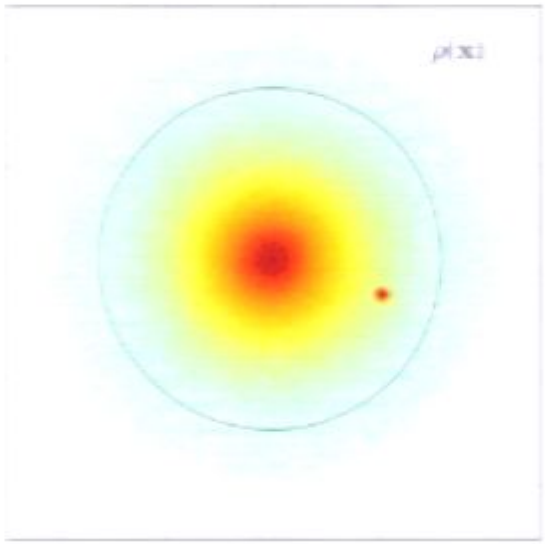
$\rho(\mathbf{x})$

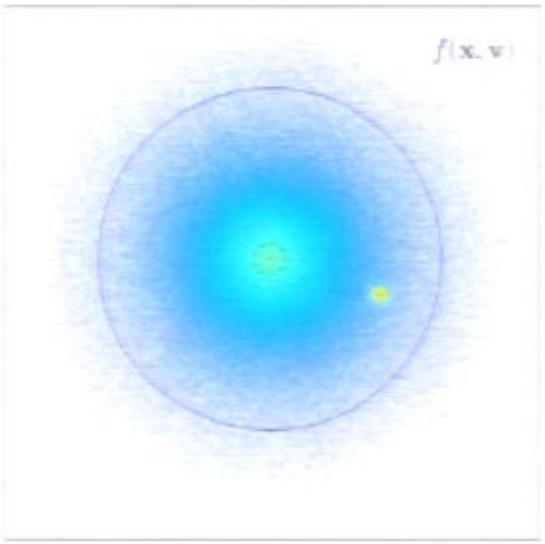
$f(\mathbf{x}, \mathbf{v})$

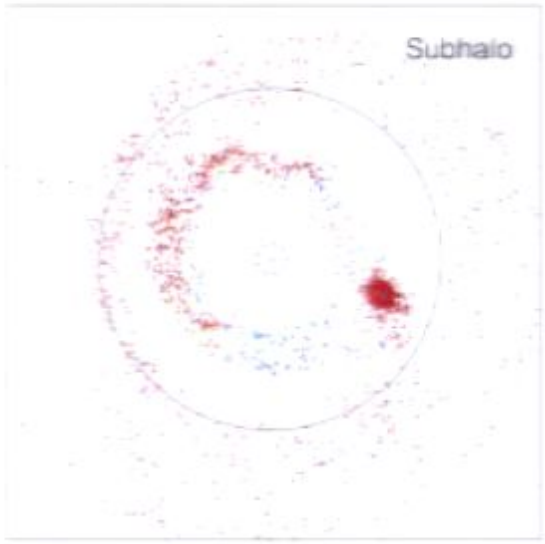
Subhalo

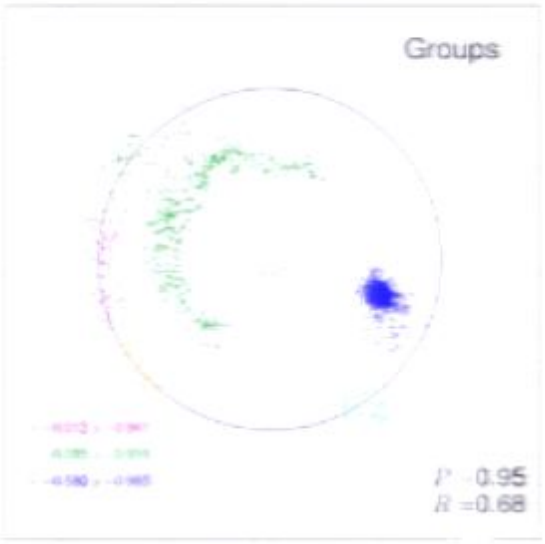
Groups
P 0.95
R =0.68

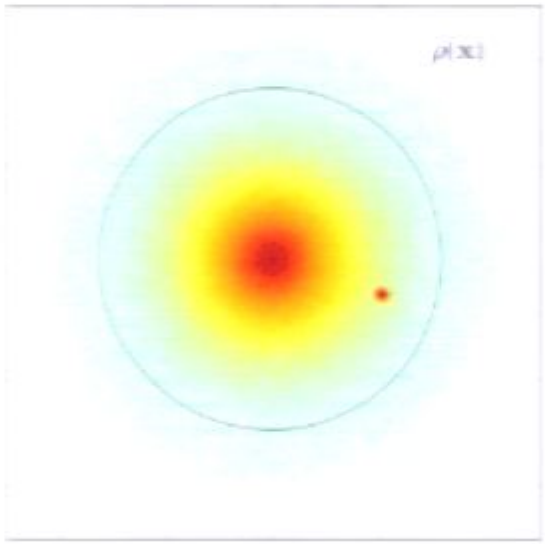
$\rho(\mathbf{x})$

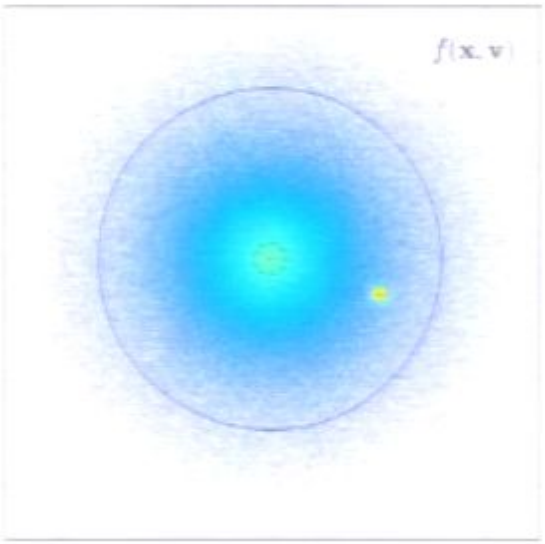
$f(\mathbf{x}, \mathbf{v})$

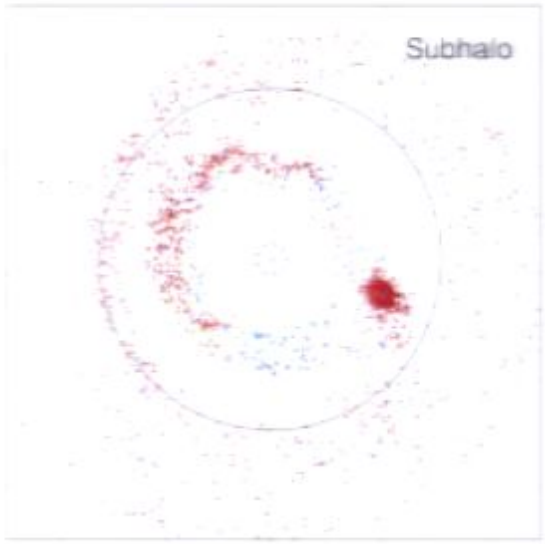
Subhalo

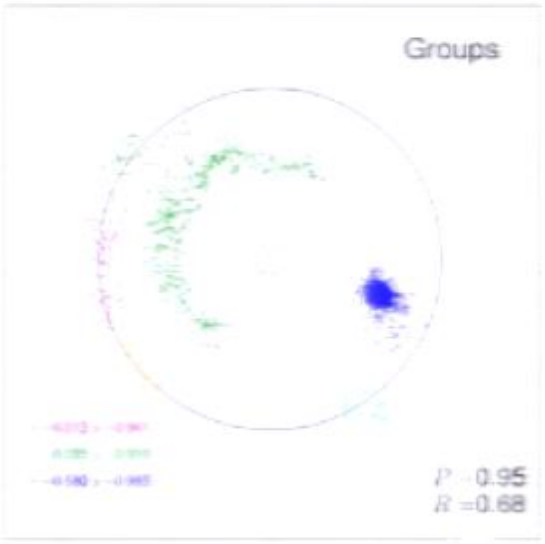
Groups
P 0.95
R 0.68

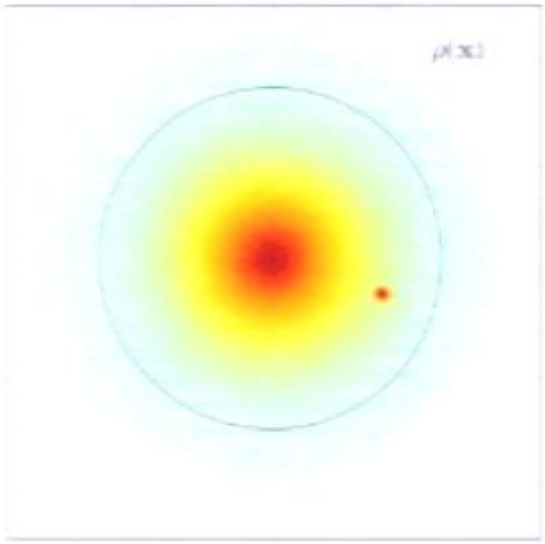
$\rho(\mathbf{x})$

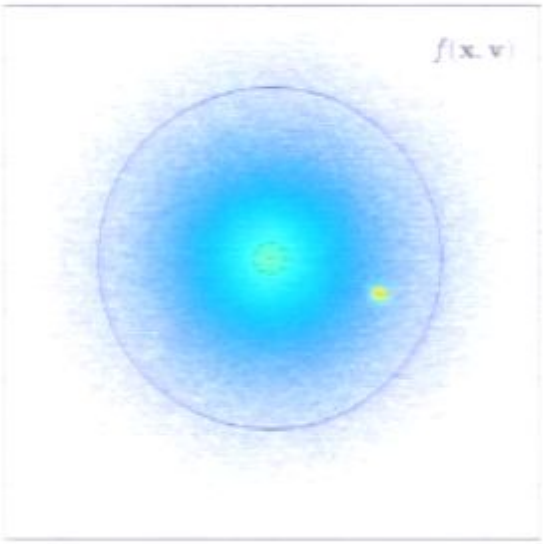
$f(\mathbf{x}, \mathbf{v})$

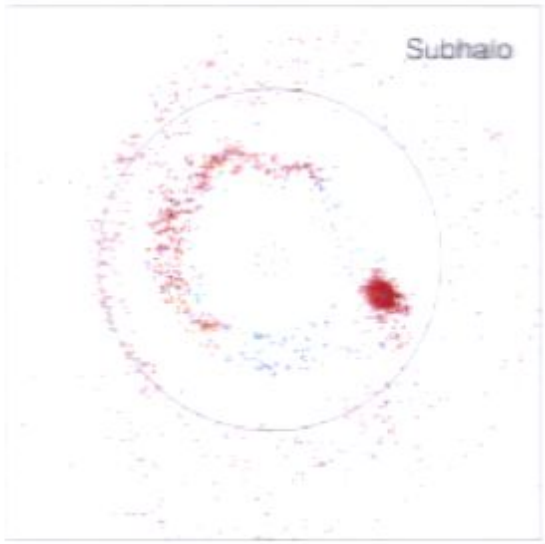
Subhalo

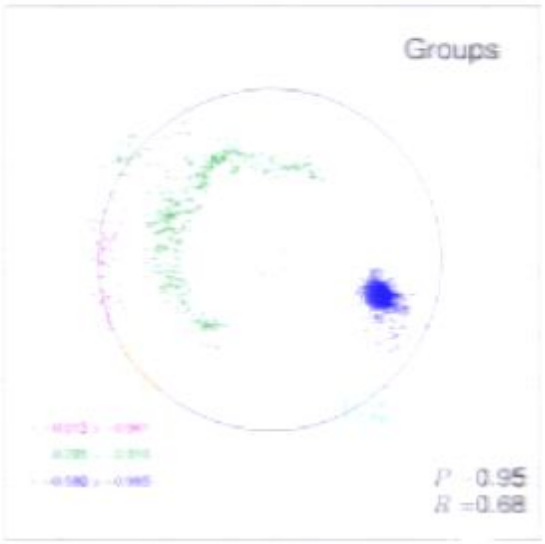
Groups
P 0.95
R =0.68

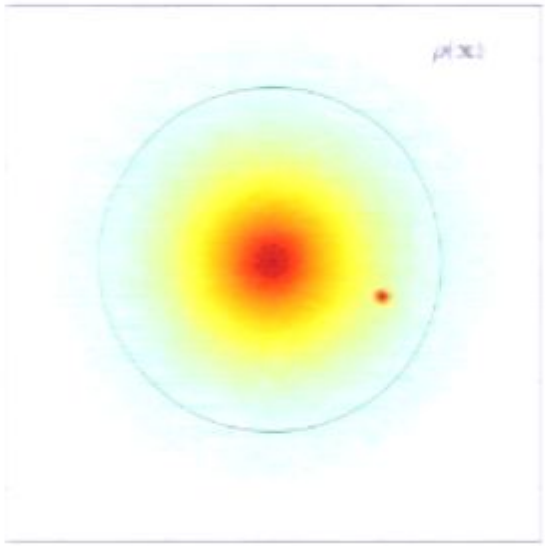
$\rho(\mathbf{x})$

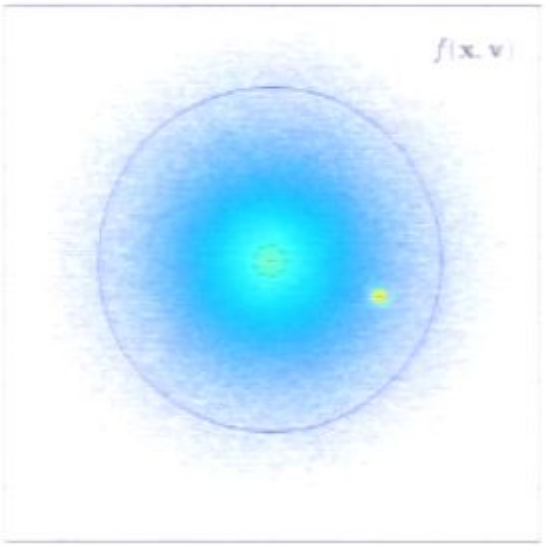
$f(\mathbf{x}, \mathbf{v})$

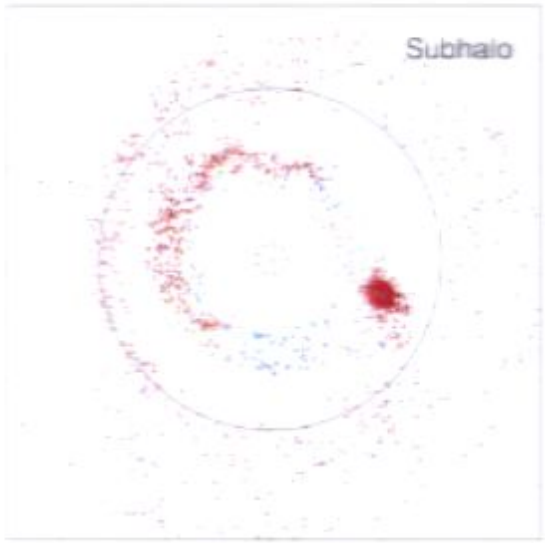
Subhalo

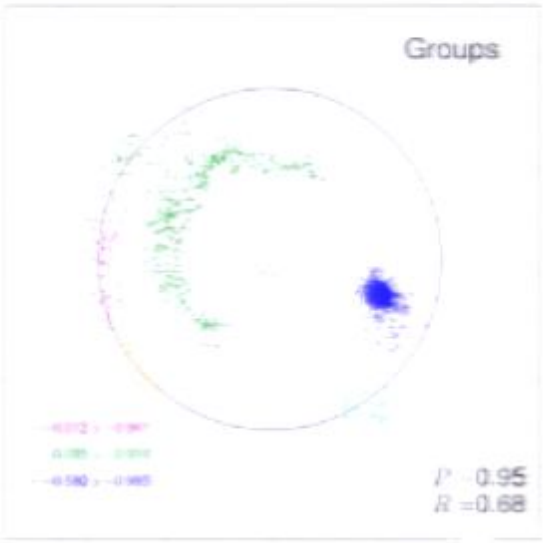
Groups
P 0.95
R =0.68

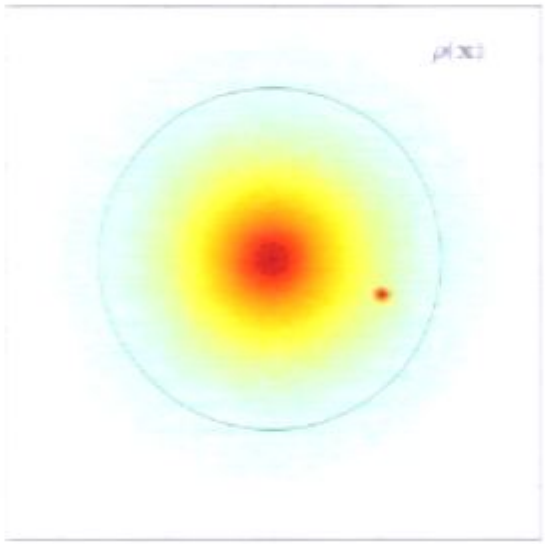
$\rho(\mathbf{x})$

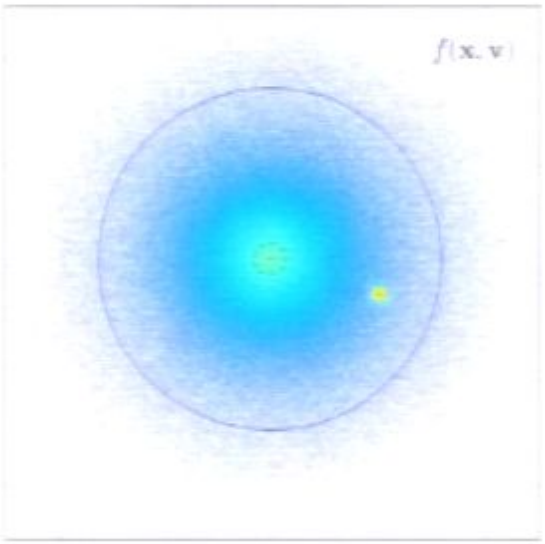
$f(\mathbf{x}, \mathbf{v})$

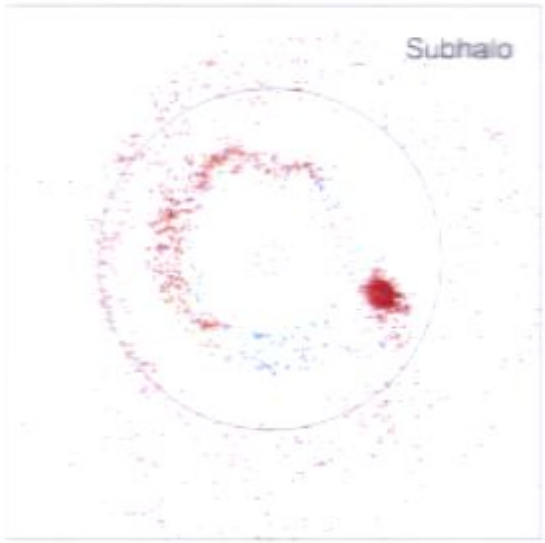
Subhalo

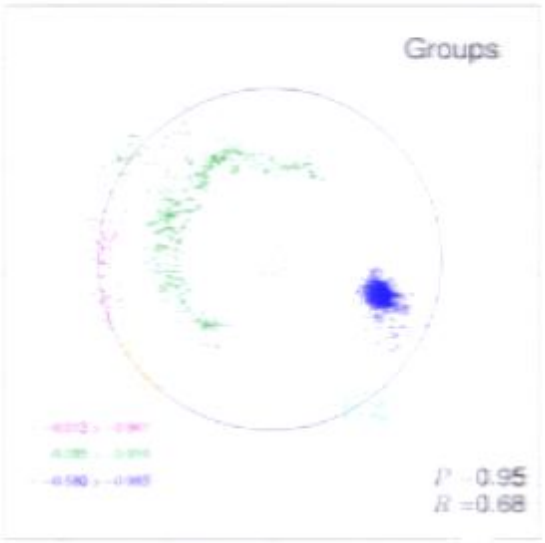
Groups
P =0.95
R =0.68

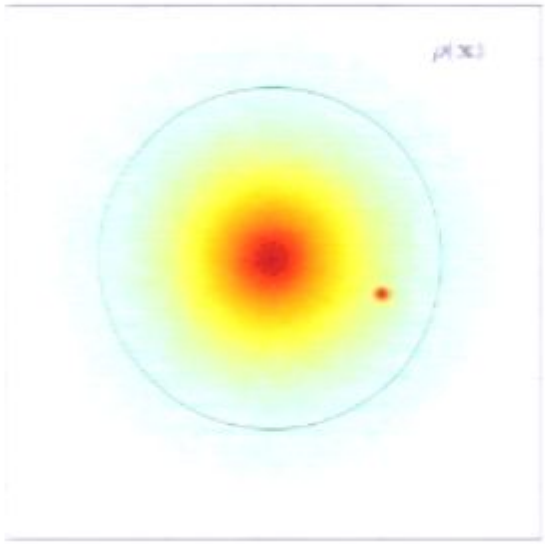
$\rho(\mathbf{x})$

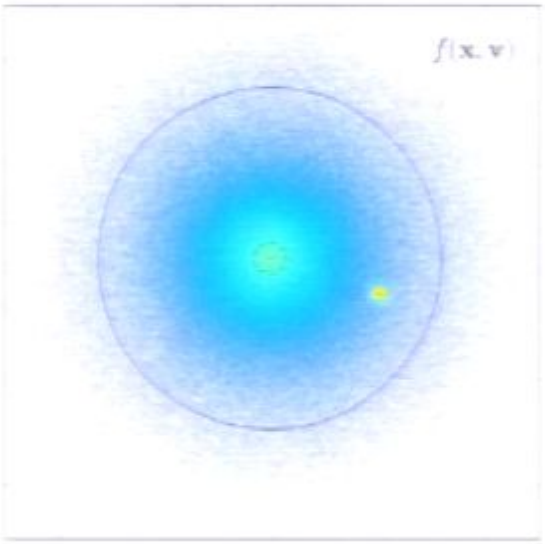
$f(\mathbf{x}, \mathbf{v})$

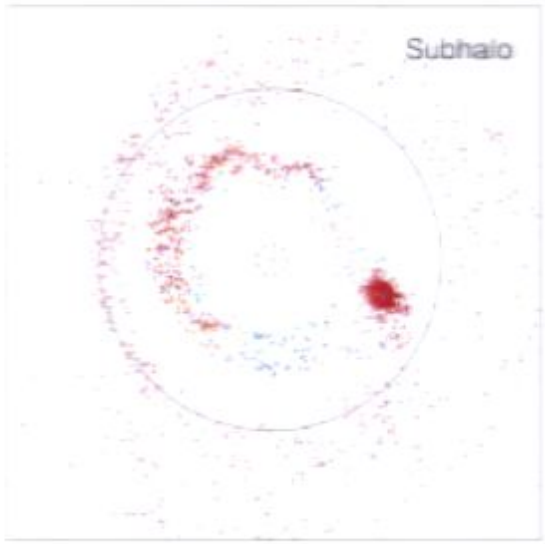
Subhalo

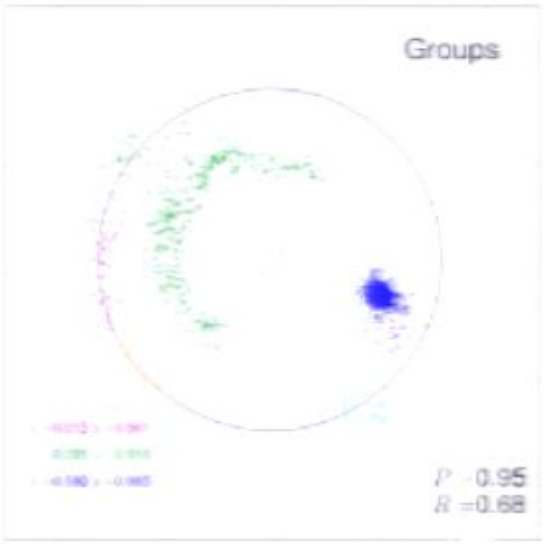
Groups
P 0.95
R =0.68

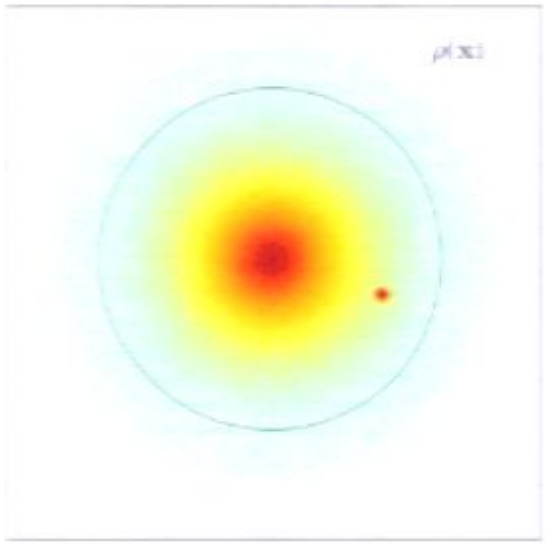
$\rho(\mathbf{x})$

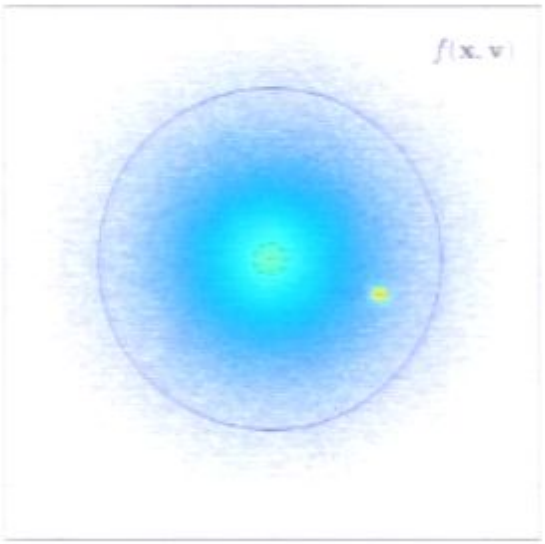
$f(\mathbf{x}, \mathbf{v})$

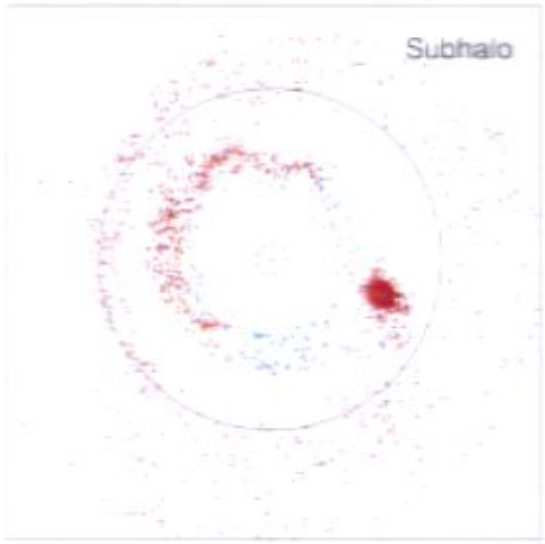
Subhalo

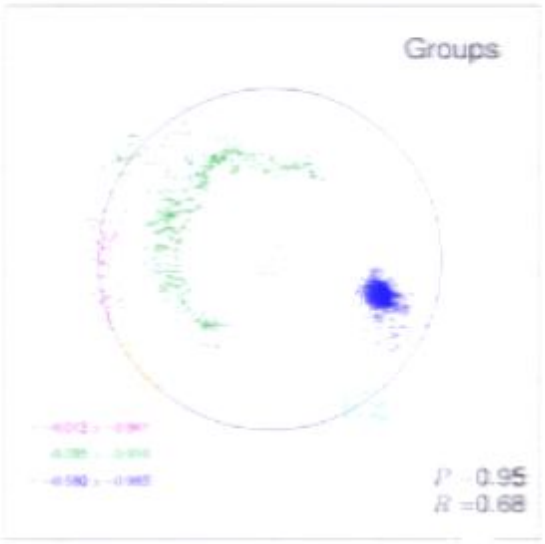
Groups
P 0.95
R =0.68

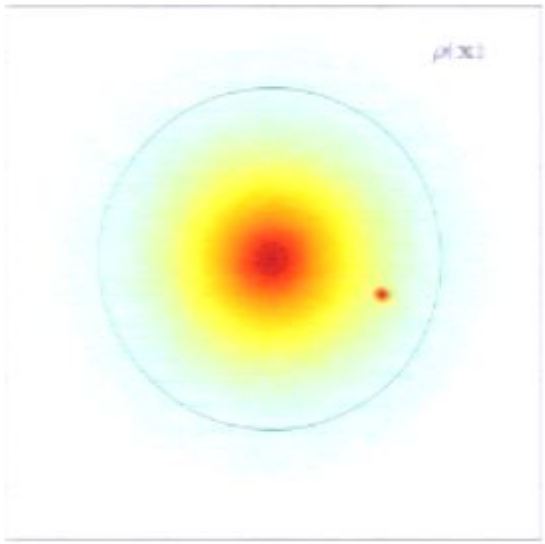
$\rho(\mathbf{x})$

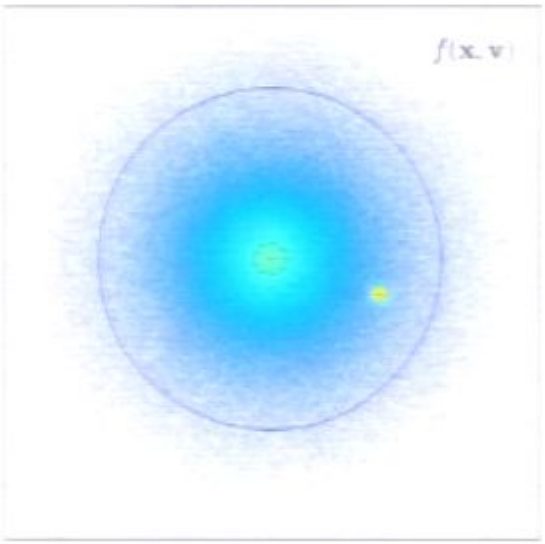
$f(\mathbf{x}, \mathbf{v})$

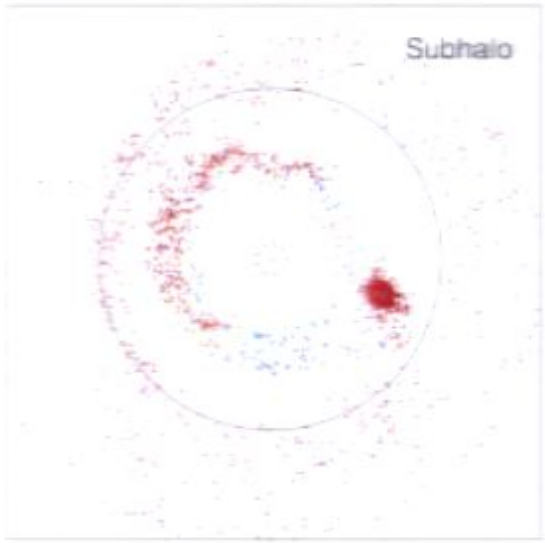
Subhalo

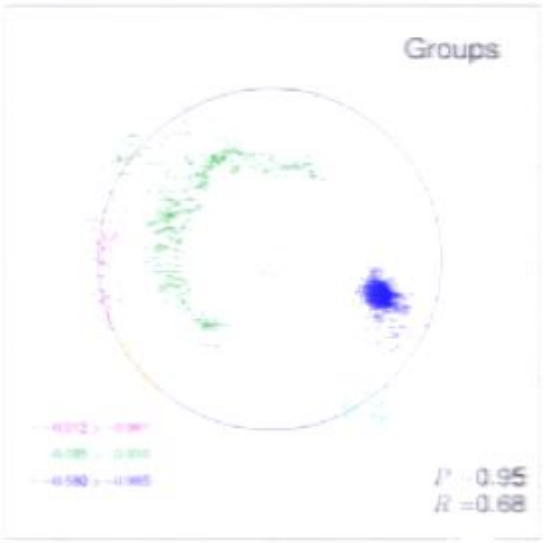
Groups
P 0.95
R =0.68

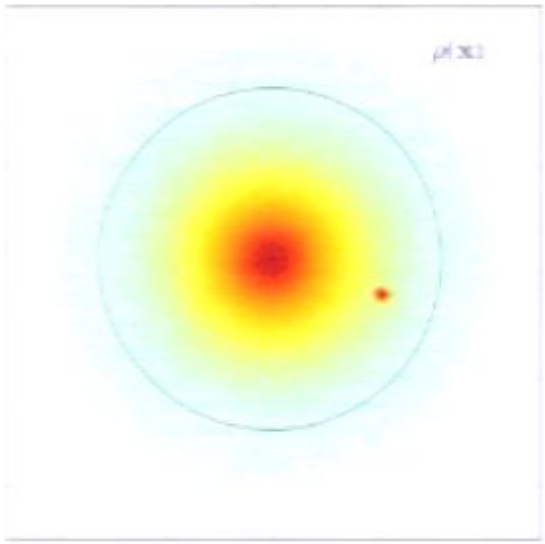
$\rho(\mathbf{x})$

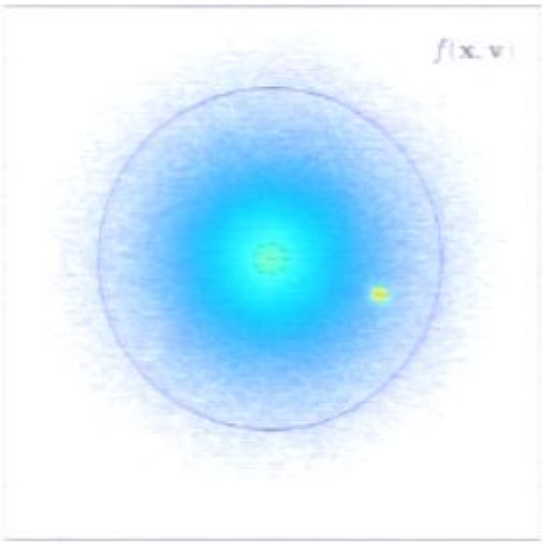
$f(\mathbf{x}, \mathbf{v})$

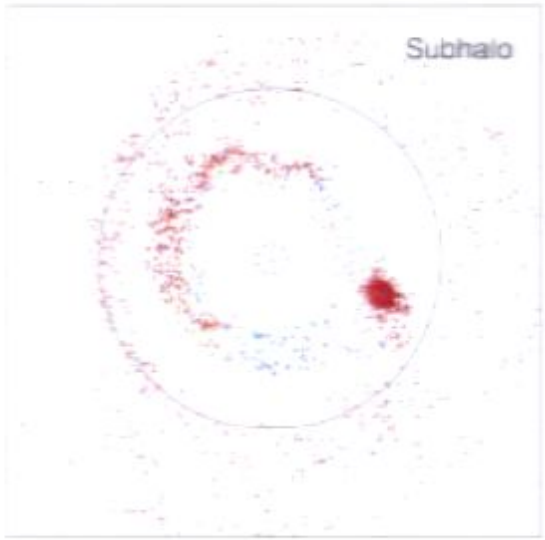
Subhalo

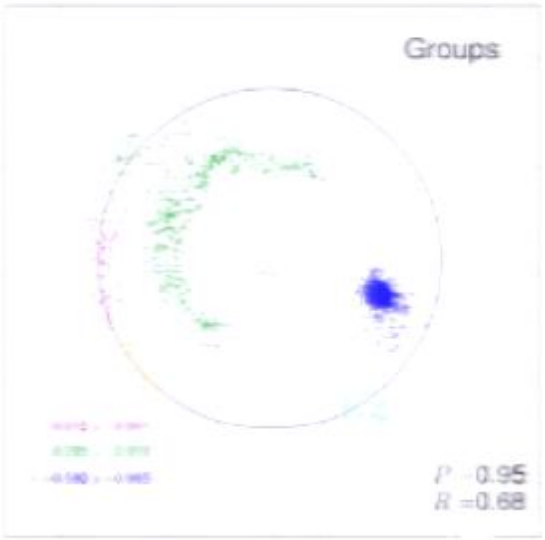
Groups
P =0.95
R =0.68

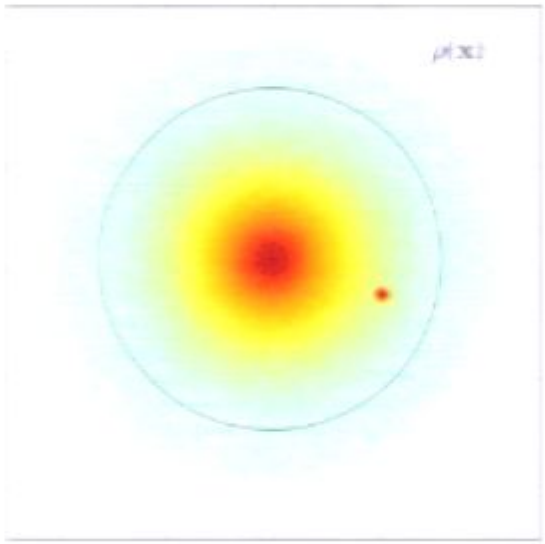
$\rho(\mathbf{x})$

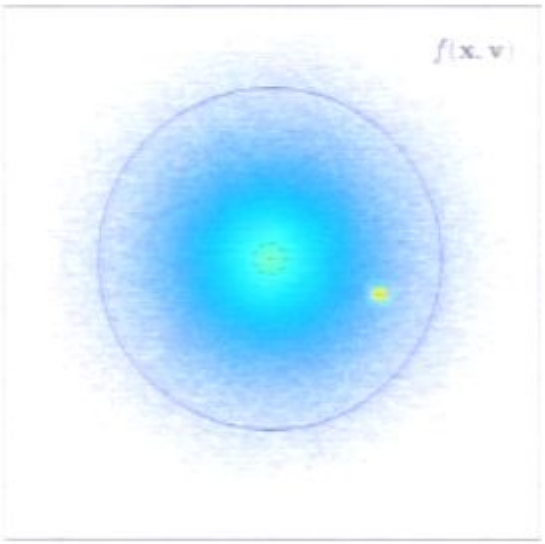
$f(\mathbf{x}, \mathbf{v})$

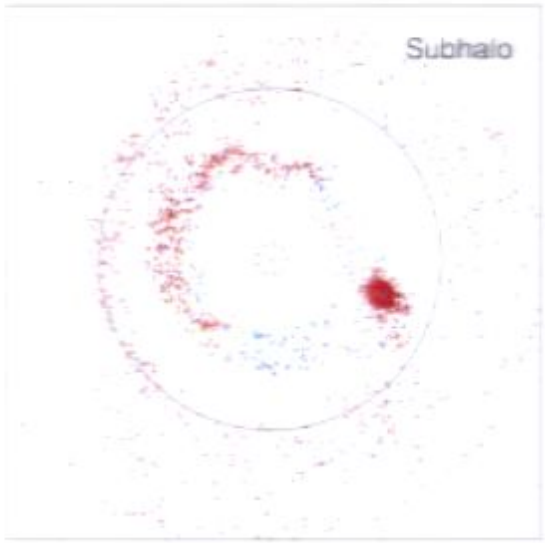
Subhalo

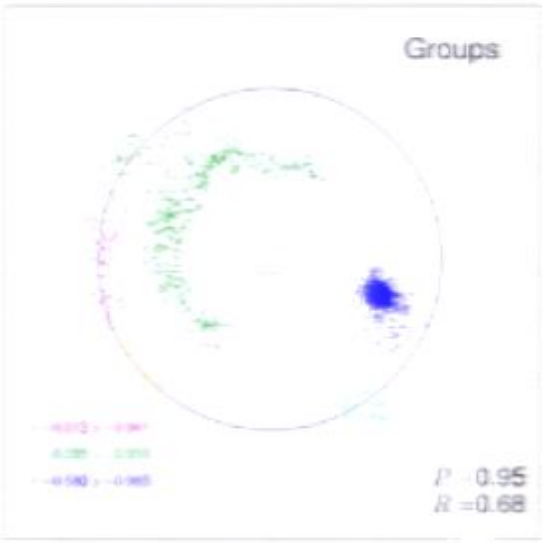
Groups
P 0.95
R =0.68

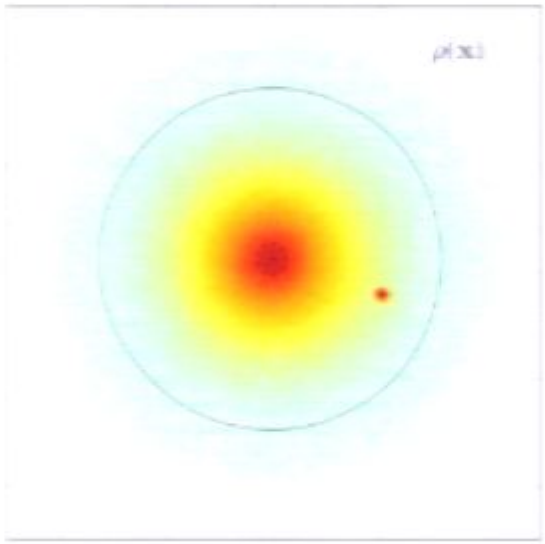
$\rho(\mathbf{x})$

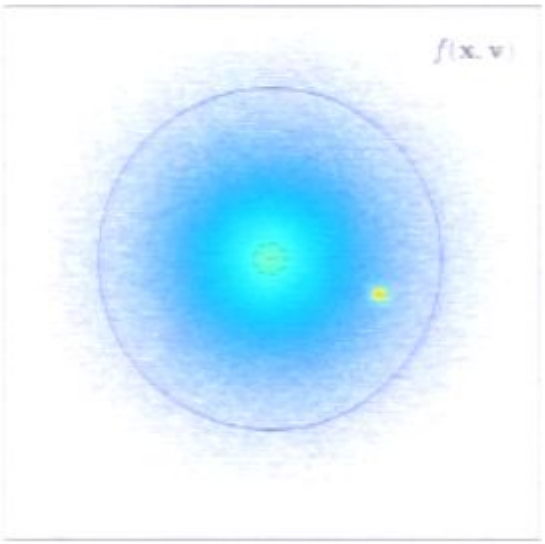
$f(\mathbf{x}, \mathbf{v})$

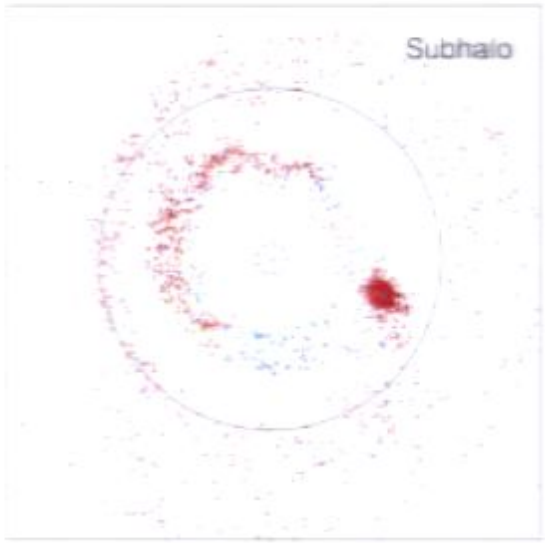
Subhalo

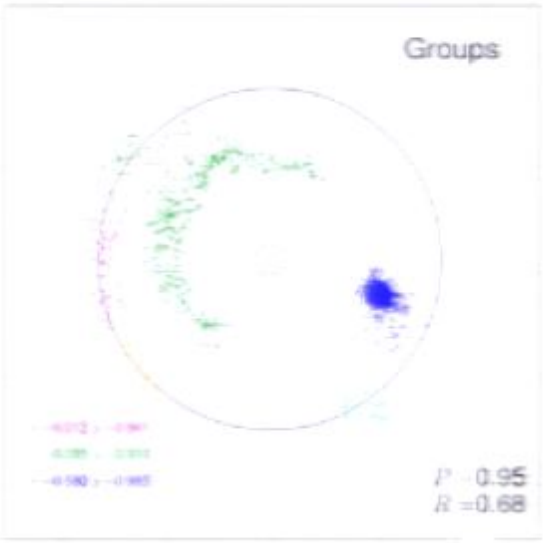
Groups
P 0.95
R =0.68

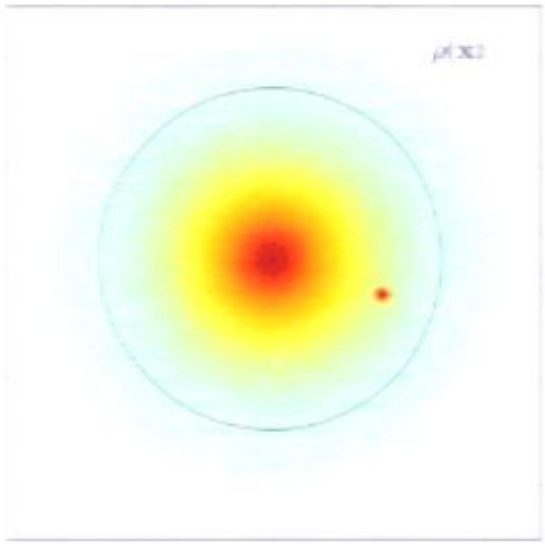
$\rho(\mathbf{x})$

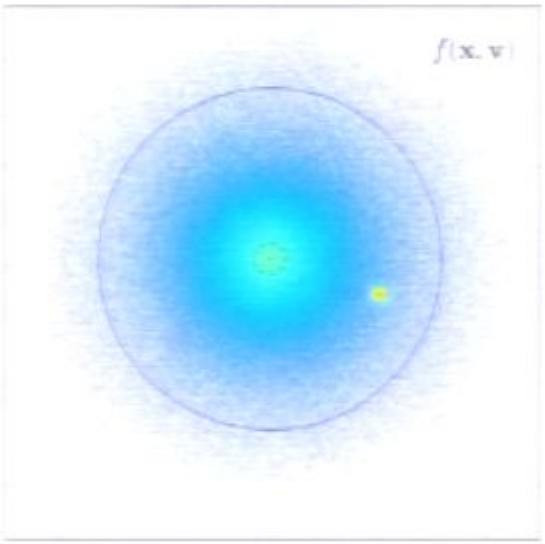
$f(\mathbf{x}, \mathbf{v})$

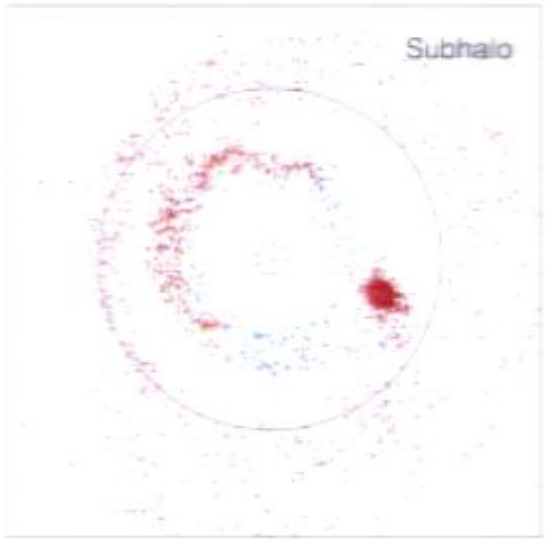
Subhalo

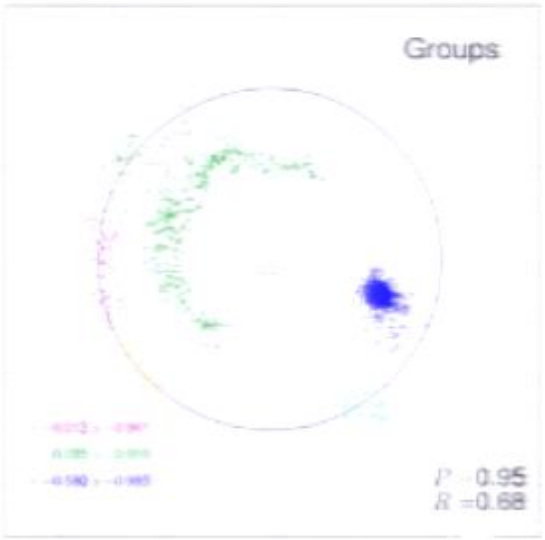
Groups
P 0.95
R =0.68

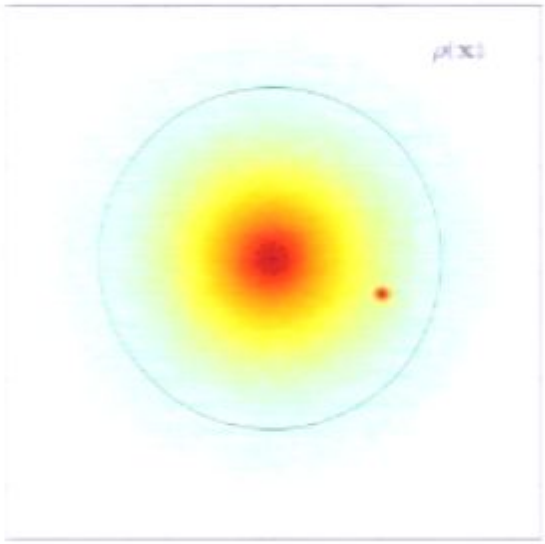
$\rho(\mathbf{x})$

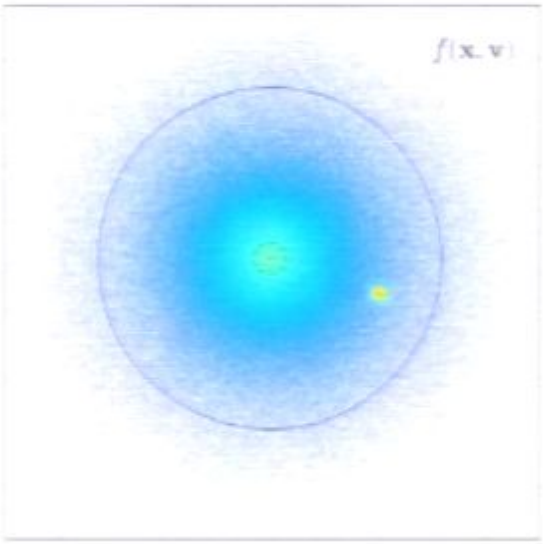
$f(\mathbf{x}, \mathbf{v})$

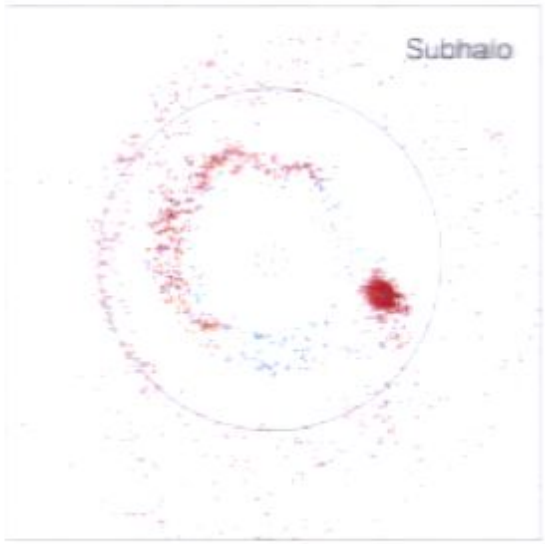
Subhalo

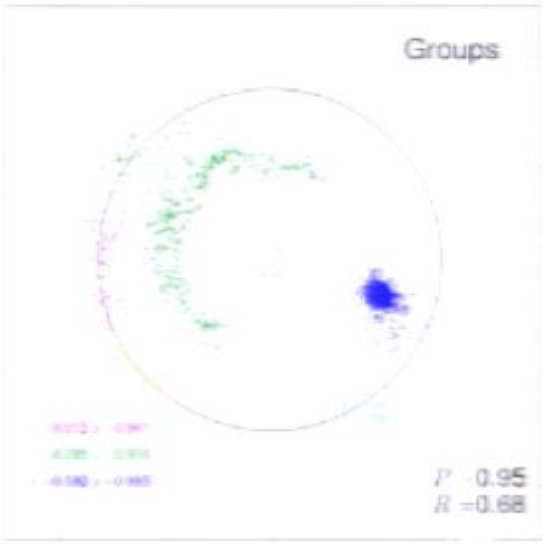
Groups
P 0.95
R =0.68

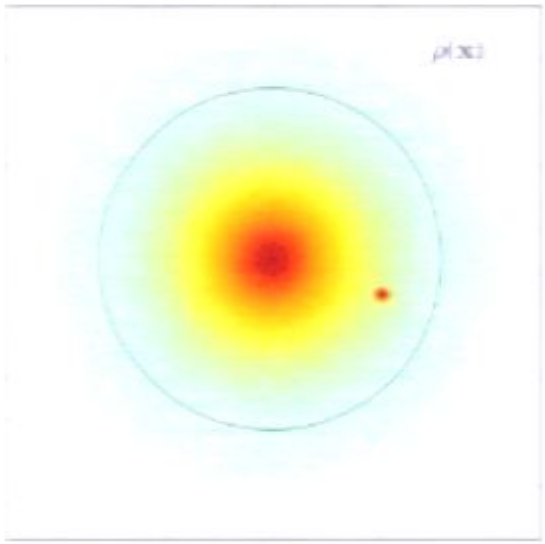
$\rho(\mathbf{x})$

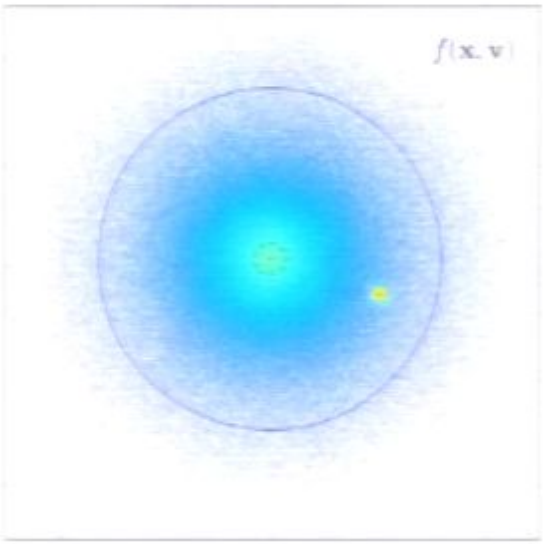
$f(\mathbf{x}, \mathbf{v})$

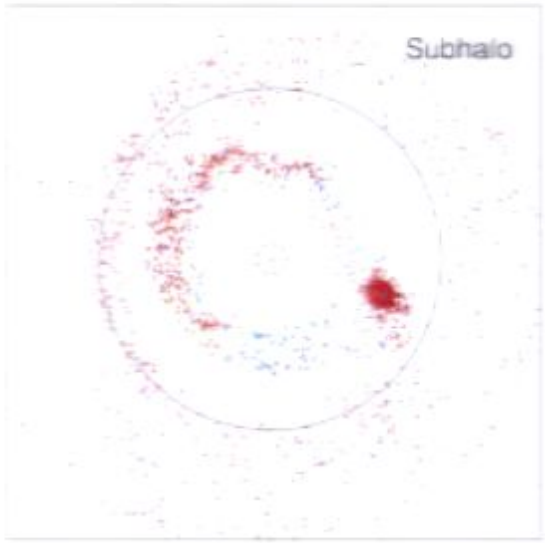
Subhalo

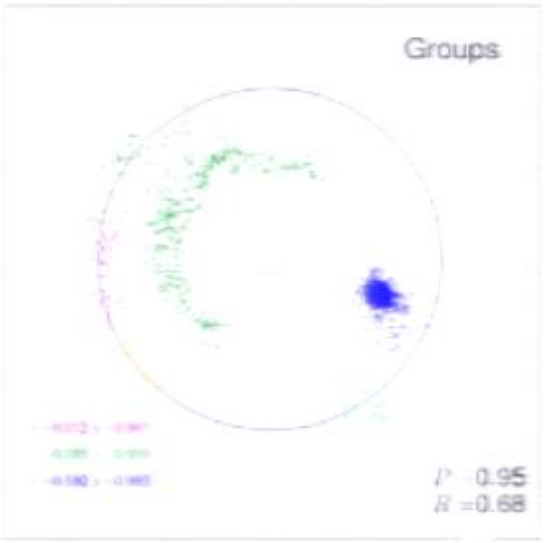
Groups
P 0.95
R =0.68

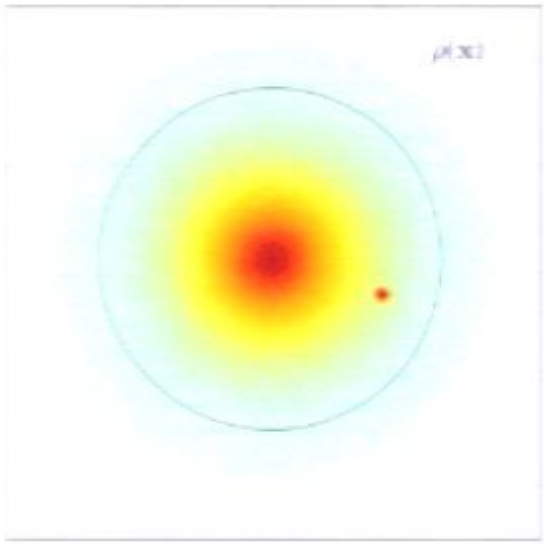
$\rho(\mathbf{x})$

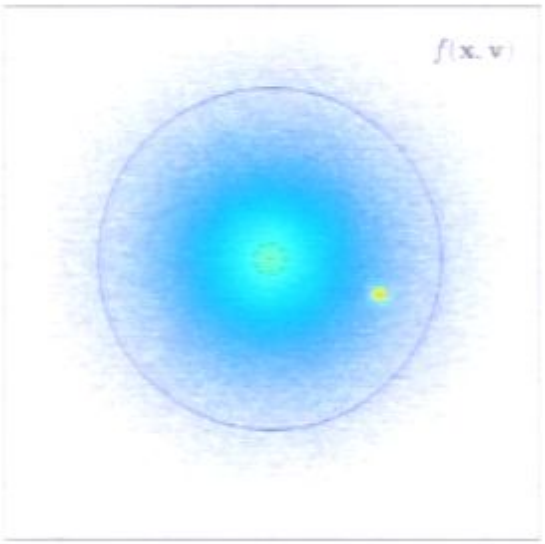
$f(\mathbf{x}, \mathbf{v})$

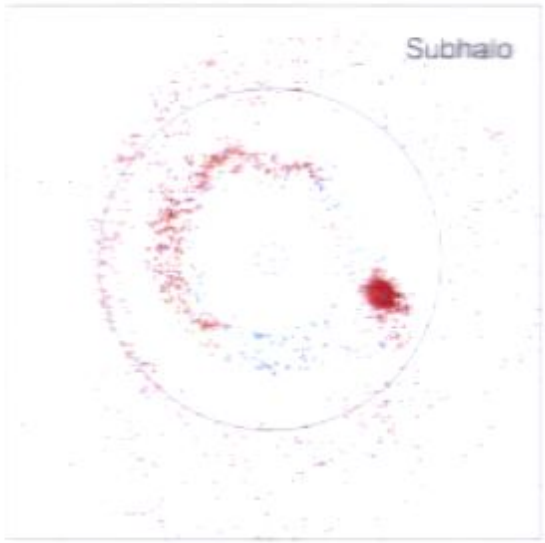
Subhalo

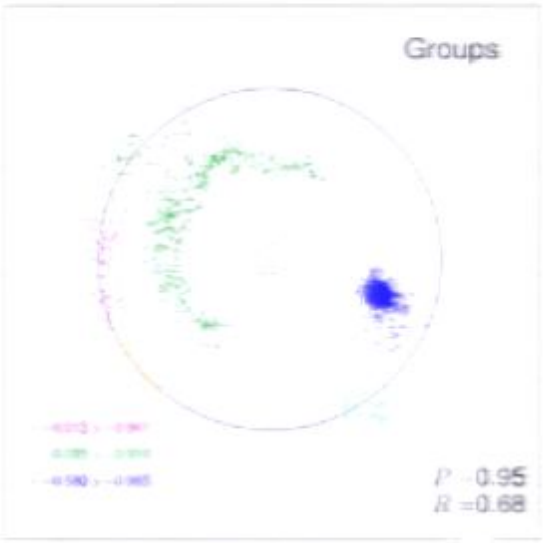
Groups
P =0.95
R =0.68

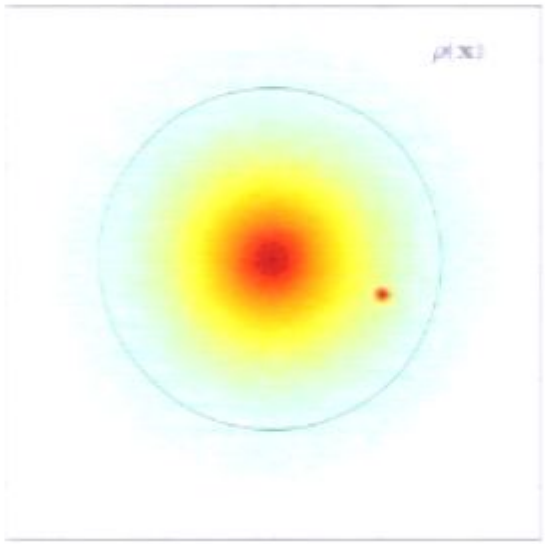
$\rho(\mathbf{x})$

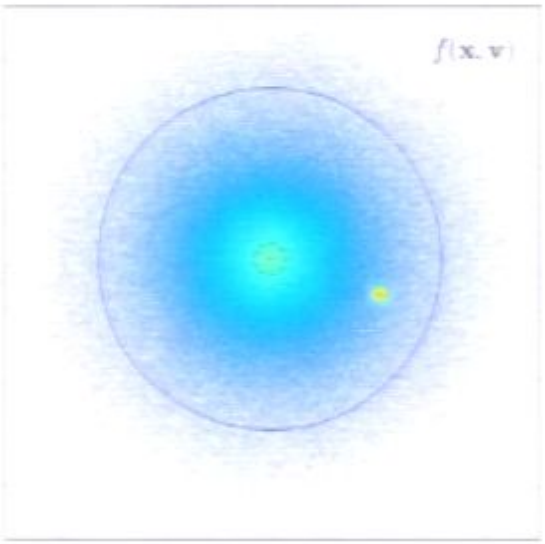
$f(\mathbf{x}, \mathbf{v})$

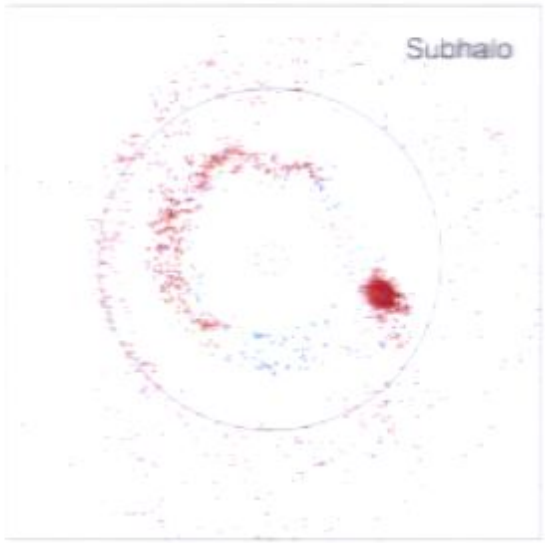
Subhalo

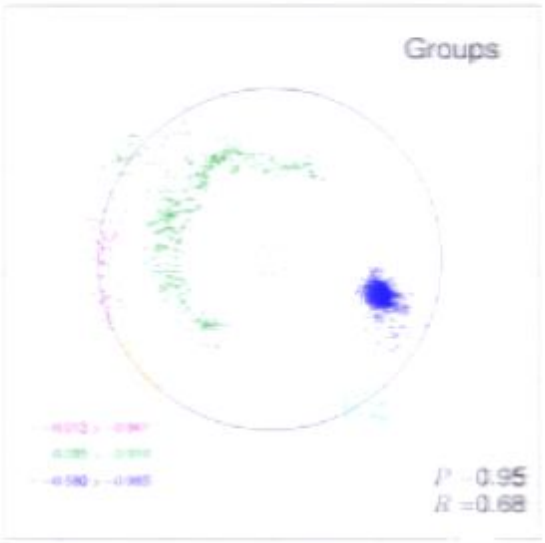
Groups
P =0.95
R =0.68

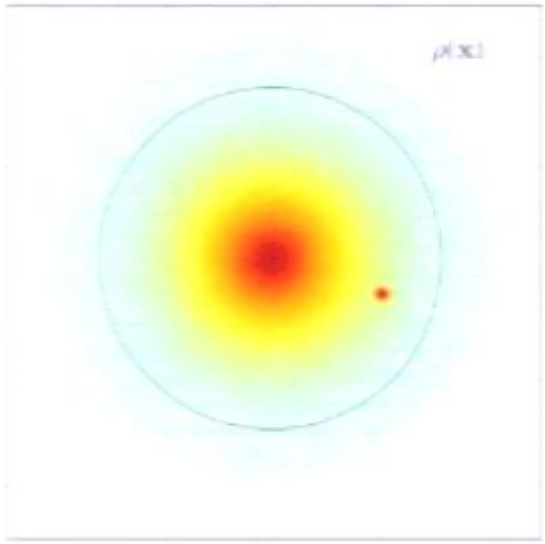
$\rho(\mathbf{x})$

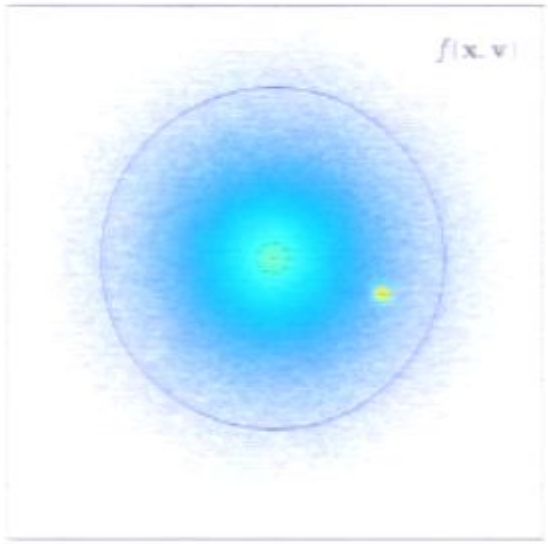
$f(\mathbf{x}, \mathbf{v})$

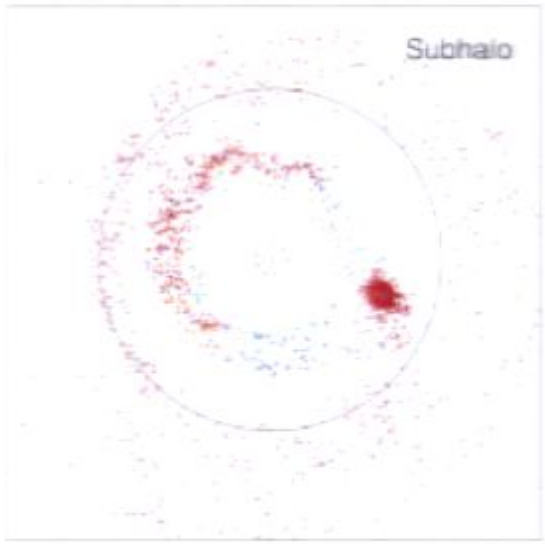
Subhalo

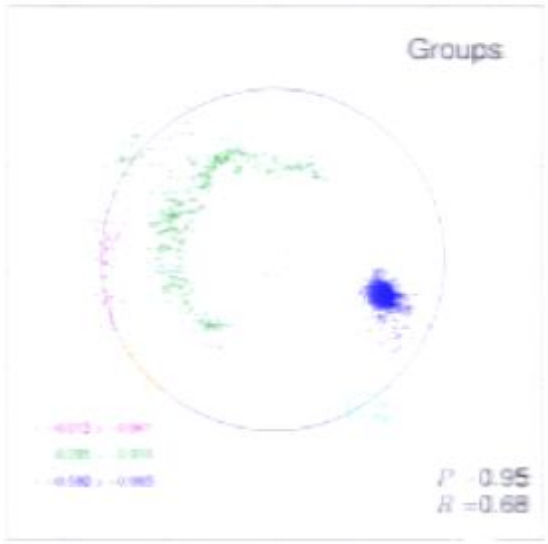
Groups
P 0.95
R =0.68

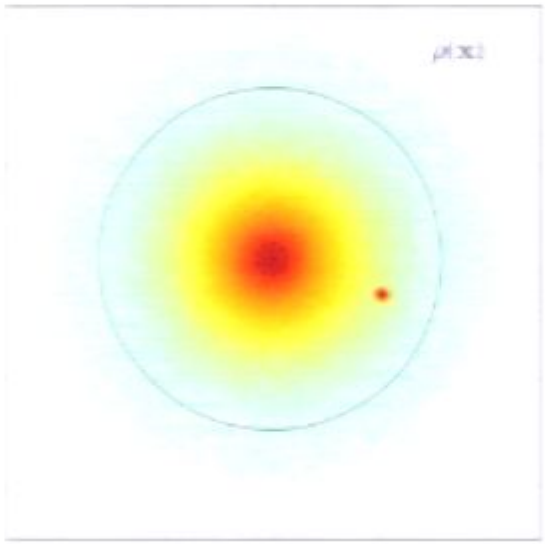
$\rho(\mathbf{x})$

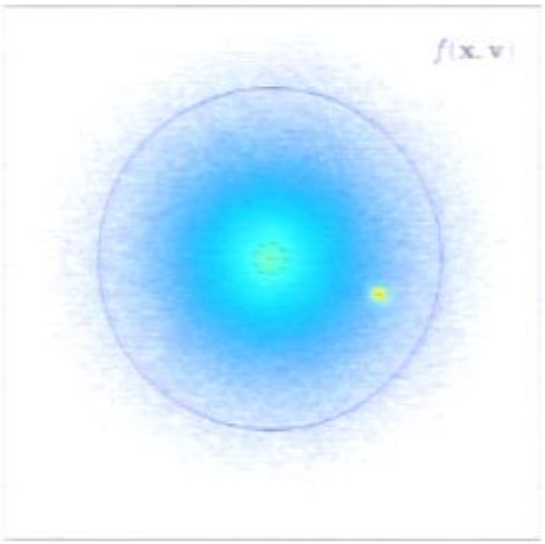
$f(\mathbf{x}, \mathbf{v})$

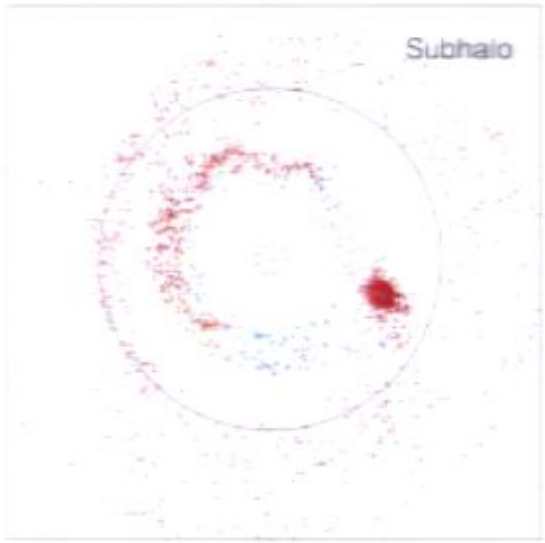
Subhalo

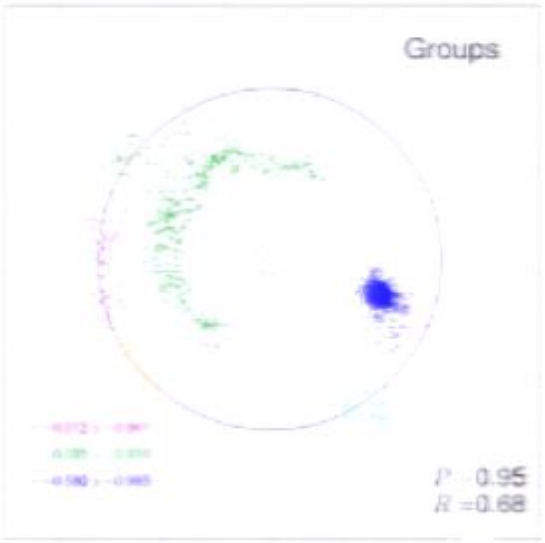
Groups
P 0.95
R =0.68

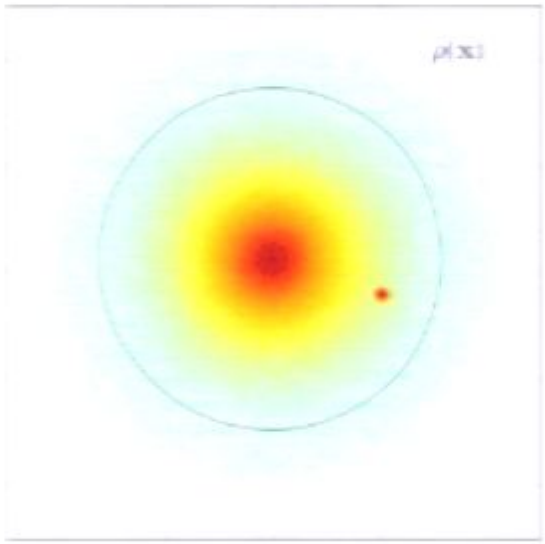
$\rho(\mathbf{x})$

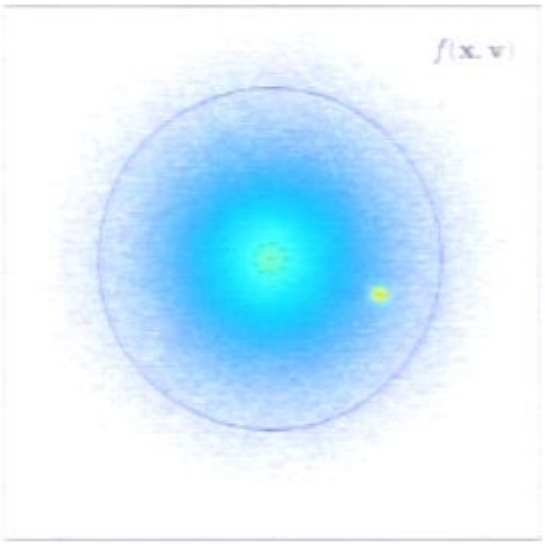
$f(\mathbf{x}, \mathbf{v})$

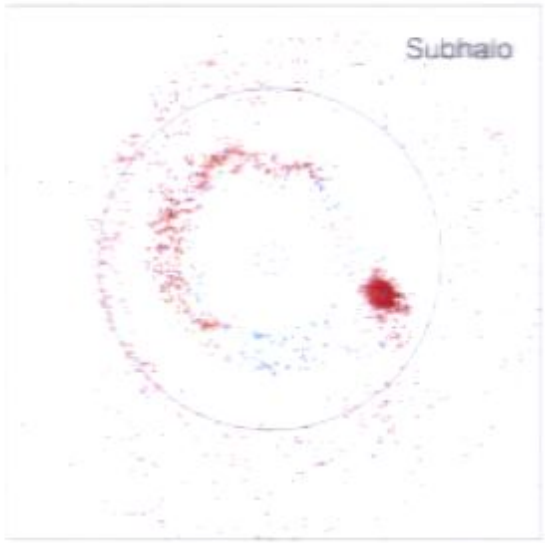
Subhalo

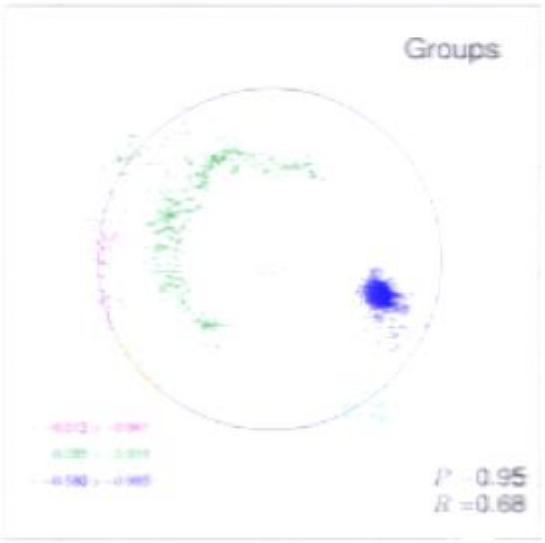
Groups
P 0.95
R =0.68

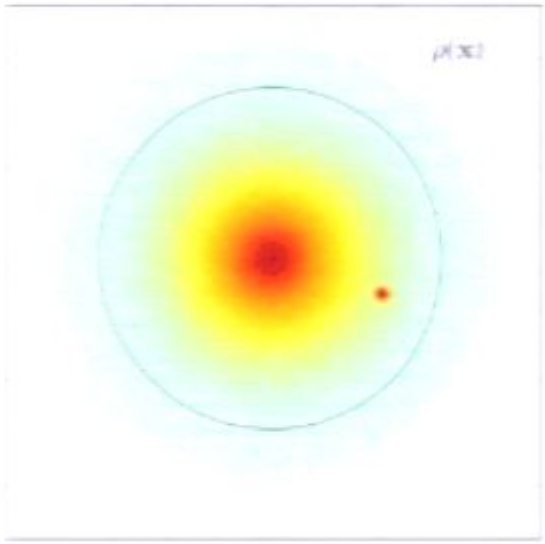
$\rho(\mathbf{x})$

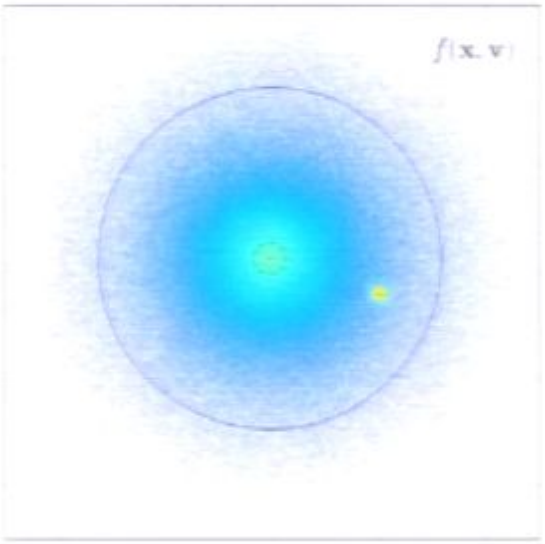
$f(\mathbf{x}, \mathbf{v})$

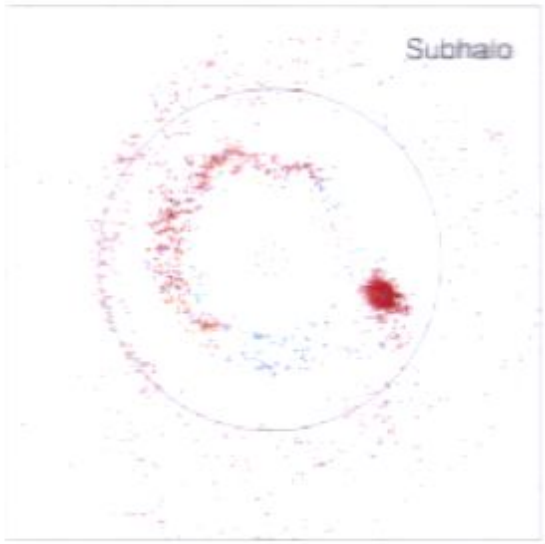
Subhalo

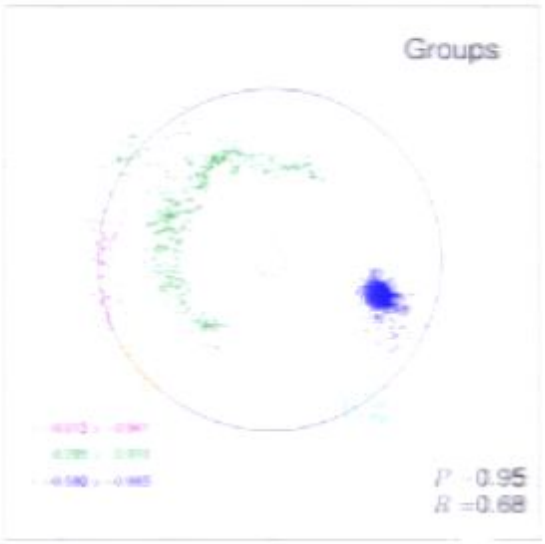
Groups
P 0.95
R =0.68

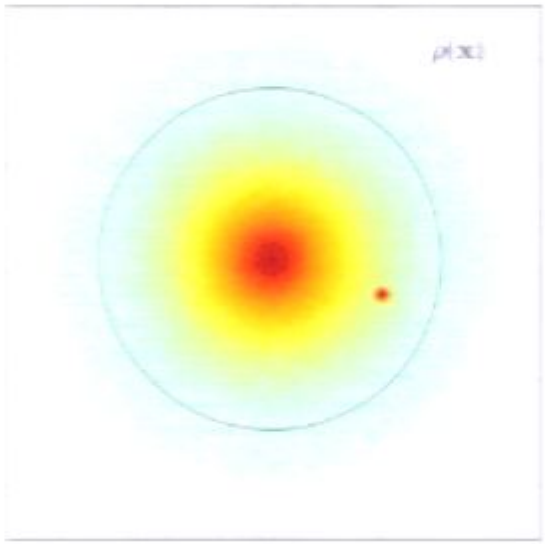
$\rho(\mathbf{x})$

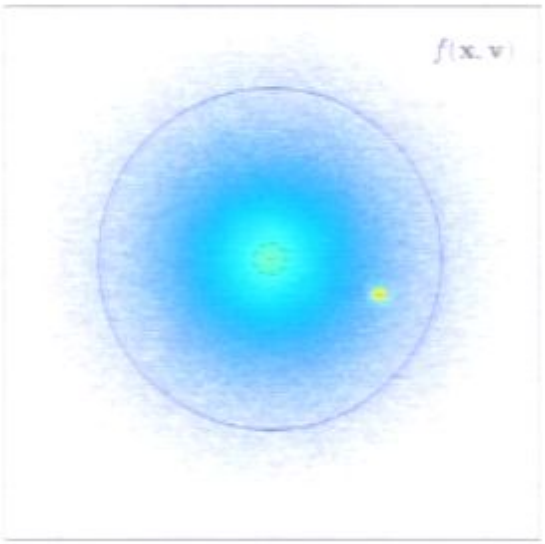
$f(\mathbf{x}, \mathbf{v})$

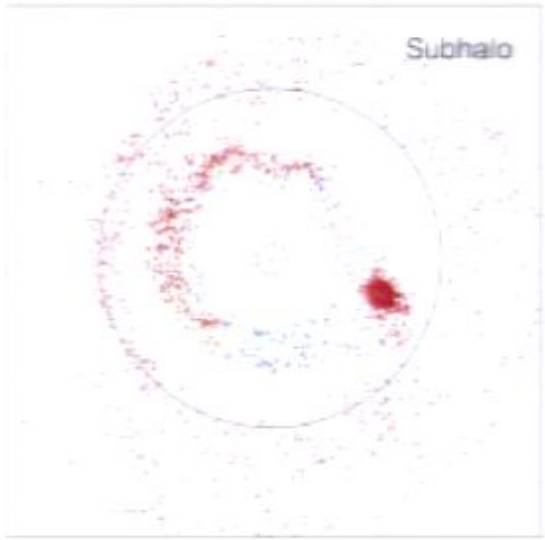
Subhalo

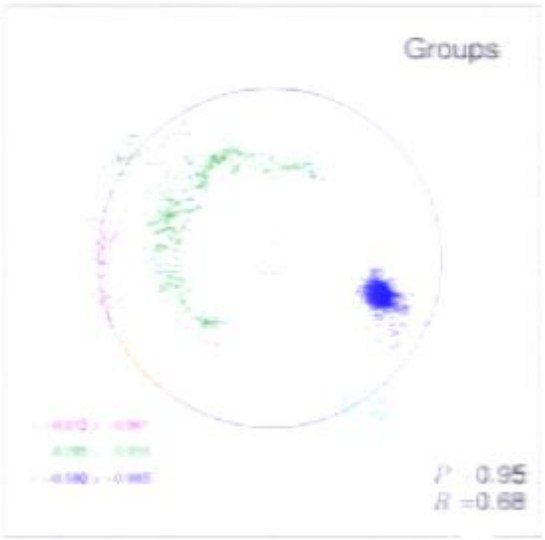
Groups
P 0.95
R =0.68

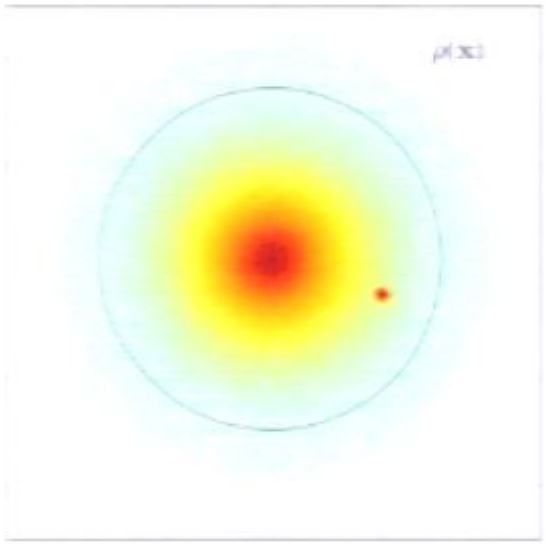
$\rho(\mathbf{x})$

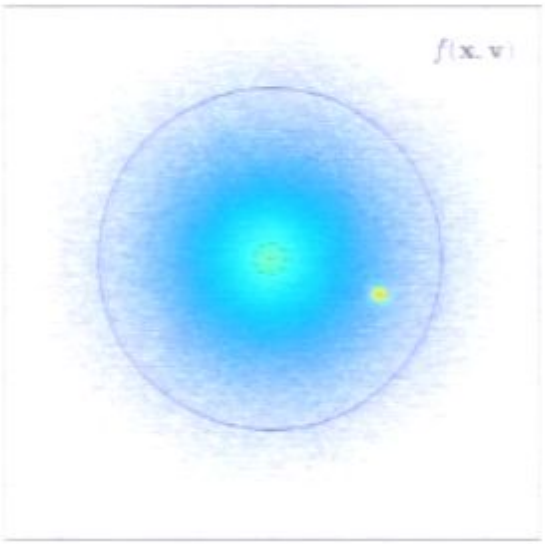
$f(\mathbf{x}, \mathbf{v})$

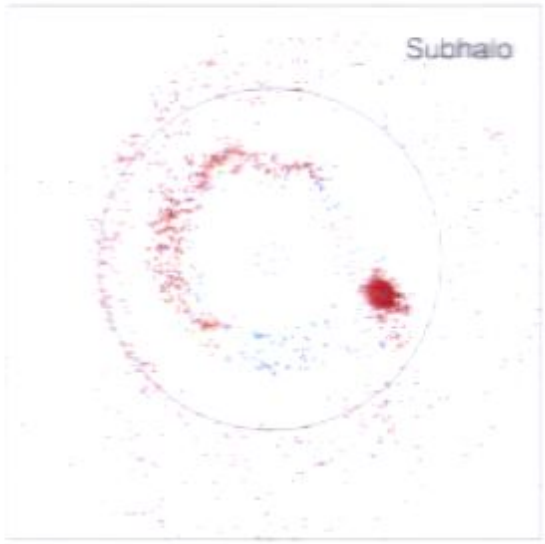
Subhalo

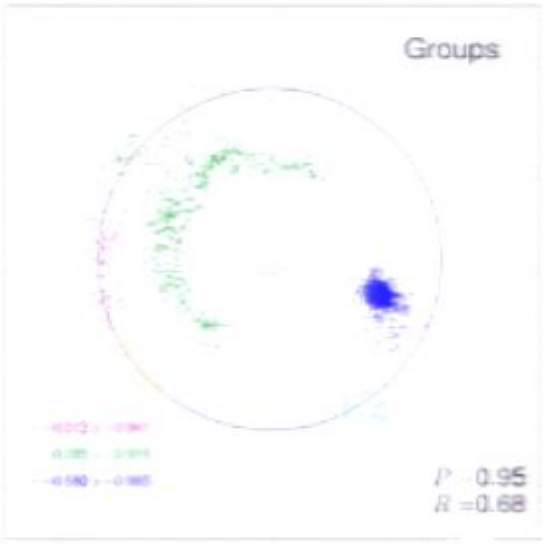
Groups
P 0.95
R =0.68

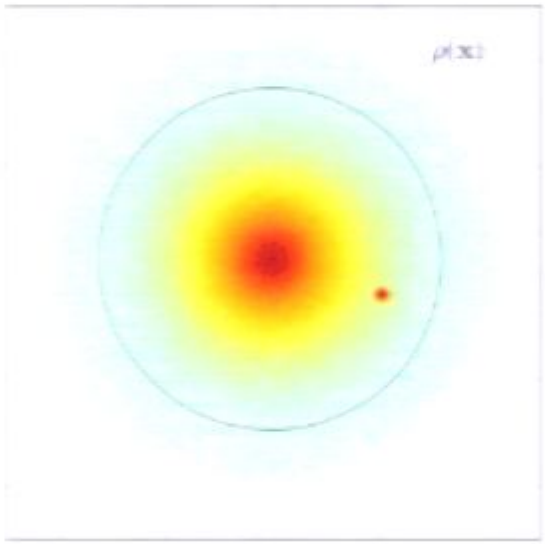
$\rho(\mathbf{x})$

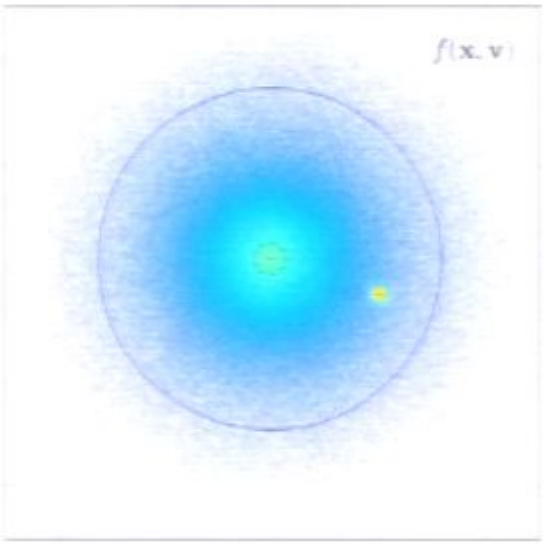
$f(\mathbf{x}, \mathbf{v})$

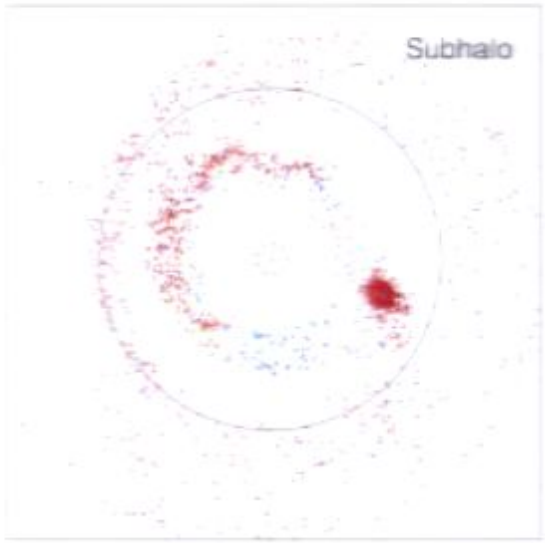
Subhalo

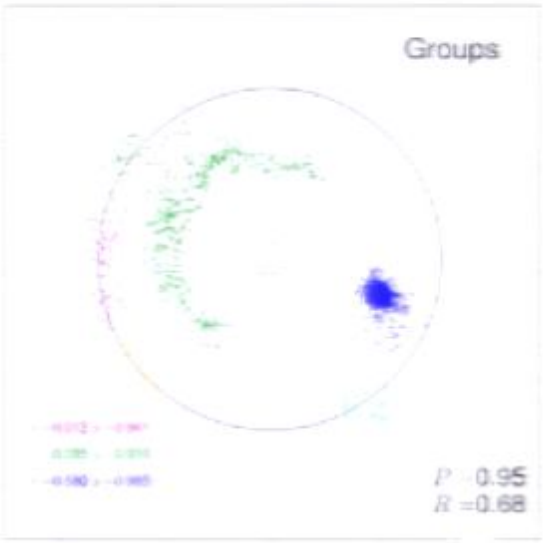
Groups
P 0.95
R =0.68

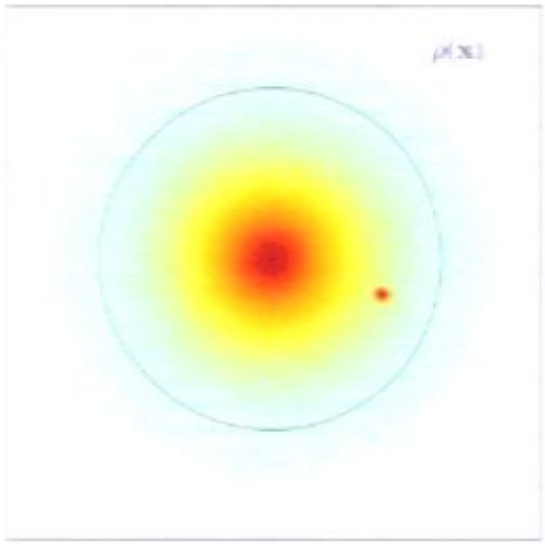
$\rho(\mathbf{x})$

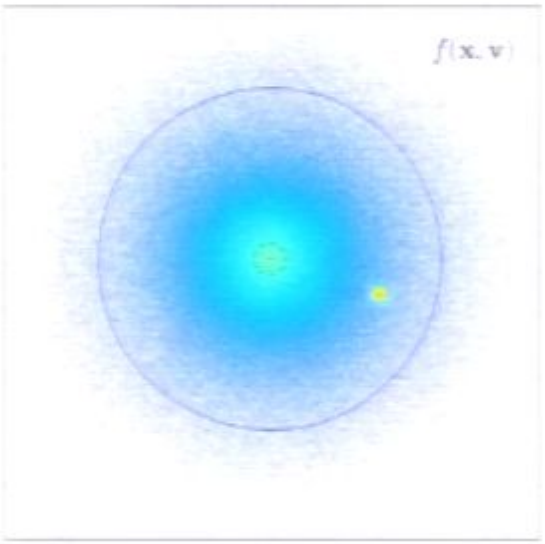
$f(\mathbf{x}, \mathbf{v})$

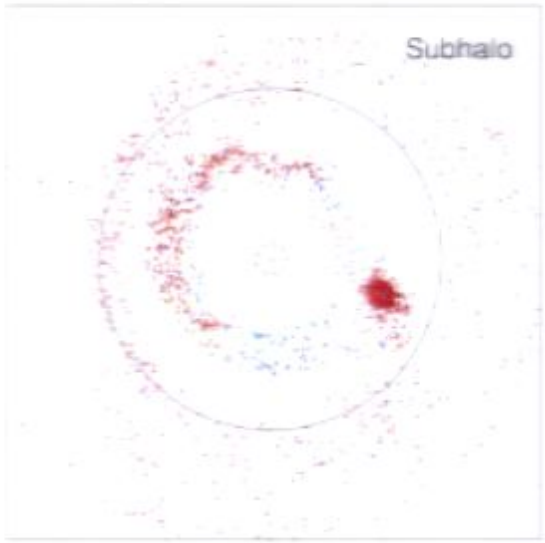
Subhalo

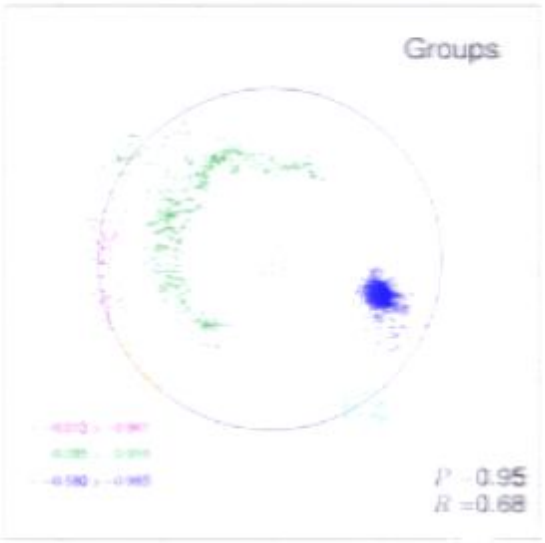
Groups
P =0.95
R =0.68

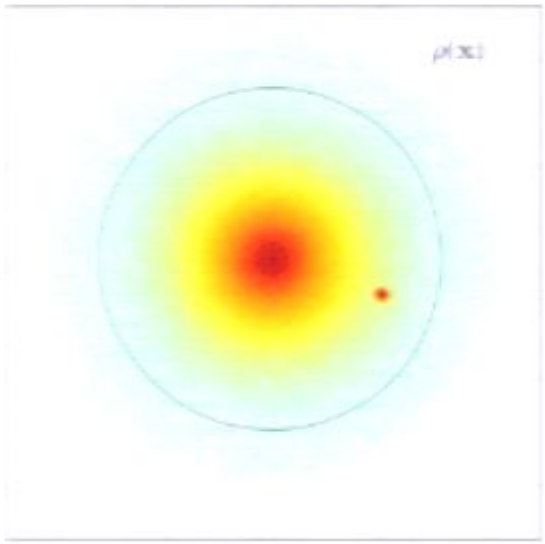
$\rho(\mathbf{x})$

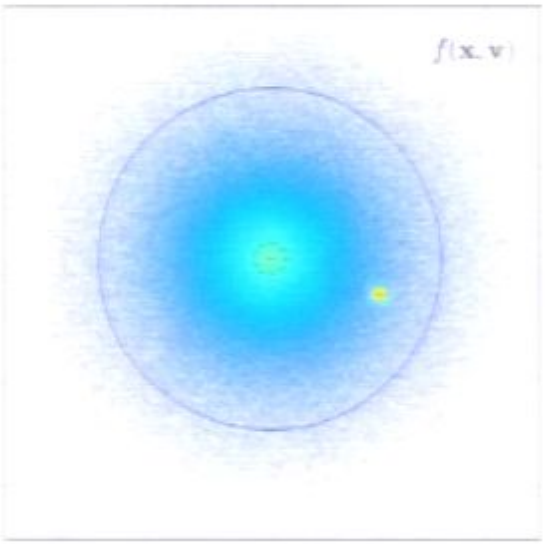
$f(\mathbf{x}, \mathbf{v})$

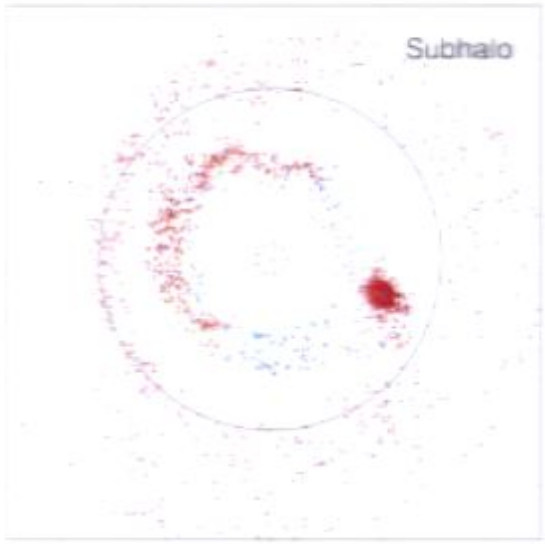
Subhalo

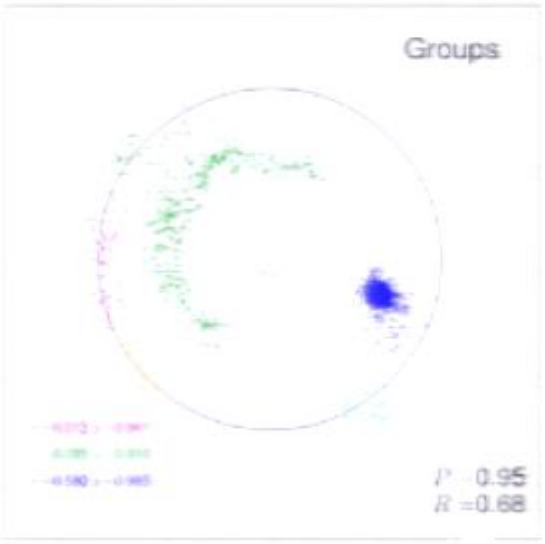
Groups
P 0.95
R =0.68

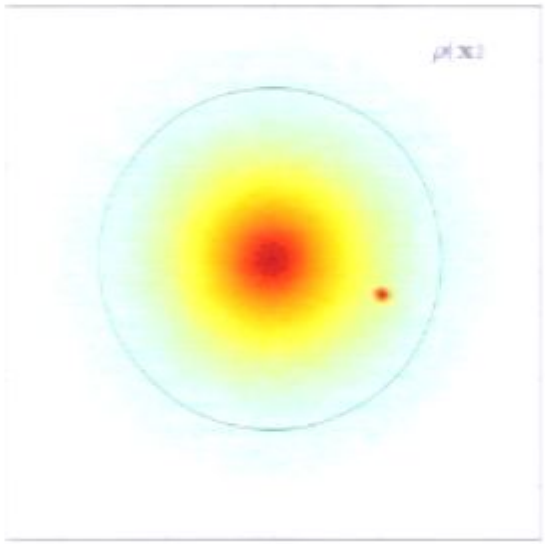
$\rho(\mathbf{x})$

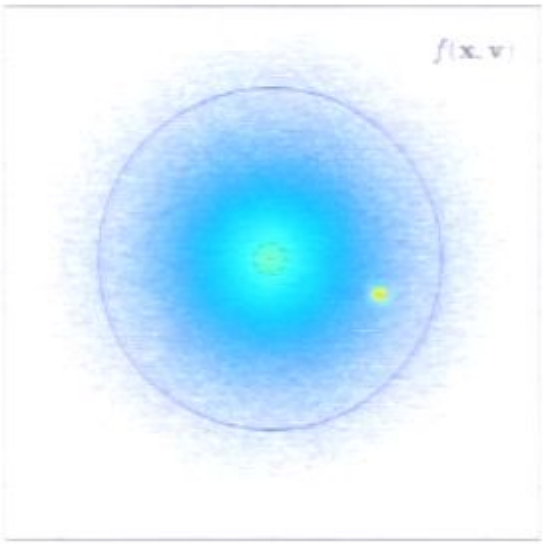
$f(\mathbf{x}, \mathbf{v})$

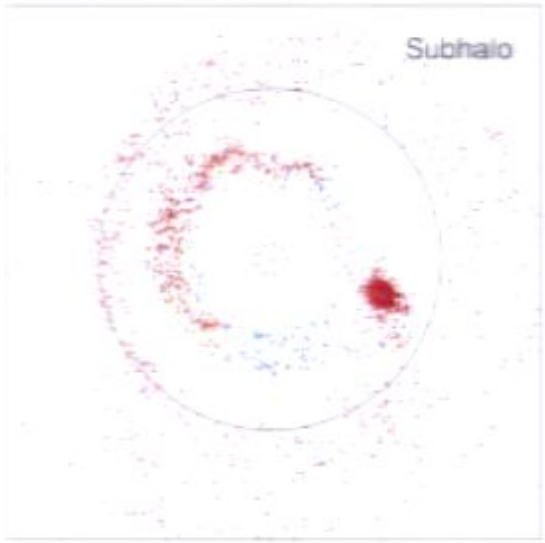
Subhalo

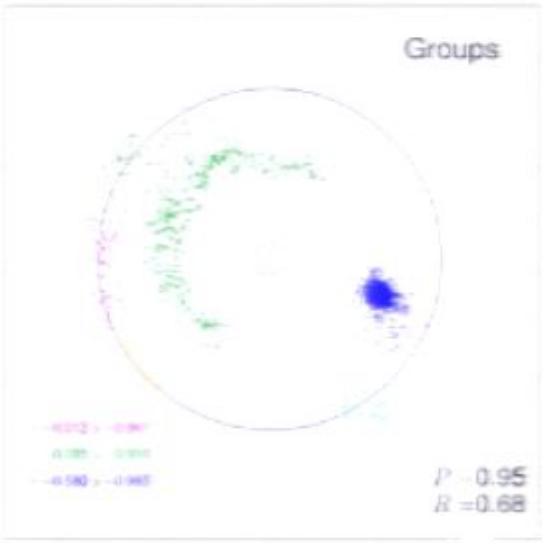
Groups
P =0.95
R =0.68

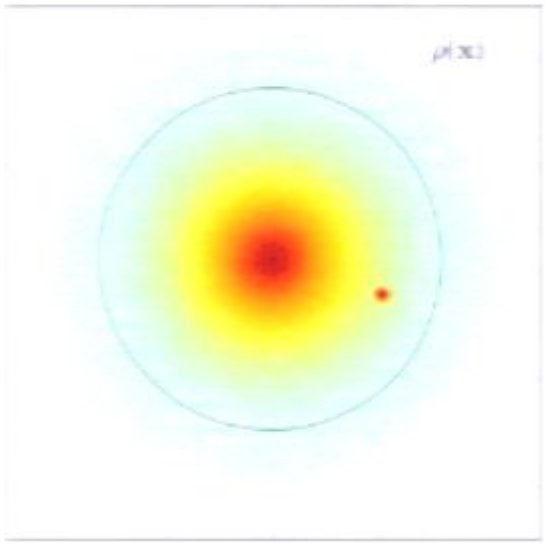
$\rho(\mathbf{x})$

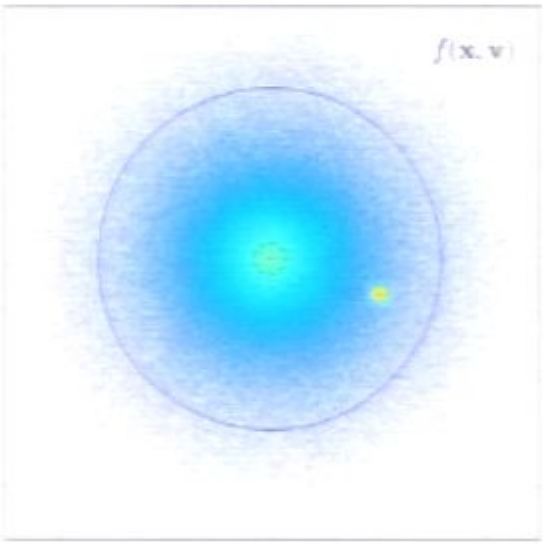
$f(\mathbf{x}, \mathbf{v})$

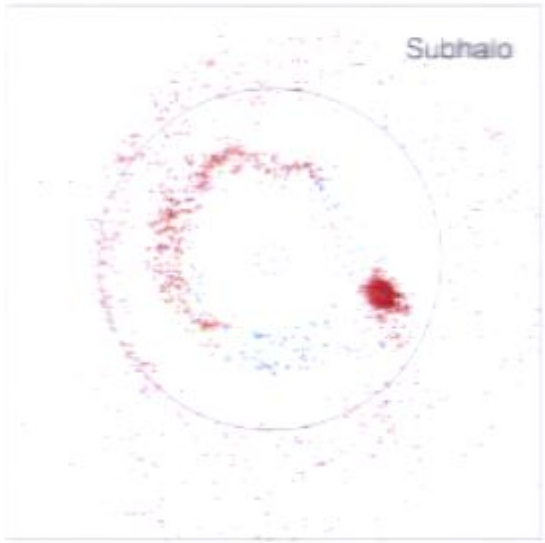
Subhalo

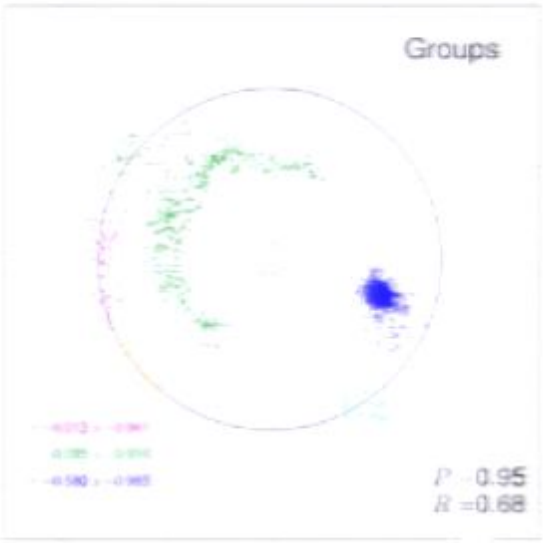
Groups
P =0.95
R =0.68

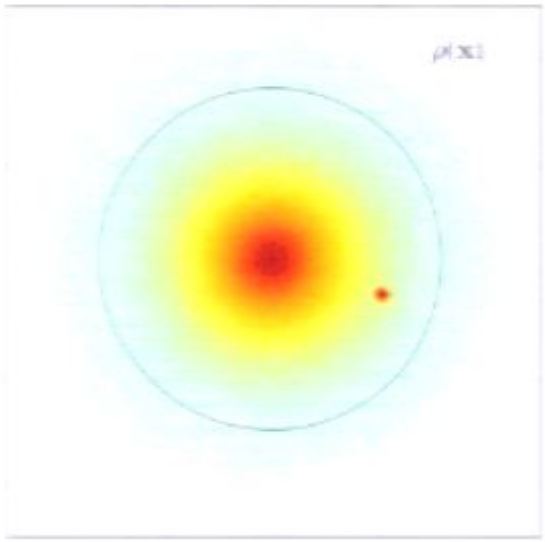
$\rho(\mathbf{x})$

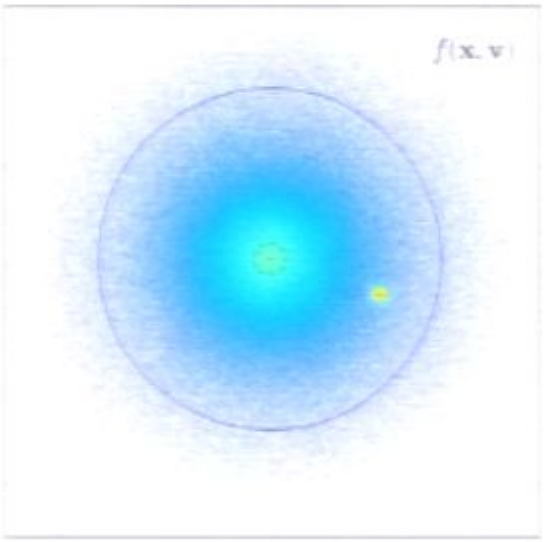
$f(\mathbf{x}, \mathbf{v})$

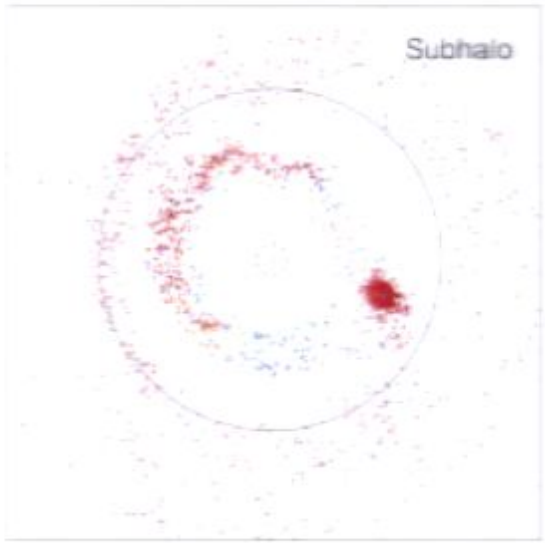
Subhalo

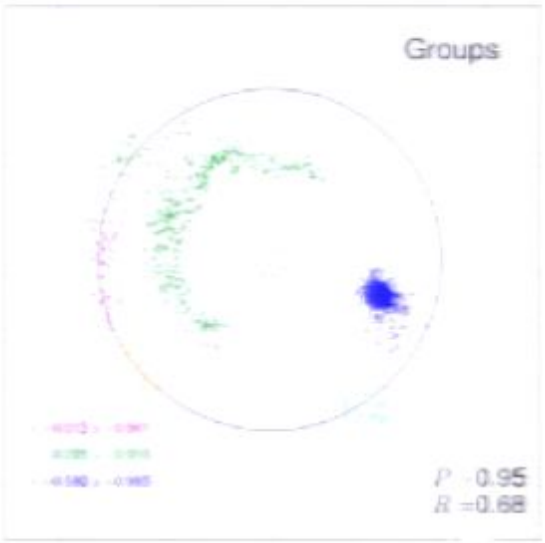
Groups
P 0.95
R =0.68

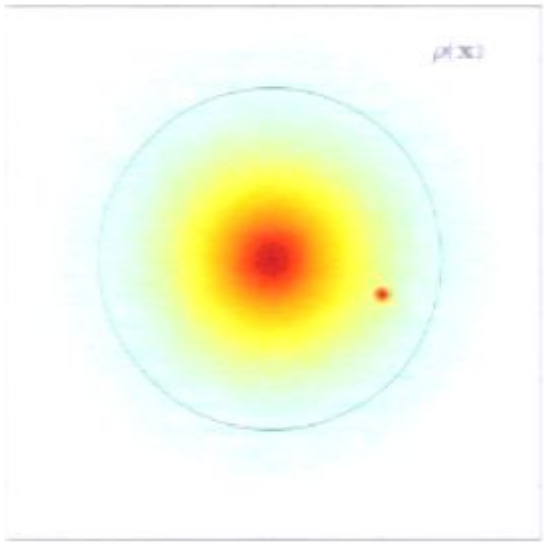
$\rho(\mathbf{x})$

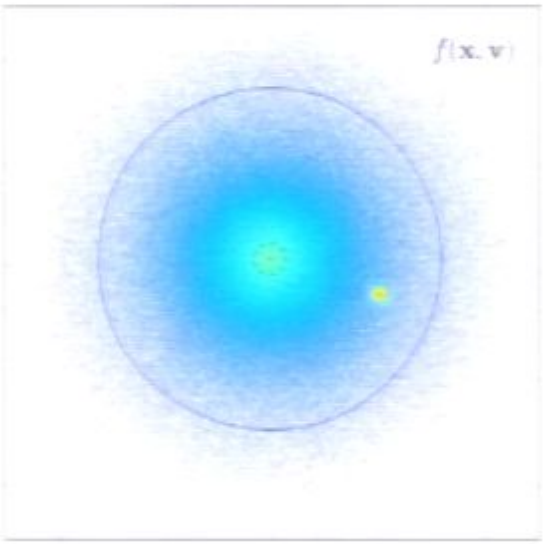
$f(\mathbf{x}, \mathbf{v})$

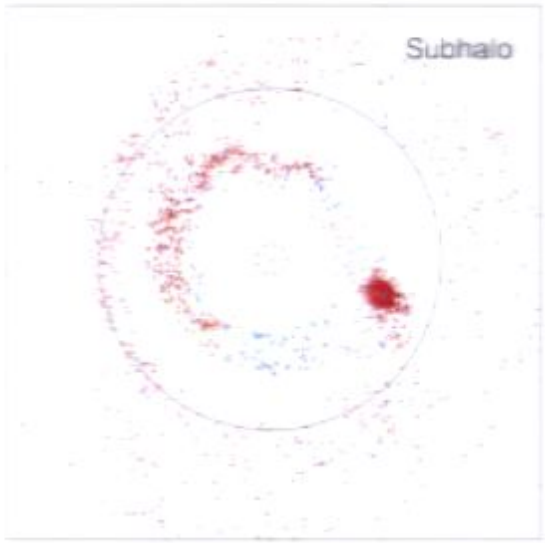
Subhalo

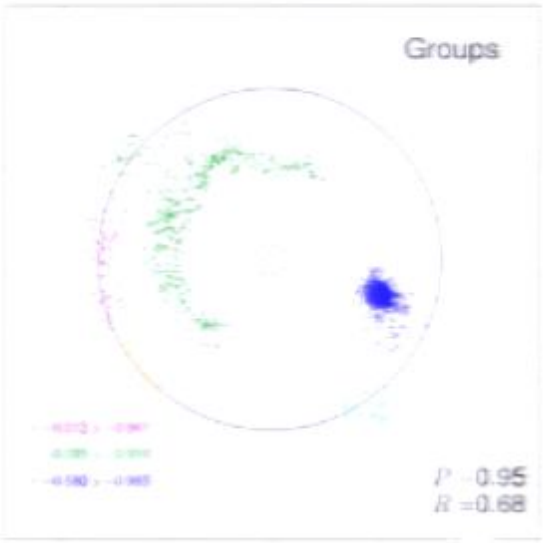
Groups
P =0.95
R =0.68

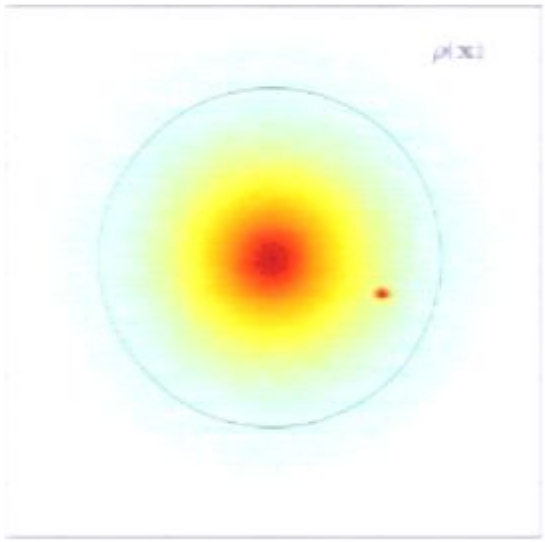
$\rho(\mathbf{x})$

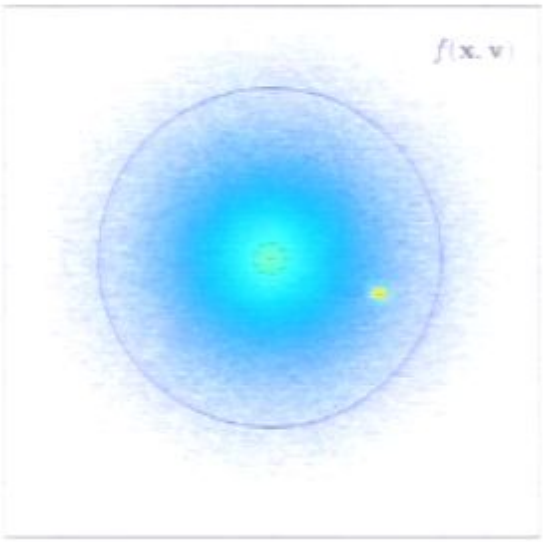
$f(\mathbf{x}, \mathbf{v})$

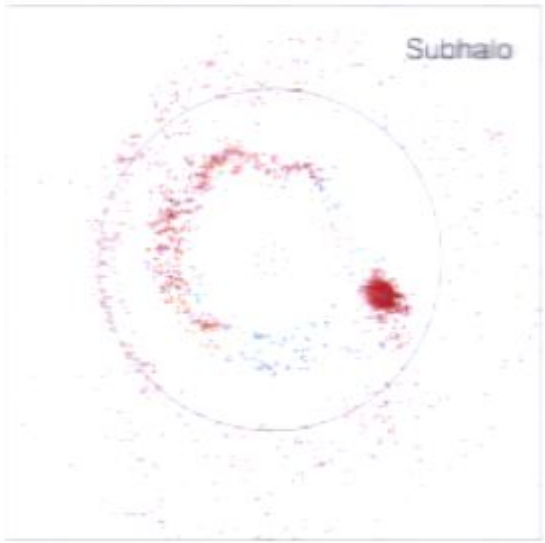
Subhalo

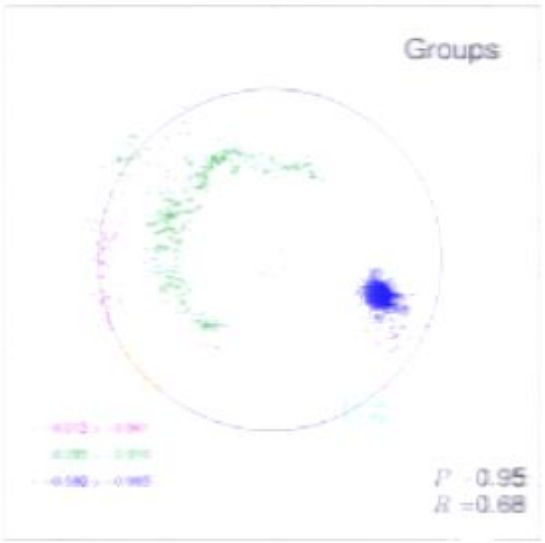
Groups
P 0.95
R =0.68

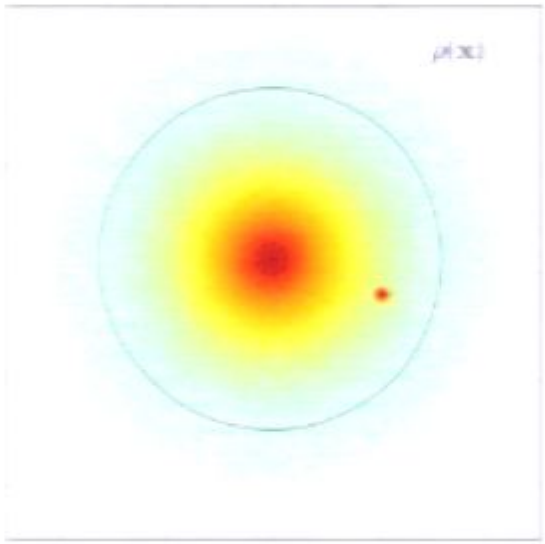
$\rho(\mathbf{x})$

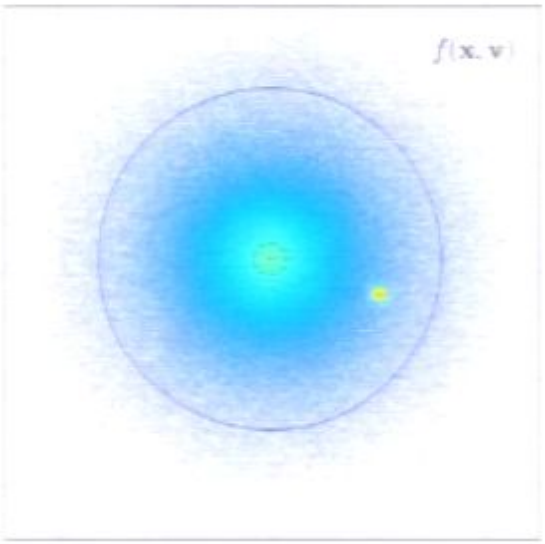
$f(\mathbf{x}, \mathbf{v})$

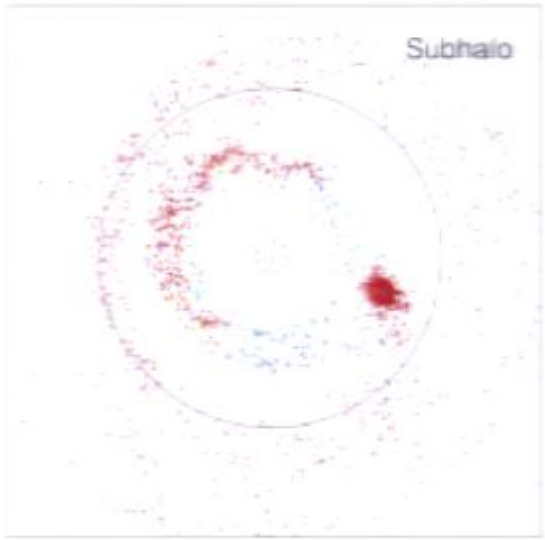
Subhalo

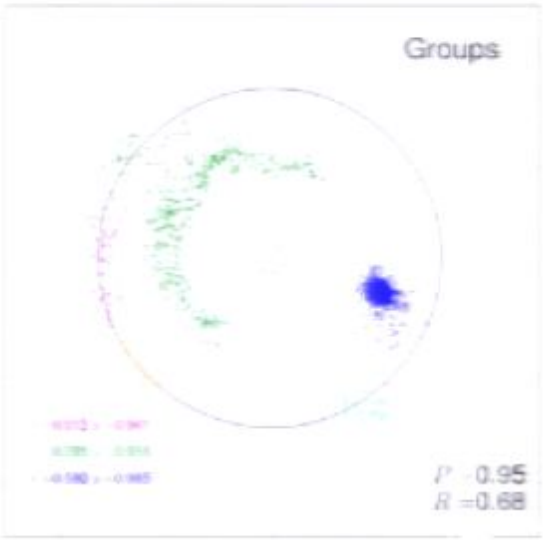
Groups
P 0.95
R =0.68

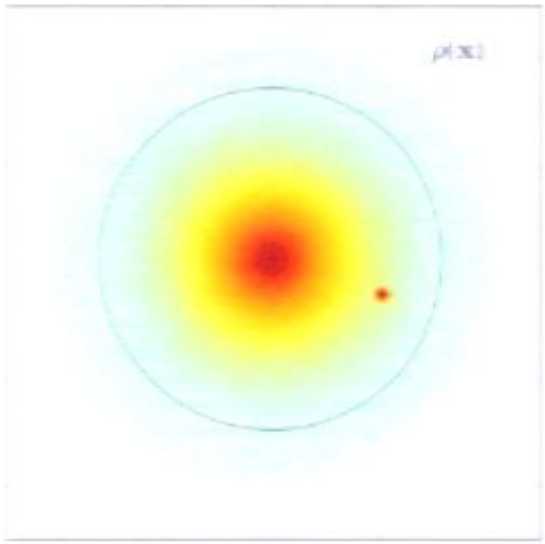
$\rho(\mathbf{x})$

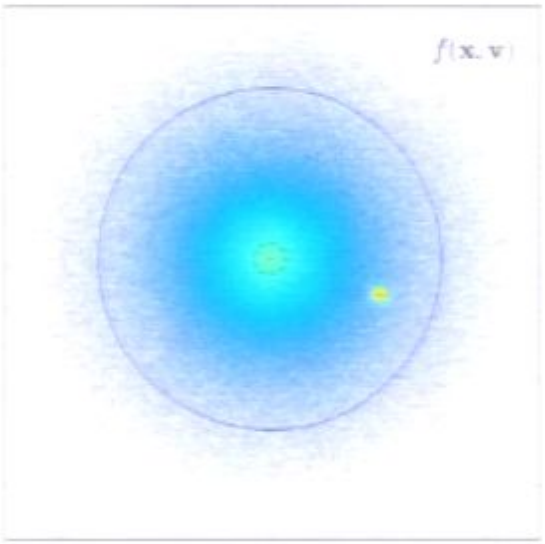
$f(\mathbf{x}, \mathbf{v})$

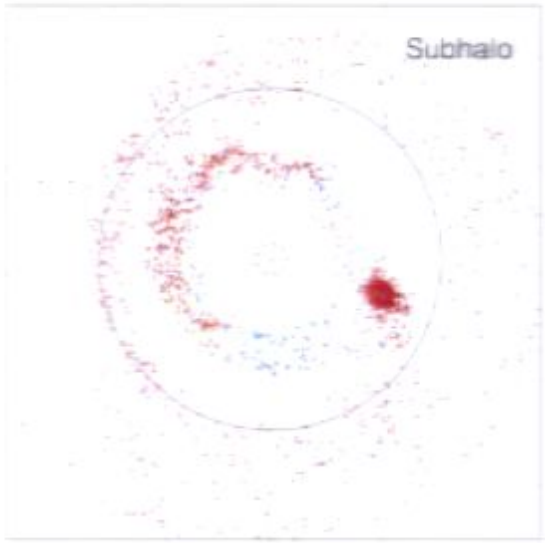
Subhalo

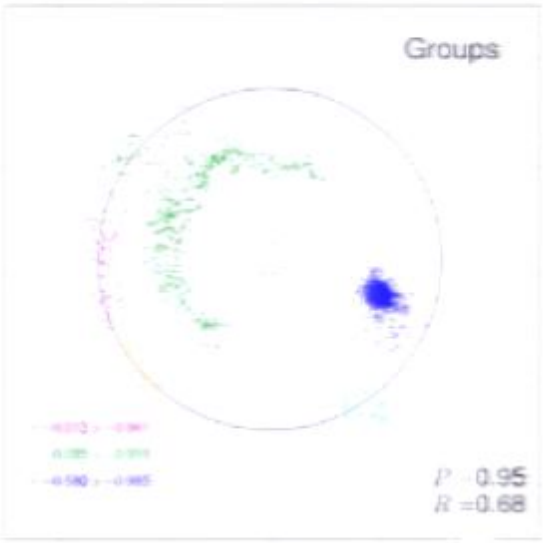
Groups
P 0.95
R =0.68

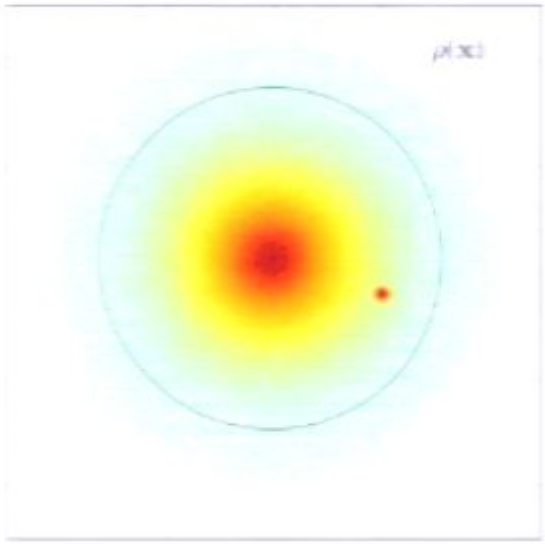
$\rho(\mathbf{x})$

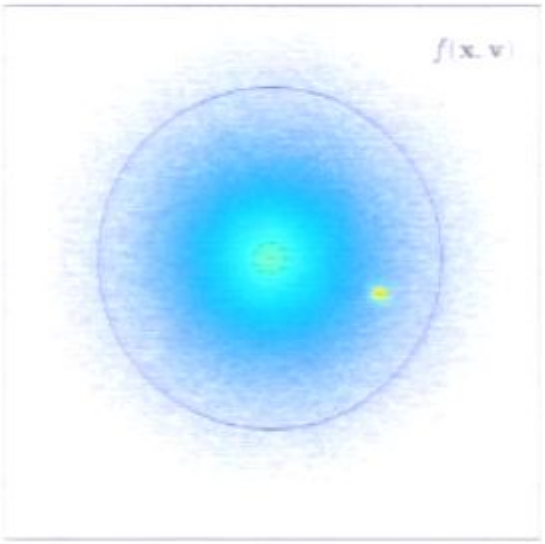
$f(\mathbf{x}, \mathbf{v})$

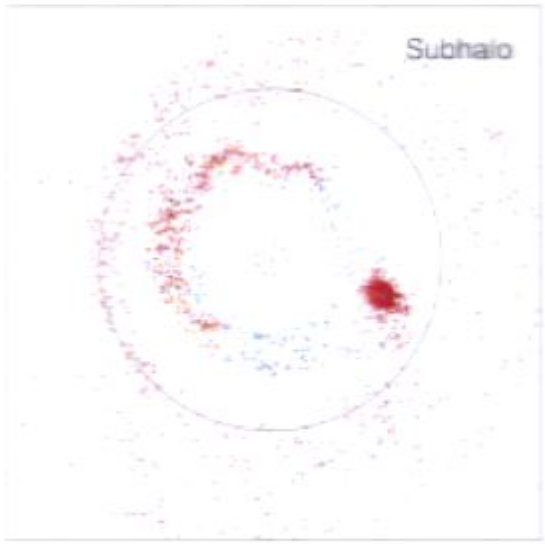
Subhalo

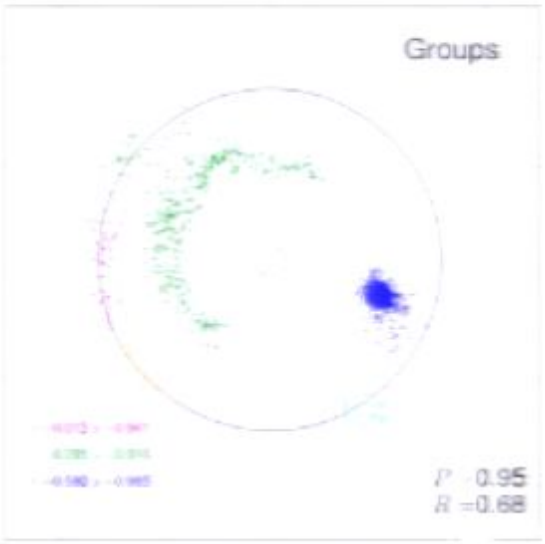
Groups
P 0.95
R =0.68

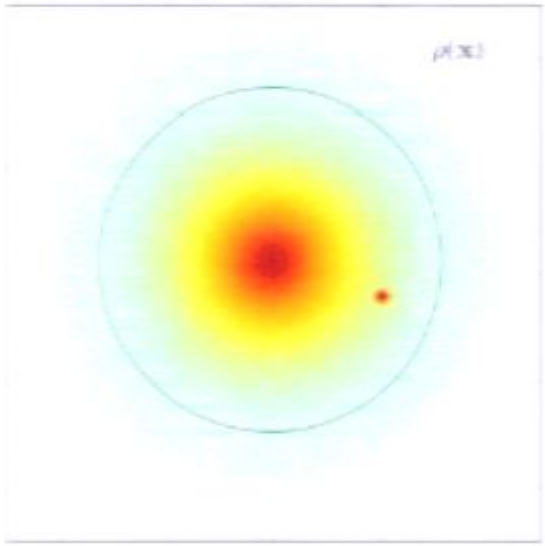
$\rho(\mathbf{x})$

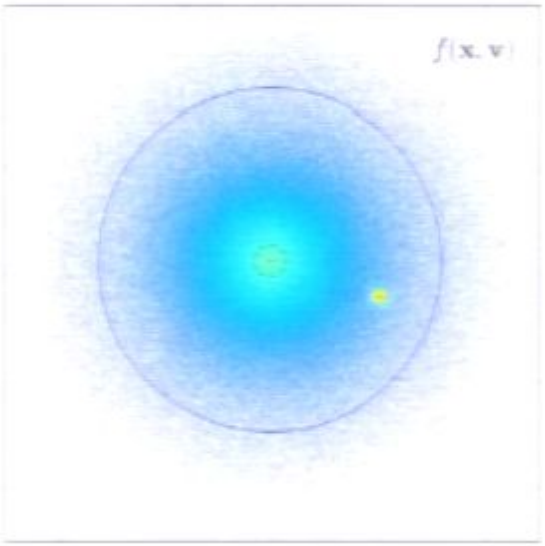
$f(\mathbf{x}, \mathbf{v})$

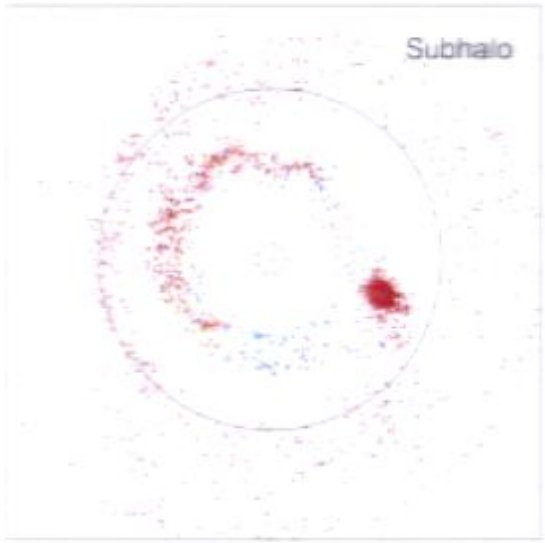
Subhalo

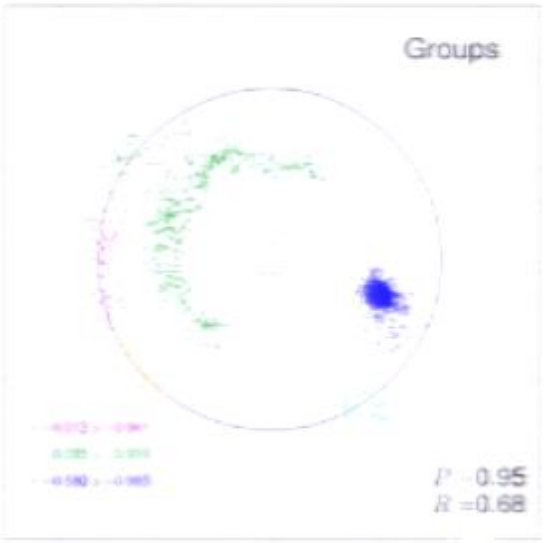
Groups
P 0.95
R =0.68

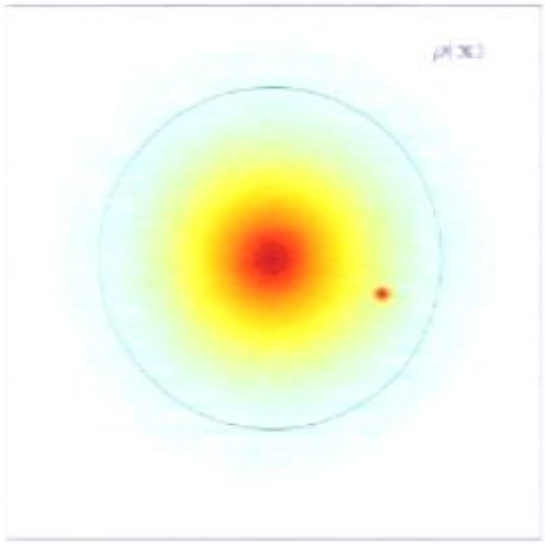

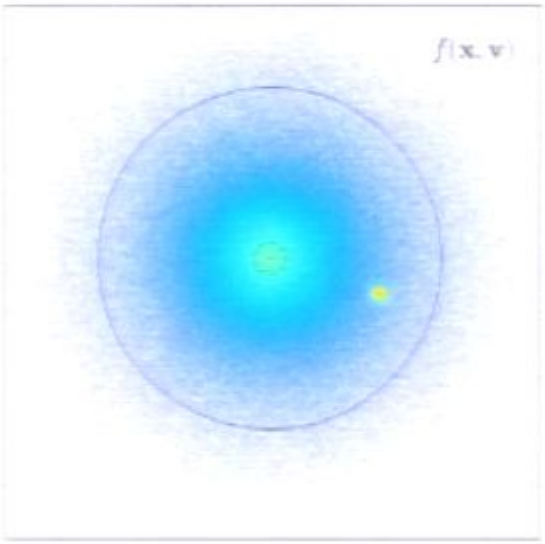
f(x, v)

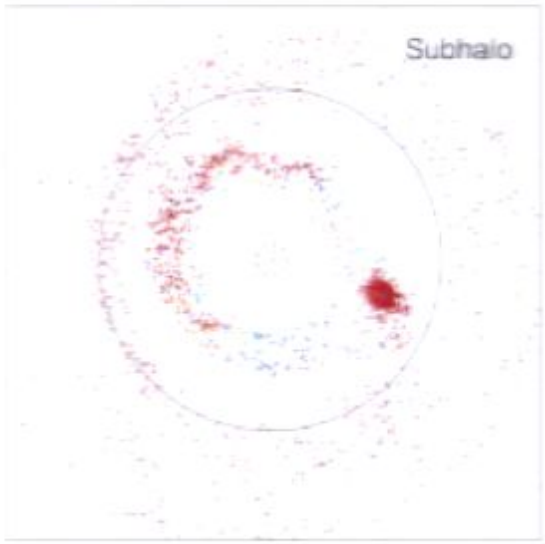
Subhalo

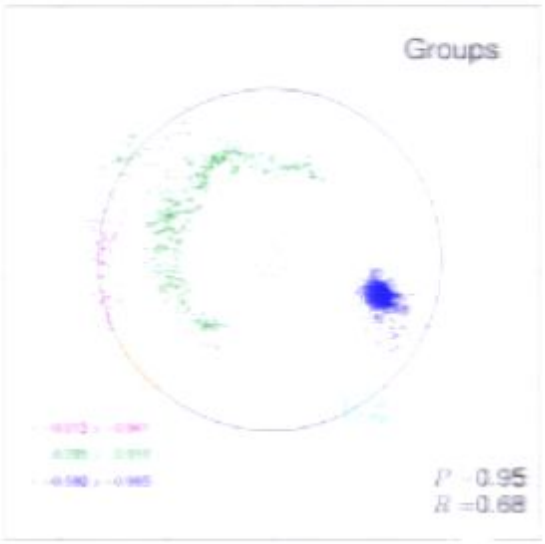
Groups
P 0.95
R =0.68

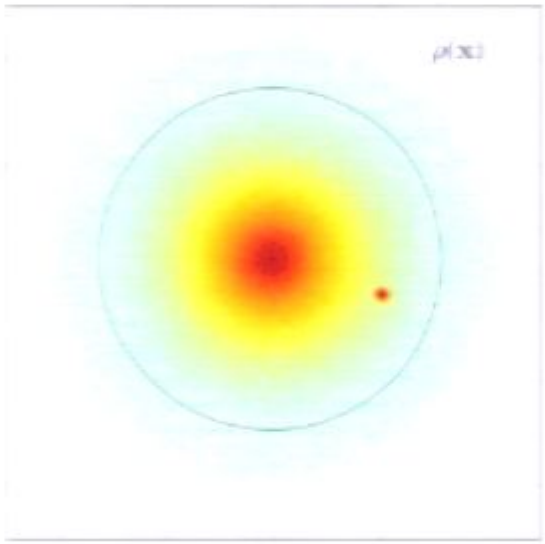
$\rho(\mathbf{x})$

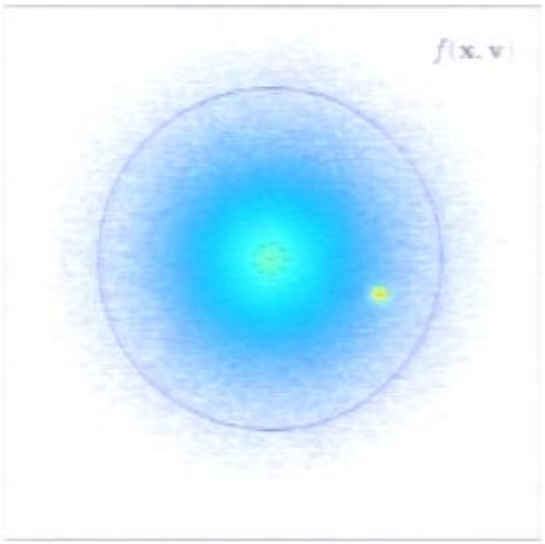
$f(\mathbf{x}, \mathbf{v})$

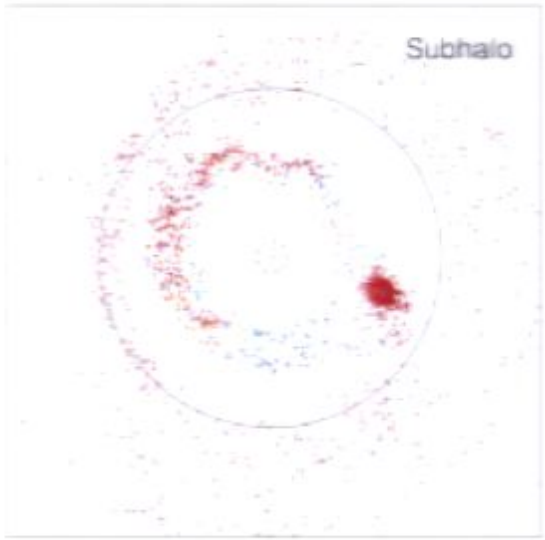
Subhalo

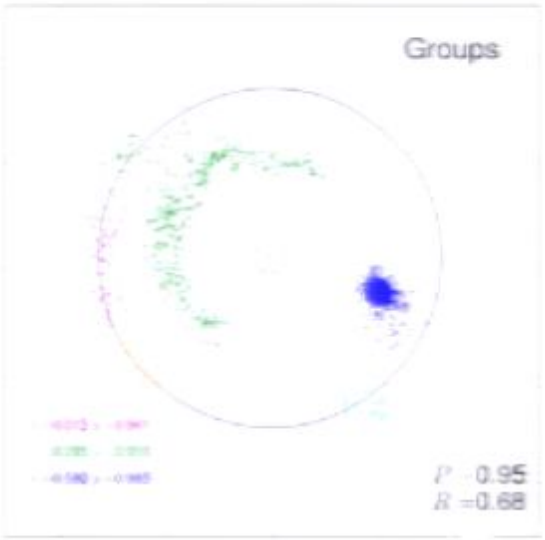
Groups
P 0.95
R =0.68

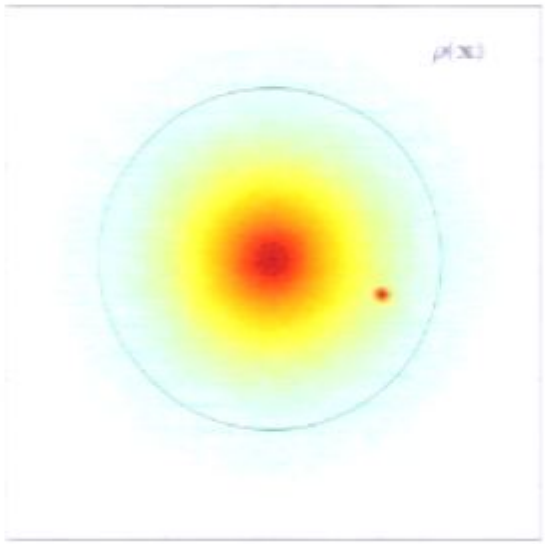
$\rho(\mathbf{x})$

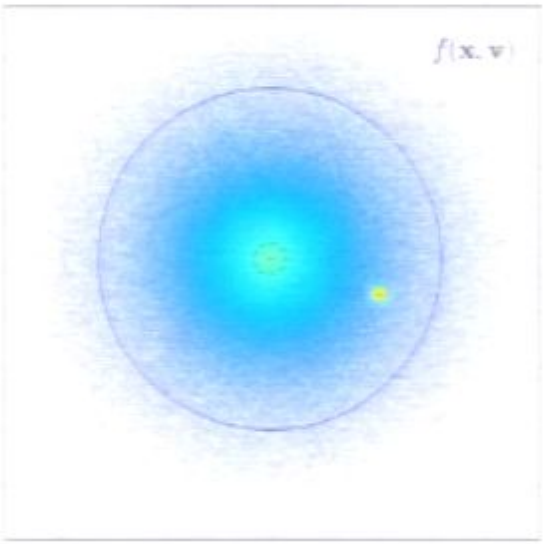
$f(\mathbf{x}, \mathbf{v})$

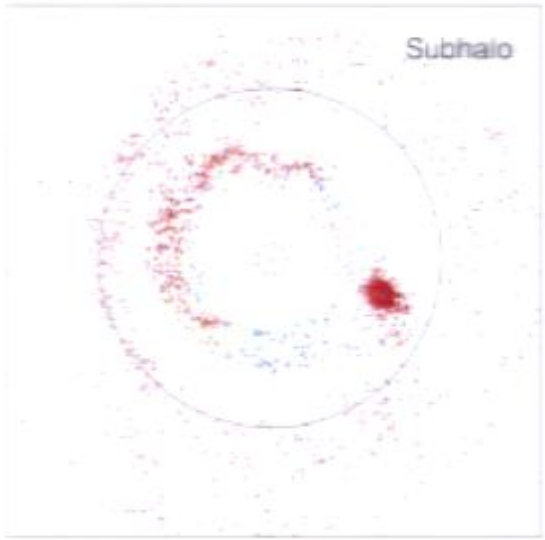
Subhalo

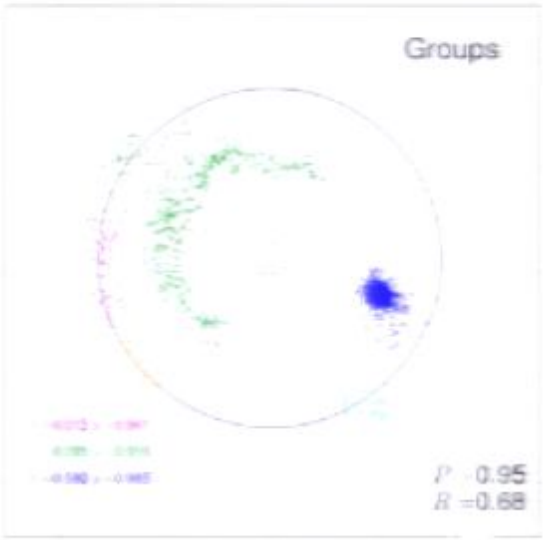
Groups
P 0.95
R =0.68

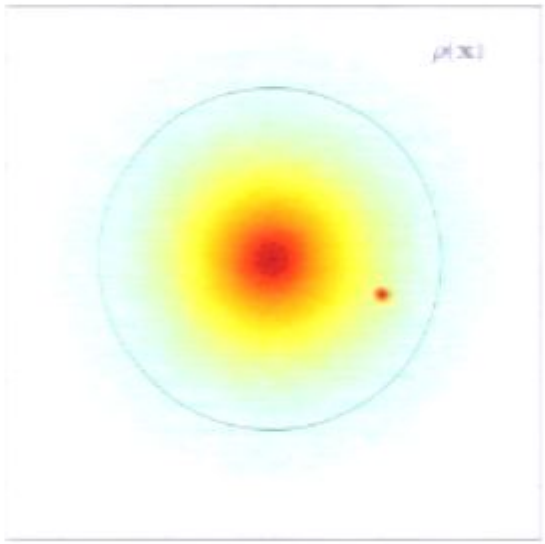
$\rho(\mathbf{x})$

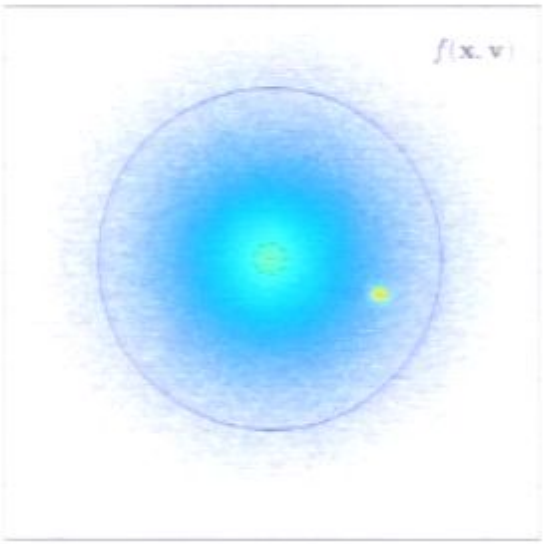
$f(\mathbf{x}, \mathbf{v})$

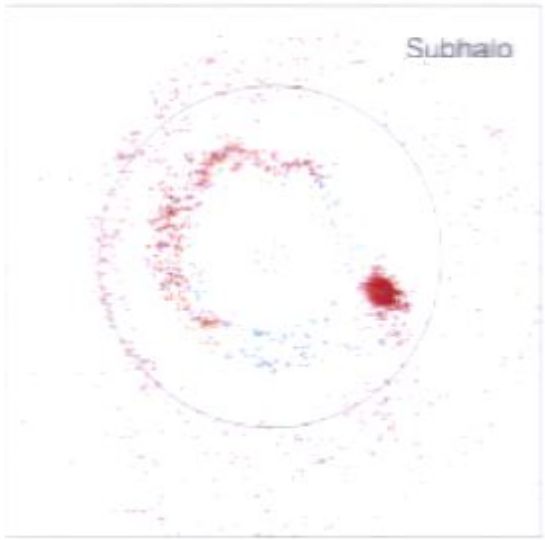
Subhalo

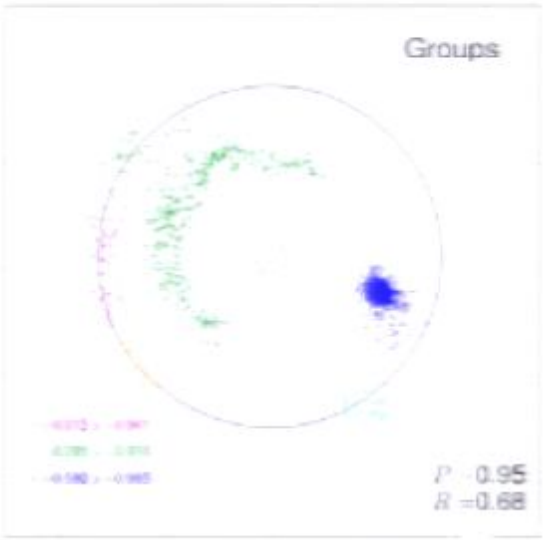
Groups
P 0.95
R =0.68

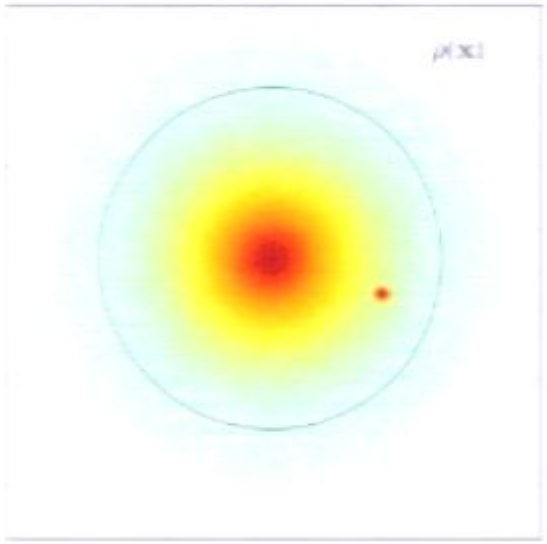
ρ(x)

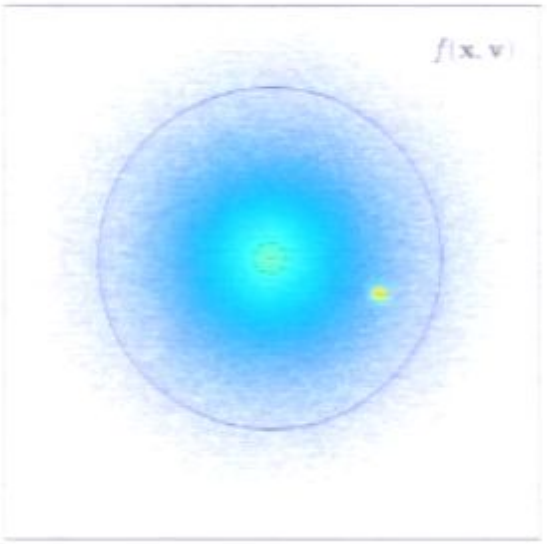
f(x, v)

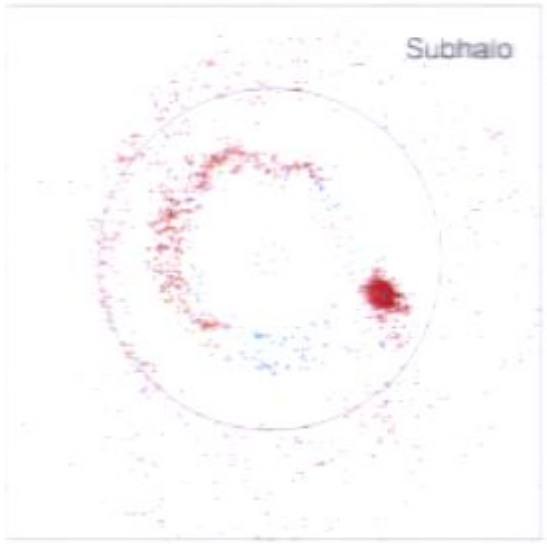
Subhalo

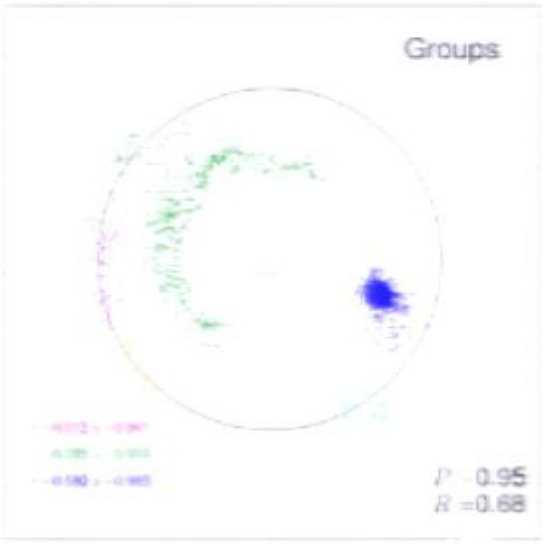
Groups
P 0.95
R =0.68

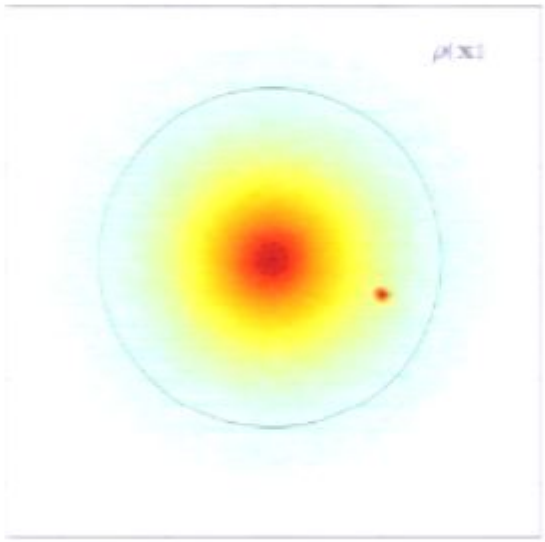
$\rho(\mathbf{x})$

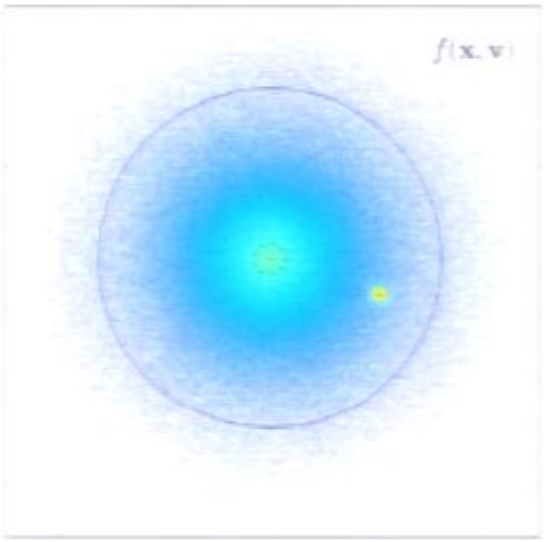
$f(\mathbf{x}, \mathbf{v})$

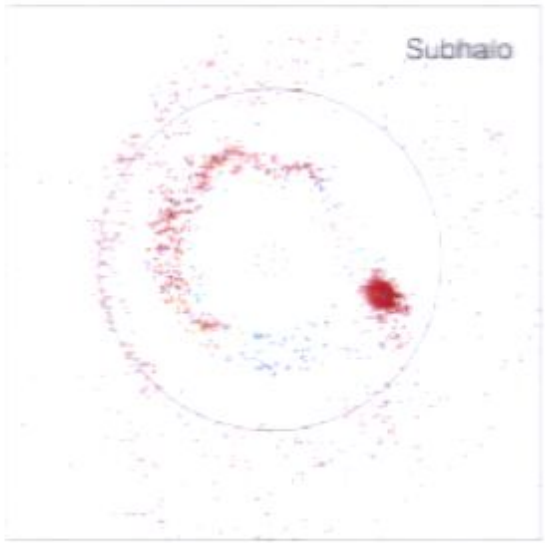
Subhalo

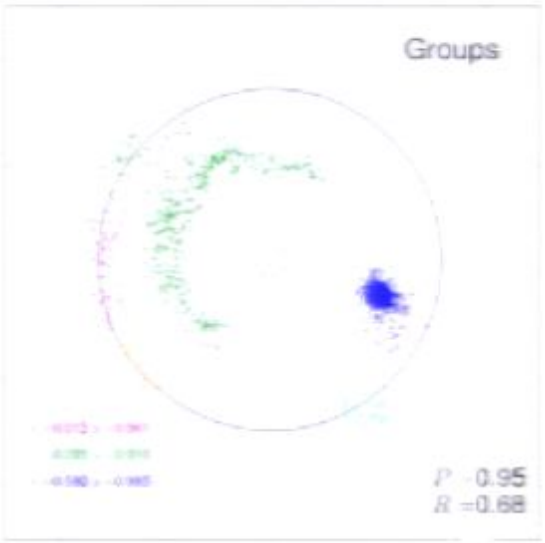
Groups
P 0.95
R =0.68

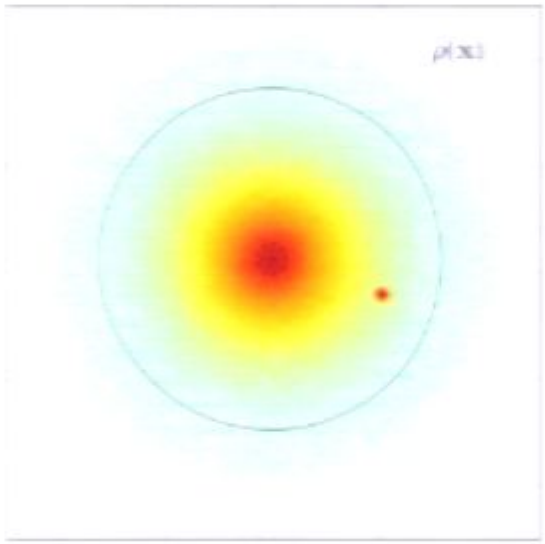
$\rho(\mathbf{x})$

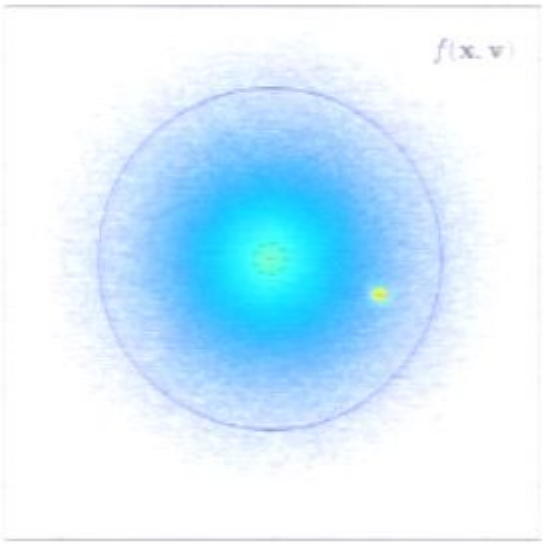
$f(\mathbf{x}, \mathbf{v})$

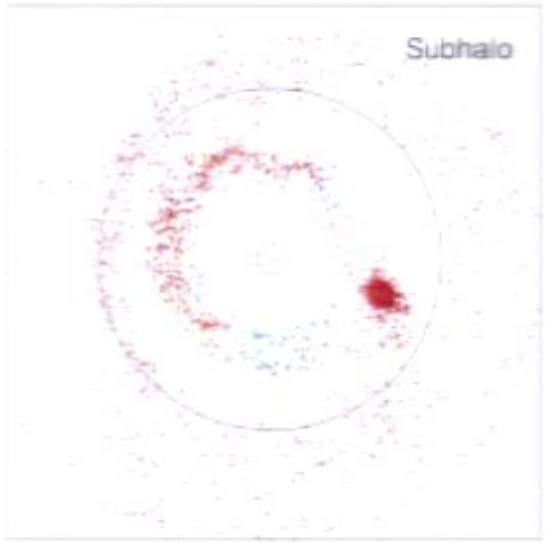
Subhalo

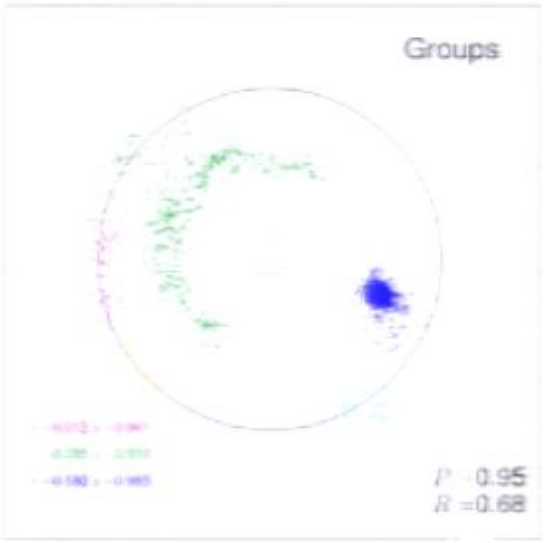
Groups
P 0.95
R =0.68

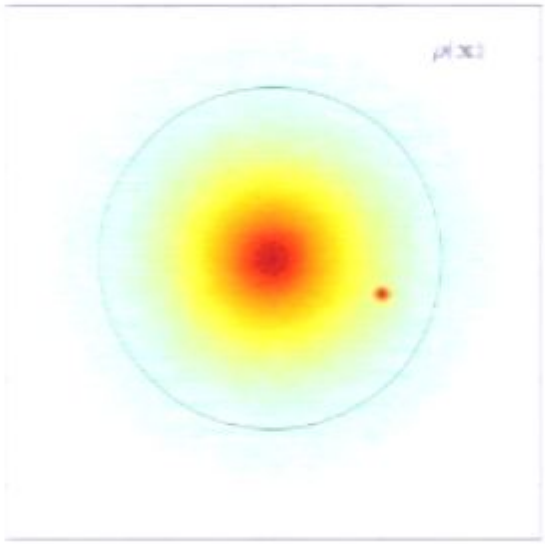

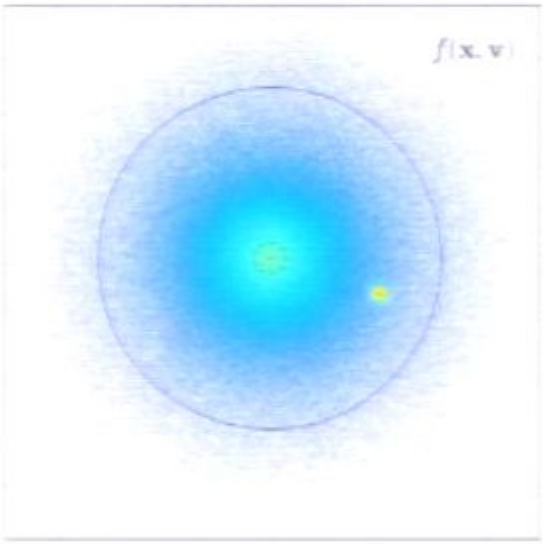

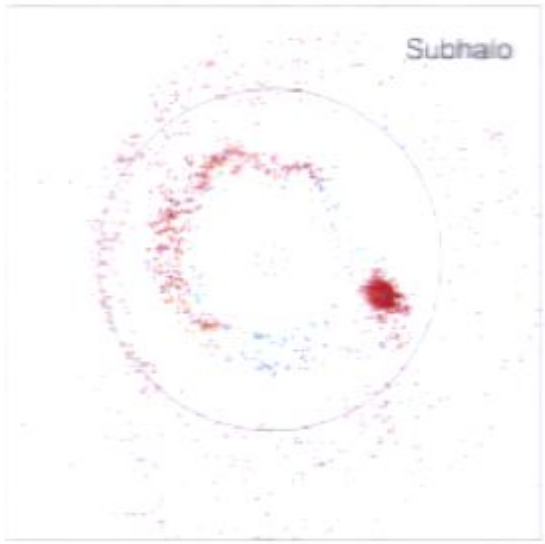
Subhalo

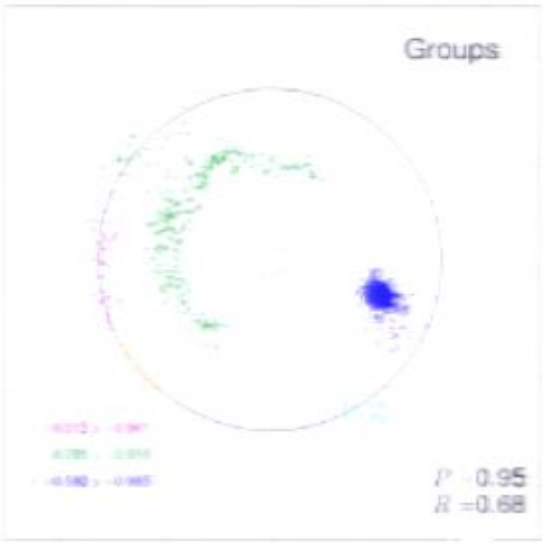
Groups
P 0.95
R =0.68

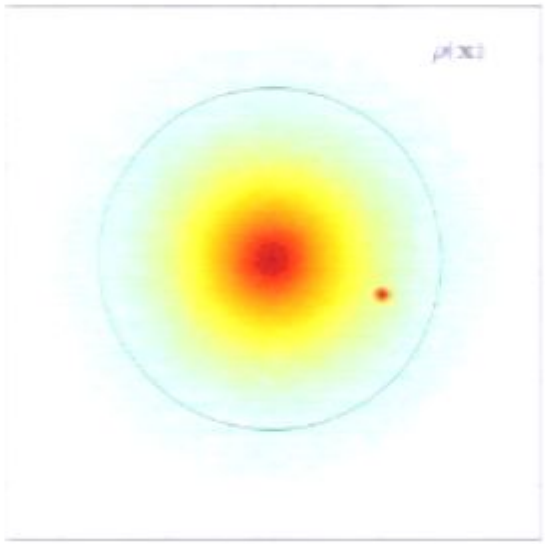
$\rho(\mathbf{x})$

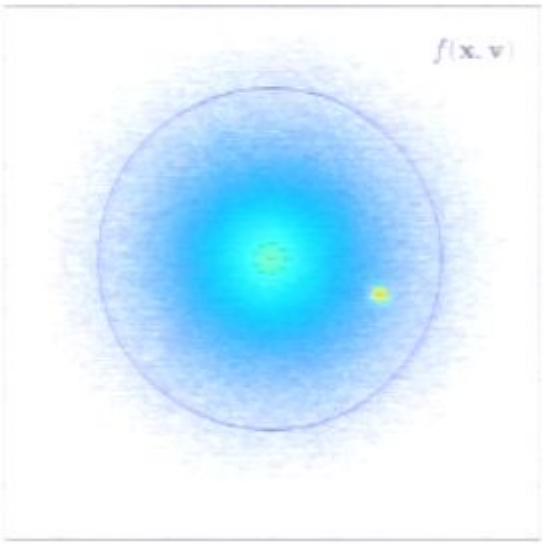
$f(\mathbf{x}, \mathbf{v})$

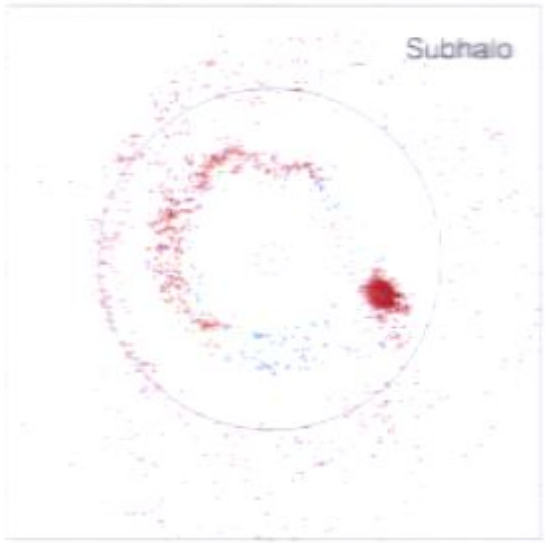
Subhalo

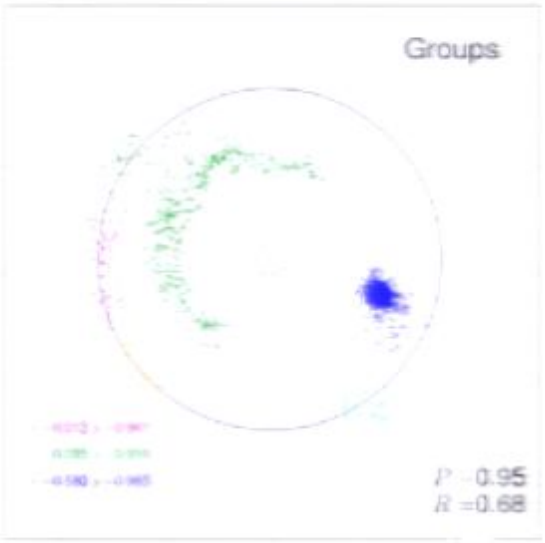
Groups
P =0.95
R =0.68

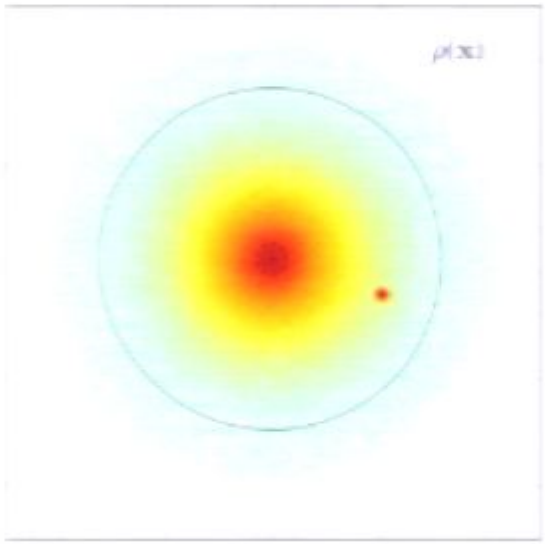
$\rho(\mathbf{x})$

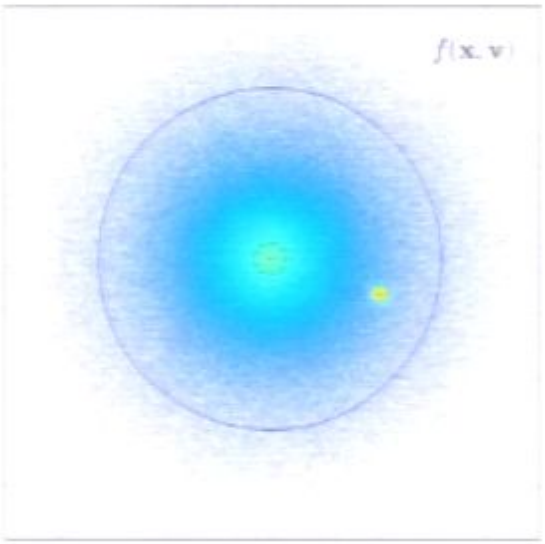
$f(\mathbf{x}, \mathbf{v})$

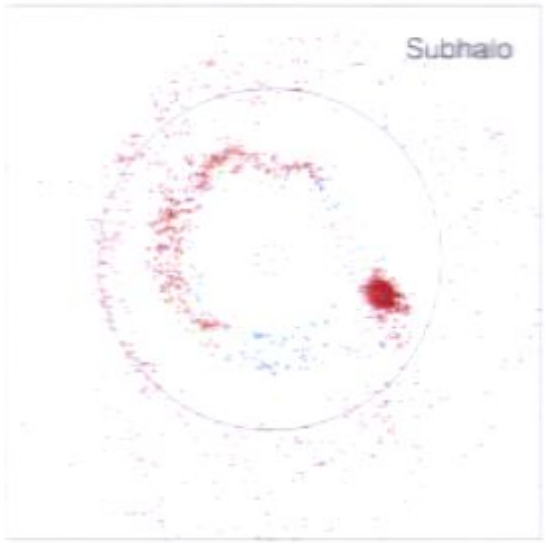
Subhalo

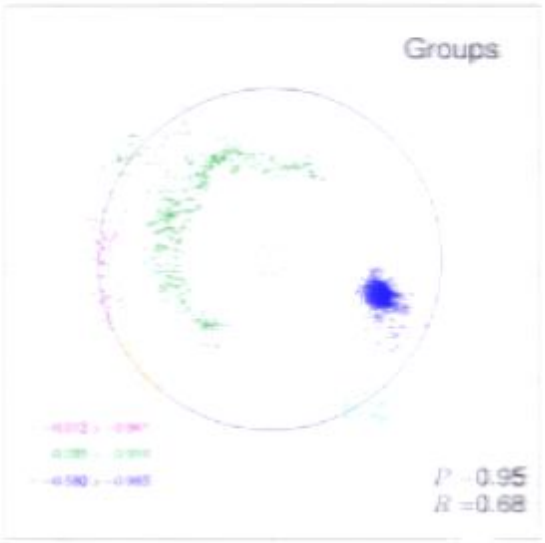
Groups
P =0.95
R =0.68

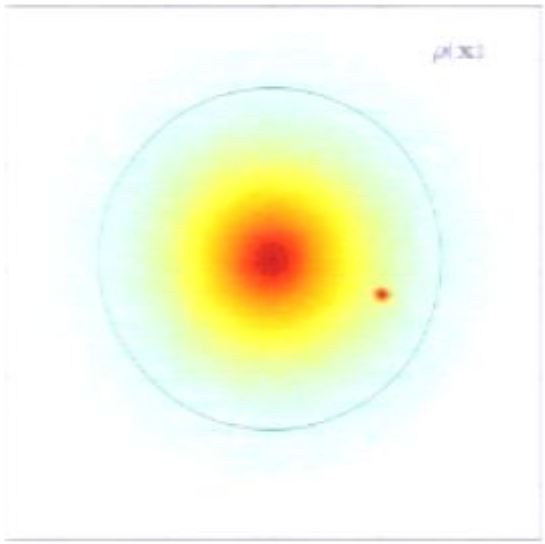
$\rho(\mathbf{x})$

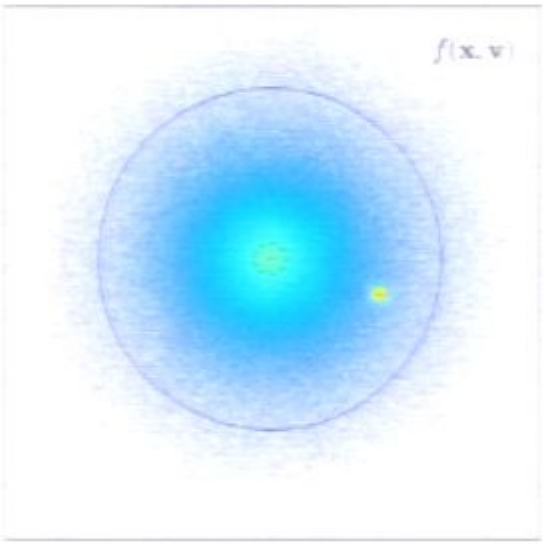
$f(\mathbf{x}, \mathbf{v})$

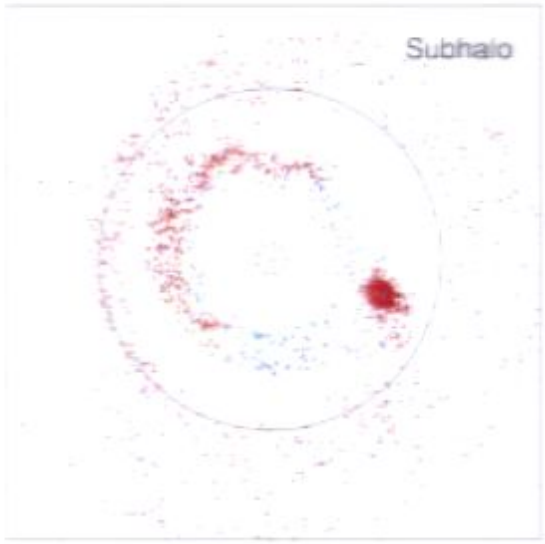
Subhalo

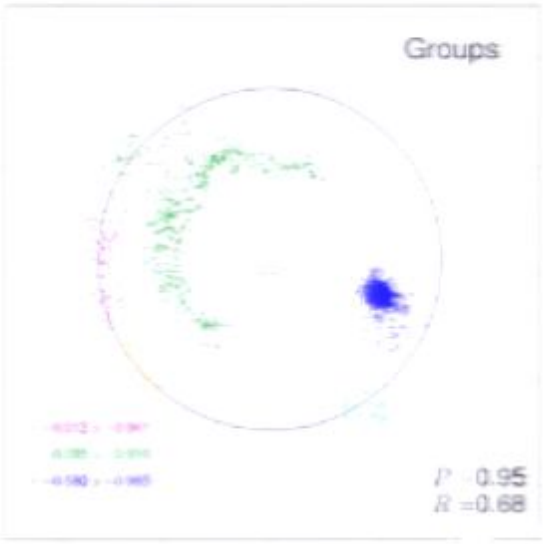
Groups
P 0.95
R =0.68

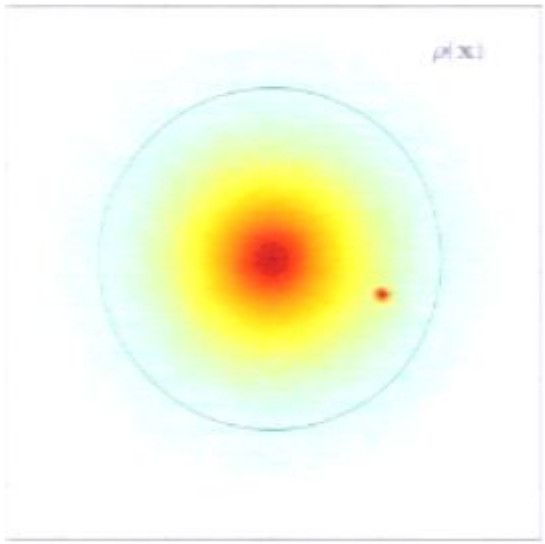
$\rho(\mathbf{x})$

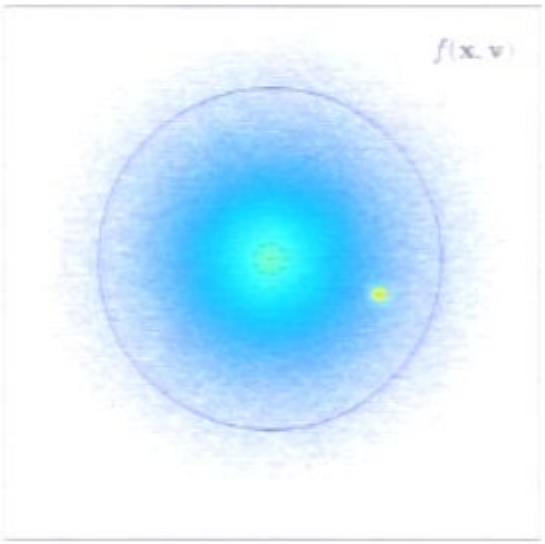
$f(\mathbf{x}, \mathbf{v})$

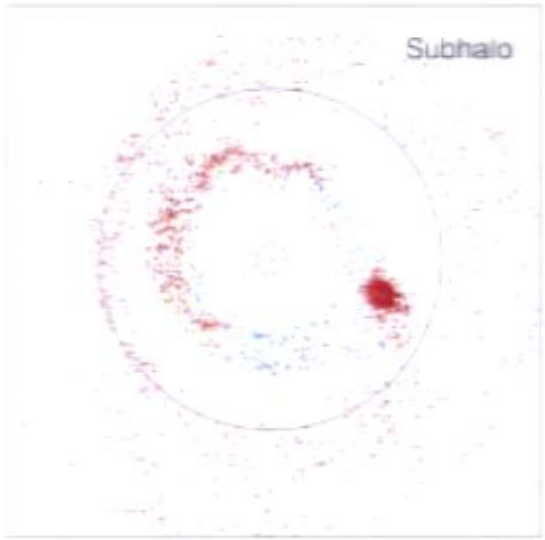
Subhalo

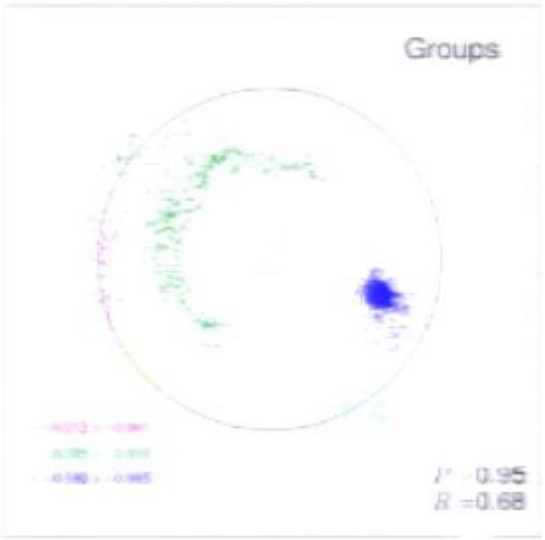
Groups
f' 0.95
R =0.68

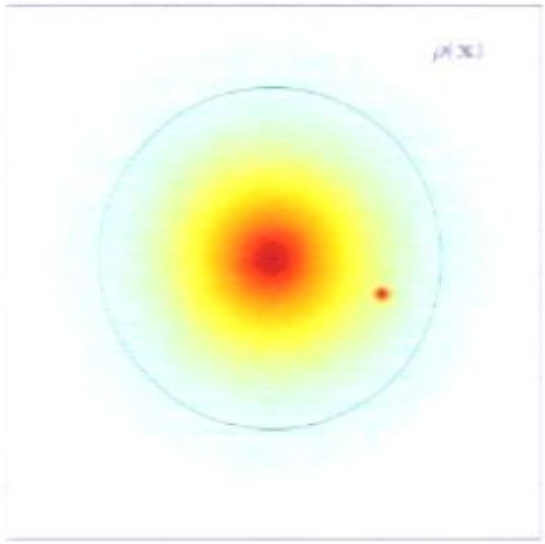
$\rho(\mathbf{x})$

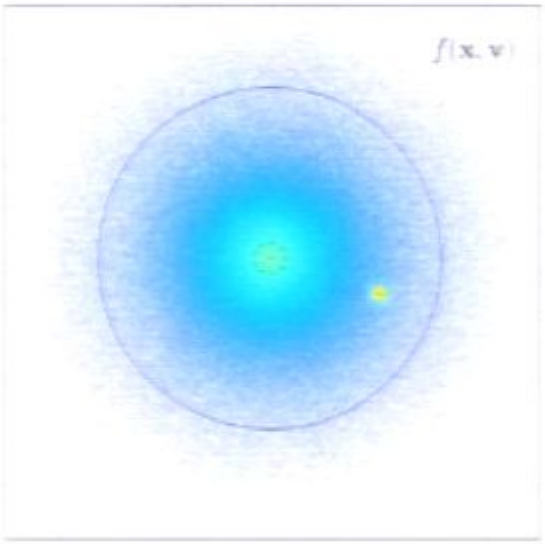
$f(\mathbf{x}, \mathbf{v})$

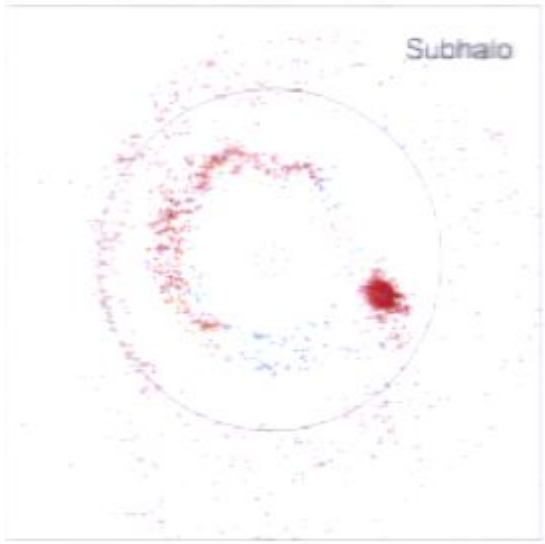
Subhalo

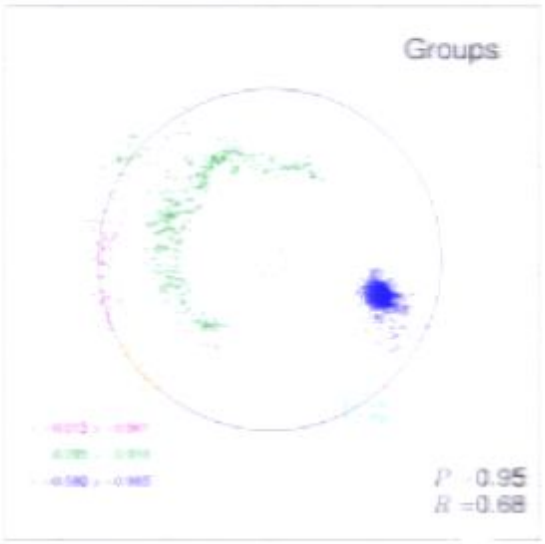
Groups
P 0.95
R =0.68

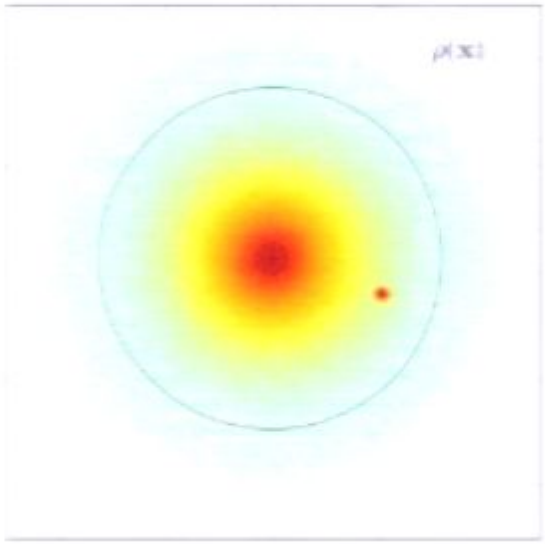
$\rho(\mathbf{x})$

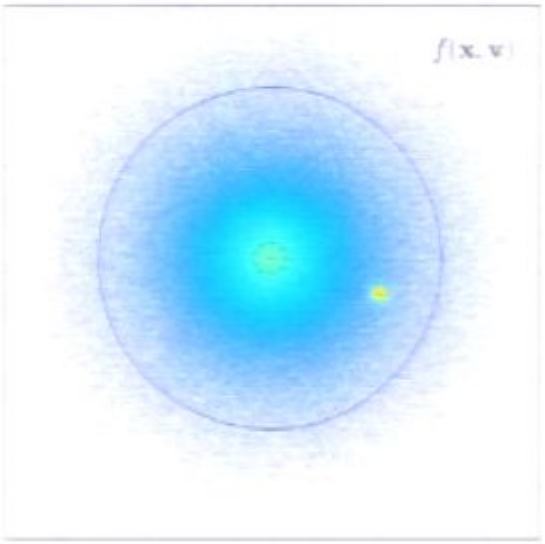
$f(\mathbf{x}, \mathbf{v})$

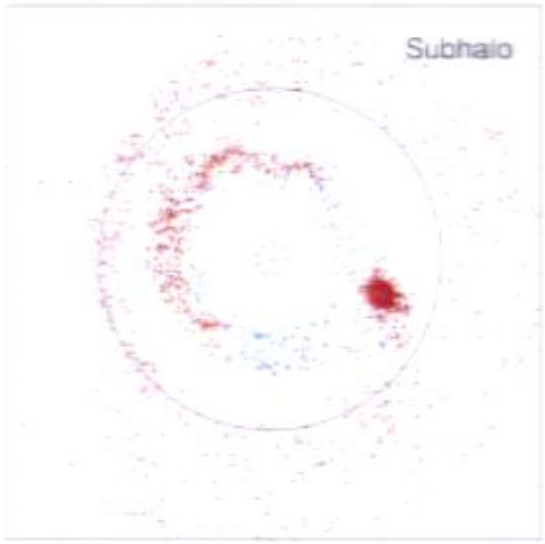
Subhalo

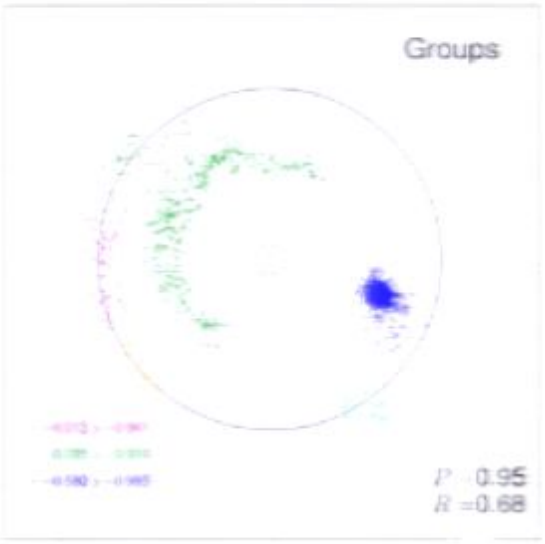
Groups
P 0.95
R =0.68

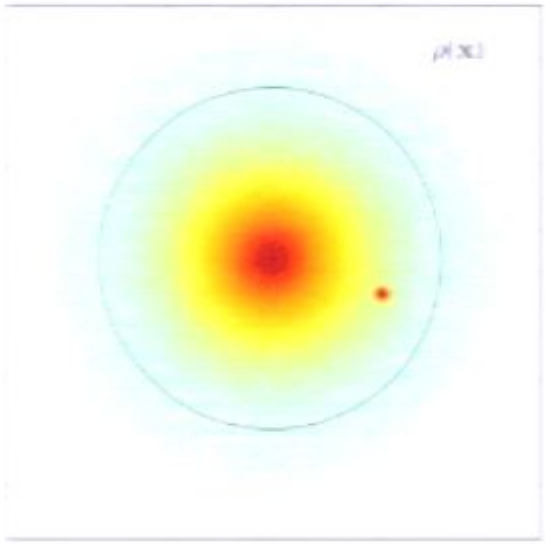
$\rho(\mathbf{x})$

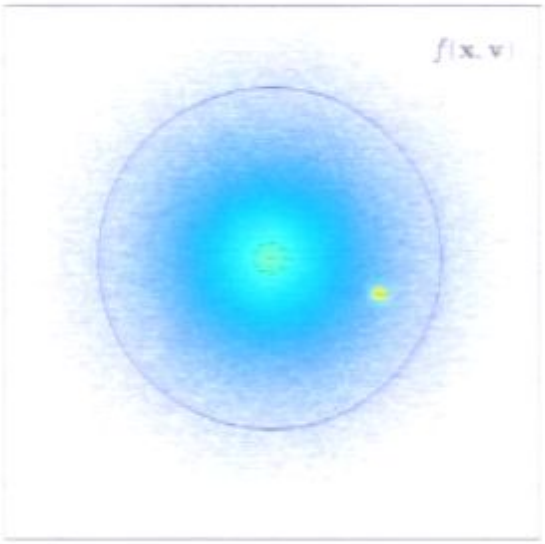
$f(\mathbf{x}, \mathbf{v})$

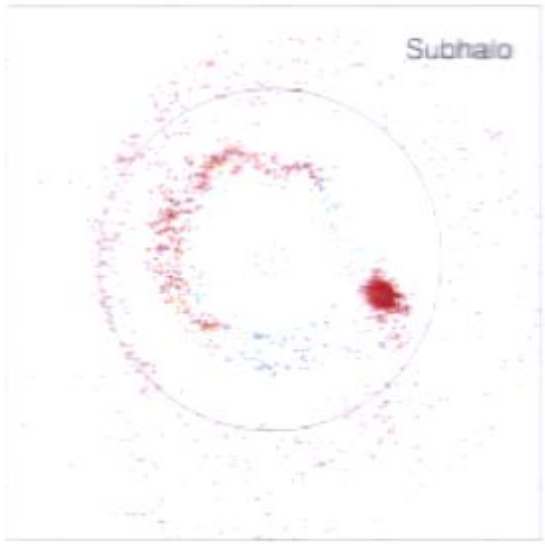
Subhalo

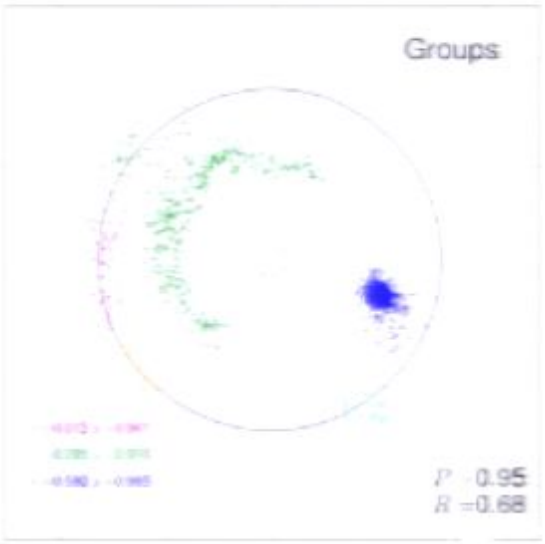
Groups
P 0.95
R =0.68

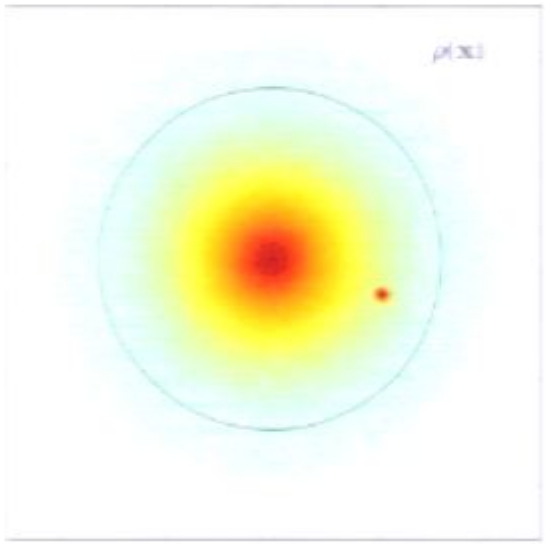
$\rho(\mathbf{x})$

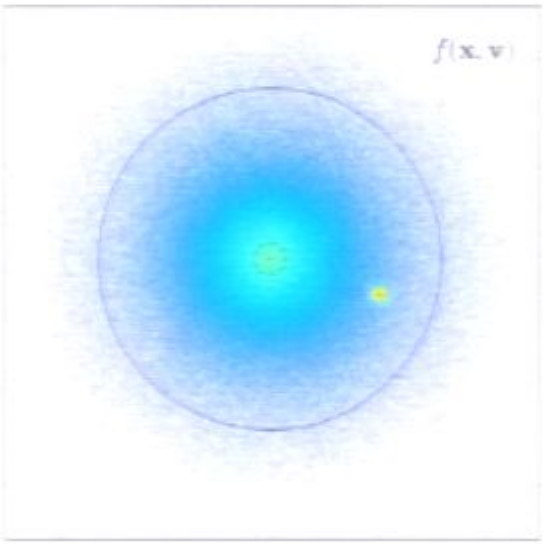
$f(\mathbf{x}, \mathbf{v})$

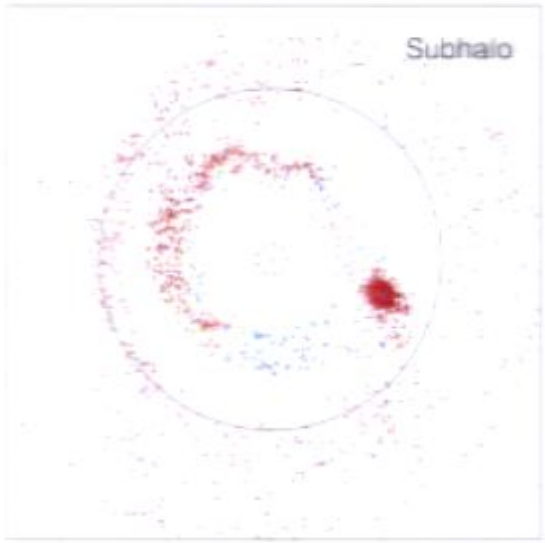
Subhalo

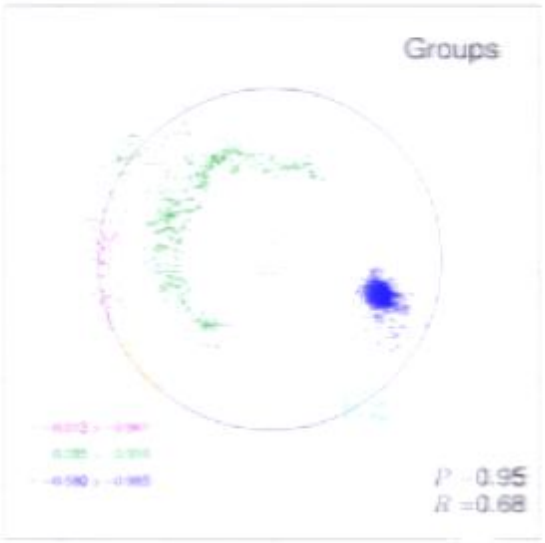
Groups
P 0.95
R =0.68

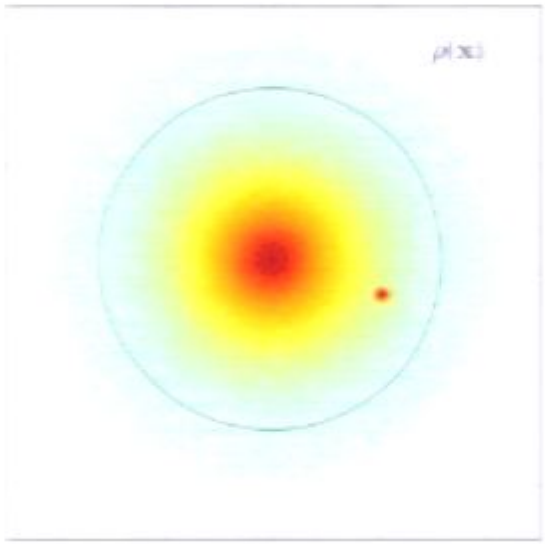
$\rho(\mathbf{x})$

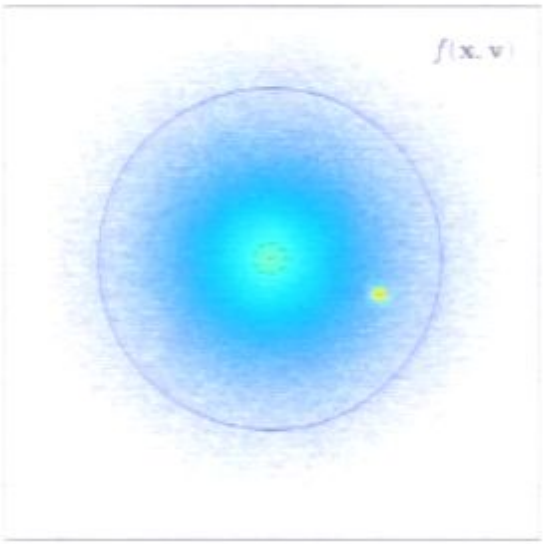
$f(\mathbf{x}, \mathbf{v})$

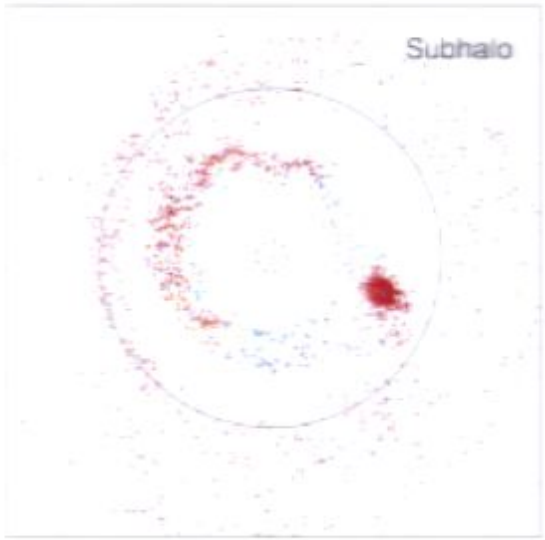
Subhalo

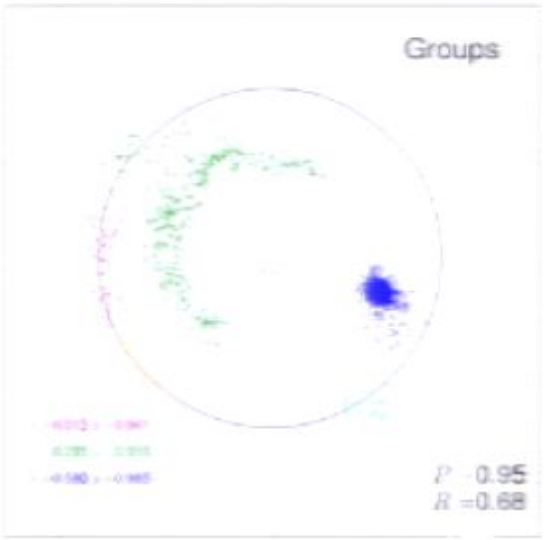
Groups
P 0.95
R =0.68

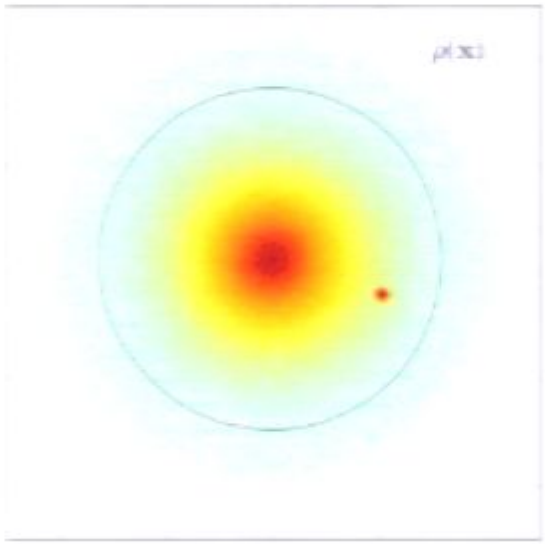
$\rho(\mathbf{x})$

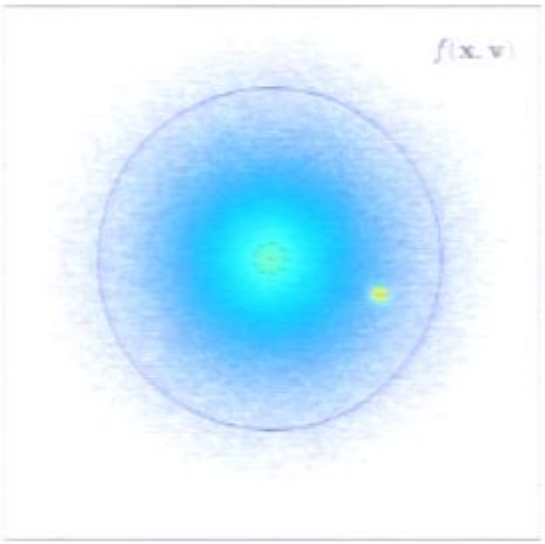
$f(\mathbf{x}, \mathbf{v})$

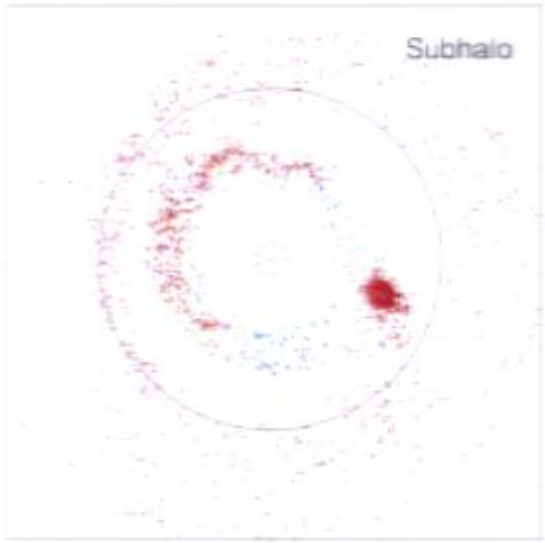
Subhalo

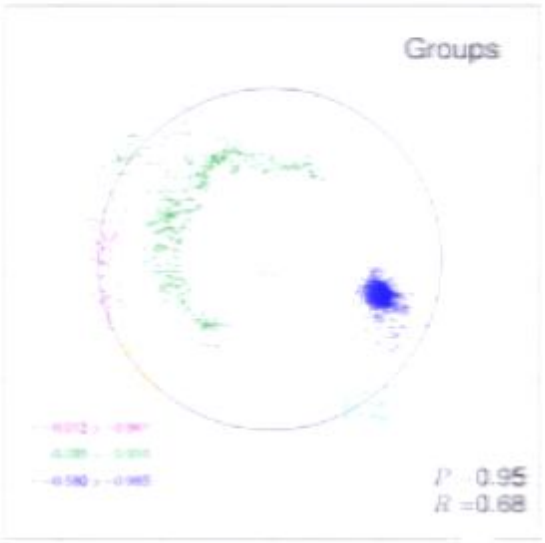
Groups
P 0.95
R =0.68

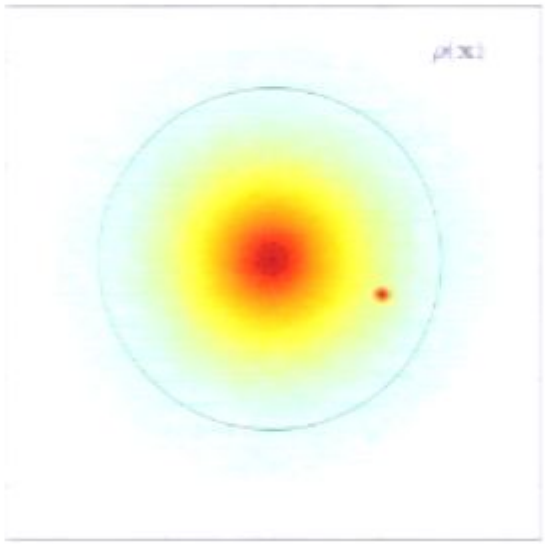
$\rho(\mathbf{x})$

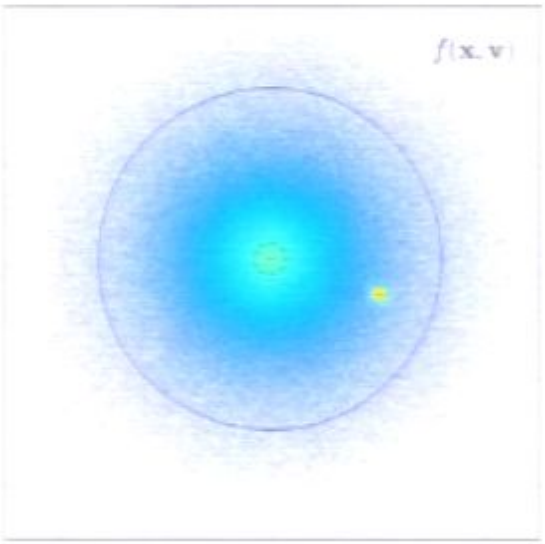
$f(\mathbf{x}, \mathbf{v})$

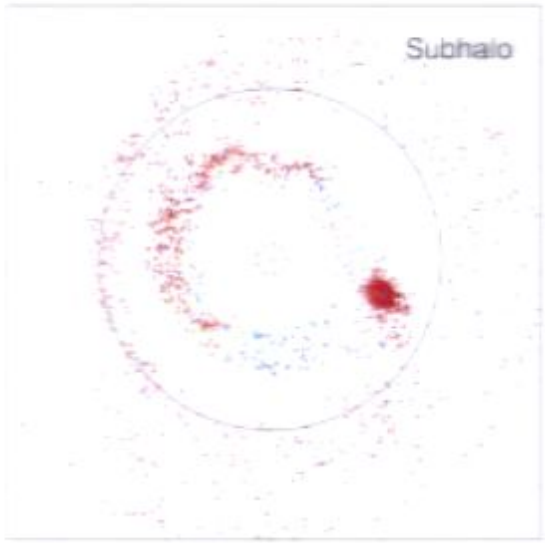
Subhalo

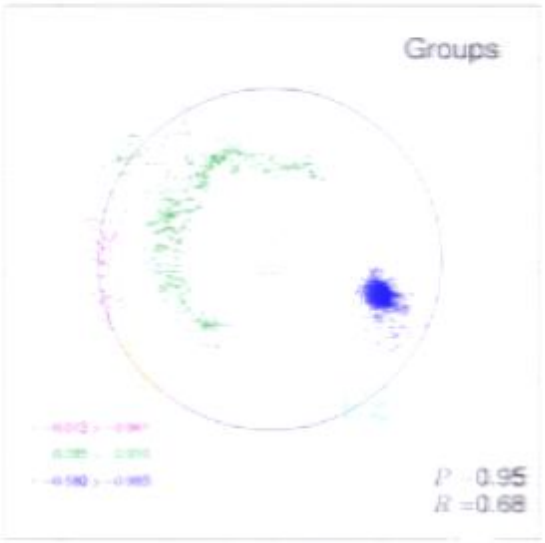
Groups
P 0.95
R =0.68

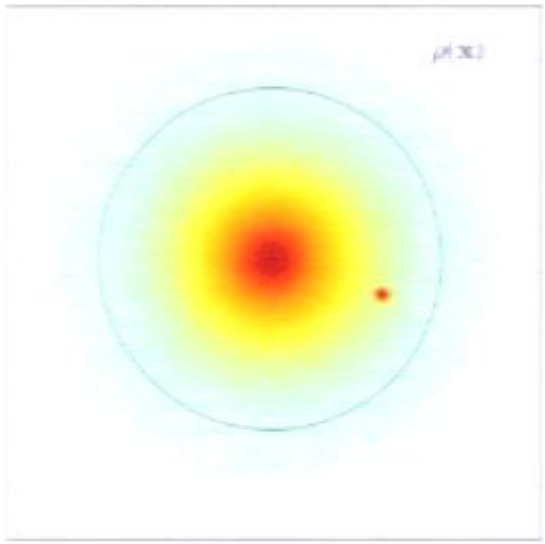
$\rho(\mathbf{x})$

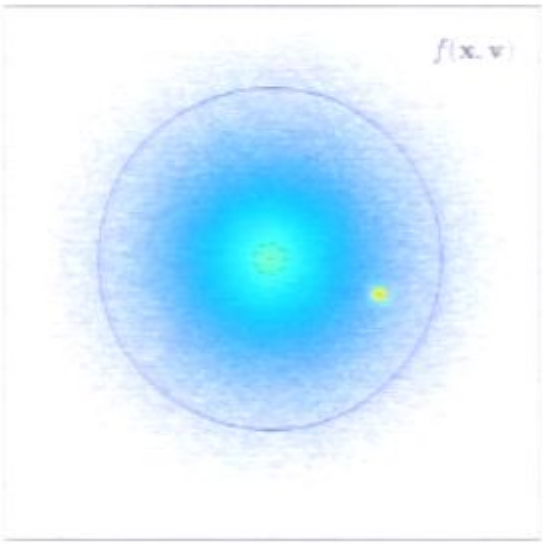
$f(\mathbf{x}, \mathbf{v})$

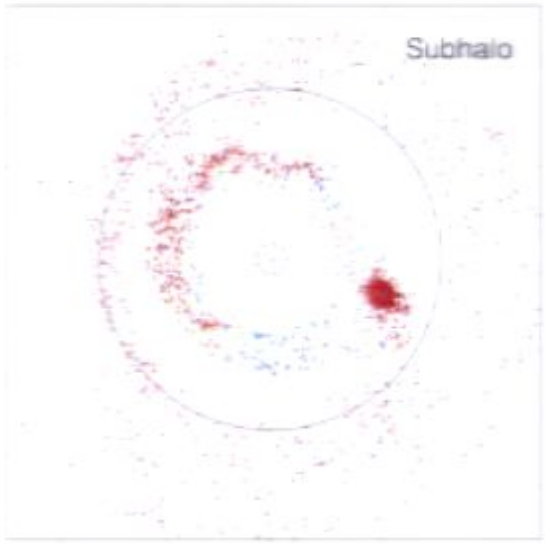
Subhalo

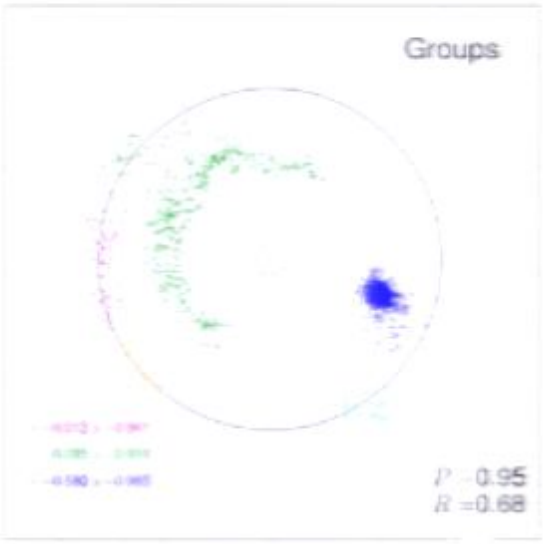
Groups
P =0.95
R =0.68

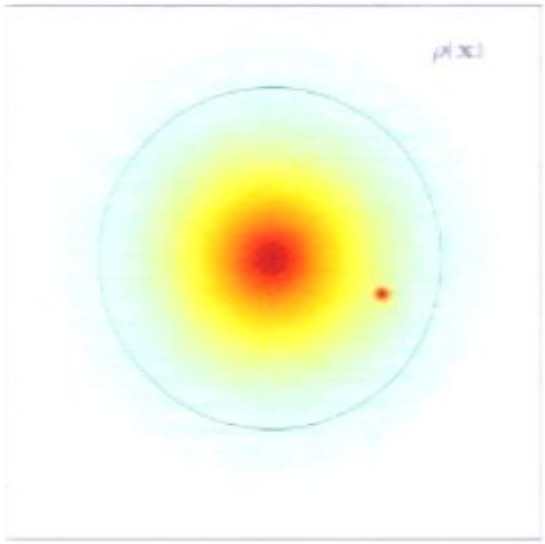
$\rho(\mathbf{x})$

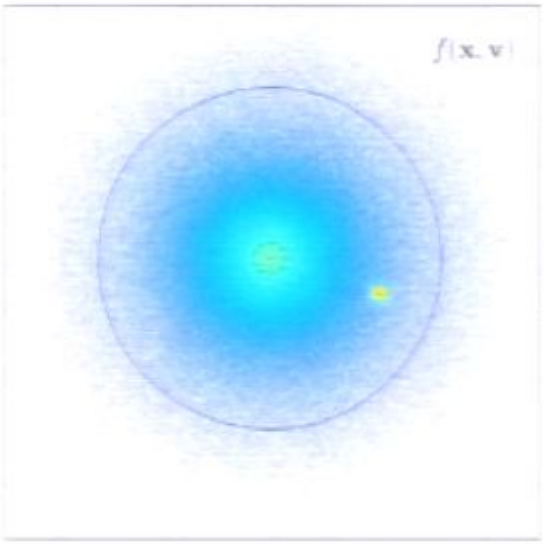
$f(\mathbf{x}, \mathbf{v})$

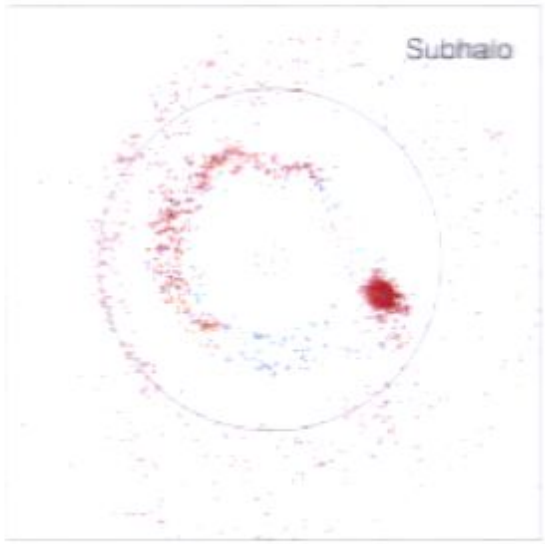
Subhalo

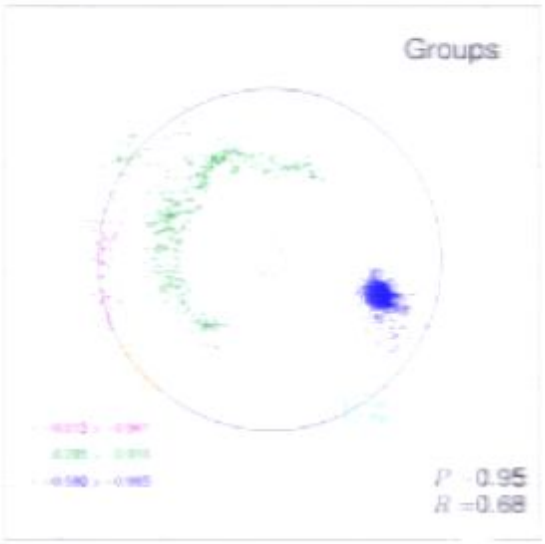
Groups
P 0.95
R =0.68

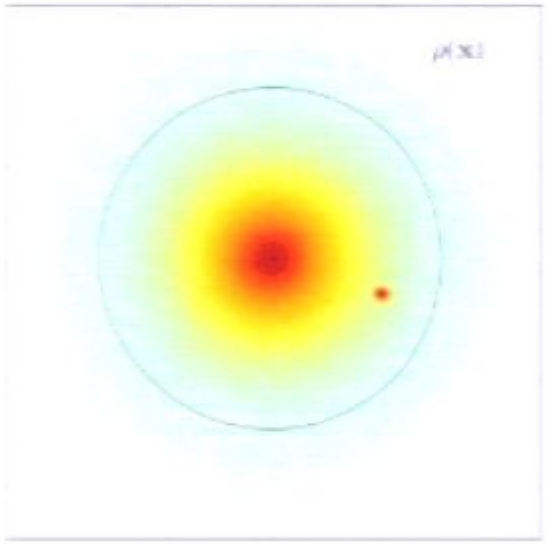
$\rho(\mathbf{x})$

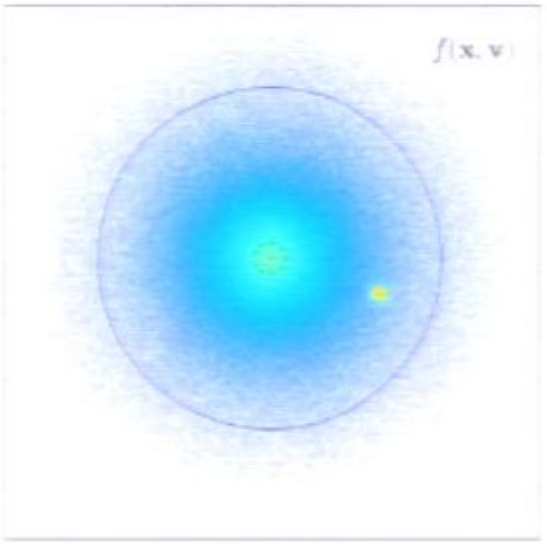
$f(\mathbf{x}, \mathbf{v})$

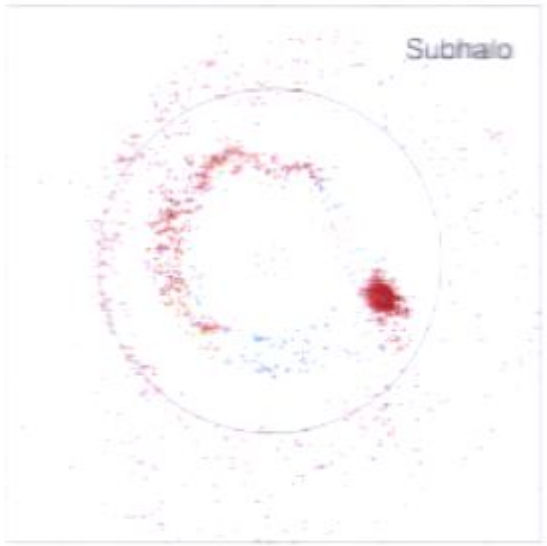
Subhalo

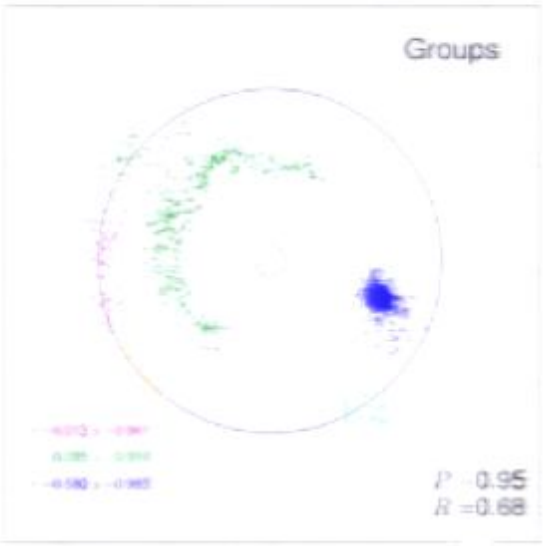
Groups
P 0.95
R =0.68

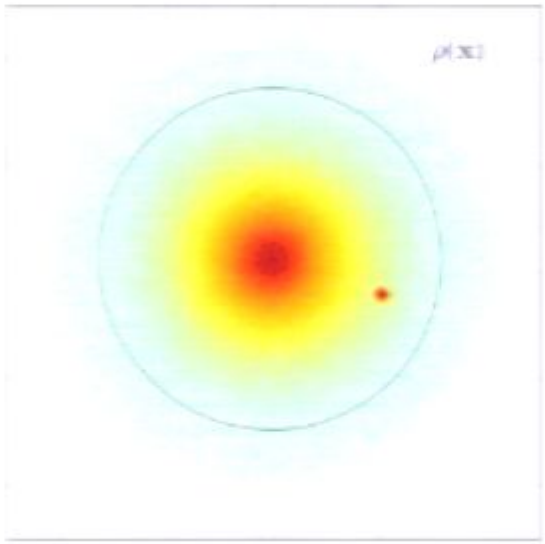
$\rho(\mathbf{x})$

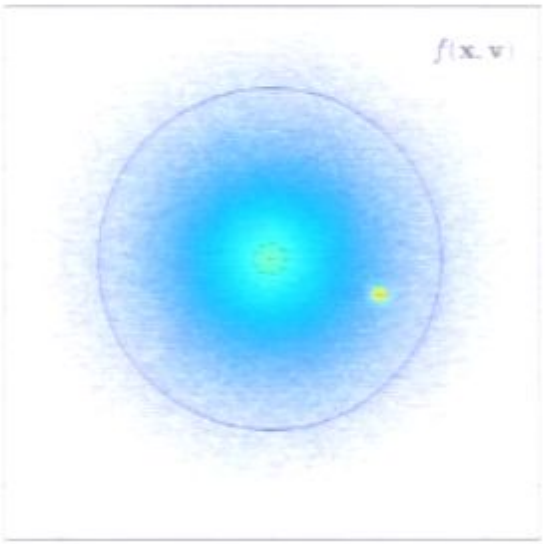
$f(\mathbf{x}, \mathbf{v})$

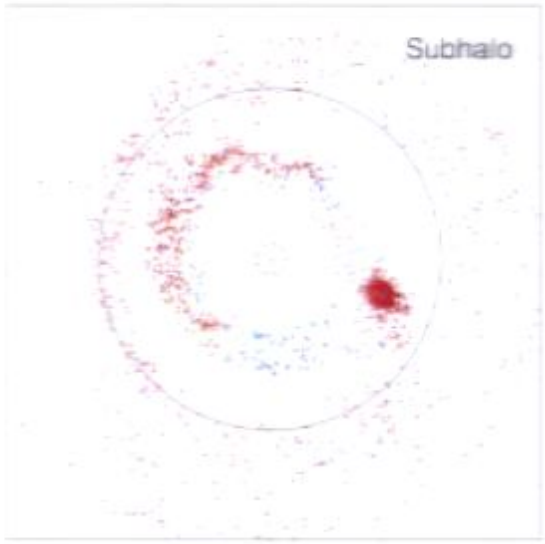
Subhalo

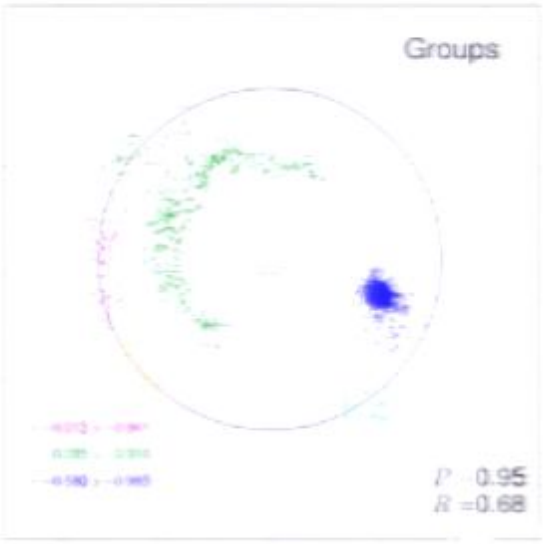
Groups
P 0.95
R =0.68

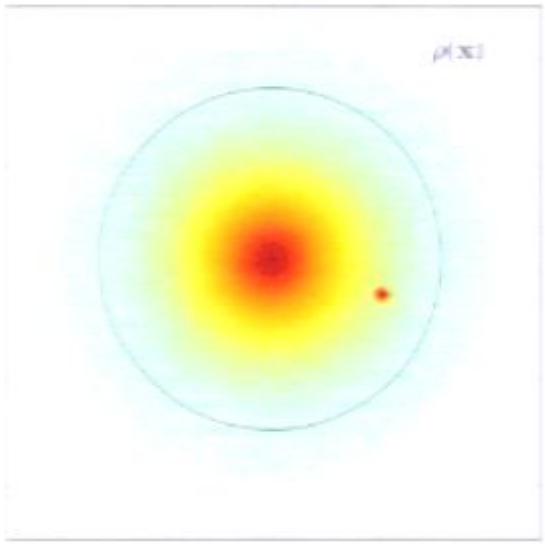
$\rho(\mathbf{x})$

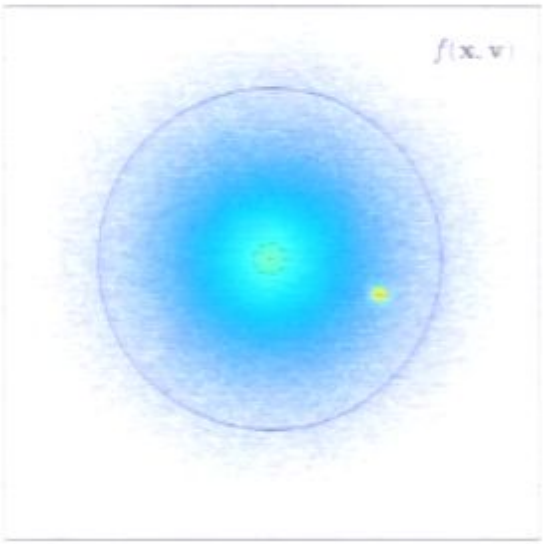
$f(\mathbf{x}, \mathbf{v})$

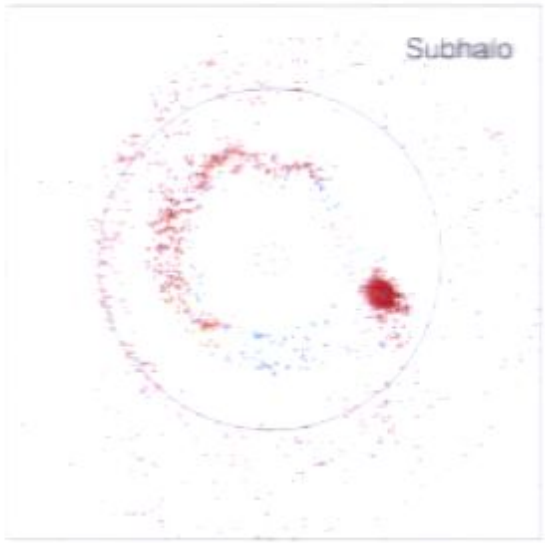
Subhalo

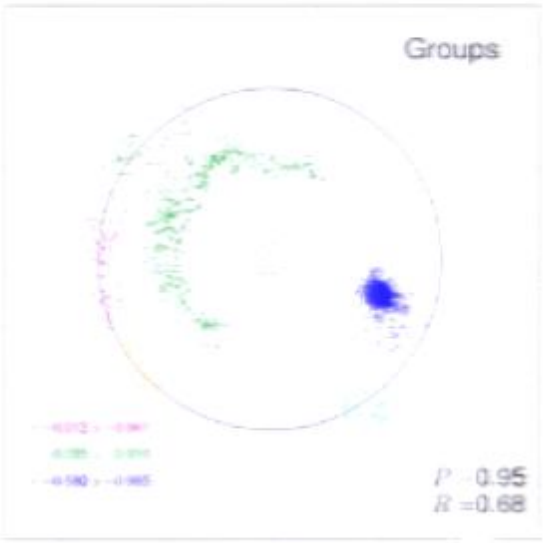
Groups
P 0.95
R =0.68

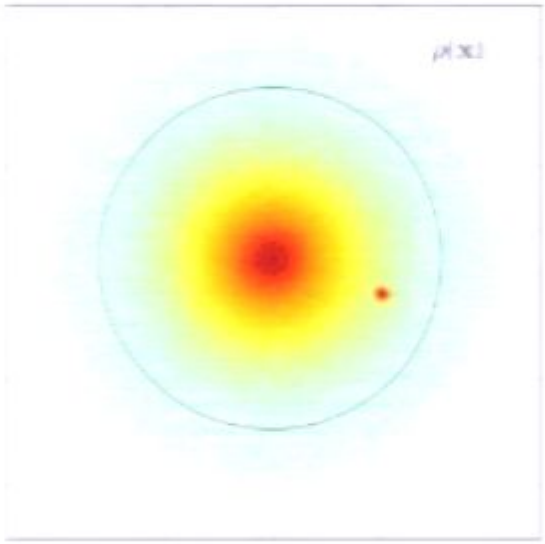
$\rho(\mathbf{x})$

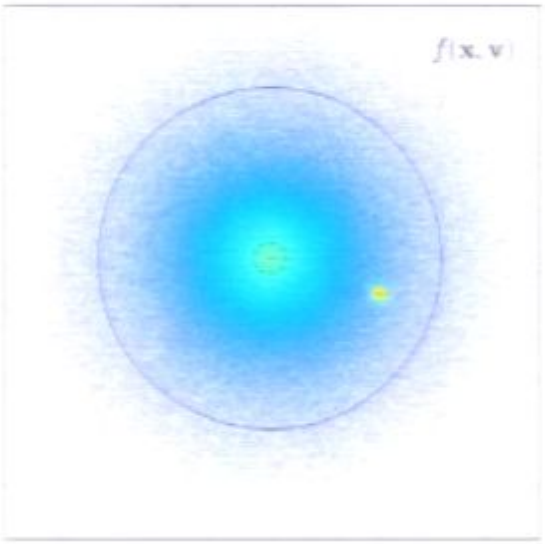
$f(\mathbf{x}, \mathbf{v})$

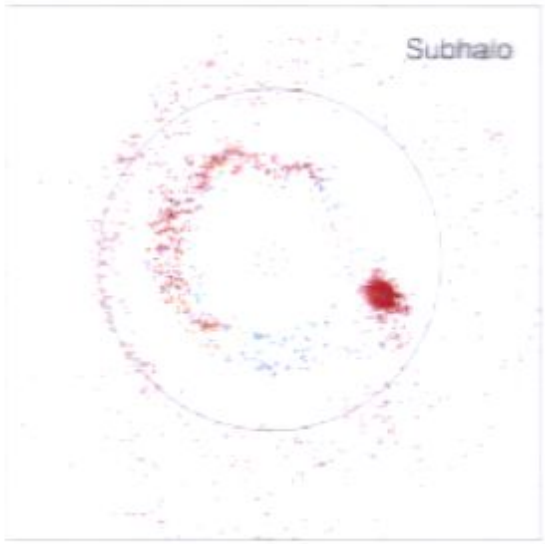
Subhalo

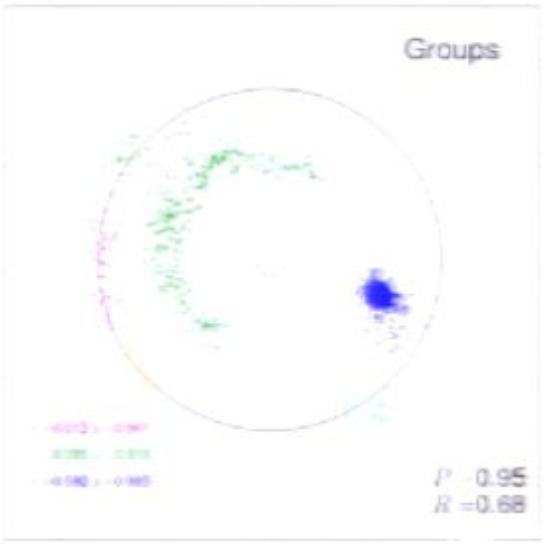
Groups
P 0.95
R =0.68

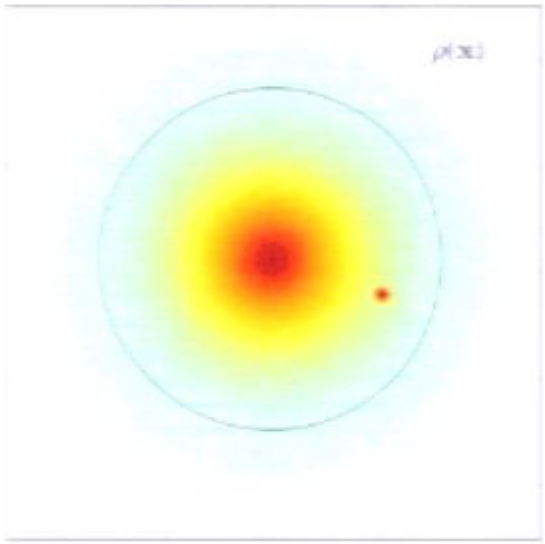
$\rho(\mathbf{x})$

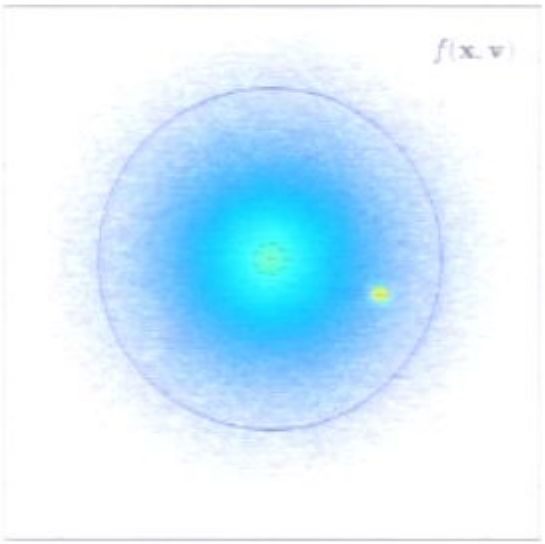
$f(\mathbf{x}, \mathbf{v})$

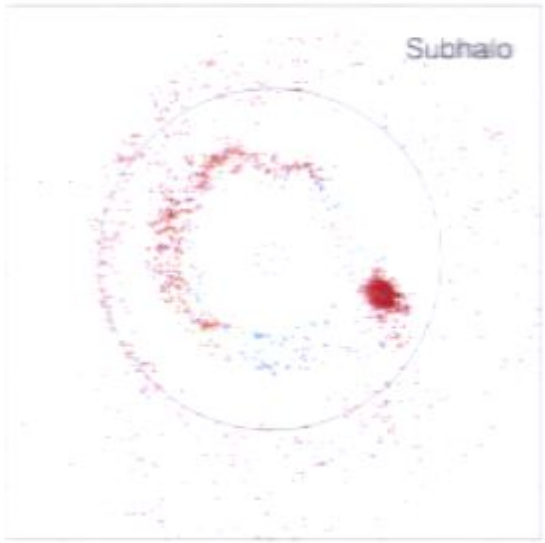
Subhalo

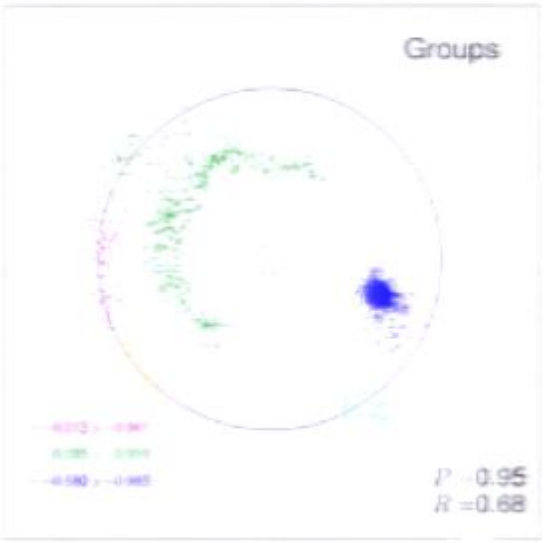
Groups
P 0.95
R =0.68

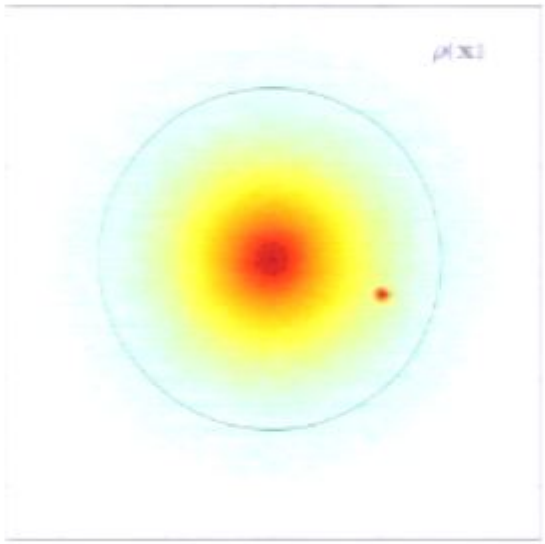
$\rho(\mathbf{x})$

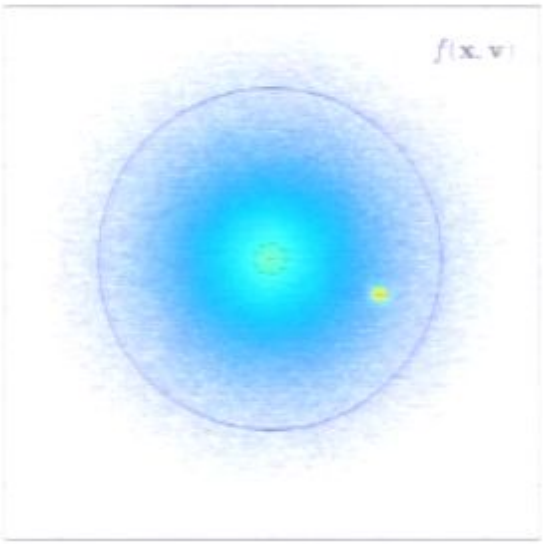
$f(\mathbf{x}, \mathbf{v})$

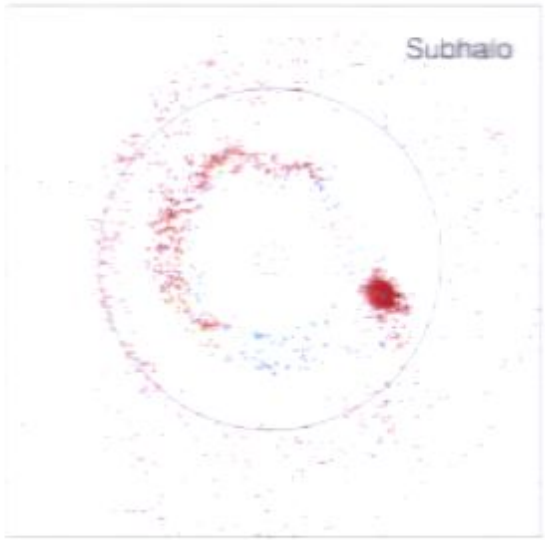
Subhalo

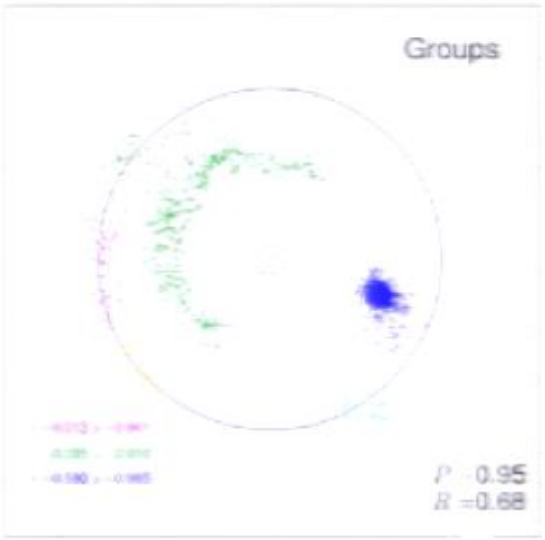
Groups
P 0.95
R =0.68

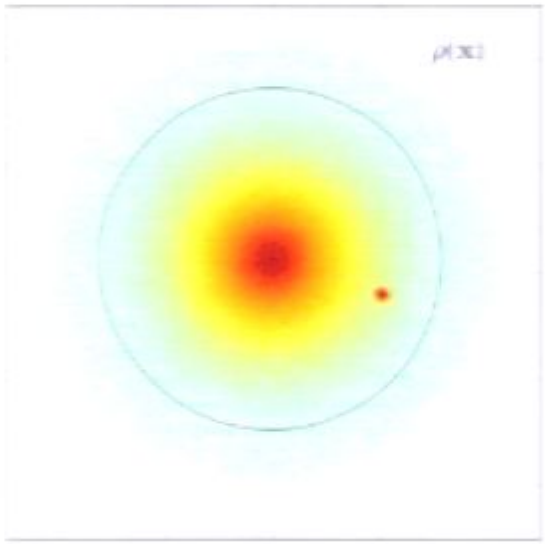
$\rho(\mathbf{x})$

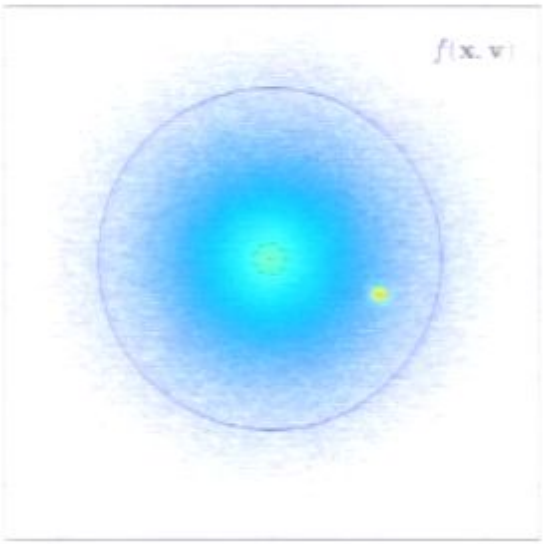
$f(\mathbf{x}, \mathbf{v})$

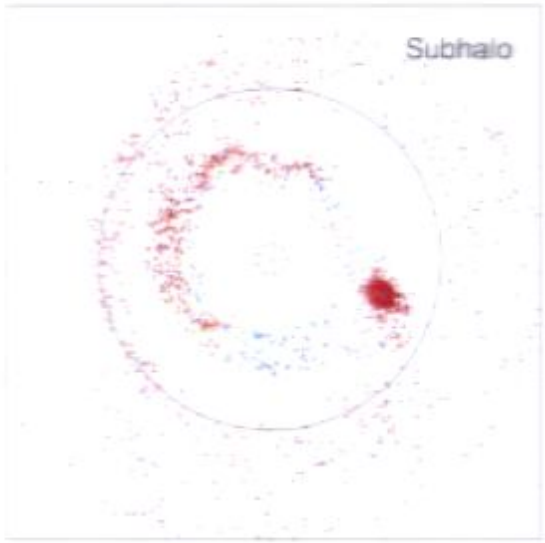
Subhalo

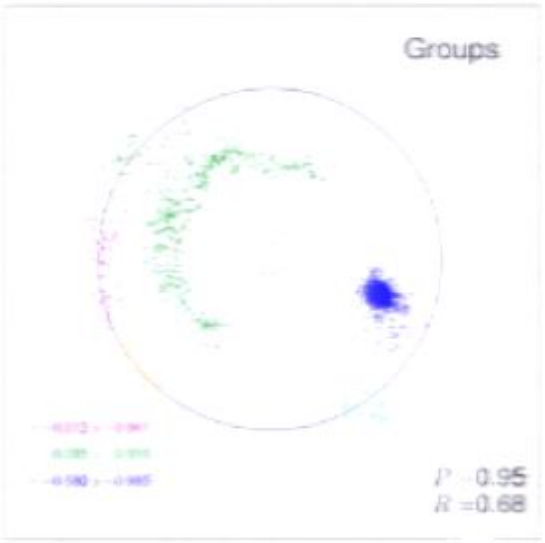
Groups
P 0.95
R =0.68

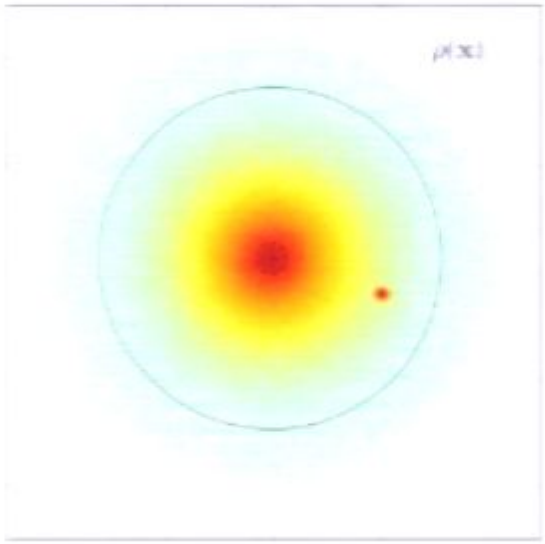
$\rho(\mathbf{x})$

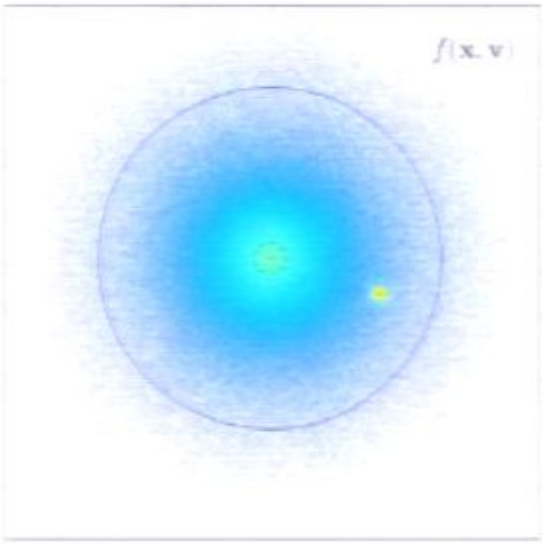
$f(\mathbf{x}, \mathbf{v})$

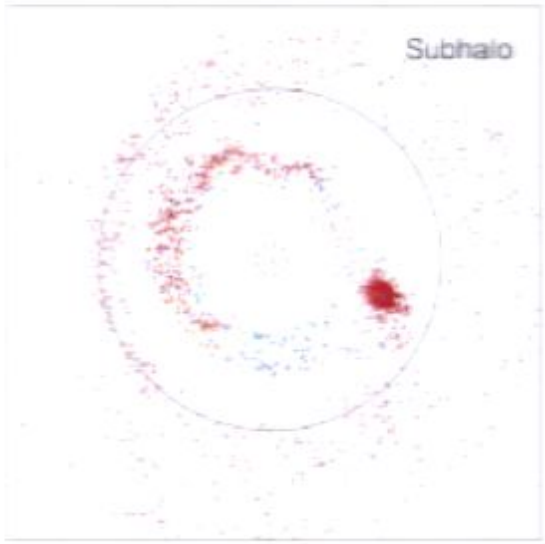
Subhalo

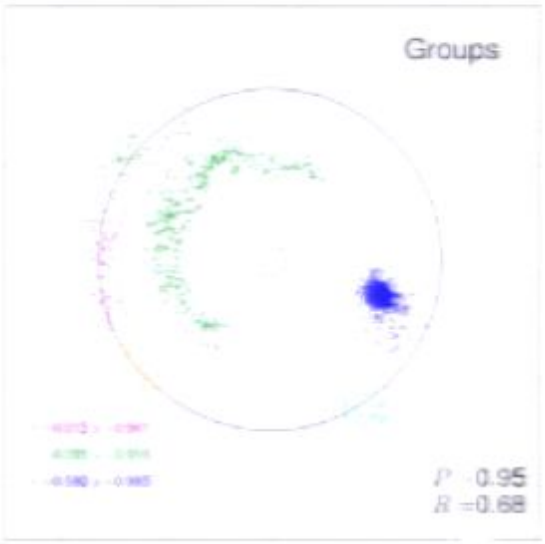
Groups
P 0.95
R =0.68

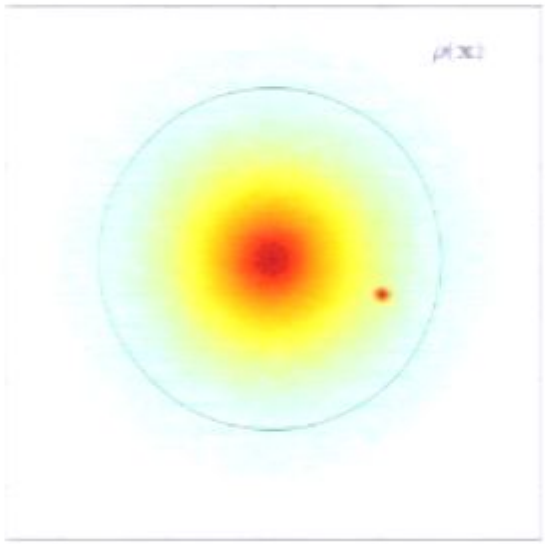
$\rho(\mathbf{x})$

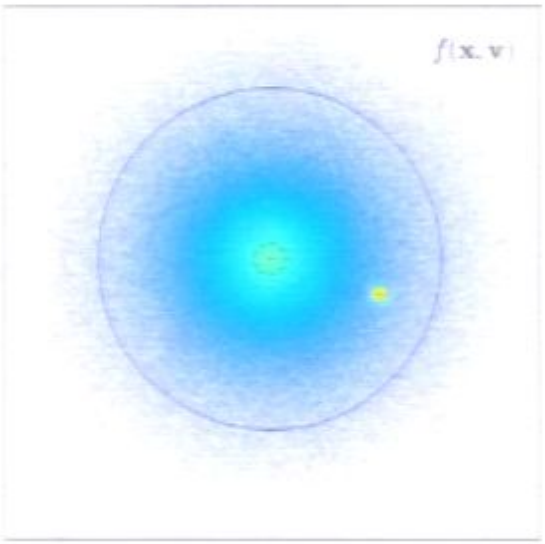
$f(\mathbf{x}, \mathbf{v})$

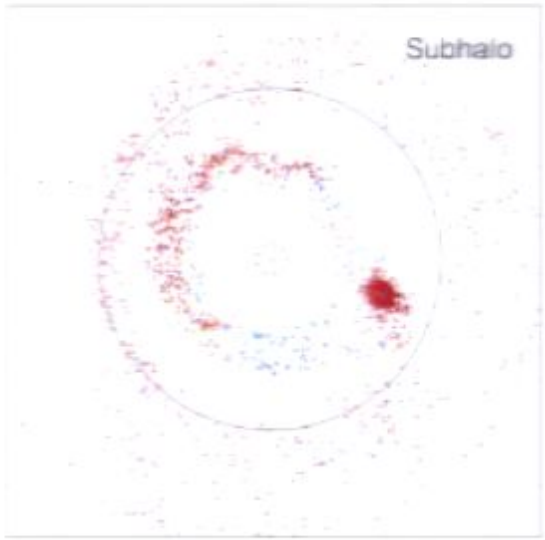
Subhalo

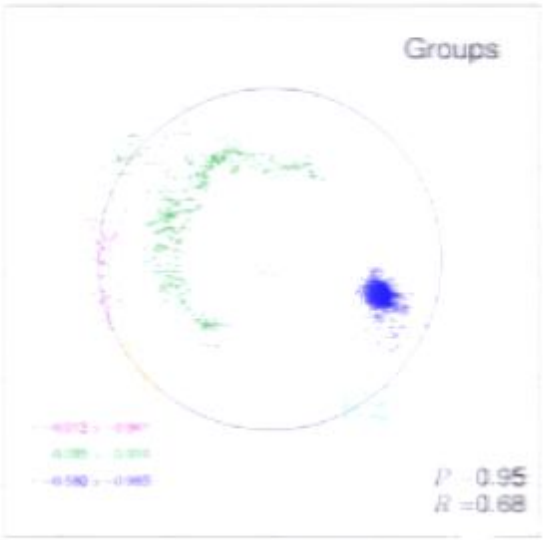
Groups
P 0.95
R =0.68

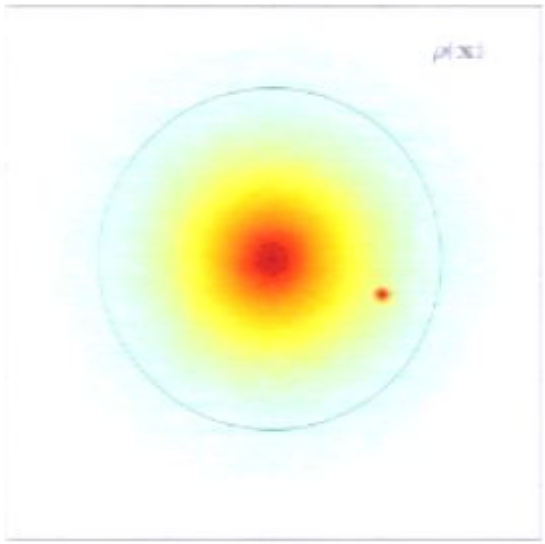
$\rho(\mathbf{x})$

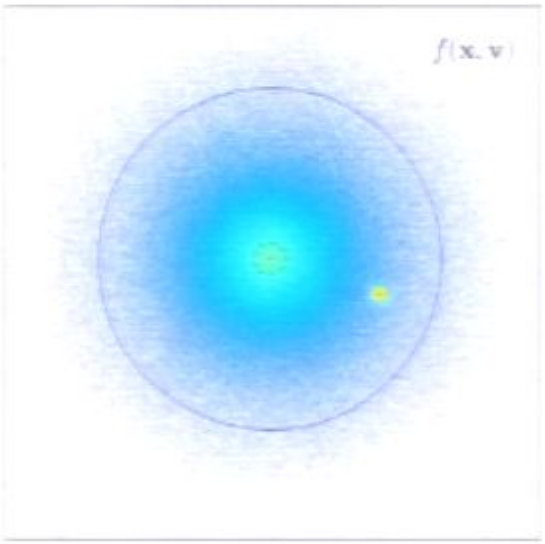
$f(\mathbf{x}, \mathbf{v})$

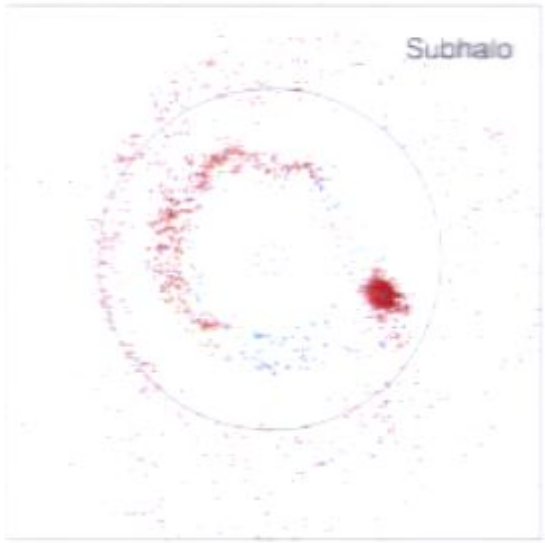
Subhalo

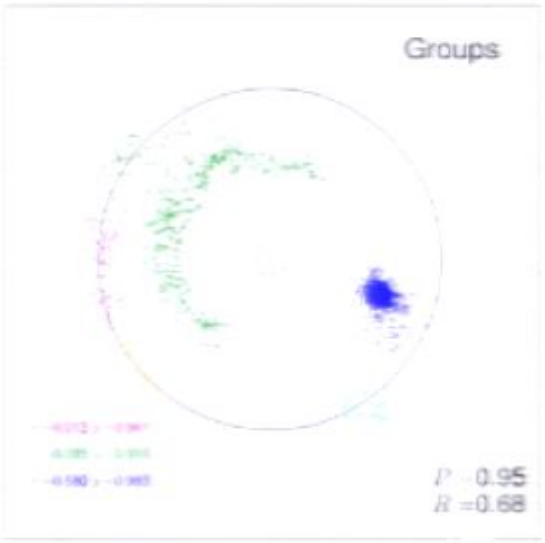
Groups
P 0.95
R =0.68

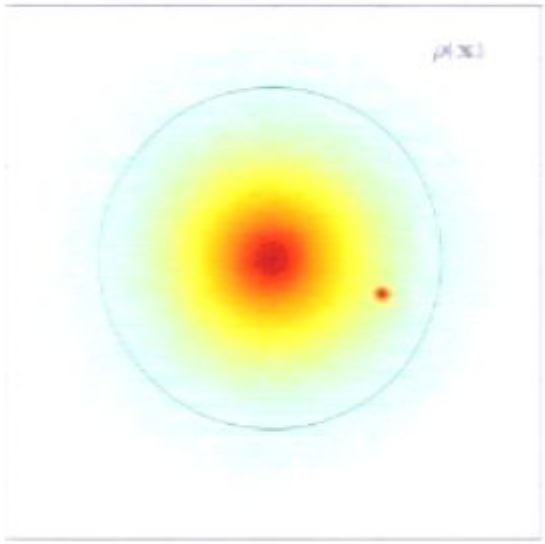
$\rho(\mathbf{x})$

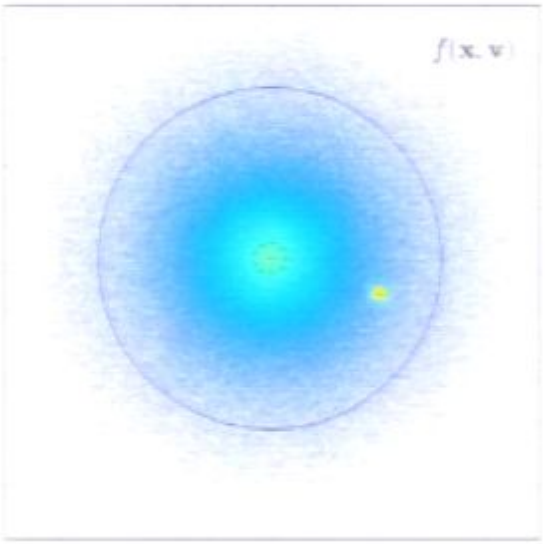
$f(\mathbf{x}, \mathbf{v})$

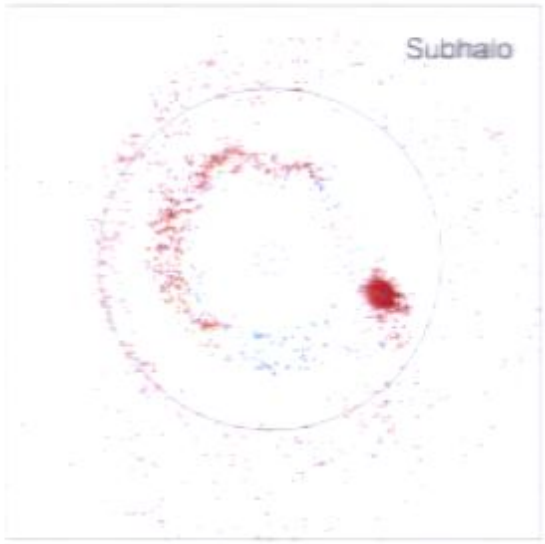
Subhalo

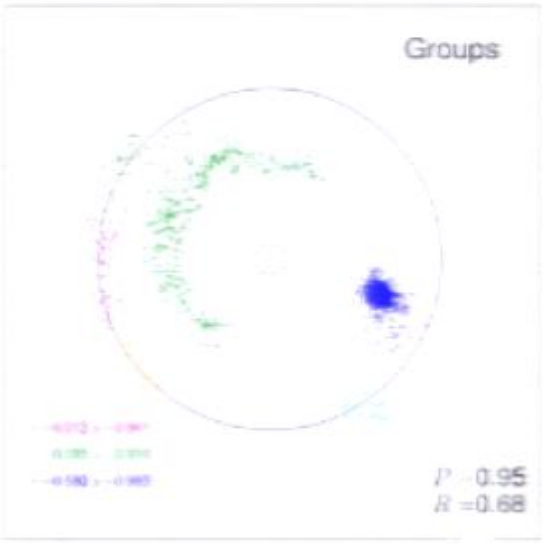
Groups
P 0.95
R =0.68

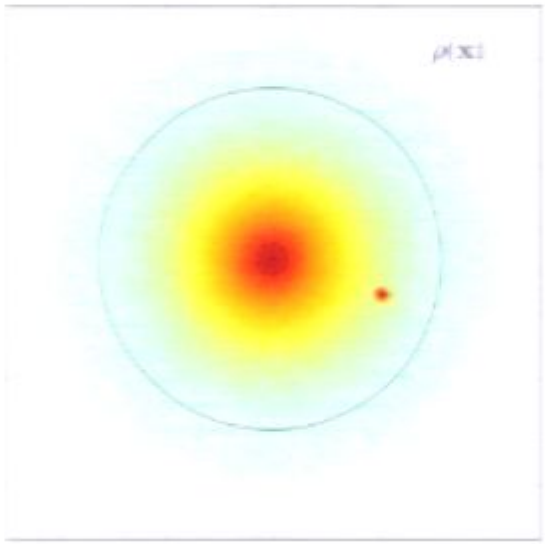
$\rho(\mathbf{x})$

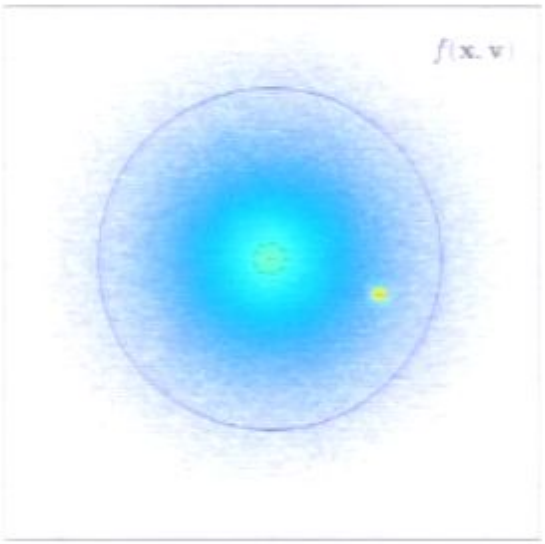
$f(\mathbf{x}, \mathbf{v})$

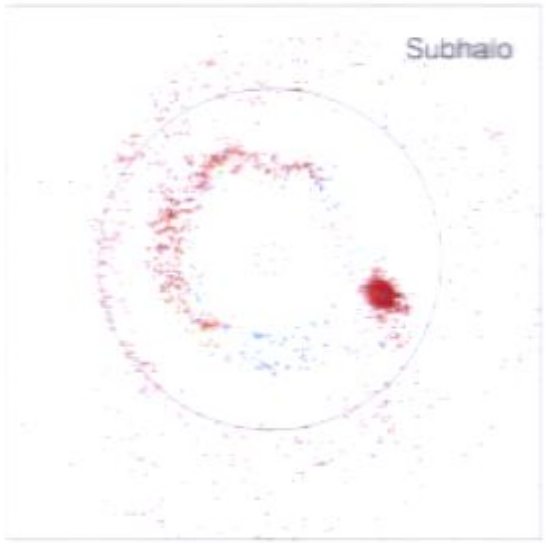
Subhalo

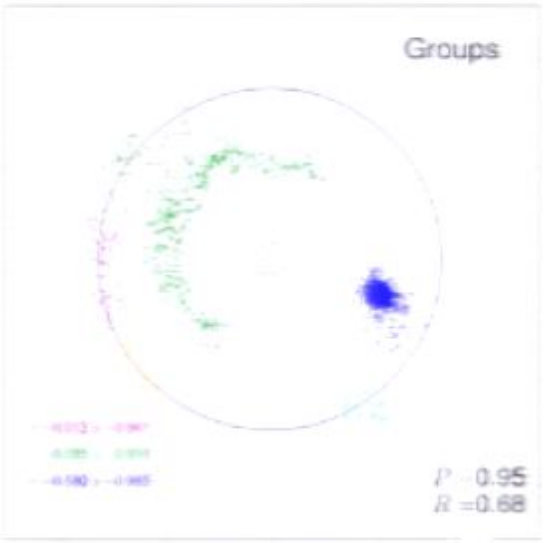
Groups
P =0.95
R =0.68

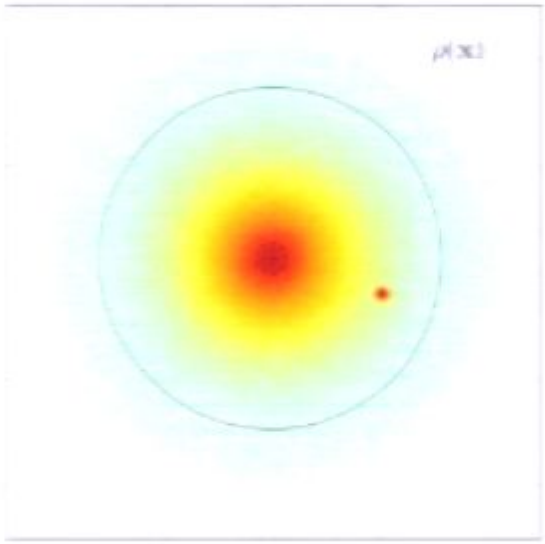
$\rho(\mathbf{x})$

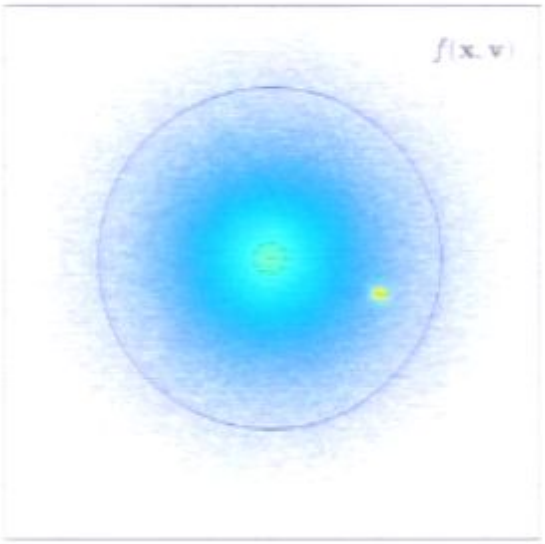
$f(\mathbf{x}, \mathbf{v})$

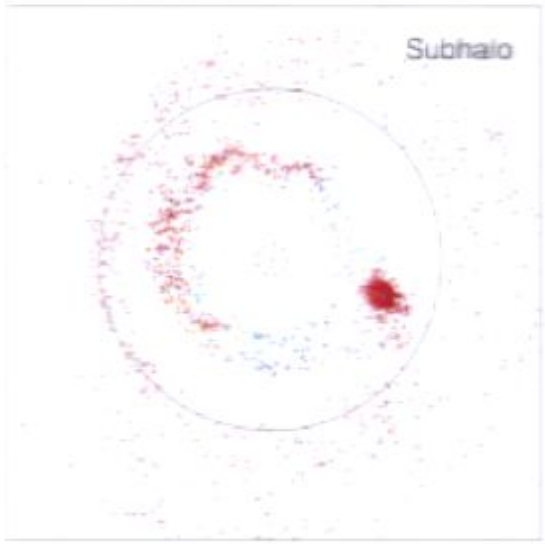
Subhalo

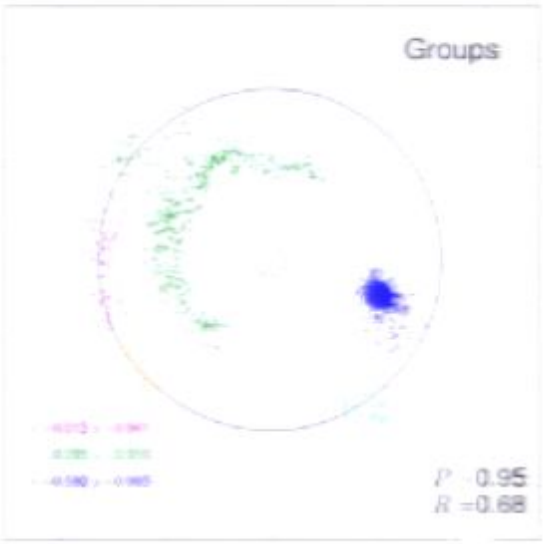
Groups
P 0.95
R =0.68

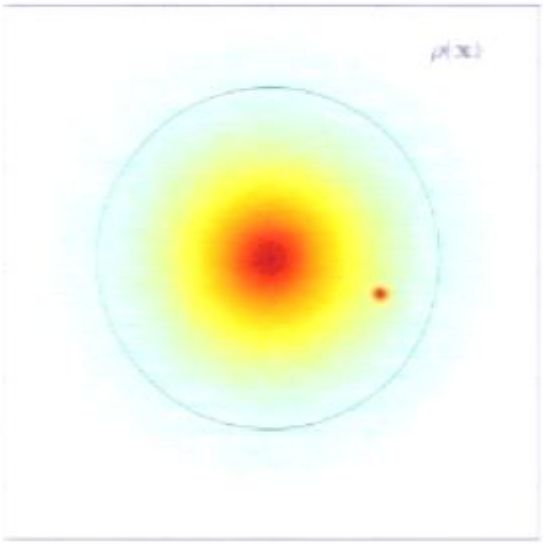
$\rho(\mathbf{x})$

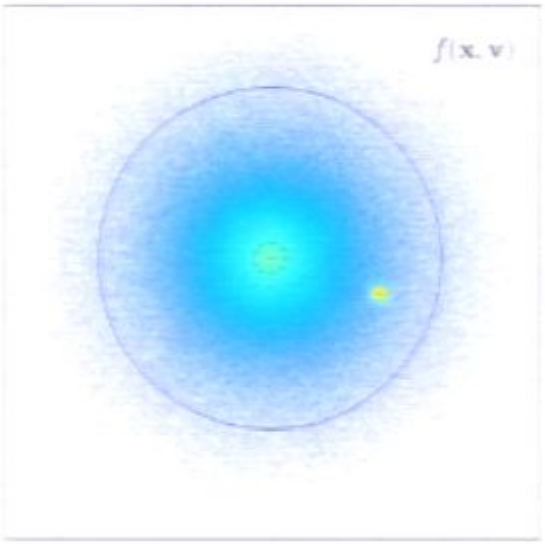
$f(\mathbf{x}, \mathbf{v})$

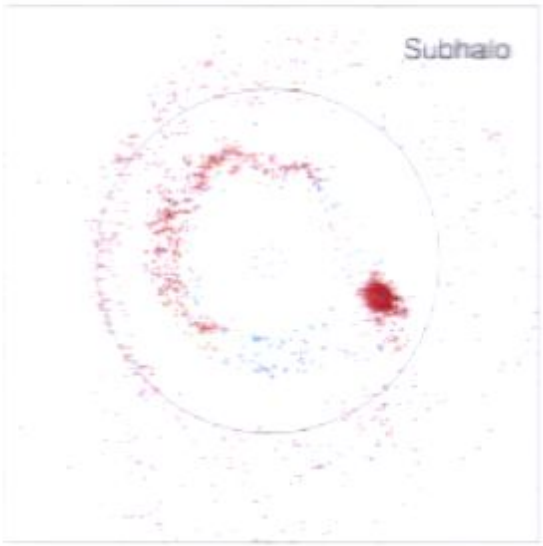
Subhalo

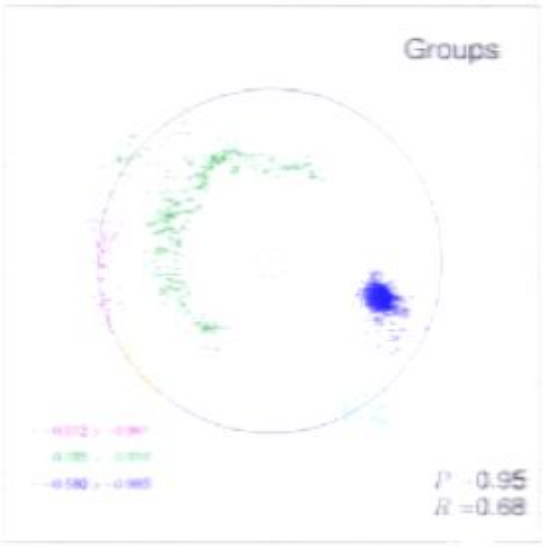
Groups
P 0.95
R =0.68

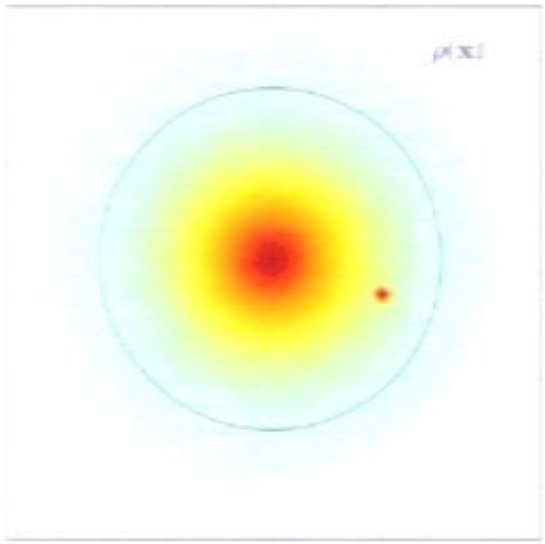
$\rho(\mathbf{x})$

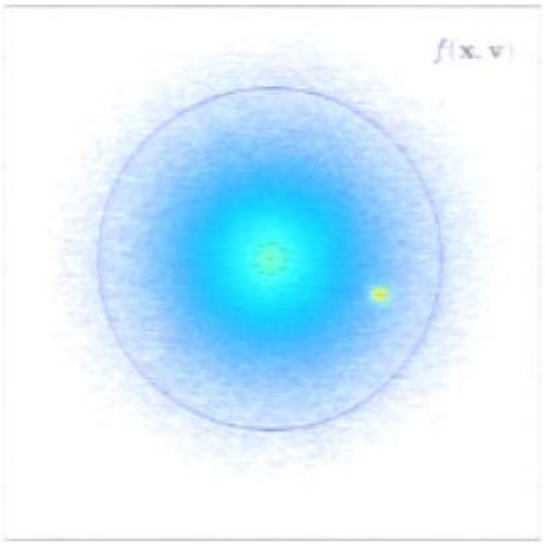
$f(\mathbf{x}, \mathbf{v})$

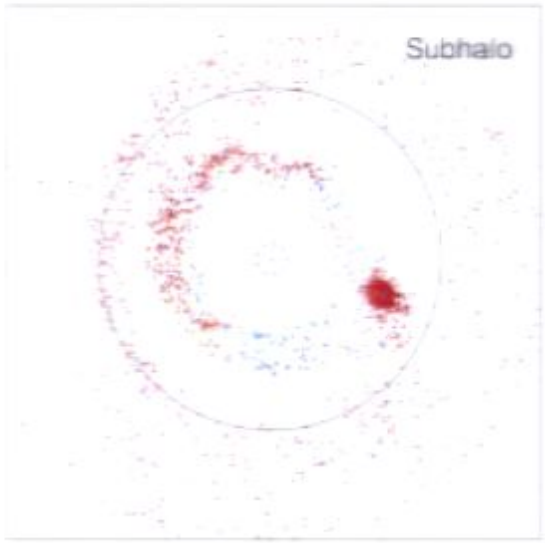
Subhalo

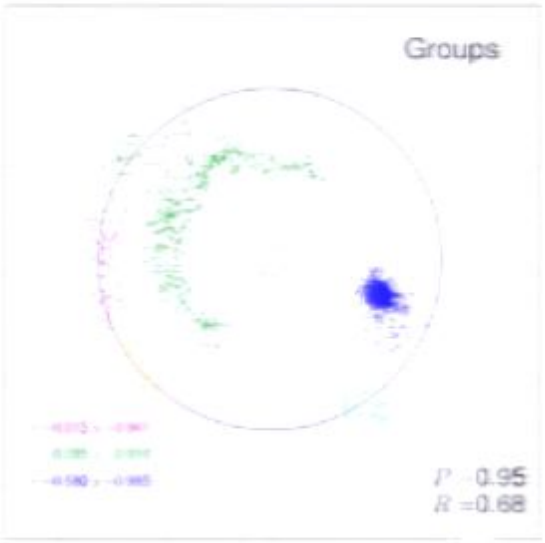
Groups
P 0.95
R =0.68

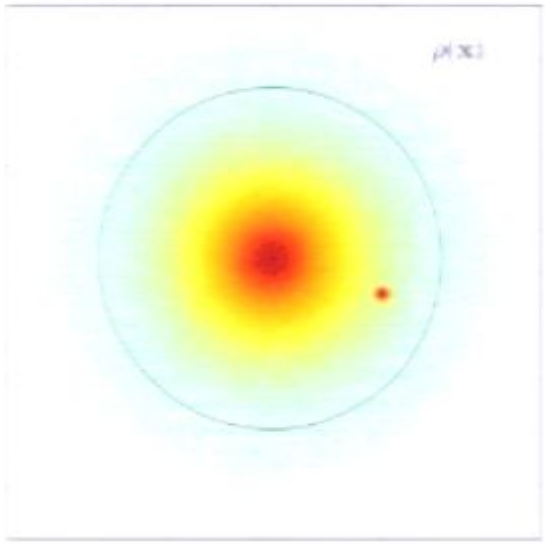
$\rho(\mathbf{x})$

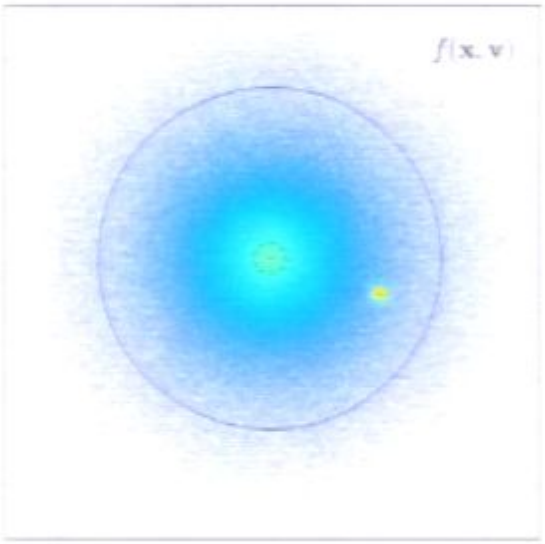
$f(\mathbf{x}, \mathbf{v})$

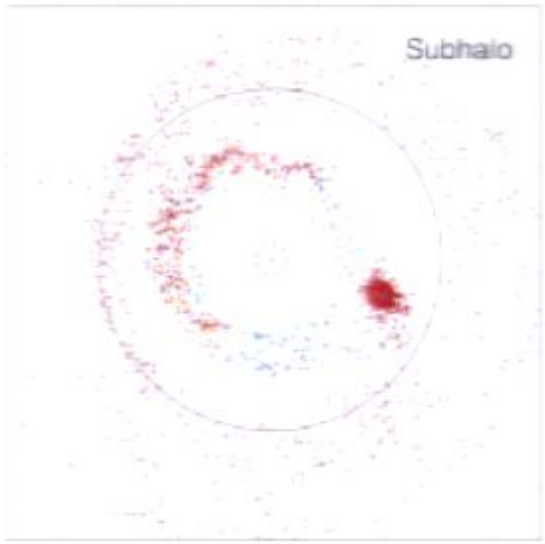
Subhalo

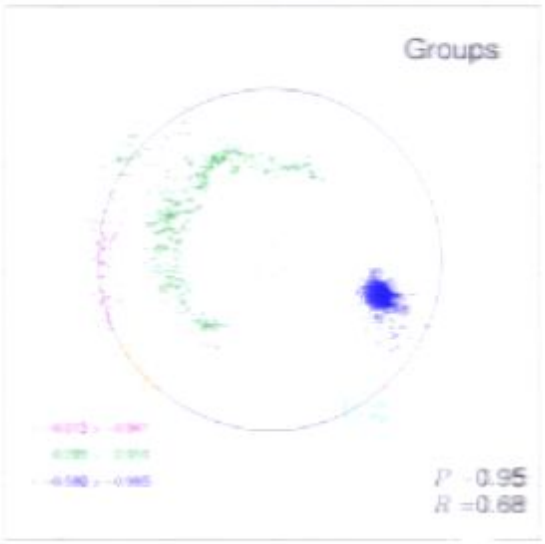
Groups
P 0.95
R =0.68

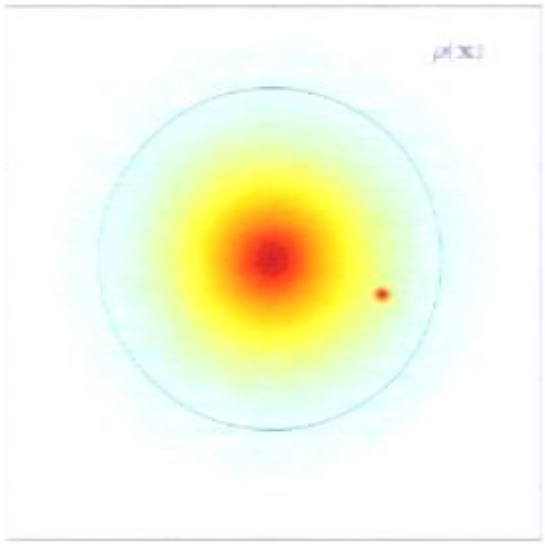
$\rho(\mathbf{x})$

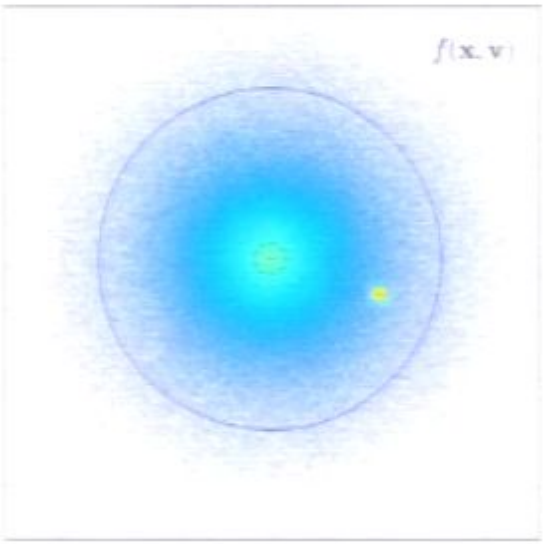
$f(\mathbf{x}, \mathbf{v})$

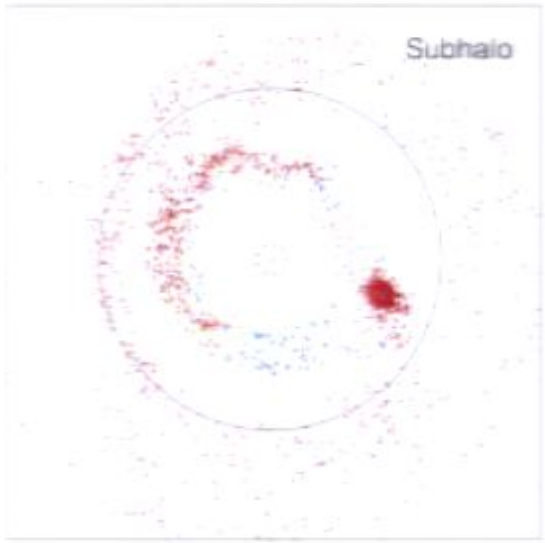
Subhalo

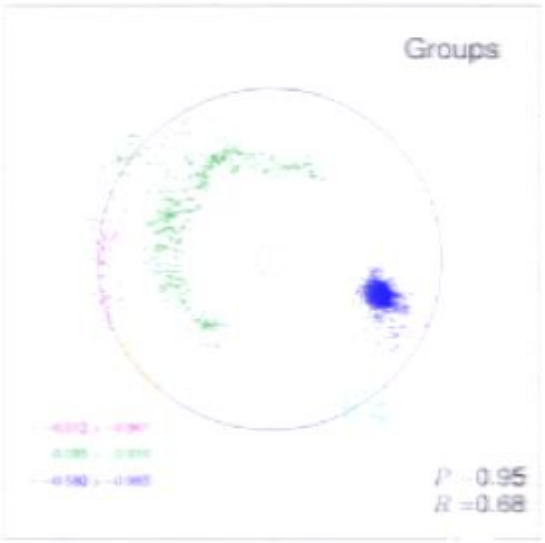
Groups
P 0.95
R =0.68

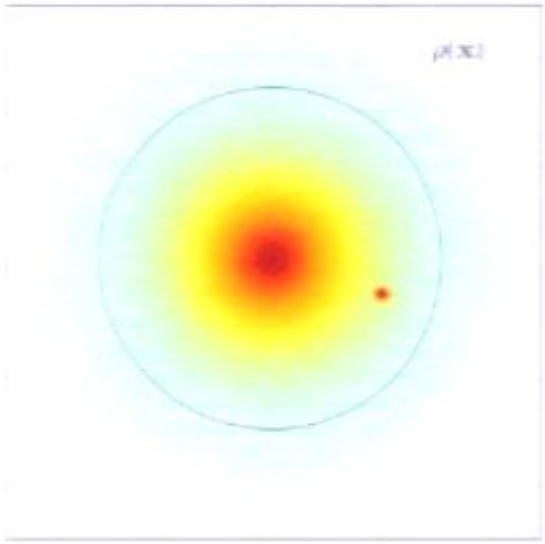
$\rho(\mathbf{x})$

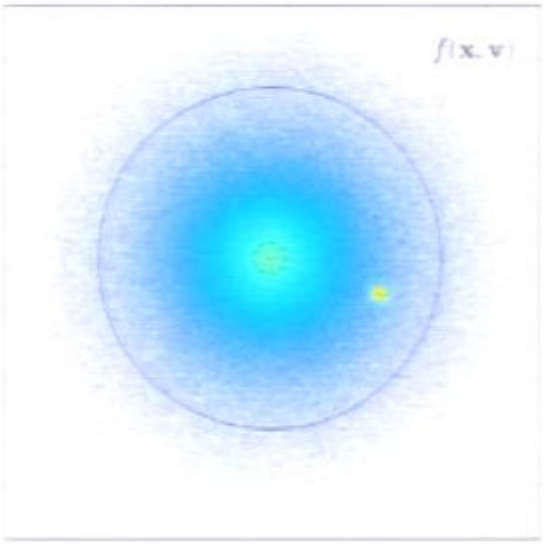
$f(\mathbf{x}, \mathbf{v})$

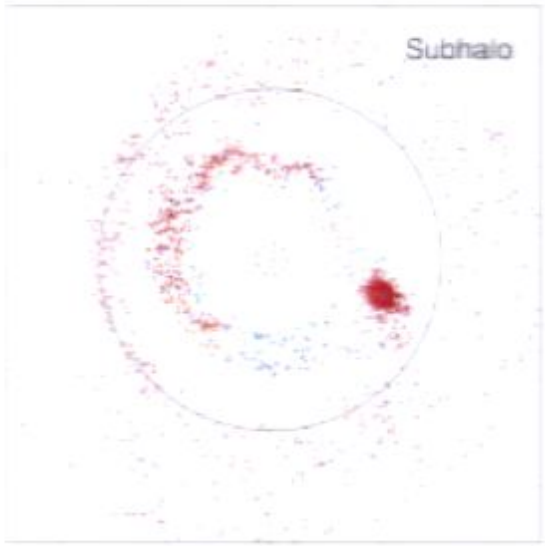
Subhalo

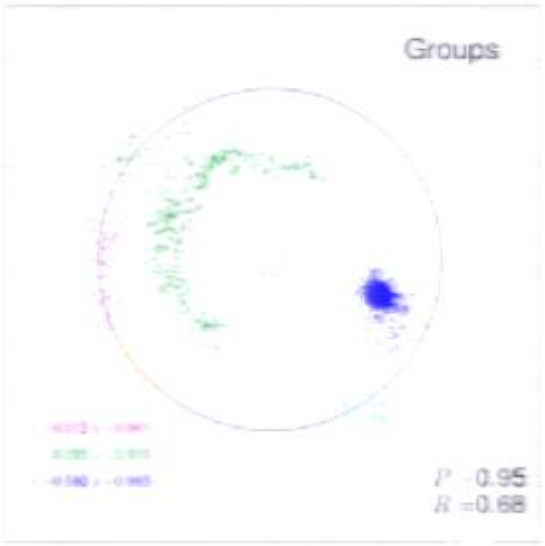
Groups
P 0.95
R =0.68

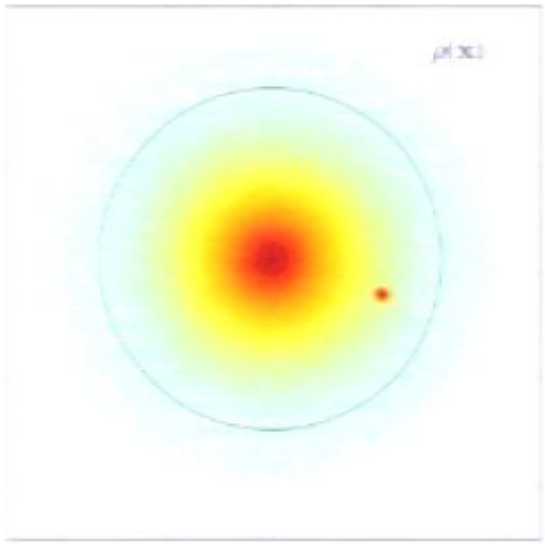
$\rho(\mathbf{x})$

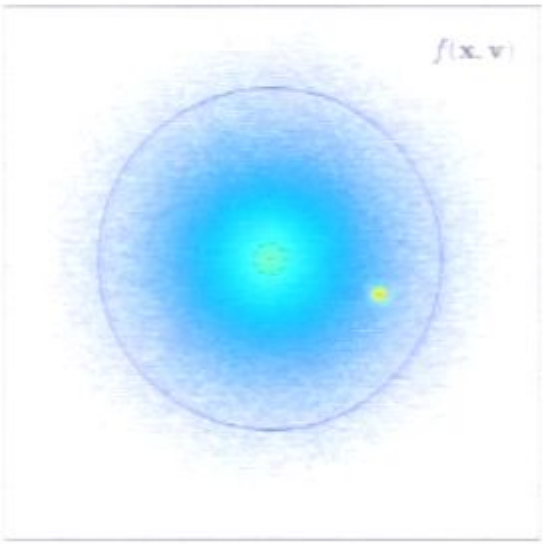
$f(\mathbf{x}, \mathbf{v})$

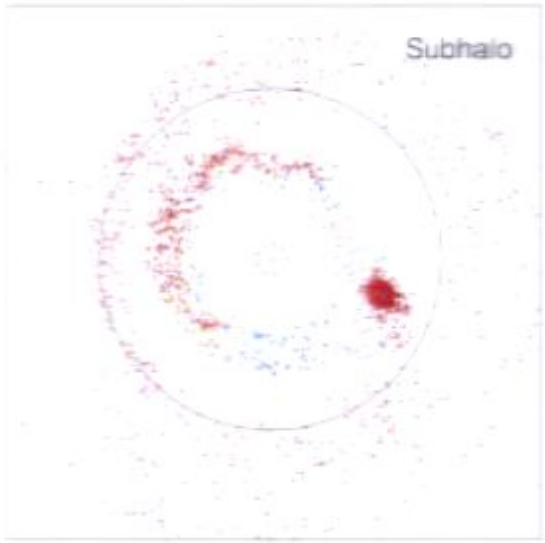
Subhalo

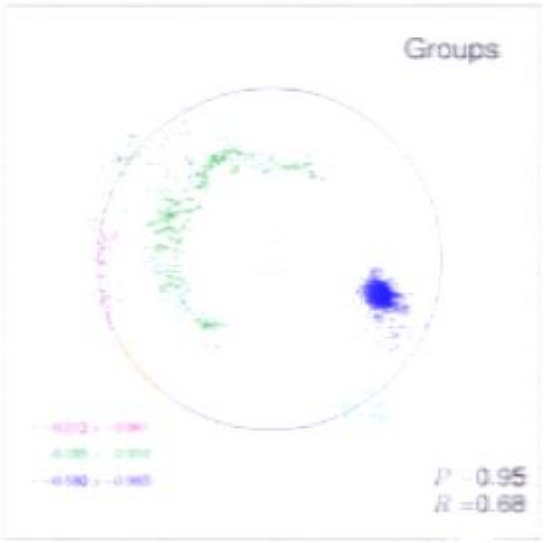
Groups
P 0.95
R =0.68

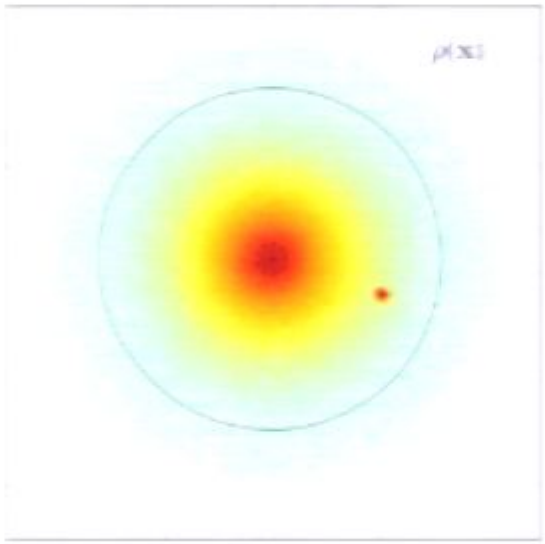
$\rho(\mathbf{x})$

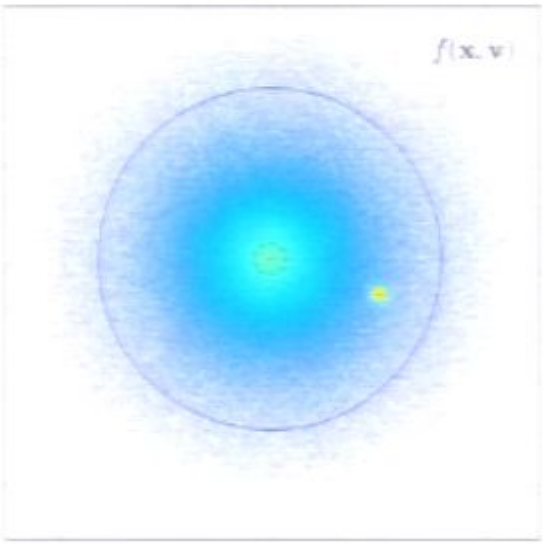
$f(\mathbf{x}, \mathbf{v})$

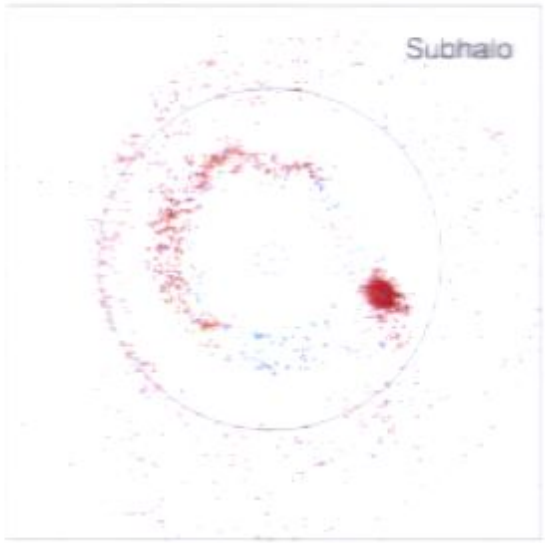
Subhalo

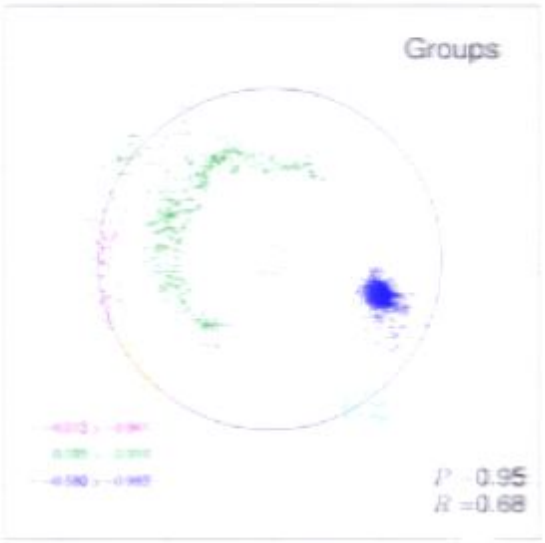
Groups
P 0.95
R =0.68

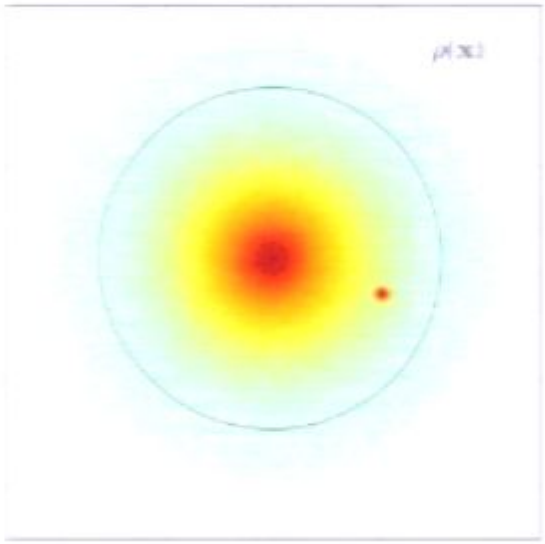
$\rho(\mathbf{x})$

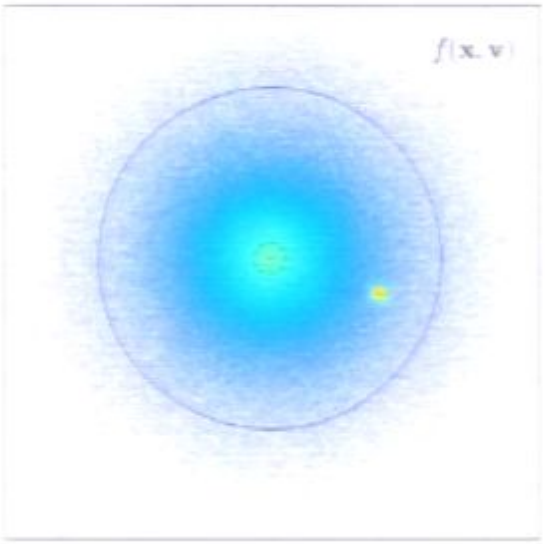
$f(\mathbf{x}, \mathbf{v})$

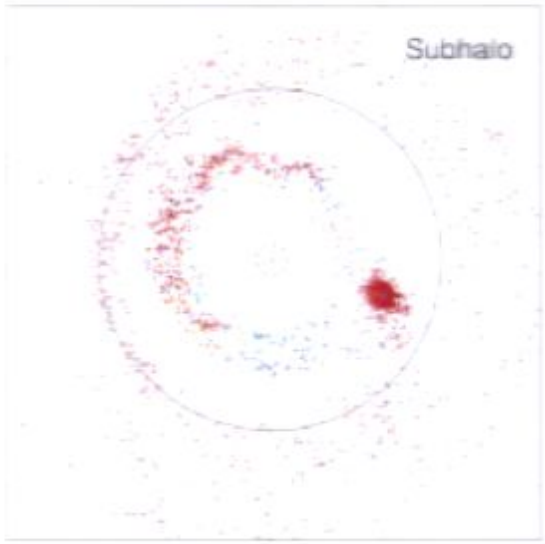
Subhalo

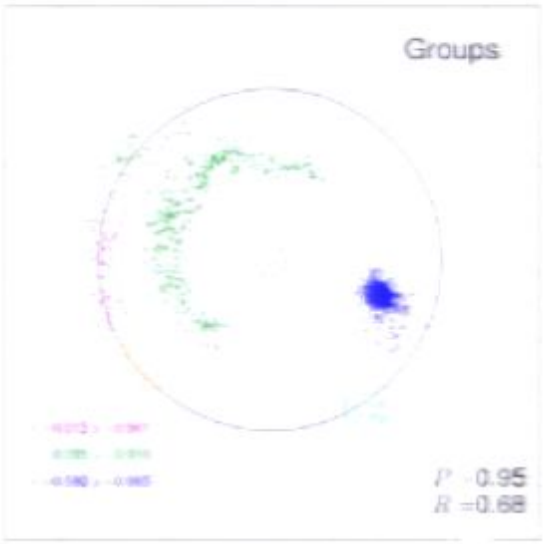
Groups
P 0.95
R =0.68

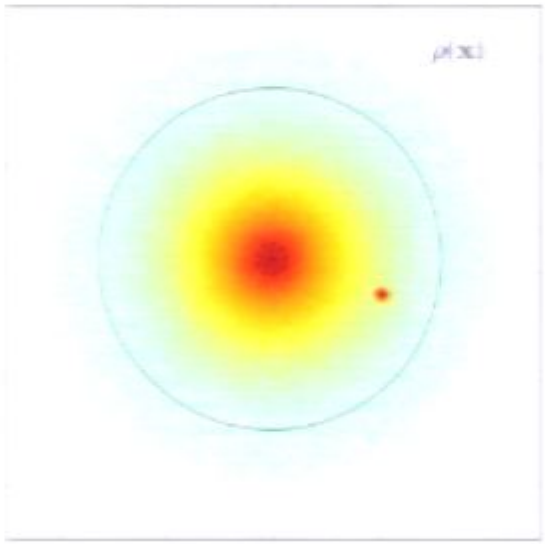
$\rho(\mathbf{x})$

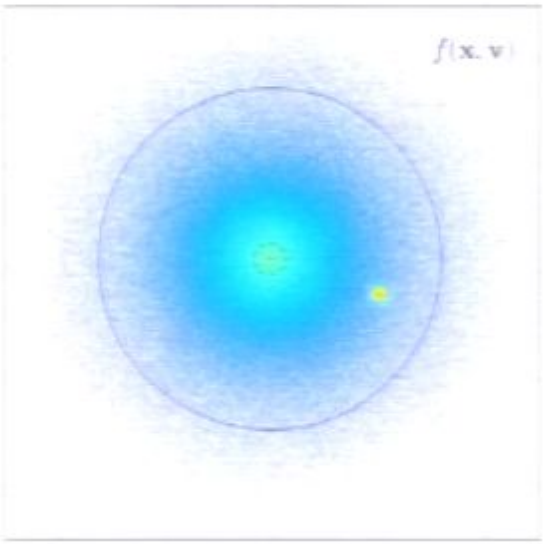
$f(\mathbf{x}, \mathbf{v})$

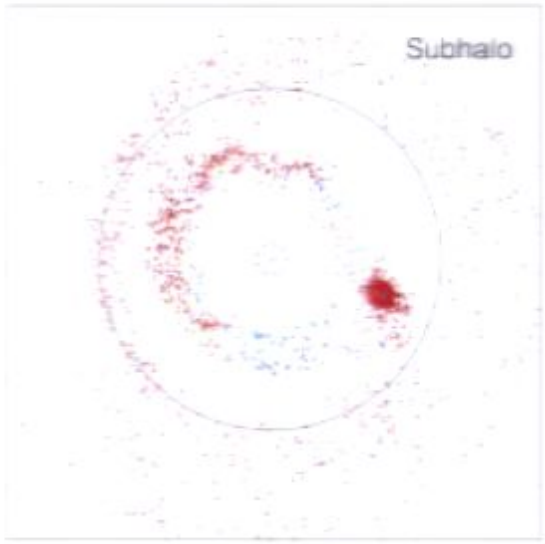
Subhalo

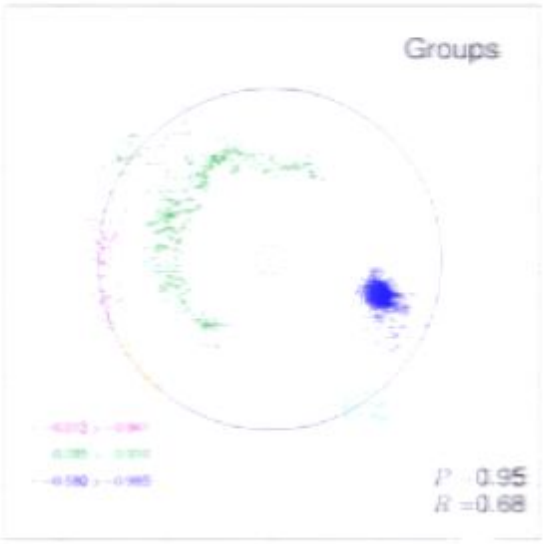
Groups
P 0.95
R =0.68

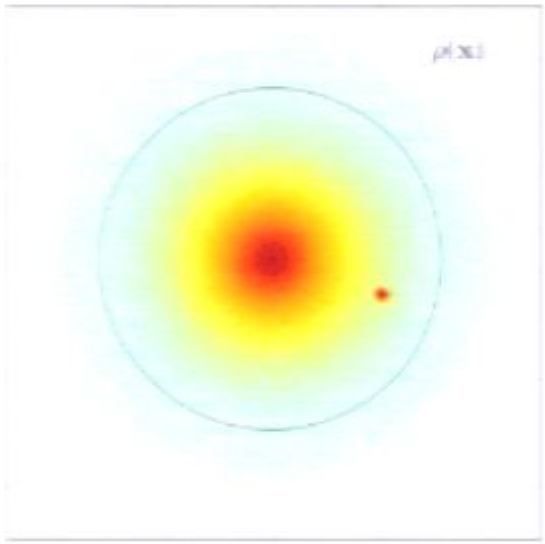
$\rho(\mathbf{x})$

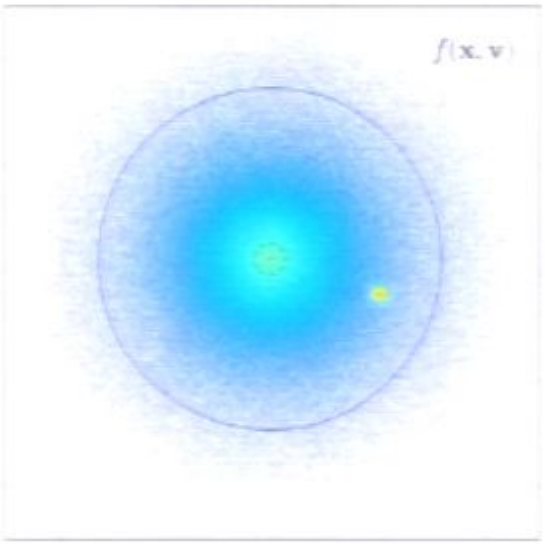
$f(\mathbf{x}, \mathbf{v})$

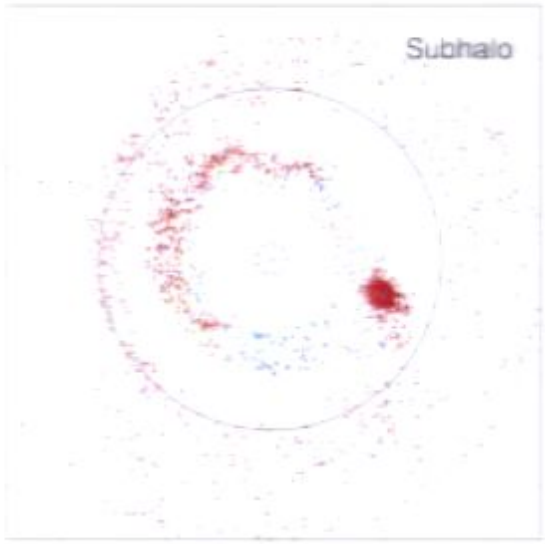
Subhalo

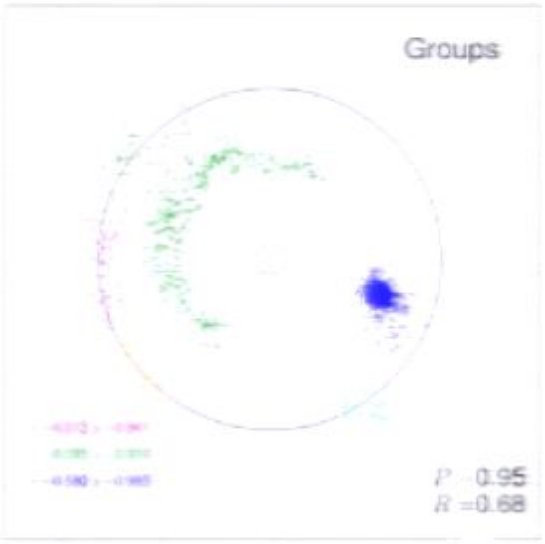
Groups
P 0.95
R =0.68

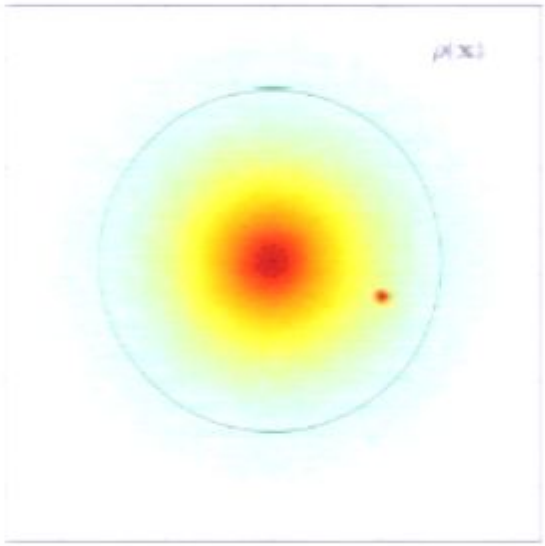
$\rho(\mathbf{x})$

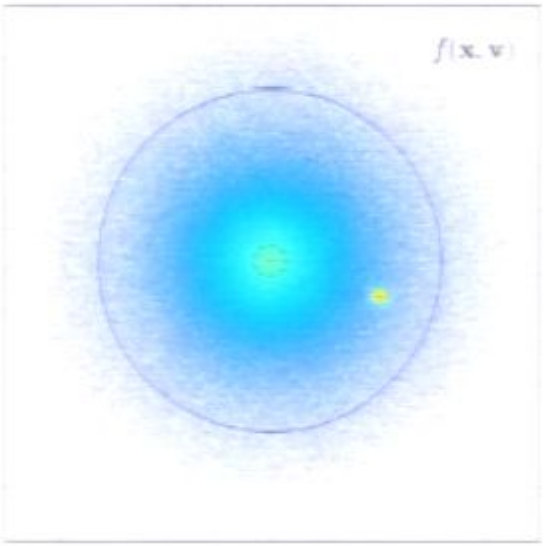
$f(\mathbf{x}, \mathbf{v})$

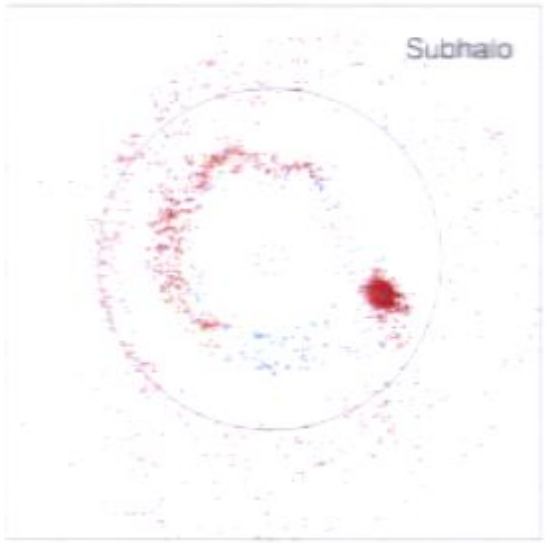
Subhalo

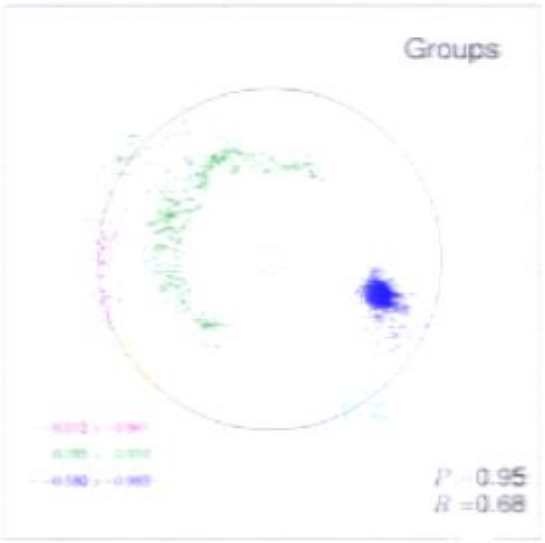
Groups
P =0.95
R =0.68

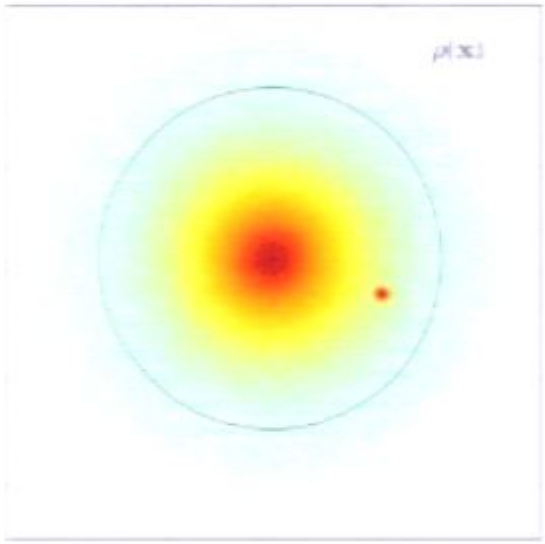
$\rho(\mathbf{x})$

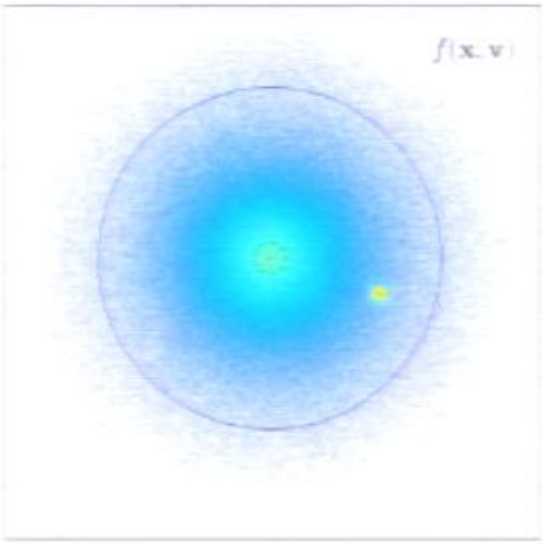
$f(\mathbf{x}, \mathbf{v})$

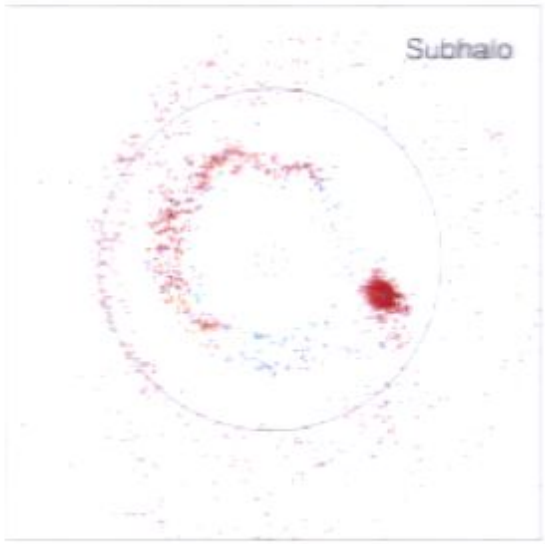
Subhalo

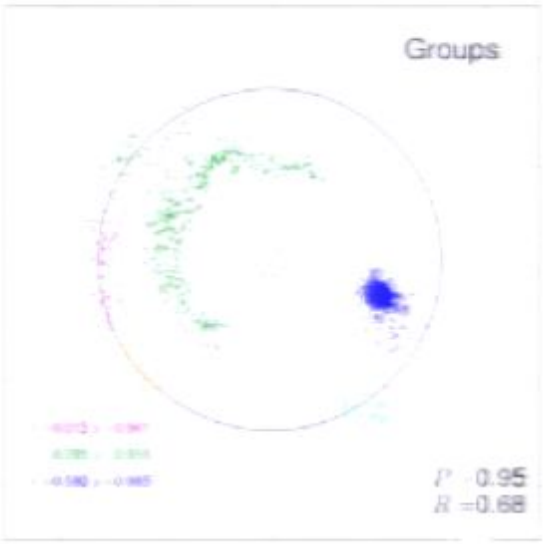
Groups
P 0.95
R =0.68

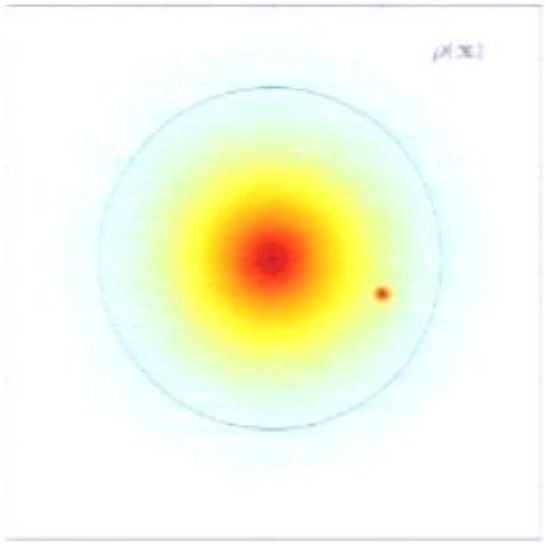
$\rho(\mathbf{x})$

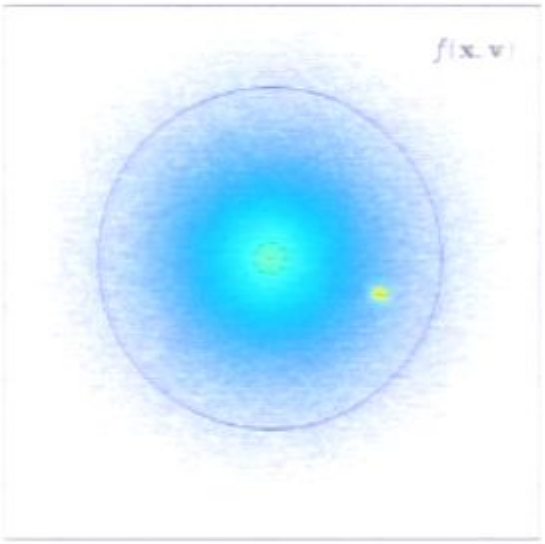
$f(\mathbf{x}, \mathbf{v})$

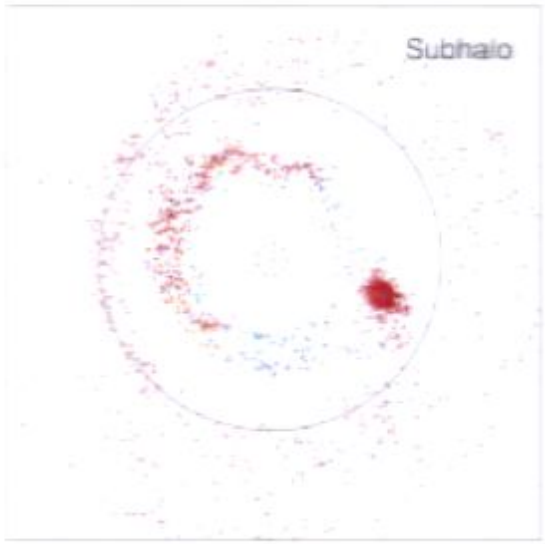
Subhalo

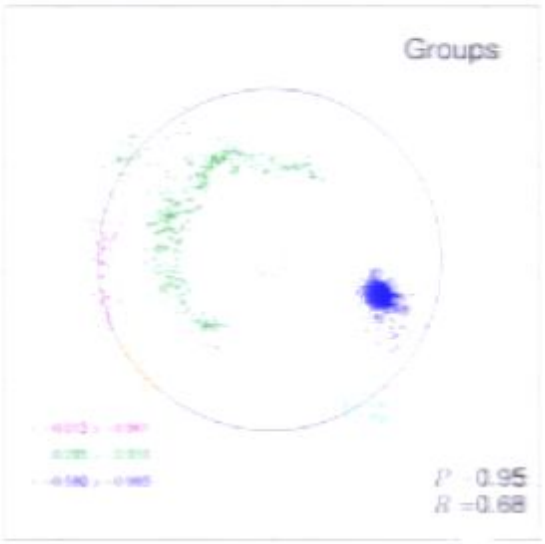
Groups
P 0.95
R =0.68

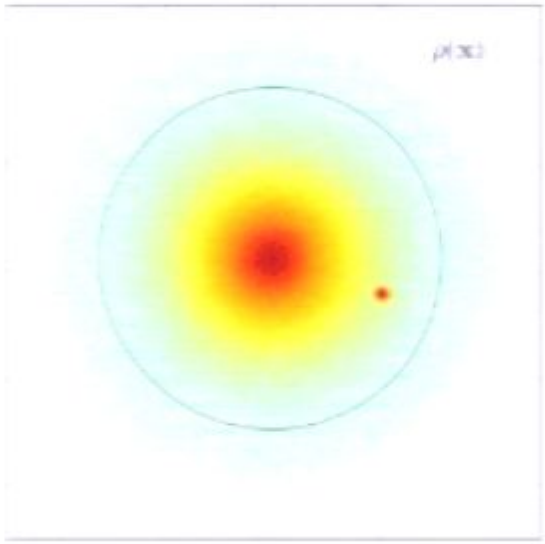
$\rho(\mathbf{x})$

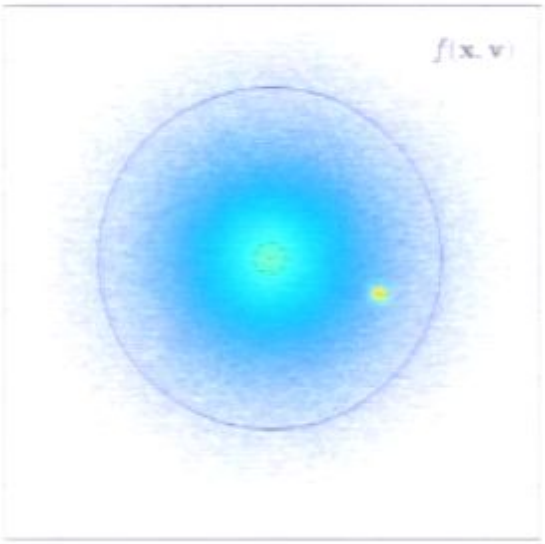
$f(\mathbf{x}, \mathbf{v})$

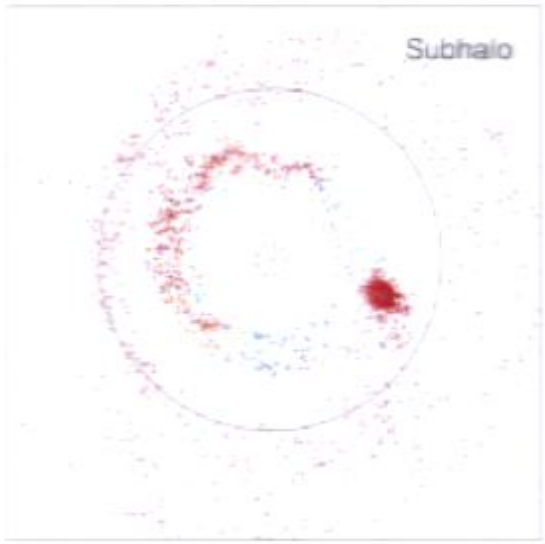
Subhalo

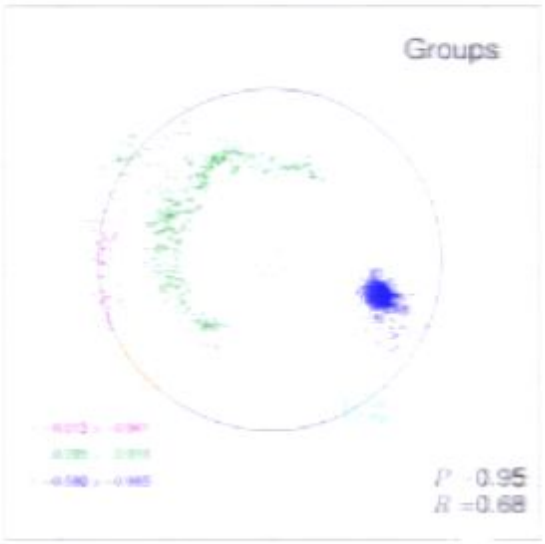
Groups
P 0.95
R =0.68

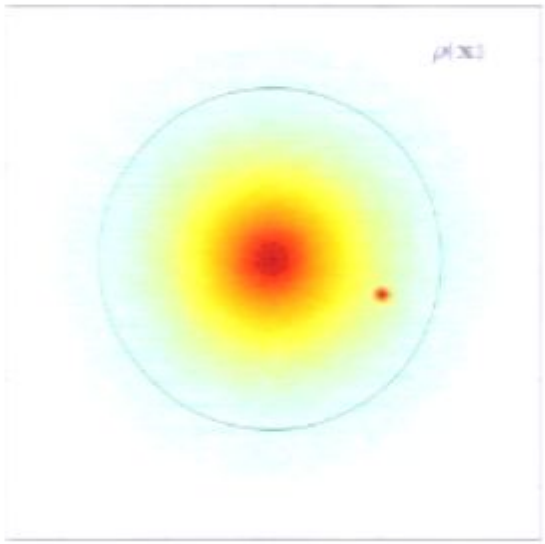
$\rho(\mathbf{x})$

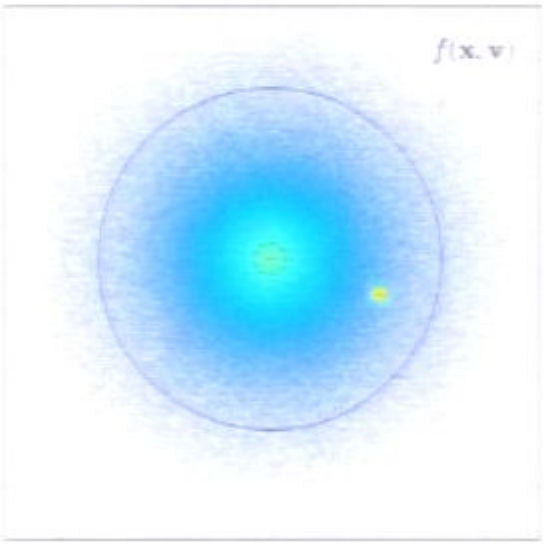
$f(\mathbf{x}, \mathbf{v})$

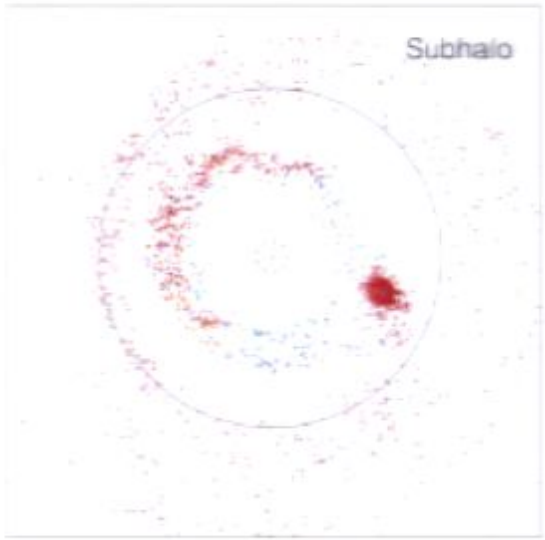
Subhalo

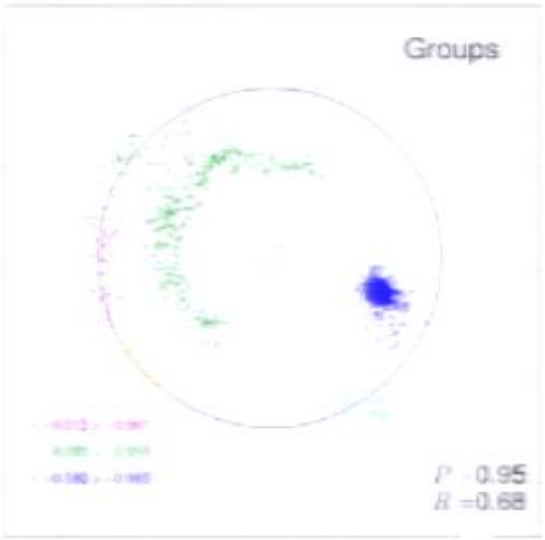
Groups
P 0.95
R =0.68

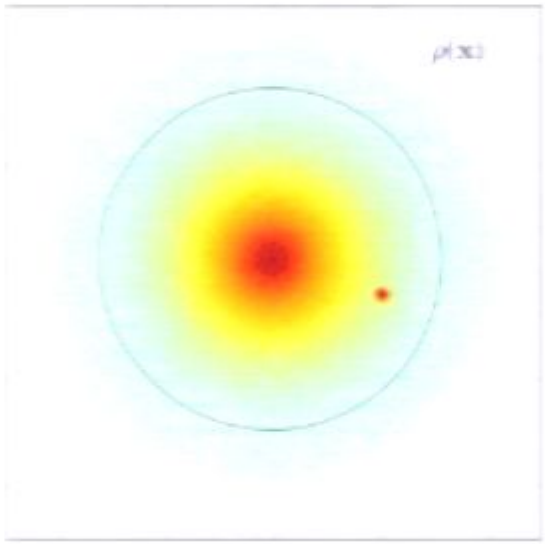
$\rho(\mathbf{x})$

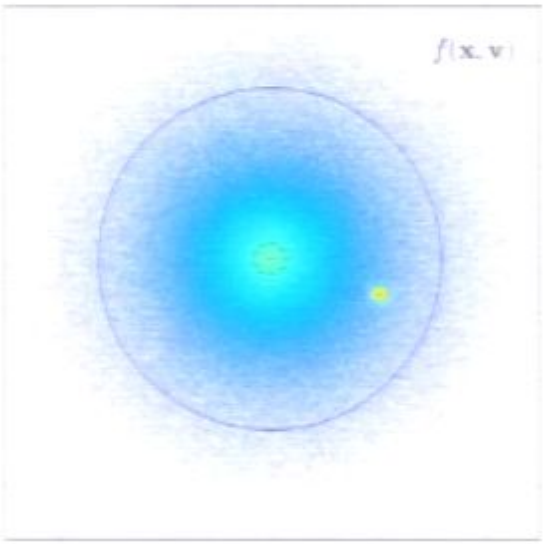
$f(\mathbf{x}, \mathbf{v})$

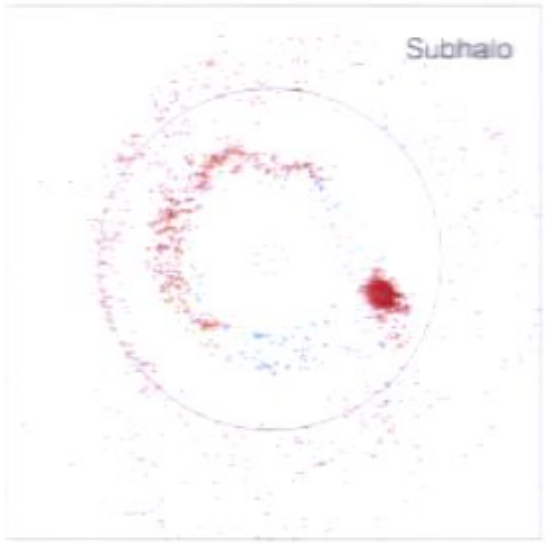
Subhalo

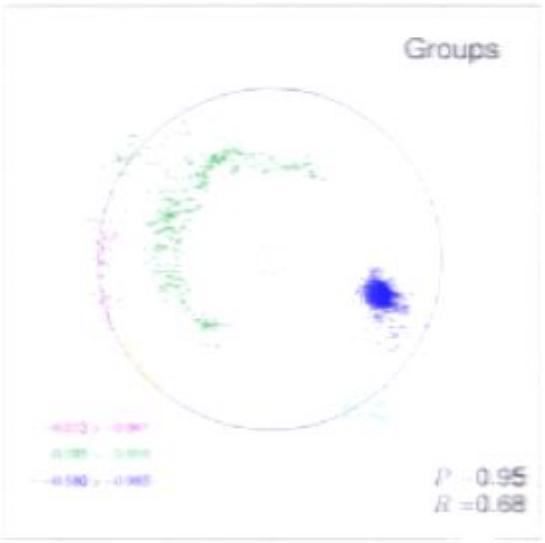
Groups
P 0.95
R =0.68

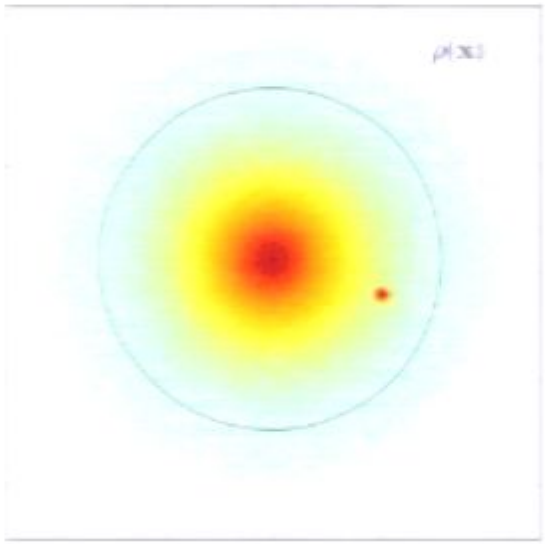
$\rho(\mathbf{x})$

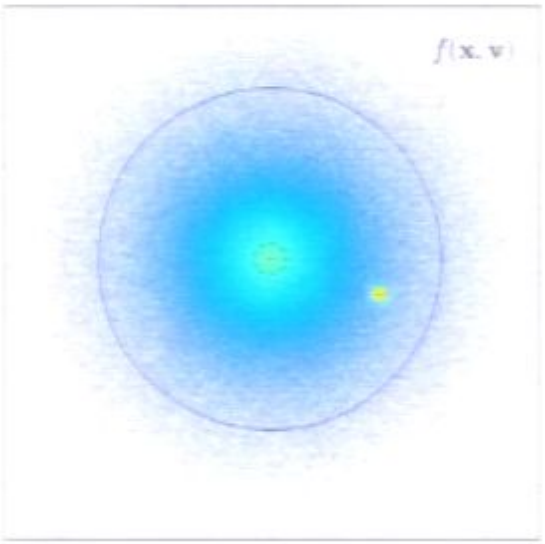
$f(\mathbf{x}, \mathbf{v})$

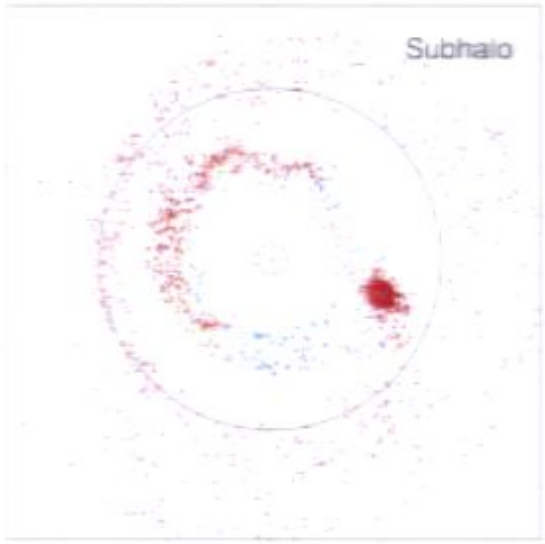
Subhalo

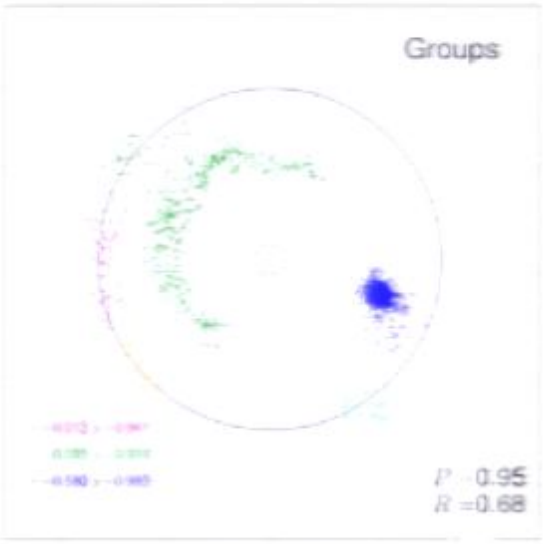
Groups
P =0.95
R =0.68

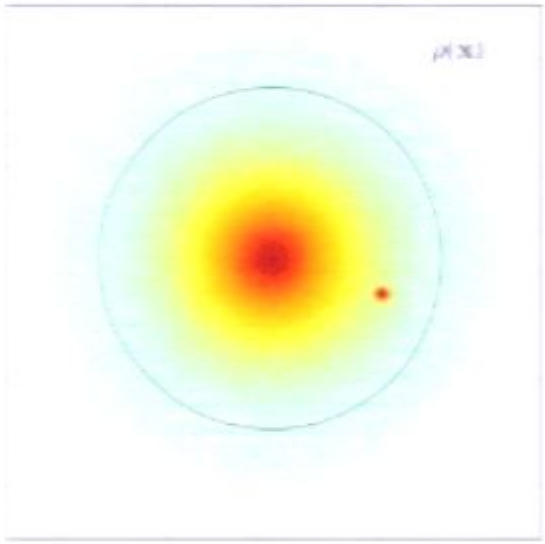
$\rho(\mathbf{x})$

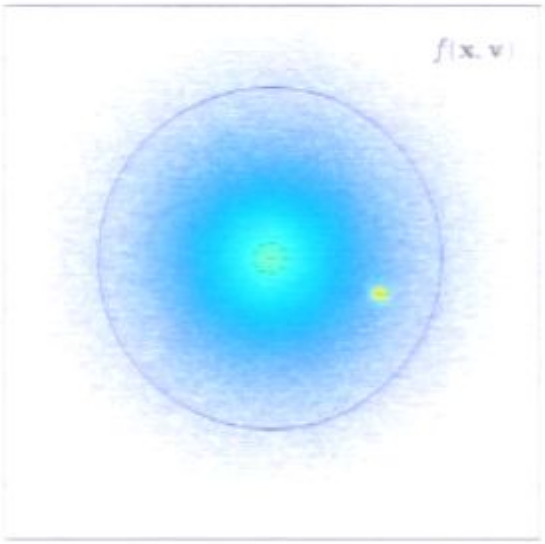
$f(\mathbf{x}, \mathbf{v})$

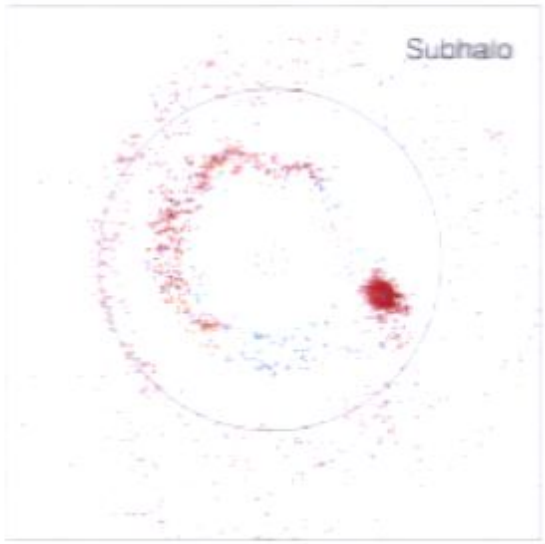
Subhalo

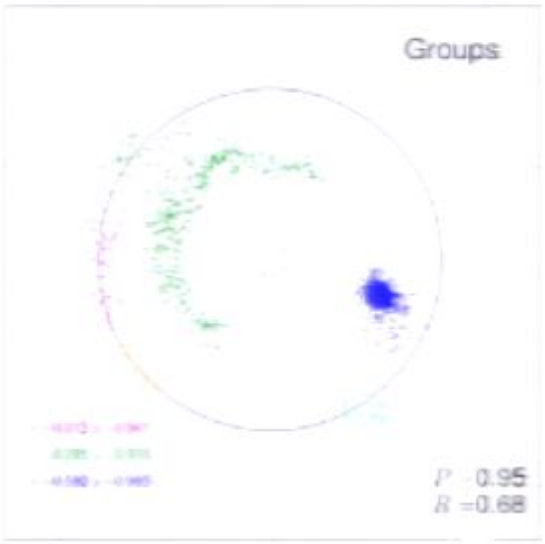
Groups
P 0.95
R =0.68

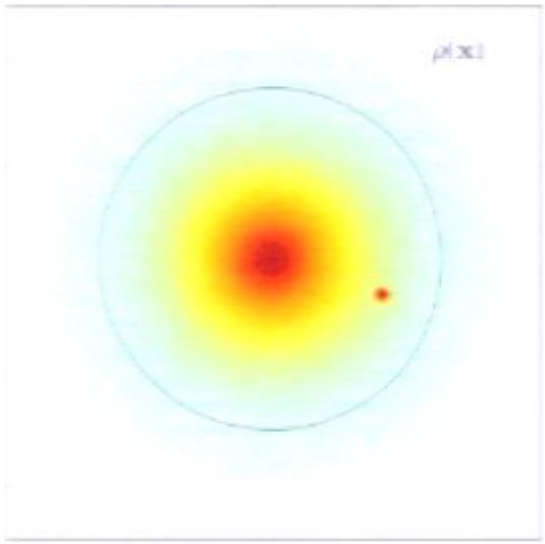
$\rho(\mathbf{x})$

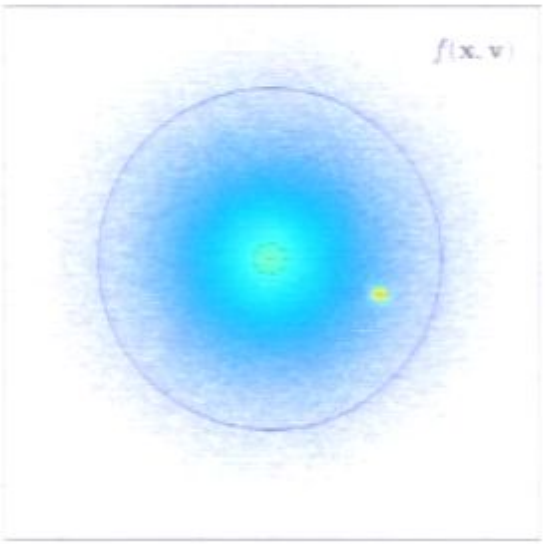
$f(\mathbf{x}, \mathbf{v})$

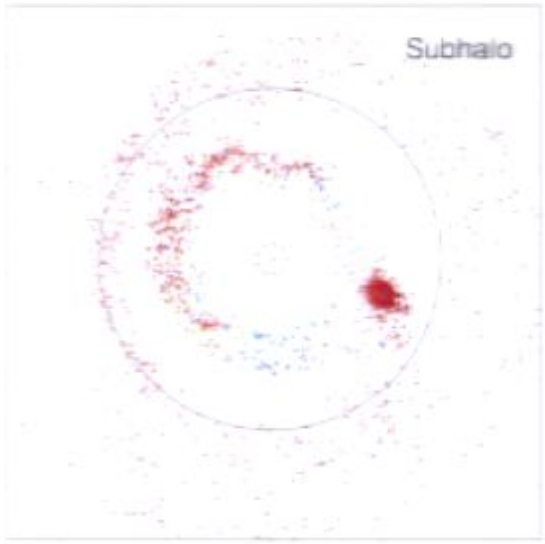
Subhalo

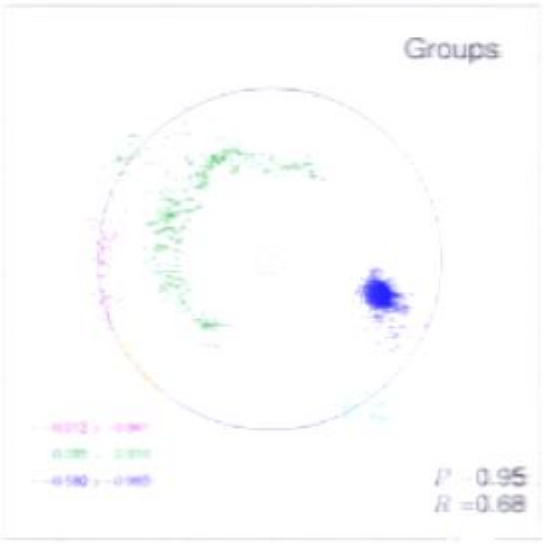
Groups
P 0.95
R =0.68

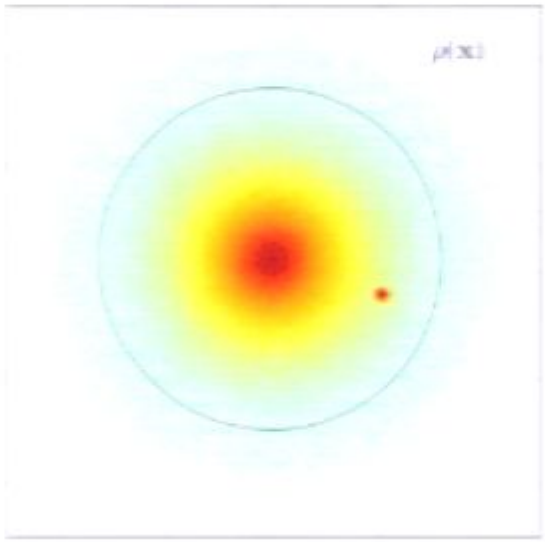
$\rho(\mathbf{x})$

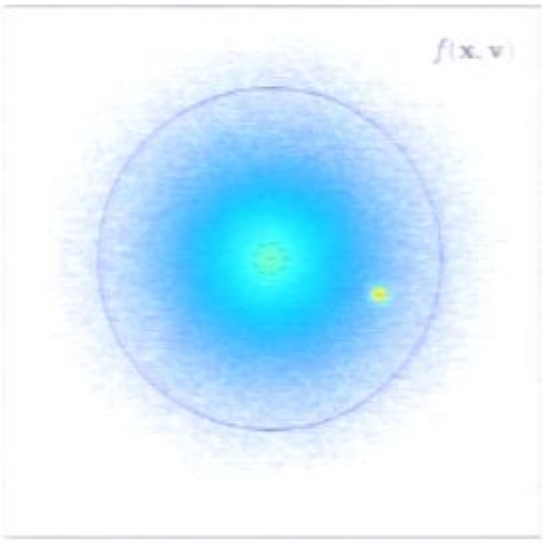
$f(\mathbf{x}, \mathbf{v})$

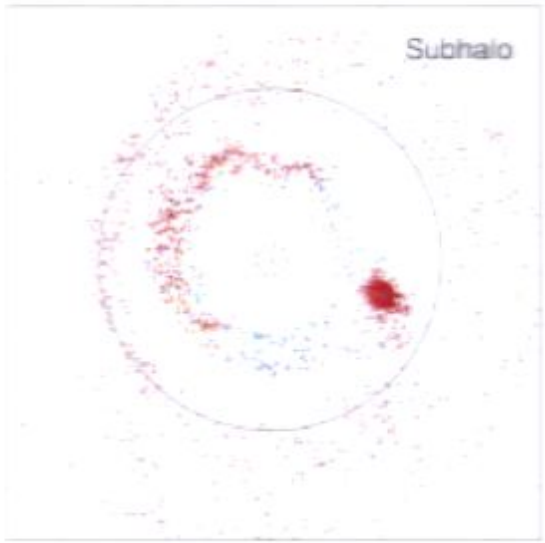
Subhalo

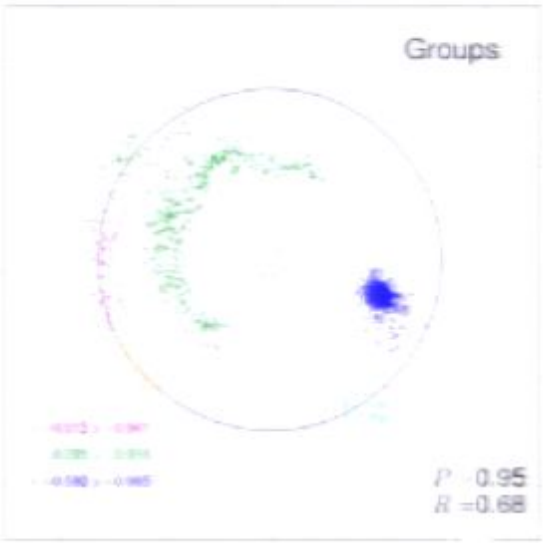
Groups
P 0.95
R =0.68

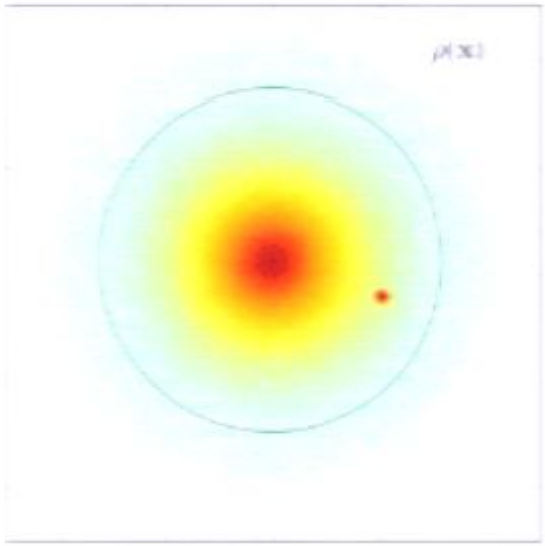
ρ(x)

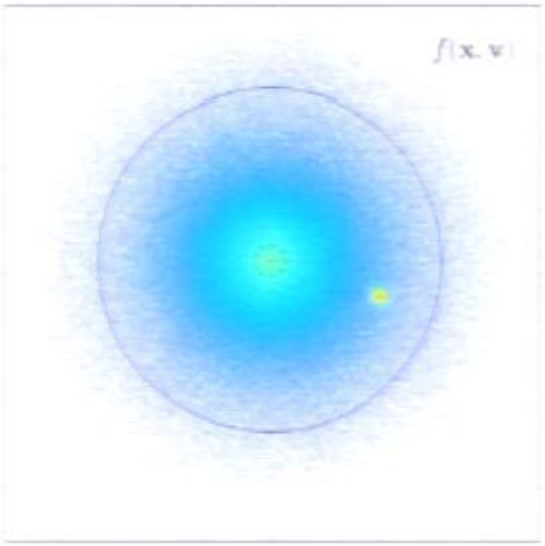
f(x, v)

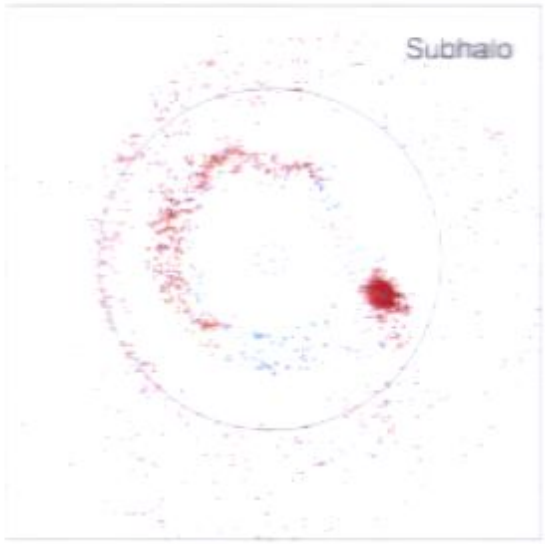
Subhalo

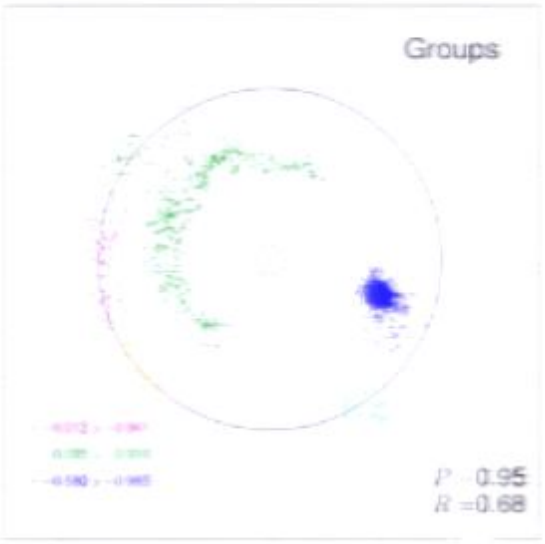
Groups
P = 0.95
R = 0.68

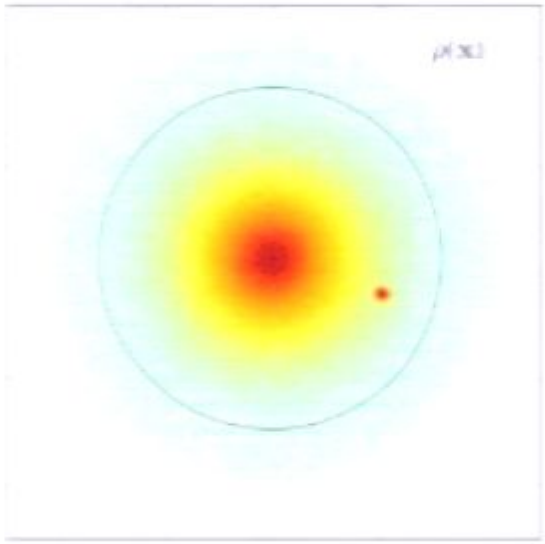

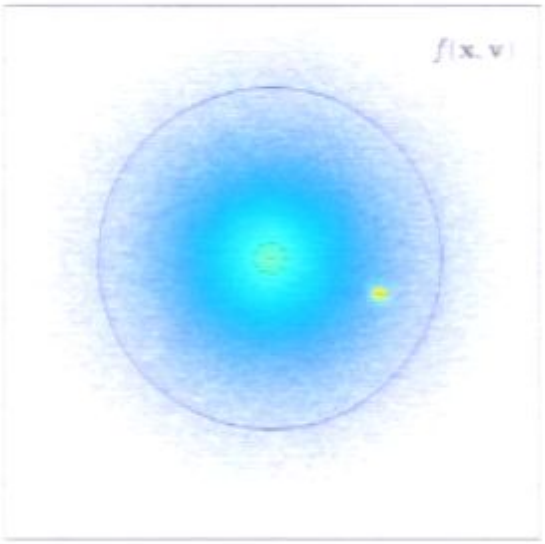

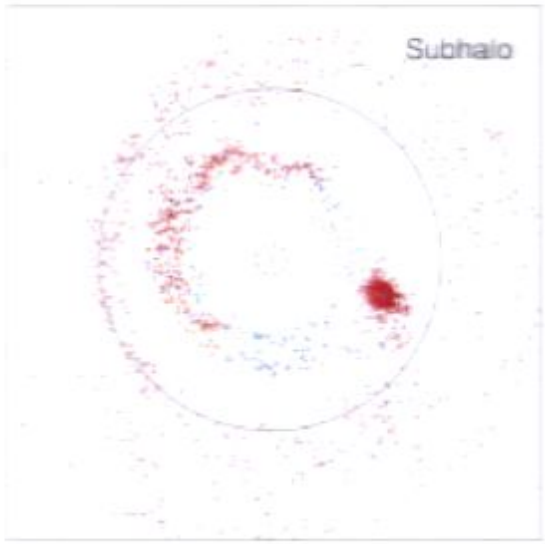
Subhalo

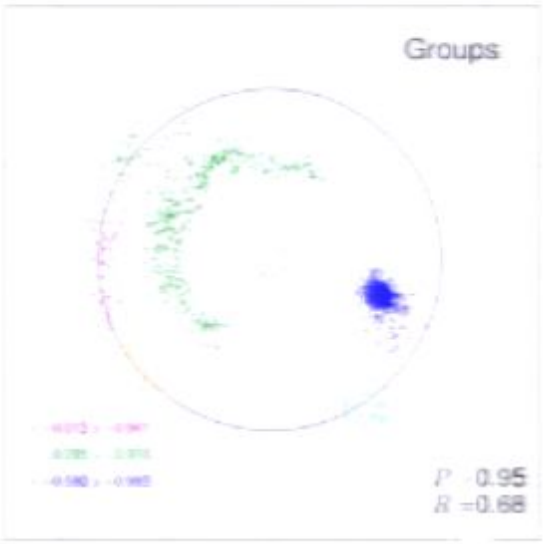
Groups
P 0.95
R =0.68

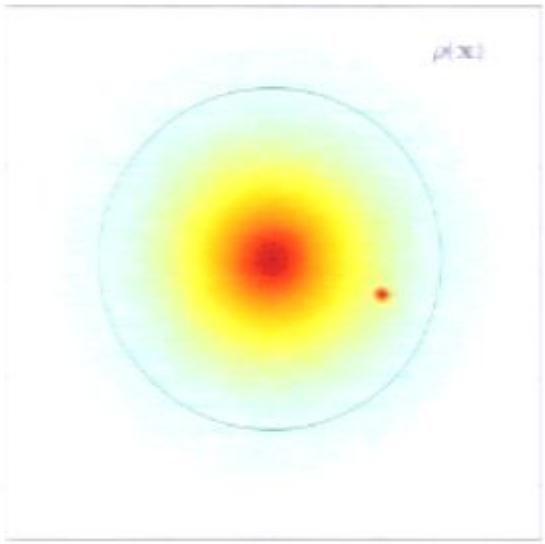
$\rho(\mathbf{x})$

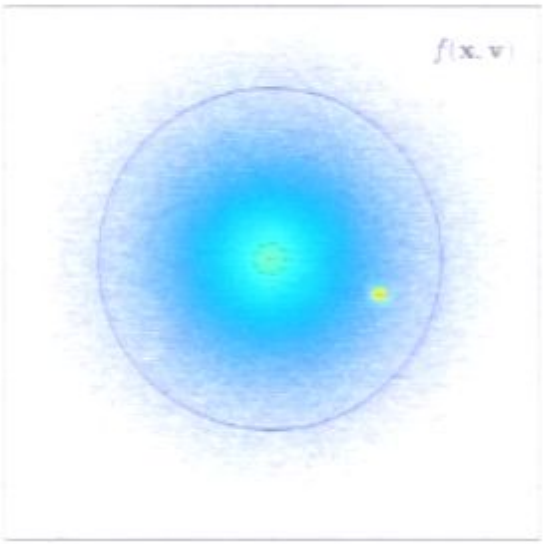
$f(\mathbf{x}, \mathbf{v})$

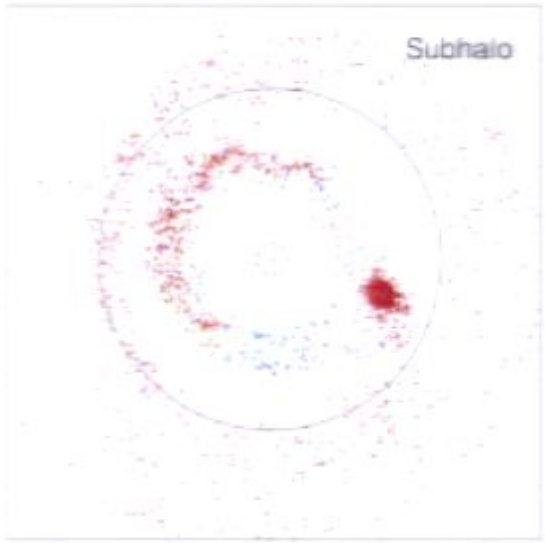
Subhalo

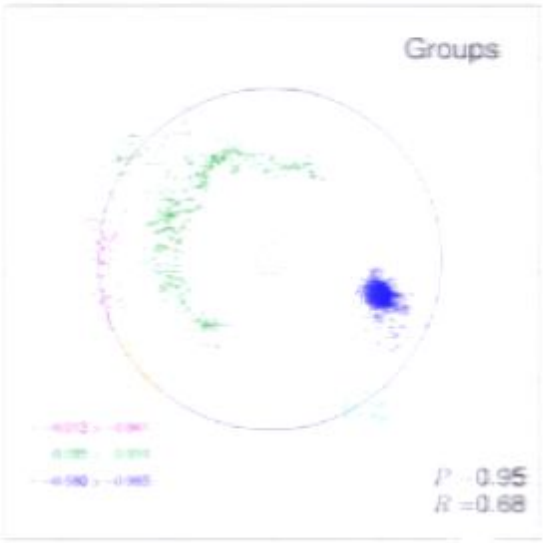
Groups
P 0.95
R =0.68

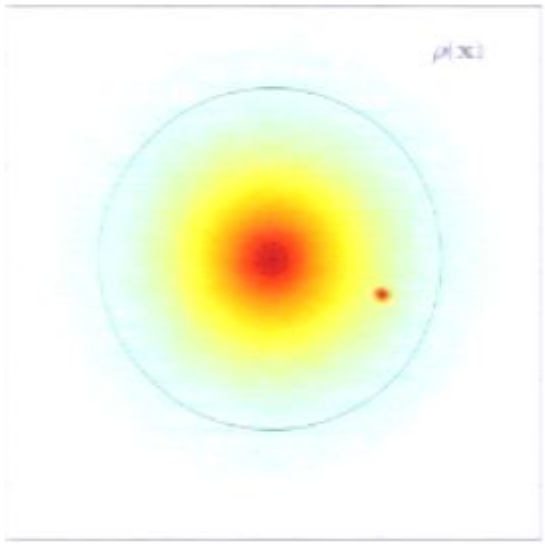
$\rho(\mathbf{x})$

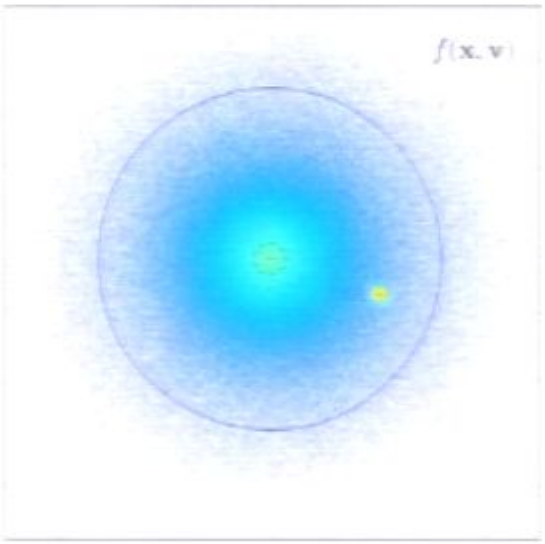
$f(\mathbf{x}, \mathbf{v})$

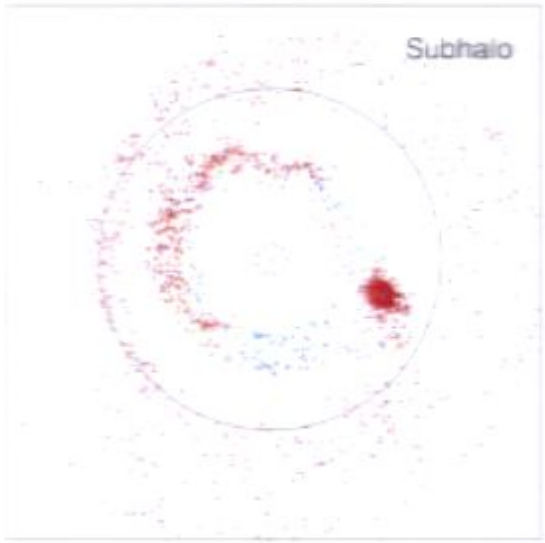
Subhalo

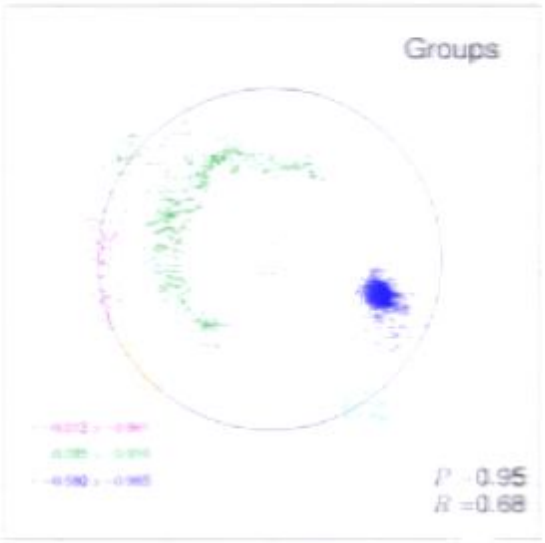
Groups
P 0.95
R =0.68

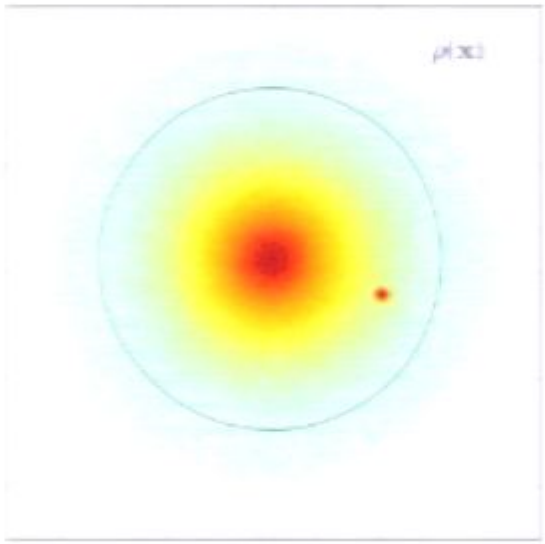
$\rho(\mathbf{x})$

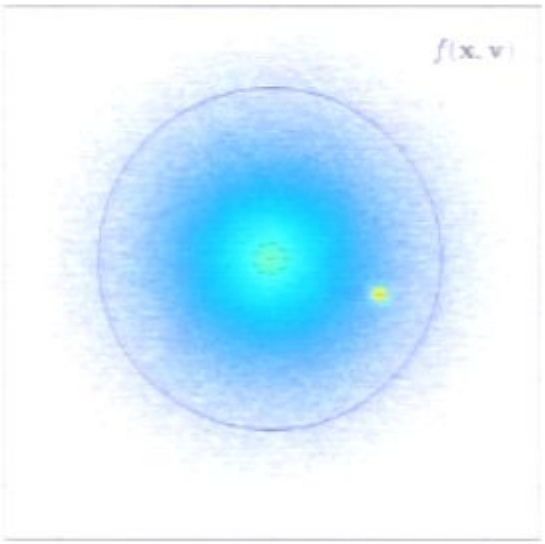
$f(\mathbf{x}, \mathbf{v})$

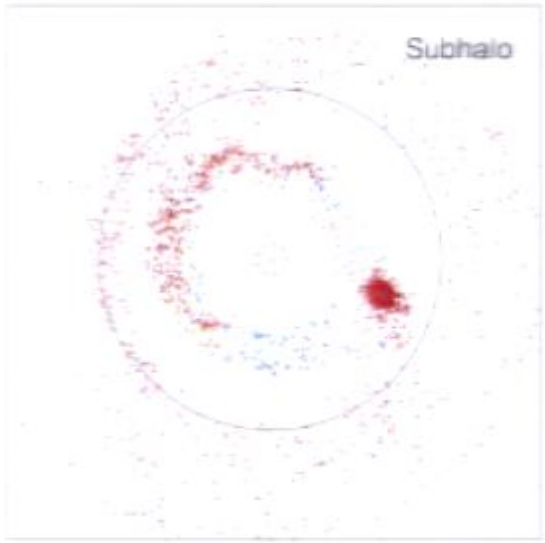
Subhalo

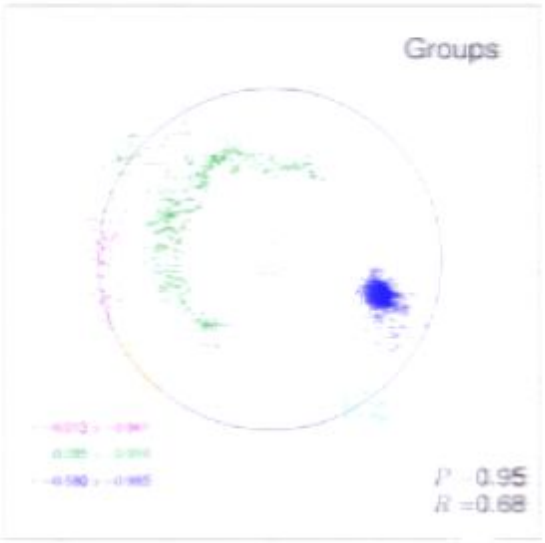
Groups
P 0.95
R =0.68

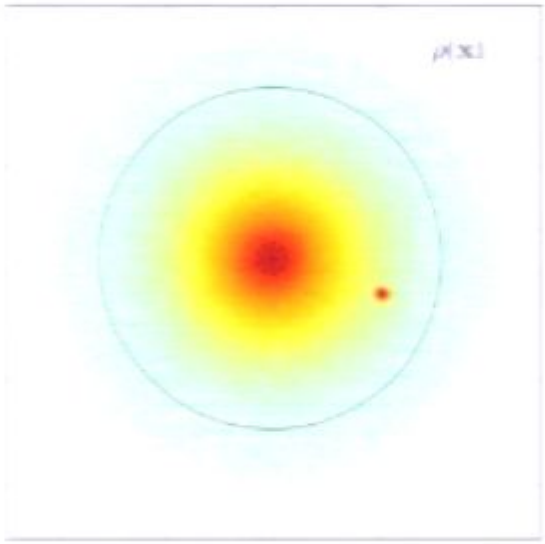
$\rho(\mathbf{x})$

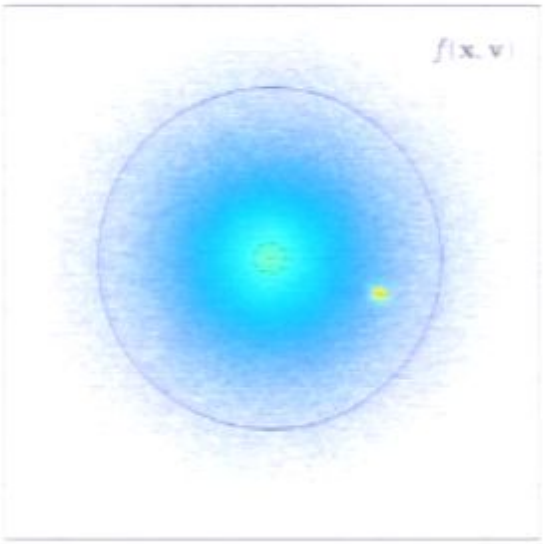
$f(\mathbf{x}, \mathbf{v})$

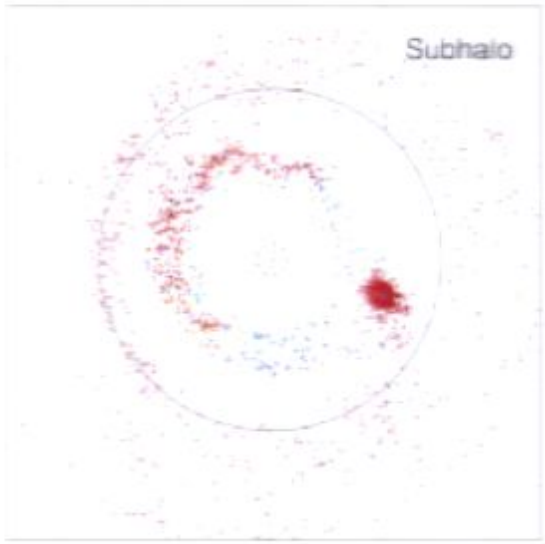
Subhalo

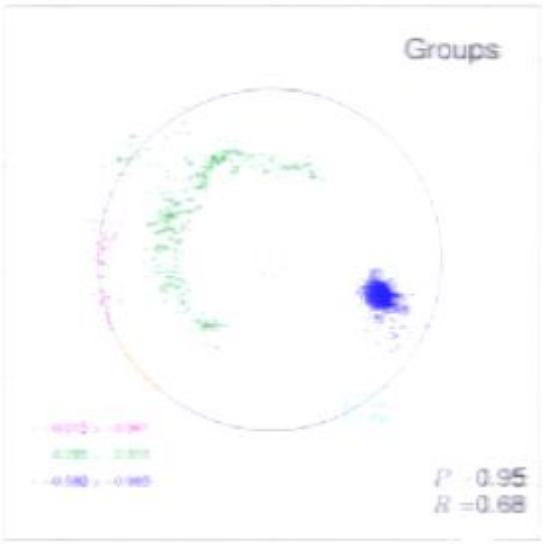
Groups
P 0.95
R =0.68

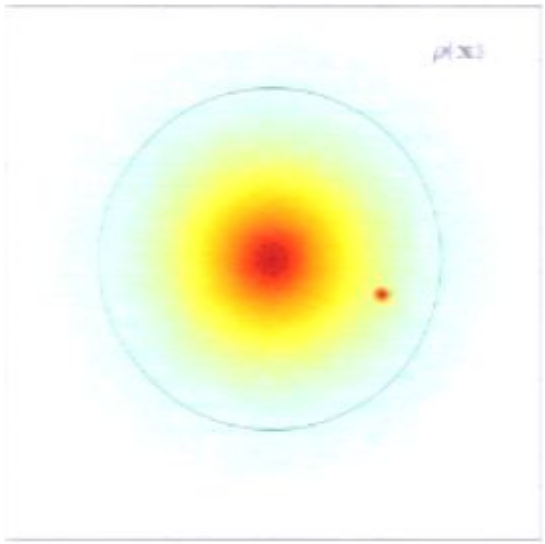
$\rho(\mathbf{x})$

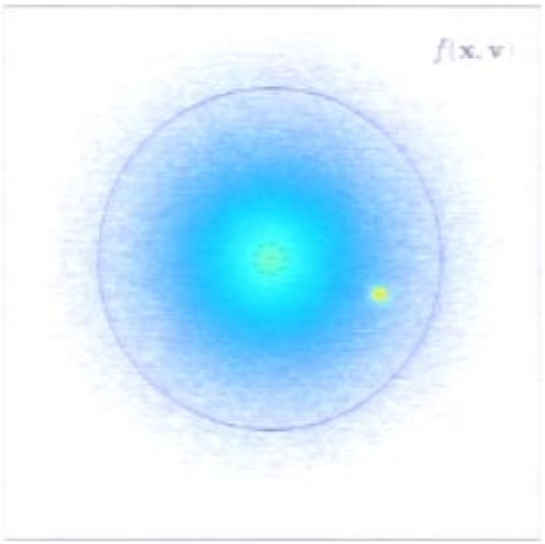
$f(\mathbf{x}, \mathbf{v})$

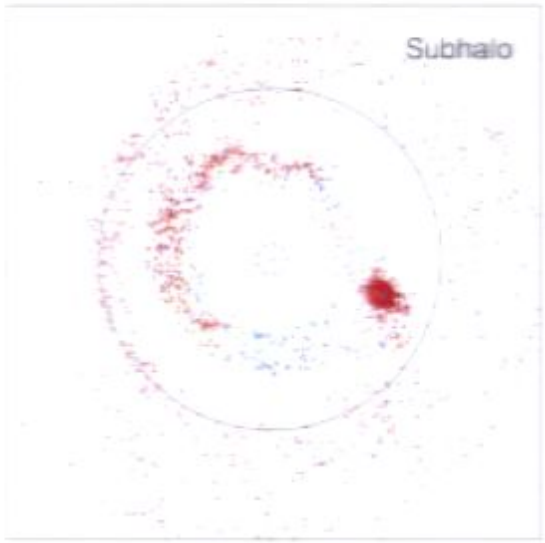
Subhalo

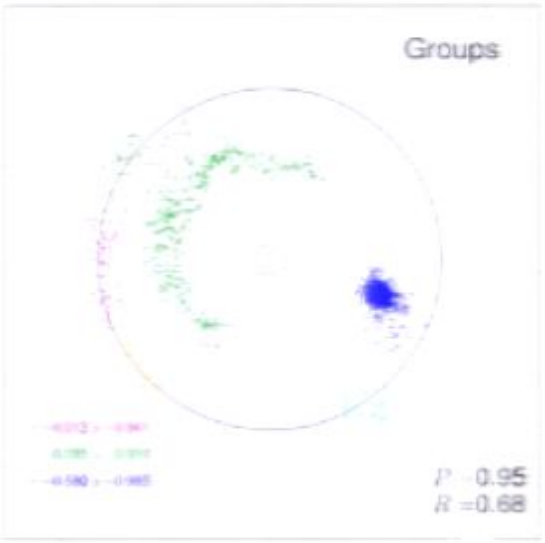
Groups
P 0.95
R =0.68

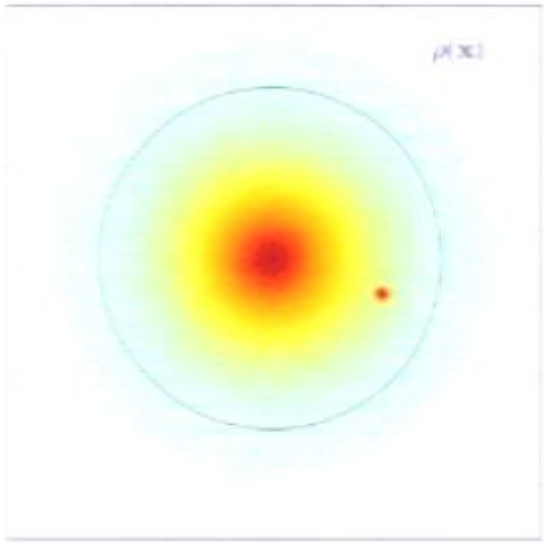
$\rho(\mathbf{x})$

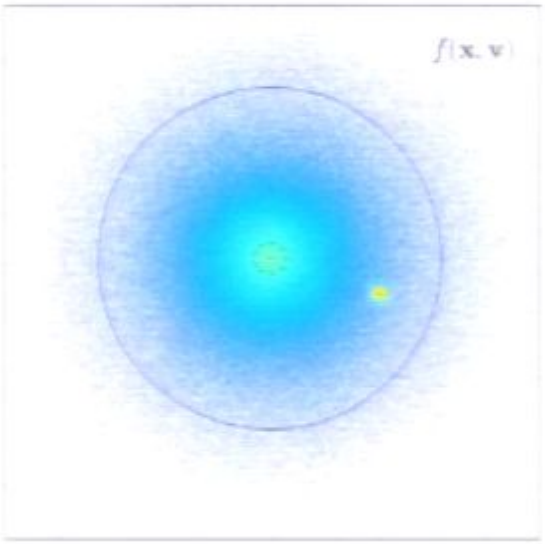
$f(\mathbf{x}, \mathbf{v})$

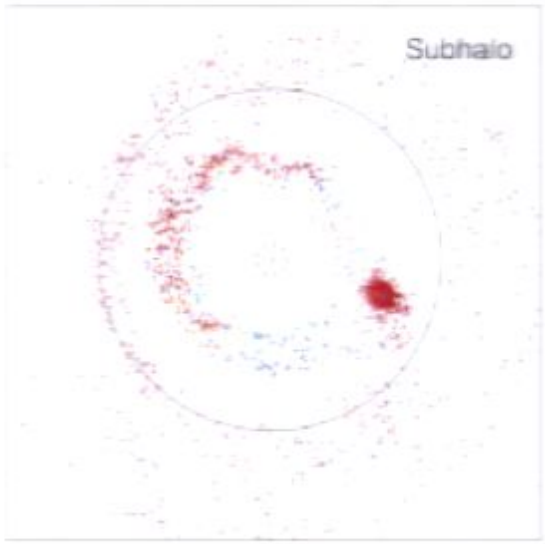
Subhalo

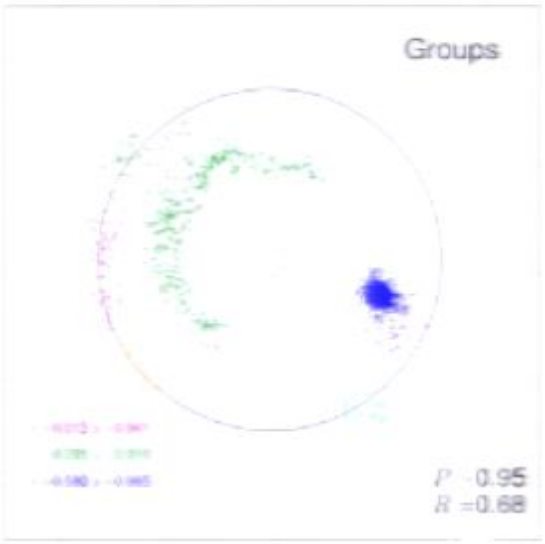
Groups
P 0.95
R =0.68

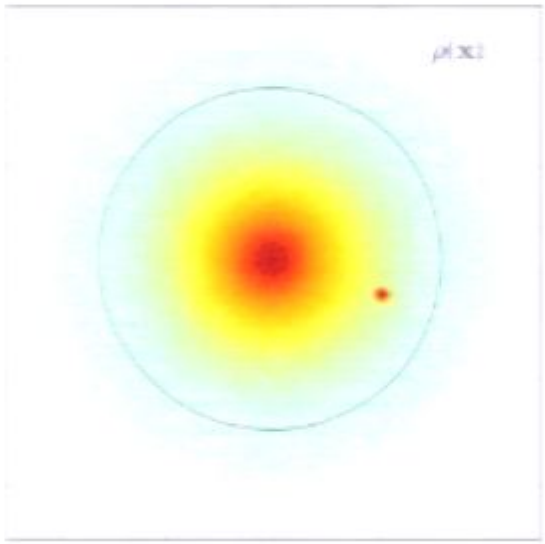
$\rho(\mathbf{x})$

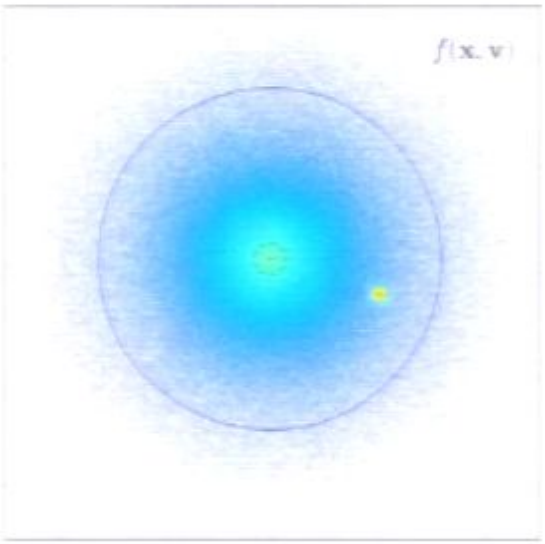
$f(\mathbf{x}, \mathbf{v})$

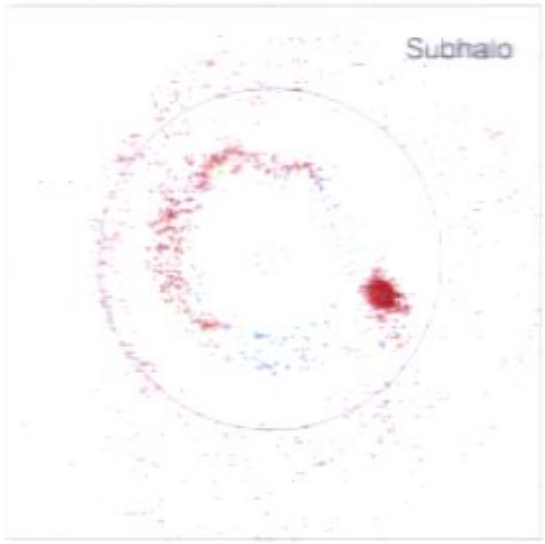
Subhalo

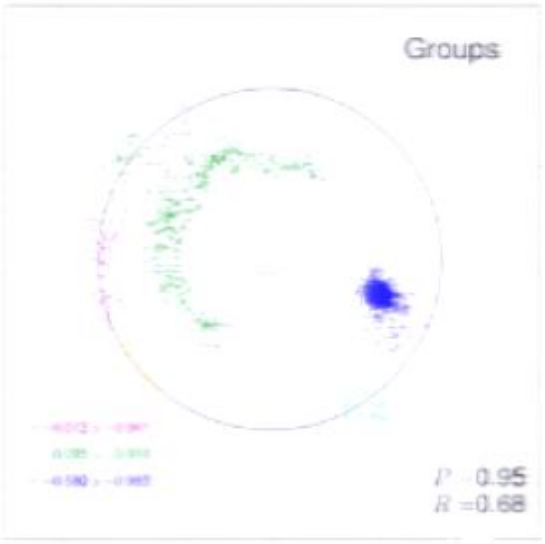
Groups
P 0.95
R =0.68

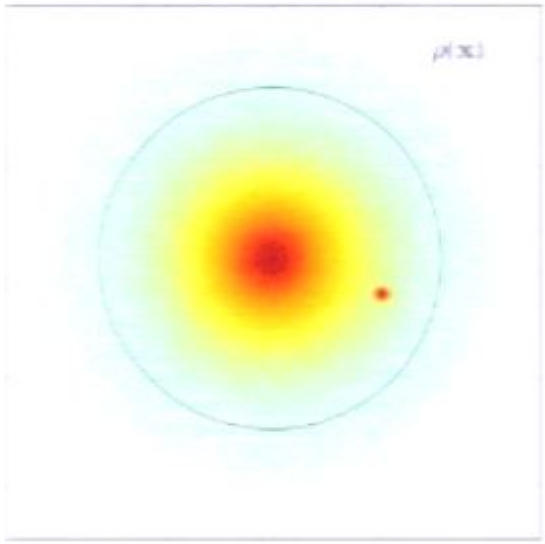
$\rho(\mathbf{x})$

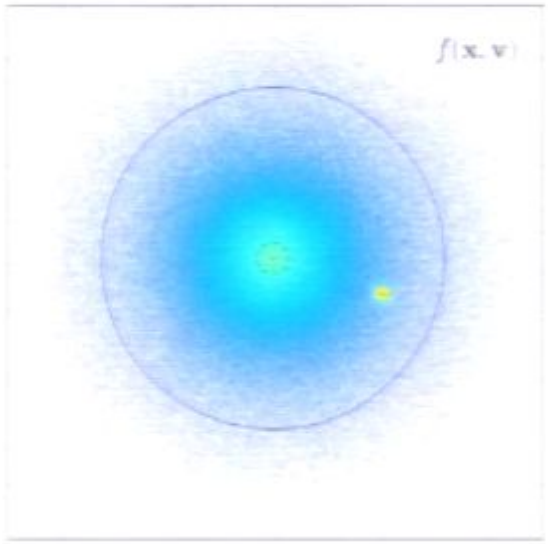
$f(\mathbf{x}, \mathbf{v})$

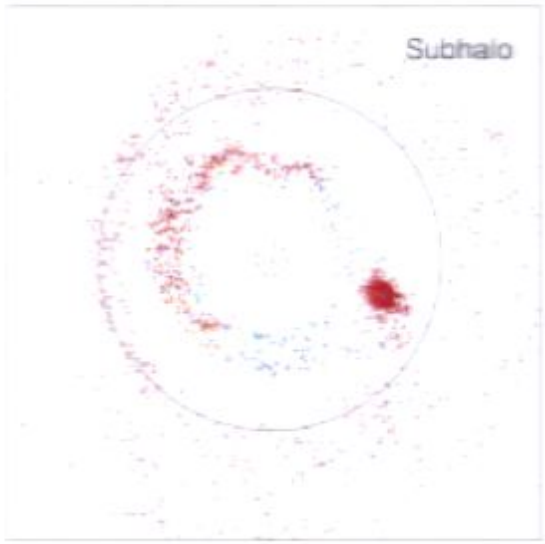
Subhalo

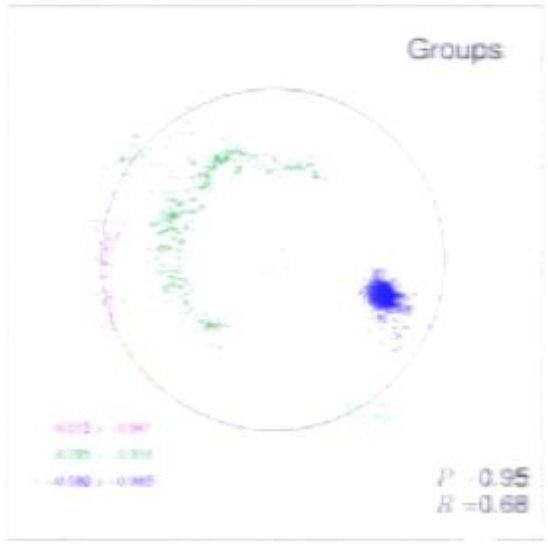
Groups
P 0.95
R =0.68

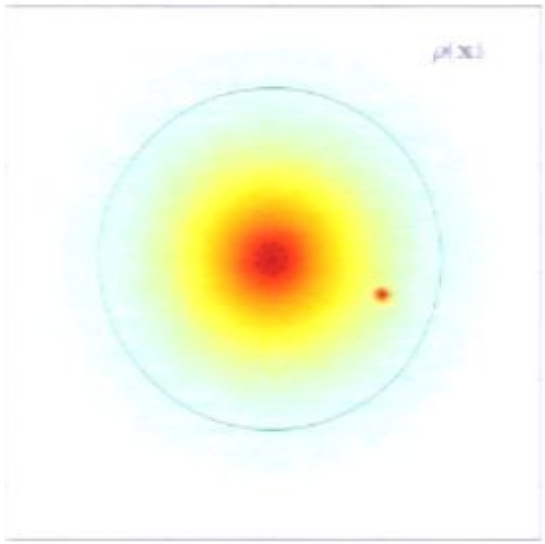
$\rho(\mathbf{x})$

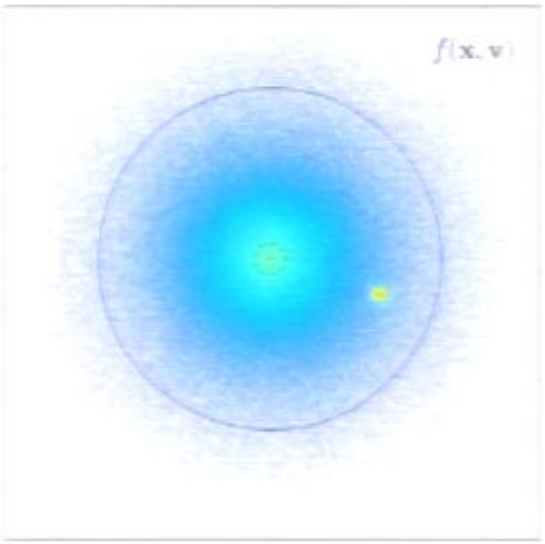
$f(\mathbf{x}, \mathbf{v})$

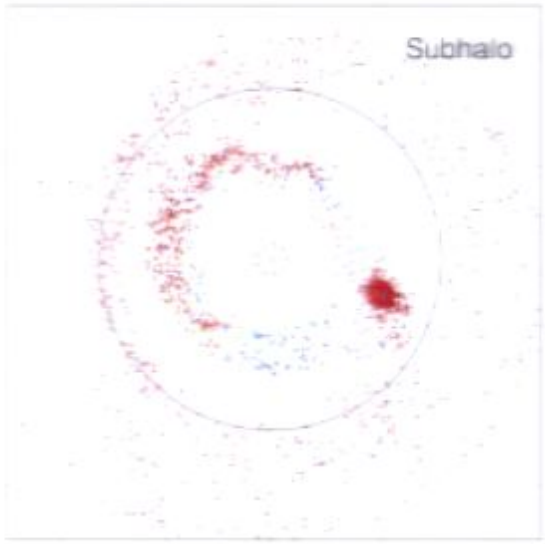
Subhalo

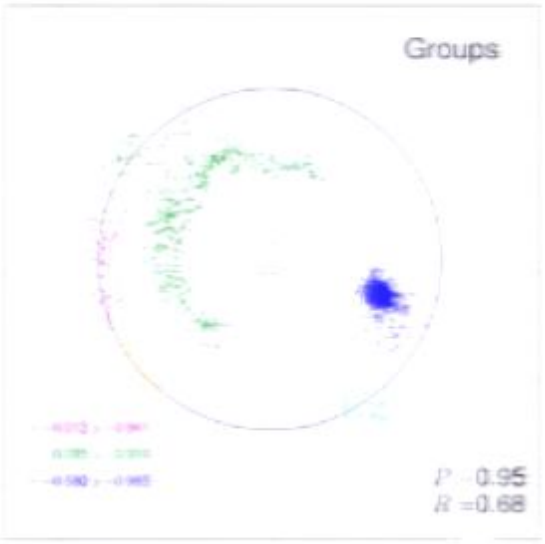
Groups
P 0.95
R =0.68

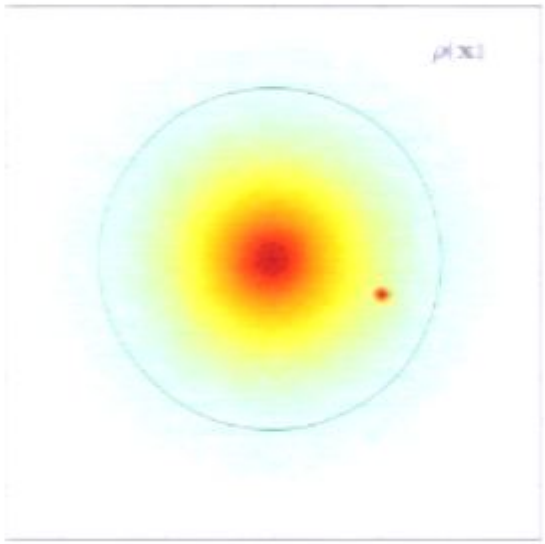
$\rho(\mathbf{x})$

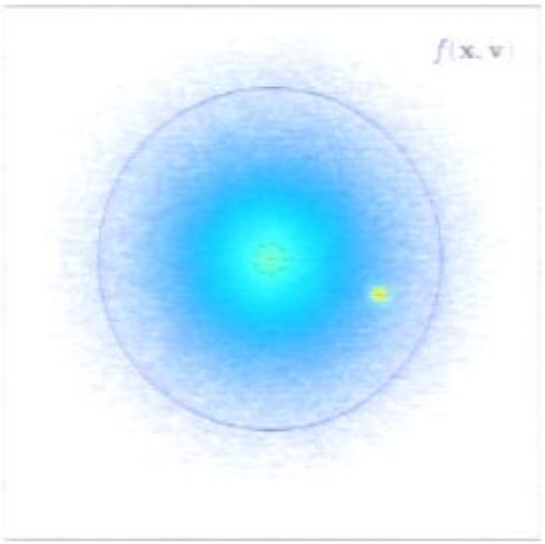
$f(\mathbf{x}, \mathbf{v})$

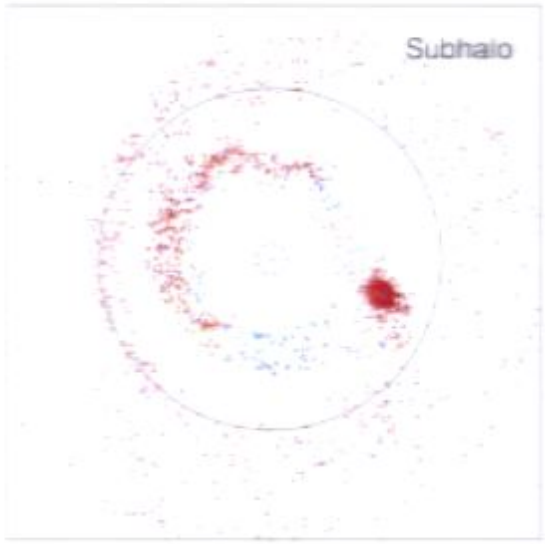
Subhalo

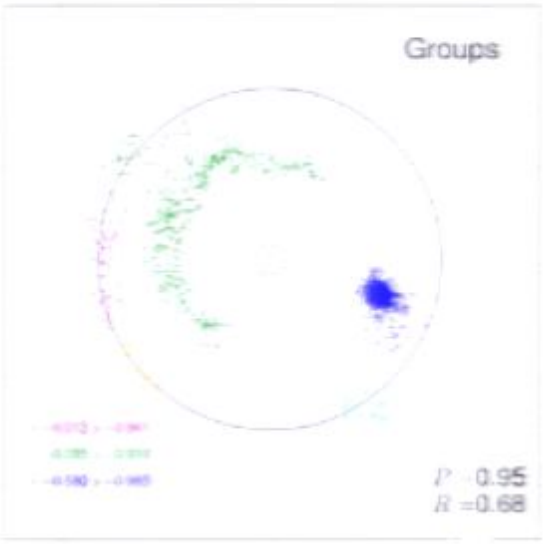
Groups
P 0.95
R =0.68

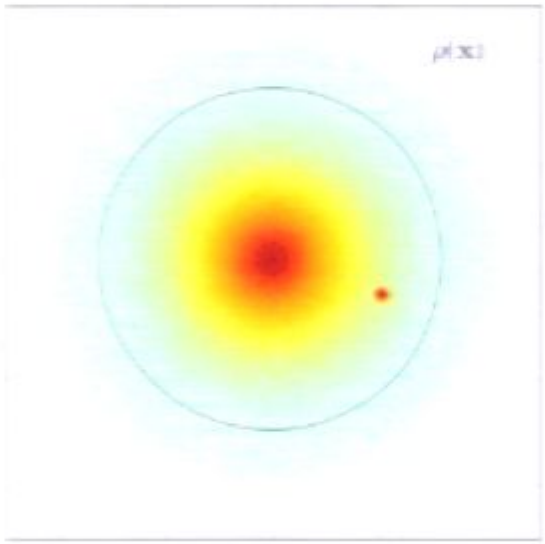
$\rho(\mathbf{x})$

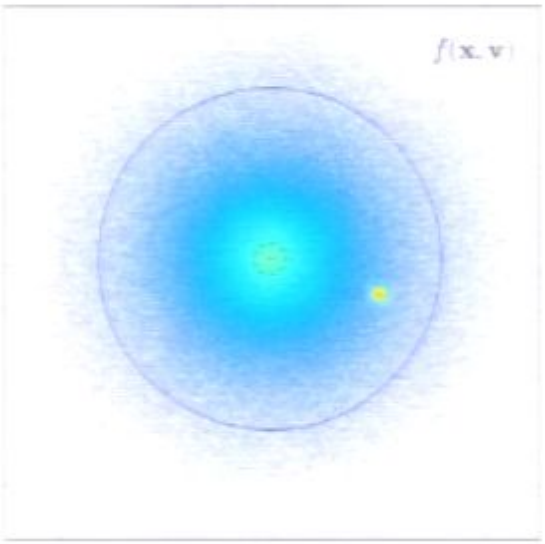
$f(\mathbf{x}, \mathbf{v})$

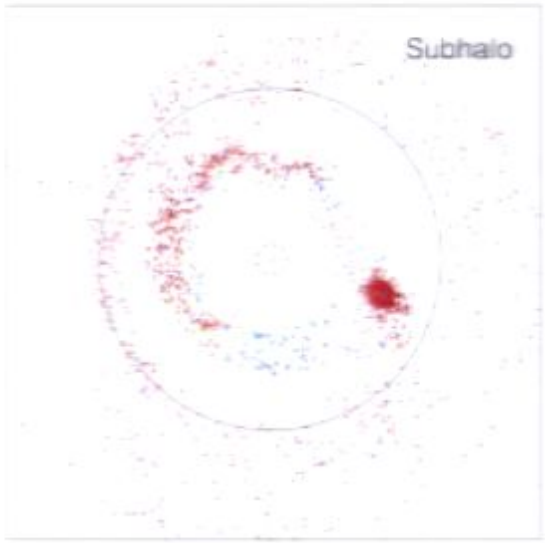
Subhalo

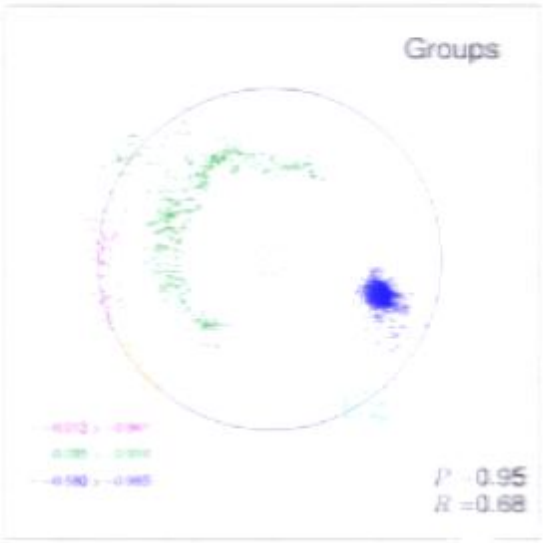
Groups
P 0.95
R =0.68

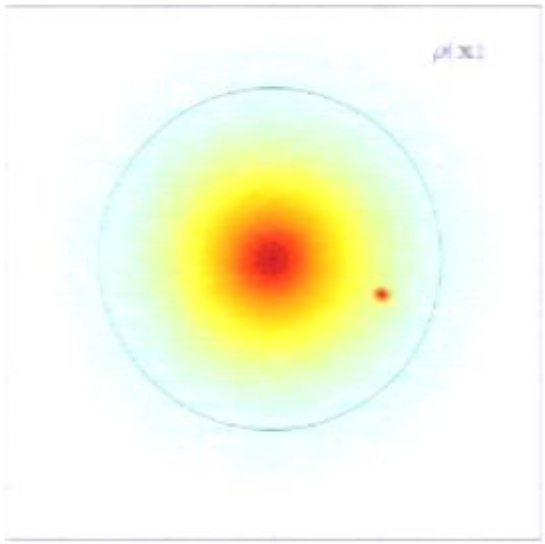
$\rho(\mathbf{x})$

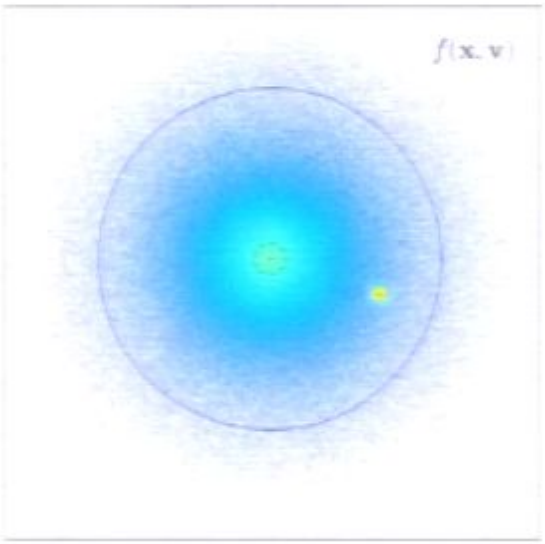
$f(\mathbf{x}, \mathbf{v})$

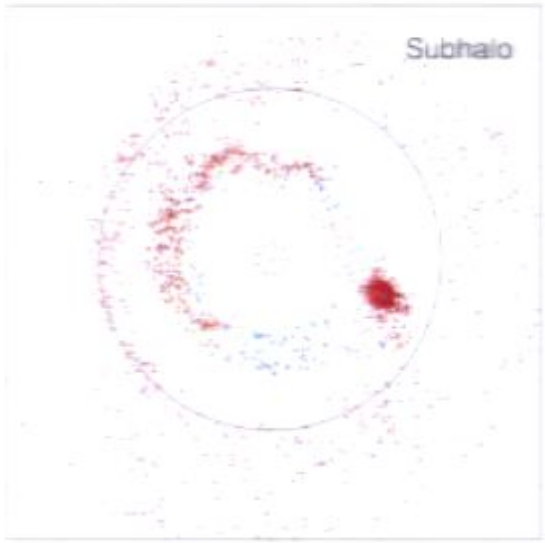
Subhalo

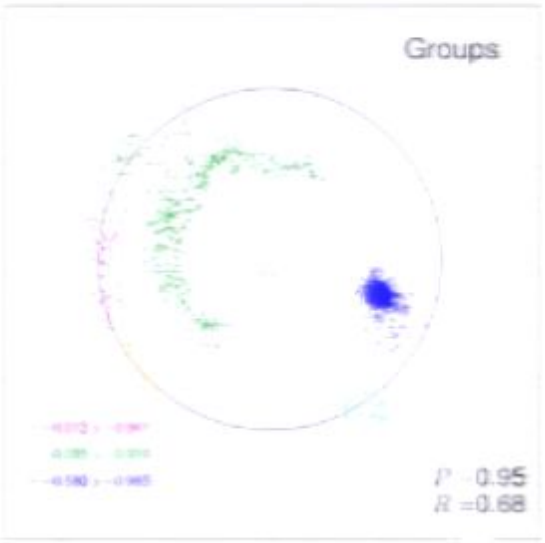
Groups
P 0.95
R =0.68

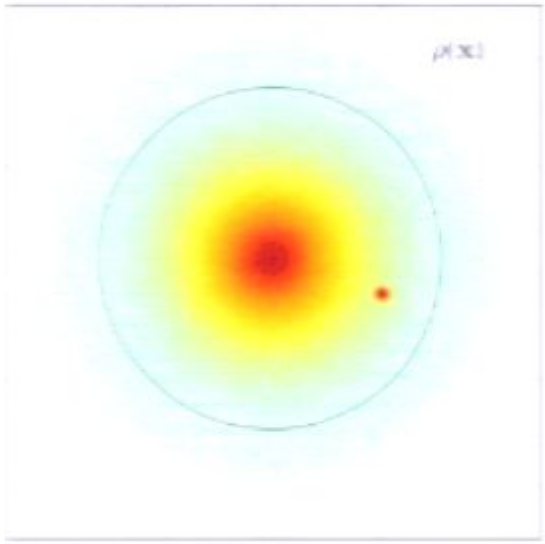
$\rho(\mathbf{x})$

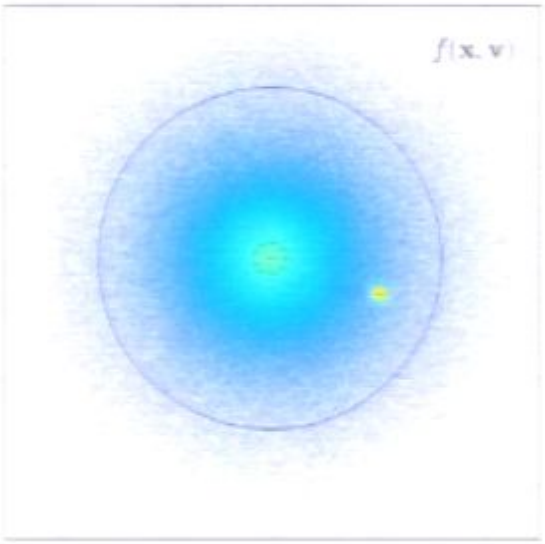
$f(\mathbf{x}, \mathbf{v})$

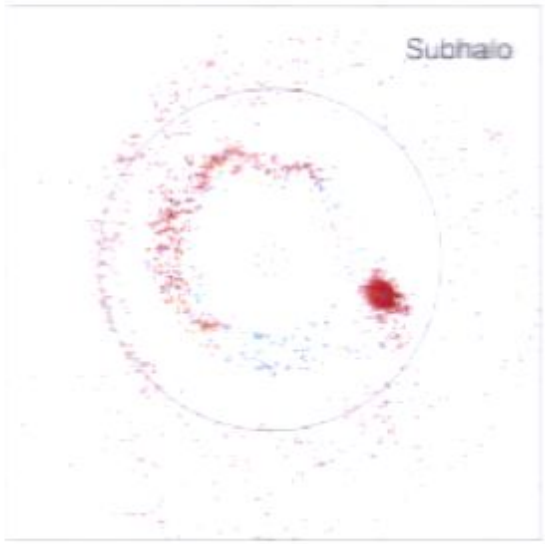
Subhalo

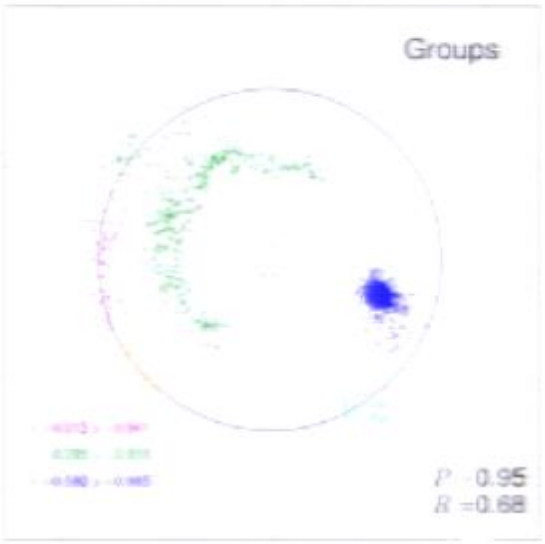
Groups
P 0.95
R =0.68

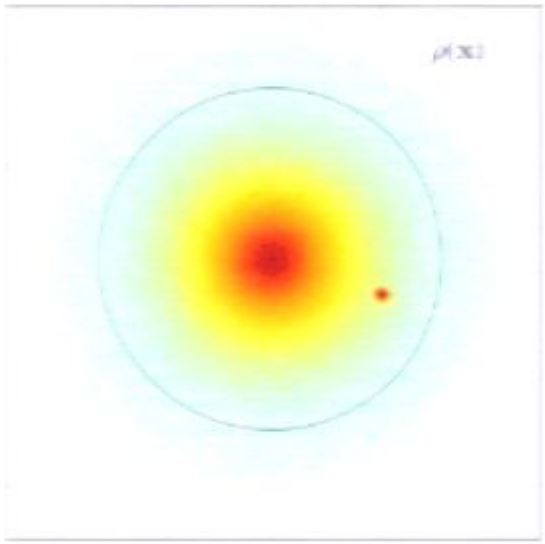
$\rho(\mathbf{x})$

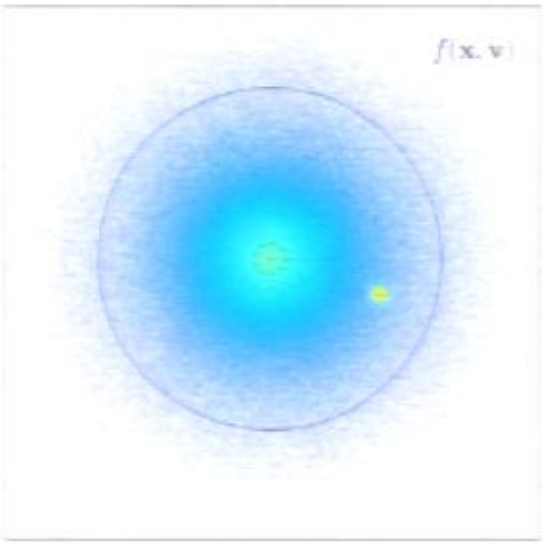
$f(\mathbf{x}, \mathbf{v})$

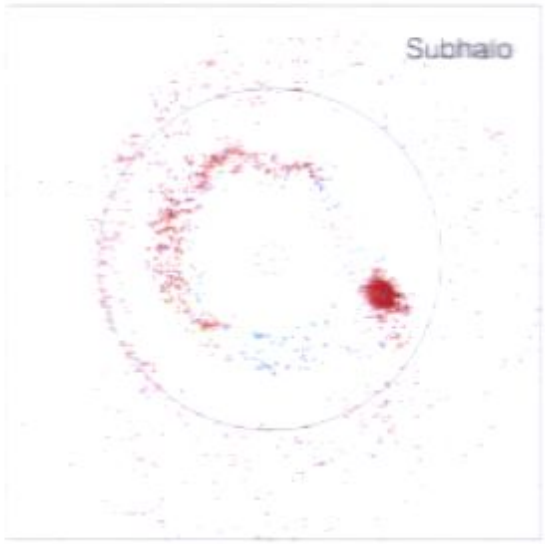
Subhalo

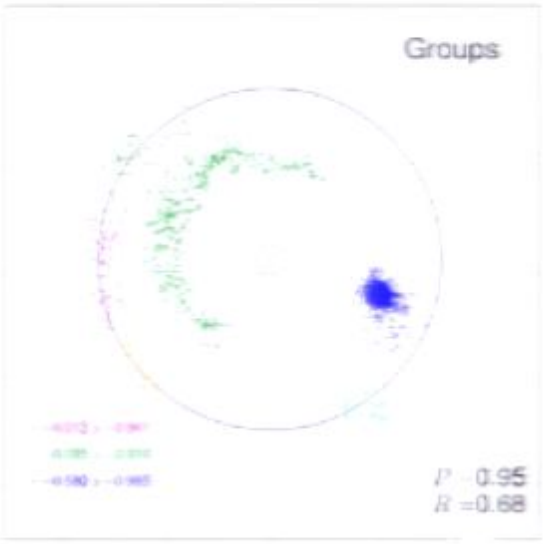
Groups
P 0.95
R =0.68

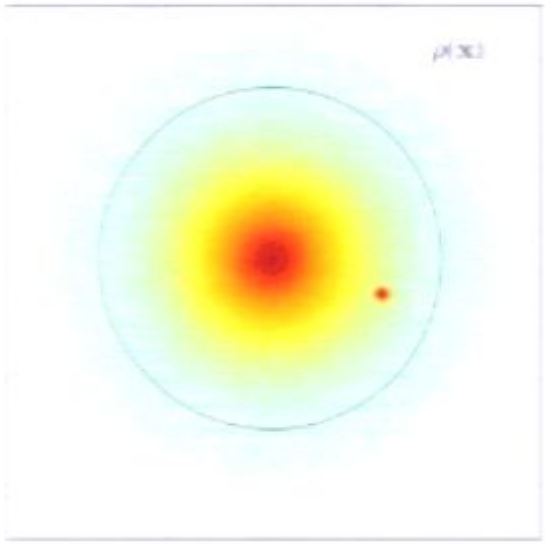

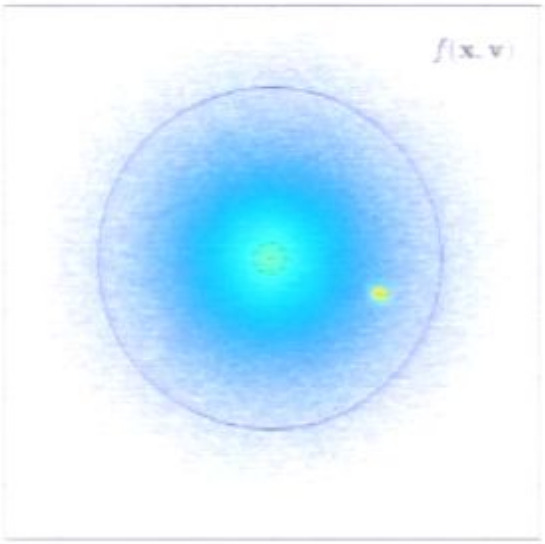

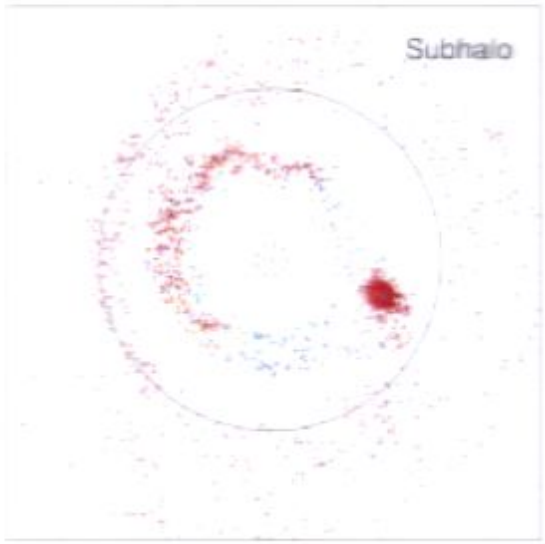
Subhalo

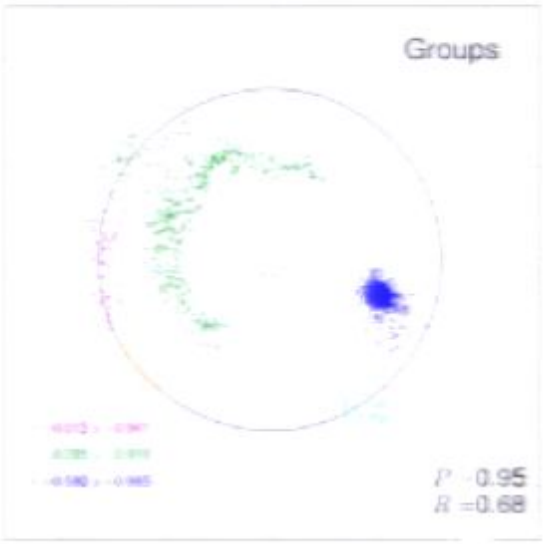
Groups
P 0.95
R =0.68

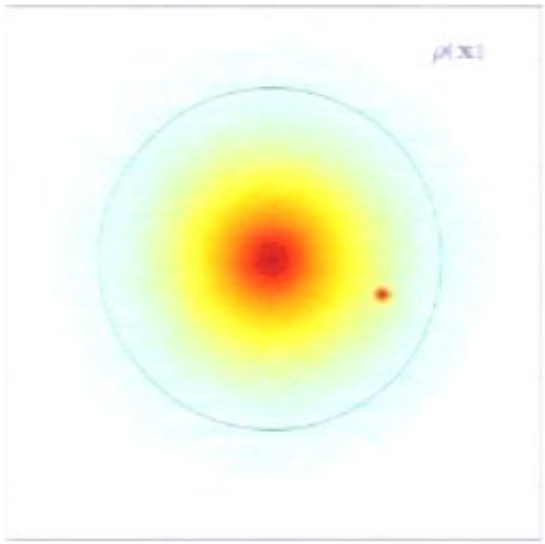
$\rho(\mathbf{x})$

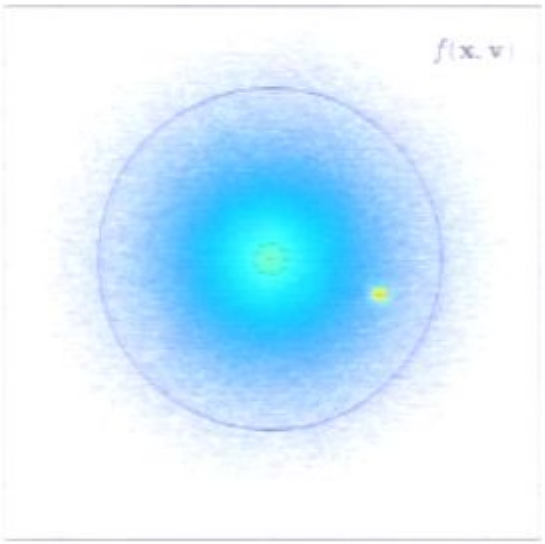
$f(\mathbf{x}, \mathbf{v})$

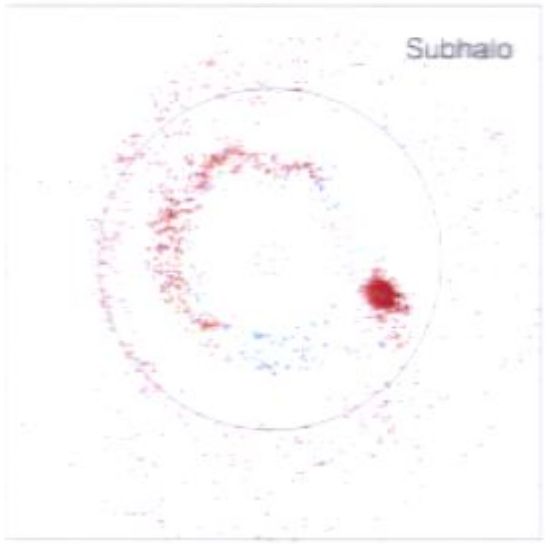
Subhalo

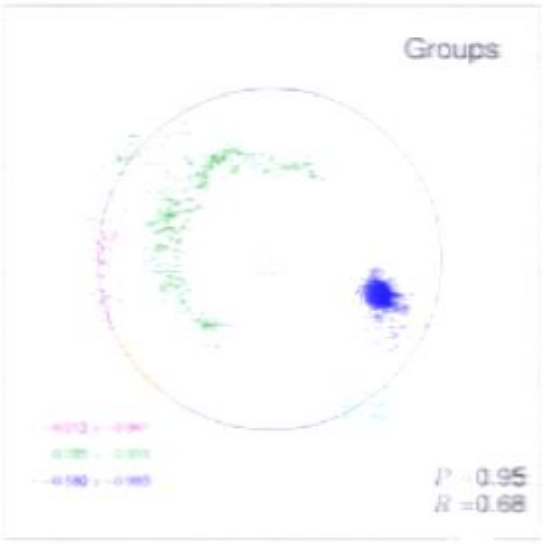
Groups
P 0.95
R =0.68

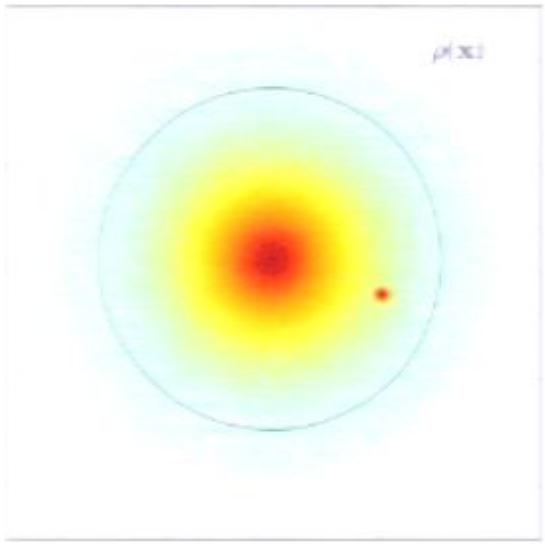
$\rho(\mathbf{x})$

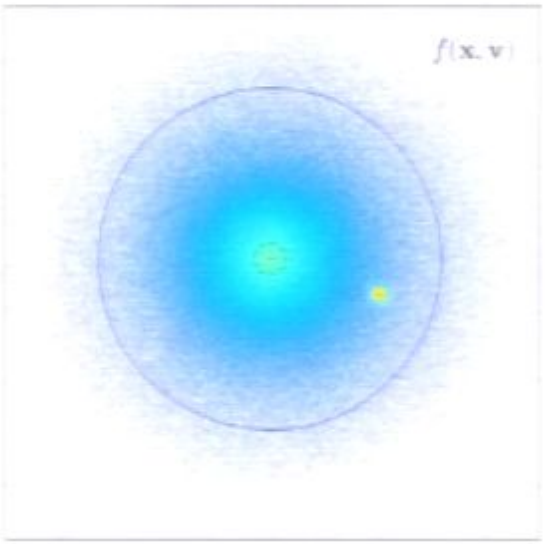
$f(\mathbf{x}, \mathbf{v})$

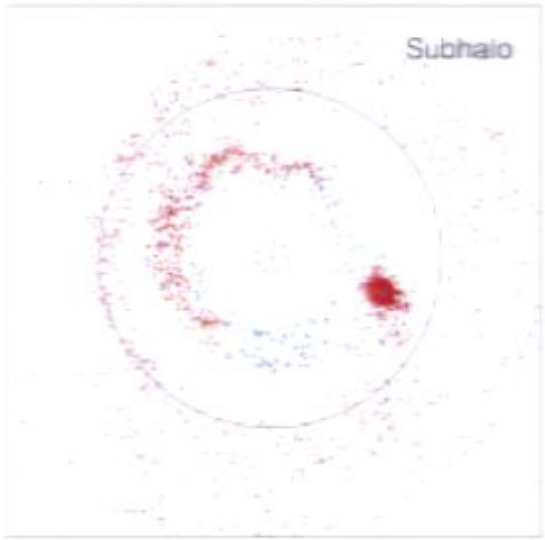
Subhalo

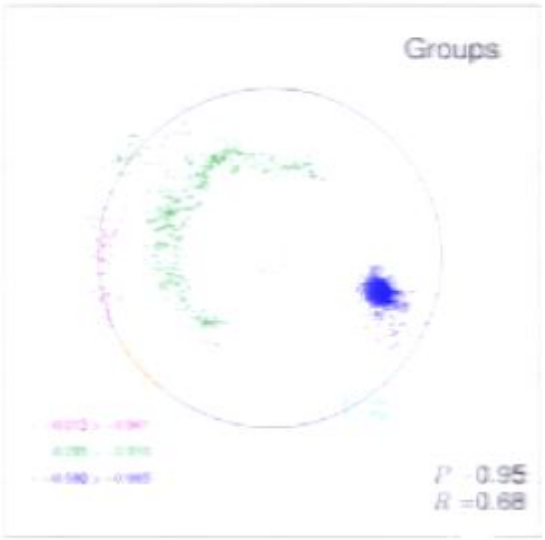
Groups
P 0.95
R =0.68

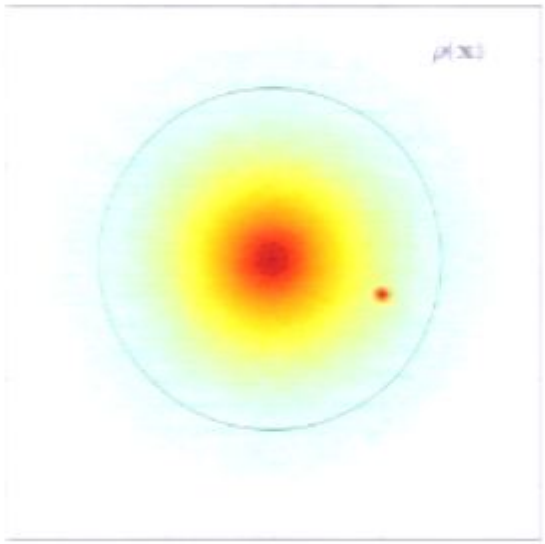
$\rho(\mathbf{x})$

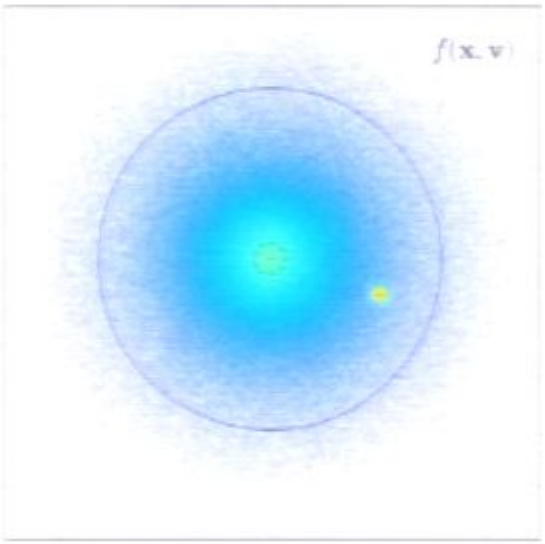
$f(\mathbf{x}, \mathbf{v})$

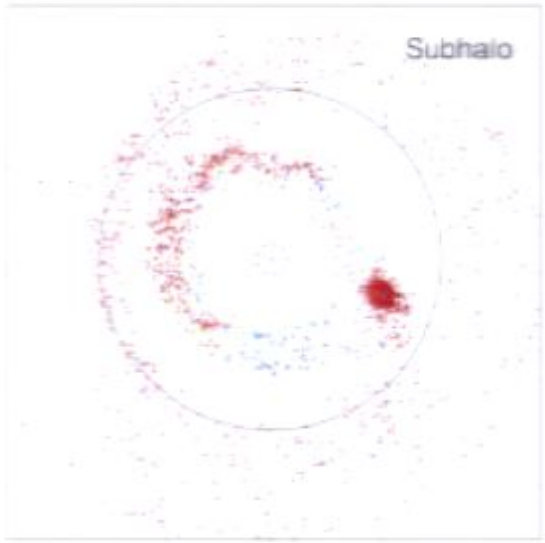
Subhalo

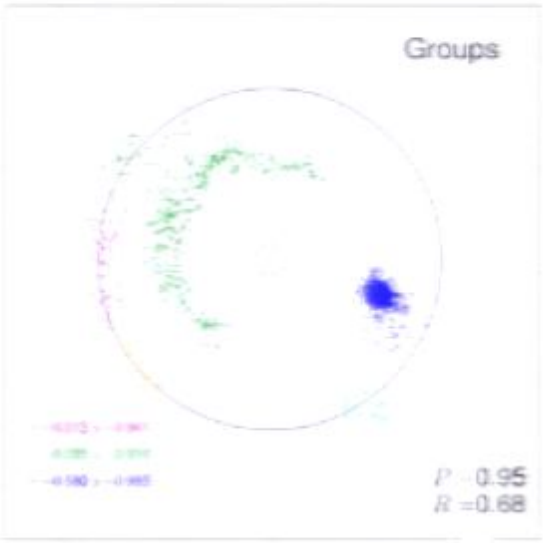
Groups
P 0.95
R =0.68

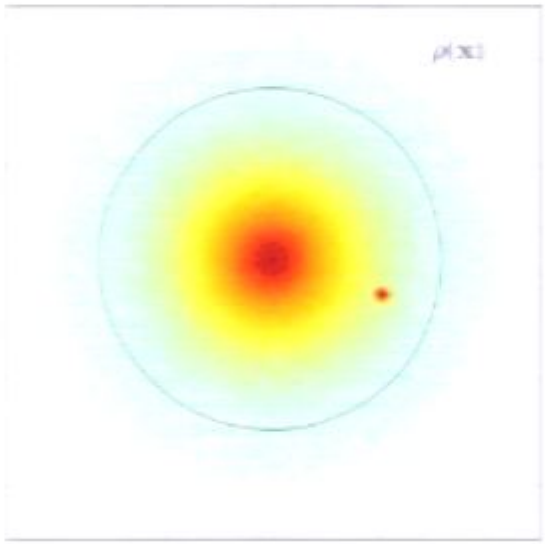
$\rho(\mathbf{x})$

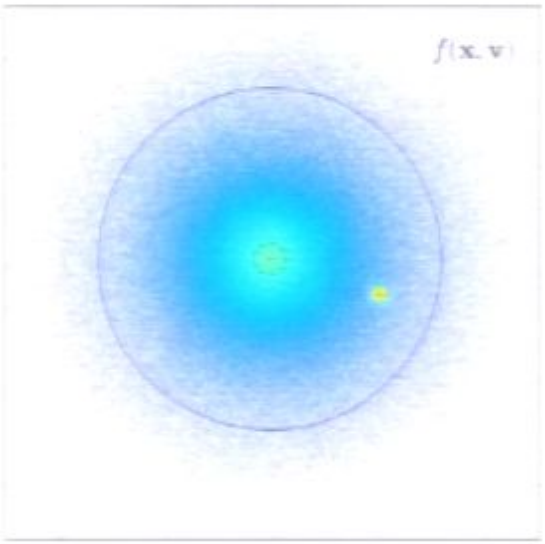
$f(\mathbf{x}, \mathbf{v})$

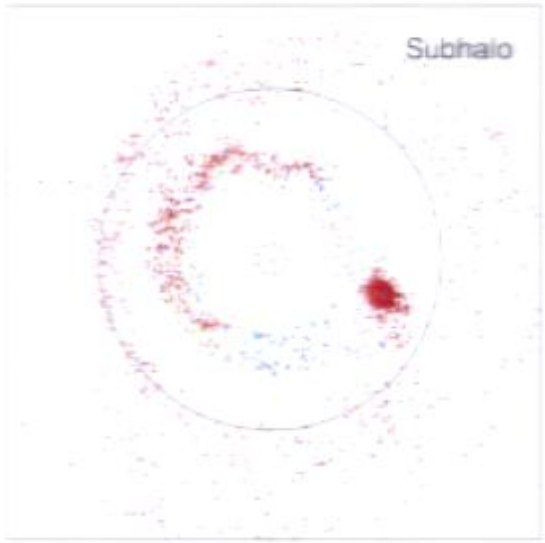
Subhalo

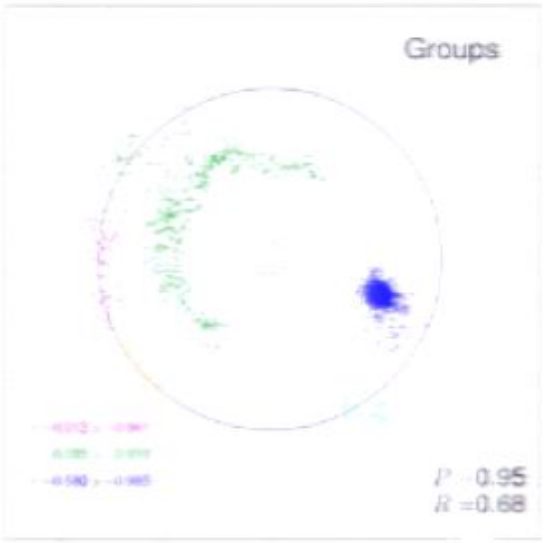
Groups
P 0.95
R =0.68

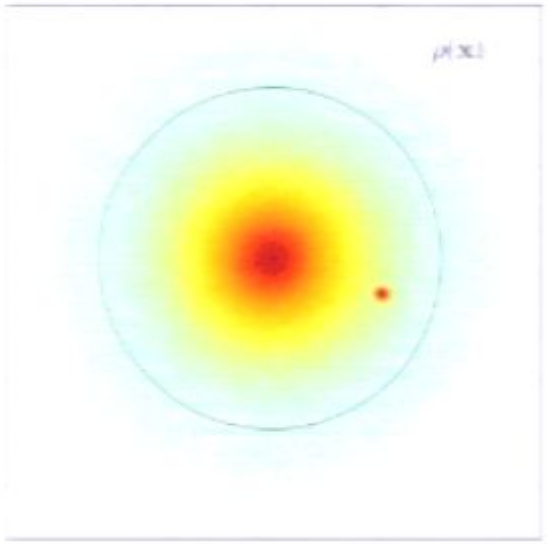
$\rho(\mathbf{x})$

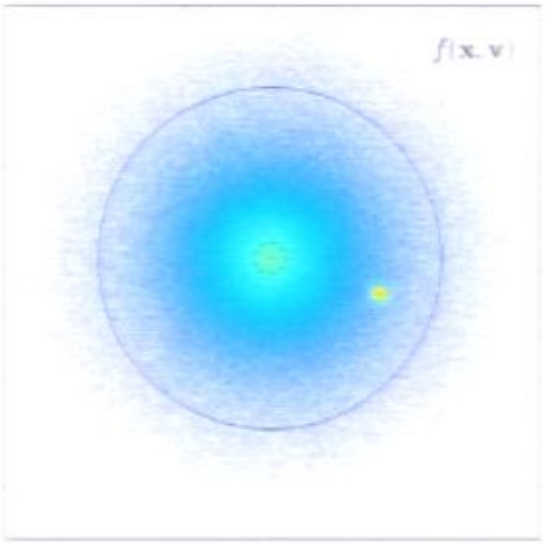
$f(\mathbf{x}, \mathbf{v})$

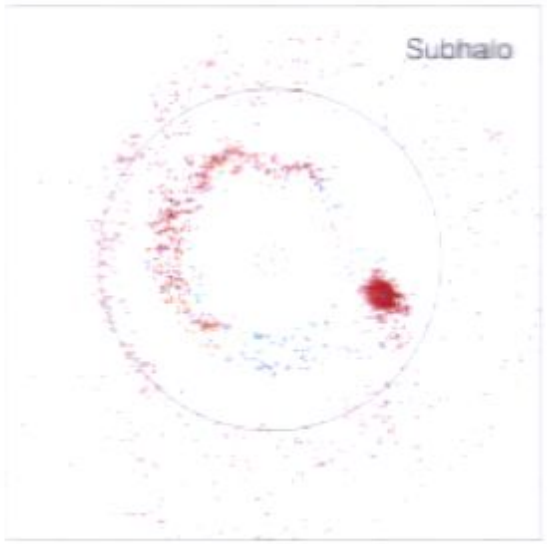
Subhalo

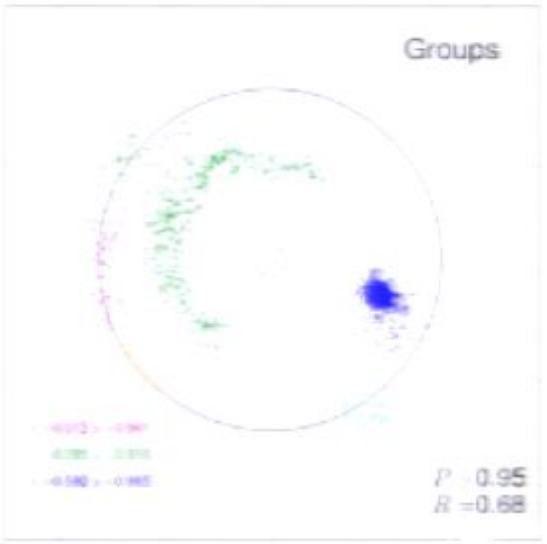
Groups
P 0.95
R =0.68

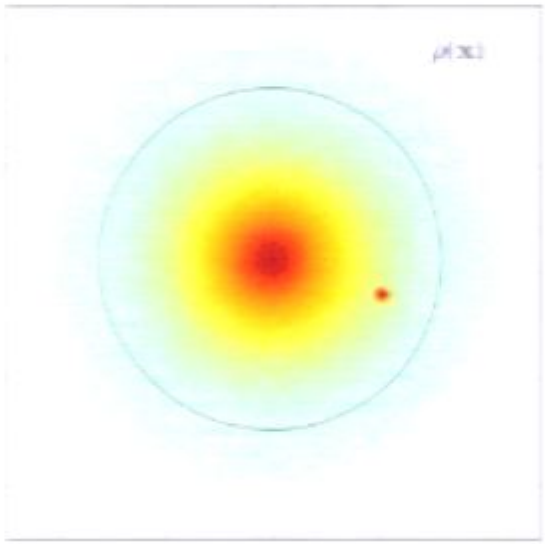
$\rho(\mathbf{x})$

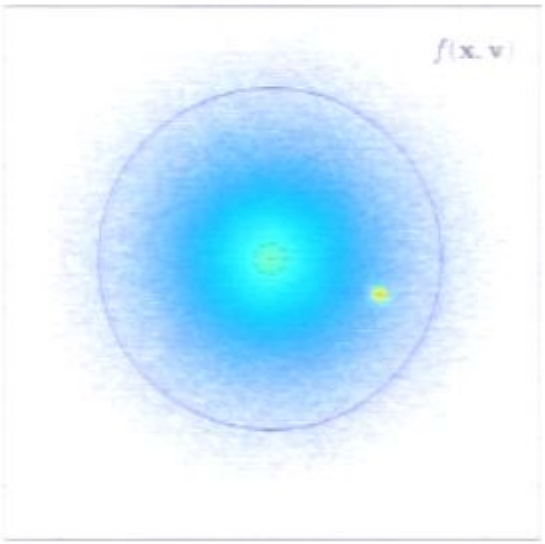
$f(\mathbf{x}, \mathbf{v})$

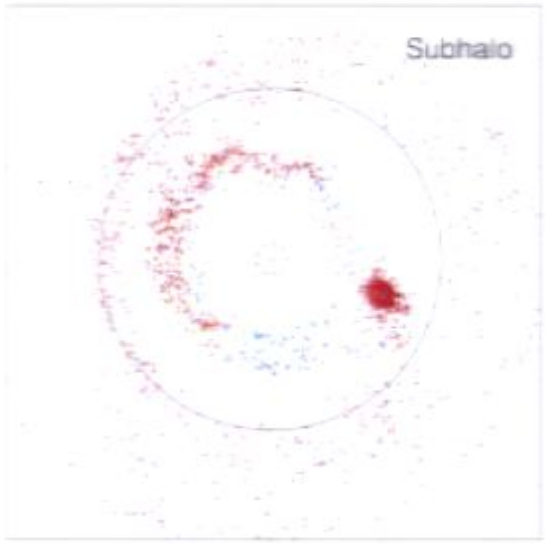
Subhalo

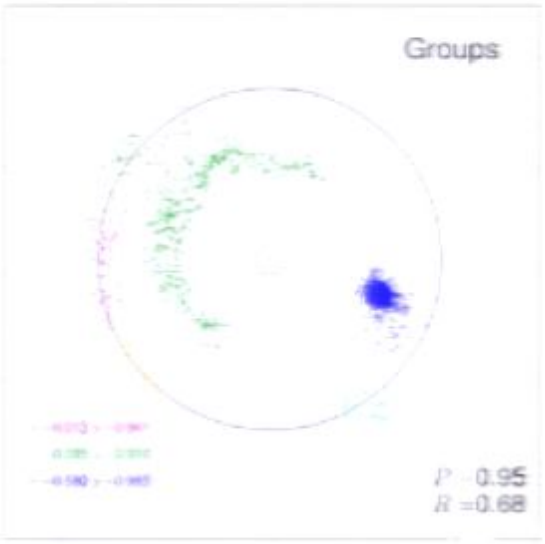
Groups
P 0.95
R =0.68

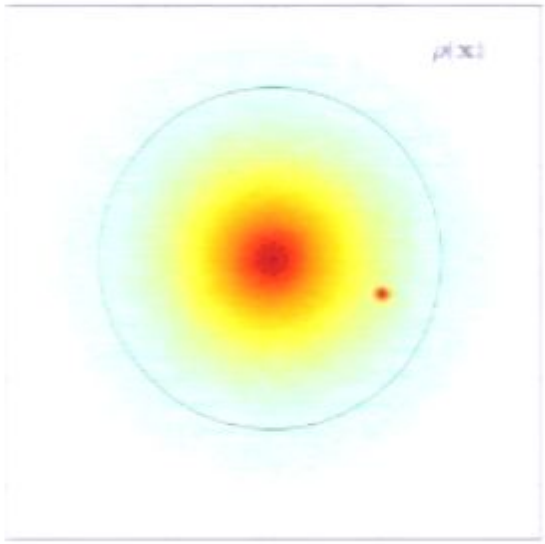
$\rho(\mathbf{x})$

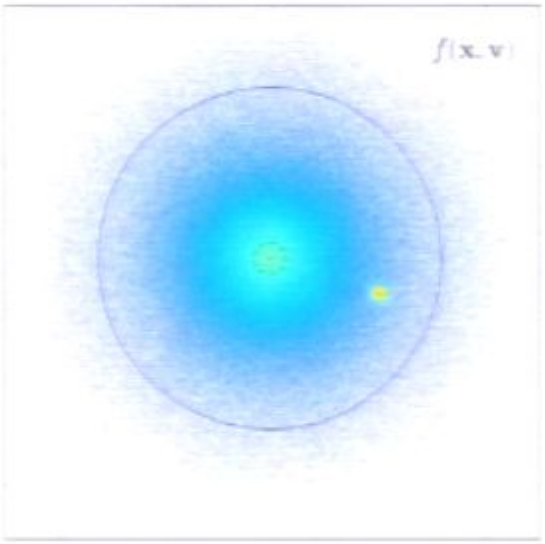
$f(\mathbf{x}, \mathbf{v})$

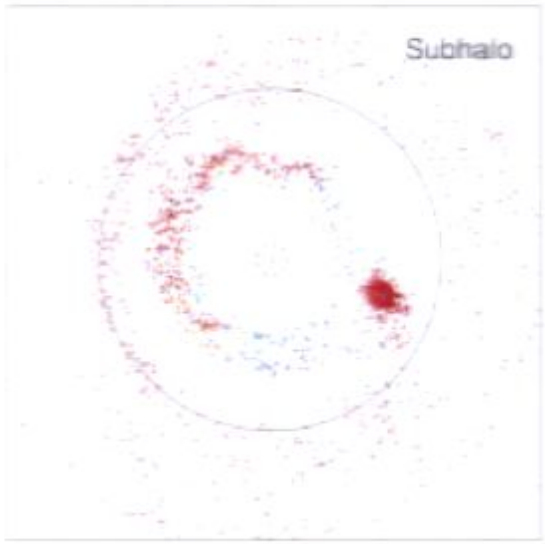
Subhalo

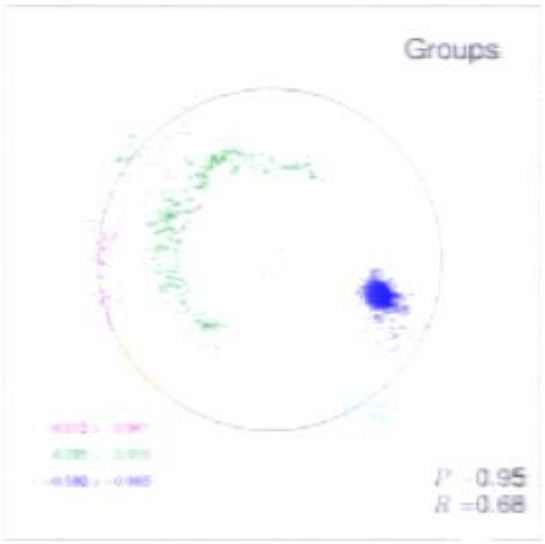
Groups
P 0.95
R =0.68